VOLUME 37, 1960

JOURNAL OF
Scientific Instruments

A MONTHLY PUBLICATION DEALING WITH THE PRINCIPLES,
CONSTRUCTION AND USE OF SCIENTIFIC INSTRUMENTS

Produced, with the co-operation of the National Physical Laboratory, by
The Institute of Physics and The Physical Society and previously by The Institute of Physics

EDITOR: **H. R. LANG,** B.Sc., Ph.D., A.R.C.S., F.Inst.P.
Secretary of The Institute of Physics

Succeeded on amalgamation by

A. C. STICKLAND, M.Sc., Ph.D.
Editor and Deputy Secretary of
The Institute of Physics and The Physical Society

THE INSTITUTE OF PHYSICS AND
THE PHYSICAL SOCIETY
LONDON

THE INSTITUTE OF PHYSICS AND THE PHYSICAL SOCIETY

OFFICERS AND MEMBERS OF THE COUNCIL, 1960–61

PRESIDENT	Sir John Cockcroft, O.M., K.C.B., C.B.E., D.Sc., F.Inst.P., F.R.S.
IMMEDIATE PAST-PRESIDENTS OF THE INSTITUTE AND OF THE SOCIETY	Sir George Thomson, M.A., LL.D., Sc.D., Hon.F.Inst.P., F.R.S.
	J. A. Ratcliffe, C.B.E., M.A., F.R.S.
VICE-PRESIDENTS	Prof. R. W. Ditchburn, M.A., B.Sc., Ph.D., F.Inst.P.
	A. J. Philpot, C.B.E., M.A., B.Sc., F.Inst.P.
	W. H. Taylor, M.A., D.Sc., F.Inst.P.
	J. Topping, M.Sc., Ph.D., F.Inst.P.
HONORARY TREASURER	J. Taylor, M.B.E., D.Sc., F.R.I.C., F.Inst.P.
HONORARY SECRETARY	C. G. Wynne, B.A., Ph.D., F.Inst.P.
ORDINARY MEMBERS OF COUNCIL	Prof. C. C. Butler, B.Sc., Ph.D., A.Inst.P.
	E. R. Davies, O.B.E., B.Sc., F.Inst.P.
	Prof. B. H. Flowers, M.A., D.Sc.
	J. M. A. Lenihan, M.Sc., Ph.D., A.M.I.E.E., F.Inst.P.
	G. R. Noakes, M.A., F.Inst.P.
	Prof. C. F. Powell, M.A., Sc.D., F.R.S.
	F. A. Vick, O.B.E., Ph.D., A.M.I.E.E., F.Inst.P.
	Prof. D. A. Wright, D.Sc., F.R.A.S., F.Inst.P.
REPRESENTING BRANCHES	M. R. Hopkins, M.Sc., Ph.D., F.Inst.P.
	Prof. H. Lipson, M.A., D.Sc., F.Inst.P., F.R.S.

EXECUTIVE OFFICERS

SECRETARY	H. R. Lang, B.Sc., Ph.D., A.R.C.S., F.Inst.P.
EDITOR AND DEPUTY SECRETARY	Miss A. C. Stickland, M.Sc., Ph.D.
DEPUTY SECRETARY	N. Clarke, B.Sc., F.Inst.P.

Journal of Scientific Instruments

SUB-COMMITTEE

M. E. Haine, D.Sc., A.M.I.E.E., F.Inst.P. (*Chairman*)
H. J. J. Braddick, B.A., Ph.D.
Prof. R. W. Ditchburn, M.A., B.Sc., Ph.D., F.Inst.P. (*Ex-officio member*)
K. J. Habell, A.R.C.S., M.Sc., F.Inst.P.
K. Kandiah, B.Sc.

CONTENTS OF VOLUME 37

PAGE

JANUARY 1960

ECIAL ARTICLE

Parametric amplification. By K. W. H. Stevens . . 1

PERS

Design and performance of a rapid-scanning X-ray diffractometer. By A. Skertchly 6
Two thermocouples suitable for measurement of temperatures up to 2800° C. By D. A. Davies . . 15
Design of laboratory furnaces. By P. L. Start and M. W. Thring 17
Apparatus for the measurement of the mechanical properties of fibres. By F. R. Morgan . . . 25
Recording weight meter. By D. J. Steele . . . 27
An electronic fluxmeter. By R. R. Birss and J. P. Fry . 31
Densitometer wedge for measurements at low optical densities. By N. R. Silvester 33

BORATORY AND WORKSHOP NOTES

High-temperature burner for working silica. By J. Conaboy 35
Double-acting reversible message register. By C. J. Sumner 35
Slow-feed dispenser for abrasive suspensions. By J. Lobb 36
Device for straining and fracturing thin foil specimens inside an electron microscope. By P. J. E. Forsyth and R. N. Wilson 37
Improved form of spring-clip for holding down a workpiece. By P. W. Harrison 38
Photoelectric refractometer. By C. W. Latey . . . 38
Simple technique for recording variations of a few centimetres in galvanometer reading. By R. G. Ackland 39

OTES AND NEWS

ew instruments, materials and tools 40

FEBRUARY 1960

APERS

X-ray diffraction by single crystals at low temperatures: a cryostat for use with liquid hydrogen. By J. H. Robertson 41
Simple device for use with platform weighbridges in the accurate determination of burning rates. By J. E. Roughton 45
An electroluminescent digital indicator with a silicon carbide coding matrix. By D. H. Mash . . . 47
Some techniques for recording and measuring time-resolved spectra. By A. H. Gabriel . . . 50
An electromicrobalance for weighing fibres. By F. R. Morgan 53
Portable airglow photometer. By B. J. O'Brien and G. de La Harpe 54
Direct method for determining the velocity of nuclear particles. By B. F. Hampton 56
Recording calorimeter for the measurement of heats of wetting, mixing, or solution. By F. A. P. Maggs and P. H. Schwabe 60
Twin-head goniometer for the study of diffusely reflected X-rays. By W. A. Wooster and G. A. Wooster . 64

ABORATORY AND WORKSHOP NOTES

Simple method of mounting and stretching thin gauze, sheet or foil. By P. A. Einstein 67
Simple refrigerant level controller for cold traps. By C. W. Nutt and A. J. Biddlestone 67
Crystal oscillation mechanism for use with automatic X-ray diffractometers. By U. W. Arndt, T. H. Faulkner and D. C. Phillips 68
Simple method of temperature control. By H. A. Vodden 69
Valve and adapter for the grease-free connexion of glass sample tubes to a mass spectrometer inlet system. By J. R. Richards 69
Diffuse-light integrator. By N. W. Wootten . . 70
Bubble method for magnetic susceptibility of liquids. By A. O. Mathai 71

NOTES AND NEWS

New instruments, materials and tools 72

MARCH 1960

PAPERS

Simple dosage meter for high-intensity thermal radiation. By P. H. Thomas and P. G. Smith 73
Design of a single electrode capacitor for use with moisture meters and similar apparatus. By D. F. Leach and J. M. M. Neilson 77
Method of measuring the angular deflexion in a dynamometer. By M. Axson and J. M. Magarshack . . 81
Apparatus for investigating total hemispherical emissivity. By J. H. Cairns 84
Oscillator measuring equipment for vibrating-wire gauges. By W. H. Ward and J. E. Cheney 88
Extensometer for semi-rigid materials. By C. D. Kinloch and N. E. Waters 93
Design criterion for correction of parallax at the best focus for definition. By G. W. Hamstead . . 95
Direct measurement of $\int i^2 dt$ by a method based on the Hall effect. By S. C. Ryder-Smith, A. E. Guile and A. E. Barrington 100
Simple ultramicro-pipette for electron microscopy. By R. Hardy, J. R. Majer and S. Travers . . . 103

LABORATORY AND WORKSHOP NOTES

Simple photoelectric demodulator. By A. Kolin and R. T. Kado 107
Gas-quenching apparatus for high-speed thermal analysis. By R. D. Garwood, J. R. Moon and B. F. Thrush . 108

NOTES AND NEWS

New instruments, materials and tools 109
New books 110
Notes and comments 112

APRIL 1960

PAPERS

Accurate direct-reading hydrostatic balance. By A. T. J. Hayward 113
Apparatus for the measurement of Young's modulus, between −200 and 700° C by transverse vibration in vacuum. By H. J. Stokes 117
Automatic decantation for routine sub-sieve sizing. By F. Horsfall and A. Jowett 120
Wax-atomizer for producing spherical dust particles. By G. K. Greenough 123

PAGE
Position transducer using a divided circle and coded scale. By I. R. YOUNG 125
Radiometer for field use. By J. H. MCGUIRE and H. WRAIGHT 128
New method of sample interchange in a solid-source mass spectrometer. By B. R. F. KENDALL . . . 130
Low-angle Geiger diffractometer for use with monochromatic radiation. By P. W. TEARE . . . 132
Improved eye-piece graticule for measuring X-ray powder diffraction patterns. By W. G. PERDOK and G. BOOM 134
Tunable galvanometer amplifier. By R. M. HUEY and B. J. LANCASTER 136
Measurement of cyclic strain. By T. M. DOWELL and J. A. MACKINNON 138
Determination of the profiles of water waves. By J. A. SANDOVER and C. TAYLOR 141
Instrument for recording the resistance during the deposition of a thin film. By J. A. BENNETT and T. P. FLANAGAN 143
Improved smoke density recorder By R. LAMBIE . 144

LABORATORY AND WORKSHOP NOTES

Electronic leak detector. By D. J. DOWLING . . 147
Filament winding machine. By D. BARKER . . . 147
Determination of the density of glass fibres. By B. D. COATES 148
Protection of diffusion pumps against inadequate cooling. By B. C. COX 148
Electromechanical low frequency oscillator. By E. W. DICKSON 149

NOTES AND NEWS

New instruments, materials and tools 150
New books 152

MAY 1960

SPECIAL ARTICLE

The Physical Society's Exhibition—London, 1960. By T. B. RYMER 153

PAPERS

Yarn-speed meter—a low-torque instrument for measuring the linear speed of low-inertia systems. By D. L. MUNDEN and T. K. MORLEY 157
Production and tensile testing of strain-free metal specimens. By G. GREETHAM and A. J. MARTIN . . 160
Primary standard barometer of range 0 to 1200 mb. By K. W. T. ELLIOTT, D. C. WILSON, F. C. P. MASON and P. H. BIGG 162
Heat transport anemometer of high stability. By A. J. DYER 166
Vacuum sublimation apparatus for preparation of thin sources of α-active materials. By N. JACKSON . . 169
Vacuum furnace for high temperature X-ray diffractometry. By J. N. VAN NIEKERK 172
Apparatus for the zone refining of copper. By E. D. TOLMIE 175

LABORATORY AND WORKSHOP NOTES

New method of cold hearth melting. By W. H. SHEPHERD 177
Automatically operated balanced filters for counter diffractometer. By H. A. MCKINSTRY and M. A. SHORT 178
Gratings for measuring separation of equidistant parallel straight lines. By R. M. DAWSON 178
Design of a small rolling mill for use at low temperatures. E. D. TOLMIE and A. C. ROBERTS 180

PAG
Two-way oil-filled dash pot. By A. W. WILLIAMS and L. RIDDIFORD 18
Grips for tensile tests on very extensible tapes. By A. G. DAY 18

CORRESPONDENCE

Effect of ambient airspeed on efficiency of thermal-precipitator. From J. R. HODKINSON, A. CRITCHLOW and N. STANLEY 18
Comments on the A.S.T.M. Powder Data File—5. From J. W. HUGHES, ISABEL E. LEWIS and A. J. C. WILSON 18

NOTES AND NEWS

Notes and comments 18

JUNE 1960

PAPERS

Compensated Wheatstone's bridge circuit for gas-chromatographic catharometry. By A. B. LITTLEWOOD 18
Transistor cup anemometer. By R. R. MCGREGOR . 18
Photoelectric comparator for Rayleigh fringe electrophoresis patterns. By C. C. CURTAIN . . . 190
Rand soil-pressure cell for low pressures, high accuracy and long-term stability. By J. E. JENNINGS and J. B. BURLAND 19
R.F. admittance bridge for liquid-dielectric measurements. By R. G. BENNETT 19
Equipment for the encapsulation of semiconductor devices. By R. D. KNIGHT 19
Tilting and rotating specimen stage for electron microscopy and electron diffraction. By R. E. BURGE and H. R. MUNDEN 19
Use of a liquid scintillator counter for beta particles. By T. B. RYVES 20
Epoxy resin joints for sealed-off, high-vacuum tubes. By J. F. SAYERS 20
High frequency light modulation. By R. L. WILLIAMS . 20
Beam method for the measurement of internal friction. By J. E. THOMPSON 208
Technique for replicating fibre surfaces by rolling. By J. MØLGAARD 21
Laboratory magnetic elutriator for purification and isolation of ferrimagnetic mineral sands. By W. R. B. MARTIN 21

LABORATORY AND WORKSHOP NOTES

Automatic polishing technique for electro-thinning metals for transmission electron microscopy. By V. A. PHILLIPS and J. A. HUGO 21
Two-valve electrometer circuit. By J. P. KEENE . . 21
Welding copper pipe to stainless-steel flanges in a laboratory workshop. By J. LEECE 21
Simple multi-position level. By C. J. SUMNER . . 22
Report on a pump-operated air aspirator. By A. NUNLIST and P. H. KITTO 221
Construction of a thermocouple for measuring surface temperatures. By L. ONGKIEHONG and J. VAN DUIJN 221
Simple agitating device for partition experiments. By L. BISHOP, H. J. DE BRUIN and R. B. TEMPLE . . 22

CORRESPONDENCE

Influence of protective paper on X-ray diffraction photographs. From H. RUCK, M. KOURIS and R. ST. J. MANLEY 22

NOTES AND NEWS

Notes and comments 22

JULY 1960

ERS

PAGE
easurement of magnetostriction within the temperature range −196 to 400° C. By R. R. Birss and E. W. Lee 225
ew high-voltage multi-stage impulse generator circuit. By T. E. Broadbent 231
agnetically operated mass-marker. By J. J. Brown, R. I. Reed and W. Simpson 236
iquid-nitrogen cryostat for single-crystal X-ray diffraction. By A. E. Attard and L. V. Azároff 238
arge storage binary-to-decimal converter. By G. Dearnaley, L. G. Lawrence and H. C. Tresise 240
rowth of single crystals of anthracene. By J. N. Sherwood and S. J. Thomson 242
ide-band detector for micro-microampere low-energy electron currents. By T. E. Everhart and R. F. M. Thornley 246

BORATORY AND WORKSHOP NOTES

Modified cylindrical cell for the microelectrophoresis of suspended particles. By E. J. Ambrose and J. Ryder 248
nstruments for measuring the temperature of a running thread-line, and of a jet of viscous liquid. By M. F. Culpin and K. A. Martin 250
akeable bellows-type differential pressure manometer. By A. E. D. Heylen 251
Method of finding the focal curve of a photographic spectrometer. By J. F. James 252
mproved sample loading technique for solid source mass spectrometry. By R. E. Powell 252
Automatic gas-sampling device for gas chromatography. By D. W. Hill and J. R. Hook 253

RRESPONDENCE

The theory of stresses in two-component glass to metal tube seals. From H. Rawson 255
Measurement of cyclic strain. From T. M. Dowell and J. A. MacKinnon 255
Apparatus for the measurement of Young's modulus, between −200 and 700° C by transverse vibration in vacuum. From H. J. Stokes 255

OTES AND NEWS

tes and comments 256

AUGUST 1960

APERS

Tomograph for industrial radiography. By D. Charles 257
A 450 J spark discharge for shadowgraph photography. By L. Whitlow 259
Moiré fringe reading head for use with a fine grating. By D. A. Palmer 261
Production of islands and dice in semiconductor slices with an ultrasonic drill. By R. D. Knight 263
Single tube sedimentation apparatus for the measurement of particle size distribution. By J. Kobak and D. J. Loveridge 266
Multipoint digital temperature recorder with punched tape output. By T. S. Holden 269
High vacuum high temperature X-ray camera. By B. A. Hatt, P. J. C. Kent and G. I. Williams 273
Sensitive and simple integrator. By J. P. Funk 276
Accurate measurements of phase differences with the Babinet compensator. By P. Hariharan and D. Sen 278
Some modifications to an oscilloscope camera, and the construction of a control unit. By M. H. Evans and G. Pierson 282
Temperature regulator for close temperature control. By E. N. Herzberg 285
PAGE
Time analyser using a crystal-controlled trochotron tube. By T. Dobrowolski and J. Walker 289
The torsiometer—an instrument for the study of gels considered as elastic solids. By W. A. Southorn 292
Portable electrometer voltmeter. By W. E. K. Gibbs 296
Novel displacement detector and its application in a recording thermobalance. By J. C. van der Breggen and H. J. Wouterlood 297
Ratiometer phase angle indicator. By K. L. Morphew 300

LABORATORY AND WORKSHOP NOTES

Transistor operation of electromechanical registers. By J. C. Barton 303
Cut-off for the vacuum manipulation of chlorine. By M. Green and K. H. Maxwell 303
Test tube adaptor for use in optical density measurements. By J. B. Dawson 304
Simple high temperature X-ray camera. By G. Farrow and D. Preston 305
Stabilized high-intensity light source. By C. M. Hurd 305
Simple detector for small leaks using a thoriated tungsten emitter with oxygen as probe gas. By R. N. Bloomer and W. C. Brooks 306

CORRESPONDENCE

Foam viscometer. From R. J. French 307

NOTES AND NEWS

New instruments, materials and tools 308
Notes and comments 312

SEPTEMBER 1960

PAPERS

Error of rectifier-type milliammeters in low-resistance circuits. By J. Wilbur-Ham and W. E. K. Gibbs 313
Daylight factor meter. By D. P. Turner 316
Time-sorter for use in the nanosecond range. By G. Jones 318
Isotopic analysis of boron in boron trifluoride by mass spectrometry, and measurement of natural boron 10 concentration. By P. G. Bentley 323
Ratiometer for low-current mass spectrometry. By F. D. S. Butement and N. P. Finkelstein 328
Measurement of space density of charge in flowing liquids. By A. Schuringa and C. Luttik 332
Reduction of dead-time in halogen-quenched Geiger counters. By B. B. Trott 336
Apparatus for the measurement of gas velocity in furnaces and models. By A. E. Pengelly 339
Simple continuous chart and integrating device for a Joyce-Loebl microdensitometer Mk. I. By G. Farrow and D. Preston 347
Measurement of thermal diffusivity of semiconductors by Ångström's method. By A. Green and L. E. J. Cowles 349
Heavy-water electrolysis unit for generation of deuterium gas provided with automatic switch-off and safety devices. By P. K. Dutt 352
Temperature-controlled permanent magnet for high-resolution nuclear magnetic resonance. By B. A. Evans and R. E. Richards 353
Improved design for an auto-focus range-finder. By H. Asher, L. Dodin and H. P. Mulholland 356

LABORATORY AND WORKSHOP NOTES

Vernier scale arrangement for the measurement of peak heights on mass spectrometer charts. By J. R. Richards 358

PAGE
Insulated terminals for high-vacuum systems using demountable glass–metal seals. By R. S. NELSON . 358
Cosine correction of a weatherproofed photovoltaic cell. By E. T. WESTON and D. PAIX 359
Automatic silver concentration control for nuclear emulsion fixing baths. By E. DAHL-JENSEN . . 360
Robust and sensitive spoon gauge. By B. J. AYLETT . 362

NOTES AND NEWS
New instruments, materials and tools 363
New books 366
Notes and comments 368

OCTOBER 1960

PAPERS

Magnetic probes of high frequency response. By S. E. SEGRE and J. E. ALLEN 369
Transistorized frequency stabilization for reflex klystrons used in magnetic resonance. By P. JUNG . . . 372
Cyclic shearing interferometer. By P. HARIHARAN and D. SEN 374
Automatic range-changing of a linear ratemeter. By S. LOVETT 376
Production of a pulsed magnetic field using an electrolytic capacitor bank. By D. G. BATE and R. F. SAXE . 378
Transformer bridges for use with resistance strain gauges and similar transducers. By L. N. CLARKE . . 381
Production of millimicrosecond current pulses using a pressurized spark gap. By J. H. ADLAM and L. S. HOLMES 385
Electronic apparatus for the study of X-rays with proportional counter. By N. PATLA 388
X-ray fluorescence method for determination of the transition-metal content in very small specimens of alloys. By P. J. BROWN 394

LABORATORY AND WORKSHOP NOTES
Pyrolytic coating of quartz and ceramic vessels used for zone melting. By R. BEELS and W. DE SUTTER . . 397
Furnace for the uniform heating and mixing of powders in controlled atmospheres. By H. MONK and F. F. KIERYS 397
Frequency stabilization of klystrons. By M. J. A. SMITH 398
Oscillating flat-specimen holder for an X-ray powder camera. By J. D. WILKINSON and L. D. CALVERT . 399

NOVEMBER 1960

PAPERS

Low-compliance diaphragm-capacitance gauge for measurement of liquid pressures of the order of 1 in. water. By A. S. LODGE 401
Lens mass-spectrometer leak detector. By D. COSSUTTA and W. STECKELMACHER 404
Apparatus for the floating-zone refining of gallium arsenide. By F. A. CUNNELL and R. WICKHAM . 410
Rapid counter for small particles in suspension. By J. B. CORNWALL and R. M. DAVISON 414
Measurement of the optical thickness of absorbing specimens with the three-beam interferometer. By P. HARIHARAN and D. SEN 417
Digito-analogue computer for solving linear simultaneous equations and related problems. By E. V. KRISHNAMURTHY 419
Inexpensive graph plotter for five-track paper tape. By L. MOLYNEUX and E. E. SCHNEIDER 425
Apparatus for measurement of sorption of reactive, condensable vapours up to 350° C. By R. M. BARRER and S. WASILEWSKI 432
Instrument for the measurement of specular reflectivity of bright metal surfaces. By B. A. SCOTT . .

LABORATORY AND WORKSHOP NOTES
Simple method for stopping a radiation chopper in a preferred position. By M. F. KIMMITT . . . .
Flap-value for long narrow apertures. By G. W. KING .
Hot tube Nylon cord cutter for balloon flights. By J. A. PHILLIPS . . . .
Film carrier for the analysis of oscillograms by means of a travelling microscope. By T. M. PARNELL . .

NOTES AND NEWS
New instruments, materials and tools . . . .
New books . . . .
Notes and comments . . . .

DECEMBER 1960

PAPERS

Further experiences with aluminium wire seals for bakeable vacuum systems. By L. ELSWORTH, L. HOLLAND and L. LAURENSON 4
Wide-angle photoelectric integrating flashmeter. By J. EDWARDS, W. R. LANE and B. R. D. STONE . . 4
Portable water velocity meter. By J. M. EDINGTON and L. MOLYNEUX 4
Swept Langmuir probe system for intense gas discharges. By H. W. JONES and P. A. H. SAUNDERS . . . 44
Photomultiplier soft X-ray spectrometer. By L. JACOB, R. NOBLE and H. YEE 44
Stability of some reactance standards. By L. H. FORD . 44
Monitor for the quantitative determination of beryllium in the atmosphere. By M. S. W. WEBB, R. J. WEBB and P. C. WILDY 44
Vibrating reed magnetometer. By D. C. DOUGHTY and P. MOSSMAN 44
Geiger counter backgrounds. By B. L. COHEN . . 4
Temperature-control system for use with a spectrophotometer. By S. W. THORNE 4
Viscometers having damped torsional oscillation. By B. S. ASHWIN, T. HAGYARD, I. C. B. SAUNDERS and T. E. YOUNG 4

LABORATORY AND WORKSHOP NOTES
Elimination of ghost images when using a Kerr-cell shutter. By D. W. GODWIN and F. R. BROOKES . 48
Improved design of portable vacuum manometer. By A. T. J. HAYWARD 48
Simple force balance for drag measurements. By G. A. HENWOOD 48
Liquid-level alarm using internally reflected light. By W. E. HOOD and E. OLDHAM 48
Improved flow-sensitive switch. By H. C. BURFORD . 49
Method for increasing the range of a flowmeter. By C. C. HARRIS 49

CORRESPONDENCE
Measurement of tellurium vapour pressure using electrical discharges. From J. C. BRICE 49

NOTES AND NEWS
New instruments, materials and tools 49
New books 49
Notes and comments 49

SUBJECT INDEX TO VOLUME 37 49

AUTHOR INDEX TO VOLUME 37 50

Parametric amplification

y K. W. H. STEVENS, M.A., D.Phil., Department of Physics, University of Nottingham

Abstract

The purpose of this paper (which is based on the lecture recently given to the Electronics Group of The Institute of Physics) is to review the underlying ideas of parametric amplification. The discussion is mainly in physical terms and passes from simple circuit amplifiers to the more complex Suhl-types of amplifier. Mention is made of some of the directions in which research is proceeding.

Introduction

The recent considerable growth of interest in the phenomenon of parametric amplification seems to have been started by a suggestion (Suhl(1)) that low-noise amplifiers for microwave frequencies could be made by using the parametric principle. Dr. Suhl had been investigating the rather complicated behaviour of certain ferrimagnetic materials under resonance conditions, using high signal powers. In consequence, a superficial reading of his earlier papers tends to suggest that there is something rather difficult in the underlying ideas. This, as it is quite clear that Dr. Suhl appreciated, is not so, and in fact the principle of parametic amplification is elementary and should have been well-known. Thus, by studying what has proved to be a complicated example of parametic amplification, and by recognizing it as such, Dr. Suhl has drawn attention to the potentialities of parametric amplification at just the time when suitable materials are available for exploiting the technique in the microwave field. The last few years have seen considerable activity in this direction: so much so that it is difficult to keep abreast of all the developments and, in a short account of this nature, it seems of most value to consider the underlying ideas and give references to the more detailed applications.

It so happened that at almost the same time that Suhl's letter appeared, Prof. Bloembergen(2) suggested that, by using the properties of certain paramagnetic salts in the solid-state maser, amplification at microwave frequencies could be obtained. The two amplifiers work on quite different principles and are being simultaneously developed. In addition the previously existing travelling-wave-tube amplifiers are being further developed (possibly because of the appearance of potential rivals), and the indications are that travelling-wave features will be increasingly introduced into both maser and parametric amplifiers. In spite of all the work that has been done, relatively little has yet been published about the performances of practical parametric amplifiers for microwaves, and it may be that some of the difficulties foreseen by Suhl have proved troublesome. It certainly seems that most progress has been made by using the principle in ways which are not, superficially, related to his original suggestion.

Simple type of amplifier

One of the most familiar oscillators which uses the parametric principle is the child's swing. Lord Rayleigh,(3) in 1883, discussed the problem of a simple pendulum in which the support is made to oscillate vertically at twice the frequency of the pendulum, and showed that the pendulum can be kept in oscillation. In the swing, an equivalent effect is obtained by varying the tension in the suspending ropes at twice the frequency of oscillation. Another well-known example is that in which a button is threaded on to a loop of string. Then, on holding a side of the loop in each hand, it is possible to get the button into rotational oscillation by applying periodic tensions to the string. In most applications, one is more interested in amplifiers than in oscillators and it turns out that, although it is simple to make mechanical oscillators, it is comparatively difficult to make mechanical amplifiers, though it has been done (Danielson(4)). The simplest amplifiers are made using electrical circuits and for this reason it is convenient to pass now to their consideration.

Consider then a resonant circuit consisting of capacitor C, inductance L and resistance R, and suppose that it has been excited so that a small, damped oscillatory current of angular frequency ω, given by $\{(1/LC) - (R^2/4L^2)\}^{1/2}$, is flowing. Suppose also that when the charge on the capacitor has its maximum value, the plates of the capacitor are pulled slightly apart, to reduce the capacitance by δC. The mechanical work needed for this is converted into electrical energy instantaneously stored in the capacitor. A quarter of a cycle later the charge will have fallen to zero and the plates can be restored to their original separation with no energy interchange. The circuit can now be subjected to a similar cycle in the next and subsequent half-cycles of oscillation of the charge. The system is such that external work is, periodically, being done on it so that, if there were no resistive losses, the energy stored would build up indefinitely. If there is a resistive loss, the stored energy will either build up or will fall to zero, for the case in which it rises to a definite stable level is exceptional. This is because both the work done in the capacitor variation and the resistive loss are proportional to Q^2, the term Q being the amplitude of the oscillating charge, and it is not possible to have the work done by the capacitor variation exactly equal to the resistive loss unless there is a definite relation between δC, ω and R. In practice, if δC is smaller than a certain value, the oscillations decay to zero: if it is greater than this value they build up indefinitely, except that Q is clearly limited by the mechanical power available. In this description, it has been assumed that the changes in C occur discontinuously at definite times in the charge cycle. Such an assumption is not necessary and it is equally possible to suppose that C is varying sinusoidally with time, thus:

$$C = C_0 + \delta C \sin 2\omega t.$$

There is again a threshold for oscillation. Alternatively the inductance can be varied at 2ω, but there is nothing to be gained by varying the resistance at 2ω, for a resistance does not store energy. For detailed discussions, the reader may be referred to Stevens(5) and Valdes.(6) It should be particularly noticed that the power supply for this oscillator is

MAR 2 3

not, as is so often the case, a steady supply, but is actually oscillating at a higher frequency than that of the oscillations it is sustaining. There can thus be no suggestion that the oscillations are being maintained by harmonics of the power supply. Also, the phase of oscillation will be determined by the phase of the capacitor variation.

Now consider what modifications are necessary if there is a signal voltage, $V \sin \omega t$ in the circuit. With δC equal to zero, the amplitude of the charge will have a stable value Q, determined by the condition that the work, proportional to Q, done by the signal voltage shall exactly equal the dissipation, proportional to Q^2, which occurs in the resistance. To increase the stored energy by means of a condenser variation, $\delta C \sin(2\omega t + \phi)$, it is necessary to phase the variation correctly so that the maximum rate of decrease of C occurs at the extreme values of capacitor charge. On the assumption that this is so, the amplitude of the oscillating charge will increase until a new stable state is reached in which the dissipation in the resistance is equal to the sum of the work done by the capacitor drive and the signal voltage. The energy balance has the form:

$$\frac{2\omega Q^2 \delta C}{2\pi(2C^2)} + \frac{\omega Q V}{2} = \frac{R\omega^2 Q^2}{2},$$

or:

$$V = Q\omega\left\{R - \frac{\delta C}{\pi\omega C^2}\right\},$$

from which it is seen that the effect of the drive, as the capacitance variation may be called, is to introduce a negative resistance into the circuit. If the drive is so great that the total effective resistance in the circuit becomes negative, oscillations occur. Below this threshold, amplification can be obtained, for the energy dissipated in R, which may be regarded as the load, is greater and proportional to the energy taken from the signal voltage. The phasing of signal and drive which is required provides a serious limitation.

If the signal voltage is not quite at the angular frequency ω, but is at $(\omega + \delta\omega)$, it can be regarded as at ω, but with a slowly varying phase. For certain phase angles it will be amplified and for others it will be attenuated, with the result that the voltage developed across R will be modulated in amplitude at $2\delta\omega$. Alternatively, the signal voltage at $(\omega + \delta\omega)$ is mixed with the drive at 2ω to produce currents at $(\omega - \delta\omega)$, which beat with the signal currents at $(\omega + \delta\omega)$ to give a beat frequency at $2\delta\omega$. There is a net power gain, but the output is such that the device can hardly be regarded as a satisfactory amplifier.

The arguments presented above were given in the literature, in a slightly different form, many years ago and are presumably well-known. Now, as a result of Suhl's work, an important new variation has been found, which eliminates the difficulty of phasing the pump and signal.

To demonstrate this, it is convenient to consider the circuit arrangement shown in Fig. 1. There are now two resonant circuits, with parameters $L_1C_1R_1$ and $L_2C_2R_2$ respectively, so chosen that their respective angular frequencies, given by

$$\omega_1 = \left(\frac{1}{L_1C_1} - \frac{R_1^2}{4L_1^2}\right)^{1/2} \text{ and } \omega_2 = \left(\frac{1}{L_2C_2} - \frac{R_2^2}{4L_2^2}\right)^{1/2},$$

are quite distinct. In addition the two circuits are to be regarded as mutually coupled by a variable reactance, which in this example takes the form of a variable mutual inductance. Suppose now that a current at ω_1 is flowing in circuit (1). Because of the constant part of the mutual inductance a voltage at ω_1 is induced into circuit (2) but, as this will be well off-resonance, its effect will be small and can be neglec
Suppose, however, that the mutual inductance is also be
varied sinusoidally with angular frequency ω. The volt
induced into circuit (2) depends on $d(Mi_1)/dt$ and
contain components at $(\omega - \omega_1)$ and $(\omega + \omega_1)$. Thus
ω is chosen to equal the sum of ω_1 and ω_2, a voltage co
ponent is induced into circuit (2) at exactly its reson

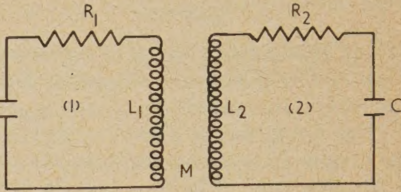

Fig. 1. Two tuned circuits of angular frequencies ω_1 and ω_2 (with $\omega_1 \neq \omega_2$) coupled through a time-dependent mutua inductance

$$M = M_0 + m \sin(\omega t + \psi)$$

frequency. Circuit (2) will respond strongly to this co
ponent and appreciable currents will flow in it, at ω_2.
an exactly similar argument these currents will react bac
through the inductance variation, on circuit (1) and t
net effect will be to change the impedance of circuit (1).
first sight, it might seem that this impedance will depend
the phase of the mutual inductance variation, but this is
so, as can be inferred from quite general arguments. Let
be supposed that the current in circuit (1) is given by

$$i_1 = i \sin \omega_1 t,$$

and the mutual inductance by:

$$M = M_0 + m \sin(\omega t + \psi).$$

In a steady condition, such as would occur if the current
circuit (1) results from a voltage source in circuit (1),
should not matter what origin of time is used. Therefo
let the origin be changed by setting t to be $(T + a)$, where
is a constant. Now unless ω/ω_1, equals an integer, whic
can be supposed not to be so, it is always possible to choos
a so that the current and inductance variations take th
forms:

$$i \sin \omega_1 T \text{ and } M = M_0 + m \sin \omega T$$

That is, to an observer using this second origin of time, th
phase angle ψ between drive and signal has disappeare
Thus, as might be expected, relative phase has no meanin
between two variations of unrelated frequency. If, however
the phase of the current in the idler circuit, as circuit (2) i
called, is also considered, in it is found that becaus
$\omega = (\omega_1 + \omega_2)$, the three phases are related, according t
$\psi_1 - \phi_1 - \phi_2 = \frac{1}{2}\pi$, where ψ_1, ϕ_1 and ϕ_2 refer to th
pump, signal and idler respectively, for any origin of time
The detailed calculations confirm this, and show that, as fa
as circuit (1) is concerned the whole of circuit (2) and th
inductance variation can be replaced by an equivalen
negative resistance $-m^2\omega_1\omega_2/4R_2$. It is also possible t
suppose that the inductance variation (the drive) is at th
difference, $|\omega_1 - \omega_2|$, rather than the sum frequency. I
this case the effective impedance is a positive resistance
$m^2\omega_1\omega_2/4R_2$. In view of the symmetry between the tw
circuits, it follows that with $\omega = (\omega_1 + \omega_2)$ the impedance
of circuit (2) is changed by $-m^2\omega_1\omega_2/4R_1$. When these
effective resistances exactly balance the natural resistances
present, the threshold for oscillation has been reached. It

will be noticed that the threshold, given by $R_1R_2 = \frac{1}{4}m^2\omega_1\omega_2$, is reached simultaneously in both circuits.

Microwave amplifiers

The circuits just discussed, while affording good examples of the phenomenon of parametric amplification, can hardly be regarded as suitable for the amplification of microwaves. Instead of using lumped tuned circuits, it is more likely that cavity resonators will be used. The two tuned circuits can then be taken as different modes of the same cavity, provided that some way is found of obtaining a time-dependent coupling between them. Suhl suggested that the resonance properties of ferrimagnetics might be used to provide the coupling.

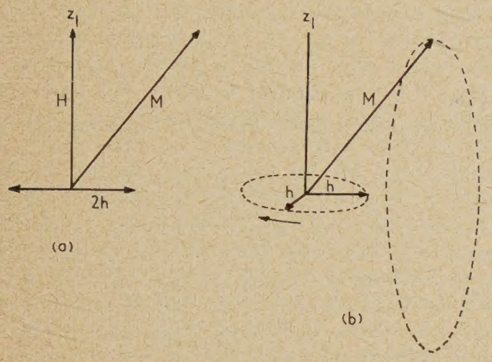

Fig. 2. Magnetic resonance; (*a*) fixed observer; (*b*) rotating observer

Suppose first that in the resonator there is a ferrimagnetic sample on which a typical resonance experiment is being carried out (Fig. 2*a*). That is, a steady external magnetic field H is applied in the z-direction and electromagnetic radiation of frequency ν is fed into a suitable cavity mode, so that the magnetic field $2h$ of the radiation, at the position of the sample, is perpendicular to H. The steady magnetic field, or the frequency of the radiation, is varied until a resonant absorption occurs. The frequency of the radiation is then the same as that of the Larmor precession of the magnetization of the sample, in the absence of the radiation. It is now of interest to consider how an observer (see Fig. 2*b*), who is made to rotate about Oz with the Larmor precession frequency, will describe what is happening. The essence of Larmor's theorem is that, to him, the effective steady d.c. field is zero, so that he is only aware of the field of the radiation. A stationary observer could regard this as composed of two oppositely rotating fields, at $\pm\nu$, each of magnitude h. To the rotating observer these will appear as a steady field h perpendicular to Oz and a field rotating at 2ν. In general, h will be very much smaller than H. The component rotating at 2ν will largely be ignored by the magnetization, which will precess, relatively slowly, about the steady component, h. Now it is probable that when the radiation field is first applied the magnetization will be directed along Oz (which is the same for a fixed and a rotating observer), so the angle of precession will be near 90 deg., and on this simple argument it appears that large changes in the orientation of the magnetization can take place. Under favourable circumstances this is true, but usually relaxation processes intervene. They operate as follows. Suppose that at some instant the magnetization is in thermal equilibrium. Then, ignoring h in comparison with H, the magnetization will be directed along Oz. The contact with the thermal bath is now broken, so that, in the rotating observer's frame of reference, the magnetization begins its precession, with angle of precession 90 deg., about h. Before very long, however, there is a "collision" with the lattice, whereby the system is restored to thermal equilibrium, and the magnetization is thereby restored to point along Oz again. This happens repeatedly. Then, instead of the rotating observer seeing a precessing moment, he sees something more like a magnetization oscillating about a mean direction which is at angle to Oz. If the oscillations are ignored, the rotating observer sees a steady magnetization, and a fixed observer regards this as a magnetization precessing steadily about Oz at an angle determined by h and the collision time. At each "collision," the energy which has been absorbed from the radiation field in the precession which has taken place since the previous collision, is given to the lattice. There is, thus, on a long time scale, a steady absorption of energy, from the radiation field, which is transmitted, through the relaxation processes, to the lattice of the sample where it appears as heat.

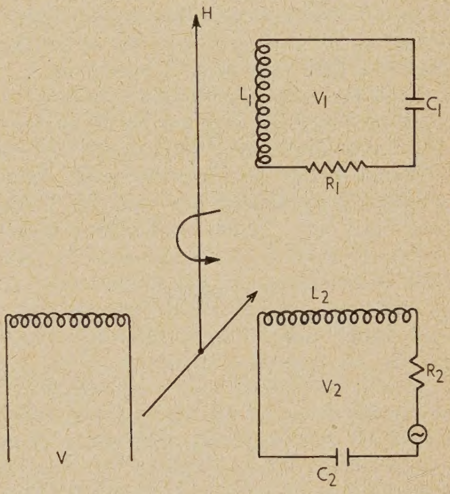

Fig. 3. Circuit analogue of ferrimagnetic amplifier

Suppose next that in addition to the mode of frequency ν (which is carrying what may be called the driving signal since it keeps the precession going) there are two other cavity modes of resonant frequencies ν_1 and ν_2 such that $\nu = \nu_1 + \nu_2$, and such that their magnetic fields at the sample are respectively parallel and transverse to H. Such an arrangement is shown schematically in Fig. 3, where suitably oriented tuned circuits are used to represent the cavity modes. In addition, a signal at ν_2 is being fed into mode (2). Returning now to the rotating observer, it is clear that he will see additional fields due to the excitation of mode (2), which will appear to him as composed of two rotating fields, at $(\nu + \nu_2)$ and $(\nu - \nu_2)$. In the resonance theory, such rotating fields are neglected as having a small effect but, in the present case, it is important not to make such an approximation. What then will be their effect? Qualitatively it seems likely that they will modulate the oscillating motion of the magnetization, as described by the rotating observer, at $(\nu_1 + \nu_2)$ and $(\nu_1 - \nu_2)$. The component of magnetization in the direction of Oz will show these modulations and, since Oz is the same for fixed and rotating observers, a fixed observer will see the same modulations. With the relation $\nu = \nu_1 + \nu_2$, one of the modulation frequencies is at precisely the right frequency (and the moment is suitably oriented) to excite mode (1). The rest of the discussion is now very similar to that of the coupled circuit example, for it is clear that there is a time-dependent coupling between modes (1) and (2) arising from the precession at ν. A detailed examination is required to determine the equivalent impedance experienced by mode (2). (See Stevens$^{(7)}$ for a lumped circuit analogue and Suhl$^{(8)}$ for the cavity case.) It is found that the equivalent impedance has a reactive part which is small and changes the resonance slightly and a resistive part which consists of two terms:

$$-\frac{\gamma^4 b^2 M^2 T_2^2 \nu_2 \lambda_1^2 \lambda_2^2}{4\nu_1 R_1} + \frac{\gamma^3 b^2 M T_2 \nu_2 \lambda_2^2}{4\nu_1}$$

where M is the magnetization, γ is the gyromagnetic ratio of the material, T_2 is a relaxation time, λ_1 and λ_2 are coupling constants which describe the interactions between the modes and the magnetization, and b represents the amplitude of the driving field. The second term gives a positive resistance and is present even in the absence of the mode (1), for it remains on putting λ_1 equal to zero. The first term is the one which gives rise to amplification, for it represents a negative resistance and it is not difficult to arrange that it more than cancels the positive term.

It will have been noticed that the cavity is required to have three modes ν, ν_1 and ν_2 such that $\nu = \nu_1 + \nu_2$, with certain geometrical relations between their fields at the sample. This requirement is not easily met, and it is experimentally simpler to let $\nu_1 = \nu_2 = \frac{1}{2}\nu$ and then dispense with the two modes (1) and (2) by having a single mode of frequency $\frac{1}{2}\nu$ with its magnetic field at a skew direction to H. Such an arrangement has been used by Weiss$^{(9)}$: presumably it suffers from the phasing difficulties discussed in the circuit analogue. Various other suggestions have been made, such as to have ν_1 and ν_2 distinct, but to eliminate the mode ν and keep the moment precessing by forcing non-resonant modes with a powerful oscillator at ν. A more interesting suggestion was made by Suhl. It depends on the fact that the moment of a ferrimagnetic is composed of the moments of very many interacting electrons. In the steady precessional motion—the so-called Kittel mode—the moments in various parts of the sample are all precessing in phase. This, however, is only one mode of excitation and it is perfectly possible to have an excitation in which the moments in different parts of the sample are not precessing in phase. These are the so-called magnetostatic modes (Walker$^{(10)}$). They have many of the characteristics of harmonic oscillators and the suggestion is to replace ν_1 by one of these internal modes of oscillation of the ferrimagnetic. Unfortunately, there is likely to be a number of pairs of magnetostatic modes such that the sums of their frequencies equal ν. Thus the possibility exists that the driving signal will excite one or more of these pairs, and so waste its power in keeping unwanted oscillations going with, effectively, no amplification in the wanted mode, ν_2. It is perhaps significant that relatively little has been published which indicates that microwave amplifiers using precessing moments can be built successfully, and it may be that the magnetostatic modes are proving troublesome.

An apparently more successful parametric amplifier relies on capacitative rather than inductive coupling by using the properties of certain semiconductors. With a suitable reverse bias it is found that the charge which they apparently store depends non-linearly on the voltage across them, and it is loosely said that their capacitance is voltage-dependent. They can be used therefore to couple resonant circuits together for parametric amplification. Most successful applicatio have been at lower frequencies than microwaves, main because the most readily available materials are not suitab for microwave frequencies. Efforts are being made develop more suitable materials (Danielson$^{(4)}$) and it seem not unlikely that there will be a move away from magnet devices.

A particular feature of parametric amplifiers of the typ described above is that no electron beams are used, whic suggests that it may be possible to avoid the sources of nois associated therewith. [Actually recent progress in electron beam techniques (Adler$^{(11)}$) has greatly reduced the bea noise.] The prospect that parametric amplifiers would hav low noise has been one of their great attractions and, to large extent, this hope seems to have been fulfilled. In an system, one must expect thermal fluctuations associated wit the dissipative elements but, provided that the temperatur can be reduced, these can be made as small as desired. How ever, it often happens that some part of the amplifier cease to work if the temperature is too low (for example, the cathod in a conventional valve). In a parametric amplifier ther seems no reason why the whole device cannot be coole indefinitely. The one element to which this may not appl is the oscillator which is providing the driving signal, and ar important question which arises is whether or not random fluctuations in the driving signal can produce excess noise in the signal circuit. Certainly such fluctuations will produce changes in the gain of the amplifier, but this is not the same as noise, for noise describes the power appearing in the signal circuit in the absence of a signal. Fluctuations in the driving signal will be centred about ν, so that fluctuations at ν_2 in the signal circuit can only arise from the mixing of the driving fluctuations with noise fluctuations in mode (1) near ν_1. There does not yet appear to be a theoretical discussion of this point, but there are experimental indications that fluctuations in the driving signal do not provide a serious limitation.

The amplification occurs because the effective resistance in the signal circuit is reduced, which means that the effective Q-factor of this circuit is increased. Thus the higher the amplification factor the less the bandwidth, according to the relation

$$GB = \textit{constant}$$

where G is the voltage gain and B is the bandwidth. For a given bandwidth there is a definite advantage in spreading the amplification over several stages and, for this reason, attention is being increasingly given to travelling-wave types of amplifier. With a ferrimagnetic substance the active material must be subjected to travelling waves in some suitable propagating structure, rather than to standing waves as in the resonator case. There is considerable scope here for ingenious circuitry.

Wave mechanical treatment

One of the features about the examples given above is that they can be understood classically. Nevertheless, it is of some value to try and describe them wave-mechanically because of the deeper insight obtained. For example, wave-mechanics shows just how detailed is the energy balance. The purpose of the driving signal is to provide quanta of magnitude $h\nu$. In the case of the precessing moment, absorption of a quantum lifts the system to a level $h\nu$ higher in energy (Fig. 4). In a steady state the system must ultimately return to its initial state, so it must get rid of the quantum ust absorbed. It can give it back to the pump, resulting in o net absorption; it can give it to the thermal vibrations of he lattice, *via* the spin-lattice relaxation processes, where it ppears as heat; or, in the parametric amplifier, it can give quantum $h\nu_1$ to mode (1) and a quantum $h\nu_2$ to mode (2). t is this last possibility which is so interesting, for it is found that the probability of the division occurring depends on the energy already in modes (1) and (2). When a quantum is given, say, to mode (1), an oscillation is set up in it and this helps to control the rate at which further quanta are given to mode (1). Thus the process differs from a simple scattering, such as occurs in the Raman effect, for here, once the scattering has occurred, say by dividing $h\nu$ into $h\nu_1$ and $h\nu_2$ (where $\nu = \nu_1 + \nu_2$) the quanta $h\nu_1$ and $h\nu_2$ represent the energies of wave-packets which are flowing away from the scattering centre and therefore cannot influence any further scattering. If a means were devised for reflecting them back to influence subsequent scatterings, the main effect in parametric amplification would be obtained.

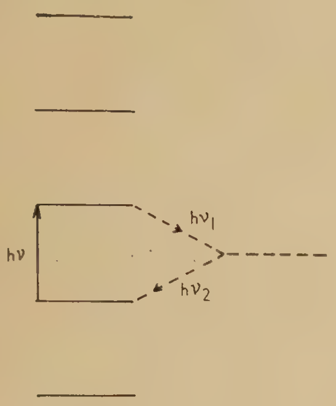

Fig. 4. Increase in energy level by absorption of a quantum

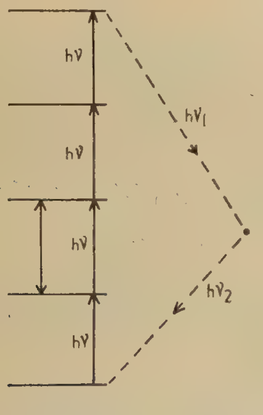

Fig. 5. Increase in energy level of ferrimagnetic material

A question which is often asked is whether or not it is possible to envisage a parametric amplifier in which the driving frequency is lower than the signal frequency. In principle there is nothing to prevent this, and several methods have been proposed, although they do not seem to have been reported as working. In terms of wave-mechanics, what is needed is a high-order process in which several quanta are absorbed from the driving signal to increase the energy of the ferrimagnetic by $nh\nu$, where n is an integer (Fig. 5). This is now passed on to two circuits tuned to ν_1 and ν_2, where $\nu_1 + \nu_2 = n\nu$. There is then no reason why ν_1 and ν_2 need be less than ν.

A practical suggestion, due to Hogan, Jepsen and Vartanian(12), is to take a parametric amplifier, such as the coupled circuit example, with no signal, and provide sufficient driving that it would be in oscillation. The circuit (2) has, effectively, a negative resistance. Next, circuit (2) is coupled, by another time-dependent mutual inductance, to circuit (3), of frequency ν_3, where $\nu_3 > \nu_2$. The second mutual inductance is to be driven at the difference frequency, $\nu_3 - \nu_2$. If circuit (2) had a positive resistance, driving at this difference frequency would give a positive resistance to circuit (3). But circuit (2) has been arranged to have a negative resistance, so that circuit (3) has a negative resistance added to it, and can therefore be used for amplification.

Conclusion

In conclusion, it may be asked what the future is likely to be with parametric amplification. It seems that the principle is capable of providing low-noise amplifiers at any frequency, provided that the circuitry and materials problems can be overcome. There are other amplifiers which are potentially as good, but there is nothing at present to suggest that parametric amplifiers will not live up to expectations. It is too soon to form really firm assessments of the relative merits of masers, travelling-wave tubes, parametric amplifiers, etc., and presumably we must look forward to interesting developments in all these devices.

References

(1) SUHL, H. *Phys. Rev.*, **106**, p. 384 (1957).

(2) BLOEMBERGEN, N. *Phys. Rev.*, **104**, p. 324 (1956).

(3) RAYLEIGH, LORD. *The Theory of Sound*, 2nd Edition, Vol. 1, p. 81 (New York: Dover Publications Inc., 1945).

(4) DANIELSON, W. E. *J. Appl. Phys.*, **30**, p. 8 (1959).

(5) STEVENS, K. W. H. *J. Electr. Contr.*, **4**, p. 275 (1958).

(6) VALDES, L. B. *J. Electr. Contr.*, **5**, p. 129 (1958).

(7) STEVENS, K. W. H. *J. Electr. Contr.*, **4**, p. 280 (1958).

(8) SUHL, H. *J. Appl. Phys.*, **28**, p. 1225 (1957).

(9) WEISS, P. R. *Phys. Rev.*, **107**, p. 317 (1957).

(10) WALKER, L. R. *Phys. Rev.*, **105**, p. 390 (1957).

(11) ADLER, R. *Proc. I.R.E.*, **46**, p. 1300 (1958).

(12) HOGAN, C. L., JEPSEN, R. L., and VARTANIAN, P. H. *J. Appl. Phys.*, **29**, p. 422 (1958).

Design and performance of a rapid-scanning X-ray diffractometer

by A. SKERTCHLY, M.Sc., A.Inst.P., Department of Textile Industries, University of Leeds

[*Paper first received* 6 *August, and in final form* 18 *September*, 1959]

Abstract

The apparatus described enables the equatorial X-ray diffraction intensity distribution from radially symmetrical specimens to be obtained over the angle range 0 *to* 20° *of Bragg* θ *in twenty seconds. Sequential scans are performed at the rate of two per minute and the X-ray intelligence is retained in the form of pulses by being recorded on magnetic tape which preserves the record with a high degree of fidelity. Also incorporated is an intensity analyser which enables the integrated count to be obtained between any two preset positions of Bragg* θ, *the limits being adjustable in steps of* 0·1° *to a high degree of precision. Although the instrument is designed primarily for the investigation of reaction kinetics in certain high polymeric substances of interest to the textile industry, there is obvious scope in other applications which involve relatively rapid changes in lattice parameters. Design details and some performance data are briefly mentioned together with an illustrative application.*

Introduction

MANY fibrous or potentially fibre-forming materials(1) are only available in the form of cylinders with an infinite longitudinal rotation axis of symmetry. Much of the data of potential interest to the X-ray diffraction crystallographer is obtained in the equatorial intensity distribution, and often the structure factors of those planes which contribute to the zero order layer lines are greater than the average, so that the magnitude of the reflexions can often be measured accurately.

The instrument reported in this paper was designed and constructed in order to obtain quickly the equatorial intensity distribution from materials in the fibre class. Since, up to a point, the accuracy obtainable in intensity measurements governed by the Poisson distribution is a function of time, increase in scanning rate will result in a diminution of accuracy. However, there are many problems where the loss in accuracy (if any) is not great enough to cause any severe disadvantage in the usefulness of the present technique.

With few exceptions(2, 3) the reported(4) applications of diffractometers have concentrated on securing high accuracy in Bragg spacings and intensity measurements, and the time taken to secure such information is often a secondary consideration.

However, as was noted by Pepinsky(5) as long ago as 1943, there is scope for the application of diffractometric measurements to investigate time-dependent lattice transformations. It is surprising how little has been reported relating to measurements of this type, and there appears to be no detailed attempt at instrumentation designed to secure quantitative X-ray diffraction data over a range of angle within a short time. It is a partial solution to this problem that is the subject matter of this paper. The solution adopte is exceedingly simple in principle, but has been developed t incorporate various extra facilities which greatly enhance th usefulness of the basic system.

Instrumental facilities

The basic technique involved is the oscilloscope display o the equatorial X-ray intensity distribution with a vertica deflexion proportional to integrated count rate, together wit a horizontal deflexion which is proportional to the Bragg position of the X-ray detector. A preliminary experimenta apparatus based on this idea has been reported,(6) but considerable elaboration has been necessary to provide th present analytical tool.

The diffractometer as finally evolved consists of two scanning arms attached to which are the radiation detector (usually Geiger or proportional counters). The arm traverse planar paths having equiangular separations from the main beam with a rate of scan that is variable between wide limits, but which is usually fixed near 1° of Bragg per second in order to make the apparatus "direct reading"

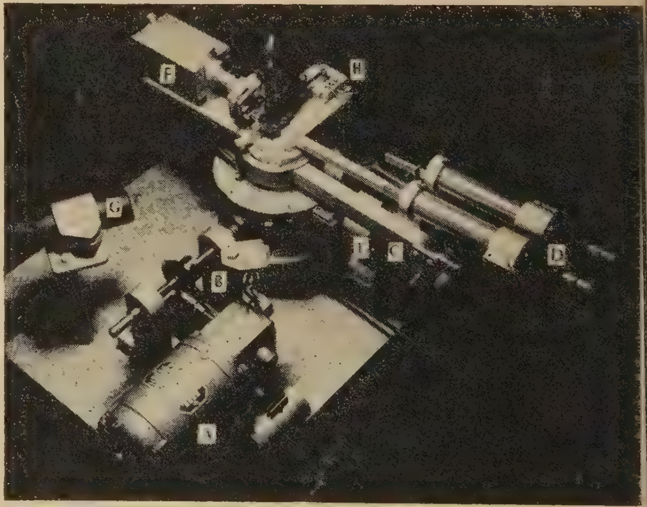

Fig. 1. Photograph of the rapid scanning X-ray diffractometer goniometer showing:

A, drive motor; *B*, gear train; *C*, scanning arms; *D*, Geiger–Müller counters; *E*, magnetic clutches; *F*, incident beam X-ray collimator; *G*, trigger photocell light source; *H*, specimen absorption, incident beam intensity monitor, and angle calibration device

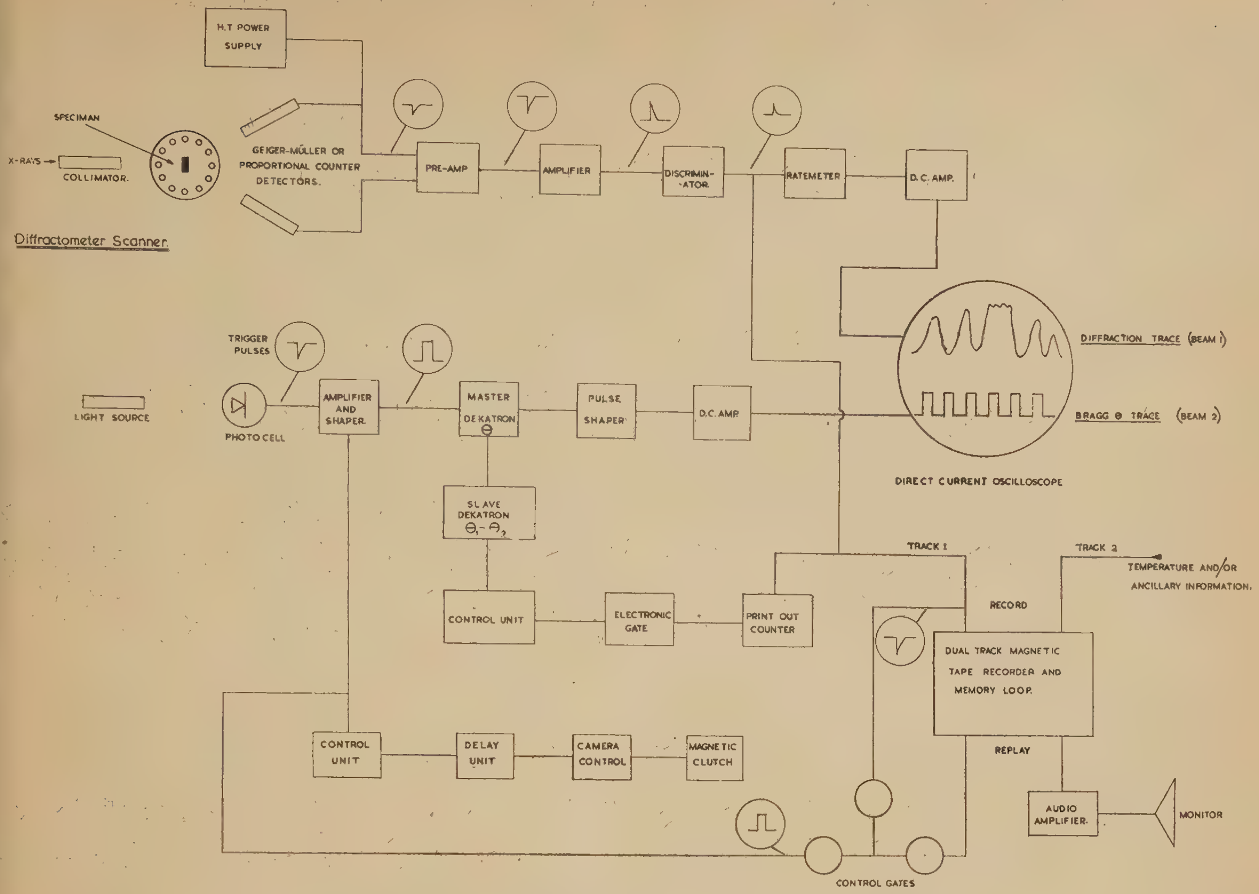
H.T POWER SUPPLY
SPECIMAN
X-RAYS
COLLIMATOR
GEIGER-MÜLLER OR PROPORTIONAL COUNTER DETECTORS
PRE-AMP
AMPLIFIER
DISCRIMIN-ATOR
RATEMETER
D.C. AMP
Diffractometer Scanner
TRIGGER PULSES
LIGHT SOURCE
PHOTOCELL
AMPLIFIER AND SHAPER
MASTER DEKATRON θ
PULSE SHAPER
D.C. AMP
DIFFRACTION TRACE (BEAM 1)
BRAGG θ TRACE (BEAM 2)
DIRECT CURRENT OSCILLOSCOPE
SLAVE DEKATRON θ1-θ2
TRACK 1
TRACK 2
TEMPERATURE AND/OR ANCILLARY INFORMATION.
RECORD
CONTROL UNIT
ELECTRONIC GATE
PRINT OUT COUNTER
DUAL TRACK MAGNETIC TAPE RECORDER AND MEMORY LOOP
REPLAY
CONTROL UNIT
DELAY UNIT
CAMERA CONTROL
MAGNETIC CLUTCH
AUDIO AMPLIFIER.
MONITOR
CONTROL GATES

Fig. 2. Block diagram of the main components of the apparatus

Mullard Geiger–Müller counters (type MX 118)
Proportional counters—author's own design, see Ref. 7
Philips high voltage supply/amplifier (type PW 4022)
Philips ratemeter (type PW 4042)
Nagard direct-current oscilloscope (type DS 103)
S.T.C. photocell (type P 50A)
Ericsson add-on counting units form master Dekatron
(Power unit and input decade, 2 × scaling decade, selector decade, register, electronic gate, 2× control unit)
Labgear programme unit forms slave Dekatrons (type D 4127)
Labgear print-out unit (type D 4123)
Ferrograph magnetic tape recorder (type 3CF/N)
Shackman autocamera (type MK3)
Mullard 5/10 monitor amplifier
Londex cross-over and delay relays

The photograph (Fig. 1) enables the salient features of the scanning assembly to be seen. The drive to the scanning arms is taken from the motor, *via* a series of reduction gears, to a pair of gears which are allowed to rotate continuously in opposite directions. The arms are engaged in the direction of increasing Bragg θ by means of magnetic clutches, with the duration of engagement controlled between $2\theta_s$ and $2\theta_l$ from the Dekatron master timer which is described later. In order to retrace their paths back to the starting place near zero angle, a spring-loaded restoring force is used at high values of Bragg θ, this being replaced by magnetic attraction when nearing and in the rest position.

The pulses from the radiation detectors are amplified, displayed, recorded and analysed by means of apparatus shown schematically in Fig. 2. The main facilities available are shown, but a brief additional description here is perhaps not amiss since there are certain novel features. The entire body of diffraction data is recorded on magnetic tape in order to facilitate permanent storage and subsequent analysis. Since a major intended use of the instrument is to enable difficult experiments involving time-dependent phenomena to be carried out, the preservation of the entire set of observations with high fidelity is highly regarded. To allow visual comparison of different diffraction patterns, the ratemeter and direct-current oscilloscope are fitted with an automatic recording camera. Normally, photographic recordings are only made of particular traces. The quantitative evaluation of the recordings (or of the current scan) is readily carried out using an intensity analyser. With this component the number of pulses (and hence the integrated intensity) occurring between any two particular Bragg θ positions may be measured, and the results printed on paper tape, from the printing-out counter.

A dual magnetic tape recording channel is used. Channel 1 carries the timing and diffraction information and channel 2 enables a simultaneous description (or associated measurement) of the experiment to be recorded.

Since one reel of magnetic tape may contain upwards of 300 separate diffraction records, the descriptive record obtained in the second track is often very important and minimizes the risk of misinterpretation of the records.

Since the normal rate of scanning is high, one scan alone may not yield a sufficiently accurate record. To enable integration of the effects of successive scans to be carried out, a memory loop integrator has been developed. This enables each new scan to be recorded on top of the previous one until a sufficient number of quanta have been received. The use of this repetitive sequence to build up records also reduces the risk of measurements being influenced by long-term drift effects caused by fluctuations in X-ray intensity.

Both sealed-off (Machlett) and continuously-evacuated (Raymax rotating anode generator by Metropolitan Vickers and Co. Ltd.) X-ray tubes have been used with success. The latter tube has, of course, a much higher output, and in operation at 50 mA and 50 kV has proved a most suitable X-ray source for the instrument. As the Raymax tube is self-rectifying, the time constant in the integrating ratemeter should not be less than about 0·3 s in order to avoid undue short term fluctuations.

Main features

The main features of the technique may thus be summarized as follows:

(i) dual fast scanning X-ray detectors of high quantum efficiency;
(ii) magnetic tape recording of the diffraction data with high fidelity and low operating costs;
(iii) a memory loop for the integration of successive traces to ensure the desired accuracy of the diffraction data;
(iv) variable scanning rates;
(v) oscilloscopic display and photographic recording of *desired* diffraction patterns;
(vi) an intensity analyser for the rapid evaluation of records;
(vii) printing-out counter to enable the analyser to perform unattended;
(viii) automatic operation during both the initial scanning and analytical functions.

Collimation of the incident and scattered X-rays

As the apparatus is designed for use under a variety of conditions, it is necessary to have a versatile system of incident X-ray beam collimation. Furthermore, the range of diffraction angles is expected to be wide—from the low-ang region where Bragg θ is less than 1° to deviation angles the region of 90°—so that the beam-defining slits nee provision for quick and easy adjustment. Details ar geometry of the collimation arrangement are shown in th diagram (Fig. 3). Since a transmission technique is employe which differs from the more usual Bragg–Brentano parafocu ing geometry, it is desirable to investigate the relationshi between resolution and diffracted intensity in order to arriv at a knowledge of optimum slit settings for particular appl cations. Usually, slit collimators are used but replacemen by pinholes is possible. The employment of a vacuu system to reduce air scatter was considered but has so fa been rejected. In order to achieve the highest possibl diffracted beam intensity to X-ray background ratio, con comitant with adequate angular resolution, recourse was ha to scanning detector slit collimators. The factors whic govern the choice of parameters for the beam collimator have been considered fully elsewhere. However, the desig of the detector collimator demands further consideration since the problems here are somewhat different from thos encountered in photographic techniques.

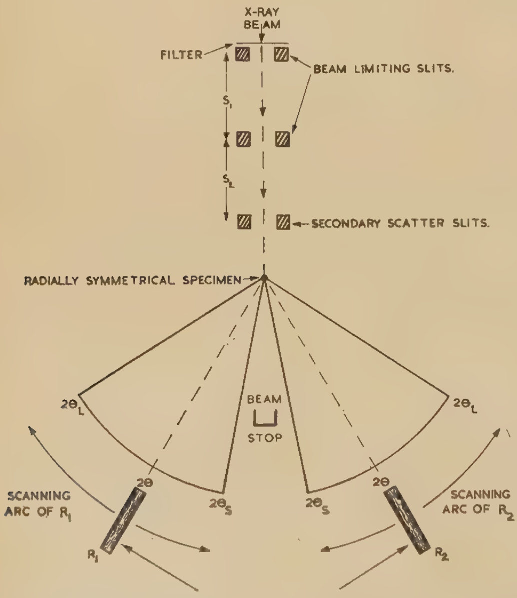

Fig. 3. Plan of geometry of the collimating and scanning assembly. The radiation detectors R_1 and R_2 perform repetitive symmetrical scans over the arcs defined by $2\theta_s$ to $2\theta_l$, $S_1 = 8$ cm, $S_2 = 5$ cm. The incident beam collimating slits are adjustable from 0–1 mm

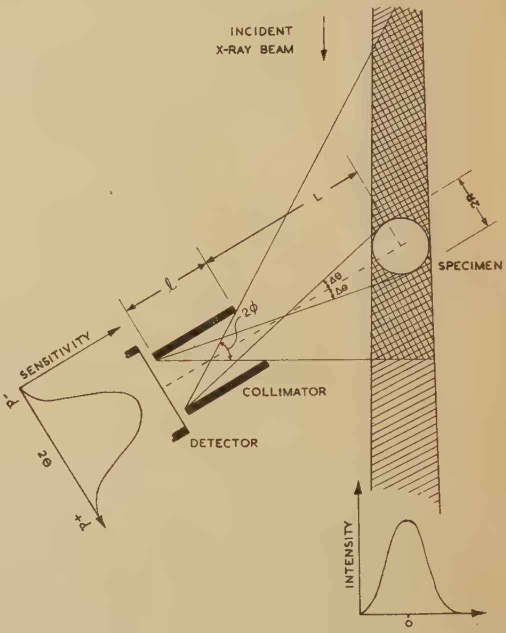

Fig. 4. Details of the factors relating to air scatter and X-ray detector collimators. The intensity distribution of the main beam and sensitivity distribution (as a function of lateral deviation d) of the detector collimator are also shown. Portions of the main beam which are double shaded contribute to the unwanted air-scattered background radiation

Reference to Fig. 4 enables an approximate relationship to be deduced for the ratio of specimen scattered radiation I_s to air scattered radiation I_n giving

$$\frac{I_s}{I_n} \propto R\left[\left(\frac{l}{2}+L\right)\left\{\frac{\sin\phi}{\sin(2\theta-\phi)}+\frac{\sin\phi}{\sin(2\theta+\phi)}\right\}-2R\right]^{-1} \quad (1)$$

where $\phi = \text{artan}\,(2R/l)$.

The maximum signal-to-noise ratio is achieved when $L \to 0$. This parameter, however, is restricted by:

(i) physical constraints;
(ii) need for accessibility to specimen;

(iii) need for the collimator to remain clear of the main beam at low Bragg angles in order to avoid direct X-ray scatter.

Because of this, L must always be greater than 0 and thus he optimum performance is never realized.

Specimen absorption, angle calibration and incident beam intensity monitoring

A suitable system of calibration for the apparatus is provided by means of two silver foils which may be simultaneously placed in position before and after the specimen. The calibration is not provided continuously but may be ntroduced during a portion of the scan that is not otherwise equired. The position of the calibration foils is controlled by means of the slave Dekatrons.

Fig. 5 shows the details schematically together with the relevant parameters for an analysis of the method. The usual specimen shape is cylindrical, but if we concern ourselves only with diffraction at the lower angles, then an analytical approximation is afforded by an infinite block.

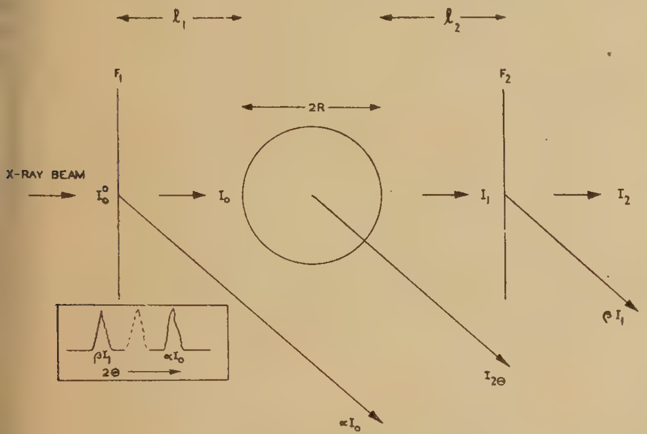

Fig. 5. Geometry of the specimen absorption and angle calibration system. F_1, F_2 silver foils; $I_0^0 \simeq I_0$; $I_1 \simeq I_2$, X-ray intensities at the indicated positions; l_1, l_2 specimen-to-foil distances; αI_0, βI_1, $I_{2\theta}$ diffracted beam intensities. The inset diagram shows the displacement (due to a translation from the centre of rotation) of the beams diffracted by the calibrating foils

In this case it is easily shown that the diffracted intensity from the specimen is given by

$$I_{2\theta} = I_0 f(2\theta) \exp(-2\mu R \sec 2\theta) \frac{\exp\{2\mu R(\sec 2\theta - 1)\}^{-1}}{\mu(\sec 2\theta - 1)} \tag{2}$$

where $f(2\theta)$ is the intensity distribution function and μ is the linear absorption coefficient.

If we assume $2\mu R(\sec 2\theta - 1)$ is small, and let S_1 equal the ratio of intensities scattered by the foils with the specimen in position and S_2 equal the corresponding ratio without the specimen, then we find

$$f(2\theta) \propto \frac{I_{2\theta} S_2 \sec 2\theta}{\alpha I_0 S_1 \ln(S_2/S_1)} \tag{3}$$

This relationship embodies corrections for:

(a) long term drift variations in incident beam intensity;
(b) specimen size.

The foils may also be used as a convenient source of Bragg θ calibration, but since the foils are not mounted coincident with the specimen there will be an apparent shift in Bragg angle due to longitudinal displacement along the incident beam axis. The change in recorded angle for the first foil is given by:

$$\Delta\theta \simeq + \frac{90(l_1 + R)\sin 2\theta}{\pi(l + L)} \tag{4}$$

and similarly for the second.

This displacement is shown in the inset diagram in Fig. 5. The calibration foils may not be used in conjunction with the detector collimators because of the limited sensitivity of the detectors to radiation originating away from the centre of rotation.

Mechanical details of scanning system

To meet the mechanical requirements great care was needed in machining the components. The main features desired of the scanning system were:

(i) a uniform dual equiangular planar scan over the desired range;
(ii) provision for securing near equal repetitive scans with the same duration, to within narrow limits;
(iii) adequate stability and rigidity of the components;
(iv) an accurately known and maintained centre of rotation.

Both supporting arms for the detectors are provided with adjustments in the form of ball and socket joints which, after alinement, may be secured in position by locknuts. Also, the detector slits are independently adjustable in the horizontal plane. In routine use the detector slit is 1 mm wide with a height of 4 mm and the radius of the scanning arc at the detector slit is 15 cm. For other applications (in particular, microdiffractometry), these dimensions may be considerably reduced. Double ball races attached to the main central pillar secure accurate alinement of the gears and scanning arms, and the central assembly is held secure by retaining plates at the top and bottom. The zero angle fiducial point and beam stop are both attached to the top retaining plate, which forms an integral part of the incident beam collimating assembly.

In order to safeguard the apparatus, limit switches are provided to cut off the motor drive at a particular preset overdrive angle.

X-ray detectors

The choice of X-ray detector is conditioned by the need for a device of high quantum efficiency. Two counters, a Geiger–Müller counter and a proportional counter (P.C.) of special design(7, 8) have been used with success. By plotting the count rate as a function of the number of uniform silver absorbing foils placed before them, the effective resolving time of the two Geiger–Müller counters in parallel was shown to be 80×10^{-6} s. This compares well with that to be expected from the literature (about 75×10^{-6} s), and leads to the expected non-linearity of response at count rates above about 600 counts/s.

For the higher counting rates, which are necessary to secure more accurate data in short times, the P.C. has decided advantages; in particular, a low rate of counting loss due to the short resolving time. Further, partial beam monochromatization may be secured with a suitable "kick-sorter". This may be useful when using non-filtered X-radiation. The P.C. used utilizes a diagonal absorption path with a high quantum efficiency. However, both these types of detector suffer from the serious drawback of bulk which precludes their use in particular applications. Thus, the use of photoconductors may be suggested, particularly as back-reflexion micro-diffraction studies of metal-impregnated polymer complexes could be investigated with their aid. Low-angle diffraction patterns at short specimen—detector distances must at present be obtained using only one detector in position.

Electronic circuitry

Most of the electrical components used are readily available commercially and are listed in the legend of Fig. 2. A number of minor modifications, such as the alteration of time constants and input and output impedances, were necessary in order to secure adequate compatability of the vario units.

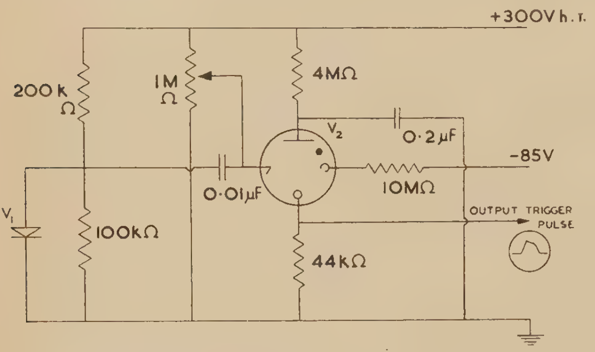

Fig. 6. Photocell trigger circuit amplifier

V_1 = S.T.C. germanium diode P 50A V_2 = Ericsson GTE 175 M

The master timer consists of four Dekatrons driven fro a 100 c/s near-constant frequency source. Added to t frequency dividers is an electronic gate, two thyratron contr units and a counting register. A slave set of Dekatrons used to control the variable period gate which is used i conjunction with the intensity analyser.

Provision of a satisfactory photocell trigger proved to b difficult because of the slow rise times involved, but wa finally achieved by means of a simple single-valve circui Fig. 6 shows this photocell circuit. The positive output puls is obtained from a thyratron cathode follower.

Relay system

Fig. 7 shows the details of the relay system incorporate in the apparatus. On receipt of a trigger pulse from th photocell amplifier or tape recording, the master Dekatron timer and electronic gate operates, thus starting the scanning cycle. Simultaneously, cross-over relay c/o R_1 instantaneously closes, operating the oscilloscope time base trigger, releasing the latching relays LR_1 and LR_2 and actuating the 0–30 s delay relay (DR_1) which controls c/o R_4, the purpose of which is to prevent spurious triggering of the system. Latching relay LR_1 controls (*a*) the camera circuits, and (*b*) the Geiger–Müller counter pulse gate, in order to suppress the trace during the "flyback" of the scanning arms. Latching relay LR_2 controls the coupling of the master and slave Dekatrons and also the resetting of the slave counters to zero before each trace. At the end of the analytical period this relay closes *via* a slave counter relay.

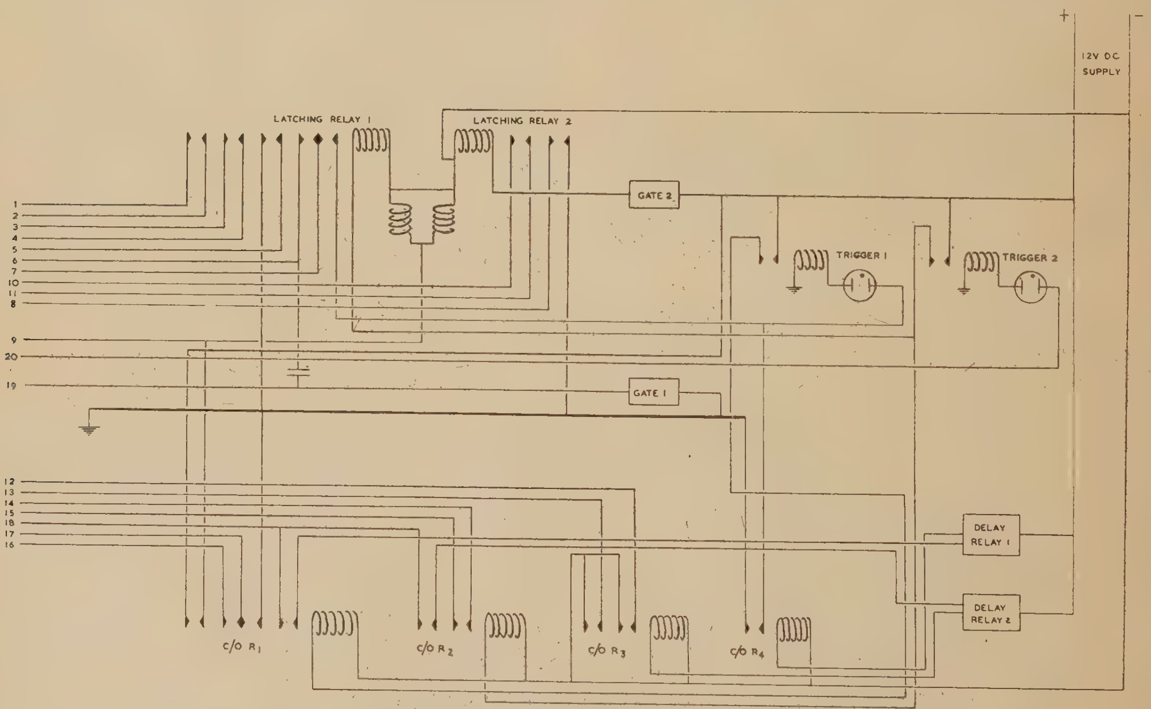

Fig. 7. Details of the basic relay system showing components and external connexions

c/o R_1, R_2, R_3, R_4 = triple cross-over relays
T_1, T_2 = thyratron triggers
LR_1, LR_2 = latching relays
DR_1 = 0–30 s delay relay
DR_2 = 0–2 s delay relay
G_1 = printing counter or calibration gate
G_2 = intensity analyser gate

Connexions

1, 2 = camera circuit
3, 4 = printing counter
5 = pulse input
6 = ratemeter
7 = amplifier output
8 = master Dekatron reset
9 = latching relay release
10, 11 = slave Dekatron coupling
12 = magnetic clutches
13 = calibration foil disengaging solenoid
14, 15 = slave Dekatron reset
16 = 50 V d.c.
17 = oscilloscope trigger
18 = line voltage 230 V a.c.
19 = intensity analyser input
20 = analyser trigger

When a complete scan ends LR_1, c/o R_2 and the 0–2 s relay DR_2 operate. Closing of LR_1 sends a pulse to the printing counter to print the results of the analysis and the camera and counting circuits are made inoperative. Relay c/o R_2 resets the master Dekatrons. The magnetic clutch operates through c/o R_3 for the period of operation of DRL_2. The time setting of both relays depends on the scanning speed. Under conditions of "direct reading" the settings are usually 27 and 1·5 s. The printing counter period is operated from relays in the slave Dekatrons.

A typical timing of the sequence for "direct reading" is as follows:

t (*s*)	*Operation*
0	Photocell trigger starts scan or analysis
t_1–t_2 ($0 \leqslant t_1 < t_2, \leqslant 20$)	Intensity analysis or calibration
20	End of scan, print result
20–21·5	Flyback of scanning arms
27	DR_I opens. Quiescent state
30	End of sequence, operation recommences

It was found that a cycling rate of two per minute provides a good compromise between speed and accuracy.

Recording system and memory loop

Suitably attenuated shaped pulses from the ratemeter circuit are used for making a recording of the diffraction patterns. The initial pulses are negative-going and this property is retained on the recording input. The trigger pulses, on the other hand, are square and positive-going. The difference in polarity facilitates the operation of the various trigger circuits. The frequency response of the recorder is sufficient to enable pulses occurring in times down to 10^{-4} s to be recorded with fidelity. This is adequate for Geiger–Müller pulses (duration 1–400 μs), but is totally inadequate for P.C. work at high intensities. If metallurgic applications of this technique were contemplated, a video-frequency magnetic tape recorder might be required. The coefficient of variation of tape velocity should be kept as low as possible. Over a short period this amounts to 0·1% and this slightly affects the analytical accuracy.

Fig. 8 shows the high degree of fidelity between the original and recorded intensity distribution. Similar correspondence is obtained up to count rates of 1000 per second.

In order to overcome the inherent statistical limitations to accuracy at low counting rates, an integrative memory loop may be used. In this application one track is used for the diffraction data and the second is used to provide accurate scan synchronization pulses. At the end of the scan there is a pause in the drive system which waits to recommence its scan until the receipt of a trigger pulse from the magnetic tape. In this way accurate integration is obtained without recourse to complex servo-mechanisms.

The usable number of successive integrations performed by the loop is limited by the counts obtained in a single scan, since the overall recorded intensity must be within the capacity of the crest of the system. A maximum of about 200 successive scans, in effect limited by the non-X-ray background count, is achievable.

Intensity analyser

The intensity analyser is controlled by the slave Dekatrons and relay system. It is normally intended as a facility for analysis of the recorded diffraction patterns but may be used directly on the scattered intensity. Since the scanning speed and master Dekatron oscillator frequency are correlated, the frequency dividers are also *per se* angle measurers. The slave Dekatrons are attached to two separate coincidence circuits that actuate relays at the end of preset intervals. The intervals correspond to values of Bragg θ chosen within the scanning range, which may be set to within 0·1° with great accuracy. It has been found that this degree of resolution of the pattern is adequate at present. The counting interval actuates a gate on the printing counter, and at the end of its analysis a further relay operates the printing sequence to produce a direct count of the number of quanta scattered between the particular chosen limits. The analytical function is automatic and sequential. Analyses of sets of recorded diffraction patterns may be carried out for a duration of up to three hours (the limiting capacity of the magnetic store).

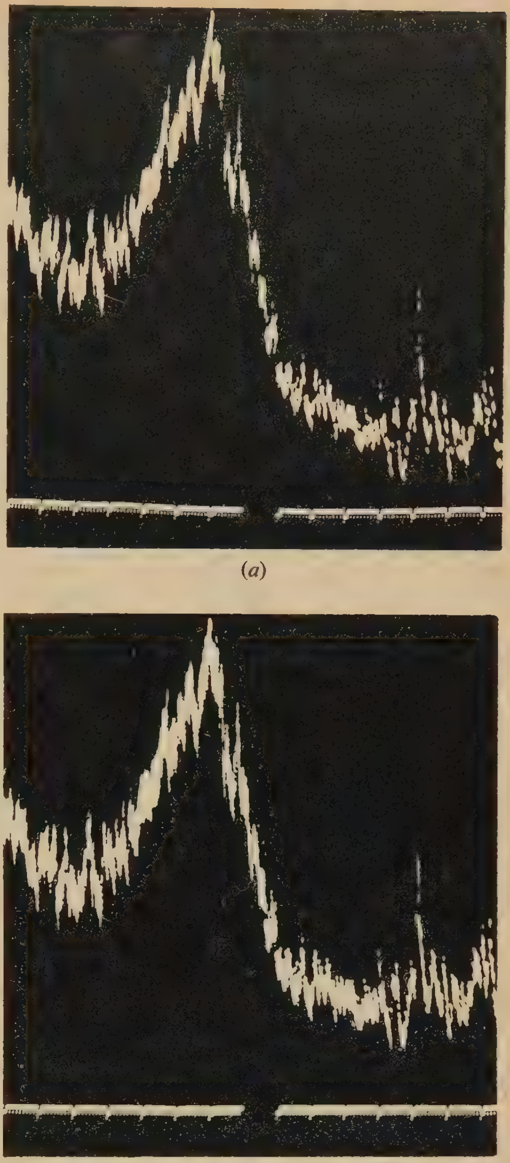
(*a*)

(*b*)

Fig. 8. Comparison of a direct (*a*) and recorded (*b*) equatorial intensity distribution

Table 1 shows the accuracy of the analyser during successive analyses of a set of diffraction patterns. The analytical system contributes an overall additional variance equal to about one-tenth of that due to the random nature of the input. This is not considered unsatisfactory and the intensity analyser provides an accurate evaluation of the records.

Table 1. *Comparison of results obtained from the original and two successive analyses of the recorded diffraction records*

Integrated counts

Original	*First analysis of record*	*Second analysis of record*
111	112	112
771	769	773
1800	1802	1810
1334	1333	1340
460	460	466
1290	1282	1293
736	736	736
1111	1110	1113
242	244	240
1084	1085	1088
48	45	51
34	31	38
964	970	966
1020	1022	1015
1048	1052	1051
986	991	990

Errors and distortions

A complete analysis of the analytical errors associated with the apparatus has not yet been made. Subsidiary errors include such factors as variation in tape speed, gating errors, lack of linearity in the oscilloscope display, optical errors and aberrations introduced during the photographic process.

However, the total of the above errors is small compared with a basic inherent limitation of the method. This is due to the random nature of arrival of quanta leading to a Poisson distribution about a mean rate x, giving the probability of recording n quanta as

$$p(n) = \frac{x^n \exp(-x)}{n!} \qquad (5)$$

and since the variance is equal to x, the coefficient of variation V is equal to $100/\sqrt{xT}$ where T is the duration of a scan.

Thus a tenfold diminution in scanning time, other things being equal, only reduces accuracy threefold. Consequently, for a number of applications where highest accuracy is not important, the fast detecting methods may be most useful. When using the ratemeter method of integration certain other problems present themselves. Consideration of the "flyback" period is governed by the fact that equilibrium of the detector response (to within σ) occurs in time.(9)

$$t = (RC/2) \ln (2NRC) \qquad (6)$$

Thus the "flyback" time for sequential traces can never be less than a value determined by the parameters of the analysis under investigation. For example, with $RC = 1$ and $N = 1000$, $t \simeq 4\cdot0$ s. Alternatively the maximum value of RC that can be used at this counting rate under the standard conditions is approximately $2\cdot3$ s.

A useful approximation to many scanned diffraction lines is a triangular waveform with a leading edge rising linearly as a function $v = kt$. In this case when $t = T_0$, the time c observation,

$$V = \frac{100\sqrt{\{T_0/2 + RC \exp(-2T_0/RC)/4 - RC/4\}}}{\sqrt{(RCk)(T_0 + RC) \exp(-T_0/RC) - RC}} \qquad (7$$

and the variation of precision along the diffraction line ma be assessed. The importance of high counting rates is evident

To facilitate the comparison of photographic records it i important to appreciate the effect of a finite time constant which causes distortion of the trace and an apparent shift i lattice spacing. The true profile $\psi(t)$ is obtained from the observed profile $\theta(t)$ by using the relationship

$$\psi(t) = \dot{\theta}(t)RC + \theta(t) \qquad (8)$$

The effect of various time constants on the observed profiles is shown in Fig. 9.

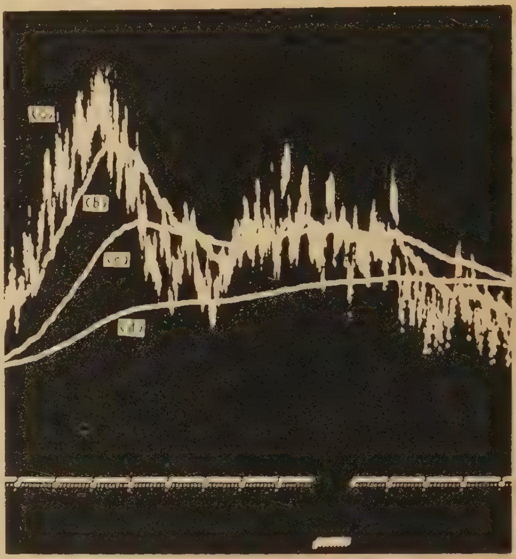

Fig. 9. Equatorial intensity distributions from α Lincoln wool keratin obtained with different time constants

(a) $RC = 0\cdot3$ s (b) $RC = 1$ s
(c) $RC = 3\cdot0$ s (d) $RC = 10$ s

The distortion of the trace due to the finite time constants is well evident

By considering a Gaussian function for $\psi(t)$ it can be shown that the observed maximum occurs at an angle approximately $0\cdot7\, RC$ after the true maximum. As an indication of the performance of the apparatus under reproducible constant frequency input conditions, measurements made at different points in the circuit are tabulated in Table 2. Again it is clear that the principal limitation is due to statistical fluctuations in the X-ray input.

Table 2. *The performance of the apparatus when operated from a uniform periodic frequency source*

Frequency input (nominal)	*Ratemeter*	*Oscilloscope deflexion (cm)*	*Intensity analyser (10 s period)*
0	0	0	0
25·0	25·1	0·25	298
50·0	50·3	0·50	556
100·0	98·1	1·03	1043
200·0	208·2	2·01	2109
300·0	310·5	2·92	3111
400·0	415·4	3·75	4113
500·0	516·5	4·40	5162

Bragg θ calibration

Although the apparatus is designed to scan at a fixed rate over the range from 0 to 20° of Bragg θ, the initial alinement is greatly facilitated if the observed angle can be calibrated against the angles of reflexion from known materials.

Table 3. *X-ray reflexions used for calibration of the rapid scanning X-ray diffractometer*

Material	*Lattice plane*	*Bragg θ°*
Cellulose I (native Ramie)	101 $10\bar{1}$ 002	7·3 8·2 11·4
Cellulose hydrate (mercerized Ramie)	101 $10\bar{1}$ 002	5·7 10·0 11·0
Polyethylene	"Amorphous halo" $10\bar{1}$ 002	9·9 10·8 12·0
Wool keratin	001 "halo"	4·5° 10·0°

Table 3 gives a list of four materials which provide a convenient calibration series. The actual calibration is carried out by successive visual measurements of the peak positions on the long persistence screen of the oscilloscope, and a regression line is plotted of true $\theta(\theta_t)$ against observed $\theta(\theta_0)$. From such an analysis the deviation of the scanning rate from that expected from a truly "direct-reading" instrument may be obtained.

In Fig. 10 the diffraction traces from the materials used for calibration are shown, and in Fig. 11 a typical plot of the observed and true Bragg θ values is given, together with the corresponding regression line. The regression equation to the line is given by $\theta_t = 1\cdot19\,\theta_0 - 0\cdot54$ with the standard error of the estimate $S_t = 0\cdot103$ and a coefficient of correlation $(r_{\theta_t\,\theta_0})$ of 0·994.

Operation and applications

The operational routine on the instrument is quite straightforward once initial alinement and a satisfactory choice of operating parameters is made. Possible applications of the

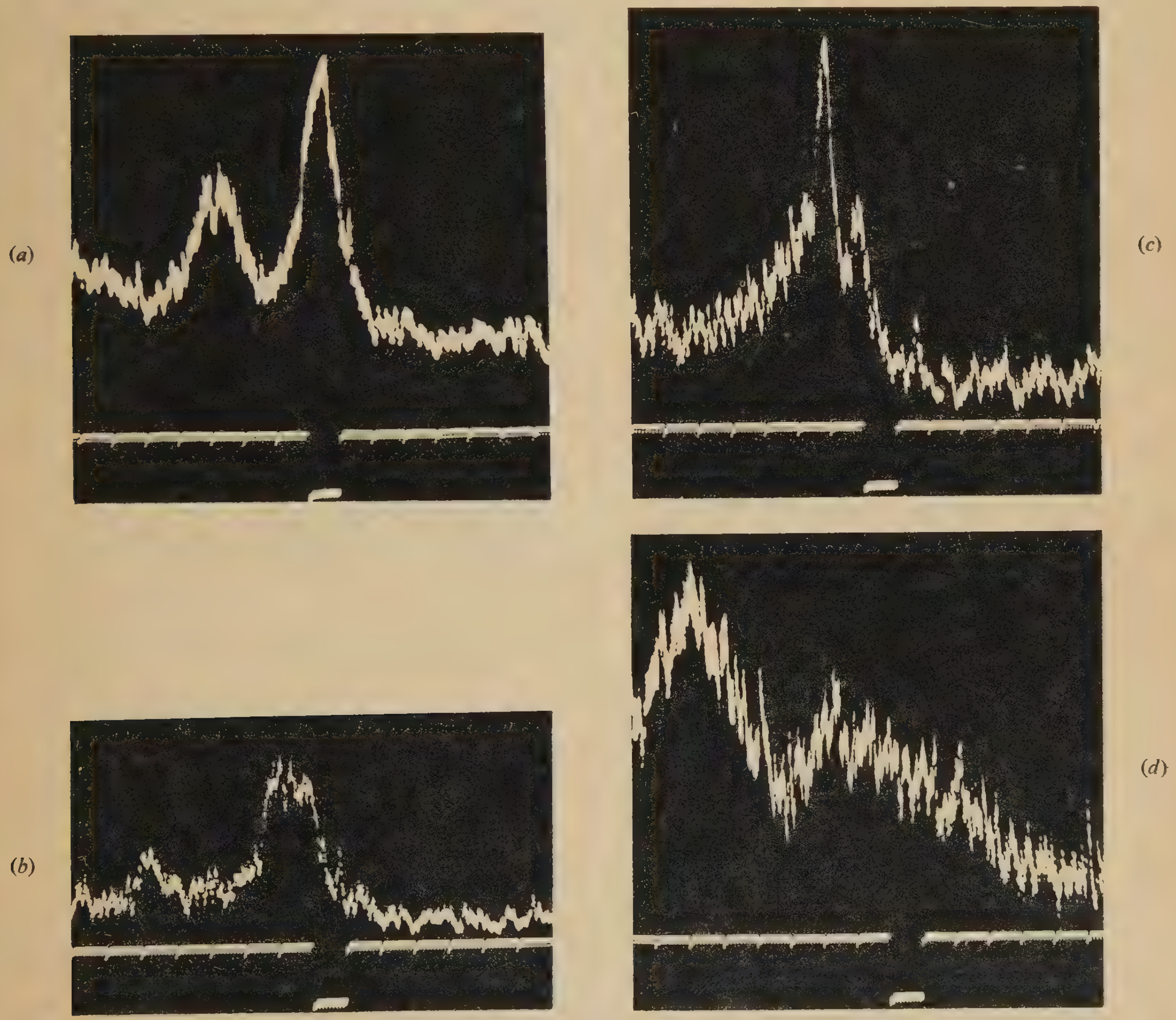

Fig. 10. Diffraction traces from the materials used for calibration of the instrument. (*a*) Native Ramie—cellulose I. (*b*) Mercerized Ramie—cellulose hydrate. (*c*) Polyethylene. (*d*) Lincoln wool keratin. ($RC = 0\cdot3$ s)

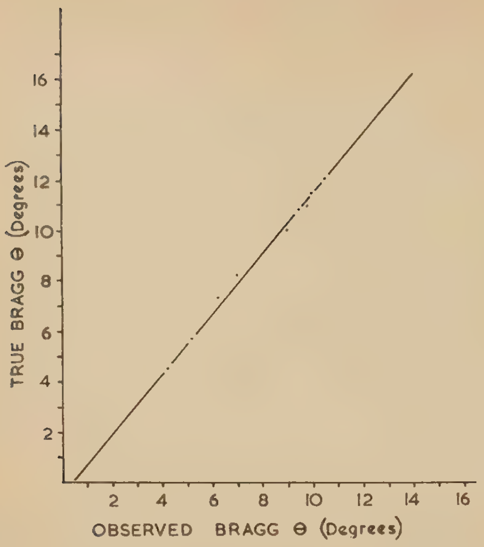

Fig. 11. The regression line and plot of a typical Bragg θ calibration run

apparatus are widespread but no systematic investigation of potentialities has yet been made. A field of particular promise concerns the analysis of phase-transformations in high polymers. As an example Fig. 12 shows the records of two experiments of this type. The ease with which the quantitative analysis of records may be made enables rate processes to be studied with facility in small and easily managed crystalline samples.

Acknowledgements

The generous advice and wise counsel of Mr. H. J. Wood is appreciatively acknowledged. To Prof. J. B. Speakman for his encouragement and durable support, to the Wool Research Council, and to all earlier workers whose ideas have been unconsciously incorporated, I express my deepest thanks.

The mechanical construction of the instrument was carried out under the direction of Mr. R. Haynes, and the drawings by Mr. M. M. Gore, to both of whom the author is deeply indebted.

References

(1) Woods, H. J. *Physics of Fibres* (London: The Institute of Physics, 1955).
(2) Little, K. *Brit. J. Appl. Phys.*, **10**, p. 225 (1959).
(3) Bendit, E. G. *Nature* (*London*), **179**, p. 535 (1957).
(4) Pike, E. R., and Hughes, J. W. *J. Sci. Instrum.*, **36**, p. 212 (1959).
(5) Pepinsky, P., and Weisz, P. *Phys. Rev.*, **63**, p. 457 (1943).
(6) Skertchly, A. R. B. *Nature* (*London*), **180**, p. 802 (1957).
(7) Skertchly, A. R. B. *J. Sci. Instrum.*, **33**, p. 209 (1956).
(8) Skertchly, A. R. B. *Rev. Sci. Instrum.*, **27**, p. 324 (1956).
(9) Schiff, N. I., and Evans, R. D. *Rev. Sci. Instrum.*, **7**, p. 456 (1936).

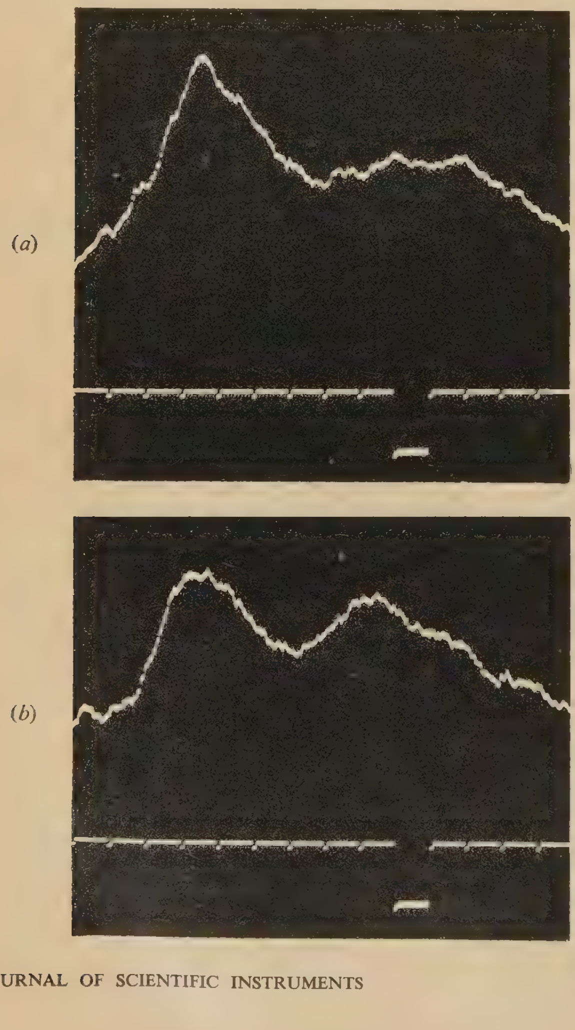

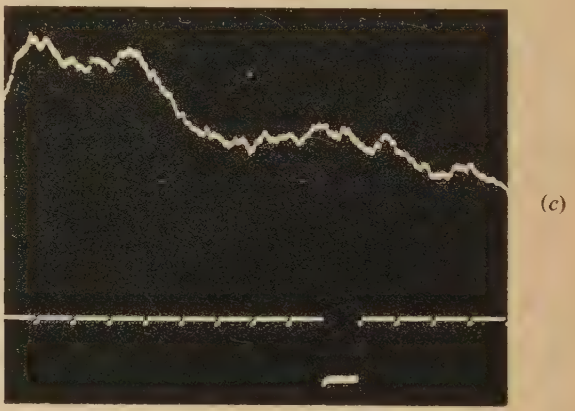

Fig. 12. (*a*) Lincoln wool keratin. (*b*) Lincoln wool keratin. The fibres of the α form have undergone a change in lattice structure on stretching to 50% in steam. (*c*) The effect of metal impregnation on the fibres of the α form. (Mercuric acetate treatment by courtesy of Dr. W. Simpson). (*d*) X-ray background without the specimen in position. ($RC = 1$ s)

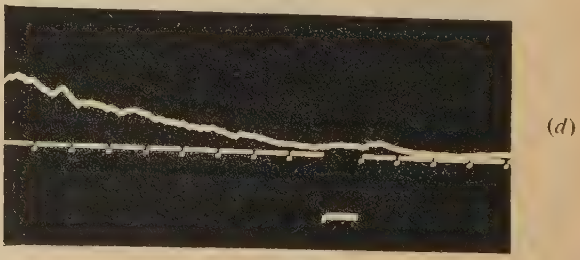

Two thermocouples suitable for measurement of temperatures up to 2800° C*

by D. A. DAVIES, A.Inst.P.,† British Thompson-Houston Co. Ltd., Rugby.

[*Paper first received* 19 *November* 1958, *and in final form*, 5 *August* 1959]

Abstract

The thermoelectric characteristics of two high-temperature thermocouples of tungsten/26% rhenium-tungsten and tantalum/26% rhenium-tungsten are described, and a method of determining the e.m.f. of the couples up to a temperature of 2800° *C is given. In the temperature range* 1000–2000° *C, the sensitivity of the tungsten/rhenium-tungsten couple is* $16\cdot2\ \mu V/{}^\circ C$ *and that of the tantalum/rhenium-tungsten couple is* $13\cdot6\ \mu V/{}^\circ C$. *The important feature of these thermocouples is their suitability for operation at much higher temperatures than existing couples, combined with a fairly high sensitivity.*

Introduction

An important drawback at present to the use of thermocouples for the measurement of high temperatures is the lack of stable couples which give a reasonably large e.m.f. gradient at temperatures above 2000° C. A material used as a thermocouple element at high temperature should have a high melting point and low vapour pressure, be stable in different atmospheres, and should not react with the thermocouple sheath at the elevated temperatures.

Platinum rhodium-platinum couples are widely used for the measurement of temperatures up to 1700° C. The characteristics of a number of thermocouples suitable for use at higher temperatures are included in a review of thermoelectric pyrometry by Hume-Rothery, Christian and Pearson(1). A general review of high temperature thermocouples is given in a paper entitled "A tungsten-iridium thermocouple" by Troy and Stevens(2). Study of the data given indicates that few thermocouples are ideally suited for operation at temperatures above those of the platinum/rhodium-platinum couples, mainly because of low e.m.f.s and, in some instances, because the e.m.f./temperature calibration shows a reversal (tungsten/tantalum, for example(3)).

The upper temperature limit of thermocouple operation is governed by the evaporation losses of the materials and, in this respect, the three metallic elements having the lowest vapour pressures and the highest melting points—namely tungsten (3380° C), rhenium (3167° C) and tantalum (3000° C)—are the most suitable. Rhenium metal work-hardens to an exceptional degree, and the practical difficulties of producing it in the form of fine wire are very great.(4) It has, however, been shown by Geach and Hughes(5) that some of the alloys of rhenium with tungsten are ductile. An alloy of tungsten and rhenium containing 26% rhenium was successfully swaged and drawn into wire (at Rugby) using techniques similar to those adopted for drawing tungsten wire. These alloy-wire samples were then used for the thermocouple experiments.

Experimental

Preliminary experiments were carried out on the alloy-wire samples to determine the evaporation rate of the material at high temperature. The experimental procedure consisted of mounting a 10 cm length of $0\cdot005$ in. alloy wire on nickel supports in a bulb, evacuating the whole, out-gassing the filament at 2000° K, and then sealing-off the bulb when the pressure had attained its minimum value of approximately 10^{-7} mm of mercury. The wire was heated by the passage of current and its temperature determined by means of a disappearing-filament optical pyrometer. It is found experimentally that the optical-pyrometer setting on fine filaments is very inaccurate because of the very small angle subtended by the filament at the pyrometer. To surmount this difficulty a strip-filament lamp was placed immediately behind the test filament and its temperature was adjusted to give disappearance of the test filament. The optical pyrometer was then set to record the temperature of the relatively wide strip filament, giving an accurate reading. Furthermore, by taking a direct temperature reading on the strip filament after removal of the test bulb, a correction for the effect of scattering at the envelope of test bulb can be obtained. It is easily shown that the correct filament-brightness temperature is given by the mean of the two optical-pyrometer readings. The correction which varies with temperature is normally small (about 20° C) but may be much larger if any appreciable evaporation of filament material on the bulb envelope has occurred.

The temperature values recorded with the optical pyrometer were "brightness temperatures" corresponding to a wavelength of $0\cdot665\ \mu$. The spectral emissivity of tungsten at this wavelength is $0\cdot43$, and shows slight variation with temperature. These emissivity values enable the true filament temperature to be calculated, the correction amounting to 175° K at a true temperature of 2200° K.

The evaporation rate of the alloy was determined from the loss in weight of the wire after maintenance at temperature for a known period of time, and also from the changes in wire resistance during operation. The evaporation rate of the alloy was found to be approximately three times that of tungsten at the same temperature. For example, at 2450° C the value was $2\cdot54 \times 10^{-6}$ g cm^{-2}s^{-1} compared with $9\cdot0 \times 10^{-7}$ g cm^{-2}s^{-1} for tungsten. It should be noted that this is approximately the order of the change in evaporation rate for a temperature change of 100° C. That is, the alloy and tungsten have approximately equal evaporation rates when the alloy is maintained at a temperature 100 degrees below that of tungsten.

The first thermocouple prepared consisted of $125\ \mu$ 26%

---

* Brit. Pat. Appl. Nos. 7103/58 and 17203/58.

† Now with Siemens Edison Swan Ltd., Harlow, Essex.

rhenium-tungsten alloy wire spot-welded on to a tungsten wire of the same diameter. The junction was brittle because of the re-crystallization of tungsten which occurred during the welding process, and the thermocouple required careful handling. This brittleness affects the whole thermocouple after exposure to high temperature and is one of the chief disadvantages of tungsten thermocouples. The thermocouple was calibrated up to 1300° C in a hydrogen atmosphere by comparing its e.m.f. with that from a standard platinum/13% rhodium-platinum couple held adjacent to it in a platinum furnace. The e.m.f. at any particular temperature was found to be the same during the heating and cooling cycle of the furnace and did not change on repeated cycling.

A different method was used to determine the e.m.f. of the thermocouple in the temperature range 1200–2800° C. A 125 μ tungsten filament *B* in Fig. 1 provided a high temperature source at an accurately determined temperature, and the thermojunction *E* consisted of a 30 μ alloy wire *D* attached to the filament. Two 30 μ tungsten wires *C* were also attached to the filament on either side of the junction at a distance of 3 mm from the junction. The tungsten filament and attached leads were mounted in a bulb on nickel supports *A*, evacuated, outgassed, and sealed-off under high-vacuum conditions.

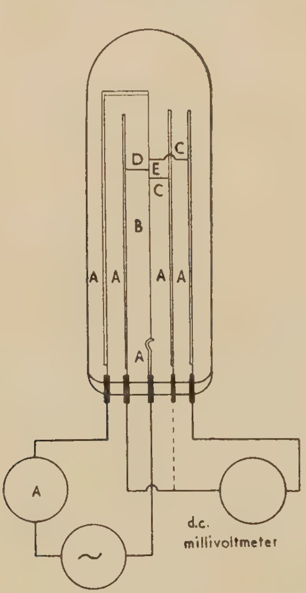

Fig. 1. Diagram of thermocouple

A = nickel supports, *B* = tungsten filament, 125 μ diam., *C* = tungsten leads, 30μ diam., *D* = rhenium-tungsten alloy leads, 30 μ diam., *E* = thermojunction

The 125 μ tungsten filament was heated by the passage of an alternating current from a Variac-controlled step-down transformer (240 to 35 V), and the filament temperature was determined by means of an optical pyrometer, as previously described. An independent check on the values of filament temperature was obtained by measuring the filament current *I* and wire diameter *d*. The quantity $I/d^{3/2}$ for a long straight tungsten wire operated *in vacuo* is a function of temperature only, and its value is accurately known for a wide temperature range (6, 7). A determination of this function can thus be used to assess the accuracy of the temperature determination by the optical-pyrometer method.

Observation of the thermojunction through the pyrometer showed that its temperature was considerably lower than the rest of the filament because of conduction of heat along the 30 μ lead wire. The difference in temperature was appro mately 150° C and did not show appreciable variation wi filament temperature.

As a preliminary test it was shown that no stray e.m. were recorded even at the highest filament temperatures wh a d.c. millivoltmeter was connected across the two 30 tungsten leads. The e.m.f. of the thermocouple was th obtained across the alloy lead and one of the tungsten lea and was recorded for a range of junction temperatures up 2800° C. The calibration curve of the thermocouple given in Fig. 2.

The thermocouple in this form (that is, a fine alloy wi attached to a tungsten filament) has been shown to mainta

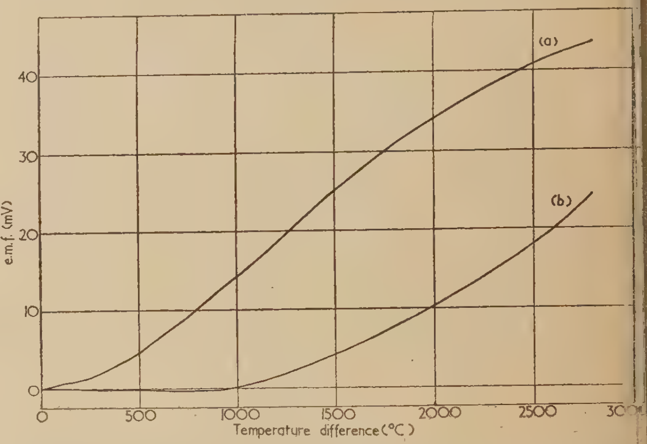

Fig. 2. Calibration graph for (*a*) tungsten/26% rhenium-tungsten couple, and (*b*) tantalum/26% rhenium-tungsten couple

its calibration unchanged after maintenance at 2750° K fo one hour (the experimental error is about ±20° C). Suc couples have been taken up to temperatures of this orde a number of times and give consistent calibrations. Experiments were confined to a single-alloy composition, that is 26% rhenium, and it was not possible to assess accurately the change in calibration expected to result from the preferentia loss of rhenium by evaporation at high temperatures. The evaporation rate data obtained, however, give the order of temperature at which calibration changes caused by rhenium loss could be expected. Thus at 2750° K a 0·020 in. wire loses 0·2% material in 80 minutes. The corresponding change in composition would be about 0·1% and the change in calibration would probably be within the limits of experimental error of measurement. At 3000° K, the evaporation rate is ten times greater, and an observable change in calibration would occur.

It is noted that there is a uniform increase of e.m.f. with temperature, with deviations from linearity at each end of temperature scale. The e.m.f. of the couple is relatively high, exceeding that of a platinum/13% rhodium-platinum couple at temperatures above 500° C., and increasing to 43 mV at a temperature difference of 2800° C. The mean sensitivity of the thermocouple for the temperature range 1000–2800° C amounts to 16·2 μV/° C.

The e.m.f. of the combination tantalum/26% rhenium-tungsten has also been determined using a similar technique. It is noted from Fig. 2 that, in this case, the e.m.f. shows a reversal below 1000° C. This reversal has been confirmed in repeat experiments and amounts to 0·2 mV. The e.m.f. gradient at temperatures greater than 1000° C is, however, fairly large, and is greater than that of the tungsten/26%

henium-tungsten couple at temperatures above 2500° C. It apparent that, except at very high temperatures where there ight be appreciable evaporation loss of tantalum, this couple an be used as an alternative to the tungsten couple. This ouple would have the additional advantage that, because of he very low e.m.f. generated below 1000° C, there is no need or control or measurement of the cold-junction temperature.

The 26% rhenium-tungsten alloy can thus be used as a hermocouple element with either tungsten or tantalum. he thermocouples would be suitable for use in a vacuum, ydrogen, nitrogen, argon or any other inert atmosphere. They would not be suitable for use under oxidizing conditions, or in the presence of hydrocarbon vapours, which will rapidly ttack tungsten at temperatures above 1000° C. The couples vould require careful handling because of the brittleness nduced by re-crystallization.

Acknowledgements

The author wishes to thank the A.E.I. Research Laboratory, Aldermaston, for providing the arc melted rhenium tungsten alloy. Thanks are also due to the Director of the British Thomson-Houston Research Laboratory for permission to publish this paper.

Note

Since this paper was prepared, Sims, Gaines and Jaffee(8) have published information regarding rhenium/tungsten and rhenium/30% rhenium-tungsten thermocouples, from which they calculate the theoretical e.m.f. expected from a tungsten/30% rhenium-tungsten couple. These values are in general agreement with the experimental values for the tungsten/26% rhenium-tungsten couple given in this paper.

References

(1) Hume-Rothery, W., Christian, J. W., and Pearson, W. B. *Metallurgical Equilibrium Diagrams*, Chap. 7, (London: The Institute of Physics, 1952).

(2) Troy, W. C., and Stevens, G. *Trans. A.S.M.*, **42,** p. 1131 (1950).

(3) Morgan, F. H., and Danforth, W. E. *J. Appl. Phys.*, **21,** p. 112 (1950).

(4) Davis, M., and Duke, J. F. *S.E.R.L. Tech. Jnl.*, **6,** p. 265 (1956).

(5) Geach, G. A., and Hughes, J. E. *Proc. 2nd Plansee Seminar*, p. 245 (Reutte Tyrol: Metallwerk Plansee A.G., 1956).

(6) Jones, H. A., and Langmuir, I. *G. E. Review*, **30,** 6, p. 310 (1927).

(7) Reimann, A. L., *Phil. Mag.*, **25,** p. 834 (1938).

(8) Sims, C. T., Gaines, G. B., and Jaffee, R. I. *Rev. Sci. Inst.*, p. 112 (Feb. 1959).

Design of laboratory furnaces

by P. L. START, B.Sc.(Tech.), and M. W. THRING, M.A., F.Inst.P., F.Inst.F., M.I.Chem.E., Department of Fuel Technology and Chemical Engineering, University of Sheffield

[*Paper first received* 2 *February, and in final form* 25 *August*, 1959]

Abstract

The paper illustrates the use of a heat balance in the design of small furnaces, and then discusses the principles of arc, arc-image, induction, electron-bombardment, resistor-heated and gas-fired furnaces. Constructional details are mentioned briefly with each type of furnace considered. A comprehensive table of resistor elements, refractory tubes, and insulating materials and their properties is included. Methods of controlling small furnaces are discussed in the final section.

Introduction

Reliable and accurately controlled small-scale furnaces have been applied in many different fields of research, and certain forms are becoming standard pieces of laboratory equipment, which can be purchased complete. Often, however, the particular application requires a special furnace, which can be built to order, but which can also be more roughly constructed by the research worker, certainly more cheaply and probably more quickly. This problem occurs frequently in post-graduate research, where financial resources are often small, and every problem is different. The idea of this paper is therefore to suggest the right approach to the basic design and, from a discussion of each particular type of furnace used, to provide a foundation on which the choice and/or the eventual construction may be based.

Small-scale furnaces are usually heated either electrically or by combustion of gas from the town's supply. (The use of solid and liquid fuels is confined to intrinsic investigations into these modes of firing.) Such units are employed in commercial production, and in both short- and long-term research programmes. Among the many applications are the melting of metals and alloys, heat treatment of metals, metallic components, and ceramic materials, the heating of fluids for processing, and for drying purposes. In selecting a furnace for a particular application, it is important to understand the potentialities, cost, and probable life of the available methods of heating, and then to ascertain whether or not the furnace could be designed and built by the intending user, or if a standard model from a manufacturer would be more suitable.

The available methods of heating for the generalized applications given above are as follows:

(i) melting of metals, glasses, and slags
    electric arc (direct and indirect)
    high-frequency induction
    resistor heated
    gas fired
    electron bombardment

(ii) heat treatment
  arc image
  high-frequency induction
  resistor heated
  gas fired

(iii) fluid heating
  resistor heated

(iv) drying
  resistor heated
  gas fired

The operating temperature range of these furnaces is given below:

electric arc (direct and indirect)
  1200–2000° C
high-frequency induction
  up to 3000° C
arc image
  up to 6000° C
electron bombardment
  2500° C (highest temperature recorded)
gas fired
  up to 1500° C (with oxygen up to 2000° C)
resistor heated
  up to 3000° C

(the range 1800–3000° C is not easily obtained by resistor-heated furnaces)

The relative cost (in pounds) of these furnaces, all designed to perform a similar heating operation such as heating a charge of small weight and volume, is given below.

electric arc	500
high-frequency induction	400
electron bombardment	500
arc image	400
gas-fired muffle	10 (min.)
resistor-heated (with transformer)	50 (min.)

The cost of the resistors increases with the increase of maximum service temperature, from nichrome to carbon tube, with exception of platinum, and this is also true for refractory tubes. These prices include all necessary electrical and vacuum equipment but do not include any manufacturing or labour costs. The cost of expendable materials (refractories, electrodes, etc.), forms a small portion of the total cost of the more expensive types, whereas the cost of element in the resistor-heated furnace forms the bulk of the cost, and it has a limited length of service.

While resistor-heated and gas-fired furnaces can be designed completely by means of a heat balance, arc, arc-image, high-frequency induction, and electron-bombardment furnaces depend on complex physical processes for their heat supply, and it is impossible to calculate the rate of heat generation. Thus, the design of such furnaces must depend to a large extent on experience. However, certain initial considerations are common to all and should form the basis of the design, although empirical and experimental relations will be employed later:

(i) The size and shape of the charge and the proposed throughput determine the dimensions of the heated chamber. The shape of the chamber will be largely determined by the method of heating chosen.

(ii) A protective atmosphere or a vacuum is often essential in the heating process, and it is sometimes necessary to prevent slags and vapours (produced by the charge) fro attacking the furnace structure by the provision of a inner container for the charge. Such considerations ca alter the conclusions drawn from (i).

(iii) The type of refractory from which the chamber is con structed will be chosen with reference to the operatin temperature level, cost and probable life in the proce under consideration.

(iv) Insulation for the chamber is chosen with regard t furnace temperature and the heating schedule (that i rate of heating or cooling). The thermal capacity of th furnace, and therefore the heat storage in the insulation should be small where high rates of heating and coolin are required.

(v) The required thermal input must be equal to the steady state heat losses and the heat required by the charge a any time. Heat losses from the external structure ca be assessed by using data and methods given in Spiers(1 or McAdams.(2)

There is no simple method for calculating the rate of ris of furnace temperature or overall heating time. The Schmi method(2) is tedious, and assumptions are essential to enabl the calculation to be made at all. The following simpl approximate method is recommended. It is assumed that:

P = average input power (kW or B.t.u.) during heatin period (1 kW = 3413 B.t.u.),
t = heating period (h),
Q = average heat losses during heating period (B.t.u./ft^2 h)
M = heat stored in furnace structure at equilibrium (B.t.u.)

For electric furnaces:

$$P = \frac{M + Qt}{3413t}$$

or

$$t = \frac{M}{3413P - Q}$$

For gas-fired furnaces:

$$t = \frac{M}{P - Q}$$

Such calculations will enable the designer to decide if the proposed furnace is suitable, but accurate values of heating and cooling rates can only be determined by experiment. The furnace should be provided with a maximum input power slightly in excess of the calculated amount—this safety factor is to allow for inaccuracies in the data used and the assumptions made. An excess of 25% is suggested. The actual power consumed will depend on the efficiency of the system. A resistor-heated furnace is the only type in which the efficiency of energy conversion is 100%. In the other furnaces listed, an overall efficiency should be used in conjunction with the heat required by the charge.

Electric-arc furnace

Small electric-arc furnaces(3, 4) are used in experimental metallurgy and melting operations, and also for instructional purposes. For the most part, they are hand-operated versions of their industrial counterparts, holding between twenty and two hundred pounds of charge and consuming between 40 and 100 kVA. The power is supplied to two or three electrodes which can be inclined together at their working end to yield an indirect arc for melting materials of low-electrical conductivity.

For a small arc furnace of this type, the heat balance hows that 50–60% of the input energy is usefully used in he melting operation, and about 25% is lost through the walls and the holes through which the electrodes are inserted. The remainder of the power input appears as heat lost to he slag, and as electrical losses. It is possible to calculate he required input power from these facts and, from this power, the cross-sectional area of the electrodes, using a current density of 200–300 A/in^2.

More specialized applications$^{(5,6)}$ have been developed for he production of gas-free ingots of rare metals, free from mpurities which they tend to pick up from the containing vessels. For these variants, the metal is melted into a water-cooled copper crucible to which the metal does not adhere. The copper hearth or crucible is $\frac{1}{4}$ in. thick and is well cooled to prevent damage by the electric arc. The electrode is usually of tungsten, and currents densities of 400–600 A/cm^2 are used. The arc is produced by touching the tip of the electrode on the specimen charge and then withdrawing the electrode to obtain an arc $\frac{1}{2}$–$\frac{3}{8}$ in. long. The electrode is movable and thus the whole of the charge can be maintained in the molten condition. Currents can be conveniently supplied from arc-welding transformers giving 40–400 A (50–100 V on open circuit). The working voltage across the arc is about 15 V. The atmosphere surrounding the arc is usually helium or argon, but if sufficient metal vapour and gases are liberated, a vacuum can be used. The characteristics (voltage against current or length) of all arcs are altered by the type of atmosphere and pressure.

In other instances, the electrode is formed from the powdered metal and pressed into shape. The electrode gradually melts to form a pool of molten metal on the hearth of the furnace and this gives rise to the name by which the process is known—the consumable-electrode arc technique. To provide extra energy for melting the electrode, the electrode-current densities are slightly higher than with the non-consumable (tungsten) arc furnace.

Arc-image furnace

The arc-image or solar furnace$^{(7,8)}$ enables small quantities of material to be heated under controlled conditions to temperatures in the region of 4000° C. The apparatus is much simpler than any of the other types of furnace described, and consists, in principle, of the concentration by an optical system of radiation from a carbon or tungsten arc on to a target.

The efficiency of the furnace depends on the efficiency of the optical system, the absorptivity of the charge for radiation from the arc, the absorptivity of the atmosphere between the arc and the charge or target, and the heat losses from the outer surfaces. The arc is formed between two electrodes, either carbon or tungsten, using current densities of 100–400 A/cm^2. The atmosphere should not absorb radiation from the arc in the temperature range to be covered. Air is quite adequate for general purposes, but the formation of nitrogen peroxide in large quantities should be avoided, because it has a high absorption coefficient. A vacuum could also be used. It is usual to create a cavity in the charge for the radiation to fall upon, thus minimizing re-radiation.

Three main types of optical system have been used:

(1) Two paraboloidal mirrors of equal focal length, arranged facing each other and coaxially, with the source at the focus of one and the sample to be irradiated at the focus of the second. One such type uses two searchlight reflectors, 36 in. diameter and 14 in. focal length, and yields a maximum irradiance of 90 cal/cm^2 s. Because there is no magnification in this system, the irradiated area is only 0·3 cm^2, and the radiator is of variable intensity (see below). In this method, losses arise because there are two reflexions, and because of the screening effect of the source and sample which must be mounted between the mirrors. The advantages of this system are the high irradiance obtained and the applicability of searchlight reflectors.

(2) An ellipsoidal mirror will overcome some of the disadvantages of method (1), but special manufacture will be required. The source is placed at the first focus and provides an enlarged image at the second focus, where the sample is placed. From a 24 in. diameter mirror, the focal lengths of which are 11 in. and 52 in. respectively, the irradiated area is 1 cm^2, with an average irradiance of 34 cal/cm^2 s.

(Reflective surfaces in methods (1) and (2) are generally aluminium, stellite, rhodium or silver.)

(3) Complete freedom from screening by the object is provided by a lens system in which one pair of condenser relay lenses provides an enlarged image as an object for a second pair of condenser lenses, providing a maximum irradiance of 30 cal/cm^2 s, but spread over an area of 97·6 cm^2. However, large heat-resisting lenses are difficult to construct, and are thus expensive, and they do not focus all wavelengths at the same point.

If the distribution of irradiance follows a Gaussian distribution function,$^{(6)}$ then:

$$H_r = H_0 \exp(-ar^2)$$

where H_r is the irradiance at a radial distance r cm from the axis (cal/cm^2 s), H_0 is the irradiance when r equals 0, and a is a constant depending on the source.

The main types of optical system are compared in Table 1, in which the following other symbols are used:

r_{90} = radius at which H_r equals 90% of H_0 (that is, at which H_r equals H_{90}),
F_{90} = the radiant flux through area $\pi(r_{90})^2$,
P = input power,
η_{90} = efficiency, and equals F_{90}/P.

Table 1. *Comparison of optical systems*

Optical system	*24 in. double parabolic*	*36 in. double parabolic*	*24 in. ellipsoida*	*Condenser relay lenses*	
positive carbon	11	16	10	16	mm
anode-current density	82	85	181	112	A/cm^2
gross power input	5·4	13·6	11·4	16·7	kW
H_0	87	90	36	30	cal/cm^2 s
a	1·1	0·3	0·15	not available	cm^{-2}
r_{90}	0·16	0·3	0·47	1·0	cm
H_{90}	83	85	34	28	cal/cm^2 s
F_{90}	6·7	24	24	84	cal/s
η_{90}	0·52	0·74	0·87	2·1	%

These arbitrarily defined efficiencies are very low because the charge is so small.

Electron bombardment furnace

It is possible to use a stream of electrons as a source of heat, provided that a vacuum of 10^{-4} mm of mercury is maintained in the system. Such a furnace is similar to a thermionic valve in operation. Electrons flow from a hot filament, are accelerated by a high potential and, in certain instances, are focused by charged shields on to the material specimen, which comprises the anode. One such unit,(9) designed to produce large crystals from such metals as silicon, tungsten, and rhenium by a zone-refining technique, consists of a single turn of tungsten wire as the cathode wound around a rod of the material with focusing shields of molybdenum above and below this filament and concentric with the rod. The shields are maintained at cathode potential. It is possible to create a molten zone, and by traversing the cathode, move this zone down the rod. Materials of low electrical conductivity can be melted by making an initial increase in the conductivity at the surface by, for example, scratching it with a pencil. The graphite will eventually burn away and will not impair the final purity. A unit(10) more suitable for all purposes constructed for the vacuum purification of metals, has as the anode, a water-cooled, earthed copper hearth on which the material to be melted is placed. Electrons flow to the charge from a movable tungsten cathode, and are focused by molybdenum shields at cathode potential (up to 9·5 kV). This method is restricted to metals of low vapour pressures, but uranium and niobium have been satisfactorily melted. The technique also permits wide control of the heating process and, as the heat is localized, a heat-resisting glass enclosure can be used, so giving unrestricted visibility of the sample.

High-frequency induction furnace

The principle of the high-frequency induction(11, 12) furnace is to generate heat by means of eddy currents set up in electrically conducting materials by a rapidly alternating field. This method has been applied to heat treatment of metallic components and to the melting of metals and alloys in a crucible. Because no electrical connexions need to be close to the crucible or component, the use of a vacuum or a controlled atmosphere is simplified. It is possible to heat by this technique to temperatures at which graphite begins to vaporize (3600° C).

The design of this type of furnace involves the following points:

(1) The shape of the crucible and energizing coil, which determines the coupling of the circuit. It is essential to make the diameter of coil as near to the diameter of the crucible as possible without allowing them to touch. The coil is made from copper, approximately $\frac{1}{4}$ in. outside diameter in small installations, and water-cooled to remove the heat generated in the energizing coil and prevent damage.

(2) The heat generated must be conserved by adequate insulation. This applies mainly to large (greater than 5 lb) melting units, for the generator is sometimes powerful enough to melt a few grammes of the charge in an uninsulated crucible. Often the insulation also forms the container for the metal charge. One widely used method is to pack the powdered refractory around the coil with a tar bond, and then burn it in to produce an impervious monolithic lining the optimum thickness of which is given by the relationship

$$a + x = \frac{k}{ah},$$

where x is the thickness of insulation (in.), k is the therm conductivity of the insulation (B.t.u. in./ft^2 h deg. F), a the radius of the chamber (in.) and h is the heat transf coefficient to the surroundings (B.t.u./ft^2 deg. F). (Th provision of a lid to prevent end losses is very important.)

(3) The high-frequency power can be obtained from valv oscillator systems or from inductor alternators. The forme system will provide from 1 to 50 kW at frequencies betwee 10 and 1000 kc/s, and have an electrical efficiency of abou 50%. They are used mostly with small apparatus requirin very high frequencies, because the valves, which have limited life, are very expensive for high power ratings. Th rotary machines are used for power consumptions of 5 t 500 kW, and frequencies up to 10 kc/s. The power factor i made to approach unity by a capacitor system, and then th electrical efficiency is about 75%.

(4) Normally, for steel making, the percentage of the inpu power used to heat the metal and slag for melting purpose is about 60%. The remainder is accounted for by electrica and radiation losses. For low temperature work, the effi ciency will be higher as the proportion of heat lost will be smaller.

(5) When an energizing coil is used for heat treatment, the effective current, and thus the heat, can be confined to a definite depth in the specimen. This depth is given by the Steinmetz equation:

$$d = \frac{1}{2\pi}\left(\frac{\rho}{\mu f}\right)^{1/2},$$

where d is the depth of penetration (cm), ρ is the resistivity (Ω cm), f is the frequency (c/s) and μ is the permeability (no units). This equation shows that the higher the frequency, the smaller the heated depth for a given material. Thus, for case-hardening, short-term high-frequency heating is used while for thorough heating, a process with a lower frequency and a longer period of process would be used.

The advantages of the method lie in the flexibility of application of the energizing coil, the attainable temperature and speed of heating, and the homogeneity of alloys produced in this process with the electromagnetic stirring that can be induced. In the purification of such metals as tungsten, tantalum, and titanium, impurities can be picked up from the crucible. Effects(13) have been directed to perfect levitation melting, in which electromagnetic forces support the specimen in an inert atmosphere and provide the heating energy as well. It is difficult to arrange these forces to hold the material in both the solid and liquid states, and then pour it, but the method is very attractive in work requiring the utmost purity.

Resistor-heated furnaces

Resistor-heated furnaces are most commonly employed in laboratory practice(14, 15, 16) and consist of a refractory tube or chamber, heated internally or externally by rods or windings or spirals, and then suitably insulated and supported. The working temperature of such furnaces is limited by the maximum service temperature of the resistor. Table 2 shows the available materials for temperatures up to 3000° C, and Table 3 shows service temperatures for refractory tubes. Larger furnaces can be made from refractory bricks or slabs made by embedding heating spirals in castable refractory concrete. The legend of a resistor-heated furnace design is shown in the figure.

Power input. The input power must be distributed evenly over the element so that the maximum working temperature

Table 2. *Resistance heating elements*

Material	*Max. service temperature (°C)*	*Remarks*
Nichrome wire or tape (80% Ni/20% Cr)	1050	Satisfactory for all low-temperature work, including reducing and oxidizing atmospheres. Corroded by sulphurous gases.
Kanthal wire or tape (an alloy of Al, Fe, Cr with some Co)	1150 to 1350	Satisfactory in reducing, oxidizing, and sulphurous atmospheres, but attacked by halogens. Becomes brittle on initial usage and must be supported with care.
Kanthal-super (a combination of Mo and Si)	1600	Softens at top temperatures and must be installed in slots or on the furnace floor on a bed of granulated alumina.
Silicone carbide resistors (globars or crusilite rods)	1550	Rods working in a hydrogen atmosphere should not be heated above 1300° C. Long rods should be placed vertically or they deform.
Platinum or platinum/rhodium containing 40% rhodium	1400 to 1540	A very expensive element, in spite of the rebate on broken ones.
Molybdenum wire	1800	A very effective element, but must be protected from oxidation by a hydrogen atmosphere, usually cracked ammonia. Although the melting point is 2612° C, the refractory materials used with it restrict its working temperature to the given value, and above 2000° C, volatilization is serious.
Granular carbon particles	1800	Contact resistance is high and an inert atmosphere is needed. Hot spots can form, which accentuate themselves with time.
Zirconia (stabilized with ceria)	2200	When heated to 1500° C, electrical conductivity high enough to allow (and short circuit the winding) its use as heating element to 2200° C. Stable in oxidizing atmospheres.
Tungsten spirals or sheets	2600 (vac.) 3200 (He)	Tubes fabricated from sheet and used in vacuum, inert atmosphere or hydrogen, because wire sags at high temperatures.
Carbon tube furnaces (graphite resistors)	3000	Resistance increased by cutting slots or spirals in tube, at the expense of mechanical strength. It is possible to fabricate a stronger high-resistance tube from machined rings. An inert atmosphere and lamp-black insulation is required with a high-current transformer.

Table 3. *Types of refractory tube*

Material	*Max. service temperature (°C)*	*Remarks*
Silica glass	1050	Good resistance to thermal shock, non-porous.
Aluminous porcelain	1500	Moderate resistance to thermal shock, very low porosity.
Mullite	1600	As above. Resistant to slag attack.
Fused alumina	1700	Slightly porous, resistant to slag and thermal shock.
Recrystallized alumina	1900	Non-porous, and as above.
Magnesia	2000	Poor resistance to thermal shock.
Stabilized zirconia	2400	Non-porous, becomes a conductor at high temperatures.

shall not be exceeded at any time. The manufacturer supplies data regarding the temperature which will be reached when a certain load (power per unit surface area) is used. It is important to adhere to such values.

If P is the input power (kW) and K is the safe loading value (W/in.^{2}) then the area of element required is $1000\,P/K$. If A is the surface area for one foot of element (in.^{2}) then the length L of element required (ft) is given by:

$$L = \frac{1000P}{KA}. \qquad (1)$$

If the resistance per unit length is $\rho(\Omega\ \text{ft})$, then the total resistance is $L\rho$, and the current through the specimen is $V/L\rho$, where V is the applied voltage. Therefore the power P is given by:

$$P = \frac{V^2}{L\rho} \qquad (2)$$

These two equations can be mutually satisfied by the choice of element gauge, the arrangement of the resistors in a series/parallel circuit, or the use of an applied voltage which can be varied. Similar equations will determine the number of silicon-carbide resistors, which will be required. When the length or number of elements is determined, the arrangement of the element in the furnace can be considered.

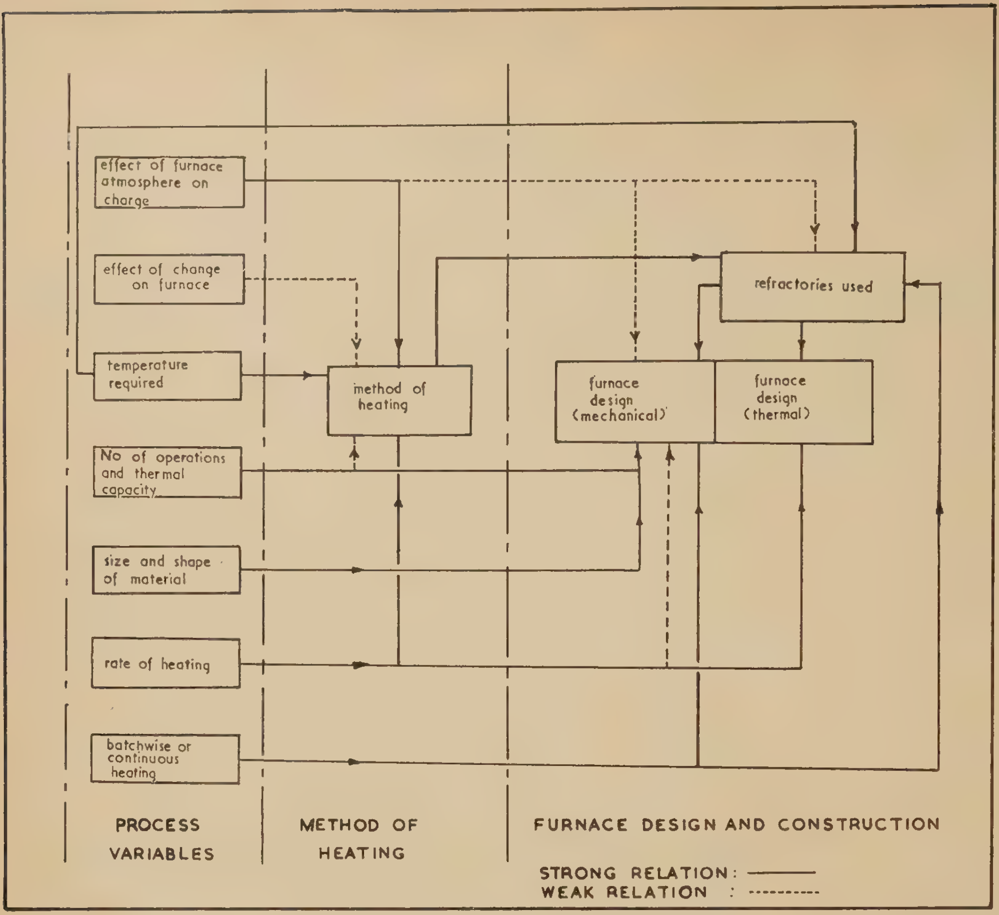
effect of furnace atmosphere on charge
effect of change on furnace
temperature required
No of operations and thermal capacity
size and shape of material
rate of heating
batchwise or continuous heating
method of heating
refractories used
furnace design (mechanical)
furnace design (thermal)
PROCESS VARIABLES
METHOD OF HEATING
FURNACE DESIGN AND CONSTRUCTION
STRONG RELATION: ———
WEAK RELATION : ---------

Scheme of resistor-heated furnace design

Wire resistors. These can be installed in two general ways:

(1) They can be installed in long spirals of small diameter, parallel to the tube axis or furnace walls and distributed to heat as evenly as possible. Such a method allows metallic furnace tubes to be used, which have certain constructional advantages but a temperature limitation of 850–1200° C. It is also simple to replace such a spiral after failure.

(2) The tube can be wound with wire. This method provides a more even heating in a circumferential direction and, by increasing the number of turns per unit length at the ends of the refractory tube, the temperature along the tube can be made more even by counter-balancing the end losses. The winding is normally held in place with some cement which will not attack the metal at working temperatures. A further winding may be installed in parallel with and on top of the first one, but careful calculation of the respective current densities should be made beforehand, or the first winding might burn out. The temperature reached with this type of winding is slightly higher than with method (1) but, in the event of failure, major reconstruction is necessary. It is possible to wind the element non-inductively so that sensitive electrical apparatus working in the immediate vicinity will not be affected, but the full potential difference will exist between neighbouring turns and, as refractory cements become more conductive at high temperatures, the danger of a short-circuiting arises. When the wire is wound, it is important to maintain an even tension and to prevent kinks and irregularities from forming, because these will become points of weakness and will cause failure at high temperatures.

Tape or strip resistors. Metallic heating elements are available as flexible tape of varying gauges and widths. While tape is somewhat more difficult to handle than wire, there is more surface over which to distribute the input power, and the tape covers the surface of the tube on which it is wound more completely. It can be installed in the form of hair-pin shaped elements, which can be fastened to the wall or roof of larger units by non-conducting pins, or laid in slots on the hearth of the furnace. In this manner, a long length of tape is accommodated neatly.

Silicon-carbide resistors. The heating section of a silicon-carbide element is arranged to have a higher resistance than the intended cooler portions, and the element is either made in a three-part construction or has a spiral cut in it to increase the path length and decrease the cross-section over which the current will flow. Certain types are available with both electrical connexions at one end, while the element has also been constructed in the form of a spiral tube to surround the refractory work tube. The manufacturer gives details of loading values, and also ways to arrange the elements to give the optimum results. It is customary to mount the elements near to and parallel to the roof in rectangular furnaces or around the circumference, on a pitch circle, in the case of cylindrical furnace tubes. The resistance of these elements increases with use and a controllable applied voltage is an advantage if constant temperature conditions are required over a long period of operation.

Molybdenum windings. This group covers tungsten, tantalum and molybdenum, which oxidize in air above temperatures of 400° C. Molybdenum is the cheapest and hence the most commonly used of these metals. The winding is prevented from oxidation by a surrounding atmosphere of hydrogen or cracked ammonia, produced by passing ammonia gas through a refractory tube at about 750° C.

Carbon resistance elements. Pure graphite carbon has a low resistance and a negative temperature coefficient of resistance. To achieve the necessary input power, low-voltage/high-current systems are necessary, involving expensive transformers. The material is used in the form of:

(1) Tube with longitudinal slots, giving several current paths, or a plain tube.

(2) A tube with a machine spiral slot, increasing the electrical resistance at the expense of mechanical strength.

(3) Machined rings, which fit together to form a tube, and the total resistance is varied by altering the axial pressure on the system, giving a secondary method of control.

(4) Carbon granules, packed together around the refractory work tube. This type of construction has a higher resistance, but the maximum operating temperature is around 1800° C, because the electrical characteristics are not very constant, and the temperature coefficient of resistance is negative in the region up to 1200° C and thereafter very low (hot spots can be formed).

After the necessary input power has been calculated, the current required depends upon the available voltage and the resistance of the element which can be measured. It is necessary to have a variable transformer in the circuit to control the heating process. The element should be protected from oxidation and thermally insulated with lampblack, which adsorbes air from outside the tube, and eventually produces carbon dioxide, carbon monoxide and nitrogen. The porosity of lampblack is about 80% and hence it is a good insulator.

Gas-fired furnaces

Many industrial small-scale furnaces(17) reaching temperatures of 1300–1400° C are fired with gas obtained from the public supply, burnt with cold air, but instances of higher temperatures are recorded in which the gas and pre-heated air, or a fuel of higher calorific value (for example, methane or acetylene) are used. In this method of heating, the hot waste products of combustion, with a slight excess of air, transfer their heat by radiation and forced convexion to the charge and/or the walls of the furnace and the furnace walls then re-radiate heat to the charge.

The best design from a heat-transfer standpoint will therefore ensure:

(1) A rapid combustion of the mixture, to produce the highest temperature practicable, and a high-velocity stream of combustion products;

(2) Scrubbing by the gases of the surface which they are intending to heat, to produce high heat-transfer coefficients;

(3) An arrangement of the inside surfaces of the furnace so that they are at a uniform temperature and the heat transferred by re-radiation is uniform.

While it is very difficult to design a furnace completely by theoretical means, it is possible to predict its performance with some success by making use of the heat balance with suitably assumed inside-wall temperatures and gas temperatures, and by knowing something of the path that the hot gases will take in the furnace. Cases occur both in industry and research where some desired flow pattern, uniform or otherwise, is required. A simple, accurate, and yet inexpensive technique is the study of the flow pattern by water models.(15, 18) The results from this practice have been invaluable in the construction of gas-fired muffle furnaces(14,16) and similar appliances.

The thermal input, and hence the size of burner required, is desired from the heat balance. Recently, several high-intensity burners have been developed (the tunnel burner, the Radiant-Cup burner, and the Cell burner(19, 20, 21)) which produce a much higher exit velocity by the use of a number of small jets and a moderate combustion air pressure. The heat-transfer coefficient from the gases to the charge is increased and, for a given size of furnace, the heating times are reduced and through-put increased. Thermal efficiencies may also be improved.

One technique has been to direct a row of these burners tangentially against the wall of the furnace, which is made cylindrical in cross-section. The furnace gas temperature and heat-transfer coefficient are approximately constant, and thus the inside surface of the furnace is practically at constant temperature.

Because the products of combustion of gas from the public supply are of an oxidizing character, and because these furnaces are often used for analytical work where the furnace gases might entrain small amounts of gravimetric samples, muffle heating, which may employ a special protective atmosphere, is used. Small industrial units, where scale formation and decarburization of the charge are to be minimized, often use a so-called reducing atmosphere, obtained by combustion with 95% of the theoretically required air. The slight reduction in thermal efficiency is more than counterbalanced by the quality of the product.

Furnace construction for gas-fired and resistor-heated furnaces

The most common form of construction employs a refractory tube as the heating chamber, placed centrally in a suitable amount of refractory insulation brick or powder, and this, in turn, is surrounded by a thin metal case, which provides a rigid basic shape. Insulation bricks are easily shaped to form the required pattern and have the additional advantage that their heat capacity is small in comparison with normal refractory bricks (for example, firebricks or fireclay refractories). This means that the furnace will heat up to the working temperature quickly and, for intermittent use, the heat stored in the furnace, which is lost when the furnace is turned off, is small. The quality of these bricks (thermal conductivity, porosity, limiting hot-face temperature and mechanical strength) has improved so much that they can be used for the internal face of many laboratory furnaces, and can support resistors in slots cut in the side or holes drilled through them. For temperatures above 1500° C, the refractoriness required can only be provided by materials with a higher alumina content or by other pure oxides. The heat capacity and cost of such refractories are increased.

Another method of insulation is to coat the winding with pure alumina cement, and then surround it with broken high-temperature insulating brick, since the average thermal conductivity and heat storage of such a material is much smaller than that of the similar solid brick. For lower temperatures, exfoliated vermiculite is a good insulator, but it tends to settle and produce void spaces unless it is well shaken down initially. Practical details of many resistor-heat

Table 4. *Types of suitable furnace brick*

Material	*Bulk density (lb/ft^3)*	*Max. service temperature (deg. C)*	*Thermal conductivity (cal/cm s deg. C)*
Asbestos slab	8·25	600	$2{\cdot}06\,.\,10^{-4}$ at 200° C
Granular vermiculite	5–7	1100	$2{\cdot}55\,.\,10^{-4}$ at 500° C
Vermiculite brick	30	1100	$4{\cdot}81\,.\,10^{-4}$ at 500° C
Diatomite powder	18	1200	$2{\cdot}06\,.\,10^{-4}$ at 1200° C
Insulating brick (various)	47	1250 1540	$8{\cdot}6\,.\,10^{-4}$ at 1000° C
High alumina brick	170	1800	$52{\cdot}9\,.\,10^{-4}$ at 500° C

furnaces are given by Okress and Wroughton,(13) Barrett,(14) and Campbell.(15) Types of furnace brick are compared in Table 4.

Control of small furnaces

It is desirable to operate small-scale furnaces at a controlled temperature, using the simplest technique which will provide the required degree of control, thus keeping cost down. The appropriate temperature level is recorded by an electrical or mechanical unit installed in the optimum position. The deviation of this reading from the set point—that is, the error signal—must be made to change the thermal input to attain the required temperature once more. This is done in two general ways:

(1) By a complete cut-off of input—that is, an on/off control.

(2) By allowing the rate of change of the deviation to be proportional to the rate of change of the input—that is, a proportional control.

This second method is applied to gas-fired furnaces, because an on/off control would require an automatic ignition system. The thermal input, or gas rate, is controlled by means of a butterfly valve operated by a lever and bi-metallic strip unit. A refinement will maintain a pre-set air-to-gas ratio. Another method controls the inlet gas valve from the reading of a temperature-recording unit through a relay system.

Occasionally, small electric furnaces can be built to run directly from the mains supply, and hence will have a fixed equilibrium temperature. The simplest improvement is to connect a variable resistance in series with the element, but the range of operating temperatures will be limited. A more efficient method is by means of an energy regulator, which switches the furnace on and off and, by providing a variable ratio of time on to time off, it varies the heating rate and final equilibrium temperature. Transformers are the simplest means of control, but are expensive when compared with the previously mentioned system. An infinitely variable transformer, or Variac, will give the widest control band, but a multi-tap transformer, in conjunction with a variable resistance, can be very useful. All these methods require experimental setting.

In furnaces with more than one current path, a control switch can be arranged to cut out certain sections, chosen so that the temperature level is satisfactorily reduced, but the temperature distribution is unaltered. In industrial units, the heating elements may form a star-connected three-phase system, and for control purposes, one or two phases may be cut out periodically. For all these methods, where making and breaking of the circuit is entailed, it is advisable to install a special contactor or automatic switch, which will obviate all problems of arcing and frequent replacement of the contacts, or overheating of the element when the contacts stick together.

The power input to electric-arc furnaces is varied by moving the electrodes and altering the resistance of the arc. It is unusual to find automatic control on small furnaces, because it must account for variation of resistance within the path of the arc and the decrease in length of the electrodes. Thus, the movement of the electrodes is manual, with the intention of maintaining a steady arc.

Small-power high-frequency induction furnaces may be controlled by varying the anode voltage in the rectification circuit by means of a Variac. This, in turn, varies the anode voltage in the amplification circuit, and thence in the inductor. In the case of larger melting units, where an inductor alternator-motor system provides the high frequency, the power input can be controlled by varying the alternator field.

Control of the electron bombardment furnace is afforded by variation of cathode-to-anode voltage, filament current or cathode-to-anode distance. It is more convenient to use the first method, because cathode movement would require an effective gland and, on the basis of electrical stability, it is better to work with the lowest cathode-to-anode potential and alter the filament current.

The arc-image furnace can be controlled by altering the radiant exposure, which is defined as the time integral of irradiance. Hence it is possible to vary the heating time or the irradiance, or both. Exposure time is controlled either by moving the specimen at a predetermined rate or by using a shutter. Diaphragms normally control the irradiance.

References

(1) *Technical Data on Fuel.* Edited by H. M. Spiers. British National Committee, World Power Conference, 1952.

(2) McAdams, W. H. *Heat Transmission.* 3rd ed. (London: McGraw-Hill Publishing Co. Ltd., 1955).

(3) Robiette, A. G. E. *Electric Melting and Smelting Practice* (London: Griffin and Co. Ltd., 1955).

(4) Otto, C. A. *Electric Furnaces* (London: George Newnes Ltd., 1958).

(5) Geach, G. A., and Summers-Smith, D. *Metallurgia*, **42**, p. 153 (1950).

(6) Pugh, J. W., Hadley, R. L., and Hennig, R. W. *Metal Progress*, **63**, p. 70 (1953).

(7) Davis, T. P. *The carbon arc image furnace.* [*High Temperature—a tool for the future*, p. 10 (Stanford: Stanford Research Institute, 1956).]

(8) Farber, J. *Images of very high temperature sources.* [*High temperature—a tool for the future*, p. 1 (Stanford: Stanford Research Institute, 1956).]

(9) Davis, M., Calverley, A., and Lever, R. F. *J. Appl. Phys.*, **27**, p. 195 (1956).

(10) England, P. G., and Jones, H. N. *J. Sci. Instrum.*, **35**, p. 66 (1958).

(11) Northrup, E. E. *J. Franklin Instn*, **201**, p. 221 (1926).

(12) Burch, C. R., and Davis, N. R. *Phil. Mag.*, **1**, p. 768 (1926).

(13) Okress, E. K., and Wroughton, D. W. *Iron Age*, **170**, p. 83 (1952).

(14) Barrett, L. R. *Research*, **6**, p. 61 (1952).

(15) Campbell, I. E. *High Temperature Technology* (New York: John Wiley and Sons, Inc., 1956).

(16) Glazebrook, R. *Dictionary of Applied Physics*, **5**, p. 309 (London: Macmillan and Co., 1923).

(17) Hayman, R. F. *The production of high temperatures in industry by Town's gas.*, Inst. of Gas Engineers, No. 396/191.

(18) Johnstone, R. E., and Thring, M. W. *Pilot Plants, Models and Scale-up in Chemical Engineering*, see, esp., p. 198 (London: McGraw-Hill Publishing Co. Ltd., 1957).

(19) Palser, J. *The Concentrated Combustion Burner.* Paper to Midland Junior Gas Association, 8 November, 1945.

(20) Francis, W. E. *The design of air blast tunnel burners.* Gas Research Council, No. G.C. 48.

(21) Wright, J. F., and Palser, J. *Furnaceless heating and small gas-fired furnaces*, Sheffield Section, Instn. Prod. Eng., February, 19.

Apparatus for the measurement of the mechanical properties of fibres

by F. R. MORGAN, B.Sc., A.Inst.P., British Leather Manufacturers' Research Association, Milton Park, Egham, Surrey

[*Paper first received* 28 *May, and in final form* 22 *July*, 1959]

Abstract

Apparatus for determining the mechanical properties of eight fibres simultaneously is described. The apparatus provides for tests to be made at different relative humidities, chainomatic loading up to about 450 g, *and measurement of extensions of the order of* 10^{-3} *cm.*

Introduction

In recent years increasing attention has been devoted to problems concerned with the mechanical properties of fibres, and some time ago an extensive programme of research on the mechanical properties of collagen fibres was started in these laboratories. Work on these mechanical properties is never easy, and collagen fibres are probably more difficult to work with than others because of their variability (which means that many fibres are needed to obtain a reliable representative result) and because even a small deformation usually results in a permanent change (so that an experiment cannot be repeated on the same specimen). Many papers describing fibre extensiometers for materials other than collagen have appeared, and it would be tedious to attempt to summarize the different designs. It might be thought that one of them could easily be adapted to test collagen fibres, but this is not the case because, in addition to the difficulties given above, a further one arises when work on collagen is attempted because measurements have nearly always to be made on fibres less than about 1·5 cm long.

Three extensiometers suitable for collagen fibres have been described. Mitton(1) used an optical lever on to which small weights were hung as required, for his studies on vegetable tanned fibres. Conabere and Hall(2) carried out investigations on vegetable and chrome-tanned fibres. They applied loads to their specimens by causing them to pull a pendulum out of the vertical, and measured the resulting extensions with a lamp and scale. Later, Hall(3) studied the tensile properties of collagen fibres in solutions of different pH values. His apparatus was designed to give continuous loading at a constant rate and operated on the same principle as a chainomatic balance. He subsequently made additions and detail alterations to this apparatus,(4, 5) but the basic design remained the same. For reasons which will become apparent later, none of these extensiometers was suitable for the extensive study of collagen fibres recently started in these laboratories. A new design, incorporating some novel features, was therefore evolved.

Description

The most important design features were the size of the programme mentioned above and the time taken to test each specimen. The programme was, in fact, expected to involve a large number of fibres—probably several thousand—before it was completed. Also, the apparatus was required in the first place, to determine the breaking load and extension of fibres in air of known relative humidity and, with the rate of loading set at a convenient value (usually 6 g/min) about 20–30 minutes were required to test each fibre. Loads of up to about 450 g were therefore necessary, and because it was necessary to work with fibres only 0·6 cm long, changes in length of the order of 10^{-3} cm had to be measured.

The apparatus is shown in the photographs of Fig. 1. A rigid framework of 1¼ in. steel-angle was built up, and on this was mounted eight short balance beams (see Fig. 2). Directly above one end of each was fixed a vertical ½ in.-diameter glass tube through which could be passed a stream of air of known humidity. The upper ends of test specimens were held in these tubes, and the lower ends were connected to the beams beneath. Loads were applied to the fibres by lowering a pair of chains connected to each beam. This was done by passing the chains over sprocket wheels bolted to a shaft which was driven through a six-speed gearbox by a synchronous electric motor. The arrangement enabled loads of up to about 450 g to be applied to each fibre at rates varying from ⅜ g/min to 48 g/min.

The fibre extensions were measured by an electronic method which depended on the change in capacitance produced by a change in separation between two metal plates. The only other way suitable for measuring the small distances was an optical one with a lamp and scale. The electronic method was preferred because it was less cumbersome and easier to operate. A rectangular aluminium plate 1¾ × 1 × $\frac{1}{16}$in. was attached to one end of each balance beam, as shown in Fig. 2. These plates were arranged above a large brass plate firmly fixed to the frame of the apparatus. Thus an extension of the fibre (connected to the other end of the balance beam) increased the separation and decreased the capacitance between the aluminium and brass plates. This decrease was measured on an instrument designed to detect small changes in capacitance (proximity meter, type PM 2 by Fielden).

Because eight fibres could be tested simultaneously, some way had to be found to connect the proximity meter to each of the eight balance beams in turn as the loads were being applied to the fibres. An automatic switching system was designed to do this. The circuit is shown in Fig. 3. The device consisted of ten change-over switches S_1–S_{10} fixed to a cylindrical cradle, mounted, together with the trimmer capacitors C_1–C_{10} and resistors R_1–R_{10}, in an earthed metal box. An electrically driven cam operated the switches so that each in turn connected one of the balance beam plates to the proximity meter. The cam rotated at 2 rev/min. Therefore two readings were taken on each balance every minute, and a series of meter readings corresponding to the settings of the beams was obtained when the apparatus was run. The switches S_9 (between S_4 and S_5) and S_{10} (between S_8 and S_1) were not returned to a balance beam. They were included for calibration purposes and to help the operator keep "in step" when taking a long run of readings.

The exact rate of loading was determined by calibrating the balance beams. The chains were lowered for a known time and the load applied to each beam was then measured. The relationship between proximity meter reading and fibre extension was determined by giving each balance beam a series of known displacements, and the meter readings were noted.

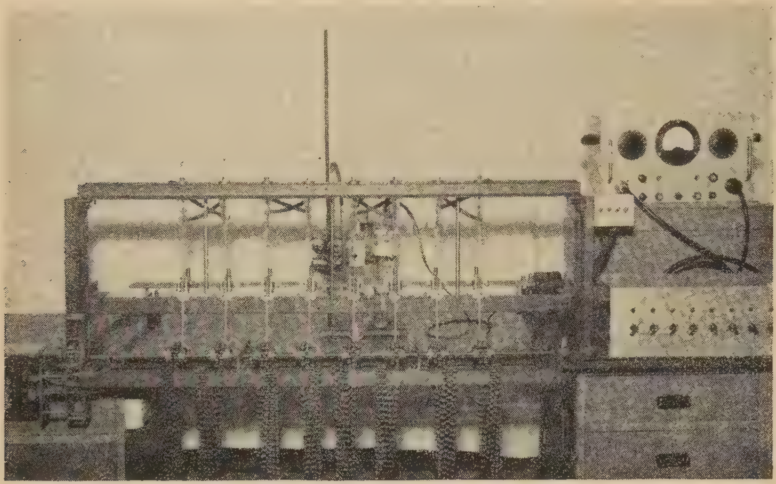

Fig. 1(*a*)

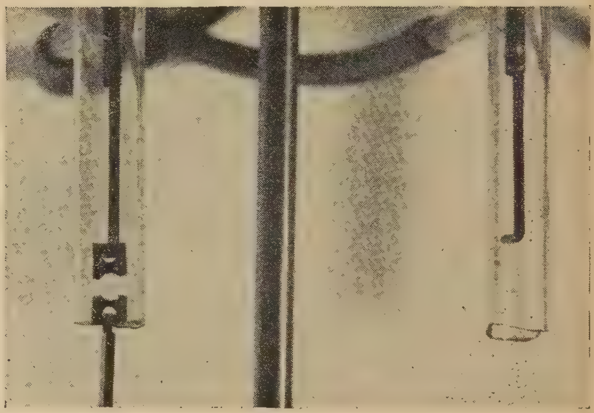

Fig. 1(*b*)

Fig. 1. (*a*) General view of extensiometer. The gearbox is on the left and the proximity meter on the right above the box containing the automatic-switching system. (*b*) Fibre mounted in apparatus and ready for testing

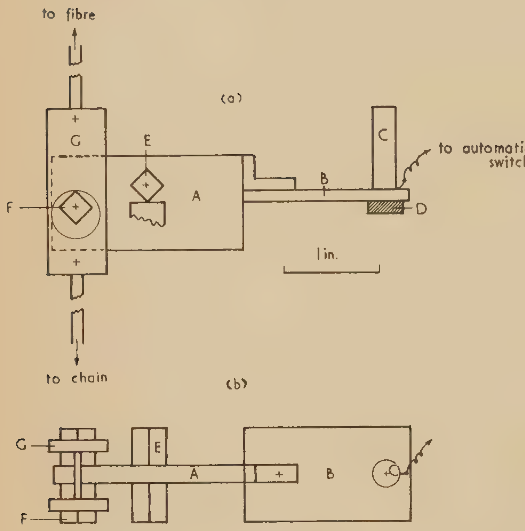

Fig. 2. Details of balance beam, (*a*) from side, (*b*) from above

A, Perspex plate; *B*, aluminium plate; *C*, counterpoise weight; *D*, Bakelite spacer; *E*, *F*, Knife edges; *G*, Vertical links. Knife edges *E* and *F* are fixed to plate *A*, and the link *G* rides on *F*.

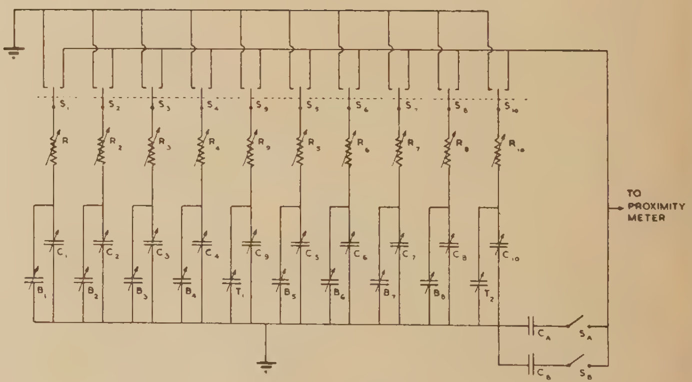

Right: Fig. 3. Circuit diagram of automatic switching system

S_1–S_{10}, change-over switches, cam operated; R_1–R_{10}, trimmer resistors; C_1–C_{10}, trimmer capacitors; T_1 and T_2, pre-set trimmer capacitors; B_1–B_8, balance capacitors; C_A and C_B, calibration capacitors.

Operation

A fibre was prepared for test by fixing its ends with nitrocellulose cement across a 0·6 cm-diameter hole punched in a piece of stout card 3 × 1 cm. A similar piece of card was then fixed over the first to ensure that the ends of the fibre were firmly held. The supporting card was cut through immediately before the test was started to leave the fibre free to extend. In this way, tests were performed on specimens of constant length, and breakages resulting from rough handling and accidents before the test were eliminated.

A fibre, prepared as described above, was hung in each of the eight glass tubes by means of a strong steel-wire hook soldered to a threaded rod passing through the metal end piece at the top of each tube. Fig. 1(*b*) shows a fibre in the apparatus and ready to be tested. The load on each balance beam was removed by adjusting the position of the chains, and the free ends of the fibres were attached to their respective beams. Each balance was then adjusted to its zero position by altering the position of the fibre to bring the bakelite spacer (shown in Fig. 2) under each aluminium plate just into contact with the earthed brass plate. All the circuitry associated with the proximity meter was next balanced-out to give a zero meter reading for each beam, and also for the blank switch positions S_9 and S_{10}. This was achieved by setting the trimmer capacitors C_1–C_{10} and resistors R_1–R_{10}. Finally, the sensitivity of the proximity meter was checked. To do this, switches S_A and S_B were closed, and the meter readings were noted. If necesssary, the gain control of the proximity meter was varied to obtain the correct reading.

When the above adjustments had been completed, the apparatus was ready for operation. Both electric motors (one driving the loading chains, the other driving the cam in the automatic switch) were switched on simultaneously and the meter readings were noted until all the fibres had been broken. By reference to the calibration curves for rate of loading and extension, it was then possible to determine the breaking load and breaking extension of each fibre, and also to draw up a load/extension curve for each of the eight fibres tested.

Acknowledgements

This paper is published by kind permission of the Director and Council of the British Leather Manufacturers' Research Association.

References

(1) Mitton, R. G. *J. Internat. Soc. Leather Trades Chem.* **29**, p. 169 (1945).

(2) Conabere, G. O., and Hall R. H. *J. Internat. Soc. Leather Trades Chem.*, **30**, p. 214 (1946).

(3) Hall, R. H. *J. Soc. Leather Trades Chem.*, **35**, p. 105 (1951).

(4) Hall, R. H. *J. Soc. Leather Trades Chem.*, **35**, p. 11 (1951).

(5) Hall, R. H. *J. Soc. Leather Trades Chem.*, **36**, p. 137 (1952).

Recording weight meter

by D. J. STEELE, The British Coal Utilisation Research Association, Leatherhead, Surrey

[*Paper first received* 7 *May, and in final form* 3 *July*, 1959]

Abstract

Modifications to a commercial platform weighing machine, to provide a continuous record of changes in weight of a standing load on the platform, are described. With this instrument, weight changes of up to 55 *lb in a maximum load of* 560 *lb can be recorded to an accuracy of* 0·5%, *i.e. less than* 5 *oz, which is the accuracy of the weighing machine itself.*

An earlier instrument, although satisfactory for short periods of operation, was found to be unsatisfactory for measuring weight changes over a time in excess of a few hours, owing to random changes of up to 2 *lb in full-scale calibration of* 50 *lb. This difficulty has been overcome in the present instrument by using photoelectric cells to detect the vertical movement of the steelyard, and a servo-operated mechanism to control the restoring force. The output, which is directly proportional to the change in weight on the platform, is in a form which is suitable for being recorded on a potentiometric recorder. It is substantially independent of normal ambient temperature changes; the calibration changes by* 0·01% *per ° F change of ambient temperature. This error can be allowed for if the ambient temperature changes are known.*

Introduction

In order to assess the efficiency of a domestic solid fuel appliance, it is essential to know the rate of fuel consumption (burning rate) so that the heat given out by the appliance may be compared with the potential heat in the fuel consumed.

The average burning rate can be obtained by refuelling the appliance at noted intervals of time, to a fixed datum line, and by weighing the amount of fuel required to do so; but in the course of appliance development work a need arose to measure the instantaneous burning rate of the fuel, and for this purpose a recording weight meter is desirable. A previous meter* built in this Laboratory was found to be satisfactory for only short-term operations over periods of a few hours, owing to inherent faults in mechanical design. These were due mainly to:

(*a*) accumulation of dirt on the contacts that were used at the sensing head, causing increased contact resistance and subsequent failure of the restoring force applied to the balancing coil;

(*b*) mechanical resistance of the contacts which imparted a varying force to the steelyard;

(*c*) excessive lateral movement of the steelyard causing the coil to rub against the sides of the magnet;

(*d*) excessive sparking of the contacts leading to their eventual welding together.

Principle of operation

The new weight meter overcomes the difficulties of an oscillating steelyard, experienced in the original model, by allowing the steelyard to "float" at a predetermined position in the "balanced" state and by eliminating the use of contacts.

---

* Bredl, J., and Marsden, K. J. *Information Circular No.* 32, (British Coal Utilisation Research Association, September 1950).

With the conventional platform machines, a weighing operation is achieved by moving an adjustable sliding weight along the steelyard until the end of the steelyard just rises after being released from its lower position. At this setting the couple on the steelyard due to the position of the sliding weight just counterbalances the effective couple due to the load on the platform.

In the recording weight meter described below, the couple due to the sliding weight is supplemented by an electromagnetic force acting at the free end of the steelyard. This force is achieved by passing a current through a coil which, attached to the free end of the steelyard, is allowed to move vertically in a magnetic field. The current can be adjusted automatically by a servo-operated potentiometer so as to provide a force which will balance any variation due to a change in load on the platform. Subject to appropriate initial adjustment, the value of the current flowing through the coil is a measure of the change of load on the platform.

The design of the commercial weighing machine used is such that it can weigh loads up to 560 lb. The modifications described below permit the automatic balancing and recording of variations of this basic load up to a maximum of 55 lb, subject to the total load not exceeding 560 lb. In setting up the weighing machine for operation it is necessary to know the maximum and minimum platform load that will be encountered during the period of test. The minimum load is then balanced by adjusting the sliding weight on the steelyard, and the electronic circuit is preset to balance automatically the load variations from minimum to maximum and simultaneously to provide a record of the variations.

Description of weight meter

Mechanical design. The general layout is depicted in Fig. 1. Attached to an extension arm of the balance frame (1) is a platform (2) and vertical column (3), the top of whic forms a fixed bridge (4) to which the photoelectric unit (5 is screwed. This is a Tufnol block carrying two photocells (6 and the lamp housing (7). The photocell and lamp housin are separated by a $\frac{5}{16}$ in. gap in which a shutter (8), attache to an extension (9) of the steelyard, can move vertically an interrupt the light paths between either cell and the lamp To a spigot (10), fixed to the end of the steelyard extensio is attached a short rod (11) carrying at its lower end th operating coil (12). This moves in the gap between th central core (13) and outer ring (14) of the magnet assembl fitted to the platform. The leads (15), (16), and (17) connec the sensing head and magnet assembly to the remainder o the electronic circuit.

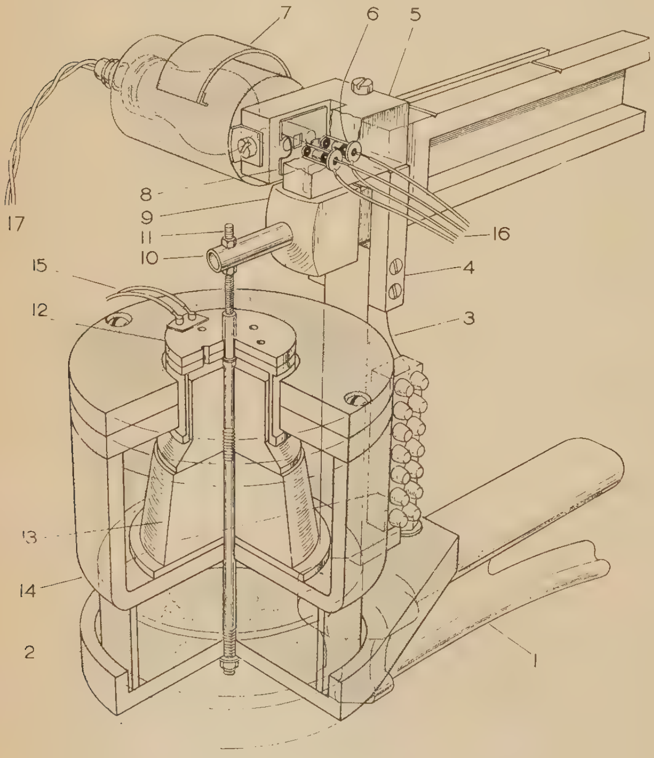

Fig. 1. Sensing head and magnet assembly

Coil and magnet assembly. The electromagnetic restorin system consists of a coil wound on a thin-walled aluminiu cylinder, which is suspended freely in the annular air ga between the pole-pieces of a loudspeaker type of permanen magnet. The air gap is machined to a dimension such tha the coil will at no time come in contact with the magne assembly when any lateral movement of the steelyard occurs

Sensing head. It was felt that the use of a photoelectri sensing head would allow greater stability of operation wit simplified electronic circuitry. At first a system using tw phototransistors (type O.C.P. 71) was tried, in which lig falling on either cell was interrupted by a shutter attach to the steelyard. This proved satisfactory at normal roo temperature, but failed at temperatures in excess of 85° F owing to the increase in "dark current" of the cells. The resultant reduction in voltage output from the phototransistors led to a failure of the servo-system.

Two germanium junction photocells (type P.50 A) were substituted for the phototransistors with appropriate circuit modifications, and a satisfactory output from the cells was obtained up to an ambient temperature of 120° F, and these photocells were therefore used in the final design of the new weight meter. In order to prevent overheating of the photocells it was found to be necessary to support the lamp housin on brackets, in such a way that the heat transferred from it to the photocells by conduction was reduced to a minimum.

The photocells are situated behind shields which allow light to pass through two holes of 0·0135 in. diameter. The shutter, which has two rectangular holes diametrically opposed, permits, at its extreme positions, either one or other of the photocells to receive light. As the shutter moves it reduces progressively the light to one photocell, so that the other cell simultaneously receives more light until a complete changeover of illumination has occurred. At the mid-position both cells receive equal amounts of light corresponding to half illumination. Thus a complete changeover of illumination to the cells occurs for a movement of the shutter of only 0·0135 in.

Circuit and operation

The circuit (Fig. 2) consists basically of (i) a sensing unit, (ii) converter unit, (iii) two-stage amplifier, (iv) servo-motor, (v) current control circuit, (vi) power supply circuits.

An out-of-balance signal obtained from the two germanium junction cells (V_1, V_2) is transformed into an alternating potential by the converter, amplified and fed as an activating signal to the servo-motor M_1. The rotation of the servo-motor, reduced by a gear ratio of 6400 : 1, positions VR_4, which varies the control current flowing through V_5 to bring the steelyard into a balanced position and so reduce to zero the signal from the sensing unit.

Sensing head. The two cells V_1, V_2, are positioned so that hey receive light from a 12 V, 24 W lamp, under-run at 10 V o prolong its life. In the balanced condition the shutter vill allow the two cells to receive equal amounts of light, nd the voltage appearing at their anodes will be equal. ince photocells of the same type have slightly different haracteristics, the potentiometer VR_1 (balance control) can e adjusted to ensure that the condition of equal voltage xists.

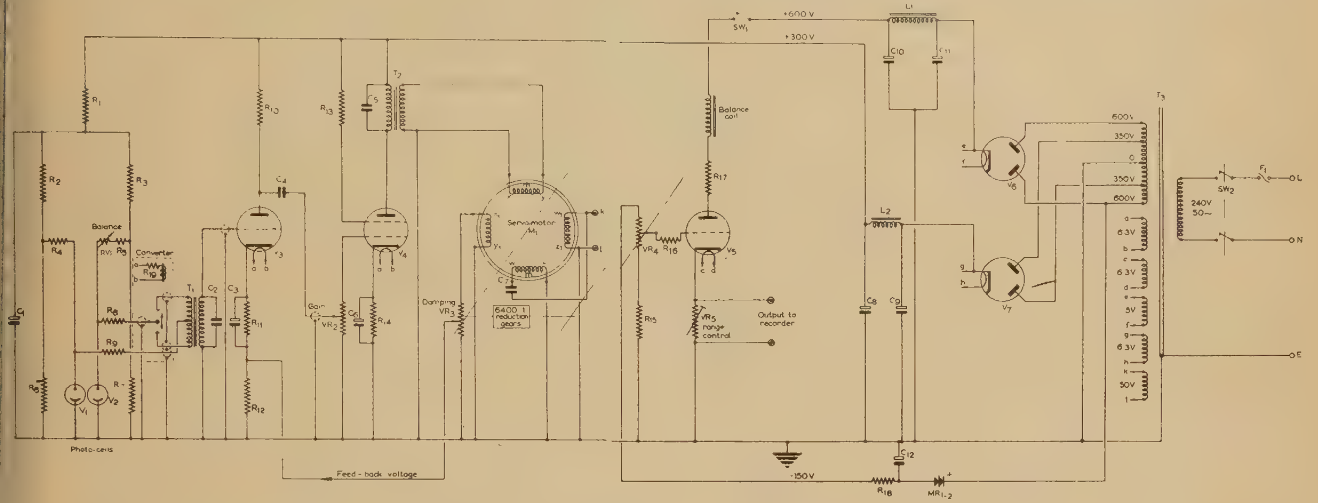

Fig. 2. Circuit diagram for recording balance

For an additional load on the platform of the weighing machine the steelyard will rise, allowing the shutter to interrupt completely the light beam to the photocell V_1, and to expose V_2 to full illumination; this causes a voltage difference to exist between the two anodes. Alternatively, a decreasing load on the platform will cause the free end of the steelyard to descend, allowing the shutter to interrupt completely the light beam falling on cell V_2 and to expose cell V_1 to full illumination. A voltage difference will again exist between the anodes of V_1 and V_2, but of opposite polarity to that in the previous condition.

Converter Unit. Any voltage difference that exists between the anodes of V_1 and V_2 is transformed from a direct to an alternating potential by the converter. This is an electro-mechanical device, in which a reed is made to vibrate by the combined fields of a permanent magnet and a coil energized at 50 c/s. When the coil is energized, the tip of the reed is magnetized alternately north and south at the 50 c/s frequency, and therefore oscillates at this frequency between the poles of the permanent magnet. By this oscillation, the reed alternately connects the anode of V_2, through resistance R_8, to the ends of the primary winding of transformer T_1. The centre tapping of this primary winding is connected, through resistance R_9, to the anode of V_1. Thus, when an out-of-balance condition exists, an alternating potential is applied to the primary winding of T_1, the instantaneous polarity of the potential depending on the sense of the out-of-balance condition.

The amplifier. Valves V_3 and V_4 form a conventional R.C. coupled amplifier. The input signal is developed across the secondary winding of T_1 and applied to the control grid of V_3.

Capacitor C_2 is connected across the secondary winding to form a tuned circuit capable of accepting the frequency of 50 c/s. This ensures the maximum signal transfer from the converter through the transformer. From the anode of V_3 the amplified signal passes through a gain control circuit VR_2 to the control grid of the power amplifier valve V_4. The primary winding T_2 is connected into the anode circuit of V_4 and the final amplified signal appears across the secondary winding.

Servo-motor. The servo-motor M_1, incorporates a tacho-generator. The supply voltage is fed direct to the generator winding w_1z_1 and through the 90° phase-changing capacitor C_7 to the motor winding $w\,z$, the phase of this voltage being such that the motor is caused to rotate in the appropriate direction when the voltage developed across the secondary winding of T_2 is applied to the winding $x\,y$. The generator output from the winding x_1y_1 provides a feedback voltage proportional to the speed of rotation of the motor. This limits the rate of change of the magnetic restoring force to the steelyard, hence excessive hunting is avoided.

Balancing system. A mechanical linkage (Fig. 3), achieved by means of 6400 : 1 reduction gearing, connects the shaft M_1 to the wiper of potentiometer VR_4. The angular rotation of the wiper of VR_4 is limited by a mechanical stop to ensure that the wiper does not exceed the limits of the resistance card, and cause the control grid of V_5 to become open circuited. A frictional clutch between the gear train and the spindle of the wiper prevents mechanical damage should any failure of the electronic system occur.

The high reduction gear ratio enables the potential of the control grid to change slowly and prevents a rapid change of the current flowing through V_5 and the balancing coil. The response time is approximately 10 s for a 1 lb change in weight on the platform of the weighing machine.

Performance

Fig. 4 shows a typical calibration obtained with the recording weight meter, and it will be seen that it is completely linear over its full range. The drift observed over substantially constant-temperature periods of 24 h continuous operation for different ranges of weights from 0 to 55 lb placed on the platform was ±0·5% of the full-scale deflexion as measured on the recording instrument. The full-scale deflexion was initially adjusted for each test operation to cover the particular range of weight used. Similar series of tests, carried out to investigate the effect of ambient temperature change on the calibration, indicated that, for a fixed preset adjustment and a temperature rise of 50° F, the weight represented by full-scale deflexion was reduced by 0·5%, i.e. 0·01% per ° F. For example, with the weight meter adjusted at 50° F to indicate 10 lb at full-scale deflexion, this deflexion represented only 9·96 lb at 90° F, with the random drift of ±0·05 lb superimposed. However, if substantial changes of ambient temperature should occur, the interpretation of the recorder chart can be adjusted accordingly, leaving only the random drift of ±0·5% as the remaining error.

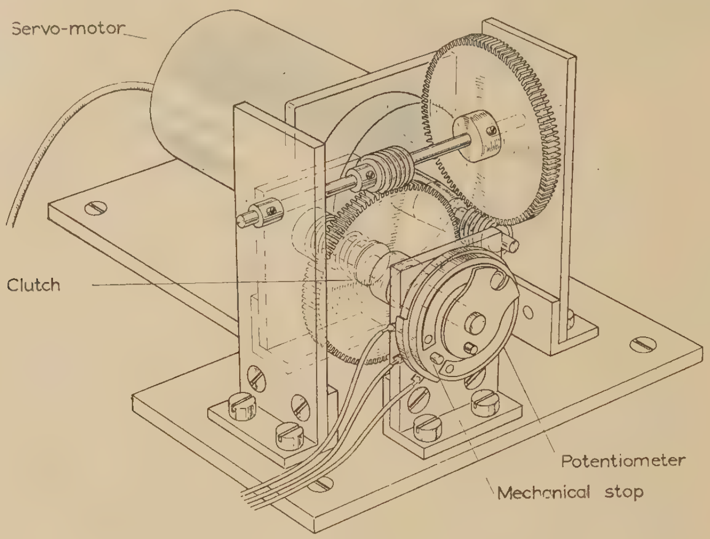

Fig. 3. Servo-unit and reduction gearing

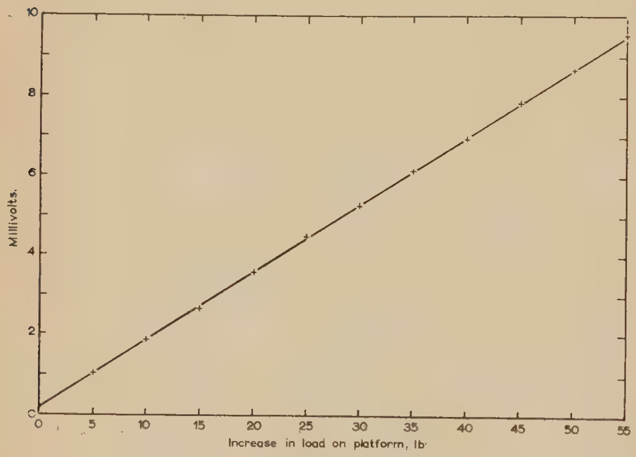

Fig. 4. Typical calibration curve obtained with recording weight meter

Setting-up procedure

An empty heating appliance is placed on the platform of the weighing machine. Switch SW_1 (Fig. 2) is switched off, to ensure that the balancing coil is de-energized. Th balance control VR_1 is adjusted so that the anode voltage V_2, when this cell is fully illuminated, is the same as th anode voltage of V_1 when this cell, in turn, is fully illuminate The damping control VR_3 is turned to the minimum positio and the gain control VR_2 to the maximum position. Th adjustable weight on the steelyard is moved until the steelyar just rises when released from its lower stop. Gain contro VR_2 is now adjusted until the servo-motor starts rotating when the steelyard is moved out of its balanced position Switch SW_1 is switched on, and VR_3 adjusted until th excessive hunting of the steelyard is damped. With th appropriate weights added to the platform, VR_5 is adjuste until a full-scale reading on the recorder is obtained for th maximum range of weight that it is required to measure.

Conclusions

The new recording weight meter has proved to be a reliabl and satisfactory method of measuring burning rates. It is semi-portable, automatic and quickly adjusted for operation the calibration of millivoltage output against weight change on the platform is linear over the full range.

Under the conditions for which it was developed, the weight meter would be required to weigh a solid fuel appliance of approximately 150 lb with a possible variation of weight of 10 lb. This is well within the range of the instrument, since, as previously stated, weight changes of up to 55 lb in a maximum load of 560 lb can be recorded. The burning rate can be measured to an accuracy of ±0·5% and this was found to be quite satisfactory, as it is within the accuracy of associated heat-measuring devices, such as thermocouples, radiometers, etc.

Acknowledgements

The paper is published by permission of the Director General, British Coal Utilisation Research Association.

An electronic fluxmeter

by R. R. BIRSS, B.Sc., Ph.D., A.Inst.P., and J. P. FRY, B.Sc.(Eng.), Imperial College, London

[*Paper first received* 28 *July, and in final form* 1 *September*, 1959]

Abstract

An instrument is described which possesses a number of advantages over a conventional fluxmeter. It has four operating ranges and may be used with a search coil of high resistance. Provision is made for self-calibration of both the sensitivity and the linearity of the instrument. The fluxmeter is suitable for operation by a non-scientist.

Introduction

A CONVENTIONAL fluxmeter exhibits a number of disadvantages. It is easily disturbed by mechanical vibration and, because of damping in the instrument, accurate measurements can only be made when it is used in conjunction with a search coil of low resistance. As the conventional fluxmeter has a low input impedance, alternative operating ranges can only be provided with difficulty and, in any event, need individual calibration. The electronic fluxmeter described below has none of these disadvantages. It is more robust than a conventional fluxmeter and, having four operating ranges, is more flexible: it is, however, more expensive. The instrument described is not as sensitive as a conventional fluxmeter when used with a search coil of low resistance, but greater sensitivity can be achieved by increasing the number of turns on the search coil. Since the sensitivity of the electronic instrument is limited by drift, which is reduced by using a high-resistance search coil, a further advantage is gained by using a search coil with an increased number of turns. An electronic fluxmeter is particularly useful for remote control operation.

Detailed description

The electronic fluxmeter is designed to measure the integrated current in a search-coil circuit. It is a multi-range instrument, and provision is made for self-calibration. A centre-zero voltmeter displays the flux measurement. The instrument is based on a Miller integrating circuit and its characteristics can be predicted by the usual methods.(1,2) Flux measurements may be made to a relative accuracy of better than $\pm 0\cdot5\%$ on the "×1" range, but with decreasing accuracy on the lower ranges. The response of the instrument is linear with flux change provided the change is completed within three seconds.

The d.c. amplifier consists of an input differential amplifier, a voltage amplifier and a cathode-follower output stage, coupled together by suitable interstage networks.

The input differential amplifier is required to compensate for drifts resulting from variations in cathode emission produced by heater-current variations, and also because it provides an output voltage without a reversal of sign referred to the input voltage. The anode currents of the two valves are approximately equal and opposite and hence cathode bias can be used without any corresponding loss in gain through degeneration. To make the output of the differential amplifier closely proportional to the difference between the two input grid voltages, a high-μ valve V_1 and large cathode resistor R_8 are used. The latter can be employed because a large negative voltage (-300 V) is used for the cathode return potential. As any grid current flowing in the input circuit produces integration errors, the operating point is chosen to correspond to zero grid-current conditions. A cathode resistor R_8 of approximately 357 kΩ is found to provide the required cathode bias with equal anode loads R_6, R_7 of 150 kΩ (each shunted by approximately 2·7 MΩ comprising the interstage network). A potentiometer RV_2 providing a further 3 kΩ in series with the cathode resistor is required to compensate for small drifts, thus ensuring that the valve works under zero grid-current conditions. With the component values given and with the grid of V_{1b} taken to earth through a 100 Ω resistor R_5, the stage gain is approximately fourteen times.

A pentode, type EF91 (by Mullard Ltd.), operating as a class A amplifier, is used as the voltage amplifier V_2. The EF91 operates at a reduced screen-grid voltage (100 V) in order to achieve higher gain and to decrease screen-grid regeneration. With an anode load R_{14} of 50 kΩ and a positive h.t. voltage of 300 V, the total anode swing is from $+26$ V to $+300$ V and is linear over the range from $+50$ V to 250 V with respect to changes in control grid voltage. The operating point is at 150 V, allowing a linear voltage swing of ± 100 V. (Since half the gain is lost in the following interstage network, this corresponds to a variation of ± 50 V at the control grid of the cathode-follower output valve V_3, so that the "×1" or "50—0—50 V" range is linear.) The stage gain is 300 times.

The cathode-follower stage is required to provide a low-impedance output to drive the meter circuit. Furthermore, it enables the output voltage to be zero with respect to earth when the amplifier is balanced, and hence minimizes the leakage current in the integrating capacitance C_1. The -300 V line is again used as the cathode return so that the control grid can follow large positive or negative voltages. Another EF91 is used in this stage, but it is connected as a triode because of a temporary unavailability of suitable single triodes.

The interstage networks are required to provide the correct d.c. reference level at the grid of the succeeding stage. The values of resistors used in the interstage networks are large compared with the anode load resistors to which they are connected, in order to minimize the loss in stage gain caused by their shunting effect.

A 0·01 μF capacitor C_6 is connected between the anode and grid of V_3 to prevent oscillation in the d.c. amplifier. A

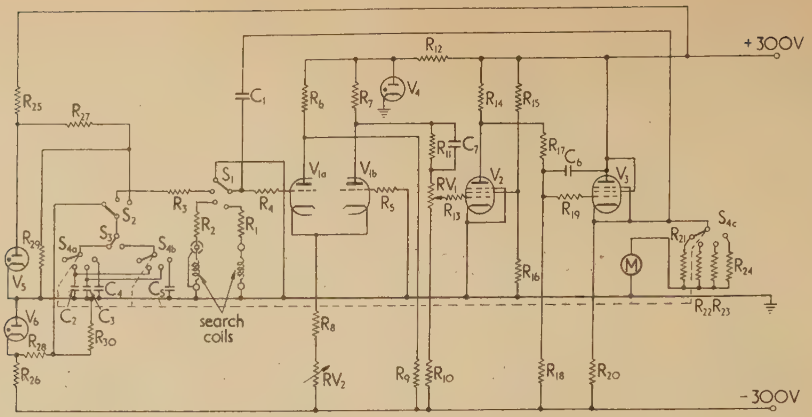

Fig. 1. Circuit diagram of the electronic fluxmeter

(All resistors are 0·75 W, high-stability type unless otherwise stated.)

R_1 = 1 MΩ
R_2 = 1 MΩ
R_3 = 1 MΩ
R_4 = 100 Ω composition
R_5 = 100 Ω composition
R_6 = 150 kΩ
R_7 = 150 kΩ
R_8 = 357 kΩ
R_9 = 2·7 MΩ
R_{10} = 2·2 MΩ
R_{11} = 500 kΩ
R_{12} = 15 kΩ (6 W)
R_{13} = 100 Ω composition
R_{14} = 50 kΩ (5 W)
R_{15} = 18 kΩ (5 W)

R_{16} = 10 kΩ (3 W)
R_{17} = 1·0 MΩ
R_{18} = 2·0 MΩ
R_{19} = 100 Ω composition
R_{20} = 100 kΩ (3 W)
R_{21} = 1 MΩ
R_{22} = meter series resistor, 50 V
R_{23} = meter series resistor, 5 V
R_{24} = meter series resistor, 0·5 V
R_{25} = 33 kΩ (3 W)
R_{26} = 33 kΩ (3 W)
R_{27} = 1 MΩ
R_{28} = 1 MΩ
R_{29} = 1 MΩ
R_{30} = 1 MΩ

RV_1 = 20 kΩ linear
RV_2 = 3 kΩ linear

C_1 = 0·1 μF Plastapack
C_2 = 0·1 μF Plastapack
C_3 = 0·01 μF paper
C_4 = 1000 pF silvered mica
C_5 = 100 pF ceramic
C_6 = 0·1 μF paper
C_7 = 47 pF ceramic

V_1 = 12AT7
V_2 = EF91
V_3 = EF91

V_4 = 150C2
V_5 = 85A2
V_6 = 85A2

S_1 = single-pole four-way (make before break)
S_2 = single-pole three-way (break before make)
S_3 = single-pole two-way (make before break)
S_4 = three-pole four-way (make before break)

M = 500 — 0 — 500 μA meter

47 pF capacitor C_7 is connected across R_{11} to compensate for the phase lag caused by the interstage coupling network R_{10}, R_{11} and RV_1.

A centre-zero meter M is connected between the cathode of the output-stage and earth, and reads zero when the amplifier is balanced. A 20 kΩ potentiometer RV_1 in the interstage coupling network between V_1 and V_2 allows the amplifier to be balanced. The four ranges of the meter (provided by switching between series resistors) are arranged in decade steps: full-scale deflexion on the most sensitive, the "×0·01", range is ±500 mV or approximately 5 × 10^6 maxwell turns; the "×10" range is provided only to prevent sudden overloading of the meter when the instrument is first switched on.

The usual precautions are taken to minimize circuit drift. Most of the resistors are of the high-stability type, and any dissipating appreciable energy are mounted on top of the chassis for better cooling. The capacitors C_1 and C_2 are of the special, low-loss "Plastapack" type (by Telegraph Condenser Co.). The valves are widely spaced and adequate ventilation is provided. The heater leads are wound tightly together and kept away from any other leads: all input grid leads are screened to minimize mains hum modulation. A 100 Ω resistor connected directly to the control grid pin of each valve base is included to prevent parasitic oscillation. A common earth line connected to the chassis at only one point is used to prevent circulating earth currents.

Operation

The general method of operation of the instrument for measuring changes in flux is sufficiently obvious to require no explanation, but the self-calibration procedure is of some interest. When the input grid is without a d.c. connection to earth, a calibrating capacitor (C_2 to C_5) at ±42·5 V can be discharged through a 1 MΩ resistor (R_3) into the input circuit. The final cathode will register a voltage change proportional to the charge injected, which can readily be calculated, thus providing a calibration for the instrument. Two calibrating capacitors can be selected for each range. One provides for approximately full-scale (coarse) calibration, the other for incremental (fine) calibration. As the calibrating charges are approximately in the ratio 10 : 1, the fine calibration can be repeated and the meter deflexion will be cumulative. By this means, the linearity of the instrument can be checked over the whole of its working range. The two appropriate calibrating capacitors are automatically selected by the meter-range switch S_4 so that accidental overloading of the meter is avoided. The positive and negative reference voltages are supplied by two neon stabilizer tubes, V_5, V_6 (type 85A2, by Mullard Ltd.), via potential dividers.

The switch S_1 selects the connections to the input, including those associated with the injection of charge from the calibrating capacitors. Two search-coil inputs are provided: screw terminals (by Belling-Lee) for normal use, and a co-axial socket for use with screened cable. The switch S_2 enables the calibrating capacitors to be charged to either a positive or negative reference voltage (35 V) and also allows the injection of charge into the input. Switch S_3 selects the coarse or fine calibration charge. Switch S_4 is the meter-range switch and also the selector of the two appropriate calibrating capacitors. The circuit, and particularly the various switches, are so arranged that the instrument can readily be operated by an unskilled person using a short series of simple operating instructions.

References

(1) Lewis, I. A. D. *Electronic Eng.*, **22**, p. 66 (1950).

(2) Korn, G. A., and Korn, T. M. *Electronic Analog. Computors*, 2nd ed., p. 169 (New York: McGraw-Hill Book Co., Inc., 1952).

Densitometer wedge for measurements at low optical densities

by N. R. SILVESTER, B.Sc., Wheatstone Physics Laboratory, King's College, London, W.C.2

[Paper first received 1 July, and in final form 1 September, 1959]

Abstract

For the quantitative evaluation of electron micrographs a continuous wedge has been simply made in which, over the range 0 *to* 1·0, *the optical density varies exponentially along its length within an accuracy of* $\pm 5\%$. *Its construction and method of use are described. An application is indicated in measurements of the mass of electron-microscope specimens and similar uses in contact microradiography and microspectrophotometry are suggested.*

In order to make quantitative deductions about image intensity from optical density measurements on electron micrographs, it has been found convenient to use low exposures and to work with that portion of the H–D curve of the photographic plate in which the density is directly proportional to exposure. The well-known advantages of this method are that the linear part of the density/exposure characteristic is inherently more sensitive to changes in exposure than the logarithmic, "gamma", part of the curve, and at the same time (for relative measurements) requires less careful standardization of the processing of the plate. The particular advantages of low exposures when used in electron microscopy are that: (i) low values of electron-beam current are employed so that contamination and disruption of the specimen are minimized; (ii) long exposure times are unnecessary, thus reducing the chance that instability in the lens currents, etc., will affect the image.

To measure optical densities of micrographs taken under the above conditions, a recording double-beam microdensitometer was used(1) in which a grey optical wedge is moved automatically across the reference light beam until the transmitted intensity is equal to that transmitted by the micrograph, which is in a similar beam. The movement of the wedge is recorded by a pen which is coupled directly to it. In normal use a wedge is employed in which the optical density D varies linearly along its length, so that at balance point in the densitometer

$$D_m - D_w + d = kx + d \qquad (1)$$

where suffixes m and w refer to the micrograph and wedge respectively, d and k are constants and x is the displacement of the pen. By adjustment of the relative intensities of the measuring beams, d can be made equal to the background density d_B of the micrograph. For micrographs where the density above background is proportional to the intensity I of the electron beam at the image plane of the electron microscope, it follows that

$$kx = D_m - d_B = gI \qquad (2)$$

where g is a constant characteristic of the photographic plate, and the pen displacement is proportional to the image intensity. In the electron microscope it has been shown(2) that $I = I_0 \exp(-Sw)$, where I_0 and S are constants and w is the mass-thickness of the specimen, and thus to find w using a linear wedge requires the calculation of $\ln(x_0/x)$, if x_0 is the pen displacement corresponding to I_0. To determine the mass of the specimen it is necessary to integrate w over its projected area in the micrograph, which involves considerable labour.

To facilitate the integration a wedge has been made in which the density varies exponentially along its length, i.e.

$$D_e = a \exp(bx) - d'$$

where a, b, and d' are constants. (3)

This was done by contact exposure of an ordinary plate of suitable size through a linear grey wedge. The intensity E of light transmitted by the linear wedge at a distance x along it is given by

$$D_w \propto \ln(1/E) \propto x \qquad (4)$$

thus

$$E \propto \exp(-bx) \qquad (5)$$

and if the plate is exposed at the part of its characteristic curve where the relation between density and exposure is approximately a linear one, i.e. in the under-exposure period,(3,4) one obtains

$$D_e + \text{const} \propto E \propto \exp(-bx) \qquad (6)$$

or

$$D_e = a \exp(bx) - d' \qquad (7)$$

on re-defining the direction of measurement of x, where d' is constant.

The plate used was an Ilford Special Lantern (contrasty) plate of size 10 by 2 in. A 20 cm linear grey wedge (density 0 to 1) was laid on it and the whole exposed from above to light from a 60 W "opal" bulb at a distance of $2\frac{1}{2}$ m for about 2 s. The plate was developed for $1\frac{1}{2}$ min in Ilford PQX2 developer at 70° F and fixed in the usual way. A densitometer trace of the wedge thus made is shown in the figure. The noise on the trace seems reasonable since the densitometer scanning aperture was about 1 mm in diameter, whereas the wedge density, on use in the densitometer, is averaged over the whole width of wedge (i.e. about 12 mm). Over the range from 1 to 19 cm a graph of log D_e against x was linear; the greatest deviations of log D_e from the straight line occurred over the last centimetre at each end of the range and were of the order of 0·02, corresponding to errors in D of about 5%. The details given here are typical of several wedges which were made in this way.

The plates produced as described above were thus the required "exponential" density wedges. On using one in the densitometer with a micrograph of density D_m, the relation holds that

$$D_m = D_e + d = a \exp(bx) + (d - d') \qquad (8)$$

where the constant d depends on the relative intensities of the densitometer beams. The constant $(d - d')$ is made equal to the background density d_B of the micrograph in the following way. From an experimental determination of a and b, a fiduciary position x_f can be found at which the x-dependent term in the density of the exponential wedge is equal to the density D_f of a given grey optical filter. The filter is inserted in the measuring beam of the densitometer together with a portion of the background of the micrograph, and the intensity of the reference beam is adjusted until the position of the pen at balance corresponds to the value x_f. In this way it is ensured that

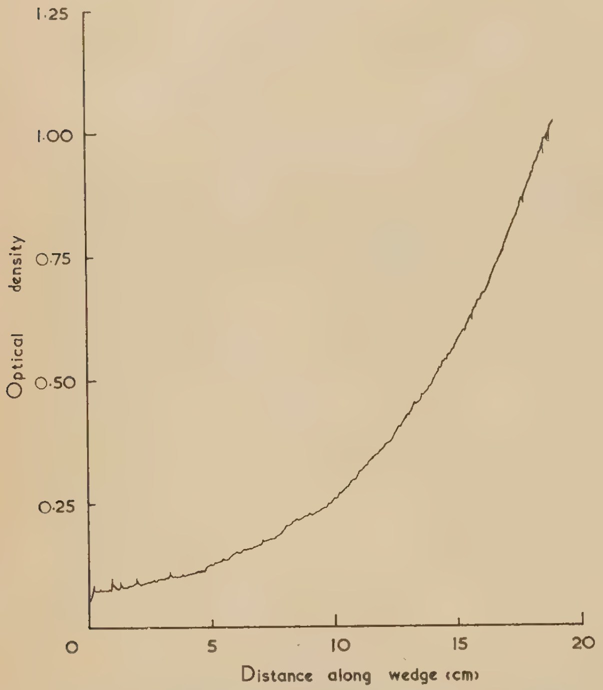

A microdensitometer trace from the "exponential" wedge described in the text.

$$D_f + d_B = a \exp (bx_f) + (d - d') \qquad (9)$$

and

$$d - d' = d_B \qquad (10)$$

The exposed part of the micrograph is then moved into the beam and the filter removed. Under these conditions of measurement

$$D_m - d_B = gI = a \exp (bx) \qquad (11)$$

i.e.

$$x = \frac{1}{b}\left(\ln I + \ln \frac{g}{a}\right) \qquad (12)$$

and

$$(x_0 - x) = \frac{1}{b} \ln \left(\frac{I_0}{I}\right) = \frac{Sw}{b} \qquad (13)$$

The displacement of the densitometer pen is directly proportional to the mass-thickness of the specimen at any point, and on integrating $(x_0 - x)$ (simply by planimetering several densitometer traces across the micrograph) the mass of the specimen may be found.⁽⁵⁾

A very similar analysis to that given above would ho
if the wedge described were used in the evaluation of conta
microradiographs⁽⁶⁾ since under certain conditions th
optical density of the radiograph, as in electron microscop
is an exponential function of the mass-thickness of th
specimen.

Apart from the limited applications given above, a wedg
made in the way described may be of more general use i
light-optical work if the well-known principle is followed o
making it from the same type of plate as the ones on whic
measurements are to be made in the densitometer. If th
plates have an H–D curve such that $D = f(E)$ then o
exposing a plate through the linear wedge its density become

$$D_e = f(E) = f\{E_0 \exp (bx)\}$$

where E_0 and b are constants. (14

On balancing in the densitometer the wedge thus mad
against a plate with a similar characteristic curve and c
density D, one has

$$D_e = D$$

i.e. $$f\{E_0 \exp (bx)\} = f(E) \qquad (15$$

and if f is a monotonic increasing function of E

$$E_0 \exp (bx) = E \qquad (16$$

thus $$x \propto \ln E + \text{const} \qquad (17$$

for all values of E.

This affords a way of using a given photographic plate in th
transition region between the low-density and "gamma
parts of the H–D curve and effectively extends the range o
measurement of ln E from either region into the other. This
application may be of use in other fields, such as micro-
spectrophotometry⁽⁷⁾, where the quantitative determinatio
of log (exposure) is of interest.

Acknowledgements

The author would like to thank Prof. J. T. Randall fo
research facilities and to acknowledge the receipt of a maintenance award from the Department of Scientific and Industrial
Research.

References

(1) Walker, P. M. B. *Exp. Cell Res.*, **8**, p. 567 (1955).

(2) Hall, C. E. *J. Appl. Phys.*, **22**, p. 655 (1951).

(3) Hurter, F., and Driffield, V. C. *J. Soc. Chem. Ind.*, **9**, p. 455 (1890).

(4) Renwick, F. F. *Photogr. J.*, **53**, p. 127 (1913).

(5) Burge, R. E., and Silvester, N. R. *J. Biophys. Biochem. Cytol.* To be published.

(6) Engström, A., and Lindström, B. *General Cytochemical Methods* (Ed. J. F. Danielli), Vol. 1, p. 1 (New York: Academic Press Inc., 1958).

(7) Walker, P. M. B. *General Cytochemical Methods* (Ed. J. F. Danielli), Vol. 1, p. 163 (New York: Academic Press Inc., 1958).

High-temperature burner for working silica

by J. Conaboy, Royal Radar Establishment, Malvern, Worcs.

[*Note received* 14 *August* 1959]

The burner described here was developed primarily for silica working but could well be useful for other applications. In conventional methods of working silica, flames of propane-oxygen or hydrogen-oxygen are commonly used, but these have certain disadvantages. For example, the temperature after radiation loss is only just high enough to melt silica slowly, and the temperature falls with increase in size of the jet thus making the working of large silica difficult. When an attempt is made to overcome the latter defect by increasing the gas flow, the force of the flame tends to push in the wall of the silica tube and the flame is less efficient as heat is lost when the burning gases bounce off the work. It has been found possible to attain a higher temperature with a softer flame by combining both types of flame, hydrogen and oxy-propane, in one burner.

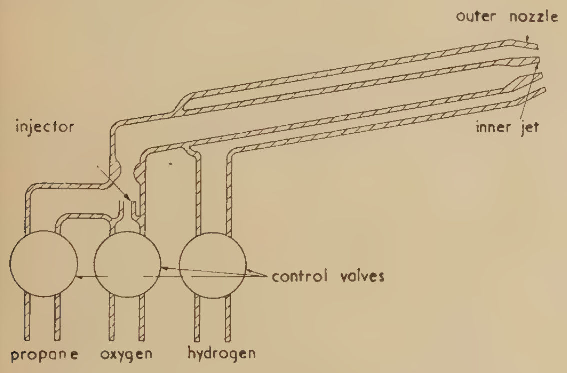

Schematic diagram of high-temperature burner

The burner head is a cylindrical outer nozzle with a concentric inner jet as shown in the diagram. The burner tips are made of stainless steel to withstand the high temperature, but otherwise the arrangement is similar to that in coal-gas/air/oxygen burners used for hard and soft glasses. If a large flame is required, a number of jets can be arranged around the circumference of the inner jet as necessary instead of the single annular jet shown in the diagram. Hydrogen is fed to the outer jet and a mixture of propane and oxygen to the inner; all the gases are controlled independently by needle valves.

In operation, the burner delivers a flame of pre-mixed oxygen and propane surrounded by a sheath of hydrogen burning in air. The layer of hydrogen next to the oxy-propane mixture burns with some of the oxygen from the mixture. Comparative tests were made with a disappearing-filament pyrometer fitted with an additional filter to extend the temperature range, and they showed that this burner gave average temperature increases of about 200° C over oxy-hydrogen flames and about 300° C over oxy-propane flames. Also, the temperature remained reasonably constant as the inner jet size was varied from 0·037 to 0·125 in. diameter, whereas both the other flames showed a falling off in temperature as the jet size was increased. It is thought that the increased temperature attained with this composite flame over the temperature reached with oxy-propane alone results from a more rapid break-up of the propane molecule inside the hot envelope of burning hydrogen.

Double-acting reversible message register

by C. J. Sumner, A.M.S.E. Commonwealth Scientific and Industrial Research Organizations, Division of Meteorological Physics, Victoria, Australia

[*Note received* 20 *July*, 1959]

This message register is an improvement on that described by Sumner.* Capable of adding and subtracting electrical impulses on a single four-wheel counter, it is, in addition, able to operate positively or negatively while the reverse solenoid remains energized. This important feature enables electrical impulses of long duration, encountered in some

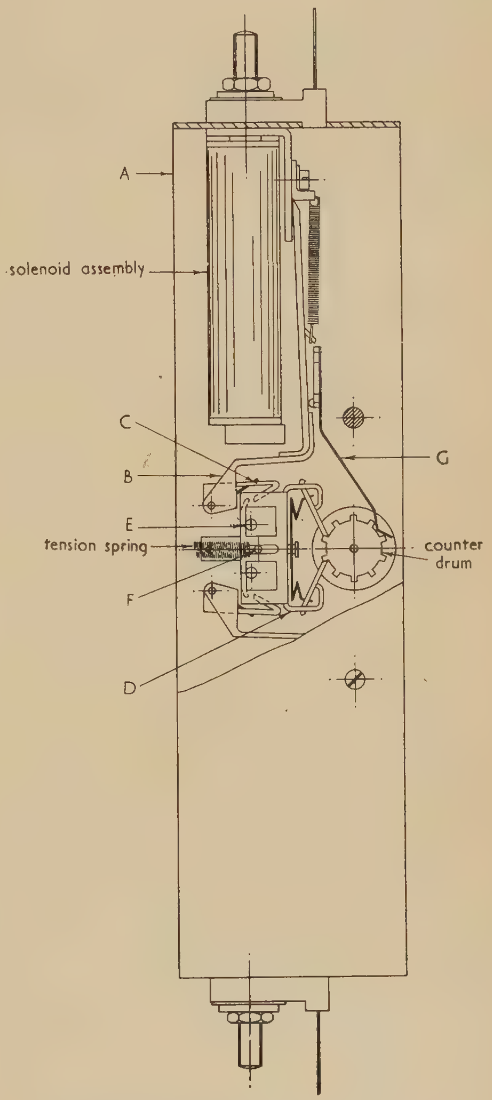

Fig. 1. Message-register assembly (cover cut away to show mechanism at rest)

differential switching mechanisms, to be directly recorded, without the need for preliminary pulse shaping.

---

* Sumner, C. J. *J. Sci. Instrum.*, **33**, p. 505 (1956).

The design includes two Post Office message registers (type 4055, by Standard Telephones and Cables Ltd). The two solenoids are mounted in opposite ends of a metal frame *A* (Fig. 1). Each armature carries an extension arm *B* on which is mounted a hinged, spring-loaded latch *C*, each of these latches being arranged to trip a rocking frame *D*. This frame is spring-loaded upwards, so that it bears on two hinge pins *E* and is centrally located by a pivot pin *F* operating in a central slot, in either side of the rocking frame. All three pins are mounted in the side plates of frame *A*. The rocking frame is constructed to carry the triggers and springs of the existing message register, one being bent the opposite way to give right- and left-hand operation. A detent spring *G* is provided to locate the counter wheels and allow them to rotate in either direction.

When the solenoids are at rest, the two-drum triggers are located on opposite sides of two adjacent projections on the primary counter-wheel sprocket, preventing the counter from being rotated in either direction (Fig. 1). When one solenoid is energized, the latch *C* causes the rocking frame *D* to rotate about the opposite hinge pin *E*, which moves the two-drum triggers so that, while one disengages from the sprocket wheel, the other advances the wheel one tooth (Fig. 2). As the armature reaches the limit of its travel the latch *C* disengages from the rocking frame *D* so that it springs back to its starting position (Fig. 3). The opposite solenoid can now operate to reverse the counter drum while the first solenoid remains energized. On the return movement of the solenoid armatures, the spring-loaded latches *C* reposition themselves above the rocking frame ready for the next impulse.

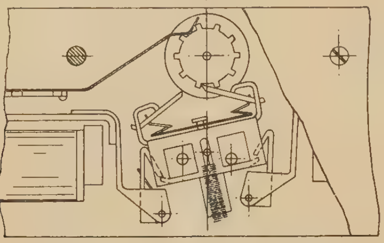

Fig. 2. Mechanism with one solenoid nearing end of movement

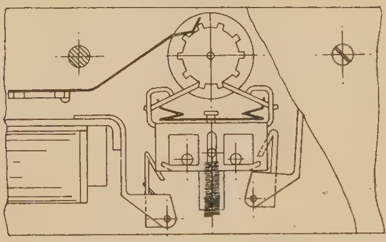

Fig. 3. Mechanism with one solenoid fully energized

Slow-feed dispenser for abrasive suspensions

by J. Lobb, Division of Metrology, National Standards Laboratory, Commonwealth Scientific and Industrial Research Organization, New South Wales, Australia

[*Note received* 13 *August*, 1959]

During the development of equipment for sharpening surgical needles by a lapping process, the problem arose of obtaining an apparatus that would feed a very small volum of a liquid containing an abrasive in suspension, witho frequent attention. The flow rate required was forty t sixty drops per minute, or approximately 50 ml/h.

All attempts to control the flow by means of a sma orifice resulted in frequent blockage of the orifice by abrasiv particles falling out of suspension. Experiments were mac with several types of orifices in an attempt to overcome th blockage, but none proved satisfactory.

In the apparatus described below, air pressure is used t lift the abrasive suspension from the lower portion of th container up a tube of relatively wide bore to the outle funnel. There being no small orifices or restrictions in th system, the flow continues without interruption and can b controlled by the air supply. As there are no bearing surface in contact with the abrasive mixture, this method is suitable for use with abrasives or slurries that would normally abrade the mating surfaces and so damage conventional mechanical devices.

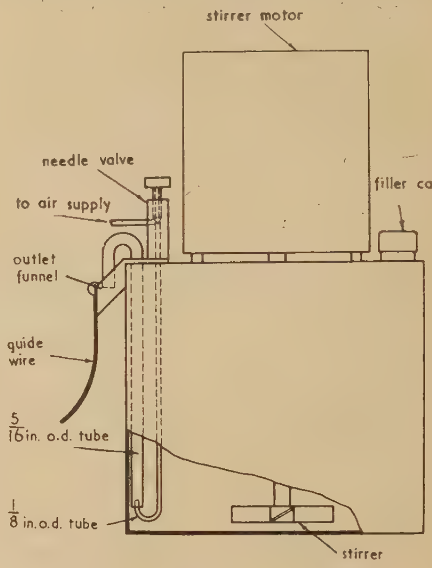

Part sectional view of apparatus

The small volume of air, at a pressure of approximately 5 lb./in.^{2}, necessary to operate the dispenser is supplied by an aquarium type aerator, comprising a simple diaphragm type pump operated by a 240 V a.c. supply. The air flow is regulated by means of a needle valve attached to the top of the abrasive container, as shown in the figure. Connected to the outlet of this valve and mounted on the top of the container is a tube of outside diameter $\frac{1}{8}$ in. and 26 s.w.g. wall thickness, which protrudes into the container and terminates in a U-shaped bend approximately $\frac{1}{2}$ in. above the container base. A second tube, similarly mounted, of outside diameter $\frac{5}{16}$ in. and 26 s.w.g. wall thickness, is positioned so that the short arm of the smaller diameter tube projects into its lower end for a distance of $\frac{3}{16}$ in. The upper end is curved to discharge into an outlet funnel attached to the outside of the container. Bubbles of air rising from the inner tube trap small quantities of the abrasive suspension, which are lifted up the larger diameter tube and delivered into the funnel. From here the abrasive suspension may be gravity fed by means of a channel, or flowed along the surface of a wire, to the desired location, such as the surface of a lap.

The container has a capacity of three litres. An electric motor, mounted on the top of the container, drives a stirrer which agitates the mixture to keep the abrasive particles in suspension.

The apparatus has been used successfully with several liquids of different viscosities carrying abrasive powders of various grades, the particle sizes ranging from 2 to 250 μ. Adjustment of the needle valve enabled steady flow rates from 1600 down to 12 ml/h to be obtained, the slowest flow corresponding to approximately twelve drops per minute.

Device for straining and fracturing thin foil specimens inside an electron microscope

by P. J. E. Forsyth, A.I.M., and R. N. Wilson, M.Met. A.I.M., Master of Metallurgy (Sheffield), Royal Aircraft Establishment, Farnborough, Hants.

[*Note first received* 6 *August, and in final form* 4 *September*, 1959]

The use of the thin foil technique for directly viewing dislocation movements in metals and alloys has opened up a new field of study of the general problem of plastic behaviour. Dislocations can be made to move in a random manner by the buckling produced in the foil by heating in the electron beam of the microscope. This buckling is indeterminate and uncontrollable, and it is obviously preferable that straining should be under the control of the operator. Moreover, fracture cannot be achieved by random buckling and some straining device is necessary.

Such a straining device should be capable of remote operation in a vacuum in the microscope stack. It should operate smoothly and should not interfere with the electron optical system. It is also essential that stereoscopic motion should be preserved in the microscope so as to develop dislocation contrast. In order to avoid modification to the stage itself, it was decided to make the "tensile machine" within the compass of the existing specimen holder. A simple method of producing controllable strain, which lends itself to vacuum use, is to make use of the distortion of a bimetal strip heated electrically *via* leads through the stack wall.

In order to minimize the lateral movement of the specimen it was decided to strain the foil by pulling from both ends, so that the point of zero lateral movement lies at the centre of the specimen.

Fig. 1 shows a cut-away view of the device. The body is made of phosphor-bronze with two bimetal strips lying in slots and attached by screws to the body at their root ends. The free ends are arranged to deflect away from one another as the temperature rises. The heater winding is 26 g manganin wire bifilar wound to a resistance of 30 Ω, the ends being terminated by soldering on to small tags. The bimetal strip is 0·45 mm thick, a common proprietary type consisting of two nickel-iron alloys of differing composition. The foil specimen is attached to the prongs with Durofix adhesive. The bimetal strips are stiff compared with the specimen, and any yielding in the specimen will not affect the spacing of the jaws, i.e. this device is effectively a hard beam tensile machine.

The behaviour of the tensile device is illustrated in Figs. 2 and 3. The rate of heating of the body of the device determines the rate of extension of the bimetal prongs. A

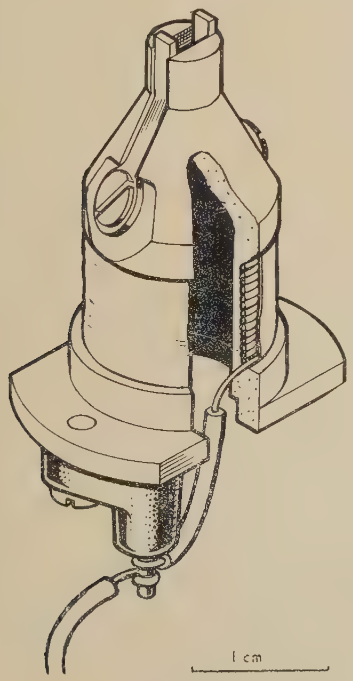

Fig. 1. Cut-away view of the micro-tensile device

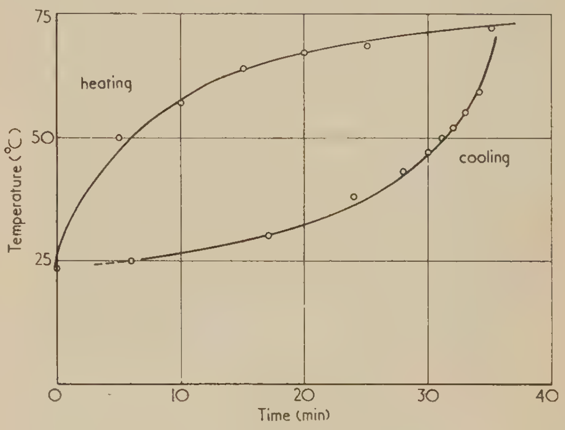

Fig. 2. Thermal response of the micro-tensile device in a vacuum. Heater current 300 mA

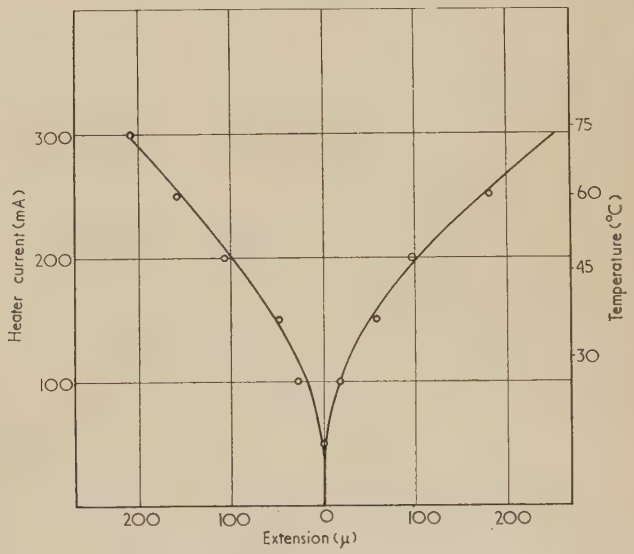

Fig. 3. Relation between heater current, body temperature and the extension of the bimetal jaws of the micro-tensile device

temperature-time curve for the device using a steady heater current of 300 mA is shown in Fig. 2. This illustrates the rapid response of the device and also the initial rapid rates of strain available if required.

The equilibrium relation between the heater current, body temperature and the extension of the prongs is shown in Fig. 3. The deflexions were measured microscopically at the tips of the prongs and these were plotted in opposition to represent total extension. It can be seen that, for a given field of view near the centre of a specimen, there is very little lateral drift because of the symmetrical behaviour of the two bimetal strips. The temperature was measured by a chromel-alumel thermocouple cemented to the body of the device and the calibration was done in a vacuum to simulate working conditions in the electron microscope.

The device has now been in use for some time in the type E.M.3.A. electron microscope, and has proved to be a simple and effective way of producing strain and fracture in thin foils. The strain can be maintained constant during a photographic exposure so that no deterioration of the photographic image is observed.

A typical micrograph obtained with the device is illustrated in Fig. 4. A foil specimen of annealed aluminium was prepared by electropolishing, and strained in the electron microscope. Slip steps due to the strain induced in the foil can be seen at *A*, and conjugate slip at *B* has produced a cross-hatching pattern. A band of heavy deformation can be seen ahead of the crack root at *C*, and also individual dislocations at *D*.

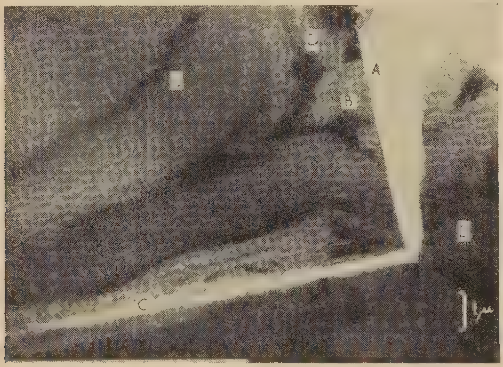

Fig. 4. Electron optical micrograph showing cracking of foil due to stressing in the micro-tensile device. (Super purity aluminium, vacuum annealed and thinned to foil.)

Note slip steps at *A*, cross-hatching due to conjugate slip at *B*, deformation band *C* and individual dislocations *D*.

Work is proceeding on a study of fracture which will be reported at greater length elsewhere. However, preliminary observations indicate that a ductile material, such as pure aluminium in the form of foil, necks down locally to a chisel edge and then fractures along a serrated path.

This note is published by permission of The Controller, H.M. Stationery Office. Crown copyright is reserved.

Improved form of spring-clip for holding down a work-piece

by P. W. Harrison, B.Sc.(Eng.), A.M.I.Mech.E., A.C.G.I., National Physical Laboratory, Teddington, Middlesex

[*Note received* 12 *August*, 1959]

The figure shows, on the left side, a clip sometimes used for holding down work-pieces. It consists of a spring-arm rigidly fixed to a block which slides freely on a shouldered column; the column fits loosely into a plain hole in the platen. When the arm is pressed down on to the work-piece it is held there by the cross-cornering of the block on the column and the column in the hole. Such a clip has the advantage that it can be used on surfaces at various heights above the platen, but has the disadvantage that it requires a force several times greater than that applied originally to release it. This may result in an undesirable disturbance of the work-piece and platen.

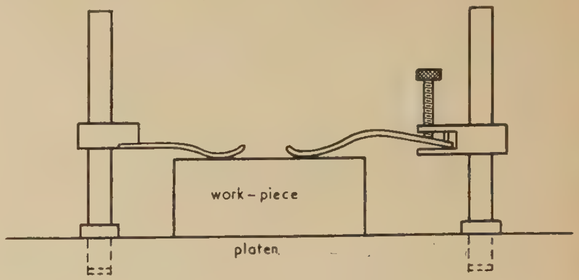

Spring clip for holding work-pieces

This difficulty is overcome in the design shown on the right of the figure which requires only a very light force to operate it both when applying and when removing the load. The spring-arm is pinned loosely in a slot in the block, but can be held against the lower face of the slot by a screw. In this condition it can be applied to the work-piece in the same manner as before. Alternatively, the block, with the screw retracted, can be moved down the column until light contact with the work-piece moves the arm to the position shown; load is then applied by advancing the screw, the clip becoming locked in position for the same reasons as before. To release the work-piece, the cross-cornering effects are readily removed by retracting the screw. Normally, only one hand is required to manipulate the clip.

This note is published by permission of the Director of the National Physical Laboratory.

Photoelectric refractometer

by C. W. Latey, B.Sc., Grad.Inst.P., National College of Food Technology, St. George's Avenue, Weybridge, Surrey

[*Note first received* 29 *May, and in final form* 30 *September*, 1959]

For certain solutions concentration of dissolved solids is indicated by refractive index, which may conveniently be monitored when the solution undergoes processing. This note describes how an air cell type of refractometer employing simple components may be combined with a photo-electric detector to indicate changes of refractive index in such cases.

The liquid flows through a vessel (*A* in the accompanying diagram) fitted with plane glass ends, and a pair of parallel glass plates *B*, cemented together and enclosing an air film, may be rotated within the liquid. Light from a sodium vapour lamp *S* passes through the vessel and its contents, and is incident finally upon the surface of a screened selenium photovoltaic cell placed in the focal plane of the convex lens *C*. The photocell is 25 mm in diameter and is divided vertically down the centre to form two cells with a common base, and the separate contacts of the two cells are connected to a taut suspension galvanometer of sensitivity 18 mm/μA. A differential refractometer employing such a photocell has been described before in this journal.*

If the air cell is rotated within the liquid under test a shadow will cross the surface of the photocell due to critical angle reflexion within the air cell. A current will then flow due to unequal intensity of illumination on the two halves of the photocell, and will rise to a maximum value when the border line of the shadow coincides with the line of division on the face of the photocell. The position of the air cell for extinction of the light over half the field of view is thus indicated by maximum current.

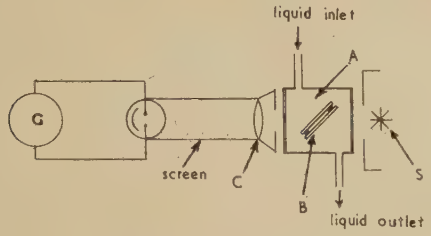

Photoelectric refractometer

In the experimental investigation of the method the refractive index of a sucrose solution flowing through the vessel was altered in successive steps within the range 1·34 to 1·40 and at each stage the new air cell setting for maximum current was determined. Angular deviations from the original setting of the air cell were found to indicate change of refractive index, but the least change of refractive index that could be detected was about 0·003 as shown by check measurements using an Abbé refractometer. This limitation (representing about 2% in terms of solids concentration of sucrose solution) appeared to be due to an uncertainty in finding the precise air cell setting for maximum current.

By this method changes of refractive index may be readily detected without setting cross-wires on a border line. Small long-period variations in light intensity and changes in photocell characteristics do not affect the results obtained.

My thanks are due to Mr. R. Wertheim for suggesting the problem and helpful discussions, and to Mr. F. G. Taylor for his assistance in the construction of the apparatus.

* Seiflow, G. H. F. *J. Sci. Instrum.*, **30**, p. 407 (1953).

Simple technique for recording variations of a few centimetres in galvanometer reading

by R. G. Ackland, B.Sc., A.Inst.P., Australian Defence Scientific Service, Defence Standards Laboratories, Department of Supply, Maribyrnong, Victoria, Australia

[*Note first received* 14 *July, and in final form* 22 *September*, 1959]

Simple galvanometer relays or amplifiers, using a differentially connected, barrier-layer type photocell arrangement, are often used to obtain high sensitivity in null-point detection, or, with negative feedback, good linearity as well as high deflexion sensitivity.(1,2,3) They are often more suitable than a sensitive d.c. amplifier of more conventional type when the very small signal arises from a source of low impedance, matching that of a galvanometer.

Sometimes, however, it may be required to observe and record variations of a few centimetres in a much larger deflexion of a light-spot, without regard to the nature of the signal or of the instrument, the deflexion of which is a measure of the signal. Of several ways in which this could be done, it has still been found very convenient and effective to use a differential photocell, but with the line dividing the two halves at an angle to the direction of excursion of the spot instead of perpendicular to it.

For example, a selenium cell of dimensions 50 × 30 mm, bisected approximately diagonally and used with a light spot masked to about 5 mm wide by 25 mm high, can provide a differential photocell output for excursions of more than ±2 cm. Obviously, larger excursions could be accommodated by using larger photocell units, and the sensitivity and linearity of response may be adjusted to some extent by varying the slope and shape of the dividing line between the two halves.

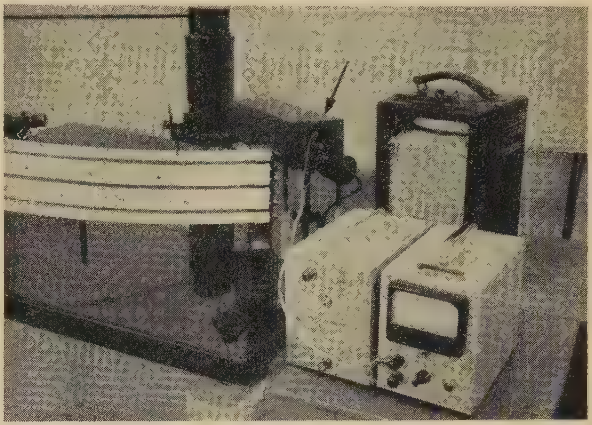

Showing diagonally cut photocell (arrow) mounted in its light hood

If the output of this photocell unit is fed to a suitable d.c. amplifier (by Pye for example), connected to a recording milliammeter, chart records of the changes in galvanometer reading can be obtained. In this way, variations of the order of ±0·1 to ±0·5% in the r.m.s. output of a line-voltage stabilizer, using a Cambridge reflecting dynamometer voltmeter, have been recorded. In this instance, it was possible to mount the photocell unit, in its hood, clear of one end of the voltmeter scale, and, by appropriate use of two lamp units, to observe visually what the photocell unit was recording. To facilitate alinement of the unit, provision was made for mounting a suitably marked-off ground-glass screen in place of the photocell.

This note is published with the permission of the Chief Scientist, Australian Defence Scientific Service, Department of Supply, Melbourne, Australia.

REFERENCES

(1) Hill, A. V. *J. Sci. Instrum.*, **8**, p. 262 (1931).
(2) Moss, E. B. *J. Sci. Instrum.*, **12**, p. 141 (1935).
(3) Preston, J. S. *J. Sci. Instrum.*, **23**, p. 173 (1946).

New instruments, materials and tools

The Editor invites manufacturers of instruments and light machine tools to keep him informed of their new or improved products. The Institute of Physics assumes no responsibility for the statements given below: information for these has been taken from literature supplied.

Production of deionized water. Elga Products Ltd., Railway Place, London, S.W.19.

Improvements have been made to an existing instrument manufactured by this firm for producing deionized water. It is stated that: (*a*) all exposed components are now made from corrosion-resistant plastic material, so that the unit may now be used in corrosive atmospheres; (*b*) "equilibrium" water (4 MΩ/cm^3) may now be drawn at the rate of up to 45 l./h; and distilled quality water (500 000 Ω/cm^3) can be drawn at the rate of 90 l./h.

Two versions of the modified instrument are available; one where the requirements are for commercial-grade distilled water, chiefly, and a capacity and exhaustion indicator is incorporated; and the other for critical applications, where a conductivity monitor forms an integral part of the unit and gives an accurate quality check throughout the exhaustion cycle. A standard modification makes it possible to pipe the water to any number of draw-off points.

Recording X-ray diffractometer and fluorescence spectrometer. Hilger and Watts Ltd., 98 St. Pancras Way, London, N.W.1.

The recording X-ray diffractometer records diffraction patterns direct on a pen recorder, and may be used with a sealed X-ray tube or with the Hilger microfocus generator. It scans in the horizontal plane up to an angle of 160° of 2θ with a choice of six scanning speeds; scanning may also be performed in small discrete steps. A second detector is used in a monitoring system to prevent variations in the intensity of the incident beam from affecting the accuracy of the measurements.

The fluorescence attachment converts the diffractometer into a fluorescence spectrometer which will analyse solid, liquid or powder samples. The X-ray tube in the spectrometer irradiates the sample with an intense beam of X-rays and causes it to emit secondary radiation or "fluorescence" which is characteristic of the elements in the sample. The radiation from the sample is collimated by Soller slits and directed on a crystal, which splits up the beam into its constituent wavelengths. A scintillation counter used as a detector may be set in any chosen position of the spectrum, to determine a single element; or it can scan the whole spectrum, to record each element in turn.

The spectrometer will determine titanium—atomic number 22—and all heavier elements; by using a helium or vacuum path, its range can be extended to magnesium. X-ray fluorescence spectrometry is a valuable complement to ultra-violet spectrography; it is often more accurate for determining major constituents in an alloy, is non-destructive and examines a sufficiently large area of the sample for the effects of sample heterogeneity to be minimized. Its sensitivity is high, though rather lower than that of ultra-violet spectrography. For routine analyses the most suitable range of concentrations is from 0·1% upwards.

Circuit magnification meter. Marconi Instruments Ltd., St. Albans, Herts.

The type TF 1245 Q-meter covers the large frequency range 1 kc/s to 300 Mc/s. It contains no internal oscillators, but there are two specially designed oscillator units TF 1246 and TF 1247, covering the frequency ranges 40 kc/s to 50 Mc/s and 20 to 300 Mc/s respectively. For frequencies below 40 kc/s, an ordinary l.f. oscillator may be used. Values of Q from 5 to 1000 can be measured directly, and the variable tuning capacitance is calibrated from 500 to 7·5 pF. Separate high- and low-frequency test circuits ensure optimum conditions throughout the whole frequency range. All Q values can be read on a triple range panel meter which is common to both test circuits. A centre zero range for measuring ΔQ is also provided for use in indirect measurements and in batch testing. A wide range of standard inductors and test jigs for dielectric and series loss measurements is available.

British Journal of Applied Physics

Contents of the January issue

PAPERS

Size distribution of airborne dust samples from British coalmines. By J. W. J. Fay and J. R. Ashford.

Some statistical aspects of dust counting. By J. R. Ashford.

CONFERENCE REPORT

Summarized proceedings of a conference on electron microscopy—Exeter, July 1959. By J. A. Chapman and M. J. Whelan.

PAPERS (continued)

Temperatures, thermal stresses and displacements in solid uranium dioxide rods. By J. P. Ellington.

Sensitive method for measurement of magneto-resistance effect with direct currents and with microwaves. By D. E. Clark and J. G. Assenheim.

Change of size of air bubbles in water containing a small dissolved air content. By D. M. J. P. Manley.

Variation with particle size of the effective X-ray absorption coefficient of heterogeneous slabs. By G. B. Mitra and A. J. C. Wilson.

Rotational hysteresis loss in grain-oriented silicon-iron. By W. F. Archenhold, W. F. Sandham and J. E. Thompson.

Measurement of tinplate thickness using fluorescent X-rays excited by a radioactive source. By J. F. Cameron and J. R. Rhodes.

THIS *JOURNAL* is produced monthly by The Institute of Physics, with the co-operation of the National Physical Laboratory. It deals with the principles, construction and use of scientific instruments. All rights reserved. Responsibility for the statements contained herein attaches only to the writers.

EDITORIAL MATTER. Communications concerning editorial matter should be addressed to the Editor, The Institute of Physics, 47 Belgrave Square, London, S.W.1. (*Telephone:* Belgravia 6111.) Prospective authors are invited to prepare their scripts in accordance with the *Notes for Authors*. (Price 3*s*. 6*d*. including postage.)

REPRODUCTION. The Institute of Physics is a signatory to The Royal Society's Fair Copying Declaration. Details may be obtained upon application from The Royal Society, London, W.1.

ADVERTISEMENTS. Communications concerning advertisements should be addressed to the agents, Messrs. George Jackson (Fleet St.) Ltd., Cliffords Inn, Fleet Street, London, E.C.4. (*Telephone:* Holborn 3611–2.)

CLAIMS FOR MISSING JOURNALS. Claims from regular subscribers to this *Journal* for missing numbers will only be considered if received within 60 days of the date of mailing plus normal outward time of transit and time for lodging the claim. Losses attributable to failure to notify a change of address or to similar omissions will not be considered.

SUBSCRIPTION RATES. A new volume commences each January. The charge is £6 per volume ($17 U.S.A.), including index (post paid) payable in advance. Single parts, so far as available, may be purchased at 12*s*. 6*d*. each ($1.75 U.S.A.), post paid, cash with order. Orders should be sent to The Institute of Physics, 47 Belgrave Square, London, S.W.1, or to any bookseller.

PRINTED IN GREAT BRITAIN BY UNWIN BROTHERS LIMITED, WOKING AND LONDON

X-ray diffraction by single crystals at low temperatures: a cryostat for use with liquid hydrogen

By J. H. ROBERTSON, B.Sc., Ph.D., School of Chemistry, University of Leeds

[*Paper received* 16 *September*, 1959]

Abstract

Techniques for cooling a single crystal in X-ray work are discussed, and the merits of the continuous gas-stream method are noted. It is shown that hydrogen gas has properties which render it especially suitable for use in this way.

A simple modification of the usual method for generating the cold gas stream is described. The apparatus is capable of maintaining a crystal at a temperature of about 23° K (using hydrogen) for periods up to 48 h, without interference with the operation of standard diffraction techniques.

Introduction

X-RAY diffraction, especially from single-crystals, has yielded a very great wealth of knowledge of the nature of the solid state. By the use of temperatures other than room temperature the range of single crystal diffraction studies can be significantly extended. In particular, the employment of low temperatures offers two kinds of advantage: on the one hand, materials which ordinarily are liquid or gaseous can, by solidification, be made accessible to the single-crystal technique; on the other hand, any substance whose atoms show strong thermal motion at ordinary temperatures may be chilled so that thermal vibrations are reduced, and more precise measurements of electron density can be made. In the first category come such simple but interesting compounds as methyl alcohol (CH_3OH), nitric oxide (NO), acetylene (C_2H_2), oxygen (O_2), etc. The second includes nearly every substance on which it is desired to measure molecular parameters with the accuracy demanded by present-day requirements, as emphasized recently by Cruickshank.(1)

General principles

For cooling a crystal specimen and maintaining it at a low temperature during diffraction of X-rays, various procedures have been proposed, based on gas cooling, liquid cooling and conduction. These have been summarized recently by Steward,(2) whose primary concern, however, was with polycrystalline material. For single crystal work there are several special requirements: thus, the specimen should be quite isolated except for the minimum necessary support, and should be free to rotate; in photography, the film should be free to move also; apart from the cooling of the crystal itself there should be the minimum of cooling action, especially on moving parts of the apparatus. Thus, for work with single crystals, the choice of suitable methods for maintaining low temperatures is restricted, and it is natural that gas cooling has now become established as the most favoured and successful technique in this field. It has been applied already to the study of single crystals by many crystallographers, notably Lipscomb and co-workers(3) and Fankuchen(4); these applications have made use of liquid nitrogen, and have attained temperatures as low as about 95° K. A commercial cooling attachment is also available (for use with liquid nitrogen),(5) giving temperatures down to about 125° K.

A crystal specimen cooled in this way has only two means of heat exchange with its surroundings, which might raise its temperature above that of the gas stream. These are conduction through its support, and radiation (we assume the absence of radiation shields). The first of these depends upon the nature and dimensions of the support: a Pyrex glass fibre is very commonly used, and entirely satisfactory; if its length and diameter are ½ cm and 20 μ respectively, it can easily be shown that the rate of conduction of heat by this route to the specimen at say 10° K is of the order of 0·002 mcal/s. The second means of heat gain might be expected to be more serious, but it is not usually realized how little is the effect of radiation on a specimen as small as is normal in X-ray work. In fact, at any temperature below, say, 100° K, a crystal of approximately 1 mm^3 dimensions (a maximum size) can receive a maximum of 0·8 mcal/s from its surroundings, if these are at 20° C. (See Fig. 1; black-body emissivity is assumed.)

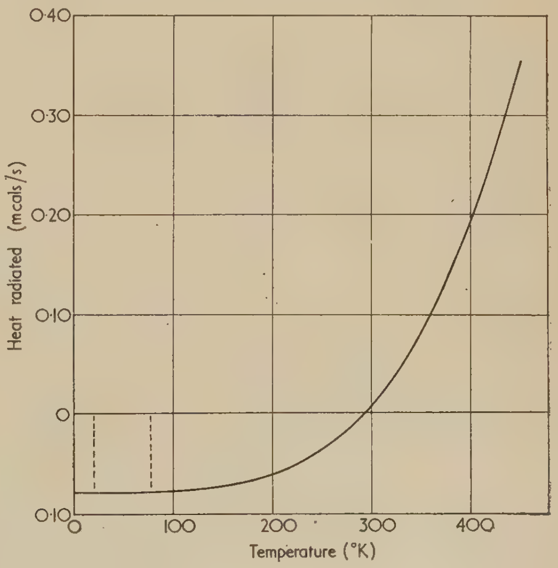

Fig. 1. Heat radiated to a small crystal as a function of its temperature, the environment being at 20° C. Crystal size: height 2 mm, diameter 1 mm

For comparison with these two sources of heat, which gas cooling must counteract, we evaluate the "cooling power" of a cold gas stream in terms of the heat capacity per unit volume, viz. millicalories of heat taken up per cubic centimetre of gas, at atmospheric pressure, when the gas temperature is altered by one degree. This is shown in Fig. 2, where curves for H_2 and N_2 gas are drawn. The variation of cooling power with temperature is primarily a consequence of the changing gas density; but it is chiefly the difference of specific heats which leads to the strikingly greater cooling power of hydrogen as compared with nitrogen. If hydrogen is used, at an operative temperature of say 25 to 30° K, the amount of heat which could be absorbed by a stream flowing as slowly as 1 cm^3/s, and rising only 1° in its temperature, would be 2 mcal/s. Heat exchange between crystal and gas stream cannot be complete or instantaneous; nevertheless the comparison between this figure and those quoted above for heat leakage into the specimen would appear to render gas cooling, by hydrogen gas especially, a promising technique. It may be added that helium gas, above 20° K, has a cooling power per cubic centimetre about equal to that of hydrogen, while below 20° K, its heat capacity per unit volume is even greater, due to the increased density.

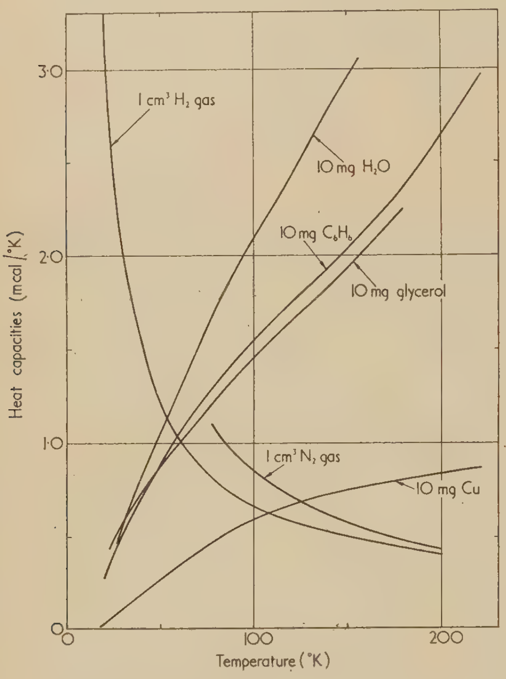

Fig. 2. Heat capacities per unit volume of hydrogen gas and of nitrogen gas compared with heat capacities of certain solids at low temperature

Hydrogen has two further advantages over nitrogen as a coolant. Its thermal conductivity, even at 25° K, is still 2½ times that of gaseous nitrogen at 80° K; thus heat exchange is more efficient. Its viscosity at 25° K is extraordinarily small ($1 \cdot 5 \times 10^{-3}$ cP)—one-fifth of that of nitrogen at 80° K; this much facilitates its flow through narrow delivery tubes. Helium shares these advantages: the conductivity and viscosity at 10° K are respectively about half and about equal to the corresponding properties of hydrogen at 25° K; the outstanding disadvantage of helium as compared with other gases as a coolant is its high cost.

A gas-flow cryostat

An apparatus for cooling a crystal by means of a strea of cold hydrogen gas, and aimed at the greatest possib economy of cold temperature has been designed as follows hydrogen gas, evolved from the gently boiling liquid an collected from near the top of the Dewar-vessel container, i led through a short metal spiral downwards, underneath th liquid, and out through the base of the Dewar. This principl is the same in essence as that employed in 1936 by Vonnegu and Warren,(6) who used liquid nitrogen. From the base c the Dewar to the point at which it emerges as a cold jet t flow over the crystal, the gas passes through a tube which i vacuum jacketed, the outer envelope being continuous wit the outside wall of the Dewar flask. This arrangement, whic we term a "gas-flow cryostat", is shown diagrammatically i Fig. 3. The reservoir section is made from a commercia Dewar vessel: the base of this is removed for constructio

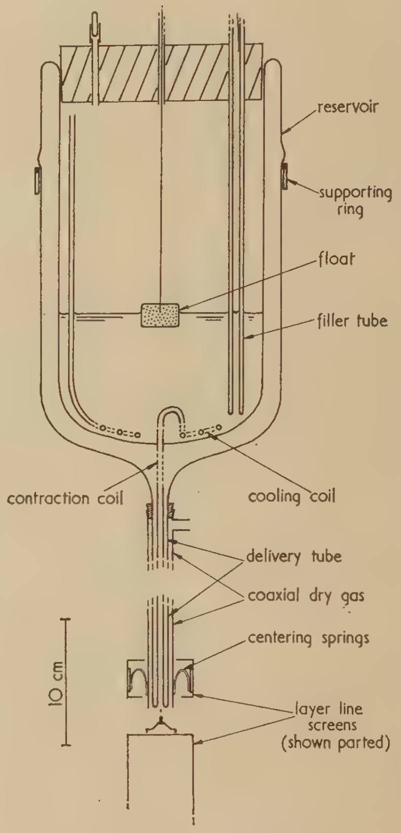

Fig. 3. Diagram showing the design of the gas-flow cryostat, and its position above a crystal in a Weissenberg goniometer

of the internal seal, and is then fused on again; after re-silvering, it is evacuated *via* a tube at the side. The bung is cut from Onazote, a vulcanized expanded rubber product. The volume held by the reservoir depends upon the choice of Dewar vessel used; that shown (Fig. 3) has a working volume of about 3 l. The internal diameter of the delivery tube is about 3·0 mm: the external diameter is about 1 cm.

In the operation of this equipment, the valve at the top is closed to prevent escape of gas through the bung; the slight pressure built up by evaporation of liquid in the reservoir causes cold gas to start flowing down the exit tube. In this way the cold gas jet is started. As heat leaks inevitably into the Dewar vessel, especially around its rim, it is carried by he flow of gas down beneath the liquid, causing further quantities of the latter to evaporate, and in this way the cold gas jet is maintained. The continual movement of gas acts s a thermal stirring device, always transporting heat leakage, rom whatever source, to the liquid; the temperature inside he Dewar reservoir is kept remarkably uniform, and the ate of boiling of the liquid is extremely constant, whether he vessel is full or nearly empty. The rate of loss of coolant, noreover, is no more than that corresponding to unavoidable eat leakage. At the same time, the temperature of the gas et is extremely low, and has been shown, in the case of liquid itrogen as refrigerant, to be only some 5 deg. above that of the liquid itself. To stop operation of the instrument, the alve at the top is opened; the cold gas jet, and thermal nixing, stop simultaneously.

The cryostat described was designed for a vertical flow ystem as required for the Leeds Weissenberg goniometer. (The vertical system has obvious advantages; however, to it a horizontal goniometer, a single bend in the delivery tube vould suffice.) The delivery tube must be positioned very accurately within the layer-line screens, 1 mm or so above the crystal. The reservoir, to which it is rigidly attached, rests in a circular hoop which is held in a robust steel stand capable of fine adjustment in the vertical direction. The delivery tube is held accurately central within the layer-line screens by three springs which bear on it near its tip. The cold gas stream flows down the camera axis until it is broken up by meeting the goniometer head. The cold jet is surrounded by a steady stream of absolutely dry gas at room temperature.(4) The most reliable and also most convenient means of obtaining this is to boil liquefied gas by means of a small electric heating coil; the vapour quickly attains room temperature as it is led to the point of use; it is far more dry than could possibly be secured with the aid of any simple chemical drying agent, and the rate of flow is steady and controllable. The dry gas is guided into the region inside the layer-line screens by means of a tube surrounding the Dewar tube co-axially.

Performance of the cryostat

(*a*) *Liquid nitrogen as refrigerant.* Measurement of the rate of boiling showed that the leakage of heat into the Dewar reservoir amounted to 1·4 cal/s (≡6·0 W). The rate of use of liquid nitrogen was, correspondingly, about 160 cm^3/h, giving a running time of about 18 h before refilling was required. This low rate of use of liquid nitrogen represented considerable economy in running costs. It may be compared with rates of the order of 4 l./h reported for other gas-flow cooling devices, when temperatures as low as 95° K are required. The rate of flow of cold gas at the jet was 8 cm^3/s. No electrical heating in the liquid was required, as this rate of boiling, determined purely by heat leakage, was fully sufficient for low temperature maintenance, and was extremely constant (to 1–2%). At this speed of running, the total delivery of "cold" into the camera, measured in terms of the calories absorbed as the entire cold gas stream rises to room temperature, amounted to 1 W only (0·25 cal/s). That this was so small was an advantage, since the goniometer and neighbouring parts of the camera were not seriously cooled. On the other hand, the cooling power of the gas jet, about 8 mcal/(s × deg.), was well in excess of the heating effects of radiation or conduction on the crystal.

The temperature of the cold gas jet was measured by three different methods. Thermocouple readings indicated a temperature of about 105° K (uncorrected), corresponding to something below 90° K when allowance was made for the error resulting from heat conduction through the wire leads. Measurements on high-angle diffraction spectra given by a sample of silver* cooled in the jet showed that the temperature was of the order of 100° K, but high accuracy was not possible by this method. The most accurate estimation of the jet temperature was provided by the use of oxygen, which could be liquefied within a narrow capillary by the cold stream. Oxygen gas from a cylinder (purity 98%), admitted at atmospheric pressure to the capillary, was quickly liquefied at the capillary tip, and the amount of liquid increased slowly till the column was about 1 cm in length. Thus the temperature was certainly below 90° K. By reduction of the oxygen pressure until the drop of liquid at the tip of the capillary was just in equilibrium it was found that the temperature at that point—inside the capillary tube—was 83° K. Fig. 4 shows the capillary tube mounted in position on a Weissenberg goniometer, with the cold gas jet streaming downwards over it, and about ½ cm length of liquid oxygen inside. The layer-line screens have been moved apart to show the tip of the Dewar delivery tube, and the coaxial tube carrying the dry nitrogen gas stream; other objects in the field are the collimator and the beam-stop. It will be seen that there is no growth of frost. The use of this technique for measurement of temperature permitted, in addition, an observation of the rate at which heat was actually abstracted from a specimen, for comparison with theoretical estimates. Observation of the rate of liquefaction of oxygen, at atmospheric pressure, showed that under the conditions of the experiment, the jet was capable of removal of 0·5 mcal/s at 90° K, even at a point 5 mm below its point of exit. Still another observation could be made in this experiment with liquid oxygen: the relative unimportance of heat radiation could be demonstrated by bringing a warm body within about 3 mm of the tube; fingers of the hand, for example, could be held as close as this and the liquid oxygen column was entirely unaffected.

Fig. 4. Oxygen, at 90° K, liquefied by a stream of cold nitrogen gas

(*b*) *Liquid hydrogen as refrigerant.* The rate of heat leakage into the Dewar reservoir was found to be about 7 W, as in the case of liquid nitrogen. The rate of boiling of liquid hydrogen, however, was about five times greater than nitrogen under these conditions (mainly because of its very low density): about 750 cm^3/h, allowing a running time of about four hours before refilling was required. The boiling rate was, as before, extremely constant. The rate of flow of gas at the jet was about 13 cm^3/s (measured as hydrogen gas at 25° K) and the cooling power of this stream, i.e. the heat absorption per 1 deg. rise in temperature, was about 32 mcal/(cm^3 × deg.) which was about four times greater than that of the nitrogen jet from the same apparatus. The total delivery of cold into the camera was similarly greater; about 70 W; this very high rate of delivery of cold was a distinct disadvantage, however, since over-cooling of the camera parts became a problem.

---

* Accurate data on the lattice parameter of silver were given by Owen.(7)

Avoidance of frost was a much more difficult matter with hydrogen than with nitrogen. The surrounding sheath of dry gas had to be of hydrogen, freed not only from traces of moisture, but also from all traces of air, which was equally capable of depositing as frost. Since liquefied hydrogen was considered too expensive to boil as a source of the pure dry gas, hydrogen was obtained from a cylinder, and purified by passage through spirals immersed in liquid nitrogen, including a tube filled with activated charcoal. This gave fairly satisfactory results, but was a tedious process, which it is hoped to improve.

Care was necessary to ensure that the gaseous hydrogen continuously evolved by the apparatus when in operation should be safely removed. This was done by means of an ordinary fume extractor. The cryostat itself released about $\frac{1}{2}$ ft^3/min measured as hydrogen gas at 20° C; the dry gas sheath added a further $\frac{1}{4}$ ft^3/min. The total was at no time greater than about 1 ft^3/min, which was small compared with the capacity of the extractor. In the extracted air the proportion of hydrogen did not exceed about 3%, which was well below the explosive limit.

The temperature of the jet was estimated from thermocouple measurements to be 30° K or less but it was checked, more reliably, by a phase-change technique, as before. Just as the liquefaction of oxygen had been used to determine a temperature below 90° K, so in this case neon was used, enclosed in a capillary. Neon liquefies at 27° K and freezes at 24° K. When the experiment was carried out, neon was observed to solidify, consistent with a temperature of 23° K inside the capillary cooled by the cold hydrogen stream.

A Weissenberg photograph obtained with radiation from a copper target, and with an ammonium oxalate crystal cooled to 23° K by the cryostat, is reproduced in Fig. 5.

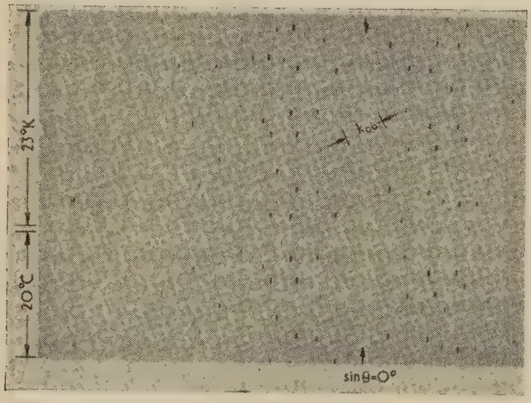

Fig. 5. Weissenberg photograph; 0-layer line of rotation about [001] of $(NH_4)_2(COO)_2$, H_2O at 23° K (upper portion) and, subsequently, at 20° C (lower portion); Cu radiation, filtered; exposure 1·2 min/deg. for each portion; the lower portion duplicates part of the range of the upper

(c) *Some difficulties and their avoidance.* As a prototype the cryostat may be regarded as satisfactory, but its operation is not entirely free from difficulties, which it is hoped will be removed by modifications to the design of future cryostats. One difficulty, that of avoidance of frost from over coolin inside the camera, has already been referred to. Sufficien reduction in the rate of boiling of liquid hydrogen wi eliminate this; this can be achieved, for example, by reductio of the rate of heat leakage into the reservoir (i.e. by bette insulation) or by the use of electrically controlled boilin under a bell within the reservoir (see below). Anothe difficulty is that the support for the cryostat in its presen form does not provide to our complete satisfaction the combination of rigidity and delicacy of adjustment necessary fo the accurate location of the gas jet above the crystal; this however, can be rectified by suitable re-design of the suppor system.

There is a remarkable phenomenon—entirely unexpecte at the outset of this work—which tends to limit the time o continuous operation of the gas-flow cryostat, in its presen form, to about 48 h. This is the slow accumulation of ic crystals around the mouth of the tube by which evaporate gas is collected and led down to the cooling spiral; the ic crystals slowly build up a resistance to gas flow, raising th pressure in the cryostat reservoir. During the first 24 h o continuous running the effect is negligible, but after abou 36 h it becomes more marked until finally the proper functioning of the apparatus is seriously impaired. That ice crystals should grow, even slowly, in an atmosphere of apparently pure nitrogen gas at a temperature near −190° C, is no easy to explain. However, the mechanism is almost certainly as follows: Condensation of atmospheric moisture aroun the rim of the Dewar reservoir during operation results i the formation of a hard layer of ice in the circular channe between the glass and the Onazote bung. (This ring of ice actually assists in the sealing of the top of the reservoir, as it blocks up any crevices at the side of the bung.) The ice becomes extremely hard; its temperature at the base of the channel must be much below 0° C. Despite its rigid condition, and despite the existence of continuous positive pressure within the Dewar vessel, slow volatilization of water molecules can take place, with subsequent condensation at the mouth of the collector-tube, because the ice at the base of the bung, although very cold, is at a temperature significantly above that of the tube.

The blockage phenomenon is interesting because mobility and volatilization of ice at temperatures close to that of liquid nitrogen would normally be discounted. In this case, however, it constitutes a nuisance. The undesirable effects can be minimized, but not altogether removed, by the use of grease round the sides of the bung. Complete elimination of the phenomenon is possible by arranging that cold gas be collected from under a bell, instead of from the space below the bung; this change would be essential for any apparatus required to operate continuously for periods over 2 to 3 days. The use of a bell has the advantage that the heat which inevitably leaks through, or across, the Dewar walls is wasted, rather than made use of; but the bell system is obviously superior for work where long periods of cooling are imperative, and it is intended to design further apparatus on this principle.

Acknowledgements

It is a great pleasure to acknowledge my debt to Prof. E. G. Cox, who originally suggested this project, and whose interest has been a constant encouragement. I am also greatly indebted to F. E. Hoare for advice, and to the Department of Physics for the liquid hydrogen used in this work.

References

(1) Cruickshank, D. W. J. Address given at Stockholm, June 1959; to be published.

(2) Steward, E. G. *X-ray Diffraction by Polycrystalline Materials*, Chap. 10 (London: The Institute of Physics, 1955).

(3) See especially Reed, T. B., and Lipscomb, W. N. *Acta Cryst.*, **6**, p. 45 (1953).

(4) Post, B., Schwartz, R. S., and Fankuchen, I. *Rev. Sci. Instrum.*, **22**, p. 218 (1951); Steinfink, H., Ladell, J., Post, B., and Fankuchen, I., **24**, p. 882 (1953).

(5) Kreuger, A. *Acta Cryst.*, **8**, p. 348 (1955).

(6) Vonnegut, B., and Warren, B. E. *J. Amer. Chem. Soc.*, **58**, p. 2459 (1936).

(7) Owen, E. A., and Williams, G. I. *J. Sci. Instrum.*, **31**, p. 49 (1954).

Simple device for use with platform weighbridges in the accurate determination of burning rates

by J. E. ROUGHTON, B.A., A.Inst.P., A.M.Inst.F.,* Radiation Ltd., Group Research Laboratories, London

[*Paper received* 11 *September*, 1959]

Abstract

The device comprises an automatically adjusted "chain rider" which permits measurement of small weight changes to better than ±½ oz with a normal 5 cwt platform weighbridge.

Introduction

Platform weighbridges are frequently used to determine the rate of burning of solid fuel fires during experimental investigations. Although these machines may be intrinsically capable of high accuracy, the normal method of adjustment, by a sliding rider on the beam arm, does not permit a measurement to closer than ±2 oz. Greater precision may sometimes be necessary, especially when low burning rates are to be measured over short intervals. A cheap and simple device has therefore been developed which increases the accuracy to better than ±½ oz. The device is automatic in operation, will measure both increases and decreases in weight and could readily be adapted as a recording instrument. It can be fitted on any beam arm weighbridge in which the arm is accessible.

Principle

The apparatus uses the principle of the "chain rider" type of analytical balance, namely that a part of the restoring force on the balance is provided by a chain, one end of which is freely suspended from a fixed point on the beam and the other from a support of variable height. The scales are adjusted so that they balance when the adjustable support is at its highest setting. Downward movement of the support then increases the restoring force by an amount proportional to the displacement, thus permitting a calibration of the support height in terms of a counter-balancing weight. A recording version of this type of balance has been described by P. D. Garn.†

In the present application, the motion of the adjustable support is automatically controlled by contacts on the beam arm such that the weighing machine is always at or close to the point of balance. As the device is normally required to measure a decrease in platform load, the zero is arranged at the lowest point of the support movement.

Description

The general arrangement of the apparatus can be seen from Fig. 1. The drive for the variable support is provided by a 12 V d.c. reversible motor with a nominal speed of 3000 rev/min. Speed reduction to approximately 10 rev/min

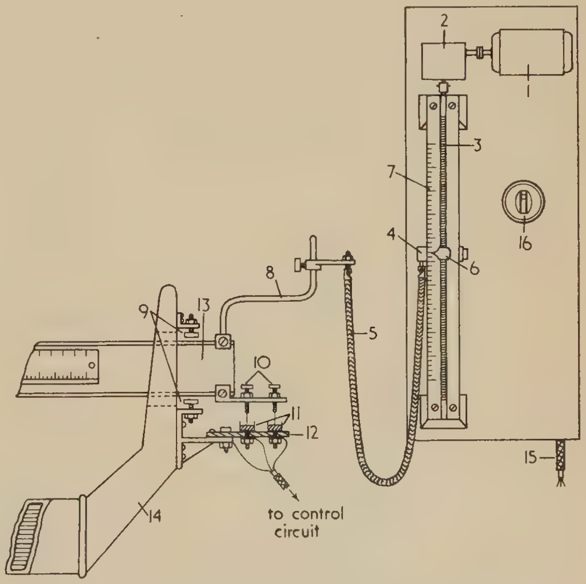

Fig. 1. General arrangement of weighing device

1, 12 V d.c. motor; 2, 300 : 1 reduction gears; 3, threaded rod; 4, rider and variable support; 5, snake chain; 6, pointer; 7, scale; 8, pre-set support; 9, upper and lower stops; 10, adjustable contacts S_1, S_2; 11, mercury pots; 12, insulation; 13, beam arm; 14, weighing-machine chassis; 15, mains connexions; 16, mains on/off switch is achieved by gear trains of 100 : 1 and 3 : 1 successively and the latter is connected to a threaded vertical rod of 26 threads per inch. Travelling on the rod is a tapped rider with a "pillar and pin" attachment from which the chain is suspended (see Fig. 2). On the front of the rider is a pointer which moves in the central slot of a scale graduated from 0–5 lb in 0·05 lb intervals (1 lb = $1\frac{1}{2}$ in.). For rapid zero setting the rider can be disengaged from the rod by the operation of a spring-loaded, push-button clutch. The whole of the drive is mounted on the outside of a rectangular box which is rigidly fixed to the weighing-machine chassis by fittings which allow a lateral adjustment for setting up purposes.

---

* Now at Central Electricity Research Laboratories, Leatherhead, Surrey.

† Garn, P. D. *Anal. Chem.*, **29**, No. 5, p. 839 (May 1957).

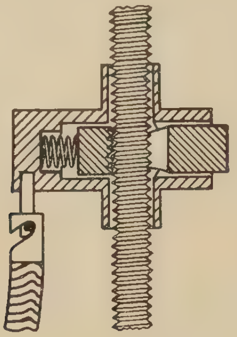

Fig. 2. Detail of rider

The chain used is an oval-section "snake" chain. This type of chain is not ideal as the manufacturing process causes a slight longitudinal twist and though this can be removed by counter twisting, the chain does not then hang in a truly vertical loop. Nevertheless, the chain is readily available in the weight required (approximately 2 oz/in.) and was found to give a performance of sufficient accuracy. The most uniform 14 in. length was selected from 30 ft of chain and was cleaned by repeated washing in trichlorethylene.

The chain support on the beam arm can be adjusted vertically, horizontally and to any desired angle with the arm, thus permitting a range of adjustment for the correct setting of the system. Also fitted to the end of the beam arm are two nichrome wire "whiskers" which dip into two separate insulated thimbles containing mercury and thus form the switches which control the drive mechanism via a double-pole, double-throw, spring-loaded relay. The control circuit shown in Fig. 3. The whiskers are pre-set so that, when th beam arm is in the balanced central position, S_2 is just close and S_1 just open, the difference in height of the whisker tip being approximately 1 mm. In this position the relay energized via S_2 but the connexion to one pole of the moto is broken by S_1, and therefore the motor does not operat If the platform load decreases, the beam arm falls, closin S_1, and switching on the motor in the direction necessary t raise the chain. Conversely, if the beam arm rises, S_2 open the relay is de-energized and the relay switch thrown ove The 12 V supply is then connected to the motor with reverse polarity, and hence the chain is lowered. By this means, th beam arm is always returned automatically to the centra position. In normal operation, the mechanism does not hun The relay and the 230 V a.c./12 V d.c. power pack are house inside the box and are mounted on a hinged panel for read accessibility.

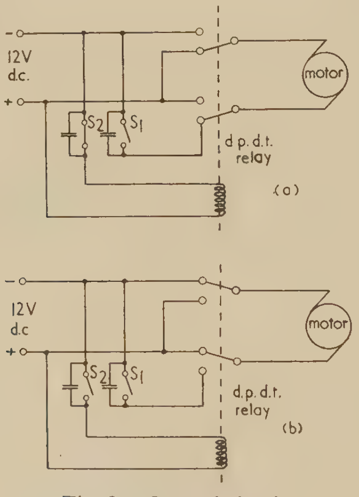

Fig. 3. Control circuit
(*a*) at balance point, S_1 open and S_2 closed;
(*b*) platform load too heavy, S_1 and S_2 both open.

Adjustment, calibration and operation

The weight of chain per unit length was so chosen that th sensitivity required could be obtained with the chain sus pended from some point close to the end of the beam arm When the device had been assembled, the position of th beam arm support and the position and angle of the contro box were adjusted simultaneously until the chain was hanging smoothly and the scale calibration was correct. With th pointer set at zero, the weighing machine was balanced by adjustment of the normal rider. Full-scale deflexion and th return to zero were then checked several times with a know 5 lb weight. When the correct maximum displacement had been obtained, the intermediate positions were checked with other known weights and the error did not exceed ±0·01 lb The repeatability of the measurements was assessed by twenty successive determinations of a weight change from 2 lb to 3 lb, and the standard deviation of the results was 0·0076 lb, which corresponds to an accuracy, on the 95% basis, of ±0·015 lb.

The performance of the device with continuous changes in weight, under normal test conditions, was investigated by running off water at a controlled rate from a reservoir on the weighing machine into a measuring cylinder. Rates of weigh change of 6 lb/h, 3 lb/h and $\frac{1}{2}$ lb/h were used. Performance was good at all rates, and the errors did not exceed ±0·03 lb or $\pm\frac{1}{2}$ oz.

Because of the inertia of the system, the scale readings lag behind the weight changes by up to 0·03 lb according to the particular zero-setting method employed. Since, for any method, the lag is constant, an appropriate allowance can readily be made.

Although the present device covers a range of weight of only 0–5 lb, extension beyond this range is readily achieved by re-setting the pointer to zero and adjusting the beam arm rider to re-balance. For other applications, of course, the weight of the chain and/or the point of suspension can be chosen to suit the weight range required. Finally, as the rider is positively driven, the device could be produced as a recorder by merely attaching a pen and fitting the necessary recording chart and drive.

Acknowledgements

The author is indebted to the engineering staff of these laboratories for assistance with the design of the chain lifting mechanism, and to the Directors of Radiation Ltd. for permission to publish this paper.

An electroluminescent digital indicator with a silicon carbide coding matrix

by D. H. MASH, B.Sc.,* Thorn Electrical Industries Ltd., Enfield, Middlesex

[*Paper first received* 8 *September, and in final form* 14 *October*, 1959]

Abstract

A digital indicator is described using an electroluminescent panel having its back electrode shaped as an array of lines, from combinations of which the digits are formed. Also described is a coding matrix which greatly simplifies the electrical switching needed for the indicator. The coding matrix utilizes the non-linear electrical properties of silicon carbide powder to discriminate between the voltage applied to wanted elements and unwanted elements, and allows a single-pole ten-way switch to be used for selecting the required digit.

The growing need to present information in the form of figures rather than as a needle displacement has led to a variety of display devices having the common feature that the digits are changed without change of position. The oldest of these is, of course, the mechanical revolution counter, which has disadvantages of inertia when used for high-speed indication, and furthermore can only operate sequentially. More recently many other indicators have been developed, including multielectrode neon lamps, projection devices and the edge-lit Perspex pack, in which a set of ten small Perspex sheets, each bearing an engraved number, is stacked one behind the other, any required number being illuminated by a small incandescent lamp set at the edge of each sheet. All of these have disadvantages—they are either bulky, or the figures lie in different planes, giving rise to the so-called "tunnel effect" which may obscure those lying farthest back.

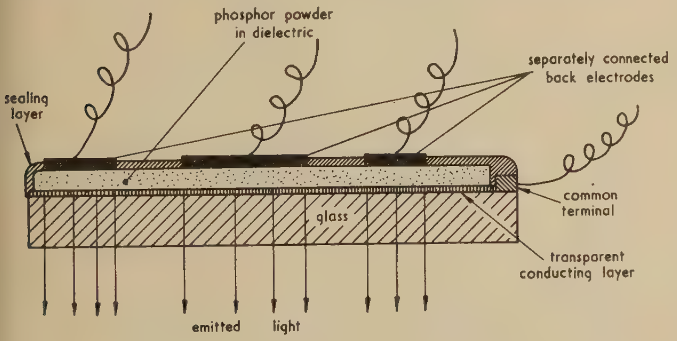
phosphor powder in dielectric
separately connected back electrodes
sealing layer
common terminal
glass
transparent conducting layer
emitted light

Fig. 1. Cross-section of electroluminescent lamp (not to scale)

In the last few years the electroluminescent lamp, or luminous condenser, has become a useful light source, and is being used in a number of applications where the particular characteristics of flatness, even illumination, low weight and power consumption are required. Much has been written about the construction and characteristics of these lamps, but the principle is shown in Fig. 1—phosphor powder suspended in a plastic dielectric is sandwiched between two plane electrodes, one of which is transparent. Under the influence of a changing electric field suitable phosphors (the most common is ZnS activated with Cu) are directly excited to emit light, and this is transmitted through the transparent electrode. The area that emits is defined by the shape of either of the electrodes, which makes it possible to have separately connected individual areas of any shape. The brightness of emission is a function of the voltage and frequency of the supply. Typical curves are shown in Fig. 2.

The special advantages of the electroluminescent lamp make it natural to consider its applications to digital display. Two general approaches are possible. In the first, the back, or opaque electrode is formed into the shape of the ten digits, each being electrically separate from the others, and connected to its own terminal. This leads to a very complicated electrode structure, with many insulating bridges where different figures cross one another, and it gives an unsatisfactory display owing to the breaks in the digits and their varying sizes. For these reasons the first system has been rejected. The second method utilizes an array of lines or dots from combinations of which the ten digits may be formed. Such a lamp is relatively straightforward to make, and gives a satisfactory display with as few as seven luminous elements, though a much better presentation is made with ten lines. A suitable ten-line array is illustrated in Fig. 3. (The two parts of the diagonal line for the figure 7 are used

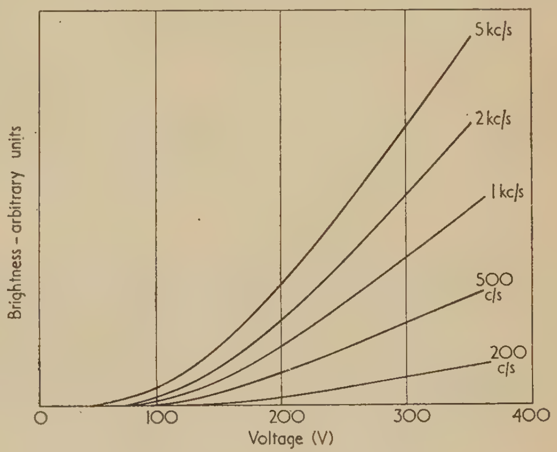

Fig. 2. Characteristics of an electroluminescent lamp

only for that digit; they are therefore permanently connected and constitute only one element.) Although the system gives formalized shapes, the numbers are unambiguous and easily recognized.

---

* Now at Siemens Edison Swan Ltd., Research Laboratory, West Road, Templefields, Harlow, Essex.

This method has one serious disadvantage. Owing to the fact that most of the elements are used in more than one digit the combinations cannot be permanently connected electrically, but must be connected by the switch or relays which provide the information to the indicator. This calls for a complicated and bulky switching circuit which defeats the object of the device, which is to minimize space requirements.

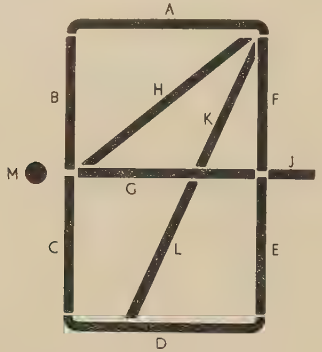

Fig. 3. Suitable ten-line array

To overcome this objection, an ancillary device has been developed known as a coding matrix.* This has the function of accepting current from one of ten channels (in other words, from a single-pole selector switch) and distributing or coding it to the required combinations of elements. The matrix is in the form of a printed circuit wafer which has the same area as the electroluminescent digital indicator and attaches directly to it, the whole device, including frame, being only $\frac{1}{4}$ in. thick. The principle on which the coding matrix works can be described with reference to the simple system shown in Fig. 4. In this there are shown two equal electroluminescent elements, P and Q, and it is required to excite one or the other or both using only a three-way selector switch S. The resistors R_1, R_2, R_3 and R_4 are equal. When S is connected to T_2, P and Q luminesce equally according to the voltage developed on them after the potential drop in R_2 and R_3. When S is connected to T_1 there is approximately the same potential drop in R_1, and hence P lights up as brightly as P and Q did before. Current also passes to Q through the extra resistors R_2 and R_3 across which a further potential drop occurs, and so Q luminesces, but more weakly than P. It can be easily shown that if $R_1 = R_2 = R_3 = R_4 = Z_P = Z_Q$ (where Z_P and Z_Q are the respective impedances of the luminous elements, and V_P and V_Q are the voltages developed across the two elements), then $V_P/V_Q = 3$. In a typical case if the applied potential is 400 V, V_P is 200 V, $V_Q = 66$ V and the ratio of the brightnesses, $B_P/B_Q = 300$. This ratio is just great enough to make Q invisible when P is brightly illuminated. The discrimination ratio B_P/B_Q increases with increasing magnitude of the resistors, but, of course, with the penalty that higher supply voltages must be used to achieve the same brightness in the wanted element.

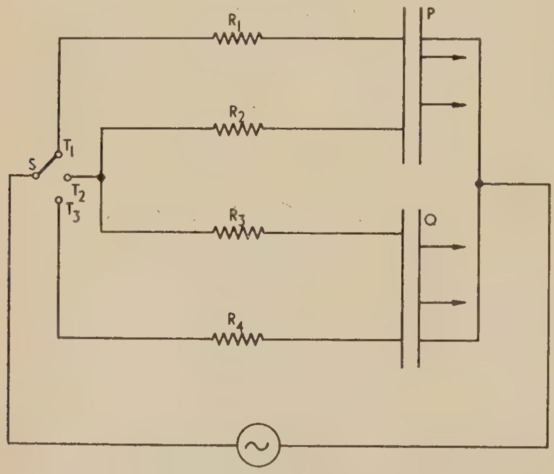

Fig. 4. Principle of the coding matrix system

As the number of elements is increased, allowing for various combinations of them, the amount of unwanted coupling also increases, and the discrimination ratio goes down. This effect is so great that if the ten elements of an electroluminescent indicator array are coupled with resistors in the manner described, the resulting display of a chosen digit is made unreadable by the excessive brightness of unwanted elements.

This difficulty has been overcome by using non-linear resistors in place of normal resistors. Many semi-conductors show non-linear characteristics, and a particularly suitable one for this purpose is silicon carbide. This exhibits a current characteristic of the form $I = kV^n$ where n is about 5. Commercially available silicon carbide powder, in a resin binder, is very suitable, and the grade may be chosen to give the required parameters.

Fig. 5 shows the relationship between brightness and applied voltage when an electroluminescent lamp is connected in series with one, two, three and four non-linear resistor elements. The direct electroluminescence characteristics with and without a series linear resistance are given for comparison. It will be seen that a family of almost parallel curves is formed, due to the tendency of the non-linear element to maintain the same potential drop across itself.

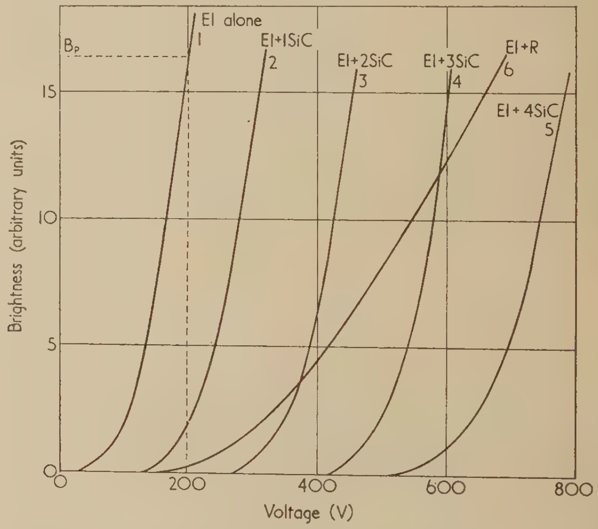

Fig. 5. Relationship between brightness and applied voltage when an electroluminescent lamp is connected in series with 1, 2, 3 and 4 non-linear resistor elements

Consider the circuit of Fig. 4 with the resistors replaced by silicon carbide elements. If the size of the silicon carbide resistors is so chosen that an applied potential of 400 V develops 200 V across P then the brightness will be B_P from Fig. 5. The brightness of element Q will be that given by curve 3 at $V = 200$, which can be seen to be vanishingly small. Hence the discrimination ratio B_P/B_Q is very large, and even when the number of elements is increased to 10, as required for the digital indicator, the discrimination remains high and unwanted lines do not luminesce.

---

* British Patent Application 27388/58.

Construction of the indicator

The basis of the indicator is an electroluminescent lamp of the general form of Fig. 1. The transparent conducting layer is a thin film of stannic oxide formed on glass at high temperature. Such conducting glass is mechanically strong and has a resistance of 500 to 1000 Ω across a square area. The dielectric in practice consists of two layers, the first (against the conducting film) being the resin-bound phosphor, and the second being a dispersion of barium titanate in a plastic. The function of this second layer is to act as a reflector, and also, through its high dielectric constant, to concentrate the field across the phosphor.* The back electrode is defined to the required array by a p.v.c. mask which is permanently attached to the reflector layer. The electrodes are of graphite which are in contact with the dielectric only through the slits in the mask, across which connecting leads of conducting paint pass to metal studs arranged on the edges. One stud is connected to the conducting glass, the others to the elements of the array. The entire back, excepting the studs, is covered with a plastic to exclude moisture. Finally the metal studs have conducting plastic pads attached to them to make connexion with the terminal areas of the matrix.

Construction of the matrix

Fig. 6 shows the basic matrix before the silicon carbide is applied. It is made by printed circuit techniques from double-surface copper-clad Bakelite. The white parts are copper, the black parts are Bakelite from which the copper has been etched. The areas marked with letters are the terminations of vertical copper strips, and when the matrix is mounted against the electroluminescent indicator, these areas make contact with studs which are connected to the back-electrode elements lettered in Fig. 3.

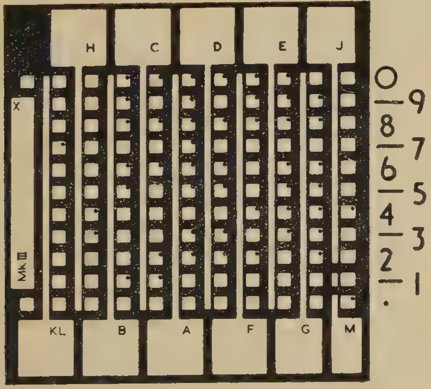

Fig. 6. Basic matrix before the silicon carbide is applied

The back surface (not shown) of the printed-circuit board is divided into a series of 11 horizontal rows (numbered 0 to 9 with a decimal point) registering with the horizontal rows of small copper squares on the front surface. Conducting rivets connect some of these squares, marked with dots, to the back rows.

When the front surface of the board is coated with resin-bonded silicon carbide powder, it covers the small gap between any vertical line and any adjacent small square. When a voltage is applied between one of the horizontal rows on the back of the board and the conducting glass of the electroluminescent panel, a current path exists along the row, through the rivets, across the gaps (*via* the SiC) to the adjacent strips, and from their terminations to a group of conducting lines of the electroluminescent array, and thence through the phosphor to the conducting glass. For example, when one side of the supply is connected to the back row marked 4, current passes through the rivets to the conducting strips *EFGHJ*, and from these to the corresponding array lines of Fig. 3. In a similar way, the other digits are formed from the following combinations:

0—*ABCDEF*
1—*BC*
2—*AFGCD*
3—*AHGED*
4—*EFGHJ*
5—*ABGED*
6—*ABCDEG*
7—*AKL*
8—*ABCDEFG*
9—*ABGFE*

As the silicon carbide extends over the entire matrix, electrical paths exist through it from every copper area to every other copper area. This does not introduce any complications, however, as the distances involved are large with respect to the wanted gap, and the non-linear property of the silicon carbide ensures that these unwanted paths have a very high resistance.

Clearly there is no restriction on the number of arrays that may be made side by side on an electroluminescent panel, nor on the number of matrices which may be similarly arranged. Fig. 7 is a photograph of a 4-in-line indicator as it appears when working. The thickness including frame is $\frac{1}{4}$ in.

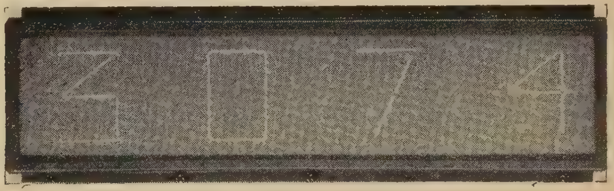

Fig. 7. 4-in-line indicator

Operating requirements

Generally speaking, the brightness of an electroluminescent lamp on mains frequency is not sufficient for viewing under normal room-lighting conditions. A supply at 400 c/s gives adequate brightness, however, and the power consumption is low enough to permit operation from a small transistor oscillator. The necessary potential drop in the coding matrix means that a higher operating voltage must be used for a digital indicator than is normally used for electroluminescent lamps. The device illustrated in Fig. 7 is being run from a 500 V 400 c/s supply, but by using thinner electroluminescent films adequate brightness has been achieved at 350 V. Under these conditions the current consumption is about 75 μA for each line of the array. Thus a figure 1 requires 150 μA while a figure 8 requires 525 μA. This current is partly capacitive and partly resistive.

---

* British Patent 798,503

The response of the device to input signals is rapid, full brightness being reached in about a millisecond when a 400 c/s supply is used, or less when higher frequencies are applied.

Present indications are that the operating life of the device will be determined primarily by the electroluminescent part, which has a lumen-maintenance of 60% after 750 hrs. running at 400 c/s.

Conclusion

The development of the silicon carbide coding matrix has made possible an electroluminescent digital indicator which is flat, can be read from any angle and consumes very littl power. It has a wide flexibility of size from the 2 in. squar which has been described, to both larger and smaller sizes and an in-line read-out of many digits may be constructe within one frame. At present, a fairly high voltage supply i required, but there is little doubt that with the use of thinne electroluminescent layers, lower voltages can be satisfactory. The principle of non-linear resistor matrices may be capable of extension to allow many other possible applications no associated with electroluminescence.

Acknowledgements

The writer wishes to thank the directors of Thorn Electrical Industries for permission to publish this work.

Some techniques for recording and measuring time-resolved spectra

by A. H. GABRIEL, Ph.D., A.Inst.P., Atomic Weapons Research Establishment, Aldermaston, Berks.

[*Paper received* 10 *August*, 1959]

Abstract

Methods are considered of recording the time-variation of the spectra of microsecond phenomena. An apparatus is described employing a rotating mirror time-resolving device before the slit of a quartz photographic spectrograph. Writing speeds of up to 5·1 *mm/μs are obtained. Consideration of possible calibration techniques involves some preliminary results on reciprocity law failure at very short exposure times. A pulsed calibration source is described in which a continuum at* 26 000° *K is maintained for* 15 *μs, and this is used to provide an absolute calibration of the records.*

Introduction

Owing to the current interest in high-temperature transient discharges for thermo-nuclear research, it is becoming increasingly important to make quantitative spectroscopic measurements on such events. Furthermore, it is desirable to time-resolve such measurements, as, in general, maximum light output will not coincide with the period of the discharge of most interest. There are a number of methods of recording such data. These can be listed:

(1) the use of a monochromator fitted with a photomultiplier and using high-speed oscilloscope display;
(2) the "gating" or shuttering of a spectrograph for a short period of the total discharge cycle;
(3) methods providing a time-scanned spectrum of a single discharge on a photographic plate.

Method (3) can be sub-divided:

(*a*) the use of a rotating mirror device before dispersion;
(*b*) the use of a rotating mirror device after dispersion;
(*c*) rotating film methods;
(*d*) the use of image-converter scanning after dispersion.

Methods (1) and (2) require an assumption that the event is reproducible, as each requires a number of similar discharges to construct a time-resolved spectrum. However, they may be desirable when there is insufficient light intensity for method (3), as method (1) is the most sensitive and method (2) allows the superimposition of a large number of flashes.

Some methods based on (3) have been described previously by Thackeray,(1) who has used a dispersing device in front of a streak camera, and by Lukyanov and Sinitsin(2) who used a rotating mirror device in front of a spectrograph. Rotating film cameras are limited to writing speeds of about 0·05 cm/μs, and image-converter techniques are inferior to direct photography in wavelength resolution. The techniques of method (3) are useful when the intensity emitted from the discharge is such as might be expected from laboratory discharges with number densities of the order of 10^{16} per cm^3, and it is on these methods that the techniques described in this paper are based.

The time-resolved quartz spectrograph

The first stage in the measurement technique is the recording of the time-resolved spectrum, and apparatus has been developed at this Establishment for obtaining such records in the quartz region, i.e. from 2200 to 8000 Å.(3) The instrument is essentially an achromatic rotating mirror device arranged in front of the slit of a Hilger medium quartz spectrograph. The optical system is as shown in Fig. 1. Light from the event (not shown) is focused by a quartz lens *A* on to the horizontal slit *S*1. This slit is imaged by a concave mirror *B* on to the spectrograph slit *S*2, after reflexion at the plane mirror *C* and the rotating plane mirror *D*. As *D* rotates, the image of *S*1, and therefore the light from the event, is swept down the vertical slit *S*2 of the spectrograph *F*. The record thus obtained is spectrallyesolved in one direction, and time-resolved in a direction at ight-angles. A quartz field lens *E*, in front of the slit *S*2, serves to ensure that the aperture of the spectrograph is filled throughout the writing period. All the mirrors used are aluminized on the front surface, with no protective coating. A photomultiplier and light source, by reflexion from the rotating mirror, are used to trigger the event when the mirror is in a suitable position. These are mounted on a cylinder around the rotor unit, so that by rotation of the assembly the timing of the output trigger can be varied with respect to the start of the record. This can be seen in Fig. 2, which is a photograph of the apparatus.

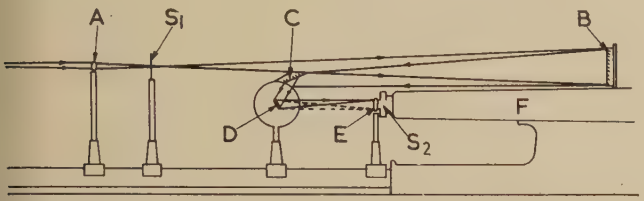

Fig. 1. The optical system of the time-resolved quartz spectrograph

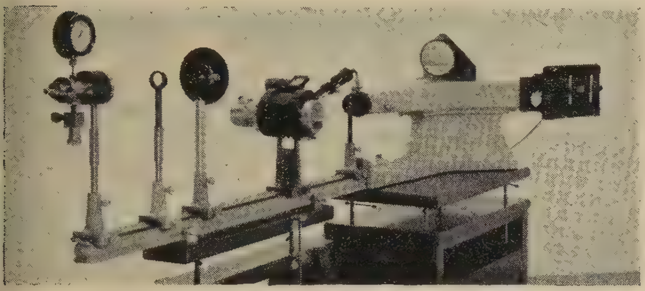

Fig. 2. The time-resolved spectrograph

The rotating mirror assembly is driven by a two-phase 1200 c/s induction motor, the armature and mirror being mounted on one shaft. The maximum speed is 57 000 rev/min, at which the writing speed along the slit *S*2 is 5·1 mm/μs. The bearings are of oil-impregnated porous bronze. The speed of rotation is measured by a magnetic pick-up coil from the shaft and indicated on a frequency meter.

A high resolution has been maintained in the focusing of the slit *S*1 on *S*2 by means of the concave mirror *B*. This is of 182 cm radius of curvature and is used with equal object and image distances. In the absence of the mirror *C* the image would lie only 7·5 cm below the slit *S*1. Under these circumstances the most severe aberration would be astigmatism. As the object is a horizontal slit, however, this will not affect its focus, but it will result in the region of the event under investigation being a small astigmatic cone.

The wavelength resolution and range of the instrument is simply that of the medium quartz spectrograph, and is not materially affected by the time-resolving system, as the prism aperture is filled at all times. Resolution in the time direction is limited by the quality of the mirrors and by coma in the spherical mirror. In practice, it is found to be better than 0·050 mm or 1/240th of the writing distance, which is 12 mm. This corresponds to 10^{-8} s at full writing speed.

The instrument has been used to make measurements on a linear pinch discharge described by Gabriel, Howell, Thornton and Wilson,(4) and on other laboratory light sources. A resolving time of 10^{-7} s has been found sufficient for these events. The assembly can be moved as a whole for lining-up, all optical components being mounted either on the spectrograph or on its accessory bar.

Calibration of records

Having recorded time-resolved spectra, using effective exposure times of about 10^{-7} s, it is necessary to record relative and absolute calibration data on these plates. This involves either making certain assumptions regarding the reciprocity law, or using a previously calibrated source exposed for the same effective exposure time as the event.

It is frequently suggested in the literature(5) that if exposure times are shorter than some critical value at about 10^{-5} s, the reciprocity law should hold well. If this were so, calibration data could be recorded at, say, 10^{-5} s, and many suitable d.c. sources could be found of sufficient intensity. Being d.c. they could then easily be calibrated against black-body sources. To test out this idea, some preliminary measurements have been carried out at this Establishment on reciprocity breakdown. An apparatus was used similar in principle to the time-resolved quartz spectrograph, and an attempt was made to construct the complete set of reciprocity curves for an emulsion. Fig. 3 shows a result for Ilford HP3 film at 5770 Å. A family of curves of log (exposure time × intensity) against log (exposure time) for a number of different developed densities is shown. It can be seen that whereas for a density of 0·1 the curve flattens below 10^{-5} s, as the density increases this point of flattening moves to shorter exposure times, so that when the density is 0·7 it occurs at 10^{-7} s. This is only a preliminary result, and much further work is required extending it to other emulsions, developers and wavelengths. However, it seems clear that it would be very difficult to make assumptions regarding the flatness of these curves in a useful exposure time region.

The possibility of using a d.c. calibration source exposed for the same time as the event is next considered. The problem is to find a source of high enough intrinsic brightness. There is some advantage in using a line source rather than continuum as, when spectrally dispersed, the light is available in a few strong lines and is likely to produce a denser record at these wavelengths. A number of sources were tried, but no significant improvement was found over

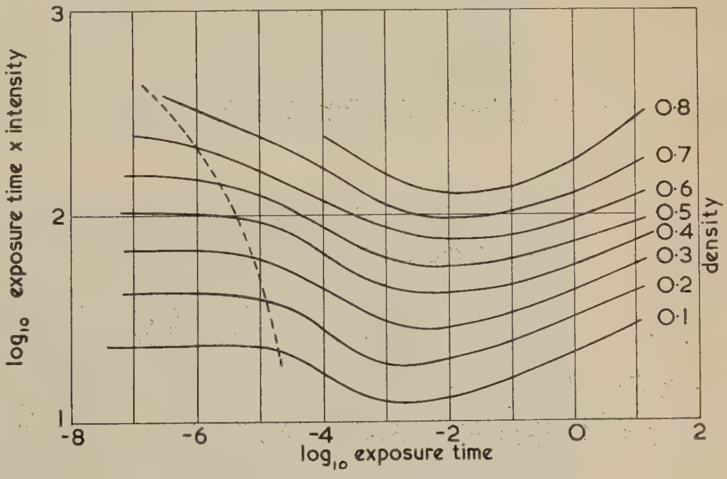

Fig. 3. A set of reciprocity breakdown curves

the cathode spot of a 250 W compact source mercury lamp. This produced a photographic density of about 0·15 when exposed for 10^{-7} s, which was not considered sufficient for use as a calibration source.

The alternative, which has been adopted, is to use a pulsed source. It will be seen that if a d.c. source were photographed in the time-resolved spectrograph using the same parameters as for the event, with the addition of a shutter to isolate one revolution of the rotor, then the record obtained would be uniform in intensity in the time direction. If now some form of known wedge or attenuator were used along the slit, the emulsion response and absolute calibration could be recorded. To use this technique with a pulsed source, it is required that its brightness remain constant for a period longer than the writing time of the instrument, i.e. longer than the effective duration of the event. No additional shutter is, of course, required in the case of a pulsed source. It was therefore decided to attempt to construct a source for use in the quartz region, which was bright enough to record a reasonable density in 10^{-7} s, and which had a constant brightness for at least 15 μs.

The calibration source

The source used consisted of an end-on view of a discharge through a ceramic capillary tube. Fig. 4 shows a cross-section through the arrangement. The capillary tube A is made from recrystallized alumina. It is 10 mm long, 10 mm in diameter and has a bore of 1 mm. The molybdenum anode B is attached to the stainless steel envelope C, while the cathode D is fixed to a tungsten rod which is sealed into the glass tube E. The arrangement consisting of the glass tube F, metal pieces G and H and O-rings J and K enable the capillary to be easily replaced when worn. Current is fed in through the e.h.t. plug L, *via* the sliding joint M, this facilitating the dismantling of the assembly. A quartz window N seals the front of the lamp with an O-ring, while the plate P seals the rear and has a glass-to-metal seal to the tube E. The side-arm Q has a dial pressure gauge attached, while R leads to a vacuum tap and union.

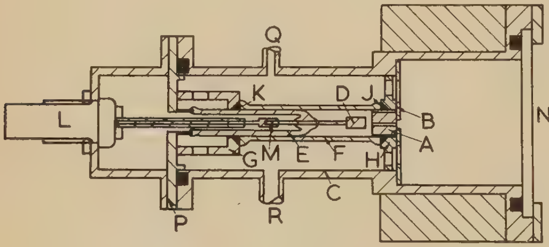

Fig. 4. The calibration source

The lamp was used filled with air to a pressure of 20 mm of mercury, but was found to be rather insensitive to the pressure or nature of the gas. The current pulse was provided by discharging a five-element artificial "line" through a matching resistor in series with the event using a series triggered spark gap. The "line" was charged to 10 kV, and when discharged through 4 Ω, gave a flat-topped current pulse of 1200 A for about 15 μs. The light output was found to be a continuum, overlaid with a few absorption lines, and a time-resolved spectrum showed it to be constant with respect to time over the period of 15 μs. Fig. 5 shows such a record, having a line spectrum in the early and later stages, and the constant continuum in between. Measurements with a monochromator and photomultiplier showed that the light output was constant to better than 5% over this time and followed the current curve closely. The monochromator was used to calibrate the lamp against a standard source consisting of a tungsten strip-filament lamp in a quartz envelope. This was done at a number of wavelengths in the visible and ultra-violet regions, and the emission was found to follow closely that of a black body at 26 000° K.

The lamp has been used for calibrating quartz spectra from the pinch discharges. An optical method is used for recording the wedge to calibrate the emulsion response. Use is made of the fact that the aperture of the spectrograph is rectangular in shape. A knife-edge is inserted in the spectrograph at a suitable position between the slit and collimating lens. This presents a horizontal edge on the optic axis of the system. Any point on the slit can then only transmit light to a portion of the aperture of the spectrograph, this portion increasing linearly from zero to the full aperture along the length of the slit. This device can be seen mounted on the side of the spectrograph in Fig. 2. This knife-edge was used when photographing the calibration lamp, and moved out of the beam for records of the event.

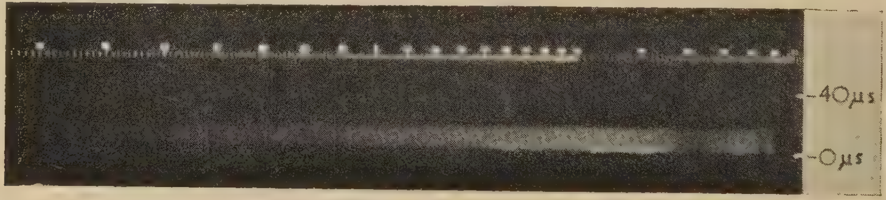

Fig. 5. A time-resolved record of the calibration source.

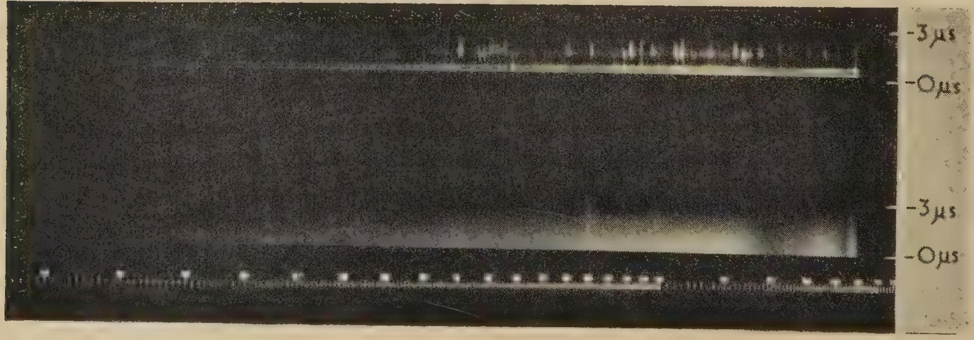

Fig. 6. A typical calibrated record

A typical calibration plate is shown in Fig. 6. This contains wo spectra, both recorded at $3 \cdot 0$ mm/μs and $0 \cdot 1$ μs esolving time. One is of an event and the other is the alibration lamp, using only the flat-topped portion and with he linear wedge in position.

The vacuum ultra-violet region

Work is now proceeding towards the extension of many of these techniques to the vacuum ultra-violet region, i.e. 500 to 2500 Å. An instrument is under construction$^{(6)}$ which is designed to record time-resolved photographic spectra in this region, and it is hoped to report further on this project at a later date.

Acknowledgements

Thanks are due to Mr. I. Maddock and Mr. R. J. Wilson of this Establishment for their continued support and discussions of this work, and also to those sections of the Establishment responsible for the construction of the rotor and for other engineering services.

The contents of this paper formed part of a contribution presented at the Fifth Conference of the International Commission for Optics, Stockholm, August 1959.

References

(1) Thackeray. *J. Sci. Instrum.*, **35**, p. 248 (1958).
(2) Lukyanov and Sinitsin. *Zh. Eksper. Teor., Fiz.* No. 4 (1958); and *2nd U.N. Conference on Peaceful Uses of Atomic Energy*.
(3) Gabriel. *U.K. Pat. App. No.* 18776/59.
(4) Gabriel, Howell, Thornton and Wilson. *J. Sci. Instrum.* To be published.
(5) Mees. *Theory of the Photographic Process*, 2nd ed., p. 212 (London: Macmillan and Co. Ltd., 1954).
(6) Gabriel. *U.K. Pat. App. No.* 14933/59

An electromicrobalance for weighing fibres

by F. R. MORGAN, B.Sc., A.Inst.P., British Leather Manufacturers' Research Association, Milton Park, Egham, Surrey

Abstract

An electromicrobalance is described that has a capacity of about $1 \cdot 5$ *mg and weighs to about* 1 μ*g*.

Introduction

To obtain a reliable estimate of the weight of a fibre it is necessary to weigh to about one millionth part of a gram. The electromicrobalance described in this paper does this quickly and conveniently. A somewhat similar balance has been described by Hales and Kynaston.*

The apparatus

The apparatus consists of a moving coil milliammeter movement used as a torsion balance. This is shown in Fig. 1, and the associated electrical control circuit in Fig. 2. The meter, *B*, was taken from a Royal Air Force visual indicator, and had a full-scale deflexion of 750 μA. It was mounted in a dust-proof Perspex box, *D*, and the pointer, *P*, was fitted with a small scale pan, *S*, made from thin aluminium foil supported by a fine nichrome wire. The suspension was approximately counterbalanced with small pieces of aluminium foil, *W*, cemented in position. The handle, *H*, mounted on top of the case, was connected to the meter zero adjustment through a length of 6 B.A. threaded rod; this allowed the final setting of the suspension to be made quickly and accurately.

The equilibrium position of the pointer was determined by alining it with the cross-wires in the eyepiece of the microscope *C*. A weight placed in the scale pan deflects the pointer, and a current is then passed through the meter movement to return it to the equilibrium position. This current was varied by altering the resistances R_{3-6} (Fig. 2) and measured on the meter *M*, a 4 in. dial Unipivot meter (by Cambridge Instrument Co.) shunted to give a full-scale deflexion of $1 \cdot 2$ mA.

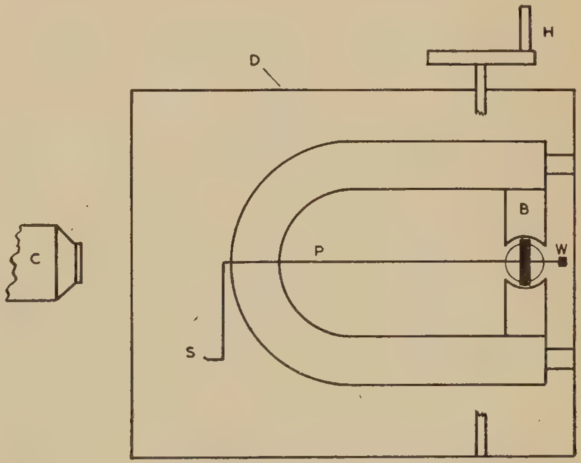

Fig. 1. Diagram of microbalance

B, meter movement; *C*, microscope; *D*, dust-proof Perspex box; *H*, zero adjustment handle; *P*, pointer; *S*, scale pan; *W*, counterbalance weights

The balance was calibrated by using small known weights of very thin copper wire. They were put on the scale pan and the current required to return the pointer to the equilibrium position was found. The balance shunt and series resistances were set so that a weight of 1 μg was equivalent to a current of approximately 1 μA. A graph of current against weight is shown in Fig. 3. A linear relationsh exists between these variables since all measurements ar made with the balance movement in the same position.

---

* Hales, H. L., and Kynaston, J, *The Analyst*, **79**, p. 702 (1954).

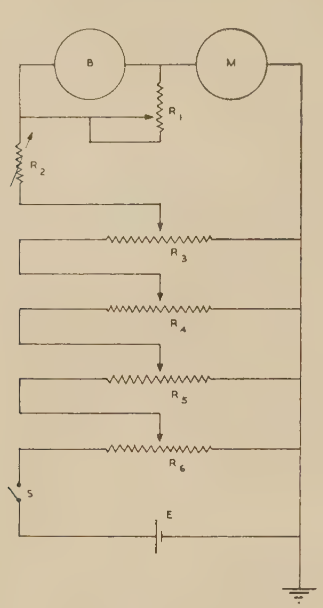

Fig. 2. Circuit diagram

B, electromicrobalance; *M*, Cambridge Unipivot meter and range box; R_1, balance shunt; R_2, series resistance; R_3–R_6, wire wound potentiometers, each 500 Ω; *S*, switch; *E*, dry cell, 1·5 V

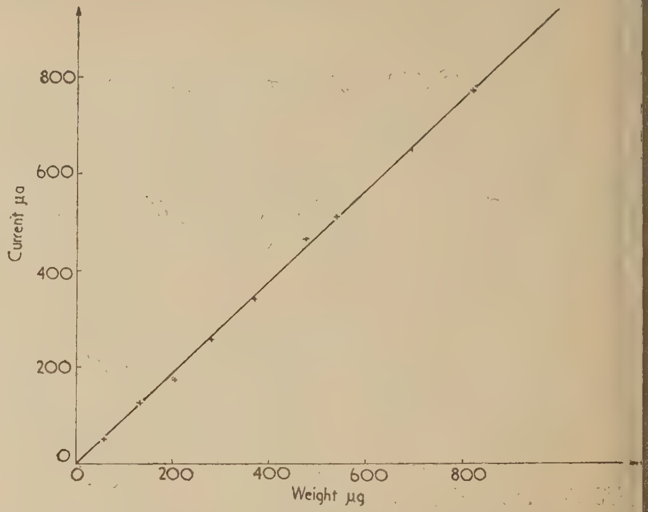

Fig. 3. Graph of current in μA against weight in μg

Acknowledgement

This paper is published by kind permission of the Directo and Council of the British Leather Manufacturers' Resear Association.

Portable airglow photometer

by B. J. O'BRIEN,* B.Sc., Ph.D., Antarctic Division, Department of External Affairs, Melbourne, and G. DE LA HARPE,† Ionospheric Prediction Service, Sydney

[*Paper first received* 6 *August*, 1959]

Abstract

A simple, direct-reading and sensitive photometer which is easily transported and is independent of external power supplies is described. Details of the optical system and the electronic circuitry are given, and the performance of the apparatus is discussed.

Many workers have used photometers to detect weak auroral and airglow emissions (see, for example, references 1, 2 and 3). In general, the instruments used in these investigations have been complex and necessarily located at a permanent station. In the studies of airglow and aurorae being carried out by the Australian National Antarctic Research Expeditions (ANARE) it has been found desirable to have a simple, direct-reading and sensitive photometer which can be transported easily and which can be operated independently of external power supplies. Such a unit has been designed and was used on the ANARE ship, m.v. *Magga Dan*, during her voyage to the Antarctic early in 1959. The apparatus is described in this paper. The basic features of the optical system are illustrated in Fig. 1.

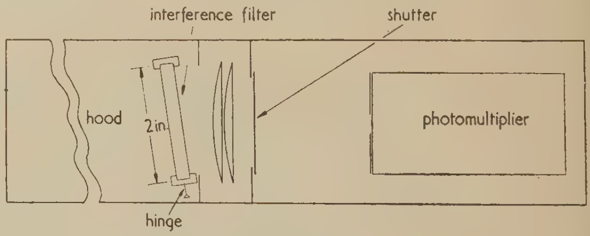

Fig. 1. Basic features of optical system of photometer

The light detector is a photomultiplier (E.M.I., type 6256 A) with very low dark current, of order 100 pulses per second at 20° C. The photocathode of nominal diameter 10 mm is the field stop of a lens of focal length 118 mm and

---

[*] Now at Department of Physics, State University of Iowa, Iowa City.

[†] Now with Australian National Antarctic Research Expedition at Wilkes.

aperture 74 mm. A camera shutter, operated by a cable release, is between the lens and the photocathode.

Spectral resolution is obtained by the use of narrow-band multi-layer interference filters (from Baird-Atomic Inc.). Three filters of less than 10 Å bandwidth (measured at half-maximum intensity) are used in measurements of Hβ and NaD, and several other filters of about 50 Å bandwidth have their peak transmission at other emissions of interest. Maximum transmission of the filters, complete with blocking filters, ranges from 25 to 70%. Most of the filters are two inches square, while several control filters are one inch square.

Filters are mounted in front of the lens, and two filters may be interchanged in about thirty seconds. A filter in its holder may be tilted rapidly to any angle of incidence θ between 0 and about 25 deg. In this way, a spectrum can be scanned over a range which is about 3% of the wavelength of maximum transmission at normal incidence ($\theta = 0$ deg.).

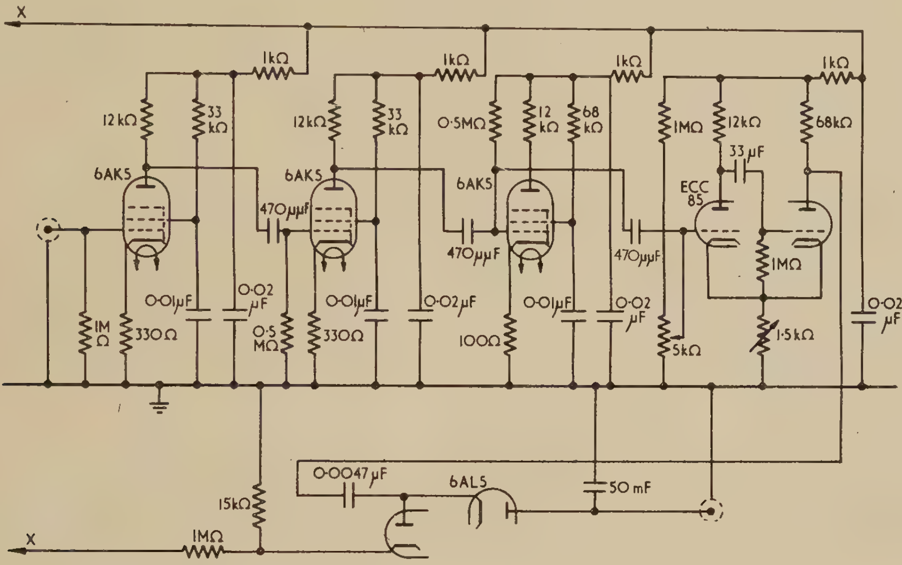

Fig. 2. Circuit diagram of portable photometer ($X = 110$ V)

The photomultiplier pulses are amplified one hundred-fold, and fed to a discriminator and univibrator. The output of the latter is taken to a ratemeter with a time constant of the order of one second. The meter is an Avometer Model 8, and the sensitivity is changed by switching to one of the 50 μA, 250 μA or 1 mA ranges. The circuit is shown in Fig. 2. The ratemeter is linear to within 5% up to 2500 pulses per second with the components as shown. This range may be extended if necessary by decreasing the time constant of the univibrator. Alternatively, for studies of bright emissions, the filter may, of course, be stopped down.

All voltages are supplied by dry cells. The useful lifetime of the batteries is dependent on their duty cycle and temperature. For instance, with continuous operation for two hours a day at about 40° F, the minimum useful life of each set is approximately three months. The batteries are placed in a box which is thermally insulated inside with sheets of Isolite two inches thick. A thermostatically controlled 100 W heater is placed in the box for use if external power should become available. Total weight of the batteries and box is about 80 lb, and the dimensions of the box are about 3 × 2 × 1½ ft.

The electronic components other than the tank circuit are mounted on the brass tube which contains the photomultiplier. This is then mounted on a stand which is fixed to the lid of the battery box. A sighting device is fitted, and the apparatus can be set quickly at any altitude and azimuth angles. Thumbscrews hold the Avometer and a box containing spare filters in position on the battery box. The box is sprayed with waterproof paint and a rubber gasket is fitted to the lid.

The use of only a single lens minimizes optical losses. The peak transmission of the filters is quite high. The two filters of least bandwidth (about 6 Å) with peak transmissions near Hβ and NaD have maximum transmission of 45 and 26% respectively. The limit to the sensitivity is set by Poissonian fluctuations in the number of pulses fed to the ratemeter, by the photomultiplier dark current, and by light of other wavelengths being passed by the filter. However, with specially selected photomultipliers, the limiting sensitivity can be brought to as low as several Rayleighs(4) of Hβ and of the order of ten Rayleighs of NaD. This instrument thus compares very favourably with others. An activated zinc-sulphide screen provides a standard light source.

The high sensitivity of the instrument was used in a study of the NaD nightglow in the summer of 1959. (In the summer, the NaD nightglow has(4) a minimum value of the order of 100 Rayleighs.) On the night of January 9, a typical signal through the NaD filter was 10·5 μA at $\theta = 0$ deg., 8·0 μA at $\theta = 5$ deg., 6·4 μA at $\theta = 10$ deg. and 6·4 μA at $\theta = 15$ deg. The dark current was 0·7 μA. The NaD intensity can then be taken as 4·1 μA. Correction for background light using this technique is not wholly satisfactory. However, it is certainly more effective than the technique which is often employed, in which a separate control filter is used with peak transmission perhaps 400 Å from the studied emission.

The instrument has also been used in NaD twilight studies in Melbourne. Since a mains power supply was available for these measurements, the electronic circuitry has been modified, and the output has been fed to a pen recorder. The versatility of the instrument is such that it has been possible to measure continuously the intensity of NaD from that in very early twilight to the residual nightglow. The results of measurements using this photometer will be reported elsewhere.(5)

Acknowledgements

The authors acknowledge with thanks the valuable assistance given by members of the Australian National Antarctic Research Expedition to Wilkes, and by the crew of the *Magga Dan*. The authors are indebted to Dr. F. Jacka for many helpful discussions, and to Messrs. J. Ballantyne and J. Nisbet for constructing the photometer so well and so rapidly.

References

(1) ELVEY, C. T., and ROACH, F. E. *Ap. J.*, **85**, p. 213 (1937).

(2) ST. AMAND, P. *Ann. Geophys.*, **11**, p. 435 (1955).

(3) OMHOLT, A. *Geofys. Publik.*, ***XX***, No. 11 (1959).

(4) HUNTEN, D. M., ROACH, F. E., and CHAMBERLAIN, J. W *J. Atmos. Terr. Phys.*, **8**, p. 345 (1956).

(5) O'BRIEN, B. J. *J. Geophys. Res.* To be published.

Direct method for determining the velocity of nuclear particles

by B. F. HAMPTON, Ph.D., D.I.C.,* Dept. of Electrical Engineering, Imperial College, London

[*Paper received* 20 *August*, 1959]

Abstract

A new method of directly determining the velocity of nuclear particles in a cloud chamber is described. It is not necessary to know the mass or charge of the particle, and measurements of radius of curvature are not involved. The principle is to make the cloud chamber in the form of a resonant microwave cavity, the electric field in the cavity being very close to breakdown. Under these conditions additional ionization takes place when the electric field is a maximum, i.e. twice per cycle, resulting in a track that is modulated in intensity. With an applied field of 3000 Mc/s *the time marks are spaced at intervals of* $2 \cdot 7$ *mm for an* α*-particle having an energy of* $5 \cdot 6 \times 10^6$ *eV. The apparatus is described, and a method of feeding* 85% *of the output of a magnetron into a resonant cavity is given. A certain amount of success was obtained using hydrogen as the working gas. Limitations of the apparatus are discussed and further improvements suggested.*

Introduction

In a Wilson cloud chamber the momentum of a nuclear particle may be determined by measuring the radius of curvature of the track when the chamber is placed in a magnetic field. If the mass of the particle is known, then its velocity follows—if it is not known, the particle must first be identified by means of characteristics such as ionization density or recoil electrons. Alternatively the mass could be directly determined from a measurement of the particle velocity, and Gabor(1) has suggested that this be accomplished by marking the particle track at known equal intervals of time. The apparatus developed to investigate this new approach will be described.

Principle

Time marks on a particle track are produced by an intense oscillating electric field, and it is evident from the high velocities of nuclear particles that fields of radio frequency must be used. The cloud chamber is made in the form of a resonant microwave cavity, and since the time marks appear at every maximum of the electric field, i.e. twice per cycle, a convenient frequency of 3000 Mc/s gives a time spacing of $1 \cdot 67 \times 10^{-10}$ s. At the velocity of light this corresponds to a distance of only 5 cm and so in principle gives no upper limit to the velocity that can be measured—for an α-particle having an energy of 5×10^6 eV the spacing would be about $2 \cdot 6$ mm.

A necessary requirement for the successful modulation of a track is that the peak electric field strength should be raised to a level at which the gas/vapour mixture in the chamber is just below the point of breakdown, since it is only then that sufficient extra ionization will take place and modulation result. Under these conditions at the peak of each half cycle an electron liberated in an ionizing collision will gain sufficient energy from the electric field to enable it to make additional ionizing collisions that it would not make in the absence of the field. This extra ionization, which appears after condensation as a periodic thickening of the track, falls so rapidly with field strength that the modulation is sharply defined and not sinusoidal in appearance.

This in itself, however, is not sufficient—it must further be ensured that *only* the electrons released at the peak of the electric field are multiplied, and that the electrons released at all previous times are not affected. Only in this way can a periodic, and not a general, thickening of the track result. In a gas having a strong electron attachment, such as chlorine or Freon, the average life of a free electron at atmospheric pressure is less than one half-cycle of the applied field. Few electrons would then survive until the next half-cycle, and a modulated track may be expected. It is unfortunate that these gases necessarily have a high breakdown strength, and the r.f. power required to achieve such an intense field was far greater than that available. Suitable powers (of the order of 100 kW) to produce such fields are of course readily obtainable in pulses of one or two microseconds, and had an accelerator been available which would have produced a few tracks of interest in that time the power source would have presented no problem. The weak radio-active source that was used, however, required about 10 ms to produce sufficient particles, and this pulse length is virtually equivalent to continuous working for r.f. power sources.

---

* Now at Vickers Research Ltd., Sunninghill, Berks.

A powerful experimental magnetron, type VX 3043, was kindly made available for this work by the General Electric Co. Ltd., but even with this it was not possible to obtain more than 2·2 kW continuous output. This limitation in power precluded the use of chlorine or Freon, and limited the experimental work to other gases, notably hydrogen, which have a very much lower breakdown strength. The electron attachment of hydrogen is negligible, but fortunately other processes become important which enable an electron in an atmosphere of hydrogen to lose energy very quickly. Due mainly to the small mass of the hydrogen molecule the energy lost by the electron in elastic collisions is high, and a calculation involving the total energy loss by both elastic and inelastic collisions reveals that in hydrogen at 0·8 atm pressure an electron starting with an energy of 2500 eV has its energy reduced to less than 9 eV in 10^{-10} s. If an electron which has such a low energy is then subjected to one half-cycle of the electric field, the energy gained from the field will not be sufficient to raise it to the ionization energy of hydrogen and therefore it cannot contribute to any further ionization. Since the application of the r.f. field results in additional ionization by only those electrons which do not have energies less than 9 eV, i.e. those that were liberated during the last 10^{-10} s, a well-modulated track can be expected.

Apparatus

Resonant cavity cloud chamber. The cloud chamber (see Fig. 1) was made in the form of a rectangular microwave cavity resonating in the H_{101} mode, with a re-entrant plunger in the centre of the baseplate. Above this plunger was a Perspex window, also re-entrant, covered on the inside with fine metal gauze having about 100 t.p.i. The electric field was concentrated in the region below the window, and this constituted the useful volume of the chamber. A small loop of wire, insulated from the chamber and raised to a d.c. potential of about 200 V, surrounded the working volume and provided the potential gradient necessary to remove unwanted charged particles from previous expansions. Expansion of the chamber was effected through the perforated baseplate, which was lapped to the body of the chamber to ensure good electrical contact, and rendered gas tight with an "O" ring. A thin latex diaphragm isolated the chamber from a vacuum reservoir, the expansion ratio being determined by the height of an adjustable platform on to which the diaphragm settled when the expansion valve was opened. The operation of this valve was performed electromagnetically and controlled from a distant switch. Microwave power dissipated in the cavity maintained its walls at a temperature slightly above ambient, thereby keeping them free from the water/alcohol mixture which preferentially condensed on the cooler walls just above the diaphragm. This ensured that the resonant properties of the cavity were not impaired by the introduction of this liquid. All metal surfaces in the chamber were rhodium plated to prevent corrosion and maintain as high a Q-factor as possible.

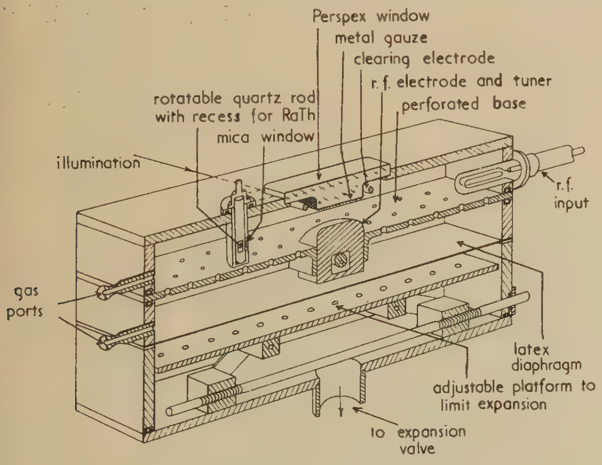

Fig. 1. Resonant cavity cloud chamber

It was decided in the first instance to attempt the modulation of α-particle tracks, because these were slow enough to undergo many half-cycles of 3000 Mc/s while passing through the small r.f. field region. Unfortunately α-particles have a maximum range in air at atmospheric pressure of only 8·6 cm, and since they also had to pass through two mica windows which reduced their range still further it was clear that the source had to be inside the chamber. The source had, of course, to be mounted and also pulsed in such a manner as not to affect the resonant properties of the chamber. This precluded the use of any metal in its construction, which would induce breakdown, and virtually limited the choice of materials to silica and polystyrene. A design that satisfied these requirements consisted basically of a silica rod attached to a ball race, so that it rotated freely inside a fixed polystyrene tube which was sealed into the chamber. The source of 0·1 mc radiothorium was contained by a flake of mica (1·5 mg/cm^2) in a small recess in the silica rod, and arranged so that at one period during its revolution it was opposite a window, also covered with mica, in the polystyrene tube. In this position a stream of α-particles was directed into the useful volume of the cavity—at all other positions of the silica rod the particles were stopped by the polystyrene tube. Rotating the rod did not affect its configuration and the resonant properties of the chamber were not affected. A remotely operated electro-magnetic system rotated the rod into the desired position to give the pulse, in synchronism with the expansion of the chamber.

The tracks were photographed through the top window, which was covered on the inside with metal gauze. A modified plate camera held in a frame above the window enabled six exposures to be taken on one $2\frac{1}{2} \times 3\frac{1}{2}$ in. HPS plate. It was required to operate the camera remotely, and this was arranged by an electro-magnetic cable release. Illumination was obtained from a 30 J xenon filled flash lamp, focused by a condenser lens on to a small window in the wall of the cloud chamber. The duration of the flash was nominally 1/600 s, and it was triggered by a synchronized switch in the camera shutter. Some difficulty was experienced due to multiple reflexions inside the highly polished cavity, and efforts were made to reduce these to an acceptable level. A certain improvement was gained by giving the wall opposite the illuminating window a matt black coating, but only at the expense of the electrical properties of the cavity. The problem was finally solved by using polarized light. A sheet of Polaroid was placed between the light source and the window in the cloud chamber, and a second sheet supported inside the cavity against the wall on to which the light fell. This sheet was polarized at right angles to the first, so that it transmitted no light. The small reflexion from its surface was not troublesome, and further since Polaroid is not very lossy the Q-factor of the cavity was little affected. Using this method of illumination, photographs were taken through the gauze window without the pattern of the gauze being seen on the plate, and with only slight reflexions from the re-entrant post.

Radio frequency system. The resonant cavity had a rather low Q of about 1000, due to the many modifications needed to convert it into a cloud chamber. R.f. power was coupled into the cavity by means of a magnetic loop, and much care had to be devoted to the design of the r.f. system to ensure that the maximum efficiency of operation was achieved. It is in general not possible to pulse a magnetron directly into a critically coupled high Q cavity because the frequency of the output is not constant during the pulse rise time. If the cavity is tuned to the stable r.f. frequency, it presents a mismatch during the initial phase of the pulse which may result in a change of mode and internal breakdown of the magnetron. During the pulse rise time the r.f. power was directed into two water loads. The loads, which were conical in shape and made of Pyrex glass, were placed in the side arms of a magic tee (see Fig. 2). All the magnetron power was dissipated here until the two r.f. switches in front of the loads fired—this probably took about a microsecond, by which time the pulse frequency was stable. The r.f. switches consisted of low pressure argon/mercury vapour discharge tubes fitted in low Q resonant irises at distances differing by one-quarter of the guide wavelength from the magic tee junction. Although these tubes were initially matched into the guide, once the discharge struck they reflected up to 90% of the incident power into the fourth arm of the magic tee. From there a coaxial cable led the power to the critically coupled cavity loop, which was cast in paraffin wax to prevent breakdown.

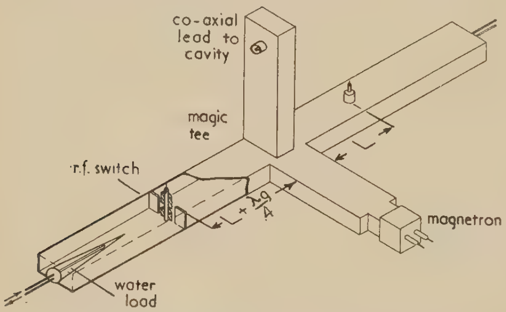

Fig. 2. Arrangement for feeding 85 to 90% of the magnetron output into a resonant cavity

In order to obtain powers of the order of 2 kW from the magnetron VX 3043, the cathode had to be maintained at a higher temperature than could be achieved by the heater alone. It was therefore operated continuously with 200 W output and pulsed four times per second with the full pulse of 5·3 kV, 0·8 A. With somewhat less than 50% efficiency, this gave an output of 2·2 kW for the 15 ms pulse.

Magnetron power supplies. The most important requirement in this work was to maintain the r.f. field in the chamber as close as possible to the breakdown level for the duration of the long pulse. This necessarily implied having the input pulse to the magnetron free from any ripple and also required means for adjustment of its level. The d.c. power was obtained from a large transformer feeding a six-phase half-wave rectifier, giving a fundamental ripple of 5·7% at 300 c/s. Smoothing was achieved by using a 50 H choke, in which an auxiliary power supply maintained a continuous direct current of the same magnitude as the pulse current taken by the magnetron (Fig. 3).

Immediately after closing switch S_1 to start the pulse, switch S_2 was opened and the auxiliary power supply P_3 open circuited. The choke instantaneously impressed its own pre-set current on the magnetron, and at the same time held the ripple to within $\frac{1}{2}$% peak to peak. The current then changed exponentially from its initial pre-set value to the ultimate value determined by the rectifier output and the magnetron characteristics, with a time constant of 5 ms Final adjustments were then made to equalize the pre-set and ultimate values of the choke current. This adjustment was helped by measuring the voltage developed across the switch S_2 when it was opened—for optimum results this must be a minimum. At the end of the pulse S_2 was closed before S_1 was opened, thus avoiding excessive transient voltages. Before every experiment a number of trial runs were made, adjusting the magnetron current until breakdown occurred in about 50% of the trials.

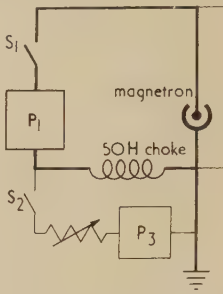

Fig. 3. Magnetron pulsing circuit

S_1, high voltage switch to pulse magnetron; S_2, auxiliary choke current switch; P_1, magnetron pulse power supply; P_2, magnetron "keep alive" power supply; P_3, choke current power supply

Timing system. A rotary spark gap S_1 was used to provide the main magnetron pulse (Fig. 4). Two fixed tungsten electrodes were bent into an arc of a circle and displaced from each other around its circumference. Two further tungsten electrodes attached radially to a rotating Perspex disk and joined at their inner ends were positioned to short out the two fixed electrodes during part of their revolution. This system had the advantage of not needing high voltage slip rings on the rotating member, and also splitting the arc formed on breaking into two smaller arcs which could conveniently be placed under the poles of a powerful permanent magnet. The shaft rotated four times per second, and the switch was dimensioned to give pulses of 15 ms duration. A second low-voltage switch operated by a cam mounted on

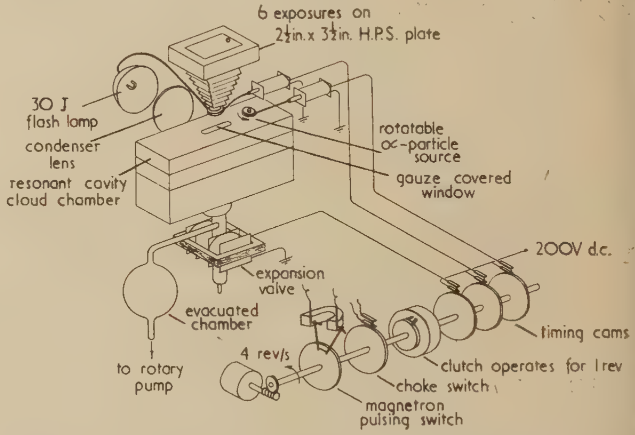

Fig. 4. Schematic arrangement of the timing system and cloud chamber ancillary apparatus

the same shaft switched the choke in and out of the circuit at the appropriate times.

The remaining operations for using the cloud chamber, namely, opening the vacuum release valve, rotating the α-particle source and operating the camera shutter, were actuated by electrical contacts closed by adjustable cams on a second shaft. This shaft, which was in line with the first, was normally stationary, but by means of a clutch mechanism could be locked on to the continuously rotating shaft in a predetermined position for one complete revolution. By this means the cloud chamber operations could be controlled relative to the magnetron pulse over a period of 250 ms.

The procedure adopted in setting up the cavity was as follows:

(1) Using continuous illumination the expansion ratio and timing of the α-particle pulse was adjusted relative to the opening of the expansion valve to give the best tracks.

(2) The flash tube was connected and the camera delay adjusted to about 75 ms.

(3) The r.f. pulse was switched on at moderate power and the cavity tuned to resonance.

(4) The magnetron switches were set to make the r.f. pulse coincident with the particle pulse.

(5) Breakdown of the gas was obtained with the chamber expanded, then the power level was reduced to just below breakdown.

(6) The chamber was flushed with clean gas, the camera shutter was set.

(7) The clutch was operated to connect the cam timing system to the rotating shaft.

Experimental results

About 400 photographs have been taken in hydrogen, and 210 of these led to gas breakdown. Of the remaining there were two photographs that showed signs of modulation (Fig. 5).(2) The measured modulation spacing of these was 2·7 mm, which is in good agreement with an expected α-particle energy of about $5 \cdot 7 \times 10^6$ eV, and an applied field of 3000 Mc/s.

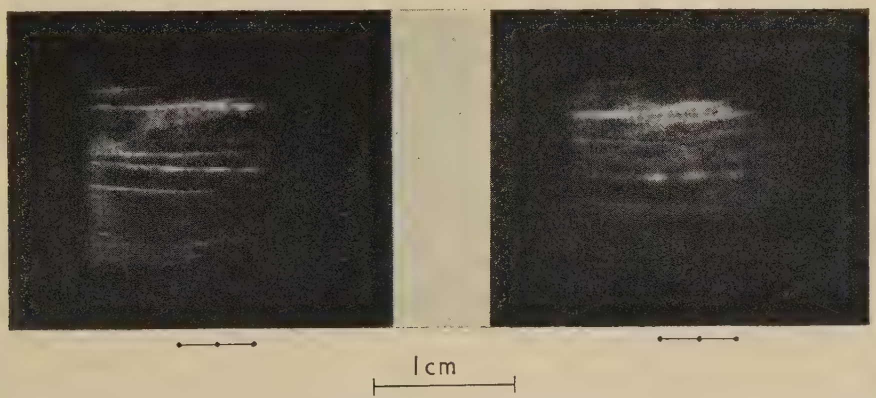

[Reproduced by courtesy of *Nature*]

Fig. 5. α-particle tracks in hydrogen, modulated at 3000 Mc/s

The evidence for modulation presented by these two photographs might not appear at first sight very convincing, and other causes such as the non-uniform expansion of the chamber through the regularly spaced holes in the perforated baseplate or some masking effect of the gauze covering the window could well be suspected. The modulation distance bears no apparent relationship to any of these dimensions, however, and none of the several hundred tracks taken without a high frequency field showed any signs of modulation. Moreover, a closer examination of the limits of experimental accuracy reveals that the result obtained is quite in keeping with what can be expected from the apparatus. The theory of avalanches shows that for modulation to occur the electric field in the cavity must be within about 1% of the intensity that would cause a breakdown in the gas—in fact the phenomenon of time marking might well be regarded as the initial stage of an interrupted breakdown. The important question is in what percentage of the tests was the field strength within this limit, and for what time?

The accuracy to which the mains input voltage to the magnetron power supply could be adjusted was approximately 1%, and this caused a change in the r.f. power output from the magnetron of no less than 13%. Since the field strength in the cavity was proportional to the square root of the input power, this variation produced a change in the electric field of 6%. By inserting a 50 H smoothing choke in series with the magnetron the ripple from the high voltage rectifiers was reduced to $\frac{1}{2}$%, which gave rise to a 3% ripple on the r.f. field in the cavity. Further, the auxiliary choke current was only controllable to within 1%. These three factors, namely, tolerance in setting the mains voltage, tolerance in setting the choke current, and ripple on the pulse voltage, were the main considerations in determining the time during which the chamber was operating within the required field limits. Taking these three factors into account, an investigation was made to determine how the field strength in the cavity varied during the pulse. This showed that there is, over a large number of pulses, a useful time of only 3% in all those pulses that did not lead to breakdown. Unless one of the half-dozen tracks which appeared in one photograph happened to occur in this period, there would be no modulation. In addition to this the field was uniform to within 1% of the maximum in not more than about 10% of the volume covered by the windows—note that the two modulated tracks appear to be in the same position.

Experimentally, two modulated tracks have been found in 190 photographs, each of which contained three or four tracks sharp enough to show modulation had it been present. This corresponds to an experimental yield of about 1/3% which, although small, is of the same order as that expected from the above considerations.

Conclusions

Because of the power limitations it has only been possible to demonstrate a somewhat marginal effect in hydrogen, a gas having a negligible electron affinity. The evidence for modulation presented here is felt to be sufficiently encouraging to warrant further work. In this respect the availability of higher r.f. powers would enable the experimental range to be extended and include promising gases having a high electron affinity, where the chance of success would be much greater. This requires the use of one or more large klystrons with a total output of 50 to 100 kW, or, alternatively, the use of strong particle bursts of microsecond duration. It may be noted here that mesons, as well as being more interesting than α-particles, are particularly suited to modulation by virtue of their less saturated tracks.

For higher powers a cylindrical cavity would be preferred, tuned as before by varying the distance between re-entrant posts. It has been found unsatisfactory to make one re-entrant post of gauze and to photograph through it, because this not only renders photography troublesome, but also makes it difficult to produce a uniform field in the gap. A better proposition would be to turn solid metal posts to their exact profile, making the surfaces very smooth, and to photograph through a window in the side wall of the chamber. Illumination through another window almost opposite to the camera would permit the use of a small scattering angle and consequent high scattered intensity. Polarized light could be used as before, although it may be preferred to allow a collimated light beam to leave the chamber through a window diametrically opposite to the illuminating window.

Acknowledgements

The author wishes to record with gratitude the enthusiasm of Prof. D. Gabor, of Imperial College, to whom this idea is due, and who gave such experienced advice and encouragement during the course of the work.

This project was financed by the Royal Society Paul Instrument Fund, and we are most indebted to the Paul Instrument Fund Committee. Our thanks are due also to Prof. J. G. Wilson for his expert advice on cloud chamber techniques, and for his constant interest.

The General Electric Company were most helpful in loaning their experimental magnetron without which the work could not have been carried out.

References

(1) Gabor, D. *Conference Report on Cloud Chamber Techniques*, University College, London, p. 211, 1956.

(2) Gabor, D., and Hampton, B. F. *Nature* (*London*), **180**, p. 746 (1957).

Recording calorimeter for the measurement of heats of wetting, mixing, or solution

by F. A. P. MAGGS, Ph.D., F.R.I.C., and P. H. SCHWABE, B.Sc., War Department, C.D.E.E., Porton, Wilts.

[*Paper first received* 24 *August, and in final form* 9 *October*, 1959]

Abstract

A calorimeter has been designed for the measurement of heat liberations of less than 50 *cal. Automatic temperature recording with variable amplification has been linked to the measuring thermocouples to produce a permanent record of temperature changes in the calorimeter. Magnetically operated stirring and reaction initiation* (*by bursting an evacuated bulb containing adsorbent or reagent*) *are employed. Electrical calibration is made for each system before and after bursting the bulb. The use of the calorimeter in measuring the heat of wetting of charcoal and the heat of mixing of water and methanol is demonstrated. Application of the calorimeter to other thermometric procedures within the mechanical limitations of the instrument is discussed.*

Introduction

In the course of examination of the sub-microscopic pore structure of charcoal, measurement of the heat developed on wetting the charcoal with various liquids was required. From such measurements information relating to the extent of the surface, the size of the pores, the heat of adsorption, and the adsorption mechanism may be derived.

A calorimeter was required, capable of dealing with gramme quantities of evacuated charcoal. For measuring heat liberations from ½ to 50 cal with an accuracy of ±2%, and for systems involving slow heat liberations, a recording calorimeter was highly desirable. No one calorimeter described in the literature complied with these requirements and the following instrument was therefore developed.

The apparatus

Constructional Details (Fig. 1)

The Dewar vessel. A glass Dewar vessel—inside diameter 2·9 cm—made from a B.34 socket, is silvered on the evacuated surface, except for a narrow observation window. It is attached by spring clips to, and is co-axial with, the solenoid which surrounds it.

A B.34 cone forms a vacuum jacketed, extended stopper and the whole calorimeter is immersed in a temperature-controlled bath.

The thermocouples. The thermel of 10 working and 10 reference junctions is made from 100 cm lengths of 40 s.w.g. enamelled copper and 40 s.w.g. constantan wires. To form a junction, a portion of the ends of the copper and constantan pair are cleaned by heating and plunging into absolute alcohol. The ends are twisted together and held in a small vice which forms the earth side of a potential of 30 V. The line side is a carbon rod which is just touched onto the ends of the twisted wires to fuse them together. As each junction s made it is electrically insulated by dipping it into a Perspex-chloroform gel. The lead wires from the thermel are 30 s.w.g. copper wire, and the total resistance is $490\ \Omega$.

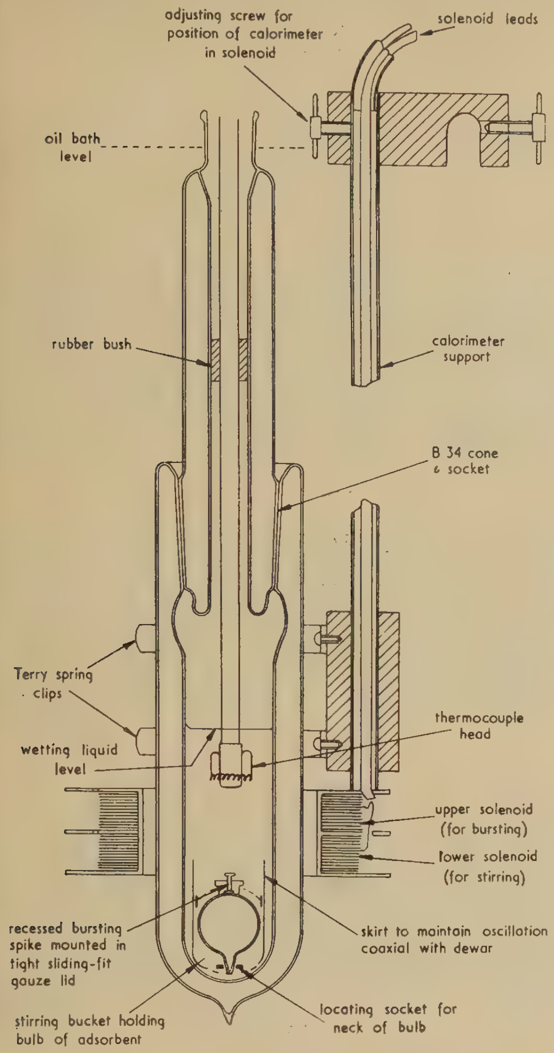
adjusting screw for position of calorimeter in solenoid
solenoid leads
oil bath level
rubber bush
calorimeter support
B 34 cone & socket
Terry spring clips
wetting liquid level
thermocouple head
upper solenoid (for bursting)
lower solenoid (for stirring)
recessed bursting spike mounted in tight sliding-fit gauze lid
skirt to maintain oscillation coaxial with dewar
stirring bucket holding bulb of adsorbent
locating socket for neck of bulb

Fig. 1. Recording calorimeter

The working junction (Fig. 2). A copper collar (1 cm long, 0·6 cm i.d., and 0·05 cm wall thickness) is cemented with Araldite to a 0·6 cm (o.d.) glass tube, 30 cm long. Into the copper collar are soldered, radially, five arms of about 3 cm length of insulated 26 s.w.g. copper wire as supports for the calibrating heater. The ten junctions are fanned out inside the copper collar and held in place by a small insulated copper cone. A copper cap is soldered to the collar to make a liquid-tight joint. The heater leads are taken up the outside of the glass stem.

The reference junction. The ten couples of the cold junction are fitted into an electrically insulated copper tube held in a mass of copper turnings (to give large thermal inertia) in a silvered Dewar vessel totally immersed in the oil bath.

The calorimeter. The adsorbent or reagent is contained in a thin walled evacuated glass bulb (diam. 2 cm). This bulb is held in a light cylindrical iron bucket which by its vertical oscillations co-axial with the Dewar vessel, under the influence of the external solenoid, also forms the stirrer. The adjustable top of the bucket carries a small spike with which the bulb is burst by applying a momentary potential of 230 V to an upper solenoid (Fig. 1) identical in construction with that described in the next section.

The thermocouple head—held coaxially with the Dewar vessel in the stopper—is immersed in 45 ml. of the wetting liquid.

The stirring. The stirring is provided by the bulb and its retaining cage being caused to reciprocate under the influence of an external solenoid consisting of approximately 650 turns 26 s.w.g. insulated copper wire on a brass skeleton 5·5 cm diam. and 2 cm depth. The lower solenoid is energized at about 30 V with on-off intervals variable between 30 and 80/min, clock controlled and adjustable to suit liquids of various viscosity and bulbs of different weight.

Fig. 2. Thermocouple head

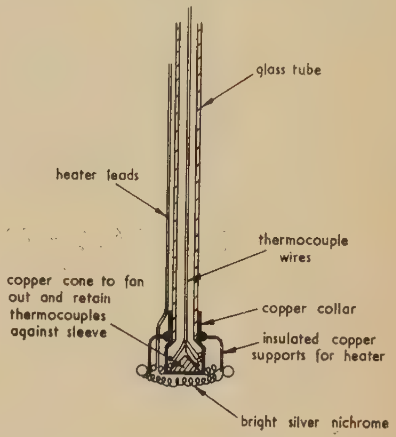
glass tube
heater leads
thermocouple wires
copper cone to fan out and retain thermocouples against sleeve
copper collar
insulated copper supports for heater
bright silver nichrome

Prior to bursting the bulb, the work required to raise the cage and bulb is less than after breakage due to the higher buoyancy of the unbroken bulb. Since an alteration of the solenoid potential during an experiment is undesirable as it affects the thermal equilibrium of the system, the minimum potential required to raise the cage after the burst is fixed by a preliminary experiment (about 30 V). The solenoid is adjusted so that the bucket has the maximum stirring movement without touching the thermocouple lead.

The calibration heater. For calibration a small coiled nichrome heater, resistance $60\ \Omega$, with 30 s.w.g. copper leads is affixed to the thermocouple head. The potential and current (supplied by a 12 V accumulator) are measured on Sangamo-Weston sub-standard instruments (readable to better than $\frac{1}{2}$% in the working range). For potential measurements, leads of fine wire are taken from the short copper current leads. For greater accuracy (better than 0·05%) current can be measured by means of the potential across a standard resistance, using a Tinsley potentiometer, which also offers an alternative measurement of heater potential.

The bath. A 25 gal iron cistern is used as a container. This is set in two surrounding wooden boxes with asbestos lagging between them. The top of the bath is screened with a Cellophane cover.

To minimize insulation trouble, paraffin oil is used in the bath. Temperature control is achieved by a benzene-mercury glass regulator of high area/volume ratio coupled with a triode operated relay(1) and is within 0·001° C. The heating element is a 12 V, 60 W bare Nichrome coil. The bath is agitated by a large paddle.

The measuring circuit. The output from the thermocouples passes into a Sunvic d.c. amplifier, via a simple potentiometer circuit R_1 for adjustment to zero output before a heat liberation. The amplifier output is fed across a $10\ \Omega$ potential divider R_2 so that a selected portion of it may be recorded by a Cambridge quick-acting recorder (2 s response) having full-scale deflexion of 1 mV (readable to 2 μV). All isolated metal parts of the apparatus are earthed with low resistance leads and screened cable is employed. R_1 and R_2 are decade boxes of high quality. All junctions are shielded from ambient temperature fluctuations.

Procedure

Sample preparation (applicable to charcoals). Tared thin walled glass bulbs are filled with oven-dry charcoal and after a preliminary evacuation at 100° C and 10^{-1} mm mercury are sealed on to weighed glass taps* and re-evacuated at 120° C and 10^{-5} mm mercury for 15 h. The bulb and tap are then reweighed to constant weight to determine the weight of dry charcoal, prior to sealing off at the construction.

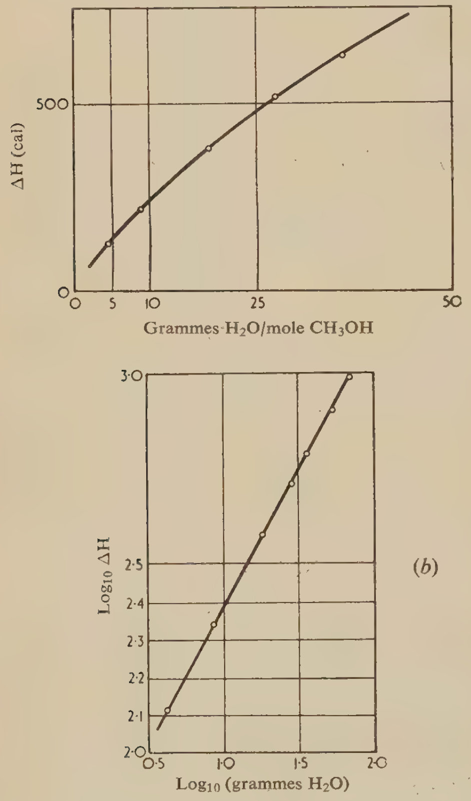

Fig. 3. (*a*) Graph showing curved relationship between concentration of water and heat of mixing. (*b*) Graph showing linear relationship between $\log_{10} x$ and $\log_{10} \Delta H$

Experimental. The bucket containing the evacuated bulb held as shown in Fig. 1 is slid into the Dewar vessel holding 45 ml. of the wetting liquid and the thermocouple head is inserted, using silicone grease to form an oil-tight seal.

The stirrer mechanism is switched on, the solenoid potential and timing adjusted and the apparatus is allowed to attain thermal equilibrium. Any e.m.f. developed from heat of stirring is backed off to zero and the trace recorded for five minutes. A measured amount of electrical energy is passed through a calibration coil, the cells having been allowed to stabilize by discharge through a dummy coil for at least an hour before use. The system is left for five minutes after calibration after which time excess e.m.f. may be backed off and a new trace started. The bulb is then burst by momentarily switching a high potential to the upper solenoid, and the temperature change due to the reaction under investigation is recorded on the chart. The calibration is then repeated.

Performance

Sensitivity. Examples of the calorimeter performance are shown in Figs. 4(*a–d*). Rapid heat liberation is typified by the system charcoal/methanol [Fig. 4(*a*)] whilst the slower penetration of benzene into a coal structure is apparent in Fig. 4(*c*). An example of the use of the calorimeter in recording very slow heat liberations is given by the heat of wetting of a carbonized coal by methanol [Fig. 4(*d*)]. Between 1 and 1·5 g carbon were wetted in these experiments. Fig. 4(*b*) records the response of the calorimeter, at high amplification, to the release of $\frac{1}{4}$ cal (electrical energy). Numerous traces have been obtained showing rapid heat liberation from well-activated charcoals.

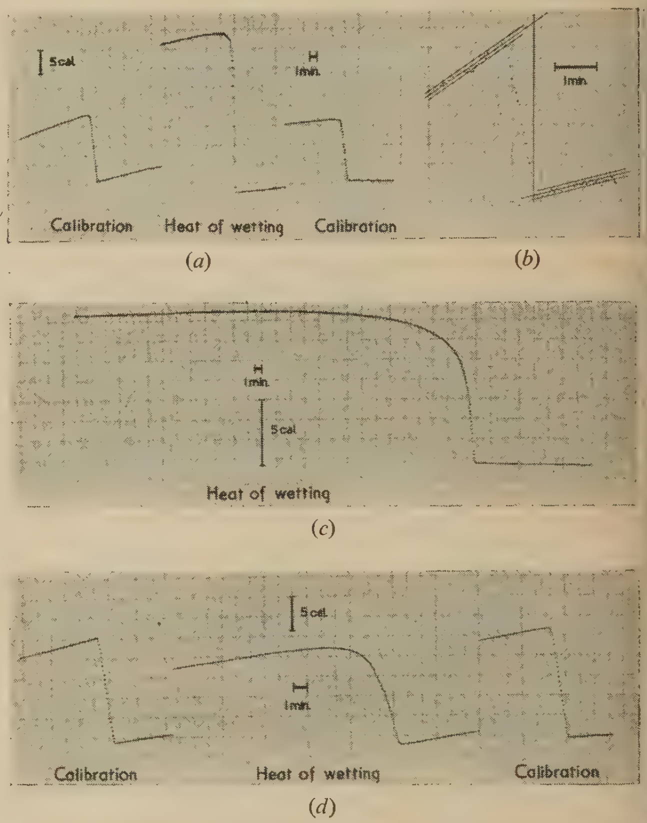

Fig. 4. (*a*) Rapid heat liberation system: charcoal/methanol (*b*) High amplification (×240): $\frac{1}{4}$ cal input. (*c*) Slow heat liberation system: coal/benzene. (*d*) Slow heat liberation system: carbonized coal/benzene

Rates of cooling before and after heat liberation are constant for an appreciable period, and the graphical cooling correction of Schulter and Nubel⁽²⁾ may be used with confidence. The correction obtained by this method rarely exceeds 1·0% of the total rise. In Table 1 figures are taken from some typical curves. Background noise increases as amplification increases but the trace width is constant at a given amplification. Percentage values of the trace width at various amplifications are given in Table 1.

---

* It has been ascertained that the weight changes in this operation are negligible.

Table 1. *Variation of trace characteristics with amplification*

Amplification	Observed sensitivity (μV/cal)	Full scale deflexion equivalent to: cal	°C*	Trace width μV	% full scale	Cooling correction % of total rise
1†	13	77	2·6	<1	—	—
1·6	20·6	50	1·7	<1	—	1·0
5·25	68·4	14·5	0·5	<1	—	0·5
15·3	199	5	0·17	8	0·8	0·5
50·4	655	1·5	0·05	20	2·0	1·8

* Using water equivalent of 30 g.
† No d.c. amplifier.

Calibration. The accuracy with which the instrument will give replicate calibrations for the same system over a range of amplification is shown in the following table:

Table 2. *Calibration reproducibility at several amplifications*

Amplification	Calibrations μV/cal input		Mean ±s.d.	% S.D.	Trace width as % of full scale
2·56	33·20	33·15	33·37	0·6	<0·1
	33·55	33·40			
	33·60	32·95	±0·2		
	33·70	33·45			
5·25	68·6	68·1	68·4	0·7	<0·1
	69·1	68·5			
	68·4	67·7	±0·5		
25·8	329·5	336·5	336·0	2·0	1·5
	334·0	333·5			
	329·5	342·0	±6·0		
	347·0	335·0			
37·8	507	476	492	3·4	2·1
	504	493			
	484	462	±17		
	513	493			

The percentage deviation from the mean increases less rapidly than does the degree of amplification, so that amplification is desirable both for ease of working and for accuracy. Moreover the width of the trace is constant at a given amplification so that a mean line may be drawn with greater confidence than is indicated by the trace width.

Confirmation of the absolute value of the calibration. A check on the operation of the apparatus is obtained from a comparison of the heat liberated on breaking a bulb containing a known weight of water into 40 ml. of methanol, with the published values for the heat of mixing of water and methanol.(3) From the literature it is seen that the relationship between the concentration of water, x, (grammes water/mole methanol) and the heat of mixing, ΔH cal, [shown graphically in Fig. 3(*a*)], is curved, so that accurate values of differential heats of mixing are absent in the region of present interest. Moreover, the water content of the anhydrous methanol* and the weight of added water becomes critical to accurate calculation of the heat liberation. To move from this critical region the anhydrous methanol was wetted by the initial addition of a known weight of water approximately 5 g/mole).

To utilize the full concentration range of the published data the regression line from the linear $\log_{10} x - \log_{10} \Delta H$ plot [Fig. 3(*b*)] was calculated as

$$\log_{10} \Delta H = 0{\cdot}7360 \log_{10} x + 1{\cdot}6437$$

Heats of mixing were measured by breaking a bulb containing a known weight of water under methanol in the calorimeter, and a comparison of the value of the heat liberation as calculated from the published data and that obtained experimentally from the measured output, translated by electrical calibration to heat units, is made in Table 3.

Table 3. *Heat of mixing, water/methanol system*

Water (g) per mole methanol initially	Weight of water in bulb (g)	Heat liberated (cal) Experimental	Heat liberated (cal) Calculated
5	0·793	17·05	16·54
5	0·440	9·35	9·23
5	2·011	45·70	45·54
4	2·132	48·5	49·3

The measured values are in good agreement with those derived from published data, showing that reliance can be placed on the absolute values determined in this calorimeter.

Replicate determinations of heats of wetting of charcoal in methanol. Measurements of the heat of wetting of two different charcoals were made in methanol. The results are given in Table 4.

Table 4. *Reproducibility of heat of wetting*

Sample	Individual detn. (cal/g)			Mean	S.D.	% S.D.
Nut shell Charcoal	35·30	34·95	35·34	35·93	1·09	3·0
	37·85	35·62	36·65			
Coal Charcoal	20·55	20·15	20·60	20·40	0·35	1·7
	20·75	19·81	20·53			

The standard deviations relate not only to the deviations associated with the calibration and the apparatus, but also include unknown factors concerned with the sample preparation and evacuation procedure.

Discussion

Calorimeter performance may be assessed in several ways, e.g.

(i) The limit of detection in terms of calories, or
(ii) Percentage deviation from the mean.

The latter will very probably vary inversely with the value of the heat liberation.

Boyd and Harkins, measuring heats of wetting of less than 3 cal, have stated(4) that their "values were good to 2% although the precision of the calorimetry was much higher". Their calorimeter held 650 ml. of wetting liquid, and between 5 and 10 g of adsorbent were wetted. Temperature measurement was by a 36 junction copper-constantan thermel which produced a galvanometer deflexion of 1 mm corresponding to 5×10^{-5} °C, i.e. about 0·03 cal. No data for an estimate of reproducibility are given. In similar work, Bond and Maggs(5) refer to a difference of 1 cal in duplicate determinations of a heat of wetting of 20 cal/g, with larger errors for smaller heat liberations; the calorimeter, which used 30 ml. of wetting liquid and about 3 g of sample, involved rotary mechanical stirring and thermometer reading estimated to 5×10^{-3} °C (i.e. reading limit of 0·1 cal). The present apparatus is capable of results showing an observed deviation from the mean of less than 3% (6 results on a nutshell charcoal heat of wetting 35·93 cal/g) and will indicate a change of 5×10^{-4} °C or 0·015 cal. The excellent agreement between our results for heat liberations between 10 and 40 cal and those of the National Bureau of Standards(3) for the heat of mixing of the methanol water system shows the potential accuracy of the calorimeter.

---

* The water content of the methanol as received from Imperial Chemical Industries Ltd. was less than 0·05% by Karl Fischer determination and was not improved upon by laboratory treatment.

The electrical calibration of the calorimeter results in a factor expressed as cal/μV scale deflexion which depends on the total heat capacity of the Dewar vessel and contents, and on the amplification employed. In a large number of experiments with a given Dewar vessel, only the wetting liquid and amplification factor have been varied substantially. It has also been ascertained by experiment that the dial settings of the decade box R_2 and of the d.c. amplifier give a linear increase in amplification (within 3%), so that the numerous experimental calibration factors may be reduced to a common basis, thus leaving the heat capacity of the liquid as the only variable in these experiments. From a plot of the reduced calibration factor against the literature values for the heat capacity *per ml.* of wetting liquid the water equivalents of two Dewar vessels and fitments are calculated as 5·3 and 6·3 g. By attention to details such as the accurate measurement* of liquid volume and the use of one setting of amplification an elegant method for the determination of the specific heat of a liquid is available. For example, the specific heats of silicone fluids have been calculated from numerous heat of wetting calibrations to be 0·44, 0·39 and 0·37 cal/g. for fluids of viscosity 1, 2 and 5 cS respectively.(6)

The calorimeter is suitable for the measurement of heats of wetting of any adsorbents in powder or granular form and for heats of mixing of liquid/liquid systems, although it cannot be used at the moment with any reagent which will attack the metal parts of the thermocouple head.

Extension of the method to heats of reaction or solution is feasible although the quantity of reactants is necessarily small. Slow heat liberations (e.g. 3 cal liberated over period of 3 h from the heat of wetting of a char with constricted pores) have been successfully measured. With liquid of high viscosity (20 cS approximately) the pumping actio of the stirring is limited.

The thermocouples have shown no evidence of instabilit and the precaution of a calibration before and after th experiment in any case guards against this contingency.

Conclusion

An electrically calibrated recording calorimeter has bee designed, and used in the measurement of heats of wettin and of mixing. The performance, assessed in terms o absolute calibration, accuracy and replicate determination of heats of wetting, is found to meet the stated requirements The absolute values of calibration have been confirmed.

Figs. 1–4. Crown copyright reserved. Reproduced wit the permission of the Controller, H.M.S.O.

References

(1) Maggs, F. A. P. *J. Sci. Instrum.*, **23**, p. 85 (1946).
(2) Schulter, W., and Nübel, R. *Brennstoff-Chem.*, **15** p. 466 (1935); Warme, **58**, p. 15 (1934).
(3) *Selected Values of Chemical Thermodynamic Properties* Circular of National Bureau of Standards, 500, p. 10 (1952).
(4) Boyd, G. E., and Harkins, W. D. *J. Amer. Chem. Soc.* **64**, p. 1190 (1942).
(5) Bond, R. L., and Maggs, F. A. P. *Fuel*, **28**, p. 169 (1949). War Department.
(6) *D.C. Silicone Fluids*, Silicone Notes, No. 2042 (Midland Silicones Ltd., 1950).

---

* In heat of wetting measurements, individual calibration for each experiment renders accurate volume measurement unnecessary.

Twin-head goniometer for the study of diffusely reflected X-rays

by W. A. WOOSTER, M.A., Sc.D., F.Inst.P., and G. A. WOOSTER, Brooklyn Crystallographic Laboratory, Cambridge

[*Paper received* 26 *August*, 1959]

Abstract

The apparatus described is a modified commercial single-crystal X-ray goniometer. Two goniometer heads are mounted on the vertical axis of the instrument so that two crystals may be placed alternately in the X-ray beam. The recording photographic film moves with the crystals and two records of diffuse reflexions, one a standard and the other the unknown, are obtained on the same film and with a known ratio of their exposure times. Thermal diffuse scattering from one (standard) crystal is used to determine the intensity of the incident X-ray beam. The thermal or structural X-ray reflexion from the second crystal may then be found in absolute measure.

Introduction

THE problem of making absolute rather than relative measurements of the intensity of X-ray reflexions arises in several kinds of investigation. Robertson(1) devised a method suitable for the absolute determination of the intensity of Bragg X-ray reflexions from single crystals. In this apparatus two goniometer heads were mounted parallel to one another so as to be able to rotate about an axis midway between them. For a certain time one crystal was in the beam and one portion of the film was exposed to the reflected beams. Then the two crystals interchanged positions so that the second crystal came into the beam. At the same time the film was covered, where before it was exposed, and uncovered, where before it was covered. An exposure in this second setting, which was not necessarily equal to the first exposure, completed one cycle. The cycles were repeated until the required total exposure was given. Wooster and Martin(2) arranged the goniometer heads on the same axis with the two crystals separated by only a few millimetres. Again the two records were obtained on the same film and during the exposure the crystals were interchanged many times.

The intensity of diffuse X-rays is often not greater than $10^{-6} - 10^{-7}$ of that of the beam incident on the crystal. It s, therefore, not practicable to use X-rays which have been monochromatized by crystal reflexion. However, filtering through a β-filter leaves enough intensity to give a satisfactory photograph in 20–100 hours. The quality of the photograph is much improved by a β-filter. The measurements nearly always involve the knowledge of the ratio of the intensities of the incident beam and the diffusely reflected beam. Because of their very unequal values they cannot be compared directly on a photographic film. The intensity of the direct beam must be reduced by a known factor of about a million to allow such a photographic comparison to be made. This is not possible using filtered radiation, as the short wavelength radiation is so little absorbed relative to the long wavelength radiation. It therefore seems necessary to compare one diffuse reflexion with a second standard diffuse reflexion, since these will have intensities not differing by more than a factor of ten. The problem is, therefore, similar to that which was solved in the apparatuses devised by Robertson and by Wooster and Martin. The apparatus described below is based on the method given by the latter authors.

Apparatus and experimental method

The present apparatus, shown schematically in Fig. 1, is based on the Unicam S-25 single-crystal X-ray goniometer. A C-shaped support D has been mounted on the base and this carries a yoke CC', supporting the two goniometer heads A and B. At its lower end the yoke CC' fits on to the spindle which normally carries the goniometer head. The shaft attached to the upper end of CC' can slide vertically in a hole bored in the support D. The two crystals, mounted one on each goniometer head, can, therefore, be brought in urn into the X-ray beam. The movement of the yoke CC' s effected by the rotation of the height adjusting screw E. A flexible drive connects this screw to a 12 V d.c. motor. An arm, fixed to the screw, strikes the rollers of two microswitches, one at its highest position and the other at its lowest position. Immediately after operating the switch the arm is arrested by a block fixed beside the switch, so that the yoke CC' stops in the same position every time. A screen with a 1 cm wide circumferential slot is fixed equatorially between the crystal and the cylindrical camera. The camera is supported on the yoke CC' and moves up and down with the crystals. A camera radius of 57·4 mm is found the most convenient size. The film is placed in a light-tight envelope and clamped by three screws, with small ball-ends, on the outside of the camera. The pressure marks made by the balls on the film accurately indicate the position of the film relative to the instrument. Use is made of this in the accurate orientation of the crystal.

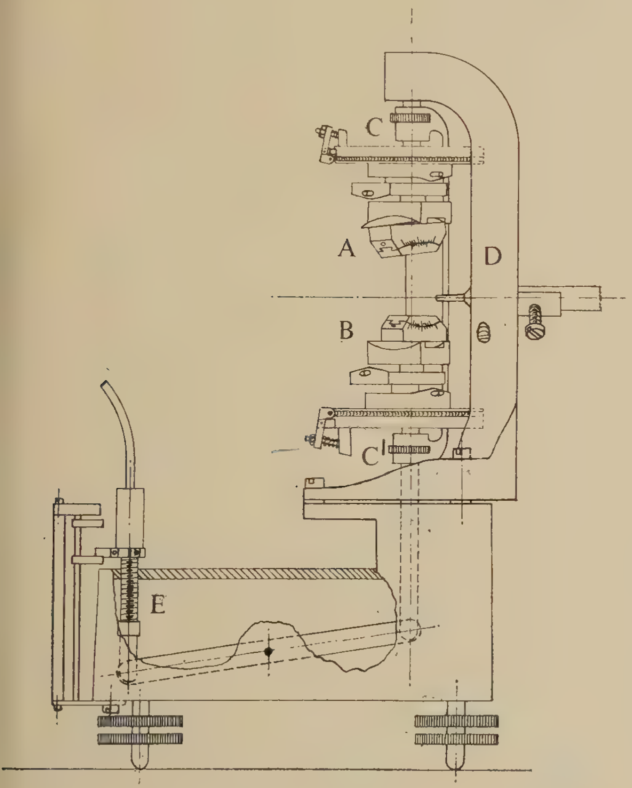

Fig. 1. Diagram of mounting of the two goniometer heads

Control of exposure times

The difference in the intensity of diffuse scattering from two crystals may be considerable, and it is therefore advantageous to be able to change the ratio of the times during which they are exposed to X-rays. The following circuit (Fig. 2) shows a particular arrangement giving a 5 : 1 ratio of exposures. The switch V is closed for a period of a few seconds, every ten minutes, by a cam driven by a synchronous motor. The closure of the contacts V operates relay R and closes switches R_1, R_2. (When any solenoid is not activated, contacts represented by two small circles with a bar above them are open.) The closing of R_1 short-circuits the switch Q_1 *via* contacts $Y_1 - Y_{10}$. (The contacts X, Y, Z are part of a Ledex rotary solenoid, operating three banks of ten-way wafer switches.) The short-circuiting of switch Q_1 operates the solenoid Q which holds Q_1 closed when R_1 is opened by the cam-contact V. The closing of Q_1 also operates the d.c. motor which raises the twin-head assembly. When the motor has rotated a few turns, the arm on screw E no longer opens microswitch T_1 (as shown in Fig. 2) and when the arm reaches its lower stopping point both T_1 and U_1 are closed. When U_1 is closed, relay P is actuated and switch P_3 is opened. This stops the motor. The lower crystal is now in the X-ray beam. After another ten minutes switch V is closed, thereby closing R_1 and R_2. Closing R_2 steps on the Ledex arm to position 3 and R_1 short-circuits Q_1. This starts the motor in the opposite direction to the previous sense of rotation. The twin-head is thereby lowered until switch T_1 is opened by the arm on the screw E. Thus an exposure of 10 min has been given to the lower crystal. The next operation of V moves the Ledex arm to position 4 but as there is no circuit through R_1 the motor does not rotate. The same occurs at positions 5 and 6 when a total exposure of 40 min of the upper crystal has been given. On the Z-bank of the Ledex switch contacts 7, 8, 9, 10 are connected to the negative terminals of the d.c. supply and the electric bell action of relay S and switch S_1 returns the Ledex switch to position 1. Another 10 min exposure is given in this position before the whole cycle is repeated. Thus the upper crystal receives five times as long an exposure as the lower crystal. By altering the contacts joined together on the banks Y and Z the ratio of the exposure times may be altered. The extreme values of this ratio are 9 : 1 and 1 : 9 respectively.

Interpretation of the photographs

An example of the photographs obtained with this apparatus is shown in Fig. 3. The upper (standard) photo-

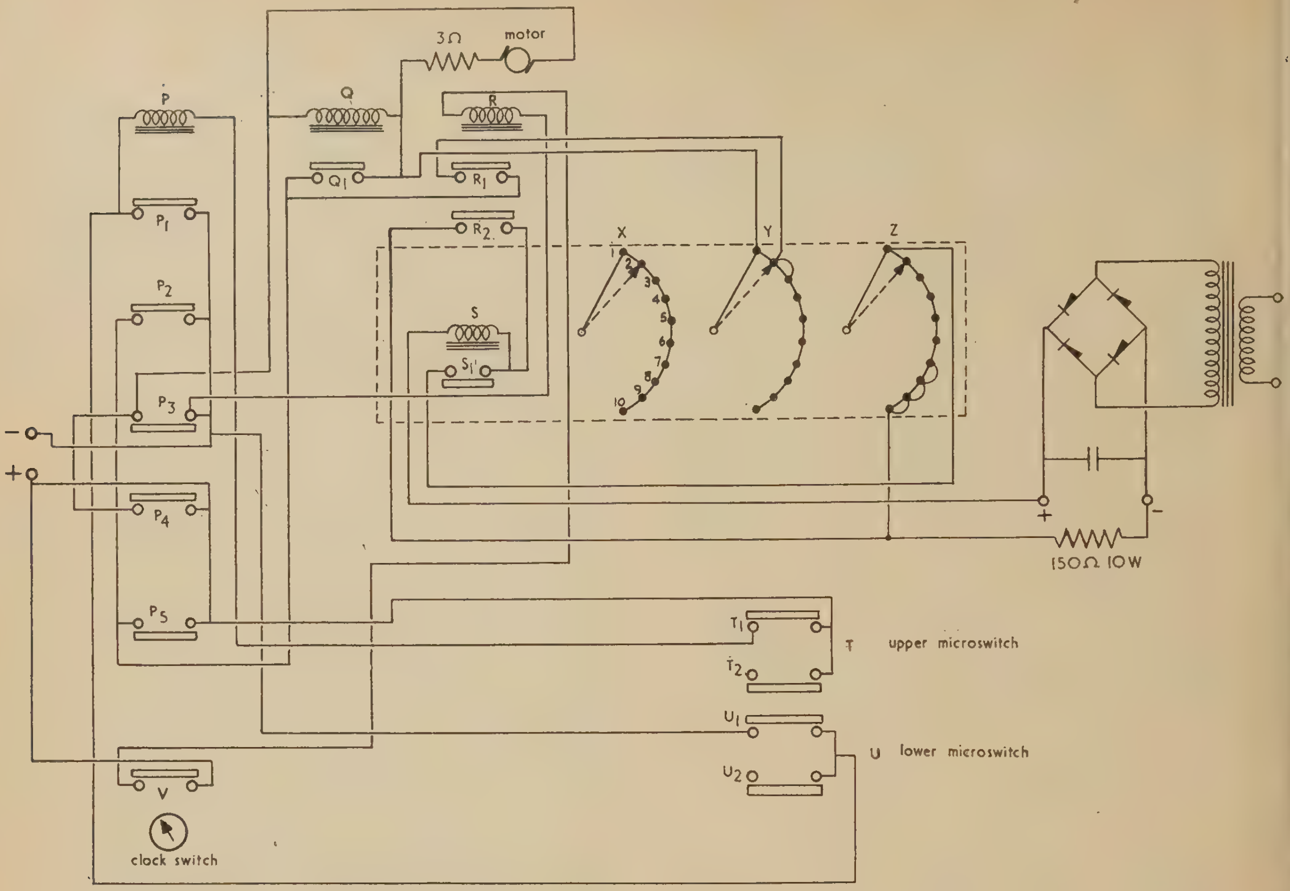

Fig. 2. Circuit diagram showing the system used for varying the relative exposures of the crystals. The stop is in the upper position, with the *P* and *Q* coils not activated

graph has been taken with an undeformed but not perfect aluminium crystal set at an angle of $(i - \theta)$ of 1° 6′ away from the Bragg 220 setting ($\theta = 32° 31'$). The heavy spot on the left-hand side is the Laue reflexion; the short vertical line on the right-hand side is a so-called S-line, which would be absent if a perfect crystal were used. Between the Laue spot and the S-line is the area of thermal diffuse scattering which may be used to calibrate the intensity of the incident beam. By measurements of the optical density at selected points on the thermal diffuse spot, it is possible$^{(3)}$ to determine the absolute intensity of the incident X-rays in terms of the elastic constants. A point or points are chosen within the thermal diffuse spot where there is no disturbance due to either the Laue spot or the S-line. The lower half of Fig. 3 contains the Laue spot and an S-line produced by deformation of an aluminium single crystal set at an angle $(i - \theta)$ of 2° 29′ away from the Bragg setting for the 220 reflexion. The density at the centre of the S-line is comparable with that of the thermal diffuse reflexion in the upper half of Fig. 3. Using the data provided by the upper half of Fig. 3 to determine the optical density corresponding to a given fraction of the incident beam, one may determine the fraction of the incident beam corresponding to any point on the lower photograph. If the crystals used were not of the same kind certain correction terms for differences in Bragg angle would be applied. This method may be applied to determine in absolute measure any thermal or structural type of diffuse X-ray reflexion.

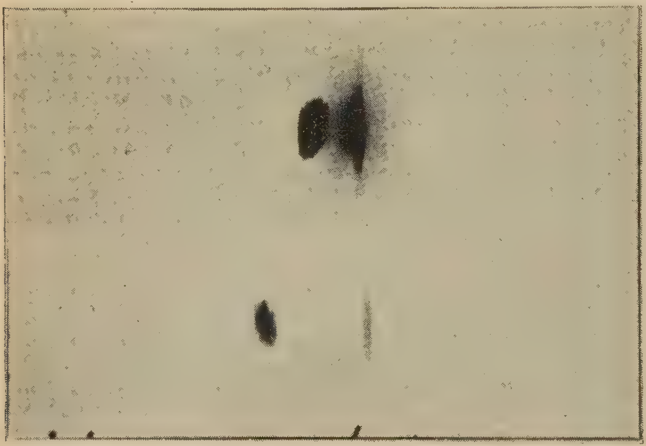

Fig. 3. The upper photograph shows a Lauė spot on the left, an S-line on the right, with a thermal diffuse spot between them. The lower photograph shows only a Laue spot and the S-line, which is stronger relative to the thermal diffuse scattering than in the upper photograph

References

(1) Robertson, J. M. *Phil. Mag.*, **18**, p. 729 (1934).

(2) Wooster, W. A., and Martin, A. J. P. *J. Sci. Instrum.*, **17**, p. 83 (1940).

(3) Hoerni, J. A., and Wooster, W. A. *Acta Cryst.*, **5**, p. 626 (1952); **6**, p. 543 (1953).

Simple method of mounting and stretching thin gauze, sheet or foil

by P. A. Einstein, Research Laboratories, Siemens Edison Swan Limited, Harlow, Essex

[*Note received* 6 *November* 1959]

In connexion with an experiment on a form of image tube, it was required to stretch tightly a rectangular mesh 750 per inch, 40 × 30 mm, and this was achieved as follows:

An overall support consisted of an aluminium annular disk some 80 mm, o.d., 70 mm, i.d. and 1 mm thick. Over this was attached a sheet of 6μ thick Melinex (I.C.I. Ltd.), stuck down around the periphery using cold-setting Araldite (C.I.B.A., Aero Research Ltd.). This was allowed to set (six hours), and the edges trimmed of excess Melinex. A central rectangular hole some 38 × 28 mm was now cut in the Melinex, using a pointed scalpel. Care was required at this stage to ensure that the cuts met neatly at points in the corners; continuation of the cuts could cause subsequent splitting of the Melinex. The edges of the hole were coated with cold-setting Araldite which was applied with a pin, and the rectangular section of gauze was carefully manœuvered into position by resting the gauze on a rectangular support just smaller than the aperture in the Melinex film and raising the aluminium ring from below, thus scooping-up the gauze in the correct position. After the Araldite around the hole had set, the whole arrangement was held in an oven at 300° C for approximately five seconds. This caused the Melinex to shrink and produce a drum tight, very flat, wrinkle free surface of both Melinex and gauze. The change thus produced was permanent and the Melinex remained tight even on cooling. Suitable electrodes or contacts could subsequently be deposited by evaporation or painted on to the Melinex faces.

Simple refrigerant level controller for cold traps

by C. W. Nutt, B.Sc., Ph.D., A.R.I.C., and A. J. Biddlestone, B.Sc., Department of Chemical Engineering, The University, Edgbaston, Birmingham, 15

[*Note received* 6 *October*, 1959]

It is often necessary to maintain continuously an adequate level of liquefied refrigerant in a cold trap for a long period of time, e.g. several days, and for this an automatic filling device is desirable. The device described here has the advantage that it employs a minimum of moving parts and requires no electricity, water, compressed air or other laboratory service.

The refrigerant level in the cold trap *A* (see figure) is maintained by an intermittent feed from a laboratory bulk storage tank *B*. The feed is regulated by the controller *C*, of which the essential component is a flexible metal bellows *D* fixed at its bottom end. To this end is attached a length of stainless steel capillary tube *E* sealed at its bottom end by a small polished stainless steel bulb or solid sphere *F*. The free upper end of the bellows actuates a simple O-ring sealed valve *G* to control the flow of gas from the vapour space of the storage tank.

When used with liquid nitrogen the mode of operation is as follows: when the refrigerant level in the cold trap is too low, the bellows are fully extended and the valve *G* closed. Heat leakage into the storage tank causes the pressure there to increase and ultimately this forces liquid through the delivery tube *H* into the cold trap. When the liquid level reaches the sphere *F*, the temperature of the bottom end of the capillary tube falls sufficiently to condense the oxygen of the air inside the bellows. The bellows are thus caused to contract and the valve *G* opens so that the pressure in the storage tank is released and the refrigerant supply is discontinued. When the refrigerant level in the cold trap falls, the sphere warms by conduction of heat down the capillary tube, the oxygen vaporizes, the valve *G* closes and the cycle of operations is repeated.

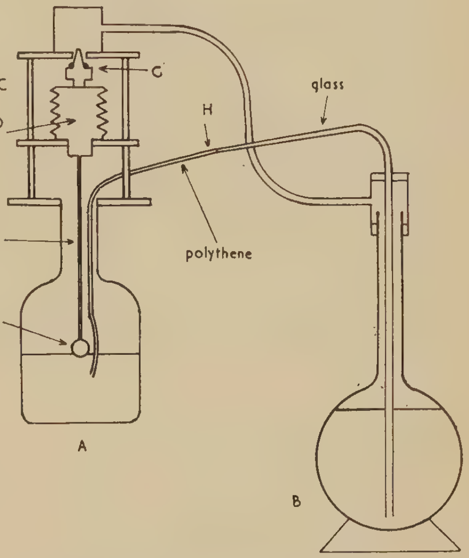

Simple refrigerant level controller for cold traps

The frequency of operation depends not only on the rate of vaporization of liquid from the cold trap but also on the rate of vaporization of the oxygen in the capillary tube, i.e. on the rate of heat flow down the tube and the volume of the bellows, and also on the volume of the vapour space of the storage tank and the rate of heat leakage into the tank. The device has been used to control the level of liquid nitrogen in an all-metal internal cold trap, capacity approximately 1 l., for which the rate of heat leakage was such that, without the controller, one filling would suffice for about 14 h. With a controller having a bellows $2\frac{3}{8}$ in. o.d. and $2\frac{1}{4}$ in. long and a capillary tube $8\frac{1}{2}$ in. long, 0·045 in. o.d. and 0·028 in. i.d. the frequency of operation was such that liquid was delivered every 2 h.

Since the bellows is normally subjected to a reduced pressure, it is essential that no leaks exist in it, or in the capillary tube, etc. Erratic operation can result if during the filling operation large splashes of refrigerant contact the capillary tube or bulb. A liquid delivery line constructed as shown in the figure from polythene and glass tube has been found to be satisfactory. U-bends in the delivery line must be avoided or violent surging may result. With these precautions the device described has given satisfactory operation for many months. Obviously it could be adapted for other refrigerants by suitable choice of gas in the bellows.

Crystal oscillation mechanism for use with automatic X-ray diffractometers

by U. W. Arndt, M.A., Ph.D., A.Inst.P., T. H. Faulkner and D. C. Phillips, B.Sc., Ph.D., F.Inst.P., The Royal Institution, 21 Albemarle Street, London, W.1.

[*Note received* 15 *September*, 1959]

In the automatic single-crystal X-ray diffractometers in use in this laboratory the method of measuring a Bragg reflexion is as follows: The crystal and X-ray detector are rotated about appropriate shafts for a given X-ray reflexion to be recorded, and the crystal is then offset by an amount ϵ sufficient for a clear background to be detected. With the crystal stationary, the incident X-ray quanta are then counted on a printing scaler for a period t and the total n_1 is printed out. The crystal is next rotated through an angle 2ϵ embracing the Bragg reflexion, the time taken for this rotation being $2t$, and at the end of this period the accumulated intensity N is printed out. Finally the crystal is held stationary for a further period t so as to record the "background count" n_2 on the other side of the reflexion. The quantity $N - (n_1 + n_2)$, which is also printed out by actuating the "total" key of the printing adding machine which acts as the output device of the scaler, is taken as the integrated intensity of the reflexion. During the whole measuring cycle, the X-ray counter, which is fitted with a wide entrance window, is held stationary.

A mechanism was, therefore, required which would impart the movement to the crystal shaft which is represented in Fig. 1 (which also shows the variation of X-ray intensity with angle). The range of angular movement 2ϵ had to be readily adjustable over a range between 1 and 5 deg. In addition, contacts were required to close at different times during the cycle, corresponding to the following signals to ancillary equipment:

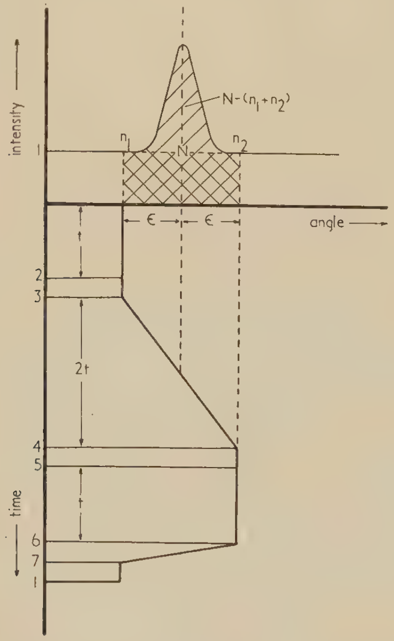

Fig. 1. Variation of X-ray intensity in a crystal reflexion with angular setting of the crystal, together with the motion of the crystal during one measuring cycle and the times of signals required by the counting circuits

1. Switch on scaler to measure the background on one side of the Bragg reflexion;
2. Print out this count and re-set the scaler;
3. Switch on scaler to measure the integrated count as the crystal sweeps through the reflecting position;
4. Print out this count and re-set the scaler;
5. Switch on scaler to measure the background on the other side of the Bragg reflexion;
6. Print out this count and re-set the scaler as the crystal turns back through the angle 2ϵ;
7. Print out $N - (n_1 + n_2)$, switch off the oscillation motor and switch on appropriate shaft-setting motors to set the crystal and X-ray detector for the next reflexion.

The mechanism evolved after some experiment is shown in Fig. 2. The synchronous motor *M* drives the cam *C* and the concentrically mounted switching cams *S* through a reduction gear-box *G* at either 1 or 4 rev/min. The cam *C* has a constant radius of 0·600 in. between the point 1 and 3 (Fig. 1), a constant positive lead of 0·002 in./deg. between 3 and 4, a constant radius of 0·888 in. between 4 and 6 and a constant negative lead of 0·008 in./deg. between 6 and 7. It was cut on a milling machine fitted with a circular table; the heel of the cam follower *F* was given a radius equal to that of the cutter used. The cam follower is pivoted at *P* and sprung against the cam. A movable pin *MP* can be clamped in the slot *SL* of the cam follower so that *s*, the distance between pivot and pin, can be varied.

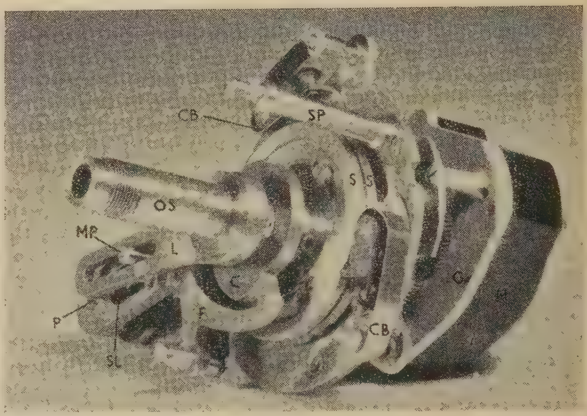

Fig. 2. Photograph of the oscillation mechanism with switching disks and contacts

The output shaft *OS* carries a slotted lever *L* in which the pin *MP* engages. *L* is held against the pin by a spring (removed for clarity). Then if l is the distance between the shaft *OS* and the pivot *P*, and α and β are the angles through which the cam follower and the lever respectively are rocked, β is given to an accuracy of better than 1% with the dimensions chosen by:

$$\beta = \frac{\alpha s}{l - s}$$

In our mechanisms α is 5 deg., so that β can be varied between 1 and 5 deg. by varying s between $l/6$ and $l/2$. The slot *SL* is calibrated in terms of the angle β in degrees.

The switching disks carry notches into which the heels of Lucas distributor-head contact breakers *CB* drop, thus closing the appropriate contacts in synchronism with the motion imparted to the crystal shaft. The whole oscillating mechanism is attached by means of three supporting pillars

SP (only one of which is shown in Fig. 2) to a plate fast with the crystal input shaft. This input shaft is set, via appropriate gearing, by the crystal-setting motors, so that, at this stage, the entire mechanism rotates with the input shaft, carrying the output shaft with it. When the crystal is set, the setting motor is at rest and the cam mechanism rotates the output shaft with respect to the motor baseplate and thus with respect to the input shaft.

Tests have shown that when the total length of the oscillation cycle is either 15 or 60 s, the lengths of the individual timing cycles can easily be kept correct to 1%; the linearity of the sweep is also of this accuracy. A "synclock" motor is used; the quality of the gears of ordinary electric clock motors is not good enough to produce a sufficiently smooth motion.

Simple method of temperature control

by H. A. Vodden, B.Sc., F.Inst.P., Monsanto Chemicals Ltd., Ruabon, N. Wales

[*Note received* 8 *July* 1959]

The need often arises to control the temperature of a system in which it is inconvenient to use a liquid heat exchange medium. In such cases, it is common practice to use metal of high thermal conductivity in the system in order to minimize temperature gradients. Even so, if a conventional electrical heater and temperature-sensing element are used in a control system, undesirable fluctuations may arise due to time lags between the feeding of power to the system and the detection of temperature change by the sensing element. It may be advantageous in such cases to utilize the electrical heater itself as its own sensing element. A simple way in which this may be done is described here.

The heater may be of any wire possessing suitable resistance/temperature characteristics. Nickel wire, for example, has been found excellent for the purpose. The circuit is shown in the figure. The heater winding R_4, which should have a resistance of not less than about 400 Ω, forms one arm of the bridge network in which R_1, R_2 and R_3 are stable resistances. The bridge is energized at 250 V, 50 c/s, either from the mains supply or from a suitable winding on a transformer. The thyratron (type EN.32) is shunted across R_3 so that, when it conducts, extra power is dissipated in the heater. When the thyratron is not conducting, the power dissipated in the heater will be limited by the value of R_3. The power limits available are, therefore, determined by the value of R_3 and the choice of this must be governed by the power requirements of the system.

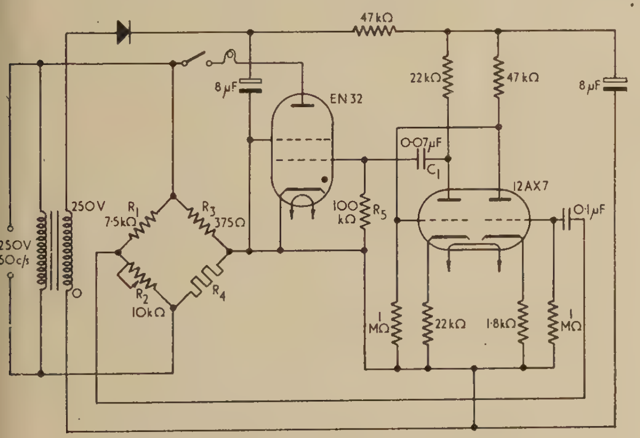

Circuit diagram of heater

The operation of the circuit is as follows. If the temperature is below that required, the resistance of R_4 will be low and the signal fed into the grid of the thyratron will be in phase, or nearly so, with that applied to the anode, since the amplifier (type 12AX7) introduces negligible phase shift. In this condition, the thyratron will conduct during each positive half cycle of the applied anode voltage. Until the thyratron discharges, the grid/cathode potential difference will be that determined by the bridge network and amplifier. After discharge, the bridge output will, of course, be very different but since the grid no longer exercises control, the operation of the circuit is not affected. If the temperature is high, the resistance R_4 will be high, and the signal to the grid will be in antiphase to the anode supply. If the amplitude of this grid signal is large enough, the thyratron will be prevented from conducting and the power dissipated in the heater will be at its lower limit. If the values of C_1 and R_5 are appropriate, the slight phase advance of the grid signal will ensure that as the amplitude of the grid signal increases, when in antiphase to the anode supply, the point of discharge of the thyratron in each cycle will be progressively retarded so that a smooth variation in power between the upper and lower limits will be obtained.

If the amplifier is omitted, the circuit will still work but will lack sensitivity, the temperature change necessary to vary the power from maximum to minimum being a few centigrade degrees. The circuit shown has been developed for controlling the temperature of a large block of aluminium. This block, of dimension 12 × 10 × 4 in. has six 12 × 1 in. holes bored vertically to form six small air ovens. The block is coated with a thin layer of epoxy resin (Shell Epikote 815) and on this is wound about 170 ft of 40 s.w.g. nickel wire insulated with Teramel enamel (by British Insulated Callender's Cables Ltd.). This heater is surrounded by about 1 in. of asbestos wool as thermal insulation. The total resistance of the heater is about 500 Ω and with $R_3 = 375\ \Omega$, $R_1 = 7{\cdot}5\ \mathrm{k}\Omega$ and $R_2 = 10\ \mathrm{k}\Omega$ the system readily controls the temperature at 110° C. Actually R_2 is a variable resistor so that the control temperature can be adjusted. Over a period of several months, this system has behaved very satisfactorily, the controlled temperature being maintained within $\pm 0{\cdot}2°$ C. It is suitable for temperatures up to about 130° C, this limit being determined by the insulating materials used. Probably the most attractive feature of this system of control is that there is virtually no time lag between the feeding of power into the system and the sensing of temperature change due to this. For this reason the design of small ovens of low thermal capacity but of good stability should be possible.

The author is indebted to Messrs. J. Selvey and D. Rickers for constructive suggestions and assistance in this development.

Valve and adapter for the grease-free connexion of glass sample tubes to a mass spectrometer inlet system

by J. R. Richards, M.Sc., Ph.D., Department of Radiochemistry, Australian National University, Canberra, Australia

[*Note received* 28 *September*, 1959]

Recent models of the Metropolitan-Vickers MS2 mass spectrometer are equipped with a double-inlet type of gas-handling system which has two methods for admission of gas samples. One is of the Taylor and Young type, with a porous sinter dipping into a pool of mercury. The other is a metal cone, of standard glass taper, size B14. The sinter inlet has been found to be unsatisfactory for the admission of tetramethyl–lead samples, possibly because the sample condenses in the sinter, thus blocking it. On the other hand, the use of grease as is customary with standard glass joints is to be avoided with samples of this type, because of the high solubility and the possibility of memory effects.

The valve adapter illustrated in the figure has been designed to accept B14 tapers, thus avoiding the need to modify the mass spectrometer. One seal is shown with a glass taper in position. The rest of the valve is shown, for clarity, in the exploded form. Each seal is achieved by two neoprene O-rings which are compressed on to the taper by means of the combination of tapered brass spacer rings and the knurled screw cap. This arrangement seems to be sufficiently vacuum-tight, even on ground glass surfaces. A similar seal, constructed to fit a C10 cone, has been used to replace the metal cup attachments at the tops of the doser manometers on the mass spectrometer, and works equally well. The valve closure consists of a stainless steel cone seating on to the edge of a brass step at the bottom of the valve well. This is the only point where care in construction is required. The step must be as nearly as possible normal to the axis, and chatter marks must be avoided. The vacuum seal at the shaft is achieved by a single compressed O-ring. The knurled head of the valve shaft is kept to a small diameter, to restrict the pressure which can be applied to the valve. The surface area of neoprene exposed to the sample is small, and absorption of sample has appeared to be negligible under normal working conditions over the period of several years in which the valves have been in use.

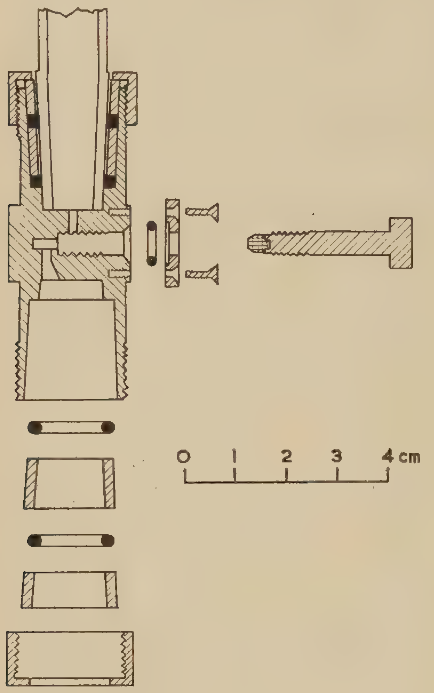

Valve adapter designed to accept B14 tapers

Thanks are due to Mr. W. van Barneveld for his assistance in the design and construction of these units.

Diffuse-light integrator

by N. W. Wootten, B.Sc., A.Inst.P., Chemical Defence Experimental Establishment, Porton Down, Wilts

[*Note first received* 24 *March, and in final form* 28 *August* 1959]

When a photo-voltaic cell is used to measure illumination the output current varies with the angle of incidence of the beam. If this angle can be measured, the intensity of the beam can be calculated from the cosine law after calibrating the photocell current against a normally incident beam of known intensity. However, when the angle of incidence is not known, or when the light is incident over a wide angle, the cosine correction cannot be applied. In order, therefore, to measure the total illumination normal to a body in a diffusing atmosphere such as fog or a smoke cloud, a measuring device is required which will give, within the forward hemisphere, an output independent of the direction from which the radiation is arriving. Such light receivers have been developed from Bennett's integrating photometer*† and others have been made for photographic exposure meters but these others, in general, are not very sensitive and are somewhat elaborate in construction.

The present simple and robust device was developed to receive light over 2π steradians. It consists of a polished Perspex cylinder mounted on a barrier-layer photocell set at the centre of a blackened metal disk. A solid 45 deg. cone of Perspex is seated on top of the cylinder which is hollowed out, also in the form of a 45 deg. cone (Fig. 1). The cone surfaces are rough-turned or ground to diffuse the light so that it is in part directed to the sensitive surface of the photocell. In this condition, the response is greater for light falling

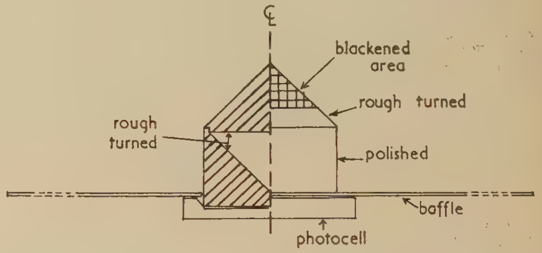

Fig. 1. Construction of diffuse-light integrator

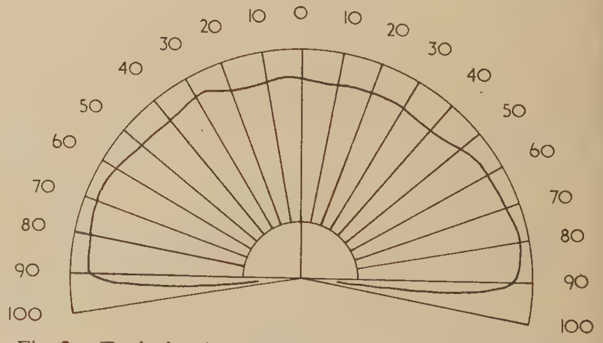

Fig. 2. Typical polar diagram of response of diffuse-light integrator

arallel to the cone axis than for that normal to the cylinder urface. The solid cone is therefore blackened sufficiently to nsure that the response is independent of the direction from vhich the light is arriving. A typical polar diagram of the esponse is shown in Fig. 2.

---

* Bennett, M. G. *Proc. Phys. Soc.*, **40**. p. 316 (1928).

† Hill, A. S. G. *Photo-electric cells and their applications*, (London: Physical and Optical Societies, 1930).

The dimensions of the cylinder and cone can be varied to uit the size of the photocell to be used. The blackened netal disk around the Perspex is necessary to ensure a sharp ut off at right-angles to the forward direction.

The light reaching the photocell varies between 10 and 5% of that falling on the integrator, according to the finish n the ground surfaces. The sensitivity will of course be lependent on the photocell and ammeter which are used.

Thanks are due to Mr. R. G. Dorman for his suggestions luring the development of this device. This note is reproluced with the permission of the Controller of Her Majesty's Stationery Office, and Crown copyright is reserved.

Bubble method for magnetic susceptibility of liquids

by A. O. Mathai, M.Sc., Dept. of Physics, University College, Trivandrum, India

[*Note received* 8 *September*, 1959]

Quincke's method and its modifications are frequently used in the absolute and comparative study of magnetic susceptibility of liquids. Although the method is noted for its simplicity, the indications are often so small that special devices are required for their accurate estimation and, except with strong paramagnetic solutions, the experiment is unsuitable for demonstrations. The bubble method dealt with in this note produces an appreciable indication of even very weak para- or diamagnetic susceptibility, and provides an easy method of comparing such susceptibilities.

A casual observation of the perceptible movement of the bubble in a spirit level when kept in a gradient of magnetic field was the origin of this work. The effect can easily be explained as a consequence of the diamagnetic susceptibility of alcohol, which is displaced by the bubble from the stronger regions of the field. The bubble is thus drawn with a force equal and opposite to that which would be experienced by the same volume of the liquid when surrounded by air and kept in the same region of the field. The final position taken up by the bubble is such that this force is balanced by buoyancy, which leads to the relationship:

$$kvdF(H, X) = vdg \sin \theta,$$

where k is the mass susceptibility of the liquid, v, the volume of the bubble, d, the density of the liquid, $F(H, X)$, a function to represent the distribution of the field in the region of the bubble and θ, the slope of the tangent at the bubble region of the tube. Thus if the susceptibility and density of air are neglected compared with those of the liquid, it follows that the susceptibility of the liquid is proportional to the tilt, which leads to an easy method for comparison.

The bubble tube closed at one end is hollow-ground inside and is graduated. It is provided with a stopper similar to that of a specific-gravity bottle. When the liquid is enclosed, the stopper is carefully pulled out to admit enough air through the exit hole of the stopper to build a bubble of reasonable size. The tube is held on a wooden lever, the tilt of which can be adjusted by a micrometer screw working at a distance of 20 cm from the pivot.

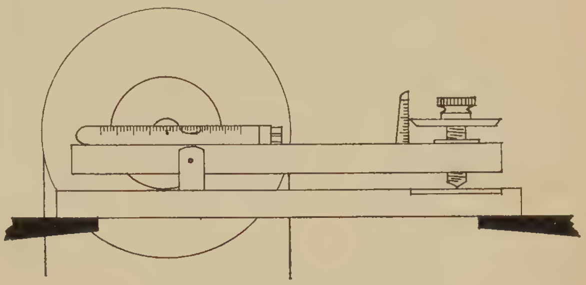

Arrangement of apparatus

This arrangement is set up between the tapering circular pole pieces of a strong electro-magnet (see the diagram) so that the bubble is about ten divisions off-centre when there is no field. When the field is applied, the bubble is drawn in or out according to the sign of susceptibility of the liquid, and it is then returned to its original position by adjustment of the micrometer screw. The difference in reading so obtained is a measure of the tilt at the bubble under conditions of equilibrium, in terms of which the susceptibilities can be compared. The table of values for a few standard liquids shows the nature of the observations.

Table of susceptibility observations

Substance	*Tilt (in scale divisions)*	*Susceptibility* ($\times 10^5$)	*Tilt/susceptibility*
Cyclohexane	86	0·81	106
Alcohol (Ethyl)	80	0·74	108
Benzene	74	0·71	104
Chloroform	52	0·49	106

The total error introduced by the sticking factor, the dependance of the shape of the bubble on surface tension and the slight change in the shape of the bubble when in the field does not seem to be appreciable.

New instruments, materials and tools

The Editor invites manufacturers of instruments and light machine tools to keep him informed of their new or improved products. The Institute of Physics assumes no responsibility for the statements given below: information for these has been taken from literature supplied.

Oscilloscope for high-frequency pulse monitoring. Mullard Equipment Ltd., Torrington Place, London, W.C.1.

The type L362 oscilloscope has been designed for the display of pulses of between 3 mμs and 3 μs duration, and with a sensitivity of 150 mV/cm. By the use of transistors, this performance has been attained with an instrument measuring 14½ × 8¾ × 18½ in. and weighing only 27 lb. The oscilloscope makes use of the sampling principle: the complete trace is built up of a series of dots, each of which corresponds to a sample taken from successive repetitions of the input. Charge storage circuits maintain the position of the dot until the next sample is taken. The instrument is therefore suitable for displaying random pulses of identical shape, such as occur with nuclear detectors. The principle of operation is as follows. The voltage stored in the X-charge store is compared with the output voltage from a fast sweep generator triggered by the signal. When these voltages are equal, the comparator circuit produces pulses which trigger the sampling circuit. Simultaneously, a pulse is passed to the X-charge storage circuit to reduce the stored charge. This causes the signal to be sampled progressively earlier, and the spot on the cathode-ray tube to be moved further to the left, for successive repetitions of the signal. When the stored charge has fallen to a certain level, the circuit is reset and flyback occurs. The signal voltage charges the input capacitance of the instrument and, when the sampling trigger pulse is received from the comparator circuit, this charge is transferred to the Y-charge store. The stored charge is thus proportional to the signal voltage at the instant of sampling. A second sampling trigger pulse causes the voltage in the Y-charge store to be applied to the Y-plates of the cathode-ray tube.

Transistorized high-speed digital printers. Venner Electronics Ltd., Kingston By-Pass, New Malden, Surrey.

Two types of high-speed printer are available, each capable of printing a line of up to eleven characters at a maximum rate of 5 lines/s. The drive circuitry is fully transistorized in both types. These printers are intended for use with both valve and transistor digital instruments such as voltmeters, counters, frequency meters and timers. The type TSA65 printer is intended for use with ten-line systems, and requires an input which varies from at least −3 to −6 V d.c. on a line to cause the respective character to be printed. This model is suitable for use with in-line readout counters using driving sources such as relays, stepping switches or multi-cathode counting tubes. The type TSA66 printer is designed for use with single-line analogue input systems and requires an input which varies from −7 V to print a zero to −2 V to print a 9, the intervening numbers being printed when the corresponding linear increment is injected. This model can be operated from parallel entry staircase voltages from a decade counter. Both models require a print command signal pulse of 3 V amplitude. The printers are of the same size (16¼ in. deep × 10 in. wide × 11½ in. high) and operate from 230 V a.c. mains.

High-stability transistorized power units. Metrix Instruments Ltd., 54 Victoria Road, Surbiton, Surrey.

A range of high-stability transistorized power supplies which are designed as sub-assemblies can now be obtained. Bench models in a case and including meters are also available, and an overload cut-out system can be incorporated in all models. The reference potentials are obtained by means of a double silicon Zener diode system, and the complete control circuit is constructed on a single printed panel which is readily accessible and removable. High stability resistors are employed throughout, and the power transistors are generously rated against overload. The units can be supplied with zero output impedance if required. The units are available with current ratings from 1 to 10 A at potentials from 0 to 30 V, and the makers claim a stability of 0·1% for models up to 2 A and better than 0·2% for 10 A models.

British Journal of Applied Physics

Contents of the February issue

CONFERENCE REPORT

Recent studies of noise problems. By G. G. Parfitt.

PAPERS

High resistivity nickel–iron alloys with rectangular hysteresis loops. A. Hart.

Viscosity and thermal conductivity of liquid boron trifluoride. A. N. Spencer and M. C. J. Todd.

Absolute intensity measurements of the carbon and aluminium X-ray K-lines with a proportional counter. R. M. Dolby.

Investigation into one of the assumptions of the Hertz theory of contact. C. Storey.

What is ferromagnetic resonance? By R. A. Waldron.

Evaporation and diffusion rate measurements on cathodes of sintered nickel containing alkaline-earth oxides. By J. F. Richardson and F. A. Vick.

Relaxation times in lead film, superconductive, storage elements. By R. F. Broom and O. Simpson.

Microcracks, and the static and dynamic elastic constants of annealed and heavily cold-worked metals. By J. R. Bristow.

Theory of the parallel plate viscometer. By A. N. Gent.

CORRESPONDENCE

Interaction between two equal-sized equal-settling spheres moving through a viscous liquid. From H. W. Matthews, F. B. Smith, and G. F. Eveson.

THIS *JOURNAL* is produced monthly by The Institute of Physics, with the co-operation of the National Physical Laboratory. It deals with the principles, construction and use of scientific instruments. All rights reserved. Responsibility for the statements contained herein attaches only to the writers.

EDITORIAL MATTER. Communications concerning editorial matter should be addressed to the Editor, The Institute of Physics, 47 Belgrave Square, London, S.W.1. (*Telephone:* Belgravia 6111.) Prospective authors are invited to prepare their scripts in accordance with the *Notes for Authors*. (Price 3*s.* 6*d.* including postage.)

REPRODUCTION. The Institute of Physics is a signatory to The Royal Society's Fair Copying Declaration. Details may be obtained upon application from The Royal Society, London, W.1.

ADVERTISEMENTS. Communications concerning advertisements should be addressed to the agents, Messrs. George Jackson (Fleet St.) Ltd., Cliffords Inn, Fleet Street, London, E.C.4. (*Telephone:* Holborn 3611–2.)

CLAIMS FOR MISSING JOURNALS. Claims from regular subscribers to this *Journal* for missing numbers will only be considered if received within 60 days of the date of mailing plus normal outward time of transit and time for lodging the claim. Losses attributable to failure to notify a change of address or to similar omissions will not be considered.

SUBSCRIPTION RATES. A new volume commences each January. The charge is £6 per volume ($17 U.S.A.), including index (post paid) payable in advance. Single parts, so far as available, may be purchased at 12*s.* 6*d.* each ($1.75 U.S.A.), post paid, cash with order. Orders should be sent to The Institute of Physics, 47 Belgrave Square, London, S.W.1, or to any bookseller.

PRINTED IN GREAT BRITAIN BY UNWIN BROTHERS LIMITED, WOKING AND LONDON

Simple dosage meter for high-intensity thermal radiation

by P. H. THOMAS, M.A., Ph.D., and P. G. SMITH, Department of Scientific and Industrial Research and Fire Offices' Committee, Joint Fire Research Organization, Fire Research Station, Boreham Wood, Herts.

[*Paper received* 15 *June*, 1959]

Abstract

A simple radiation dosage meter which uses the melting of a temperature-sensitive paint as an indicator is described. Calibration curves are given for two versions, one suitable for 5–18 *cal* cm^{-2}, *the other for* 16–60 *cal* cm^{-2}. *An approximate theoretical analysis is also given.*

Introduction

This note describes the construction and calibration of a simple robust instrument, originally suggested by D. I. Lawson, for measuring the total amount of radiant heat falling on a given area in a short time. This dosage meter is self-contained, needs no power supply, and will retain indefinitely any radiation which has fallen on it. If thermal radiation is allowed to fall on a restricted area on the front of a sheet of material, heat will subsequently spread outwards. If the unexposed surface of this sheet is coated with a paint which melts or changes colour at a definite temperature, then the area of paint melted can be taken as a measure of the dose applied.

Construction of the dosage meter

A meter is illustrated in Figs. 1 and 2 and the appearance of the paint after exposure in Fig. 3. A 38 s.w.g. copper plate is used for doses in the range 5–18 cal cm^{-2} and a 26 s.w.g. steel plate for the range 16–60 cal cm^{-2}. The rear surface is coated with a paint which melts at 66° C and the exposed surface is coated with candle black so that it absorbs the incident radiation. In front of this plate is a shield of 16 s.w.g. polished aluminium with a central circular hole 1·9 cm diameter.

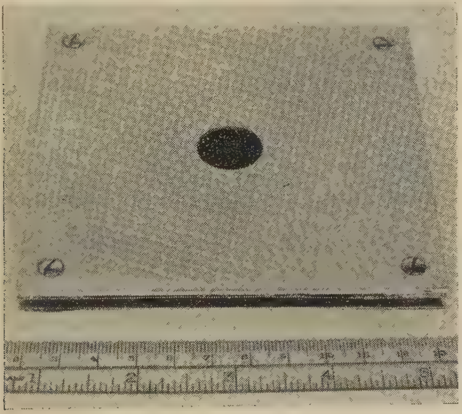

Fig. 1. Front view of dosage meter

The polished aluminium and the painted plate are separated by two vertical strips of asbestos paper 0·05 in. (0·13 cm) thick. In addition, a rear shield is necessary to minimize cooling effects caused by draughts. This shield is separated from the plate by about $\frac{1}{10}$ in. and may be made of any convenient thin metal sheet. The whole assembly is secured together by four 4 B.A. bolts. Even if the rear shield is made of highly reflecting aluminium, a screen may be

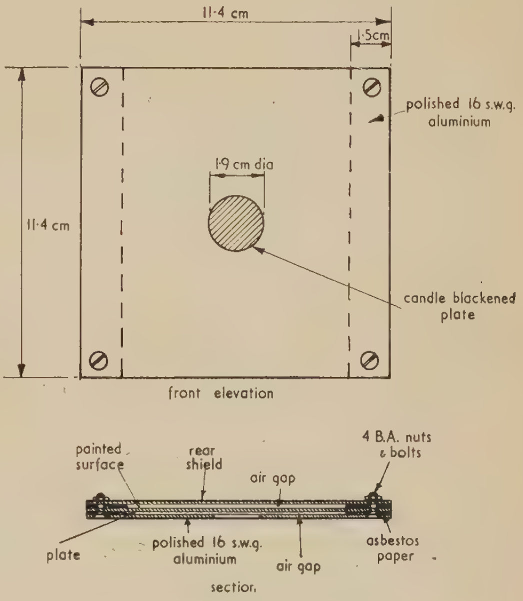
11·4 cm
1·5cm
polished 16 s.w.g. aluminium
1·9 cm dia
11·4 cm
candle blackened plate
front elevation
painted surface
rear shield
air gap
4 B.A. nuts & bolts
plate
polished 16 s.w.g. aluminium
air gap
asbestos paper
section

Fig. 2. Diagram of meter

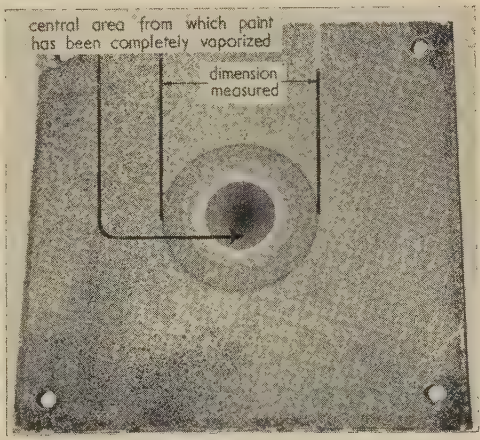
central area from which paint has been completely vaporized
dimension measured

Fig. 3. View of painted plate of dosage meter after exposure

required to protect the instrument from radiation from the sun. Such a screen should not interfere with the free flow of air from the atmosphere to the spaces between the painted plate and the front and rear shields.

Theory of dosage meter

The general radial conduction problem which is involved in the theory of this instrument is not readily amenable to analytic solution, except in terms of infinite integrals. Nevertheless, it is possible to establish quite simply some useful criteria to be observed in the design of a meter and to derive the approximate form of its calibration. To consider the idealized problem of a sheet across which the temperature remains uniform when heated and allowed to cool, it is assumed that the pulse of thermal energy is delivered to the sheet over a circular area of radius R. Therefore:

$$\frac{\partial^2\theta}{\partial r^2} + \frac{1}{r}\frac{\partial\theta}{\partial r} = \frac{1}{k}\frac{\partial\theta}{\partial t} + \frac{2H\theta}{\Delta K} - Q'_m\frac{f(t/t_m)}{\Delta K}, \qquad (1)$$

where: θ is the temperature of the sheet above ambient at radius r and time t,
K is the thermal conductivity,
k is the thermal diffusivity ($=K/\rho c$),
Δ is the thickness of the sheet,
Q'_m is the peak value of the incident flux,
t_m is a time characteristic of the duration of the pulse (for example, the time to maximum flux),
f describes the pulse shape,
H is the surface cooling coefficient,
ρ is the density,
c is the specific heat.

The boundary condition is:

$$Q'_m = 0, \quad r > R,$$

$$Q'_m = Q_m, \quad r < R$$

and

$$\theta = 0 \quad \text{when} \quad t = 0$$

General solution

The solution to equation (1) with the above conditions can be shown to be:

$$\theta = \frac{Q_m}{\rho c\Delta}\int_0^\infty J_1(z)J_0\left(\frac{r}{R}z\right)dz\int_0^t f\left(\frac{\lambda}{t_m}\right)\times$$

$$\times \exp\left\{-k\left(\frac{t-\lambda}{R^2}\right)\left(z^2+\frac{2hR^2}{\Delta}\right)\right\}d\lambda, \qquad (2)$$

where h equals H/K, and J_0 and J_1 are Bessel functions of the first kind of zero and first order.

It can be written quite generally:

$$\theta = \frac{Q_m t_m}{\Delta\rho c}F_1\left(\frac{r}{R}, \frac{t}{t_m}, \frac{kt_m}{R^2}, \frac{hR^2}{\Delta}\right) \qquad (3)$$

where F denotes "a function of". The energy dose received by the sheet is:

$$E = Q_m\int_0^\infty f(\lambda/t_m)d\lambda = (A,\ Q_m,\ t_m),\ \text{say},$$

where A depends on the pulse shape only and not on its magnitude or duration, so that in the above equation $Q_m t_m$ can be replaced by E/A.

The purpose of the thermal dosage meter is to measure the energy E received by recording the radius r_1 of the area of melted paint. If θ_p is the ambient temperature at which the paint melts and if any effects resulting from latent heat of melting are neglected, then θ_p is the maximum temperature occurring at radius r_1. Hence:

$$\frac{E}{\Delta\rho c\theta_p} = F_2\left(\frac{r_1}{R}, \frac{kt_m}{R^2}, \frac{hR^2}{\Delta}\right). \qquad (4)$$

This is the general form of the calibration.

It should be noted that as $(kt_m/R^2) \to 0$, equation (2) tends to:

$$\theta = \frac{E}{\Delta\rho c}\exp\left(\frac{-2hR^2}{\Delta}\cdot\frac{kt}{R^2}\right)\int_0^\infty J_1(z)J_0\left(\frac{r}{R}z\right)\exp\left(\frac{-z^2kt}{R^2}\right)dz. \qquad (5)$$

Only if kt_m/R^2 is small can the calibration be truly that for a dosage meter and independent of pulse shape and duration. In fact, the condition is not as stringent as this; it is shown below that the conditions required are:

$$\frac{kt_m}{r_1^2} \ll 1 \quad \text{and} \quad \frac{Ht_m}{\rho c\Delta} \ll 1.$$

Approximate square law

The limiting form of the function F_2 when hR^2/Δ and kt_m/R^2 are effectively zero is now considered. The heated plate behaves as if the temperature were instantaneously raised to $E/\rho c\Delta$ over the exposed area. The maximum temperature just beyond $r = R$ is $E/2\rho c\Delta$ (Fig. 4). Since this result is obtained for $t \to 0$, it must be independent of cooling and therefore:

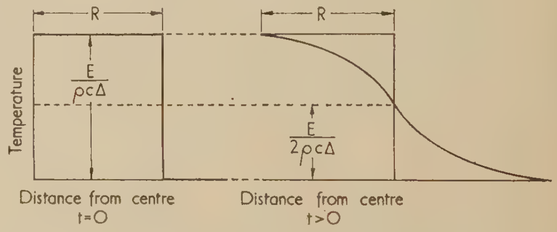

Fig. 4. Initial distribution of temperature

$$\frac{E}{\Delta\rho c\theta_p} \to 2 \quad \text{as} \quad r \to R.$$

High values of E are now considered so that r_1/R is large. With no surface cooling, the radiant-temperature distribution is similar to that in an infinite medium and the small value of R/r_1 makes the distribution similar to that from a line source of strength $\pi R^2 E/\rho c\Delta$. The solution for this problem is readily available and so:

$$\frac{\Delta\rho c\theta r^2}{ER^2} = \frac{1}{4\tau}\exp(-1/4\tau), \qquad (6)$$

where $\tau = kt/r^2$.

The maximum value of the left-hand side occurs when τ is equal to $\frac{1}{4}$, so that

$$\frac{ER^2}{\Delta\rho c\theta_p r_1^2} \to 2{\cdot}72 \quad \text{as} \quad \frac{r_1}{R} \to \infty$$

This value of $ER^2/\Delta\rho c\theta_p r_1^2$ differs by only 36% from its value for $r_1/R = 1$ and this suggests that a "square law" between E and r_1 would be a first approximation for a calibration.

Effect of cooling and a finite exposure time

The above result does not take cooling or finite times of exposure into account. For the special case of a large distance of spread and a short, but finite, application time it is possible to take the theory further, thus allowing for these effects, without undue complexity. A "square pulse" will be discussed, for which can be written:

$$f\left(\frac{\lambda}{t_m}\right) = 1 \quad \text{for} \quad \lambda < t_m.$$

For large values of r_1/R, the integral in equation (2) can be solved by writing:

$$J_1(z) \simeq \frac{z}{2} \qquad z \to 0$$

by which is obtained:

$$\frac{\Delta\rho c\theta r^2}{ER^2} = \frac{1}{2}\exp\left(\frac{-2hr^2\tau}{\Delta}\right) \times$$

$$\times \int_0^\infty yJ_0(y)e^{-\tau y^2}\left(1 + \frac{T_mW^2}{2!} + \frac{T_m^2W^4}{3!} + \ldots\right)dy \qquad (7)$$

where
$$T_m = \frac{kt_m}{r^2},$$

and
$$W^2 = y^2 + \frac{2hr^2}{\Delta}.$$

For small values of T_m, only the first two terms of the series need be discussed. From integrals given by Watson(1):

$$\frac{\Delta\rho c\theta r^2}{ER^2} = \exp\left(\frac{-2hr^2\tau}{\Delta}\right)\left(1 + \frac{hr^2T_m}{\Delta}\right)\frac{1}{4\tau}\exp\left(-\frac{1}{4\tau}\right) +$$

$$+ \exp\left(-\frac{2hr^2\tau}{\Delta}\right)\cdot\frac{T_m}{8\tau^2}\left(1 - \frac{1}{4\tau}\right)\exp\left(-\frac{1}{4\tau}\right) \qquad (8)$$

The value of τ can now be found for any value of hr^2/Δ and a small value of kt_m/r^2 that makes the left-hand side of equation (8) a maximum. After some rearrangement:

$$\frac{ER^2}{\Delta\rho c\theta_p r_1^2} = \frac{2\exp\{1 + (2hr_1^2/\Delta)\}^{1/2}}{1 + \{1 + (2hr_1^2/\Delta)\}^{1/2}} \times$$

$$\times \left(1 + \frac{kt_m}{r_1^2}[\{1 + (2hr_1^2/\Delta)\}^{1/2} - 1] + \text{higher powers of } \frac{kt_m}{r_1^2}\right) \qquad (9)$$

This gives the correction for a finite value of t_m. The equation is plotted in Fig. 5 for $t_m = 0$ and is discussed below. The term θ_p is a temperature above ambient so that, in practice, if the paint melts at 66° C, the value of θ_p is $66 - \theta_{amb}$ where θ_{amb} denotes the ambient temperature.

In order to use equation (9), a value must be assumed for H. This was taken as the value appropriate to radiation and convection from a vertical plate in free space. Because the receiver is in fact partially enclosed and the temperature of the plate is not uniform, this value of H is not strictly correct, but it is sufficient for a first approximation to the cooling correction. The correction term for finite values of t_m is always less than $Ht_m/\rho c\Delta$, irrespective of the value of r_1.

Calibration

The source of radiation used for calibration had a maximum intensity of radiation of about 12 cal cm^{-2} s^{-1}. The steel-plate dosage meter was exposed to this intensity for various times so that, for a dosage of 90 cal cm^{-2}, the exposure time was 7·5 s and, for a dosage of 18 cal cm^{-2}, was 1·5 s. It was possible to calibrate the copper-plate dosage meter for dosages below 12 cal cm^{-2} by altering the intensity of radiation, while keeping the exposure time at approximately 1 s. For higher doses it was necessary to increase the exposure times slightly to a maximum of 1·5 s.

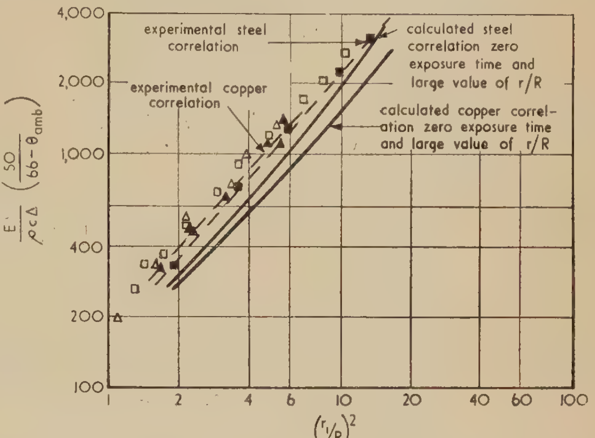

Fig. 5. Correlation of data for calibration of dosage meter

■ Steel 12 cal cm^{-2} s^{-1}
▲ Copper 12 cal cm^{-2} s^{-1}
□ Steel 6 cal cm^{-2} s^{-1}
△ Copper 6 cal cm^{-2} s^{-1}

The lines through the points are based on the 12 cal cm^{-2} s^{-1} results only

To investigate the effect of the use of long exposures at low intensities to simulate short exposures at high intensities, a calibration of the steel plate was carried out with the output of the radiation source halved, the exposure times being doubled. The calibrations obtained in this way are also shown in Fig. 5. The value of T_m was approximately constant and, for the steel dosage meter, was about 0·09 for exposure at 12 cal cm^{-2} s^{-1} and twice this for exposure at 6 cal cm^{-2} s^{-1}. For the copper dosage meter, the values of T_m were respectively 0·015 and 0·031. These values are all small compared with unity. For steel, the largest value of $Ht_m/\rho c\Delta$ was 0·08 and for copper 0·06. The conditions for the approximate theory given above may therefore be regarded as being largely fulfilled.

The effect of the finite exposure time is to increase the value of the calculated ordinate for a given value of r_1/R by less than 8% at the largest value of r_1/R. This would bring the calculated line and experimental points in Fig. 5 even closer together at large values of r_1/R where the calculations should be most accurate.

Discussion

The practical difference between exposure at 12 and 6 cal cm^{-2} s^{-1} is small and the calibrations at 12 cal cm^{-2} s^{-1} for both the steel and the copper plates have been taken as the best calibrations. According to the approximate theory leading to equation (9), the difference between the two copper calibration curves made at intensities of 12 and 6 cal cm^{-2} s^{-1} should be less than that between the corresponding calibrations using steel sheets, and the copper calibration should lie below the steel on Fig. 5 because of the smaller value of hr_1^2/Δ, but this was not found to be so. However, it is considered that the approximate theory is sufficiently accurate to provide a basis for designing dosage meters for other ranges of thermal dose.

It has been shown that the direct effect on the calibration of sideways conduction during the exposure is assessed by kt_m/r_1^2 which is small and is a much less stringent condition than that kt_m/R^2 should be small. The physical reason for this is that, at large distances from the heat source in the centre of the plate, the distribution of heat is not critical, the source behaving more like a point source the greater the distance of final spread.

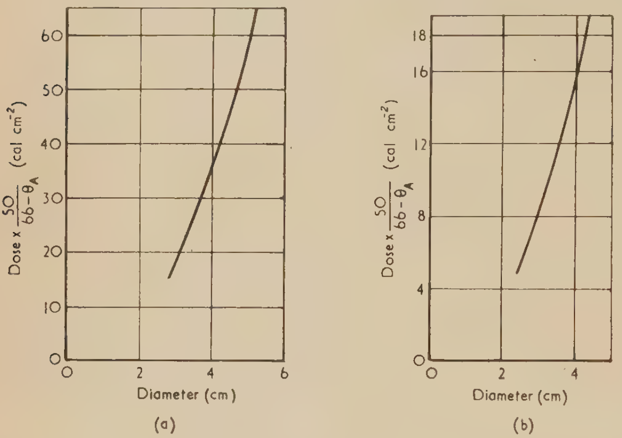

Fig. 6. Diameter of melted area (*a*) for steel plate, and (*b*) for copper plate

Conduction sideways during the exposure markedly affects the actual temperature reached by the plate and, when exposure times are short, the temperatures more nearly approach the theoretical limits of $E/\rho c\Delta$. As will be seen from Fig. 5, this means that the field performance of the thermal dosage meters is limited by the melting of the metal.

The steel plate, slightly roughened and oxidized, was blackened and then exposed to a high radiation intensity to burn off the carbon black. It was then allowed to cool and was re-exposed to a dose of 20 cal cm^{-2}; the area of melted paint was the same as for a plate on which the carbon black had not been destroyed. The copper plate behaved in the same way. The performance of the meters is therefore no limited by the burning of the carbon black. It would, in principle, be possible to reduce this effect by increasing the sideways conduction during exposure, but this would require exposure areas which are too small (approximately 1 mm diameter) for the measure of the melted area to be accurate. Fig. 6 shows the dotted lines of Fig. 5 replotted directly in terms of energy and diameter of the melted area.

The apparatus can also be used to measure the value o the heat flux, if this is constant for some time. It is worth noting that, in principle, use could be made either of radial flow or linear flow, the first from a circular area and the second from a long strip. The theory for linear flow is somewhat simpler than that for radial flow, and the calibration will be approximately linear between dose and distance of spread instead of between dose and area. Practical difficulties arise in calibrating strip-type radiometers because of the small areas of the available high-intensity sources but, being linear, they may be more suitable for some uses, although the range of any such instrument will be less than for a radial-flow instrument of equal size and aperture.

Acknowledgements

The work described in this paper forms part of the programme of the Joint Fire Research Organization of the Department of Scientific and Industrial Research and Fire Offices' Committee. The paper is published by permission of the Director of Fire Research. The authors would like to acknowledge the assistance of J. H. McGuire.

Reference

(1) WATSON, G. N. *Treatise on the Theory of Bessel Functions*, p. 393 (Cambridge: C.U.P., 1944).

Design of a single electrode capacitor for use with moisture meters and similar apparatus

by D. F. LEACH, B.Sc., Grad.Inst.P., and J. M. M. NEILSON, B.Sc.,* The British Jute Trade Research Association, Dundee

[*Paper first received* 7 *May, and in final form* 21 *September* 1959]

Abstract

Measurements of the capacitance of a single cylindrical electrode in air have been made for each of the three variables, length, radius and height above earth. The effect of surrounding it by dielectric masses of various sizes was also investigated, and the change of capacitance with increase in dielectric volume determined. The influence of these factors when designing a capacitor of this type is discussed. This electrode has been successfully used for measuring the moisture content of textile packages, and could be used for similar applications involving measurement of dielectric properties.

Any conducting cylinder will possess a capacitance dependent upon its physical dimensions, disposition to earth and the dielectric constant of the surrounding medium. If the radius of the cylinder is sufficiently small compared with its length, a needle-like electrode is obtained suitable for plunging into a mass of dielectric, the change of capacitance which takes place giving a measure of the dielectric constant.

Mention of this type of capacitor was found in standard textbooks,† but these do not deal specifically with the case of a finite dielectric and contain no reference to agreement of the theory with experimental results. In view of this it was thought worth while to examine further the properties of the probe in both infinite and finite dielectrics.

Interest in the use of a capacitor of this type arose from attempts to determine the moisture content of jute packages by dielectric methods. Spools of jute yarn are commonly about 8 in. in diameter and 9 in. long, and are wound on a hollow wooden centre of 1 in. diameter. Initially these were examined by inserting them in a cylindrical capacitor, so that the central electrode was inside the spool centre, but it was found that as the wooden centre was closest to the central rod electrode it greatly influenced the results. It was also found that removal of the exterior earthed electrode made very little difference to the capacitance of the system. These observations suggested that the cylindrical capacitor could be replaced by a "probe" electrode of the type described above, which could be inserted directly into the jute.

The capacitance of a probe electrode

The capacitance of the probe will be influenced by its length, radius, height above earth and the size of the surrounding dielectric.

For a thin right circular cylinder of total length l and radius r, in a dielectric of permittivity K, the capacitance may be shown to be

$$C = 1\cdot 11Kl\bigg/\left\{2\log_e\left(\frac{4h}{r[1+\{1+(16h^2/l^2)\}^{1/2}]}\right)\right\}\text{pF} \quad (1)$$

provided $h \gg r$ and $l \gg r$, and if $h \gg l$

$$C = 1\cdot 11Kl/\{2\log_e(l/r)\}\ \text{pF} \quad (2)$$

in which case C is independent of h.

Consideration of finite dielectrics must be based upon an examination of the equipotential surfaces. Let P be a point in the field due to a thin right circular cylinder with a charge of q electrostatic units per unit length and other dimensions as indicated in Fig. 1.

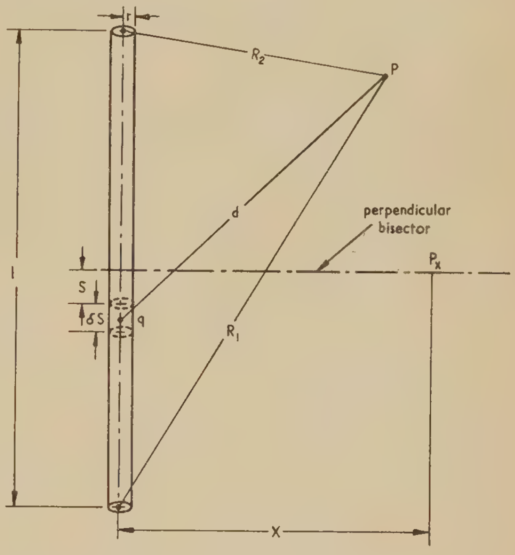

Fig. 1. Field at a point due to an element of the probe

Then the total potential V, and P due to the whole cylinder may be shown to be

$$V = (q/K)\log_e\{(R_1+R_2+l)/(R_1+R_2-l)\}\ \text{e.s.u.} \quad (3)$$

and thus V is constant when $R_1 + R_2$ is constant. As $R_1 + R_2$ is the sum of the distances from P to the ends of the cylinder, the equipotentials are ellipsoids with the ends of the cylinder as foci.

To see how the potential falls with distance from the cylinder axis, it is convenient to examine the behaviour along the perpendicular bisector of the cylinder. Let the potential at a point P_x, a distance x along the perpendicular bisector, be V_x (see Fig. 1); then as

---

* Now at University of Edinburgh.

† See, for example, Attwood, S. S. *Electric and Magnetic Fields*, 3rd ed., p. 82 (New York: John Wiley and Sons, Inc., 1949).

$$R_1 = R_2 = \{(x^2 + l^2)/4\}^{1/2}$$

$$V_x = (q/K) \log_e [\{(4x^2 + l^2)^{1/2} + l\}/\{(4x^2 + l^2)^{1/2} - l\}] \quad \text{e.s.u.}$$

and if $x = \beta l$

$$V_x = (q/K) \log_e [\{(4\beta^2 + 1)^{1/2} + 1\}/\{(4\beta^2 + 1)^{1/2} - 1\}] \quad \text{e.s.u.} \quad (4)$$

Thus the potential is determined by the ratio of the distance from the cylinder to its length. The nature of equation (4) is shown in Fig. 2 by the full line, where it will be seen that at first the potential falls off very rapidly.

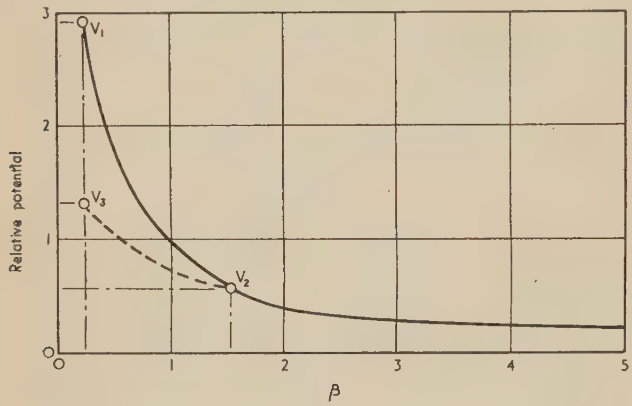

Fig. 2. Change of potential with position in field
—— = potential in uniform infinite dielectric $K = 1$
– – – = potential in finite ellipsoidal dielectric $K = 3$

Provided $h \gg r$, equation (4) can be used to find the capacitance of a probe in an ellipsoidal dielectric. Let V_1 be the potential of a probe in a vacuum and V_2 the potential for an ellipsoidal equipotential, the minor axis of which is in the ratio β to the length of the probe. Then if V_3 is the potential of the probe when a uniform dielectric of permittivity K fills the ellipsoid out to the equipotential, the equivalent series capacitor arrangement gives

$$\frac{V_2}{V_3} = K/K - 1 + \frac{V_1}{V_2} \quad (5)$$

From this the capacitance for any particular size of dielectric may be found.

The effect of a dielectric of $K = 3$ filling an ellipsoid of minor axis 1·5 times the probe length is shown by the dotted line in Fig. 2.

Experimental

The above equations apply to an idealized probe and no allowance is made for distortion of the field caused by the electrical connexion to a measuring circuit. Further, a practical probe may need a handle to enable it to be plunged into dielectric masses, and also these dielectrics will rarely approximate to ellipsoids.

To examine the magnitude of the influence of these factors, experiments were conducted for the following four variables:

(*a*) the effect of length in an infinite dielectric;
(*b*) the effect of height above earth on an infinite dielectric;
(*c*) the effect of radius in an infinite dielectric;
(*d*) the effect of the size of the dielectric.

Air was used as the infinite dielectric and for variables (*a*), (*b*) and (*c*) capacitance measures were made with a Marconi circuit magnification meter at 100 kc/s, but for variable (*d*) special arrangements were required.

It was found that the method of holding the probe influenced the results obtained; if the connexion was made at one end of the rod the capacitance was lower than predicted, but if the connexion was by a miniature crocodile clip to the centre results were in better agreement with the theory. As the method used will depend on the application, the clip at the centre was used unless otherwise stated.

(*a*) *Effect of length.* Probes of lengths between 10 and 70 cm, and of 0·159 cm radius, were examined at one height above earth, and the results are shown in relation to the calculated curve in Fig. 3. Up to 50 cm the experimental values agree moderately well with the calculation, but above 50 cm the experimental values are greater, probably because of the presence of objects other than the plane earthed sheet.

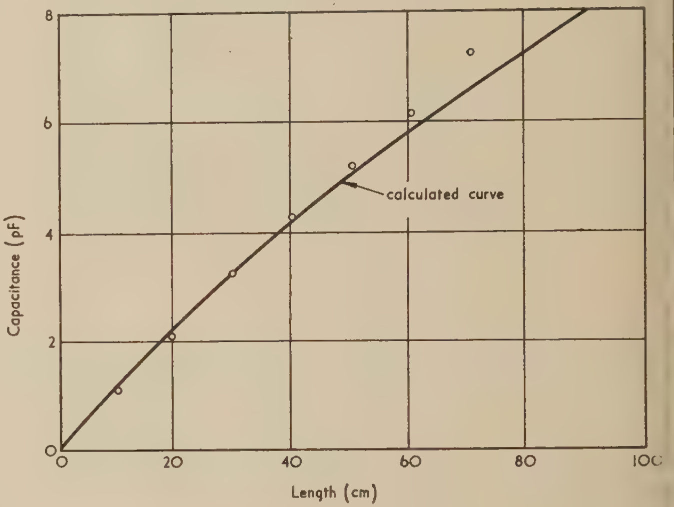

Fig. 3. Variation of capacitance with length of probe ($h = 100$ cm, $r = 0·159$ cm)

(*b*) *Effect of height.* The variation of capacitance with height above an earthed sheet is shown in Fig. 4, and the results are in good agreement with the calculated curve (solid line). Results are also shown for a probe supported at one end by insertion into an axial hole in a ½ in. diameter brass

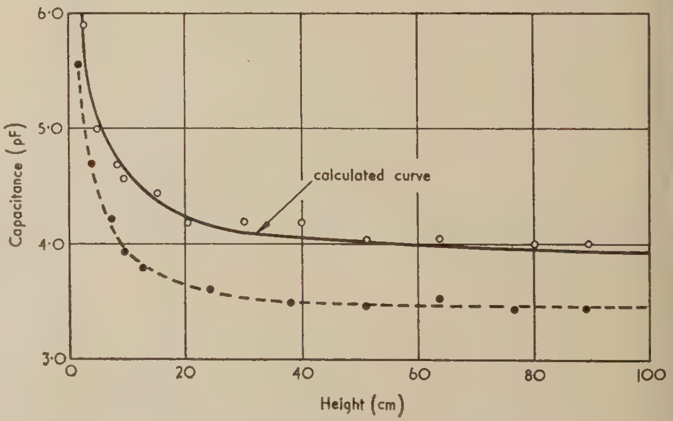

Fig. 4. Variation of capacitance with height above earthed sheet. (1 = 38·1 cm, $r = 0·159$ cm)
○ = supported at centre
● = supported at end

cylinder, the projecting length being taken as the probe length. It will be seen that, whilst the shape of the curve is the same, the values are lower, the difference at 100 cm being 0·55 pF.

(*c*) *Effect of radius.* From equation (1) it will be seen that $(\text{capacitance})^{-1}$ is directly proportional to $\log r$, and the results in Fig. 5 are shown on this basis. The results are in good agreement with the calculation for the range investigated, $0{\cdot}03 < r < 1{\cdot}0$ cm.

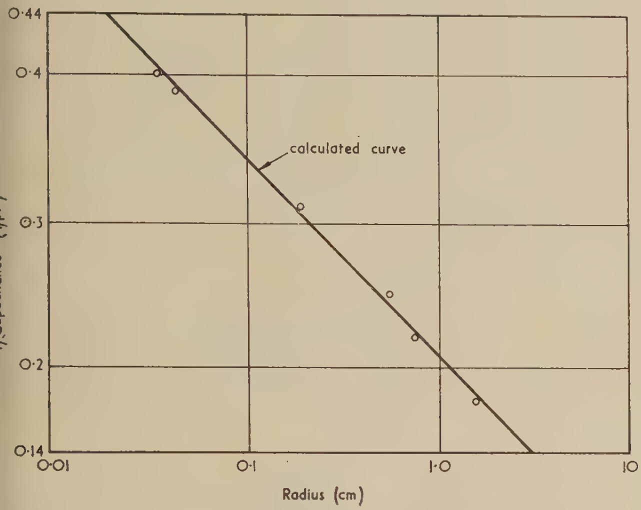

Fig. 5. Variation of capacitance with radius of probe. (1 = 30 cm, h = 100 cm)

(*d*) *Finite dielectrics.* For the purposes of the present investigation, it is only necessary to consider the case where a material in contact with the probe has a higher dielectric constant than the surrounding medium.

The theoretical examination of the effect of size of the dielectric on the capacitance of the probe postulated a probe lying between the foci of an ellipsoidal dielectric. Experimentally this was not practicable, but as the theory indicates that above small radii increases of capacitance with radius are small, the shape of the dielectric should become unimportant, thus allowing dielectrics in the form of right circular cylinders to be used, the radius of the cylinder being taken as equivalent to the minor axis of an ellipsoid.

The probe was supported by insertion into an axial hole in a larger rod, so that the projecting length was the nominal probe length. It has already been shown in paragraph (*b*) that this method gives results lower than those calculated, but this should not influence the manner in which the field decreases with distance from the probe axis.

Ideally, materials covering a range of dielectric constant should have been investigated, as this quantity influences the decline of the field, but suitable dielectric substances which are easily obtained in cylindrical form are not readily available. Liquids would be suitable, as the container need have little influence, and would cover a wide range of dielectric constant. Unfortunately, many of these liquids also have high conductivities, but transformer oil is an exception, and this was used.

The experimental arrangement is shown in Fig. 6. The probe was supported in a length of $\frac{1}{2}$ in. diameter threaded rod and the end of the rod lay $\frac{1}{4}$ in. below the surface to eliminate positioning errors. The thread on the rod allowed adjustment to suit the container depth. The capacitance changes measured were small, 0·15 to 0·75 pF, and care was necessary to maintain conditions constant; the observer had to remain in one position whilst taking readings (about 4 ft from the probe) and the final lead to the probe was made with unscreened wire, so that its position relative to the probe was unimportant.

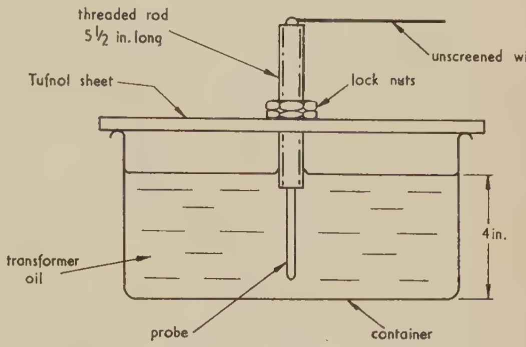

Fig. 6. Arrangement for dielectric experiments

So as to measure only the capacitance effects due to the probe the supporting rod was always kept in the position shown in Fig. 6 and the probe removed to find the capacitance due to its presence in the dielectric. The Marconi circuit magnification meter used for the other experiments was not sufficiently sensitive, and the capacitance change was measured by substituting a calibrated capacitor, a Fielden proximity meter being used as the null detector. Two probe lengths, 1·25 and 2·50 in. both $\frac{1}{8}$ in. in diameter, were examined.

The capacitance found for a probe in a dielectric cylinder was denoted by C_D and the values of C_D for various dielectric radii were expressed as percentages of the maximum value KC_0, where C_0 is the capacitance of the probe in a vacuum (air in practice). The permittivity K for the transformer oil was 2·2, and Fig. 7 shows the experimental results together with the calculated curves. It will be seen that the results for the 2·5 in. probe are in good agreement with the calculations, and those for the 1·25 in. probe fit a curve of similar shape to that calculated. The less satisfactory nature of the results for the 1·25 in. probe is, perhaps, to be expected,

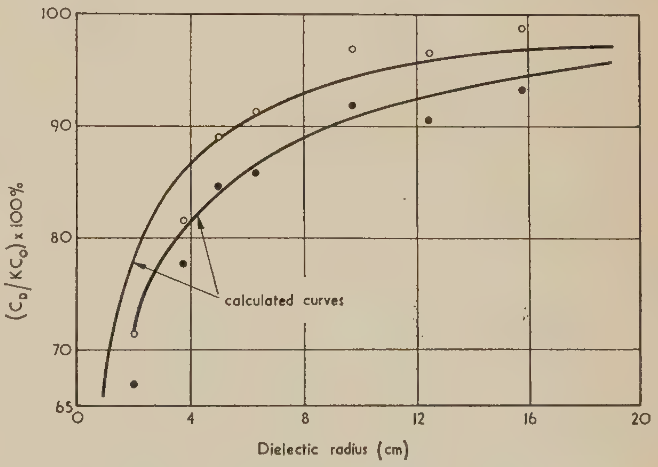

Fig. 7. Effect of varying dielectric radius

○ = 1·25 in. probe
● = 2·5 in. probe

as the experimental conditions become progressively less ideal as the probe becomes shorter. The general measure of agreement confirms the essential correctness of the assumption, that the difference between the ellipsoidal dielectric assumed for the calculation and the cylinders used in the experiments was not important.

Design considerations

For applications such as the measurement of moisture in textile packages, it is not necessary to be able to determine the actual permittivity, and calibrations are made empirically. It is sufficient to ensure that factors, other than the moisture content, which influence the capacitance are either under control or of negligible extent. The degree of accuracy required will vary with the application envisaged, but an error of ±5% in the capacitance measurement would not be serious in many cases.

The factors of importance for the probe were discussed above and the practical implications are stated below.

(*a*) *Effect of height.* From Fig. 4 (probe supported at end) it can be seen that, provided the probe is more than 30 cm above the ground, errors will be small; approximately a 0·2% change in capacitance for a 10 cm change in height.

(*b*) *Effect of length and radius.* The ratio of probe length to radius is important, because the greater this ratio the greater is the field strength at the surface of the probe. The longer a probe the farther out will the strong regions of the field extend, thus necessitating larger volumes of dielectric. It is desirable that the field within the dielectric should be as strong as possible and that the field at the surface of the material should be as weak as possible. Thus a probe should be as thin and short as is practicably consistent with obtaining sufficient mechanical strength, reasonable penetration and a capacitance change large enough to be accurately measured.

(*c*) *Size of the dielectric.* The dielectric should be as large as possible, so that the capacitance change measured is large, and also to keep the effect of the supporting surface, i.e. the floor or bench top, to a minimum. For packages which are large compared with the length of the probe the effect of changes in size will be small (see Fig. 7) and may be neglected, but with smaller packages dimensions would be more important. However, for many industrial processes the packages would have consistent dimensions, and size should not be a great problem. For cylindrical packages the effect of the supporting surface may be minimized by inserting the probe perpendicular to this surface.

(*d*) *Packing density.* The permittivity of a material is directly related to its packing density and, as with all tests based on capacitance measurements, this property must be controlled. This is usually a matter of adequate maintenance of the device which forms the packages.

(*e*) *Conductivity effects.* The simple theory given above takes no account of the effect of the conductivity of the dielectric, a factor which may be appreciable in certain materials or with conditions of high moisture content. This conductivity effect can be utilized in suitable circuits to give greater equivalent changes of capacitance. For instance, if the probe is included as part of the tuned circuit of an oscillator, the conductivity of the dielectric will have a considerable influence on the frequency of the oscillator. For large changes in conductivity it may be necessary to limit the change with a series capacitor; this will also reduce the power loss which might otherwise prohibit the oscillator from functioning.

Use in the jute industry

The probe has been successfully used in the jute industry to measure the moisture content of a wide range of jute packages, including bales of fibre $4 \times 1\frac{1}{2} \times 1\frac{1}{2}$ ft; rolls $2\frac{1}{2}$ ft in diameter and 5 in. thick; and spools of yarn, 8 in. in diameter and 9 in. long.

The probe was made of carbon steel and its construction is shown in Fig. 8. It was used in conjunction with a heterodyne capacity meter, operating at 200 kc/s, where it formed part of the tuned circuit of one oscillator. The measuring capacitor was part of the same tuned circuit and the second oscillator was provided with a tuning capacitor for obtaining zero beat. The beat frequency was indicated on a "magic eye" tuning indicator. The instrument had three measuring ranges, 0–14, 0–28 and 0–600 pF, the latter being restricted to a measured change of 0–14 pF, by a series capacitor. This enabled the range 10–30% moisture content (expressed on wet weight) to be covered.

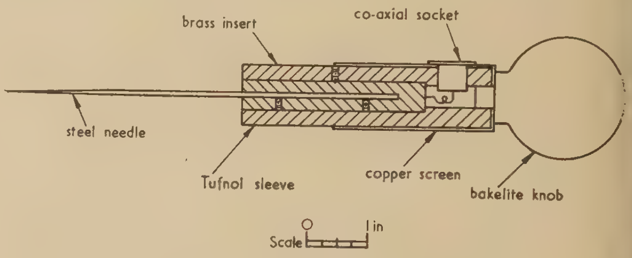

Fig. 8. Construction of probe

At 10% moisture content the circuit discriminates to 10 ± 0·25%, and at 30% to 30 ± 0·05%. These values are small compared with the moisture variations often present within packages. It is difficult to put a figure on the inherent accuracy of the probe because the standard tests against which it was evaluated use samples of less than 100 g, and are thus subjected to large sampling errors. However, the standard deviation of results on packages of relatively uniform moisture distribution is 0·3%, and it may thus be taken that a single probe reading will give the moisture content x% of a package to within x ± 0·75% (98·8% of all tests). This figure may, of course, be improved by taking more tests.

The empirical calibration was made for one size of roll and one size of spool, and this was found to apply satisfactorily to other sizes of rolls and spools and also to bales. (Allowance was made for differences in packing density between the various packages.) The higher conductivity present with material above 16% moisture content did not present a problem, as it is only the large rolls which normally exceed this figure.

Conclusions

The probe electrode is well suited for use as the transducer in an industrial instrument where it is desired to measure either the dielectric constant, or some property which affects the dielectric constant, of material available in bulk. It enables tests to be made at the point of production without the laborious process of removing samples—a disadvantage inherent in many other methods of test.

Acknowledgements

The authors express their thanks to the Director and Council of the British Jute Trade Research Association for permission to publish this paper.

Method of measuring the angular deflexion in a dynamometer

by M. AXSON, B.Sc., and J. M. MAGARSHACK, B.A., British Cotton Industry Research Association, Shirley Institute, Manchester

[*Paper received* 21 *September*, 1959]

Abstract

In the method to be described, unidirectional square-wave current pulses are produced with a mark-to-space ratio proportional to the deflexion of the spring system in a dynamometer. The pulses are fed to a moving-coil meter which has a sufficiently slow response to read the mean current. The reading is then proportional to the deflexion. Two systems for producing the square-wave pulses are discussed. The first is robust and simple in construction and can be applied when the forces to be measured are large. The second system can be used for the measurement of small forces where it is undesirable to make any physical contact with the dynamometer.

Introduction

The use of a dynamometer to find the torque acting on a rotating shaft usually involves the measurement of an angular displacement between driving and driven portions of the system. In the simplest form of dynamometer, the deflexion is observed by using a stroboscope, but in general it is more convenient to obtain an indication of the deflexion at some distance from the shaft and possibly to record it at the same time. For these purposes, it is customary to use an electronic technique involving either strain gauges, capacitative pick-up heads or some other type of transducer. A method which can sometimes be applied with advantage is to produce unidirectional square-wave current pulses of constant amplitude with a mark-to-space ratio depending upon the deflexion to be measured. If such pulses are fed to a moving-coil meter with a natural frequency much lower than the pulse frequency, the mean current reading is directly proportional to the time for which current flows during any one cycle, and is therefore proportional to the angular displacement. It has been shown by Pearce* that if square-wave current pulses with a 1 : 1 mark-to-space ratio are fed to a critically damped meter the natural frequency of which is half that of the pulse frequency, the fluctuation in the reading above the mean level is less than 5%.

As the frequency ratio is reduced, the fluctuations rapidly become negligible. If the pulse frequency is not sufficiently high, it will be immediately obvious by the visible needle fluctuations which will be of the same frequency as the square-wave pulses. The square-wave pulses are produced by the rotation of the loaded shaft and, provided the pulse frequency remains much greater than the natural frequency of the meter, any variation in the speed of the shaft has no effect on the meter reading. The square-wave frequency must also be greater than the rate of change of the angular deflexion to be measured. Two dynamometer systems using this principle are described in this paper.

Dynamometer using slip rings

The dynamometer described in this section can be used when the torque to be measured is sufficiently great for the frictional forces inherent in the measuring system to be neglected, the main advantage being that it can be made simply and robustly. The torque acts on a spring which transmits the drive, and the angular deflexion of this spring is measured.

The detecting system acts as a switch which is continually making and breaking, and the on-to-off time ratio of this switch is proportional to the angular displacement which it is required to measure. The switch is connected in series with an energizing voltage V, a limiting resistance R and a meter, the resistance of which is R_m. If the switching frequency is sufficiently high, therefore, the meter will read:

$$\bar{i} = PV/(R + R_m),$$

where P is the on-to-off ratio.

The complete detecting system has two separate switches each consisting of a brush and commutator system. One switch is attached to the driving member and one to the driven. The relative sizes of the conducting and insulated commutator segments and their total number are determined by the conditions to be described. There are several alternative ways of connecting these switches and these are illustrated in Fig. 1.

In the circuit (*a*), the two brush-commutators are connected in series with the meter. The relative position of the brushes with respect to their commutators is adjusted so that when there is no angular displacement between the driving and driven members the switch *B* switches on as *A* switches off, as shown in the brush-timing column. When there is some relative displacement, *B* switches on before *A* switches off and a square-wave current pulse flows through the meter. In the undeflected condition, *B* switches off before *A* switches on again. This is necessary in order to avoid current flowing for negative deflexions if there is some vibration in the drive that is not transmitted by the spring. This overlapping "off" region must be of an amount not less than the amplitude of the vibration. The number of segments per ring, which must be large enough to ensure that the switching frequency is much greater than the natural frequency of the meter, is restricted by the vibration present. Depending on the speed of the shaft and the maximum torque applied to it therefore, the minimum spring strength can be determined for the maximum angular deflexion consistent with a reasonable number of segments. The conducting segments of each commutator are connected together and are either connected to earth through the machinery or the commutators are joined by means of a lead which is sufficiently flexible for it to exert no restraining force on the spring. In this case, no current need pass through the mechanical parts.

---

* Pearce, S. F. *J. Sci. Instrum.*, **27**, p. 203 (1950).

In circuit (*b*), the two brushes are in parallel with each other and the meter, and their timing is out of phase, current flowing through the meter only when both brushes are off. In this case, the earth return must be either through the machinery or through an extra slip ring. Only one brush is needed with this system if it is made to overlap on to both commutators.

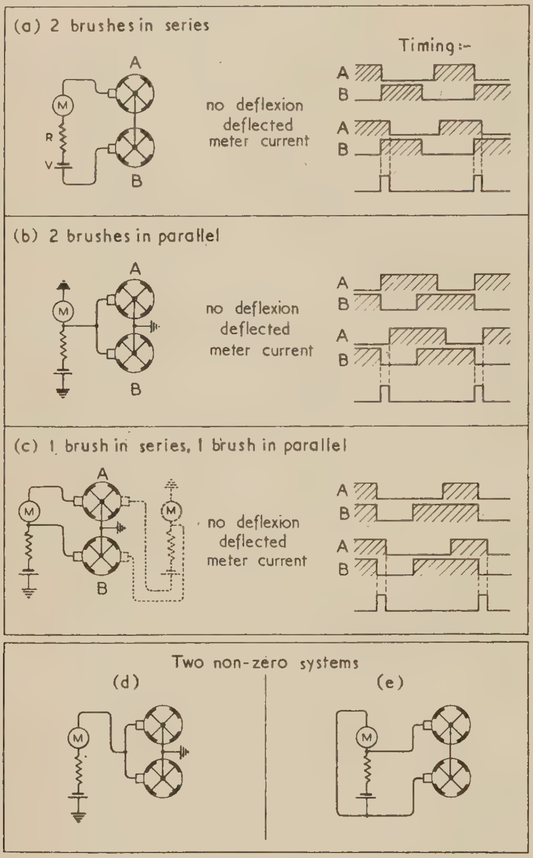

Fig. 1. Alternative ways of connecting switches

In circuit (*c*), two alternatives are shown with one brush in series and one in parallel. The timing here is in phase, current flowing through the meter when the series brush switches on before the parallel brush short circuits the meter, and can be adjusted more easily for this reason than in the other systems.

If there is some brush resistance the meter will read high for systems (*b*) and (*c*) and low for system (*a*). The current passing through the brushes will be smallest in the first system.

To include all the types of series and parallel switches, two other possible systems {(*d*) and (*e*)} might be mentioned. These, however, give a non-zero minimum current which increases linearly with the deflexion with the appropriate timing.

Fig. 2 shows an example of a dynamometer applied to a pulley-shaft system which rotates at about 800 rev/min. The pulley has been mounted in ball bearings on the shaft and a leaf spring which is clamped to the pulley transmits the drive. Two standard d.c. motor commutators, each of 48 segments. are attached one to the end face of the pulley and the other to a stub which is fixed to the end of the shaft. Every third commutator segment is connected to a common lead, each intermediate pair remaining insulated. The brushes are mounted at 90 deg. for convenience and are connected as i the first system. The width of one brush was reduced s that the switch-on time is suitable for the vibration presen There is also a scale and pointer for calibrating the deflexio of the spring (see final section).

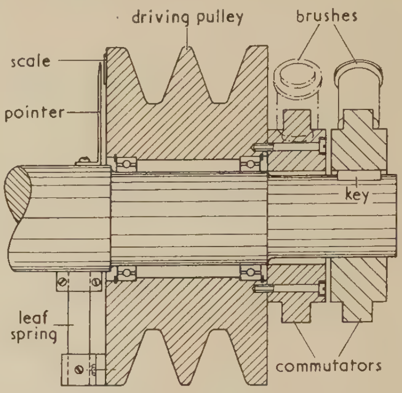

Fig. 2. Dynamometer applied to pulley-shaft system

All the main components used in this dynamometer are standard parts and it was found to give reliable performance in spite of a complicated vibration in the drive.

Dynamometers without direct connexion to the rotating system

If a dynamometer is to be used to measure small forces, the frictional drag imposed by the brush and commutato systems used in the method described in the previous section cannot be tolerated and it is necessary to produce the square- wave current pulses without making any direct connexion to

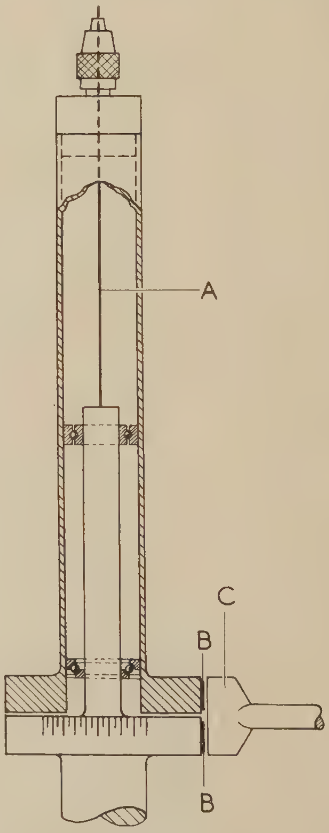

Fig. 3. Method for producing square-wave current pulses without making direct connexion to the rotating system

the rotating system. The roller or bobbin upon which the torque is to be measured, is coupled to the driving shaft by a light spring or torsion wire (*A*. Fig. 3), A disk is attached to both driving shaft and roller, the two disks being adjacent to each other, and the same size. One disk has a scale on it and the other an index mark. In addition, each disk carries a projecting lug *B*, and these projections separate when the torque is applied. Mounted in a fixed position near the roller is a thin plate *C* with its edge lying in the same plane as the two lugs, and separated from them by a small gap of about 1 mm. The edge of the plate and the two disks form an electrical capacitor and, as each lug passes the plate, there is a change in the electrical capacitance. The capacitor controls the positive feedback of an oscillator so that any change in its capacitance alters the amplitude of the oscillation. The oscillator output is rectified and each passage of a lug past the flat plate produces a voltage pulse. If there is an angular separation between the two lugs, a train of voltage pulses is produced, as shown in Fig. 4(*a*).

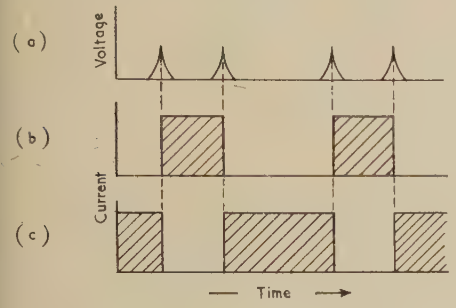

Fig. 4. Voltage and current pulses

The pulses are amplified and shaped to a form suitable for the operation of an Eccles–Jordan circuit, which contains two valves, one of which is passing current while the other is practically cut off. When triggered by a negative pulse, the first valve becomes non-conducting and current begins to flow in the second valve. The next negative pulse restores the original condition. Therefore, each pair of pulses produces a square-wave current pulse at the anode of the second valve, the duration of which is the time interval between the triggering pulses [Fig. 4(*b*)]. If a milliammeter is placed in series with the anode of the second valve, the current indicated will depend upon the mark-to-space ratio of the square-wave current pulses, provided the natural frequency of the meter is much lower than the frequency of the square waves.

There is obviously a danger that the Eccles–Jordan circuit will start out of phase, thus giving the square-wave pattern shown in Fig. 4(*c*). This is overcome by choosing the coupling spring so that the maximum deflexion is never likely to exceed 120 deg. Therefore, current will never be passing through the indicating meter for more than one-third of the time if the Eccles–Jordan circuit is operating in the correct phase, but will be passing for more than two-thirds of the time if the circuit is out of phase. A low-current, high-speed relay is placed in series with the meter and is shunted by a small resistance which is adjusted until the relay operates when current is passing for more than half the time. The relay contacts are in series with the relay, and they open when the relay operates, thus breaking the anode circuit. This brings the Eccles–Jordan circuit automatically into the correct phase. The complete circuit is shown in Fig. 5.

The dynamometer was designed to measure forces when rotating at 6000–10000 rev/min, but it can, of course, be used at much slower speeds by increasing the number of projections on the disks.

Calibration

The calibration of both systems is carried out in two stages. Various known torques are applied to the roller or bobbin when stationary and the corresponding deflexions are read

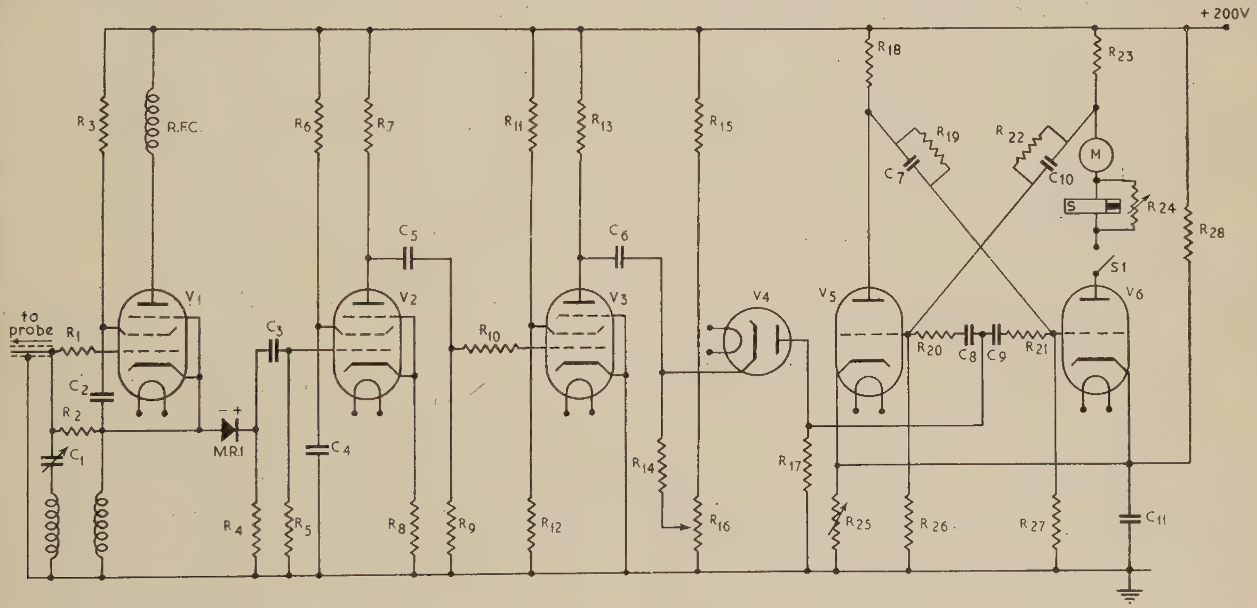

Fig. 5. Low torque dynamometer circuit

R_1 = 10 kΩ
R_2 = 470 kΩ
R_3 = 100 kΩ
R_4 = 470 kΩ
R_5 = 470 kΩ
R_6 = 2 MΩ
R_7 = 470 kΩ
R_8 = 2·2 kΩ
R_9 = 470 kΩ
R_{10} = 10 kΩ
R_{11} = 4·7 kΩ
R_{12} = 22 kΩ
R_{13} = 100 kΩ
R_{14} = 470 kΩ
R_{15} = 68 kΩ
R_{16} = 25 kΩ
R_{17} = 470 kΩ
R_{18} = 28 kΩ
R_{19} = 470 kΩ
R_{20} = 100 kΩ
R_{21} = 100 kΩ
R_{22} = 470 kΩ
R_{23} = 28 kΩ
R_{24} = 1 kΩ
R_{25} = 10 kΩ
R_{26} = 100 kΩ
R_{27} = 100 kΩ
R_{28} = 100 kΩ

C_1 = 100 pF
C_2 = 0·1 μF
C_3 = 0·01 μF
C_4 = 0·5 μF
C_5 = 0·01 μF
C_6 = 500 pF
C_7 = 33 pF
C_8 = 33 pF
C_9 = 33 pF
C_{10} = 33 pF
C_{11} = 0·2 μF
V_1 = 6AM6
V_2 = 6SJ7
V_3 = 6SJ7
V_4 = 6H6
V_5 = 6J5
V_6 = 6J5
MR_1 = W6
M = 0·5 mA (f.s.d.)

S = 2000 Ω coil

from the scale, so that a calibration curve of deflexion as a function of torque can be obtained. The roller is then locked to the driving shaft at a particular deflexion and the meter reading obtained with the roller rotating. This is repeated for several values of the deflexion and a calibration curve of deflexion plotted against the meter reading is obtained. Alternatively, if the height of the current pulse is known, a calibration curve of deflexion against meter reading can be calculated. From the two calibrations it is then possible to calculate a calibration curve for torque against meter reading. In general, the calibration curve may be expected to be linear. As the forces measured using the second technique are small, it may be necessary to take account of the air drag by running the roller without applying a torque and subtracting the resulting meter reading from that obtained when the torque is applied.

Apparatus for investigating total hemispherical emissivity

by J. H. CAIRNS, M.Sc.Tech., Ph.D., A.I.M., Department of Chemical Engineering and Metallurgy,
Faculty of Technology, University of Manchester

[*Paper first received* 6 *August, and in final form* 22 *September*, 1959)

Abstract

An apparatus is described for measuring the total hemispherical emissivity of highly polished metals and alloys over the temperature range 100 to 900° C. The apparatus consists essentially of a highly polished, hollow, cylindrical sample supported within an evacuated enclosure of only slightly larger dimensions. Provision is made for raising the temperature of the sample above that of the enclosure by means of an internal heater contained within the hollow sample. Emissivity values are obtained by observing the rate of loss of heat from the sample after switching off the heater, and substituting this observed value in a specially derived radiation equation. An accuracy of better than ±8% and a reproducibility of ±5% are claimed for the emissivity values. Experimental data for titanium are included as an example. The apparatus is also capable of direct measurement of specific heat over the same temperature range to an accuracy of ±2%.

THE physical properties of metals and alloys have, in general, been widely investigated and evaluated by many workers, but little attention has been given to the emissive properties, particularly to the total hemispherical emissivity. Total hemispherical emissivity is defined as the ratio of the total energy radiated by a body throughout the hemisphere above each element of surface to that radiated by a black body of equal surface area at the same temperature. The reported values of total hemispherical emissivity, which are limited to a few isolated metals, differ widely, and have been reported for only limited ranges of temperature.(1–5) Over the last decade, the lack of an exact knowledge of the emissivity of high-temperature metals and alloys has become an increasingly important problem in the design of supersonic aircraft, rockets, and nuclear reactors, for which an accurate prediction of the radiant-heat dissipation is essential. The apparatus described here was designed and constructed for a twofold purpose; firstly to evaluate accurately the total hemispherical emissivity of the important high-temperature metals and alloys, thus providing the engineer with the values essential to accurate high-temperature design, and secondly, to attempt to correlate the observed emissivity values with other fundamental properties of metals and alloys, such as electrical conductivity and electronic structure. The results of this work will shortly be published elsewhere.

Principle of operation

A sample of the metal under investigation was prepared in the form of a hollow cylinder closed at both ends, highly polished on its outer surfaces and contained within a cylindrical copper enclosure, as shown in Fig. 1. The temperature of the specimen was caused to rise above that of the enclosure by the input of electrical energy to an internal heater contained within the hollow specimen. On switching off the heater, the specimen temperature falls as a result of heat loss to the enclosure. This heat loss results from a com-

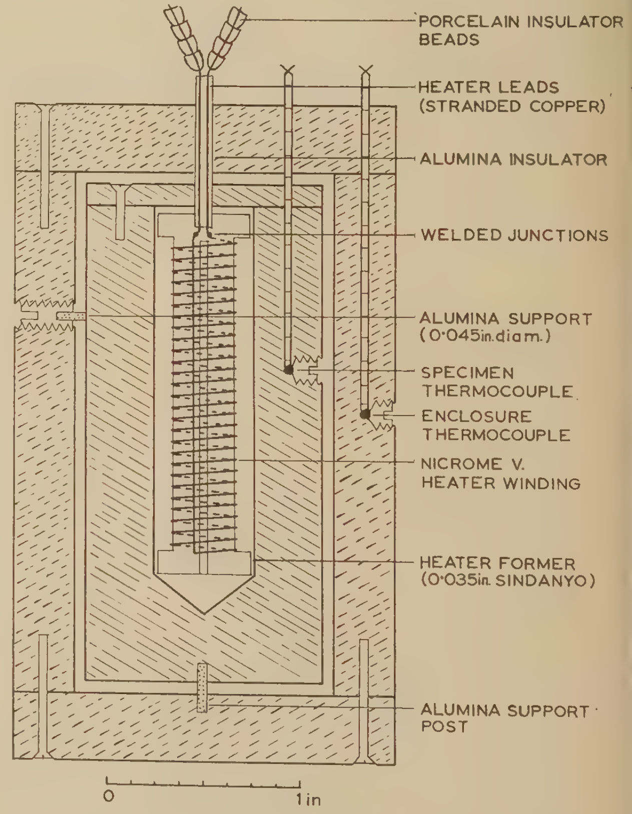
PORCELAIN INSULATOR BEADS
HEATER LEADS (STRANDED COPPER)
ALUMINA INSULATOR
WELDED JUNCTIONS
ALUMINA SUPPORT (0·045in.diam.)
SPECIMEN THERMOCOUPLE
ENCLOSURE THERMOCOUPLE
NICROME V. HEATER WINDING
HEATER FORMER (0·035in. SINDANYO)
ALUMINA SUPPORT POST
0
1 in

Fig. 1. Vertical section through specimen/enclosure assembly

bination of the following factors: (*a*) radiation, (*b*) molecular conduction by the residual gases, (*c*) conduction along the specimen supports and the heater and thermocouple leads. Of these three factors, the first may be shown to be predominant under conditions of high vacuum. Experimental evaluation of (*b*) and (*c*) and the inclusion of an experimentally determined correction factor H, the non-radiant transfer (see Appendix), allowed the heat loss to be considered as resulting from radiation alone.

If the mass of the specimen, m, and its specific heat, s, are known, and if its rate of fall of temperature, $d\theta/dt$, is observed, then the loss of heat from the specimen is $msd\theta/dt$ cal/s. Incorporating the non-radiant transfer factor H, the radiant-heat loss from the specimen is $\{(msd\theta/dt) - H\}$ cal/s. It has, however, been well established that the energy radiated by a hot body at T° K is $A\sigma T^4$ cal/s for a black body, and $AE\sigma T^4$ cal/s for a non-black body, where A is the surface area of the body, E its total hemispherical emissivity, and σ the Stefan constant. These values represent simply the heat emitted by the body. To arrive at the net heat loss, it is necessary to take into account also the heat which the body receives. This includes what it gains from the radiation emitted from its surroundings and from such part of its own radiation as is reflected back to it by the surroundings. For complex shapes of hot body in restricted surroundings, a precise formulation of the net radiation is not possible, but for concentric spheres or cylinders, an exact equation can be derived. In the present investigation, the geometrical arrangement of concentric cylinders in which the specimen size is only slightly less than that of the enclosure was used. For this geometrical arrangement, the problem of the reflective nature of the surrounding surface was resolved, for it can be shown that the net radiation from the specimen is the same irrespective of the nature of the reflective surface, be it specular or diffuse. Since most practical surfaces are intermediate between these two extremes, a radiation equation which is exact for all conditions of enclosure surface was derived. A further advantage of the adopted geometrical arrangement is that the ratio of radiant/non-radiant heat transfer is a maximum.

The radiation equation was derived by considering the radiation from the specimen and from the enclosure separately. The net radiation from the specimen was obtained by summation, and is given by:

$$J = \frac{A\sigma(T_S^4 - T_E^4)}{(1/E_E) + (1/E_S) - 1} \text{ cal/s,} \qquad (1)$$

where A is the surface area of the specimen and is approximately equal to the surface area of the enclosure, T_S and T_E are the absolute temperatures, and E_S and E_E are the total hemispherical emissivities of the specimen and enclosure.

Rearrangement of equation (1) for solution of the specimen emissivity gives:

$$E_S = \frac{J}{A\sigma(T_S^4 - T_E^4) + J - J/E_E}. \qquad (2)$$

However, since the radiant-heat loss from the specimen is $\{(msd\theta/dt) - H\}$ cal/s, then substitution for J in equation (2) above gives:

$$E_S = \frac{(msd\theta/dt) - H}{A\sigma(T_S^4 - T_E^4) + \{(msd\theta/dt) - H\} - \{(msd\theta/dt) - H\}/E_E}, \qquad (3)$$

from which the specimen emissivity can be computed.

Apparatus

The specimen under investigation was supported within a copper enclosure by alumina posts, as shown in Fig. 1. The alumina side supports, of which there were three symmetrically disposed at 120 deg. spacings, were adjustable by means of the grub-screw holders which allowed accurate axial location of the specimen with respect to the enclosure. Provision was made for observing the specimen and enclosure temperatures by means of thermocouple hot junctions located

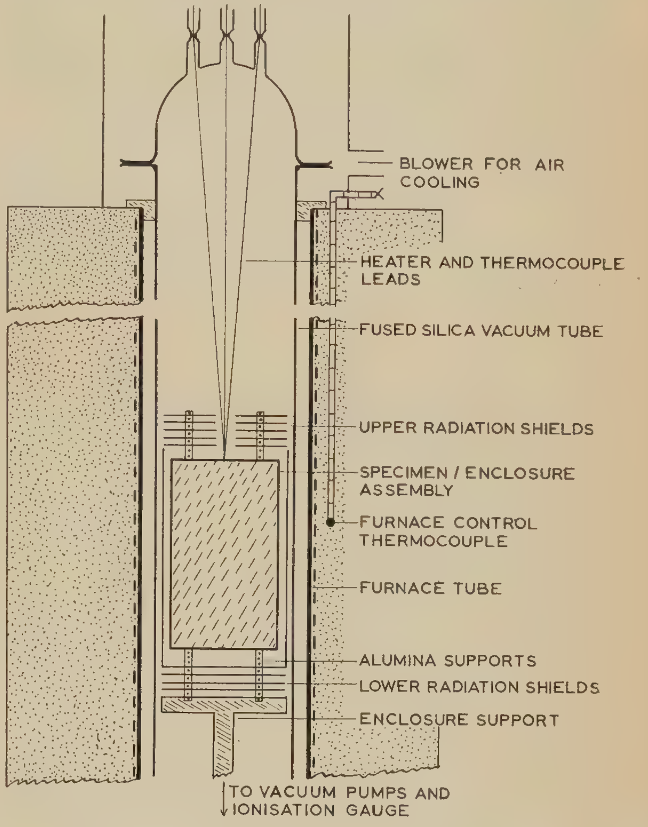

Fig. 2. Vertical section through furnace assembly

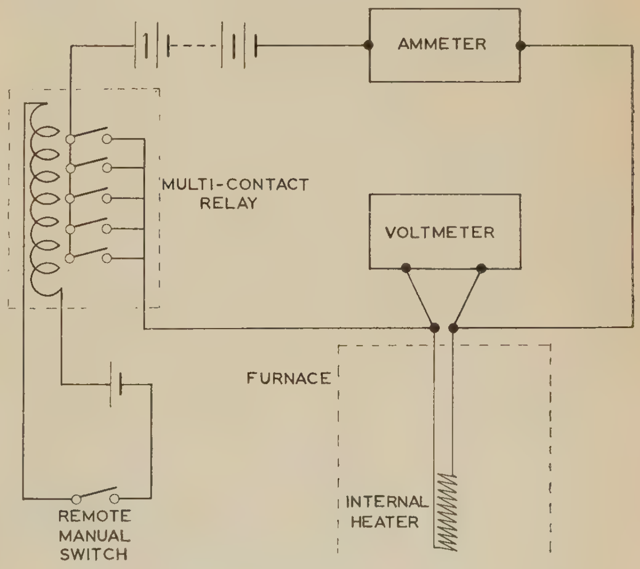

Fig. 3. Internal heater circuit

in the specimen and enclosure walls. The thermocouple e.m.f.'s were measured by means of a matched pair of Cambridge vernier potentiometers. The heater leads were enclosed in a twin-bore alumina insulator and passed through the enclosure and specimen tops. Radiation shields were placed around the enclosure to ensure uniformity of enclosure temperature, and the whole specimen-enclosure assembly was located centrally within a vertical furnace tube of fused silica, as shown in Fig. 2. The internal heater circuit, Fig. 3, included a substandard ammeter and voltmeter which enabled the energy input to the specimen to be measured accurately. The heater was wound with 0·0125 in. diameter Nichrome V wire on a cruciform framework of 0·035 in. Sindanyo, and the junctions of the copper heater leads and the Nichrome element were made by arc-welding under argon. The heater circuit was switched by means of a silvered, multi-contact relay which ensured minimum variation of contact resistance. Evacuation of the system was achieved by a three-stage oil diffusion pump backed by a double-stage rotary pump, and residual pressures of the order of 10^{-5} mm of mercury (as measured with an ionization gauge) were obtained.

Operating procedure

The specimen was positioned within the enclosure and the combined assembly located within the furnace tube as shown in Fig. 2. The Pyrex adaptor through which the heater and thermocouple leads passed was sealed to the silica furnace tube with Picien wax. The system was then evacuated for fifteen hours in order to ensure thorough degasification before taking the first readings. The furnace was then raised to the chosen temperature of investigation and allowed to stabilize. The internal heater of the specimen was switched on, and the current and the potential drop across the heater were noted. When the specimen temperature had risen by approximately 12° C, the heater was switched off, and the duration of the "heater-on" period was noted. The temperature of the specimen continued to rise slowly, because of a levelling of the thermal gradients resulting from the rapid heating. The maximum temperature of the specimen and the corresponding enclosure temperature at that instant were recorded and the total time taken for the specimen to attain its maximum temperature was noted. From these results the specific heat of the specimen, which was required for inclusion in the emissivity equation, was obtained in accordance with the following theory.

Specific-heat theory

The energy supplied to the internal heater causes the specimen temperature to rise from its initial value θ_{S1} to a maximum value θ_{S2}. During the time required for the specimen to attain its maximum temperature, it loses a small amount of heat to its surroundings, namely the enclosure, by reason of the imperfection of the insulating media. This causes the enclosure temperature to rise slightly from its initial value θ_{E1} to θ_{E2}. The presence of the series of radiation shields surrounding the enclosure reduces the heat loss from the enclosure to a negligible value. A further source of heat loss from the specimen is by conduction along the heater and thermocouple leads during the heating period. This represents not more than 5% of the total energy input, and is a function of the time t required to attain maximum specimen temperature, the final temperature difference between the specimen and the enclosure, and the thermal conductivity k of the heater and thermocouple leads.

Thus, all the energy input to the specimen is accounted fo and the specimen specific heat is obtained from the equation

$$\frac{\mathrm{CV}d}{4\cdot 19} = m_S(\theta_{S2} - \theta_{S1})S_S + m_E(\theta_{E2} - \theta_{E1})S_E + k(\theta_{S2} - \theta_{E2}) \qquad (4$$

where C and V are the current and potential drop in the heate circuit, d the duration of the heater-on period, and m_S, m and S_S, S_E are the masses and specific heats of the specime and enclosure. The specific-heat/temperature relationship c the enclosure was obtained experimentally by an initia determination using a specimen prepared from the sam batch of copper as that used for the enclosure, so that th specific heats of the specimen and enclosure could be assume to be equal. The results obtained agreed to within ±2% with the latest reported mean values of specific heat fo copper.

Emissivity procedure

On attaining maximum temperature as a result of th energy supplied in the specific-heat determination, the speci men begins to cool and loses heat by radiation to its sur roundings, namely the enclosure. When sufficient time fo the cooling rate to become fully established has been allowe the enclosure and specimen temperatures and the rate of fal of the specimen temperature were measured, thus providing data for the evaluation of the specimen emissivity, in accordance with equation (3). The rate of fall of the speci men temperature, $d\theta/dt$, was measured for a specimen-to enclosure temperature difference of approximately 12° C The time required for a fall of specimen temperature corre sponding to a decrement of 0·02 mV (that is approximately 0·5° C) was normally measured, except in the higher tem perature range where the rate of cooling was so fast that in order to reduce the effect of errors in time measurement, a decrement of 0·04 mV was used. As a result of the inciden radiation from the specimen, the enclosure temperature rises during the emissivity determination. This temperature rise is very small because of the much larger mass of the enclosure but by a slight reduction of the furnace temperature, it was possible with practice to maintain a constant enclosure temperature for the duration of the emissivity determination. It should be noted that constancy of enclosure temperature is not a necessary requirement of the emissivity equation, but was maintained for ease of experimental observation. The specimen and enclosure temperatures observed, that is, T_S and T_E, were those corresponding to the mid-point of the specimen temperature decrement.

Example of use

The experimental data given below are for a titanium specimen at a starting temperature of 606° C.

Specimen starting temperature θ_{S1} = 606·00° C
Corresponding enclosure temperature θ_{E1} = 606·40° C
Mean heater current C = 1·755 A
Mean heater voltage V = 11·92 V
Heater duration d = 127·8 s
Maximum specimen temperature θ_{S2} = 624·42° C
Corresponding enclosure temperature θ_{E2} = 606·60° C

Time to reach maximum specimen temperature t = 150·0 s
Rate of fall of specimen temperature $d\theta/dt$ = $5{\cdot}2313 \times 10^{-3}$ deg./s
Mean specimen temperature T_S = 618·24° C (891·24° K)
Corresponding enclosure temperature T_E = 606·27° C (879·27° K)
Non-radiant transfer factor H = $0{\cdot}0527 \times 10^{7}$ erg/s
Mass of specimen m = 202·0 g
Specimen surface area A = $80{\cdot}79\ \text{cm}^2$
Vacuum = $0{\cdot}92 \times 10^{-5}$ mm of Hg
Enclosure emissivity E_E = 0·051

Substitution of the experimental data in the specific-heat relationship of equation (4) gives:

$$(1{\cdot}755 \times 11{\cdot}92 \times 127{\cdot}8)/4{\cdot}19 = 202(624{\cdot}42 - 606{\cdot}00)S + 980(606{\cdot}60 - 606{\cdot}40)0{\cdot}105 + 0{\cdot}0038(624{\cdot}42 - 606{\cdot}60)150$$

Therefore the specific heat S is 607·43/3720·84 or 0·1632 cal/g deg. C at a mean temperature of 615·2° C.

If this experimental value of the specimen specific heat, together with the additional experimental data, is substituted in the emissivity equation, equation (3), then first:

$$(msd\theta/dt) - H = (202 \times 0{\cdot}163 \times 5{\cdot}231 \times 10^{-3} \times 4{\cdot}19 \times 10^{7}) - (0{\cdot}0527 \times 10^{7}) = 0{\cdot}6687 \times 10^{7},$$

and second:

$$A\sigma(T_S{}^4 - T_E{}^4) = 80{\cdot}79 \times 5{\cdot}6699 \times 10^{-5}\ (891{\cdot}24^4 - 879{\cdot}27^4) = 15{\cdot}2165 \times 10^{7}.$$

Therefore the specimen emissivity E_S is given by:

$$E_S = \frac{0{\cdot}6687 \times 10^{7}}{\{15{\cdot}2165 + 0{\cdot}6687 - (0{\cdot}6687/0{\cdot}051)\} \times 10^{7}} = 0{\cdot}241, \text{ at mean temperature of } 618^\circ\ \text{C}.$$

The enclosure emissivity incorporated in the above calculation was obtained from an enclosure calibration curve. This was compiled from the results of three investigations using a copper specimen prepared from the same batch of copper as the enclosure and having the same thermal history and surface finish. Thus the specimen and enclosure emissivities could safely be considered equal and substitution of E_E for E_S in equation (3) allowed evaluation of the enclosure emissivity.

Accuracy

The main sources of error are thought to be:

(*a*) Temperature measurement, which is to the nearest 0·001 mV (that is, 0·025° C) for chromel-alumel couples. Allowing for an error of opposite sign in the specimen and enclosure thermocouples, and considering the fourth-power difference of temperature, this source of error is not greater than 1%.

(*b*) Specific-heat values which are determined experimentally to ±2%. This factor may be responsible for an error of ±2% in the computed emissivity.

(*c*) The use of a radiation equation based on the assumption that the specimen and enclosure surface areas are equal. The smaller surface area of the specimen necessary for clearance will cause an error in the computed emissivity only in the case of diffuse reflexion. For highly polished metals, this error is less than 1%.

(*d*) Slight variation in the non-radiant transfer factor H caused by vibration of the specimen against the alumina locating posts. This is responsible for an error of not more than ±2% in the lower temperature range and ±1% in the higher temperature range.

(*e*) The inclusion of the enclosure emissivity in the specimen emissivity equation. Any error in the enclosure calibration will be cumulative in the computed specimen emissivity. However, by taking the enclosure calibration as the mean of a number of carefully performed determinations, it is thought that this error can be reduced to less than ±2%.

The maximum total error in the apparatus is therefore ±8%, but in view of the closer reproducibility of the experimental results, that is, to ±5% in the worst case, it is considered that the ultimate accuracy of the emissivity results is somewhat better than ±8%.

Appendix. Experimental evaluation of non-radiant transfer factor *H*

Because of the imperfection of the insulating media, a small percentage of the heat transfer from the specimen to the enclosure during the emissivity determination occurs other than by radiation. This non-radiant transfer consists of conduction along the thermocouple and heater leads and the alumina locating posts, and conductance by the residual gases, that is, molecular conductance. In the higher temperature range, this non-radiant transfer is less than 5% of the total, but an accurate experimental evaluation is essential to the accuracy of the emissivity results. This was achieved by undertaking two series of experiments, the first with a copper specimen of standard size and the second with a specimen of the same material and surface finish, but of half the standard surface area. In order to preserve the same geometrical relationship as for the standard specimen, the bottom of the enclosure was filled with a copper insert for the second series of experiments. The locating posts and the heater and thermocouple leads were, however, identical with those used for the standard specimen. This reduction of the specimen surface area reduces the radiation transfer to half the standard value, while the non-radiant transfer remains unaltered. (In practice, the molecular transfer, being area-dependent, is also reduced to a half, but this is compensated for by doubling the residual pressure. This is justifiable because molecular transfer is directly dependent on both surface area and residual pressure.) The emissivities of the standard and the half specimens are, however, the same. Therefore, by equating the experimental data from the two series of experiments in accordance with equation (3), the non-radiant transfer H (the only unknown quantity), may be evaluated.

References

(1) Davisson, C., and Weeks, J. R. *J. Opt. Soc. Amer.*, **8**, p. 581 (1924).

(2) Worthing, A. G. *Phys. Rev.* (2), **28**, p. 190 (1926).

(3) Michels, W. C., and Wilford, S. *J. Appl. Phys.*, **20**, p. 1223 (1949).

(4) Best, G. *J. Opt. Soc. Amer.*, **39**, p. 1009 (1949).

(5) Zimmermann, F. J. *J. Appl. Phys.*, **26**, p. 1483 (1955).

Oscillator measuring equipment for vibrating-wire gauges

by W. H. WARD, B.Sc.(Eng.), A.M.I.C.E., and J. E. CHENEY, Department of Scientific and Industrial Research, Building Research Station, Garston, Watford, Herts.

[*Paper first received* 10 *September, and in final form* 17 *November*, 1959]

Abstract

Vibrating-wire gauges are well known for their versatility in the measurement, not only of strain, but of many other physical quantities. It has been found that for some purposes the usefulness of the gauges has been restricted by limitations in the traditional reference-wire method of measurement. The design, construction, calibration and use of a new instrument which measures the frequency of vibrating-wire gauges is presented. It utilizes a variable-frequency electronic oscillator, which is continuously checked against a tuning-fork and regularly checked by time signals. Two models of the present version of the instrument have given very satisfactory performance under difficult conditions on civil engineering projects. The new instrument is cheaper and simpler to make than the traditional type and covers a frequency range of about 250 *to* 2500 *c/s.*

Introduction

This paper describes the design, construction, calibration and use of an instrument* for measuring the frequencies of vibrating-wire gauges. These gauges are used for measuring strains and, indirectly, can measure many other physical quantities such as stress, load and temperature. The measurement depends on the well-known property of a flexible elastic wire, tensioned between two supports as in a stringed musical instrument, that any change in axial strain produces a proportional change in the square of the frequency of vibration.† Normally a high-tensile steel wire is used and an electromagnet is placed alongside for pulsing the wire and reading its frequency from a distance.

The vibrating-wire gauge is essentially a very simple *mechanical* gauge which is capable of maintaining its dimensions and frequency to a degree comparable with the stability of a tuning fork. The electromagnetic circuit is not an essential part of the gauge, but it is a very useful adjunct which provides a simple means of operating and recording the gauge from a distance. In contrast to the various types of strictly electrical strain gauges, any change in the properties of the electrical circuit of a vibrating-wire gauge does not alter the gauge and its frequency. The high degree of stability of the gauge is also a very valuable asset, particularly when it is not possible to make independent checks on the stability at frequent intervals. For these reasons, the vibrating-wire gauge is particularly useful in field work where electrical circuits become prone to damage and deterioration. In the authors' experience, the vibrating-wire gauge is to be recommended as a reliable instrument for use in the field on civil engineering projects. No insurmountable problems have been encountered when operating gauges remotely under such adverse conditions as in a water-filled tunnel under a head of 140 ft of water,(1) in compressed air at the dew point, in tube railway tunnels,(2) and in a large excavation in the Thames marshes.(3)

In the past,(4, 5, 6) the frequencies of vibrating-wire strain gauges have been measured by reference to another wire, the frequency of vibration of which can be adjusted to correspond with the gauge frequency by straining with a screw micrometer. This method possesses the theoretical simplification that differences in micrometer readings are directly proportional to the strain changes in the gauge wire, but in our experience this method has not proved satisfactory. For example, the gauges themselves proved to be more stable than the reference-wire device and the frequency range of the device was inadequate.

In the light of these experiences it was decided to develop a new instrument using a valve oscillator to measure the frequencies of vibrating-wire gauges. The variable-frequency oscillator contained in the new instrument has, in its present form, a frequency range of about 250 to 2500 c/s (range of strain-unit values* 60–6000). Means are provided for exciting the gauge, and the oscillator can be tuned to the strain gauge frequency, either visually by means of signal traces on a cathode-ray tube, or audibly on earphones. A maintained tuning-fork, incorporated within the instrument, is used in the calibration of the oscillator and to keep a subsequent check on its calibration. The tuning-fork is checked against Post Office time signals.

Two versions of the complete instrument have been built in the last few years, and two models of the latest version, which is described below, have been in continuous field use for two years. Their performance has amply justified the departure from the traditional reference-wire system and they are considerably cheaper to construct since almost all the components are regular products of the radio industry.

Experience has shown that with this instrument 150–200 strain gauges, and an adequate number of checks on the frequency calibration, can be observed in an hour. There is no difficulty in measuring strains to an accuracy of 10^{-6} during a period of several months on a gauge in common use, and, when necessary, measurements to an accuracy of 10^{-7} can be made over shorter periods. The instrument is as stable as the strain gauges and in tests for their stability such small strains that are recorded may be natural movements of the materials to which the gauges are fixed.

---

* Covered by British Patent Application No. 169/60.

† This is not strictly true because every wire has some stiffness, but, provided the tension is not allowed to fall below some minimum value which reduces the influence of rigidity to insignificance, the relation is sufficiently accurate for most practical purposes.

* The strain-unit value is obtained by squaring the frequency (in cycles per second) and dividing by 1000; it is a convenient unit when working with vibrating-wire strain gauges.

Circuit

Fig. 1 shows a block diagram of the instrument. The auge wire is plucked by means of a manual switch which onnects either the single pulse or the resonant plucking ystem to the electromagnet alongside the gauge wire. The ibrations of the wire are then picked up by the same electronagnet which is now connected to the gauge-signal amplifier. he signal from the variable-frequency oscillator is amplified nd matched with the gauge frequency, either visually on the athode-ray tube by obtaining the 1 : 1 ratio Lissajous figure r aurally by eliminating the beats produced in earphones. he calibration of the oscillator is checked by substituting the signal from the tuning-fork for the gauge signal and observing the appropriate Lissajous figures on the cathode-ray tube. The complete circuit diagram and a list of components are given in Fig. 2.

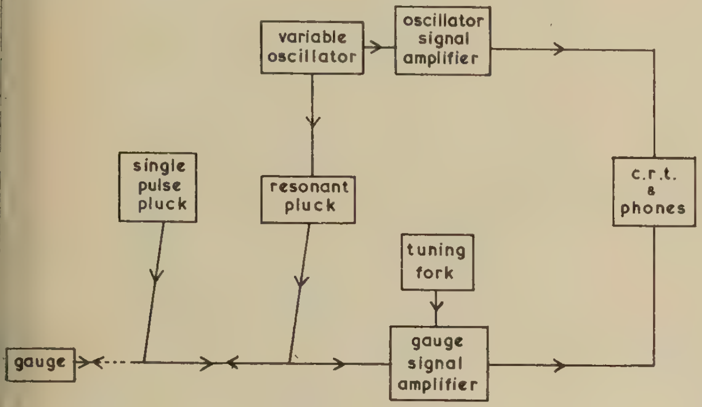

Fig. 1. Block diagram of circuit

Oscillator. The resistance-capacitance oscillator is based on a variation⁽⁷⁾ of the Wien bridge circuit with 360 deg. phase shift and automatic amplitude control. The pairs of resistors R_1, R_2, and the pairs of capacitors C_1, C_2 and C_3, C_4 in the bridge are made as nearly equal as is practicable so that the resonant frequency f is given by the equation:

$$f = \frac{1}{2\pi R_1(C_1 + C_3)}.$$

The strain recorded by a vibrating-wire gauge is proportional to the change in the square of the wire frequency and it is therefore desirable for the oscillator to have a control giving a linear scale in terms of the square of the frequency, that is a control which gives a linear variation in $\{1/R_1(C_1 + C_3)\}^2$.

A two-gang capacitor (C_1, C_2) was chosen as the continuously variable component and, to obtain a steady linear variation in f^2 over a series of bands, it is necessary to switch both resistors and capacitors. In the present version of the instrument, this elaboration was not attempted, and only resistors are switched for a series of eleven bands labelled A to L, with the result that the strain-unit sensitivity decreases from band to band as the frequency is increased. The variable-capacitor dial divides the 180 deg. rotation accurately into 1000 parts, and the sensitivity of the bands varies from about 0·05 to 5·0 strain-units per dial division from band A to band L respectively (see table).

Oscillator-signal amplifier. The oscillator signal is fed through R_{11} and C_{10} to a conventional single-stage valve amplifier (V_5); amplitude control is provided by the potentiometer R_{17}.

Gauge excitation. The gauge is excited, or plucked, by means of the manual switch *SD* which, at the same time, temporarily disconnects the gauge from its amplifier. The type of excitation is chosen by pre-setting the switch *SF*, the three positions of which provide for single pulse, single pulse with reversed polarity, or resonant excitation.

Single-pulse plucking of the gauge is effected by discharging the capacitor C_{35} through the coil of the gauge magnet, the energy discharged to the coil being controlled by pre-setting R_{54} which, with R_{53}, forms a potential divider across the h.t. supply. R_{53} limits the charging voltage to a maximum of about 60 V on the earthed side of the h.t. supply.

Resonant excitation is obtained by feeding a resonant frequency to the gauge from the oscillator. The oscillator signal is taken from C_{10}, amplified by V_4 and applied to the gauge for about two seconds. The amplitude of the signal is controlled by R_{12}.

Maintained tuning-fork. The tuning-fork is maintained in oscillation when required by means of a junction transistor with a common emitter. Power for the transistor is provided by the potential divider R_{56}, R_{57}, and switch *SE*; the switch also connects the fork output to the gauge-signal amplifier in place of a gauge. The fork amplitude is controlled by the potentiometer R_{57}.

Gauge-signal amplifier. This is a two-stage amplifier (V_6 and V_7) of conventional design, the signal amplitude being controlled by the potentiometer R_{25}.

Cathode-ray tube and earphones. The oscillator signal, after amplification, is fed by C_{16} to one of a pair of plates of the cathode-ray tube and arranged to give a horizontal trace on the screen. The gauge or tuning-fork signals coming from C_{25} are connected to give vertical deflexions of the trace. The oscillator, and the gauge or fork, signals are mixed at C_{26}, R_{36}, C_{27}, R_{37} and fed to earphones at JK_2. Independent control of the earphones volume is given by R_{38}.

Power supply. The power supply arrangements are conventional. Resistance-capacitance smoothing (R_{39-42}, C_{28-31}) is employed, as the equivalent choke would be heavier and take more space. The screen-grid voltage to the oscillator valves V_1 and V_2 is stabilized at 150 V by the neon stabilizer V_3.

Construction, screening and filters

A compact arrangement of the instrument was aimed at, and close attention had to be given to circuit layout and screening in order to avoid the pick-up of signals between one circuit and another. The finished instrument is shown in Fig. 3. Most of the controls are on the front panels, but the frequency-band switch *SA* is alongside the carrying handle, and there is a subsidiary panel at the back. The instrument is divided vertically into three compartments separated by tinplate sheets. These compartments contain (*a*) mains transformer, rectifier and stabilizer valves, (*b*) oscillator bridge circuit and its associated switches, and the tuning-fork with its transistor circuit within a separate dust-proof box of mu-metal, and (*c*) the remaining components. The walls of compartment (*b*) are thermally insulated with fibreboard.

In order to prevent the oscillator locking on a multiple of the mains frequency or on the gauge frequency, additional smoothing of its h.t. supply is provided by R_{10}, C_8, and the oscillator amplifier is kept away from the remaining components. The network R_{22}, C_{17}, R_{23}, C_{18} filters out ripple between the h.t. supplies to the two amplifiers. R_{36}, R_{37}

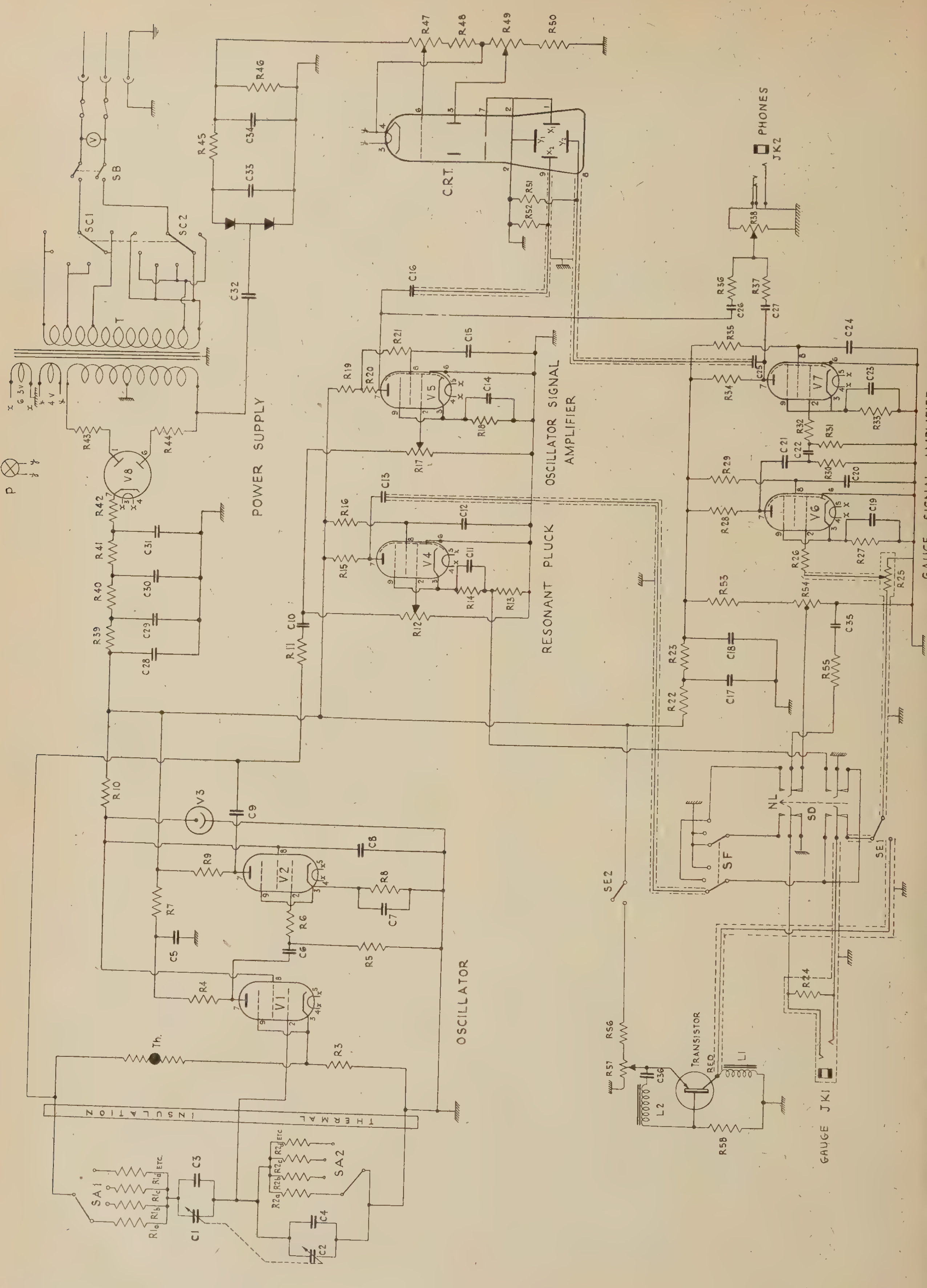
POWER SUPPLY
OSCILLATOR
RESONANT PLUCK
OSCILLATOR SIGNAL AMPLIFIER
GAUGE SIGNAL AMPLIFIER
C.R.T.
PHONES
JK2
GAUGE
JK1
TRANSISTOR
RED
THERMAL INSULATION
P
6·3V
4V
T
SB
SC1
SC2
SA1
SA2
SE1
SE2
SF
SD
NL
Th.
V1
V2
V3
V4
V5
V6
V7
V8
L1
L2
R1a
R1b
R1c
R1d ETC.
R2a
R2b
R2c
R2d ETC.
C1
C2
C3
C4
R3
R4
R5
R6
R7
R8
R9
R10
R11
R12
R13
R14
R15
R16
R17
R18
R19
R20
R21
R22
R23
R24
R25
R26
R27
R28
R29
R30
R31
R32
R33
R34
R35
R36
R37
R38
R39
R40
R41
R42
R43
R44
R45
R46
R47
R48
R49
R50
R51
R52
R53
R54
R55
R56
R57
R58
C5
C6
C7
C8
C9
C10
C11
C12
C13
C14
C15
C16
C17
C18
C19
C20
C21
C22
C23
C24
C25
C26
C27
C28
C29
C30
C31
C32
C33
C34
C35
C36
X1
X2
Y1
Y2

Fig. 2. Detailed circuit diagram of oscillator measuring equipment (See opposite page for list of

and the method of connexion of R_{38} effectively stop interferences of the cathode-ray tube signals through the mixing circuit to the earphones. The resonant plucking signal from V_4 proved a source of interference at switch SD, and so the switch is arranged to cut off V_4 except when resonant plucking is used. The pick-up of low-frequency signals by the gauge leads joining at JK_1 is filtered out by C_{21}, R_{30}, C_{22}, R_{31} in the gauge-signal amplifier between valves V_6 and V_7. The screening necessary for the particular layout used is shown by the broken lines in Fig. 2. A tube of mu-metal is fitted closely around the cathode-ray tube.

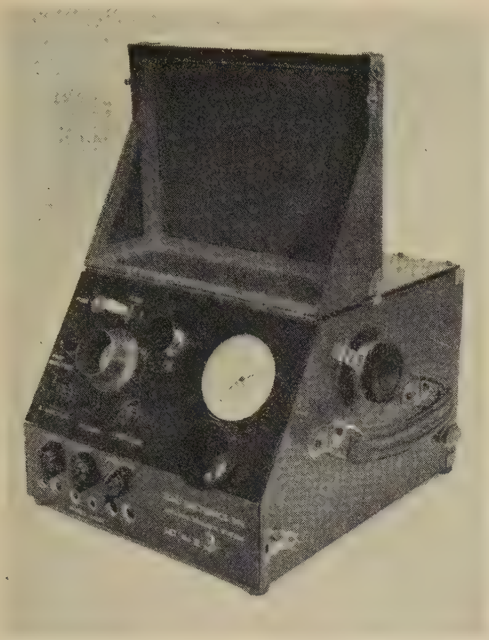

Fig. 3. Front view of instrument showing front panels and, on one side, the frequency band change knob and carrying handle

Frequency calibration

In the measurement of strains in civil engineering structures, for which this equipment was developed, it is very often necessary to maintain continuity of observations for several years and, in this event, the frequency calibration of the oscillator must be referred to an accurate time standard. The tuning-fork within the instrument is calibrated, after initial adjustment and careful sealing, by amplifying its output to drive a synchronous clock for several hours, and at intervals the differences between the times given by the Post Office speaking clock and by the synchronous clock are recorded with a stop-watch. The tuning-fork is then used as a substandard for calibration of the oscillator and as a frequent check on its stability.

The oscillator is calibrated against the tuning-fork with the complete instrument fully warmed up. Its frequency is defined at several points on the dial, and on each frequency band, by obtaining simple fractional and multiple Lissajous figures on the cathode-ray tube. As soon as the dial has been set at one of these calibrated points, the signal from a good-quality decade oscillator is substituted for the fork and its frequency adjusted to the frequency of the instrument oscillator by obtaining the 1 : 1 ratio Lissajous figure. The linearity of the decade oscillator is then used to interpolate the instrument oscillator readings between one point fixed by the tuning-fork and the next, and a calibration is obtained for every twenty dial divisions to an accuracy better than 0·1 c/s.

For strain measurements with vibrating wires, a calibration is required in terms of f^2 and it has been found convenient to work in terms of a unit of $f^2/1000$, which is conveniently called a "strain-unit" ($10^{-3}\,\mathrm{s}^{-2}$). From the above calibration, tables are prepared relating every ten dial divisions on each band to strain-units and interpolation tables are provided for single dial divisions. It is sufficiently accurate for many purposes to work to the nearest strain-unit, but greater accuracy can be obtained if necessary.

Operation of the instrument

The instrument is normally used for recording observations on groups of about 20 to 200 gauges, the intervals between observations varying from about half a day to several months. Although in the present version of the instrument a small change in the frequency of its oscillator occurs as it warms up, it is not necessary that the instrument should be switched on for a long period before it is used. The change is allowed for in normal use by observing the dial positions of suitable Lissajous figures obtained between the oscillator and the tuning-fork. Only those Lissajous figures within the range of the gauge observations need to be recorded and they are read at suitable times in the course of a set of gauge observations. These times are determined by the accuracy required in the gauge observations and the rate at which the oscillator frequency is changing. It may not be necessary for many purposes to make any corrections for the small frequency drift of the oscillator. Nevertheless, dial readings of the

---

List of components of circuit diagram (Fig. 2) opposite

R_{1a}, R_{2a} = 317 kΩ
R_{1b}, R_{2b} = 252 kΩ
R_{1c}, R_{2c} = 200 kΩ
R_{1d}, R_{2d} = 159 kΩ
R_{1e}, R_{2e} = 126 kΩ
R_{1f}, R_{2f} = 100 kΩ
R_{1g}, R_{2g} = 79·4 kΩ
R_{1h}, R_{2h} = 63·0 kΩ
R_{1j}, R_{2j} = 50·0 kΩ
R_{1k}, R_{2k} = 39·7 kΩ
R_{1l}, R_{2l} = 31·5 kΩ
R_3 = 5·1 kΩ
R_4 = 100 kΩ
R_5 = 470 kΩ
R_6 = 2·2 kΩ
R_7 = 47 kΩ

R_8 = 470 Ω
R_9 = 8·2 kΩ
R_{10} = 15 kΩ
R_{11} = 1 MΩ
(all above h.s.)
R_{12} = 0–50 kΩ
R_{13} = 220 kΩ
R_{14} = 470 Ω
R_{15} = 47 kΩ
R_{16} = 330 kΩ
R_{17} = 0–50 kΩ
R_{18} = 1 kΩ
R_{19} = 22 kΩ
R_{20} = 100 kΩ
R_{21} = 680 kΩ
R_{22} = 470 Ω

R_{23} = 470 Ω
R_{24} = 22 kΩ
R_{25} = 0–50 kΩ
R_{26} = 47 kΩ
R_{27} = 2·2 kΩ
R_{28} = 470 kΩ
R_{29} = 2·2 MΩ
R_{30}, R_{31} = 1 MΩ
R_{32} = 2·7 kΩ
R_{33} = 2·2 kΩ
R_{34} = 470 kΩ
R_{35} = 2·2 MΩ
R_{36}, R_{37} = 1 MΩ
R_{38} = 0–50 kΩ
R_{39} = 330 Ω
R_{40} = 390 Ω

R_{41}, R_{42} = 470 Ω
R_{43}, R_{44} = 150 Ω
R_{45} = 220 kΩ
R_{46} = 10 MΩ
R_{47} = 0–100 kΩ
R_{48} = 4·7 kΩ
R_{49} = 0–500 kΩ
R_{50} = 2 MΩ
R_{51}, R_{52} = 1 MΩ
R_{53} = 220 kΩ
R_{54} = 0–50 kΩ
R_{55} = 10 Ω
R_{56} = 168 kΩ
R_{57} = 0–5 kΩ
R_{58} = 100 kΩ

C_1, C_2 = 490 pF
C_3, C_4 = 1500 pF
C_5 = 8 μF
C_6 = 0·05 μF
C_7 = 5 μF
C_8 = 8 μF
C_9 = 0·02 μF
C_{10} = 0·01 μF
C_{11} = 5 μF
C_{12} = 0·01 μF
C_{13} = 0·002 μF
C_{14} = 5 μF
C_{15} = 0·01 μF
C_{16} = 0·002 μF

C_{17}, C_{18} = 8 μF
C_{19} = 5 μF
C_{20} = 0·01 μF
C_{21}, C_{22} = 860 pF
C_{23} = 5 μF
C_{24} = 0·01 μF
C_{25}, C_{26}, C_{27} = 0·002 μF
C_{28}, C_{29}, C_{30}, C_{31} = 8 μF
C_{32} = 0·1 μF
C_{33} = 0·01 μF
C_{34} = 0·1 μF
C_{35} = 4 μF
C_{36} = 10 μF

V_1, V_2, CV2127; V_3, CV2225; V_4, V_5, V_6, V_7,; CV4006 V_8, CV4005; Transistor CV7005; C.R. tube CV1522.
SA, 2-pole, 11-way; SB, 2-pole, 2-way; SC, 2-pole, 6-way; SD, 4-pole, 2-way (non-lock); SE, 2-pole, 2-way.
P, 6·3 V, 0·3 A lamp; MR_1 and MR_2, rectifiers (Sentercel type K3/20); T, transformer 300–0–300 V, 80 mA: 6·3 V, and 4 V, 4 A; Th, thermistor (Stantel type A5513/100); V, voltmeter, 0–300 V; L1, L2, 150 Ω d.c. (S. G. Brown type D/A); Precision drive (Microdial 57, Transradio Ltd.); Tuning fork, 500 ± 0·1 c/s at 20° C, low tem. coeff. alloy steel, overall length 3·5 in., depth of tine $\frac{5}{16}$ in. (Ragg); Headphones, high-impedance.

Lissajous figures are always taken to ensure that there has been no damage to the instrument, and they are used in conjunction with the calibration tables to interpolate the strain-unit values.

A typical set of observations of the effect of warming-up of the instrument on the changes in frequency in terms of strain-units for bands *B* to *H* are given in the table. This table gives also the frequency range, the strain-unit range and the average sensitivity (in terms of strain-units per dial division). Bands *B* to *H* are the only bands which it has been found necessary to use to date. The bands most frequently used are *C*, *D*, *E* and *F*, because it is more accurate to operate the gauge at as low a frequency as is practicable. In this region, even if the effects of warming-up are neglected in any period of one hour, the error is not greater than about two strain-units, or approximately $1{\cdot}5 \times 10^{-6}$ strain on a gauge in common use. If a gauge moves into the region of the higher-frequency bands of the oscillator, the strain will have been substantial and greater attention must be paid to warming-up changes to give the same degree of accuracy in measurement. Often it is not necessary to know the strains so accurately when they are large.

Resonant circuit band ranges, sensitivities and effects of warming-up

Band	Theoretical range		Measured frequency range (c/s)	Mean band sensitivity (strain-units per dial division)	Changes in strain-unit values due to warm-up from 68° F ambient temperature											
	Frequency (c/s)	Strain-unit values $(1/1000\ s^2)$			0·5*h*			1·0 *h*			2·0 *h*			7·0 *h*		
A	252 334	64 112	254 328	0·048	—	—	—	—	—	—	—	—	—	—	—	—
B	317 421	101 177	317 412	0·067	+0·5	+0·2	+0·2	+0·3	+0·1	+0·1	+0·2	−0·1	− 0·3	+0·0	−0·2	− 0·6
C	400 531	160 281	396 516	0·122	+0·4	+0·2	+0·2	+0·1	−0·1	−0·3	−0·1	−0·3	− 0·6	−0·3	−0·6	− 1·2
D	504 668	254 447	495 649	0·193	+0·4	+0·3	+0·3	−0·2	−0·4	−0·8	−0·6	−0·6	− 1·5	−1·1	−1·3	− 2·4
E	635 842	403 709	622 811	0·306	+0·5	+0·3	+0·3	−0·3	−0·6	−1·1	−0·7	−1·1	− 2·2	−1·5	−1·8	− 3·5
F	800 1060	639 1130	787 1026	0·486	+0·5	+0·2	+0·2	−0·7	−1·4	−2·3	−1·9	−2·6	− 4·3	−3·0	−3·8	− 6·2
G	1010 1340	1020 1790	982 1280	0·772	+0·4	0	0	−1·7	−2·3	−3·7	−3·1	−3·7	− 6·2	−4·6	−5·4	− 9·0
H	1270 1680	1610 2840	1240 1620	1·22	+0·6	0	0	−2·7	−3·1	−6·7	−4·9	−5·5	−11·0	−7·0	−8·0	−15·9
J	1600 2120	2560 4500	1560 2040	1·94	—	—	—	—	—	—	—	—	—	—	—	—
K	2020 2670	4060 7150	1960 2470	3·09	—	—	—	—	—	—	—	—	—	—	—	—
L	2540 3370	6450 11350	2470 3220	4·70	—	—	—	—	—	—	—	—	—	—	—	—

1 The changes in strain-unit values with warm-up are given for three nominal positions on the dial of approximately 200, 350 and 800.
2 The maximum increase in strain-unit value is given under the 0·5 h heading; it occurs earlier on some bands.

Most of the manual controls on the instrument will be self-evident, but several points on their manipulation are worthy of mention. Single-pulse plucking is normally used to excite a gauge. The plucking switch *SD* is biased and it is only necessary to flick it in one direction for single-pulse plucking. Resonant plucking is used only on the rare occasions when the gauge is faulty or has a poor response. It will only excite the gauge when the oscillator is set very close to the gauge frequency, and the plucking switch is held on for two or three seconds before being released. Resonant plucking has been used to detach dust or magnetic particles from between the magnet and the wire, but the method is not always successful.

As a rule, no gauge is plucked more times than is absolutely essential to adjust the oscillator to its frequency. Normally, the balance point will be known approximately and can be determined precisely in the course of two or three flicks of the plucking switch. Most frequently, the oscillator is balanced to the frequency of the gauge by obtaining the 1 : 1 ratio Lissajous figure (an ellipse or circle) in the cathode-ray tube. The elimination of beats between the two signals on the earphones is not generally so convenient and many noisy situations are encountered where it is not possible to use this method.

Acknowledgements

Mr. T. R. M. Wakeling and Mr. T. K. Chaplin were associated with the construction of the earliest model of the oscillator and its application to vibrating-wire gauge measurements. Mr. Chaplin also helped in the design and construction of the first model of the complete instrument. The Radio Research Station and Mr. W. Wilson of the National Physical Laboratory gave valuable advice at several stages of the work.

The instrument was developed as part of the research programme of the Building Research Board of the Department of Scientific and Industrial Research and is published by permission of the Director of Building Research. A limited number of copies of a more detailed note on the construction and calibration of the instrument are available on application to the Building Research Station, Watford, Hertfordshire.

References

(1) Tattersall, F., Wakeling, T. R. M., and Ward, W. H. *Proc. Inst. Civil Engrs*, **4**, p. 400 (1955).

(2) Ward, W. H., and Chaplin, T. K. *Proc. Fourth Int. Conf. Soil Mech. and Found. Eng., London* 1957, **2**, p. 256 (1957).

(3) Skempton, A. W., and Ward, W. H. *Géotechnique*, **3**, p. 119 (1952).

(4) Anonymous. *The Engineer*, **158**, p. 142 (1934).

(5) Jerrett, R. S. *J. Sci. Instrum.*, **22**, p. 29 (1945).

(6) Mainstone, R. J. *Engineering*, **176**, p. 153 (1953).

(7) Scroggie, M. G. *Wireless World*, **55**, pp. 294 and 331 (1949).

Extensometer for semi-rigid materials

by C. D. KINLOCH, A.M.I.E.E., and N. E. WATERS, B.Sc., The British Rubber Producers' Research Association, Welwyn Garden City, Herts.

[*Paper first received* 14 *July, and in final form* 27 *August*, 1959]

Abstract

A differential capacitance extensometer is described which is capable of measuring extensions between 1 *and* 50% *on an unstrained gauge length of one inch. With this instrument, complete tensile stress-strain curves to the point of rupture of the test piece may be obtained on semi-rigid materials.*

---

1. Introduction

VARIOUS extensometers are available for measuring small extensions, as in the testing of metals⁽¹⁾ or for large extensions, as in the testing of rubber-like materials,⁽²⁻⁵⁾ but, so far as the authors are aware, no equipment is available commercially in this country for materials having an extension break of 50%, although at least one such is available in the U.S.A. from the Baldwin–Lima–Hamilton Corp.

The extensometer described has been designed for use with dumb-bell shaped specimens of semi-rigid materials, which have an elongation at break of below 50%. The principle used is that of a variable electrical capacitor, the change in capacitance being accurately proportional to the change in separation of two arms attached to the test portion of the dumb-bell. The extensometer is robust and is designed to withstand the impact caused by fracture of the test piece.

2. The capacitance extensometer

The extensometer is shown in Fig. 1 and in a diagrammatic form in Fig. 2. Two arms of insulating material *A*, having cranked ends, of aluminium alloy, each carry a fixed steel pin *B* of $\frac{1}{32}$ in. diameter with a hemispherical end. Each pin rests in a 90° V-shaped groove $\frac{1}{32}$ in. deep machined in the upper surface of a spring-loaded clip (Fig. 3), which is attached to the test piece and forms a gauge mark.

The two arms are rigidly fixed to two $\frac{1}{8}$ in. diameter steel rods *C* and *D*, which run in bearings *E* of polytetrafluorethylene carried in two vertical brass pillars. One end of each rod projects into a central brass electrode *F* $2\frac{1}{4}$ in. long, and is insulated from it by a liner of suitable dielectric constant. The brass electrode and pillars are carried by a sheet of polymethyl methacrylate. A brass screen *G* encases the capacitor, except for $\frac{3}{16}$ in. holes at both ends through which the steel rods pass. The assembly is fixed rigidly to a baseplate.

It is necessary to ensure that the two steel rods *C* and *D* are a good sliding fit in the dielectric liner *F* and bearings *E*, as any side play can cause non-linearity in the response of the extensometer. A clearance of 0·002 in. was found satisfactory in practice in minimizing side play whilst allowing free running of the two steel rods, which is essential if the two steel pins *B* are to remain centrally within the V-shaped grooves on the spring-loaded clips.

Following Vinycomb and Martyr,⁽⁶⁾ fringing effects at the extreme ends of travel are avoided by ensuring that the ends of the moving steel rods do not come within a distance from the ends of the capacitor less than ten times the thickness of the dielectric.

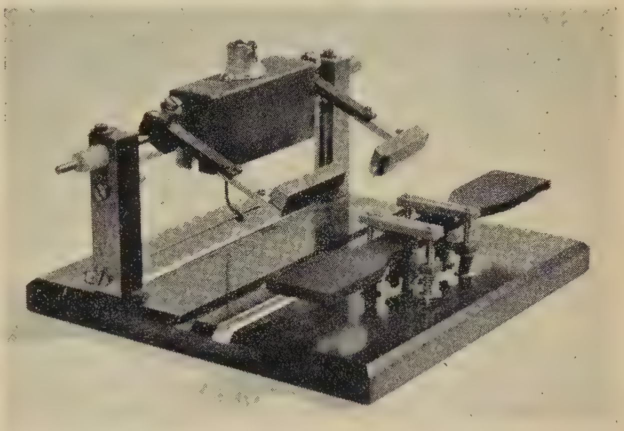

Fig. 1. General view of capacitance extensometer

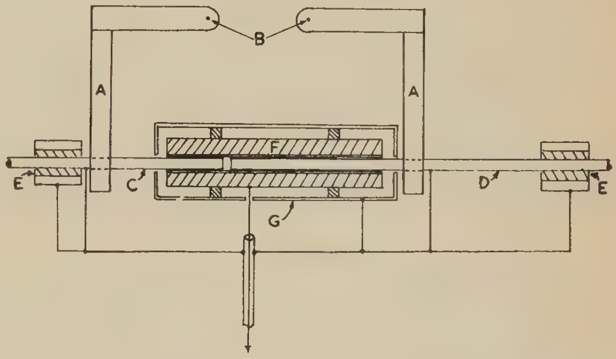

Fig. 2. Capacitance extensometer in diagrammatic form

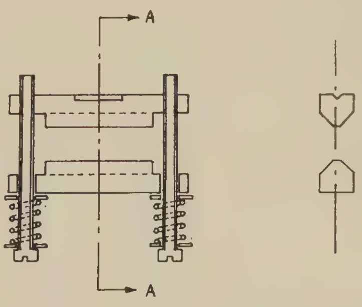

Fig. 3. Diagram of spring-loaded specimen clips

The capacitance of a length L of a long coaxial capacitor is given by

$$C = \frac{KL}{1 \cdot 8 \log_e (D/d)} \text{ pF}$$

where K = dielectric constant of liner; D = internal diameter of outer cylinder; and d = diameter of central electrode.

This expression may be used directly to give the capacitance variation of the extensometer if L is taken as the change in separation of the gauge arms (assuming the air gap between the central electrodes and the dielectric liner to have a negligible effect on the capacitance).

Using a liner of paper-based phenolic material, approximately 0·03 in. thick, a capacitance change of 13 pF/in. separation of the gauge arms was obtained at a measurement frequency of 2 Mc/s.

3. The measuring unit

It is necessary to convert the change in capacitance of the extensometer into a proportional voltage change. The electronic equipment used for this conversion is marketed by Southern Instruments Ltd. as equipment type E7A. Alternative commercial equipment is known to be available in this country and other suitable circuits have been published in the literature, e.g. Ref. (7). The Southern Instruments equipment comprises one MR.202 power supply panel, one MR220F frequency-modulated pre-amplifier and one M700L gauge oscillator. The capacitance extensometer forms part of the tuned circuit of the oscillator, which operates at about 2 Mc/s. Any alteration in the separation of the gauge arms thus alters the frequency of the oscillator. The change in frequency is detected by a frequency discriminator circuit, which gives a voltage output proportional to the change in capacitance of the extensometer. With this equipment an output of approximately 0·5 V/pF change in capacitance on the 20 pF range, or 2·0 V/pF on the 5 pF range can be obtained. For the work described in this paper the units referenced MR220F and M700L were duplicated so that the tensile stress in the test piece could also be measured; the technique adopted is given in Section 4.

The elongation and load outputs are fed to the X and Y plates, respectively, of a cathode-ray oscillograph to give a continuous tensile stress-strain curve, up to the point of rupture of the specimen under test if required.

4. The testing machine

For the tests described in this paper use was made of a Hounsfield tensometer fitted with lock-jaw chucks for textiles and films (Code Fig. 37), as manufactured by Tensometer Ltd.

On this machine, the load on the test piece is measured by means of a spring beam, the deflexion of which actuates a piston which moves a mercury thread in a capillary tube against a scale calibrated in load units. By placing a strip of metallized paper behind the capillary tube, a capacitance change proportional to the load on the test piece could be detected by a second amplifier channel; the accuracy is adequate for most purposes, except at loads below 20 lb where friction in the mercury system may become appreciable. If required for light loads, the spring beam could be replaced by a proof-ring fitted with a transducer.(8)

5. Calibration and performance

The displacement of the extensometer arms can be measured accurately by means of a micrometer head fitted to the outer ends of the two steel rods (C and D, Fig. 2). Alternatively, if the Hounsfield tensometer is being used, the extensometer may be calibrated by fixing to the movable cross-head a rigid strip having a transverse groove for locating one arm of the extensometer. With the second arm in some fixed position, the movement of the first arm can be measured from the rotating drum on the tensometer, which allows a magnification of ×16 to be obtained.

On examining the output obtained from the extensometer by moving the two arms independently, it was found that the deviations from linearity in each case were less than 1%, although a discrepancy of 4% existed between the outputs of the two arms, probably due to a small difference in the diameter of the two rods. Since in practice the shorter arm, which follows the movement of the gauge mark nearest to the load measuring device, only moves a small amount in comparison with the second arm, this discrepancy was unimportant. The overall linearity of the device thus appears to be within the value of ±2% quoted as being attainable with capacitance displacement transducers.(6) It is estimated that the zero error, due to initial play between the central rods and the dielectric liner, is less than 0·2% based on an unstrained gauge length of one inch.

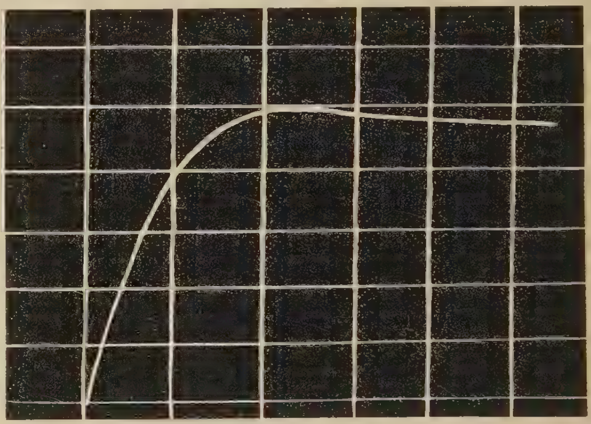

Fig. 4. Load-extension curve for Mix A

x axis: one division = 2·2%
y axis: one division = 25 lb
Breaking load = 117·5 lb (tensile strength = 120 kg/cm^2)
Elongation at break = 12·1%

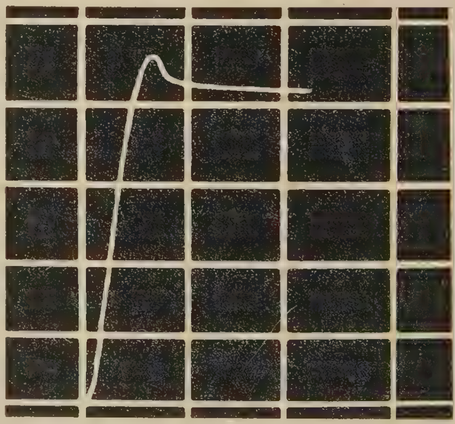

Fig. 5. Load-extension curve for Mix B

x axis: one division = 2·2%
y axis: one division = 50 lb
Breaking load = 258 lb (tensile strength = 225 kg/cm^2)
Elongation at break = 4·9%

Calibration of the load scale is simply effected, if the technique described in Section 4 is used, by adjusting the length of the mercury thread by suitable increments and observing the displacement of the spot on the cathode-ray tube.

To avoid the effects of non-linearity in the cathode-ray oscillograph, it is desirable to superimpose a calibration grid on the stress-strain curve.

Figs. 4, 5 and 6 show the stress-strain curves of three hard rubber compounds measured at a cross-head speed of 3 in./min. The composition of these mixes is given in the Appendix.

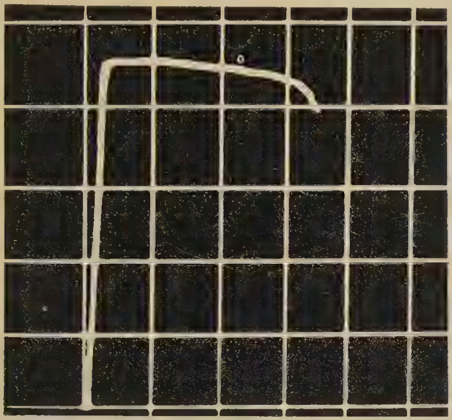

Fig. 6. Load-extension curve for Mix *C*
x axis: one division = 4·4%
y axis: one division = 25 lb
Breaking load = 100 lb (tensile strength = 68 kg/cm^2)
Elongation at break = 15·0%

Acknowledgements

The authors are indebted to Mr. R. F. Blackwell who undertook the preliminary development work and to Mr. A. Giles for the construction of the extensometer. This work forms part of a programme of technological research undertaken by the Board of the British Rubber Producers' Research Association.

References

(1) For a description of some of these instruments see Morley, A. *Strength of Materials* (London: Longmans, Green and Co., 9th ed., 1940).
(2) British Patents Nos. 673,203 and 677,391, 1952, Imperial Chemical Industries Ltd.
(3) Gehman, S. D., and Clifford, R. P. Special Technical Publication No. 136: *Symposium on Recent Developments in the Evaluation of Natural Rubber* (American Society for Testing Materials, 1952).
(4) Eagles, A. E., and Payne, A. R. *Research Memorandum R.*405 (Research Association of British Rubber Manufacturers, 1957).
(5) Farlie, E. D., Hawkes, J. F., and Waters, N. E. *Rubber J.*, **132**, p. 648 (1957).
(6) Vinycomb, R. K., and Martyr, F. E. *Instrument Practice*, **10**, p. 986 (1956).
(7) Frommer, J. C. *Electronics*, p. 104 (July 1943).
(8) Payne, A. R., and Smith, J. F. *J. Sci. Instrum.*, **33**, p. 432 (1956).

Appendix

Composition reference	*A*	*B*	*C*
Smoked sheet	—	—	100
Heveaplus M-G 50*	100	—	—
Cyclized rubber (50/50 master batch)	—	100	—
Zinc oxide	5	5	200
Stearic acid	2	2	2
Sulphur	1·5	1·5	1·5
Mercaptobenzthiazole	1	1	1
Tetramethylthiuram disulphide	1	1	1
M.P.C. black	15	15	—
China clay (Stockalite)	75	75	—
Manosil AS7	—	—	200
Nonox EXN	1	1	1

Vulcanization: 10 min at 153° C

* 50 : 50 methyl methacrylate, natural rubber graft polymer.

Design criterion for correction of parallax at the best focus for definition

by G. W. HAMSTEAD, B.Sc., A.R.C.S., F.Inst.P., W. Watson and Sons Ltd., Barnet, Herts

[*Paper received* 10 *August*, 1959]

Abstract

Parallax is the angular aberration of an optical system. Conventional balance of primary against secondary aberration does not give the best definition with freedom from parallax. A design criterion is established to obtain this desirable condition and tolerances calculated.

PARALLAX is defined as the apparent change in the position of an object due to change in the position of the observer. In optical systems it may be detected by movement of the eye about the exit pupil. In sighting instruments where an image is formed on a graticule, parallax gives rise to errors in the line of sight. Parallax due to residual aberrations and errors of focusing will be considered in this paper.

Definition

The so-called Strehl definition of the image is taken as the criterion of the definition, *D*, of an optical system. Then

$$D = \frac{I}{I_0} = \left(1 - \frac{2\pi^2}{\lambda^2}E_0\right)^2 \tag{1}$$

where *I* is the intensity at the centre of the diffraction image that the system produces of an ideal point object, I_0 being the intensity in the ideal case of the system being free from aberration.

$$E_0 = \int_0^1 W^2 dV - \left[\int_0^1 W dV\right]^2 \tag{2}$$

where W is the wave-front aberration$^{(1)}$ with respect to the reference sphere centred on the selected focus and V is the square of the fractional aperture. The validity of equation (1) depends on the aberration being small, but as we are concerned with good definition where the correction of the system is within the so-called Rayleigh limit where $D \geqslant 0 \cdot 8$ this condition may be assumed to be fulfilled.

Angular aberration

The angular aberration$^{(2)}$ of an optical system is the difference between the ideal direction of a ray and its true path. In Fig. 1 O is the selected focus on the axis AO of an optical system, AE represents the plane of the exit pupil, APQ is the section of the reference sphere centred on O, ARS is the section of the wave-front, RM is a ray, defined as a normal to the wave front, RO is the normal to the reference sphere and is the ideal direction of RM, and RT is an arc of a centre on O cutting QO at T.

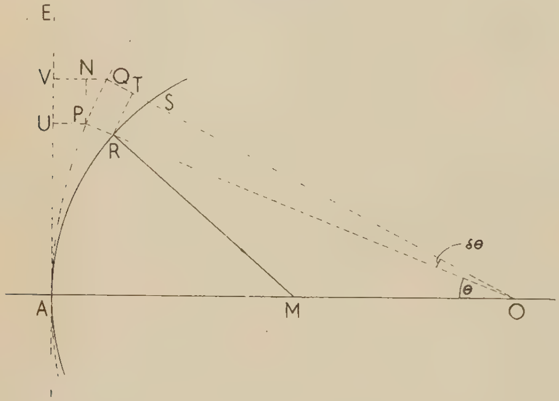

Fig. 1. Wave front and reference sphere at exit pupil

The angular aberration ψ is measured by the angle MRO.

Let the angle $AOR = \theta$ and the angle ROS be a small increase in θ then considering the triangle RST

$$\tan \psi = TS/TR \tag{3}$$

The wave-front aberration W at θ, is defined as

$$W = N \,.\, PR = [PR]$$

the medium having a refractive index, N.

At $\theta + \delta\theta$, the wave-front aberration becomes $W + \delta W$, whence $\delta W = [TS]$,

so that $$TS = \frac{1}{N}\delta W. \tag{4}$$

Provided $W \ll AO$ we have, very nearly

$$RT = PQ \tag{5}$$

and $$PN \doteq PQ \cos \theta \tag{6}$$

with $$PN = UV \tag{7}$$

Taking $AU = \rho =$ zonal aperture (with ρ_0 the maximum value of ρ defining the radius of the exit pupil) we have

$$UV = \delta\rho \tag{8}$$

Combining in equation (3) the equalities in equations (4), (5), (6), (7) and (8), we obtain

$$\tan \psi = \frac{1}{N}\frac{\delta W}{\delta \rho} \cos \theta$$

allowing $\delta\rho \to 0$, we have $\tan \psi = \dfrac{1}{N}\dfrac{dW}{d\rho} \cos \theta$

For small aberrations ψ is not large and $\tan \psi \to \psi$, while $\cos \theta$ may be taken as unity. (For an $f/3 \cdot 5$ system the error is about 1%.)

Thus $$\psi = \frac{1}{N}\frac{dW}{d\rho}. \tag{9}$$

Focusing error

The wave-front aberration introduced by a change in focus may be taken as

$$W = a_2(\rho/\rho_0)^2 \tag{10}$$

so that for a system in air

$$\psi = \frac{2a_2}{\rho_0}\left(\frac{\rho}{\rho_0}\right) \tag{11}$$

In this case $E_0 = a_2^2/12$

and for $D \geqslant 0 \cdot 8$, $E_0 \leqslant \lambda^2/187$

or conventionally $|a_2| \leqslant \lambda/4$

giving $$|\psi| \leqslant \frac{\lambda}{2\rho_0}\left(\frac{\rho}{\rho_0}\right) \tag{12}$$

The maximum value of ψ is thus $\lambda/2\rho_0$. For an objective of 25 mm diameter this is about $4\frac{1}{2}$ seconds of arc and is independent of the relative aperture.

Conventional balance of aberrations

Many optical systems have their axial spherical aberration with respect to the paraxial focus adequately represented by a two-term formula. Denoting the wave-front aberration with respect to the paraxial focus as W_p we may take

$$W_p = a_4\left(\frac{\rho}{\rho_0}\right)^4 + a_6\left(\frac{\rho}{\rho_0}\right)^6 \tag{13}$$

The coefficients a_4 and a_6 conventionally represent the primary and secondary spherical aberration respectively.

In selecting a focus different from the paraxial focus the change in focus term (10) must be added to W_p to give the general wave front aberration W, so we have

$$W = W_p + a_2(\rho/\rho_0)^2 \tag{14}$$

or $$W = a_2(\rho/\rho_0)^2 + a_4(\rho/\rho_0)^4 + a_6(\rho/\rho_0)^6 \tag{15}$$

minimizing E_0 with respect to a_2 and a_4 gives the well-known result

$$a_2 = 3/5 a_6,\ a_4 = -3/2\, a_6$$

with the design condition that the marginal ray is brought to the paraxial focus. The non-zero value of a_2 shows that the common marginal-paraxial focus is not the focus selected for best definition.

These values of a_2 and a_4 give

$$W = a_6\left\{\frac{3}{5}\left(\frac{\rho}{\rho_0}\right)^2 - \frac{3}{2}\left(\frac{\rho}{\rho_0}\right)^4 + \left(\frac{\rho}{\rho_0}\right)^6\right\} \tag{16}$$

the value of E_0 in this case being $a_6^2/2800$, giving the (conventional) tolerance

$$|a_6| \leqslant 4\lambda \tag{17}$$

From equation (16) for a system in air we obtain

$$\psi = \frac{a_6}{\rho_0}\left\{\frac{6}{5}\left(\frac{\rho}{\rho_0}\right) - 6\left(\frac{}{\rho_0}\right)^3 + 6\left(\frac{\rho}{\rho_0}\right)^5\right\} \tag{18}$$

which has zeros at $\left(\frac{\rho}{\rho_0}\right) = 0$ and $\left(\frac{\rho}{\rho_0}\right)^2 = \frac{5 \pm \sqrt{5}}{10}$

the values of ψ at these points are $\pm\left(\mp\frac{12}{125}\frac{a_6}{\rho_0}\right)$

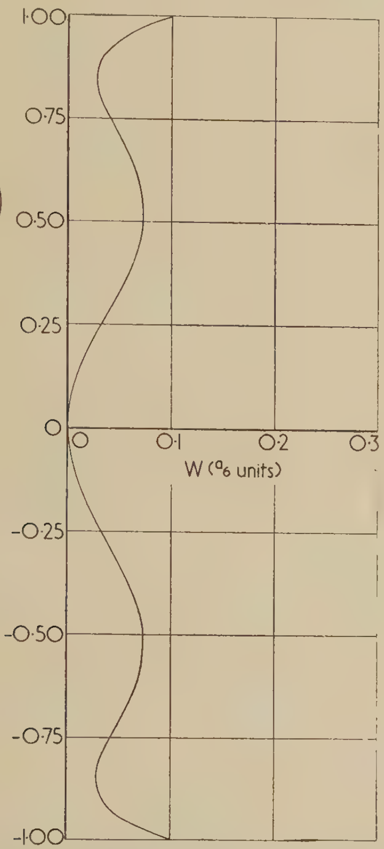

Fig. 2. Wave front with respect to best definition focus for conventional correction of spherical aberration

Fig. 2 shows equation (16) plotted, with W in units of a_6. Fig. 3 shows equation (18) plotted with ψ in units of a_6/ρ_0.

The largest value of ψ is at the edge of the pupil where

$$|\psi| \text{ maximum} = \frac{6}{5}\frac{|a_6|}{\rho_0} \tag{19}$$

For $|a_6| = 4\lambda$ which is the limit given by the expression (17) then

$$|\psi| \text{ maximum} = \frac{24}{5}\frac{\lambda}{\rho_0} \tag{20}$$

For an objective of 25 mm diameter this is about 44 seconds of arc, while the zonal maxima are about 8 seconds of arc. a_6 is limited to approximately $\lambda/10$ per second of arc of parallax.

If the region of focus is searched to obtain zero parallax then the common marginal-paraxial focus may be chosen as this gives zero angular-aberration at the edge of the pupil.

Then
$$W_p = a_6\left\{-\frac{3}{2}\left(\frac{\rho}{\rho_0}\right)^4 + \left(\frac{\rho}{\rho_0}\right)^6\right\} \tag{21}$$

and
$$\psi_p = \frac{a_6}{\rho_0}\left\{-6\left(\frac{\rho}{\rho_0}\right)^3 + 6\left(\frac{\rho}{\rho_0}\right)^5\right\} \tag{22}$$

with
$$E_{0p} = 17/560a_6^2 \tag{23}$$

Setting
$$D \geqslant 0\cdot8 \text{ we find } a_6 \leqslant 0\cdot42\lambda \tag{24}$$

ψ_p is zero for $(\rho/\rho_0)^2 = 1$ and $(\rho/\rho_0) = 0$ and has turning values at $(\rho/\rho_0)^2 = 3/5$ and $(\rho/\rho_0) = 0$. The corresponding values of ψ_p are $\mp\frac{36\sqrt{15}}{125}\frac{a_6}{\rho_0}$ and zero.

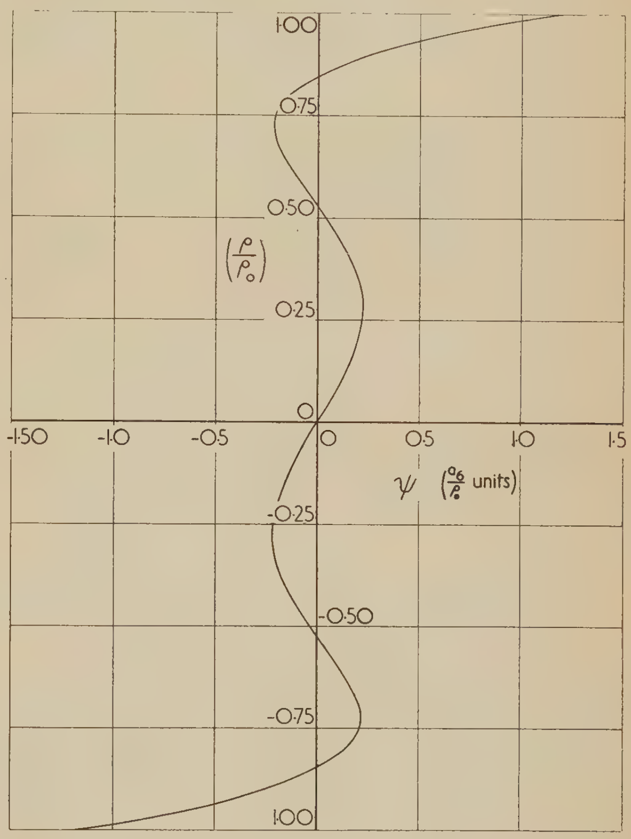

Fig. 3. Angular aberration with respect to best definition focus for conventional correction of spherical aberration

Fig. 4 shows equation (21) plotted with W in units of a_6. Fig. 5 shows equation (22) plotted with ψ in units of a_6/ρ_0.

If $|a_6|$ is taken as $0\cdot42\lambda$ the limit given by the expression (24) then

$$|\psi_p| \text{ zonal} = 0\cdot47\ \lambda/\rho_0 \tag{25}$$

For an objective of 25 mm clear aperture this has the value of about 4 seconds of arc. a_6 is limited to $\lambda/10$ per second of arc (with an upper limit on a_6 of approximately one-tenth of the conventional amount).

An important criticism of the conventional balance of primary against secondary spherical aberration such that the marginal ray is brought to the paraxial focus is that the focus for best definition is not the focus for zero parallax. We may either have good definition with the centre of the pupil having little parallax with a large amount of parallax on the edge of the pupil, or poor definition with zonal parallax and no parallax on the edge of the pupil. The former setting is normally chosen where very precise correction of parallax is not required, say one minute of arc. For good definition with parallax corrected to a few seconds of arc across the entire pupil a new type of balance of primary against secondary aberration is necessary.

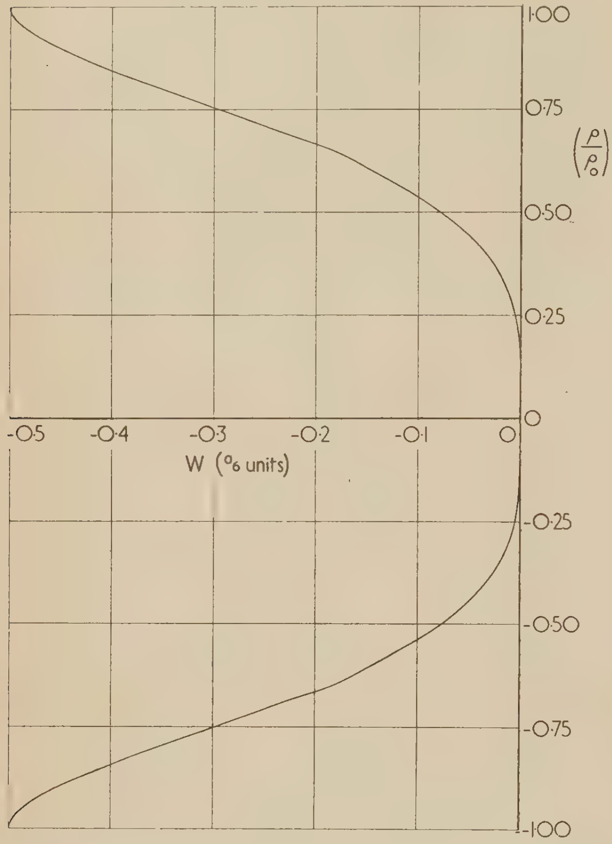

Fig. 4. Wave front with respect to paraxial focus for conventional correction of spherical aberration

Combined focus for definition and parallax

We take equation (6) as the general form of the wave-front aberration. Minimizing E_0 with respect to a_2 we obtain the condition

$$a_2 = -(a_4 + 9/10a_6) \tag{26}$$

For zero parallax at the edge of the pupil we set $\psi_M = 0$, which gives us $a_4 = -21/10a_6$, so that $a_2 = 6/5a_6$ and

$$W = a_6\left\{\frac{6}{5}\left(\frac{\rho}{\rho_0}\right)^2 - \frac{21}{10}\left(\frac{\rho}{\rho_0}\right)^4 + \left(\frac{\rho}{\rho_0}\right)^6\right\} \tag{27}$$

with $$\psi = \frac{a_6}{\rho_0}\left\{\frac{12}{5}\left(\frac{\rho}{\rho_0}\right) - \frac{42}{5}\left(\frac{\rho}{\rho_0}\right)^3 + 6\left(\frac{\rho}{\rho_0}\right)^5\right\} \tag{28}$$

and $$E_0 = \frac{33}{14\,000}a_6^2 \tag{29}$$

For $D \geqslant 0\cdot 8$ equation (29) gives $|a_6| \leqslant 1\cdot 5\lambda$ (30

ψ has zeros at $(\rho/\rho_0)^2 = 1$, $(\rho/\rho_0)^2 = 2/5$ and $\rho/\rho_0 = 0$ with turning values at $(\rho/\rho_0)^2 = \dfrac{21 \pm \sqrt{241}}{50}$.

Fig. 6 shows equation (27) plotted with W in units of a_6 Fig. 7 shows equation (28) plotted with ψ in units of a_6/ρ_0.

For the limiting value for $|a_6|$ of $1\cdot 5\,\lambda$ given by th expression (30) the larger zonal value of ψ for an objectiv of 25 mm clear aperture is about 7 seconds of arc. Thus a is limited to about $\lambda/5$ per second of arc of parallax. This i double the amount permitted in the previous cases. It i interesting to note that if a_6 is limited to $1\cdot 5\,\lambda$ in the conventional balance of primary against secondary spherica aberration the maximum value of ψ obtained is about 16 seconds of arc.

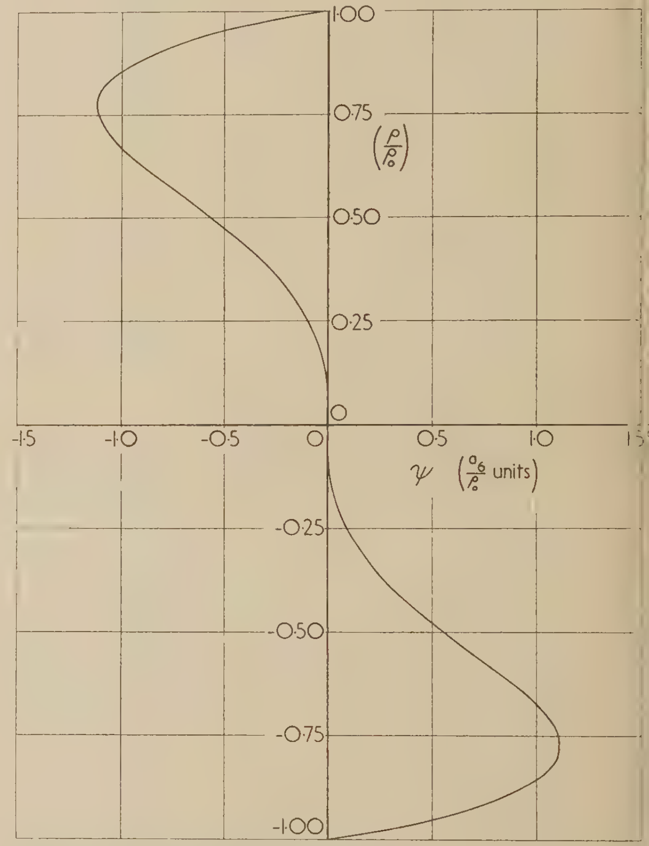

Fig. 5. Angular aberration with respect to paraxial focus for conventional correction of spherical aberration

The design criterion to obtain this balance of aberration is obtained by considering equation (28). If we measure ψ with respect to the paraxial focus we have

$$\psi_p = \frac{a_6}{\rho_0}\left\{-\frac{42}{5}\left(\frac{\rho}{\rho_0}\right)^3 + 6\left(\frac{\rho}{\rho_0}\right)^5\right\} \tag{31}$$

For zero longitudinal spherical aberration $\psi_p = 0$ and for this condition we have

$$(\rho/\rho_0)^3 = 0 \text{ or } (\rho/\rho_0)^2 = 7/5.$$

The desired design criterion is that the ray at the $\sqrt{7/5}$ zone is brought to the paraxial focus. We may note that the correction for parallax in a system having the conventional balance of primary against secondary aberration may be obtained by stopping down the aperture to about 85% (slight refocusing is also necessary).

It may be easily shown that the design criterion established above is equivalent to the condition that the spherical aberration of the marginal rays is 8/9 that of the $\sqrt{\frac{1}{2}}$ zonal rays. (This condition may be preferred in practical computing when considering other aberrations.)

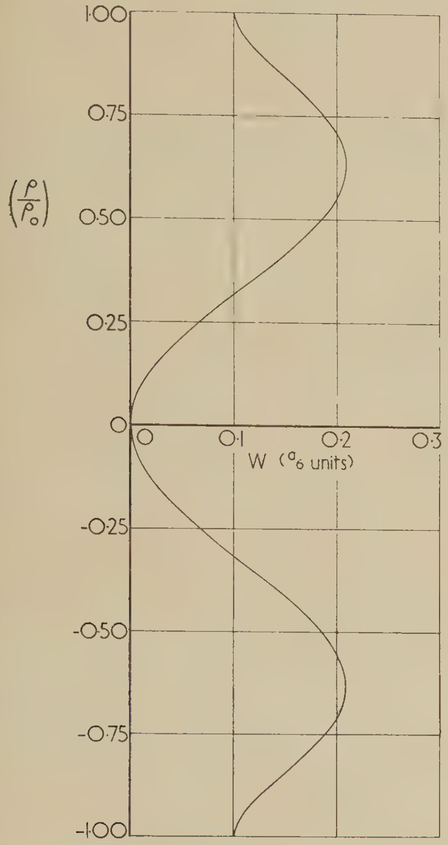

Fig. 6. Wave front with respect to combined focus for definition and parallax

Conclusion

The advantage of having the best focus for definition at the same point that parallax is eliminated is highly desirable, particularly in sighting instruments, since the eye automatically searches the region of focus for best definition. Conventionally designed systems do not have this characteristic and differences of opinion as to the "best" focus occur. By adopting the criterion established above these differences are eliminated making focusing easier and more accurate. In addition the limit placed on the secondary aberration is doubled, allowing greater freedom in design.

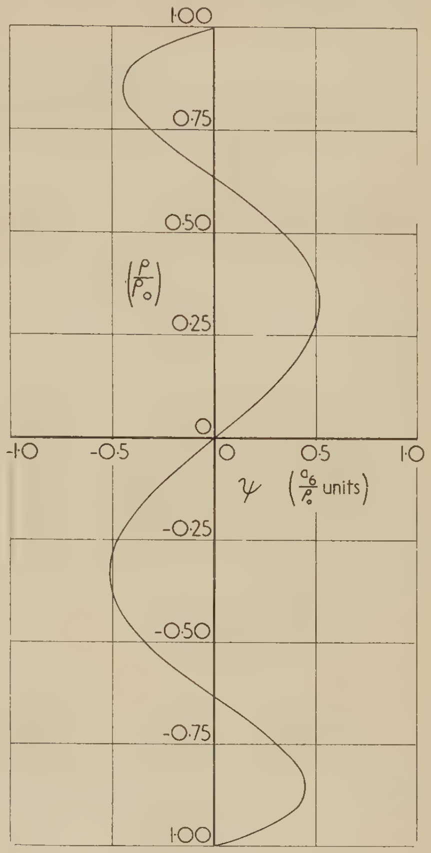

Fig. 7. Angular aberration with respect to combined focus for definition and parallax

Acknowledgement

This investigation was initiated by the requirement of the Fighting Vehicles Research and Development Establishment for a muzzle boresight with less than 0·05 mils (10 seconds of arc) of parallax (F.V.R.D.E. Specification 1108, sub-section 4·5).

References

(1) Hopkins, H. H. *Wave Theory of Aberrations* (London: Oxford University Press, 1950).

(2) Conrady, A. E. *Applied Optics and Optical Design* (London: Oxford University Press, 1929).

Direct measurement of $\int i^2 . dt$ by a method based on the Hall effect

by S. C. RYDER-SMITH, B.Sc.(Eng.),* A. E. GUILE, Ph.D., B.Sc.(Eng.), A.M.I.E.E.,†
and A. E. BARRINGTON, Ph.D., B.Sc.(Eng.), A.M.I.E.E.,‡ Queen Mary College, University of London

[*Paper first received* 31 *July, and in final form* 23 *September*, 1959]

Abstract

A squaring unit based on the Hall effect is used to give an a.c. output, the amplitude of which is proportional to the square of an input current. The input impedance is low, so that the unit may conveniently be fed from a shunt. The output is amplified in a tuned amplifier, and fed through a rectifying circuit to an integrating instrument such as a fluxmeter, so that a direct reading of $\int i^2 . \mathrm{dt}$ *is obtained. A modification is suggested to enable* $\int eidt$ *to be measured, giving the arc energy in a circuit breaker or fuse. Thus, direct and immediate readings of these integrals can be obtained, and the need to apply time-consuming graphical techniques to records of the appropriate current or voltage waveforms is avoided. The accuracy is shown to be better than 2%.*

British Standard 2692 : 1956 for fuses lays down that when specifying the characteristics of a fuse, it is necessary to give a value for the "virtual total operating time" of the fuse. This is calculated from the value of $\int i^2 . dt$ for the fuse, where i is the instantaneous current through the fuse from the instant when the current is first switched on to the point where the current ceases. The value of this integral for a given fuse does not vary over a wide range, because, above a certain current where heat loss from the element is negligible, its value is constant. At lower currents the integral depends largely on the degree of overloading.

In the instrument described in this paper, a specially developed squaring unit based on the Hall effect is connected across a shunt in series with the fuse, and the output from this is amplified and fed to a fluxmeter, which therefore reads directly $\int i^2 . dt$. British Standard 2692 : 1956 suggests the use of a direct-reading instrument for this purpose, but no satisfactory method has previously been described. It is possible to use the quadrant electrometer as a ballistic energy meter.(1) However, this only yields accurate results if the period of energy flow is short (the published experimental results were obtained using a time of 0·02 s), as the assumption is made that no deflexion occurs during the energy pulse.

Previous methods of squaring

Devices containing square-law elements are frequently used in analogue computers, particularly for multiplication problems. There are four types of element in general use, and these are as follows:

(1) Thermal instruments, such as temperature-limite diodes,(2) having an output voltage proportional to the temperature of a wire, which is in turn proportional to the squar of the current passing through it. The time constant of suc devices is high, sometimes up to several seconds.

(2) Instruments in which square-law characteristics a synthesized from segments of diode characteristics.(3) A large number of elements are needed; for example, Chance(used fifteen diodes to cover an input voltage range of 0 to 25 V

(3) Beam-deflexion square-law tubes,(5,6) in which th current in an electron beam is made to be proportional t the square of the deflexion, and hence to the square of th deflecting voltage, by using a suitably designed anode shape

(4) Instruments in which triodes and pentodes are operate on the range of their characteristics which is approximatel square-law. These are suitable where only moderate accurac is required.

In the present application, a squaring element is require which is both accurate and reliable, and which will operat from a comparatively small input voltage (say less than 2 V) In addition it should be able to respond to inputs havin frequencies from zero up to, say, 1 kc/s, and should hav characteristics which will not vary with age from tru squaring. Squaring by means of the Hall effect in semiconductors can offer all these advantages.

Hall effect in a semiconductor

If a piece of semiconductor lies in the xy-plane of a Cartesian co-ordinate system with the origin at its centre then, when a magnetic field of strength B is set up along the z-axis, with a current I flowing through the specimen along the y-axis, a voltage of magnitude V due to the Hall effect will arise along the x-axis. The equation relating these three quantities is

$$V = RIB/t$$

where R is the Hall coefficient and t is the thickness of the specimen in the z-direction. A Hall crystal may thus be regarded as a multiplying device, with the two inputs at (a) the current contacts, and (b) the field-coil terminals, and the output being taken from the Hall contacts. If the crystal and field coil are connected in series, the arrangement can be made into a squaring device.

Hall-effect squaring unit

It was found that with the simple squaring arrangement described above, there was insufficient power available at the Hall contacts to drive the fluxmeter directly, and some means of amplification had to be found.

To avoid the necessity of using a d.c. amplifier, a method has been devised in which an a.c. tuned amplifier can be used. In this method the output of the Hall unit is in the form of an a.c. signal, the amplitude of which is modulated by the required voltage waveform of i^2. The a.c. tuned amplifier is then used, and the i^2-waveform is obtained at the output by means of a rectifying circuit. The multiplication is performed in two stages, so that two specimens of semiconductor are required. In the first stage, the current i is multiplied by the a.c. output i_{osc} of an oscillator, producing an output proportional to $i \times i_{osc}$. This output is fed to the second stage, where it is again multiplied by i, giving an output which is proportional to $i^2 \times i_{osc}$. An alternative arrangement would be to use the first stage in the normal way to produce an output proportional to i^2, and then to multiply this in the second stage by the a.c. signal to produce an output, as before, proportional to $i^2 \times i_{osc}$.

---

* Now with Standard Telephones and Cables, Ltd., Footscray, Kent.
† Now at Rangoon University, Burma.
‡ Now at Harvard University, U.S.A.

Of the five possible circuit arrangements, the one chosen as being the simplest to operate is shown in Fig. 1. It has the advantages (i) that the Hall output of the first crystal is fed into the low-resistance load of the second crystal, rather than being taken into a field coil, so that a greater current transfer takes place, (ii) that only one field coil is used, thus reducing the error arising from pick-up between the two stages, and (iii) that the current input is isolated from the main circuit. The semiconductor used was indium antimonide, since, although it has a lower Hall coefficient than germanium, its very much lower resistance means that a greater current will be transferred from the first to the second stage.⁽⁷⁾

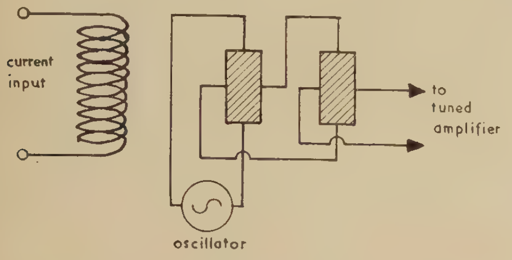

Fig. 1. Hall squaring unit

Both Hall-effect crystals are mounted in the field of the field coil.

It should be noted that this arrangement has an inductive input, so that the accuracy can be improved by connecting it to a shunt having the same time constant. This is particularly so when periods of less than one cycle are being used. In the tests described below, however, times corresponding to one cycle or more were used, and a wire-wound resistance was used as a shunt, no attempt being made to match it to the input.

Complete instrument

As the time that could be spent on this project was limited, existing equipment was used wherever possible. An oscillator giving an undistorted output of 0·5 A at 10 kc/s was used, the choice of frequency being dictated by the fact that this was the highest frequency to which the only suitable amplifier could be tuned. The output from the Hall unit was fed through a 60 : 1 step-up transformer to the input of a frequency-selective amplifier, and the output from this was taken through a 2 : 1 step-down transformer to the bridge rectifier, which used four medium-power germanium rectifiers. The rectified output was fed to a fluxmeter with a sensitivity of 50 μV . s per division when fed from a source of 7 Ω. The circuit is shown in Fig. 2, together with the circuit used for making some fuse tests in which the fluxmeter readings could be compared with the results obtained from the current record taken on an oscillograph.

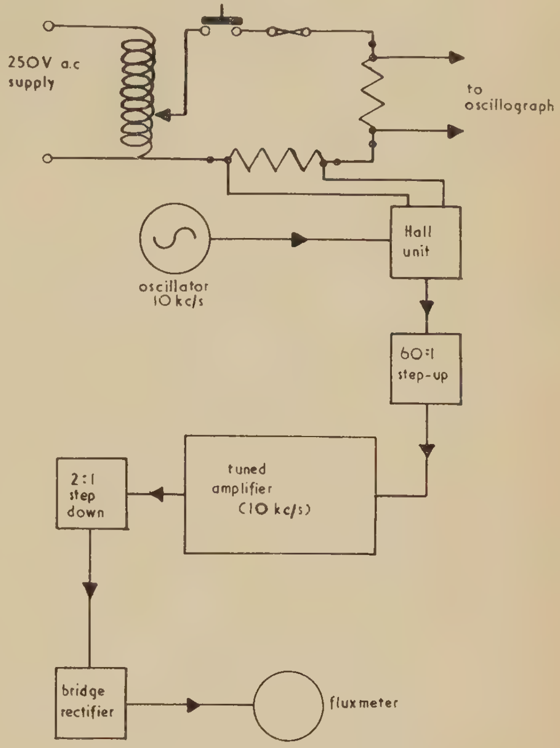

Fig. 2. Complete instrument

Results

A total of twenty fuse tests were made, but the range of fluxmeter deflexions obtained was insufficient to allow a graph to be usefully plotted. The tests were made with 6 A fuse wire in all but five of the tests, where 2 A wire was used. The maximum peak current varied from 21 to 38 A, and the number of cycles before current ceased varied from one to nine. In the tests using the 6 A fuse wire, the ratio of fluxmeter reading to oscillograph reading varied by ±5%, with a standard deviation of 2·9%. The low-deflexion tests (up to only 4% of full-scale fluxmeter deflexion) made with the 2 A wire gave results which were between 10 and 15% low, because of the inaccuracy of the reading of the fluxmeter in this range. In addition there will be somewhat less accuracy in the measurements on the oscillograph record when only one cycle, which departs considerably from being a true sine-wave, is being dealt with. Such low deflexions with consequent inaccuracy would be avoided by a range changing circuit at the input.

To examine the range of linearity of the instrument more thoroughly, two more tests were performed, and the results of these are shown graphically in Figs. 3 and 4. In the first, a constant alternating current of 200 mA was passed through the field coil for varying periods of time, measured on a time interval meter, and the fluxmeter deflexion has been plotted against the time for which the current was passed in Fig. 3. In the second test, currents of varying magnitude were passed through the field coil for a period of approximately 1 s. The fluxmeter reading was then corrected (by dividing it by the time in seconds for which the current had actually flowed) to be a reading per second of current flow, and the logarithm of this value has been plotted against the logarithm of the current in Fig. 4.

Fig. 3 shows that there is linearity over the whole range of times for which the apparatus was tested, and the standard deviation is 1·1 %. From Fig. 4, it is clear that there is a range of input currents, from 150 to 350 mA, over which true squaring occurs. Above 350 mA, the amplifier is overloaded, and the output is no longer proportional to the square of the input current. The output from the bridge rectifier when the input current is 350 mA is about 5 V, so that the output voltage for an input current of 150 mA would be $5(150/350)^2$, or 0·9 V. For voltages below this value the bridge will be working on the non-linear portion of the rectifier characteristics, and this accounts for the non-linearity of Fig. 4 in the region for currents below 150 mA. The standard deviation of the readings over this range of linearity is 1·9%.

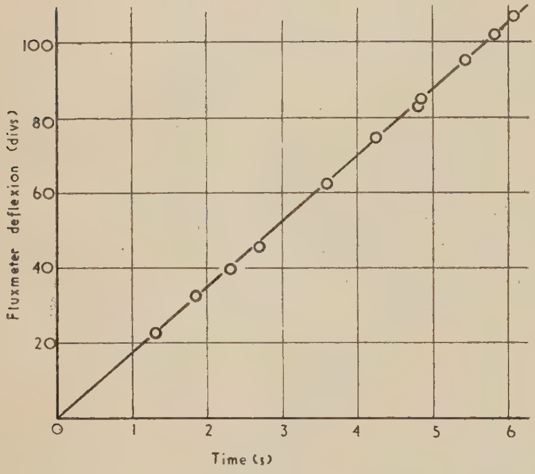

Fig. 3. Variations of fluxmeter readings with time for a steady current of 200 mA

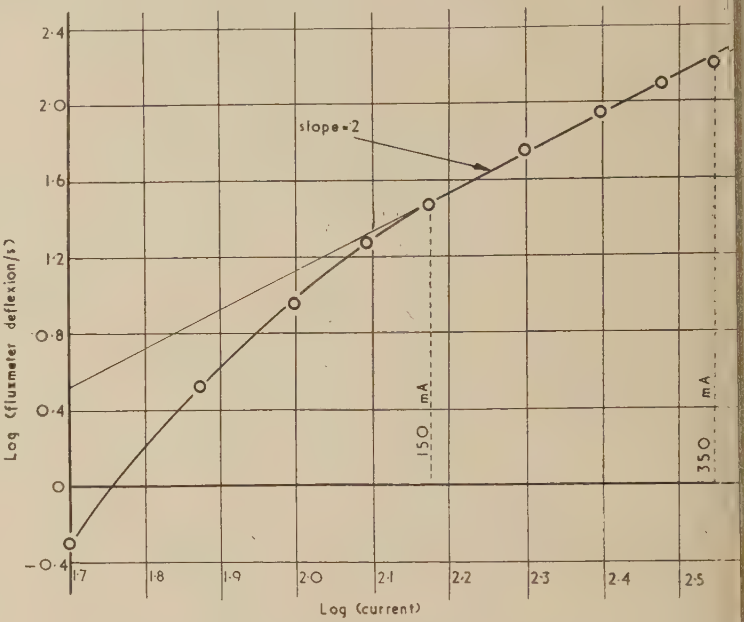

Fig. 4. Curve showing the range of linearity of squaring of the instrument

Conclusion

Deviations between fluxmeter readings and graphical integrals have been 2·9% with variations from the mean of ±5%. That some of this difference is the result of the inaccuracy of the graphical method is shown by the results of Figs. 3 and 4, where deviations between fluxmeter readings and integrals obtained by the time-interval meter have been below 2%. The method described has therefore produced results of good accuracy over a limited range of input currents. With specially designed equipment it would be possible to make a number of modifications which would extend considerably the range of input currents over which the instrument will operate satisfactorily, and would also make it more flexible and accurate in operation.

The circuit of the Hall unit described above was chosen for its simplicity, but the one given in Fig. 5 would have many advantages in operating a final working instrument. An amplifier (shown dotted) would probably be required between the output of the first crystal and the field coil the second to make the field in the second stage sufficient large, and more elaborate screening would be needed betwee the two stages. The advantages of this circuit in operatio however, are great. There are two inputs which may connected in series for squaring a current, or which can operated separately to multiply two currents together. Thu without the necessity of altering the internal circuitry, would be a simple matter to use the instrument for th measurement of either $\int i^2 . dt$, or $\int eidt$. The latter measurement would give circuit-breaker or fuse-arc energy. I addition, the two inputs are isolated, and are purely resistive as compared with the inductive input of the circuit given i Fig. 1. Thus there would be no problems of matching the shunt and input time constants.

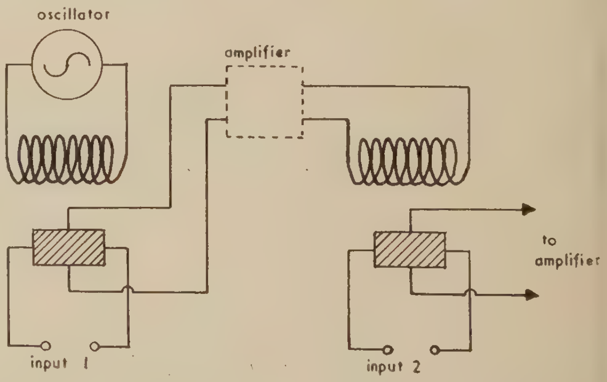

Fig. 5. Suggested circuit for a Hall-effect multiplying unit

It is often desirable to split up the reading of the values of $\int i^2 . dt$ into its pre-arcing and arcing components. When arcing begins, there is a sharp rise in voltage, and this could be used to actuate some form of electronic switch. If this switch were used to divert the signal from one fluxmeter to another, or simply to make or break the circuit to a single fluxmeter, then readings of the pre-arcing and arcing integrals could be obtained.

The maximum input current for accurate squaring is determined in the amplifier design by the voltage at which it will be overloaded, and the minimum input current is determined in the design of the rectifier circuit. Thus, a high h.t. voltage in the amplifier might be used in order to increase the overloading output voltage. A Hall-effect detector has been described,(8) in which the voltage to be rectified is multiplied by a constant voltage of identical frequency and phase. This voltage could be taken through a phase-adjusting network from the oscillator feeding the Hall squaring unit. The output from this detector consists of the second harmonic of the oscillator frequency (which has a zero integral, and may be ignored) and a d.c. signal proportional to the magnitude of the signal to be detected. As this is a linear detecting device, it should be possible, by using this in place of the bridge rectifier, to reduce considerably the minimum input current for accurate squaring.

Additional modifications might include a range-changing circuit, to accommodate a range of shunt voltages, so that fuses of different ratings could be tested with the same shunt. This circuit should be fitted in the input to the Hall unit, so that the input to this unit can be kept within the range of linearity.

A circuit which could be made to give one pulse of a known form and magnitude (say a square pulse of known height) could be incorporated into the instrument for use in checking the calibration, and a pre-set gain control in the amplifier could be used to adjust the calibration constant to a convenient value.

Acknowledgements

The authors wish to thank the Association of Short-Circuit Testing Authorities for a maintenance grant to one of them; Mr. C. Hilsum of S.E.R.L. for help in obtaining samples of indium antimonide; and Dr. A. K. Jonscher of G.E.C. Research Laboratories for helpful suggestions.

References

(1) Morgan, P. D., and Whitehead, S. *J. Sci. Inst.*, **6**, p. 241 (1929).

(2) Campbell, R. D. *Electronics*, **23**, p. 93 (1950).

(3) Kelner, R., Proctor, W., and Berger, F. B. *Rad. Lab. Series*, p. 315 (New York: McGraw-Hill, 1949).

(4) Chance, B., *et al.*, *Rev. Sci. Inst.*, **22**, p. 683 (1951).

(5) Soltes, A. S. *Electronics*, **23**, p. 122 (1950).

(6) Miller, J. A., Soltes, A. S., and Scott, R. E. *Electronics*, **28**, p. 160 (1955).

(7) Saker, E. W., Cunnell, F. A., and Edmond, J. T. *Brit. J. Appl. Phys.*, **6**, p. 217 (1955).

(8) Bogomolov, V. N., and Vasil'ev, V. A. *Zur. Tekh. Fiz.*, **27**, p. 260 (1957).

Simple ultramicro-pipette for electron microscopy

by R. HARDY, Ph.D., J. R. MAJER, Ph.D., and S. TRAVERS, Chemistry Department, University of Birmingham

[*Paper first received* 7 *September, and in final form* 2 *November*, 1959]

Abstract

A design for an ultramicro-pipette which permits the controlled delivery of droplets down to 2 μ *in diameter is described. After measurement by means of a screw-micrometer eyepiece, the droplets are deposited directly upon film-covered electron-microscope grids by means of a micro-manipulator. This technique allows particle counts of suspensions of submicroscopic particles to be made with greatly increased precision.*

Introduction

Estimates of the numbers of submicroscopic particles in suspensions are most commonly made with the aid of the electron microscope. To achieve satisfactory counts, it is necessary to examine the trace remaining upon a film-covered electron-microscope grid after a droplet of known size deposited upon the grid has evaporated, and to count the individual particles remaining within the trace. The comparatively small field of view provided by the electron microscope at magnifications sufficient to resolve particles below 0·1 μ in diameter limits the size of droplets which may be examined in this manner to a diameter of 40 μ. Droplets of this size are produced very readily by atomization with either a spray gun(1) or a rapidly rotating disk.(2, 3) The rotating disk in the form designed by May(3) gives a relatively homogeneous aerosol provided that the air jets used to rotate it are carefully controlled. Estimates of particle number may be made by sampling the aerosol produced by either of these methods with a sensitive surface such as magnesium oxide,(4) soot,(5) petrolatum-mineral oil,(6) dyed gelatin,(7) or polyvinyl alcohol containing silver nitrate,(8) and assuming a relationship between the impressions left upon the sensitive surface and the droplets whose dried traces are examined on the electron microscope grid. The uncertainty inherent in this method was avoided by Backus and Williams(9) who calculated the volume of droplets produced by the spray gun directly from the dried trace. This was achieved by adding to the original suspension a known volume of a calibrating suspension containing a known number of easily recognized particles (Dow Standard latex particles). A further refinement of this method has been carried out by Nixon and Fisher(10) who used a cascade impactor to separate an aerosol produced by a spray gun into close size ranges. These methods are limited by the statistical sampling variation and by the absence of a suitable calibrating suspension when polymer latex particles themselves are being counted. The need for a dispenser capable of producing droplets of known size down to 2 μ in diameter and a means of measuring the size of the droplet before placing it upon the electron-microscope grid was recognized by Sugar,(11) who also described a dispenser which used mercury pistons. While many micro-pipettes have been described, only that designed by Kopac(12) was sufficiently sensitive to allow the production of droplets having volumes in the 10^{-10} to 10^{-12} ml range. In this design, the droplet was ejected by the movement of a piston 0·005 in. in diameter driven by a differential thread. Since it was impossible to calibrate the differential thread to a sufficiently high degree of accuracy, the position of the piston was indicated by an electronic device of the Proximity Meter type. A very high standard of engineering is demanded in the construction of the instrument because the piston, which has the dimensions and strength of fine wire, must fit the barrel in which it slides with a tolerance very much better than the diameter of the orifice through which the droplet is ejected, otherwise leakage past the piston occurs. As the diameter of the orifice is of the order of 1–2 μ, the tolerance which can be accepted is far outside that commonly attained in precision engineering. To avoid the necessity of high-precision machining and complex electronic equipment, a much simpler design was adopted.

The ultramicro-pipette

The pipettes from which the droplets were ejected were made in the manner described by A. A. Benedetti-Pichler(13) from Pyrex glass tubing, using a de Fonbrune Microforge. The diameter of the tip ranged from 1 to 5 μ, and the overall length was about 10 cm. The pipettes, when prepared, were glassblown to ¼ in. diameter glass-to-metal seals and the assembly was soldered into a brass block having a horizontal hole. A length of copper capillary tube 0·016 cm in diameter connects the pipette to the piston assembly (Fig. 1). The production of small droplets by pipettes with small orifices is made difficult by the high surface-tension forces which occur at the tip. The pressure is equal to $2\gamma/R$, where R is the radius of the tip and γ is the surface tension of the liquid being ejected. With aqueous suspensions, this can rise to as high as three atmospheres, so that a hydraulic pressure equal to this must be established within the pipette before th droplet can be ejected. Kopac(12) found that two piston were needed to carry out the formation of the droplet, on large piston to raise the pressure until the surface-tensio forces were balanced and one small piston to expel th droplet. We have found that the first process is best carrie out in two stages because it is difficult to find the exact poin of balance with a large piston and the droplets were fr quently ejected while attempting to balance the surfac tension forces. The piston assembly therefore containe three separate pistons, one coarse, to permit rapid raising o the internal pressure, one small, to permit accurate balancin of the surface-tension forces and a third differential pisto to eject the droplet.

Piston assembly

The piston assembly is shown in Fig. 1. A brass bloc 9 × 4 × 4 cm. (*D*) has a horizontal hole 2 cm in diamete At one end of the hole, the block is recessed to carry a end plate which is soldered to the block. The end plat carries a union (A) containing a conical Teflon washe which is compressed by a brass nut. A piece of stainles steel rod 0·5 cm in diameter passes through the union an washer into the hole and provides the second balancin piston. The piston is moved through the Teflon seal b means of a differential thread (B) giving a movement of 25 μ per revolution.

A stainless steel rod 0·6 cm in diameter passes into th hole in the brass block at the other end, carrying a Teflo washer at one end to form a seal inside the hole. The othe end of the rod is pegged to a stainless steel rod 1·25 cm in diameter having 12 threads per inch (*G*) and passing throug a brass block having a similarly threaded hole. This pisto is used to raise the pressure within the pipette rapidly. The hole in the brass block is connected *via* a side hole to a second smaller brass block (*H*) 3·8 × 3·8 × 2 cm with the aid of copper capillary tubing (*E*). The second block has a central hole 0·16 cm in diameter connecting the two threaded extensions. These contain conical Teflon washers which are

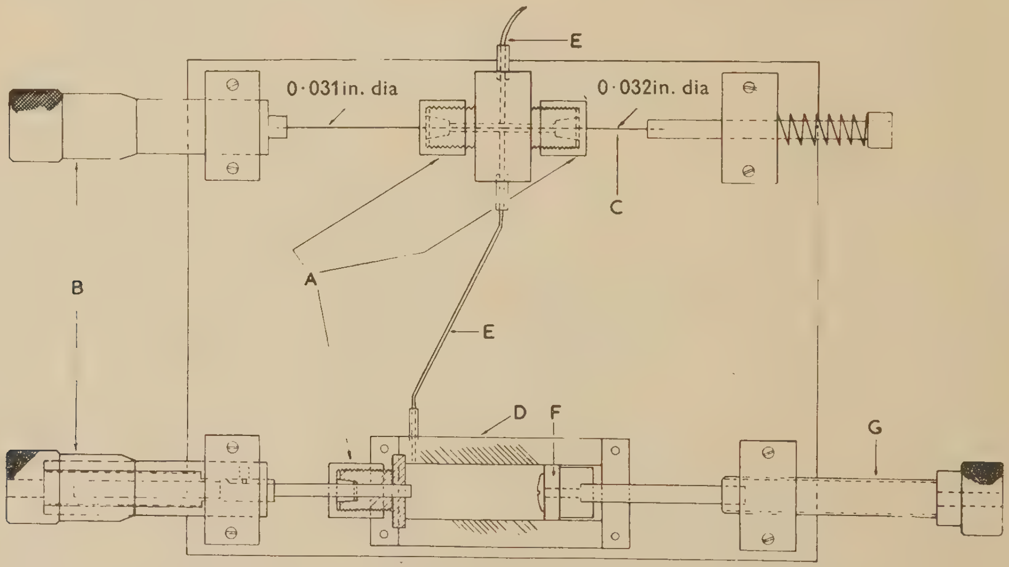

Fig. 1. Piston assembly

A, Union nut and Teflon washer; *B*, differential screw; *C*, differential piston; *D*, coarse piston; *E*, copper capillary; *F*, Teflon disk seal; *G*, coarse adjustment; *H*, differential piston chamber compressed by brass nuts. A stainless steel rod (C) 0·08 cm in diameter passes through both washers and along the axis of the hole. It is moved through the hole by means of a differential thread (B) similar to that described above. A 0·16 cm diameter hole drilled at right-angles permits connexion of the block to the coarse piston assembly on one side and to the pipette on the other. One half of the length of the rod was lightly rubbed with very fine emery paper so that it had a slightly smaller diameter than the other. Thus when the rod moved through the hole a reduction in volume, corresponding to the difference in cross-sectional areas of the two halves of the rod multiplied by the distances moved through, was achieved. No attempt was made to measure the difference in diameter or to relate the linear movement of the rod to the volume of liquid expelled because of irregularities in both rod and differential thread. Instead, the droplets were measured directly with a screw-micrometer eyepiece. The cross-sectional area of a piston 0·0125 cm in diameter is of the order $10^4\ \mu^2$ so that a movement of less than a micron is required to expel a droplet of 20 μ diameter. With the differential piston, a movement of about 10 μ was permitted to expel the same size droplet. Even so, only very small displacements of the differential were required to expel droplets below 5 μ in diameter. The smallest droplets were obtained by continuously ejecting liquid from the pipette tip until only sufficient remained for the small droplet which was then expelled instantaneously by rotating the differential knob rapidly. The entire piston assembly was filled with silicone oil which served as the hydraulic fluid. An air gap separated it from the sample and the pipette.

All the components of the piston assembly were mounted upon a Dural sheet which was mounted in turn upon a large slate bed to ensure rigidity and freedom from vibration.

Method of operation

In practice, the pipette was mounted upon a robust micromanipulator having movements in three directions. Because of the possibility that the pipette tip might pierce the thin carbon film covering the electron microscope grid if any vibration were introduced during the process of deposition of the droplet on the grid, the micro-manipulator was made very heavy and rigid. It consisted of a brass baseplate mounted upon three screw feet which were located in metal grooves screwed to the slate bed and served to level the pipette. Upon the base is mounted a tower of heavy V-slides moved by screw threads (40 per in.). These permit movement of the pipette vertically, laterally and transversely. A coarse rack and pinion was also provided to allow rapid removal of the pipette from the field of view of the microscope. The microscope itself was also mounted upon a heavy tripod with adjustable feet located in V-grooves screwed to the slate bed. The microscope had a small mechanical stage and focusing was by vertical movement of the whole stage.

The electron-microscope grid, covered with a thin carbon film, was placed upon a special slide (Fig. 2) consisting of a block of Perspex 7·5 × 4·2 × 0·8 cm with a trough 5·5 × 3·8 × 0·6 cm milled from its centre. In the centre of the trough, there is a small island 1·8 × 1·0 × 0·6 cm having a small recess to accommodate several electron-microscope grids and two vertical holes 0·2 cm in diameter and 0·5 cm deep at one side. A Perspex block 2·5 × 3·7 × 2·0 cm has a central hole 1·7 cm in diameter which is a close fit upon the microscope objective. When the electron-microscope grids are being viewed the Perspex block dips into a layer of water in the trough thus forming a moist chamber which minimizes evaporation of the droplets during manipulation. A narrow slit in the block attached to the objective allows the pipette to be inserted from the side without a perceptible drop in humidity. When the grids are placed on the island in the trough and the microscope objective is in position the samples to be measured are placed in the holes at the side of the island by means of a hypodermic syringe protruding through the side slit. The syringe is then withdrawn and replaced by the pipette. From now on, all operations in the field of view of the microscope, at a magnification of 400 times, are carried out with the micro-manipulator. The tip of the pipette is centred in the field of view of the microscope and brought into focus by means of the micro-manipulator. The mechanical stage is then used to locate the holes containing the samples and the stage raised until the tip of the pipette touches the surface of the suspension. A quantity of the suspension is then drawn into the pipette by capillary forces. The stage is then lowered and the mechanical stage used to position the selected electron-microscope grid aperture below the pipette tip. The stage is then raised until the grid itself is in focus and, at this point, the tip is just above the surface of the carbon film. The coarse and balancing piston controls are then operated until the meniscus in the shank of the pipette just begins to move. The differential piston control is then operated to eject a droplet of the preferred size. The diameter is measured as the droplet hangs from the tip. The stage is then raised until the droplet touches the carbon film, when it immediately becomes detached from the tip. Difficulties were encountered at first, as the droplet tended to run back along the outside of the pipette, but this tendency was prevented by dipping the pipette into a solution of trichloroethyl-silane in chloroform before use. Diameters are measured by means of a Watson screw micrometer eyepiece. An alternative procedure is to calibrate each pipette before use by measuring the column of liquid drawn up into the pipette shank by means of the micrometer eyepiece and then ejecting the whole of the column into an immiscible liquid. The diameter of the droplet can then be measured and its size related to the length of the column originally in the pipette. A number of droplets of different sizes can be placed upon grids without removing the pipette from the moist chamber. Fig. 3 shows a number of droplets of water resting upon a carbon film which has been contaminated to make it visible.

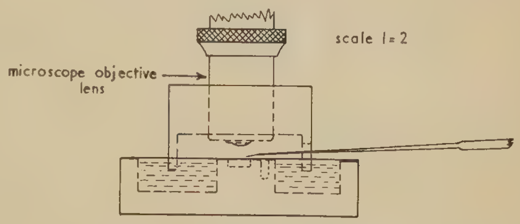

Fig. 2. Moist chamber

When deposition of the droplets is complete, the grids are removed from the moist chamber and the water allowed to evaporate. The specimens are then shadowed with palladium metal in a vacuum coating plant and examined in the electron microscope.

The magnification required varies with the size of the particles being counted. In the study of emulsion-polymerization systems, the polymer-latex particles range from about 500 to 1200 Å in diameter, and the magnification of the final photographic print from which the particle counts are made varies from 6000 to 8000 times. The concentration of the polymer latex is adjusted so that a droplet 30 μ in diameter contains about 20000 particles. Counts done on a series of similar droplets were remarkably uniform. This is attributed to the fact that significant populations were being counted, so that statistical variations were reduced. The limiting feature of the method is the accuracy with which the diameter of a droplet may be measured with the screw-micrometer eyepiece.

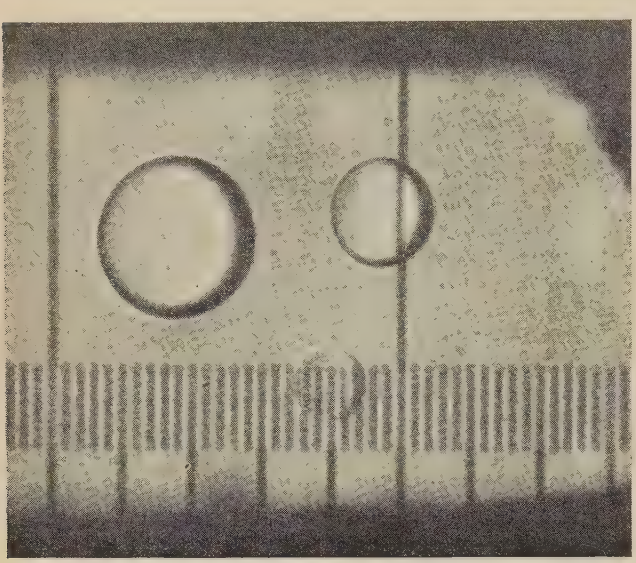

Fig. 3. Water droplets resting upon film-covered electron-microscope grid

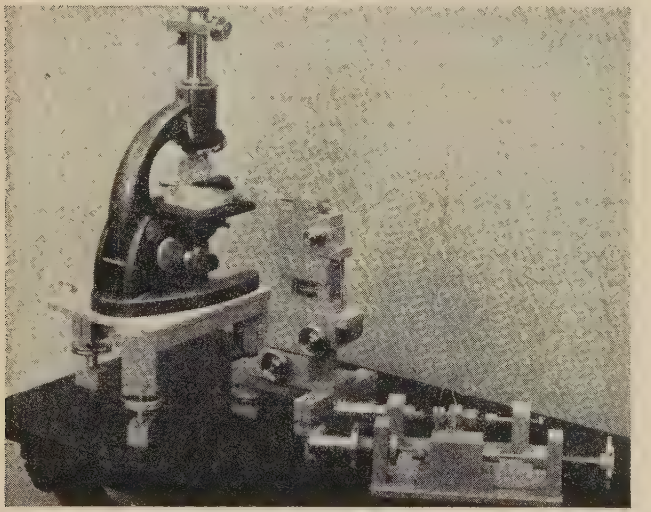

Fig. 4. General view of ultramicro-pipette

Applications

The ultramicro-pipette was constructed to facilitate the evaluation of polymer lattices and the results obtained with it are reported fully elsewhere. Particle counts on polymer lattices can provide information concerning the rate and mechanism of the polymerization and this technique has been found most useful in the study of polymerizatio
initiated by γ-irradiation.

A second application of the instrument is in the calibratio
of sensitive surfaces used for sampling aerosols. It has bee
found that gelatin surfaces, such as those provided by fixe
photographic plates, retain the impressions created by th
contact of water droplets. These impressions are readil
visible in the optical microscope without the use of phase
contrast methods or staining techniques. The relationshi
between the diameter of the impression in the gelatin surfac
and volume of the droplet producing it may be determine
by measuring the impressions created by a series of droplet
of known size ejected from the ultramicro-pipette and allowe
to impinge upon the gelatin surface.

As the larger polymer molecules (above 50000 MW) ar
readily visible in the electron microscope, it is possible, wit
considerably greater difficulty, to make an estimate of th
number average molecular weight of a polymer by electro
microscope examination of the trace left by a droplet of
polymer solution (in a poor solvent). A similar techniq
may be used to estimate the weight of individual viru
particles.

Finally, the ultramicro-pipette provides a unique direc
method of dispensing very small samples of organic liquid
for testing the ultimate sensitivity of gas-chromatograph
detectors.

Acknowledgements

The authors are indebted to Professor J. C. Robb for hi
advice and encouragement and to Courtaulds Educationa
Trust for financial support.

References

(1) Cravath, A. M., Smith, A. E., Vinograd, J. R., and Wilson, J. N. *J. Appl. Phys.*, **17**, p. 309 (1946).

(2) Walton, W. H., and Prewett, W. C. *Proc. Phys. Soc. B*, **62**, p. 341 (1949).

(3) May, K. R. *J. Appl. Phys.*, **20**, p. 933 (1949).

(4) May, K. R. *J. Sci. Instrum.*, **27**, p. 128 (1950).

(5) Stokes, R. L. *J. Appl. Phys.*, **17**, p. 243 (1946).

(6) Fuchs, N., and Petrjanoff, I. *Nature*, **139**, p. 111
(1937).

(7) Schaeffer, V. J. *General Electric Co., A.A.F. Technica
Report No.* 5539. A.A.F. Air Materials Command
Wrightfield, Dayton, Ohio, 1947.

(8) Farlow, N. H. *J. Coll. Sci.*, **11**, p. 184 (1956).

(9) Backus, R. C., and Williams, R. C. *J. Appl. Phys.*, **21**,
p. 11 (1950); *J. Amer. Chem. Soc.*, **71**, p. 4052 (1949).

(10) Nixon, H. L., and Fisher, H. L. *Brit. J. Appl. Phys.*, **9**
p. 68 (1958).

(11) Sugar, I. *Proceeding of Conference on Electron Micro-scopy, Stockholm*, 1956, p. 118.

(12) Kopac, M. J. *Trans, N.Y. Acad. Sci., Series* 2, **15**,
p. 290 (1953).

(13) Benedetti-Pichler, A. A. *Microchem. J.*, **2**, p. 3
(1958).

Simple photoelectric demodulator

by A. Kolin and R. T. Kado, Department of Biophysics, University of California, Los Angeles, U.S.A.

[*Note first received* 16 *February*, *and in final form* 23 *July*, 1959]

The simple device described below proved very convenient in many laboratory applications. It proved especially useful in permitting the flow signal of an electromagnetic blood flowmeter displayed on an oscilloscope screen to be recorded on a standard pen-recording electrocardiograph. This application will be used to illustrate the use of this device.

The flow signal is a sinusoidal alternating voltage induced in conductive liquid flowing through an alternating magnetic field. Variations in flow during the cardiac cycle modulate the amplitude of the sinusoidal voltage output. It is this amplitude which is to be recorded as a measure of the instantaneous rate of flow. The phase of the output is determined by the direction of flow, so that a reversal of flow reverses the phase of the flow signal. This phase reversal should be indicated by reversal of the ordinate in the recording.

Phase sensitive detection of the flow meter signal is desirable not only for the purpose of indicating the direction of flow; it can also serve to facilitate the task of eliminating the "transformer e.m.f.", induced by the changing magnetic field in the unavoidable loop which is formed by the ends of the twisted pair of leads connected to the electrode pins. This e.m.f. can be eliminated completely as previously described.* This is, however, a tedious process with miniature flowmeters designed for implantations into an animal. A great simplification in the design and construction of such flow transducers could be achieved if a reduction in magnitude of the transformer e.m.f., rather than its complete elimination, would suffice. The fact that the transformer e.m.f. is 90° out-of-phase with respect to the magnetic field, and thus to the flow signal, suggests the idea of sampling the flow signal at the moment when it is at its maximum, at which time the transformer e.m.f. vanishes. The demodulating device described below makes it possible to approximate the suggested sampling conditions.

Fig. 1 shows the sinusoidal flow signal displayed on the oscilloscope screen. An opaque mask M in which a double slit (Sl_1 and Sl_2) is cut is positioned so as to sample a narrow zone at the apex of the sine pattern. A slit angle of about 3° is used.

Two rectangular selenium photocells PC_1 and PC_2 (type B10 by the International Rectifier Corp.) connected in parallel opposition, as shown in Fig. 1, are placed behind the mask M with the photosensitive surface facing the oscilloscope screen. As the amplitude of the sine wave changes, the time interval during which the oscilloscope spot sweeps across the photosensitive surface bared by the mask M changes porportionally. The photocell output voltage is thus proportional to the amplitude of the signal displayed on the oscilloscope screen. When the phase of the signal is reversed, the apex of the sinusoidal signal is transferred from triangular window Sl_1 to Sl_2 thus reversing the polarity of the photocell output voltage which is recorded with a standard pen recorder.

Fig. 2 shows a record of blood flow in the carotid artery of a conscious dog obtained with this demodulator and a Sanborn pen-writing electrocardiograph.

The stability of the demodulator depends on the quality of the oscilloscope used. Most modern oscilloscopes are adequately stabilized against line voltage fluctuations. A test of the demodulator output for a constant input signal, performed with a type 531 Tectronix oscilloscope, showed a maximum fluctuation of the photocell output of about 4% as compared to a 17% maximum fluctuation of a deliberately varied line voltage energizing the oscilloscope. This simple arrangement thus provides good stability in its performance, combining the functions of a phase-sensitive rectifier, demodulator and sampling device.

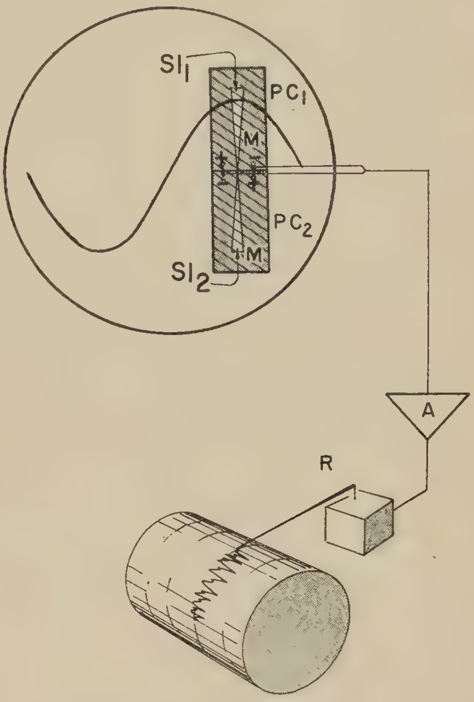

Fig. 1. Application of photocells PC_1 and PC_2 and mask M to the screen of an oscilloscope. Sl_1 and Sl_2, triangular slits in the mask M which is located between the cells and the screen. A, d.c. amplifier; R, recorder

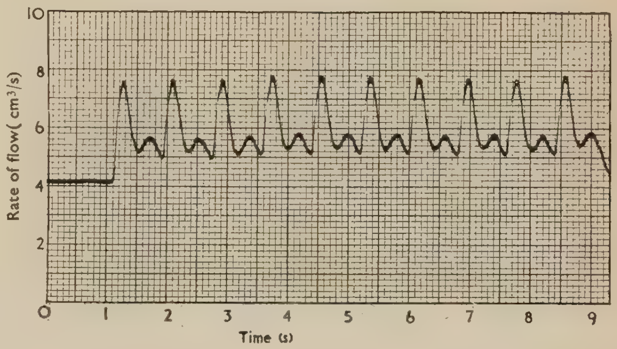

Fig. 2. Tracing of blood flow in the carotid artery of a dog; obtained with an electromagnetic flowmeter using the recording arrangement shown in Fig. 1

This work was supported by a grant from the Office of Naval Research.

---

* Kolin, A., Herrold, G. and Assali, N. *Proc. Soc. Exp. Biol. Med.*, **98**, p. 550 (1958).

Gas-quenching apparatus for high-speed thermal analysis

by R. D. Garwood, M.Sc., J. R. Moon, B.Sc., and B. F. Thrush, Metallurgy Department, University College, Cardiff

[*Note received* 26 *October*, 1959]

The heat treatment of certain metals and alloys is possible in practice because the phase transformations which take place under conditions of slow cooling are modified or prevented when the cooling rate is increased. The highest speeds of cooling are obtained by quenching the parts into liquid cooling media, such as oil, water or brine. Phase changes during quenching may be detected by thermal analysis but the discontinuities on the curves due to the various stages of cooling in liquids(1,2) tend to mask the true thermal arrest points. This difficulty was overcome b Greninger(3) and Duwez(4) who employed gaseous quenchi media in order to study the transformation characteristics steels and titanium alloys respectively. The apparatu described in this note was developed from that used b Greninger. An automatic device has been incorporate for the removal of the heating coil from the vicinity of th specimen at the instant of quenching.

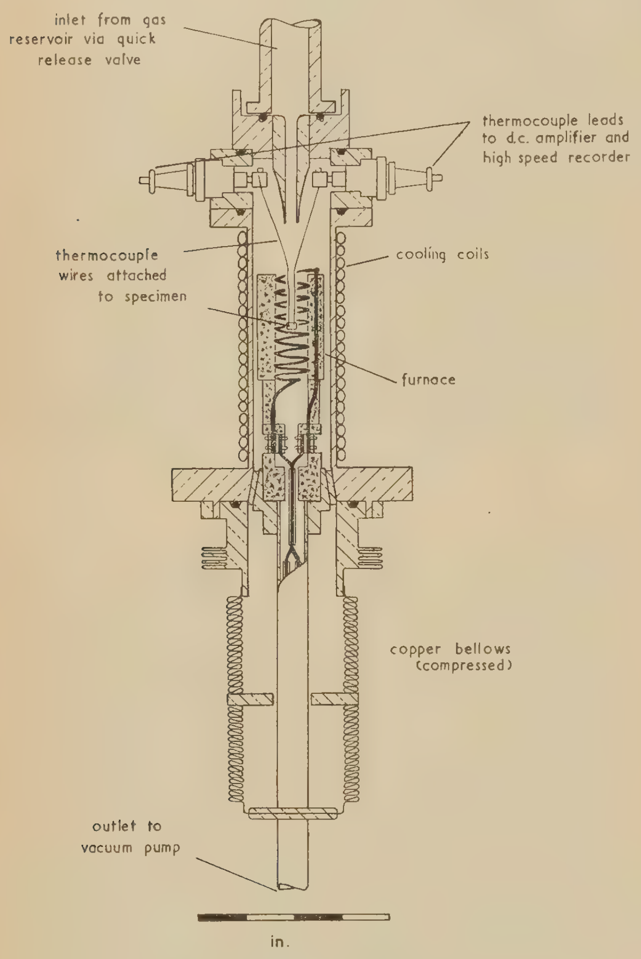
inlet from gas reservoir via quick release valve
thermocouple leads to d.c. amplifier and high speed recorder
thermocouple wires attached to specimen
cooling coils
furnace
copper bellows (compressed)
outlet to vacuum pump
in.

Gas-quenching apparatus

The general arrangement is shown in the figure. Th specimen is heated in a small furnace consisting of 0·5 in diameter coil of 20 s.w.g. nichrome wire and is supported o the chromel/alumel thermocouple. It is advisable to spo weld these wires to the specimen but where this is not possibl beads of the thermocouple wires may be caulked into sma tapered holes in the specimen. On closing the valve to th pressure tank containing the quenching gas, the vacuu pump causes the copper bellows to contract and carry th furnace into a position surrounding the specimen, that is, i the centre of the water-cooled jacket. The specimen is the given the required solution treatment, after which it quenched by opening the quick-release valve to the gas tank This destroys the vacuum and causes the bellows to expand thereby removing the furnace to a point 4 in. below th specimen. The incoming gas streams over the specimen at rate determined by the size of the orifice and the initia pressure, and produces a rapid fall in temperature. A d.c amplifier of the push-pull type is used to feed the output o the thermocouple into a high-speed pen recorder with response time of 2·5 ms for full-scale deflexion.

It was found that the cooling rate could be varied b changing the diameter of the gas inlet, the initial pressure o the quenching gas and the size of the specimen, the last metho being the most effective. Cooling speeds measured at 500° on quenching a 4 × 3 × 1·5 mm specimen of aluminiu bronze from 900° C are given in the table.

Cooling speeds of aluminium bronze

Diameter of orifice (in.)	*COOLING SPEED (° C/S)*		
	Initial nitrogen pressure (lb/in²).		
	10	20	30
0·125	330	355	480
0·250	375	535	640
0·530	265	335	320

References

(1) Pilling, N. B., and Lynch, T. D. *Trans. Amer. Ins Min. Met. Engrs.*, **62**, p. 665 (1920).

(2) Scott, H., *Trans. Amer. Soc. Metals*, **22**, p. 577 (1934

(3) Greninger, A. B., *Trans. Amer. Soc. Metals*, **30**, p. (1942).

(4) Duwez, P., *Trans. Amer. Inst. Min. Met. Engrs.*, **191** p. 765 (1951).

New instruments, materials and tools

The Editor invites manufacturers of instruments and light machine tools to keep him informed of their new or improved products. The Institute of Physics assumes no responsibility for the statements given below: information for these has been taken from literature supplied.

Microwave generator. M.O. Valve Co. Ltd., Hammersmith, London.

A microwave generator embodying a new focusing principle is named the Ophitron. The valve is an electrostatically-focused backward-wave oscillator in which the electron beam follows an undulating path. The advantages claimed for the new oscillator are its small size (6 in. long × $\frac{3}{4}$ in. diameter), low weight (7 oz.) and simple construction. A single stamped-out periodic structure and two flat focusing plates form the propagating path for the radio-frequency wave and set up the periodic electrostatic field which focuses the electron beam. This system brings the crests of the undulating electron beam into the region of maximum radio-frequency field, thus providing good coupling between beam and wave and resulting in greater bandwidth than can be obtained with a magnetically-focused oscillator. The present valve tunes electronically over at least a 40% band in the 10 000 Mc/s region. The range covers the most important centimetric bands. It is expected that noise will be less than that of magnetically-focused oscillators owing to the ion drainage from the electron beam produced by the electrostatic focusing system.

L-band signal generator. Winston Electronics Ltd., Shepperton, Middlesex.

The type 957 signal generator provides a source of unmodulated or pulse-modulated power over the frequency range 800–2100 Mc/s, which is covered in one band with single dial control directly calibrated to within 1%. The output power is continuously variable by a calibrated control over the range 0 to -100 dB relative to 1 mW; the absolute accuracy of power readings is stated to be ± 2 dB, the power being monitored by a temperature-compensated thermistor bridge operating a panel meter. The modulating pulses have a width variable between 0·5 and 10 μs, a delay variable between 3 and 300 μs and a repetition rate between 40 and 4000 pulses/s. The internal pulse generator can be synchronized to external pulses or to sine waves.

Portable potentiometer recorder. Mervyn Instruments, St. John's, Woking, Surrey.

This recorder is operated by internal batteries having a life of 250 h. It is contained in a cabinet measuring 7 × 7 × 10 in. and weighs only 10 lb. This small size and weight is made possible by the use of transistor circuitry, printed wiring and a permanent magnet d.c. motor drive for the potentiometer. The chopping system is transistorized, and chopping is done at 1 kc/s, thus eliminating 50 c/s interference. The reference potential is a Zener diode. The recording chart has a width of 4 in., and speeds from 1/25 to 6000 in./h are available. The drive is by an eight-day clockwork motor and indication is by wax paper. The ranges available are 0–5 mV and 0–1 V with zero suppression up to 20 mV and 0·8 V respectively. An accuracy of 0·5% is claimed with a pen speed of 3 s full-scale travel. The instrument can also be supplied for mains operation at a.c. voltages from 26 to 250 V and frequencies from 50 to 2400 c/s; the power consumption of the mains model is 10 W.

Permanent magnet. Schlumberger Well Surveying Corporation, Ridgefield Instrumentation Division, Ridgefield, Connecticut.

This precision permanent magnet has a field strength of 1717·5 G and maximum field inhomogeneity at gap centre of 40 mG over a 2 in. maximum dimension region. The field is stated to be accurate to 0·1%. The model, which is, in effect, a secondary magnetic standard is suitable for magnetic analysis by nuclear magnetic resonance, and semiconductor studies. It has a 2 in. thick and 10 in. diameter gap which permits the use of large material samples and cryostating equipment; and over a region of 1 cm^3 the maximum field inhomogeneity is claimed to be 10 mG. The overall size is 15·5 in. wide × 20 in. deep × 12 in. high.

Neutron spectral measurements. Aerojet General Nucleonics, San Ramon, (nr. San Francisco), California, U.S.A.

It is stated that accurate, reproducible spectral determinations for neutron energies are now possible by using a system of neutron detection foils. The spectrum is measured by foils in six energy increments, as follows:

(1) Thermal neutrons are measured with gold or cobalt foils.
(2) Neutron energies greater than 1 keV are measured by ^{239}Pu foils.
(3) Energies greater then 1·5 MeV, by ^{238}U foils.
(4) Energies greater than 2·9 MeV by ^{32}S foils.
(5) Energies greater than 5·3 MeV are measured by analysing the products of the (n, p) reaction on ^{27}Al foils.
(6) Energies greater than 8·6 MeV, by analysing the products from the (n, p) reaction on ^{27}Al foils.

A ^{10}B shield is used to protect the fission foils from the thermal neutrons during irradiation. Cadmium covers are available for use with the gold and cobalt foils for determining the cadmium ratio. Sulphur foils are repackaged in "cold" aluminium after their irradiation, thus eliminating the possibility of mistaking certain reactions in aluminium for those in sulphur.

These accessories, together with high-precision counting equipment, are available from the firm. Calibrated irradiated foils can also be supplied for cross-checking the results, or alternatively, a calibrated detector and sample holder may be used. The detector includes photo-multiplier tube, cathode follower and cables, and is delivered ready for use with the amplifier and scaling equipment. The firm will undertake the entire analysis if desired.

An alternative analysis, from foils consisting of neptunium, plutonium, and ^{238}U in boron shields, of bare and cadmium covered gold, and of sulphur, is available for monitoring nuclear reactor excursions.

The foil dimensions for the first analysis are as shown in the figure. The thickness is of the order of 0·010 cm except for the sulphur, and in addition it contains graphite for eliminating charge build-up. The gold, aluminium, and sulphur are stated to be pure to 0·001%, and the uranium contains 0·4039% ^{235}U by weight.

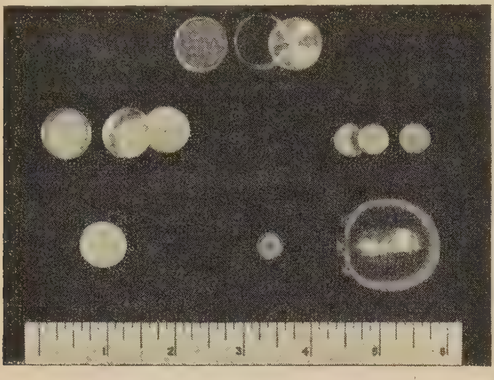

Foil dimensions for the first analysis

This analysis makes it possible to compare results from the various radiation studies for, it is stated, these studies depend for their completeness on a complete neutron spectra data.

Vibrator pressure transducer. Solartron Electronic Group Ltd., Thames Ditton, Surrey.

The pressure-sensitive element of this transducer is a mechanical vibrating system, the natural frequency of whi is dependent upon the applied pressure. This vibrati element determines the frequency of an electronic feedba oscillator, which therefore provides an output voltage constant amplitude but with a frequency varying parabolica with the pressure. The oscillator uses a printed circuit wi a transistor and is encapsulated in epoxy resin. The who transducer is encased in stainless steel and measures $1\frac{1}{2}$ i diameter by $2\frac{1}{2}$ in. length. The unit is available in pressu ranges from 25 to 600 lb/in.^{2}. A repetition accuracy 0·1% is claimed, and it is stated that the device is unaffect by vibrations of 10 g; at frequencies up to 2 kc/s stead accelerations of 20 g change the sensitivity by 0·015%.

Directional coupler for measurement of power in coaxial cabl Sir W. G. Armstrong Whitworth Ltd., Baginto Coventry.

The directional coupler type DC1/52 is of the loop type ar is intended for insertion in 52 Ω coaxial cables. The couplin consists of a single loop terminated at each end by resistanc of equal value. For forward-going power, the curren induced by the electric and magnetic fields add in the resis ance nearest the generator and cancel in the other. The currents are rectified and measured on two microammeter The coupler therefore serves to measure both radio-frequenc power and standing-wave ratio. The instrument is fitte with a two-range switch and, at the calibration frequency, t ranges are 1 and 5 W with an accuracy of 0·1 and 0·2 d respectively. The attenuation produced by the unit stated to be less than 0·2 dB. The power measurements a correct only at the calibration frequency, since the mete readings are proportional to frequency, but the coupl may be used as an aid to obtaining optimum termina tion of a 52 Ω coaxial system over the frequency rang 300–600 Mc/s.

New books

Techniques modernes et applications de la cryométrie. By Y. Doucet. (Paris: Dunod Éditeur, 1959.) Pp. ix + 225. Price 1450 fr.

In the first 120 pages the author describes the techniques available for determining the depression of freezing-point in solutions, including both methods that involve supercooling and those that employ analysis of an equilibrium mixture. Practical details are given. There is a 6-page table of solvents with their cryometric constants. The use of fused salts, strong salt solutions, and eutectics as solvents is described. In the remaining 93 pages the author sketches the application of cryometry to various problems: the determination of molecular weights, entropies of fusion, activity coefficients, association, ionic dissociation, solvation, hydrolysis, analysis of mixed crystals, titrations, and the strengths of weak acids. There is a bibliography but no index. In a short book selection is inevitable, but the reviewer noted some surprising omissions, e.g. recent work on solutions in sulphuric acid. The book will be very usef as a guide to practical techniques.

E. F. Caldin

The cathode-ray tube and its applications. 3rd ed. B G. Parr and O. H. Davie. (London: Chapman an Hall Ltd., 1959.) Pp. xii + 433. Price 50*s*.

This book is primarily intended for those who wish to us cathode-ray oscillographs without necessarily having t acquire on the way, for example, any great knowledge of th more philosophical aspects of electron optics and circui theory. It is the third edition and contains much ne material not given in the earlier editions.

There are introductory chapters on historical aspects an development and on tube construction and performance, i which only the essential elementary aspects of electron optic are given. Various types of tube are briefly described The third chapter begins what is probably by far the mos portant and useful part of the book, namely a compre-ensive collection of information on the circuits necessary r the construction and use of cathode-ray oscillographs in any fields of work. These chapters are clearly written and ontain much valuable information. Many of the circuit agrams recommended for specific uses also show the com-onent values but unfortunately there are exceptions. This ifficulty could easily be corrected in the next edition, but therwise references must be made to the original papers, omprehensive lists of which are given at the ends of chapters. atters dealt with in this part of the book include power upplies, amplifiers, time bases of many and various kinds nd auxiliary circuits, e.g. pulse generators. The section on illimicrosecond pulse generators is perhaps disappointingly rief. There is the usual, and probably unnecessary, chapter n photographic recording followed by a description of arious transducer devices and then chapters on mechanical nd electrical engineering applications which, in my view, ould have been better omitted. It is customary in works f this kind to include brief descriptions of such applications ut there are so many of them and they bear little relation n general to the day-to-day uses of cathode-ray oscillographs hat there seems to be a good case for their complete omission, specially in view of the high cost of books in general. Much he same could be said about the chapter on measurements in adio engineering, although this is unusually interesting, lthough again necessarily superficial. Finally there are hapters on oscillographs for television measurements, appli-ations to general and nuclear physics and miscellaneous pplications, including electro-medical and computer pplications.

There is no doubt that the book should be widely used.

J. D. Craggs

Adhesives guide. By J. Hurd. (Chislehurst: British Scientific Instrument Research Association, 1959.) Pp. viii + 138. Price 20*s.*

Mrs. Hurd has given a great deal of thought to the compilation of this reference book. Although written as a comprehensive answer to inquiries received by The British Scientific Instrument Research Association from its member firms, the book is issued as an open publication for all to buy. And there is no doubt that a great many people will buy it, because it supplies a need no other book does.

Adhesives guide makes it clear that it does not pretend to be a treatise on adhesion; instead, it gives "tabulated data on 400 individual adhesives made by about 100 firms". It starts with a useful Introduction which includes a number of do's and don'ts (but not in those words), a page on testing adhesives, and a few words on such things as surface preparation. Considering the number of patents on the subject, perhaps something might have been said about creating a wettable surface on polyethylene to make it adhesionable with a wider range of adhesives.

The contents proper begin with a section on selecting the right adhesives for the job. The part dealing with wood adhesives shows that note has been taken of the doctrines of the Forest Products Research Laboratory.

Another section is called "Encyclopaedia of basic types of adhesive"; and at the back of the book is a bibliography showing from where most of this information was obtained.

Section 3 is called "Classification of manufacturers by basic types of adhesive made". Only one or two omissions were noticed.

Sections 4 and 5 contain an alphabetical list of manufacturers and an alphabetical list of adhesives by their trade names. When read in conjunction with the earlier chapters, the user is supplied with all the general information he needs, except the more specific advice that only the adhesives manufacturer can give.

Finally there is an appendix which includes the formulations of a dozen or so different types of adhesives, some quite modern and some time-honoured.

Collecting all the information and presenting it in such an easy-to-get-at manner is a praiseworthy effort, and *Adhesives guide* will thoroughly deserve the blessings its readers will bestow on it.

C. A. A. Rayner

Electronic components handbook. Vol. 3. Edited by K. Henney, H. Mileaf and C. Walsh. (London: McGraw-Hill Publishing Co. Ltd., 1959.) Pp. 180. Price 77*s.* 6*d.*

This is the third and final volume of a Handbook dealing with electronic components. It provides data on transformers and inductors; connectors; wire and cable; terminals; tube shields; hardware. Volumes 1 and 2 were reviewed in this *Journal* for November 1957 and January 1959.

There is much factual information about every type of component that will be of value to the designer of electronic equipment and will assist in the selection of the component most suited to the particular function it has to perform. This general information comprizes a large part of the text and is applicable outside the strictly military equipment field of the U.S.A., though it is this field to which the detailed specifications strictly apply.

In the chapter on transformers are discussed those for power, communication, pulse, hybrid, logic, and tuned, as well as magnetic amplifiers: connectors include jacks, plugs and sockets: whilst hardware deals with knobs, dials, indicating lights, flexible shafting and fasteners.

A. J. Maddock

Tools of biological research. By H. J. B. Atkins. (Oxford: Blackwell Scientific Publications Ltd., 1959.) Pp. xvi + 183. Price 37*s.* 6*d.*

At a meeting of the Surgical Research Society in 1958 a number of scientists explained the principles and potentialities of research techniques employed in biology that they had themselves exploited with distinction. This book is expanded from the proceedings. It provides, on the whole, admirable introductions to a number of specifically biological techniques, e.g. tissue culture and transplantation, and to others, e.g. electron-microscopy and mass spectrometry, of more general application but of profound importance to biologists.

The beliefs and procedures of surgeons are not generally noted for the soundness of their scientific foundations, a state of affairs no doubt sustained by those surgeons who so vociferously claim their trade to be more Art than Science. So it is a matter for regret that problems so fundamental to research as experimental design and analysis were not felt worthy of more than 10 of 183 pages.

D. W. James

Notes and comments

Index of Crystallographic Supplies

In September 1956 the first edition was published of the *Index of Manufacturers of Apparatus and Materials Used in Crystallography.* The second edition has recently been published under the title *Index of Crystallographic Supplies.* A limited number of copies of this publication are available free of charge to *bona fide* crystallographers who are resident in the United Kingdom, and who have not already received a copy. Applications will be dealt with in strict order of receipt and should be made to The Institute of Physics, 47, Belgrave Square, London, S.W.1, as soon as possible.

Proceedings of Comité Consultatif de Thermométrie

It has been announced that the proceedings of the 1958 meeting of the Comité Consultatif de Thermométrie of the Comité International des Poids et Mesures have now been published by Gauthier–Villars of Paris. The 230-page book comprises the minutes and report of the meeting, together with reprints of the documents which were considered. These include accounts of the international intercomparisons which have been made to verify the agreement between the scales realized by the different national laboratories and show an agreement of about 0·001 deg C at 100° C and of two or three degrees at 2200° C. An account is also given of work with platinum resistance thermometers in the range 11° to 90° K, whereby it is hoped to extend the international scale into this region. Resistance thermometer measurements of the freezing point of zinc made at the National Research Council in Canada, the Mendeleev Institute of Metrology in Leningrad and the National Physical Laboratory agree on a figure of 419·505° C (Int. 1948) to within ±0·001 deg C.

Instrument Abstracts

Instrument Abstracts is a monthly journal devoted to abstracts of the world's technical literature relating to scientific and industrial instruments. It is prepared by the British Scientific Instrument Research Association and is now printed and published by Messrs. Taylor and Francis Ltd., of London.

The publishers state that *Instrument Abstracts* is to cover a wider field than it has done previously and in more detail. The subscription price is £4 p.a. ($12.00), including postage.

The Royal Society's Fair Copying Declaration

The Institute, in common with more than 70 other scientific and learned societies, has subscribed to the Royal Society's Declaration on Fair Copying which reads as follows:—

We will regard it as fair dealing for the purpose of private study or research when a non-profit-making organization, such as a library, archives office, museum or information service, owning or handling scientific or technical periodica published by us makes and delivers a single reproduction a part of an issue thereof to a person or his agent representi in writing that he desires such reproduction in lieu of a lo or manual transcription and that he requires it solely for t purpose of private study, research criticism or review, a that he undertakes not to sell or reproduce for publicati the copy supplied, provided:

1. The recipient of the copy is given notice that he is liab for infringement of copyright by misuse of the copy, a that it is illegal to use the copy for any further reproductio
2. The organization making and furnishing the copy do so without profit to itself.
3. Proper acknowledgement is given to the publicati from which the copy is made.
4. Not more than one copy of any one excerpt shall b furnished to any one person.

The exemption from liability of the library, archives offic museum or information service herein provided shall exte to every officer, agent or employee of such organization the making and delivery of such reproduction when acti within the scope of his authority of employment. Th exemption for the organization itself carries with it respons bility to see that employees caution those receiving copi against the misuse of material reproduced.

We reserve the right to take action against any person c organization copying or misusing for any purpose whate the whole or part of a work published by us without abidi by the conditions laid down herein unless the person c organization has our special permission in respect of the ite to be copied.

We reserve the right to withdraw this declaration.

British Journal of Applied Physics

Contents of the March issue

CONFERENCE REPORT

Summarized proceedings of a conference on X-ray analysis, Leeds, April 195 By A. Skertchly and R. Steadman.

PAPERS

Influence of instrumental aberrations on the Schultz technique for the measun ment of pole figures. By B. Gale and D. Griffiths.

Fourier series associated with duty cycles. By C. G. Mayo and J. W. Head.

NEW BOOKS SECTION

Reviews and notices.

PAPERS (continued)

Inter-observer checks on standards of performance in evaluating thermal pr cipitator slides. J. W. J. Fay, P. H. Smith, and J. R. Ashford.

Anode surface effects in diodes containing oxide-coated cathodes. By B Hopkins.

Purification of organic materials by zone refining. J. H. Beynon and R. Saunders.

Stroboscopic radiography with a linear accelerator. B. J. Vincent.

NOTES AND NEWS

Notes and comments

THIS *JOURNAL* is produced monthly by The Institute of Physics, with the co-operation of the National Physical Laboratory. It deals with the principles, construction and use of scientific instruments. All rights reserved. Responsibility for the statements contained herein attaches only to the writers.

EDITORIAL MATTER. Communications concerning editorial matter should be addressed to the Editor, The Institute of Physics, 47 Belgrave Square, London, S.W.1. (*Telephone:* Belgravia 6111.) Prospective authors are invited to prepare their scripts in accordance with the *Notes for Authors.* (Price 3*s.* 6*d.* including postage.)

REPRODUCTION. The Institute of Physics is a signatory to The Royal Society's Fair Copying Declaration. Details may be obtained upon application from The Royal Society, London, W.1.

ADVERTISEMENTS. Communications concerning advertisements should be addressed to the agents, Messrs. George Jackson (Fleet St.) Ltd., Cliffords Inn, Fleet Street, London, E.C.4. (*Telephone:* Holborn 3611–2.)

CLAIMS FOR MISSING JOURNALS. Claims from regular subscribers to this *Journal* for missing numbers will only be considered if received within 60 days of the date of mailing plus normal outward time of transit and time for lodging the claim. Losses attributable to failure to notify a change of address or to similar omissions will not be considered.

SUBSCRIPTION RATES. A new volume commences each January. The charge is £6 per volume ($17 U.S.A.), including index (post paid) payable in advance. Single parts, so far as available, may be purchased at 12*s.* 6*d.* each ($1.75 U.S.A.), post paid, cash with order. Orders should be sent to The Institute of Physics, 47 Belgrave Square, London, S.W.1, or to any bookseller.

PRINTED IN GREAT BRITAIN BY UNWIN BROTHERS LIMITED, WOKING AND LONDON

Accurate direct-reading hydrostatic balance

By A. T. J. HAYWARD, B.Sc.(Eng.), Fluid Mechanics Division, National Engineering Laboratory,
East Kilbride, Glasgow

[*Paper first received* 20 *July, and in final form*, 8 *October*, 1959.]

Abstract

An apparatus has been built to enable the specific gravity of the water in the sump of the N.E.L. Hydraulic Machinery building to be read directly, with an accuracy of 1 *in* 50000. *A watertight, hollow, stainless-steel sphere,* 15 *in. in diameter, loaded with shot so that it just sinks in water, hangs from a semi-automatic balance in a Perspex tank through which sump water is circulated. Tables, based on a previous calibration of the apparatus with distilled water, enable balance readings to be converted directly to specific gravity values for any given temperature from* 13·0 *to* 21·0° *C. A cheap form of the apparatus for use in hydraulics laboratories is suggested. The possibility is discussed of increasing the accuracy to better than* 1 *part per million for research on the density of liquids.*

In the Hydraulic Machinery building at N.E.L., the absolute measurement of water flow is performed by weighing the discharge during a measured time interval. Weight measurements are then converted to volumes by the use of temperature/density tables for distilled water, due allowance being made for the specific gravity of the water used, which is significantly different from unity because of the presence of sodium nitrite, a corrosion inhibitor. The sodium nitrite solution is slightly unstable chemically, and although efforts are made to maintain its concentration at a constant level, it is found that the specific gravity varies slightly from day to day. Extreme values of 1·001 and 1·003 have been recorded. To reduce the error arising from this to insignificant proportions, it is necessary to measure the specific gravity at frequent intervals to an accuracy of about 1 part in 10000. This accuracy is beyond the reach of hydrometers and almost beyond the specific gravity bottle method, unless great care is taken. To obtain accurate measurements quickly, the apparatus described below has been developed.

Apparatus

Requirements. It was required that the apparatus should be:

(*a*) accurate to at least 1 part in 10000;
(*b*) direct-reading over the range 1·000 to 1·003;
(*c*) sufficiently robust for permanent installation in an engineering laboratory.

It was decided to employ the method of the "hydrostatic balance", by which the specific gravity of a liquid is calculated from the results of weighing the same object three times, first in air, second in distilled water, and third in the liquid being tested. This is regarded by physicists as the most accurate method available, but in its normal form it is neither direct-reading nor robust. These requirements were met by using as the "sinker" (that is, the object to be weighed) a very large body with a specific gravity only very slightly more than that of the water to be tested, and by using a relatively insensitive but robust semi-automatic balance.

Description of apparatus. The apparatus shown in Fig. 1 consists essentially of a hollow, stainless-steel sphere, immersed in a Perspex tank containing water, and suspended by a stainless 32 gauge wire from a $\frac{1}{2}$ kg semi-automatic balance which has a 10 g dial graduated in 0·1 g divisions. The sphere is made from a non-magnetic stainless steel, with an outside diameter of 15 in. and a wall thickness of $\frac{1}{4}$ in. The two halves of the sphere were machined from cast shells and joined with a decay-free stainless weld before finally machining and polishing the outer surface. Access to the interior of the sphere is only by a $\frac{1}{2}$ in. diameter screwed hole, which is sealed by a stainless cap bearing on a rubber O-ring. Embodied in this cap are two hooks, a large one for man-handling purposes and a small one for suspending the

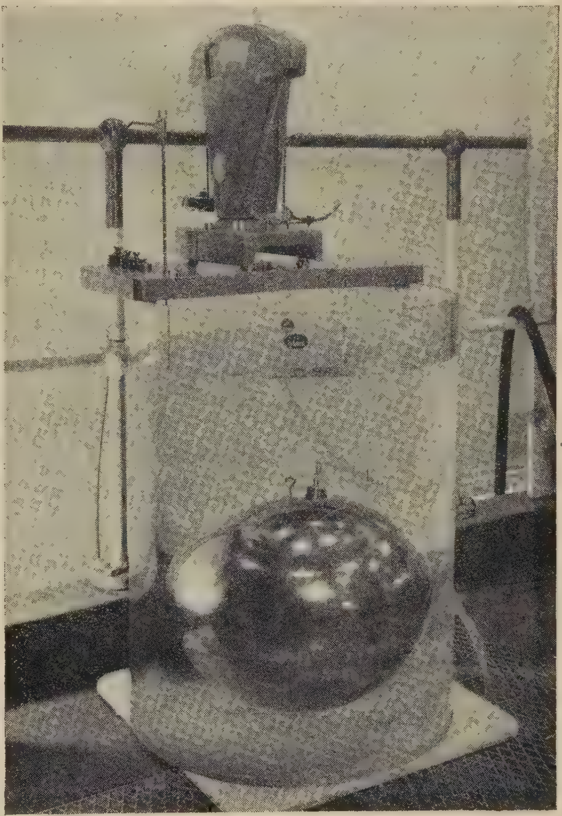

Fig. 1. General arrangement of apparatus

immersed sphere from the balance. The sphere is loaded internally with lead shot so that it would just sink in water of a specific gravity of 1·003. It weighs nearly 30 kg.

Water from the main sump in the Hydraulic Machinery building is circulated continuously through the Perspex tank, as shown in Fig. 2. This water is drawn from the "clean" side of the by-pass filtration system to avoid fouling the sphere with grease and dirt which may be present in small quantities in the sump. When the filter pumps are switched off, the contents of the tank are liable to siphon out. If this is allowed to occur, the whole weight of the sphere will be applied to the balance, thus grossly overloading and probably damaging it. To prevent siphoning, a very small hole has been drilled in the inlet pipe, 1 in. below surface level.

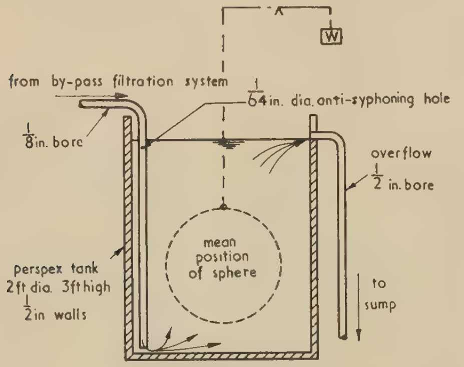
W
from by-pass filtration system
$\frac{1}{64}$in. dia. anti-syphoning hole
$\frac{1}{8}$in. bore
overflow
$\frac{1}{2}$ in. bore
mean position of sphere
perspex tank 2ft dia. 3ft high $\frac{1}{2}$in walls
to sump

Fig. 2. Circulation system

Calibration of apparatus. It is assumed that:

V = volume of the sphere,
W = true weight of the sphere (that is, weight *in vacuo*),
W_d = apparent weight of the sphere when immersed in distilled water at 15° C,
W_t = apparent weight of the sphere when immersed in the water being tested at 15° C,
σ = specific gravity of the water being tested (15°/15° C),
ρ_d = density of distilled water at 15° C,
ρ_t = density of the water being tested at 15° C.

Then V which equals the volume of water displaced is given by:

$$V = \frac{\text{apparent loss of weight}}{\text{density of water}}.$$

That is,

$$V = \frac{W - W_d}{\rho_d} = \frac{W - W_t}{\rho_t}.$$

Therefore:

$$\sigma = \frac{\rho_t}{\rho_d} = \frac{W - W_t}{W - W_d} \qquad (1)$$

Over the range of temperatures experienced in practice, the coefficients of thermal expansion of distilled water and sump water have been found, within the limits of accuracy of measurement, to be identical. Hence, as long as W_d and W_t are both measured at precisely the same temperature, it does not matter what that temperature is: the results will be the same as for 15°/15° C.

To calibrate the apparatus, the tank was filled with distilled water and the apparent weight of the sphere was measured at about fifty different temperatures over the range 13 to 21° C. The semi-automatic balance is graduated in tenths of a gramme, and a thermometer graduated in fiftieths of a degree was used for the calibration test. Fig. 3 shows the calibrati curve thus obtained. From this curve and equation (tables have been prepared from which specific gravity m be read directly for any combination of the apparent weig W_t in the test water and the temperature of the test wa likely to arise in practice. An extract from these tab appears in Fig. 4.

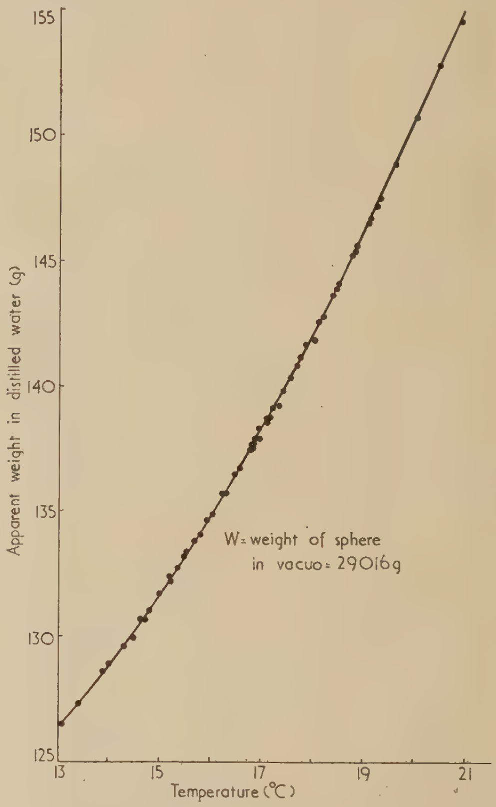

Fig. 3. Calibration curve for apparatus

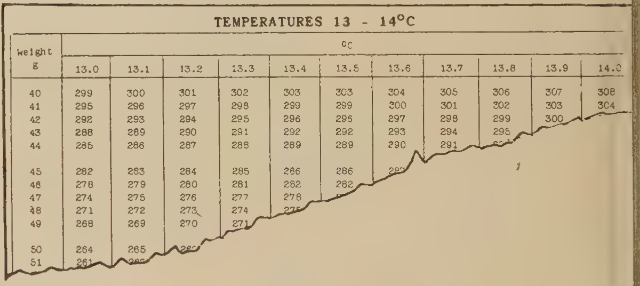

TEMPERATURES 13 - 14°C

weight g	13.0	13.1	13.2	13.3	13.4	13.5	13.6	13.7	13.8	13.9	14.0
40	299	300	301	302	303	303	304	305	306	307	308
41	295	296	297	298	299	299	300	301	302	303	304
42	292	293	294	295	296	296	297	298	299	300	
43	288	289	290	291	292	292	293	294	295		
44	285	286	287	288	289	289	290	291	[illegible]		
45	282	283	284	285	286	286	[illegible]				
46	278	279	280	281	282	282					
47	274	275	276	277	278	[illegible]					
48	271	272	273	274	[illegible]						
49	268	269	270	271							
50	264	265	[illegible]								
51	261	[illegible]									

Fig. 4. Extract from tables
(Complete tables are given in N.E.L. Fluids Note No. 67)

Use of apparatus. Because of the insensitivity of the sem automatic balance, the apparatus is extremely easy to us During calibration it was necessary to stir the water in th tank vigorously and then to allow five minutes to elaps before taking each reading. At the end of that time th movement of water was not sufficient to cause any fluctuatio of the balance needle, and the temperature of the water wa uniform throughout. During the day-to-day use of th apparatus, however, stirring was found to be unnecessary the continuous circulation through the tank indicated in th description of the apparatus is sufficient to maintain un formity of temperature, but the movement of the water i o slow that it has no effect on the reading of the balance. he apparatus is therefore always ready for immediate use; is necessary only to read the balance and the thermometer which is kept permanently immersed in the tank, and then ead off specific gravity from the tables.

The water fed into the apparatus is normally almost aturated with dissolved air. (Because the difference between he densities of saturated water and air-free water at the emperatures encountered is only of the order of 1 part per million,* the exact degree of saturation is of no significance.) Occasionally a rapid rise in temperature of one or two degrees occurs, and the consequent reduction in air solubility is enough to cause air bubbles to form on the surface of the phere. These can be cleared in a few seconds by the simple expedient of lifting the sphere just out of the water and mmediately lowering it in again. The use of a transparent ank enables any bubbles to be detected as soon as they appear.

Typical reading.

Temperature of water (by thermometer No. 5541034):	13·5° C
Thermometer indication:	0·1° C high
True temperature:	13·4° C
Weights on pan:	45 g
Dial indication:	2·25 g light
True apparent weight:	42·75 g
Appropriate figure from Table (see Fig. 4):	293
Specific gravity:	1·00293

Accuracy of results

Analysis of possible errors. The total differentiation of equation (1) gives:

$$d\sigma = \frac{\partial\sigma}{\partial W}\cdot dW + \frac{\partial\sigma}{\partial W_t}\cdot dW_t + \frac{\partial\sigma}{\partial W_d}\cdot dW_d,$$

that is:

$$d\sigma = \frac{(W_t - W_d)dW}{(W - W_d)^2} - \frac{dW_t}{(W - W_d)} + \frac{(W - W_t)}{(W - W_d)^2}dW_d,$$

or:

$$d\sigma \simeq \frac{(W_t - W_d)dW}{W^2} - \frac{dW_t}{W} + \frac{dW_d}{W},$$

(since W_t and W_d are very small compared with W).

Now $W \simeq 30$ kg, $(W_t - W_d) \simeq 100$ g and errors in weighing are likely to be well within the following limits:

$$dW = \pm 50 \text{ g, max.}$$
$$dW_t = 2\,dW_a = \pm\, 0{\cdot}3 \text{ g max.}$$

(dW_d will be much less than dW_t, since it is taken from a smooth curve through 50 points, so that it may be assumed that $dW_t = 2dW_d$). Then, in the worst possible case:

$$d\sigma = 100 + \frac{50}{(30000)^2} + \frac{0{\cdot}3}{30000} + \frac{0{\cdot}15}{30000},$$

or $$d\sigma = 0{\cdot}000005 + 0{\cdot}00001 + 0{\cdot}000005,$$

or $$d\sigma = 0{\cdot}00002,$$

which is the maximum likely error in specific gravity resulting from errors in weighing.

No allowance has been made for the effect of surface tension on the suspension wire. The mean diameter of the wire is 0·028 cm, so that the force due to a surface tension of 75 dyn/cm around the circumference of the wire is 6·6 dyn. This corresponds to a weight of 0·0067 g, which is negligible compared with the contemplated weighing error of 0·3 g.

There will also be an error arising from inaccuracies in temperature measurement. During calibration of the apparatus, temperatures were read to 0·02° C, but when testing sump water, it is regarded as adequate to use a less accurately calibrated thermometer (graduated in fifths of a degree) which will be read to 0·05° C. A possible error of 0·12° C in testing and 0·06° C in calibration will therefore be envisaged. This is equivalent to an error of 0·5 g on W_t and 0·25 g on W_d, corresponding to errors of 0·000017 and 0·000008 on σ, that is, a combined error of 0·000025 which is the maximum likely error in specific gravity due to errors in temperature measurement.

An estimate of the worst possible combination of errors is shown in Table 1 and is conservative—the actual error on any one reading is likely to be considerably less. It should be noted that the worst possible error is well within the requirements stipulated above.

Table 1. *Summary of maximum possible errors*

Source of error		*Maximum error (g or ° C)*	*Effect on specific gravity*
Weighing	W	50	0·000005
	W_t	0·3	0·000010
	W_d	0·15	0·000005
Temperature measurement	W_t	0·12	0·000017
	W_d	0·06	0·000008
Rounding-off tables			0·000010
Surface tension			<0·000001
Total (= worst possible combination)			0·000055

Note: the errors in W_d are taken as half those in W_t because the former are based on a smooth curve obtained from a large number of readings.

Comparison with the N.P.L. hydrostatic balance. The tables are constructed to give specific gravities to five decimal places. Comparative tests with a specific-gravity bottle have confirmed the accuracy of the first four places, but the bottle method is not sufficiently sensitive to provide any information about the accuracy of the last figure.

Arrangements were therefore made to compare the N.E.L. apparatus with the hydrostatic balance at the National Physical Laboratory, which is probably the most sensitive instrument for the measurement of liquid density in the country. 7-litre samples of water were taken from the tank of the N.E.L. apparatus (which holds 180 litres) on six different occasions, and these samples were subsequently tested in the N.P.L. apparatus. The results obtained are shown in Table 2.

The agreement between the two instruments is very good and indicates that the accuracy of the N.E.L. instrument is in fact substantially better than the analysis in Section 3.1 suggests, as would be expected from statistical considerations of the combination of small errors. Since the accuracy claimed for the N.P.L. measurements is ±5 parts per million, it appears that the error in the N.E.L. instrument will not often exceed 10 parts per million, and may confidently be regarded as less than 20 parts per million.

---

* Dorsey, N. E. *Properties of ordinary water substance*, pp. 198, 251 (New York: Amer. Chem. Soc. Monograph Series, 1940).

Table 2. *Results of comparative tests*

Water sample No.	*N.E.L. test results* *Individual* *Temp. (° C)*	 *Weight (g)*	 *Specific gravity*	 *Mean specific gravity*	*Specific gravity N.P.L. result*	*Discrepancy N.E.L.—N.P.L. (parts per million)*
2	19·45	83·1	1·002 26	1·002 26	1·002 256	+4
	19·45	83·0	1·002 26			
3	19·4	78·9	1·002 38	1·002 38	1·002 393	−13
	19·4	78·85	1·002 38			
4	19·3	74·7	1·002 53	1·002 53	1·002 527	+ 3
	19·3	74·8	1·002 53			
5	19·35	70·9	1·002 66	1·002 655	1·002 658	− 3
	19·4	71·2	1·002 65			
6	19·4	67·3	1·002 79	1·002 79	1·002 796	− 6
	19·4	67·4	1·002 79			
7	19·45	63·8	1·002 93	1·002 93	1·002 930	0
	19·45	63·85	1·002 93			

Discussion

Present instrument. The present instrument has amply fulfilled the requirements. It is robust: since being installed more than a year ago in an engineering laboratory containing heavy vibrating machinery, it has shown no signs of deterioration. It is very easy to use: the time taken to read the immersed weight and the temperature, and then to look up the corresponding specific gravity in the tables, is normally only about one minute. It is highly accurate, with an error of less than 1 part in 50 000.

This degree of accuracy is unnecessarily high for routine measurements, and a modified apparatus, simpler and cheaper in construction, could be adopted for laboratory use. Alternatively, the present sinker could be used in conjunction with more accurate weighing and temperature-measuring equipment, and would then be suitable for research of the highest precision into the physical properties of liquids. These two possibilities are briefly considered below.

Simplified instrument for hydraulic laboratories. By far the most expensive part of the present equipment is the spherical sinker, which proved quite difficult to manufacture. An accuracy of 1 in 10 000 is regarded as adequate for normal laboratory purposes, and this could be achieved with a smaller sinker of a more convenient shape. It is thought that a satisfactory cylindrical sinker could be made much more easily by welding end-plates to a length of non-magnetic stainless-steel tube.

A cylindrical sinker with the following dimensions could be expected to provide results with an accuracy of at least 1 in 10 000:

diameter = 8 in.
height = 8 in.
wall thickness = 3/16 in.

An inexpensive alternative, which might give equally go results, would be to load a Winchester bottle with shot a seal its neck with a rigid insoluble adhesive such as "Araldit

An instrument for physical research. The use of the 15 diameter sinker has enabled an accuracy of 20 parts million to be obtained with a balance graduated in tenths a gramme and a thermometer graduated in fifths of a degr It is evident that by adopting more accurate weighing a thermometric equipment with this sphere, and by calculati each result separately instead of employing tables, an instr ment of very high precision should result. This might comparable in accuracy with the finest instruments so used by physicists for research connected with liquid densi and would certainly be very much easier to use.

As an illustration of the potentialities of the apparatu the computation of the worst possible combination of erro which was summarized for the present instrument in Table is repeated in Table 3 for a hypothetical instrument to t following specification:

Thermostatic control to ±0·01° C.
Temperature measurement by electrical resistance therm meter to 0·001° C.
Sphere weighed in air to 1 g.
Sphere weighed in liquid on a 200 g semi-automatic balan 0·5 g dial, graduated in 0·005 g divisions.

Table 3. *Maximum possible errors—modified apparatu*

Source of error	*Maximum error (g or ° C)*		*Effect on—specific gravity*
Weighing	W	1	0·000 000 01
	W_t	0·01	0·000 000 33
	W_d	0·005	0·000 000 17
Temperature measurement	W_t	0·002	0·000 000 27
	W_d	0·001	0·000 000 14
Surface tension	W_t	0·0067	0·000 000 22
	W_d	0·0033	0·000 000 11
Total (= worst possible combination)			0·000 001 25

Among the possible fields of research employing a apparatus of this type, it is planned to use it at the Nationa Engineering Laboratory to study the effect of dissolved ai on the density of various mineral oils and of water.

Acknowledgements

Thanks are due to Mr. P. H. Bigg of the National Physica Laboratory, Teddington, for arranging the comparativ tests with the N.P.L. hydrostatic balance. The work describe has been carried out in the National Engineering Laborator of the Department of Scientific and Industrial Research This paper is published by permission of the Director.

Apparatus for the measurement of Young's modulus, between − 200 and 700°C by transverse vibration in vacuum

by H. J. STOKES, B.Sc., A.Inst.P., Research Department, Imperial Chemical Industries Limited, Metals Division, Birmingham

[*Paper first received* 31 *August*, *and in final form* 2 *November*, 1959]

Abstract

The construction and use of apparatus for the determination of Young's Modulus by means of transverse vibrations of specimens in strip form four inches long are described. Two vacuum chambers are employed, one for immersion in liquid nitrogen and the other incorporating a small furnace for operation at temperatures up to 700° C, the electronic units being common to both. Typical results are included to illustrate use of the equipment, the accuracy of which is claimed to be within ±1% for absolute values.

Introduction

BECAUSE of loading and temperature-range limitations of static methods for the determination of Young's Modulus of Elasticity, attention has been given by a number of workers to alternative means of evaluation. Methods involving measurement of the resonance frequency of specimens of known dimensions are accurate and lead to the introduction of strains only of the order of 10^{-5} or less. Such acoustic methods for the determination of Young's Modulus have been fully described by Cabarat(1) and by Bordoni.(2) It is the object of this paper to describe, and illustrate with typical results, sensitive apparatus for operation at high and low temperatures and in vacuum, which has been most successfully used for several years in the laboratories in which the author is employed. Other equipment using longitudinal vibrations is being developed for higher temperature use in evaluating Young's Modulus even more accurately, and encouraging results have been obtained.

Principle of operation

Of the several methods of specimen excitation and vibration detection which can be used, viz. mechanical,(3) magnetostrictive,(4) electromagnetic,(5) piezoelectric,(6, 7) and electrostatic,(8–10) the last mentioned was chosen for the apparatus to be described on the grounds of being most easily applied at elevated temperatures and in vacuum and not leading to any significant mechanical loading of the sample. In essence, a small plate electrode is placed near one end and parallel to one face of a strip specimen which is supported at nodal points on two knife edges. The specimen is maintained at earth potential and an alternating voltage applied between this driving electrode and the specimen so that forces of electrostatic attraction are set up and cause the specimen to vibrate, whilst detection of vibration is carried out by a similar electrode connected as a capacitance microphone.(11)

From a knowledge of the resonance frequency of a specimen, which can be determined with accuracy, the modulus can be calculated using the expression(12):

$$E = \frac{1}{(1{\cdot}028)^2}\,\rho\frac{L^4}{b^2}f^2,$$

where E = Young's Modulus (dyn cm^{-2}),
ρ = density (g cm^{-3}),
L = specimen length (cm),
b = specimen thickness (cm),
f = specimen resonance frequency (c/s),

and correction may be made, if necessary, for the effects of rotary inertia and anticlastic bending. At elevated and depressed temperatures, further correction must be applied to accommodate the changes caused by thermal expansion. The value obtained from dynamic measurements and the above expression is the adiabatic modulus E_a, which is related to the isothermal modulus E_i, as determined in static methods, by the relation(13):

$$E_a = \frac{E_i}{1 - \alpha^2 T E_i/\rho c}$$

where T = absolute temperature,
α = coefficient of thermal expansion,
c = specific heat.

The adiabatic modulus for the materials examined is generally higher than the isothermal by about a half per cent.

Apparatus

The apparatus depicted in block schematic form in Fig. 1 comprises the three main groups of units described below, viz. I, specimen holder and its vacuum enclosure; II, electronic units for maintaining the strip specimen in oscillation and for detecting its point of resonance as the frequency is varied; and III, temperature and vacuum monitoring units.

Alternative specimen-holding assemblies are employed, (*a*) that used in the range of room temperature to 500° C, or occasionally 700° C, which necessarily includes a furnace and thermal radiation shields, and (*b*) a low-temperature assembly incorporating a similar specimen mounting jig, surrounded by a chamber suitable for evacuation or filling with dry gas, which may be immersed in a carbon dioxide/acetone mixture or liquid nitrogen for use at temperatures down to −200° C.

I(*a*) *Vacuum furnace and specimen holder.* The vacuum chamber, 6 in. dia. × 24 in. long, shown in section, Fig. 2, is horizontally mounted, water cooled and fitted with removable end plates. A small electric furnace of about 1 kW

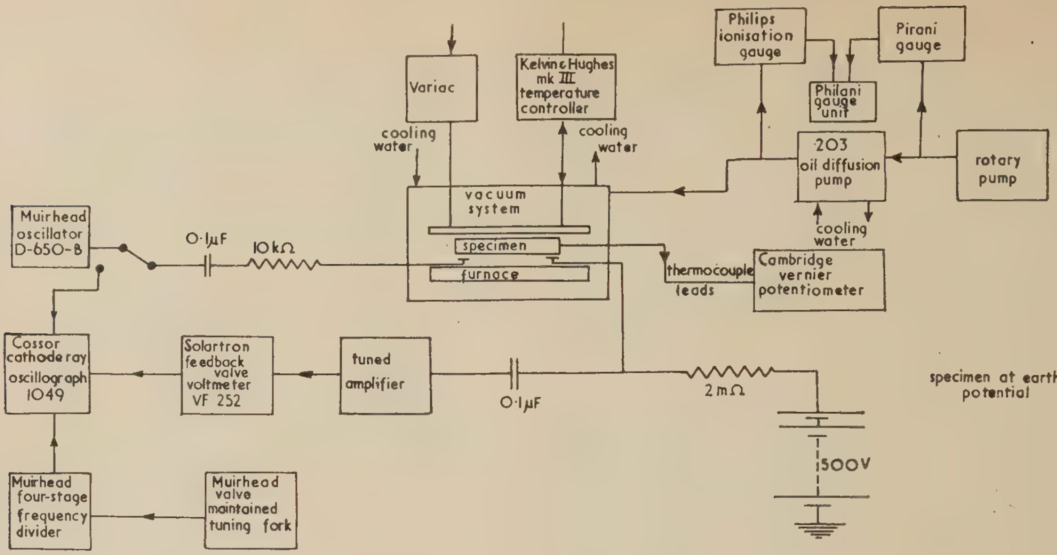
Variac
Kelvin & Hughes mk III temperature controller
Philips ionisation gauge
Pirani gauge
Philani gauge unit
cooling water
cooling water
203 oil diffusion pump
rotary pump
vacuum system
specimen
furnace
cooling water
Muirhead oscillator D-650-B
0·1μF
10kΩ
thermocouple leads
Cambridge vernier potentiometer
Cossor cathode ray oscillograph 1049
Solartron feedback valve voltmeter VF 252
tuned amplifier
0·1μF
2mΩ
specimen at earth potential
500V
Muirhead four-stage frequency divider
Muirhead valve maintained tuning fork

Fig. 1. Block diagram of apparatus

rating is fixed concentrically within the chamber and consists of a Nichrome winding in a helical groove ground in a large bore silica tube. Two concentric radiation shields surround the furnace, which is electrically insulated by means of a silica-cloth jacket, and transverse shields reduce the end heat losses. Introduction and accurate positioning of a sample are facilitated by arranging that one end plate of the vacuum chamber, to which the whole specimen mount assembly is attached, can slide to and fro on guides.

The specimen holder, also included in Fig. 2, consists of two vertical knife edges, separated by a distance 0·552 times the length of the sample, which in the present apparatus is 4·000 in. long × 0·500 in. wide × approximately 0·05 in. thick. Two pointed screw clamps, situated immediately above the knife edges, may be adjusted to minimize the risk of the specimen being displaced by movement of the electrodes. In order to accommodate dimensional changes of the specimen and apparatus as the temperature is raised, the electrode/specimen gaps are made adjustable by means of a lever and push-rod system operated by fine-thread adjusting screws on top of the chamber. The present specimen mount introduces some energy loss at the points of support, and provision has been made in the design for an alternative method of mounting in which the specimen may be suspended by two wires. Such a system is known to introduce appreciably lower losses and should enable determinations of internal friction to be carried out.

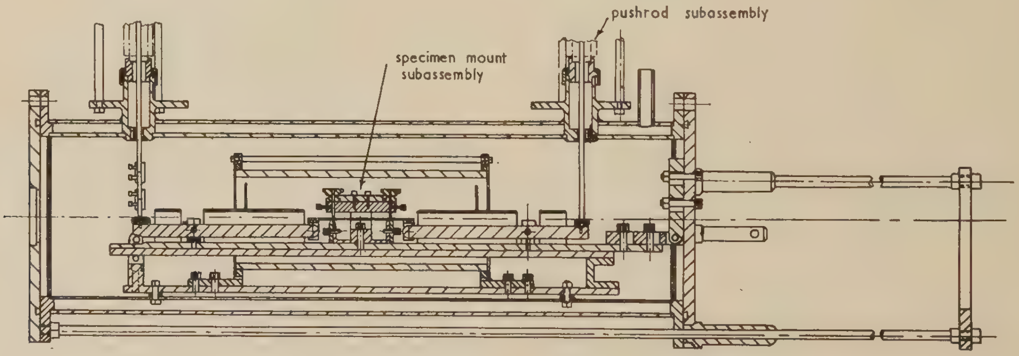
pushrod subassembly
specimen mount subassembly

Fig. 2. General layout of vacuum and specimen-mount assembly

The leads interconnecting the electrodes and the electron units, and those from a regulating transformer pass into th vacuum chamber *via* vacuum electrode seals (type 7A b Edwards). Pumping down is achieved by means of a rotar pump (type 1SC50, by Edwards) backing a diffusion pum (type 203 by Edwards) connected to the chamber by mean of a bellows. Monitoring of the pressure (usually bet than 0·1 μ) is effected by means of a Philips gauge in ass ciation with a Philani gauge unit (Edwards).

I(*b*) *Low-temperature specimen mount and chamber* Essentially, this specimen mount is very similar to tha described above, viz. the specimen is supported on two knif edges. However, in this assembly, two mounting units ar incorporated side by side so that two samples can be evaluate at any temperature attained by the chamber. To avoid th difficulties which would arise in maintaining several vacuum seals at low temperature, the moving controls are brough out of the vacuum system through thin walled Nimonic tubes, which extend into a region at room temperature, an orthodox "O" rings are employed in these seals. Cooling o specimens may be accelerated by bringing a plate, which is attached thermally to the walls of the chamber, into contact with the specimens by means of a control on top of the unit. Evacuation of the chamber to a pressure of less than 50 μ is effected by means of a rotary pump (type 1SC50, by Edwards).

II *The electronic units.* The variable-frequency specimen drive is obtained from a decade oscillator (type D-650B, by Muirhead–Wigan), in the output of which are included in series a 10 kΩ resistor to limit the current on short circuit, and a $0{\cdot}1\ \mu$F capacitor to protect the oscillator from accidental application of a direct bias voltage. The specimen vibrates at twice the input frequency, as there is electrostatic attraction on both half cycles of the alternating driving voltage. Frequency-calibration checks are effected by oscillographic comparison of the decade oscillator output with those from a 2 kc/s valve-maintained tuning fork (type D-630B, by Muirhead), which has an error not greater than $0{\cdot}001\%$, and a four-stage frequency divider (type D-694, by Muirhead) providing additional frequencies of 1000, 500, 250 and 125 c/s.

The vibration-detecting capacitance microphone, biased at 540 V by means of twelve 45 V dry cells, includes a 2 MΩ resistor and a $0{\cdot}1\ \mu$F blocking capacitor in one of its leads to prevent the bias being applied to the subsequent stage. The signal generated across the resistor, on specimen oscillation, is applied *via* a coaxial cable to a flatly tuned amplifier and thence to a valve voltmeter (type VF252, by Solartron). The flatly tuned amplifier is used to reduce the effect of direct pick-up of the driving frequency, and for convenience, a cathode-ray oscilloscope is used to monitor the output of the valve voltmeter, to facilitate the finding of the resonance point.

III *Temperature measurement.* In the high-temperature equipment, two platinum/platinum, 13% rhodium thermocouples, attached to the specimen mount, are brought out of the vacuum chamber through quadruple-bore silica tubing in an "O" ring seal. A preliminary control experiment has indicated that the temperature difference between the specimen and mount does not exceed ±2° C over the whole temperature range of the apparatus. One of the couples only is used for actual temperature evaluation, the other being employed in conjunction with a temperature controller (MKIII, by Kelvin and Hughes). For operational convenience, a time switch is incorporated in the furnace circuit, so that the maximum temperature required may be obtained before the working day commences, and evaluations made as the furnace slowly cools. Temperature measurements are effected for both specimens in the low-temperature assembly, but no temperature controller is employed.

Experimental results

The apparatus described has been used extensively for measurement of the modulus of aluminium, copper, titanium and manganese/copper alloys, but brief results for only three materials, Fig. 3, are included here to illustrate its use and its sensitivity. More results will be published elsewhere.

Although super pure aluminium has an approximately linear variation of modulus with temperature over the range −200 to +300° C, at about 360° C a rapid decrease of about 10% commences, the rate of decrease returning to about its original rate above 420° C. The temperature at which this inflexion occurs is not quite in accordance with that reported elsewhere,(14, 15, 16) but this is probably caused by the different resonance frequency, about 1 kc/s, used in this investigation. It is suggested that the shape of the curve in this region is due to a transition from the unrelaxed to the relaxed modulus in a manner described by Zener(15) and Kê.(17) Similar variations are shown for the O.F.H.C. copper, but, on the other hand, the results for the mild steel decrease regularly over the whole temperature range −200 to +500° C.

Accuracy of measurement

Although evaluation of the resonance frequency, of the order of 1 kc/s, can be made with an error of less than $0{\cdot}1\%$, the length measurement (4 in. specimen) with an error of less than $0{\cdot}025\%$ and the density correct to within $0{\cdot}1\%$, the limiting parameter in this transverse vibrational method lies in the determination of thickness of the specimen (about 0·05 in.). It is estimated that the total error is somewhat less than 1% in making absolute measurements, but that changes from one reading to another can be obtained to an order of accuracy ten times better than this, since a change of 1 c/s in the oscillator setting can reduce the signal amplitude at resonance by as much as 90%, and adjustment can be made to better than 0·05 c/s.

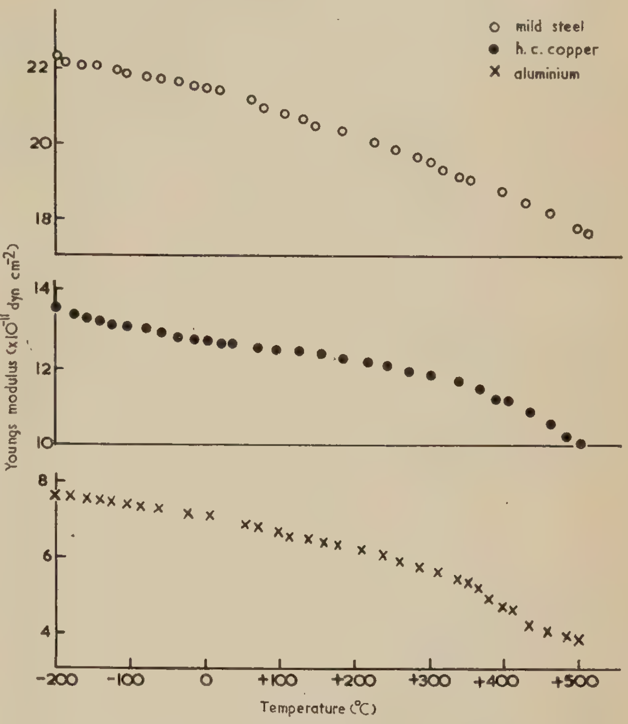

Fig. 3. Variation of Young's modulus with temperature

References

(1) Cabarat, R. *Bull. du Lab. d'Essais du Conservatoire National des Arts et Métiers* (B27–B30), p. 275 (1948).

(2) Bordoni, P. G. *Nuovo Cim.*, **4**, p. 177 (1947).

(3) Vidal, G., Lescop, P., and Raymondin, L. *Rev. Métall.*, **48**, p. 864 (1951).

(4) Bennett, G. E., and Davies, R. M. *J. Inst. Met.*, **75**, p. 759 (1948–49).

(5) Fusfeld, H. I. *Rev. Sci. Instrum.*, **21**, p. 612, 1950.

(6) Quimby, S. L. *Phys. Rev. Series, ii*, **25**, p. 558 (1925).

(7) Vidal, G., and Lescop, P. *Rev, Gén. Mécan.*, **34**, p. 170 (1950).

(8) Cabarat, R., *et al. J. Inst. Met.*, **80**, p. 151 (1951–52).

(9) Bancroft, D., and Jacobs, R. B. *Rev. Sci. Instrum.*, **9**, p. 279 (1938).

(10) Ide, J. M. *Rev. Sci. Instrum.*, **6**, p. 296 (1935).

(11) Kolsky, H. *Proc. Phys. Soc. Lond. B*, **62**, p. 676 (1949).

(12) Timoshenko, S. *Vibration problems in engineering*, p. 324, 3rd ed. (New York: D. Van Nostrand., 1955).
(13) Newman, F. H., and Searle, V. H. L. *The general properties of matter*, p. 138, 4th ed. (London: Edward Arnold and Co., 1949).
(14) Stanford, E. G. *Research, Lond.*, **6**, p. 21 (1953).
(15) Zener, C. M. *Elasticity and anelasticity of met* (Chicago: Chicago University Press, 1948).
(16) Kê, T.-S. *Phys. Rev.*, **71**, p. 533 (1947).
(17) Kê, T.-S. *Phys. Rev.*, **72**, p. 41 (1947).

Automatic decantation for routine sub-sieve sizing

by F. HORSFALL and A. JOWETT, B.Sc., Ph.D., Department of Mining, Leeds University

Paper received 4 *December*, 1959]

Abstract

Electronic equipment used to control sizing analysis by the beaker-decantation method is described. Capacitor-resistor circuits are used to give appropriate sedimentation times and also to control draining and filling of the decantation apparatus. Except for adjusting a control to alter the sedimentation time when necessary, the operator is free to attend to other duties.

Introduction

Of the various sedimentation processes used for sizing analysis in the sub-sieve range, decantation after settling is one of the most accurate if properly carried out with temperature control and accurate timing. Cadle* discusses in detail the relative merits of numerous methods of size analysis. For routine sub-sieve sizing of only moderate accuracy, decantation is less convenient to use than other methods such as the sedimentation balance, the Andreasen pipette, or elutriation methods in air or water. These latter methods combine rapid analysis with moderate accuracy. The decantation method suffers the big disadvantage that decantation of the liquid after a specified sedimentation time must be repeated many times before all undersize particles have been poured off. Heywood† has estimated that 45 decantations would be necessary to eliminate 99% of particles near to the size of separation. The sizing analysis is consequently a protracted operation, especially at very fine sizes where sedimentation times of an hour or more may be required. Not only that, it must continuously have the attention of an operator to time the sedimentation and to decant, fill and stir the suspension.

In order to overcome some of these difficulties, a decantation apparatus has been constructed in which the operations are carried out automatically. Except for adjusting a control to alter the sedimentation time after the requisite number of decantations at a specified particle size, the operator is free to attend to other duties.

Apparatus

Essentially, the apparatus consists of a sedimentation vessel in which filling, stirring, sedimentation and decantation are automatically controlled by an electronic circuit. It w necessary to design a controller which would give thr operational times of predetermined length in sequence. Th centre of operation is a one-litre vessel with an inlet/out tube set at a suitable distance from the base so as to dra away supernatant liquid without extracting sediment. Th sample for size analysis, after being suitably dispersed in small amount of water, is washed into the vessel and th procedure is then:

(i) beaker fills to preset level while being stirred (0–100 s
(ii) water is cut off, stirrer stops, sedimentation perio commences (0–55 min);
(iii) supernatant liquid is drawn away at conclusion o sedimentation period (0–100 s).

It is desirable that this sequence shall be repeated day an night, without attention if necessary. To satisfy the firs operation, various methods may be used to attain the neces sary accuracy of upper level of liquid. Examples of thes are photoelectric beaming, fluid contact with electrode, ba valve with contacts, etc. However, to minimize compl cation, it was decided to use a three-way tap for filling an draining the sedimentation vessel, and to draw the feed wate from a constant head tank for a set time.

The operational features for the first stage of control ar therefore to turn a three-way tap and to turn the motor of stirrer on and off. The three-way tap must be turned throug 90 deg. from the draining to the filling positions, and ther through a further 270 deg. before the draining position i again reached. The tap is operated by means of a four-wa cam switch driven by a 1/100 h.p. induction motor geare to give 15 rev/min (that is 90 deg./s).

Timing circuit

The essential features of the timing circuit are shown in Fig. 1. The anode of the triode valve V is connected directl to the a.c. mains. Between the grid and cathode is a resistance R. In the cathode lead is a relay coil RLA, a variable ballast resistance B and a switch of suitable form to break the circuit at X. The capacitor C has one lead con- nected to the cathode and the other to a change-over contac RLA_1 operated by the relay coil. With zero bias, the valve will be conducting heavily and will develop a potentia difference across the cathode circuit proportional to the values of RLA and B, since the valve acts as its own rectifier of the a.c. mains.

---

* Cadle, R. D. *Particle size determination* (New York: Interscience Publishers Inc., 1955).

† Heywood, H. Fundamental principles of sub-sieve particle size measurement. Symposium on recent developments in mineral dressing, *Inst. Min. Met., London*, p. 31 (1952).

If the circuit be momentarily broken at X, the relay coil will de-energize and change over the contacts at RLA_1. This witch puts the voltage on the capaciter C in the form of a negative bias on the grid of the triode thus cutting off the current through the valve even if the switch X remakes contact. The relay coil will not re-energize until C has discharged through R sufficiently to increase the cathode current to the operational value again. When this occurs, the contacts at RLA_1 will be reset automatically, the switch at X being closed. The total time for which the coil is de-energized is governed solely by the values of C and R, and these times can be calculated from the well-known relationship governing the discharge of a capacitor through a resistor.

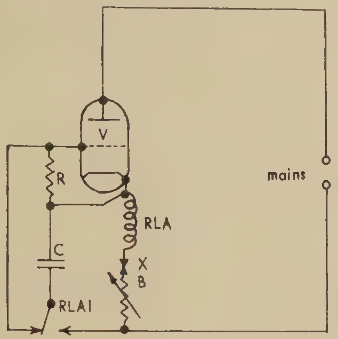

Fig. 1. Timing circuit

The full circuit is given in Fig. 2. The beam tetrode, type 6V6, strapped as a triode was used because it has the best characteristics for the duty: an entirely suitable triode is not available. The 6V6 fits the requirements of a long grid base reaching a high anode current. This enables the relay to operate before the voltage on the capacitor is so low as to give too small a rate of change of bias voltage for the required accuracy. The 6V6 also has the advantage of being an extensively used valve which is frequently held in stock.

The full sequence of operations is as follows. With the relay-coil RLA in a non-energized condition, contact RLA_1 is switched to the left in the diagram and contacts RLA_2 are in open circuit. Assuming operations to commence with the filling of the sedimentation vessel, the switches, S_1, S_2, S_3, will be in the positions shown and the three-way tap will be turned to "inlet". The sequence motor, when running, turns these switches, the tap and the contactor in a clockwise direction as viewed in the diagram. When the valve conducts, the relay coil is energized, contacts RLA_1 change over and contacts RLA_2 close. This starts the sequence motor, and S_1 puts the cathode in open circuit as its switch contact traverses from position 1 to position 2. This de-energizes the relay coil and again the contacts RLA_1 change over; in the meantime capacitor C has been fully charged. RLA_2 is also put in open circuit, but conditions are adjusted so that the cam contactor takes over from RLA_2, and consequently the sequence motor is kept running until 90 deg. have been traversed. The contactor then switches off the motor. During this period, S_2 will have changed to the first sedimentation position, selecting R_2 as discharge resistance; S_3 will have switched off the stirrer motor and the tap will be closed. Also, S_1 will have closed the cathode circuit, but the relay coil will not be energized until after the required time, given by the reduction of bias on the discharge of the capacitor C. After the appropriate time set by the combination of R_2C, relay coil RLA again operates the contacts RLA_1 and RLA_2, and the process repeats itself for the next sequence.

The switch S_4 is a reset switch operated by a push button on the front panel of the chassis, and when closed will discharge C in a fraction of a second. This is used as a sequence-cancellation switch to enable the correct stage to be brought into operation quickly when starting a sizing analysis.

For simplicity in the diagram, R_2, R_3 and R_4 are shown as rheostats, but in the actual circuit, Yaxley switches of the 12-way 1-pole type are used. These connect into the circuit 1% tolerance high-stability resistors of the appropriate value. For the inlet times, resistors of 100 kΩ each are fitted at R_4 to give a total of 110 s in steps of 10 s with a minimum of 10 s. A fine control of the upper level of fluid is effected with a tap fitted in the feed pipe from the constant head tank. Although

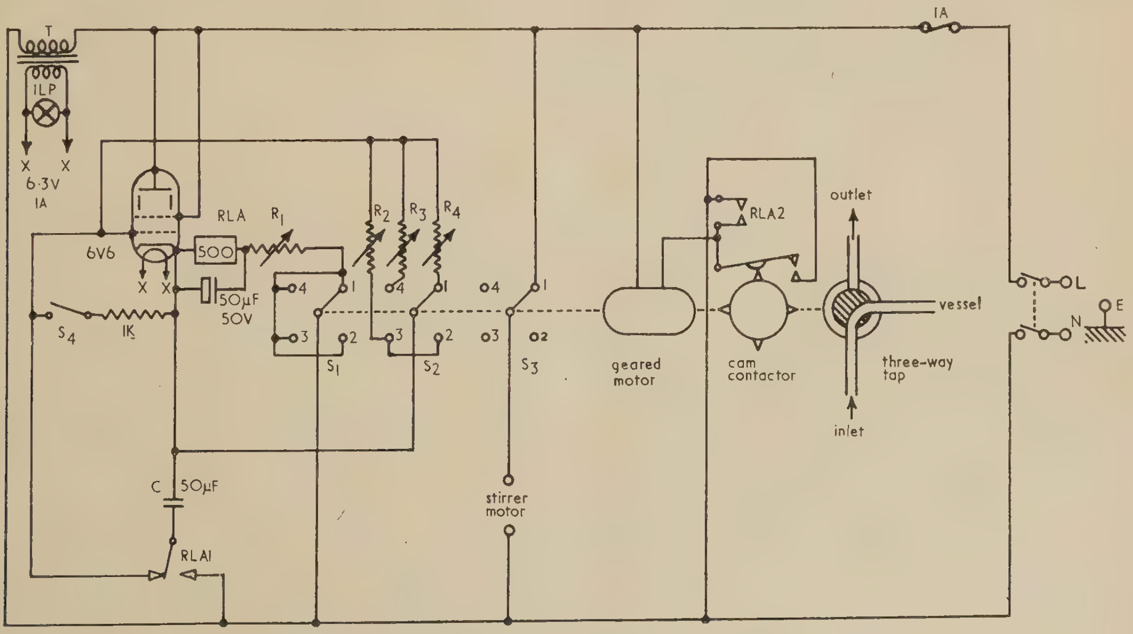

Fig. 2. Complete circuit

the outlet time is not critical, similar resistors are fitted at R_3, the switch being set to a time just long enough to ensure that the lower level is reached. R_2 consists of three of these switches connected in series and individually controlled. One is made up of ten resistors each of 1·5 MΩ (2·5 min. each), one with ten resistors each of 150 kΩ (15 s each) and one with ten resistors each of 15 kΩ (1·5 s each). The corresponding dials are calibrated in times, 0–50 min in 5 min steps, 0–5 min in 30 s steps, and 0–30 s in 3 s steps; these doubled time periods are available because of the repeat sedimentation step afforded by the switch S_2. Instructions must be given to the operator not to switch all these resistors to zero together, since this would short-circuit the capacitor and probably also damage the contacts of RLA_1 and S_2. The 50 μF, 50 V (d.c.) electrolytic capacitor across the relay coil is to suppress relay chatter which can be troublesome, especially on half-wave rectification. Although R_1 is a ballast control to limit valve current and ensure correct energization of the relay coil, it can also be used as a fine control of sequence times to aline the dials because it controls the maximum charge that can be acquired by capacitor C.

The complete apparatus comprising three identical sedimentation vessels all controlled by the same timing circuit is illustrated in Fig. 3. With this apparatus, three decantation-sizing analyses can be run simultaneously. For separati at very fine sizes the apparatus may be left on overnight.

The circuit may be criticized in using a CR discharge f such long time periods in the sedimentation step. With 1 tolerance high-stability resistors and a good-quality capacito it was found possible to obtain an accuracy within 2% f the sedimentation periods. The sizing-analysis resu obtained with this method of timing have been wholly ad quate, good agreement being obtained between duplicate For greater accuracy and reliability on the longer times th circuit may be modified to switch in an electric-clock mechanism in place of the discharge system.

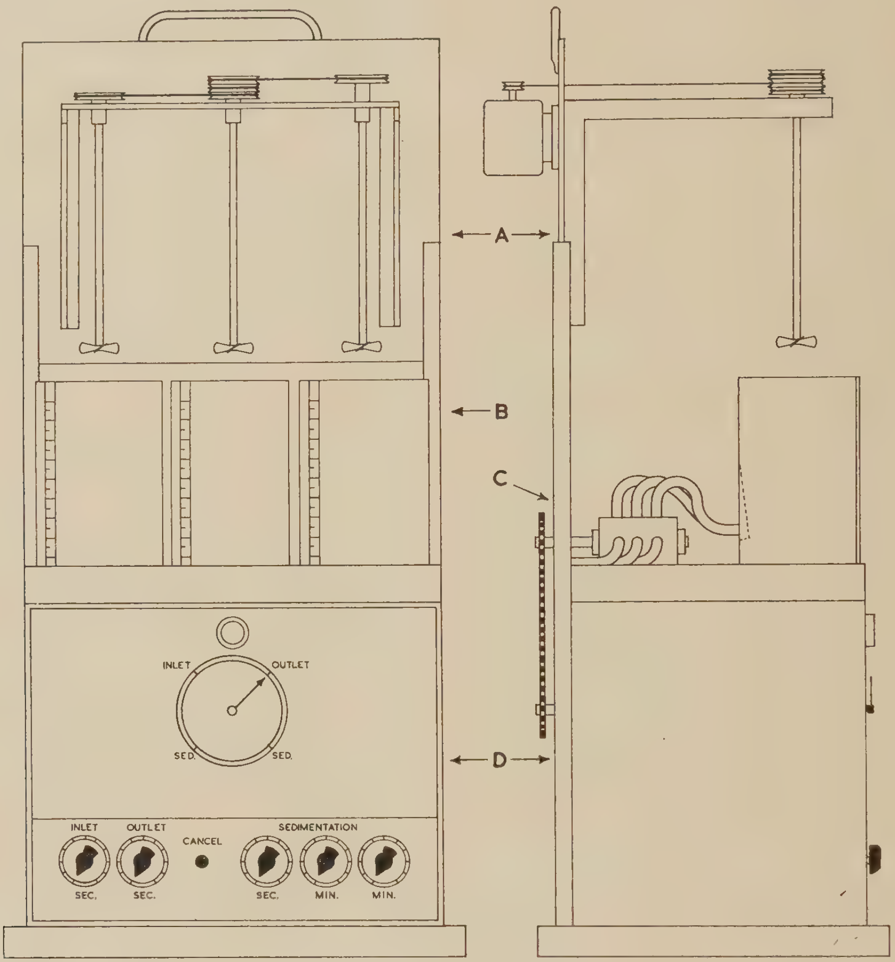

Fig. 3. Complete apparatus

A, stirrer assembly in raised position; *B*, sedimentation vessels; *C*, three-way tap assembly (one three-way tap for each sedimentation vessel); *D*, electronic sequence controller.

The electronic principles employed in this circuit may be applied to any problem involving a series of timed operations in sequence. There is no theoretical limit to the number o steps which may be controlled, but difficulty in finding suitable switch gear is likely to impose practical limits.

Acknowledgements

The authors gratefully acknowledge the encouragement and advice given by Professor J. T. Whetton, and the late H. G. Smith, formerly Senior Lecturer in Metal Mining and Mineral Dressing, and also the assistance of colleagues in the Department of Mining.

Wax-atomizer for producing spherical dust particles

by G. K. GREENOUGH, B.Sc., B.Sc.(Eng.), Safety in Mines Research Establishment, Ministry of Power, Sheffield

[*Paper received* 14 *October*, 1959]

Abstract

An airblast atomizer is described which produces spherical wax particles suitable for use in the investigation of the aerodynamic behaviour of dust particles.

The aerodynamic behaviour of spherical dust particles is easier to treat theoretically than that of irregular dust particles, and experiments requiring theoretical treatment are therefore best performed using such "ideal" particles. One means of producing spherical particles is by atomization of molten wax in an airblast atomizer, the droplets being drawn into spheres by surface tension, prior to solidification. Fig. 1 depicts an atomizer which gives a dust cloud of controllable concentration and size-distribution. It is designed to be mounted on the top of a wind tunnel and to spray into the centre of the cross-section.

Wax is stored in the container *a* and melted by the heating-element *b* to flow down the tube *c* to the jet *d*. A second element *e* heats the projecting stem of the atomizer and is controlled by the regulator *f*; the jet temperature is indicated by the thermocouple *g*. The atomizer is both lagged and electrically insulated by layers of asbestos cloth and heat-resisting cement *h*. Compressed air passes through a filter *l* and is fed through the control valve *i* to the outer jet *j* to atomize the wax; the mercury manometer *k* monitors the air-flow. The air is heated in passing through the atomizer and this prevents solidification of the wax in the turbulence of the jet which could result in irregular particles. The gauge *n* indicates the input air-pressure, and heater-element warning-lights *o* are incorporated. For ease of maintenance, the container has a full-diameter lid held in place by studs, and a smaller, screw-on lid for filling. A removable wire-

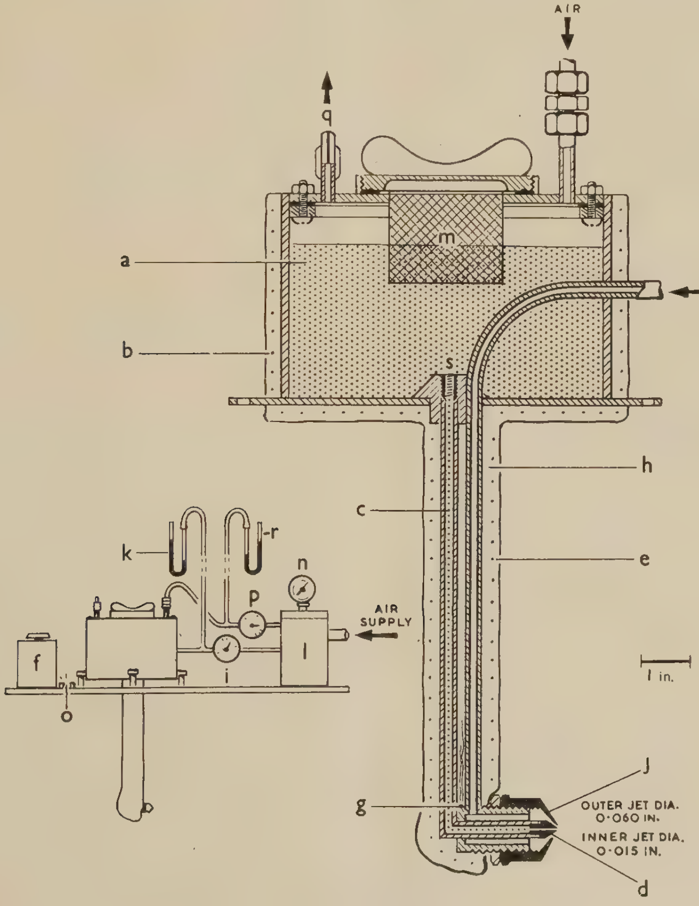

[Crown copyright]

Fig. 1. Diagram of atomizer

gauze filter basket *m* filters the wax when filling. The atomizer is made of brass, all joints being brazed. Two 500 W heating elements are employed and the metal parts of the atomizer are well earthed. A compressor having a displacement of 2½ ft³/min and a maximum pressure of 15 lb/in² is used with the atomizer.

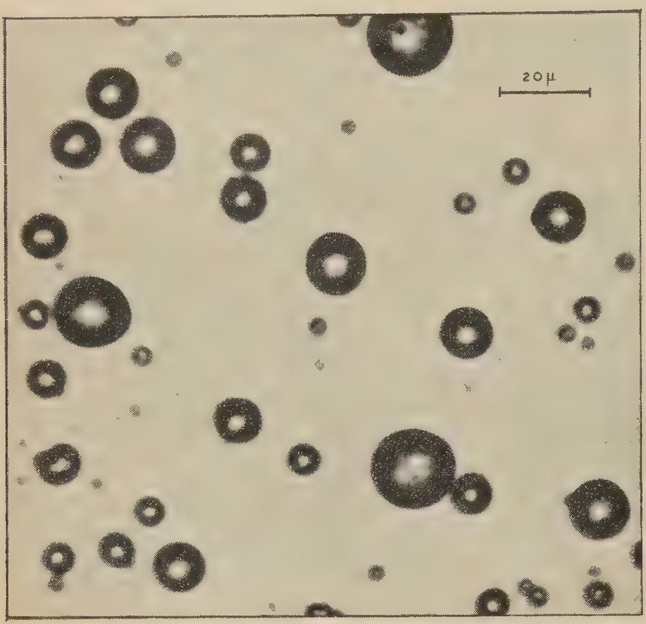

[Crown copyright]

Fig. 2. Typical sample of atomized wax particles

The wax flow-rate is determined by the difference between the pressure at the wax-surface and that at the inner jet. The pressure at the wax-surface is controlled by bleeding air through the top of the container *via* valve *p* and the narrow-bore outlet *q*, and is indicated by the manometer *r*. The pressure at the inner jet is determined by the air-flow through the outer jet and the relative positions of the two jets. In adjusting the atomizer initially, valve *p* is closed, the container lid is unscrewed and valve *i* is set to an intermediate position. The outer jet is screwed inwards until wax just begins to flow and then screwed out again until the wax-flow just ceases and air bubbles through the wax in the container. The outer jet is then locked in position by a locknut. This ensures maximum sensitivity of the manometer *r* and also enables the wax to be shut off at the termination of an experiment by closing valve *p*. High sensitivity in setting the wax-flow can be obtained by inserting a capillary tube within the tube *c* using the threaded connexion *s* and this also minimizes the effect of change of wax-level in the container. In practice, however, this has not been found to be necessary.

In use, the regulator *f* is set to maintain a suitable jet temperature and the concentration and size-distribution are adjusted using the valves *p* and *i*. Opening the valve *p* increases the concentration and coarsens the size-distribution; opening the valve *i* makes the size-distribution finer. When the concentration and size-distribution are as required, the readings of manometers *k* and *r* are noted, and are maintaine constant by using the appropriate valves. The wax used a mineral wax having a melting-point of approximately 90° to prevent the particles being melted when sampled by thermal precipitator.

Fig. 2 shows a typical sample obtained by allowing th particles to settle on a glass slide placed on the floor of th wind-tunnel 30 ft from the source; the size-distribution at th source was obtained by counting and sizing such depositio samples supplemented by thermal-precipitator samples fo

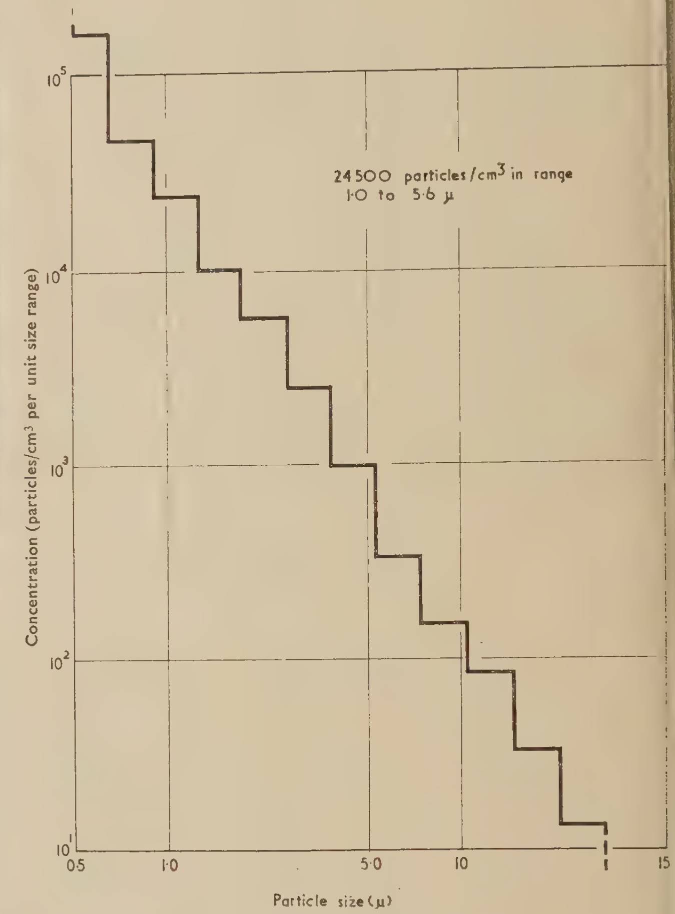

[Crown copyright]

Fig. 3. Size-distribution at source

the smaller particle sizes, and then correcting for sedimentation losses upwind of the sampling point. Fig. 3 shows the size-distribution at the source obtained with a wax-pressure of 6 cm of mercury and an air-pressure of 10 cm of mercury. The wind-tunnel was of square section, 1 × 1 ft, and the wind speed was 100 ft/min.

Acknowledgement

The help of Messrs. S. R. Howarth and B. Bancroft in constructing and testing the atomizer is gratefully acknowledged.

Position transducer using a divided circle and coded scale

by I. R. YOUNG, B.Sc., Grad.Inst.P.,* Hilger and Watts Ltd., London, S.E.5

[*Paper first received* 4 *September, and in final form* 9 *November,* 1959]

Abstract

A small transducer is described in which a coded scale is used to distinguish the lines on a divided circle. This unit is intended as a positional reference in a large data-collecting system. The circle and code are both detected photoelectrically, though using very different cells and lamps. In order to keep the instrument diameter small, the coded scale is made in drum form.

Introduction

Most present-day measuring systems use time as a reference to initiate any action to be taken. However, there are those in which position is a better reference, assuming a suitable transducer is available. This article describes such an instrument, intended as the master reference in a wind tunnel monitoring scheme, in which readings of parameters like pressure and strain are to be taken at pre-determined positions of the model. The unit contains a scale marked at the desired places, the marks being distinguished by a coded scale. This approach has many applications: for example if a large number of identical parts are to be turned, special scales, with the appropriate dimensions marked on them, may be attached to the lathe and used with a relatively simple control system to facilitate production.(1)

Principle of operation

Fundamentally the instrument has to define eighty positions equispaced at 4° 30′ to an accuracy of ±5′ of arc. This is conveniently done using an accurately divided circle which is detected photoelectrically.

To distinguish the lines on it, a coded scale is associated with the circle, which, because of space considerations, takes the form of a drum. This is also read photoelectrically, the signals from the rulings on the circle being used to trigger its detecting system, as well as initiating the rest of the reading process in the tunnel.

Description of the instrument

The unit is a cylinder 1·125 in. in diameter and 2·5 in. long with a 0·187 in. diameter shaft protruding from one end. For convenience of mounting the instrument, the shaft end was made identical with that of a motor made to the international size 11 specification, and the end of the shaft was threaded and splined accordingly (*A*, Fig. 1).

The circle *B* was divided on a glass blank 0·75 in. in diameter and 0·032 in. thick. The rulings are 0·000 30 in. (±0·000 05 in.) wide, 0·060 in. long and are on a mean diameter of 0·625 in. These lines are equispaced at 4° 30′ (±15″ of arc), and were engraved in evaporated silver by a standard Watts' precision dividing engine. After dividing, the circle was protected by an evaporated layer of silicon monoxide.

The circle was centred on a boss on the shaft using a pair of microscopes, and correcting repeatedly across two diameters at 90° in the usual way. The maximum relative displacement of the centre of rotation of the shaft and the centre of the rulings did not exceed 0·0001 in.

The circle is illuminated by a "grain of wheat" filament lamp (type All by Rimmer Bros. London Ltd.) held in a Tufnol bush by a spring bearing on the contact at the end of the lamp (*C*, Fig. 1). The other contact is made between a shoulder on the brass cap of the bulb and a brass light shield with an aperture in it to allow light through to the circle.

On the other side of the circle, a slit in a small graticule (*D*, Fig. 1) limits the part of the circle which can be "seen" by the detector. This is a Ferranti silicon photovoltaic cell type MS1, which is encapsulated in Araldite. The slit is 0·000 30 in. wide, ruled in aluminium on a small glass blank.

The rear section of the instrument contains the coded scale, produced in an etched metal foil, which is stuck on the outside of a hollow Perspex drum, polished inside and out (*E*, Fig. 1). The code used is pure binary with the divisions numbered 0 to 79 inclusive. The drum is attached to the instrument shaft at its front end.

The cells reading the code are in two banks at opposite ends of a diameter (*F*, Fig. 1). They are "staggered" so that every other track is read by neighbouring cells at one end of the diameter. The cells, which are Hilger Schwarz cells, are in pellicle form; stuck down on a small printed circuit and contacted to it with conducting glue. They are 2·5 by 2·25 mm in total size with the sensitive area, 0·2 mm wide, parallel to the longer edge and roughly central. In practice, these pellicles are difficult to position on the printed circuits and, as the cells are primarily sensitive to intensity (a narrow beam of light of a given intensity and spectral distribution, covering only a fraction of the length of the sensitive area, produces nearly as much effect as a similar beam covering the whole cell), they are mounted with their sensitive areas perpendicular to the defining slits between them and the scale (*F*, Fig. 1).

This means, in practice, that only 0·5 mm out of about 3 mm of scale width can be usefully employed, unless the cells are staggered in the way described. In practice, the code tracks are pitched at 1·5 mm and are 1 mm wide.

The slits in front of the cells are 0·010 in. wide and 0·040 in. long, etched in lead sulphide deposited chemically on 0·030 in. thick glass blanks. Illumination for the Schwarz cells is provided by a neon indicator tube. This is a special type used in one design of Hilger and Watts coded commutators; it is electrically similar to other such tubes but has an electrode length (12 mm) suited to the design of those instruments.

---

* Now at Evershed and Vignoles Ltd., London, W.4.

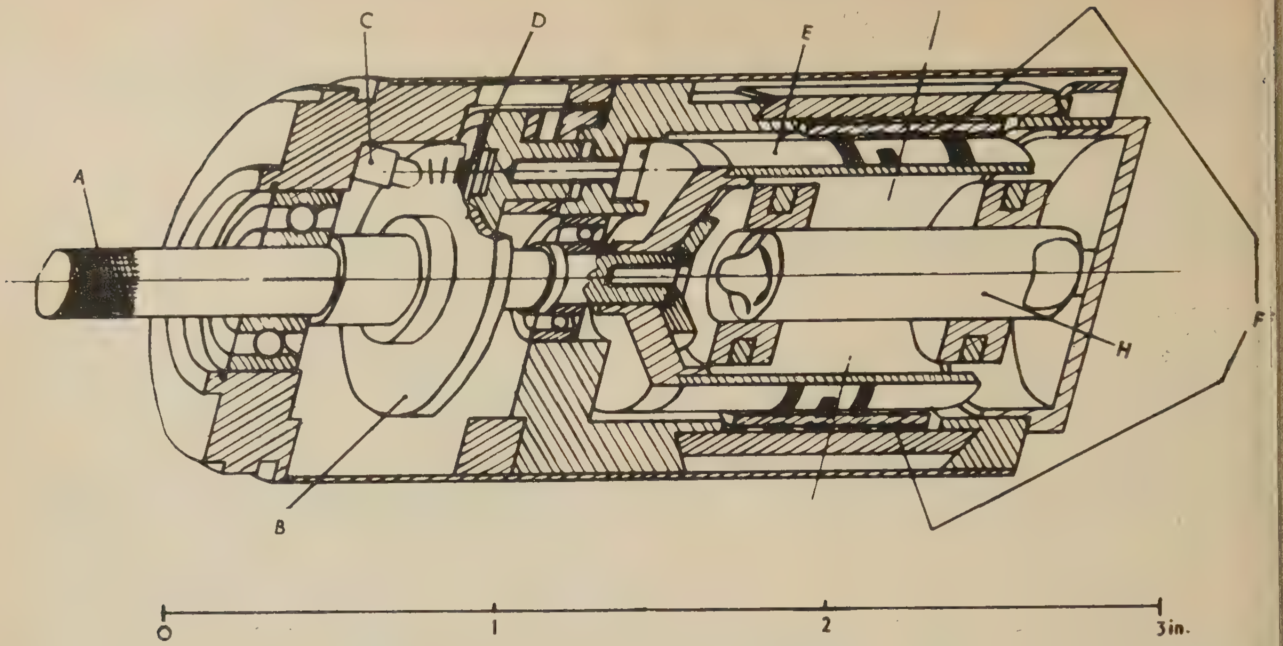

Fig. 1. Exploded drawing of the transducer

It is mounted in grommets supported from the rear of the instrument (*H*, Fig. 1). A photograph of an instrument is shown in Fig. 2.

Performance

The primary function of this unit is to provide the trigger signals for the remainder of the system of which it is part. In order to achieve the angular accuracy needed for these (±5′ of arc), the apparent width of the lines as recorded by the cells must not be too great if the level in the system electronics at which a line is indicated as present is not to be too critical. This is undesirable as the variation existing in the width of the rulings is a considerable fraction of the nominal value, and the amplitude of the signals from the cell fluctuates by about 15% from line to line.

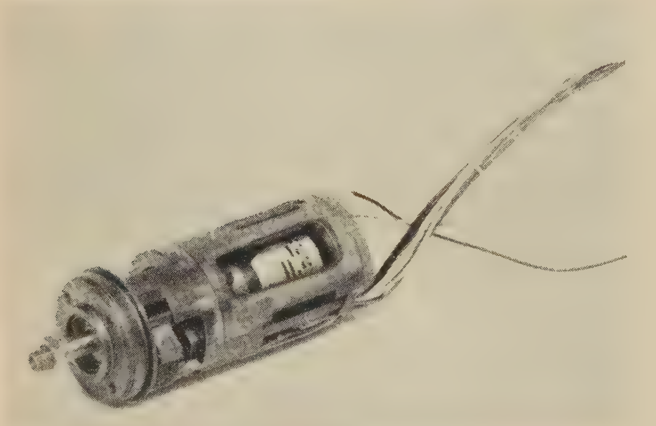

Fig. 2. Photograph of the transducer

As the light is not collimated and as the angle subtended by the sensitive region of the cell at the slit (about 45°) is large, increasing the gap between the slit plate and the circle can result in an appreciable apparent broadening of the line as seen by the cells. The apparent width of a line (at half the peak signal amplitude) is approximately $d + 2x \tan \alpha/$ where x is the distance between the circle and graticule. is the width of a ruling and α the angle subtended by t source at the ruling. With $x = 0{\cdot}0015$ in., $d = 0{\cdot}0003$ in and $\alpha = 30°$, the full apparent width of a line is $0{\cdot}0010$ in The width of a line at half the signal amplitude is about 9· on this argument alone.

Another effect tending to broaden the lines is due to th rulings in the circle and graticule not being parallel whe they are nominally so. Displacement of one end of th graticule slit by 0·0003 in. (the width of a line) from a tru radius results in an increase in the width of the signal at ha amplitude of about 30%.

In the present instrument the latter effect makes much th smaller contribution to line spread. No precise measuremen of the angle between the graticule and circle slits when the are nominally coincident was possible, but the graticule ti appeared to be less than 30′. (The relevant graticule adjust ment is a rotation about an axis which cuts the circle on th mean diameter of the ruled track.) This results in a theoretica line broadening of about 1·5′ of arc.

As x varied between 0·0015 and 0·0020 in., owing to fluctuation in glass thickness, the spread due to the larg source area was the dominant one. The practically deter mined width of a line fluctuated between 15 and 19′ of arc This is satisfactory as the peak of any line can then be com fortably determined to better than ±5′ of arc.

The signal amplitude was about 30 mV (on a standing leve of 15 mV, due to stray light) and fluctuated by about 15% owing to variations in line thickness, which could not be controlled to better than 0·000 05 in. The lamps were run at 2·5 V, d.c. (compared with the rated 3·5 V) and the signals measured on a valve voltmeter. The positions of the peak signals from the lines relative one to another were accurate to better than 1′ of arc.

Coded section

The Schwarz cells used are small and very sensitive—and therefore, quite suitable for this instrument—but they are ery slow. (The time constant varies widely but usually lies etween 10 and 40 ms.) This disadvantage can be minimized y using a flashed source of light, to which the cells can only espond if they are illuminated whilst light is present. The output signal, characteristically, for a flash of up to about ms in duration, rises nearly linearly, then decays exponenially.

In this instrument the code is pure binary, and it is, thereore, essential that the flash, which is triggered by the signal rom a line on the ruled circle, should be completed before he edge of the digit corresponding to the line passes in front of the slits before the cells—even if the shaft is turning at its maximum speed.

The width of the slits is 0·010 in. and the digit size is about 0·029 in. Assuming that the angular centre of a digit coincides with the corresponding line on the circle to better than digit, and that the maximum shaft rotation speed is 2 rev/s, the flash may be up to a little over 1 ms in duration. Since, with the light source used, the cells do not respond appreciably to flashes shorter than 0·25 ms and, as it is possible to trigger from the leading edge of a line signal pulse, a flash length of 1·5 ms may be used without any danger of errors arising in the code output.

The other difficulty with the cells lies in their widely different outputs with equal incident illuminations. In the case of the flashed light this is due partly to a spread in sensitivity, but also to the variation in response time. In practice, selection of the cells to give any considerable uniformity is economically wasteful, as it is even more desirable to select for stability and freedom from random noise. It is necessary to aim for as great a signal/noise ratio as possible; and to guarantee a reasonable minimum signal. In this context, "noise" includes any undesirable output of the same polarity as the signal, and the ratio which decides the quality of the instrument is struck between the smallest signal in any output and the noisiest channel. In this instrument the ratio was 12·5 : 1. The smallest signal with a 1·5 ms flash from the lamp was 105 mV, measured across a 330 kΩ resistance in series with the cell and with 10 V d.c. applied. The lamp passed 10 mA current during the flash.

At this current lamp life would be very short, were it not for the favourable duty cycle; at the worst the lamp is ignited for only one fifth of the running time of the system.

Conclusion

This paper has described a transducer intended for use in a digital measuring system as the master instrument, as all other readings are taken in accordance with signals from it. In systems where it is possible to make a relatively simple transducer such as that described, the scales needed are much easier to make than those for a coded commutator, and the electronics much less than for a fringe counter. The main disadvantage of the approach is that the reference positions, once the transducer is made, cannot be easily changed.

Since the scale in this type of instrument can be read by a photoelectric microscope,$^{(1)}$ precision is no difficulty. However; since existing microscopes$^{(2, 3)}$ need relatively long times to find the centre of a line, the speed of movement of the scale is seriously limited. Where an accuracy which corresponds with a linear displacement of 0·0001 in. or greater is concerned, a simple arrangement such as that used here is to be preferred. Where space is available it is advisable to image the scale on the slit optically as the effects tending to spread the line width are then more easily eliminated.

There is a limit on the closeness of neighbouring lines, which depends on the method used to read the scales, though in general, that limitation is set by the coded section. Much of the point of the technique is that scale digits should be large enough to avoid the added electronic complication of a cyclic code and the need for precision divided scales. Though in the instrument described the scale graduations are uniformly spaced, this is often not so.

Acknowledgements

My thanks are due to Mr. E. Patterson of the English Electric Co. Ltd. (Luton Airport), who suggested the problem, to the Directors of Hilger and Watts Ltd. for their permission to publish this article and to Mr. L. E. Parker for his help in designing the instrument.

References

(1) *Machinery*, **89**, p. 82 (1956).
(2) *Machinery*, **84**, p. 1334 (1954).
(3) Clark, J. S., and Cook, A. H. *J. Sci. Instrum.*, **33**, p. 341 (1956).

Revised edition of *Notes for authors*

The Institute of Physics has recently published a 36-page revised edition of its booklet intended to assist less-experienced authors and to serve as a reference booklet for all those who wish to contribute to the Institute's publications. Under its new title *Notes for authors*, it gives hints on the preparation of scripts and diagrams, on the layout of mathematics, the correction of proofs and so on. In addition to a bibliography of reference books and works on technical writing, the pamphlet also contains lists of the spellings, symbols and abbreviations used by the Institute. These conform with British Standard 1991: Part I: 1954: *Letter symbols, signs and abbreviations, Part I, General* which authors of mathematical papers are also advised to consult.

Authors preparing contributions for submission to this *Journal* are invited to make use of the guidance available in the booklet, copies of which may be obtained from The Institute of Physics, price 3*s.* 6*d.* (including postage).

Radiometer for field use

by J. H. McGUIRE, B.Sc., A.M.I.E.E., A.Inst.P.,* and H. WRAIGHT, B.Sc., Department of Scientific and Industr
Research and Fire Offices' Committee, Boreham Wood, Herts.

[*Paper first received* 22 *September, and in final form* 29 *October*, 1959]

Abstract

A shielded, gold-disk radiometer, specially designed for field use, is described. It measures thermal radiation in the range $0 \cdot 01$ *to* $1 \cdot 2\ cal\ cm^{-2}\ s^{-1}$. *The calibration is not greatly affected by ambient temperature or by prolonged exposure and the error introduced by winds of up to 25 mile/h is less than* 8%.

Introduction

Most cellulosic materials may be exposed to radiation intensities of less than $0 \cdot 1$ cal cm^{-2}s^{-1} without any likelihood of their igniting or even charring, but if they are subjected to an intensity greater than $1 \cdot 0$ cal cm^{-2}s^{-1} ignition takes place within a few seconds. To determine the hazard to buildings exposed to fires, an instrument is therefore required which will measure thermal radiation in the range $0 \cdot 05$ to $1 \cdot 5$ cal cm^{-2} s^{-1}. Instruments such as the Moll Thermopile† or the asbestos-faced copper disk,‡ although suitable for laboratory measurements, are too susceptible to draughts in the field, and the error introduced by, say, a 10 mile/h wind would be over 100%. It is necessary for any instrument to have as robust a construction as possible and be simple to operate without, for example, frequent zero adjustments.

Design and construction of radiometer

A radiometer which has been developed for field use is illustrated in Fig. 4. It consists basically of a gold disk to which is attached a 40 s.w.g. chromel-constantan thermocouple. The front face of the disk is coated with candleblack to increase its absorptivity and hence raise the thermoelectric output. The gold disk is mounted behind a thin ($0 \cdot 0010$–$0 \cdot 0015$ in.) mica window within a chromium-plated brass enclosure. A second disk is mounted within the enclosure and is shielded from the window. The thermocouple attached to this disk is connected in opposition to the other.

The blackened gold disk is only $0 \cdot 004$ in. thick to give a rapid response time and the 40 s.w.g. chromel and constantan wires are silver-soldered to it. The assembly is supported on ceramic posts which are secured by epoxy resins. Diagrams of the radiometer are shown in Fig. 1. On one version of the radiometer provision is made for cooling by drilling a ¼ in. diameter hole diametrically through the radiomet body through which water can be passed if the radiometer to be exposed to high intensity radiation for periods of mo than about 5 min.

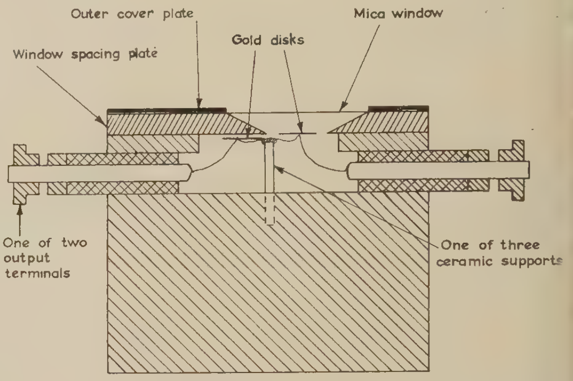

SECTION THROUGH RADIOMETER

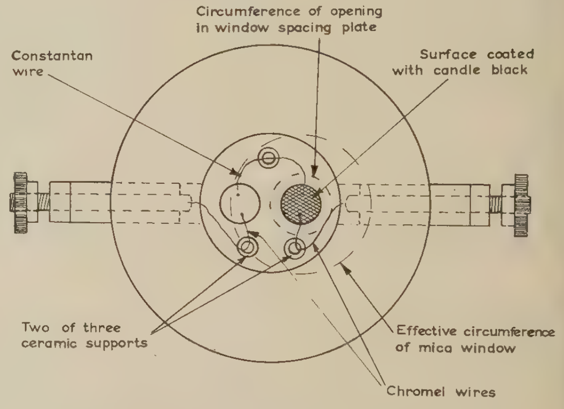
Circumference of opening in window spacing plate
Constantan wire
Surface coated with candle black
Two of three ceramic supports
Effective circumference of mica window
Chromel wires

RADIOMETER WITH COVERS REMOVED

Fig. 1. Diagrams of radiometer

Performance of radiometer

A typical calibration is given in Fig. 2 (curve *B*). The upper and lower curves (*A* and *C*) show the upper and lower limits obtained using twelve radiometers nominally of the same design. The factor limiting the maximum intensity to which the radiometer may be subjected is the temperature a which the candleblack on the exposed gold disk deteriorates. For short periods of exposure (that is, up to 5 min), radiation intensities of up to $1 \cdot 2$ cal cm^{-2} s^{-1} may be tolerated, while for an indefinitely prolonged exposure (that is, exceeding 60 min), the intensity should not exceed $0 \cdot 7$ cal cm^{-2} s^{-1}.

---

* Now with National Research Council, Div. of Building Research, Ottawa, Canada.

† Moll, W. J. H. *Proc. Phys. Soc. Lond. A*, **35**, p. 257 (1922–3).

‡ Webster, C. T., and Gregsten, M. J. "A disk-type radiometer", Department of Scientific and Industrial Research and Fire Offices' Committee, *Joint Fire Research Organization F.R. Note* No. 160/1955.

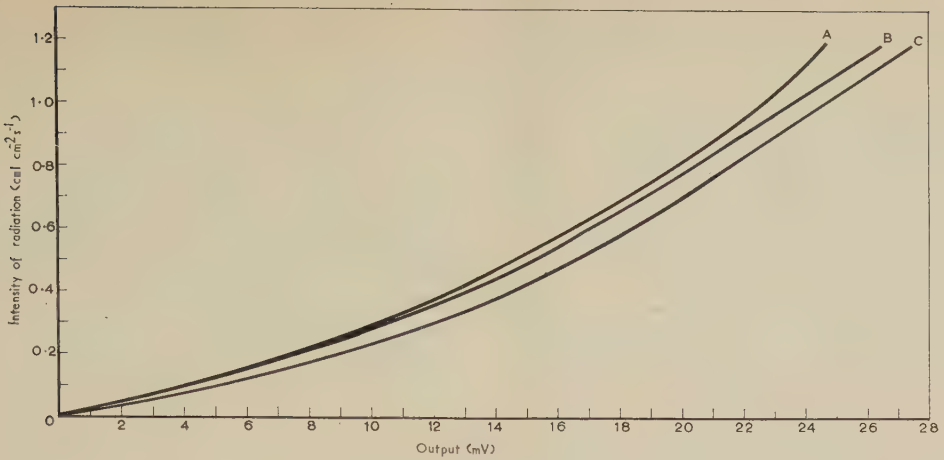

Fig. 2. Calibration of twelve radiometers
A typical curve with upper and lower limits

Fig. 3 gives the output of the radiometer when it is subjected to a constant level of radiation of $0\cdot5$ cal cm^{-2} s^{-1}. From this figure, it is seen that the response time of the radiometer for a 95% true-scale reading is 10 s. It can also be seen that prolonged exposure reduced the output by 3% with water running and about 15% without water running. The slight variations superimposed on the gradual decline of output result from fluctuations in the radiation source.

The temperature attained by the disk is a function not merely of the incident radiation, but also of the body temperature of the instrument. However, when a radiometer was removed from a refrigerator at −10° C and immediately subjected to radiation its output remained within the limits of the normal calibrations. This suggests that the radiometer calibration is substantially unaffected by ambient temperature.

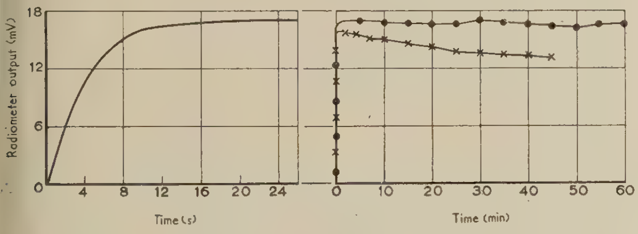

Fig. 3. Variation of radiometer output with time
● with water flow
× without water flow

It was then found that the effect of wind was greatly reduced by increasing the separation between the exposed disk and the mica window. The final design, in which the mica window is sandwiched between two front plates bolted to the radiometer body, is illustrated in Fig. 4. Provided that the exposed disk is not less than ⅛ in. behind the mica window, the effect of wind up to 25 mile/h was to reduce the radiometer output by less than 8%. For lower wind speeds, the reduction was correspondingly less. The wind effect can be diminished still further by using a thicker mica window, but this is of doubtful benefit as the selective absorption of incoming radiation is thereby increased.

The wind effect was found to be slightly affected by changes in the incident radiation intensity, the radiometer body temperature, the thickness of the mica window and its separation from the exposed disk.

Field use of radiometers

An essential feature of any instrument designed for use in the field, is its ability to withstand rough usage. The robustness of this instrument is aptly illustrated by an accident to several radiometers which were substantially identical with

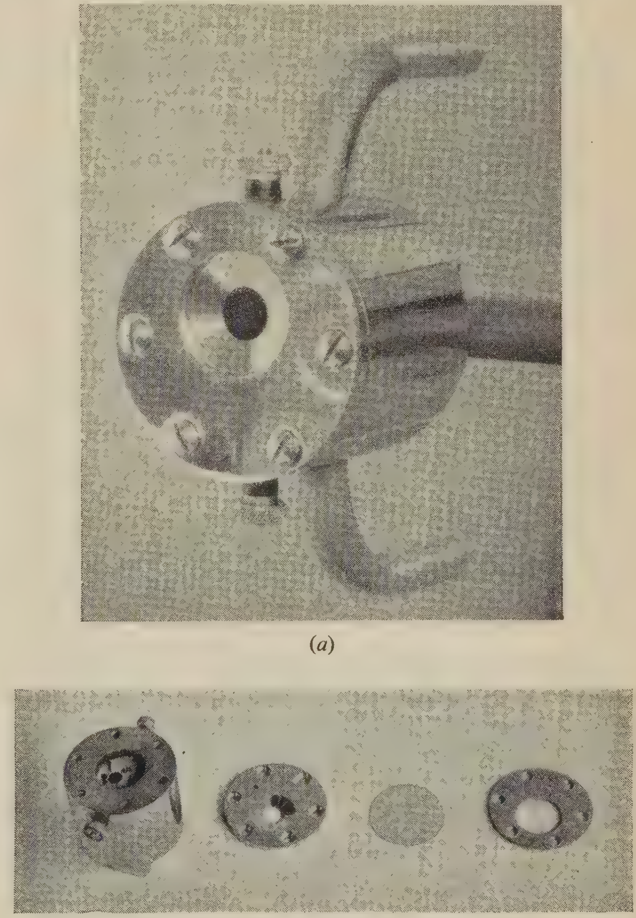
(a)

(b)

Fig. 4. (a) Assembled radiometer with tube for water cooling.
(b) Radiometer without provision for water cooling with front plates and mica window detached

the type illustrated in Fig. 4. These were to be used in a series of experimental building fires on the banks of the St. Lawrence River in Canada during January and February, 1958. During transit, the containing box was broken and several radiometers received blows of sufficient force to dent the solid brass enclosures to a depth of 1/32 in. As a result, the disks were of course displaced. They were relocated approximately in the field, and it was later found in the laboratory that the calibrations had not been affected.

Conclusion

The instrument will measure thermal radiation levels in the range 0·01 to 1·2 cal cm^{-2} s^{-1} and is convenient for use in the field since it is robust and is not greatly affect by wind. For exposures of less than 5 min or intensiti less than 0·7 cal cm^{-2} s^{-1}, no water supply is required f cooling.

Acknowledgement

The apparatus described in this paper was designed in t Laboratory of the Joint Fire Research Organization of t Department of Scientific and Industrial Research and Fi Offices' Committee; this paper is published by permission the Director of Fire Research.

The radiometer described in this note is based on o designed by P. L. Hinkley and R. J. French for use wi intensities of radiation up to 0·25 cal cm^{-2} s^{-1}.

New method of sample interchange in a solid-source mass spectrometer

by B. R. F. KENDALL, B.Sc.,* Department of Physics, The University of Western Australia, Nedlands, Western Australia

[*Paper first received* 2 *October, and in final form* 29 *October*, 1959]

Abstract

An ion source is described in which any one of a number of samples on a single filament can be analysed at will. The operation of the source is based on the effects of potential variations along the length of the filament. Results obtained with this and other experimental sources are discussed.

Introduction

The changing of samples in conventional solid-source mass spectrometers involves the mechanical removal of the sample, followed by the mechanical introduction of the succeeding sample. If the complications of vacuum locks are to be avoided, the body of the spectrometer must be returned to atmospheric pressure and then pumped down again to operating pressure when the fresh sample has been loaded. Thus a complete loading and pumping cycle, lasting several hours, is required for the analysis of a single sample. A technique is described here whereby a number of samples can be analysed during a single loading and pumping cycle. No modifications need be made to the structure of a conventional surface ionization instrument to which the technique is to be applied.

Principles of operation

The operation of the new multiple-sample source is based on the fact that samples mounted at different positions along an electrically-heated filament are in general at differen potentials. This leads to two effects which accompany the normal processes of surface ionization:

(1) variations in the efficiency with which ions are extracte from the regions of the various samples;
(2) variations in the kinetic energy of ions extracted from these samples.

The first effect allows the attenuation of ion currents from samples other than that which is being analysed. The secon effect, because the conventional sector-field mass spectrometer is a momentum analyser and will resolve ions of the same mass but different energies, leads to a relative displacement of the mass spectra from the different samples. This attenuation and displacement of unwanted ion beams allows ready identification of ion beams from the sample being analysed.

Experimental ion sources

Illustration of Effect 1 (*Extraction-efficiency variation*). Investigations were carried out to determine the extent to which the ion current from a sample of potassium salt loaded on a tungsten filament could be controlled by variation of its potential relative to the adjacent electrodes. It was found that potential variations of 0·5 and 2 V could change the ion current by factors of 8 and 50 respectively. It follows that, if two identical samples were placed on a constant-temperature filament at positions differing in potential by 2 V, adjustment of the mean filament potential would allow either sample to be selected as the source of 98% of the emitted ions.

---

[*] At present a Fellow in the Radio and Electrical Engineering Division of the National Research Council, Ottawa, Canada.

Tests with a source of this type showed that satisfactory peration could be obtained only when the emission from the vo samples was adequately balanced. In other cases, the atio of the emissivities of the samples was sometimes as igh as 25, because of slight temperature differences. Under hese conditions, the most strongly emitting samples could ot be prevented from supplying a substantial fraction of the otal ion current emerging from the source.

Illustration of Effect 2 (*Kinetic energy variation*). Tests vere carried out to determine whether or not the kinetic-nergy difference of ions from adjacent samples was sufficient o obtain adequate resolution between ion beams of the same nass number. Displacements of 0·2 m.u. at mass 39 were btained between mass spectra of adjacent samples. The nass spectrometer used in this work had a resolving power f several hundred, so that adjacent ion beams of the same nass were easily resolved.

Combination of Effects 1 *and* 2. Tests were carried out n a source in which Effects 1 and 2 were applied simultaneously. In this case, the potential difference between the samples was used to give a relative displacement of the mass spectra, and also to attenuate the unwanted ion currents. Filament heating was by alternating current, gating of the ion gun being used to ensure that ions were passed only while the filament heating current was passing through a maximum in one direction. The r.m.s. filament voltage was 2·5 V. For compactness the filament was coiled. Two samples, *A* and *B*, with ^{39}K/^{41}K ratios of 1·05 : 1 and 13·5 : 1 respectively, were loaded on the filament, one at each end. The mean filament potential could be switched so that end *A* or end *B* of the filament could be set in turn to the same potential during the period when the ion gun was passing ions. This preset potential was that at which most efficient extraction of the ions occurred.

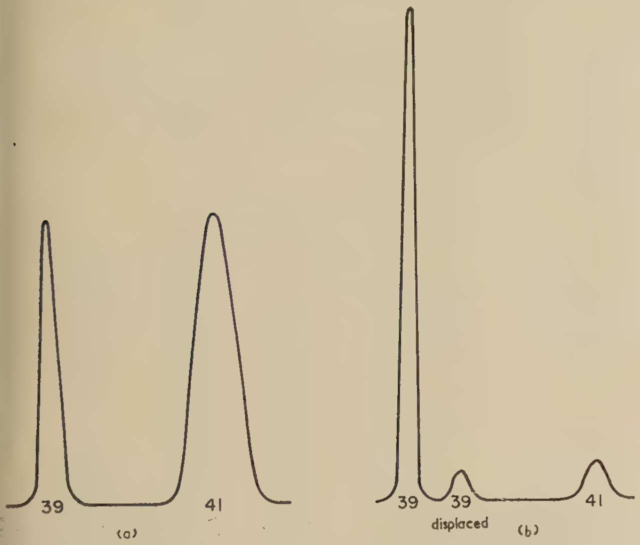

Mass spectra obtained with two samples on single filament

With end *A* at the preset potential, the mass spectrogram (*a*) (see figure) was obtained by varying the magnet current. The variation in peak shape results from a non-linear sweep rate. There was no sign of emission from the sample at *B*, presumably because of the high attenuation combined with a somewhat lower emissivity for this sample. The two peaks obtained in the mass 39 and 41 regions, respectively show a ^{39}K/^{41}K ratio of approximately 1 : 1, corresponding with the known composition of sample *A*.

With end *B* at the preset potential, the mass spectrogram (*b*) was obtained. This shows a small displaced ^{39}K peak shifted about 0·3 m.u. from the "normal" ^{39}K position and reduced in true height relative to the ^{39}K peak in spectrogram (*a*) by a factor of about 50. (The two spectrograms are not to the same scale.) From its position in spectrogram (*b*), the displaced peak is readily identified as originating from sample *A*. The ^{39}K/^{41}K ratio for the two remaining peaks is approximately 13 : 1, corresponding with the known composition of sample *B*.

Conclusion

A technique has been developed which allows isotopic analysis of more than one sample from a single-filament ion source. The method effectively allows interchange of samples without mechanical movement. The multiple-sample source can easily be used in existing solid-source mass spectrometers of conventional design. A small amount of additional electronic circuitry may be required if the filament is heated by alternating current.

It appears likely that the multiple-sample source may be useful in some industrial applications where a high rate of analyses is required from simple instrumentation. With a sample on every turn of a coiled source filament and a potential difference of 1 or 2 V per turn, relatively large numbers of samples could be analysed at each loading. Heating the filament with pulsed current would allow the necessary peak voltages to be obtained across filaments of any desired cross-section.

The ability of the source to analyse the emission from selected portions of the filament may also be valuable in studies of surface effects, diffusion of sample material over filaments, distribution of impurities in the filament material, and similar problems. The origins of ions emerging from an experimental ion source have been investigated using similar methods.*

The multiple-sample technique is inherently suitable for application to any type of ion source in which ionization occurs from well-defined and well-separated sites. Thus, the technique could be applied to a source in which molecular beams from the various samples fall on different portions of the filament. In this way it might be possible to combine multiple-sample operation with the comparative freedom from isotopic fractionation reported by Palmer† for sources of the multiple-filament type.

Acknowledgements

The Solid Source Mass Spectrometry Project was supported by grants from the New South Wales State Cancer Council, Dr. K. W. Starr, the University of Western Australia Research Grants Committee, and the Australian Atomic Energy Commission, to which the writer is also indebted for a Postgraduate Research Studentship.

---

* Kendall, B. R. F. *Rev. Sci. Instrum.*, **29**, p. 1089 (1958).
† Palmer, G. H. *J. Nuclear Energy*, **7**, p. 1 (1958).

Low-angle Geiger diffractometer for use with monochromatic radiation

by P. W. TEARE, B.Sc.,* Aluminium Laboratories Ltd., Banbury, Oxfordshire

[*Paper received* 31 *December*, 1959]

Abstract

An X-ray diffractometer has been designed to study low-angle scattering from precipitation-hardening aluminium alloys. The special problems of design that arise with this type of instrument are discussed, and their practical solution illustrated by the low-angle diffractometer finally built. The performance of the diffractometer is critically reviewed and a table of results quoted to show the reproducibility obtainable. It is thought possible that proportional counting could greatly improve the diffractometer.

Introduction

THE theoretical aspects of low-angle diffractometer design have, to a large extent, been surveyed by Guinier and co-authors† in their book on low-angle scattering. The practical problems which arise with the various methods of studying low-angle scatter can, however, be easily overlooked or underestimated at the design stage. In this paper, some of the major design problems are analysed and an account is given of a new diffractometer designed to solve some of these problems.

Design factors

The diffractometer should be so designed that the adjustments associated with its installation, or re-adjustment, following any modification of the instrument, are straightforward, reasonably rapid and precise. The emphasis is on precision. Where a series of delicate adjustments has to be made, any lack of precision will make it difficult to find the settings for optimum performance, particularly in the monochromator.

Operation of the instrument should be simple and as free as possible from external effects such as vibration, thermal motion and shock movements caused by operation of the controls. Provision should be made for centring the axis of rotation of the Geiger counter in the reflected beam from the monochromator, and for adjustment of the Geiger counter along the beam path so as to locate the focus of the monochromatic beam. The angular scale measuring displacement of the Geiger counter from the point of incidence of the direct X-ray beam should be adjustable; that is, it should be possible to zero the scale by means of a clutch or similar device to any new setting of the instrument. Provision for automatic and/or step-wise scanning is usefu although not essential for low-angle studies.

Because the scattering to be studied often extends onl some 4 deg from the direction of the incident X-ray beam it is essential that the angular settings of the counter be both precise and reproducible. This means complete freedom from backlash in angular motion. Because the intensity o the radiation scattered from the sample is usually very low the parasitic background should be reduced to a minimum If this is not achieved, the usable angular range of the instru ment is curtailed, both near the incident beam and at large angles, where the scattered intensity tends to merge into th background. The minimum angle observable depends on counter-slit design. This is discussed fully by Guinie (see reference, p. 121).

Table of observed scatter

Scattering angle	*Expt.* (1)	*Expt.* (2)	*Expt.* (3)	*Mean*
0·3	1236	1198	1203	1212
0·4	658	663	650	657
0·5	522	526	534	527
0·7	462	468	478	469
0·9	473	459	489	474
1·1	465	468	468	467
1·3	436	452	448	445
1·6	388	375	392	385
1·9	310	305	312	309
2·3	244	209	214	222
2·8	125	117	124	122
3·4	69	66	67	68
4·1	37	33	35	36

The alloy used was aluminium—2½ % silver—8 % zinc, annealed for 30 min at 460° C, water quenched and aged for 48 h at room temperature

The parasitic background is largely controlled by the scatter slits both on the monochromator and immediately in front of the specimen. It is difficult to obtain a minimized background of constant intensity, as trouble can arise from several sources. Motion of the focal spot on the anode of the X-ray source will cause a small rotation of the reflected beam from the monochromator. This is observed as a change in intensity of the reflected beam and a change in intensity of the parasitic background because the beam in its changed position strikes the preset scatter slits. Motion of the anode assembly with respect to the cathode has a similarly small effect. Motion of the monochromator with respect to the beam or thermal expansion of the monochromator crystal itself is the major source of trouble. If these sources of error are not countered, they will give incorrect plots of ntensity against angle and a lack of reproducibility. There seems to be no complete solution to these problems for an instrument of this type. A stabilized d.c. X-ray source operating in a room which is reasonably constant in temperature, coupled to an instrument which has a high inertia, does however provide usable results. An X-ray source should be chosen that will produce a sharply defined high-intensity line focus of X-rays, with a very small line width at the anode. The width of the beam determines the width of the reflected beam from the monochromator, and hence the minimum angle observable.

---

* Now at Central Electricity Research Laboratories, Leatherhead, Surrey.

† GUINIER, A., FOURNET, G., WALKER, C., and YUDOWITCH, K. *Small-angle Scattering of X-Rays* (New York: John Wiley and Sons Inc., 1955).

The height of the focal line on the anode of the X-ray source is of importance. On leaving the anode, the X-ray beam diverges vertically—a factor of 20 between the dimension of the beam at the anode and at the receiving slit of the Geiger counter is not uncommon. The size of the slit on the Geiger counter is determined by the dimensions of the counter window; the slit is normally about 1 cm long. A focal spot should thus be about 0·5 mm if the loss of intensity caused by vertical divergence is to be minimized.

As stated above, the scatter slits in front of the specimen largely control the parasitic background. In the design stage it is almost impossible to predict the magnitude of this background. However, by making the distance between the specimen and the counter variable whilst still maintaining the scatter slits in their position immediately in front of the specimen, it is possible to achieve the best compromise between the sensitivity, determined by the specimen-to-counter distance and the parasitic background. It is advisable, for some purposes, to provide for evacuation of the air path between the specimen and the counter. The author has not found this essential for low-angle studies of age-hardening effects in aluminium alloys containing 10% or more of a solute such as zinc, but in the studies of the aluminium–magnesium–zinc alloys and the more dilute aluminium–zinc alloys, it would certainly be a considerable improvement.

Description of the diffractometer

The diffractometer shown in the figure has a base plate with three triangulated levelling screws on the point, line and plane basis, resting on a bed plate positively located on the X-ray console. Two additional screws just out of contact with the bed plate are used to prevent accidental tipping of the instrument about the apex of the triangle formed by the levelling screws. The base plate carries a bracket on which the monochromator is mounted, this bracket is also locked transversely to the tube head carrying the X-ray source. On top of the base plate are two further superimposed plates which can move in two directions at right-angles to the base plate, the upper plate carrying the diffractometer.

The various motions of the instrument are probably best illustrated in terms of the setting-up procedure. This procedure will now be described with reference to the figure. The monochromator, *M*, is first adjusted in the normal manner to give a sharp focal line of high brilliance, uniform illumination and sharp extinction on rotation about the monochromator axis. A fluorescent screen, which carries a thin wire cross, is mounted on the specimen arcs *A*. By means of the various motions built into the arcs, the wire cross is brought into coincidence with the cross wire of the telescope *T* the focus of which intersects a vertical axis passing through the centre of rotation of Geiger counter G_1. The cross is now illuminated by the reflected beam from the monochromator. In general, the beam will not strike the screen uniformly about the cross wire; that is, the centre of rotation of the Geiger counter G_1 will not be coincident with the centre of the X-ray beam. By means of the screws S_1 and S_2, which move the diffractometer independently of the monochromator, the beam is centred on to the centre of rotation of G_1. The counter G_1 is rotated by means of the micrometer drum *MD* until the electronic counting equipment shows that the receiving slit of the Geiger counter lies in the path of the beam. The angular scale on *MD* is set to zero at this position by means of a clutch. The Geiger counter is traversed along the beam by S_5 in millimetre increments, and a plot of intensity against distance is made. The maximum of the curve so obtained will correspond to the true focal position of the beam, provided that the distance traversed is not large enough to introduce large errors from vertical divergence and that the receiving slit used has the same width as the beam at its focal position. Scatter slits L_1 are set to reduce the beam to the desired width. Slits L_2 are then set to be just out of contact with the beam. This setting is made with the aid of Geiger counter G_1, which records the variation in level of the parasitic background with the angle for a given setting of L_2. The minimum value of the background will correspond to a correct slit setting. The level of parasitic background found in this manner is then compared with the background obtained for various other specimen-to-counter distances. The specimen-to-counter distance can be varied by screws S_2 and S_4. For each new specimen-to-counter distance, the setting-up procedure

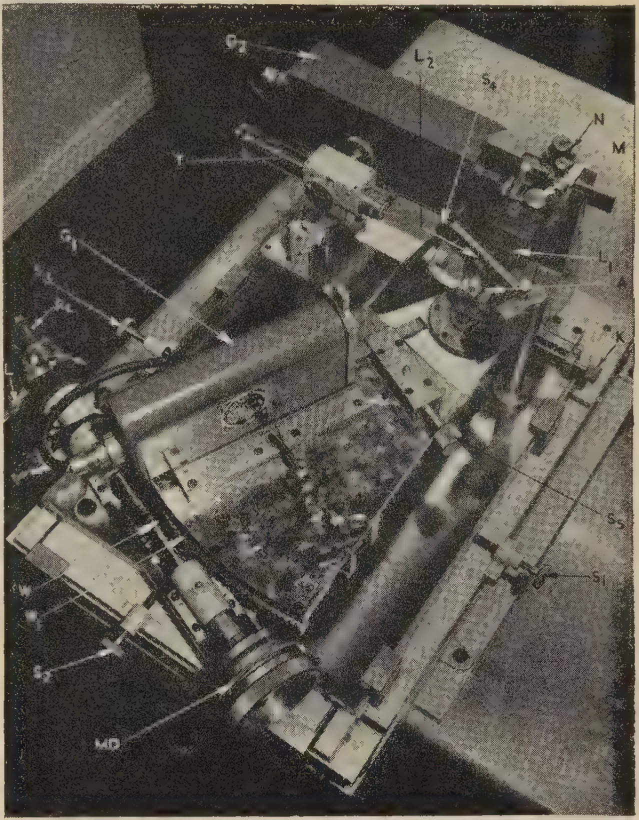

Low-angle Geiger diffractometer for use with monochromatic radiation described above is repeated. The results so obtained may be used to select the best compromise between background and specimen-to-counter distance, that is, the best compromise between background and sensitivity. The instrument is now ready for use.

Micrometer drum *MD* is calibrated in one two-hundredths of a degree and drives a worm *W* actuating a sector W_1 of 14·33 in. radius. This gives a motion of $\frac{1}{4}$ in./deg. at the wheel. The lever *L* controls a ratchet which may be preset to give a semi-automatic scan through a known increment of angle. A revolution counter *RC* is connected to the worm shaft by an eccentric motion and will count clockwise or anticlockwise revolutions of the micrometer drum. The knurled knob *K* is connected to a gear mechanism which rotates the specimen arcs, one revolution of *K* being equivalent to 4 deg. The knurled knob *N* carries a thin piece of nickel foil; the foil causes a Debye–Scherrer line from the nickel spectrum to fall on to the Geiger counter G_2. This counter is a monitor on the tube output.

Some observations on the operation of the diffractometer

When the diffractometer was first installed, a series of experiments was carried out to examine the reproducibility of the instrument. A rather large source of error was found to lie in the effect of varying temperature on the monochromator crystal. If, during the winter months, a window was opened during an experiment, the blast of cold air blowing over the monochromator crystal was sufficient to cause a serious change in the intensity reflected by the monochromator. It is extremely difficult to eliminate this trouble. The only solution is to use a thermostatically controlled laboratory. If, however, the unit is run for several hours before making an experiment, a fair degree of reproducibility is obtainable. Small irregular intensity fluctuations, which are probably still caused by local thermal changes, occur even after this stabilizing treatment.

The parasitic background has been carefully studied. To obtain a reasonable background, it was found that the aperture of the monochromator crystal had to be set to pass rather less than half the available beam. In fact, the only real advantage one obtains from the monochromator is the very sharply defined focus. The parasitic scatter effects arising from the "white" radiation scattered from the area of the crystal under irradiation almost nullify the gain in intensity expected from a focusing monochromator.

The life of a filament in the X-ray source used is usually about 200 h. It was found however that, after about 80–100 h, the target had developed a small pit which reduced the intensity of the beam as seen by the monochromator. Consequently, both the target and filament should be replaced after being used for about 70 h. Targets should be polished as for a normal metallographical microscopic examination. The extra flatness so obtained gives a significant increase in X-ray output.

The reproducibility obtained is demonstrated in the table. This shows a series of three experiments performed over a period of about two days. During this period, the output of the source changed because of filament ageing. The results were, therefore, scaled to constant output. As can be seen, the reproducibility was quite good.

Future development of the diffractometer

The main source of parasitic background is known to be "white" radiation scattered by the monochromator crystal. In the previous section, it was shown that, to reduce this background to a reasonable level, a small monochromator aperture must be used. This causes a marked loss of intensity in the monochromated beam. The problem of small apertures could probably be overcome by the use of a proportional counter. "White" radiation, by virtue of its shorter wavelength and higher energy than copper $K\alpha$, can be mostly eliminated by an electronic discriminator attached to a proportional counter. In this manner, lower parasitic backgrounds and greater intensities could be obtained because it would then be possible to use the full width of the monochromated beam.

Improved eye-piece graticule for measuring X-ray powder diffraction patterns

by W. G. PERDOK and G. BOOM, University of Groningen, Kristallografisch Instituut, Melkweg 1, Gröningen, Netherlands

[*Paper received* 28 *September*, 1959]

Abstract

The accuracy of measuring Debye–Scherrer lines can be improved by a slight modification of the cross-wire system in the microscope. The new graticule can be made simply by photographing a large-scale drawing.

For precision determinations of lattice parameters from X-ray powder photographs, it is necessary to have a measuring device allowing readings to 0·01 mm or less. Measuring is generally done by setting one of the cross wires—or their point of intersection—in the eye-piece of a travelling microscope as accurately as possible on the centre of a diffraction line, but an accuracy of 0·01 mm can only be attained for this setting on strong and narrow lines. The inadequacy of cross wires for measuring diffraction lines has been pointed out before and, instead, an illuminated glass fibre* or a collimator slit† have been proposed, the image of which was projected on the film as a reference mark. Although this method was found to be quite satisfactory, it requires a rather clumsy attachment to the measuring device. The graticule described here is as convenient as cross wires and gives measuring results comparable with illuminated-slit methods.

---

* Lees, C. S. *J. Sci. Instrum.*, **32**, p. 17 (1955).

† Armstrong, W. E., and Davis, R. J. *J. Sci. Instrum.*, **35**, p. 59 (1958).

Principle of new graticule

The use of very thin cross wires as a reference mark is perfectly sound for measuring a series of sharp, straight lines on a photograph. The setting of the cross wires on the middle of such a line is performed so easily because of the sense for seeing bilateral symmetry when the symmetry plane is parallel to the observer's vertical mirror plane. But when the lines are strongly curved, as in the case of high-angle powder lines in a Debye–Scherrer camera, this sense of symmetry counteracts rather than helps the accurate setting: there is a trend to mis-setting towards the concave side of the line, irrespective of whether the cross wires are vertical and horizontal (+) or inclined to the vertical and horizontal (×).

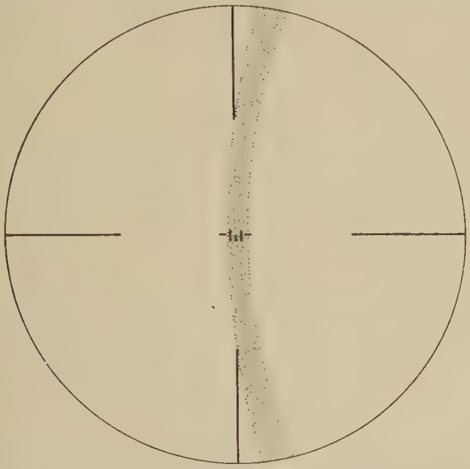

Fig. 1. Curved diffraction line in microscope field

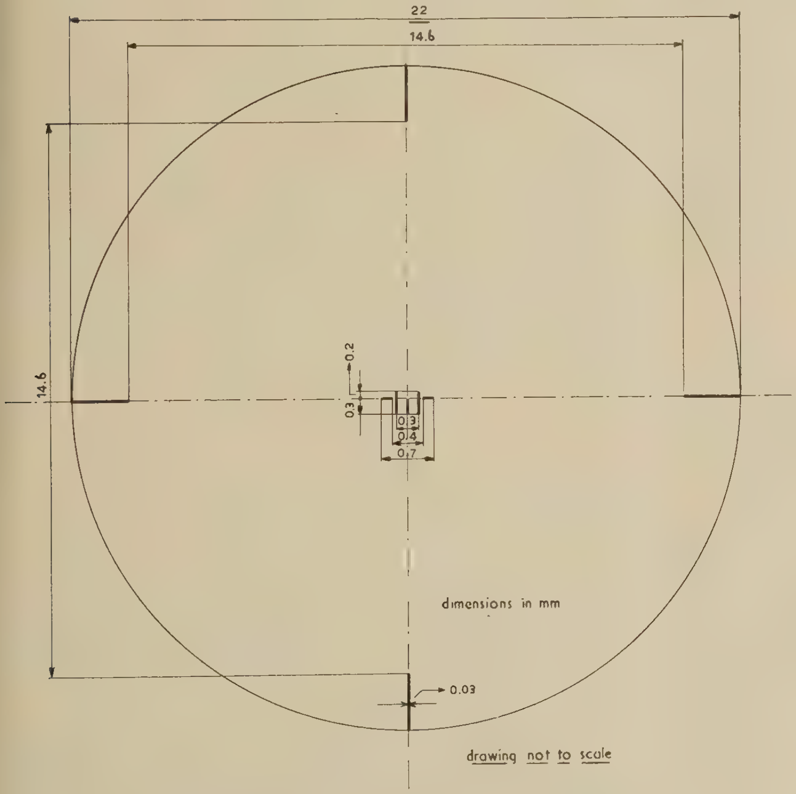

Fig. 2. Dimensions for constructing graticule

As the lines have to be measured on the equator of the film, the graticule has to be modified in such a way that the field does not accentuate the vertical symmetry plane of the reference mark at both sides of the equator. Therefore the cross wires have been erased around their point of intersection, leaving only a very short vertical line, the top of which indicates the centre of the field. In addition, the graticule has been extended in the horizontal direction for convenience in setting broader lines (Fig. 1 and 2). Very sharp powder lines are measured by using the short central vertical line of the graticule. Somewhat broader diffraction rings are set between the two longer vertical lines, and diffuse powder lines are set by using the small horizontal lines. Obviously, these lines and the top of the central line must be collinear, and the graticule must possess a strict symmetry in the horizontal direction. As the ends of the cross wires remaining in the outer half of the field are used for adjusting the film position prior to line measurement, these ends have to be exactly equidistant from the centre, that is, the upper end of the central small vertical line. Moreover, this small vertical line and the (ends of the) vertical cross wire must be collinear. The (end of the) horizontal cross wire, the small horizontal lines, and the upper end of the small central vertical line must also be collinear.

Measuring procedure

The eye-piece of the measuring microscope is adjusted in such a way that the horizontal cross wire is parallel to the travelling direction. This can easily be achieved by following the path of a spot on the film in the field. A (nearly) straight diffraction line on the photograph in the region $\theta = 45^\circ$ is located and brought into the centre of the field. The film is adjusted (by rotation) so that the two ends of the vertical cross wire and the powder line are collinear. This brings the film equator parallel to the travelling direction.

The film is next translated in a vertical direction, until the central ends of the vertical cross wire are simultaneously touching a curved diffraction line, that is brought into the field (Fig. 1). When this can be achieved for all the lines of the photograph, the film has its equator exactly underneath the horizontal cross wire and the distances between the powder lines measured in this way are true equator distances.

Making the graticule

The graticule is made by photographing an enlarged drawing (20 times) on the right scale of 1 : 20. The negative serves for making a contact print on document film. The diapositive is cut out and mounted between glass plates in the eye-piece of the measuring microscope. The enlarged drawing has to be prepared carefully and all dimensions given in Fig. 2, multiplied by 20, must be strictly maintained.

Tunable galvanometer amplifier

by R. M. HUEY, B.Sc., B.E., and B. J. LANCASTER, B.E.,* School of Electrical Engineering, University of New South Wales, Sydney, Australia

[*Paper first received* 6 *August, and in final form* 2 *November,* 1959]

Abstract

The construction and performance of a tunable galvanometer amplifier using a photomultiplier tube are described. A tuning range of a little over two octaves with resonant voltage gains of over 10^4 *times and Q-values ranging from* 1·7 *to* 7·5 *were obtained.*

Introduction

The galvanometer amplifier is inherently a resonant device. Its resonance is determined by the rotational inertia and the spring constant of the galvanometer. If it is desired to change the resonant frequency, it is necessary to alter the value of the inertia or the spring constant. To effect any such change in the value of the inertia appears difficult, unless the instrument is made demountable and this method is thus inconvenient for tuning. The effective value of the spring constant may be varied by the application of current feedback round the galvanometer plus amplifier, and the device is tunable by this means. The degree of feedback that may be applied depends upon the gain of the photoelectric amplifier. The availability of very high gain photomultiplier tubes has given rise to the possibility of the design of an amplifier that would be tunable over a relatively large range of frequencies and which would also have a high gain at resonance.

Low-frequency selective devices

The authors' interest in the galvanometer amplifier was occasioned by the fact that the amplifier shows selective properties in the sub-audio frequency portion of the spectrum.(1) However, many other selective devices in this range of frequency exist, and it is not out of place to review some other low-frequency systems.

Many mechanical systems are analogues of the galvanometer amplifier, possessing inertia of the vibrating mass, spring constant of the member supporting the mass, and some form of damping. It is common experience that mechanical systems having resonances in the sub-audio frequency range are easily constructed. Tuning may be achieved by mechanical variation of a parameter, such as the length of the member supporting the mass. A number of vibration-measuring devices (for example the Frahm tachometer and the Westinghouse vibrometer) are commercially available.

Most of these systems are governed by the general equation:

$$J\ddot{\theta} + F\dot{\theta} + k\theta = P_0 \cos pt,$$

whence it follows that the resonance frequency is given by:

$$\omega_0 = \left\{\frac{k}{j} - \left(\frac{F}{2J}\right)^2\right\}^{1/2}.$$

Various electrical networks have been used as filters in the sub-audio frequency range. The symmetrical twin-T network has zero transmission at a frequency given by:

$$\omega_0 = I/RC.$$

This type of network has been used(2) as a selective element in the feedback path of a d.c. amplifier. The feedback is made negative so that, at the zero transmission frequency for the filter, the amplifier has a maximum gain. During the past few years, a transistor impedance convertor has been developed,(3) and it is now possible to produce filters, with given Butterworth characteristics, employing the convertor as a perfect one-to-one transformer. It is unfortunate that most of these filter techniques necessitate the use of accurately ganged potentiometers or capacitors to achieve a shift in the relative position of the pass band. Apart from amplifiers using frequency-sensitive elements in a feedback loop, there is another set of purely electronic devices. This second set uses valves (or transistors) in circuits which depend upon the reactive valve effect. For a resonant effect to be obtained electrically, it is necessary to have two reactive elements, one the complement of the other, and to arrange for an interchange of energy between these two elements. It is possible to utilize the phase shift between the anode-cathode and grid cathode circuits of a valve to produce complementary reactive components. In effect, the valve converts the reactance of one type into reactance of the complementary type and then compares this converted reactance with the initial type. It may be shown(4) that such a circuit has a resonance with maximum gain at a frequency given by:

$$\omega_0 = \text{constant}/m^{1/2},$$

where m is the stage gain. It is worth noting that this circuit may be tuned by purely electronic means.

Experimental amplifier

The amplifier is arranged so that, as the galvanometer deflects, the image of the slit forming the light source is moved across a similar slit in front of the photomultiplier. The zero is set so that half the image of the source falls across the second slit (see Fig. 4).

If an alternating signal is applied to the input terminals, (Fig. 1), the galvanometer deflexion will cause the image to oscillate across the second slit. The photomultiplier output signal will consist of a steady potential with the alternating potential superimposed upon it. The value of the alternating potential will depend upon the value of anode load, the light flux to the cell and the angle of deflexion of the galvanometer. If current feedback is introduced, it becomes necessary to remove the direct component in the photocell circuit from the feedback circuit and hence from the primary circuit. This is achieved by the balance circuit shown in Fig. 1, the resistor R_B being adjusted so that with no signal at the input the voltage between point C and earth is zero. The fractional feedback may be adjusted by potentiometer R_F. Fig. 2 shows the equivalent circuit of the photomultiplier amplifier, where $gL = dI_a/dL$ is the transfer function of the multiplier, R_B is the anode resistance of the multiplier and dL is the incremental light flux. Finally, dL may be given in terms of dI_{in} by writing the transfer function of the galvanometer plus slit and light source (assumed constant in intensity), and hence, the open loop gain becomes:

---

* Now with the P.M.G.'s. Dept., Australia.

$$A = \frac{dI_a}{dI_{in}}.$$

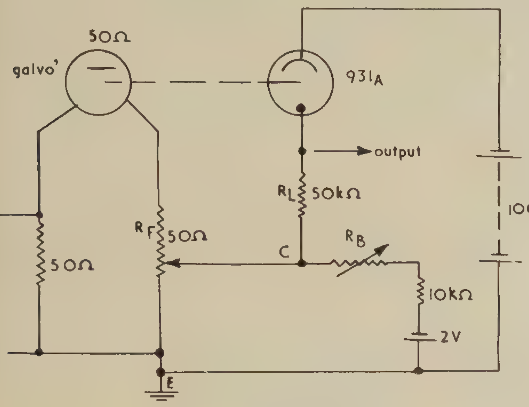

Fig. 1. Circuit diagram

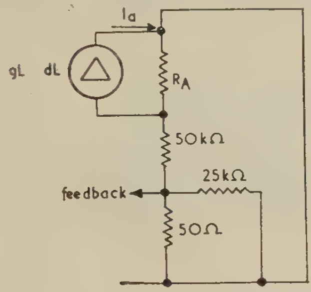

Fig. 2. Equivalent circuit of photomultiplier load and feedback

Apart from the unconventional forward path, the circuit behaves, electrically, as a normal negative feedback amplifier. The optical system and the Cambridge galvanometer (type 41157/1) were solidly mounted to a 1 in. diameter, 18 in. long brass bar. The photomultiplier that was used is the R.C.A. type 931-A, the response of which covers the range 3000–6000 Å. The multiplying process is carried out by nine dynodes with intervening electrostatic screens which shape and direct the streams of primary and secondary electrons.

The final dynode is shaped partially to enclose the anode, and serves as a shield to prevent signals at the anode interfering with the focusing in the inter-dynode regions. The shape of dynode nine also ensures that practically all the emission from this dynode is collected by the anode. Hence the anode current tends to be independent of the anode voltage over a wide range. As a result of this, the 931-A can be coupled to any practical load.

It was found that the spectral response matched quite well the tungsten filament lamp used as the source. However, this particular cell is very sensitive to light produced by normal fluorescent tubes, since the maximum light sensitivity is at about 4000 Å. Consequently, the whole amplifier was very carefully light-insulated from the fluorescent room lighting, although the photomultiplier need not be so carefully shielded from the exciter lamp. The active area of the cell is 5/16 in. wide by 15/16 in. high, and the slit width is considerably less than the aperture width. The slit height of a little over half the aperture height is limited by the lens available.

During development, emphasis was placed on stability, and the maximum anode current was chosen at 250 μA with a quiescent value of 125 μA. Since the multiplier cell is very sensitive to changes in dynode voltage, a well-regulated power supply using cascaded voltage-regulator valves is necessary. The voltage is stabilized to 70 V between dynode nine and earth, and 95 V between all other dynodes.

Performance

An analysis of the amplifier, treated as a feedback control system, shows that:

(1) The resonant frequency is increased from the natural resonant frequency of the galvanometer by negative feedback.
(2) The sensitivity, and hence the resonant amplitude, are decreased by negative feedback.
(3) The Q-factor of the circuit is increased with feedback and hence with resonant frequency.

During measurements on the experimental equipment, the input attenuation networks, the feedback resistor and the load were all 0–100 000 Ω decade boxes. A calibrated twin-channel d.c. oscilloscope (by Cawkell) was used to measure input and output voltages simultaneously, and to test for the presence of distortion and noise. To ensure that there were

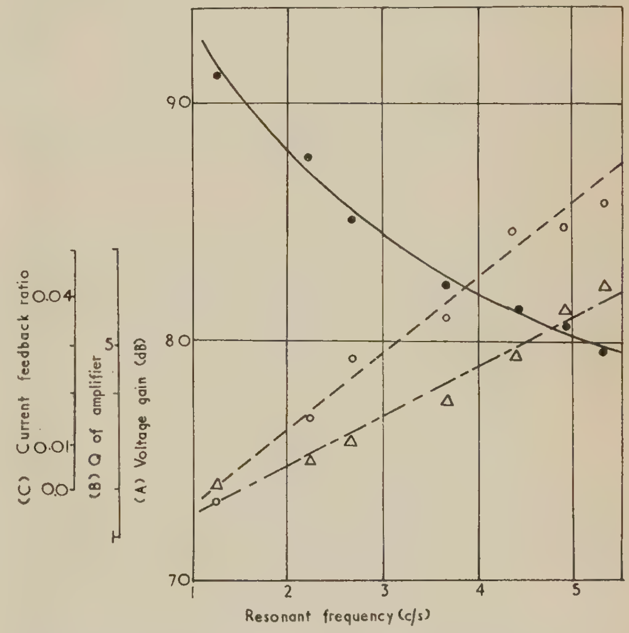

Fig. 3. Performance as a function of resonance frequency
● Voltage gain
○ Q-factor of amplifier
△ Feedback ratio

no fluctuations in the light flux from the lamp, the supply to this lamp consisted of a secondary cell floated across a half-wave rectifier.

The gain of the amplifier was measured for a number of different settings of the feedback control. The fractional feedback (β), the resulting Q-values and the resonant gai are plotted against resonant frequency in Fig. 3, and th shape of these curves verifies the three results of the analys as stated above. Transient effects were observed by th application of a step function to the input while the outpu of the amplifier was traced out by a pen recorder. An inpu voltage was chosen so that the amplifier did not saturate A satisfactory step response was obtained for the whol range of values of feedback.

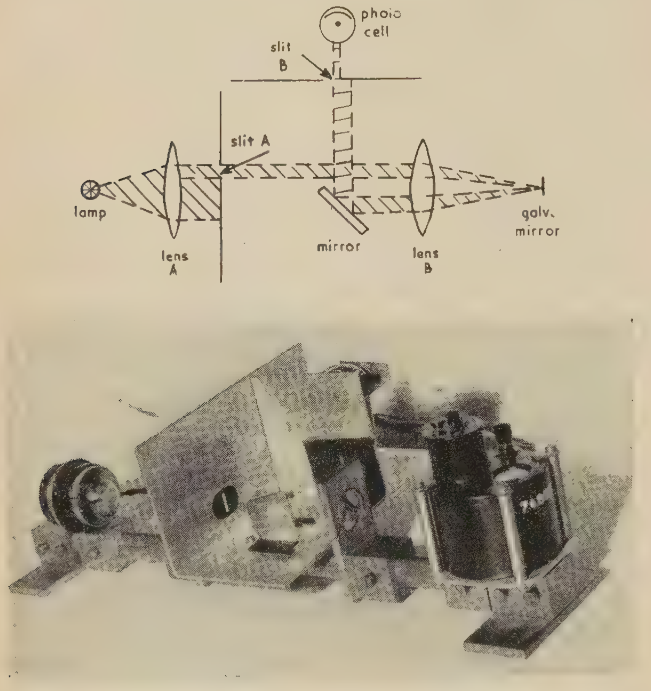

Fig. 4. Details of construction and mounting of the amplifier

To measure the noise levels in the amplifier, the oscillato was replaced by a 2500 Ω resistor and the output wa measured on the oscilloscope. With no feedback the d.c gain was $1\cdot79 \times 10^5$ times, while the equivalent-noise inpu current (in 25 Ω) was $5\cdot6 \times 10^{-8}$ A.

The dynamic characteristic of the amplifier was obtaine by slowly increasing the level of the sinusoidal input, an measuring input and output deflexions on the oscilloscop trace. The characteristic was linear up to output voltage of 12 V. Distortion was measured at the same time b observations of the output wave shape with the oscilloscop timebase connected.

Acknowledgement

The authors are indebted for the use of facilities to Pro-fessor R. E. Vowels, in whose school this project was carrie out.

References

(1) Beatie, J. R., and Conn, G. K. T. *Rev. Sci. Instrum*., **25**, p. 888 (1954).
(2) Battye, C. K. *J. Sci. Instrum.*, **34**, p. 263 (1957).
(3) Linvill, J. G. *Proc. I.R.E.*, **42**, p. 555 (1954).
(4) Schneider, E. E. *Phil. Mag.*, **36**, p. 371 (1954).

Measurement of cyclic strain

by T. M. DOWELL, B.Sc., A.M.I.E.E.,* and J. A. MACKINNON, National Engineering Laboratory, East Kilbride, Glasgow

[*Paper first received* 18 *August, and in final form* 16 *November*, 1959]

Abstract

The paper describes a versatile multi-way instrument for measuring periodic strain gauge signals. The strain is either shown on a meter or can be accurately measured on an oscilloscope in terms of resistance change. Full-scale deflexion of the meter is obtained for strains in the order of $\pm 10^{-4}$.

Introduction

In normal laboratory fatigue testing, cyclic, as distinct from random, strains are induced in the specimen under test. Cyclic strains are also frequently encountered in engineering components under normal operating conditions. These strains may be simply and accurately measured by feeding a strain-gauge signal to an amplifier-rectifier type of valve voltmeter and calibrating the meter scale in terms of strain. When the strain cycle is sinusoidal, as in resonant systems, it does not matter whether the meter responds to the peak, average, or root-mean-square value of the strain cycle since these all bear a constant relation to each other in simple harmonic motion. An instrument for the measurement of cyclic strains was constructed at the National Engineering Laboratory as part of a versatile fatigue-testing rig in which resonant vibrations are induced in engineering components by means of electromagnetic vibration generators.(1) It consists essentially of a d.c. energized Wheatstone bridge with a.c. amplifier and bridge rectifier feeding a sensitive microammeter. The meter responds approximately to the average value of the strain cycle but is calibrated in terms of the peak value. The calibration is effected by the standard method used in the Laboratory for the calibration of fatigue-testing machines.(2, 3) The principle involved is illustrated in Fig. 1.

The bridge is energized by a direct voltage and the output taken *via* a short-circuiting vibrator and electronic amplifier to a cathode-ray oscilloscope. If the short-circuiting vibrator were omitted, the trace on the oscilloscope would simply be a reproduction of the load cycle as shown at (*a*) in Fig. 1. The purpose of the short-circuiting vibrator is to produce on the oscilloscope a reference line which corresponds to the bridge-balanced condition. This condition, no output from the bridge, is indistinguishable from a short circuit across the amplifier input since, under both conditions, the points x and y are at the same potential. The waveform produced at the input to the oscilloscope when the amplifier input is intermittently short-circuited is as shown at (*b*). By adjustment of the oscilloscope timebase, a trace as shown at (*c*) is obtained. Here the trace of the strain cycle is superimposed on a horizontal line which, while being independent of the bridge output, is nevertheless the trace which would be obtained were the bridge balanced. At the instant when the alternating trace coincides with the reference line the bridge is, in fact, balanced. Adjustment of the variable resistor in the bridge circuit will have the effect of altering the d.c. level of the bridge output and will, therefore, move the alternating trace on the oscilloscope vertically. The reference line, being independent of the bridge output, will, of course, remain unaltered. It is therefore possible, by adjustment of the calibrated resistor, to balance first one peak and then the other against the reference line as shown at (*d*) and (*e*). The difference between these two resistance readings gives the peak-to-peak resistance change of the strain gauge and, therefore, the strain.

---

* Now with the South of Scotland Electricity Board.

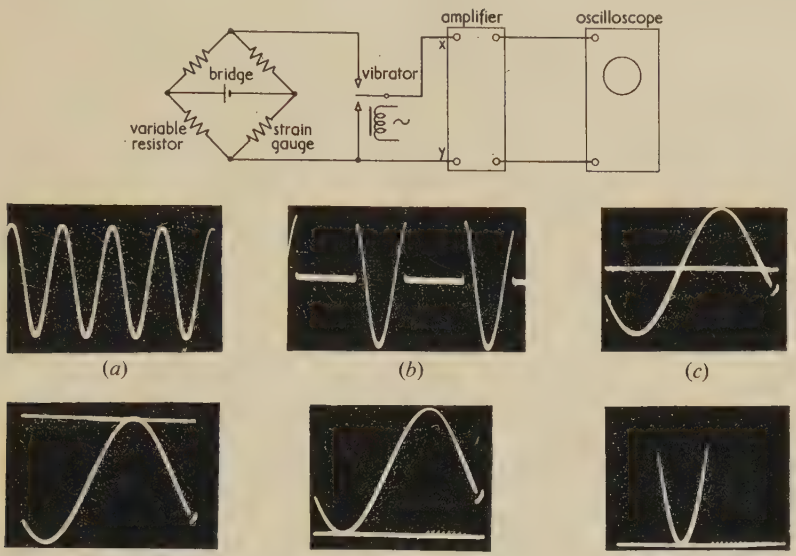

(*a*) (*b*) (*c*)

(*d*) (*e*) (*f*)

Fig. 1. Principle of dynamic calibration

As the bridge is balanced at the instant when the peak of the trace is coincident with the reference line, the measurement is, in fact, a "null" measurement. This can easily be verified by varying the gain of the amplifier. The only effect is to alter the sensitivity of measurement. Trace (*f*) in Fig. 1 shows how the bridge balance may be performed at increased sensitivity by increasing the oscilloscope gain.

The possible accuracy by this means of measurement of periodic resistance changes is much better than the accuracy to which the gauge factor is known. The calibrating device just described could, of course, be used for measuring strain without using a meter indicator at all. The process would, however, be tedious and lengthy if a large number of points were being investigated. A fair amount of care is needed in balancing the bridge and two readings have to be taken and the difference obtained in order to get the resistance change of a single gauge.

The circuit diagram of the multi-way cyclic-strain indicator with built-in calibration facilities is shown in Fig. 2. The gauges, which should have a resistance of 2000–10 000 Ω, are selected by means of a switch of low and constant contact resistance. Associated with this switch is a set of auxiliary contacts which short-circuit the meter while selecting gauges. If the meter is not so protected, damage may occur when used at its maximum sensitivity because of the large transients which are set up at the amplifier output on operating the gauge selector switch. The calibrate key switches the bridge output for strain measurement by the "null" deflexion method. There are facilities for measuring the bridge-supply voltage, which must be kept constant when using the meter indicator, and adjusting it when necessary.

With the component values shown and the bridge supply set to 80 V, the amplifier gain may be adjusted, by means of the feedback control in the cathode of V_1, to give meter full-scale deflexion with strains of $\pm 10^{-4}$. Larger strains, such as those encountered in fatigue testing, may be accommodated by providing an attenuator or by increasing the degree of feedback. This latter method will not only increase the overall stability but, by increasing the amplifier output impedance, will improve the linearity of the scale.

Since the calibration is in terms of "peak-to-peak" strain, the indicator may be used for measurements on non-sinusoidal cyclic strains containing odd harmonics only (see Appendix). It is not suited for use on strain cycles containing even harmonics. This application would require the use of a half-wave peak-reading rectifier instrument with facilities for separately inspecting the positive and negative half-cycles.

The advantages of the method described are best seen by comparison with the available alternatives. It is unnecessary to employ any recording instrument where every strain cycle is identical. Carrier-wave instruments are needlessly complex for all but the lowest frequencies, say below 5 c/s, and the difficulties of drift associated with directly coupled amplifiers are best avoided where possible. As already stated, the

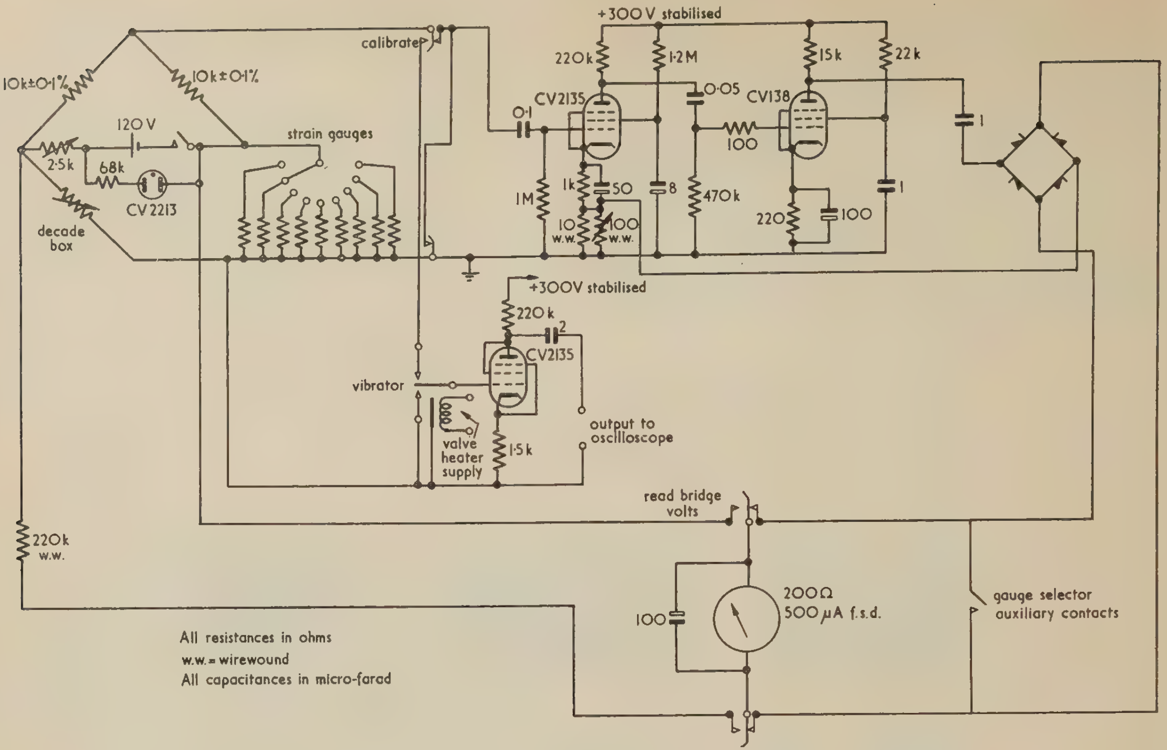
+300 V stabilised
calibrate
10k±0·1%
10k±0·1%
120 V
strain gauges
2·5k
68k
CV 2213
decade box
220k
1·2M
15k
22k
CV2135
0·1
0·05
CV138
100
1M
1k
50
8
470k
220
100
1
1
10 w.w.
100 w.w.
+300V stabilised
220 k
2
CV2135
vibrator
valve heater supply
1·5 k
output to oscilloscope
read bridge volts
220k w.w.
200Ω
500 μA f.s.d.
100
gauge selector auxiliary contacts
All resistances in ohms
w.w. = wirewound
All capacitances in micro-farad

Fig. 2. Cyclic-strain indicator

instrument described forms the basis of the strain measurements on a resonant fatigue-testing rig in the Laboratory. It has proved itself particularly useful for rapidly determining the strain distribution over a test component and then accurately measuring the maximum strain by the null method provided. In this way it has been used for determining fatigue limits in engineering components such as rolling-stock axles.

Acknowledgements

The work described has been carried out in the National Engineering Laboratory of the Department of Scientific and Industrial Research. This paper is published by permission of the Director.

References

(1) DOWELL, T. M. *N.E.L. unpublished report*, AB Div. No. 5/59.

(2) BILLING, B. F. *J. of the Roy. Aero. Soc.*, **58**, No. 523 (1954).

(3) DOWELL, T. M. *Engineering*, **185**, p. 693 (1958).

Appendix

Steady-state stresses arise in steady-state motions governed by the equation:

$$x = X_0 + \sum_{1}^{N} X_n \sin (n\omega t + \phi_n)$$

where X_0 is the static displacement giving rise to static strain and X_n is the amplitude of vibratory motion of the nth harmonic. If attention is confined to the periodic part of the motion, there exist three different conditions which lend themselves to slightly different measuring techniques. The first condition is the important case where parts are being excited at resonance (where dangerous fatigue stresses may exist). At resonance, the only harmonic of any real importance is the periodic motion to which the structure is resonating and, at or near this frequency, the strain cycle is not only periodic but is a very pure sine wave. The equatio of motion for this case is simply:

$$x = X_n \sin (n\omega t + \phi_n).$$

The second case of interest is the one in which only od harmonics are present. Let the positive half-cycle be x given by:

$$x_1 = X_1 \sin (\omega t + \phi_1) + X_3 \sin (3\omega t + \phi_3) + \\ + X_5 \sin (5\omega t + \phi_5) + \ldots$$

The negative half-cycle, x_2, is obtained by substitutin $(\omega t + \pi)$ for ωt. Therefore:

$$x_2 = X_1 \sin (\omega t + \pi + \phi_1) + X_3 \sin (3\omega t + 3\pi + \phi_3) + \\ + X_5 \sin (5\omega t + 5\pi + \phi_5) + \ldots$$

that is,

$$x_2 = - X_1 \sin (\omega t + \phi_1) - X_3 \sin (3\omega t + \phi_3) - \\ - X_5 \sin (5\omega t + \phi_5) - \ldots$$

Therefore, x_2 equals $-x_1$ and full information concerning the strain amplitude arising from such a motion is obtained from the peak-to-peak value of the wave or from the peak value of one half-cycle.

The third case of periodic strain is where even harmonics are present. As before:

$$x_1 = X_1 \sin (\omega t + \phi_1) + X_2 \sin (2\omega t + \phi_2) + \\ + X_3 \sin (3\omega t + \phi_3) + \ldots$$

and:

$$x_2 = X_1 \sin (\omega t + \pi + \phi_1) + X_2 \sin (2\omega t + 2\pi + \phi_2) + \\ + X_3 \sin (3\omega t + 3\pi + \phi_3) + \ldots$$

or:

$$x_2 = - X_1 \sin (\omega t + \phi_1) + X_2 \sin (2\omega t + \phi_2) - \\ - X_3 \sin (3\omega t + \phi_3) + \ldots$$

Therefore, x_2 does *not* equal $-x_1$ and full information concerning the strain amplitude arising from such a motion requires separate examination of the positive and negative half-cycles.

Determination of the profiles of water waves

By J. A. SANDOVER, B.Sc., Ph.D., and C. TAYLOR, B.Sc., Engineering Department, University College of Swansea, Singleton Park, Swansea

[*Paper received* 17 *November*, 1959]

Abstract

The capacitor type depth gauge, described in this paper, facilitates accurate recordings of the profiles of three dimensional water waves propagated in prismoidal open channels. The circuitry, principle and calibration of the gauge are outlined, with particular reference to the advantages of using standard industrial equipment.

Introduction

When waves are formed in laboratory open channels, the crest heights and trough depths of uniform and repetitive waves may be measured, with reasonable accuracy, using micrometer depth gauges fitted with sharp pointers. This type of depth gauge is of little value, however, when the waves are irregular, or if the complete wave profile is required. Floats have been used with moderate success, but the inertia of the float and scribing device is usually too large. This state of affairs induced the investigators of wave phenomena to consider the advantages of depth measurement which utilizes the electrical properties of the medium. A number of different electronic gauges have been developed, the two principal types being the resistance gauge and capacitance gauge. Some of the resistance gauges have been highly successful, notably those designed by Brebner,(1) Killen,(2) and Nougaro.(3)

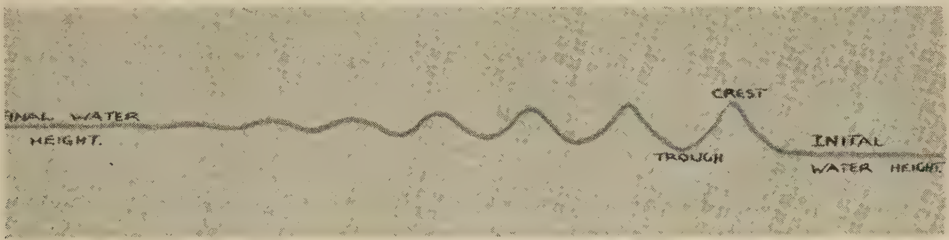

Fig. 1. Sample of wave record from oscillograph

The authors of this paper preferred the capacitance type gauge, as it entails the use of only one extremely thin probe. Polarization does not occur and the design of the circuitry does not appear to present greater difficulties than those involved in the circuitry of resistance type gauges. In fact, the major portion of the electronic apparatus used is standard industrial equipment, the gauge alone being of original design. Similar gauges have been developed by Tucker(4) and S.O.G.R.A.P.H., at Grenoble. The original gauge has already been described,(5,6) when it was applied to the determination of the profiles of waves in rectangular channels. Problems arose, however, when the gauges had to be adapted for use in prismoidal channels, and it is these gauges that are the subject of this paper. A very brief outline of the investigations and a description of the remainder of the apparatus will be included.

The depth gauge and standard equipment are used to record the longitudinal profiles and cross-sections of undular surge waves produced in a prismoidal channel. These waves are produced when a sudden sustained quantity of water is discharged into the channel, which contains an initial level of still water. The wave cross-section is obtained by compiling the records from a number of probes on and offset from the centre line of the channel.

Fig. 1 shows a typical recording of an undular surge wave using the apparatus which consists of the components shown in Fig. 2.

Construction of depth gauge

The depth gauge, Fig. 3, consists of a copper wire 0·0148 in. diameter, with a p.v.c. covering of overall diameter 0·031 in., which passes through a solid Perspex base. The lower end of the wire is knotted to prevent withdrawal, the tail fits into a recess in the underside of the base and is insulated using a proprietary insulating glue. The base is secured by means of screws to a slotted brass insertion in the bed of the channel. The upper framework of the gauge consists of four Perspex supports (outstands, Fig. 3*F*) fixed to a central Perspex block. These outstands are joined in pairs by aluminium plates and rest on the tops of opposite sides of the channel.

A brass rod passes downward through the upper Perspex block and is threaded into a small Perspex cylinder which supports the central wire of the depth gauge. The wire passes diagonally through the cylinder and is either knotted

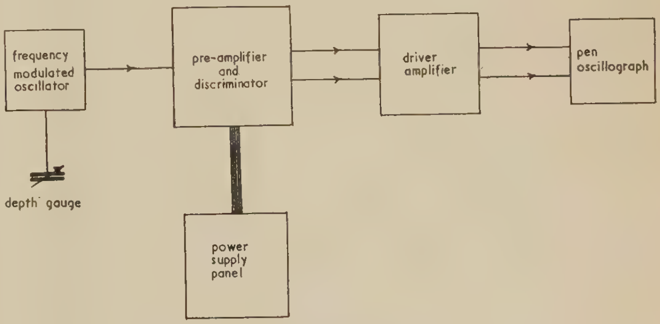
frequency modulated oscillator
pre-amplifier and discriminator
driver amplifier
pen oscillograph
depth gauge
power supply panel

Fig. 2. Diagrammatic representation of the detector and recording circuit

or bent downwards to prevent withdrawal. The wire is tensioned by turning a nut, threaded on the rod, against the upper surface of the block. The free end of this wire is attached to the terminal of a coaxial socket fixed to the upper surface of the Perspex block.

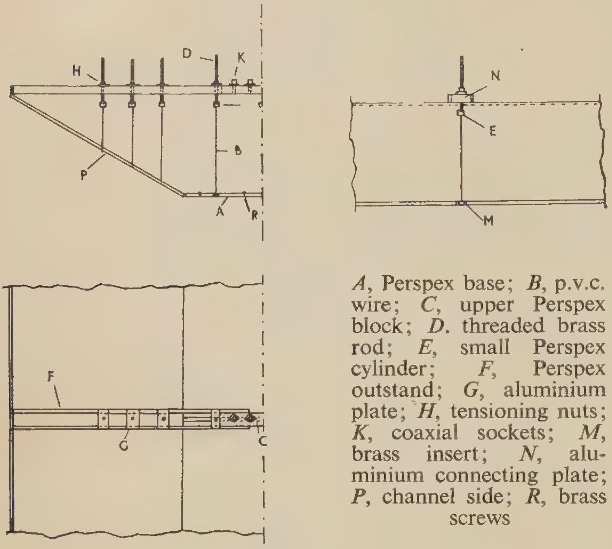

A, Perspex base; *B*, p.v.c. wire; *C*, upper Perspex block; *D*. threaded brass rod; *E*, small Perspex cylinder; *F*, Perspex outstand; *G*, aluminium plate; *H*, tensioning nuts; *K*, coaxial sockets; *M*, brass insert; *N*, aluminium connecting plate; *P*, channel side; *R*, brass screws

Fig. 3. Depth gauge

The probes which are offset from the centre line of the channel are tensioned in a similar manner, the tensioning nut bearing on the aluminium plates fixed to the outstands. These wires pass through similar Perspex cylinders and thence to the terminal of a coaxial socket. Holes are drilled through the sloping sides of the channel so that the relevant gauge wires can be secured and insulated in air, the tension being applied as before. This arrangement of the probes or wires of the depth gauge is used to obtain the cross-section of a wave at any point along its length, as well as the longitudinal profile at various distances from the centre line of the channel.

One coaxial socket is connected to a frequency modulated oscillator (M.700), which employs a nominal carrier frequency of 2 Mc/s, and has a linear frequency range 0 to 30 kc/s. The output from the oscillator is connected to a pre-amplifier (M.R.220), embodying a frequency modulated system with a conventional frequency discriminator and a double diode rectifier. The output from the discriminator is directly proportional to the oscillator output frequency variation and the oscillator input capacitance, within the limits of its full range of 0 to 10 V. The pre-amplifier, which has a total capacity range of either 800 or 200 pF, and the oscillator obtain their h.t. supply from a power supply panel (M.R.202) connected directly to the pre-amplifier. The supply stability is better than 0·1% under all normal mains fluctuations, an essential requirement if zero drift is to be avoided.

A driver amplifier (M.R.209), which has a maximum gain of 850, a linear output swing of 400 V and response of 0 to 30 kc/s, provides the necessary amplification of the d.c. voltage from the pre-amplifier, and the resulting signal is recorded by a pen oscillograph (M.942), which has a linear frequency response of 0 to 55 c/s and a maximum swing of 300 V, both of which are well within the limits required.

The (M.942) pen oscillograph is used in preference to an oscilloscope as the frequency response is adequate, and an immediate permanent record is obtained; other advantag of this equipment are zero stability and good sensitivit Undesirable effects, which are almost invariably associat with high amplification, are kept to a minimum and th characteristics of the frequency discriminator are almc linear when correct "setting up" adjustments have bee made. Further, although the oscillator has to be plac within 20 ft of the depth gauge, the remainder of th equipment may be situated at some distance away.

The five pieces of apparatus, oscillator, pre-amplifie power supply panel, driver amplifier and pen oscillograp are manufactured by Southern Instruments Ltd. and a standard commercial models.

Principle of depth gauge

The copper wire and the water form the two plates and th p.v.c. covering the dielectric of a capacitor. A change the depth of the water induces a corresponding change the overall capacitance of the capacitor. These fluctuatio give rise to variations in the signal frequency transmitted the discriminator from the oscillator. The resulting d. voltage variation from the discriminator is amplified an applied to a pen oscillograph. If the gauges have bee calibrated the oscillograph record represents the variation c the water depth at the gauge. It is assumed that a sho length of the record will represent the wave profile at particular instant at the gauge.

When performing a static gauge calibration it is of gre importance that a sustained effect should produce a sustaine deflexion on the pen oscillograph, otherwise accurate dynami recordings cannot be obtained. If an alternative electric system involving a time constant is used, where the deflexio decreases while the effect is sustained, this characteristi would be a serious shortcoming in these investigations. static calibrations can be successfully carried out, the overa characteristics of the system may be studied to detect non linearity and hysteresis, and to ensure the accurate repro duction of low frequency variations encountered in th measurement of undular surge wave profiles.

Calibration of depth gauge

The datum of the static calibration is undisturbed wate level, which is maintained for a suitable instrument "warmin up" period, usually 8 to 10 h, to ensure consistent results A micrometer depth gauge, fitted with a sharp pointer, i used to measure the initial water depth. When contact i made between the pointer and the water an electrical circui is completed (Fig. 4), which results in the deflexion of on pen of the pen oscillograph. The zero position of the secon oscillograph pen, which is connected to the probe, is chose to indicate datum level, and the pointer is raised 0·1 in. Th paper speed is then adjusted to 1 mm/s, and a gradual influ of water is fed into the channel. The instant of contac between the water and point gauge is indicated by th deflexion of the first pen and the rise of 0·1 in., is represente by the deflexion from zero of the second pen. The micro meter gauge pointer is again raised 0·1 in., and the proces repeated, the influx of water and the traverse of the pape being continuous, until a suitable calibration curve is obtained A steady discharge from the channel enables a calibratio curve to be plotted as the water depth decreases. Bot curves are found to be linear and the discrepancy less tha 1%. This is probably due to the increased meniscus effect on the gauge wire as the depth of water is decreased. I addition, it has been checked that identical calibration curve are obtained when the water level is kept constant and the depth gauge is respectively lowered or raised.

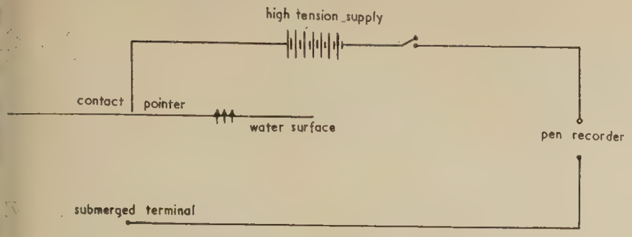

Fig. 4. Electrical circuit for gauge calibration

Under certain conditions (which fortunately did not prevail in these investigations) unless suitable precautions, such as the screening of the probe, are taken, the characteristics of the gauge may not be linear.

The accuracy of the calibration may be checked photographically for any type of wave or by the use of the micrometer screw gauge to check the first wave crest height. The maximum differences between the electrical recording and the other two methods are found to be less than 2%. These differences are probably due to a combination of experimental errors, parallax and meniscus effects.

Conclusion

The gauges are easily manufactured, inexpensive, reliable and need little attention. In addition, the gauge wire has such a small overall diameter that the surface disturbances are negligible. The present design of the depth gauge may be readily adapted for use in a channel or waterway of any cross-section. "Setting up" and calibrating techniques are simple, effective and an immediate permanent record is made. The equipment is reliable and consistent results have been obtained. This apparatus has been assembled by the authors in connexion with their investigations into the behaviour of undular surge waves in prismoidal channels at the University College of Swansea.

References

(1) Brebner, A. *J. Sci. Instrum.*, **34**, p. 506 (1957).
(2) Killen, J. M. Technical Paper, 11B, Univ. of Minnesota, Hydraulics Laboratory.
(3) Nougaro, J. Thésis Presentées a la Faculté des Sciences de L'Universite de Toulouse (1952).
(4) Tucker, M., and Charnock, H. Fifth Conference on Coastal Engineering, Grenoble (1954).
(5) Sandover, J. A. *Water Power*, **9**, p. 213, June 1957.
(6) Sandover, J. A., and Zienkiewicz, O. C. *Water Power*, **9**, p. 418, November 1957.

Instrument for recording the resistance during the deposition of a thin film

by J. A. BENNETT, B.Sc., Grad.Inst.P., and T. P. FLANAGAN, M.Sc., A.Inst.P., A.M.I.E.E.,
British Scientific Instrument Research Association, South Hill, Chislehurst, Kent

[*Paper first received* 11 *November, and in final form* 7 *December*, 1959]

Abstract

The instrument described enables a decrease in the electrical resistance of a metallic film to be followed during the deposition of the film. This is achieved by recording the instant at which certain fixed resistance values are attained. When one balance point is reached the value of the reference resistance in one arm of a Wheatstone bridge is changed to the next balance point by a uniselector actuated by a valve amplifier.

In connexion with an investigation into the electrical properties of vacuum deposited thin films, it was required to observe the decrease in electrical resistance of a film during its growth. The films were deposited upon an insulating substrate and the resistance was measured between two contacts that had previously been attached to the substrate surface. Initially the resistance was very high, but as the condensation proceeded the resistance decreased, rapidly at first and then more gradually. It was required to measure the change in resistance over the range 10 MΩ to 10 Ω at a constant value of the applied potential.

Resistance values can be continuously measured over a range of several decades by utilizing a thermionic diode with the anode maintained at a negative potential with respect to the cathode. Such a system will require an accurately stabilized power supply to prevent serious zero drift.

For this reason, in the present system it was not attempted to obtain a continuous trace of the variation of resistance with time, but rather to record the instant at which certain resistance values were obtained. This enables a resistance/time curve to be constructed. The number of balance points that can be obtained with the present system is 25 and these balance points must be separated by a time interval in excess of 35 μs. These limitations are not serious in the application for which the apparatus was constructed. An advantage of the present system is that the pen recorder acts only as an event marker and the magnitude of the deflexion is not a function of the resistance under investigation.

The apparatus, illustrated in the figure, can be considered as being a simple servo-system, consisting of a transducer, an amplifier and a feed-back control system.

The transducer is a Wheatstone bridge circuit, consisting of the two fixed ratio arms, the resistance of the film under investigation and in the fourth arm of the bridge a chain of resistors, the values of which are determined by the values for which balance points are required.

Initially, the resistance across the surface of the substrate, before the deposition of the film, is very large. The value of the resistance in the fourth arm of the bridge is set to the value for which the first balance point is required. The potential difference between A and B is a function of the difference in resistance between the film and the first balance point. This out-of-balance potential between A and B is amplified and used to actuate a high-speed relay. During the deposition of the film the value of its resistance decreases, and when it becomes equal to the first balance point, the

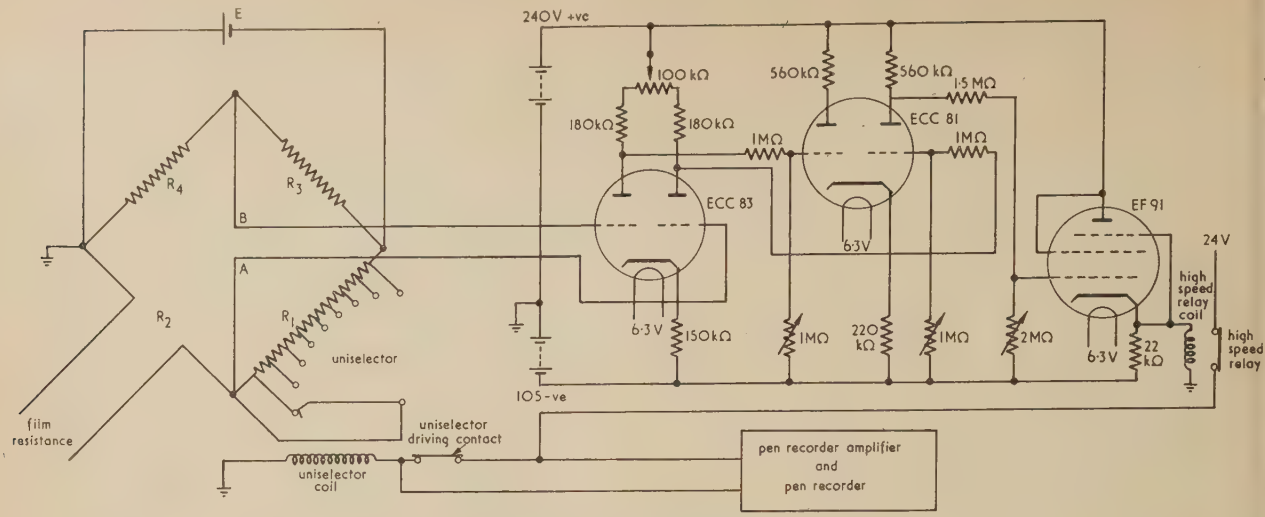

Circuit diagram of apparatus

potential between A and B is zero, the output from the amplifier is also zero. As the output from the amplifier falls to zero the relay is de-energized, which produces a signal that is recorded on the trace of a pen recorder; at the same time it actuates a uniselector which reduces the value of the resistance in the fourth arm of the bridge to the second balance point. The bridge is now out of balance, and a potential exists between A and B which is amplified and hence re-energizes the relay.

An analysis of the bridge circuit shows that the sensitivity of the bridge is independent of the value of the balance resistance, provided the balance resistance is less than the input impedance of the amplifier. It can also be shown that the sensitivity is greatest at the balance point, which is a desirable condition.

The amplifier is a conventional differential d.c. amplifier using long tailed pair triodes with consequent high rejection for in-phase signals. The two input grids A and B of the amplifier are connected to the detector terminals of the bridge. No attempt was made to obtain a high degree o linearity of output since the output is used to actuate relay, and the uniselector changeover action only occur when the amplifier output is approaching zero. The outpu is derived from a cathode follower stage. The amplifier i balanced initially by adjustment of the 100 kΩ variabl resistor in the anode supply to the first stage.

The relay actuated by the cathode follower circuit was hermetically sealed high-speed relay. The uniselector was standard G.P.O. type with five banks of 25 contacts. It wa driven by means of its own make and break contacts whic were also used to produce the event marker pulse.

The time required to actuate the high-speed relay and rese the uniselector was 35 μs. It is considered that if the standar G.P.O. uniselector was replaced by a miniature uniselector the speed of operation could be increased.

The event marker pulse generated by the uniselector contact was recorded on a four-channel recorder that could be operated at either 2 or 4 in./s.

Improved smoke density recorder

by R. LAMBIE, Fuel Research Station, Blackwall Lane, Greenwich, London

[*Paper first received* 23 *May, and in final form* 15 *December*, 1959]

Abstract

A smoke density recorder is described in which high stability is achieved by the use of stabilized circuits for the light source and head amplifier. A method of calibration by means of optical-density screens standardized for the type of photocell used is given. Drift caused by deposition of smoke on the optical system was overcome by the use of hot air jets. During extended tests on laboratory and industrial installations, stable operation with negligible drift was obtained.

Smoke-meter requirements

DURING an investigation concerned with the amount of smoke emitted from the stack of a hand-fired Lancashire boiler, accurate readings were required of the amount of smoke emitted over long periods. To carry out this investigation, it was necessary to use a smoke meter that would meet the following requirements:

(1) there should be no appreciable drift in the amplifier over long periods;

(2) the light source should remain constant over long periods;

(3) the control panel should be remote from the photocell at least 150 yards distant;

(4) there should be the facility for calibration with optical-density screens over a wide range.

As no instrument existed which was able to meet all these requirements, the instrument described below was developed.

Description of instrument

The complete instrument consists of a light source, a photocell and head amplifier, which enables the amplified photocell signal to be fed to a recorder over long distances without measurable losses. The voltages supplied to the head amplifier are stabilized and the light-beam source is controlled by a constant-voltage transformer. In the tests carried out on the Lancashire boiler stack, the light source consisted of a 6 in. parabolic mirror and a 6 V, 24 W bulb. To obtain accurate focusing, the mirror was made adjustable, and the beam was projected through a glass screen, along a 4 ft length of tubing, 2 in. in diameter with a 2 ft gap in the centre (see Fig. 1). This enabled a sensibly parallel beam of light to cover a 2 ft column of smoke, and also cut down eddy currents of smoke which caused deposition on the glass screens shielding the optical system. Finally, the beam passed through a lens and was focused on to the cathode of the photocell. The photocell was of the vacuum type with a caesium/silver-oxide cathode, this cell being chosen because it has a linear response to light intensity, and its output is independent of the applied voltage. The photocell was coupled to a double-triode head amplifier, which enabled the amplified photocell current to be fed into the control panel at a distance. In these tests, a cable 200 yards long was used. As the valve amplifier registers voltage changes, it will be seen that any variations in the supply voltages to the anode of the amplifier valve or heaters will be recorded on the instrument which records the smoke density and would therefore give a false measurement. To overcome this, a voltage-stabilized power supply was essential.

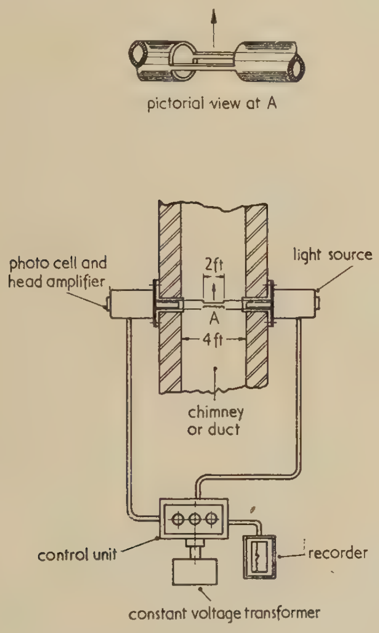

Fig. 1. Diagrammatic arrangement of smoke meter

In the circuit shown in Fig. 2, a constant-voltage transformer is connected between the supply mains and the stabilizer input. This transformer stabilizes the heater supply to the valves of the amplifier and stabilizer. Briefly the operation of the stabilizer circuit is as follows. The smoothed, d.c. voltage from the rectifier circuit flows through the valve V_1 across which the voltage drop is determined by the grid-to-cathode potential. This voltage drop is used to control the output voltage. The valve V_2 has its cathode potential held constant by a neon stabilizer, whilst the grid observes any fluctuations in the output voltages (nominally +210 V). In this way, an amplified correction voltage appears across the resistance R_1, and is applied to the grid of valve V_1 in a manner which materially reduces the voltage change which would otherwise be caused by either fluctuations in mains voltage or variations in the current drawn from the stabilized supply. The regulated voltage is then fed to a "Stabilivolt" neon tube, which acts as a potential divider, where voltages for the amplifier and photocell are taken off.

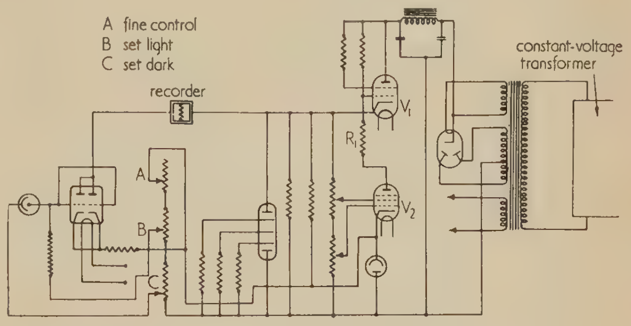

Fig. 2. Circuit of photocell amplifier and power pack

Construction and assembly

The instrument consists of three units: the head amplifier, the light source and control unit which contains the stabilized voltage pack, and the recorder. The head amplifier unit consists of the photocell, valve amplifier and resistance chain. The whole is enclosed in a small metal cabinet, at the front of which is mounted a lens, which focuses the light beam on to the photocell cathode. The amplifier unit is mounted on a movable platform which is easily removed for servicing and enables the beam to be accurately focused on to the photocell. The resistance chain which is mounted underneath the platform is encapsulated in epoxy resin, to prevent any skin effects caused by moisture affecting the resistance of the chain. All connexions from the amplifier are taken to a terminal strip and from the strip to a six-pin socket. A six-way cable is taken from a plug at the rear of the cabinet to the control unit. The control unit houses the stabilized voltage pack and the variable resistances for the "set light" and "set dark" positions. The recorder is fed from the six-pin plug. The control unit is fed by a constant-voltage transformer. The light source is contained in an airtight box and, when the back of this box is removed, there is access to four centering screws for focusing the bulb in the parabolic mirror. A measure of control of light intensity is provided by a 10 Ω rheostat wired in series with the lamp in the secondary winding of a low-voltage, constant-voltage transformer.

Mounting on stack. In order to measure the smoke at a representative position the instrument was mounted on the stack at a distance of approximately five diameters from the point at which the flue gases enter the stack.

Calibration of instrument

The instrument was calibrated by means of neutral-density filters, which consist of gelatine sheets impregnated with varying amounts of graphite, the gelatine sheet being cemented between sheets of glass. Since a caesium/silver-oxide photocell is most sensitive to radiation in the red and infra-red region of the spectrum, it is considered essential that the optical density of the filters are determined for the particular light source and the photocell used. The filters themselves were calibrated at the N.P.L. for a tungsten light source and a caesium/silver-oxide photocell. It is assumed that the small changes in the light source used to set the zero of the instrument, and the ageing of the photocell do not affect the calibration of the filters to any appreciable extent.

The instrument was set up so that with a clear chimney (that is, no smoke), the reading on the recorder was zero. This was carried out by means of a variable resistance which controls the bias voltage to the amplifier valve. The light was then obscured from the photocell and a second variable resistance which controls the photocell voltage was adjusted until the recorder reads to its upper limit of 10 mA. The instrument was then ready for use, a final check on the set-zero position being made by means of a third variable resistance which acts as a fine control for the set-zero.

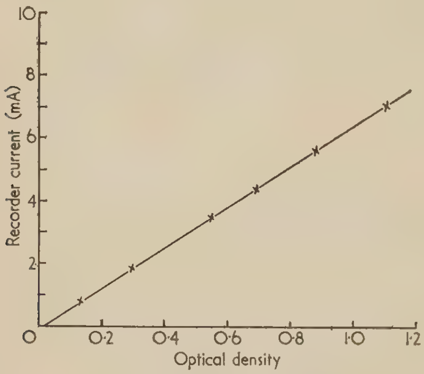

Fig. 3. Instrument calibration

In all the tests, a calibration of the instrument with optical-density screens was made every day during each boiler tests. A calibration typical of readings taken over a three months' period is given in Fig. 3. To check variation of the light source, an optical screen of 0·68 density was inserted in the light beam and correction was made to 4·4 mA on the recorder; any variation that was noted was found to result from deposits on the glass screens.

Special tests on a Lancashire boiler

In tests carried out on a Lancashire boiler to determine the correlation of optical density with the concentration and composition of the smoke emitted, the instrument was connected to a duct 1 ft in diameter and the smoke was drawn through the duct by means of a fan. It was possible with the shorter light path, to use a more accurate type of light beam. In this method, the light from a 6 V, 24 W bulb was focused by a lens on to an opal glass screen, which covered an aperture $\frac{1}{32}$ in. in diameter in a metal plate and thus ac as a point source. The light from this source passes throug a second lens placed at a distance equal to its focal lengt from the aperture, giving a sensibly parallel beam 1 in. i diameter. The function of the opal glass screen is to diffus the filament image. It was found possible in these tests o the duct to eliminate the effect of dust deposition by passin a jet of hot air at a temperature of 100° C over the surfac of windows which were sealed into the side walls of the duc and flush with their surface. A diagram of the light sourc is shown in Fig. 4.

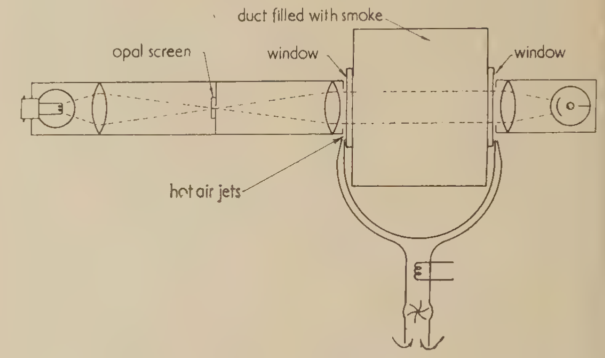

Fig. 4. Section of horizontal test duct

Conclusion

Tests were carried out on the equipment to ascertain the effectiveness of the voltage stabilization. For these tests, a variable auto-transformer was inserted in the input to the supply mains. Variations of input voltage between 190 and 250 V were made and no change in output voltage could be detected. To measure drift, the apparatus was set up with a neutral-density filter in position in the light path, its optical density being such as to give a reading about half full-scale deflexion. When the instrument was allowed to run for a period of 24 h, the drift recorded in the output was negligible, being less than 2%.

The constancy of the light source and the stability of the amplifier (or the absence of drift) have been confirmed by practical operation with the equipment installed in a number of industrial boiler stacks. It is important to note that, unlike most commercial instruments, the method of amplification adopted in this system enables the recorder to be installed at long distances from the photocell unit. In some installations, the instrument has been situated over 200 yards from the photocell unit without any inaccuracy occuring as a result of changes in the impedance of the lead arising from changes in humidity or other atmospheric conditions.

The instrument described was developed as part of the program of the Warren Spring Laboratory of the Department of Scientific and Industrial Research and this paper is published by permission of the Director. The illustrations are Crown Copyright and are reproduced by permission of the Controller H.M. Stationery Office.

Electronic leak detector

by D. J. Dowling, Ph.D., Mining and Chemical Products Ltd., Alperton, Middlesex

[*Note first received* 3 *July*, 1958 *and in final form* 8 *January*, 1960]

For a rough indication of the degree of vacuum in a glass vacuum system, and for the detection of pinhole leaks, a Tesla discharge is commonly used. It is not, perhaps, generally realized that an electronic high-voltage generator of the high-frequency transformer type can be conveniently used as a leak detector. Such an arrangement has often been used to supply e.h.t. for a television cathode-ray tube and, for this resaon, coils of this type are easily obtainable. Any conventional circuit is suitable, and the actual one used is shown. The electronic components used were of the normal radio type. Suitable radio-frequency e.h.t. transformers are advertised regularly in the technical press. The coil used had a rated output of 10 kV which seems to be sufficient in this application.

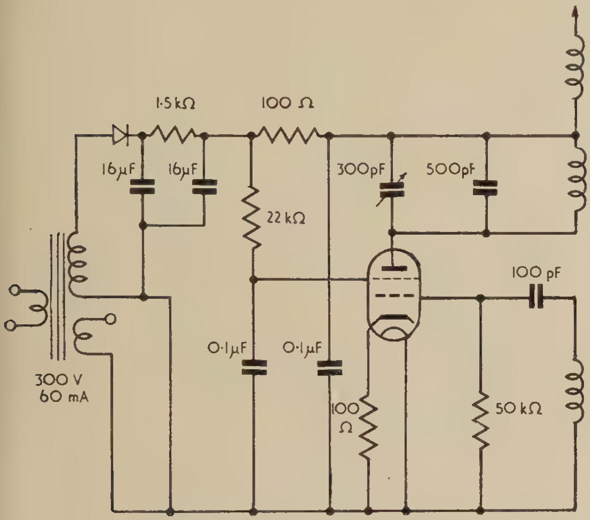

Circuit diagram of leak detector

The power unit, consisting of a half-wave rectified supply, is entirely orthodox. A single transformer supplies h.t. voltage to the oscillator valve, and a 6·3 V supply to the valve heater. The output required is about 350 V at 30 mA. Good smoothing is not important.

The oscillator circuit is simpler than that necessary for a cathode-ray-tube power supply. No rectification of the output is necessary. The oscillator valve used was a tetrode type 6V6 (by Brimar) but the 6L6 or more modern equivalents are suitable.

The unit was made in two sections each on a separate chassis. One carried the power supply, while the other carried the oscillator circuit, and could be held in the hand to make it possible to probe for leaks and, at the same time, to keep the high voltage lead down to the shortest possible length. This is necessary, as it is very difficult to insulate. In general, insulation of the high voltage coil must be good. In the unit constructed, Perspex was used and proved to be satisfactory.

The setting up of the circuit is straightforward. The oscillator is tuned by varying C5 to give the largest possible spark discharge. The condenser can be of the preset type, as further adjustment is not necessary.

Filament winding machine

by D. Barker, Vacuum Coating Laboratory, Edwards High Vacuum Ltd., Manor Royal, Crawley, Sussex

[*Note received* 13 *January*, 1959]

The vacuum evaporation of metals has become an established process requiring the production of large numbers of tungsten wire heaters. A small machine has been constructed in this laboratory for making helical and basket filaments from stranded tungsten wire.

The heating elements are made from several strands of 0·5 mm diam. wire twisted together at a temperature of 100° C because it has been shown by Strong* that non-crystallized wire has a maximum ductility at this temperature. The usual method of preparing filaments has been to twist the wire strands with a hand-brace, whilst heating the wires with a gas flame. The stranded wire is then reheated whilst winding into the desired form on a mandrel. The intense heating by the flame may result in oxidized and brittle filaments which have a greatly reduced working life. A small winding machine is described here in which the tungsten wire is electrically heated by a 12 V power supply controlled with a Variac transformer.

The winding machine is shown in schematic drawing in the figure which is self-explanatory. To prepare the stranded wire, three 75 cm lengths of 0·5 mm tungsten wire are connected to the adaptor (*a*), the other ends being held taut in the hand-set. The power supply is switched on and the current set to about 20 A, which heats the wire to about 100° C. After preparation, the stranded wire is cut into lengths corresponding to a particular type of filament and wound on one of the different types of mandrel. The power supply output voltage must be reduced to suit the needs of the smaller wire length. While the filament is being formed the wire must be held taut

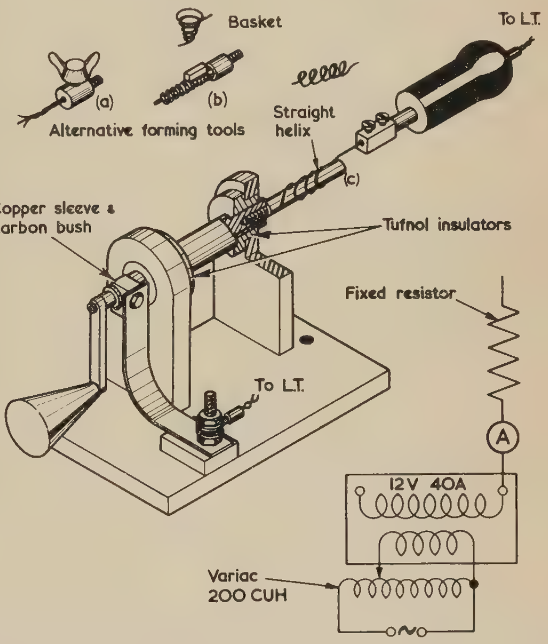

Apparatus for winding filaments for vacuum evaporation with the hand-set to ensure accurate forming on the mandrel. If the surface of the mandrel is not electrically insulated the heating current tends to rise as the free length of wire shortens. Undue change in current can be prevented by fitting a resistor in the l.t. output as shown in the figure.

---

* Strong, J. *Modern physical laboratory practice*, p. 444 (London: Blackie and Son, 1944).

Acknowledgements are made to Edwards High Vacuum Ltd., for permission to publish this letter.

Determination of the density of glass fibres

by Beryl D. Coates, Pilkington Brothers Ltd., Research Laboratories, St. Helens, Lancs.

[*Note received* 26 *October*, 1959]

The measurement of glass fibre density to an accuracy of 1% would appear to be straightforward, because all that is necessary is a knowledge of mass and volume. The method of obtaining the mass requires no discussion, but the measurement of volume is difficult because of the small diameter of the individual fibres which is of the order of 20 μ. It is possible to calculate the volume from the dimensions, but the degree of precision required in the diameter measurement, and the number of such measurements necessary along the length, make this method both difficult and laborious. A modification of the density-bottle method has been used to overcome this difficulty.

The use of a density bottle in the normal manner with a bundle of fibres gave erroneous results because of the air which was trapped with the fibres. These bubbles were extremely difficult to remove, but the problem was solved by displacing the air in the bottle by a gas which was soluble in a suitable liquid. In this case, the air was displaced by carbon doxide and a solution of potassium carbonate, approximately 0·1 Normal, was used as the liquid. A preliminary test was carried out on the effect of "dissolved" carbon dioxide on the density of the liquid by "dissolving" a bottle of carbon dioxide in its own volume of potassium carbonate solution. It was found that the increase in density was less than 0·05%. Because most of the gas was displaced and not "dissolved", when fibre density was measured, this factor was neglected.

A bottle made of fused silica was used so that volume changes with temperature were small, and the temperature of the liquid was noted immediately after each weighing so that the appropriate density could be applied. Errors arising from evaporation were minimized by using a semi-automatic balance, with which rapid measurement was possible.

The following results have been obtained on E- and sheet-glass fibres of various diameters:

Fibre density of E-glass = 2·56 g/ml. ± 1%,
Fibre density of sheet-glass = 2·47 g/ml. ± 1%.

No change in density could be detected with changing diameter over a range of 10–40 μ. The diameter was varied only by changing the speed of drawing, the bushing temperature remaining constant.

The permission of the Directors of Pilkington Brothers Limited to publish this note is gratefully acknowledged.

Protection of diffusion pumps against inadequate cooling

by B. C. Cox, B.Sc., Ph.D., A.R.I.C., Welsh College of Advanced Technology, Cathays Park, Cardiff

[*Note received* 16 *November*, 1959]

Inadequate cooling of diffusion pumps either by failure of the water supply or gradual choking of the circulation system is an unwelcome hazard in the operation of high vacuum systems. Only one device[(1)] has been described which w give foolproof protection against choking and the cessatio of water supplies, whilst several[(2–5)] pressure operate mechanisms have been used which give protection on against failure of the supply of cooling water.

This note describes an easily constructed pressure operate device which will give protection against both possibl circumstances, and which, because of no water spillage danger, does not need to be mounted away from electrica equipment.

The figure shows that the apparatus consists of a mercury filled U-tube manometer with one closed limb. To each limb is attached a mercury cup and tungsten through Pyrex electrical connexion. In operation, water from the diffusion pump P passes through the impedance I and when the flow is adequate the pressure developed at the junction of P and I raises the mercury in the closed limb so that an electical connexion is made between A and B. Total failure of the water supply and choking of the diffusion pump cooling system will cause this pressure to fall with a consequent break in the electrical circuit at a. An increase in the pressure will result from a blockage or choking of I, and will cause the electrical circuit to be broken at b.

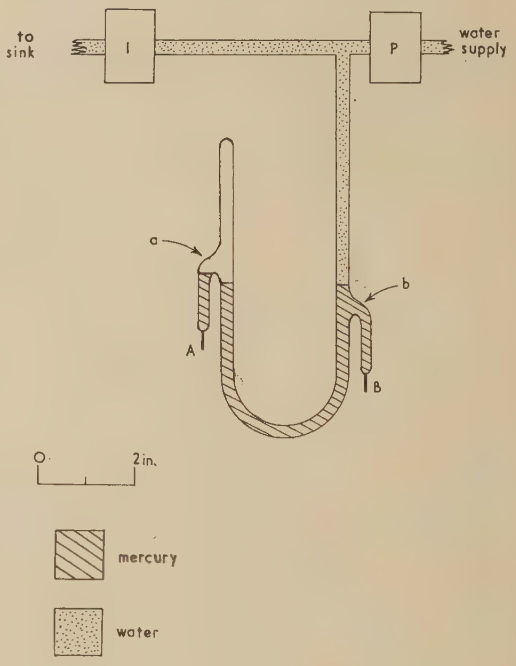

Closed manometer water relay

In the apparatus in use I consists of a length of rubber pressure-tubing fitted with a conventional screw clip. With a water supply head corresponding to 35 cm of mercury, and I set to limit the flow through two Edwards type 102 oil diffusion pumps to 600 ml.min^{-1}, the electrical circuit is broken when the flow falls below 500 ml.min^{-1} due to choking of P or I or water supply failure.

The water supply used is also subject to pressure transients when other taps in the building are operated. To prevent these tripping the relay energized through the contacts A and B a large capacitor is connected across the relay coil so that the relay contacts do not open unless the electrical circuit is broken for at least 3 seconds.

REFERENCES

(1) Poole, J. H. J. *J. Sci. Instrum.*, **20**, p. 49 (1943).
(2) Croft, P. G. *J. Sci. Instrum.*, **25**, p. 386 (1948).
(3) Houghton, G. *J. Sci. Instrum.*, **33**, p. 199 (1956).
(4) Green, G. W. *J. Sci. Instrum*,. **35**, p. 147 (1958).
(5) Preston, J. *J. Sci. Instrum.* **36**, p. 98 (1959).

Electromechanical low frequency oscillator

by E. W. Dickson, B.Sc., Ph.D., A.Inst.P.,* Tube Investments Research Laboratories, Hinxton Hall, Cambridge

[*Note first received* 20 *November, and in final form* 30 *December*, 1959]

An electromechanical oscillator (0·1–0·001 c/s) has been constructed which is comparatively simple and, though it has certain limitations, produces a waveform which differs in amplitude by less than 1% from a true sine wave. The sinusoidal output signal is derived from a mechanical simulation of the definition of a sine wave, namely, the projection on to a diameter of a circle of a radius rotating at constant angular velocity. A slider is constrained in such a manner that its movement along its bearing rods is exactly equal to the projection of a fixed radius of a constant-speed driving wheel in the direction of the bearing rods. The sinusoidal linear motion of the slider is then converted into a sinusoidal angular motion which is applied to the contact arm of a rotary potentiometer.

The essential details of the mechanical construction are illustrated in Fig. 1. The driving wheel is driven by a synchronous motor through a potter's wheel and stepped gear-box. This system provides continuous regulation of the speed of the driving wheel between the motor speed M and $M/125$. The driving wheel carries a pin on which is mounted a ball race. The slider is maintained in contact with this ball race by a spring placed between the end of an extension arm attached to the slider and a collar on the pin which supports the ball race. The spring suffers maximum extension when the pin is vertically above or below the axis of the driving wheel. The variation in spring tension produces a cyclic loading of the gearing and to reduce the magnitude of this effect an extension arm is fitted to the slider and the spring length increased. The slider carries a rack which engages a spring-loaded pinion coupled directly to the potentiometer shaft. The spring-loaded pinion eliminates backlash between the slider and potentiometer contact arm. Any rotary potentiometer can be fitted to this apparatus but, to reduce the magnitude of the discontinuity as the contact arm moves from one turn of the resistance wire to another, the product of the radius of the toroid and the number of turns of resistance wire per unit length of its circumference must be large. The output signal is obtained directly from the contact arm when a d.c. supply is connected to the ends of the potentiometer resistance.

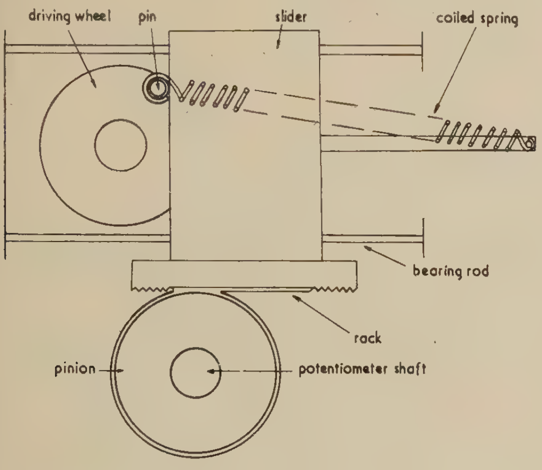

Fig. 1. Mechanical construction

To record the waveform for analysis the output of the oscillator was applied to a potentiometric pen recorder having an 11 in. wide chart and an accuracy of ±0·2%. Arbitrary axes were drawn on a portion of the chart record as shown in Fig. 2. Points corresponding to a true sine wave were calculated and plotted on the same graph. The total deviation from the calculated curve was found to be always less than 1% of the zero-to-maximum amplitude of the signal. The waveform was very smooth except in the neighbourhood of the peaks where a stepwise change in output signal was just resolved. The stepwise variation of the output signal results partly from the discontinuous nature of the potentiometer resistance. The total error from this effect and the accuracy of the recorder could account for the stepwise changes observed and the slight flattening of the signal peaks. The frequency of the output signal was dependent on mains frequency and, making due allowance for this factor, no change in the output waveform has been observed over periods of several hours.

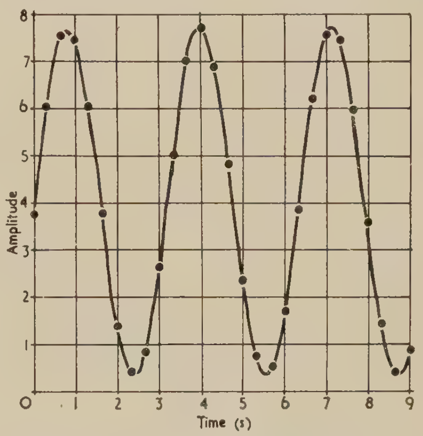

Fig. 2. Pen-recorder trace of output waveform

The complete oscillator which is compact and relatively simple to construct has been built into a case 12 × 9½ × 6½ in., which includes sufficient space for a battery to be used as the d.c. source. By suitable choice of potentiometer and supply voltage, a sinusoidal waveform can be obtained of any desired amplitude and source impedance in the frequency range 0·1–0·001 c/s. It has been shown that the deviation of the waveform from a mathematically true sine wave can be reduced to less than 1% of the signal amplitude. This level of distortion compares favourably with much more complicated, purely electronic oscillators. A variety of output waveforms can be obtained over the same frequency range by replacing the driving wheel by suitably shaped cams.

The author wishes to acknowledge the valuable assistance of Mr. H. Nightingale in constructing this device and to thank the Chairman of Tube Investments Ltd. for permission to publish this paper.

---

* Now at Associated Engineering Limited, Leamington Spa, Warwickshire.

New instruments, materials and tools

The Editor invites manufacturers of instruments and light machine tools to keep him informed of their new or improved products. The Institute of Physics assumes no responsibility for the statements given below: information for these has been taken from literature supplied.

Thermo-switch. A. M. Lock and Co. Ltd., 79 Union Street, Oldham, Lancs.

The temperature elements of this thermo-switch are interchangeable and very sensitive. Each consists of a platinum winding housed in a stainless steel tube, which can be located remotely from the control unit.

The instrument is designed to maintain temperatures at a pre-set value, and gives immediate relay action for any tendency to deviate from this value. A variation will result in the platinum "sensing" element producing an out-of-balance signal in the electrical bridge network. This will be either in or out of phase with the bridge voltage, depending upon the sense of the temperature change. The signal is then amplified and applied to a phase-sensitive detector; this, in turn, operates a heavy duty relay, making or breaking it according as to whether the measured temperature is lower or higher than the pre-set position of the control knob.

It is stated that this instrument has the following features: (*a*) a long-term calibration accuracy, (*b*) operates when the temperature varies by ±0·1% of the range span covered by the instrument; (*c*) a temperature range from −200 to +500° C; (*d*) an alarm operating on the high- or low-temperature side as required, or when there is any component failure.

The instrument has a plug-in electronic chassis for easy and rapid replacement. The terminal panel is robustly designed and easily accessible, and there is a locking device to prevent unauthorized interference with the controls.

Low voltage soldering iron. Electrical Remote Control Co. Ltd., Harlow, Essex.

The range of type SMS "Sub-miniature" soldering irons are rated at 10, 15, 20, 25, 40, 55 and 75 W and are conveniently fed from an 80 VA, 230 V transformer built into the primary side, which is also supplied by the firm. The weight of the tool with the copper bit is 1 oz. There is a range of 20 standard types of exchangeable copper bits with $\frac{1}{16}$–$\frac{5}{16}$ in. diameter tips. The makers state that, with suitable bits, gauge 10 brass sections can be soldered.

Electric oven. Stabilag Co. Ltd., Mark Road, Hemel Hempstead, Herts.

A high-grade refractory brick lining is used on the interior of the oven, except for the internal surface of the vertically sliding door which is faced with Marinite. Behind the brickwork is a secondary thermal insulation consisting of 3 in. thick slabs of caposil. Further insulation is provided by an air space between the Caposil and the metal sheathing of the oven. Air-space insulation is also used in the observation window of the door, which consists of two layers of quartz. It is claimed that a temperature of 1000° C in a volume of $4\frac{1}{2}$ ft^3 is obtained with an electrical loading of 12 kW. Th whole unit stands on a folded and welded steel base. Th central portion includes a control panel which gives a easy view of the controls from a standing position. On th sides of the oven are two terminal covers through which is possible to withdraw all the heating spirals. The spira themselves are high-quality resistance wires which fit in grooves in the base of the refractory brick lining.

Digital-reading slide-wire potentiometer. Howell Instrume Co., 3101 Trinity Street, Fort Worth 7, Texas, U.S.A.

The type H5600 potentiometer is shown in the figure. Th basic element is a resistance wire bonded within the edge o a laminated Mylar tape 120 in. long. The resistance wi may be straight or helical according to the total resistanc required; resistance ranges from 100 Ω to 100 kΩ are avai able. The potentiometer is read through a window on th front of the case from calibration marks stamped on th tape; these figures may be spaced to correspond to any linea or non-linear function. Each potentiometer is individual calibrated on an automatic system which compares the unit under test with a master tape 60 ft long. Calibration is made at 1000 points, and the digital values are automatically printed on the tape. The makers claim that conformity between true resistance value and the specified function of the calibration is 0·05%, resolution is better than 0·01%, total resistance tolerance is 0·25% and end resistance is less than 0·005 Ω. The device is rated at 2 W. The instrument case measures 2 × $2\frac{1}{4}$ × $2\frac{3}{4}$ in. The straight sides and interlocking drive shaft ends permit the adjacent ganging of units for single-knob setting of related functions.

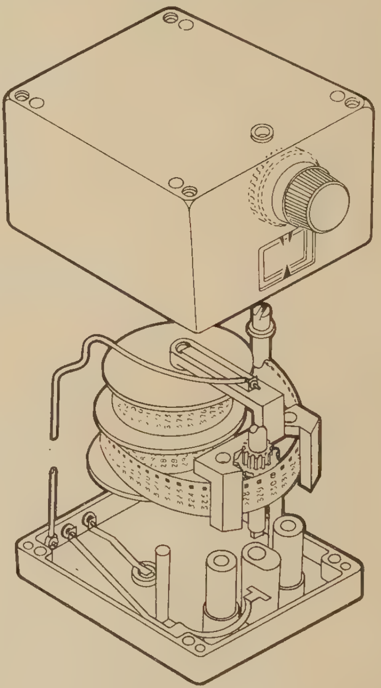

Exploded view of digital-reading, slide-wire potentiometer

dgewise electric meter. Taylor Electrical Instruments Ltd., Montrose Avenue, Slough.

he model 220 meter, illustrated in the figure, has been eveloped for use in crowded control panels where panel pace must be kept to a minimum. The meter movement s of the centre pole pattern, which provides inherent magnetic shielding. The meter readings are therefore unaffected by other meters or magnetic material in the immediate icinity. The meter is housed in a transparent case, which allows the maximum amount of light to fall on the scale without shadows. The panel area occupied is only 2·5 × 0·62 in., and the meter can be arranged for either horizontal or vertical mounting. Voltmeters, milliammeters and microammeters are available with right-hand, left-hand, displaced or centre zeros. The instruments can also be supplied with rectifiers for a.c. measurements.

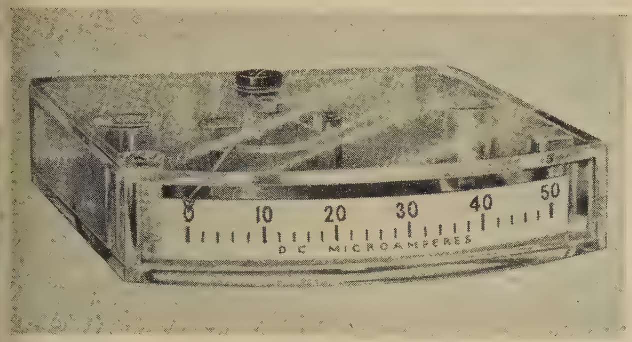

Edgewise electric meter (full size)

Low-voltage power supply unit. Allied Electronics Ltd., 28 Upper Richmond Road, London, S.W.15.

The type LS353–H supply unit is designed as a compact stabilized d.c. source for heater supplies in d.c. amplifiers, exciter lamps in photoelectric measuring instruments and similar applications. The basic unit is a germanium junction rectifier circuit with a transistor voltage stabilizer and a reference potential device; it is available in chassis or cabinet form. The nominal voltage is 6·3 V and a stability of 25 mV against a mains voltage variation of 10% is claimed. The full load ripple is given as 3 mV r.m.s. The unit operates from 50 c/s mains supply at from 190 to 250 V.

Signal generator. Taylor Electrical Instruments Ltd., Montrose Avenue, Slough.

The model 68 A/M signal generator covers the frequency range 100 kc/s to 240 Mc/s in eight ranges without the use of harmonics. The scale length is 58 in., and a calibration accuracy of 1% is claimed. The normal radio-frequency output is 100 mV and is monitored by a built-in meter. A coarse attenuator, having five steps of 20 dB, and a fine control, variable to 20 dB, are fitted. It is claimed that leakage into the output and into the power lines is negligible. The output can be either unmodulated or sine-wave modulated to 30%. Direct connexion can be made to the modulator, giving an audio-frequency output variable up to 1 V maximum. The output impedance is 75 Ω *via* a coaxial cable. A dummy aerial is supplied with the instrument, and there is a further choice of five terminations, including an output with both leads isolated (for use with a.c./d.c. receivers) and a minimum loss pad matching 75 Ω unbalanced to 300 Ω balanced.

Radiation pyrometer. General Electric Co. Ltd., Magnet House, Kingsway, W.C.2.

This instrument consists of a thermocouple enclosed in a cavity in an aluminium block. It responds to a wide range of source temperatures and is almost independent of the ambient temperature. It can be used with a radiation collecting probe—made of fused silica—or directly with the help of limiting stops. It is stated that the calibrated instrument is consistent in its readings.

A target body is mounted inside a cavity in the aluminium block, which because of its diffusivity, can be regarded as at uniform temperature. A narrow pencil of heat radiation falls on the target from the source through a small hole in the cavity wall. The temperature of the target is thus raised above that of the rest of the cavity; and it is stopped down until this difference is only a few degrees centigrade. This steady temperature rise is a measure of the radiation entering the cavity and hence of the temperature of the source. This temperature difference is found to change only slowly with the *ambient* temperature, as for example with a source at 300° C, and an ambient change from 15 to 50° C, the change is only −6° C.

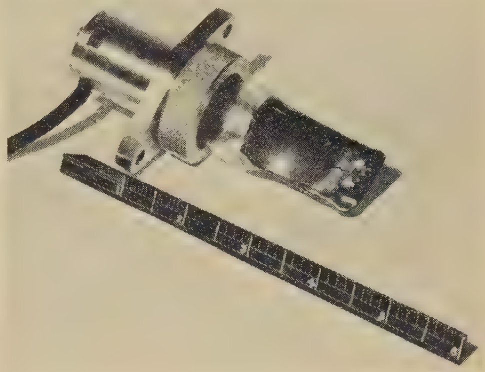

Radiation pyrometer (rule in inches)

The target body consists of a number of thermojunctions of 0·004 in. diameter wires, disposed radially in the cavity within the instrument. The cold junctions are welded to a segmented annular ring, insulated from the pyrometer case by a thin layer of resin. The ring serves to connect the wires in series and give good thermal contact at the cold junction. At the aperture end of the case, is a screwed clamping ring by which the probes and aperture disks may be attached: and the connecting leads come out at the other end.

The silica probe is composed of polished rods of fused silica, $\frac{1}{4}$ in. in diameter, and have been used successfully up to 12 in. in length. It is sometimes necessary to shield the air silica surface from contamination, and for this a fused silica sheath has been used. Because of the poor transmission of fused silica, the probe is efficient only at temperatures above 400 to 500° C.

In operation the instrument is stopped down to give about a millivolt output; which is read off on a millivoltmeter or light-spot galvanometer. The response time is dependent entirely on the voltmeter for the response time of the thermocouple is very rapid, being of the order of 0·1 s.

New books

The properties, physics and design of semiconductor devices. By J. N. Shive. (London: D. Van Nostrand Co. Ltd., 1959.) Pp. xxi + 487. Price 73*s*.

This book is an introduction to semiconductor device physics written primarily for advanced students and scientists entering the subject, although it might be read with enjoyment and interest by workers already in the field, for the area of study is larger than is usually found in one volume and the treatment authoritative.

The book is divided into two parts, the first dealing empirically with the action and uses of devices without going too deeply into the solid state physics involved. This is left to the second part which is itself a useful introduction to that aspect of the subject. Many introductory courses become too involved in the initial stages with such problems as the meaning of holes and effective masses and the arrangement of this book successfully avoids this difficulty. This is accomplished with such lively writing and the inclusion of just enough historical detail that the treatment is convincing and useful throughout.

The subject is developed through the devices discussed, starting with thermistors and continuing with varistors, photoelectric devices, and transistors. Transistors are dealt with extensively from the simple alloy types to the pnip and diffused base structures, tetrodes, and pnpn switches. Basic circuit theory is also developed. The author deliberately omits some devices such as gyrators and masers. It is a pity that the book is a little too early to include a mention of the Esaki diode.

From the number of courses on semiconductors being arranged by Technical Colleges and other organizations in this country, it is clear that there are increasingly large numbers of scientists wishing to improve their acquaintance with this subject. To them this book is recommended.

J. Houghton.

Photomicrography. 2nd ed. By R. M. Allen. (New York: D. Van Nostrand Co. Inc.; London: D. Van Nostrand Co. Ltd., 1958.) Pp. xiii + 441. Price 67*s*. 6*d*.

There are few good books, in spite of numerous attempts, on the use of the microscope and still fewer on the special art of photographing through it. Dr. Allen's book, in its original edition, has long been recognized as one of the best and now, brought up to date after an interval of 17 years, it must rank as the most complete treatment available. One of its principal merits is the operational approach of the author, who has clearly had first-hand experience of a wide variety of types of modern equipment. The basic principles of the optical microscope are set out in the first chapter, and those of phase and interference microscopy in a later one, but most of the text is concerned with the description of microscopes and the way to get the best results with the There is also an interesting and unusual chapter on hom made equipment, which will be of special help to sma laboratories and to the amateurs of microscopy, who a still legion. The author interprets his title in the prop sense of photography through the microscope, but includ also a chapter on microphotography, in view of the growin interest in recording information in ultra-small forma There is in addition a short chapter on the electron micr scope which, however, hardly does justice either to th instrument or to its applications. Here, as also in one two other sections such as that on ultra-violet microscop the reader would welcome a list of references for furth reading.

In all the techniques of optical microscopy there is remarkably full treatment, illustrated with many line diagram photographs of apparatus and micrographs, which sho what to avoid as well as what to aim at. There is also compilation of practical techniques and formulas for dar room work covering all relevant aspects of photograph Not least, the book ends with a selection of 54 photomicro graphs, at magnifications ranging from 4× to 4500× Many of these are works of art in their own right, as we as illustrating different practical problems of microscopy full exposure details are given with each. Only a lifetim spent in the subject, and a deep affection for it, could hav produced such a comprehensive account. The book can b recommended to all involved in the practice of microscop and particularly to that great majority who have had to pic up the subject as they went along, in the absence of a reliab handbook. Here is what we have been looking for, and th author is to be congratulated on meeting this long-felt nee

V. E. Cosslett.

British Journal of Applied Physics

Contents for the April issue

CONFERENCE REPORT

Summarized proceedings of a conference on solid state physics—Melbourne August 1959. By J. F. Nicholas.

SPECIAL ARTICLE

Very high energy ultrasonics. E. A. Neppiras.

PAPERS

The spectral emission of radiation by glass. J. R. Beattie and E. Coen.

Reflexion electron microscopy using diffracted electrons. J. S. Halliday and R. C. Newman.

X-ray microbeam study of deformation bands in aluminium. D. Lewis.

Simple rotary dynamic testing machine. A. N. Gent.

CORRESPONDENCE

Annealing silicon monoxide films on aluminium mirrors. From L. Holland, T. Putner and R. Ball.

THIS *JOURNAL* is produced monthly by The Institute of Physics, with the co-operation of the National Physical Laboratory. It deals with the principles, construction and use of scientific instruments. All rights reserved. Responsibility for the statements contained herein attaches only to the writers.

EDITORIAL MATTER. Communications concerning editorial matter should be addressed to the Editor, The Institute of Physics, 47 Belgrave Square, London, S.W.1. (*Telephone:* Belgravia 6111.) Prospective authors are invited to prepare their scripts in accordance with the *Notes for Authors*. (Price 3*s*. 6*d*. including postage.)

REPRODUCTION. The Institute of Physics is a signatory to The Royal Society's Fair Copying Declaration. Details may be obtained upon application from The Royal Society, London, W.1.

ADVERTISEMENTS. Communications concerning advertisements should be addressed to the agents, Messrs. George Jackson (Fleet St.) Ltd., Cliffords Inn, Fleet Street, London, E.C.4. (*Telephone:* Holborn 3611–2.)

CLAIMS FOR MISSING JOURNALS. Claims from regular subscribers to this *Journal* for missing numbers will only be considered if received within 60 days of the date of mailing plus normal outward time of transit and time for lodging the claim. Losses attributable to failure to notify a change of address or to similar omissions will not be considered.

SUBSCRIPTION RATES. A new volume commences each January. The charge is £6 per volume ($17 U.S.A.), including index (post paid) payable in advance. Single parts, so far as available, may be purchased at 12*s*. 6*d*. each ($1.75 U.S.A.), post paid, cash with order. Orders should be sent to The Institute of Physics, 47 Belgrave Square, London, S.W.1, or to any bookseller.

PRINTED IN GREAT BRITAIN BY UNWIN BROTHERS LIMITED, WOKING AND LONDON

The Physical Society's Exhibition—London, 1960

By T. B. RYMER, M.A., Ph.D., F.Inst.P.

Abstract

A general survey is given of the newer developments of nstruments and apparatus exhibited, together with some bservations on the Exhibition, and the prize list of the Craftsmanship and Draughtsmanship Competition.

Introduction

The annual Exhibition of The Physical Society was originally conceived as a scientific gathering at which physicists could meet to discuss new ideas in scientific nstruments and techniques. Inevitably, the bulk of the exhibits have always come from scientific instrument manufacturers, and fears have been expressed by many people that the Exhibition was becoming indistinguishable from other trade shows. It is therefore pleasant to be able to record that this year there was a marked improvement in the general quality of the Exhibition, and few visitors can have failed to be inspired by some new idea. Government research establishments continued to provide numerous exhibits showing research in progress, and industrial research associations were also well represented. University and hospital physics departments—organizations which a year ago seemed to be in danger of disappearing from the Exhibition—provided this year no less than 29 exhibits on 7 stands. Besides this increased contribution by non-commercial organizations, a further factor which provided added interest was the praiseworthy tendency of many manufacturers to devote more of the available space to prototype instruments and exhibits from their research departments, and less to older, well-established lines. A striking illustration of this tendency was that electron microscopes and X-ray diffraction equipment, in which there has been no major advance during the last twelve months were, for the first time for many years, missing from the Exhibition; and electron diffraction apparatus was represented by a single Swiss exhibit. On the other hand, the Associated Electrical Industries Research Laboratories demonstrated the electron beam focusing properties of magnetic quadrupoles and octupoles.

Last year's experiment of inviting foreign exhibitors was repeated this year, and resulted in an interesting group of instruments from Swiss manufacturers procured through the co-operation of the Swiss Physical Society and the Swiss Office for the Development of Trade. Prominent among the foreign exhibits was an electron diffraction camera by Trüb, Täuber and Co. of Zürich. This instrument was notable for the high standard of engineering and the numerous accessories provided for heating and cooling the specimen, its bombardment by electrons or ions, and the preparation of specimens by evaporation within the camera. A novel exhibit by Metrohm A.G. of Herisau was an apparatus for the automatic recording of titration curves in which the reagent is added continuously and in synchronism with the advance of the recording paper.

It is impossible in a short article to deal with the whole Exhibition, and the selection of exhibits for mention will be partly determined by the author's own interests. It is hoped that an account of what impressed one visitor may be of interest to those who were unable to see the Exhibition.

Materials, components and techniques

Advances in instruments and techniques depend ultimately on the provision of new materials with improved properties, and it is therefore natural to enquire what new materials have become available during the past year. Semiconductors formed the largest class of new materials. Gallium arsenide should theoretically be superior to germanium and silicon for transistors, power rectifiers and solar energy conversion, but the purity of the best material currently available limits its application to devices for which a short carrier lifetime is not a disadvantage. The Services Electronics Research Laboratory demonstrated the refining and growth of single crystals of gallium arsenide by the floating zone method, and also showed examples of the use of this material in a switching diode, an Esaki diode and a photocell converting radiant energy from an electric lamp into an electric current to drive a motor. Texas Instruments Ltd. showed a gallium arsenide Zener diode operating in the 11 V range with a power dissipation of 0·8 W and at ambient temperatures between -65 and $+325°$ C.

Indium antinomide is a material which is being increasingly used because of its large Hall and magnetoresistance coefficients. Some applications of this material are referred to in the section dealing with electronic devices.

The use of semiconducting oxide films as resistive elements was exhibited by G. V. Planer Ltd. The oxide can be coated on 25 μ diameter glass fibres, which are then wound on ceramic formers to produce stable, compact resistors of high value. Other applications shown of these oxide films were a miniature potentiometer, and a switch in which a globule of mercury running over an oxide film provides a continuous variation of resistance with angle of tilt.

Among the new alloys exhibited by Johnson Matthey and Co. Ltd. was Platinax II, a 50% alloy of cobalt and platinum used for permanent magnets and having a $(BH)_{max}$ value of $9{\cdot}2 \times 10^6$ gauss-oersted. Two machinable, tungsten-base alloys, Mallory 1000 and 2000, having specific gravities of 16·9 and 18 respectively, were also exhibited; these are intended for counter-balance weights and for γ-ray radiation screening.

Electron microscopists will be interested in the precision aperture disks of platinum and molybdenum shown by Engelhard Industries Ltd. These disks can be supplied with holes of diameters from 5 to 500 μ in steps of 1 μ, and in diameters up to 1 mm in 10 μ steps.

An interesting technique for working hard metals was shown by the Armament Research and Development Establishment. The work piece is clamped to the work table and fully submerged in paraffin. A succession of sparks between the work piece and an electrode erodes the former in a controllable manner. The production of a 0·007 in. diam. hole in a 0·015 in. diam. hardened steel ball was demonstrated.

An exhibit by the Royal Radar Establishment showed the microminiaturization of electronic circuits by repeated vacuum evaporation on to an insulating substrate. Resistors consist of a nickel–chromium film about 75 Å thick; values up to $10^5\ \Omega$ are obtained in an area of $\frac{1}{4}$ cm^2. Capacitors are made in the form of a sandwich of thin metal films with magnesium fluoride as a dielectric, capacitances of 2000 pF being obtained in an area of $\frac{1}{4}$ cm^2. Transistors and diodes are fabricated in the form of flat units.

An alternative approach to the problem of microminiaturization was shown by Texas Instruments Ltd. This is based on the selection and shaping of conducting paths upon and through a semiconducting wafer. Resistances are formed by the bulk resistance of the material, capacitors by utilizing capacitor forming techniques, and transistors and diodes by diffusion methods. The exhibit showed a multivibrator circuit measuring $\frac{1}{4} \times \frac{1}{8} \times \frac{1}{32}$ in.

An interesting example of miniaturization using standard components was shown by H. S. Wolff of the National Institute for Medical Research. This consisted of an electric transducer connected to a radio transmitter powered by a Mallory cell. The whole system was encapsulated and measured only 19 mm long × 8 mm diam. It could be swallowed as a pill and during its passage through the digestive tract transmitted indications of temperature, pressure or pH. The position of the pill in the tract could be determined by radio direction-finding methods using a small pick-up aerial a few inches from the body.

Electronic devices

It is possible to mention only a few of the many new cathode-ray tubes displayed. 20th Century Electronics Ltd. showed tubes using travelling-wave deflexion systems for the presentation of transient and repetitive phenomena in the millimicrosecond range. The same firm also showed prototypes of direct viewing storage type cathode-ray tubes for recording single transients. The English Electric Valve Co. Ltd. showed a storage tube for use in analogue or digital computer systems, in which the target consists of 2000 gold strips deposited on a thin glass plate backed by a continuous metal film forming the signal output electrode. The strips are scanned by a beam from an electron gun, and the information is written as negative charges on the strips. The information is read by scanning with a beam from a lower potential electron gun, which neutralizes the stored charge and induces an output signal on the backing electrode. A storage tube of the barrier-grid type was displayed by E.M.I. Electronics Ltd. Among the specialized cathode-ray tubes shown by Electronic Tubes Ltd. was a 1 in. diam. tube designed for operating potentials as low as 350 V. Another interesting exhibit by the same firm was a cathode-ray tube having a fine screen grid between the deflexion and post-deflexion acceleration systems. In the usual post-deflexion acceleration system, a converging electron lens is formed by the post-deflexion acceleration field penetrating the region between the deflector plates. This effect increases with the post-deflexion ratio, and limits the permissible value of this quantity. Greater sensitivity with reduced distortion is obtained by placing a high transmission grid to screen the post-deflexion acceleration field from the deflector plates. When this grid is correctly placed, the fields are so shaped that the sensitivity is substantially independent of the post-deflexion acceleration ratio.

The Hall and magneto-resistance effects in thin films of indium antinomide and arsenide formed the basis of magnetic field measuring devices shown by G. V. Planer Ltd. and by The Plessey Co. Ltd. With these materials, Hall potenti exceeding 4 V are obtained, and twenty-fold resistan changes are produced by a field of 10^4 oersted. The use these devices as multipliers, amplifiers and oscillators w demonstrated.

The National Research Development Corporation show a portable susceptibility meter using the Hall effect in indiu antimonide. This depended on the detection of a change reluctance of part of a magnetic circuit; it consisted of magnetic network with an air gap in which is inserted t specimen whose susceptibility is to be measured. The n work is so arranged that two points at equal magne potential are joined by a magnetic link containing the H effect detector. The network is adjusted so that in t absence of a specimen there is no flux through the detecto On placing a specimen in the gap, the balance is upset a flux passes through the detector. The instrument has linear response, and will detect a susceptibility of 10^{-8}.

The National Research Development Corporation al showed a displacement meter based on the magneto-resista effect in indium antimonide. The unit is in the form of a.c. operated Wheatstone bridge, the arms of which lie the non-uniform field of a magnet. Movement of the magn changes the resistances of the arms and disturbs the balan of the bridge. With suitable amplification of the brid output, displacements of the order of 1 A can be detected.

Parametric amplifiers of various kinds were displayed on number of stands. The English Electric Valve Co. Lt showed a development example of a transverse field electr beam parametric amplifier operating at a signal frequency 200 Mc/s, and having a noise figure of 2 dB. The Gener Electric Company's Research Laboratories used a demoun able vacuum system to demonstrate the action of the long tudinal space-charge wave type of parametric amplifier. Th demonstration showed the existence in an electron beam a growing wave caused by the interaction between the field created by the bunching processes at the signal and pum frequencies. Parametric amplifiers using solid-state diod were shown by Ferranti Ltd., The General Electric Compa Ltd. and the Admiralty Surface Weapons Establishment.

No developments in solid-state masers were shown in th year's Exhibition, but the ammonia maser which was show last year by Glass Developments Ltd. has now been produce in a sealed-off form consisting of a reservoir of ammoni and a cavity chamber. The reservoir contains sufficie ammonia to run continuously for 100 hours, after which th gas may be returned to the reservoir by cooling the latter.

The increasing use of complicated electronic compute has led to a search for new bistable systems for elements c the computer "memory". Since a large computer ma contain thousands of such elements, compactness, cheapnes and speed are all-important. Mullard Ltd. and the Roya Radar Establishment demonstrated the magnetic properti of thin films of ferromagnetic alloy deposited by vacuu evaporation on an insulating substrate; such films seem likel to prove useful as memory elements. If the film is deposite in the presence of a magnetic field, it will have a near rectangular hysteresis loop when examined by fields in th same direction, and is therefore a bistable system capable o storing a binary digit.

Digital instruments

It is becoming increasingly common to design instrument so that the readings are presented as a row of figures instea of by a pointer moving over a scale. This is found to lea less error in recording observations. Typical of this trend s the frequency meter shown by J. Langham Thomson d. which covered the range 0–100 kc/s with an accuracy of /s or 5 parts in 10^5. The reading was displayed as a row figures in special neon tubes. A similar meter with optical ojection of numbers for the display was exhibited by nner Electronics Ltd. Digital voltmeters and similar vices, with an accuracy of the order of 0·2%, were shown Racal Instruments Ltd., Burndept Ltd., Nash and omson Ltd. and The Solartron Electronic Group Ltd. A ore elaborate 5-digit voltmeter reading up to 159·99 V was so shown by the last-named firm.

Numerous kinds of display unit are now available for use digital equipment. The digits may be displayed by wire ectrodes stacked one behind the other in a neon glow tube ricsson Telephones Ltd.); by engravings in a series of erspex plates stacked one behind the other, the appropriate ate being illuminated from the side (Ferranti Ltd.); by a t of projector lamps focused on to the same part of a anslucent screen (R. B. Pullin and Co. Ltd.); by com- nations of lines and curves on an electroluminescent panel horn Electric Industries Ltd.); or by a special cathode-ray- be system (Research Laboratories of the General Electric o. Ltd.). Digital instruments can readily be arranged to rint out readings, and printers for this purpose were shown y Venner Electronics Ltd. Electronic circuits for converting oltages to binary digits were shown by the Royal Aircraft stablishment, and by The Solartron Electronic Group Ltd. he first-named exhibit was designed for feeding accurate formation down a standard elementary link; it could take 000 independent readings per second, each with an accuracy f 0·01%. The second exhibit read voltages up to 15·999 V the nearest mV in about 0·01 s.

Among the other exhibits incorporating digital devices ay be mentioned the comprehensive range of linear and ngular displacement measuring equipment shown by Hilger nd Watts Ltd., a planimeter with digital display by dekatron ounters shown by W. F. Stanley and Co. Ltd., and a measur- g instrument of advanced design by Ferranti Ltd. in which isplacements were measured by photoelectric detection of oiré fringes using transistorized decade counters.

Moiré fringes in conjunction with photo-electric detectors re well adapted to the accurate recording of displacements digital form. The National Physical Laboratory showed n interesting example of this in the form of a Michelson nterferometer for the study of infra-red spectra. The nterferometer had large mirrors and beam-splitting plate so s to have good light-gathering power. The moving mirror vas attached to a grating, and moiré fringes were formed by his and a fixed grating; as the mirror moved uniformly long the carriage, the passage of each moiré fringe over the hotocell opened a gate to permit a second photocell to record he intensity of the radiation passing through the interfero- neter. The resulting digitalized record of intensities at qually spaced mirror positions could be fed into a large lectronic computer, which performed a Fourier trans- ormation to produce an intensity-wavelength table.

The use of digital methods for control purposes was xemplified in an exhibit by the British Iron and Steel esearch Association. The demonstration made use of the alf-cycle-response type of magnetic amplifier, which, when sed as an on-off device, has the property that there is a elay of a half-cycle between the input and the corresponding utput. A number of such amplifiers in cascade will form a elay line. If the first stage of such a line has an inhibit ircuit connected to the outputs of the even stages, it will allow single pulses to pass along. From the passage of a single pulse along the line, a pulse pattern may be generated by selecting outputs from some or all of the odd stages. Such patterns of pulses can be used for controlling the grids of a 6-phase grid-controlled mercury arc rectifier. With this method of control, each individual rectifier either conducts during the whole of a half-cycle or not at all. Consequently, by changing the pulse pattern, the wave-form of the output can be varied. In this way, the mean d.c. output can be varied within wide limits while keeping the current and voltage always nearly in phase and producing a minimum of higher harmonics.

Ultra-high vacuum apparatus

The production of ultra-high vacuum, with residual gas pressures of the order of 10^{-9} mm of mercury, was until recently a difficult laboratory art. Edwards High Vacuum Ltd. had an extensive exhibit showing the whole range of pumps, gauges, valves and unions which are now available as standard items and can be fitted together to form a reliable, demountable system capable of producing pressures of this order. The first essential is to be able to bake out the whole system at a temperature of about 450° C so that the walls are thoroughly outgassed. This requires that the whole vacuum system be constructed of a good vacuum metal such as stainless steel, and that the usual organic O-ring seals be replaced by specially designed metal seals using copper, aluminium or lead gaskets. Pressure down to 10^{-9} mm of mercury or less can be obtained in well outgassed systems by an oil or mercury diffusion pump fitted with water-cooled baffles and a stainless steel liquid air trap. The latter is fitted with a heating jacket for baking out the trap at 450° C during the preliminary outgassing period. An alternative method of producing a low pressure is by means of a getter pump. Such a pump consists of a chamber 24 in. high and 12 in. diam. fitted with a 9 in. diam. pumping port. After baking and preliminary pumping down to 10^{-6} mm, the titanium getter is evaporated from a molten bead suspended by a frozen zone from a water-cooled copper block. The bead is heated by electron bombardment and replenished by a continuously fed wire. A Penning type ionization gauge fitted with titanium electrodes was also shown; this acts as a pump capable of reducing the pressure from 10^{-1} to 10^{-8} mm.

The fact that Penning and ionization type gauges both have a pumping action implies that they will not give correct pressure readings if they are connected to the main vacuum system by tubes having appreciable resistance. A wide bore, all metal, demountable ultra-high vacuum ionization gauge head was shown which is free from this disadvantage.

The practical value of ultra-high vacuum technique is in the production of clean, vacuum-evaporated surfaces. A vacuum coating plant was shown, capable of producing pure, thin metal films at pressures of 10^{-8}–10^{-9} mm of mercury.

Dr. P. C. Banbury of Reading University showed another example of the use of ultra-high vacuum for the production of clean surfaces. In this case, a clean germanium surface was obtained by cleaving a crystal in a residual gas pressure less than 10^{-9} mm of mercury. This was achieved in a continuously pumped system with diffusion and ion pumping using a special glass jig. The crystal is bent by a magnetically operated lever until cleavage starts from a diamond scratch. Because of the healing effects of the vacuum baking, it is necessary to make the scratch after baking by means of a magnetically operated, diamond tipped lever.

Mullard Ltd. showed development work proceeding on the design of ultra-high vacuum equipment. A getter-ion pump was shown consisting of a multi-cell Penning cold-cathode tube with titanium cathodes, together with a filament from which titanium may be evaporated. Two types of expendable getter-ion pumps were shown. One consisted of a Bayard–Alpert ion gauge with a filament from which zirconium could be evaporated. The other was a Penning type of pump consisting of a single loop of wire, from which titanium could be evaporated, and a side contact sealed through the glass envelope. A magnetic field is applied at right angles to the loop. Titanium is evaporated from the loop during pumping, and the film thus produced forms the cathodes on either side of the loop. The pumping speed is about 1 litre/s and the starting pressure may be several mm of mercury.

A radio-frequency mass spectrometer was shown for the analysis of residual gases in the pressure range 10^{-3}–10^{-6} mm of mercury. This operated on the principle of the linear accelerator and had a mass resolution of about 30. Its advantage over the omegatron, which uses the principle of the cyclotron, is that it does not need a powerful magnetic field.

Craftsmanship and Draughtsmanship Competition

The winning entries in the annual Craftsmanship and Draughtsmanship Competition were, as usual, displayed in the entrance hall. The judges' report on the entries was follows:

A satisfactory number of entries was received in classes for general scientific instruments and componen for optical components and systems, and for blown gl and silica ware and the craftsmanship shown in all corresponding basic techniques for the construction physical apparatus reached the very high standard that have come to expect in this Competition. It is, howev disappointing to find that the Silvanus P. Thomson Pr which calls for draughtsmanship as well as craftsmansh attracted only two entries, though the level reached was w up to standard.

The newer classes for microwave components and electronic circuitry have not yet attracted more than half t number of entries usually received in the older classes b this year has shown an encouraging improvement in t workmanship of the microwave components. The standa is still rather below that of the best of the entries in the cla for general instruments, particularly in the fine details finish, but the prize-winning entries showed very good wo

The few items of electronic circuitry received show commendable craftsmanship but of a kind that is difficult assess and it is not yet clear whether the young workers this rapidly growing field will establish their right to ra with their fellow-craftsmen in the other classes of t Competition.

Craftsmanship and Draughtsmanship Competition

PRIZE LIST

Silvanus P. Thomson Prize

(for Draughtsmanship and Craftsmanship combined)

C. Samms (Marconi's Wireless Telegraph Co. Ltd.). Mechanical drive unit.

Scientific instruments and components (Junior grade)

First prize: R. Jolley (Cambridge Instrument Co. Ltd.). High temperature creep extensometer.

Second prize: M. A. Shearman (Marconi's Wireless Telegraph Co. Ltd.). Turret indexing mechanism.

Third prize: R. J. Warner (Cambridge Instrument Co. Ltd.). Callendar radiation balance.

Third prize: K. G. McCarthy (Hilger and Watts Ltd.). Optical Besel protractor.

Scientific instruments and components (Senior grade)

First prize: C. F. White (Hilger and Watts Ltd.). Biological microscope.

Second prize: A. W. Brett (Hilger and Watts Ltd.). Grating monochromator.

Third prize: T. A. Winter (Marconi's Wireless Telegraph Co. Ltd.). Focusing mechanism.

Optical components and systems

First prize: T. Renwick (Hilger and Watts Ltd.). 60° regular glass polygon.

Second prize: G. Glass (Optical Measuring Tools). Pentagonal roof prism.

Third prize: F. C. Turvell (Hilger and Watts Ltd.). Rutherford prism for Raman spectrograph.

Blown-glass and silica ware (blown-glass)

First prize: R. W. Crook (G.E.C. Research Laboratories). Three-stage diffusion pump.

Second prize: K. G. Wornham (Mullard Research Laborator Spiral condenser.

Third prize: D. W. Lanman (British Thomson-Houston Co. Lt Crystallization unit.

Blown-glass and silica ware (silica ware)

First prize: D. W. Lanman (British Thomson-Houston Co. Ltd Single-stage mercury diffusion pump.

Second prize: K. Robson (Thermal Syndicate Ltd.). Two-sta mercury diffusion pump.

Third prize: J. Mathieson (Thermal Syndicate Ltd.). Single-sta pump.

Instructional items, models, etc.

First prize: D. H. Jackson (Standard Telephones and Cables Ltd 0–4 in. diam. measuring machine (floating carriage).

Electronic circuitry (Junior grade)

First prize: J. G. Butler (Hilger and Watts Ltd.). Digi coincidence unit.

Second prize: J. A. Mills (Marconi's Wireless Telegraph Co. Ltd Vision modulator.

Electronic circuitry (Senior grade)

Second prize: D. L. Elliot (Marconi's Wireless Telegraph C Ltd.). Ranging unit assembly.

Microwave components (Junior grade)

First prize: J. Danbury [Services Electronics Research Laborato (Admiralty)]. O-band puller.

Microwave components (Senior grade)

Second prize: R. J. Tucker (Hilger and Watts Ltd.). Prototy Q-band adjustable matching assembly.

Third prize: A. Short [Services Electronics Research Laborato (Admiralty)]. Section of delay line for travelling-wave tube.

arn-speed meter*—a low-torque instrument for measuring he linear speed of low-inertia systems

y D. L. MUNDEN, B.Sc.,† and T. K. MORLEY, The Hosiery and Allied Trades Research Association, Nottingham

aper first received 26 *October, and in final form* 14 *December*, 1959]

Abstract

small portable low-torque tachometer is described hich has been designed to measure linear speeds of unning yarns or threads. The instrument is a simple apacitor-switching circuit, power being provided by a mall mercury-amalgam cell contained in the handle of he instrument. The instrument has been used to measure arn speeds of up to 1200 *ft/min to an accuracy of* ±1% *ithin the calibrated limits.*

Introduction

TACHOMETERS are, at present, commercially available which depend on either frictional or electromagnetic effects to give a reading on a meter indicating the rotational speed of a shaft or machine. Most of these instruments have been designed to measure the rotational speed of mechanical systems of high inertia or where reserves of power are sufficient to overcome any effect that the addition of the tachometer may have on the rotational speed of the mechanical system. In many rotational or linearly moving systems, the inertia of the moving body is low and the speed of the system is readily affected by the addition of extra load. Under these conditions the torque required to operate the tachometer becomes of critical importance.

This is usually the case in the manufacture of textile materials, where the moving member may be a light thread or yarn, and where any increase in tension on the yarn as it is fed to the machine affects its speed and, in extreme cases, may even cause the running thread to break. Under these conditions the torque required to operate the tachometer is the prime factor limiting the accuracy of the instrument.

The knitting action is particularly sensitive to such yarn-tension changes. For example, an addition of 10 g tension may affect the speed of the yarn fed to the machine by as much as 15%. The instrument described below, the yarn speed meter, has been designed to add the minimum tension to a running yarn, in order that the measured yarn speed may be within 1% of the undisturbed yarn speed.

General design of instrument

The instrument is, in principle, a simple capacitor charge/discharge switching circuit; the circuit and component values are shown in Fig. 1. Fig. 2(*a*) shows a front view of the instrument and Fig. 2(*b*) a back view when the back plates are removed.

The moving element (for example, the yarn as it is fed to the knitting machine) engages a light plastic pulley *P* [Fig. 2(*a*)]. Mounted rigidly on the same shaft as the pulley is a metallic contactor disk *C* [Figs. 1 and 2(*b*)] which contains three insulator segments equally spaced angularly. Electrical contact to the disk is made by three wipers, W_1, W_2 and W_3.

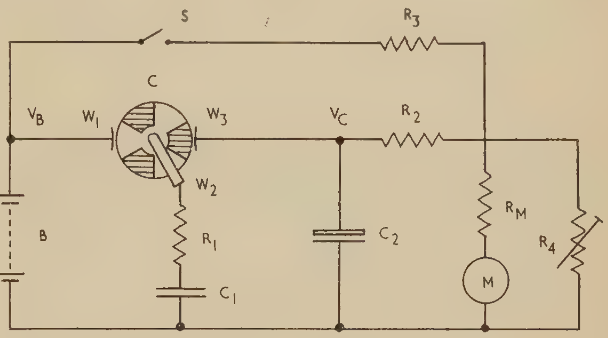

Fig. 1. Circuit diagram of yarn-speed meter

$R_1 = 100\ \Omega \pm 5\%$
$R_2 = 2{\cdot}2\ \mathrm{k}\Omega \pm 5\%$
$R_3 = 320\ \mathrm{k}\Omega \pm 1\%$
$R_4 = 100\ \mathrm{k}\Omega$ linear carbon rheostat
R_M = resistance of meter, 1000 Ω
$C_1 = 0{\cdot}0266\ \mu\mathrm{F} \pm 1\%$, silvered mica
$C_2 = 50\ \mu\mathrm{F}$, 12 V, electrolytic
B = 27 V mercury cell, Mallory type SKB360

C = contactor, 0·2 in. draw; silver rod with Tufnol or Araldite inserts
M = d.c. microammeter scaled in ft/min (full-scale deflexion, 100 μA)
S = switch, 250 V, 1 A
W_1, W_3 = periphery wipers, 20 × 2 thou. strip, gold alloy
W_2 = centre wiper, 50 × 2 thou. strip, gold alloy

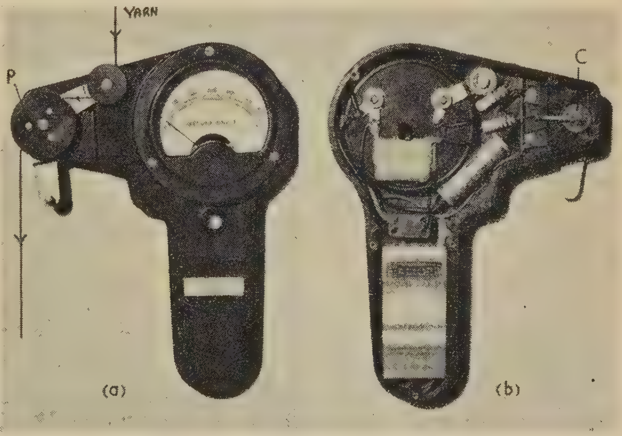

Fig. 2. (*a*) Front view of yarn-speed meter

(*b*) Back view of yarn-speed meter with rear panels removed

---

* Brit. Pat. No. 743182; Prov. Brit. Pat. No. 13026/56.

† Now Lecturer in Textile Engineering, University of Leeds.

The central wiper W_2 makes contact continually, whilst wipers W_1 and W_3, which are diametrically opposite one another, make contact continually with the circumference of the disk, but are connected to W_2 alternately through the conducting sectors of the disk.

The sequence of operations as the disk rotates is therefore as follows:

(i) W_1 makes contact with W_2. Capacitor C_1 is charged through R_1 from battery B.
(ii) Contact is broken. Capacitor C_1 retains charge.
(iii) W_2 makes contact with W_3. Capacitor C_1 is discharged through R_1 into capacitor C_2.
(iv) Contact is broken. Capacitor C_2 continues to discharge through meter M and R_2.

In operation, therefore, the capacitor C_1 is charged from the battery through resistor R_1 three times per revolution of the contactor disk and discharged three times per revolution through R_1 into capacitor C_2.

The average discharge current (i_d) flowing from C_1 into C_2 is given by:

$$i_d = C_1(V_b - V_c)f,$$

where V_b is the maximum voltage attained by capacitor C_1 during charge, V_c is the voltage across C_2 when C_1 is discharged into it, and f is the number of charge and discharges per second.

If there is no current lost through C_2, the current through the meter (i_M) is given by:

$$i_M = C_1(V_b - V_c)f \cdot \frac{R_4}{R_4 + R_M}. \qquad (1)$$

To obtain a linear response, the circuit components are chosen so that (i) the capacitor C_1 is charged to the full battery voltage (V_B) each charge cycle, that is, $V_b = V_B$ (battery voltage), and (ii) the steady voltage V_c across C_2 necessary to give full-scale deflexion on the meter at maximum, linear yarn speed is small compared with V_B (see section on the smoothing circuit, below). Therefore:

$$i_M \simeq C_1 V_B f \cdot \frac{R_4}{R_4 + R_M}. \qquad (2)$$

Under these conditions, therefore, for fixed values of C_1, V_B, R_4 and R_M, the meter current is proportional to the frequency of charge and discharge, which in turn is proportional to the linear speed of the running yarn.

Circuit details

Battery. Under these conditions of operation, the output current is directly proportional to the battery voltage. For the instrument to remain in calibration, therefore, it is necessary to select a battery of characteristics and capacity such that its voltage will remain constant over a reasonable time period. Dry, Leclanché-type cells are not satisfactory from this point of view because their voltage falls off gradually with time. Mercury-amalgam cells, however, possess a steady voltage characteristic throughout the greater part of their life, although the voltage falls rapidly at the end of life period. Mercury-amalgam cells are available commercially, and a small and convenient pack unit has been made to give 27 V which fits into the handle of the yarn-speed meter [see Fig. 2(*b*)]. This battery unit ha life of 12–24 months whether stored or used intermitte to give currents up to 100 μA.

Meter. The selection of the meter for the instrument been a matter of compromise since increase in m sensitivity offers certain advantages, but also has attend disadvantages. A sensitive meter movement is to be ferred for the following reasons

(1) The current drain on the battery is reduced, wh results in increased battery life and makes possible the of a small battery pack, thus making possible a more porta unit.
(2) The switching currents are reduced, hence keep wear at the contactor because of arcing to a minimum.

Against these advantages must be set the follow disadvantages:

(1) Meter costs increase rapidly with sensitivity for sen tivity greater than 1 mA full-scale deflexion.
(2) For increased meter sensitivity, robustness of meter movement is reduced, so that the meter is more lia to damage from vibration, shock, etc.
(3) With increased sensitivity, the characteristics of co mercial meters become increasingly non-linear.

Consideration of all these points led to the final selecti of a meter having a full-scale deflexion sensitivity of 100 μ Use of a meter of this sensitivity permitted the smal mercury-amalgam cell to be used as power source, givi an expected life of 12–24 months under storage intermittent-use conditions. The cost of the meter is n excessive and linearity of characteristic and robustness a not seriously impaired at this sensitivity.

C_1R_1 charge and discharge circuit, and calibration of *by resistor R_4.* The current-limiting resistor R_1 has be introduced into the circuit to prevent wear at the conta point caused by arcing. A resistance of value 100 Ω h been found suitable for this purpose.

To allow for variation in the component values and order to make it possible to calibrate each unit individuall a rheostat R_4, which may be preset, is included in the circu Component variations have been reduced to a minimum the accurate grinding to size of the yarn-driven pulley ar by the use of a low tolerance silvered-mica capacitor for C The use of these low-tolerance components permits the value of R_4 for all units to be large compared with R_M, that the current lost through R_4, and hence the current dra on the battery, is kept to a minimum. In practice, it ha been found possible to achieve calibration on all units wi R_4 always greater than 25 kΩ.

Each instrument is calibrated initially at 300 and 600 ft/mi Calibration is achieved by engaging the yarn pulley with yar travelling at these fixed speeds, and R_4 is adjusted until th meter reads within ±1% (or ±5 ft/min) of these fixed speed This tolerance is necessary since the non-linearity of th meter movements makes it impossible to set all meters t the absolute speed of the yarn at both levels of yarn speec Any meter which is not sufficiently linear in characteristic t allow setting to these tolerances is discarded. These point of calibration have been selected since the normal operationa range of the instrument is between these limits, and it ha been found that the meter characteristics are such that unit set to this accuracy at these limiting speeds will measure t an accuracy of greater than ±1% at all speeds within thes limits.

Battery-checking circuit S_1R_3. The switch S and resistor $_3$ have been included in the circuit in order to check the ttery voltage. Immediately after calibration, the switch S depressed and the meter reading taken. This is noted on e body of the instrument [see Fig. 2(*a*)]. Subsequently, efore using the instrument, this switch may be depressed order to check the battery voltage. Recalibration is ecessary when the meter reading on depressing the switch S 1% lower than the calibration figure. Since the calibration gure is usually 480/500 ft/min, a fall in reading of 5 ft/min elow the calibration figure is normally accepted as the mit for recalibration. The need for frequent recalibration f the unit is an indication that the battery is coming to the nd of its useful life, and the battery should be replaced.

Smoothing circuit C_2R_2. This section of the circuit is ecessary to prevent needle flicker at normal operating peeds. The values of R_2 and C_2 are determined by simple ircuit considerations. In order to obtain linearity of meter urrent with frequency, it is necessary to ensure that at full-cale deflexion (that is, maximum frequency) the voltage across apacitor C_2 (V_c) is small compared with V_B. (If a 1% lack f linearity is allowed at this point $V_c = 0{\cdot}01\ V_B$.) Now:

$$V_c = i_M \frac{R_2(R_M + R_4) + R_M R_4}{R_4}.$$

f $R_4 \gg R_M$, this reduces to:

$$V_c \simeq i_M(R_2 + R_M).$$

For the instrument described, V_B is 27 V and R_M is 1000 Ω. At full-scale deflexion, i_M is 100 μA, V_c is 0·27 V and a value for R_2 of the order of 2000 Ω is obtained.

The value of C_2 is determined by time-constant considerations. A suitable time constant for the smoothing circuit is 0·1 second, which provides sufficient smoothing to enable yarn speeds as low as 100 ft/min to be accurately measured. With R_2 fixed at 2000 Ω, this gives a value for C_2 of 50 μF.

Mechanical details

The drive-pulley contactor unit was designed for ease of assembly, and for use of components which did not need to be made to very close limits. Reference to the drawing (Fig. 3) will show that the assembly consists of a spindle (1), $\frac{5}{64}$ in. diameter, which is supported by two $\frac{5}{64} \times \frac{1}{4}$ in. R.C. bearings separated by a spacer (5). From left to right, the spindle assembly consists of a 9 B.A. slotted nut, driving pulley, a spacer, bearing, spacer, bearing, spacer, contactor and silver contact mounted on a 9 B.A. nut. Tightening the slotted nut causes the bearing to be gripped firmly on to the spindle without the need for a closely controlled interference fit. The bearings are retained in the housing (6) by end covers (3) and (8). The outer cover (3) carries the rotatable guide pulley which is held against a friction washer by disk (2).

The housing (6) is moulded into the plastic case (4), its length being such that it allows some 0·002 in. clearance on the overall length of the bearings and spacer. This is to ensure that the bearings are not nipped tightly together by the outer race. In the drawing, this clearance is exaggerated in order to show an alternative method of retention. Here one bearing is held with retaining rings, whilst the other bearing is allowed to "float" endwise in order to take up its own position. It will be seen that by removing the slotted nut and pulley, the spindle and contactor may be withdrawn or by also removing the two screws (7) the spindle and bearings may be taken out.

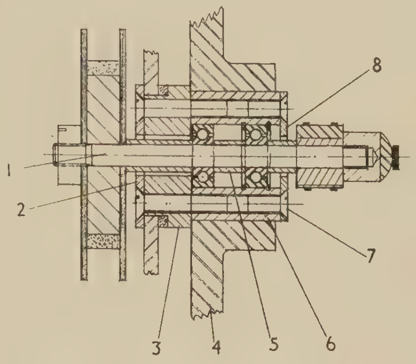

Fig. 3. Detailed drawing of contactor assembly

The pulley P is lined with a cork-rubber bonded material accurately ground to size ($\frac{3}{4} \pm 2/1000$ in. diameter) and of high friction so as to prevent yarn slippage.

The contactor disk, which is about 0·2 in. diameter, is made in silver for best results, although copper and brass, which is not free cutting, have been used successfully. Three inset Tufnol insulators, equally spaced angularly, are laid into the circumference. The wipers are of gold alloy, 0·002 × 0·020 in., with a centre wiper of similar material 0·005 × 0·050 in.

Cleaning and oiling of bearings. The extremely low-torque characteristics necessary for the satisfactory application of this instrument to measure yarn speeds on knitting machines means that over-lubrication of the miniature bearings must be avoided. This necessitated the development of a technique for cleaning even new bearings since they were supplied in capsules filled with oil. A satisfactory cleaning and lubrication technique has been evolved in which the bearings are cleaned in watch-cleaning solution by rotation at high speed, are dried on an electrically heated plate, and are lightly lubricated using a light watch oil applied *via* a stylus-type oiler, as used in horological work.

Acknowledgements

The authors wish to thank the Director of Research and Council of the Hosiery and Allied Trades Research Association for permission to publish this paper.

Production and tensile testing of strain-free metal specimens

by G. GREETHAM, B.Sc.,* English Electric Co., Whetstone, and A. J. MARTIN, B.Sc., Ph.D., Atomic Weapons Research Establishment, Aldermaston, Berks

[*Paper first received* 10 *November, and in final form* 7 *December*, 1959]

Abstract

Details are given of equipment which has been used to prepare and mechanically test single crystal specimens of beryllium from zone refined rod. An electrolytic etching machine is described whereby the test-pieces may be prepared without mechanical deformation, and details are given of a modified Polanyi apparatus in which specimens may be tested in tension at temperatures up to about 600 °*C*.

1. Introduction

Any investigation concerning the mechanical deformation of metals consists of two distinct stages. Firstly the metal must be fashioned into a shape applicable to the mode of testing and secondly the shaped specimen must be tested on a suitably designed machine.

The shaping of metal specimens is usually done mechanically, e.g. turning, grinding. This invariably work-hardens the specimen surface and an annealing treatment is necessary prior to mechanical testing. There are instances, however, when it is undesirable to mechanically work the specimen or give an anneal before mechanical testing. Examples of these two cases are single crystal work, where prior accidental deformation would invalidate the mechanical test results, and precipitation investigations, where an anneal would alter the metallurgical state of the specimen. The electrolytic method described below provides a means of producing shaped strain-free specimens, and deals specifically with beryllium single crystals.

A small Polanyi tensile machine is also described. The design employed enables the specimen temperature to be changed rapidly and easily. The load is measured by a dynamometer, the output of which is fed into a converted temperature recorder. This provides a continuous record of load and extension of the specimen during the tensile test.

Both pieces of equipment were designed as part of an investigation at A.W.R.E. into the deformation characteristics of beryllium single crystals.

2. Anodic machining equipment

As mechanical work is to be avoided an electrolytic turning technique has been developed. This consists of a 3 in. diam. stainless steel wheel *A* (Fig. 1) rotating at 0·2 rev/min, and a counterbalanced chuck *B*, rotating at 1 rev/min. The beryllium single crystal *C* is held in this chuck and made to rest lightly on the stainless wheel by adjusting the counterweight.

Electrolyte from the dish *D* is carried up to the specimen, surface tension retaining a layer between the wheel and the crystal. A 5 V potential is applied between the wheel cathode and the specimen as anode. With this electroly technique beryllium is removed preferentially from the "hig spots" of the crystals as they rotate close to the stainle steel wheel, and the profile of the wheel slowly cuts into th crystal. Fig. 2 gives the dimensions of the finished test piec The electrolyte used is one containing 900 ml. H_3PO_4, 300 m ethanol, 300 ml. conc. H_2SO_4, and 300 ml. glycerol. Crysta are produced having a reasonably bright, smoothly polishe surface and need only a short final electro-polish befor examination.

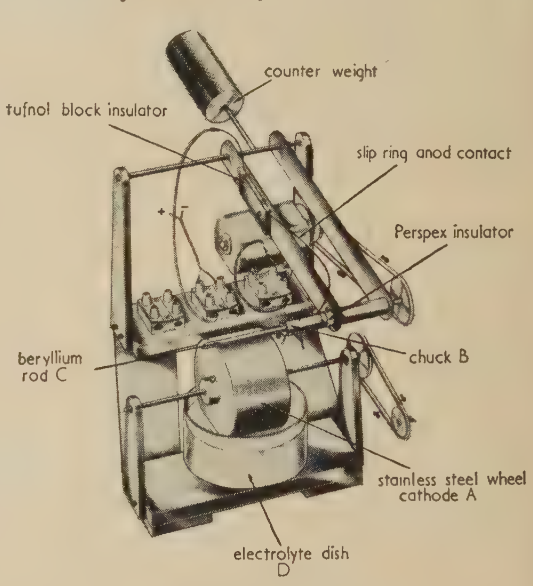

Fig. 1. Electrolytic turning machine

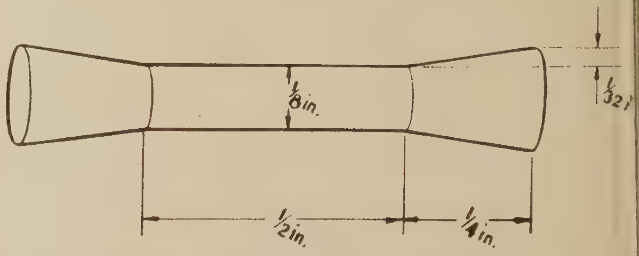

Fig. 2. Dimensions of finished crystal

Although conically shaped ends are shown in Fig. 2 it i possible to produce various shapes, providing they are no too elaborate, by simply altering the profile of the stainles steel wheel *A*.

There is also no reason why other metals should not b fabricated in exactly the same way as for beryllium, providing the correct electrolyte and anode (profile wheel) are used.

---

* Seconded to the Beryllium Section, S.R.M., A.W.R.E., Aldermaston, during the course of this work.

he method is particularly useful when brittle or hard metals ve to be shaped.

3. Tensile testing equipment

3.1 *General description of tensile machine and autographic cording.* A modified Polanyi type tensile machine has been esigned. The design generally is based on fine engineering lerances giving the advantage of greater robustness.

The crosshead *E*, Fig. 3, slides in bushes on the side pillars C and *D*. Two compression members, *F* and *G*, extend hrough the bottom plate *B*. The upper central tensile nember, *H*, passes upwards through a hole in the lead screw, , to the load measuring device. This arrangement enables n oil bath or furnace to be placed easily and quickly round he specimen, *S*.

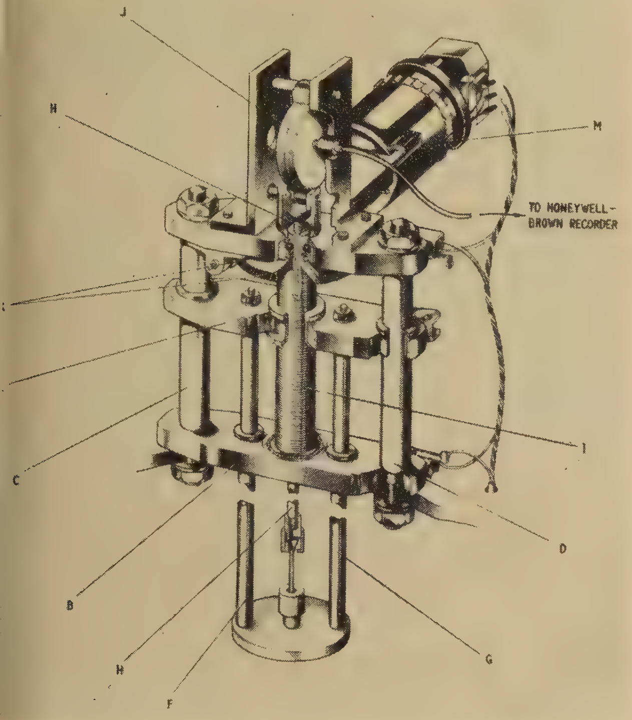

Fig. 3. Details of tensile testing machine

Strain rate is governed by the number of threads per inch f the lead screw *I*, the reduction ratio of the crown wheel nd pinion *K*, and the speed of motor *M*. Only the last wo are variable. The crown wheel and pinion used at resent has a reduction ratio of 60 : 1, with a motor speed of 2 rev/min. This, combined with a 20 teeth/in. lead screw, ives a strain rate of $5 \cdot 5 \times 10^{-5}$/s for a $\frac{1}{2}$ in. gauge-length pecimen. This rate can readily be altered by altering the eduction ratio of the crown wheel and pinion and/or the notor speed.

Load is measured by a dynamometer,* *J*, of 500 lb capacity. The output from this instrument is then fed into a Honeywell-Brown millivolt recorder.

As the chart speed of the recorder and the rate of straining f the specimen are known, the strain in the specimen can be eadily obtained from the recorded load-elongation curve.

The recorder used is, in fact, a 0 to 1000° C temperature ecorder, modified in the following ways:—

(1) The instrument has been altered to read from right to left. Stress-strain curves are then obtained as plotted conventionally, with strain increasing from left to right and the stress increasing vertically.

(2) The automatic standardization mechanism has been disconnected and replaced by external variable resistors. The recorder can be adjusted thereby to give the millivolt range required.

(3) Finally, using an external battery circuit, the input from the dynamometer can be "backed-off" in steps in order to extend the range of the recorder.

3.2 *Details of dynamometer supply and backing-off circuit.* The dynamometer consists of four matching resistance strain gauges, *P*, *Q*, *R* and *S* attached to a brass ring (Fig. 4). When the ring is strained the resistance of two of these gauges increases and the resistance of the remaining two gauges decreases, producing an increase in the potential drop across *Y* and *Z*.

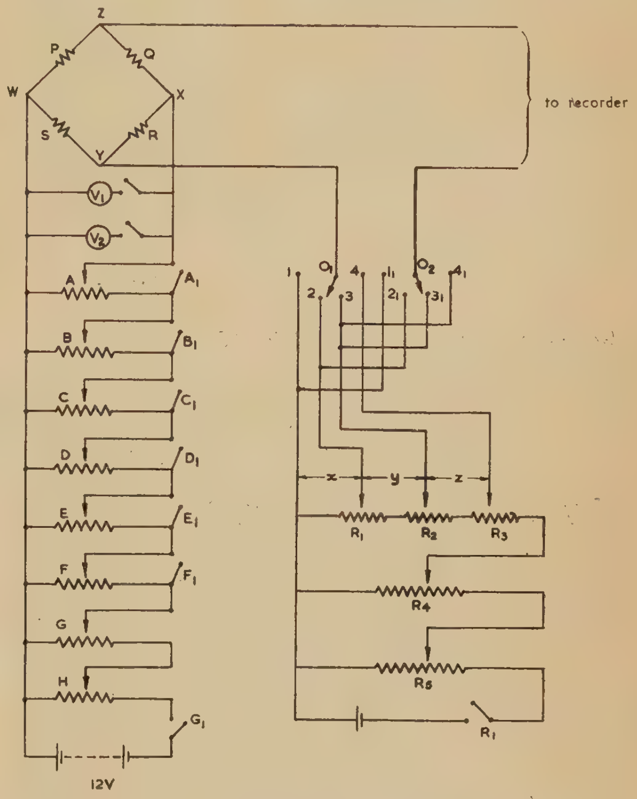

Fig. 4. Circuit diagram of dynamometer supply and backing-off circuit

The output from *YZ* may be backed-off using the circuit indicated. With the rotary switches 0_1, 0_2 in position, 1, 1_1 the circuit is shorted out. In position 1, 2_1 x mV are subtracted from the output across *YZ*. This in effect depresses the zero of the recorder and therefore increases the length of its scale. With the switches in position 1, 3_1 the zero is depressed by $(x + y)$ mV, and so on, depending on the length of scale required.

It is also possible, by using rotary switches, to alter the zero position of the recorder. This is sometimes necessary since some dynamometers give a negative reading when completely unloaded. The switches may be set in position 2, 1_1 to alter the zero, by adding x mV to the output from *YZ*.

The supply to *WX* consist of a series of potential dividers, each capable of being shorted out by a switch. These resistors, A, B, C, D, E and F, may be set to give an output from YZ which will match the millivolt range of the recorder or give some simple multiple of it. Hence it is possible to change from one range to another easily and quickly.

---

* J. Langham Thompson Ltd., Bushey Heath, Herts.

The recorder is calibrated in the following way. A known weight is suspended from the dynamometer and the input voltage set. The standardizing resistors are adjusted until the pointer of the recorder comes to rest at some required mark on the scale. As the dynamometer output is linear the scale is now calibrated for any other load.

The backing-off circuit may now be set. With the rotary switches in position 1, 2_1, resistor R_1 is adjusted to move the pointer of the recorder back to zero, i.e. the zero has been depressed and the length of the scale increased. Now w switches in position 2, 3_1, R_2 is adjusted to move the poir back to zero. Similarly for switch position 3, 4_1 and resis R_3. Then $x = y = z$ mV and the scale is increased fourf

The above system produces a most flexible arrangeme easily adaptable to different capacity dynamometers a enabling the required scale to be selected quickly.

Acknowledgements

The authors would like to thank Dr. M. A. Adar A.E.R.E., for his advice on the design of the tensile machi and Mr. G. C. Ellis, Superintendent, Metals Research, his encouragement during the course of this work.

Primary standard barometer of range 0 to 1200 mb

by K. W. T. ELLIOTT, D. C. WILSON, F. C. P. MASON, A.M.I.Mech.E., and P. H. BIGG, B.Sc., F.Inst.P.,
National Physical Laboratory, Teddington, Middlesex

[*Paper received* 17 *November*, 1959]

Abstract

A primary standard barometer covering all pressures in the range 0 *to* 1200 *mb has been designed and constructed at the National Physical Laboratory. A feature of the instrument is the use of optical probes*(1) *as fiducial indicators which assess, from overhead, the positions of* 11-*cm diameter mercury surfaces in the barometer U-tube, thus permitting the mercury columns to be fully water-jacketed. The two probes use a single mercury pool as a common reference surface and their movements are assessed in terms of readings on associated line standards of Invar by means of fixed micrometer microscopes. The U-tube assembly is supported on an anti-vibration mount. The accuracy of height measurement of barometric columns was estimated by reference to measurements on end-gauges mounted in the empty U-tube and found to be better than* 0·003 *mm* (*standard deviation*). *Taking into account the small uncertainties in mercury density and local gravity the overall accuracy of a single pressure measurement is estimated to be about* ±0·01 *mb on a* 99% *certainty basis. At about* 1000 *mb, check comparisons with N.P.L. primary barometers of earlier design support this assessment.*

1. Introduction

A PRIMARY standard barometer has been designed, constructed and installed at the National Physical Laboratory to meet the need for an instrument which will measure, from first principles, pressures covering the entire range 1200 to 0 mb found in the free air, namely, from those experienced, say, one mile below mean sea level to those existing beyond the outer limits of the atmosphere. Such an instrument is required as the basis of the accurate calibration of pressure-measuring instruments used in mining, aviation and rocket research.

Hitherto, the accuracy of calibration of the N.P.L. standard barometers used in this work has been limited by the need to calculate the corrections from those at about 1000 r (known by reference to the first N.P.L. primary standa barometer(2)), from precise scale and bore measuremen etc., supplemented by the use of an experimental merc column and length comparator. This left much to be desire however, as regards both certainty and ease of measureme

The new instrument is, essentially, a mercury U-tube w one limb evacuated, changes in mercury-level being measur from above the mercury surfaces by a pair of optical prob which have already been described.(1) This arrangeme avoids the necessity of long, blemish-free and optically f windows mounted in the sides of the U-tube, and genera facilitates the solution of the problem of achieving unifor temperature conditions. The instrument was initially co ceived as being capable of 0·03 mb accuracy and it w designed accordingly. The high precision of performance the probes, however, encouraged the investigation of the fu potentialities of the instrument, and it was found th throughout its range the accuracy of pressure measureme is ±0·01 mb on a 99% confidence basis. This is appro mately the same as that given at about 1000 mb by t original N.P.L. primary standard barometer which it no supplements.

2. Description

In the photograph (Fig. 1) the barometer is seen after i initial assembly and prior to its enclosure within a metal ar Perspex draughtproof case. On the right is the U-tube un supported on an anti-vibration mount, and on the left is t measuring machine, running on a massive concrete supp bedded into the ground.

The general arrangement of the U-tube assembly is show in Fig. 2. The upper and lower working sections of t U-tube are formed by two 11 cm diameter tubes; the lar diameter is necessitated by the dimensions of the optic probes but it serves, incidentally, to eliminate capilla depression from the operative, central, parts of the mercu surfaces. These large-bore tubes, together with the narrow vertical connecting tube which is placed adjacent to the complementary limb, are water-jacketed for good thermal conditions. Both working sections are of Inconel, a material containing 76% nickel, 15% chromium, 9% iron, which is considered to be free from mercury and water attack and can be spun-cast for homogeneity. The connecting tube is of stainless steel. Both limbs are provided with 16-mm thick optically flat and parallel coverplates, through which the mercury surfaces are viewed. The top of the upper limb is normally connected, through a flexible stainless steel tube, to a mercury diffusion pump whereby a vacuum may be produced and maintained as required. The residual pressure in this limb is measured by a directly-attached Pirani gauge head. The lower limb may be connected to any enclosed volume of air, the pressure of which is to be measured. The barometer contains approximately 55 kg of mercury, and with equal pressures above the mercury in the two sections, the common mercury level is 2·5 cm below the top of the lower section and 2·5 cm above the bottom of the upper section. Both sections are 51 cm high and any pressure corresponding to a head of mercury of up to 92 cm can be measured.

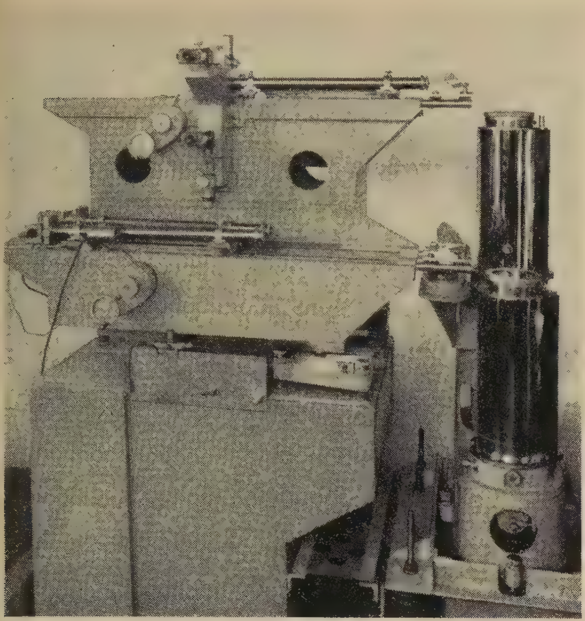

Fig. 1. The barometer before enclosure in its protective case in which the vacuum and electronic equipment are also contained. (The flat perforated anti-tilt strips were later replaced by strips each having a single large corrugation; see text)

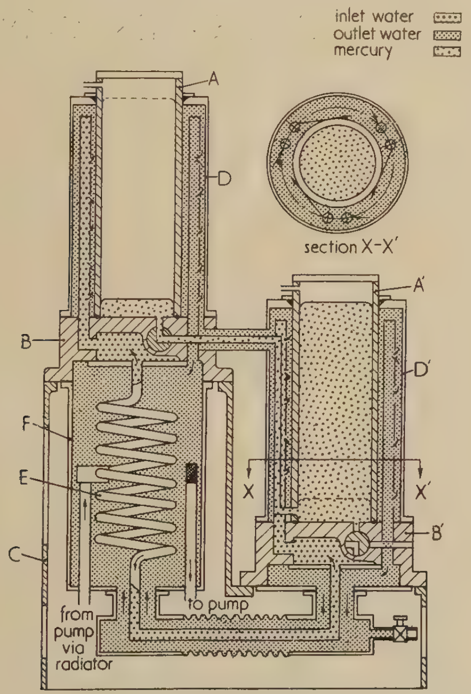

Fig. 2. Diagrammatic representation of the U-tube assembly and water circulation. (*Inset*, cross-section at *XX′*)

The simultaneous positions of the mercury surfaces in the U-tube are ascertained by optical probes which have been described previously.(1) The probes can be seen in Fig. 1 mounted on a stiff casting supported on a kinematically designed ball trackway. They are supported between horizontal parallel guideways formed in the upper surfaces of the casting, fast- and slow-motion positional controls being provided. Briefly (see Fig. 3), each optical probe consists of an arrangement by which the image of an illuminated grating of special construction is formed on the surface to be observed, and light reflected from this surface then forms, on an exactly similar grating, an image of equal size. The incident and reflected rays are each inclined to the normal at an angle of 5°, and because of this the lateral disposition of the final image relative to the grating on which it is formed depends upon the position of the probe relative to the reflecting surface. Changes in this disposition cause variations in the amount of light which passes through the receiving grating to a photocell. A probe can therefore be set at a reproducible distance from the reflecting surface by moving it axially until a predetermined amount of light is received on the photocell; it is thus used as a fiducial indicator. Further details may be found on reference to the original publication. In the barometer the gratings are housed in the rectangular boxes seen in Fig. 1 attached at the left of the converging tubes, which carry at their opposite ends the projection lenses. The horizontal optical paths of the probes are deflected into vertical planes by inclined mirrors freely supported on adjustable mountings fixed to the casting at the end of the guideways. The whole casting can be translated along its trackway by pneumatic pressure so that the two probes can be brought to operate simultaneously either on the U-tube or (as in Fig. 1) on a common mercury reference pool, contained in the chamber which can be seen fixed to the left-hand side of the U-tube assembly. The reference level closely coincides with the mean surface level in the U-tube. Displacements of the optical probes along their ways between settings on the U-tube and the reference pool are referred, by means of micrometer microscopes attached rigidly to the casting,

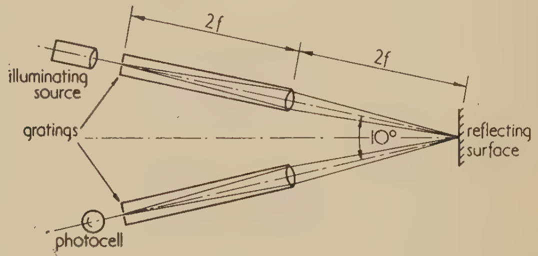

Fig. 3. Principle of optical probe

directly to verified line standards mounted on the probe carriages.

The construction of the U-tube unit is shown diagrammatically in Fig. 2 which also indicates the water circulation. The barometer tubes *A*, *A′* are sealed with O-rings to the bases *B*, *B′* mounted on the casting *C*. Each of the barometer tubes is enclosed within a water-jacket *D*, *D′* which is chromium-plated to minimize radiation. The delivery from a small water-circulating pump is connected *via* a car-type radiator to the midpoint of the coil *E*, whence water passes into the two water-jackets. Thence it returns to the reservoir *F* and finally to the pump. Water enters the jackets through three symmetrically disposed vertical tubes perforated so that it flows at all levels round the mercury tube to three similar exit tubes (see Fig. 2, inset). The horizontal connecting mercury tube and the tube conveying water to the jacket of the lower mercury limb are water-jacketed and the coil E is of corrugated metal. This arrangement ensures adequate uniformity of temperature distribution within the water-jackets (see Section 3), good heat transference between the incoming and outgoing water streams, and high thermal capacity with thorough mixing in the reservoir. Cocks are provided in the bases to isolate the working sections when desired, and to assist in filling and draining. Care was taken to avoid the contact of electrochemically dissimilar metals.

The U-tube unit, which weighs about 285 kg when filled with mercury, is supported on an anti-vibration mount. This consists of a concrete block weighing about 680 kg carried by four helical compression springs, the natural frequency of the system in the vertical direction being about $1\frac{1}{3}$ c/s. A special requirement of the mount was that the barometer should not tilt by more than 0·2° due to the transference of mercury from one limb of the barometer to the other. This condition was achieved by fitting four horizontal restraining strips of brass sheet, each having a large single corrugation running parallel to the plane of the U-tube. Small open dashpots, filled with a silicone fluid, were added to reduce the amplitude of the residual low-frequency oscillation.

3. Temperature measurement

Initial thermocouple measurements having shown that after the water had been circulating for a few minutes the temperature in each jacket was uniform within about ±0·005 deg C, its mean temperature is taken to be the temperature at a point halfway up the jacket, where it is measured by a mercury-in-glass thermometer with its bulb set in a brass block. The thermometer is divided to 0·01 deg C and verified, by reference to the International Temperature Scale, to ±0·002 deg C in conditions similar to those occurring in service.

Most of the pump energy transferred to the water is removed from the radiator by air circulation within the barometer case; the rate of rise of temperature is thus kept down to 0·1 deg C/h and the water and air temperatures are equalized to about 0·1 deg C. The pump is switched off immediately prior to an observation and the thermometer readings then remain steady within ±0·002 deg C for some minutes. The thermal lagging time of the mercury in the working sections being $2\frac{1}{2}$ min relative to the water, the thermometers, read 3 or 4 min after switching off, indicate the mercury temperature extremely closely. Due perhaps to an accident of circulation or to unequal heat losses, the upper jacket is usually a few hundredths of a degree colder than the lower jacket, but this difference is appropriately allowed for.

Fully adequate thermal control of the various parts of th measuring machine is ensured by the circulation of the a within the barometer case. The line standards carried on th optical probes are of Invar and have coefficients of expansio less than 1 × 10^{-6} per deg C. The greatest combined lengt used is 920 mm and hence the greatest length change due t temperature is less than 1 μm per deg C (1 μm = 10^{-3} mm = 10^{-6} m). Therefore it is quite adequate to regard th temperature of the line standards as being the same as tha of the circulating air. The very small and slow effects o temperature on other components of the measuring machin are eliminated by associating a reference pool measuremen with each U-tube measurement.

4. Assessment of effects of refraction and instrumental imperfections

Each optical probe is required to make two settings, on on the mercury surface in the reference pool and one on tha in the appropriate limb of the U-tube, and any change in th length of the probe between these two settings will affect th assessment of the vertical distance between the surfaces. Th length of a probe depends on the point of intersection of th optical axes and this is influenced by:

(*a*) slight curvature of the mirrors and coverplates;
(*b*) differences of refractive index of the air on either sid of the coverplates;
(*c*) elastic yield of the coverplates due to pressur differences across them.

The mirrors depart from flatness by about 0·05 μm an therefore each mirror alters the probe length, the magnitud of the change being dependent upon the parts of the mirro being used. The errors arising from this cause were assessed by using the probes to measure both directly and *via* the mirrors special combination end-gauges of several lengths. To each end of the gauges were wrung projecting blocks having parallel, polished plane surfaces facing in the same direction and so disposed that by moving a probe along its runway the apex could be set on either face. Each combination of gauges was first held vertically in the empty U-tube (without coverplates) and measured *via* the mirrors, and secondly, horizontally on the probe axes and measured directly. It was necessary to make allowance for the tilting of the main casting which is due to elastic yield of the supports, which occurs when the probes are moved along the runways, and causes a vertical displacment of the mirrors. This affects the vertical measurement but not the horizontal one. The effect of this tilting was assessed by observing the change in the set position of one probe when the other probe was traversed along its ways. By combining the results obtained in this manner for various dispositions of the probes, it was possible to derive the magnitude of the appropriate allowance in the above test and also the net effect of the probe movements that occur in actual barometric observations. A 450 mm movement of one probe causes a vertical displacement of the mirrors of about 12 μm, whilst the net effect of moving both probes in opposite directions, as when taking a barometric observation, is only about 2 μm on a column height of 900 mm.

The glass coverplates, also, show sufficient departures from flatness to affect the probe lengths. To measure the errors due to this cause the gauges used in the mirror tests were set up in the U-tube and measured with and without the coverplates in position. The results were independent of mirror imperfections because corresponding observations involved he same parts of the mirror surfaces. The main casting ilted by the same amount whether or not the coverplates were in position, and therefore did not affect the results.

When there is a pressure difference across a coverplate as n use on the barometer, the refractive indices of the air above and below the plate are different and the plate bends slightly. The first of these effects can be calculated theoretically in terms of the pressures and temperatures of the air above and below the plate. This is a relatively large effect, amounting to nearly 0·13 mm under certain conditions of use. To calculate the change in probe length to an accuracy of 1 μm one must know the refractive indices of the air on both sides of the plate to about 1 part per million (p.p.m.); it is sufficient for this purpose to assume an average value for the humidity and to ascertain the appropriate pressures and temperatures to 1 mb and 1 deg C respectively which presents no difficulty. The distance between the plate and the surface being detected must be known to 1 mm, and in the case of barometric observation this can be derived from the uncorrected height of the column.

The slight bending of the coverplate when subject to pressure differences introduces small additional refraction effects. The allowance, which is a function of both the distance of the probe apex below the plate and the pressure difference, does not exceed 6 μm in normal use of the barometer, and does not vary significantly with ambient conditions. The combined refraction errors were assessed by measuring the combination end-gauges in the U-tube with and without various pressure differences across the coverplates.

Subsequently, the U-tube was filled with the correct quantity of mercury, and with no coverplates in position the zero height was measured in the normal way against the reference pool. This provided a check on the motion of the measuring machine between settings on the reference pool and the U-tube. The coverplates were then placed in position, and, still with atmospheric pressure on both limbs, the zero height was again measured to show the effect of the slight differences in thickness of the coverplates. Finally, the combined correction at zero barometric height due to the different thicknesses of the glass plates and to their bending under the associated pressure differences was confirmed. The errors pertaining to the measurement of any particular column height were thus assessed from first principles.

The magnitudes of the corrections due to imperfections of the optical components are shown in Fig. 4 relative to those at zero height of barometric column. Apart from the refraction corrections the total correction including the zero correction (−1·3 μm) rises to +13 μm when measuring a column height of about 900 mm.

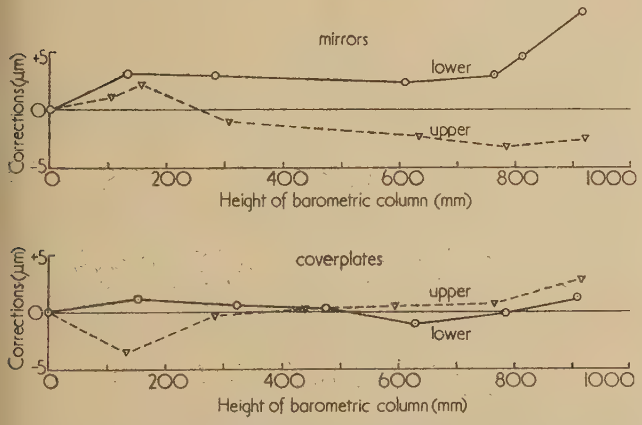

Fig. 4. Corrections due to the residual imperfections of form of the mirrors and coverplates; these corrections are relative to the correction at zero height of barometric column

5. Accuracy

Each measurement of the height of the barometric column requires two length measurements, one with each probe. It has previously been reported⁽¹⁾ that the standard deviation of a length measurement not subject to error due to the optical effects discussed above is not larger than 0·7 μm.

From the degree of consistency of measurements made on different occasions and the extent of the irregularities in the curves in Fig. 4 it is estimated that the assessments of the optical effects have the following standard deviations:

due to curvature of a mirror, 0·8 μm;
due to departure of a coverplate from flatness, 1·2 μm.

The zero correction and the refraction correction are each thought to be known with a standard deviation of 0·5 μm. A standard deviation of 1·0 μm is associated with the bending of the plates.

Taking the total variance associated with a single measurement of a barometric height to be $2(0{\cdot}7^2 + 0{\cdot}8^2 + 1{\cdot}2^2) + 1{\cdot}0^2 + 0{\cdot}5^2 + 0{\cdot}5^2\ \mu\text{m}^2$, i.e. $6{\cdot}6\ \mu\text{m}^2$, the standard deviation is 2·6 μm. On a barometric height of 760 mm this corresponds to 3·5 p.p.m.

To derive the pressure from the height of the barometric column the density of the mercury and the local value of gravity need to be taken into account. The density at 20° C of the mercury used was measured by Cook and Stone⁽³⁾ and it is considered that by adopting a standard deviation of 0·4 p.p.m., both random and systematic errors of the density determination are adequately covered. It is considered that the temperature of the mercury is known well within 0·01 deg C corresponding to a standard deviation of 0·003 deg C or 0·6 p.p.m. in the mercury density. All barometric observations are made with the mercury within two or three degrees of 20° C and the observations of column height are adjusted to 20° C by means of the expansion data published by Beattie and others⁽⁴⁾ and reviewed by Cook⁽⁵⁾; this adjustment does not introduce significant error. Consequently the mercury density brought into the final calculation is regarded as having the standard deviation of 0·7 p.p.m. It is not known for certain yet how much the mercury density is likely to change through contact with the barometer, but any change is confidently expected to be extremely small and it will be disregarded for the time being. The acceleration due to gravity was determined at the N.P.L. by Clark⁽⁶⁾ with a standard deviation of 0·6 p.p.m.⁽⁷⁾ by means of absolute pendulum measurements. A further re-assessment of this estimate will be necessary when the results of a new absolute determination by a symmetrical ballistic method, now in progress, become available; current indications are that Clark's value is very close indeed to reality and for the present it will be assumed to hold good.

Combining the above estimates of uncertainty, the standard deviation of a single measurement of about 1000 mb is found to be 0·0036 mb. The contribution of the uncertainties associated with the density and with gravity being very small relative to those of the height measurements, this standard deviation may be taken to apply at all pressures. A single determination of pressure with the instrument described may in consequence be considered as accurate, at the confidence level of 99%, within ±0·01 mb, i.e. within one hundred-thousandth part of one atmosphere.

6. Comparison with other primary standard barometers

As a check the barometer was compared both with the original (1933) N.P.L. primary standard barometer (1) and a recently constructed similar instrument (1*A*). Apart from the provision of special anti-vibration mounts for the mercury columns and an improved method of temperature measurement in the newer instrument these barometers are essentially as originally described.(2)

Barometers 1 and 1*A* were set up in a temperature-controlled enclosure near to the long-range primary barometer (l.r.p.) and the three instruments were connected by an airtight system which included a stabilizing ballast volume. The mercury contained in the three barometers came from stocks known to have the same density within 1 p.p.m. and it was assumed that the instruments were subject to the same gravity.

Twenty measurements of common pressures (about 1000 mb) were carried out with each of the three possible pairs of barometers and the following results were obtained:

	Mean (*mb*)	*Variance* (*mb*^{2})
1 minus l.r.p.	$-2{\cdot}1 \times 10^{-3}$	$8{\cdot}4 \times 10^{-6}$
l.r.p. minus 1*A*	$-1{\cdot}3 \times 10^{-3}$	$6{\cdot}8 \times 10^{-6}$
1*A* minus 1	$+2{\cdot}3 \times 10^{-3}$	$3{\cdot}7 \times 10^{-6}$

Assuming normal distribution of error one may deduce that the standard deviation associated with the new primary standard barometer in these comparisons is approximately 0·0024 mb, which compares favourably with the conclusions drawn in Section 5.

Acknowledgements

The work described above has been carried out as part the research programme of the National Physical Laborato and this paper is published by permission of the Director the Laboratory. The late Mr. F. D. Jones, who conceiv the idea of the optical probe, worked until his death on th development of the barometer; it was then in an advance stage of construction. The precision constructional wor was carried out by Mr. J. Wilson. The authors acknowledg the assistance given them by other colleagues, particular Mr. H. L. Cox and Mr. N. B. Owen who advised on the ant vibration mount and Mr. J. S. Clark with whom muc helpful discussion took place.

References

(1) Elliott, K. W. T., and Wilson, D. C. *J. Sci. Instrum* **34**, p. 349 (1957).
(2) Clark, J. S., and Sears, J. E. *Proc. Roy. Soc. A*, 13 p. 130 (1933).
(3) Cook, A. H., and Stone, N. W. B. *Phil. Trans A*, 25 p. 279 (1957).
(4) Beattie, J. A., Blaisdell, B. E., Kaye, J., Gerry, H. T and Johnson, C. A. *Proc. Amer. Acad. Arts Sci.*, 71 p. 371 (1941).
(5) Cook, A. H. *Brit. J. Appl. Phys.*, **7**, p. 285 (1956).
(6) Clark, J. S. *Phil. Trans A*, **238**, p. 65 (1939).
(7) Jeffreys, H. *Monthly Not. Roy. Astron. Soc., Geophys Suppl.*, **5**, p. 398 (1949).

Heat transport anemometer of high stability

by A. J. DYER, M.Sc., Ph.D., F.Inst.P., Division of Meteorological Physics, Commonwealth Scientific and Industrial Research Organization, Melbourne, Australia

[*Paper received* 21 *October* 1959]

Abstract

An anemometer is described based on the principle of detecting the wake behind a heated wire by means of a thermometric bridge. An earlier design of this type of anemometer required a servo-amplifier having a gain of 10^6 *times. A new principle enables the desirable features of the former method, namely linearity and unidirectivity, to be preserved with an amplifier gain of* 80 *times with a corresponding improvement in stability and simplicity. The measured response time of the instrument is approximately* 0·1 *second.*

Introduction

Taylor(1) has described an anemometer having certain unique advantages for micro-meteorological studies in that it is of rapid response, is unidirectional, and has an output linearly related to wind velocity. A form of this instrument also described by Taylor, measuring the vertical component of the wind in the lowest layers of the atmosphere, has now been in operation for a number of years. An additional anemometer was recently required to determine the corresponding horizontal wind component for the purpose of obtaining the turbulent transfer of momentum by the eddy correlation method. It was essential that this instrument should be compatible with existing equipment measuring the eddy transfer of water vapour (Taylor and Dyer(2)), and the opportunity was taken of reviewing the anemometer design to see if significant improvements could be effected.

In the original method, a servo-amplifier having a gain of 10^6 times is required as the bridge output signals (1200 c/s) are of the order of a few microvolts. The signal frequency for the new anemometer had to be that of the mains supply for the reasons of compatibility referred to above, and the possibility was evident of spurious signals and noise causing severe limitations in operation. A design principle was therefore sought which avoided the use of an amplifier of such high gain. A corresponding improvement in stability was expected. The method evolved on this basis raises the level of performance of this type of anemometer considerably above that of the conventional type of hot-wire instrument.

Theory of basic design

The various elements of the sensing device are shown schematically in Fig. 1. *XX* and *YY* are two fine wires having a large temperature coefficient of resistance (λ) and *A* is a long heater wire running perpendicular to the plane

XYY. It can readily be shown (Taylor[(1)]) that the difference resistance (δr) between the two sensing wires for a wind mponent u in the plane $XXYY$ and perpendicular to the ne XX is given by:

$$\frac{\delta r}{r} = \frac{k}{u - \eta} \tag{1}$$

here $k = \lambda H/C_p \rho l$ and $\eta = \alpha H/C_p \rho$ (η is a second-order rm and is retained merely for completeness). H is the rate f heat input per unit length of heater, l the length of the nsing wires, C_p the specific heat of air at constant pressure nd ρ the air density. The term α is a small quantity related the width of the wake of the heated air.

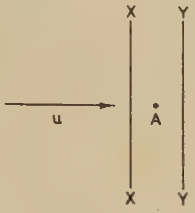

Fig. 1. Schematic representation of sensing device

If the two sensing wires are placed in the opposite arms f a Wheatstone bridge (input voltage E) in a servo-circuit Fig. 2), the following equations can be written:

$$E = \gamma(e_0 - \beta G e), \tag{2}$$

$$e \approx \frac{E}{4r}(\delta r - \delta r_0). \tag{3}$$

The term γ is a factor determined by the attenuation in the nixing circuit in which the feedback voltage $\beta G e$ is subracted from the source voltage e_0. The term δr represents he unbalance of the bridge varying with wind speed according o equation (1), and δr_0 represents an initial unbalance ntroduced in the bridge, so arranged that the bridge comes nto balance when in operation at the mid-point (u_0) of the vind-speed range, that is:

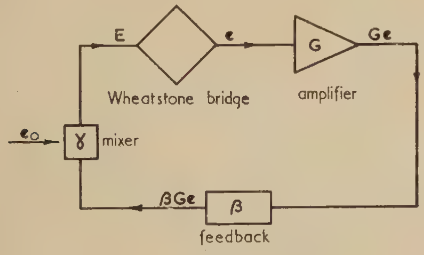

Fig. 2. Basic circuit design

$$\frac{\delta r_0}{r} = \frac{k}{u_0 - \eta}. \tag{4}$$

Solution for E gives:

$$E = \frac{\gamma e_0}{1 + \frac{k\gamma\beta G}{4}\left(\frac{1}{u - \eta} - \frac{1}{u_0 - \eta}\right)}.$$

f the relation:

$$\frac{k\gamma\beta G}{4(u_0 - \eta)} = 1, \tag{5}$$

can now be satisfied, then the desired linear relation is obtained,

$$E = \frac{4e_0(u - \eta)}{k\beta G} = \frac{\gamma e_0(u - \eta)}{u_0 - \eta}. \tag{6}$$

The above criterion for linearity (equation 5) expresses essentially the relation between total servo-loop gain and the value of windspeed (u_0) at which the bridge is balanced. It will be readily seen that the higher the value of u_0, the greater is the amount of gain required to achieve linearity.

In the Taylor design, the bridge comes into balance at a wind speed close to infinity and this is a fundamental reason for the high servo gain required. This difficulty is avoided in the present method by causing the bridge to balance at the mid-point of the wind-speed range. Minor modifications of circuit design render the latter approach feasible. If similar sensing and circuit elements to the earlier scheme are used, it is found that equation (5) accurately predicts that an amplifier gain of approximately 80 times is required (compared with 10^6 times required previously).

It is of interest to assess the effect on performance of a variation in total loop gain, that is, if equation (5) is not exactly satisfied. If:

$$\frac{k\gamma\beta G}{4(u_0 - \eta)} = 1 + \zeta,$$

where $\zeta \ll 1$, then the error δE in E as a result of ζ not being zero is given by:

$$\frac{\delta E}{E} \simeq \frac{\zeta(u - u_0)}{u_0 - \eta}.$$

Hence the percentage variation in E is less than the percentage variation in loop gain in the design range $\eta < u < 2u_0 - \eta$. At the centre of the range near $u = u_0$, the variation in E is obviously negligible if the loop gain is held constant to within a few per cent.

Practical circuit details

The detailed electronic circuit is shown in Fig. 3. The servo amplifier V_1, V_2 consists of two stages of total nominal gain 6×10^3 times with overall feedback providing a stable amplifier of gain 80 times. A cathode follower V_3 supplies the feedback to the bridge in series with the source voltage. This feedback voltage should have zero phase shift and suitable corrections are applied at two points. The input voltage E to the bridge is measured by a phase detector V_5 after a single stage of amplification V_4.

The setting-up procedure is simplified by means of a five-position master switch with a single adjustment in each position as described in the following:

(1) Phase-detector zero (*phase*).

(2) Bridge balanced at u_0 (*bal*).

Wind speed u_0 is simulated by a 10 kΩ high-stability resistor in parallel with a 200 Ω resistor in the bridge arm.

(3) Output signal adjusted to standard sensitivity (50 μA) at u_0 (*sens*).

(4) Feedback adjusted to give desired linearity (*lin*). Wind speed $2u_0$ (100 μA) simulated by 20 kΩ shunt.

(5) In position *run*, the heater current can then be turned on and an adjustment (*run*) is provided to adjust the mean wind speed for zero output. (This was necessary in the particular context in which the equipment was used.)

The linearity adjustment (4) does not affect the sensitivity adjustment (3) since the latter is carried out with the bridge

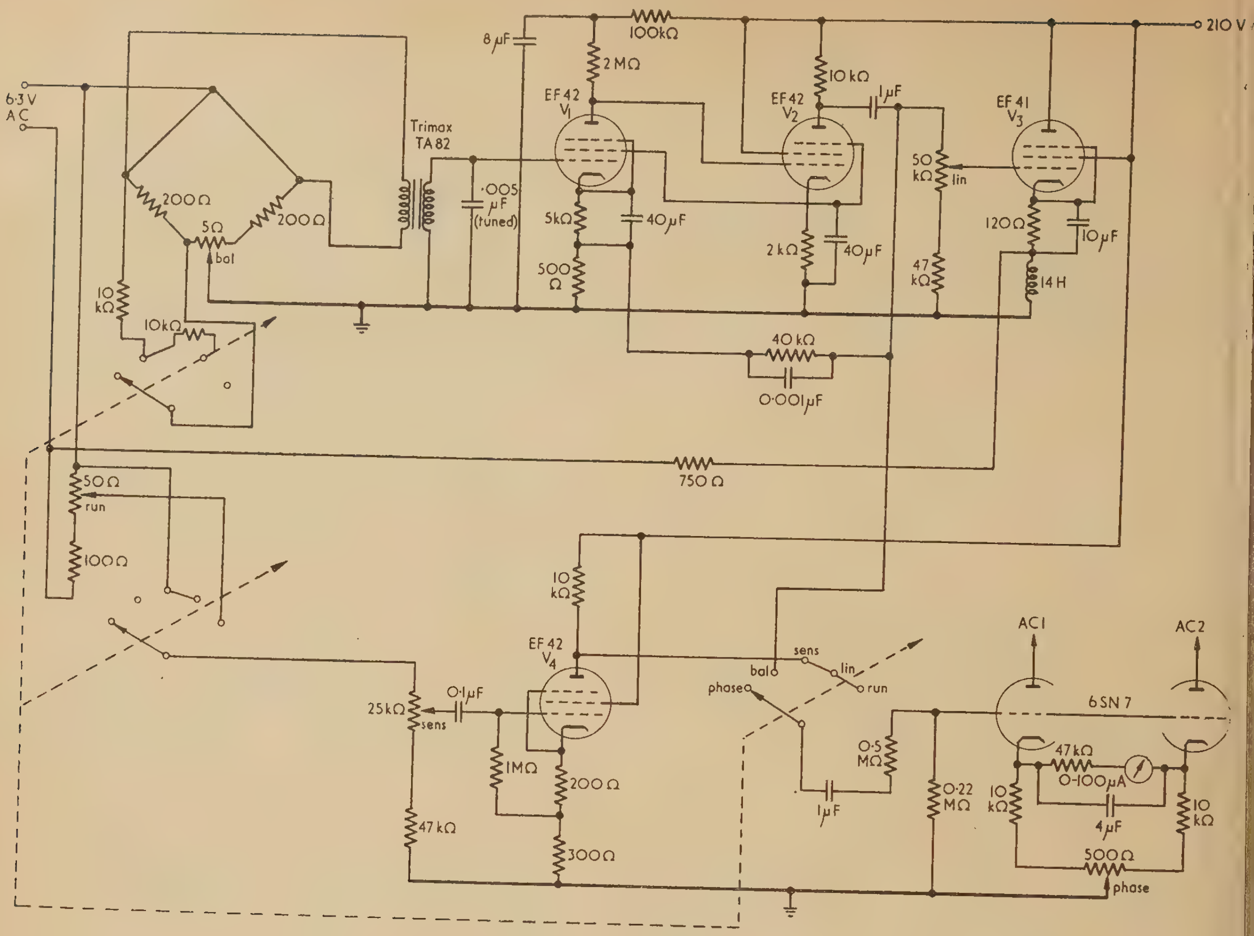
210 V
6·3 V AC
100kΩ
8μF
2MΩ
EF 42 V1
10kΩ
1μF
EF 42 V2
EF 41 V3
Trimax TA 82
200Ω
200Ω
5Ω
bal
·005 μF (tuned)
5kΩ
40μF
500 Ω
50 kΩ
lin
2 kΩ
40μF
120Ω
10μF
47 kΩ
14 H
10 kΩ
10kΩ
40 kΩ
0·001μF
750 Ω
50Ω
run
100Ω
10 kΩ
EF 42 V4
0·1μF
25kΩ
sens
1MΩ
200Ω
47 kΩ
300Ω
sens
bal
lin
run
phase
AC1
AC2
6SN 7
0·5 MΩ
1μF
0·22 MΩ
10 kΩ
47kΩ
0-100μA
4μF
10 kΩ
500Ω
phase

Fig. 3. Detailed circuit diagram

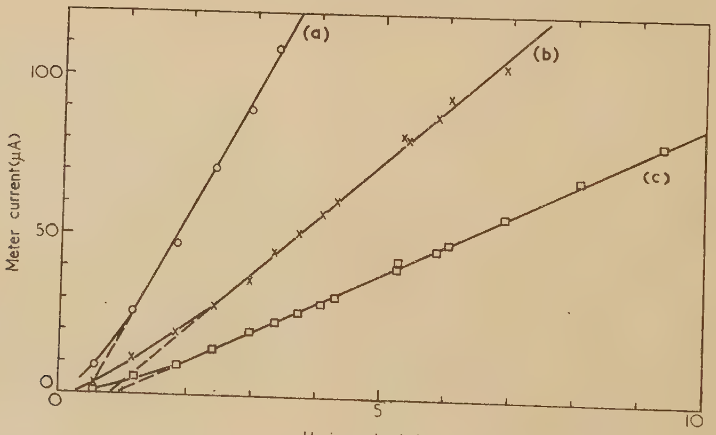

Fig. 4. Calibration data for anemometer
(*a*) 3·8 W/cm; (*b*) 8·4 W/cm; (*c*) 14·9 W/cm

balanced and the feedback is then zero. The anemometer sensing wires each consisted of 26 strands of nickel (diam. 0·001 in.) giving a resistance of approximately 200 Ω, and the heater was made up of 14 strands of 42 s.w.g. nichrome wire. The sensing head itself was so constructed as to allow an unimpeded flow of air for variations in wind directions normally encountered. Tests indicated that the departure from standard calibration (head-on to the wind) was less than 2% up to angles of azimuth and elevation of 20 de

An almost unlimited range in azimuth could be achieved b mounting the sensing head on a slow moving vane. Great range in elevation could be obtained if required by a suitabl modification of the sensing-head geometry.

A number of calibrations for different heat inputs ar presented in Fig. 4. The degree of linearity is excellen except at very low wind speeds which in practice occur ver rarely. The departure from linearity probably results from harmonic components in the mains supply for which the necessary linearity criterion (equation 5) is not satisfied. From equation (6) it will be seen that $E = 0$ for $u = \eta$. The effect of this second order term is apparent in Fig. 4 in that the linear calibrations do not pass through zero. This is of no consequence in practice. The response time of the instrument is decided almost entirely by the aerodynamics of the sensing head; the electronic time constant being much smaller than this. For average values of wind speed the response time has been found to be approximately 0·1 s. The anemometer has proved to be very simple to use in practice and, as expected, possesses a very high degree of stability.

Acknowledgements

Some of the practical circuit details evolved out of discussion with Mr. R. R. McGregor.

References

(1) Taylor, R. J. *J. Sci. Instrum.*, **35**, p. 47 (1958).
(2) Taylor, R. J., and Dyer, A. J. *Nature*, **181**, p. 408 (1958).

Vacuum sublimation apparatus for preparation of thin sources of ∝-active materials

by N. JACKSON, Atomic Energy Research Establishment, Harwell, Berks

[*Paper first received* 20 *July, and in final form* 16 *October*, 1959]

Abstract

This paper describes a method of preparing sources for α-pulse analysis, by subliming the oxide at 2000° C from a tantalum filament. Sources so prepared gave good uniform resolution with a peak width at half height of 35 keV or better.

Introduction

The identification and quantitative estimation of α-emitters by α-pulse analysis requires (*a*) an ion chamber and electronic equipment which is stable and has a high resolution, and (*b*) thin uniform sources so that there is no degradation of the emitted α-particles by self absorption.

The need for thin sources is reflected in the preparative techniques which have been described in the literature. These include the use of tetraethylene glycol as a spreading agent,⁽¹⁾ the ejection of an organic solution from a fine capillary by the application of an electric field and collection of the source material on a metal plate,⁽²⁾ the painting of a dilute organic solution of the source material on to a metal plate with ignition between paintings⁽³⁾ and vacuum sublimation.⁽⁴, ⁵⁾ Sources prepared by spreading with tetraethylene glycol are tedious to make and show enormous variations in resolution from source to source even when prepared by an experienced person. The ejection by an electric field (3000–10 000 V d.c.) and the painting technique both require the source material to be soluble in organic solvents. This is not always possible or convenient. The painting technique is time-consuming for it needs several coats to prepare a source.

The vacuum sublimation apparatus described by Milsted⁽⁴⁾ was the most innocuous, least time-consuming and gave reproducible sources even when used by inexperienced operators. Continual use of the apparatus, however, showed it to have a few deficiencies which tended to slow down source preparation; these are described below:

(i) the pumping down of the chamber to a vacuum at which firing could take place was slow;
(ii) the firing filament was fixed below an immovable baffle plate making it difficult to pipette aliquots on to it; and this arrangement necessitated evaporating the aliquot by passing a current through the filament;
(iii) it was found necessary to use a sector plate carrying two disks, one of which was to act as a check that the firing on to the first had been complete;
(iv) after several firings the whole chamber became contaminated, increasing the risk of cross-contamination since decontamination between firings was impossible.

The vacuum sublimation apparatus described in this paper was designed to eliminate these deficiencies; sources prepared in this apparatus gave good resolution, approaching that obtained by a test pulse generator or the ultimate of the electronic equipment.

Description

Sublimation chamber. The vacuum sublimation apparatus (Fig. 1) consists of a brass body (1), 3 in. diameter × 3½ in. long, with a Tufnol base (2) held in position by studs (12). The top is a glass plate ¼ in. thick, (16) fitted into a brass retaining ring (3), which is positioned by three studs (15). The O-rings (13) provide a vacuum seal. The tantalum

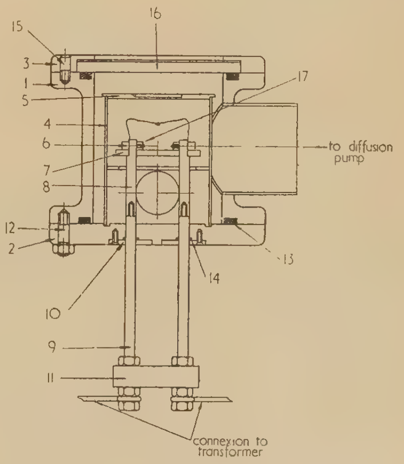

Fig. 1. Vacuum sublimation chamber

firing filament (0·005 in. ribbon, 0·125 in. wide, 3 in. long) has a small depression $\frac{1}{16}$ in. diameter at the centre and is fixed to electrode rods (8), (9) by bushes (6), (17). The electrode rods, which pass through the Tufnol base, are made vacuum tight with O-ring seals (14) and electrode retaining rings (10). The electrode rods are clamped together by a Tufnol coupling bar (11), and are free to move vertically. This allows adjustment of the filament height for firing, permits the filament to be raised clear of the brass body for pipetting and evaporating solutions on to the filament, and also for replacement of the filament.

The filament is enclosed inside the body of the apparatus by a shield tube (4), which supports the source disk holder (5), and by silica baffle plate (7), resting on the electrode rods (8). The electrode rods are made in two parts, a top (8), and a base (9). By enclosing the firing filament as above, the spread of scattered activity is confined. The above parts (4), (5), (6), (7) and (8) can easily be removed for decontamination or replacement, so preventing cross-contamination of sources.

Vacuum assembly. The arrangement of the pumping system and ancillary equipment is shown in Fig. 2. The sublimation chamber is attached to the system shut-off valve, through the cold trap chamber on to the baffle valve of a diffusion pump (Edwards type 203). The backing pump is a Metrovac type DR1. An air bleed valve is fitted between the system shut-off valve and the chamber. A by-pass lin is provided from the baffle chamber through the roughin valve and into the backing valve. This enables the chambe to be rapidly evacuated by the backing pump after it has bee opened to atmosphere. An isolation valve and second ai bleed valve are placed in the backing line, so that the syster may be left under vacuum when not in use.

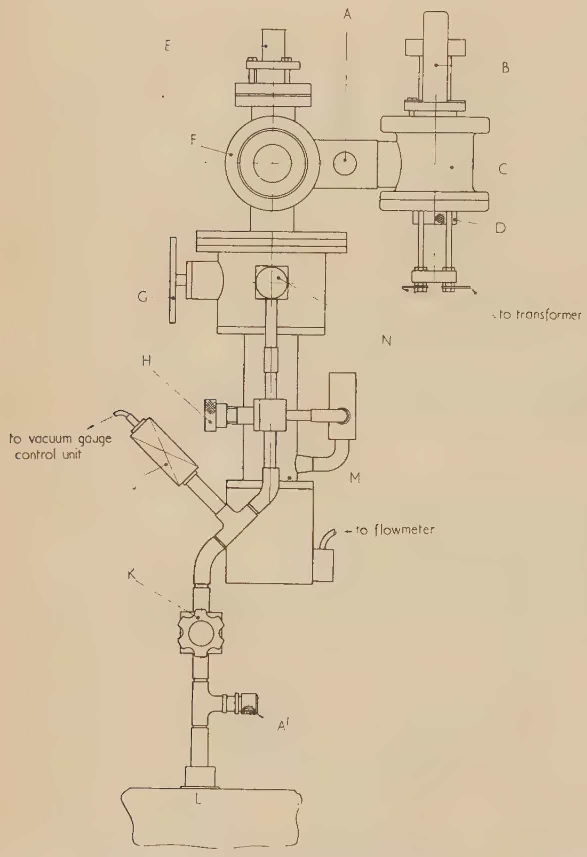

Fig. 2. Vacuum sublimation apparatus

AA', air bleed valve, Edwards type RS2; *B*, Philips ionization gauge; *C*, vacuum sublimation chamber; *D*, Philips ionization gauge, shut-off valve; *E*, cold trap; *F*, system shut-off valve; *G*, baffle valve; *H*, backing valve; *J*, Pirani gauge head; *K*, isolation valve, Edwards Speedivac ½ in.; *L*, vacuum pump; *M*, diffusion pump Edwards type 203; *N*, roughing valve

The pressure in the chamber is measured by a Philip ionization gauge (P.I.G.) (power unit 1126A) connecte through a P.I.G. shut-off valve. The backing line pressure i measured by a Pirani gauge head (Edwards type B4 vacuun gauge control unit). The cooling water for the diffusion pum passes through an Edwards type F.S.I. Flowtrol control uni as a safety measure.

Electrical power for the tantalum filament is provided b a transformer, the primary being fed from a 2 kVA Variac while the secondary is capable of supplying 100 A at 10 V All electrical switches and controls are grouped on a contro panel. The whole assembly is mounted on a mobile frame work such that the sublimation chamber can be placed insid a standard fume cupboard with all the controls outside.

Cold trap chamber. The cold trap is of the cold finge type, Fig. 3, and consists of a glass tube (18) 1$\frac{1}{10}$ in. outsid diameter and 9½ in. long. It is held in a flanged Harwell vacuum coupling (19) by two rubber rings (20). The whole assembly rests on a similar flange (21) on the main vacuum line, and is located by three studs (22). Vacuum sealing is provided by an O-ring (23).

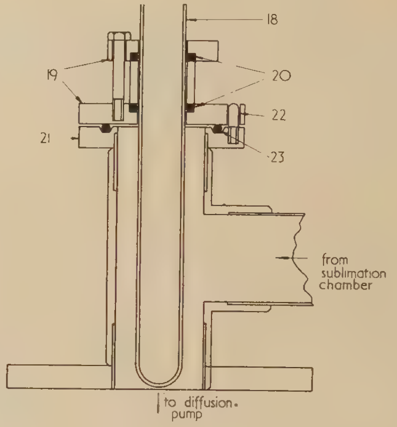

Fig. 3. Cold trap

Results

General. The apparatus described above has been used mainly to produce sources 1 in. in diameter on 1$\frac{1}{16}$ in. diameter stainless steel disks, but the size of the source may be varied by altering the size of the hole in the source disk holder (5, Fig. 1). In the existing apparatus with the filament ¼ in. from the source disk, one third of the starting material is deposited as an adherent film on the disk. The remainder is scattered on the disk holder (5) silica baffle plate (7) and shield tube (4). The maximum aliquot which can be evaporated on the filament at any one time is 0·01 ml. and this must contain only a few microgrammes of solid matter.

Sources can be prepared in less than half an hour, the limiting factor being the time taken to pipette and evaporate the aliquot to dryness, and operate the valves in the apparatus.

α-pulse analysis. The stainless steel discs used in these xperiments are polished on one side and all have their olished surfaces marred with fine scratches. The effect on ne resolution produced by these scratches and by the gnition of the prepared sources to red heat, in order to roduce a more adherent oxide film, has been investigated.

Several steel discs with a minimum of scratches were elected. Some were hand-polished on nylon fabric, using iamond cutting paste, in an attempt to remove surface nperfections. Several sources of ^{233}U were then prepared y subliming the source material on to these disks. All were ubjected to α-pulse analysis and some of each were heated o a dull red heat in a Bunsen flame and re-analysed. A ridded ion chamber(6) and a ninety-nine channel pulse nalyser were used to check the quality of these sources, the uality of a source being defined, in terms of resolution, as he width of each α-peak at half height.

The results are shown in Figs. 4 and 5. A peak width at half height of 30 keV was obtained for ^{233}U sources (Figs. 4 and 5); the variation in width between normal, hand-polished and ignited sources, 29–32 keV, was insignificant.

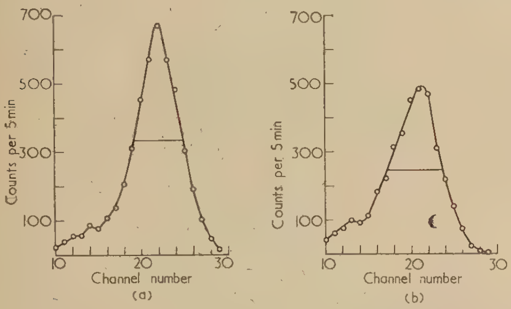

Fig. 4. Scans showing the effect of re-heating stainless steel trays ^{233}U peak from source prepared by vacuum sublimation on to a stainless steel tray (*a*) prior to ignition in air and (*b*) tray ignited to red heat in air

Peak width at half height: (*a*), 5·8 channels or 29 keV; (*b*) 6·5 channels or 32 keV

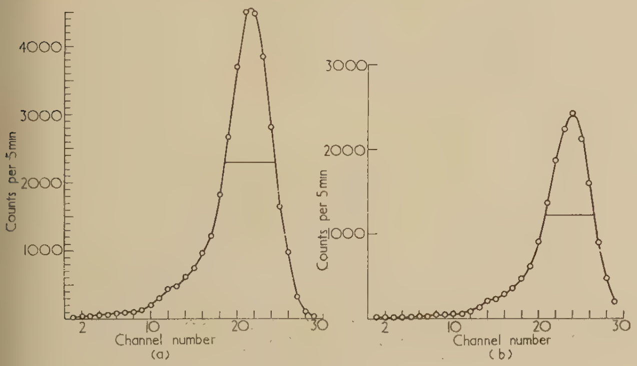

Fig. 5. Comparative scans on ^{233}U sources prepared by vacuum sublimation. One channel is equivalent to 5·20 keV

(*a*) ^{233}U sublimed on to a stainless steel disk width at half height = 5·9 channels or 30·7 keV

(*b*) ^{233}U sublimed on to a stainless steel disk repolished before use

Width of peak at half height = 5·7 channels or 29·7 keV

A mixed calibration source (Fig. 6) containing ^{233}U, ^{239}Pu, ^{238}Pu and ^{241}Am, ^{244}Cm, ^{242}Cm, was prepared by sublimation on to a stainless steel disc and may be compared with a similar quantity of material evaporated on to a similar disc (Fig. 7). The symmetry of the peaks in Fig. 6 illustrates the uniformity and thinness of the sources which can be produced in this way. In the thick source, Fig. 7, the low energy half of the peak drops down to zero much more slowly than the high energy half, producing a "low energy tail" which is caused by the degradation of the energy of the α-particles due to self-absorption in the source.

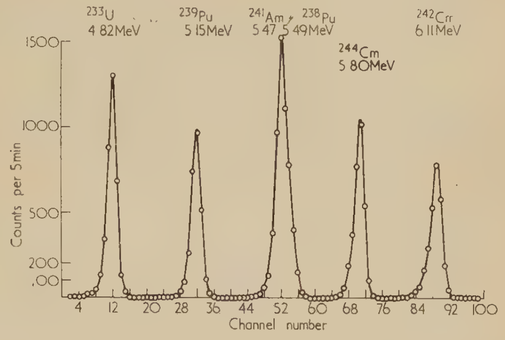

Fig. 6. Sublimed calibration source

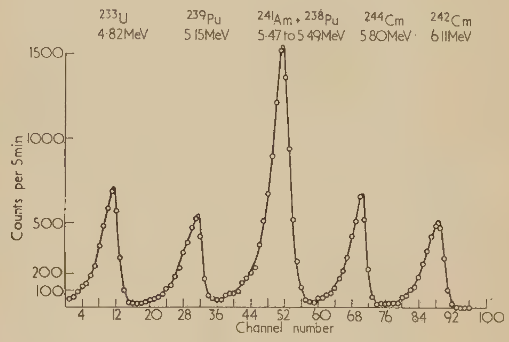

Fig. 7. Evaporated calibration source

Acknowledgements

The author is indebted to Mrs. K. M. Glover and Mr. F. J. G. Rogers for the α-pulse analysis, to Dr. J. Milsted and Mr. A. B. Beadle for suggestions in design and to Mr. A. Mason, Engineering Services who assembled the apparatus.

References

(1) Hurst, R., and Glover, K. M. *Atomic Energy Res. Establ. (Harwell)*, C/M 100 (1951).

(2) Carswell, D. J., and Milsted, J. *J. Nuclear Energy*, **4**, pp. 51–4 (1957).

(3) Glover, K. M., and Borrell, P. *Atomic Energy Res. Establ. (Harwell)*, C/R 1359 (1954).

(4) Milsted, J. *Atomic Energy Res. Establ. (Harwell)*, C/R 1379 (1954).

(5) Furby, E., and Wilkinson, K. L. *Atomic Energy Res. Establ. (Harwell)*, C/R 2441 (1958).

(6) Glover, K. M. *Atomic Energy Res. Establ. (Harwell)*, C/R 2091 (1957).

Vacuum furnace for high temperature X-ray diffractometry

by J. N. VAN NIEKERK, M.Sc., Ph.D., National Physical Research Laboratory, Council for Scientific and Industrial Research, Pretoria, South Africa

[*Paper received* 17 *November*, 1959]

Abstract

A vacuum furnace, to be used in conjunction with an X-ray diffractometer, for studying phase changes and solid state reactions at high temperatures is described. The sample is heated, primarily by radiation, from a platinum/20% rhodium heating element. The present temperature range is from room temperature to 1200° C, but a slight modification to the sample holder should allow temperatures of about 1600° C to be reached. Cooling of the furnace jacket is so efficient that simple O-ring principles are used to obtain the desired vacuum conditions. The sample holder is controlled from the outside and can be removed without in any way disturbing the rest of the furnace components. Data on temperature calibration and the experimentally determined inversion temperatures of quartz and iron are given. Decomposition studies of potassium and silver permanganates and phase changes in the iron carbide system, which are now in progress, illustrate the type of investigations which can be undertaken with this instrument.

Introduction

THE convenience and increasing popularity of diffractometers for recording X-ray diffraction patterns has led to the construction of a number of high-temperature devices[1–15] which can be used in conjunction with such instruments for studying phase changes and solid state reactions in position at elevated temperatures and also for measuring thermal expansions along specific crystallographic directions.[16–22] However, nearly all these designs suffer from the disadvantage that it is not possible to examine or change the specimen without allowing the apparatus first to cool down and then to partially dismantle the furnace, thereby disrupting its alinement. Furthermore, in the majority of cases these instruments have not been designed for operating with the specimen in a vacuum. In other cases the possibility of such operation at elevated temperatures becomes problematical because of the inefficient cooling of the outer jacket and the possible effect of this on the rubber sealing rings.

In the apparatus described in this paper these difficulties have been overcome as the specimen holder can be removed from the furnace without disrupting the electric and water-flow controls, and without in any way disturbing the positions of the rest of the furnace components such as heating elements, radiation shields and windows. Cooling of the furnace base, body and cap is, moreover, so efficient that these regions remain substantially cool during operation so that rubber gaskets and O-rings can be used to make the furnace vacuum tight.

Furnace geometry

The geometry according to which the furnace operates
best explained by reference to Fig. 1 which represents

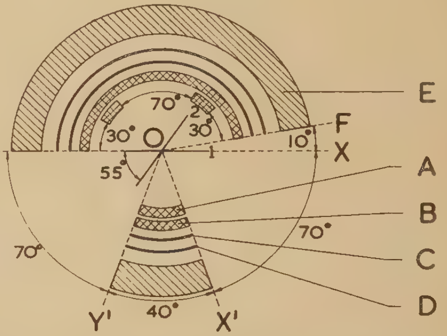

Fig. 1. Cross-section of furnace at window level
A, *B*, alundum heating coils; *C*, *D*, radiation shields; *E*, furna
body; *O*, centre of specimen

horizontal section through the furnace at window level;
and *B* are two concentric alundum cylinders which carry t
heating element. The inner radiation shield *C* is an 80
platinum/20% rhodium cylinder of thickness 0·25 mm, wh
D is a second radiation shield made of stainless steel. T
furnace jacket *E* is made of brass. Portholes, 1 cm high, a
cut in the five cylinders to allow the free passage of t
incident and reflected X-ray beams. As shown on t
diagram the portholes in *B*, *C*, *D* and *E* subtend angles
70° and 80° at the centre *O* of the specimen when these fo
components are alined with respect to one another. T
corresponding portholes in the inner alundum cylinder
subtend angles of 100° and 110° at the centre of the specime
This cylinder has an additional symmetrically located po
hole cut into it which subtends an angle of 70° at the centr
The reason for this additional porthole is to allow the heati
coils to be wound in such a manner that the specimen hold
will receive uniform and direct irradiation from in front a
from behind, while the two supporting pillars lend streng
and rigidity to the construction. (This will become cle
when referring to Fig. 4 where the two cylinders are show
separated.)

The plane of the specimen can be accurately adjusted
coincide with either position 1 or position 2 (Fig. 1). The
two positions are inclined at an angle of 55° and can
accurately located by means of an arm on the specime
holder cap which rests against two adjustable stops locat
on the furnace cap. With the furnace in the zero positi
and the specimen in position 1, the incident X-ray bea
goes along *XOY*, the opening *XF* eliminating any possib
edge effects. Anti-clockwise rotation of the furnace throu

)° gives the incident beam the direction $X'O$ while the flected beam goes along OY'. The angular range which n be recorded is therefore 140° in 2θ. With the furnace gain set at the zero position, but with the specimen now in osition 2, the incident direction XO makes an angle of 5° with the specimen surface; the reflected beam is therere along OX', i.e. 110° in 2θ. Anti-clockwise rotation of e furnace now permits the range 110°–164° to be recorded, hich is the maximum possible with the Philips high angle oniometer. The instrument can therefore be used for cording either the low- or the high-angle region, with an verlap of 30° in 2θ between the two regions.

Furnace construction

The external dimensions of the furnace have been chosen that it will fit either the 90° Norelco diffractometer or e Philips high angle goniometer. In Fig. 2 the main tructural features are drawn approximately to scale. The nain body E of the furnace is made of brass. The base, vhich has an annular recess to permit the entrance and irculation of cooling water, is fitted with a spigot H and a lamping block J. This latter arrangement replaces the egular specimen holder supplied with the goniometer and nsures accurate and firm location of the furnace on to the goniometer. From the annular recess in the base the water s ducted along a spiral groove K which runs around the main urnace wall. The water stream then passes through a union L to encircle the furnace cap M before it flows out through he exit connexion. This method of cooling is so effective hat an O-ring O can be incorporated between the furnace ap and body before screwing the two parts together.

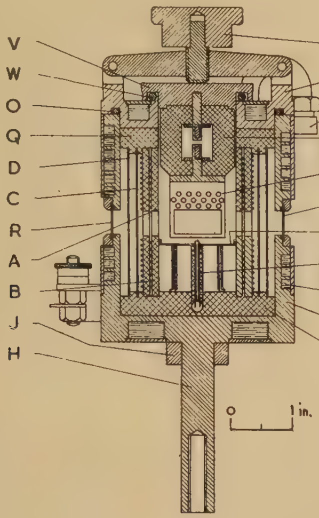

Fig. 2. Vertical section along furnace axis

A, B, alundum heating coils; C, D, radiation shields; E, furnace body; H, spigot; J, clamping block; K, spiral groove; L, union; M, furnace cap; N, ceramic disk; O, O-ring; P, retaining dish; Q, ceramic ring; R, S, beryllium windows; T, U, V, specimen holder; W, O-ring; X, clamping screw

On the furnace base rests a ceramic disk N which has grooves cut into it to accommodate the two alundum ylinders A and B and the two radiation shields C and D. A slot in these grooves and a corresponding lip on the lower idge of the radiation shields ensures exact location. On the eramic disk N rests a tripod stand which supports a dish P. The object of this dish is to catch the powder sample should this fall out of the specimen holder when the furnace is used in a vertical position, as is the case with the 90° diffractometer. At the top end the cylinders A, B, C and D are spaced and held in position by a ceramic ring Q with locating grooves cut into it.

The furnace body has two slots (1 cm high) cut into it at positions as shown in Fig. 1. These slots accommodate the two preformed beryllium windows R and S (Fig. 2). The two windows, with dimensions 54 × 15 × 0·38 mm and 47·5 × 15 × 0·38 mm, are laid on two neoprene gaskets into recesses on the main furnace wall and are then firmly secured with suitable clamping frames and screws (see Fig. 3).

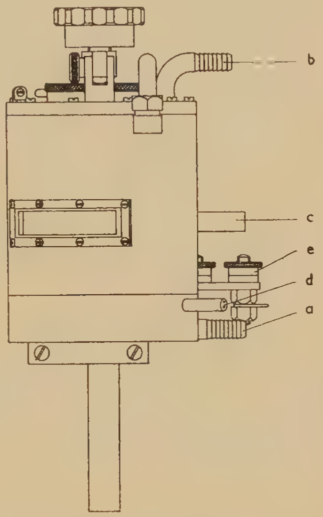

Fig. 3. Side view of furnace illustrating window mount and lead-in connexions

a, b, water inlet and outlet connexions; c, exhaust connexion; d, thermocouple connexion; e, electrical terminals

This method of clamping ensures a vacuum-tight mount, while the windows can be readily removed for purposes of cleaning. The double window thickness has been so chosen that it will transmit 83% of incident CuKα radiation; the experimentally determined value was found to be 81%.

The heating element consists of an 80% platinum/20% rhodium wire, wound in series and joined at the top of the two coaxial alundum cylinders. Fig. 4 shows a schematic diagram of the two separated cylinders with the windings located in grooves on the outer and inner surfaces. On the

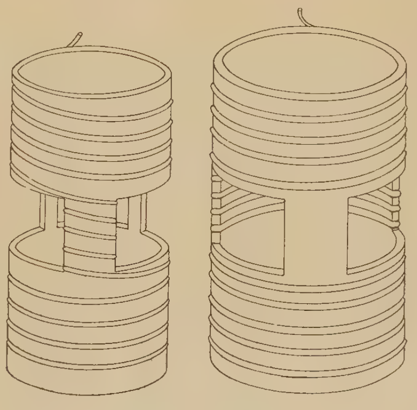

Fig. 4. Schematic drawing of the two separated alundum cylinders showing grooves and heating element

inner cylinder, that part of the wall located between the window ports has the wire placed on both sides, while on the outer cylinder the wire is doubled back on the rear section of the wall corresponding to window level. The winding of the coils is similar to the scheme adopted by Van Valkenburg and McMurdie.(2) This way of winding the heating elements, together with the two enlarged portholes and the third additional porthole at the rear of the inner cylinder, ensures that the specimen holder is heated directly and uniformly from in front and from behind. In a vacuum the heating is almost entirely by radiation.

The sample holder is a completely separate construction and can be inserted from the outside through an opening in the furnace cap. The holder consists of three parts as shown in Fig. 2: a high temperature resistant steel plate *T*, with a recess for accommodating the powder specimen, a ceramic insulator *U* and a cap *V*, fitted with a locating arm. By means of wedges the steel plate is secured to the sample holder cap *via* the ceramic insulator and this, together with holes in the plate, partially isolates the specimen cap from undue heat transfer. This manner of securing *T* to *V* leads to a completely rigid construction. The sample holder, which fits snugly into the opening in the furnace cap, is also fitted with an O-ring *W*, thus affording a vacuum-tight seal between the sample holder and the furnace cap when the former is squeezed down with the knurled knob screw *X*. The knurled screw is hinged to the furnace cap and a single locating pin locks it into position, in readiness to be screwed down after the accurately machined flat surface of the sample holder has been set by means of the locating arm and adjustable stops (see Fig. 5). Once this setting has been accomplished, the specimen holder can be readily removed from the furnace without interfering with any of the furnace components and then replaced to take up its exact position again.

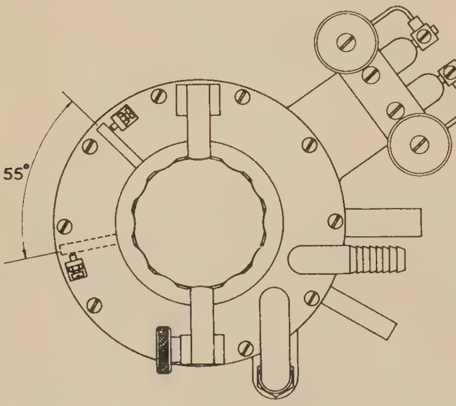

Fig. 5. Top view of furnace

In Fig. 3 the positions of the water inlet *a* and outlet *b* connexions can be seen. The exhaust connexion is at *c* and two separate pipes lead into this connexion. If one pipe is shut off the furnace can be evacuated through the other pipe. Alternatively, by passing an inert gas through one pipe, flushing the furnace and out again through the other pipe, recordings under a controlled inert atmosphere can also be obtained at elevated temperatures.

The platinum–platinum/10% rhodium thermocouple leads are led in through a ceramic sleeve through the connexion at *d* and here the vacuum is effected by making use of a rubber seal and a suitable sealing wax. The thermocouple wires run up the centre of the furnace through a second cera sleeve (*Y* in Fig. 2) which passes through a hole in retaining dish *P*, and finally terminate just below the lo portion of the sample holder. In Fig. 3 *e* shows the locat of the electrical terminals which are connected to Kov glass insulators soldered in place to meet the necess vacuum requirements (see Fig. 5). The furnace is hea with 220 V alternating current, controlled by two varia autotransformers so that the secondary of the first feeds primary of the second which gives finer control.

Furnace performance

The most serious limitation to the highest temperat attainable with this instrument in its present form is impo by the sample holder which is made of a special heat resista steel; for this reason temperatures in excess of 1200° C ha not been attempted. At this temperature the power co sumption is about 600 W and within this range of tempe tures the performance is most satisfactory. A modifica of the present sample holder, such as replacing the st portion by platinum–rhodium or by making the entire hol of a suitable ceramic material, should make it possible reach temperatures up to 1600° C.

Within the temperature range 25–1200° C, the furnace been calibrated against a standard thermocouple, the juncti of which was buried in a powdered quartz sample. A grea reduced plot of the temperature calibration curve which w actually obtained is shown in Fig. 6. By using data obta from this curve, the transition temperature of α-quartz β-quartz was investigated. The following table illustrates t results which were obtained when the sample was alternate heated and cooled and a diffraction pattern was run when steady temperature was reached.

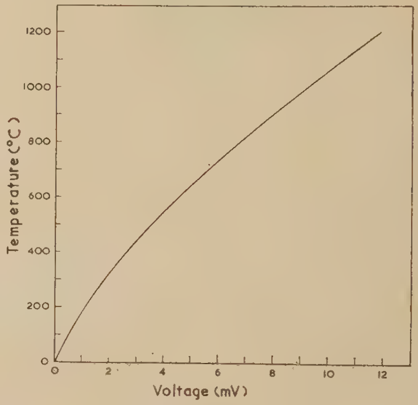

Fig. 6. Temperature calibration curve

Phase change of quartz with temperature

Voltage (mV)	*Temperature (° C)*	*Phase*
4·35	588	β
4·28	582	β
4·20	574	β (with a trace of
4·22	575	β
4·14	567	α
4·18	572	α
4·22	575	β

From these values the transition point lies between 5 and 575° C, a value which agrees well with the value 573° cited in the literature.

The transition temperature of α–γ iron was similarly nvestigated and in this case it was found to lie within the ange 907–913° C, which again agrees well with the value of 909·5° C given in textbooks.

An investigation into the changes in composition with temperature of various iron carbides, within the temperature range 300–700° C, has recently been undertaken. The phases investigated were Fe$_3$C, pseudo cementite,(23) Fe$_2$C and FeC and the experiments were carried out both under vacuum and under an inert atmosphere. The results of this investigation will be reported on elsewhere.

Decomposition studies of potassium and silver permanganates, within the temperature range 200–900° C, are now in progress. In such cases, where a gas is one of the decomposition products, its evolution often disrupts the smooth sample surface as the powder grains are inclined to jump. It is in cases like these that an externally controlled sample holder has proved its value, as the sample can be inspected at any stage of the investigation without disrupting the rest of the furnace components. The requirement of a smooth sample surface could probably be simply achieved by clamping a thin beryllium sheet on to the flat surface of the sample holder. Dr. F. H. Herbstein will report elsewhere on the results of this investigation.

Acknowledgements

It is a pleasure to thank Mr. J. Kidd of the Central Workshop for his expert workmanship in making the furnace and also for many helpful discussions during the early design stages.

References

(1) Birks, L. S., and Friedman, H. *Rev. Sci. Instrum.*, **18**, p. 576 (1947).

(2) Van Valkenburg, A., Jr., and McMurdie, H. F. *J. Res. Nat. Bur. Stand.*, **38**, p. 415 (1947).

(3) Birks, L. S. *Rev. Sci. Instrum.*, **25**, p. 963 (1954).

(4) Chiotti, P. *Rev. Sci. Instrum.*, **25**, p. 683 (1954).

(5) Butters, R. G., and Parr, J. G. *Canad. J. Technology*, **33**, p. 117 (1955).

(6) Mauer, F. A., and Bolz, L. H. Report 3148 (1953); Report 4685 (1956) (Washington: National Bureau of Standards).

(7) McKeand, I. J., and Hursh, R. K. *J. Amer. Ceram. Soc.*, **38**, p. 63 (1955).

(8) Weiss, E. J., and Rowland, R. A. *Amer. Mineralogist*, **41**, p. 117 (1956).

(9) Williamson, G. K., and Moore, A. *J. Sci. Instrum.*, **33**, p. 107 (1956).

(10) Wood, E. A. *Rev. Sci. Instrum.*, **27**, p. 60 (1956).

(11) Perri, J. A., Banks, E., and Post, B. *J. Appl. Phys.*, **28**, p. 1272 (1957).

(12) Bassett, W. A., and Lapham, D. M. *Amer. Mineralogist*, **42**, p. 548 (1957).

(13) Kennedy, S. W., and Calvert, L. D. *J. Sci. Instrum.*, **35**, p. 61 (1958).

(14) Rowland, R. A., Weiss, E. J., and Lewis, D. R. *J. Amer. Ceram. Soc.*, **42**, p. 133 (1959).

(15) Spreadborough, J., and Christian, J. W. *J. Sci. Instrum.*, **36**, p. 116 (1959).

(16) Richards, J. W. *Amer. Soc. Metals*, **30**, p. 326 (1942).

(17) Rosen, C., Banks, E., and Post, B. *Acta Cryst.*, **9**, p. 475 (1956).

(18) Fischmeister, H. F. *Acta Cryst.*, **9**, p. 416 (1956).

(19) Beals, R. J., and Cook, R. L. *J. Amer. Ceram. Soc.*, **40**, p. 279 (1957).

(20) Feder, R., and Nowick, A. S. *Phys. Rev.*, **109**, p. 1959 (1958).

(21) Engberg, C. J., and Zehms, E. H. *J. Amer. Ceram. Soc.*, **42**, p. 300 (1959).

(22) Bernstein, B. T., and Smith, J. F. *Acta Cryst.*, **12**, p. 419 (1959).

(23) Louw, J. D., Malan, O. G., and Ferreira, L. C. *J. Amer. Chem. Soc.* To be published.

Apparatus for the zone refining of copper

by E. D. TOLMIE, B.Sc., Research Laboratories, The General Electric Company Limited, Wembley, England

[*Paper received* 3 *December*, 1959]

Abstract

An apparatus has been constructed to enable a small molten zone to be formed and maintained at a constant length while being made to travel along a copper bar. Zone-refining performance is indicated for commercial O.F.H.C. copper after ten passes with speed of travel 11 *mm/h.*

Introduction

The maintenance of a short and stable molten zone in copper bars is more difficult than in bars of other metals having melting points up to about that of iron, because of the high thermal and electrical conductivity of copper. If a radiant-heat emitter is employed, its temperature must be considerably higher than the melting point of the copper, and a reflector is necessary for concentrating as much heat as possible into the small volume to be melted.

In the apparatus to be described, copper bars of length 16 cm and diameter 7 mm are refined: a molten zone of length 1·5 ± 0·15 cm can be maintained. The heating element consists of a strip of tungsten foil 1 cm wide and 0·06 mm thick hung in the form of a vertical loop from copper clamps (Figs. 1 and 2). Horizontal platforms on either side of the element support and guide the graphite boat containing the charge, so that the clearance between boat and loop is about 3 mm. A reflector of molybdenum foil bent into the form of a "U" surrounds the tungsten strip with a spacing of 0·5 cm (Fig. 2). A second reflector is fitted concentrically round the first with a spacing of 1 cm. These reflectors are held in position by wires between the parallel walls of a molybdenum casing. The top of the heat

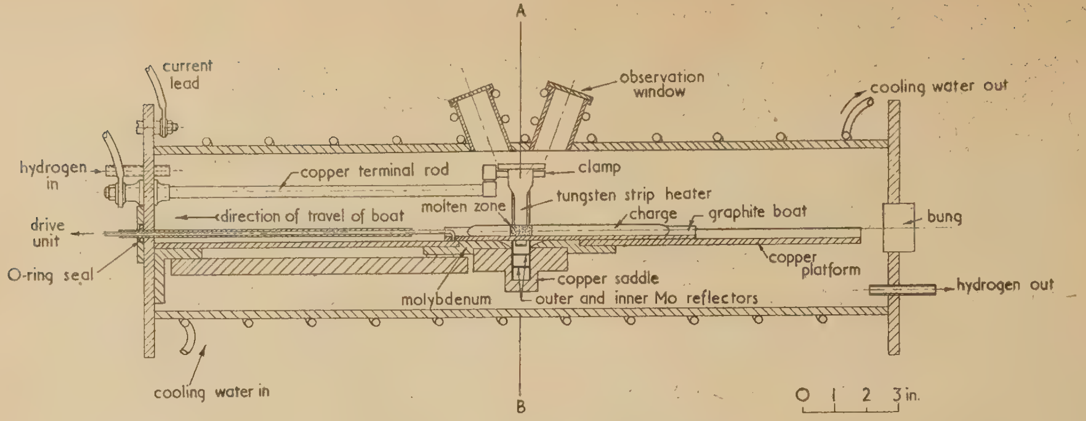
A
current lead
observation window
cooling water out
hydrogen in
copper terminal rod
clamp
tungsten strip heater
drive unit
direction of travel of boat
molten zone
charge
graphite boat
bung
O-ring seal
copper platform
copper saddle
hydrogen out
molybdenum
outer and inner Mo reflectors
cooling water in
B
0 1 2 3 in.

Fig. 1.—Heater assembly for zone-refining treatment

shield is necessarily open to accommodate the tungsten heater and its supports.

The copper platform along which the boat is drawn consists of three sections together forming a rigid horizontal structure supported from one end only by a fixture in one of the end plates of the containing vessel (Fig. 1). The central section acts as a saddle for the heat shield and is joined to the other sections by thick molybdenum strips secured with steel bolts. Copper was chosen for the platform material to ensure a sufficiently steep temperature gradient in the specimens and thus maintain a short molten zone.

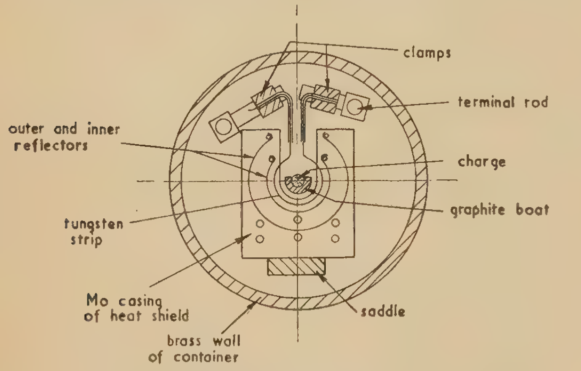
clamps
terminal rod
outer and inner reflectors
charge
graphite boat
tungsten strip
Mo casing of heat shield
saddle
brass wall of container

Fig. 2. Arrangement of heater as viewed from the right of plane *AB* in Fig. 1

The assembly as described above is completely enclosed by a metal casing consisting of brass tubing of $5\frac{1}{2}$ in. in diameter closed at the ends by brass plates. The joints are made with Woods Metal so that the casing can be opened with little difficulty if necessary. The end-plate supporting the platform also has passing through it the two copper terminal rods which extend inside as far as the position for the heater. Only one of these rods is electrically insulated from the plate.

A copper rod for drawing the boat passes through an O-ring seal mounted into the end plate and is connected at its outer end to the drive unit (a 1/50 h.p. electric motor) by means of a universal joint. For zone refining copper in an atmosphere of dry hydrogen a speed of travel of 11 mm/h has been used (see reference).

The power for the heater is obtained from a 240/20 V transformer, and the average power required for maintaining the molten zone is about 1·65 kW, which corresponds to a current through the tungsten heater of 137 A. Conduction losses are least when the bar is at either end of its traverse and a variation of about 30% in power occurs over the period of a complete pass. The approximate form of the variation is shown in Fig. 3 in terms of supply voltage (Variac reading) and distance of the molten zone from the starting end. A plot of this graph made for any one pass may differ from the average by an amount which will depend on irregularities introduced by the previous passes in the cross-section of the bar.

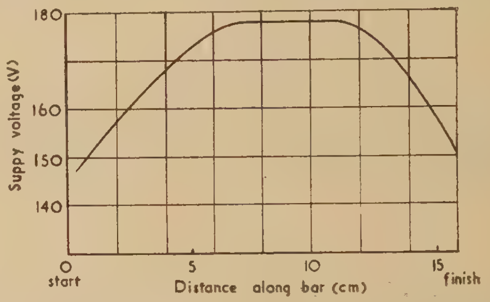

Fig. 3. Variation of supply voltage with respect to position of molten zone along the bar

To avoid the necessity for frequent adjustment, a device is employed to give approximate but effective control to the power (Fig. 4). A rigid metal cam is made to rotate by a sprocket connexion with the drive unit so that the time of one rotation coincides with that of one complete pass of the molten zone. The cam is so shaped that a loaded lever clamped to the Variac spindle follows its profile and causes

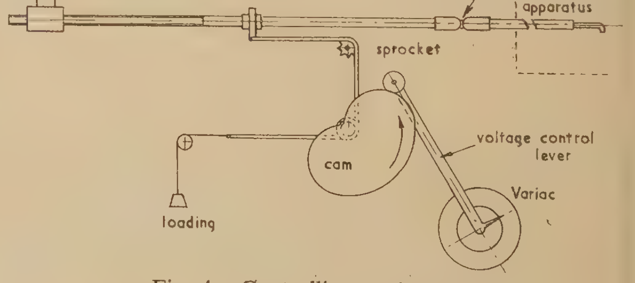
universal pivot
drive unit
direction of travel
zone refining apparatus
sprocket
voltage control lever
cam
Variac
loading

Fig. 4. Controlling mechanism

Table of spectrographic values of impurity concentration

	Ag (%)	*Ca* (%)	*Fe* (%)	*Ni* (%)	*Pb* (%)	*Total imp.* (%)
Before treatment	0·003	0·003	0·0002	0·001	0·0003	0·0075
Starting end after 10 passes	n.d.	0·001	0·0005	0·002	n.d.	0·0035
Middle after 10 passes	n.d.	0·001	n.d.	0·0003	n.d.	0·0013
Finishing end after 10 passes	0·01	0·001	n.d.	0·0001	n.d.	0·0111

n.d. signifies "not detected".

he supply voltage to vary in the manner indicated in Fig. 3. nly occasional adjustments are necesary.

The table gives spectrographic values of impurity concentration, before and after treatment of 10 passes in the pparatus, in samples taken from the starting end, middle nd finishing end of a bar of commercial O.F.H.C. copper. Silver, iron and nickel behave as one would expect: the level distribution of the calcium and apparently complete disappearance of lead suggest loss of these two elements by evaporation.

Reference

Tolmie, E. D., and Robins, D. A. *J. Inst. Metals*, **85**, Part 5, p. 1738 (1957).

LABORATORY AND WORKSHOP NOTES

New method of cold hearth melting*

by W. H. Shepherd, B.Sc., A.R.C.S., The Plessey Co. Ltd., Caswell Research Laboratories, Towcester, Northants

[*Note received* 9 *December*, 1959]

The melting of highly reactive refractory metals on a water cooled copper hearth is by no means new, the principle is used industrially, for instance, in vacuum and argon arc melting furnaces.† The first experiments with electron bombardment melting were, it is believed, carried out on a water-cooled copper table. However at the time this work was carried out metal melting on a cold copper hearth by means of r.f. heating had not been reported.

The success of the method relies largely on the high values of electrical and thermal conductivity for copper. The first leads to relatively poor heating in an r.f. field and the latter allows any heat that is produced to be removed rapidly.

The original apparatus, designed for melting small (3 to 5 g) buttons of refractory alloys is illustrated in the diagram. The power unit had an output of 9 kW at 400 kc/s. The heating rate of the sample, in this case initially in the form of a pressed powder compact, was controlled by varying the output of the work coil and the position of the hearth along the principal axis of the coil. The most effective position was found to be at the centre of the coil as might have been expected in the absence of the copper hearth.

Using the apparatus illustrated here refractory metal alloys were melted at temperatures in excess of 2000° C. Although examination of the buttons showed that melting had been complete, apart from a very thin skin in contact with the hearth, the buttons were turned over and remelted at least once. Whether this was necessary in view of the violent stirring action experienced by the melt in the r.f. field was not determined.

An enlargement of the illustrated apparatus with a hearth diameter of 1 in. was used to prepare larger buttons but at a lower efficiency which resulted in a reduction in the maximum temperature available for a given melt. For hearths of this size or larger a horizontal "inverted saucer" coil suspended directly over the melt would probably be more efficient.

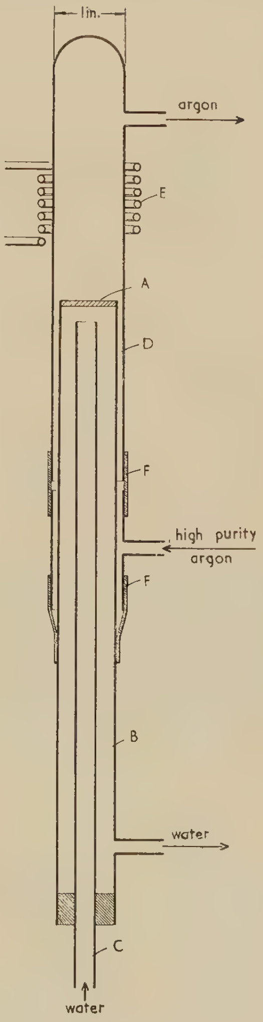

Apparatus for melting on a cold copper hearth

A, circular copper hearth $\frac{1}{8}$ in. thick; *B*, copper tube; *C*, copper tube for water cooling; *D*, silica melting chamber; *E*, r.f. coil $\frac{1}{8}$ in. outer diameter copper tube; *F*, rubber connexion

Thanks are due to the Plessey Company Ltd. for permission to publish this note.

---

* Patent applied for December 1958.

† Newhall, H. S., and Lee, J. R. *High Temperature Technology*—Chap. 14 (New York: John Wiley and Sons Inc., 1956).

Automatically operated balanced filters for a counter diffractometer

by H. A. McKinstry, M.S., and M. A. Short, M.Sc., A.R.I.C., College of Mineral Industries, The Pennsylvania State University, University Park, Pennsylvania

[*Note received* 4 *January*, 1960]

In the quantitative X-ray diffractometric study of non-crystalline materials, it is usually necessary to use monochromatic radiation. Because of the low intensity of the scattering, it is generally best to achieve this by using balanced or Ross* filters. It has been shown elsewhere† that these filters must be placed in the primary beam to avoid counting the fluorescent radiation arising from the filters. The purpose of this note is to describe the design, operation and automatic control of a pair of balanced filters attached to a diffractometer.

The filters themselves consist of thin uniform nickel and cobalt (for isolation of CuKα radiation) metal foils, each mounted in a vertical plane through a diameter of a cylindrical stainless-steel holder (see inset in Fig. 1). These stainless-steel holders fit into cylindrical slots, spaced 180 deg apart, machined near the edge of one face of an aluminium wheel, as shown in Fig. 1. Holes are cut through the wheel so that the X-ray beam is directly incident upon the filters. The wheel is mounted so that one filter is held immediately in front of the beam slit, and it is driven by a dynamic brake motor *via* a series of gear wheels. The filters are balanced by rotating the cylindrical holders about a vertical axis in the plane of the X-ray beam, thus varying their effective thickness.

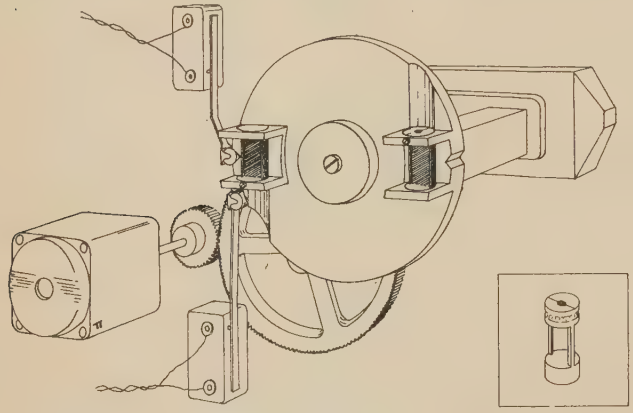

Fig. 1. Balanced filter unit, as attached to a diffractometer type XRD-3, by General Electric Co.
(Inset, Filter holder)

The filter wheel and its control unit operate in conjunction with a scaler and a digital printer. At the beginning of a cycle, counting commences with one filter held in front of the beam slit. After a given length of time, preset on the scaler, counting ceases. The count is sent to the digital printer and, at the same time, the print-out signal is used to activate the filter control unit. This unit causes the filter wheel to turn through half a revolution, thus bringing the second filter into position. The counting for the second half of a cycle is then started by a time-delay mechanism, which removes the possibility of error resulting from variations in print-out time and in the time required to change the filter. The time delay is set at 1·5 s. As currently used, the counter is continuously scanning the specimen, and the intensi recorded is thus due to a finite angular interval. In the stu of non-crystalline materials, $\delta I/\delta\theta$ is generally small and, f reasonably slow rates of scanning, no error is introduced considering each recorded intensity as arising from the mi point of the angular interval. Alternatively, it should n be difficult to adapt the system to step-wise scanning.

The signal sent by the scaler to the printer to initiate t print-out sequence is used to close a relay in the filter-whe control unit, the circuit of which is shown in Fig. 2. Th relay starts the time-delay mechanism and also energizes second relay. This second relay, which is self-latchin inhibits the scaler reset and also starts the motor which caus the filter wheel to rotate clockwise at a rate of 30 rev/mi It was found that the dynamic brake motor did not stop dea when its phase-splitting capacitor was short-circuited, b coasted slightly. Because of this, a special braking circu was devised. The operation of this circuit is controlled b two microswitches actuated by a V-notch on the circum ference of the filter wheel. After almost half a revolutio the lower microswitch (see Fig. 1) is closed, slowing the moto by sending a d.c. pulse of controlled duration through on of the windings and reducing the size of the phase-splittin capacitor. The upper microswitch then stops the whe dead by putting a continuous d.c. signal through the moto Finally, the time delay mechanism switches off the current t the second relay, which then unlatches, cutting off the powe to the circuit.

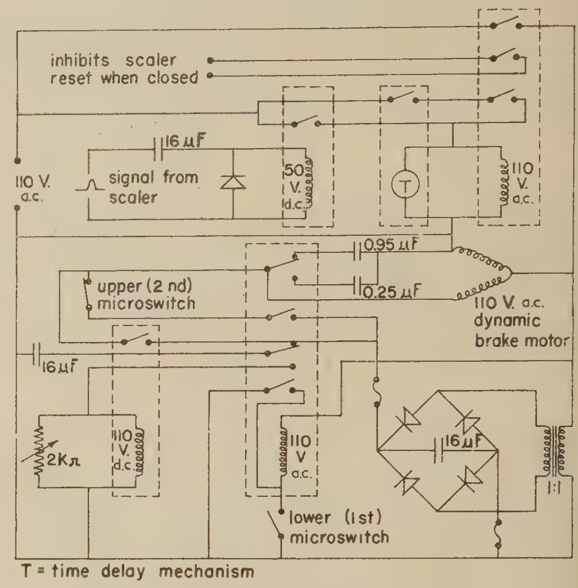

Fig. 2. Electrical control circuit

We would like to express our thanks to Dr. R. Diamon who participated in the construction of a prototype filte changer.

---

* Ross, P. A., *Phys. Rev.*, **28**, p. 425 (1926).
† McKinstry, H. A. and Short, M. A., to be published.

Gratings for measuring separation of equidistant parall straight lines

by R. M. Dawson, B.Sc., The British Jute Trade Research Association, Dundee

[*Paper received* 25 *November*, 1959]

Various methods are available for measuring the perpend cular separation, or its reciprocal, of equidistant parall traight lines, by observing the moiré pattern resulting from he superimposition of a grating on the lines.$^{(1-4)}$ This note liscusses only cases in which rectilinear propagation alone ieed be considered and gratings which may be represented y a strictly monotonic function.

If patterns represented by $y - f_1(x, n_1)$ and $y = f_2(x, n_2)$, vhere $n_1, n_2 = 0, \pm 1, \pm 2 \ldots$ are superimposed, then if hese equations may be rewritten as $n_1 = F_1(x, y)$ and $_2 = F_2(x, y)$, the resultant moiré fringes are given by

$$n_1 \pm n_2 = F_1(x, y) \pm F_2(x, y),$$

he sign depending on the directions of numbering lines in he component patterns.$^{(5)}$

If the lines whose spacing k is to be measured are:

$$y = mx + kn_1(1 + m^2)^{1/2}, \tag{1}$$

or $n_1 = 0, \pm 1, \pm 2 \ldots$, $m =$ constant; and the grating:

$$y = n_2 f(x), \tag{2}$$

where $n_2 = 0, \pm 1, \pm 2 \ldots$; then, if the fringes are lines of onstant $(n_1 - n_2) \equiv \Delta$:

$$y = f(x) \, . \left\{ \frac{mx + \Delta k(1 + m^2)^{1/2}}{f(x) - k(1 + m^2)^{1/2}} \right\},$$

and the separation in the y-direction of adjacent moiré fringes, δy, is given by:

$$\delta y = \frac{1}{[\{1/k(1 + m^2)^{1/2}\} - \{1/f(x)\}]}.$$

Thus, if $f(x)$ is a strictly monotonic function, δy will increase as x tends to the one value at which:

$$f(x) = k(1 + m^2)^{1/2}. \tag{3}$$

In this case a moiré pattern will be formed, as indicated by Fig. 1 (Fig. 2 being an example of a complete pattern), in which the fringe perpendicular to the x-axis (that is, the vertical arm of the central cross of the pattern) is that at which:

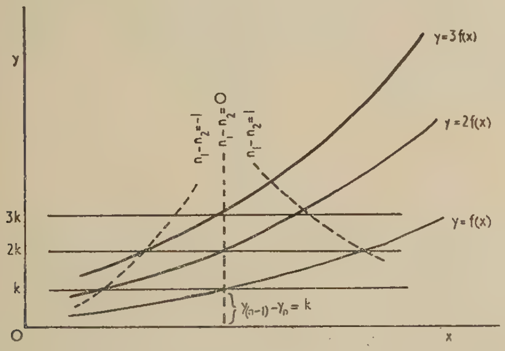

Fig. 1. Form of moiré pattern obtained with monotonic grating

Full lines represent component patterns; broken lines, the moiré fringes

$$f(x) = k(1 + m^2)^{1/2},$$

and

$$\delta y = \infty,$$

since

$$y_{(n+1)} - y_n = f(x).$$

Therefore, at this position, k is equal to the grating spacing divided by $(1 + m^2)^{1/2}$. Consequently, if the grating carries a scale of $f(x)$ the value of k may be read off directly from it, adjustment being made so that m is approximately zero.

Any grating of this type will be suitable for making the measurement in so far as the moiré pattern will be distinctive and readily interpreted, but a criterion for choosing a particular grating form is required. Normally a linear scale is desirable, and this is given by the grating represented by the solution of:

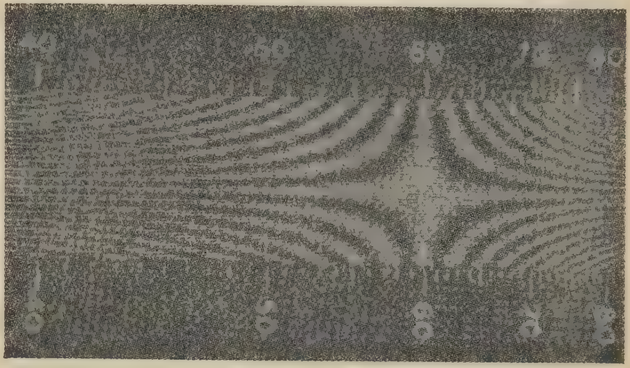

Fig. 2. Moiré pattern obtained with taper grating, scale of $1/k$

$$\frac{d(1/k)}{dx} = c,$$

that is, $y = n/cx$ for $1/k$, and of:

$$\frac{dk}{dx} = g;$$

that is, $y = ngx$ for k (n equals $0, \pm 1, \pm 2 \ldots$ in both cases; c and g are constants). Thus, k may be measured on a linear scale with the Taper Grating,$^{(1,2)}$ and $1/k$ with a grating the lines of which are rectangular hyperbolae (Fig. 3).

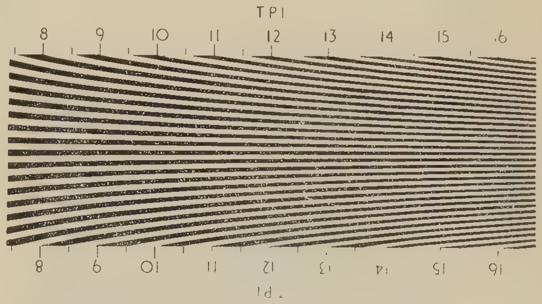

Fig. 3. Hyperbolic grating, with scale of $1/k$ (T.P.I. = threads per inch)

The moiré patterns obtained with this hyperbolic grating may be completely analysed using Lehmann and Wiemer's method,$^{(5)}$ but in the case of the Taper Grating the equation of the fringes can only be reduced to standard form by eliminating y and n_1 from equations (1) and (2) (instead of n_1 and n_2). Secondary patterns can be accounted for by a simple extension of the analyses, and it may be shown that although parallax might affect the appearance of the patterns, the locations of their centres are independent of the observer's position.

If $x = x_c$ is the solution of equation (3), the sensitivity of a grating can be defined as dx_c/dk, or $dx_c/d(1/k)$, as the case may be. A grating of a particular type is completely specified by quoting this sensitivity, its scale range, and the grating width.

For convenience the centre of the pattern has been mentioned as indicating the required spacing, but the measurement is made by noting the intersections of the more well-defined arms of the central cross of the pattern on both scales, which are then averaged. From equation (3), it can be decided whether or not tilting gives rise to an appreciable error.

Thanks are due to the Director and Council of the British Jute Trade Research Association for permission to publish, and to the British Cotton Industry Research Association for supplying Fig. 2.

References

(1) B.S. 2862: 1957.

(2) "Shirley" Line Gratings, Shirley Developments Ltd.

(3) "Lunometer", Peter Luhn, Wuppertal Barmen.

(4) Valyus. *Rastrovaya optika* (Moscow 1949). Quoted by Kaczer, J., and Kroupa, F. *Czech. J. Phys.* (edn. for Western Countries), **1**, p. 80 (1952).

(5) Lehmann, R., and Wiemer, A. *Feingerätetechnik*, **2**, p. 199 (1953).

Design of a small rolling mill for use at low temperatures

by E. D. Tolmie, B.Sc., and A. C. Roberts, B.A.,
Research Laboratories, The General Electric Co. Ltd.,
Wembley, England

[*Note received* 26 *November*, 1959]

In a study of the annealing of point defects in copper, it has been necessary to give specimens a uniform and large deformation at low temperatures, so that electrical resistance measurements can be used to follow the annealing which occurs on subsequent heating. The most suitable way of deforming small specimens is by rolling and we have developed a rolling mill which operates satisfactorily at 77° K.

A photograph of the mill is shown in Fig. 1 and a plan in Fig. 2. The frame L consists of two "L" shaped mild steel blocks held rigidly together by dowels and the screws S. A mild steel block K split in order to allow insertion of roller R_1, is free to slide through a 1 cm length in the rectangular slot formed by the outer frame: its alinement is maintained by a close fit between it and the frame L and by having four guiding plates P, three of which are shown in Fig. 1. The other roll
R_2 is carried by the outer frame: both rollers are of stainle
steel (EN.57 stainless S80) and are mounted in bronze bush
T with an accuracy better than 0·0005 in. The lubricant
molybdenum disulphide; graphite would also be suitab

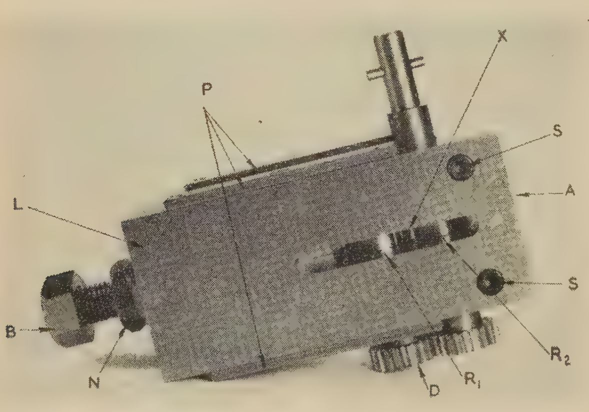

Fig. 1. Photograph of rolling mill

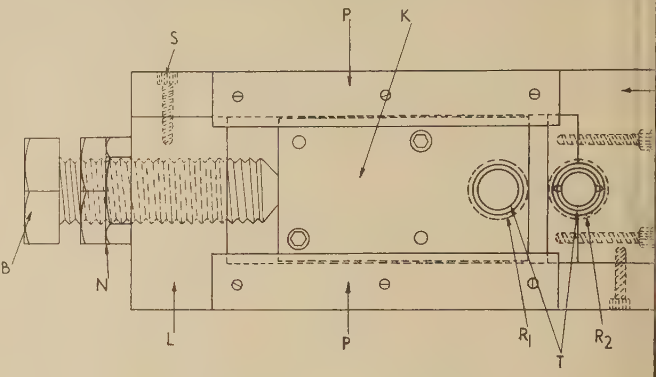

Fig. 2. Plan of rolling mill

The spindle of R_2 is continued in one direction so that
stainless steel handle may be fitted using a bayonet ty
connexion. The possibility of independent movement
the rollers is eliminated by the pinion drive D. The spaci
between the rollers is governed by the adjustment screw
which screws into a thread in the outer framework and caus
the block K to slide. The roller spacing may be fixed by me
of two locking nuts N.

The mill is supported from a vice by a steel strip bolted
face A, and immersed several inches in liquid nitrogen, ca
being taken to ensure that the mill is dry to prevent ice formi
in the bearings. Metal strip up to 0·5 cm wide may be f
between the rollers through the aperture X. The rollers a
easily turned by hand but if required may be driven by
motor. The dimensions of the mill, not including handle
supporting strip, are 16·5 × 10 × 5 cm.

So far the mill has been used at 77° K to roll copper f
from 0·25 mm to 0·14 mm thick and gold foil from 0·20 m
to 0·125 mm. There is no reason why these metals, at leas
should not be rolled to smaller thicknesses.

Two-way oil-filled dash pot

by A. W. Williams, Ph.D.,* and L. Riddiford, Ph.D.,
Department of Physics, University of Birmingham

[*Note received* 7 *December*, 1959]

A double-acting oil-filled dash pot was constructed for use
the expansion system of a liquid-hydrogen bubble chamber
The device may prove of value in other applications. T
chamber is expanded and re-compressed by means of a lar
stainless-steel bellows within the vacuum tank, actuated fro
outside by a compressed-air cylinder. The extension of t
bellows is limited; to make the best use of it the deceleratio
stroke should be short, but not so short that the control r
is damaged. The fast cycle requires a light-weight system.

The figure is a line drawing of the dash pot. The stainles
steel piston P starts from position A and is propelled by
force of about one ton towards position B. As it enters t

---

* Now at The English Electric Co. Limited, Leicester.

† Colley, D. C., Kinson, J. B., and Riddiford, L. *Nucle*
Instruments, **4**, p. 26 (1959).

perture at *B*, compression of the oil starts and the piston omes to rest in about 0·4 in. For a 2 in. acceleration stroke nd a piston area of 2 in.^{2}, the decelerating force is 5 ton and he oil pressure 2·5 ton in.^{2} or 380 atm. The pressure is vithstood by the brass cylinder *C* and the flanges *F* sealed to it by rubber gaskets *G*. The flanges are clamped by eight $\frac{3}{8}$ in. bolts *R*, and act as limiting stops for the system. The shaft oil seals are of the U-ring type.

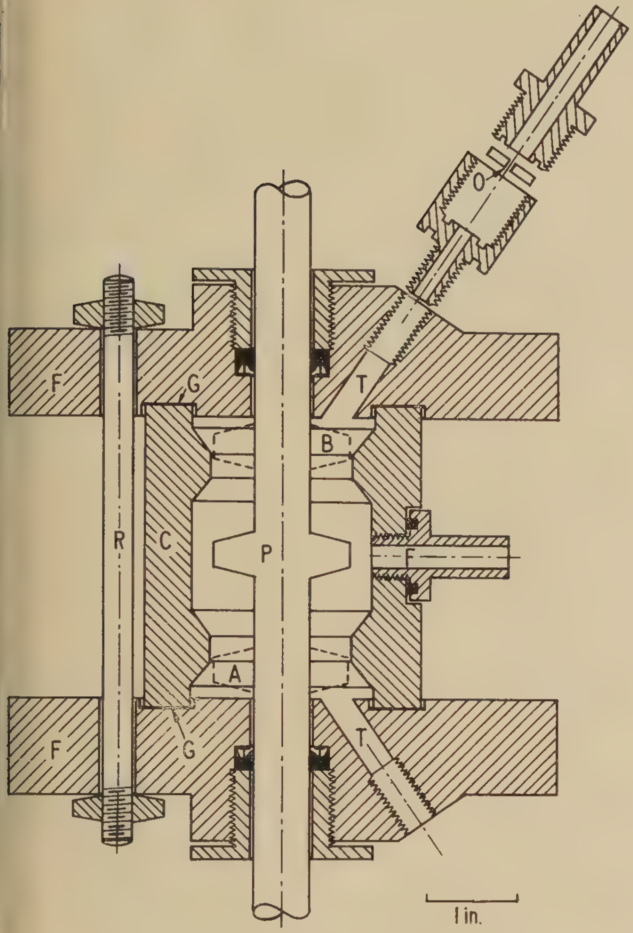

Line drawing of dash pot

The clearance of the piston in the apertures is about 0·002 in. to insure freedom of movement and yet maintain the pressure. The correct deceleration is obtained by a trial and error determination of the size of the orifice *O* in the vent tube *T* ($\frac{1}{8}$ in. long and 0·045 in. in diameter). During re-compression from *B* to *A* the piston is brought to rest in a similar way at the base of the dash pot. The vent tubes *T* and the filling tube *F* are connected to an oil reservoir which permits expansion and prevents the admission of air. Any air initially present is removed by a few preliminary low-pressure expansions.

To assist in testing and adjusting the device the out of balance voltage from a radio-frequency capacitor bridge was displayed on an oscilloscope, the variable capacitance being dependent on the position of the control rod. The capacitor vanes attached to the rod were interspaced between other vanes attached to a fixed part of the assembly.

We are grateful to Mr. A. E. Bingham of Dowty Equipment Ltd. (Cheltenham) for a discussion which assisted considerably in the design.

Grips for tensile tests on very extensible tapes

by A. G. Day, Ph.D., A.Inst.P., The British Electrical and Allied Industries Research Association, Leatherhead

[*Note received* 23 *November*, 1959]

Measurement of the tensile strength of a very extensible tape is difficult if the extension is accompanied by a considerable reduction in width. Flat, or serrated vice-type grips, as generally used for sheet or fabric specimens, do not allow a uniform reduction in width along the whole free length of the specimen. There are short lengths at either end, where the grips restrict the narrowing, and breaks occur at the grips, or in these restricted regions, due to stress concentration where the width of the tape changes rapidly along its length.

This difficulty was met during the testing of varnished fabrics cut on the bias for use as electrical insulation. Extensions of 100% and reductions in width of nearly 50% were measured when a constant rate of extension of 2 in./min was used. A new type of grip was designed which almost eliminated breaks at the grip or in the restricted regions.

Fig. 1(*a*) shows the grip as designed for testing 1 in. tape. The body of the grip was machined from cast steel, and the $\frac{1}{2}$ in. diameter clamping bar made from silver steel and highly polished on its curved surface. The end of the specimen is clamped between the body of the grip and a flat area machined on the polished bar. Fig. 1(*b*) shows how the tape is wrapped round the bar for about two thirds of its circumference before being completely free of the grip. The short lengths at the ends of the specimen where the change in width occurs as shown in Fig. 2 are slightly restrained by the polished surfaces of the bars and breaks seldom occur outside the remaining free, and uniformly narrow length of the specimen.

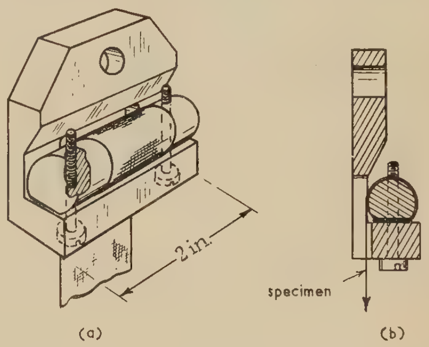

Fig. 1(*a*) Tensile grip. (*b*) Section showing position of specimen

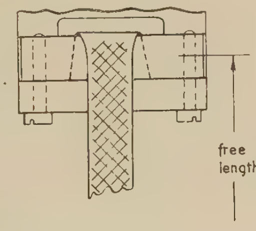

Fig. 2. The narrowing of a stressed tape

The free length of tape between its points of contact with the bars is made a minimum of 6 in. for a 1 in. tape. This free length and the diameter of the bar may have to be changed for tapes of different widths, but this has not been investigated.

The successful operation of the grips depends on the specimen sliding freely over the clamping bars during the extension. A specimen which is tacky must be dusted wi talc before fitting it in the grips, otherwise the narrowing restricted to the free part of the specimen.

This note is communicated by permission of the Director The British Electrical and Allied Industries Researc Association.

CORRESPONDENCE

Effect of ambient airspeed on efficiency of thermal-precipitator

In his account of the standard thermal-precipitator, Watson^(1) states that its efficiency in sampling airborne-dust is satisfactory for ambient airspeeds up to 600 ft min^{-1}. Later investigations by Simons^(2) in a coal-dust cloud in a wind-tunnel suggested that the number of 1–5 μ particles collected by a thermal precipitator sampling moving air, compare with one sampling stationary air, rose to 120% as the ai speed increased to 500 ft min^{-1} and then declined to 80% the airspeed increased further to 900 ft min^{-1}. Such variation would not, in fact, be very serious for routi airborne-dust measurement in mines. However, sinc

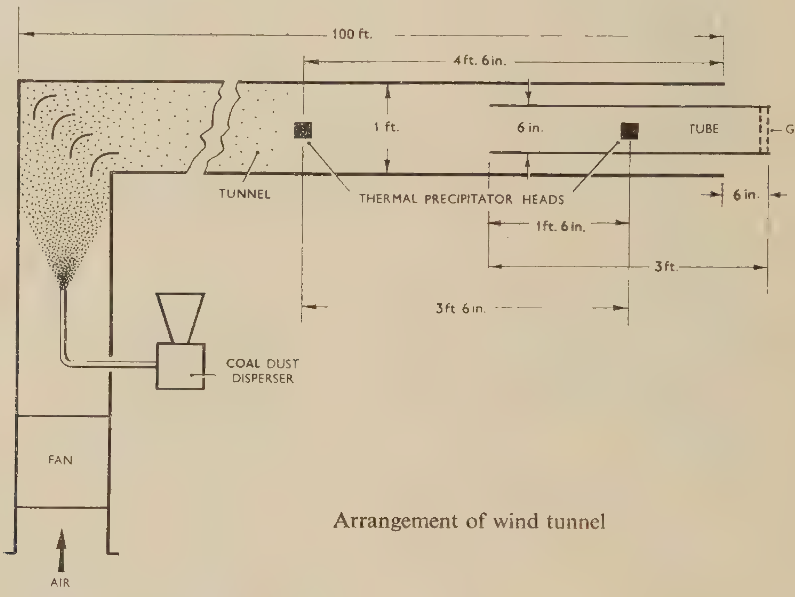

Arrangement of wind tunnel

Table of dust concentration measurements

Airspeeds, ft min^{-1}		*Standard thermal precipitator (1–5 μ particles)*					*Long-period thermal precipitator (1–5 μ particles*		
		Tunnel		*Tube*		*Geometric mean ratio of tunnel to tube concentrations*	*Concentration particles cm^{-3}*		*Geometric mean ratio of tunnel to tube concentrations*
Tunnel	*Tube*	*Concentration particles cm^{-3}*	*Cover-glass count ratio*	*Concentration particles cm^{-3}*	*Cover-glass count ratio*		*Tunnel*	*Tube*	
200	40	2850	0·75	2870	1·08	1·03	2270	2120	0·99
		2840	0·88	2670	0·96		1950	2150	
400	90	1640	0·94	1570	0·94	1·06	2750	2830	1·03
		1680	0·94	1570	0·97		2820	2590	
600	150	2090	0·83	2020	1·03	1·05	3360	2680	1·07
		2010	1·03	1900	0·92		2570	2900	
800	205	2380	0·73	2450	0·74	1·05	2530	2790	1·09
		2790	1·14	2480	0·88		2900	2230	
1000	265	1910	0·90	2000	1·12	0·97	2300	2770	1·00
		2100	1·07	2140	0·88		2790	2330	
1200	340	2470	0·95	2560	1·03	0·99	2210	2680	1·04
		2450	0·70	2390	0·85		2950	2250	
Means			0·89		0·94	1·025			1·035

[illegible] observed a similar increase in sampling efficiency [illegible] thermal [illegible](3) in which the [illegible] air [illegible] at more than a thousand times [illegible] than at the thermal [illegible]. It seemed possible that this result might be an effect of the experimental arrangement. We have therefore made another wind-tunnel arrangement using a different means of producing test clouds of equal concentration [illegible] at different airspeeds.

[illegible] tunnel was [illegible](4) with a [illegible] of 1.5 square [illegible] section (see figure). Near the outlet 100 ft away, where [illegible] dust concentration had become uniform, an open [illegible] 6 in. in diameter and 15 ft long, with [illegible] each [illegible] down-stream end, was placed along the axis [illegible] the tunnel. The induced air velocities in the tube were [illegible] by a fixed [illegible] velocity [illegible] in the tunnel, [illegible] velocities in both cases being measured by a 4-in. vane anemometer on the axis of the tunnel or tube. The two [illegible] measured in this way would not be very accurately comparable, but this in no way invalidates the conclusions drawn from the dust measurements. The air velocities were too low to produce any appreciable increase in the [illegible] of 1 μ particles in the tube because of the [illegible] of the particle trajectories from the [illegible].

The [illegible] was sampled simultaneously [illegible] by two standard thermal precipitators, and in a [illegible] series of experiments by two long-period thermal precipitators,(5) the sampling heads of which were, for this purpose, detached from the bodies of the instruments. The [illegible] of all the instruments were always at right angles [illegible] the airstream and faced upwards, that is, sampled the air [illegible] in the usual fashion. Two sets of measurements were made at each airspeed, interchanging the instruments. [illegible] counts were made in the size range 1–5 μ, both for the standard thermal precipitator and for the long-period precipitator.

Application of "Student's" t test to the two measurements [illegible] shows no significant increase in the sampling efficiency of the [illegible] or long-period thermal precipitator over the [illegible] range of 40–1200 ft min^{-1}. The ratios of the particle counts on the A and B cover glasses of each short-period thermal precipitator sample are also [illegible] in the table, and show no significant variation.

Acknowledgement is given to Mr. G. Barker and Mr. B. [illegible] who assisted in the experiments.

Safety in Mines Research
Establishment,
Ministry of Power,
Sheffield.

J. R. Hodkinson
A. Critchlow
N. Stanley

(1) Watson, H. H. Trans. Inst. Min. Met., 46, p. 176 (1936).
(2) [illegible], F. Ph.D. Thesis, University of Sheffield (1955).
(3) Watson, W., Ltd. Leaflet 1039 (Barnet, Herts, 1957).
(4) [illegible], R., [illegible], R. A., and [illegible], D. L. Research Report No. 103, Safety in Mines Research Establishment, Sheffield (1954).
(5) Hamilton, R. J. J. Sci. Instrum., 33, p. 395 (1956).

Comments on the A.S.T.M. Powder Data File—5

The writers have now prepared a fifth booklet bearing the above title, which contains further additions to the lists previously published and described in the Institute's Journals.* Copies of the present booklet have been distributed in the same way as were the others. Those who have not received copies of the booklets in this way may obtain them (free of charge) on request from the Institute or from us.

It is hoped that similar lists of comments will continue to be published at approximately annual intervals. Users of the Data File are urged to send to the writers any material that they feel should be included in future issues.

It would help considerably in the work of extending the File if those who are working on structures by single-crystal methods could send us the crystallographic data and sufficient of their material to permit the production of a powder pattern from it. Full acknowledgement of the source would, of course, appear on the published card.

Viriamu Jones Laboratory,
University College, Cardiff,
Great Britain.

J. W. Hughes
Isobel E. Lewis
A. J. C. Wilson

[8 January, 1960]

---

* Hughes, J. W., Lewis, Isobel E., and Wilson, A. J. C. Brit. J. Appl. Phys., 10, p. [illegible] (1959); J. Sci. Instrum., 36, p. [illegible] (1959).

Revised edition of *Notes for authors*

The Institute of Physics has recently published a 16-page revised edition of its booklet intended to assist less-experienced authors and to serve as a reference booklet for all those who wish to contribute to the Institute's publications. Under its new title, *Notes for authors*, it gives notes on the preparation of scripts and diagrams, on the layout of mathematics, the correction of proofs and so on. In addition to a bibliography of reference books and works on technical writing, the pamphlet also contains lists of the spellings, symbols and abbreviations used by the Institute. These conform with British Standard 1991: Part 1: 1954 *Letter symbols, signs and abbreviations: Part 1. General* which authors of mathematical papers are also advised to consult.

Authors preparing contributions for submission to this Journal are invited to make use of the guidance contained in the booklet, copies of which may be obtained from The Institute of Physics price 1s 6d including postage.

Notes and comments

The postgraduate training of physicists in British universities

A distinguished committee appointed by The Institute of Physics and The Physical Society has now issued its report *The postgraduate training of physicists in British universities*, in which it records its opinion that the Ph.D. degree in physics is severely criticized by employers of physicists. In the committee's opinion this criticism is often justified. A strong recommendation is made that universities should require postgraduate students to attend co-ordinated courses of lectures in physics as part of their preparation for the Ph.D. Universities should be more critical in their selection of research students and should be willing to fail candidates who do not show evidence of an appropriate degree of scientific originality. Copies of the report are available (price 2*s*., including postage) from The Institute of Physics, 47 Belgrave Square, London, S.W.1.

Contemporary physics

In announcing this new periodical the publishers say "This new journal has been established to publish review articles on various aspects of physics of a standard suitable for teachers in schools and in technical colleges, scientists in industry, and others striving to keep in touch with modern developments. It is hoped to maintain the highest level of scientific content, and at the same time to interpret this content in a way that the ordinary graduate can understand. The Editorial Board has in mind the kind of treatment given in lectures at refresher courses organized by the universities, and indeed the real object of the *Journal* is of comparable intent".

The *Journal* will appear six times a year. The main features will be: major articles of about 6000 words, which will be descriptive surveys of advances in physics, relatively elementary interpretations of theoretical matters, and papers on the historical, philosophical, and educational aspects of the subject; articles of about 2000 words, which will deal with individual topics in greater detail; essay reviews, which will interpret the contents of outstanding publications, either books or original papers; book reviews, for which reviewers, as well as commenting by their own specialist standards, will try to assess a book's usefulness to the ordinary reader of the journal.

The Editor is Mr. G. R. Noakes, and he is supported by an Editorial Board of five distinguished physicists. The first issue of eighty pages contained the following contributions: "Molecular beams," by O. R. Frisch: "Nuclear structure," by R. J. Blin-Stoyle; "Alexander von Humboldt and the beginnings of geophysical research," by C. Kellner; "The selection of experiments for the Cavendish Laboratory alternating-current course," by E. V. Beck; "Skidding friction," by B. Sabey, and "Atomic light sources," by E Wilson and J. D. H. Hughes. In addition there are th essay reviews and seven other book reviews.

The price of single parts is 5*s*. (75 cents) excluding posta There are to be six parts to the volume. The subscripti price per volume is £1 7*s*. ($4.00), including postage. T publishers are Taylor and Francis Ltd., Red Lion Cou Fleet Street, London, E.C.4.

The Electronic Guide

This new directory is to be published annually to ass workers in electronics to locate articles in which they mig be interested. The articles are listed by titles only and ha appeared in nearly fifty periodicals published in the Weste world. The guide is easy to follow and contains a bibl graphic section which lists the names, addresses, and su scription prices of all the periodicals mentioned.

Further details may be obtained from References Research Division, Electronic Guide Publishing Co., B bank, California, U.S.A. The price is $7.50 per volume.

Glass Technology; Physics and Chemistry of Glasses

From the beginning of this year The Society of Gla Technology's *Journal* has been divided. *Glass Technolog* contains reports of applications of science in indust *Physics and Chemistry of Glasses* has reports of orig studies of physics and chemistry of glass both experimen and theoretical. It is to include such items as electric properties, infra-red absorption relaxation processes, therm dynamics of the glassy state, viscosity and X-ray diffractio

Both periodicals contain abstracts, letters and book review They are well produced and we congratulate the Society Editor Professor R. W. Douglas and the Assistant Edit Mr. R. Haresnape on the results of their efforts and wi them all success with this new venture of the Society.

British Journal of Applied Physics

Contents of the May issue

SPECIAL ARTICLES

Electron probe methods of X-ray microanalysis. By P. Duncumb.
Location of *p-n* and *l-h* junctions in semi-conductors. By P. A. Iles and P. Coppen.

PAPERS

Accuracy of selected-area microdiffraction in the electron microscope. A. W. Agar.
Vibration phenomena in detonation waves in hydrogen-oxygen mixtures. D. H. Edwards and T. G. Jones.
High alloy steels for use as a thermal conductivity standard. By R. W. Pow and R. P. Tye.
Correction of errors in electron stereomicroscopy. By O. C. Wells.
Contact electrification and polarization of nylon threads. By R. G. C. Arrid
Resistance-temperature relationship of platinum at low temperatures and influence on precision thermometry. By G. C. Lowenthal and A. F. Harper.

THIS *JOURNAL* is produced monthly by The Institute of Physics, with the co-operation of the National Physical Laboratory. It deals with the principles, construction and use of scientific instruments. All rights reserved. Responsibility for the statements contained herein attaches only to the writers.

EDITORIAL MATTER. Communications concerning editorial matter should be addressed to the Editor, The Institute of Physics, 47 Belgrave Square, London, S.W.1. (*Telephone:* Belgravia 6111.) Prospective authors are invited to prepare their scripts in accordance with the *Notes for Authors*. (Price 3*s*. 6*d*. including postage.)

REPRODUCTION. The Institute of Physics is a signatory to The Royal Society's Fair Copying Declaration. Details may be obtained upon application from The Royal Society, London, W.1.

ADVERTISEMENTS. Communications concerning advertisements should be addressed to the agents, Messrs. George Jackson (Fleet St.) Ltd., Cliffords Inn, Fleet Street, London, E.C.4. (*Telephone:* Holborn 3611–2.)

CLAIMS FOR MISSING JOURNALS. Claims from regular subscribers to this *Journal* for missing numbers will only be considered if received within 60 days of the date of mailing plus normal outward time of transit and time for lodging the claim. Losses attributable to failure to notify a change of address or to similar omissions will not be considered.

SUBSCRIPTION RATES. A new volume commences each January. The charge is £6 per volume ($17 U.S.A.), including index (post paid) payable in advance. Single parts, so far as available, may be purchased at 12*s*. 6*d*. each ($1.75 U.S.A.), post paid, cash with order. Orders should be sent to The Institute of Physics, 47 Belgrave Square, London, S.W.1, or to any bookseller.

PRINTED IN GREAT BRITAIN BY UNWIN BROTHERS LIMITED, WOKING AND LONDON

Compensated Wheatstone's bridge circuit for gas-chromatographic catharometry

by A. B. LITTLEWOOD, B.A., Department of Chemistry, King's College, University of Durham, Newcastle upon Tyne

[*Paper first received* 9 *November*, 1959, *and in final form* 12 *February*, 1960]

Abstract

Drift of the base line caused by imperfect control of temperature or voltage of a gas-chromatographic catharometer may be eliminated by including one shunt and one series resistance with the catharometer hot elements in the Wheatstone's bridge circuit. Equations enabling the positions and values of the resistances to be calculated from the observed drift are given. Experience shows that use of the compensating resistances enables a catharometer to be used more sensitively without the trouble and expense of careful temperature and voltage control.

Introduction

In gas-chromatographic catharometry, a unit for detecting vapours which emerge from the chromatographic column has two cavities, each containing one of two similar electrically heated resistances, or "hot elements". The effluent from the column flows through one cavity and pure carrier gas flows through the other; both cavities are usually in the same metal block, so that their walls are at exactly the same temperature. The hot elements (R_1 and R_4, Fig. 1) are used in a Wheatstone's bridge circuit together with R_2 and R_3, which are constant resistances whose values are such that the bridge is in balance.

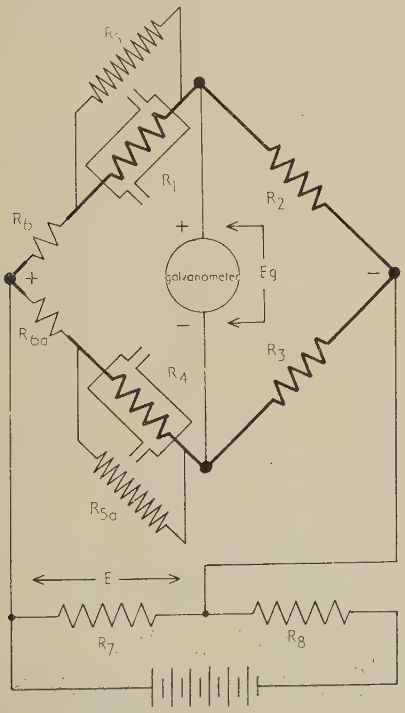

Fig. 1. Compensated Wheatstone's bridge circuit

In what may be termed an "ideal" bridge, that is, comprising R_1–R_2–R_3–R_4 (shown in heavy lines in Fig. 1) in balance ($E_g = 0$), a change in applied voltage E or in the temperature T of the block containing the cavities should not alter the balance, for, in either case, R_1 and R_4 should both change in the same proportion. In practice, this is not so, because the hot elements are not quite identical and cannot be made so to a sufficient degree of accuracy. In practical gas chromatography, therefore, where the galvanometer is a strip-chart recorder, inevitable slight changes in E and T cause an undesirable drift in the base line. This paper describes how drift resulting from changes in *either* E *or* T can be eliminated by incorporating a suitable constant shunt *or* series resistance R_5, R_{5a}, R_6, *or* R_{6a} (Fig. 1), and how drift resulting from changes in *both* E *and* T can be eliminated by incorporating one shunt resistance *and* one series resistance suitably chosen from R_5, R_{5a}, R_6, and R_{6a}.

To compensate for drift, one must first find which of the possible resistances are required, and then find their values. This may be achieved by trial and error, but it would be tedious. Therefore, a theory of the compensation is outlined below, and equations are given which enable the correct resistances to be chosen, and their values roughly calculated from measurements of the drift of a non-compensated circuit.

Theory

To calculate equations for the compensating resistances, the non-ideality of the bridge can be expressed in terms of coefficients of R_1 and R_4 with respect to change in temperature and applied voltage as follows. Let:

$$\alpha_1 = \frac{1}{R_1}\frac{\partial R_1}{\partial T}, \tag{1}$$

$$\alpha_4 = \frac{1}{R_4}\frac{\partial R_4}{\partial T}, \tag{2}$$

$$\beta_1 = \frac{1}{R_1}\frac{\partial R_1}{\partial E_1}, \tag{3}$$

$$\beta_4 = \frac{1}{R_4}\frac{\partial R_4}{\partial E_4}, \tag{4}$$

where E_1 and Es are voltages across R_1 and R_4. Also let:

$$\frac{\alpha_1}{\alpha_4} = 1 + a, \quad \frac{\beta_1}{\beta_4} = 1 + b.$$

In an ideal bridge, $\alpha_1 = \alpha_4$, $\beta_1 = \beta_4$, so that $a = b = 0$.

In a real bridge, it is assumed that (either actually or in effect) α_1 and α_4, β_1 and β_4 are slightly different, so that a and b are numbers, small compared with unity, which may be either positive or negative. It is also assumed that a and b are sufficiently small that the approximate numerical values of α_1, α_4, β_1 and β_4 may be given by:

$$\alpha_1 \simeq \alpha \simeq \alpha_4, \quad \beta_1 \simeq \beta \simeq \beta_4,$$

where α is the temperature coefficient of resistance of the material of the hot elements, and β is a coefficient, the value of which may be found from a graph showing how the resistance of the hot elements changes with applied voltage.

The observed drift due to changes in temperature and/or voltage may be measured and specified numerically by the quantities $\partial E_g/\partial T$, $\partial E_g/\partial E$. If it is assumed that the resistance of the galvanometer is high compared with the resistances of the arms of the bridge, application of Ohm's law yields the following equations for a and b in terms of the observed drift; the signs being correct for the polarities indicated in Fig. 1:

$$a = -\frac{1}{E\alpha} \cdot \frac{\partial E_g}{\partial T} \cdot \frac{(R_1 + R_2)^2}{R_1 R_2}, \tag{5}$$

$$b = -\frac{1}{E\beta} \cdot \frac{\partial E_g}{\partial E} \cdot \frac{(R_1 + R_2)^2}{R_1 R_2}. \tag{6}$$

In these equations, all the quantities on the right-hand side are known or measurable. It should be noted that if $2R_2 > R_1 > \frac{1}{2}R_2$, as is common practice, then

$$(R_1 + R_2)^2/R_1 R_2 \simeq 4.$$

The numbers a and b may now be related to the positions and values of compensating resistances by means of Ohm's law and the rules of partial differentiation. The values of the resistances arise from the conditions that, for compensated circuits, $\partial E_g/\partial T = 0$ and/or $\partial E_g/\partial E = 0$. The positions of the resistances are determined by the obvious fact that only circuits of which the equations give positive values for compensating resistances for given values of a and b are acceptable.

When a single compensating resistance is used, either $\partial E_g/\partial T$ or $\partial E_g/\partial E$ may be made equal to zero, but not, in general, both. The compensating resistance is a function of a for temperature compensation, and of b for voltage compensation. Four cases can be distinguished. These are listed in Table 1, together with the required equations and the conditions in a and b which define whether the compensating resistance should go with R_1 or R_4.

Table 1. *Values and positions of single compensating resistances*

Case number	*Compensation such that:*	*If* a *or* b *are positive, incorporate:*	*If* a *or* b *are negative, incorporate:*
1	$\partial E_g/\partial T = 0$	$R_5 = R_1/a$	$R_{5a} = -R_4/a$
2	$\partial E_g/\partial T = 0$	$R_6 = R_1 a$	$R_{6a} = -R_4 a$
3	$\partial E_g/\partial E = 0$	$R_5 = R_1/b$	$R_{5a} = -R_4/b$
4	$\partial E_g/\partial E = 0$	$R_6 = R_1 b/2$	$R_{6a} = -R_4 b/2$

When two compensating resistances are used, one shunt and one series, both $\partial E_g/\partial T$ and $\partial E_g/\partial E$ may be made zero. Again, four possible cases can be distinguished, the relevance of each depending on the values of a and b. These are listed in Table 2, together with the equations for the values of the compensating resistances and their ranges of application. Study of Table 2 shows that if, by chance, $a = b$, compensation for both variables is obtained with R_6 (or R_{6a}) equal to zero, that is, with a shunt resistance only. This i also apparent by comparison of cases 1 and 3. Simlarly, i $2a = b$, a series resistance alone will compensate for both variables; this is apparent from cases 2 and 4.

From the above discussion, therefore, the procedure fo calculating the positions and values of the compensatin resistances consists of (*a*) calculating a and/or b by equations 5 and/or 6; (*b*) using Tables 1 or 2.

Table 2. *Values and positions of two compensating resistances*

Case number	*R_5 or R_{5a}*	*R_6 or R_{6a}*	*Conditions of applicability*
5	$R_5 = R_1/(2a - b)$	$R_{6a} = R_4(a - b)$	$0 \leqslant a \geqslant b$ or $0 \geqslant 2a \geqslant b$
6	$R_{5a} = R_4/(b - 2a)$	$R_6 = R_1(b - a)$	$0 \geqslant a \leqslant b$ or $0 \leqslant 2a \leqslant b$
7	$R_5 = R_1/(2a - b)$	$R_6 = R_1(b - a)$	$0 \leqslant a \leqslant b \leqslant 2a$
8	$R_{5a} = R_4/(b - 2a)$	$R_{6a} = R_4(a - b)$	$0 \geqslant a \geqslant b \geqslant 2a$

Experimental methods and results

Several catharometers of different design and operating in different conditions have been compensated for drift, and the values and positions of the resistances required have been correlated with the drift through the quantities a and b.

(*a*) *Compensation for temperature drift only.* Cells were heated and cooled a few degrees above and below their temperature of operation, and the drift $\partial E_g/\partial T$ was measured for the uncompensated circuit. The position and value of the compensating resistance was then determined as described from the drift and from α, which was measured in a separate experiment (α for the thermistors was obtained from published data). The value of the compensating resistance required to make $\partial E_g/\partial T = 0$ was then found by trial, using the calculated value as a guide. There is a considerable range of values of the compensating resistances in which the drift is smaller than can be conveniently measured, so that experimental values of the compensating resistances are approximate, but since the object of the resistances is achieved when the drift is too small to measure, the difference between their values and the values required for perfect compensation is immaterial. Calculated and experimental values are shown in Table 3.

With a shunt resistance (case 1), the calculated and experimental values agree fairly well, results 4 and 5 exemplifying the worst that may be expected. When a series resistance is used (case 2), experimental and calculated values sometimes agree well, but there are some cases in which the resistance required is abnormally large. In these, the calculated value considerably reduces the drift, but further increase in the value has comparatively little effect. In all cases, the sign of a correctly determines the position of the compensating resistance.

A gross change in temperature may necessitate a change in the value of the compensating resistance, though not always. Thus the conditions pertaining to results 4 and 5 were similar apart from temperature, and R_5 remains the same. Results 1 and 2, however, the conditions for which also differed only in temperature, show a difference in the required compensating resistance. A gross change in E has a gross effect on the required compensating resistance; this is shown by results 8 and 9 in which conditions were similar apart from change in E.

(*b*) *Compensation for voltage drift only.* The voltage applied to the bridge was varied a few per cent above and below the operating voltage by adjustment of the potential

Table 3. *Compensation for temperature drift*

Result number	*Type of elements*	*Carrier gas*	T (° C)	E (V)	R_1 (Ω)	α (*per* ° C)	$\partial E_g/\partial T$ (mV/° C)	a	*Calc.* (Ω)	*Exper.* (Ω)
Case 1									R_5 *or* R_{5a}	
1	Pt wire	H_2	50	12	93	0·0033	+0·19	−0·019	4900	5050
2	Pt wire	H_2	100	12	114	0·0027	+0·30	−0·039	2900	3700
3	Pt wire	N_2	50	6	85	0·0033	+0·085	−0·019	5000	5000
4	Pt wire	N_2	100	6	105	0·0027	+0·085	−0·021	5000	3500
5	Pt wire	H_2	50	6	85	0·0033	+0·082	−0·019	5000	3500
6	Pt wire	H_2	41	18	103	0·0034	+1·95	−0·127	810	800
7	Thermistor	N_2	100	12	8500	−0·05	+0·35	+0·003	$1·9\times10^6$	$0·8\times10^6$
Case 2									R_6 *or* R_{6a}	
8	Pt wire	H_2	100	6	105	0·0027	+0·058	−0·015	1·5	1·5
9	Pt wire	H_2	100	12	114	0·0027	+0·30	−0·039	4·4	4·5
10	Pt wire	H_2	50	12	93	0·0033	+0·19	−0·019	1·8	7·0
11	Pt wire	N_2	100	6	105	0·0027	+0·085	−0·021	2·2	12·0

Table 4. *Compensation for voltage drift*

Result number	*Type of elements*	*Carrier gas*	T (° C)	E (V)	R_1 (Ω)	β (*per V*)	$\partial E_g/\partial E$ ($\times 10^3$)	b	*Calc.* (Ω)	*Exper.* (Ω)
Case 3									R_5 *or* R_{5a}	
12	Pt wire	H_2	50	18	106	+0·014	+3·7	−0·059	1 800	1 750
13	Pt wire	H_2	20	18	94	+0·016	+0·61	−0·0085	11 000	10 000
14	Pt wire	N_2	50	10	106	+0·027	−1·0	+0·15	7 100	7 500
15	Pt wire	N_2	100	6	105	+0·038	−6·9	+0·12	875	1 150
16	Pt wire	H_2	20	6	78	+0·012	−3·2	+0·16	490	500
17	Pt wire	H_2	100	12	114	+0·018	−5·8	+0·107	1 060	810
18	Pt wire	H_2	50	12	93	+0·020	−7·2	+0·12	770	740
Case 4									R_6 *or* R_{6a}	
19	Pt wire	H_2	50	18	106	+0·014	+3·7	−0·059	3·1	3·0
20	Pt wire	H_2	20	18	94	+0·016	+0·61	−0·0085	0·40	0·4
21	Pt wire	N_2	50	10	106	+0·027	−1·0	−0·015	0·80	0·8
22	Pt wire	N_2	100	6	105	+0·038	−6·9	+0·12	6·3	4·6
23	Pt wire	H_2	50	6	85	+0·012	−2·44	+0·125	5·2	4·0
24	Pt wire	H_2	100	12	114	+0·018	−5·8	+0·107	6·1	5·0
25	Pt wire	H_2	50	12	93	+0·020	7·2	+0·12	5·5	4·6
26	Thermistor	N_2	100	12	8 500	−0·015	−1·9	−0·053	150	47
27	Thermistor	N_2	50	12	35 000	−0·062	−5·0	−0·028	500	160

Table 5. *Compensation for temperature and voltage drift*

Result number	*Type of elements*	*Carrier gas*	T (° C)	E (V)	R_1 (Ω)	α (*per* ° C) β (*per V*)	$\partial E_g/\partial T$ (mV/° C) $\partial E_g/\partial E$ ($\times 10^3$)	a b	*Calc.* (Ω)	*Exper.* (Ω)
									R_5 *or* R_{5a} R_6 *or* R_{6a}	
28	Pt wire	H_2	33	18	100	+0·0034 +0·014	+1·95 +3·7	−0·127 −0·059	540 6·8	700 5·0
29	Pt wire	N_2	50	10	106	+0·0033 +0·027	0·00 1·0	0·00 +0·015	7000 1·6	7000 1·5
30	Pt wire	N_2	100	6	105	+0·0027 +0·035	+0·085 −6·9	−0·021 +0·12	650 14·8	1400 8
31	Pt wire	H_2	50	12	93	+0·004 +0·024	+0·19 −7·2	−0·019 +0·12	590 12·9	1260 7·2
32	Pt wire	H_2	100	12	114	+0·004 +0·024	+0·19 −7·2	−0·019 +0·12	560 10·6	1200 9·0
33	Thermistor	H_2	50	12	35K	−0·07 −0·062	−0·30 −5·0	+1·5 −0·028	1M 800K	1M 330K

divider R_7, R_8 (Fig. 1), and the drift $\partial E_g/\partial E$ for the uncompensated circuit was measured. As in the previous case, the compensating resistance was calculated from this and from β, which was determined separately; these values were then used as a guide in determining actual values. Calculated and experimental values are shown in Table 4. The figures agree within about 10% on average and often within much narrower limits for both shunt- and series-compensating resistances. As with temperature compensation, discrepancy between calculated and experimental values is greatest for the thermistor. In all cases, the sign of b correctly determines the position of the compensating resistance.

In the cases studied, gross changes in the applied voltage, the carrier gas, or the temperature have not produced gross changes in the compensating resistances required. Thus results 15, 16, 17, 18, 22, 23, 24 and 25 were all obtained with the same hot elements in the conditions tabulated, and the compensating resistances are all within about 25% of 750 or 4·5 Ω. In cases where the same cell in the same conditions has been compensated with both series and shunt resistances in two separate experiments, for example, results 12 and 19, 13 and 20, 14 and 21, 15 and 22, the relation $2R_6R_5 = R_1^2$, derived from the equations for cases 3 and 4 by elimination of b, is approximately maintained.

(*c*) *Compensation for temperature and voltage drift.* Table 5 shows examples of cases 5 and 6. No cells requiring compensation according to cases 7 or 8 were encountered; it is impossible to say whether this is coincidence or is general. In all examples, theory predicts the correct case, but the quantitative predictions are only approximate, especially when a and b are greater than a few hundredths.

The improvement in drift produced by compensation is illustrated in Fig. 2, which shows a tracing of a base line A from a compensated metal catharometer cell which was being continually heated; both time and temperature are marked on the abscissa. The periodic deflexions in the curve were produced by changing the applied voltage by 0·3 V for 20 s. Also constructed in Fig. 2 are the base line that would have appeared from the uncompensated cell similarly heated (line B), and an indication of the deflexion that would have occurred on similarly changing the applied voltage to the uncompensated cell (C). The diagram shows that the compensation is almost perfect over a range of about 10° C and is effective over 50° C or more. As may be expected, the range of temperature over which given compensatin resistances are effective is smaller when the hot elements ar thermistors; in the cases studied it was not greater than 10° C

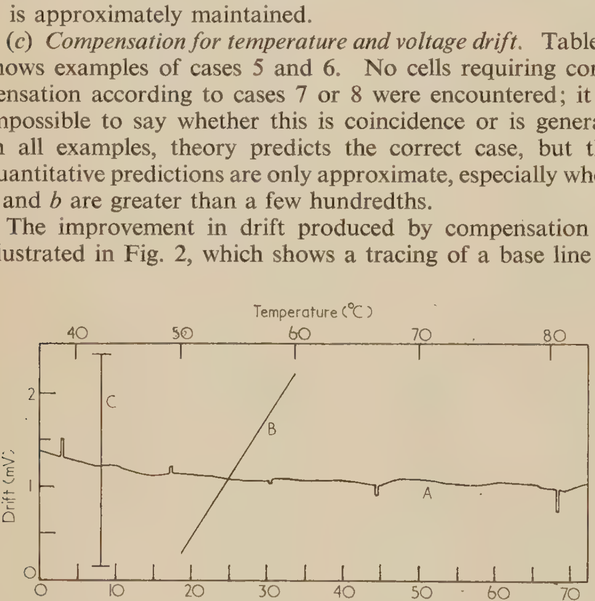

Fig. 2. Illustration of improvement in drift resulting from compensation

Discussion

The results indicate that the drift due to changes in E an T can be completely eliminated by adding suitable compensating resistances. In the experiments reported, the limit o detection of the drift was such that the compensating resistances needed only to be within ±5% of the true value fo its complete elimination; more accurate elimination of th drift would presumably only require more careful adjustmen of the values of the compensating resistances, unless dri were caused by changes in quantities other than E and T of which there is no evidence. Agreement between th observed values of the compensating resistances and thos calculated by theory is often but not always good. However in all cases the theory predicts the correct position and th correct order of magnitude of the compensating resistances and to this extent it is useful in practice. The quickest an most satisfactory way of compensating the drift in a give catharometer circuit is to measure $\partial E_g/\partial T$, $\partial E_g/\partial E$, α and β very roughly, whence one may calculate positions an approximate values of the compensating resistances. Whe these are inserted, exact values may easily be found by trial If only one compensating resistance is to be used, a shun is preferable to a series resistance, since with a shunt resistance imperfect contacts are less likely to produce noise.

In a given catharometer, the importance of the drift depend on (*a*) whether or not the noise is bigger than the drift, an (*b*) whether or not the catharometer is to be used at such sensitivity that the drift is appreciable compared with th chromatographic peaks to be measured. Answers to thes questions cannot, of course, be given in general, but experienc is that, unless elaborate and expensive temperature- an voltage-control methods are used, the drift is certainly greate than the noise, and that the elimination of the drift enable the catharometer to be used to detect and measure much smaller concentrations of vapour if required. This can b illustrated by the following data pertaining to the cell used for results 6, 12, 13, 19, 20 and 28. With E equal to 18 V and hydrogen carrier gas, its sensitivity towards *n*-heptan vapour was such that a concentration of 1 μg of heptan per millilitre of hydrogen produced ΔE_g equal 1 mV. In these circumstances, the noise was invisible on a 2 mV strip chart recorder, so was less than about 10 μV. Thus, the limit of detection was about 10^{-8} g/ml. According to the data of runs 6 and either 12 or 19, 0·1° C change in T in the uncompensated circuit caused a drift of 195 μV, and 0·1 V change in E caused a drift of 370 μV, both of which figures are very much greater than the noise, and both o which are caused by not unreasonable changes in E and T Also in the above example, the drift produced by the change in T is equivalent to a heptane vapour concentration o approximately 0·195 μg/ml. and that produced by the change in E to a concentration of 0·370 μg/ml., both of which figures are very much greater than the limit of detection With regard to both criteria above, therefore, the compensation is very desirable.

Transistor cup anemometer

by R. R. McGREGOR, Dip. Appd. Sci., Division of Meteorological Physics, Commonwealth Scientific
and Industrial Research Organization, Aspendale Victoria, Australia

[*Paper first received* 27 *July*, 1959, *and in final form* 12 *February*, 1960]

Abstract

A remote indicating cup anemometer is described in which transistor electronics have been applied to obtain a compact instrument, operating off small dry batteries and capable of registering wind speeds down to 0·2 *m/s.*

Introduction

In meteorological work it is often useful to employ a sensitive cup anemometer capable of operating an electric counter at a distance from the instrument. With a direct electric contact in the anemometer it is difficult to secure fully reliable contacting while maintaining a small enough friction for operation at wind speeds less than 0·5–0·75 m/s. As a bearing friction small enough for operation down to 0·2 m/s can be secured, photoelectric switching is sometimes employed,(1,2) but this has the disadvantage of a rather large power consumption which is inconvenient in work at sites without an electric power supply. For such applications an anemometer, with a shielding vane controlling a transistor oscillator switching circuit, has been found useful and is described below.

Description of apparatus

The anemometer employs the Sheppard type of cup rotor, spindle, bearings, bearing tube and movement case of the Casella sensitive anemometer, as in the instrument described by Crawford.(3) The 16-tooth spindle pinion *A* (see the figure) meshes with a 64-tooth fibre gear wheel *B*, carrying a kidney-shaped piece of Stalloy sheet *D*. Wheel *B* is drilled for balancing and half of it protrudes into a slot in a cylindrical Neosid former carrying the windings L_1, L_2, L_3. The tuning slug is divided into halves and mounted securely within L_1 and L_2. When *D* is within the windings its shielding reduces the positive feedback between L_1 and L_2 sufficiently to stop oscillation and only the preset forward bias current flows which is insufficient to hold relay *K* operated; L_3 is a small winding (approximately one turn) which enables the minimum value of feedback to be adjusted. When *D* is withdrawn the feedback increases to a sufficiently large value that the resulting oscillations cause bottoming of the transistor collector current. In this condition a large mean current flow is obtained at a modest voltage. As long as the current gain α' for each transistor exceeds 70% of the rated average value for each transistor no other matching is required.

Temperature compensation is a necessity with transistors, and in this instance attention to three points provided satisfactory operation. A grounded base circuit gives the advantage of a very small output leakage (I_{co}). The temperature dependant diode e.m.f. between base and emitter (E_{be}) is balanced by a suitably connected junction diode, a strapped type OC73 or OC71, and finally a temperature-sensitive resistor (copper) in the emitter circuit prevents runaway. The following random variations in currents were obtained between 32 and 140° F.

Supply voltage (V)	*Minimum relay current (mA)*	*Maximum relay current (mA*
11·75	−0·18/−0·25	−6·3/−6·6
16·0	−0·26/−0·32	−8·5/−8·9

The three transistors and the copper resistor are placed together to reduce temperature differences, and the case and face of the anemometer are painted white. The whole left-hand part of the circuit in the figure fits neatly into the anemometer movement case.

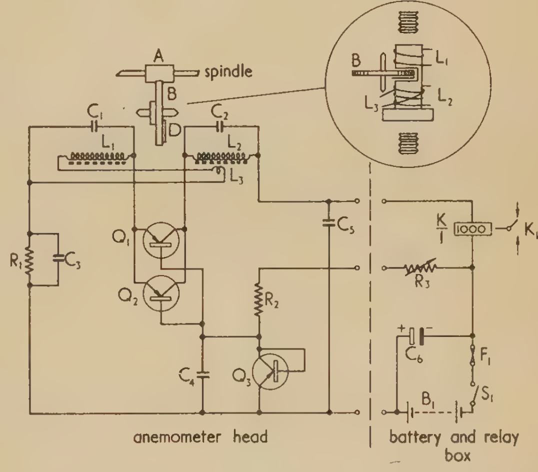

Circuit of transistor cup anemometer

C_1 = 1700 pF, silver mica
C_2 = 5000 pF, silver mica
C_3–C_5 = 6000 pF, mica
C_6 = 100 μF

R_1 = copper resistor 70 Ω at 60° F
R_2 = 10 kΩ, 1 W carbon
R_3 = 20 kΩ, 2 W carbon

Q_1, Q_2 = OC44
Q_3 = OC73 or OC71

S_1 = single-pole, single-throw switch

F_1 = 60 mA fuse

K = British Post Office 3000 type relay 1 kΩ coil, 1 changeover set

L_1 = 6 turns, 22 s.w.g. close wound
L_2 = 11 turns, 22 s.w.g. close wound
L_3 = 1 turn, 22 s.w.g.

B_1 = 18 V dry cell

A = 16-tooth spindle gear
B = 64-tooth fibre gear
D = Stalloy vane 0·014″ arc for equal make and break approximately 210°
L_2, C_2 tune 1400–1600 kc/s

The forward bias current, necessary to obtain an operating point sufficiently sensitive for oscillation to commence, is developed across Q_3 and controlled by R_3 which can compensate for different values of Q_1, Q_2. A single setting allows a 1·5 : 1 change in supply voltage. This setting should be tested over the voltage range it is intended to use whenever the batteries are changed. An endpoint of 1·0 V per cell is normal, which gives a working range of 18 V to 12 V. The supply consists of three batteries of four cells in series so that a convenient 12 V tap is available for testing.

The counting rate of the anemometer in a wind of 5 m/s is approximately 50 counts per minute and the calibration is nearly linear. For some micro-meteorological purposes it is desirable to have a greater counting rate for greater resolving power with runs of short duration. The geometry of the movement case of the Casella anemometer precludes the use of a lower gear ratio than the 4 : 1 reduction used here, but the counting rate can be doubled by using a capacitor discharge method of operating the counter; it is then easy to arrange for the changeover contacts on relay K to give counts in both positions.

The instrument has fulfilled all requirements and the four in service for the past three months have not required mo fication. The power consumption is very low at 3–4 m from 18 V and allows a light economical battery to la 5–6 weeks.

Acknowledgement

Thanks are due to Mr. G. Grauze for constructing the instruments.

References

(1) Deacon, E. L. *J. Sci. Instrum.*, **25**, pp. 44–47 (1948).
(2) Kassander, A. R., and Stewart, R. M. *Bull. Am Meteorol. Soc.*, **36**, pp. 384–387 (1955).
(3) Crawford, S. G. *J. Sci. Instrum.*, **28**, pp. 36–37 (195

Photoelectric comparator for Rayleigh fringe electrophoresis patterns

by C. C. CURTAIN, M.Sc., Ph.D., A.R.A.C.I., The Baker Medical Research Institute, Alfred Hospital, Melbourne, Australia

[*Paper received* 25 *January*, 1960]

Abstract

A photoelectric fringe comparator for scanning electrophoresis plates, based on a microdensitometer, a Schmitt-trigger operated counter and a recording milliammeter is described. The basis of the microdensitometer is a standard Zeiss binocular microscope with a mechanical stage driven by a reduction gearbox. A considerable simplification in the electronic circuit of the densitometer is achieved by using highly sensitive type ORP 90 *cadmium sulphide photoconductive cells.*

Introduction

A number of commercially available electrophoresis instruments can be fitted with interferometric optical systems. Owing to the absence of diffraction effects, and the fact that a minimum of optical density may be located more reproducibly than the edge of a shadow, interference fringe patterns are more accurate than those of the conventional Schlieren systems.

Perhaps the major disadvantage of interference optical systems is the strain imposed upon the operator by visual methods of fringe measurement. This paper describes the design of a simple photoelectric comparator which has proved most useful in replacing visual methods in the routine measurement of large numbers of electrophoresis and diffusion plates.

Design considerations

The basis of the instrument is a photoelectric microdensitometer, with a resolving power of approximately one-tenth of the finest fringe separation likely to be encountered. The electrophoresis instrument used was the Perkin-Elmer Model 38A fitted with the phase-plate-gradient Rayleigh interferometer optical system of Moore and Opperman.⁽¹⁾ A typical pattern is shown in Fig. 1. The maximum co centration gradients encountered in normal electrophore and diffusion runs in this instrument are of the order of 2 g per cm. Assuming $\eta = 0{\cdot}00184$ for a 1 g % prote

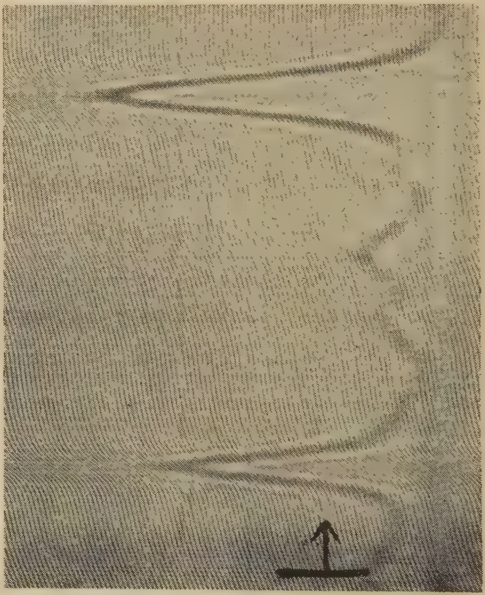

Fig. 1. An electrophoresis pattern obtained with the phase-plate gradient interferometric optical system of the Perkin-Elmer Model 38A Tiselius electrophoresis apparatus. The pattern is from the ascending limb of a run on the serum of a patient suffering from macroglobulinaemia. The photograph was taken after electrophoresis for 5000 s at 25 V cm^{-1} in pH 8·6, $I = 0{\cdot}1$ veronal buffer at 2° C. The arrow and vertical line indicate direction of migration

lution, each fringe deflected across the baseline in the
oore and Opperman optical system corresponds to a con-
ntration increment of 0·02 g %. A maximum concen-
ation gradient of 2 g% per cm corresponds to 100 fringes/cm,
r a minimum fringe separation of 50 μ in the focal plane
f the camera at a cell magnification of unity. The resolving
ower of the photometer should therefore be 5 μ. At the
aximum concentration gradient of 2 g% per cm this corre-
onds to a concentration increment of 0·002 g%. At lower
oncentration gradients and greater fringe separations it
orresponds to proportionately smaller concentration incre-
ents. Kodak contrast process orthochromatic plates were
sed for recording patterns in the electrophoresis instrument.
eveloped in Kodak D72 developer, these plates have an
verage grain size of 1·5 μ.

Constructional detail

To achieve the desired resolution the photometer was
ased on a Zeiss binocular microscope fitted with a vernier
tage. A 100 W projection lamp was used as a light source.
ne ocular was replaced by a Zeiss No. 2 projection ocular,
asked so that the field viewed in the focal plane was 5 μ in
iameter, with an oil immersion objective (H.I. 90) in position.
he objective was used dry, having sufficient resolution for
he purpose. The phototube was placed in the focal plane
f the projection ocular on top of an extension tube.

The other ocular (×12) was fitted with cross hairs and
sed for alinement and focusing. As the microscope stage
ernier could be read to only 0·1 mm, further scale magni-
ication was obtained by using a reduction gearbox with a
atio such that one rotation of the input shaft moved the
tage a distance of 25 μ. The gears were obtained from a
endix azimuth indicator. A dial calibrated in microns was
laced on the input shaft and the main dial of the azimuth
ndicator was recalibrated in tens of microns.

For routine fringe counting and evaluation of electrophoresis patterns (particularly of serum) the photometer was connected to a discriminator and counter and a chart recorder. The stage traverse of the microscope was then driven by a synchronous motor (Bodine type KYC-23, 1 rev/s speed) coupled to the input shaft of the gearbox. A block diagram of the instrument is shown in Fig. 2.

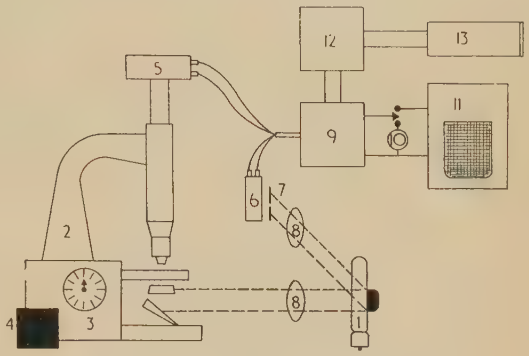

Fig. 2. Block diagram of the comparator

(1), 100 W projection lamp; (2), Zeiss binocular microscope; (3), gearbox (adapted from a Bendix azimuth indicator); (4), Bodine KYC 23 synchronous motor; (5), ORP 90 photocell in focal plane of projection ocular; (6), ORP 90 balance cell; (7), neutral density filter; (8) lens; (9), d.c. amplifier; (10), 0–1 mA meter; (11), recording milliammeter (Evershed and Vignoles); (12), trigger; (13), electromechanical counter

Electronic circuits

The photometer, discriminator and counter circuits are given in Fig. 3. Two Philips type ORP 90 cadmium sulphide photoconductive cells were used in a bridge circuit. One cell was located in the focal plane of the projection ocular. The other cell was used to compensate for fluctuations in the light

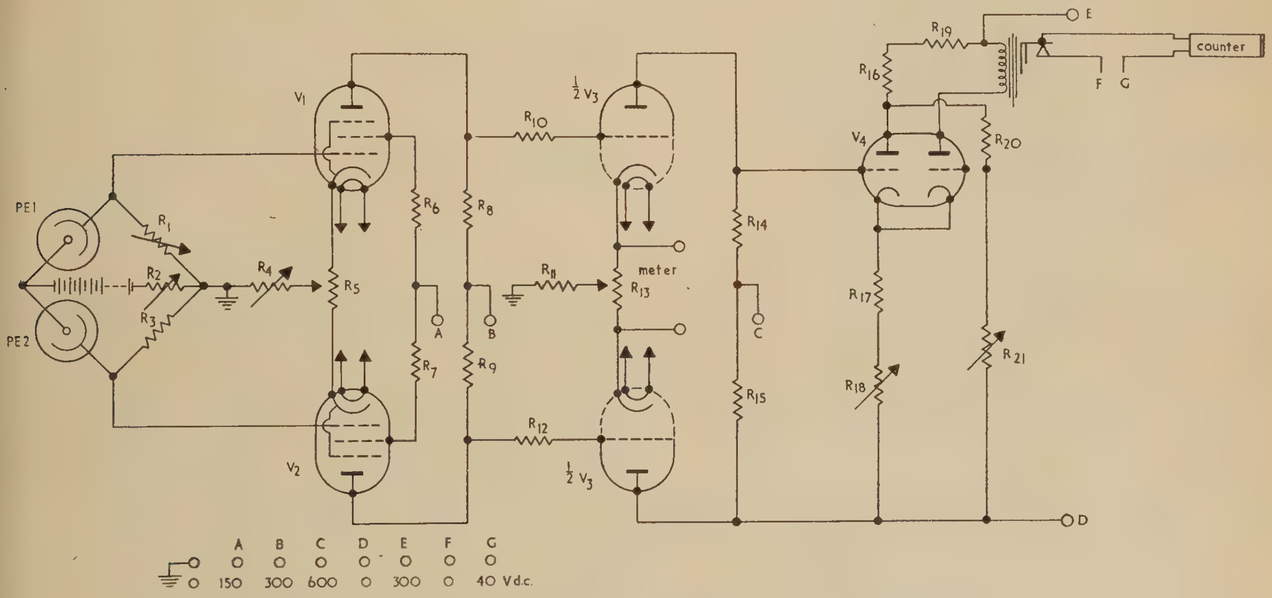

Fig. 3. Circuit diagram of densitometer and trigger. All resistances and potentiometers were of 10% tolerance. V_1 and V_2 were a matched pair of valves supplied by S.T.C. (Australia) Ltd.

$R_1 = 150\ \text{k}\Omega$
$R_2 = 50\ \text{k}\Omega$
$R_3 = 100\ \text{k}\Omega$
$R_4 = 1\cdot5\ \text{k}\Omega$
$R_5 = 600\ \Omega$
$R_6, R_7 = 600\ \text{k}\Omega$
$R_8, R_9 = 470\ \text{k}\Omega$
$R_{10} = 25\ \text{k}\Omega$
$R_{11} = 1\cdot5\ \text{M}\Omega$
$R_{12} = 25\ \text{k}\Omega$
$R_{13}, R_{14}, R_{15} = 100\ \text{k}\Omega$
$R_{16} = 120\ \text{k}\Omega$
$R_{17} = 500\ \Omega$
$R_{18} = 1\ \text{k}\Omega$
$R_{19} = 15\ \text{k}\Omega$
$R_{20}, R_{21} = 500\ \text{k}\Omega$
PE_1, PE_2 = Philips type ORP90 cadmium sulphide cells
V_1, V_2 = 6 AU 6
V_3 = 12 AX 7
V_4 = 6 SN 7
Relay = 1 mA, 5 kΩ Post Office movement

source. The image of the source was projected on to this cell by a simple lens through a neutral density filter (made from a piece of processed, exposed X-ray film) so that the light intensity on, and hence the resistance of the cell, was approximately the same as that of the ocular cell.

As cadmium sulphide photocells are very sensitive (10 A/lm at 100 lx) it was possible to use a simple direct-coupled amplifier to drive the output meter (0–1 mA movement). The output from the amplifier also operated a Schmitt trigger circuit which was connected through a 1 mA relay to an electromechanical counter. To allow for variations in the intensity of illumination over the field of the electrophoresis instrument, and the resulting variations in the optical density of each fringe, the trigger was set to fire when the photometer had reached approximately 30% of its maximum output. A typical densitometric curve is shown in Fig. 4.

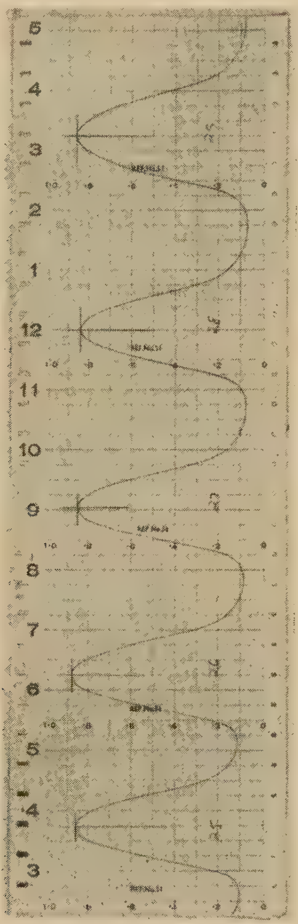

Fig. 4. Densitometer recording. The numbers 25–29 are fringe numbers which have been written on the chart by the operator

For automatic photometric recording the output meter was replaced by a recording milliammeter (Evershed and Vignoles Murday-type recorder).

Power supplies

A 90 V dry battery was used for the bridge. With the exception of the d.c. voltage for the counter, which was obtained from a transformer and dry rectifier, the other voltages indicated in the circuit were obtained from conventional electronically stabilized supplies.

Methods of use

The instrument can be used in two ways.

(1) *To measure fringe separation.* The synchronous mot is disconnected, the stage traverse operated manually a the maximum in the curve of each fringe is obtained observing the output meter. The distances between t maxima are read from the gearbox dials.

Alternatively, with the motor connected it is possible record with the chart recorder the photometric curves all the fringes on a given plate. Fringe separation may easily measured on this record.

A plot of the fringe separation $d_{x+1} - d_x$ (where d is t distance of a given fringe from the origin, and x is the frin number) against x gives the protein concentration as function of the height in the electrophoresis cell. If t reciprocal of the fringe separation $I/(d_{x+1} - d_x)$ is plott against the mean position, a gradient curve is obtaine This is free of the diffraction and tracing errors which acco pany Schlieren gradient curves, including those obtained wi a diagonal phase-plate. This higher accuracy is of co siderable value in the study of boundary asymmetry, par cularly at low protein concentrations (0·3 g% or less).

(2) *Combined use of the counter and chart recorder.* F analysis of complex patterns, such as serum, it is not necessa to plot all the d_x values. A minimum in the gradient cur occurs at each maximum in the separation of the fringe These minima may be taken to represent the limits of ea component in the system,(2) and it is therefore only necessa to count fringes between successive minima in the gradie curve to determine the refractive increment due to each these components. The fringe number δd_{max} at which e minimum occurs may be obtained by numerical inte polation.(3)

If
$$\delta d_1 = \delta d_x - \delta d_{x-1}$$
$$\delta d_2 = \delta d_{x+1} - \delta d_x$$
and
$$\delta d_3 = \delta d_{x+2} - \delta d_{x+1}$$

where d_2 is a maximum, that is

$$\delta d_1 < \delta d_2 > \delta d_3$$

The fringe number x_m at the minimum in the gradie curve is given by

$$x_m = \frac{(2x+1)\delta d_2 - x\delta d_3 - (x+1)\delta d_1}{2\delta d_2 - \delta d_1 - \delta d_3}$$

A typical procedure using the counter and recorder is t make marks with a red grease pencil at the top of the pla at positions corresponding to the minima in the phase-pla gradient curve. The stage motor and counter are started the origin on the plate and as each minimum is approache (as indicated by the approach of the red mark to a wi "sight" fixed to the frame of the microscope) the recorder started. Each fringe number is noted on the recording cha as its curve is traced. This is quite easy, as near the minim the fringes are well spaced and the rate of counting is lo As the minimum recedes the recorder is stopped, and restarte as the next minimum approaches. The usual practice is t record five fringes on each side of a minimum. The valu for d and x are obtained from the chart and x_m is calculate to the nearest 0·2 fringe. The concentration of each co ponent (in grammes per cent) is obtained by multiplying t number of fringes between successive values of x_m by 0·02.

This procedure can be adapted readily to the plates fro ny auto-collimating interferometric optical system where is possible to locate the minima approximately from a uperimposed Schlieren-gradient curve.

Acknowledgement

The author is grateful to Mr. S. Hart for suggesting and dapting the azimuth indicator, and to Mr. J. Bremner for dvice and criticism concerning the electronic circuits.

References

(1) Moore, D. H., and Opperman, K. *Biochim. Biophys. Acta*, **22**, p. 136 (1936).

(2) Tiselius, A., and Kabat, E. A. *J. Exper. Med.*, **69**, p. 119 (1939).

(3) Longsworth, L. G. *Electrophoresis theory, methods, applications*, edited by M. Bier, p. 161 (New York: Academic Press, Inc., 1959).

Rand soil-pressure cell for low pressures, high accuracy and long-term stability

by Prof. J. E. JENNINGS, B.Sc.(Eng.), S.M., M.I.C.E., and J. B. BURLAND, B.Sc.(Eng.),
University of the Witwatersrand, Johannesburg, S. Africa

[*Paper received* 6 *October*, 1959]

Abstract

The cell is of a "balanced pressure" type and a linear differential transformer is used as a null point indicator to maintain a diaphragm in its zero position. The deflexions of the diaphragm during pressure measurement may be kept very small, well within the limits required for soil pressure cells. The cell is used for direct and tangential pressures on the face of a rigid wall containing consolidating silt. The accuracy of observing the pressures lies within ±0·04 *in. head of oil.*

Introduction

The apparatus has been designed for the measurement of soil pressures on a rigid, rough boundary. It is being used initially for measurements during sedimentation, the same principles being employed for the observation of normal and tangential pressures on the rigid boundary and for the porewater pressures in the consolidating mass of soil. This is the problem of pressures on a dam wall during silting of the dam.

For the proper measurement of soil pressures on a rigid face, it is necessary that distortions of the soil mass in the vicinity of measuring instrument be limited to a small order. This requires that the maximum deflexion at the face of any circular measuring cell shall be less than one two-thousandth of the diameter.* In the cell described a movement of 0·0005 in. over a diameter of 3 in. is easily achieved, i.e. the ratio concerned is 1 : 6000.

Further requirements of the instrument are a high accuracy of pressure measurement, of the order of ±0·1 in. water head, tightness to leakage of oil, water or air, and a stable zero setting, allowing tests of long duration.

Description of the cell

The cell is shown in Fig. 1. A brass membrane, 0·005 in. thick is arranged to be flush with the face of the retaining wall. This membrane is stretched and locked into place by the holding ring. The cell is operated on a "null-deflexion" principle, the external pressure due to the soil being balanced by an equal oil pressure on the inside of the membrane. [Transformer oil to B.S.S. 148 (1951) is used.] The balancing pressure is measured on a manometer or pressure gauge.

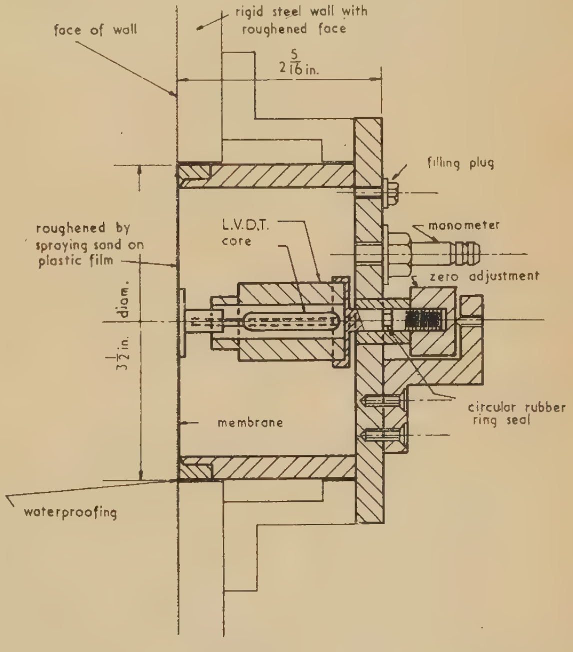

Fig. 1. General arrangement of the Rand soil-pressure cell

A good quality linear differential transformer (L.V.D.T.) such as type 0605–LD by Schaevitz, is used as a null point indicator. The electrical circuit is shown in Fig. 2. Mains current, 50 c/s 220 V., is transformed to 5 V and used for exciting the central coil. The differential output current from the L.V.D.T. is rectified by two germanium diodes before passing through a good quality spot galvanometer

---

* *Triaxial Shear Research and Pressure Distribution Studies on Soils*, Progress Report. (U.S. Waterways Experiment Station, 1947.)

(such as the Pye "Scalamp" type 7901/5 galvanometer, 22 Ω, 16 mm/μA). The capacitor and resistor serve to reduce secondary currents not completely rectified by the diodes. The diodes are sensitive to light and temperature changes and are mounted in transformer oil to reduce variations to a minimum. The circuit is very sensitive to voltage variation in the mains, and at present a variable resistance is being employed with a high quality voltmeter, but a constant voltage transformer will soon be used to replace this. It is then proposed to raise the input voltage from 5 to 6 V, thereby increasing the sensitivity of the apparatus.

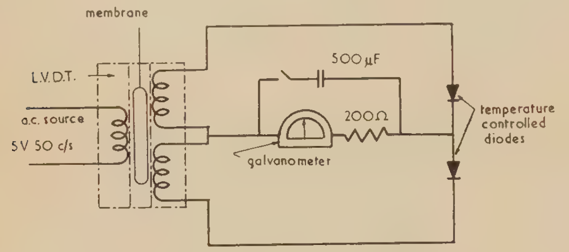

Fig. 2. Circuit diagram for linear differential transformer indication in the Rand soil-pressure cell

The core of the L.V.D.T. is fixed to the membrane and the coils are mounted on an adjustable base attached to a rigid housing. The coils are set to give zero out-of-balance current with known conditions of equal pressure inside and outside the cell. When pressure is applied by the soil outside the membrane, this balance point is again found by adjusting the pressure of the oil inside the cell. The mounting of the cell and arrangements for rapid application of pressure to the transformer oil are shown in Fig. 3.

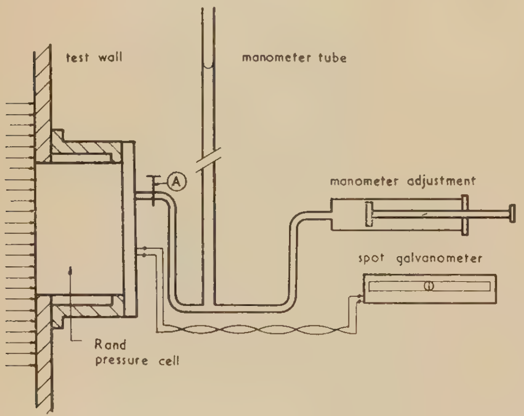

Fig. 3. Layout of apparatus for measuring normal pressures against a rigid wall

Extensive tests were performed to determine whether there were any hysteresis or other effects involved in securing the balance point. A typical calibration curve is shown in Fig. 4(*a*) and no discernible external effects were found to exist.

Test results

(*a*) *Accuracy.* A test bed was constructed which permitted a known oil pressure to be applied to the outside of the cell, and this pressure was then compared with the measured internal oil pressure. The external pressure was set at three predetermined heads, namely −27 in., +3 in. and +31 in. of oil and the test was repeated until thirty readings at eac stage had been obtained. The mean differences and standar deviations at each stage were obtained and the root mea square error for all ninety readings was calculated.

The results of the tests showed that at −27 in. of oil th cell gave a reading 0·036 in. too low, while at +31 in. c oil the reading was 0·072 in. too high. These difference are due to distortion of the cell back plate and are found t remain constant within the limits described in the nex paragraph. They may be taken into account by calibratio correction.

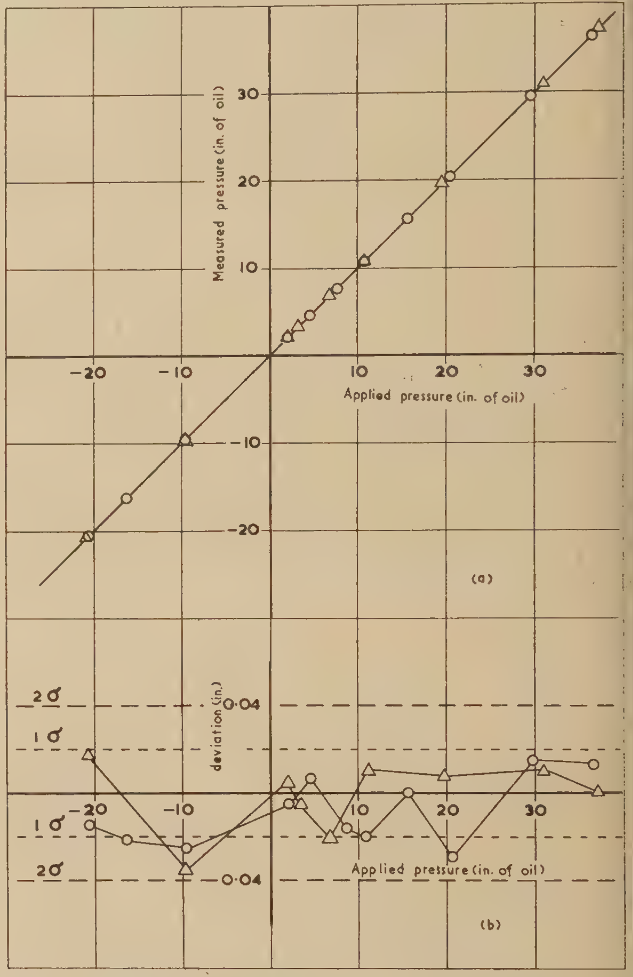

Fig. 4. (*a*) Typical calibration curve
(*b*) Statistical variations in observations of pressures with the Rand soil pressure cell

The standard deviations at −27 in., +3 in. and +31 in. external heads of oil were 0·021, 0·024 and 0·014 in. respectively. The root mean square error of all the readings was 0·020 in. This gives an accuracy of 0·040 in. with 95% confidence. The accuracy of the cell was then tested over the range −20 to +36 in., readings being taken at various applied pressures throughout this range. The measured pressures were adjusted using the back plate distortion figures quoted above as a basis for calibration. The deviations of the measured pressures from the applied pressures are plotted on Fig. 4(*b*). All the readings lie within twice the standard deviation given above.

(*b*) *Water, oil and air-tightness.* After a short period necessary for the insulating fibre washers to become soaked ith transformer oil, no perceptible leakage was observed. s a final test the cell was left for a few days with an internal ressure lower than atmospheric and no air was found to nter the cell.

(c) *Stable zero setting.* The L.V.D.T. type indicator is ell noted for its stable characteristics, and its stability is onsiderably improved when it is used as a null point indiator for a condition of zero out-of-balance current. The ell was tested by making the zero adjustment to the coils, reviously described, and observing the galvanometer eflexion at regular intervals over a period of about two weeks. he tests were conducted in a laboratory which was not emperature controlled. The variations were very small and ere due almost entirely to the effects of ambient temperature hanges on the diodes.

Operation of the cell

The cell is very sensitive and small deflexions of the diahragm are immediately indicated on the galvanometer. his feature is very useful for securing quick readings of ressures since there is no need to wait for off-balance quilibrium conditions to be established before readjustment s made. In operation a "no-volume change" valve, *A*, ig. 3, is normally closed when readings are not being taken. When a reading is taken the valve is opened a small amount. ny flow of oil is immediately accompanied by a deflexion f the diaphragm and an indication on the galvanometer which can be counterbalanced with the piston-type manometer adjustment. When approximate balance has been chieved the valve is opened fully and final adjustment made o bring the galvanometer back to zero. Calculations based n volume changes have shown that with this method of djustment it is possible to keep the membrane within $\times 10^{-4}$ in. of the neutral position.

With modifications, the same cell is being used to measure the tangential pressures on the wall face. In this case a floating disk, flush with the wall face, is attached to a spring-loaded lever as shown in Fig. 5. A L.V.D.T. is used to maintain a neutral position of the disk and the oil pressure in the cell is used to measure the drag or shear force on the face of the disk. When used for pore water pressure measurements, a porous disk is placed in contact with the soil water. Flow of water through the disk is observed as a deflexion of the diaphragm and the internal pressure is again adjusted to maintain zero flow. In both additional applications the feature allowing rapid adjustment of pressures without having to wait for equilibrium conditions to become established is of very great importance.

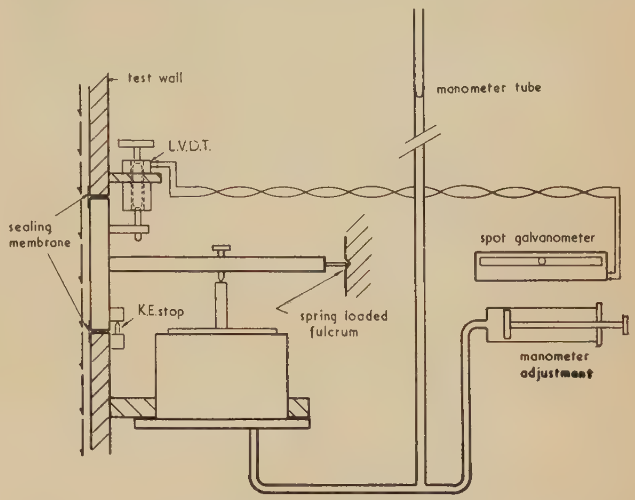

Fig. 5. Layout of apparatus for measuring the tangential pressure against a rigid wall

---

R.F. admittance bridge for liquid-dielectric measurements

by R. G. BENNETT, B.Sc., A.M.I.E.E., Department of Electrical Engineering, Royal Technical College, Salford

[*Paper first received* 21 *January, and in final form* 12 *February*, 1960]

Abstract

An admittance bridge is described suitable for the measurement of the complex permittivity of liquid dielectrics at frequencies between 100 *kc/s and* 3 *Mc/s. The unknown capacitance is compared directly with a standard capacitor, while the conductance arm may be simply calibrated on a direct current supply. Component values are given suitable for use with a cell having an empty capacitance of* 5 *pF. No Wagner earth is necessary when using a* 3*-terminal cell, since the balance condition is independent of admittances between the electrodes and the guard electrode.*

Introduction

THE admittance bridge described in this paper has been designed to determine the real and imaginary components of the complex permittivity of a liquid dielectric at frequencies between 100 kc/s and 3 Mc/s by measurement of the capacitance and conductance of a capacitor using the liquid as dielectric. If C_x and G_x are the measured values of capacitance and conductance respectively, and C_0 is the capacitance of the empty cell, the real part ϵ' of the complex permittivity is equal to C_x/C_0 and the imaginary part ϵ'' is equal to $G_x/\omega C_0$.

To avoid errors arising from the lead capacitance and the variation of liquid volume with temperature, it is advantageous to employ a three-terminal capacitor. This type of cell has a large capacitance between each electrode and the guard electrode and it is therefore necessary to employ a Wagner earth when making measurements with a conventional four-arm bridge. The bridge described here measures the direct admittance between the electrodes, and the balance is unaffected by admittances to the guard electrode. It is constructed of components which are readily available and has the advantage that it is possible to calibrate the conductance arm with a direct-current supply.

Component values have been chosen for use with a capacitor with an empty capacitance (C_0) of 5 pF.

The circuit is as shown. The *T*-network composed of the two capacitors *C* and the resistor *R* has an effect equivalent to connecting a capacitor and negative conductance between *A* and *B*. At balance, the equivalent capacitance of the *T*-network plus the standard capacitor C_s, the variable capacitor C_1 and the capacitance of the cell has a susceptance equal in magnitude but of opposite sign to that of the inductor *L*. Also, the equivalent negative conductance of the *T*-network is equal to the sum of the conductance of the cell, the equivalent loss conductance of the inductor and the equivalent conductance between *A* and *B* produced by R_1 and R_2. Under these conditions, the admittance between *A* and *B* is zero, and the source and detector are effectively isolated. The condition of balance is independent of admittances between *D* and either *A* or *B*, so that the effect of admittances between the electrodes and the guard electrode is eliminated if the latter is connected to *D*. With the cell connected to the bridge, an initial balance is made with C_s at the minimum value by means of R_1 and C_1 with *L*, *R* and R_2 switched to appropriate values. The cell is now disconnected and balance restored by addition of capacitance and conductance across *AB* to replace the admittance of the cell by readjustment of C_s and R_1 only. The cell capacitance is given by the change in C_s and the conductance by the change in setting of R_1, which may be calibrated in equivalent conductance across *AB*.

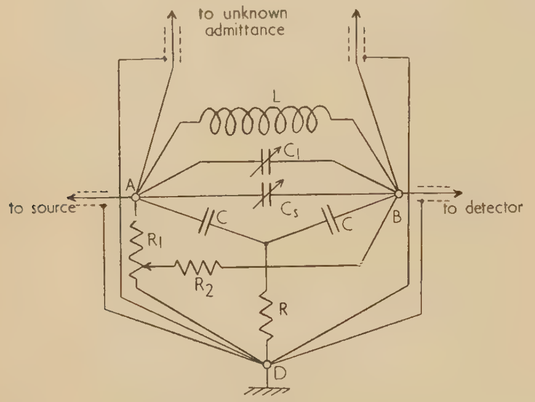

Component values of bridge circuit

C = 700 pF.
C_s = standard capacitor.
C_1 = 1000 pF. Two-gang, air-spaced variable, 500 pF per section.
L = 3, 9·1, 27·2, 81·5, 245, 733 μH, 2·2 mH, selected by rotary switch with provision for plug-in coil.
R_1 = 100 Ω wire-wound, Reliance, type TW/1, linear, non-inductively wound.
R_2 = 250, 750, 2000, 7500 Ω, high-stability carbon, selected by rotary switch. Common connexion of resistors to *B* and switch rotor to slider on R_1. Unused resistors connected to *D* by short-circuiting contact on switch. The resistors should have as low a reactance as possible. Those used in the model were manufactured by LAB (by Radio Resistor Co. Ltd.) and proved satisfactory.
R = 50, 100, 250, 500, 1000, 2000, 4000, 7500, 10 000, 20 000, 50 000, 100 000 Ω high-stability carbon, selected by rotary switch.

T-network

This is equivalent to a π-network with the admittance of the branch between *A* and *B* equal to

$$\omega^2C^2R(j2\omega CR - 1)/(1 + 4\omega^2C^2R^2)$$

At any frequency, the maximum negative conductance has value of $\omega C/4$ and is obtained when *R* is equal to $1/2\omega$ *C* must be chosen so that this may exceed the maximu positive conductance it is intended to connect across *A* The maximum value of ϵ'' it was proposed to measure was 1 giving a maximum value of G_x equal to $\omega C_0\epsilon''$ 60 × $10^{-12}\omega$ mho. The equivalent loss conductance of is $\omega C_{tot}/Q$ where C_{tot} is the total effective capacitance acro *AB*. If C_{tot} is assumed to have a maximum value of 2000 p and *Q* a minimum value of 25, the loss conductance und these conditions will be 80 × $10^{-12}\omega$ mho. If the negati conductance is to equal the sum of these, *C* will be 560 p The value of 700 pF chosen allows for *R* not being of exact the optimum value and the additional conductance added b the R_1, R_2 combination. For maximum negative condu tance, *R* should be 76 Ω at 3 Mc/s and 2280 Ω at 100 kc/ Switched values of *R* are available to give suitable value for frequencies between these limits, and also higher valu for use when lower conductances are being measured.

Conductance-measuring network

The equivalent conductance across *AB* of the R_1 and combination is K/R_2 where *K* is the fraction of the potenti difference across R_1 appearing between the slider and *D* whe *B* is at the same potential as *D*. The system used has th advantage over the connexion of a variable resistor betwee *A* and *B* that the inductance of R_1 has a negligible effec providing it is uniform per unit length of resistor windin and the loading by R_2 is not excessive. R_1 is fitted with scale which is calibrated by the following procedure. Th inductor selecting switch is turned to a blank contact so tha there is no d.c. connexion between *A* and *B* other than R_1 and R_2. *B* is connected to *D*, a 2 V cell is connecte between *A* and *D*, and an accurate high resistance voltmete between the slider on R_1 and *D*. For various angul positions of R_1, the voltmeter reading is expressed as fraction of the total voltage across R_1, from which th equivalent conductance across *AB* for each position may b calculated. The procedure is repeated for all values of *R*

Standard capacitor

The capacitor used was a General Radio, type 722D, whic has two ranges of 25–115 and 100–1150 pF, respectively, bu any stable calibrated capacitor would be suitable. Measure ments were generally made on the lower range and, in th case, the capacitor was set to 30 pF when the initial balanc was made. An error is introduced by the inductance of th capacitor and its leads, the fractional error being ω^2L_c where L_c is the value of inductance. With the syste of substitution measurement used in this bridge, the frac tional error in the measured value of cell capacitance $\omega^2L_c(2C_A + C_x)$, where C_A is the initial setting of th standard capacitor (30 pF in this case). Measurement indicate that, in this particular case, L_c is about 0·24 μH giving an error of 1% when a 50 pF capacitor is measure at 3 Mc/s. It could be reduced by employing a standar capacitor more suitable for high-frequency use.

Inductor

The variation of capacity of C_1 was assumed to give ratio of maximum-to-minimum total capacity across *AB* 3 to 1, and the inductors were chosen in this ratio to giv a continuous coverage. They were made from Wearite coils, type PA, by choosing a value higher than that required and removing a suitable number of turns. The coupling coils were removed. A socket is provided for external plug-in coils to provide for possible operation outside the normal frequency range of the instrument.

Constructional details

All the components except the standard capacitor are mounted on a heavy brass panel. It is important that connexions should be made directly to the three points A, B and D. This particularly applies to connexions to the source, detector and cell where coaxial connectors are employed. Sockets on the panel are provided for these and must be mounted on insulating bushes to remove multiple earth paths. The layout is such that the connexions to the standard capacitor are as short as possible.

Conclusion

In operation, this bridge has been found to give adequate capacitance discrimination using a signal generator as source and a converted Government-surplus receiver as detector. The conductance discrimination is limited by the fineness of adjustment of R_1, which is about 0·25 deg. At 100 kc/s, this represents an error in ϵ'' of 0·04, when R_2 is set at 7500 Ω, while errors will be correspondingly less at higher frequencies. The bridge is mainly intended for use in the region of the critical relaxation frequency, where values of ϵ'' will be high, and for this purpose the performance is adequate.

Equipment for the encapsulation of semiconductor devices

by R. D. KNIGHT, A.M.I.Mech.E., A.M.I.Prod.E., Services Electronics Research Laboratory, Baldock, Herts

[*Paper first received* 29 *September*, 1959, *and in final form* 12 *February*, 1960]

Abstract

A hydraulically operated ram carries the semiconductor device and its envelope, loosely assembled, into a Pyrex chamber. Here the two are separated while the envelope is outgassed by e.c.h. in vacuum. They are then brought together, in vacuum or in gas, and the residual heat in the envelope melts a ring of tin in the mount collar to make the final seal. During the process the device is warmed sufficiently to drive off any moisture. A novel three-port valve controls the gas and vacuum supplies to the chamber. The equipment has been designed with a view to ultimate automation.

Introduction

It is generally accepted that most semiconductor devices require gas-tight protection, particularly against the attack of moisture. This protection is being satisfactorily provided by various methods of encapsulation. The method and equipment described here were designed to combine clinical cleanliness with a high degree of control in a production process which would lend itself to ultimate automation.

Outline of method

Fig. 1 shows the envelope and mount before assembly. These are loosely assembled for introduction into the encapsulation chamber, where they are again separated so that the envelope can be outgassed in vacuum by e.c.h. without overheating the device. The seal is made by lowering the mount into the envelope whilst the residual heat in the latter is sufficient to melt the tin or alloy in the mount collar. The equipment provides for the seal to be made with the chamber either evacuated or gas-filled. It will be appreciated that in outgassing the envelope the mount itself is warmed sufficiently by radiation to drive off any moisture and to discourage condensation of impurities on the device.

Equipment and operation

The chamber shown in Fig. 2 is formed by retaining a Pyrex sleeve between the upper- and lower-bearing bodies; rubber or indium rings seal the ends. In order that the two bearings will operate satisfactorily under vacuum, they are tin-lined and the tin is impregnated with molybdenum

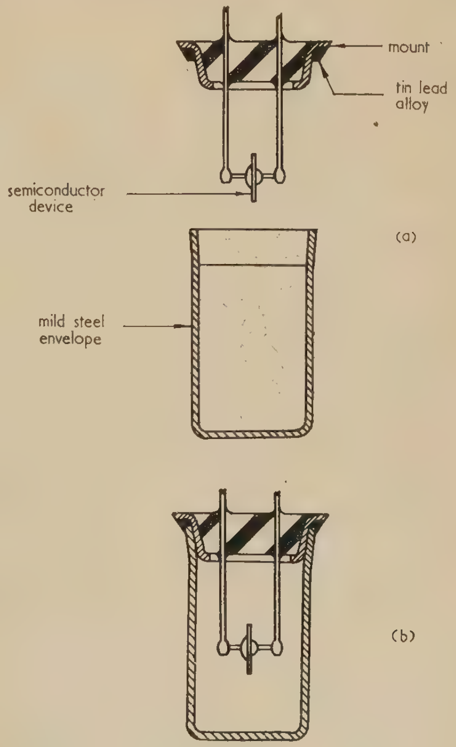

Fig. 1. Mount and envelope (*a*) before, (*b*) after encapsulation

disulphide. As the lower ram, which is hydraulically operated, enters the lower bearing, it trips both a micro-switch to interrupt its own upward movement and a valve to evacuate roughly the chamber *via* an annulus in the bearing. After about seven seconds, when the chamber is evacuated, the lower ram continues upwards, coming to rest with the envelope situated in the field of an e.c.h. coil, whilst the mount is held in the upper ram. The upper ram, operated by a lever from the lower hydraulic system, then moves upwards to carry the device clear of the envelope, while the lower ram rises a further 0·020 in. This last movement is designed to allow the upper ram to exert sealing pressure on the mount and envelope when the downward stroke is made for, if the pressure were exerted on the upward stroke, it would cause the mount to stick to the envelope prematurely. The chamber is then connected to a mercury pump for hard evacuation. The annuli in the bearings are continuously evacuated by separate pumps to reduce air leakage down the bearings and so make it unnecessary to use bellows or Wilson seals. The envelope is outgassed by e.c.h. and, if encapsulation in vacuum is required, the upper ram is now lowered so that the tin in the mount collar is melted by the residual heat in the envelope to make the seal. When, however, gas encapsulation is required, the evacuated chamber is filled with the desired gas (dry nitrogen in this instance). The envelope is again heated slightly, and the mount lowered to make the seal. The lower ram descends, after a short pause for cooling, taking with it the encapsulated device. During the descent it automatically closes the annulus cut-off valve to prevent the pressure in the roughing pump becoming atmospheric. The complete cycle, loading to unloading, occupies about 2½ minutes.

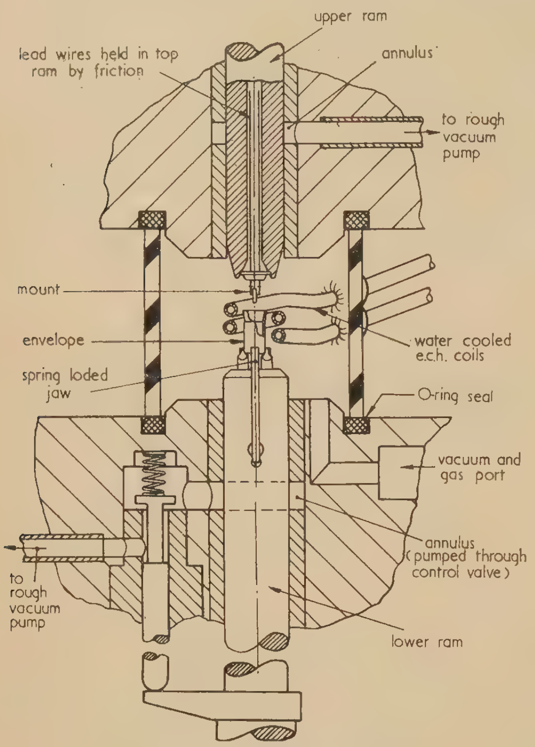

Fig. 2. Encapsulation chamber

The method of loading and gripping has been designed to allow scope for variations of the mount and envelope design. Thus, almost any lead wire arrangement, including a double-ended system, can be accommodated as well as envelopes o non-circular section.

The method of controlling the vacuum and gas is novel as no standard equipment could be found to do this in th desired manner. A special valve was designed to meet th requirements. This valve is illustrated diagrammatically in Fig. 3. The operating lever on the control panel has it three positions marked "Vacuum", "Isolated" and "Gas" respectively. In the "Vacuum" position, the chamber por is connected to the mercury pump and the gas line is sealed. In the second or "Isolated" position, the vacuum line, gas line and chamber port are all isolated. In the third or "Gas" position, the chamber port is connected to the gas line, an the vacuum line is sealed. Corrugated beryllium–copper diaphragms separate the compartments of the valve whilst providing a flexible seal between plunger and valve body. In addition, the upper diaphragm centralizes the upper plunger. There is no friction in the gas or vacuum regions and therefore no lubrication is required. In the present application, the diaphragm and apertures are sealed wit rubber and are giving very satisfactory service, but where a better vacuum is required, aluminium and indium would be used as sealing materials and the diaphragms could be soldered to the valve body. In this instance, the centre and outside seals above the upper diaphragm were made with a single sheet of rubber; this forms an additional safety diaphragm so that, in the event of the beryllium–copper diaphragm fracturing, there would not be a sudden rush of gas into the mercury pump.

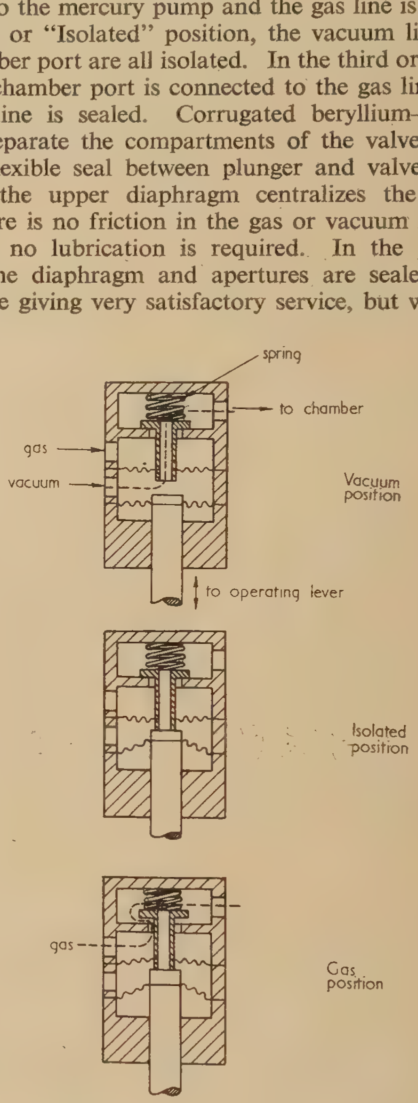

Fig. 3. Operation of main valve

It will be seen that the lower diaphragm has about twice the stroke of the upper one and might, therefore, be expected to have a shorter life. To counter this, provision has been made to evacuate roughly the area below the lower diaphragm, so reducing diaphragm ripple. So far, it has not been found necessary to utilize this.

In order that correct working of the valve will not depend pon accurate setting of the manual control lever, provision made for override of the lever in both directions. The aximum gas pressure that can be used is mainly governed y a coil spring housed in the top of the valve body. he present arrangement allows for a pressure of three mospheres.

Difficulties encountered

Although vacuum encapsulation presented no difficulty, rst attempts at gas encapsulation using straight-sided nvelopes resulted in about 20% leaky seals because the tin as sucked into the envelope at the instant of making the eal. This condition was partly remedied by the replacement f pure tin in the collar by the tin–lead autectic. The lower nelting point reduced the difference between the internal and xternal pressures at the instant of sealing while the short lastic range gave the advantage of quicker freezing.

The seal was finally made reliable by the introduction of the ared envelope shown in Fig. 1. The flared mouth fits the ollar taper to provide a reasonable mechanical closure estricting the inflow of molten metal. The brim of the collar was originally curled to accommodate a large amount of tin. It was discovered, however, that in tin-dipping the collar, air pockets would occasionally form, leaving portions of the brim untinned. This was remedied by the introduction of the flat brim shown in Fig. 1. A minor difficulty was caused by the fillet of tin in the collar brim making initial location in the envelope somewhat uncertain when loading into the bottom ram. This was overcome by the introduction of a trimming operation to square-off the fillet and so provide a flat seat for the envelope.

Acknowledgements

In designing this equipment the author was able to draw on the basic principles laid down by Mr. A. R. Rangabe* for a vacuum encapsulation chamber designed and built under his leadership at S.E.R.L. some years ago. This most valuable assistance is gratefully acknowledged. Acknowledgement is also made to the Admiralty for permission to publish this paper.

---

* Now with Messrs. Leigh Electronic Development Ltd.

Tilting and rotating specimen stage for electron microscopy and electron diffraction

y R. E. BURGE, B.Sc., Ph.D., and H. R. MUNDEN, Wheatstone Physics Laboratory, King's College, University of London

Paper first received 13 *January, and in final form* 12 *February*, 1960]

Abstract

The importance of tilting and rotating the specimen in electron microscopy and electron diffraction is discussed. The design and construction of a specimen stage, allowing a maximum tilt of 35 *deg. of the plane of the specimen from a plane perpendicular to the electron beam, and providing a* 360 *deg. rotation at all angles of tilt are described. Though the stage has been designed specifically for the Metropolitan-Vickers type E.M.*3 *electron microscope,*⁽¹⁾ *the principles involved may have application to other microscopes.*

Introduction

In electron stereo-microscopy and sometimes in the electron microscopy of fibres and thin tissue sections, it is desirable to adjust the orientation of a region of the specimen before photography. In electron diffraction by the selected-area transmission technique, it is of great importance to adjust the position of a selected crystal so that the diffraction from a given set of crystallographic planes may be recorded. Specimen manipulation in diffraction is both more important and more stringent than in microscopy since, ideally, it is required to record the diffraction from all the possible diffracting planes in a given crystal.

The changes in orientation necessary to record all the diffracted beams corresponding to the reciprocal lattice points of a single crystal within the sphere of reflexion can in principle be achieved by means of a tilting and rotating specimen stage. The reciprocal lattice points may be conveniently sampled by a stage which allows the plane of the specimen supporting film to be tilted up to an angle of 45 deg. with a plane perpendicular to the incident electron beam, an independent 360 deg. rotation of the specimen about an axis normal to the plane of the specimen and operative at any angle of tilt, together with the lateral traverse of the specimen stage normally used in electron microscopy. In the specimen stage described below, a maximum angle of tilt of 35 deg., a complete rotation at any angle of tilt, and the usual lateral traverse have been attained.

The specimen stage was developed for the Metropolitan-Vickers type E.M.3 electron microscope,⁽¹⁾ but similar design considerations may be valid for other types of commercially available electron microscope. The specimen stage described by Riecke and Stöcklein⁽²⁾ for specimen manipulation in reflexion diffraction has been designed for use on an electron optical bench.

In the design of the stage the following points were considered:

(1) That the stage should be interchangeable with the standard fitment.
(2) The desirability of maintaining the operating focal length of the objective lens as close as possible to its

normal value, and to minimize the changes in focal length necessary for image formation when the specimen is tilted. The first condition is necessary to retain as far as possible the normal operating characteristics of the objective lens, and the second to reduce changes in image magnification, and electron diffraction calibration during specimen tilt.

(3) The need for a different specimen holder since the normal holder is of a design which severely limits the maximum possible angle of tilt.

(4) To maintain the tilting and rotatory motions, and the lateral traverse of the specimen stage as a whole, independent of one another.

(5) The necessity for an objective-lens limiting-aperture system for use with the stage, to increase contrast in electron microscopy.

Description

The complete specimen stage is shown mounted on the objective lens in Fig. 1(*a*) and the components are shown in detail in Figs 1(*b*) and 1(*c*).

The control rods. The rectangular metal box shown in Fig. 1(*a*) replaces the usual specimen-chamber door and effectively increases the space available for the stage. The rods controlling the tilting and rotatory motions pass through O-ring seals in the front face of the box, and in this face a central lead-glass window is provided to allow observation of the specimen. The box is held in place on a rubber vacuum seal by two stirrups. To change the specimen, the box is removed by drawing it off the control rods; for this purpose the quick-release adjusting knobs, shown resting on the box in Fig. 1(*a*), were provided.

The control rods are mounted on the vertical carrier plate (*A*) shown *in situ* in Fig. 1(*a*) and in more detail in Fig. 1(*c*). Access to the specimen stage is possible through the rectangular $2\frac{1}{2} \times 1\frac{1}{4}$ in. aperture in this plate. The carrier plate (*A*) is held in position on a vacuum seal by Allen-screws penetrating the sides of the plate. At the back of this plate is mounted the rack-and-pinion mechanism providing the specimen tilt.

The specimen holder. The specimen holder (*D*) is shown in position in Fig. 1(*b*) and has the form of a truncated cone $\frac{3}{10}$ in. deep, with a base of diameter $\frac{6}{10}$ in., and a semi-angle of 40 deg. The specimen grid is held in position by a split-ring in a plane distant 0·02 in. from the plane defining the top of the truncated cone. The specimen holder is suspended just above the face of the objective lens to allow sufficient clearance for the full 35 deg. tilt to be possible without fouling the lens. The line about which the specimen is tilted is in the same plane as the untilted specimen. In this way, the objective lens operates at the minimum focal length (6·5 mm instead of the usual 4 mm) commensurate with a 35 deg. tilt, and the changes in specimen height during tilting are minimized.

The specimen holder is inserted in the microscope by the tool (*B*) shown in Fig. 1(*c*); the specimen cone is firmly held in a pair of suitably shaped spring-loaded jaws and is released by depressing the plunger.

Tilting mechanism. The specimen holder is tilted by means of a vertical rack and pinion (*E*) shown in Fig. 1(*c*). A horizontal projection from the rack (*F*) bears on the ball-ended lever (*G*) [Fig. 1(*b*)] which is attached to the C-shaped specimen-holder carriage. The carriage is spring-loaded to the base of the specimen stage where it is pivoted on a knife-edge working in a V-slot on one side and a pin in a cone-shaped depression on the other. The specimen holder received by and located in the C-shaped carrier by thr equally spaced $\frac{2}{10}$ in. diameter pulleys around its circumf ence. One of the pulleys is mounted on a spring-loaded a and the rim of the specimen holder is tightly gripped betwe

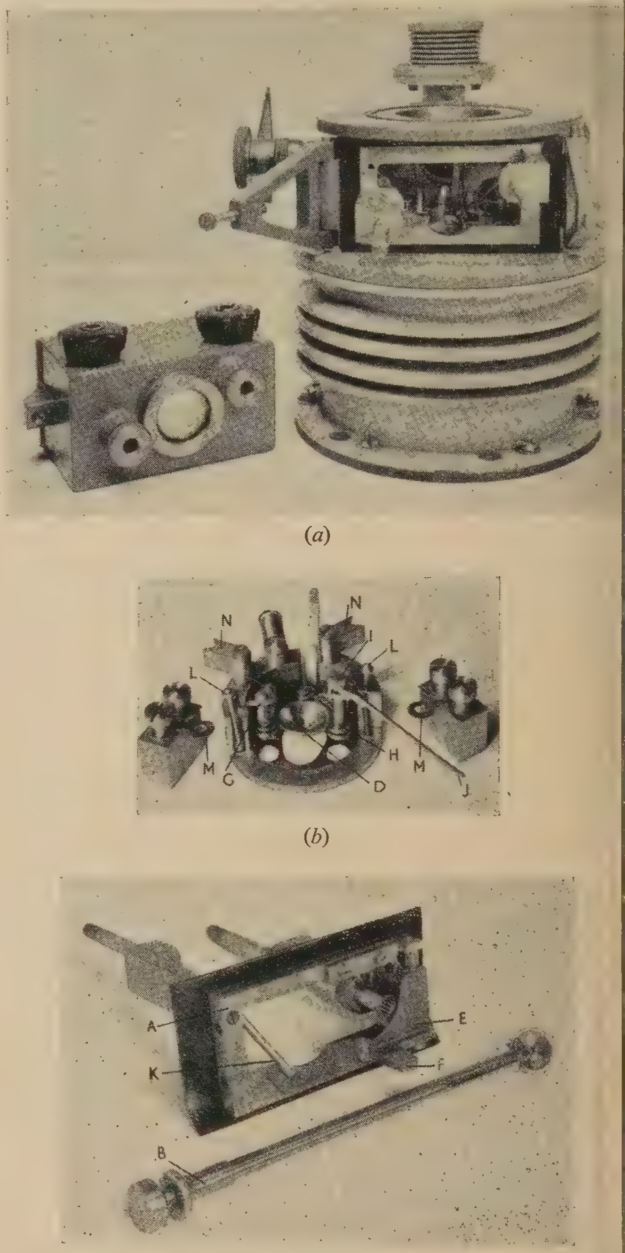

(*a*)

(*b*)

(*c*)

Fig. 1. (*a*) Specimen stage in position on the objective lens; the specimen-chamber door is also shown

(*b*) Mechanism for communicating the tilting, rotating and traversing motions to the specimen holder

(*c*) Control rods and specimen holder insertion tool

the pulleys. A horizontal fiduciary position for the specim is maintained by means of a stop fitted to the control rod.

Rotating mechanism. The specimen is rotated by rotati the axle of one of the pulleys (*H*) which communicates friction-drive to the specimen holder. The lower end of th axle supplies the pin which helps to locate the C-shap rrier during tilting. Since the mechanism controlling the tation also tilts with the specimen a 360 deg. rotation is ossible at all angles of tilt. For the pulley-drive to be fective at all angles of tilt, the drive is made by a universal upling (*I*) connected to a keyed piston (*J*) which moves side a tube (*K*) connected by another universal coupling the main control rod passing through the vacuum seal.

Specimen-stage traverse. The entire specimen stage is held place on the surface of the objective lens by two dumbells (*L*) working under the phosphor-bronze tongues (*M*) tached to the small separate blocks shown to the left and ght of Fig. 1(*b*). The traverse motion is communicated by e usual plungers bearing in the V-blocks (*N*) at the rear the specimen block as in the commercial instrument.

Objective-aperture system. The design of the objective lens n the E.M.3 electron microscope allows the insertion of an bjective-lens limiting aperture from either the top or the ottom of the lens. The design of the new specimen-stage recludes the insertion of the aperture from the top. A tisfactory system was found in which the objective aperture as located at the top of a tube extending upwards from the ectrostatic astigmatism corrector (stigmator), which is laced immediately below the objective lens. This stigmator of a similar design to that published by Haine and ulvey.(3) The position of the aperture is varied by means f the lateral-adjustment controls for the stigmator. It was ound that this position for the aperture neither affected the ase of setting the stigmator nor the degree of astigmation orrection attainable.

Performance of the specimen stage. The tilt, rotation and raverse of the specimen stage were found to be independent f one another, and the general stability of the stage sufficient to achieve a similar revolving power (about 20 Å as judged by the Fresnel fringe test(3)) to that found with the normal stage. The need to remove the front of the specimen stage to change the specimen was not found to be tedious, while the vacuum attained is as good as with the normal stage.

The tilt of the stage was calibrated by an optical-lever method, and for this purpose the specimen was replaced by a platinum objective aperture disk (which acted as a mirror) of the same diameter as a specimen grid. The tilt is expressed in terms of a 0–360 deg. scale (not shown) attached to the control rod. For movements in the same direction, the reproducability of the tilt was found to be ±1 deg. The rotation is also measured on a 0–360 deg. scale. The reproducibility of the rotation may be judged in terms of the traverse necessary to regain a given region of the specimen after a 360 deg. rotation. This was found to be about 20 μ. The new stage has been in regular and satisfactory use for a period of 18 months.

Acknowledgements

The authors wish to thank Prof. J. T. Randall for facilities and Mr. L. Pitches who made the specimen stage.

References

(1) Haine, M. E., Page, R. S., and Garfitt, R. G. *J. Appl. Phys.*, **21,** p. 173 (1950).
(2) Riecke, W. D., and Stöcklein, F. *Z. Phys.*, **156,** p. 163 (1959).
(3) Haine, M. E., and Mulvey, T. *J. Sci. Instrum.*, **31,** p. 326 (1954).

Use of a liquid scintillator counter for beta particles

y T. B. RYVES, B.Sc., Atomic Energy Research Establishment, Harwell, Berks

Paper first received 4 *December*, 1959, *and in final form* 10 *February*, 1959]

Abstract

simple counting technique is described for absolute ounting of beta particles using a 4 π *liquid scintillator ounter technique. The radioactive sample is deposited n a thin backing film of transparent material, which is hen immersed in the liquid scintillator. It was found that or samples with a maximum beta particle energy greater han 0·7 MeV the detection efficiency was close to 100% omparing favourably with other methods of absolute ounting.*

Introduction

DURING the course of work on activation measurements in the fast reactor ZEUS the need arose for accurate measurements of low energy emitters of β-rays. The method adopted for most materials, i.e. the use of end-indow Geiger-counters, was unsatisfactory for low energy -particles from such materials as ^{60}Co, for which the window bsorption is very high, and an accurate measurement of the ounter efficiency is difficult. An attempt was therefore made to develop a scintillation method of counting of high efficiency in which the sample to be measured was contained within the body of the scintillator.

The first method tried was that of counting an active solid suspension in a scintillating gel (toluene, PPO, POPOP and Thixin).(1) This method was found unsatisfactory because of difficulty in forming a uniform fine suspension of known total mass in the thixotropic gel, and moreover the absolute efficiency was not 100%, e.g. ^{56}Mn as MnO_2 suspension had an efficiency of only 90%.

These difficulties were overcome by coating the active material on a fine Zapon film and inserting this into the centre of a liquid scintillator.

Experimental technique

A Mullard photomultiplier (type 6260) with 2 in. end window was mounted vertically. On top of the window was placed a cylindrical tank containing a liquid scintillator, optical contact being made with silicone grease. The tank was a quartz tube (thickness 0·1 in., height 1 in., diameter

1 in.) with a thin quartz end-plate cemented on with Araldite. Around the tank was a removable reflector made of plaster of Paris, and the tank lid was a plane disk of aluminium, painted with MgO (Fig. 1).

The liquid scintillator used was rectified toluene containing 5 g/l. PPO and 0·1 g/l. POPOP which was made up in bulk, each tank filling being about 20 ml. solution. It was found that liquid evaporation was small with the lid on the tank, activities being followed for 24 h without much loss of scintillator.

The active sample was deposited on a thin backing film which was immersed in the tank. The film was supported by a simple frame made of fine wire. This frame consisted of a wire loop supported by three short legs, with a carrying handle above as indicated in Fig. 1. The thin film was made from a drop of Zapon (by Imperial Chemical Industries Ltd., Paints Division) which spread over a large surface of clean water, the wire frame being used to scoop up the film to cover the wire loop. Films used were about 0·2 mg cm^{-2} and showed interference fringes when illuminated by an extended light source. The active sample was dissolved in a known mass of aqueous solution and a few millilitres of solution introduced into a U-tube with one arm drawn out into a fine jet. This was weighed and then several drops were forced out onto the centre of the thin film, the U-tube being reweighed to determine the mass of active material counted. The drops of solution on the film were evaporated to dryness using a weak lamp and a slow stream of warm air, leaving an adherent sample ready for counting in the centre of the thin film.

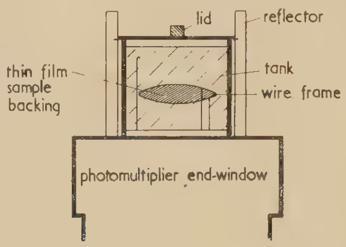

Fig. 1. Photomultiplier assembly

The counting technique involved a preliminary set of background counts followed by counts with the sample in the tank. It was found that the counting liquid became weakly contaminated so that a final background count was impossible, and the liquid had to be renewed for further sample determinations.

The method of counting adopted was to plot a discriminator bias curve for various settings of amplifier gain and time constants, extrapolating the bias curves back to give the count-rate at zero bias (bias voltages were measured with a meter) (Fig. 2). In general, for each sample about nine bias curves were measured (time constants 0·16 μs, 0·32 μ 0·8 μs with gain about −14 to −6 dB) at any one tim the measurements being repeated after 24 h in some cas before discarding the sample. The initial background w measured similarly. At the high gain used (e.h.t. abo 1750 V) the noise was fairly large and sample activity about 10^3 counts/s was necessary to reduce errors due small variations in background to about 1%.

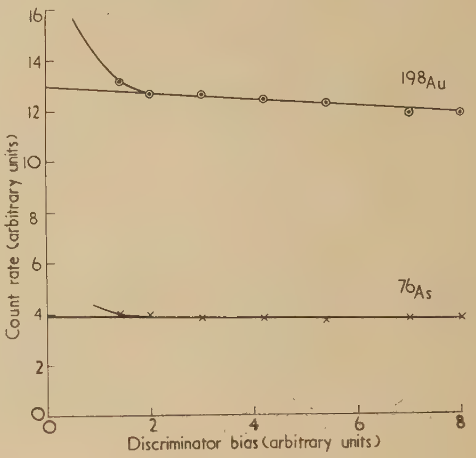

Fig. 2. Discriminator bias curves, extrapolation

For upper curve e.h.t. = 1760 V; time constant = 0·16 μs; gain = −14 dB

For lower curve e.h.t. = 1760 V; time constant = 0·16 μs; gain = −18 dB

Results

Measurements were made with liquid samples calibrat by the Isotope Division of the Atomic Energy Researc Establishment to ±3%. In general the count rates for an one sample were self-consistent to within ±3% or bette The bias curves were easy to extrapolate to zero bias, major portion of the curve being nearly horizontal, with rapid rise at small bias levels due to noise (Fig. 2). β-partic counting efficiencies are given relative to the Isotope Divisio calibration in the table.

^{198}Au (maximum β-ray energy 0·96 MeV, other β- an γ-rays present) was counted as two samples giving efficienci 90% and 110% which suggested experimental error. ^{76}A (several β-rays with energies >1·7 MeV) was also counte twice and disagreed widely with the Isotope Division ca bration. However, in this case it was found that the AsC used was unsuitable for the 4π Geiger counter calibratio

Discussion

The results indicated that for activities with maximu β-energy >0·8 MeV the detection efficiency was about 100

Experimental results

Isotope	*Maximum β-energy (MeV)*	*Other activity*	*β-particle counting efficiency (%)*	*Remarks*
^{24}Na	1·39	Two γ-ray pulses in coincidence	103 ± 1	Two samples counted. Ten bias curv measured over a period of 15 h.
^{204}Tl	0·76	^{204}Hg X-rays from orbital electron capture	98·5 ± 1·5	Two samples counted. Fourteen bi curves measured.
^{32}P	1·71	No γ-rays: ^{33}P present 1·3%	103 ± 4	One sample counted. Five bias curv measured.
^{60}Co	0·31	β- and γ-rays present	80 ± 1	One sample counted. Nine bias curv measured.

within the errors. In the present work the estimated errors were ±3%, while Isotope Division calibrations were ±3%. The results were sensitive to contaminating activities, but any γ-ray pulses in coincidence with β-rays would merely increase the signal pulse height. The efficiency for ^{60}Co (0·31 MeV maximum β-energy) was only 80%. The ^{198}Au results were inconsistent and indicated experimental errors. Thus to obtain a reliable result it is necessary to do a repeat run, taking several bias curve extrapolations for each run. No dead time correction was applied for the relatively low count rates measured.

To improve this method of absolute β-particle counting a number of refinements could be used. Thinner backing ilms would reduce the absorption of low energy β-particles n the spectrum. An external source could be used to monitor the gain of the counting channel. To produce a better bias curve extrapolation to zero bias, two photomultipliers in coincidence could be used, thus eliminating much of the noise, assuming that each β-particle absorbed n the liquid scintillator is certain to be detected by both photomultipliers. The high background in these experiments (300 to 20 counts/s) entailed using relatively active sources (about 1000 counts/s or more). To prevent evaporation of liquid and improve the top reflector the level of liquid in the tank should be raised to the lid with a small overflow capillary tube let into the lid. The tank sides should be painted internally to give more efficient reflexion. Finally, if the toluene were redistilled and dried before use the performance should improve and contamination of the liquid scintillator be eliminated (since this was presumably due to traces of water in the toluene). This would much facilitate the experimental procedure and enable a background measurement after each sample measurement.

Acknowledgements

The author wishes to thank Dr. R. D. Smith (A.E.R.E.) for his helpful advice, Dr. W. La Page (A.W.R.E.) for advice and supplies of scintillators, and Mr. B. Slade (Isotope Division, A.E.R.E.) for calibrated isotopes.

Reference

(1) Furst, B. L. *Nucleonics*, **14**, No. 8, p. 83 (1956).

Epoxy-resin joints for sealed-off, high-vacuum tubes

by J. F. SAYERS, Grad.I.E.E., Grad.Inst.P.,* Northampton College of Advanced Technology, London

[*Paper first received* 9 *June*, 1959, *and in final form* 25 *January*, 1960]

Abstract

The paper describes how joints may be made in the envelope of sealed-off, high-vacuum tubes using a synthetic resin adhesive, permitting unusual forms of construction. A pressure of 10^{-6} *torr may be maintained in such a tube for several years. Success depends on suitable design and processing and on the use of getters. A special television camera tube and a vacuum photocell have been made using this technique.*

Introduction

The use of synthetic resins is well known in the construction of low-vacuum, sealed-off devices such as proportional counter tubes⁽¹⁾ and photoconductive cells,⁽²⁾ but little has been published on their successful use in high-vacuum, sealed-off electron tubes.⁽³⁾ It has been found that, provided suitable precautions are taken, electron tube envelopes may be glued together and working pressures of 10^{-6} torr maintained in them for several years after they have been sealed off from the pumps. These techniques were evolved during the construction of a Sokoloff⁽⁴⁾ ultrasound microscope at the Northampton College, London, and may be of interest to others concerned with electron tube construction.

The microscope contains a special electron tube resembling an Orthicon television camera tube, in which the photoelectric surface is replaced by a crystalline quartz plate. One side of the plate is in contact with the ultra-sound transmitting medium, normally a liquid; the other side is scanned by an electron beam. A quartz plate of suitable cut has widely different coefficients of thermal expansion (7·5 and 13·7 parts in 10^6 for an "X" cut plate) in the length and breadth directions, making a good vacuum seal to the tube envelope difficult. A continuously pumped tube would appear the most satisfactory solution, had it not been decided that a photoemissive surface would probably be required, and for this reason it was decided to develop a sealed-off tube.

Following experiments with a variety of sealing methods, seals using epoxy resins have been found to be the most satisfactory. A sealed-off camera tube which has been in use for two years has the crystal plate sealed to the envelope with Araldite type 1 adhesive [by Ciba (A.R.L.) Ltd.]. The vacuum in the tube shows no sign of deterioration, the oxide-coated cathode of the electron gun maintaining ample emission during this period.

Some of the alternative sealing methods which have been considered are listed below, together with their advantages and disadvantages:

(i) direct fusion of glass to quartz⁽⁵⁾;
(ii) sealing to ductile metal with "solder" glass powder⁽⁶⁾;
(iii) soldering to glass with tin/indium alloy⁽⁷⁾;
(iv) sealing to ductile metal with silver chloride⁽⁸⁾;
(v) sealing to silver foil using silver "spotting paste"⁽⁹⁾;
(vi) soldering to metal after vacuum deposition of metal layer and electroplating⁽¹⁰⁾;

None of the above methods were found satisfactory as at least one of the following limitations was present:

(*a*) the support for the crystal is not sufficiently yielding so that fracture of the crystal or bond occurs due to differential expansion between crystal and the support caused by changes in temperature;

---

* Now at the Atomic Energy Research Establishment, Harwell, Berks.

(*b*) the bonding temperature is higher than 573° C and twinning of the quartz occurs on cooling;

(*c*) the seal limits the temperature of the vacuum bake-out, resulting in a poor final vacuum.

Araldite is least satisfactory as regards (*c*), the maximum vacuum bake temperature being 200° C. For this reason experiments were conducted using silicone resins, which may be baked at 300° C, but satisfactory vacuum-tight joints could not be made owing to the low strength of the bond between quartz and the resin.

Technique

The first tubes constructed using Araldite did not have a very satisfactory performance, the pressure rising to about 10^{-5} torr in a month, because of the following factors:

(i) an appreciable area of resin was exposed to the vacuum causing degassing by desorption and by breakdown of resin from electron bombardment;

(ii) degassing of the tube envelope due to low vacuum bake-out temperature.

The evolution of gas due to factor (i) was reduced by making the surfaces to be joined flat, to within about three wavelengths of light, clamping them together and only applying the resin to the outside. The area of adhesive exposed to the vacuum is then very small. Despite the small gap between the surfaces the resin always penetrated the joint. The surfaces are polished in order to gauge their flatness by interference of light. Polishing these surfaces also prevents the migration of a thin film of resin over the surface exposed to the vacuum, which may occur if they are left rough.

Degassing of the tube envelope may be reduced if parts of the tube remote from the adhesive are at a much higher temperature during the vacuum bake-out, produced by a suitable temperature gradient in the oven. A further reduction in degassing is achieved by only half curing the resin during assembly of the envelope and completing the cure on the pumps.

The use of getters

Efficient getters are essential if a good vacuum is to be maintained in an electron tube sealed with synthetic resin, as the getter has to absorb gas released from the tube walls, vapours from the resin and gases and vapours that diffuse through the resin from outside. Barium flash getters and a heated zirconium contact getter were used in the camera tube, which has given satisfactory service for two years. The pressure in this tube is about 10^{-5} torr. Much superior results can be obtained by using a titanium flash getter in combination with an ionization gauge to form an ion pump. Working pressures of 10^{-7} torr can be obtained.

Construction of glued joints

Fig. 1 shows a seal between quartz/stainless steel/Kodial glass. Other expansion mismatch combinations such as quartz/Kodial glass and Kodial/soda glass may be jointed successfully; provided they are not greater than about three inches in diameter, but joints between Pyrex glass and brass crack on cooling.

The parts to be joined are ground and polished, baked in air at about 300° C to remove final traces of contamination and then assembled, using jigs to hold the parts together. The assembly is warmed with air at about 120° C from an oven, and stick Araldite No. 1 applied to the outside of the joint. The joint is then partly cured in an oven by baking at 200° C for twenty minutes, the rate of heating being not more than 4° C/min between 100 and 200° C, if bubbles in the joint are to be avoided. Temperatures may be measured by using thermocouples clamped to suitable points on the envelope. After completing the assembly, the tube is exhausted and, during the bake-out, the temperature of the resin joint raised to 200° C for half an hour.

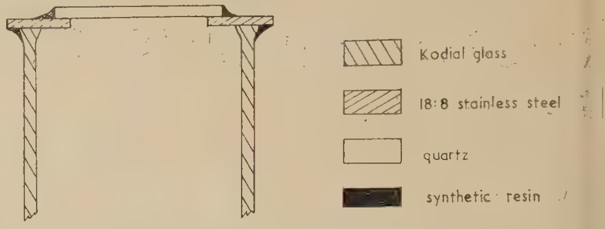

Fig. 1. A quartz/stainless steel/Kodial glass seal for an ultrasound camera tube using synthetic resin adhesive

The titanium ion-pump

The ion pump in use consists of a suitably shielded titanium source and an Alpert type ionization gauge. The titanium layer is deposited on the inside of a Pyrex tube and on the wall of the electron tube, away from surfaces where electrical insulation is required. After a layer of titanium has been deposited, switching on the ion gauge reduces the pressure from 5×10^{-5} to 10^{-6} torr in 30 s, 10^{-7} torr in 2 min and

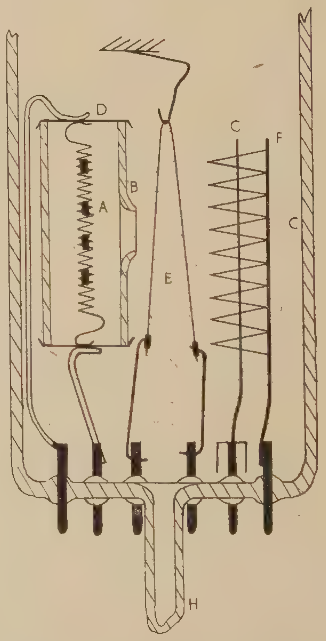

Fig. 2. A titanium ion-pump

A, spiral of 0·35 mm tungsten wire, formed by winding on a 1 mm diameter mandrel, and containing short lengths of 0·5 mm titanium wire; *B*, Pyrex tube 18 mm diameter with hole blown in wall; *C*, titanium film on wall of tube; *D*, nickel end plates, *E*, tungsten filament of ion gauge; *F*, ion gauge grid, a helix of molybdenum wire welded on to a nickel support strip; *G*, ion collector tungsten wire; *H*, tip-off

× 10^{-8} torr in half an hour in a typical tube. The amount f gas that may be absorbed in this way is very much greater ian from a similar area of barium getter. If a very large mount of gas is absorbed, such as that from a poorly out-assed Aquadag wall coating, and the efficiency of the getter ills, it may be restored by flashing off a new layer of titanium rom the tungsten spiral. The author used a hot cathode onization gauge as a source of ionization in preference to a enning gauge, as it did not produce disturbing radio-equency fields.

Photoelectric surfaces

A trial photoelectric cell was constructed having a vacuum window sealed with Araldite. The photocathode was ntimony/caesium and the tube contained an ionization gauge nd a titanium source similar to that shown in Fig. 2. No other getters were employed.

The photosensitivity obtained was lower than that expected rom this type of cathode. This may be due to the presence of the adhesive, but may also be due to the inexperience of the onstructor in preparing this type of cathode. The variation n photosensitivity with time is small, being about ±20% over a period of three months. After a further period of torage of eighteen months the sensitivity had increased to wice the initial value.

Acknowledgements

I wish to thank Dr. C. N. Smyth of University College Hospital Medical School and Mr. F. Y. Poynton of the Northampton College for guidance while carrying out this work; thanks are also due to the Principal and Governors of the Northampton College for the provision of laboratory facilities and to the Committee of the R.W. Paul Instrument Fund of the Royal Society for the grant for ultra-sound research, of which this worked formed a part.

References

(1) Buchanan, J. S. *J. Sci. Instrum.*, **31**, p. 136 (1954).
(2) Roberts, V. *J. Sci. Instrum.*, **31**, p. 251 (1954).
(3) Gale, A. J. *A Symposium on Vacuum Technique*, p. 12 (London: Pergamon Press, Ltd., 1957).
(4) British Patent Appn. No. 477, 139 (1937).
(5) Rawson, H. *J. Sci. Instrum.*, **28**, p. 208 (1951).
(6) Dale, A. E., and Stanworth, J. E. *J. Soc. Glass Technol.*, **33**, p. 167 (1949).
(7) British Patent No. 737,162.
(8) Frank and Stow. *Rev. Sci. Instrum.*, **25**, p. 251 (1954).
(9) Private communication from the Scientific Instrument Research Association.
(10) Partridge, J. H. *Glass-to-metal seals.* Chapter VI (Sheffield: Society of Glass Technology, 1949).

High frequency light modulation

by R. L. WILLIAMS, B.Sc., M.A., Ph.D.,* Canadian Armament Research and Development Establishment,
P.O. Box 1427, Quebec, Canada

[*Paper first received* 17 *December*, 1959, *and in final form* 8 *February*, 1960]

Abstract

High frequency light modulation has been realized using a magnetically driven rotor suspended by a magnetic field in a vacuum chamber. With a rotor 1 *in. in diameter having* 180 *reflecting faces, modulation frequencies in the megacycle region are readily obtainable. Design considerations are given for the rotor described, together with details of the driving and suspension circuit employed. A time constant measurement for an indium antimonide sample is given as an illustration of the system.*

Introduction

The response times of long-wavelength infra-red detectors are frequently in the submicrosecond range. Rotating slotted disks, as light modulators, are not suitable for investigating response times much shorter than 10 μs. Garbunny, Vogel and Hansen(1) have described a rotating mirror system with which they measured the time constant of a p-type gold-doped detector to be 2×10^{-7} s. The apparatus, using a six-sided rotating mirror, had a response time of about 10^{-8} s.

Spark gaps have been described by Porter and Wooding(2) which give light pulses lasting 20 mμs, and by Kerns, Leisten and Cox(3) having a light pulse as short as 5×10^{-10} s. In the testing of materials sensitive to infra-red rays it is not sufficient that the light pulse be fast. It must also contain sufficient radiation in the required wavelength region to give a signal larger than noise. This latter consideration has led to the design and construction of a high-speed rotor which, although it modulates a light beam in the conventional manner, runs so fast that it can be used to measure response times down to approximately 0·02 μs.

System

The time constant of a semiconductive material can be determined from a knowledge of its frequency response to an optical signal. The system employed is shown schematically in Fig. 1, which is not drawn to scale.

A light beam is focused on the surface of a rotor which has alternate reflecting and absorbing facets. To obtain the highest possible modulation frequency, for a given speed of rotation, a good image must be produced on the rotor face. Therefore, a mirror was employed to avoid chromatic aberrations, with a small off-axis angle to prevent excessive image distortion. After the light has been reflected from the rotor surface, however, the harmonic content of the signal has been determined so that glass optics can be used to direct the light further on to the material being studied. For wavelengths greater than 2·7 μ, arsenic trisulphide lenses

---

[*] Now at RCA Victor Research Laboratories, 1001 Lenoir St., Montreal, Canada.

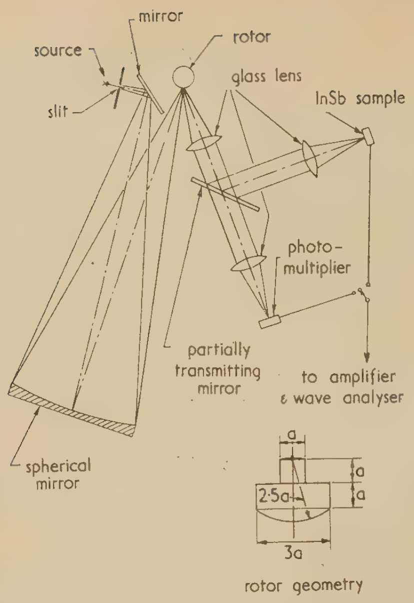
mirror
source
rotor
slit
glass lens
InSb sample
photo-multiplier
partially transmitting mirror
to amplifier & wave analyser
spherical mirror
a
2·5a
a
a
3a
rotor geometry

Fig. 1. Schematic diagram of light-modulating system. Insert shows rotor geometry

could be substituted for the glass. Generally, a portion of the optical signal was focused on to a photomultiplier to provide a monitoring signal for checking the performance of the electrical measuring equipment, and to detect variations of the light intensity.

The rotor is magnetically suspended and magnetically driven, in a way similar to that devised by Beam.(4,5,6) The electrical circuits, however, have been modified to give higher stability. The geometrical rotor configuration is shown as an insert of Fig. 1.

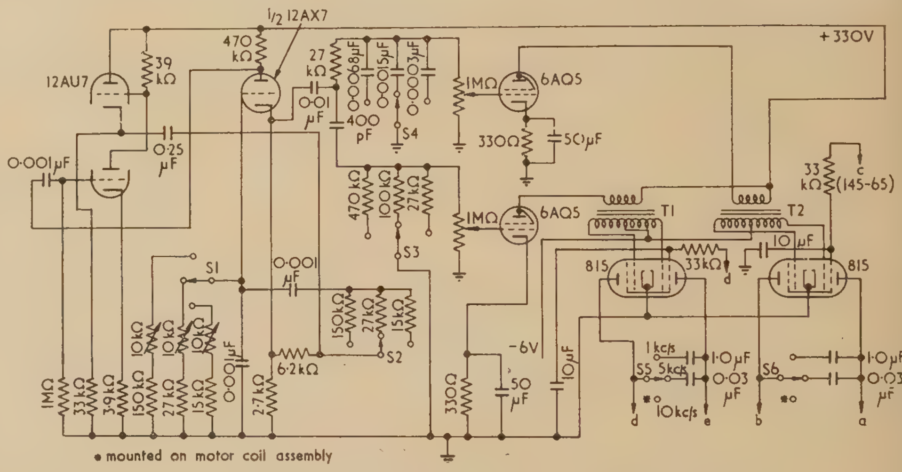
½ 12AX7
12AU7
39 kΩ
470 kΩ
27 kΩ
0·0068 μF
0·0015 μF
0·0003 μF
0·01 μF
400 pF
S4
1MΩ
6AQ5
330Ω
50μF
+330V
0·001μF
0·25 μF
470kΩ
100kΩ
27kΩ
S3
1MΩ
6AQ5
T1
T2
33 kΩ
c (145-65)
10μF
815
33kΩ
d
815
S1
0·001 μF
150kΩ
27kΩ
15kΩ
S2
6·2kΩ
-6V
1MΩ
33kΩ
3·9kΩ
150kΩ
10kΩ
27kΩ
10kΩ
15kΩ
10kΩ
0·001μF
2·7kΩ
330Ω
50 μF
10μF
1 kc/s
S5 5kc/s
10kc/s
1·0μF
0·03 μF
S6
1·0μF
0·03 μF
d
e
b
a

• mounted on motor coil assembly

Fig. 2. Electrical drive circuits used to accelerate the rotor

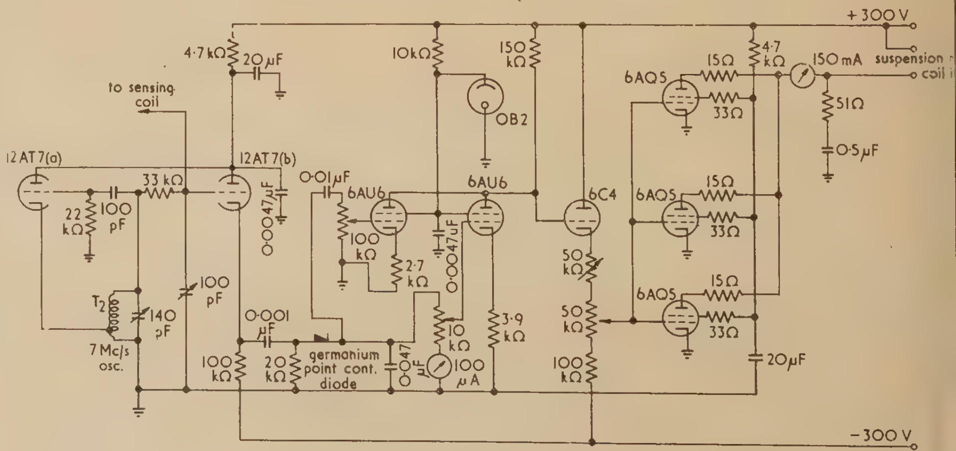
+300 V
4·7 kΩ
20μF
to sensing coil
10kΩ
150 kΩ
OB2
4·7 kΩ
15Ω
150 mA
suspension coil
6AQ5
33Ω
51Ω
0·5μF
12AT7(a)
12AT7(b)
33 kΩ
22 kΩ
100 pF
0·0047μF
0·01μF
6AU6
6AU6
100 kΩ
2·7 kΩ
0·0047μF
6C4
6AQ5
15Ω
33Ω
50 kΩ
100 pF
T2
140 pF
7 Mc/s osc.
0·001 μF
100 kΩ
20 kΩ
germanium point cont. diode
0·047
10 kΩ
100 μA
3·9 kΩ
50 kΩ
100 kΩ
6AQ5
15Ω
33Ω
20μF
-300 V

Fig. 3. Rotor suspension circuit

Electrical circuits

The primary advantage of a light-pulse system over a frequency-response system is the speed with which a reading may be accomplished. Thus one of the prime practical requirements for a frequency-response system is high acceleration. The circuits have been designed to this end. Beams used hollow-cored driving coils, so that the light beam used for checking rotor speed could pass through them. In the present work it was found that the light beam could be passed between the coils so that the coil could be wound on a high permeability core to increase the concentration of the driving field at the rotor. Since a range of frequencies was required, an attempt was made to use class A amplification and drive circuits. This was abandone in favour of the more efficient class C operation. Th problem of obtaining various frequencies was solved b accelerating to the frequency required and then turning o the drive power. As the rotor was suspended in a vacuu system it decelerated slowly, permitting the desired measurements. The magnitude of the deceleration is discussed i Beams's(5) paper.

The electrical drive circuit and suspension circuit used ar given in Figs. 2 and 3. With these circuits a 1 in. rotor, t be described subsequently, could be accelerated to th nominal top frequency in two to three hours. Sierra wav analyser models 121 and 158 were employed to measure th amplitude of the signal fundamental or harmonic in question

Rotor

The maximum operating frequency depends directly o the maximum speed of the rotor and the latter is determine by the strength of the rotor material. The rotors used wer of steel hardened to a Rockwell C scale value of 60.

The shape of the rotor found to be stable in the magneti field is indicated in Fig. 1. A rotor with this configuration made of the material mentioned above, $\frac{1}{2}$ in. in diameter an having six faces, was accelerated to $1{\cdot}0 \times 10^6$ rev/min. Th peripheral velocity of such a rotor is $1{\cdot}3 \times 10^5$ cm/s. Thi is slightly higher than the average self-destroying value o $1{\cdot}0 \times 10^5$ cm/s quoted by Beams,(5) suggesting perhaps a slightly stronger material. No rotor made of hardened steel has burst, but speeds 50% lower than a 10^5 cm/s peripheral velocity were not normally exceeded.

From the analysis which follows, the maximum signal for a particular frequency is always obtained from the rotor with the largest number of faces. For comparison purposes consider the slit width and the rotor speed to be fixed. Using the maximum number of faces the slit width would be equal to the dimension of the reflecting face. The resulting waveform is triangular and the fundamental amplitude is $4\,A/\pi^2$, A being the intensity of the optical signal when the face is completely illuminated. This amplitude signal must be compared to that obtained from the third harmonic derived from a rotor with one-third the number of faces, that is, $\frac{10A}{9\pi 2} \sin \frac{6}{10}\pi$. The ratio of the first amplitude to the latter is $3 \cdot 6/\cos \pi/10$ or about a factor of 4.

Early rotors were made with polished flat faces as the divergence of the light beam of the size used would have been large for a cylindrical surface. With a large number of faces this problem no longer arises, and the design considered best is a 1 in. rotor with 180 reflecting and 180 absorbing faces, the surfaces being cylindrical. The work to be described employed such a rotor. The absorbing or black sections of the rotor are found to be sufficiently absorbing or scattering as machined.

Measurements

A measurement using the fundamental components obtained with a 180-face rotor is shown in Fig. 4. This was performed with a piece of p-type indium antimonide with a free hole concentration of 8×10^{14} per cm^3 at 77° K. It is seen from the curve that some deviation from the form $(1 + w^2\tau^2)^{-1/2}$ is found near the point $w\tau = 1$, but the slope of the curve above this point is very nearly w^{-1}; the intersection of the w^{-1} line with the maximum relative amplitude was taken as the point $w\tau = 1$, and the time constant of 3×10^{-7} s evaluated therefrom. This is in fair agreement with an approximate value of $0 \cdot 2\ \mu$s for τ derived from the magnitude of the photoconductivity. Earlier experiments were performed with comparable success using a ninety-face rotor and the seventh harmonic of the optical signal.

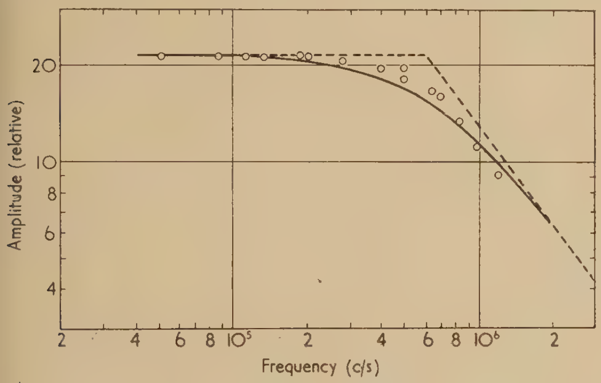

Fig. 4. Frequency response of a sample of indium antimonide
Time constant $= 3 \times 10^{-7}$ s. $\tau\rho = 1 \cdot 7 \times 10^{-7}$ s.
$P_0 = 8 \cdot 0 \times 10^{14}$ holes per cm^3. $T = 77°$ K

The disagreement between the theoretical curve and the actual frequency response measurements just mentioned was found for all indium antimonide samples measured. This is not believed to be due to frequency distortion in the amplifier, since the time constant of the amplifier was estimated to be $2\,\theta$ times smaller than the cell time constant. Good agreement with theory was obtained for samples of germanium and lead sulphide.

Discussion

It is felt that 180 is probably about the largest number of faces that is practical with the present rotor system. The faces are then about $0 \cdot 22$ mm wide. Small movement of the rotor would prevent stable alinement of smaller slits and faces. With the 180-face rotor third harmonics were normally quite large. Using a peripheral velocity of 10^5 cm/s as the maximum speed obtainable, the frequency of the third harmonic from a 180-face rotor is $6 \cdot 9 \times 10^6$ c/s, corresponding to a 3 dB point for a response time of $2 \cdot 3 \times 10^{-8}$ s. The system described uses only the simplest of optics and an 80 W incandescent lamp, so that higher frequencies or time constants shorter than 10^{-8} s could be measured with a slightly more elaborate system.

It is to be noted that with a ninety-face rotor, frequencies as low as 10 c/s could be obtained of sufficient stability for measurements to be made.

The system described does not replace pulsed-light systems where such provide adequate intensities for usable signal-to-noise ratios. The advantage of the present system comes from its higher light-collecting power, as f numbers of the order of 2 can be realized. A second gain in signal-to-noise is realized through the use of narrow-band wave-analyser detectors.

Another advantage of the frequency-response system is in its use in measurements on fast-detectors having high impedance. A material such as n-type gold-doped germanium has a very high resistance, and for normal operation the series resistance is comparable in magnitude. In measuring the response time of such material, however, the cell circuit RC time constant must be small, so the series resistance has to be reduced in value to the low kilohm range. To obtain usable electrical signals it is then necessary to use such large optical signals that the test material resistance is changed appreciably. This point has been discussed by Beyen *et al.*(7)

Response times of n-type gold-doped germanium have been measured with the frequency response system and, because of the reduction in bandwidth possible, smaller optical signals were employed compared to those necessary to perform the same measurement with a spark gap. It is also possible to gain in signal amplitude by using series resistances which give RC time constants longer than the cell time constants. The cell time constant is then obtained from the point of intersection of the w^{-1} and w^{-2} portions of the curve. This condition also represents the minimum optical signal that can be employed for a given bandwidth analyser system and a particular signal-to-noise ratio.

Acknowledgements

The author wishes to express his gratitude to R. Porter, J. Vannier and G. I. Turner who assisted in various phases of the work.

References

(1) Garbunny, M., Vogel, T. P., and Hansen, J. R. *Rev. Sci. Instrum.*, **28**, p. 826 (1947).

(2) Porter, G., and Wooding, E. R. *J. Sci. Instrum.*, **36**, p. 147 (1959).

(3) Kerns, Q. A., Leisten, F. A., and Cox, G. C. *Rev. Sci. Instrum.*, **30**, p. 31 (1959).

(4) Beams, J. W., Smith, E. C., and Watkins, J. M. *J. Soc. Motion Picture Televis. Engrs*, **58**, p. 159 (1952).

(5) Beams, J. W. *Science*, **120**, p. 619 (1954).

(6) Beams, J. W. *Phys. Today*, **12**, p. 20 (1959).

(7) Beyen, W., Bratt, P., Davis, H., Johnson, L., Levingstein, H., and MacRae, A. *J. Opt. Soc. Amer.*, **49**, p. 686 (1959).

Beam method for the measurement of internal friction

by J. E. THOMPSON, Ph.D., The English Electric Co. Ltd., Nelson Research Laboratories, Stafford

[*Paper received* 8 *January*, 1960]

Abstract

The oscillatory motion of a swinging beam used to measure the internal friction of a silicon–iron strip has been found to be complicated, and to consist of a small amplitude, higher frequency oscillation superimposed on the main oscillation, so that difficulty arises in obtaining a unique value for the logarithmic decrement of the strip oscillation. The motion has been analysed and reasonable agreement is found between the experimental results and the theory developed.

Introduction

The determination of interstitial nitrogen by the damping of an oscillating system due to the conversion of mechanical energy into heat energy in the suspension material, commonly referred to as "internal friction," was first discussed in detail by Snoek.* He described methods by which the measurement of the nitrogen content could be made in metal strips, using an oscillating beam apparatus, and in metal wires, using a disk in torsional oscillation. It was shown that the method enables the interstitial impurities to be determined accurately. The technique has since been used for a large number of investigations, principally with the torsional apparatus.

The beam method appeared to be the most convenient method available for measurements on silicon–iron strip, though it was found that the motion was complex under certain conditions. The results of the measurements, together with the relevant theory, are given and discussed.

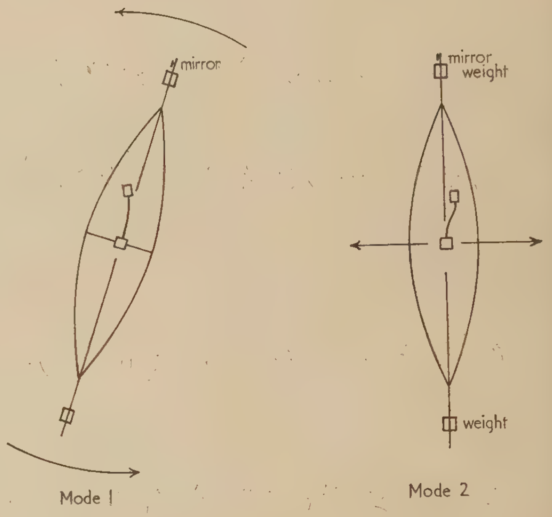

Fig. 1. The two modes of vibration of the beam

The beam

The beam was made from a light aluminium framework with adjustable weights at each end which could be moved relative to the centre. The centre of the beam was clamped to the metal test strip, about 10 cm long, which was itself firmly clamped to a fixed support. The weights could be moved so that the centre of gravity of the beam could lie anywhere within limits about 15 cm above or below the geometric centre of the beam.

The diagram of Fig. 1 shows the structure of the beam, together with two possible modes of oscillation. It is important to note that the mirror, lamp and scale measure the slope or inclination of the strip to the vertical at the lower suspension point, which for motion in mode 2 is constant.

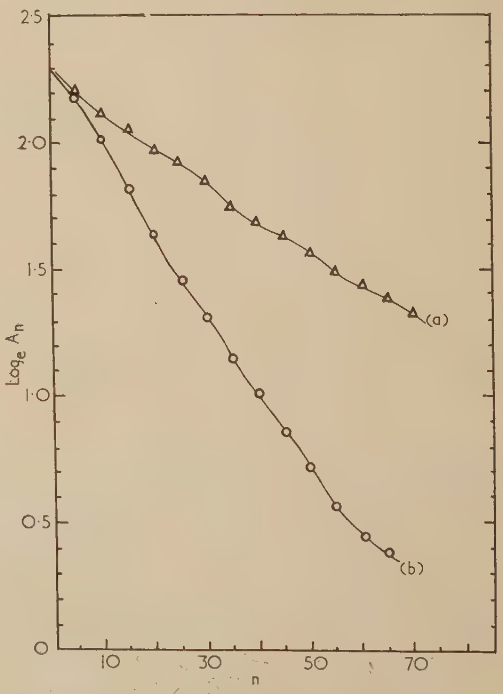

Fig. 2. Graph of $\log_e A_n$ and n for a silicon–iron strip
Curve (*a*), centre of gravity at the clamping point; curve (*b*), centre of gravity displaced below the clamping point

Experimental results

Fig. 2 shows the value of $\log_e A_n$ (where A_n is the amplitude of the nth swing) plotted against the swing number for a silicon–iron strip with (*a*) the beam weights symmetrically placed, and (*b*) asymmetrically placed. It is convenient generally to measure the logarithmic decrement by the slope of this line.

---

* Snoek, J. L. *Physica*, **8**, p. 711 (1941).

Two disturbing features emerged from the results: firstly, the logarithmic decrement or slope varied with amplitude, and secondly, there was an oscillation on the curve, the amplitude and frequency of which varied appreciably with the total weights and their distribution on the beam, and strip thickness. These effects were due to a complex oscillation in the two modes.

Theory

The simpler case is with the two weights $m/2$ placed so that the centre of gravity of the beam coincides with the beam clamping point. Let W be a horizontal force and M the moment acting at the end of the metal strip, l the length of the strip, I_s the inertia of the cross-section of the strip, x the distance from the fixed clamping point, y the horizontal displacement, and E Young's modulus for the strip material.

The equation for the bending moment across the strip section at the distance x is

$$(EI_s)(d^2y/dx^2) = W(l-x) + M \tag{1}$$

using the conditions:

$$y = 0, \quad dy/dx = 0 \quad \text{when} \quad x = 0,$$

and denoting (EI_s) by K.

$$K(dy/dx) = (Wl^2/2) + Ml \tag{2}$$

and

$$Ky = (Wl^3/3) + (Ml^2/2) \quad \text{at} \quad x = l \tag{3}$$

Now

$$W = -m\ddot{y} \quad \text{and} \quad M = -I_b\ddot{z} \tag{4}$$

where I_b is the inertia of the beam system, m the mass of the end weights, $\dot{y} = dy/dt$, $\ddot{y} = d^2y/dt^2$ and $z = (dy/dx)_{x=l}$. Whence equation (2) becomes

$$Kz = -\frac{ml^2}{2}\ddot{y} - I_b l\ddot{z}$$

and equation (3) becomes

$$Ky_l = -\frac{ml^3}{3}\ddot{y} - \frac{I_b \,.\, l^2}{2}\ddot{z}$$

Using the D operator notation, and re-arranging

$$\left(D^2 + \frac{K}{I_b l}\right)z = -\frac{ml}{2I_b}\cdot D^2y \tag{5}$$

and

$$\left(D^2 + \frac{3K}{ml^3}\right)y = -\frac{3}{2}\frac{I_b}{ml}\cdot D^2z \tag{6}$$

Let

$$\frac{3K}{ml^3} = \alpha^2, \quad \frac{K}{I_b \,.\, l} = \beta^2 \quad \text{and} \quad \gamma = \frac{ml}{2I_b}$$

then

$$(D^2 + \alpha^2)y = -\frac{3}{4}\frac{1}{\gamma}\cdot D^2z \tag{7}$$

and

$$(D^2 + \beta^2)z = -\gamma D^2y \tag{8}$$

From the Laplace transform and the initial conditions

$$y = y_0, \quad z = z_0, \quad dy/dt = 0, \quad dz/dt = 0 \quad \text{at} \quad t = 0$$

the equations give

$$Z(p) = \frac{p^3z_0 + 4\alpha^2(\gamma y_0 + z_0)p}{p^4 + 4(\alpha^2 + \beta^2)p^2 + 4\alpha^2\beta^2} \tag{9}$$

whence

$$Z(p) = \frac{\lambda p}{p^2 + a^2} + \frac{\mu p}{p^2 + b^2} \tag{10}$$

where $-a^2$, $-b^2$ are $2[-(\alpha^2 + \beta^2) \mp \sqrt{\{(\alpha^2 + \beta^2)^2 - \alpha^2\beta^2\}}]$

The solution is

$$z = \lambda \cos at \quad + \mu \cos bt \quad \text{with} \quad a > b \tag{11}$$

For given initial values of the displacement and slope, the amplitude factors λ, μ governing the motion are

$$\lambda = \frac{\{\sqrt{(\alpha^4 + \alpha^2\beta^2 + \beta^4)} - \alpha^2 + \beta^2\}z_0 - 3\beta^2(y_0/l)}{2\sqrt{(\alpha^4 + \alpha^2\beta^2 + \beta^4)}} \tag{12}$$

$$\mu = \frac{\{\sqrt{(\alpha^4 + \alpha^2\beta^2 + \beta^4)} + \alpha^2 - \beta^2\}z_0 + 3\beta^2(y_0/l)}{2\sqrt{(\alpha^2 + \alpha^2\beta^2 + \beta^4)}} \tag{13}$$

Discussion of the solution

The term β contains the inertia of the beam system, and considering this to be due entirely to two masses $(m/2)$ placed near the ends of the beam equidistant (d) from the clamping point, the ratio α^2/β^2 is $3d^2/l^2$, which is independent of the mass of the weights.

In practice l/d should be made as small as possible (i.e. $\alpha \gg \beta$ and $l \ll s\sqrt{3}$) when the approximate solution is given by (after some re-arrangement)

$$z \doteqdot \frac{l^2}{4d^2}\left(z_0 - \frac{2y_0}{l}\right)\cos 2\alpha t + z_0 \cos \beta t \tag{14}$$

so that the ratio of $\lambda/\mu \ll 1$ and, moreover, the oscillation is not complicated by the initial conditions.

As l/d is made large, the motion becomes more dependent on the initial conditions until with $l/d \gg 1$, the motion is complex, and is given by

$$z \doteqdot \left(z_0 - \frac{3}{2}\frac{y_0}{l}\right)\cos 2\beta t + \frac{3}{2}\frac{y_0}{l}\cdot \cos \alpha t \tag{15}$$

For the particular beam system used for Fig. 2, $d/l > 1$, so that the motion contains a small amplitude, higher frequency oscillation superimposed on the main oscillation, which shows up as a lower frequency variation on the logarithmic decrement curve.

Experimentally (as in Fig. 2) the effect of this more rapid oscillation of smaller amplitude is to cause the measured peaks of the slower oscillation to be increased or decreased by a frequency component corresponding to the difference factor $(a - nb)$, where n is an integer such that this difference is the smallest value possible. Theoretically and experimentally, the period of the slow oscillation ($\cos bt$) was about one second.

The general equation

Consider the beam weight distribution being such that the centre of gravity does not coincide with the beam fixing point. If S is the distance of the centre of gravity from the beam-strip clamp, and ϕ is the inclination of the beam to the vertical, then the total kinetic energy of motion of the frame is

$$T = \tfrac{1}{2}I\dot{\phi}^2 + \frac{m}{2}(\dot{y} + S\dot{\phi})^2$$

The Lagrange equations of motion are (16)

$$\left.\begin{aligned} \frac{d}{dt}\left(\frac{\partial T}{\partial \dot{y}}\right) - \frac{\partial T}{\partial y} &= -W + p\dot{y} \\ \text{and} \qquad \frac{d}{dt}\left(\frac{\partial T}{\partial \dot{\phi}}\right) - \frac{\partial T}{\partial \phi} &= -M + q\dot{\phi} \end{aligned}\right\} \tag{17}$$

introducing damping proportional to $\dot{y}$ and $\dot{\phi}$, which becomes

$$m(\ddot{y} + S\ddot{\phi}) = -W + p\dot{y} \qquad (18)$$

$$I\ddot{\phi} + mS(\ddot{y} + S\ddot{\phi}) = -M + q\dot{\phi} \qquad (19)$$

If $S = 0$, and with no damping, the equations reduce to the form given previously in equation (4). Substitution into equations (2) and (3) gives a solution of the form

$$\phi = A \exp(-K_1 t) \cos(K_2 T + K_3) + B \exp(-K_4 t) \cos(K_5 t + K_6)$$

Conclusion

It has been found that complications arise in determining the logarithmic decrement of the swinging beam apparatus in certain cases due to the presence of two modes of oscillation and their interaction, and to the difficulty in starting a satisfactory oscillation. The torsion method is superior in use to the beam method, since the mode of vibration is essentially a simple oscillation. Good agreement has been obtained between the experimental results and the theory given here.

Acknowledgements

Thanks are expressed to Mr. V. A. Hughes for his encouragement and interest in this study, and to Mr. J. K. Brown, Director of Research, for his interest and permission to publish this paper.

Technique for replicating fibre surfaces by rolling

by J. MØLGAARD, B.Sc., Research Department, British Nylon Spinners Limited, Pontypool, Monmouthshire

[*Paper first received* 16 *February, and in final form* 14 *March* 1960]

Abstract

Short lengths of fibre with cylindrical cross-section are placed on a plastic film and rolled, thereby replicating the entire fibre surface. The apparatus to do this is described. The replicas are examined by phase contrast. Nylon fibre surfaces are illustrated.

Introduction

A PROCEDURE for rolling impressions of animal-fibre surfaces for the purpose of fibre identification and classification from the overall scale pattern has been described by Wildman.(1,2) A technique having the same principle is being used in these laboratories for the study of fine detail of synthetic-fibre surfaces of approximately cylindrical cross-section.(3,4) Instead of the curved surface of static, embedding-replica techniques in electron and light microscopy, a flat impression is obtained of the entire fibre surface. The examination of replicas in phase contrast microscopy is in general advantageous(5,6) and particularly so on rolled fibre impressions.(3,4) Details are given here of the apparatus and procedures which have been used for producing, fairly consistently, good rolled-fibre replicas. The application of phase-contrast microscopy to replicas of nylon-fibre surfaces is illustrated.

Method

Three pieces, approximately 2 mm long, are cut from a fibre of the yarn to be examined and placed on a microscope slide which is coated with a partially dried film of the replica medium, still in the plastic state. The fibres are arranged as shown in Fig. 1 in a position to roll along the slide. Another glass slide is placed on the fibres and slowly moved to roll the fibres, while a weight is applied to the top slide. In this manner, flat impressions are made by the fibre surfaces on the replica film, which in the meantime dries out and hardens, thereby retaining the imprints.

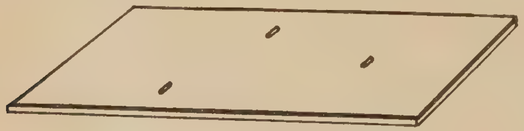

Fig. 1. Arrangement of fibres

Preparation of the replica film

Five per cent (v/v) polystyrene dissolved in benzene with $1\frac{1}{2}$% (v/v) di-butyl-phthallate as plasticizer is at the moment preferred as replica medium. Clearer replicas are obtained than with the acetone solution of Necol cement (by I.C.I. Ltd.) referred to previously.(3)

Standard drying conditions are required for reproducible preparation of suitable replica films. The slide, after dipping in the replica-medium solution, is allowed to drain in the presence of solvent-laden air for 2–3 min with a flow of 2·3 l./min through a drying chamber of volume 1·5 litres.

Placing and rolling fibres on the replica film

The glass slide is taken from the drying jar; any thick rim of polystyrene along the bottom edge is scraped off, and the fibres are placed on the slide by means of a glass nozzle connected to a vacuum line. The nozzle has a fine capillary at its end and a larger hole at the side. On placing a finger over the larger hole a fibre can be picked up and held transversely across the capillary.

Fig. 2 shows diagrammatically the principal parts of the apparatus used for rolling the fibres. *O* is the coated slide carrying the fibres *T*. A flexible coupling (flexible in bending, *not* extension) connects the upper slide *P* to a trolley *Q* driven, via rack and pinion, by a highly geared-down, 1 rev/min Drayton motor, type RQR (by Drayton Regulator Instrument Co. Ltd.). Two gear ratios are available providing the slide *P* with speeds of 0·01 and 0·08 mm/s; 0·01 mm/s is usually used. The motor and gearing are not shown in Fig. 3. The weight *R*, attached to *P* by steel wire running over a pulley, takes up any backlash in the gears. The tension is always applied to *P* before it touches the fibres.

Illustrations of fibre replicas

Two widely differing surfaces of nylon multi-filament yarn are shown in Figs. 3 and 4. Both replicas are photographed

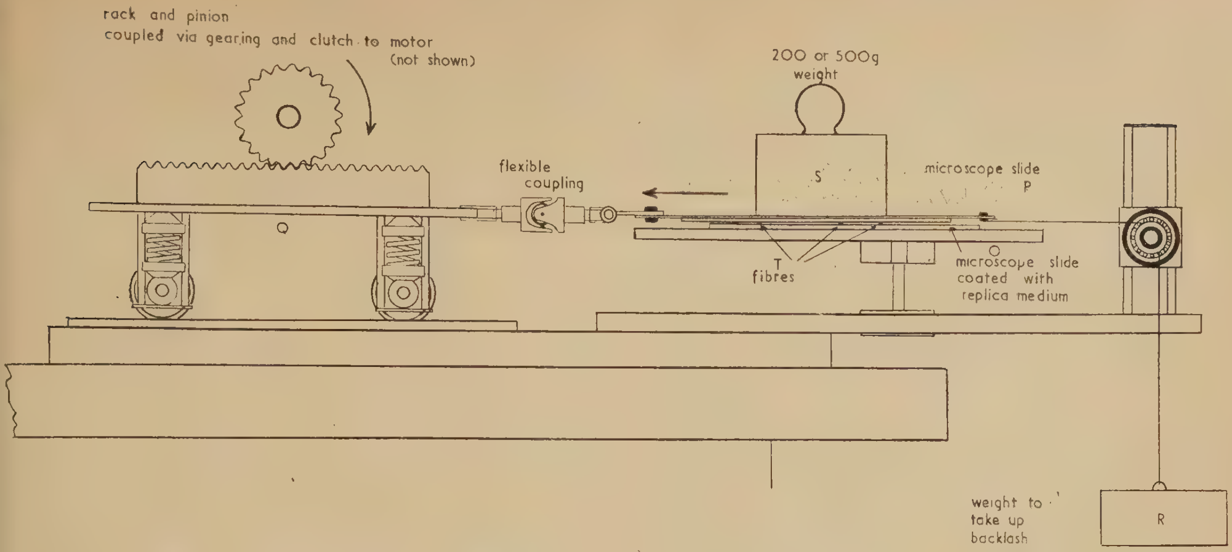
rack and pinion
coupled via gearing and clutch to motor
(not shown)
200 or 500g
weight
S
flexible
coupling
microscope slide
P
T
fibres
microscope slide
coated with
replica medium
Q
weight to
take up
backlash
R

Fig. 2. Replicator, to roll fibres on replica film

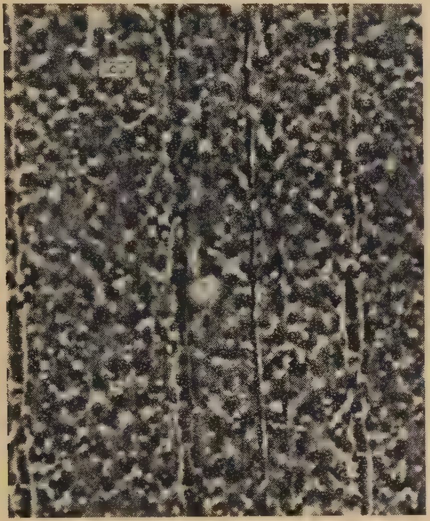

Fig. 3. Highly delustred, undrawn nylon filament

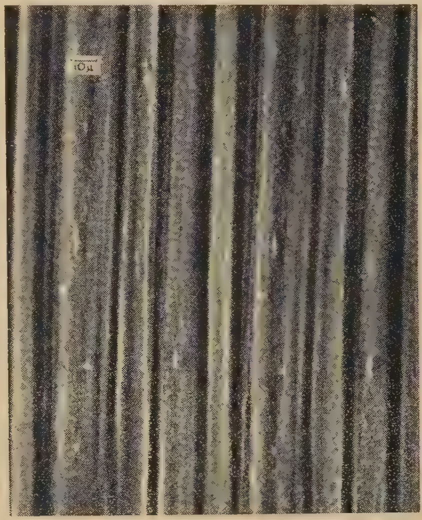

Fig. 4. Drawn nylon filaments with low-delustrant content

in phase contrast, with a 4 mm objective lens of numerical aperture 0·65. Fig. 3 shows the surface of a highly delustred, undrawn filament, clearly demonstrating the protrusion of a large number of delustrant particles. Fig. 4 is the surface of a drawn filament with a low delustrant content. Only a few particles are protruding. A fine, elongated granular structure is also seen. The lines running along the length of the fibre are presumed to originate from contact with various yarn guides during processing. Some marking of this type is also seen in Fig. 3.

Both photographs demonstrate clearly the repeated replication of the entire fibre circumference. Just over one revolution of the fibre is included in Fig. 3, two revolutions in Fig. 4. The diameters of the fibres are 0·037 and 0·021 mm respectively.

Acknowledgements

The author is indebted to Mr. J. F. Williams for valuable assistance, and to British Nylon Spinners Limited for permission to publish this paper.

References

(1) Wildman, A. B. *The microscopy of animal textile fibres*, p. 36 (Leeds: Wool Industries Research Association, 1954).

(2) Wildman, A. B. Proc. International Wool Textile Conference, Australia, 1955, Vol. F, p. 162 (Melbourne: Commonwealth Scientific and Industrial Research Organization, Australia, 1956).

(3) Mølgaard, J. *Nature* (*London*), **184**, p. 264 (1959).

(4) Woods, H. J.
Mølgaard, J. *Nature* (*London*), **184**, p. 1478 (1959).

(5) Marx, T., and Diehl, F. *Naturwissenschaffen*, **35**, p. 91 (1948).

(6) Bennett, A. H., Jupnik, N., Osterberg, H., and Richards, O. W. *Phase microscopy*, pp. 175, 216, 235 (New York: John Wiley and Sons, Inc.; London: Chapman and Hall, Ltd., 1951).

Laboratory magnetic elutriator for purification and isolation of ferrimagnetic mineral sands

by W. R. B. MARTIN, M.Sc., A.M.I.Mech.E., A.M.I.Chem.E., Victoria University of Wellington, New Zealand

[*Paper first received* 20 *May, and in final form* 10 *December,* 1959]

Abstract

An apparatus is described which allows almost total removal of not-completely homogeneous magnetic grains from ferrimagnetic mineral sand, and will further separate strongly remanent from weakly remanent grains. Magnetic-field strengths and water-flow velocities required for material of size 60 *to* 200 *B.S. mesh, and a scale drawing of the separation tube are given.*

Introduction

MANY different types of magnetic separators are well reviewed by Dean and Davis.(1) A small laboratory Roche-type separator built by the author(2) has proved efficient for extracting ferrimagnetic minerals rapidly from field samples, but has little discrimination against "composite" particles which have up to a 25% occurrence in some of the New Zealand titanomagnetite deposits.

In the hope of obtaining high-purity samples as free as possible from these composite grains, an apparatus was built to the specifications of Roe.(3) It did not have sufficient discrimination for the author's purpose, but it appeared that, with some modifications, it should allow almost perfect separation. The modified form as described can yield a product with fewer than one grain of gangue or composite per thousand.

The modifications were to the shape of the tube and consisted essentially of provision of a gently tapered section at the lower end just beyond the effective range of the magnetic field, thus converting the tube to the shape of a Schöne elutriator,(4) and a turbulence-producing bowl at th bottom of that section.

Principles of operation

It would appear from the fundamental principles involv that, if an axial magnetic field was applied to particl previously "hydraulically sized" which were suspended in a uprising stream of water in a vertical elutriator tube, it shou be possible to so regulate the field and rate of flow of th stream that ferrimagnetic particles of different degrees magnetization could be separated, and all composite particle even those with only very small gangue inclusions, be rejecte in the overflow. The form of apparatus developed (Fig. shows this to be practicable.

The apparatus consists essentially of a vertically oriente Schöne elutriator tube connected to a suitable turbulenc producing bulb at its lower end; a suitably wound c around the elutriator tube that can produce a controllabl steady axial field across the tube; the means of feeding i samples and of collecting and disposing of overflow wat and "tails", and a constant-pressure, constant-temperatu water supply (low-head tank) free of any suspended matte

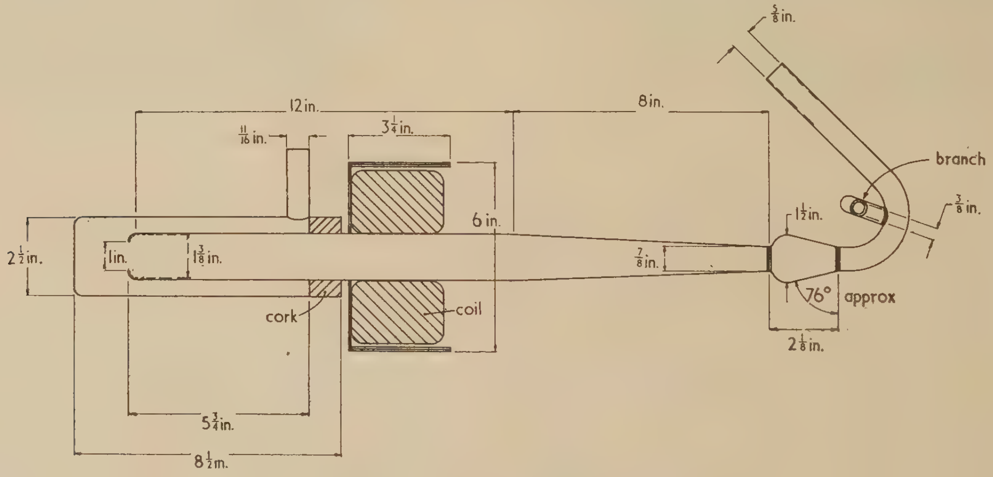

Fig. 1. Details of separator

At a particular rate of flow of water up the separator tub there will be some "hydraulic size" of particle that will ten to remain just suspended in the stream. With streamlin flow, conditions in the parallel portion of the tube hydraul lift depends primarily on shape; opposing this is gravit which depends only on size; long thin grains align with th tube axis and behave like much larger, nearly spherical grain

If an axial magnetic field is applied to a sample so sized, ferrimagnetic particles have poles induced, and they align themselves in "chains" parallel to the axis and hence to the flow stream lines. Gravitational force on a chain is the sum of that on the individual particles, but the hydraulic lift is much less than the sum of that for the individuals. These chains thus sink and, because of magnetic retentivity, descend beyond the range of effective influence of the field down into the bulb.

The purpose of the bulb is to generate vigorous turbulence in the water stream at this point and so break up the chains continuously falling into it. The purpose of the long, gently tapered section is twofold: to convert the turbulent flow to streamline flow, and to hold hydraulically oversized particles in suspension during the "hydraulic sizing" part of the separation cycle.

If, with the axial magnetic field energized, the rate of the stream flow is increased beyond the "sizing" velocity, the non-magnetic particles will be carried out, but the ferrimagnetic ones alternately joining and being torn from chains will be continuously recycled in the tube.

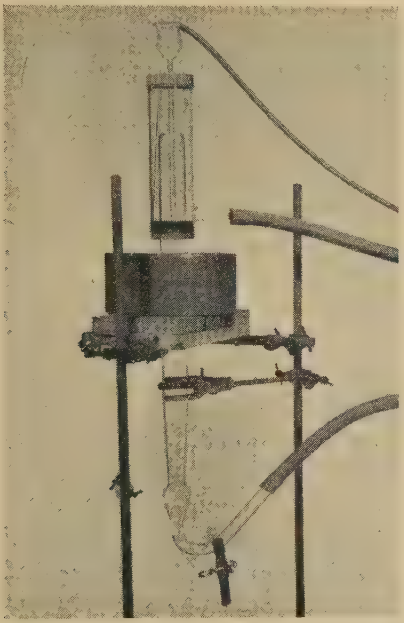

Fig. 2. Photograph of essentials of separator

Because of fluid friction, there is a lower stream velocity against the sides. Chains, which because of curvature of the field at the coil outlet have their lower ends against the walls, tend to fall in this annular zone and to leave the central regions clear for the freer passage of unpartnered rising particles.

Statistical rather than individual behaviours govern the fate of composite grains. Over nearest neighbour distances the field can be considered uniform. Individual hydraulically sized grains of similar magnetic-mineral content can be considered as of some equivalent size and shape; the pure grains are of smaller average size. Resistance to movement, following Stokes Law, depends on diameters. Hence, on the average, composite particles, which approach more slowly, tend to be excluded from chains or to be less strongly attached. It is possible to adjust the field so that, while retaining most of the pure grains, almost all others are eliminated.

When the exciting field is removed and the flow rate decreased until it is just a little greater than that necessary to carry over all the particles in a fully demagnetized condition, chains then in existence fall into the turbulence bowl and tend to be broken up. The extent of the break-up is dependent on the retentivity of the magnetic minerals present. If magnetically soft, the chain fragments rapidly disappear and the unflocculated sample overflows into the tails. If the sample contains magnetically hard mineral, chain fragments become smaller, flocculi of irregular shape and the groups persist or reform in the tapering portion of the tube to sink along the sides into the turbulent bowl again. In the process, weakly remanent grains tend to be excluded and to be swept out, thus effecting a separation between strongly and weakly remanent grains.

It is important that a sample be fully demagnetized before preliminary hydraulic sizing; otherwise composite grains of borderline size are partnered with a small number of strongly remanent grains into flocculi of sufficient hydraulic size to be retained when the composite particles alone would have been rejected. It is easy to see the behaviour of particles in the present apparatus, except within the limits of the solid coil. When the apparatus is finely adjusted for good separation, single particles above the coil are always carried onwards, pairs of particles are also rejected unless they come close to the sides and enter the lower velocity zone, but groups of more than three particles do not escape. It is observed that, within the influence of the magnetic field, the magnetic particles form chains up to three or four grains wide and about an inch long.

In the early work with a parallel tube and perforated flow-distribution plate as given by Roe, chains which sank along the walls tended, at low velocities, to settle as a flocculated high-density zone above the perforated plate. Application (where shown by Roe) of a 50 c/s a.c. magnetic field of 150 oersteds maximum effected little if any improvement. Only by keeping the velocity relatively high could the bottom plate be kept reasonably clear of settled flocculi. At these velocities and the fields necessary to retain the magnetic particles, there was little or no selective rejection of composites containing any appreciable amount of magnetic mineral. This experience suggested turbulent chain breaking (which permits operation at lower velocities) and weak fields so that almost all unhomogeneous grains can be rejected over the size range tested (− 60–+ 200 B.S. mesh).

It must be stated that free gangue and many composite grains were removed by Roe's apparatus and nothing in the foregoing is incompatible with his claims; this apparatus was developed to give a refinement which, for the purposes of Roe's work, would probably have been unnecessary.

Construction

The elutriator tube (Fig. 1), made from Pyrex glass tubing, was reduced in diameter at the top overflow lip to increase the velocity of the stream so that particles reaching the top were not recirculated down the walls. The side tube (normally closed by a clip on a piece of rubber tubing) taken off the upper part of the bottom bend was the best means found of quantitatively removing cleaned samples lying in the bend after a separation.

The magnetic field was modified by a 16 G mild-steel disk with a central hole fitting close to the elutriator tube sitting on top of the coil, and a 16 G band of mild steel wrapped twice around its perimeter. The sharp cut-off of the field above the coil produced by the disk results in a steep field gradient in this region; acting as a screen, this brings any small groups of two or three particles tending to escape from the field quickly to the side and prevents their loss with the tails.

Filtered water, at four feet of head, was drawn from a constant-level tank. If unfiltered water was used, small filaments became attached to small groups of magnetic grains and provided extra hydraulic lift which caused loss of the particles. The water flow was controlled by means of a stop valve and two metal seat valves in parallel, a $\frac{3}{8}$ in. needle valve and a $\frac{1}{2}$ in. gate valve. The preliminary flooding was done with the larger valve; the smaller one could be left set at the proper flow rate for a particular particle size and would require little, if any, adjustment to repeat a flow rate. The stop valve up stream of the control valves allowed the set flow to be stopped for the removal of samples. The flow was measured by passing the water through a glass orifice plate with manometer tubes either side and carried up to beyond the level of the constant-head tank.

Operating procedure

Preliminaries. The sample, contained in a glass tube, was demagnetized by placing in an alternating magnetic field which was decreased over a period of a minute from 2000 oersteds to zero. Under the microscope, even strongly-remanent material showed no evidence of grains attracting each other after this treatment. The material was then sieved and the fraction to be separated stood under water with a drop or two of Teepol to ensure thorough wetting of all particles.

Preparation of elutriator to receive a sample. The bottom drain-off tube was closed with a pinch cock and the water was turned on to flood the elutriator fast enough to sweep *all* air bubbles from the system; otherwise pulsating flow was liable to spoil separation. The flow was then adjusted to a rate which would suspend most of the sample of the particular size range well up in the tapering transition tube of the elutriator and the sample, in the form of a slurry, was introduced about two inches below the level of the bottom of the coil by means of a central, long, slender funnel.

Hydraulic sizing. The rate of water flow was increased until the dense bed concentrated in the tapered transition section just expanded into the parallel, constant-velocity parts of the elutriator tube. It was then successively increased at intervals and a series of products, three usually sufficing, of increasing hydraulic size was collected.

In general, as soon as a sample was introduced, a proportion would sink even through the turbulence bulb, to lie on the bottom of the inlet bend, because the initial rate, even in the throat, was too slow to suspend the particles of the last product size, and in the zone of slow flow against the walls, some grains would sink to the bottom along with the really hydraulically over-sized material. When mixed with over-sized material the last fraction of sized particles could not subsequently be lifted from among the heavier neighbours by a velocity of flow that would normally suspend them. Reintroduction of this material, together with the "dregs" from the final sizing, at the same velocity as the last product was collected, allowed the trapped material to be recovered. As would be expected, hydraulically over-sized particles were always elongated grains that were much heavier than the particles of average shape passing the same sieve. Simple hydraulic elutriation got rid of a lot of gangue and composite over-sized material very easily.

Removal of gangue and composite grains by magnetic elutriation. The rate of flow of water through the apparatus was first adjusted so that the uprising velocity was two to two and a half times that at which the particular fraction had previously been carried out of the elutriator. This rate was not critical. The magnetic field was then energized and the sample introduced and allowed to recycle for some 20 minutes, or until it was free of composite particles. Complete removal of the sample from the elutriator and a microscope check of a small, dry portion was a satisfactory quick way to assess the degree of purity.

It was necessary to stop the flow about half-way through a magnetic run, withdraw the sample from the bottom and reintroduce it, because chain fragments tended to escape turbulent break-up and accumulated at the bottom bend. This was not a rapid settling as with the hydraulically over-sized grains, but is believed to be a direct result of the slow velocity flow near the walls of the elutriator passages. When the product was of the required purity, the flow was stopped, the field removed and the sample withdrawn and immediately treated as follows.

Separation of magnetically soft and hard fractions. The slurried fraction to be separated into its magnetically different components was well diluted and shaken to break up temporarily any close knit chains or rings of grains, and so to free weakly remanent grains. Water flow was restarted and the rate adjusted to that at which the sample had been originally carried over in hydraulic sizing. The sample was reintroduced. In the general case, free grains, small groups and short chains could be seen. The single particles would immediately rise and were carried out; these were collected as the weakly remanent (W.R.) fraction. The flow rate was then approximately doubled when the smaller groups of particles were carried over; it is assumed that small groups contained both non-remanent and strongly remanent grains, though for convenience the fraction was called intermediately remanent (I.R.) material. The material remaining in large groups and chains was collected as the strongly remanent (S.R.) fraction. The importance of prior removal of hydraulically over-size grains is evident.

Field strength. The strength of field found suitable for magnetic elutriation of −120–+200 B.S. mesh, New Zealand ferrimagnetic minerals was between 30 and 75 oersteds as measured on the axis in the plane of the free end (bottom) of the coil. If the field was too strong, it was found that much material would hold up on the sides of the tube within the coil and hence not recycle. The weakest field that would just muster the majority of magnetic grains into chains was aimed for. That was ascertained by watching the small unobstructed clear zone immediately above the magnet and under the overflow collector vessel; the minimum fields at which excessive carrying-over of particles cease are fairly sharply defined.

To check the behaviour of weakly magnetic minerals, ilmenite at tetering velocity was subjected to a field of approximately 600 oersteds. There was no sign of flocculation, indicating that the principle is not applicable to such minerals and confirming that it is the interaction between the local fields set up around strongly permeable grains that is essentially responsible for flocculation.

Results

Table 1 shows the uprising velocities in the elutriator tube found satisfactory for the operations of hydraulic sizing, magnetic elutriation, collection of weakly remanent material and elimination of material of intermediate remanence from ypically ferrimagnetic-ore mineral sands in the size range −120–+240 B.S. mesh. These data should serve as a guide o the requirements in other separators built to use this principle, though of different mechanical dimensions. Performance was judged by the macroscopic purity of the samples when examined under a low-power microscope. The working standard that could in most cases be achieved by 20 minutes magnetic elutriation was, a maximum of one composite grain in a closely packed field, counted in the circumstances to be around a thousand grains.

The true significance of the resolution into weakly and strongly remanent grains was only revealed by chemical analysis. Only the end members—the weakly and strongly remanent grains—are considered significant as, in any deposit, apart from a mixture of individuals of both end types in the "intermediate" cut from the machine, there is probably a series of intrinsically intermediate minerals. As previously mentioned, the machine was built to obtain pure specimens of titanomagnetite mineral from many places along the west coast of the North Island of New Zealand. Even for samples a hundred miles apart, the ratios of ferric to ferrous iron in the strongly remanent fraction separated were remarkably close; so also were the ferric/ferrous ratios for the weakly remanent fractions, while the consistent ratios for both series were different. Table 2 shows typical ratios of ferric to ferrous iron in strongly remanent and weakly remanent fractions of titanomagnetite from several localities on the west coast of the North Island of New Zealand. There were other less-pronounced differences between weakly and strongly remanent types.

These results leave little doubt that the machine can reproducably separate ferrimagnetic mineral grains of different magnetic remanence.

Table 1. *Operating data for elutriator*

Sieve size (B.S. mesh)	*Water flow velocities (cm/s)*				*Field current (A)*	*Field at centre of tube (oersteds)*
	"Hydraulic sizing"	*Magnetic elutriation*	*Collection of W.R.*	*Removal of I.R.*		
−150 +200	1·1–1·7	2·2–4·2	1·2–1·7	2·2–3·5	0·07–0·1	50–75
−120 +150	1·6–2·4	3·2–6·0	1·7–2·5	3·2–4·8	0·05–0·1	37–75

Table 2. *Typical results*

Locality	*S.R.*	*W.R.*
Patea	1·54	1·37
Marakopa	1·57	1·30
Taharoa	1·57	1·37
Kawhia	1·55	1·39
Piha	1·56	1·37

Acknowledgements

Acknowledgement is made to the Council of Scientific and Industrial Research for a grant of funds to Victoria University of Wellington, to Victoria University of Wellington for accommodation and facilities, and to the University of New Zealand for a Senior Research Fellowship during the tenure of which the work was carried out.

References

(1) Dean, R. S., and Davis, C. W. *Bull. U.S. Bur. Min.*, No. 425 (1941).

(2) Martin, W. R. B. *N.Z.J. Sci. Tech.*, **B31**, p. 5 (1949).

(3) Roe, L. A. *Min. Engng*, **5** p. 312 (1953).

(4) Krumbein, W. C., and Pettijohn, F. J. *Manual of Sedimentary Petrography* (New York: D. Appleton-Century Co., 1938).

Automatic polishing technique for electro-thinning metals for transmission electron microscopy

by V. A. Phillips, A.R.S.M., A.I.M., B.Sc., D.Eng., and J. A. Hugo, General Electric Research Laboratory Schenectady, New York, U.S.A.

[*Note received* 18 *January*, 1960]

Electrolytic polishing appears to be the most generally applicable method for the preparation of thin foils from bulk samples for direct examination in an electron microscope. Previous techniques for electrolytic thinning(1–5) suffer from the disadvantage of being relatively slow, tedious and difficult to control. In addition, due to a marked tendency to edge attack, it is necessary to mask off edges repeatedly during thinning and often to use fairly large samples of up to 1 in. square. Mirand and Saulnier(6) described a rapid method using an automatic polisher. In their method the sample 0·001 in. or less in thickness, backed by a piece of the same metal, was placed against a 5-mm diaphragm of an automatic polisher. The sample polished through in $\frac{1}{2}$–1 min and the fragments were afterwards recovered from the electrolyte and washed. This method suffers from the disadvantages that the sample cannot be observed during polishing, that edge attack occurs and that the fragments become entrained in the electrolyte and tend to become etched. The present method of electro-polishing has been devised to overcome these disadvantages.

The instrument used was a Disa-Electrolpol type 53A (by Stoners Scientific Instruments, Copenhagen), although any similar instrument could be used. Fig. 1 shows the arrangement employed. The standard mask design was altered to eliminate edge attack. The new thinning mask is made of $\frac{1}{8}$ in. Teflon and retains the standard 11·5 mm diameter hole next to the specimen, but is stepped down to a $\frac{5}{16}$ in. diameter hole part way through the mask. A further alteration lies in the cutting of an air escape slot, $\frac{1}{32} \times \frac{1}{32}$ in., from the polishing hole to the air escape hole.

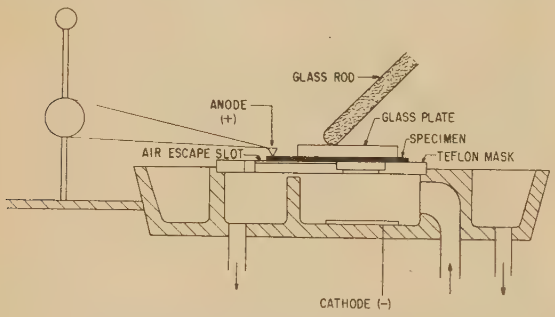

Fig. 1. Schematic section showing specimens and mask in position on the automatic polisher

The method of clamping the specimen to the mask, by means of a hand-held glass rod pressing a glass plate on to the specimen, is of great advantage because it enables one to observe the last stages of thin film preparation, namely, the holes formed when the sample is "polished through." The specimens used are usually 0·003 to 0·005 in. thick.

The thinning of a specimen is carried out as a routine polishing operation with the exception that the specimen is turned over when it is brightly polished and about half of its original thickness. After turning, the remaining side i polished until the specimen polishes through. Staining o the top polished surface may occur at this point but thi stain is usually of little consequence. Experience will show just how much further polishing is permissible after th initial break through. At the completion of thinning, th specimen is quickly removed from the apparatus, washed dried and immediately stored in a vacuum desiccator. Thin fragments may then be cut from the specimen and examined in the electron microscope. Deterioration occurs durin storage at a rate varying with the metal. Pure iron is parti cularly difficult to store and should be examined within few hours.

The following materials have been successfully thinne using the conditions shown:

	Copper–4% tin	*Pure iron*	*"Nickel silver"*	*Stainless steel*
Initial surface	as rolled	as rolled	as rolled	as rolled
Disa electrolyte	D-2	A-2	D-2	A-2
Flow rate	2	3	2	3
Polishing time interval (s)	20	10	20	15
Current (A)	1·0	1·8	1·8	1·8

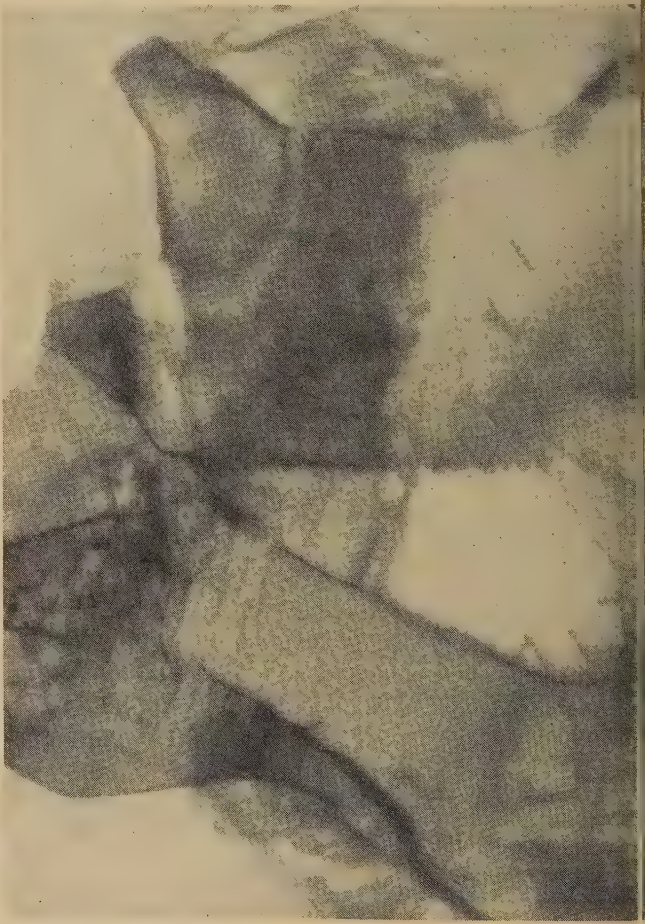

Fig. 2. High-purity vacuum-melted iron, cold rolled heavily and subsequently annealed for 1 h at 690° C and water quenched. Thin foil (×60 000)

The total time to thin a 0·003 in. thick sample varies from about 30 s to 4 min depending on the material and the electrolyte. Polishing is carried out in an intermittent fashion in order to avoid a "hill-valley" structure; the automatic timer is set to the time interval indicated above and reset manually.

The results described below were obtained by examining thin foils of iron and copper–4% tin alloy in a Siemens Elmiskop I electron microscope operated at a voltage of 100 kV.

A number of grain boundaries in annealed and quenched high purity iron are shown in Fig. 2. Some of these are low angle boundaries in which the individual dislocations are clearly resolved. In others all that can be seen are interference fringes running parallel to the boundary; this is typical of a high angle grain boundary. Many dislocations will be seen inside the grains, in fact, this particular region had an unusually high dislocation density for an annealed sample. A number of dislocations emanating from a source near the upper right-hand corner of the micrograph have moved towards the low angle boundary at the centre of the micrograph and some have passed through.

A very high dislocation density is apparent in a heavily rolled copper–4% tin alloy shown in Fig. 3. No grain boundaries are visible, probably because the area is within a single grain. Many irregular Bragg fringes are visible due to variations in thickness and complex buckling. Six or more stacking faults may be seen running through the thickness of the foil, apparently on the same type plane. These are bounded by the two surfaces of the foil giving the parallel-sided appearance. Such faults have been studied in detail in stainless steel, but have not previously been observed in copper–tin alloy.

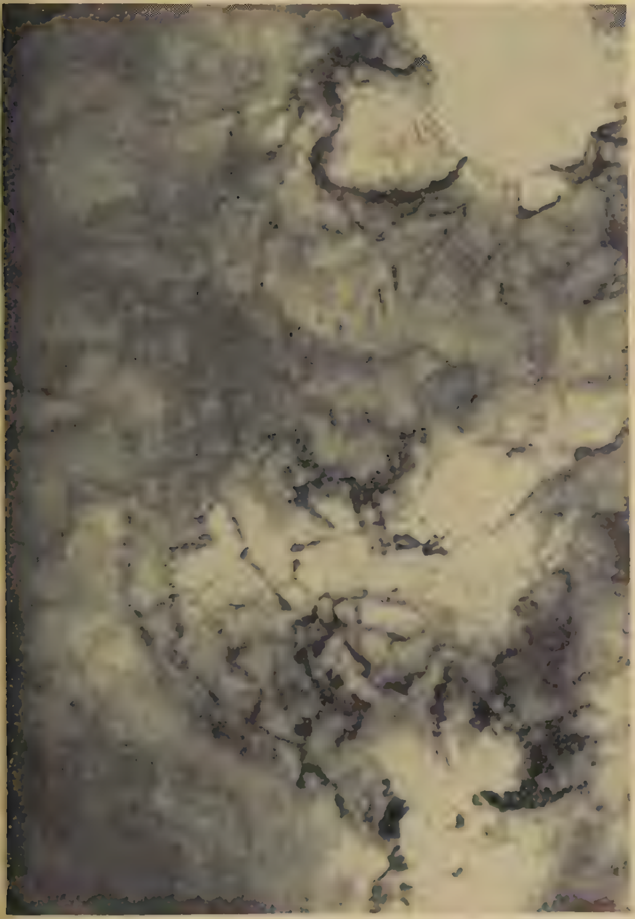

Fig. 3. High-purity copper–4% tin alloy cold rolled to 96% reduction. Thin foil (×60 000)

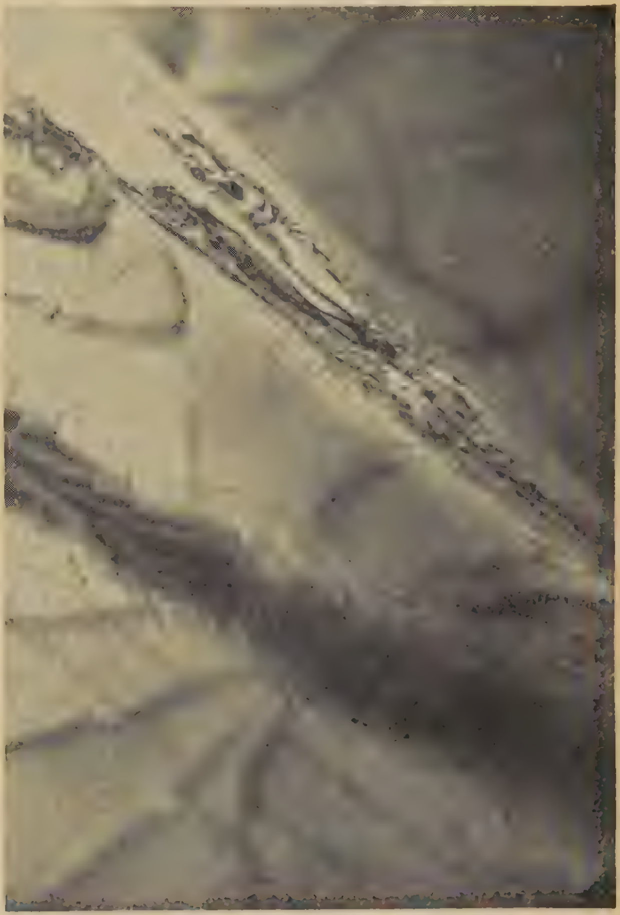

Fig. 4. As Fig. 2, but annealed for 1 h at 600° C. (×60 000)

In the annealed condition (Fig. 4) the copper–tin alloy shows a tremendous decrease in the dislocation content. Dislocations on at least three different types of slip planes are visible. It was possible to move dislocations in this foil by means of thermal stresses induced by heating in the beam. Many of the dislocations as they pass through the foil from surface to surface show the typical variations in contrast which has been previously observed in other materials and theoretically interpreted by Whelan and Hirsch.$^{(7-8)}$

References

(1) Heidenreich, R. D. *J. Appl. Phys.*, **20**, p. 993 (1949).

(2) Bollman, W. *Phys. Rev.*, **103**, p. 1588 (1956).

(3) Nicholson, R. B., Thomas, G., and Nutting, J. *Brit. J. Appl. Phys.*, **9**, p. 23 (1958).

(4) Tomlinson, H. M. *Phil. Mag.*, **3**, p. 867 (1958).

(5) Brandon, D. G., and Nutting, J. *Brit. J. Appl. Phys.*, **10**, p. 255 (1959).

(6) Mirand, P., and Saulnier, A. *C. R. Acad. Sci.* (*Paris*), **246**, p. 1688 (1958).

(7) Whelan, M. J., and Hirsch, P. B. *Phil. Mag.*, **2**, p. 1121, (1957).

(8) Whelan, M. J., and Hirsch, P. B. *Phil. Mag.*, **2**, p. 1303 (1957).

Two-valve electrometer circuit

by J. P. Keene, Ph.D., Physics Research Department, Christie Hospital and Holt Radium Institute, Manchester

[*Note first received* 16 *September, and in final form* 9 *December*, 1959]

This note describes a simple electrometer circuit the linearity output impedance, input impedance, voltage swing and zero-stability of which are adequate for many purposes. A battery and a mains operated version are shown and it is suggested that more complicated circuits are unnecessary in many applications.

Two valve-electrometer circuits using an electrometer pentode stage of high gain coupled to a cathode follower have been described by Moody,* Fedoruk, Johns and Watson,† and Steele.‡ In these circuits, the maximum possible loop gain (several hundred) is obtained (*a*) by coupling the anode of the electrometer directly to the grid of the cathode follower and inserting a battery in the feedback connexion, and (*b*) by supplying the anode voltage of the electrometer from a battery connected to the cathode of the cathode follower. The first of these expedients eliminates attenuation in the interstage coupling, and the second provides the electrometer valve with an apparent anode load of approximately infinite value. For many applications, these refinements are unnecessary since adequate loop gain can be obtained by using a voltage-dividing chain to couple the electrometer to the cathode follower, and by supplying the electrometer and cathode follower from the same h.t. supply. This procedure considerably simplifies the circuit and has the advantages of eliminating two batteries and of making the circuit easily adaptable to mains operation. Sufficiently high loop gain to ensure good linearity, low output impedance and considerable reduction in input capacity is still obtained.

Fig. 1 and 2 show a battery and a mains-operated version of this modified circuit. The latter is shown with a double triode which combines the function of output cathode follower (V_{2A}) and h.t. regulator (V_{2B}). Input voltage, developed across a high resistance or a capacitor, is applied between *A* and *B*, and the output between *C* and *B* is $\alpha/(1+\alpha)$ times the input, where α is the loop gain. With a large value of α, the circuit can be regarded as an impedance-changing device of almost infinite input impedance and relatively low output impedance. A value of α of about 60 is obtained in the circuits shown, and results in linearity better than that of most moving-coil voltmeters, and a time constant of 1·5 s with an input resistance of 10^{12} Ω provided cable capacitances do not exceed 20 pF. Over the operating range, the output impedance of the battery version is 30 Ω and of the mains version 2 Ω. The former will thus easily drive a 10000 Ω/V meter (100 µA full-scale deflexion) and the latter a 1000 Ω/V meter. In the battery version, zero fluctuations are less than 0·2 mV over short times but the zero drifts a few millivolts per hou as the batteries run down. In the mains version with th regulated supply shown in Fig. 2, the zero changes 2 mV fo a change of 1 V in mains voltage. This can be brough down to 0·05 mV/V by using a series regulated h.t. supply and a constant voltage transformer for V_2 heater, but mechanical shock is still liable to cause zero shifts of a few millivolts. In Fig. 1, cathode current of V_2 is 900 µA. This

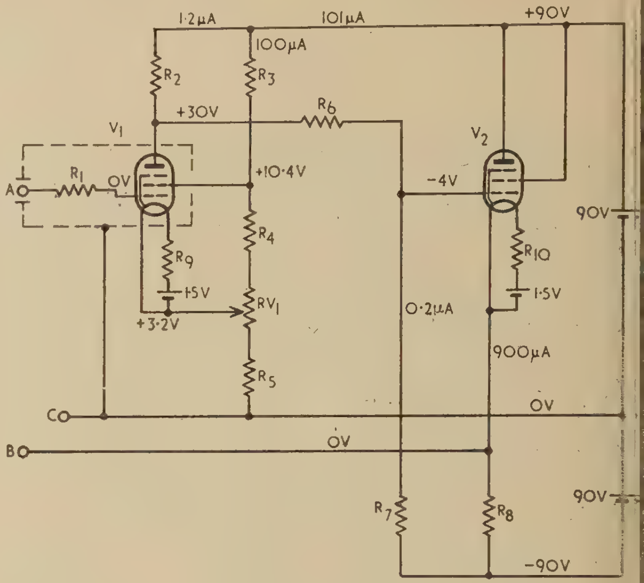

Fig. 1. Battery circuit

V_1 = ME1403 (Mullard)
V_2 = DL69 (Mullard)
R_1 = 10 MΩ
R_2 = 50 MΩ
R_3 = 820 kΩ
R_4 = 68 kΩ
R_5 = 30 kΩ
R_6 = 150MΩ
R_7 = 500 MΩ
R_8 = 100 kΩ
R_9 = 30 Ω
R_{10} = 10 Ω
RV_1 = 5 kΩ

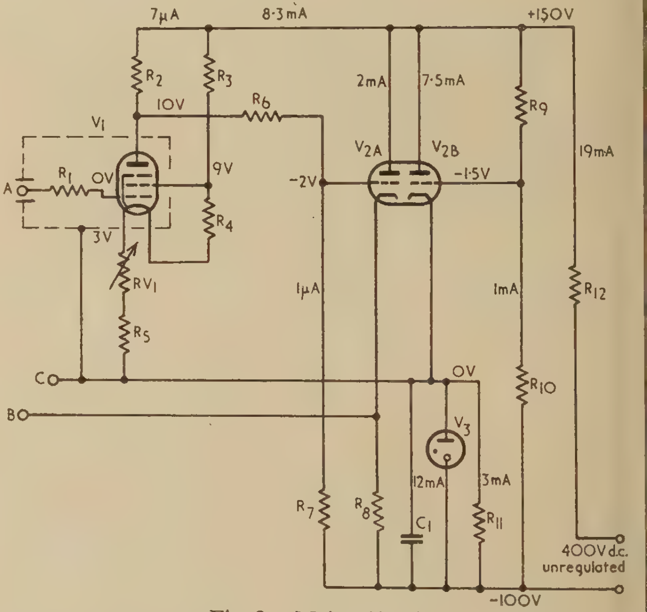

Fig. 2. Mains Circuit

V_1 = ME1403 (Mullard)
V_2 = ECC81 (Mullard)
V_3 = 108C1 (Mullard)
R_1 = 10 MΩ
R_2 = 20 MΩ
R_3 = 17 kΩ
R_4 = 750 Ω
R_5 = 300 Ω
R_6 = 10 MΩ
R_7 = 100 MΩ
R_8 = 50 kΩ
R_9 = 140 kΩ
R_{10} = 100 kΩ
R_{11} = 33 kΩ
R_{12} = 8 kΩ
RV_1 = 100 Ω
C_1 = 1 µF

---

* Moody, N. F., *Rev. Sci. Instrum.*, **22**, p. 236 (1951).

† Fedoruk, S. O., Johns, H. E., and Watson, M. B. *Radiology*, **62**, p. 177 (1954).

‡ Steele, R. E. *Radiology*, **72**, p. 242 (1959).

can be reduced to about 200 μA (by increasing R_8) when low battery drainage is of importance, provided an increase in output impedance can be tolerated. Zero setting is by means of RV_1, and part of R_5 can be made variable for use as a coarse preset zero control. Alternatively the zero setting can be done by varying the screen grid voltage of V_1. A three-position on-off switch is required in order to supply filament current to V_1 before the application of screen grid and anode voltages. This switch should also short the output meter in the intermediate and off positions.

The maximum allowable voltage swing of the electrometer valve anode is 40 V (5–45 V with respect to filament negative). This limits the output swing of the circuit to about 30 V. The anode voltage with zero input can be set initially to any value by adjusting R_6. If only negative inputs are anticipated, it should be set to a low value (about 6 V), while for positive inputs, a high value (up to 45 V) is required. The grid current varies considerably from valve to valve and depends on anode voltage. Typical values are 10^{-14} A with the anode at 9 V and 10^{-13} A at 45 V. This limits the usefulness of the circuit for large positive inputs when the anode is at a high voltage with zero input. The grid current increases more rapidly with anode voltage than a linear relationship would give, so that it is only at values considerably greater than 9 V that the increase is of significance. When a larger grid current can be tolerated and a bigger voltage is to be measured the ME1403 can be replaced by an ME1400 which has a grid current in the region of 10^{-11} A and a maximum anode voltage of 90 V. Values of α considerably greater than 60 can be obtained with this valve. It is indirectly heated, and requires 0·16 A heater current. With the heater supplied from an unregulated transformer and with the regulated h.t. supply shown in Fig. 2, the variation of zero with mains is 5 mV/V. This can be reduced to 1 mV/V by using a small constant-voltage transformer to supply both heaters.

The circuits can be earthed at either *B* or *C*, but *C* should normally be connected to cable screening in order to degenerate cable capacitance. It is also sometimes convenient to earth the negative supply to provide a polarizing voltage for an ionization chamber. For this, the earthed negative line is connected to the outer electrode and the point *C* to the cable screening and the chamber guard electrode. Cable capacitance and chamber capacitance are then both degenerated.

Voltage-range switching is best achieved by varying the sensitivity of the output meter rather than by the more common method of altering the feedback factor. This has the advantage that the loop gain is the same on all ranges instead of becoming smaller on the more sensitive ranges. A high loop gain is very desirable at the limits of sensitivity since it is then that degeneration of input capacitance is most valuable. However, it is sometimes convenient to arrange for the feedback factor to be variable between say 0·7 and 1·0 to compensate for variations in a set of input capacitances or resistances.*

The circuits described here are adaptable to many uses and several instruments based on them have been constructed in this department. They include a general purpose multi-range voltmeter as well as instruments for the measurement of ionization-chamber currents, vacuum ionization-gauge currents, photomultiplier anode currents, and the charges on an array of high-insulation capacitors used with a multiple geiger-counter chromatogram scanner.

---

* Stuart, S., and Osborn, S. B. *Phys. Med. Biol.*, **3**, p. 255 (1959).

Welding copper pipe to stainless-steel flanges in a laboratory workshop

by J. Leece, U.K. Atomic Energy Authority (Development and Engineering Group), Research and Development Branch, Capenhurst, Chester

[*Note first received* 6 *January, and in final form* 8 *March*, 1960]

Methods of brazing stainless steel to copper in high vacuum by means of an r.f. induction heater have already been described, for example, by Liebson.† Such methods usually involve performing the operation within a glass vessel to allow the operator to control the progress. However, if the components to be brazed are large or made unwieldy by jigs, the size of the glass vessel may become prohibitively large. In addition, the presence of jigs may lead to poor r.f. coupling. To overcome these difficulties, a method has been evolved in this laboratory for welding copper pipe to stainless-steel flanges by means of a conventional argon-arc non-consumable electrode welding set in normal workshop conditions.

A sectional view of the machining necessary to the stainless-steel flange is shown in Fig. 1. A spigot of twice the wall thickness of the copper pipe is machined: the depth and width of the recess are unimportant, but $\frac{1}{8}$ in. is a convenient dimension for both. The edge of the copper pipe is bevelled as shown, and a ring of 0·020 in. diameter fine gold wire is laid in the resulting groove. With a direct current of 35–40 A, used with a thoriated-tungsten electrode tapered to a needle point, the copper, stainless steel and gold are fused together; at the same time, a gold wire of 0·020 in. diameter is fed into the point of melt as one would use a filler rod. The amount of gold fed in is comparatively small: 3–4 in. of 0·020 in. diameter wire are required per inch of weld. Although the weld is normally made with complete success with wire of this diameter laid in the groove, it is inclined to run away from the arc, and 0·030 in. diameter wire would probably be easier to work with.

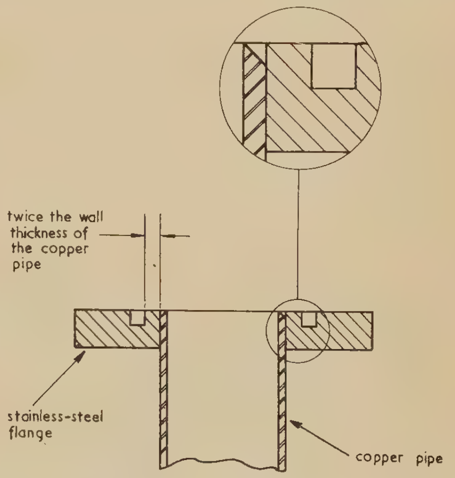

Fig. 1. Machining required on stainless-steel flange

Fig. 2 shows test-pieces of 1 in. nominal-bore copper pipe welded to 2 in. diameter stainless-steel flanges by this method, before and after the weld was dressed. Since the joint is an edge weld, care must be exercised when the weld is cleaned up. Fig. 3 shows the analyser tube of a mass spectrometer, consisting of a 90-deg. arc of 6 in. radius made from 1 × ½ in. copper waveguide, before the weld was dressed.

---

† Liebson, M., *Rev. Sci. Instrum.*, **30**, p. 369 (1959).

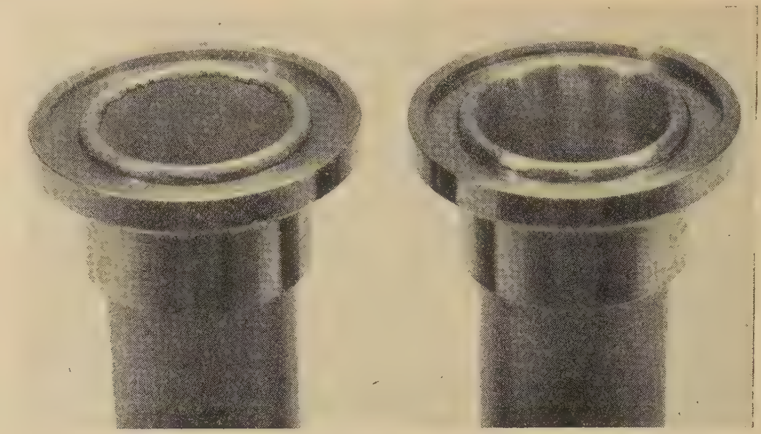

Fig. 2. Weld before and after machining

To assess the strength of such welds, a copper and a stainless-steel plate, each of dimensions 3 × 3 × 1/16 in., were placed face to face and welded along one edge. The plates were prised apart, and folded back against the weld in a vice. The plates were almost completely folded back before the weld tore. Further tests with similar samples showed a high uniformity of behaviour, and indicated a weld strength comparable with that between mild steel plates welded by conventional methods.

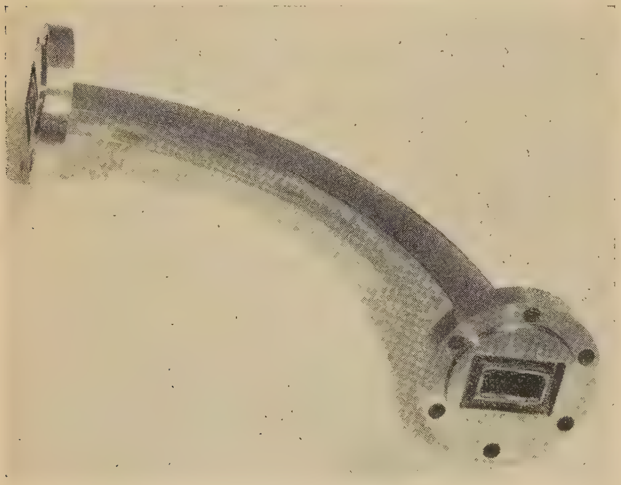

Fig. 3. Analyser tube for mass spectrometer, showing weld before dressing

To assess the weld for use in high-vacuum systems subjected to heat cycling, test-pieces as shown in Fig. 2 were heat-cycled as follows: the copper pipe was rapidly heated to bright red by a blow-torch, thus giving rise to a considerable temperature gradient across the weld and also across the stainless-steel flange. The test-pieces were then quenched in water and vacuum-tested by means of a helium leak detector supplied by Consolidated Electrodynamics Corporation. None of the test-pieces leaked, even after five or six similar heat cycles.

The co-operation of Messrs. J. R. Kent and C. Rawbone is gratefully acknowledged. This Note is published by permission of Sir William Cook, Managing Director, and Dr. H. Kronberger, Director of Research and Developmen of the U.K.A.E.A. (Development and Engineering Group).

Simple multi-position level

by C. J. Sumner, A.M.S.E., Division of Meteorological Physics, Commonwealth Scientific and Industrial Research Organization, Victoria, Australia.

[*Note first received* 12 *August*, 1959, *and in final form* 15 *February*, 1960]

In many scientific operations it is necessary to be able t adjust equipment accurately in a number of attitudes; this i usually done by mounting separate level bubbles for eac position required, or by fitting an adjustable bubble capabl of being set to the required positions. The simple levellin device described below was designed to avoid the use o numbers of bubbles, or an adjustable bubble which may b in error due to faulty setting.

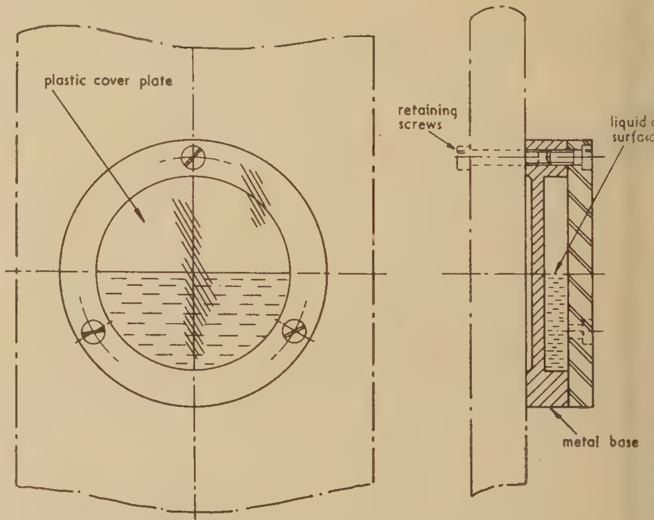

Two views of the multi-position level

As shown in the figure, the level consists of a metal block having a circular cavity machined in it, approximately 2 in inside diameter by ¼ in. depth. A clear plastic cover plat having radial lines engraved on the back, at the require angles, is fitted centrally over the cavity. This is then partially filled with coloured liquid (e.g. alcohol) so that its leve oincides with one of the engraved lines. When the unit is ounted in a suitable position on the equipment the latter n then be adjusted to the required positions by lining up the ppropriate engraved lines with the liquid surface. The btainable accuracy of setting is governed by the diameter of vity, being with the above dimensions within ±9′.

Report on a pump-operated air aspirator

by A. Nunlist and P. H. Kitto, M.Sc., Dust and Ventilation Research Laboratory, Transvaal and Orange Free State Chamber of Mines, Johannesburg, South Africa

[*Note received* 17 *August*, 1959]

he most accurate dust-sampling instruments for collecting ust of respirable size in order to examine it with the light microscope or the electron microscope, are those using the rinciple of thermal precipitation. One of the difficulties ssociated with this type of instrument, particularly when ong-period samples are required, is the production of a slow teady flow of air through the instrument. In the standard orm of thermal precipitator a water aspirator is usually sed for this purpose, and for the modified thermal pre-ipitator a bellows-operated aspirator was developed. This nd other types of aspirator have been adopted for various modifications of the thermal precipitator, but there was still need for a smaller, lighter and more reliable type of aspirator which could operate for long periods without attention. The iaphragm pump described in this note was developed to meet this need, but it might prove useful in many other ields. Details of the pump are shown in the figure.

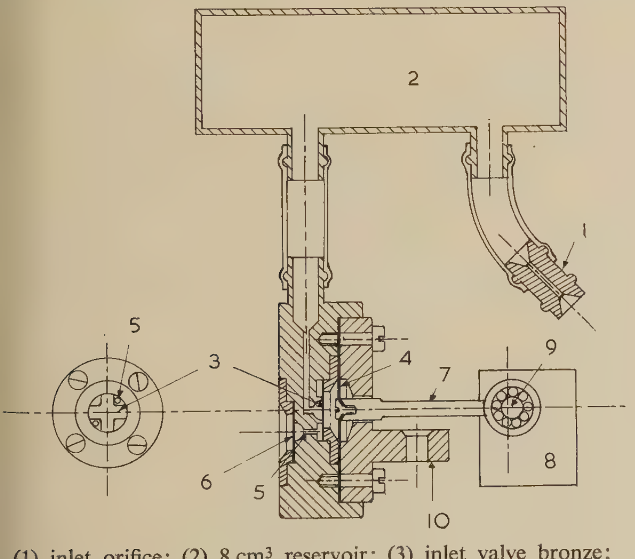

(1) inlet orifice; (2) 8 cm³ reservoir; (3) inlet valve bronze; (4) pump diaphragm; (5) outlet ports; (6) outlet valve; (7) reciprocating arm; (8) motor; (9) eccentric; (10) mounting bracket

Inset: Diagram of pump with diaphragm removed showing inlet valve and outlet ports

A crank giving a throw of 0·5 mm is fitted to the shaft of motor revolving at 960 rev/min. The reciprocating arm uns on a miniature ball-bearing; at the small end the arm s fixed to a diaphragm of reinforced plastic sheet, 9 mm in diameter. Both valves are made of beryllium bronze.

The pump intake is connected to a damping reservoir of pproximately 8 ml. capacity, and the inflow rate of air to the reservoir is controlled by a baffle to give slightly more than the required airflow. The orifice diameter of the baffle depends on the size of the reservoir and is fairly critical. These conditions proved successful in reducing the pulsations from the pump to a negligible amount. A small needle valve is fitted on to the reservoir as a bleeder, in order to make the final adjustment in the rate of aspiration.

The first pump made was intended to be used with a modified thermal precipitator, and it has been thoroughly tested at an aspiration rate of 10 ml./min. Used in conjunction with a 20 ml. Rotameter, the airflow was shown to be remarkably steady even for hours of continuous running, the float of the Rotameter remaining practically stationary. The different conditions of temperature and humidity met with underground appeared to have no effect on the operation of the pump.

A 3 V d.c. miniature motor is used to drive the pump. It runs at 15 mA when geared from 2500 to 960 rev/min without the pump, and 18·5 mA with the pump, so that the pump consumption is only about 10 mW.

Acknowledgement is made to the Transvaal and Orange Free State Chamber of Mines for permission to publish this note, and to the members of the staff of the Dust and Ventilation Laboratory who assisted in this project.

Construction of a thermocouple for measuring surface temperatures

by L. Ongkiehong, and J. van Duijn, Koninklijke/Shell-Laboratorium, Amsterdam (Shell Internationale Research Maatschappij N.V.)

[*Note first received* 1 *February, and in final form* 3 *March*, 1960]

For static and dynamic temperature measurements on the inner wall of a running combustion engine, a thermocouple construction of small dimensions was required, in order to cause the least possible disturbance of thermal conditions.

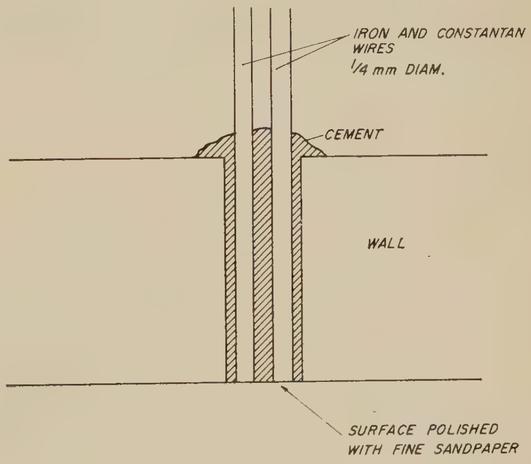
IRON AND CONSTANTAN WIRES
1/4 mm DIAM.
CEMENT
WALL
SURFACE POLISHED WITH FINE SANDPAPER

Construction of thermocouple

The construction also has to be as flush as possible with the surface, otherwise damage will be caused by moving piston rings. Bendersky* has described a thermocouple with favourable properties. Through a small hole perpendicular to the wall he inserts a steel tube containing an insulated nickel wire. The end is covered with nickel by vacuum deposition. As it is difficult to make the front of this couple flush with the surface and as, moreover, the bonding properties of nickel, especially to the cement used to fix the thermocouple in position, were unsatisfactory for the present application, the following modified procedure was developed.

---

* Bendersky, D. *Mech. Engng*, **75**, p. 117 (1953).

Through the wall, a hole with a diameter of about 1 mm is drilled. Two bare thermocouple wires (iron and constantan, 0·25 mm, diam.) are inserted, so as to protrude a few millimetres at the other end. The wires are cemented with a heat-resistant material.* During cementing, care must be taken to avoid electric contact between the wires, or between one of the wires and the wall. The cementing material can be considered as an ideal insulator compared with the impedance of the thermocouple. After the cement has hardened, the protruding part is polished flush with the surface by means of fine sandpaper.

The hot junction is made by plating the ends of the wires and their immediate surroundings. To obtain the required resistance to wear, good adhesion of the plating to the thermocouple wires and to the cement is essential. Tests with vacuum and electrolytic deposits of various metals gave unsatisfactory results; especially, the bonding to the cement was poor. Excellent results were obtained with an electroless nickel process† in which nickel chloride is reduced according to:

$$NiCl_2 + NaH_2PO_2 + H_2O \longrightarrow Ni + NaH_2PO_3 + 2\,HCl.$$

The surface to be plated must be very clean and, accordingly, the following procedure, which includes an activation treatment, is applied:

1. Polishing with very fine sandpaper;
2. Polishing with MgO or $MgCO_3$;
3. Removal of grease with a solution of 30 g of sodium triphosphate in 1 l. of distilled water at 90° C;
4. Removal of rust with 1 : 1 HCl;
5. Immersion for 1 min in a solution of 10 g of $SnCl_2$ plus 10 ml of HCl in 1 l. of distilled water;
6. Immersion for 1 min in a solution of 1 g of $PdCl_2$ in 1 of distilled water.

After each manipulation, the surface is cleaned carefully wi distilled water before the next is started.

For plating, the following bath composition was used:

$NiCl_2 \cdot 6\,H_2O$	30 g;
NaH_2PO_2	10 g;
Sodium lactate (60% aqueous solution)	30 g;
Distilled water	1 000 g.

Deposition of nickel starts at about 90° C, at a fairly consta rate of 13 μ/h. If a very large amount of nickel has to deposited, the acidity (pH) must be kept at a value of about The addition of sodium lactate considerably improves t adhesion of nickel, especially to the Devcon cement.

After plating, the surface is polished. Satisfactory lengt of life were obtained with nickel layers having a thickne of 25 μ.

If surface temperatures must be measured in places whe no mechanical load is present, the nickel layer can be ke much thinner, and the time constant of its response to ter perature fluctuations is then reduced. This thermocoup construction may also be suitable for measuring the he flux through a metal plate. In this case two thermocoupl should be mounted, one on either side of the plate.

The errors in the measurement of rapid temperatu fluctuations are mainly determined by the thickness of t nickel layer. When measured under static conditions, possible errors are very small as long as the hole diamet is small in comparison to its length. The isotherms rema essentially straight lines in the transition from the ir into the cement.

---

* Devcon WR Special, a product of Devcon Corporation, Danvers, Massachusets, U.S.A., was used. It consists of 80% steel and 20% plastics. The hardener provided is added between 100 and 125° C. An additional treatment at 175° C is necessary to make the material stable up to 205° C.

† De Minjer, C. H., and Brenner, A. *Plating*, **44**, p. 1297 (1957).

Simple agitating device for partition experiments

by L. Bishop, H. J. de Bruin, M.Sc., and R. B. Temple, D.Phil., Australian Atomic Energy Commission Research Establishment, Sydney, Australia

[*Note received* 1 *December*, 1959]

During a series of solvent extraction investigations, a simp shaking device was needed which would allow several reacti vessels to be agitated simultaneously in a constant temperatu

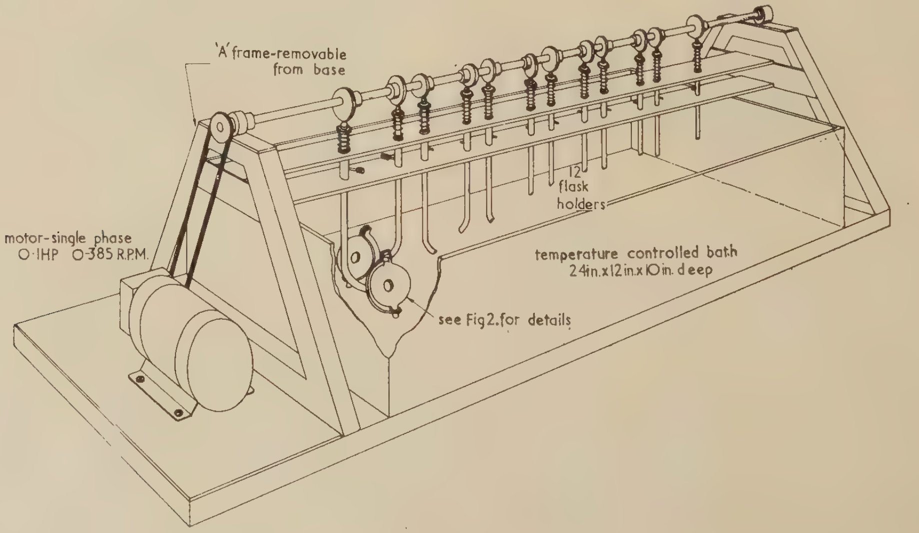
'A' frame-removable from base
12 flask holders
motor-single phase O·IHP O·385 R.P.M.
temperature controlled bath 24in.x12in.x10in. deep
see Fig2.for details

Fig. 1. Complete assembly of agitating device

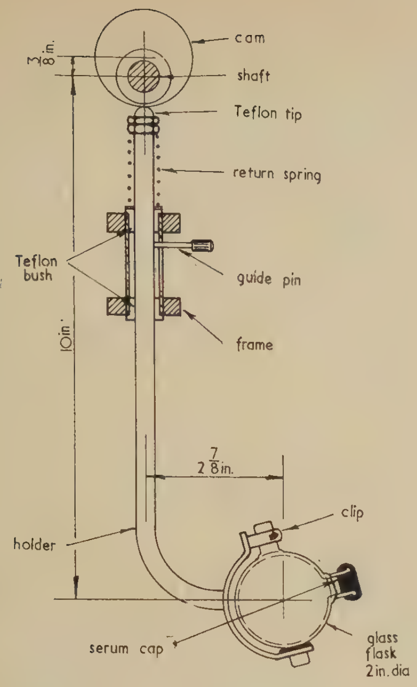

Fig. 2. Flask holder

ath. Because of the need to produce intimate mixing of an rganic and an aqueous phase, vigorous movement is needed ithout splashing. In addition, in experiments involving the measurement of reaction-rates it is necessary to be able to sample any one vessel without interrupting the mixing of the others. Since no commercial shaking machine appeared suitable one was developed, in which simplicity was made a special feature.

In principle the shaker operates similarly to the valves of an internal combustion engine. Each reaction vessel is held on a vertical rod which is spring-loaded to press against an eccentric cam operated by an overhead camshaft. Rotating the camshaft causes the reaction vessels to oscillate in a vertical direction. The cams are staggered so as to reduce the variations in load on the motor.

The diagrams are self-explanatory. Provision is made for up to twelve glass reaction bulbs (Fig. 1), which are held in place by a stainless steel spring-clip. The sliding mechanism and bearing-members which are immersed in the water bath are of stainless steel and the bearings have Teflon inserts. The movement on any slide can be stopped independently of the others by depressing the shaft against the spring and turning it to engage a simple catch.

Using a 0·1 h.p. single-phase motor geared down to 385 rev/min, the frequency of oscillation can be varied from zero to 385 strokes per minute. This range of frequencies has been found to be completely adequate for the solvents used. These included chloroform, benzene, butex and hexone.

The reaction bulbs are constructed as shown in Fig. 2. The glass rods at top and bottom are used for positioning the bulb in the cradle of the sliders. Filling and sampling is done through the side, which is closed by a rubber serum cap. Samples of both phases are withdrawn using a hypodermic syringe.

ORRESPONDENCE

Influence of protective paper on X-ray diffraction photographs

n X-ray diffraction studies, the film is often protected against xposure to light by a layer of black paper. We have found hat this protective paper is a potential source or error when ccurate intensity measurements are required. The errors in uestion are due to the following factors. (1) Many protective papers are not lightproof but contain a large number of inholes. This can be demonstrated readily by examining he paper against a bright background. Spots due to these inholes may easily be superimposed on the diffraction attern. (2) The mass per unit area of the protective paper s not constant, and consequently the absorption of the iffracted rays varies over its surface.

Photometer traces of a fine-grained film irradiated through various protective papers are shown in the figure. Ilford C ilm was placed in a cassette about 10 in. from the point focus window of the X-ray tube. Uncollimated nickel-filtered copper radiation was used, and the time of exposure was adjusted to give an optical density in the range of 0·3–0·9.

It is seen that the almost smooth curve for the uncovered ilm (curve 1) gives way to progressively more pronounced irregularities as the surface density variations in the covering material increases. Sharper irregularities are observed under reduced target loads.

To avoid the need for the protective paper, the camera was enclosed in a lightproof cloth bag which could be closed by means of a zip-fastener.

As a consequence of these observations, the possibility may

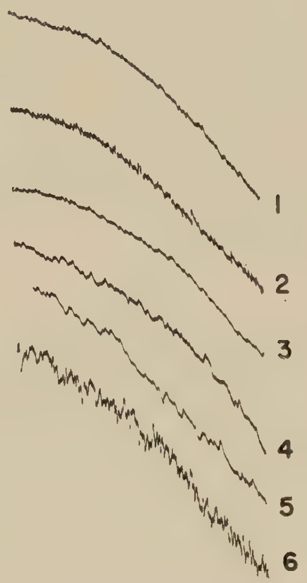

Photometer traces of Ilford C films protected with the following materials during irradiation. (Experimental conditions: 200 kVs 5 mA)

Curve (1), bare film; curve (2), Ilford C film previously fully exposed and developed; curve (3), Supronyl foil (thin lightproof super-polyamide, by Kalle and Co. A.G., Wiesbaden); curve (4), Kodak yellow paper (not light-proof, more of a surface protector of X-ray films); curve (5), Ilford black paper; curve (6), Nylon camera-shutter cloth have been found for using X-radiation in the study of surface density variations in paper. This has previously been investigated by scanning with a beam of visible light.* However, in such methods an appreciable amount of the incident light is converted into Raleigh scattering and, since Beer's law is not obeyed, the fluctuations in intensity of the transmitted light cannot be related directly to the surface density variations of the scanned sheet. In contrast, preliminary X-ray investigations of pulp sheets indicate th soft or medium radiation might overcome these limitatio of visible light.

Physical Chemistry Division,
Pulp and Paper Research Institute
of Canada,
and Department of Chemistry,
McGill University,
Montreal,
Canada

H. Ruck
M. Kouris
R. St. J. Manle

[9 *February*, 196

---

* Favis, D. V., Robertson, A. A., and Mason, S. G. *Canad. J. Tech.*, **30**, p. 280 (1952.)

NOTES AND NEWS

Notes and comments

Journal of Nuclear Energy: Part C

We have received the first issue of the *Journal of Nuclear Energy: Part C* which combines Numbers 1 and 2 of Volume 1. This new journal, edited by Dr. J. V. Dunworth, covers plasma physics, accelerators and thermonuclear research. It is intended to publish translations of the numerous and important papers produced in Russia in order to make them available for physicists unable to read the originals. Among the contributions contained in the first issue are the following: M. A. Leontovich: Some investigations on the physics of a heated plasma and its containment; J. W. Burren, D. Morgan and W. Walkinshaw: Production of high density proton currents for colliding beam accelerators; Mitsuo Imoto: Essential limitations and *T-Nt* diagram for self-sustaining fusion systems; J. D. Lawson: On the classification of electron streams; P. Reynolds and H. M. Skarsgard: A plasma betatron; B. Lehnert: On the confinement of charged particles in a magnetic field; E. W. Laing, S. J. Roberts and R. T. .P Whipple: Equilibrium configurations of a toroidal plasma; P. F. Smith: An experimental and theoretical investigation of the magnetic field produced by ridged pole-pieces.

The journal is to be published quarterly and the subscription is £7 per volume (U.S.A. $20). The publisher is Pergamon Press Ltd.

Coke and chemistry, U.S.S.R.

The Russian technical journal *Koks i Khimiya* is now being translated into English and published monthly under the above title at an annual subscription rate of £5 5*s*. This journal is sponsored by the Department of Scientific and Industrial Research and is produced by the Coal Tar Research Association in collaboration with the British Cok Research Association.

Each issue consists of approximately 60 pages and th original tables and diagrams are reproduced in the Engl version. Current advances in Russian coking technolog are described and should be of interest to technical staff co cerned in the production of metallurgical and gas coke an the recovery and refining of the by-products of co carbonization.

Further information, specimen copies and order for may be obtained from the Intelligence Officer, The Coal Ta Research Association, Oxford Road, Gomersal, Leeds, c from the Information Officer, The British Coke Researc Association, Chesterfield, Derbyshire.

British Journal of Applied Physics

Contents of the June issue

SPECIAL ARTICLE

Principles of thermoelectric devices. By H. J. Goldsmid.

PAPERS

Choice of frequency for eddy-current tube testing. By F. R. Bareham.
Charge localization on the surfaces of oxide-coated cathodes. By B. J. Hopki and F. A. Vick.
New technique for measurement of low dissolved-air content of water. E D. M. J. P. Manley.
Determination of orientation of bismuth single crystals using back-reflexio technique. By H. D. Mallon and C. G. Wilson.

NEW BOOKS SECTION

Reviews (and notices).

PAPERS (continued)

The measurement of surface stress in austenitic steel. By J. C. Moore.
Analogy between the slow motion of a viscous fluid and the extension and flexu of plates; a geometric demonstration by means of Moire fringes. By T. F Richards.
Determination of the elastic moduli of tin single crystals, and their variation wit temperature. By D. G. House and E. V. Vernon.
Measurement of atomic differential scattering cross-sections. By J. S. Halliday

NOTES AND NEWS

Notes and comments

THIS *JOURNAL* is produced monthly by The Institute of Physics, with the co-operation of the National Physical Laboratory. It deals with the principles, construction and use of scientific instruments. All rights reserved. Responsibility for the statements contained herein attaches only to the writers.

EDITORIAL MATTER. Communications concerning editorial matter should be addressed to the Editor, The Institute of Physics, 47 Belgrave Square, London, S.W.1. (*Telephone:* Belgravia 6111.) Prospective authors are invited to prepare their scripts in accordance with the *Notes for Authors*. (Price 3*s*. 6*d*. including postage.)

REPRODUCTION. The Institute of Physics is a signatory to The Royal Society's Fair Copying Declaration. Details may be obtained upon application from The Royal Society, London, W.1.

ADVERTISEMENTS. Communications concerning advertisements should be addressed to the agents, Messrs. George Jackson (Fleet St.) Ltd., Cliffords Inn, Fleet Street, London, E.C.4. (*Telephone:* Holborn 3611–2.)

CLAIMS FOR MISSING JOURNALS. Claims from regular subscribers to this *Journal* for missing numbers will only be considered if received within 60 days of the date of mailing plus normal outward time of transit and time for lodging the claim. Losses attributable to failure to notify a change of address or to similar omissions will not be considered.

SUBSCRIPTION RATES. A new volume commences each January. The charge is £6 per volume ($17 U.S.A.), including index (post paid) payable in advance. Single parts, so far as available, may be purchased at 12*s*. 6*d*. each ($1.75 U.S.A.), post paid, cash with order. Orders should be sent to The Institute of Physics, 47 Belgrave Square, London, S.W.1, or to any bookseller.

PRINTED IN GREAT BRITAIN BY UNWIN BROTHERS LIMITED, WOKING AND LONDON

Ieasurement of magnetostriction within the temperature ange −196 to 400° C

R. R. BIRSS, B.Sc., Ph.D., A.Inst.P., Imperial College of Science and Technology, London
d E. W. LEE, B.Sc., Ph.D., Physics Department, University of Sheffield

aper first received 6 *November*, 1959, *and in final form* 25 *January*, 1960]

Abstract

n apparatus is described which permits the magnetorictive behaviour of small single-crystal or polycrystalline ecimens to be investigated over a range of temperatures om −196 *to* 400° *C. Resistance strain gauges are nployed and the performance of a number of gauges has en investigated at these temperatures. Details are ven of the techniques used to obtain a reliable overall rain sensitivity of* 2×10^{-7} *per mm deflexion of the dicating galvanometer. The procedure by which the ngle-crystal magnetostriction constants may be obtained om strain measurements at saturation is outlined for e case of a disk-shaped crystal in which the plane of e disk is normal to one of the three principal crystalloaphic directions.*

1. Introduction

THE magnetostriction constants of a ferromagnetic substance are, like the spontaneous magnetization and crystal anisotropy, intrinsic, and not structure-sensitive roperties of the material. They may be defined as the onstants C_1, C_2 in equation (3) or by analogous equations, nd should not be confused with the various other magnetotrictions, longitudinal, linear, transverse and so on. These uantities are invariably a measure of the fractional change f length with respect to a reference state, the so-called lemagnetized state, which from a magnetostrictive point of iew is not merely arbitrary but unknown. They are thereore structure sensitive in so far as the demagnetized state is tself structure sensitive.

Magnetostriction constants are of interest both from a undamental and an applied standpoint. Since the magnetotriction is believed to arise from psuedo-dipolar interactions etween atoms, the magnitude of the observed magnetotriction is a measure of the strength of these. Further, the nagnetostriction constants determine many of the secondary nagnetic properties such as initial permeability and coercive orce, and it is also believed that the response of a ferronagnetic alloy to magnetic annealing is determined by its nagnetostriction constants.(1) Experimental data on magnetostriction constants are still surprisingly meagre although umerous measurements at room temperature exist. Unortunately, however, magnetostriction constants do not vary vith temperature in any systematic or predictable manner, o that room temperature measurements are of limited nterest to the theoretical physicist whose calculations isually refer to absolute zero; nor do they offer any definite ndication of the likelihood of successful magnetic annealing it, say, 500° C. Measurements at low and high temperatures have, of course, been made but, with very few exceptions, these are only of the longitudinal magnetostriction and hence are subject to the uncertainties in the demagnetized state mentioned previously. In an attempt to remedy this state of affairs an apparatus has been developed which permits accurate determinations of magnetostriction constants over a wide range of temperature. It has been successfully used for a large number of materials, both single-crystal and polycrystalline. It is hoped that the following description may prove of use to those contemplating similar measurements.

2. General design of apparatus

The function of the apparatus is to permit the measurement of magnetostrictive strains in ferromagnetic crystals over ranges of temperature and magnetic field. It is also required that the directions of measurement and applied field shall be independently capable of variation relative to the axes of

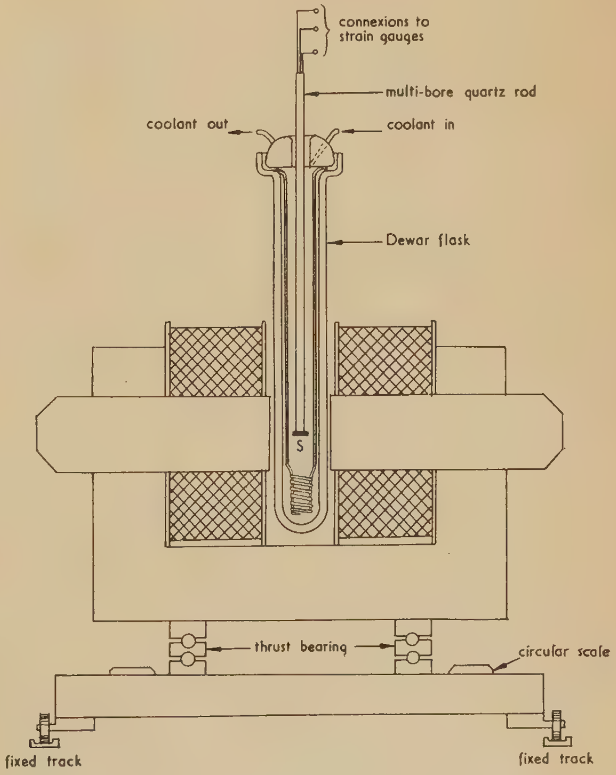

Fig. 1. General design of the apparatus

the crystal. The use of a flat disk-shaped specimen approximating to an oblate spheroid with the equatorial plane coinciding with a principal crystallographic plane is desirable, since this greatly facilitates the mathematical interpretation of the results. It will be shown in Section 5 that, for a given direction of measurement in the equatorial plane, the magnetizing field is to be applied in various directions in this plane. Hence either the specimen or the magnetic field should be capable of rotation. Rotation of the specimen, although the simpler procedure, would be likely to involve disturbance to the associated measuring and temperature control arrangements, whereas rotation of the magnetic field can readily be arranged to avoid such disturbances. The arrangement adopted was therefore to mount the electromagnet on a thrust bearing as shown in Fig. 1. This was mounted on a carriage as shown, thus enabling the magnet to be moved clear of the Dewar flask. In order to accommodate this Dewar flask, a pole gap of not less than 2 in. is required and, to ensure the uniformity of field necessary to prevent large translational forces on the specimen, a magnet with a pole diameter of not less than 4 in. is required. A 4 in. magnet was considered suitable since preliminary design calculations showed that the magnetic field should be constant under these conditions to 0·75% over a central spherical region $\frac{1}{2}$ in. in diameter. The specimen and its associated equipment was rigidly supported from directly above the working position of the magnet.

3. Detailed design considerations

The magnetostrictive strains which are likely to be encountered are small, frequently no greater than 1×10^{-6}. Since this is rather less than one-tenth of the strain that would accompany a temperature change of 1° C, considerable care must be exercised if errors due to spurious effects are to be avoided. This can be achieved only by paying careful attention to points of detail.

3.1 *Specimen support arrangements.* It is required that small disk-shaped specimens be rigidly supported at the centre of the pole gap of the electromagnet, the plane of the disks being horizontal. The support for the specimen is a multi-bore quartz tube which passes through a heavy slate slab surmounting brick pillars built on either side of the magnet.

This tube is rigidly clamped in a mounting fixed to the slab, but a movable member carrying the tube may be unlocked to allow small vertical and horizontal adjustments of the position of the specimen. The temperature enclosure is independently fixed to the lower side of the slab.

The specimen is fixed to the lower end of the quartz tube. Since it is necessary to ensure that one face of the specimen is available for mounting the strain gauges, the upper face could with convenience be fixed to the lower end of the tube. This is open to the objection, however, that the magnetostrictive distortion of the specimen might thereby be restricted. It is necessary therefore to interpose between the specimen and the rod a small degree of flexibility in the horizontal plane. This is achieved by cementing the specimen to an asbestos pad, approximately 1 mm thick, which is in turn cemented to the tube. The texture of the pad is, however, sufficiently close to prevent significant translation or rotation of the specimen. Before fixing the specimen the wall of the tube is slit at each bore sufficiently to allow the conducting leads to be brought out above the asbestos pad.

3.2 *Strain measuring equipment.* The problem of the measurement of small changes in dimension over a temperature range has produced a number of different techniques.(2, 3) The considerable success of the resistance strain gau technique(4) at room temperature suggested that its appli tion, if it could be employed successfully over a temperat range, should offer rewarding results. The chief difficul to be surmounted were ignorance of the temperature variati of gauge factor and failure of both the gauge and its fixat at high temperature. Recent work by Day and Sevan showed, however, that the variation in gauge factor fr room temperature to −183° C was of the order of 5% ordinary commercial gauges supplied for use at ro temperatures. The development by Messrs. H. Tinsley a Co. of experimental gauges for high temperature wo together with a suitable cement, was a further factor favouri this approach to the problem. It appeared, therefore, th the strain gauge technique might be profitably employ provided that the performance of the gauges over t temperature range involved could be accurately establish Such a technique is attractive because it allows a particula simple experimental arrangement. The fractional resistan changes which correspond to magnetostrictive strains may easily and accurately measured with a Wheatstone brid The use of a strain gauge method secures advantages arisi from its particular applicability when dealing with sm specimens. Because the strain is measured directly, particular advantage accrues from the use of specime which exceed appreciably the length of the gauge. Th method does not therefore rely for its accuracy upon the u of large specimens with a correspondingly large magnet strictive displacement. When dealing with single crysta the use of small specimens has an obvious appeal, which heightened when both specimen and associated temperatu enclosure must be accommodated between the poles of electromagnet. Since the strain gauges are cemented to t specimen, this method is insensitive to small translation movements of the specimen as a whole. Thus there is n the possibility, as there is with mechanical methods, of th measurements being affected by such movements arising fro inhomogeneity of the magnetic field.

In the experimental arrangement adopted two stra gauges, forming adjacent arms of a Wheatstone bridge, a used. One of these (*A*, Fig. 2) is the active gauge and cemented in the desired position, to the lower surface of th specimen *S*. The other gauge *D* is a dummy and is place adjacent to the active gauge within the temperature enclosur It is similarly orientated to *A* and is cemented, at one en only, to the corresponding end of the active gauge. Th dummy gauge, whilst being unaffected by the distortion the specimen, is nevertheless at the same temperature and the same magnetic field as the active gauge. Since the gauge are chosen so that their nominal resistances are equal, erro due to temperature variations are thereby considerab reduced and those due to magnetoresistance in the gauge are almost completely eliminated. Each of the gauges use was tested in position for magnetoresistance by replacing th other gauge with a resistance box placed some distance fro the magnet. In no case was a magnetoresistive effe observed, but these measurements could only be performe at room temperature.

The remaining arms of the bridge *B* and *C* are variab resistances placed outside the temperature enclosure. A four arms are of approximately the same resistance.

Resistance *C* is made up of two elements, one an ordinar resistance box and the other the familiar arrangement of large resistance box in parallel with a 10 Ω resistor. Wit such an arrangement it is possible not only to balance th bridge accurately, but also to compensate for resistanc anges in the active gauge induced by thermal expansion the specimen.

The choice of a galvanometer *G* is governed primarily by consideration of its periodic time, rather than its sensitivity its internal resistance. At temperatures other than room emperature, it is difficult to preserve the temperature of the pecimen within limits such that the balance of the bridge is ot sensibly disturbed by changes in the resistance of the ctive gauge arising from the thermal expansion of the pecimen. It is therefore desirable that the galvanometer hould have as short a periodic time as practicable, and the nstrument employed is a Cambridge galvanometer of period ·7 s. The sensitivity is 336 mm/μA at 1 m and the internal esistance 21·8 Ω.

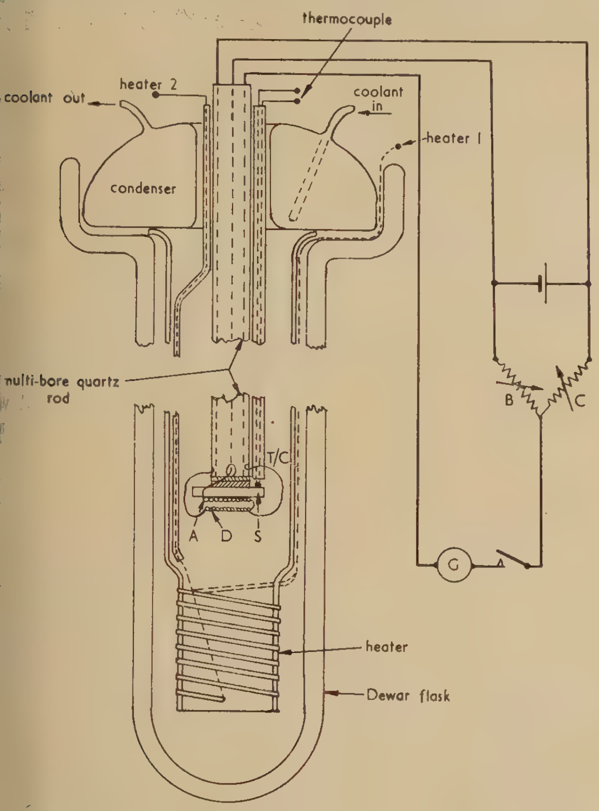

Fig. 2. Arrangement of the apparatus within the temperature enclosure

The stability of the bridge circuit is of considerable mportance; further, it is important to ensure that the ensitivity of the bridge is uninfluenced when the specimen s at a temperature other than room temperature and also hat the stability of the bridge is unaffected by changes in oom temperature. The connexions from the top of the nulti-bore tube to the resistors *C* and *D* are kept as short as possible and consist of brass strips of cross-section 0·5 by ·1 in. In addition, all the components of the bridge, except he galvanometer, are contained within an enclosure mounted n the slate slab. The stability of the bridge is consequently naffected by changes in room temperature. As mentioned bove, the performance of the bridge is continually monitored, luring high and low temperature operation, by making nown changes in the resistance of *C*. Such a procedure vill not, however, reveal any difference which may exist etween the sensitivity of the active gauge to strain at the operating temperature and the corresponding value at room emperature. The dependence of the strain sensitivity factor, or gauge factor, on temperature must be determined independently. This is described briefly in Section 4. It may be noted, however, that the temperature variation of gauge factor is not usually large except near the temperature at which the gauge breaks down completely.

3.3 *Temperature control.* In considering the control of the specimen temperature it was appreciated that a method of high temperature stability was essential. Although the temperature variation of magnetostriction is usually small except near the Curie point, the strains introduced by thermal expansion can dominate those caused by magnetostriction. Factors essential to high temperature stability are efficient thermal insulation and high thermal capacity. The efficiency of the insulation minimizes the flow of heat between the enclosure and its surroundings, and the effects of these flows on the specimen temperature are reduced by filling the enclosure with a medium of high thermal capacity per unit volume. To satisfy the first requirement the specimen is accommodated in a long Dewar vessel which forms the temperature enclosure. The medium used to increase the thermal capacity must be homogeneous, in order to avoid temperature gradients within the enclosure, and it is also desirable that it should be an electrical insulant. A fluid is therefore indicated and Corner and Hunt(6) have shown that a silicone fluid (M.S. 550) and isopentane possess respectively the stability required to cover extended temperature ranges above and below room temperature. Both fluids, by reason of their electrical insulating properties, permit considerable simplification of the heating and measuring arrangements within the enclosure. Details of the arrangement of the specimen and the associated equipment in the temperature enclosure are shown in Fig. 2.

The liquids are contained in a Dewar vessel and, to provide a source of heat within it, a heating element is located below the specimen as shown in Fig. 2. An annular water-cooled glass condenser which closes the top of the Dewar vessel serves to condense the vapours evolved during high temperature operation.

The temperature of the specimen is controlled in the upper and lower ranges by different methods. Above room temperature the upper limit is set by the boiling point of the silicone fluid, which is a little over 400° C. Throughout this range, loss of heat from the system is small so that the specimen temperature is readily stabilized by a small dissipation of power in the heating element. Switching the heater current on and off affords confirmation of the absence of spurious electromagnetic effects.

Below room temperature the lower limit is the freezing point of the isopentane, which is quoted as −159° C. It is found, however, that although the liquid becomes rather viscous at this temperature, solidification does not occur until the temperature is reduced considerably below this value. The freezing point is slightly different for samples of isopentane supplied by different manufacturers, and the lowest value attained was −170° C. Over the lower range measurements are taken from the lowest temperature up to room temperature. To attain the lowest temperature, the enclosure is removed from the specimen and both are precooled with liquid nitrogen. The isopentane is similarly cooled to its freezing point and sufficient is solidified for the latent heat to counterbalance the heat losses which occur in reassembling the equipment. Thereafter, the temperature may be maintained at this value by the addition of further solid isopentane. When this has liquefied the specimen temperature gradually increases. Because of the efficient insulation and high thermal capacity of the enclosure, the temperature rises slowly enough to permit reliable measurements to be taken. Nearer room temperature the rise is so slow that the heating element may be employed with advantage to facilitate more rapid measurements over the remaining temperature range.

3.4 *Sensitivity.* The sensitivity of the apparatus will, naturally, depend to a certain extent on the resistance of the gauges employed. With 100 Ω gauges and with 2 V across the bridge, a resistance change of $4{\cdot}0 \times 10^{-4}\,\Omega$ produced a scale deflexion of the galvanometer of 1·0 cm. Assuming a nominal gauge factor (defined below) of 2, the strain sensitivity is about 2×10^{-7} per mm deflexion.

4. Strain gauge calibration

In the strain gauge technique a strain is measured as a fractional change in resistance and, in order to calculate the strain, the gauge factor g defined by

$$\Delta R/R = g\Delta l/l \qquad (1)$$

must be known. The gauge factor g depends in an unknown manner upon Poisson's ratio and upon the change in resistivity with pressure, both of which may be expected to be temperature dependent. It follows that the gauge factor will be a function of temperature. Although the investigations of Day and Sevand(5) indicate that the variation of gauge factor with temperature is small, it was felt that the variation may be different for different gauges and, moreover, their measurements do not extend above room temperature. It was therefore decided to measure the gauge factor of all the gauges used over the required temperature range.

The gauges used were of three types, all manufactured by H. Tinsley and Co. Ltd. Type 6J consists of a grid of fine nickel–chromium wire cemented to a paper backing having an active area of 0·8 × 0·15 cm and a nominal resistance of 100 Ω. This type of gauge is supplied for use at room temperature. In practice, however, it has been extensively employed at temperatures down to −196° C and up to the point at which it breaks down completely. This latter temperature is rather unpredictable and seems to depend upon the length of time for which the cement (Durofix) has been allowed to dry: a maximum value is about 170° C. Type 20A were specially supplied and were only half the normal breadth of this type of gauge. They are miniature gauges having an active area of 0·32 × 0·24 cm, which renders them of great use when small samples only are available. They suffer from a number of disadvantages however. A greater thickness of paper is used for the gauge backing and this increases the drying time for the cement to 2–3 weeks. The method of construction of the 20A gauge, in which the gauge wire is wound on a slip of paper impregnated with cellulose nitrate, renders the gauge liable to failure above 100° C.

The 40A gauges were experimental high temperature gauges. They consisted of a grid of fine nickel–chromium wire mounted on a Japanese tissue base. A silicate cement is employed to fix the gauge to the specimen and both gauge and fixative have proved quite satisfactory for use below room temperature and up to the highest temperature (400° C) at which measurements of magnetostriction have been attempted.

The gauges were calibrated using an electromagnetically-operated thin phosphor-bronze cantilever with the gauge cemented to one surface. The temperature is varied by immersing the whole apparatus in a Dewar vessel containing isopentane or silicone fluid. Thus, since a dummy gauge is also employed, the further advantage is afforded that the gauges are tested under closely similar conditions to tho obtained during the magnetostriction measurements. A apparatus almost identical with this has recently be described by McClintock.(7)

Typical curves relating the variation of g with temperatu for 6J, 20A and 40A gauges are presented in Fig. 3. It ma be seen that, below room temperature, g is constant to with about 1% of the room temperature value. Above roo temperature g changes by approximately 0·03% per deg. C Also included in Fig. 3 for comparison is a curve, supplie by the manufacturers, for type Y1 gauges. These a Bakelite impregnated gauges consisting of a grid of fi nickel–chromium–third metal wire mounted on a fibre gla base. The Y1 gauges were not used for magnetostrictio measurements as they only became available after the measurements were completed. They were, howeve employed to provide a useful check on the accuracy of th calibrating system described above.

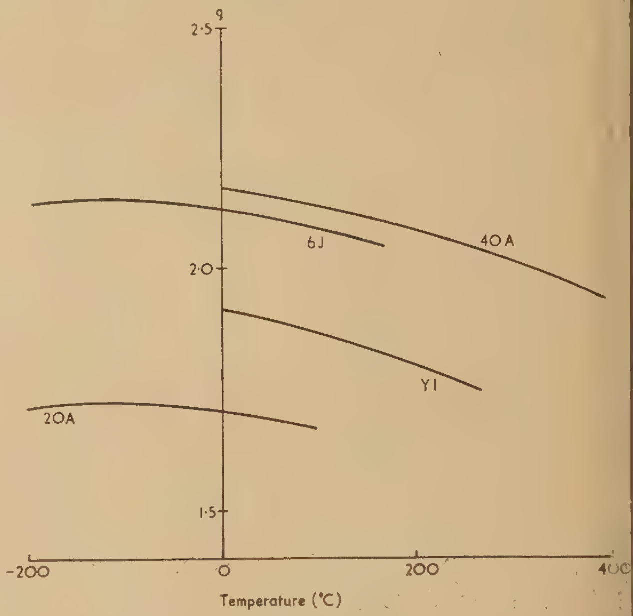

Fig. 3. The variation of gauge factor g with temperature fo four gauges 20A, 6J, 40A and Y1 described in the text

5. Evaluation of magnetostriction constants

The magnetostriction constants are the constants in th expressions for the spontaneous lattice deformation as function of the direction cosines of the spontaneous magnet zation, α_1, α_2, α_3, and of the measuring direction β_1, β_2, β relative to the crystal axes. The equations reflect the sym metry of the crystal lattice since they may be derived b expanding the lattice deformation as a power series in th α_i and rejecting those terms which do not have the sam symmetry properties as the crystal. For cubic crystal form which has been widely used is

$$\lambda = B_0 + B_1S(\alpha_1^2\beta_1^2) + B_2S(\alpha_1\alpha_2\beta_1\beta_2) + B_3S(\alpha_1^2\alpha_2^2) + \\ + B_4S(\alpha_1^4\beta_1^2) + B_5S(\alpha_1\alpha_2\alpha_3^2\beta_1\beta_1) \qquad (2$$

in which the operator $S(\ \ )$ denotes the sum of the thre quantities obtained by a cyclic permutation of suffixes o the expression within the brackets. A procedure fo evaluating the magnetostriction constants B_1–B_5 involvin measurement of magnetostrictive strain at various azimutha angles in a definite crystal plane has been described in deta by Bozorth and Hamming.(8) It does not appear feasible t e this method at any other than room temperature because the errors which are likely to be introduced by minute uctuations in temperature. In any case Bozorth and amming concluded that the constants B_3–B_5 for nickel e "not certainly different from zero"—a conclusion which ems to have been confirmed by work on other materials. ne may therefore express results in terms of a two-constant uation, namely,

$$\lambda = C_0 + C_1 S(\alpha_1^2\beta_1^2) + C_2 S(\alpha_1\alpha_2\beta_1\beta_2) \qquad (3)$$

his is the simplest equation consistent with anisotropic agnetostriction and is often written in the alternative form

$$\lambda - \lambda_i = \tfrac{3}{2}\lambda_{100}\{S(\alpha_1^2\beta_1^2) - \tfrac{1}{3}\} + 3\lambda_{111}S(\alpha_1\alpha_2\beta_1\beta_2)$$

which λ_i is the magnetostriction in the ideal demagnetized ate. This equation has frequently been a source of con-usion owing to mis-interpretation of the significance of the onstants λ_{100} and λ_{111}. It thus seems desirable to use the riginal form [equation (3)], regarding C_1 and C_2 as constants f the material.

For hexagonal crystals the equation corresponding to quation (3) is

$$= R_0 + R_1\beta_3^2 + (R_2 + R_3\beta_3^2)(1 - \alpha_3^2) + \{R_4\alpha_3\beta_3 + R_5(\alpha_1\beta_1 + \alpha_2\beta_2)\}(\alpha_1\beta_1 + \alpha_2\beta_2) \qquad (4)$$

n which the subscripts 1, 2 and 3 refer to the [1$\bar{2}$·0], [10·0] nd [00·1] crystallographic axes respectively. The equation onforms to cylindrical symmetry.

For cubic crystals, the saturation magnetostriction con-tants C_1 and C_2, occurring in equation (3), may be evaluated rom measurements in the three principal planes as follows. Let the planes be, for convenience, the (001), (1$\bar{1}$0) and (1$\bar{1}$1) lanes, and let the measuring direction make an azimuthal ngle β with the [110] direction. [The sense of β is such hat the position $\beta = +90°$ defines the axes [$\bar{1}$10], [001] and [$\bar{1}$12] respectively as shown in Figs. 4(*a, b* and *c*).] A rotation of the saturation magnetization vector from the direction β into the direction $\alpha = \beta + x$ is accompanied by a strain in the direction β which may be evaluated as a function of x, for various values of β. This quantity may be designated by $\lambda_x - \lambda_0$, where the suffix indicates the angle between the magnetization vector and the measuring direction. For all three principal planes it may be written in the form

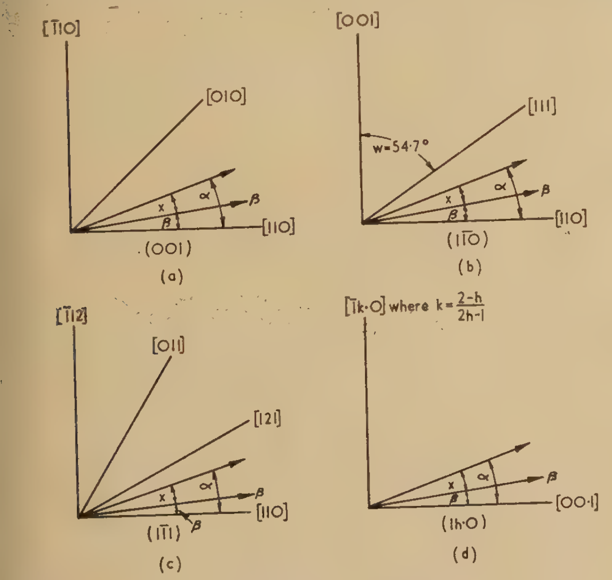

Fig. 4. Angles associated with magnetization in various crystallographic planes

$$\lambda_x - \lambda_0 = q(\cos 2x - 1) + 2r\sin 2\beta \sin 2x \qquad (5)$$

where the functions $q = q(\beta)$ and $r = r(\beta)$, which depend only upon C_1, C_2 and β, may be found from the equations

(001) plane
$$\left.\begin{aligned} 8q &= (2C_1 + C_2) - (2C_1 - C_2)\cos 4\beta \\ 8r &= (2C_1 - C_2)\cos 2\beta \end{aligned}\right\} \qquad (6)$$

(1$\bar{1}$0) plane
$$\left.\begin{aligned} 32q &= (6C_1 + 5C_2) - \\ &\quad - (2C_1 - C_2)(2\cos 2\beta - 3\cos 4\beta) \\ 32r &= (2C_1 - C_2)(1 - 3\cos 2\beta) \end{aligned}\right\} \qquad (7)$$

(1$\bar{1}$1) plane
$$6q = (C_1 + C_2), \quad r = 0 \qquad (8)$$

These expressions may therefore be employed to determine the values of C_1 and C_2 which correspond to the best agreement between the experimental data and the values obtained from equation (5). It may be noted at this point that equation (5) predicts the occurrence of alternate maxima and minima of $\lambda_x - \lambda_0$ at positions $x = \frac{1}{2}\tan^{-1}(2r\sin 2\beta)/q$ which are separated by intervals of 90°. It therefore follows that such an extreme position will coincide with the direction of measurement only if $r\sin 2\beta = 0$. This condition is always satisfied in the (1$\bar{1}$1) plane since $r = 0$. In the (001) and (1$\bar{1}$0) planes, however, an *extremum* will coincide with the measuring direction only if the latter is one of the principal crystallographic directions lying in the plane of the specimen.

If equation (5) is regarded as being an exact equation for the quantity $\lambda_x - \lambda_0$ rather than an approximation, then a pair of measurements suffices to determine C_1 and C_2. For example, in the (001) plane, if $\beta = 0$ and $x = 90°$ then $\lambda_x - \lambda_0 = \frac{1}{2}C_2$, whilst if $\beta = 45°$ and $x = 90°$ then $\lambda_x - \lambda_0 = -C_1$. It is this which makes evaluation of C_1 and C_2 over a wide range of temperature, technically feasible. Superimposed on the galvanometer deflexion due to magnetostrictive strains there is, at low temperatures, a slow steady drift associated with the tendency of the system to approach room temperature and a rapidly fluctuating deflexion due to small temperature fluctuations. The effect of the latter can be greatly minimized by taking a large number of pairs of measurements at a single temperature and taking the average reading.

For a hexagonal crystal, the constants R_2–R_5 occurring in the expression (4) may all be determined by observations in any plane containing the [00·1] hexagonal axis. Since the second-order equation conforms to cylindrical symmetry, it is immaterial what orientation this plane possesses with respect to the other crystal axes. In the basal plane $\lambda_x - \lambda_0$ vanishes identically for the same reason. If β is now the angle between the measuring direction and the hexagonal axis [Fig. 4(*d*)] then $\lambda_x - \lambda_0$ is again given by equation (5) together with the relations

$$\left.\begin{aligned} 8q &= (R_4 + R_5 - R_3) - (4R_2 + 2R_3 + 2R_5)\cos 2\beta - \\ &\quad - (R_3 + R_4 - R_5)\cos 4\beta \\ 8r &= (2R_2 + R_3 + R_5) + (R_3 + R_4 - R_5)\cos 2\beta \end{aligned}\right\} \qquad (9)$$

As before, the most satisfactory method of evaluating the magnetostriction constants is by adjusting the values of q and r to obtain the best agreement with the experimental observations. If the measuring direction is parallel to the hexagonal axis ($\beta = 0$) then

$$\lambda_x - \lambda_0 = \tfrac{1}{2}(R_2 + R_3)(1 - \cos 2x) \qquad (10)$$

and only two of the magnetostriction constants are involved.

6. Accuracy of the method

Inaccuracies in the measurement of magnetostriction constants are of two kinds and arise from different origins.

First, there are experimental errors, which are usually involved in any measurement. With specimens of moderate size it is quite difficult to ensure complete absence of translational forces, especially in very high fields; and in mechanical methods such forces are liable to give rise to a movement of the free end of the specimen which is superimposed upon the magnetostrictive change in length. In the strain gauge method, however, the magnetostrictive strain is measured directly and errors due to translational motion are therefore small. Moreover, since the strain gauge method permits the use of smaller specimens than is usual with mechanical methods, the problem of maintaining a uniform field strength over the entire sample, with the consequent elimination of translational forces, is, in general, much less severe. It might be thought that the field within the flat disk-shaped specimen described in section 2 would be substantially non-uniform, since the boundary of the specimen is not a complete surface of the second degree. However, the specimen diameters were commonly 1·12 cm, whilst the thicknesses were usually in the range 50 to 500 μ so that, at the values of applied field which were employed (up to 15 000 oersted), the consequent non-uniformity of the internal field was considerably less than that resulting from the non-uniformity (less than 0·75%) of the applied field. Any possible errors arising from errors in the (purely) resistive arms of the bridge can be eliminated by the use of high quality components. Purely observational errors are thus negligibly small. The ultimate accuracy is set by the accuracy to which the gauge factor is known and by its constancy from one gauge to another. This can be estimated by measurements of magnetostriction with different gauges having *different* gauge factors. The authors' observations are that measurements made in this way agree amongst themselves to better than 3%. Additional confirmatory evidence of this conclusion is presented below.

The second source of error arises not from the measurement itself but rather from the manner in which the measurement is made. Magnetostriction is a change in length and the magnetostriction constants may be measured as changes of length between two well-defined magnetic states. A demagnetized state is, magnetically, not well defined. Evidence for this comes from the fact that the initial permeability is frequently found to depend upon the manner in which a substance has been demagnetized and, more directly, from Bitter pattern observations.(9) The values of the saturation magnetostriction constant for polycrystalline nickel—the material which has been most extensively studied—when measured between saturation and a demagnetized state, vary from $-24{\cdot}8 \times 10^{-6}$(10) to $-46{\cdot}8 \times 10^{-6}$.(11) Such measurements may give some information regarding the nature of the demagnetized state but very little about the magnetostriction constant. Two convenient well-defined magnetic states may be obtained by applying a saturating magnetic field parallel and perpendicular to the direction of measurement. By measuring the magnetostriction between these two states, errors due to ambiguities of the reference state are eliminated. For polycrystalline nickel, the values of the saturation magnetostriction constant (at room temperature) obtained in this manner are

$\lambda_s = (-35 \pm 1) \times 10^{-6}$ (Strauss(12))
$\lambda_s = -35{\cdot}5 \times 10^{-6}$ (present work)

The very close agreement between these values and th calculated from the saturation magnetostriction constan obtained in the same way,(8) for nickel single crystals, name $(-34{\cdot}2 \pm 1{\cdot}7) \times 10^{-6}$ indicates that most of the spread the values obtained from mechanical methods of measur ment arises from errors associated with the use of a dema netized state as a reference state. Once this is eliminat there is a close consistency in the results obtained usi different samples and different gauges, a fact whic strengthens the belief that errors due to errors in gau factor are small.

7. Conclusion

Provided sufficient care is used in the design and co struction of the apparatus, the electrical resistance stra gauge technique may be used very satisfactorily to measu magnetostriction accurately over the range from −196 400° C. The single-crystal constants may be determine using the procedure outlined in section 5. The accuracy the method is limited by the accuracy with which the stra gauge may be calibrated and this should be at best as high that using displacement techniques. The use of strain gaug can serve to eliminate possible systematic (yet neverthele temperature-dependent) errors due to uncertainty of magnetic reference state (the demagnetized state), a measurements made in this way are inherently more relia than those in which the demagnetized state forms o measurement. The method has been successfully used on number of polycrystalline and single-crystal samples and th results will be presented elsewhere.

Acknowledgements

This work was carried out whilst both authors wer members of the Physics Department of Nottingham Universit and they would like to place on record their gratitude t Prof. L. F. Bates for useful suggestions and for so generous providing the facilities which made this investigation possib Thanks are also due to the generous co-operation of Mess H. Tinsley and Co. Ltd. for providing experimental hig temperature and other strain gauges.

References

(1) Néel, L. *J. Phys. Radium*, **15**, p. 225 (1954).
(2) Bates, L. F. *Modern Magnetism*, 3rd ed., p. 40 (Cambridge: University Press, 1951).
(3) Bozorth, R. M. *Ferromagnetism*, p. 628 (New York D. Van Nostrand Book Co. Inc., 1951).
(4) Goldman, J. E., and Smoluchowski, R. *Phys. Rev.* **75**, p. 140 (1949).
(5) Day, E. E., and Sevand, A. H. *Proc. Soc. Exptl. Stres Anal.*, **8**, p. 133 (1950).
(6) Corner, W. D., and Hunt, G. H. *Proc. Phys. Soc (London) A*, **68**, p. 133 (1955).
(7) McClintock, R. M. *Rev. Sci. Instrum.*, **30**, p. 71 (1959).
(8) Bozorth, R. M., and Hamming, R. W. *Phys. Rev.*, **89** p. 865 (1953).
(9) Sommerkorn, G. *Tech. Mitt. Krupp*, **13**, p. 71 (1955)
(10) Schulze, A. *Z. Phys.*, **50**, p. 448 (1928).
(11) Masumoto, H. *Sci. Rep. Tôhoku Univ.*, **17**, p. 945 (1927)
(12) Strauss, H. E. *J. Appl. Phys.*, **30**, p. 1648 (1959).

ew high-voltage multi-stage impulse generator circuit

T. E. BROADBENT, M.Sc., Ph.D., A.M.I.E.E. Electrical Engineering Department, University of Manchester

aper first received 6 November, 1959, and in final form 16 February, 1960]

Abstract

new high-voltage multi-stage impulse generator circuit described. The circuit is based on conventional multi-age impulse generator circuits but trigatrons are used each stage in place of the sphere gaps used in conven-onal circuits. The triggering pulse necessary to fire each igatron is derived from the breakdown of the previous age. For all multi-stage impulse generators of this type ther than very small ones), the stray capacitance coupling etween stages is sufficient to operate the trigatrons, and extra coupling capacitance is required. With the new rcuit, multi-stage generators operate over a much greater inge of voltage for given gap spacings in the various stages ian is the case with the conventional circuits. The need r the spark gaps in each stage to be critically set is ereby eliminated. The results of an experimental com-arison between the new and conventional circuits are escribed.

Introduction

THE basic circuit of a conventional n-stage impulse generator is shown in Fig. 1. Many modifications of this circuit exist(1) but the principle is the same in each ase: This principle is that the capacitors $C_1, C_2 \dots C_n$ are harged in parallel to a steady voltage V. The spark gap S_1 s then caused to spark over using a trigatron(2) or any other orm of triggered spark gap. The use of two trigatrons in the irst stage, as shown, ensures satisfactory operation of this tage with either charging polarity. The voltage across S_2 s thus suddenly increased, and provided the setting of this ap is such that it just withstands the steady charging voltage V, the increase in voltage is sufficient to cause breakdown f S_2. By a similar process the gaps $S_3, S_4 \dots S_n$ spark over n rapid succession, causing an impulse voltage of peak value $-nV$ to be produced at P.

It might appear at first sight that the gaps subsequent to he first have available, at the moment they are due to break lown, voltages of about 2 V, 3 V . . . nV. However, the ffect of stray capacitance on these voltages is of major mportance and it has been shown(1) both experimentally nd theoretically that the available overvoltage on the econd and subsequent gaps is small and of short duration. Thus, the second and subsequent gaps cannot be set to break lown at a voltage much higher than that at which the first ap breaks down. On the other hand, the dispersion of the reakdown values on direct voltages in the presence of xcessive dust may be so great that if the difference in settings s small, any one of the gaps may fail irregularly at less than he intended voltage. Further, irradiation from the first gap n to the other gaps is necessary if erratic operation is to e avoided.

The above circuit has been used for many years and perates satisfactorily, provided the spark gaps are carefully set. In view of the facts given in the previous paragraph, however (all of which are given in Section 5.4 of the paper already quoted(1)), the circuit clearly possesses certain disadvantages. These may be summarized as follows:

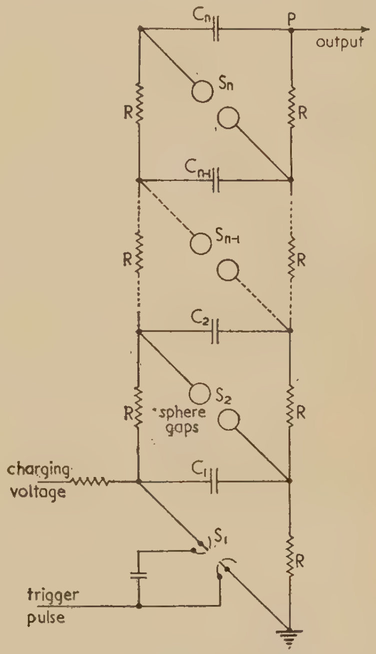

Fig. 1. Conventional n-stage impulse generator circuit

(1) If reliable operation of large multi-stage generators is to occur, the spark gaps $S_1, S_2 \dots S_n$ must be arranged exactly in line, so that ultra-violet light from the first gap S_1 irradiates all the other gaps. If the gaps are not in line, breakdown in the first gap may not necessarily initiate breakdown in the subsequent gaps.(1)

(2) Each of the gaps $S_2 \dots S_n$ of large generators must usually be set to break down at a voltage only slightly greater than that at which S_1 breaks down, otherwise $S_2 \dots S_n$ do not break down when S_1 breaks down.(1)

(3) Since the impulse-generator spark gaps must be critically set (that is, set to just withstand the charging voltage prior to triggering), spurious breakdowns may occur in the gaps, causing an impulse voltage to be produced at the output terminal of the generator. Such spurious impulse voltages are undesirable whatever the application of the generator may be.

In this paper, a new circuit is described which, it is believed, overcomes the above inherent disadvantages of the circuit shown in Fig. 1. Experiments have been carried out to compare the new circuit with that of Fig. 1 and the results are described in a subsequent section.

New circuit and its principle of operation

It is well known⁽³⁾ that a trigatron spark gap (when triggered) has a breakdown voltage considerably less than that of a two-sphere gap having the same electrode diameter and spacing between electrodes. The breakdown voltage under d.c. conditions (that is, with the trigatron untriggered) is about the same as for the sphere gap. It therefore follows that, for a given breakdown voltage, the spacing between the electrodes of a trigatron spark gap (when triggered) is much greater than that between the electrodes of a two-sphere gap. Under these latter conditions the d.c. breakdown voltage of the trigatron (that is, when untriggered) is considerably greater than that of the two-sphere gap. In view of these facts a new multi-stage impulse generator circuit has been devised and investigated experimentally. The circuit is shown in Fig. 2 and it is this circuit⁽⁴⁾ which is the subject of the present paper. The circuit differs basically from that of Fig. 1 in that trigatrons, working in air, are used in each stage of the generator instead of the conventional two-electrode spark gap. The capacitances drawn with broken-line connexions (C_{2a}, C_{2b}, etc.) represent stray capacitances. Extra capacitance may, however, be connected in these positions, as described later. Stray capacitance also exists from each stage of the impulse generator to earth. The principle of the circuit is that, when the first stage is triggered, the capacitance coupling C_{2a} causes the potential of the sphere of T_{2a} to fall; the trigger rod of T_{2a} tends to be held at potential V by the stray capacitance from C_2 to earth. Thus, a high overvoltage (its magnitude depending on the charging voltage, the value of C_{2a}, the capacitance between the rod and sphere of T_{2a}, and the stray cpacitance from C_2 to earth) suddenly appears across the annular gap of T_{2a}, causing this annular gap to spark over. Similarly, the capacitance coupling C_{2b} simultaneously gives rise to a spark in the annular gap of the trigatron T_{2b}. Thus, the trigatrons T_{2a} and T_{2b} are triggered simultaneously when breakdown occurs in S_1. This enables the second stage gap S_2 to fire with the spacing of this gap much greater than would be the case in the generator shown in Fig. 1. When S_2 fires, similar effect takes place in S_3, and so on. Thus all the ga fire in rapid succession, producing the impulse at the point

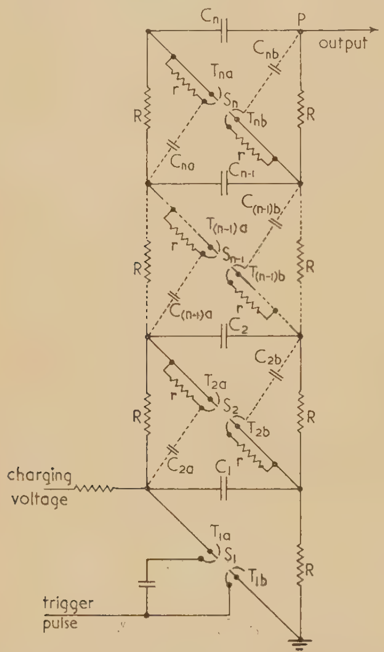

Fig. 2. New n-stage impulse generator circuit

The values of the time constants of the trigger circu ($C_{2a}r$, $C_{2b}r$, etc.) in Fig. 2 are not important in the operati of the circuit. The reason for this is that, once S_1 fires high overvoltage appears across the annular gaps of T_{2a} a T_{2b}, giving very rapid breakdown in these gaps. Once brea down of the annular gaps occurs, the resistors r are sho circuited and therefore do not affect the speed of operati of the system. The purpose of these resistors is only hold the potential of each sphere the same as that of t trigger rod it surrounds prior to triggering.

It has previously been shown⁽²˒ ³⁾ that a trigatron spark-g works best when the electrode containing the annular gap positive with respect to the other main electrode. The use two trigatrons in each stage of the circuit shown in Fig. is thus to ensure effective operation with either chargi polarity.

Therefore, the advantage of the system shown in Fig. 2 that the generator will operate satisfactorily with the spar gaps $S_2 \dots S_n$ much less critically set than is the case wi the circuit of Fig. 1. The circuit of Fig. 2 thus overcom the various disadvantages of the circuit shown in Fig. 1. T establish the degree of improvement derived with the ne circuit, an experimental investigation has been carried o and is described in this paper.

A mathematical analysis of the circuit shown in Fig. has been given elsewhere⁽¹⁾ and is therefore not reproduc here. In the circuit of Fig. 2, a large number of stra capacitances have a bearing on the operation of the circu (for example, C_{2a}, C_{2b}, etc., the stray capacitance from ea stage to ground, the capacitance between rod and sphere f each trigatron, and the self-capacitance of the gaps S_2, S etc.). The value of each of these capacitances is unknow and it is therefore considered that, since any estimate these capacitances must be highly inaccurate, a mathematic treatment of the circuit would be of negligible practical val Such a mathematical treatment is therefore not given.

Experimental methods

If the maximum charging voltage which the spark-gaps a multi-stage impulse generator will withstand without th triggering mechanism in operation is V_{dc}, the impuls generator will operate satisfactorily (that is, all the gaps wi break down simultaneously when a trigger pulse is applie over a range of voltage from V_{dc} down to a voltage V_{min} Thus V_{min} is the minimum value of voltage at which sati factory operation of the generator is assured on the appl cation of a trigger pulse. The range of voltage ($V_{dc}-V_{min}$ therefore represents the range of satisfactory operation the generator and is termed the "working range". Expresse as a percentage of V_{dc}, the working range equa $100(V_{dc}-V_{min})/V_{dc}$. For given spark-gap spacings, it clearly desirable for the working range to be as high a possible.

The technique used in this investigation was to compar the working range obtained using the circuit of Fig. 1 wit that of the circuit of Fig. 2 for various spark-gap spacings For each of the two circuits in turn, the spacings of th gaps $S_2 \dots S_n$ were all made equal to each other, at a serie of fixed values greater than S_1. The working range was the investigated as a function of S_2/S_1 for the circuits of Figs. and 2. The choice of S_1 as the shortest gap was arbitrary the two circuits could be compared equally well with othe relative spacings of S_1, S_2 and S_3. It is desirable from th nsiderations discussed in the Introduction that the working ıge should be high for high values of S_2/S_1. The greater value of S_2/S_1 for which a high working range occurs, less critically may the gaps $S_2 \ldots S_n$ be set.

Experimental equipment

In the experiments described in this paper, two impulse nerators were used, each of three stages. The first operated charging voltages up to 50 kV. The trigatrons T_{2a}, T_{3a} ıd T_{4a} (Fig. 2) of this generator were each 5 cm in diameter ıd the trigatrons T_{2b}, T_{3b} and T_{4b} were each 6·25 cm in ameter. The two different diameters were used, since six heres of the same diameter were not available. The cond impulse generator was smaller, operating at charging oltages up to 20 kV and using trigatron electrodes 0·5 in. diameter. The working range of these impulse generators as investigated first with the circuit connected as in Fig. 1 y short-circuiting the trigatron rods to the spherical ectrodes) and then as in Fig. 2. It was decided that the se of more than three stages for the comparison of Figs. 1 ıd 2 was not necessary, since it was found that whenever ıe gap S_2 broke down, breakdown also occurred in S_3. It likely that breakdown would also have occurred in any ırther stages having gap spacings equal to S_2 and S_3.

In all the experiments, a steep-fronted, negative voltage-ulse of 10 kV peak value was used for triggering the first tage. All the trigatrons used were made from spheres, not emispheres: previous work[(5)] has shown that trigatrons ive best performance when the main electrodes are spherical ather than hemispherical. The annular gap length was bout 1 mm for each of the trigatrons. Throughout the xperiments, the resistors R (Figs. 1 and 2) were 30 kΩ each. xcept where otherwise stated each of the resistors r (Fig. 2) onsisted of three 3·3 kΩ carbon resistors connected in eries directly between the trigger rods and the spherical lectrodes of the trigatrons. All the experiments were arried out with the impulse-generator output open-circuited, xcept where otherwise stated.

Experimental results

It should perhaps be stressed that the results quoted in his paper are for typical impulse generators used in this aboratory, and are in no way claimed to be representative of all impulse generators. The results are included to show the approximate magnitude of the improvement obtained with the new circuit in two typical cases. Since the action of the new generator circuit is dependent on its complex stray-capacitance distribution the exact degree of improvement obtained in any particular generator will depend on the geometrical arrangement of the components. Experiments were first carried out with the larger of the two impulse generators (working at charging voltages up to 50 kV) using a capacitance per stage of 0·25 μF.

Preliminary experiments. Preliminary experiments showed that with the circuit of Fig. 2, the same working range was obtained whether the gaps S_2 and S_3 were screened or unscreened from the irradiation produced by S_1. With the circuit shown in Fig. 1, the working range obtained with S_2 and S_3 unscreened from S_1 was up to about 2·5% better than that obtained with S_2 and S_3 screened from the irradiation produced in S_1. Previous observations[(1)] suggest that, with very large impulse generators, the increase in working range produced by allowing the spark in the first-stage gap to irradiate the subsequent gaps might be greater than the above figure of 2·5%. For any particular impulse generator, the precise increase in working range produced by such irradiation will probably depend on the intensity of background radiation. With the circuits of both Figs. 1 and 2, the working-range curves described in the following text were obtained with the gaps S_2 and S_3 unscreened from the irradiation produced by the breakdown of S_1.

Although the value of the resistors r is not critical (within wide limits), it was found that very high values, of the order of 1 MΩ or more, were unsuitable as corona from the trigger rods of the trigatrons caused a large enough voltage drop across the resistors r to cause spurious breakdown in the trigatron annular gaps under d.c. conditions.

Effect of coupling capacitance magnitude. Experiments were carried out under the following conditions:

(1) With the circuit connected as in Fig. 1.
(2) With the circuit as in Fig. 2. Extra coupling capacitances of 500 pF connected in each of the positions shown dotted in Fig. 2 (C_{2a}, C_{2b}, etc.).
(3) As condition 2, but with extra coupling capacitances of only 50 instead of 500 pF.
(4) As condition 2, but with no extra coupling capacitance (that is, stray-capacitance coupling only).

The results of all these tests, showing working range as a function of S_2/S_1 (for positive and negative charging voltages) are shown in Fig. 3. The gap spacing S_1 was 1·7 cm throughout the tests, corresponding to an experimentally measured breakdown voltage of 50 kV (under d.c. conditions) for both positive and negative charging voltage. Since S_2 and S_3 were equal to each other and greater than S_1, this d.c. breakdown voltage of 50 kV corresponded to the maximum possible charging voltage of the impulse generator, that is, V_{dc}.

It will be seen from Fig. 3 that, for each of the four conditions investigated, the results for negative charging voltage

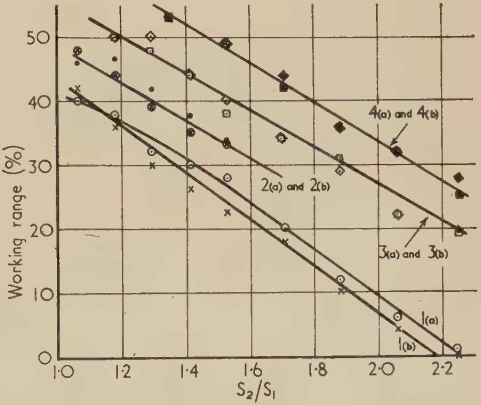

Fig. 3. Comparison between performance of circuits shown in Figs. 1 and 2. Three-stage impulse generator; charging voltages up to 50 kV; stage capacitance, 0·25 μF

Curve 1(*a*) ⊙ Positive } Conventional circuit
Curve 1(*b*) × Negative } (as in Fig. 1)

Curve 2(*a*) ⊗ Positive } New circuit
Curve 2(*b*) ● Negative } (as in Fig. 2)
(Extra coupling capacitors, 500 pF each)

Curve 3(*a*) ⊡ Positive } New circuit
Curve 3(*b*) ⟐ Negative } (as in Fig. 2)
(Extra coupling capacitors, 50 pF each)

Curve 4(*a*) ⊠ Positive } New circuit
Curve 4(*b*) ◈ Negative } (as in Fig. 2)
(No extra coupling capacitors, stray capacitance only)
Polarities quoted above are those of charging voltage

closely resemble those for positive. For Cases 2, 3 and 4 (above), results for positive and negative voltage are so similar that a common curve has been drawn for the two polarities in each case, while in Case 1 the maximum difference between the working range obtained with positive and negative polarity is not more than 3%. It is also seen that the working range obtained with the circuit of Fig. 2 is substantially better than that obtained with the circuit of Fig. 1. The degree of improvement is dependent on the value of the coupling capacitance between stages. The best result occurs (Curve 4) when no extra coupling capacitance is used, the stray-capacitance coupling alone being used to fire the trigatrons. This is clearly a most satisfactory result since no extra high-voltage capacitors are required. It will be seen from Fig. 3 that for all values of S_2/S_1 up to 2·2, the working range with the circuit of Fig. 2 with stray-capacitance coupling only between stages (Curve 4) is about 25% greater than that with the circuit of Fig. 1 (Curve 1). The significance of this can best be grasped by considering as an example a particular value of S_2/S_1. For instance, with S_2/S_1 equal to 2·0 (that is, $S_1 = 1 \cdot 7$ cm, $S_2 = S_3 = 3 \cdot 4$ cm), the circuit of Fig. 1 has a working range of 9·5% for positive charging voltage and 6% for negative charging voltage. Thus the range of voltage for which the impulse generator operates with these gap spacings is 45·25–50 kV with positive charging voltage and 47–50 kV with negative charging voltage. With the circuit of Fig. 2 and only stray-capacitance coupling between stages, the corresponding working range is 33·5% for both positive and negative charging polarity. Thus, the range of voltage over which the generator operates is now 33·25–50 kV. These figures clearly demonstrate the magnitude of the improvement obtained by using the circuit of Fig. 2 instead of that of Fig. 1.

The fact that the circuit of Fig. 2 works best with relatively small values of coupling capacitance (C_{2a}, etc.) may be explained by a consideration of the various stray capacitances in the system. When the coupling capacitances (C_{2a}, etc.) are high compared with the stray capacitance from each stage to earth, the spherical electrodes of S_2 tend to remain at the same relative potential when S_1 and the annular gaps of T_{2a} and T_{2b} fire. Thus the likelihood of S_2 firing is reduced. A similar argument applies to the breakdown of each stage when the preceding stage breaks down.

The assumption that the stray-capacitance coupling between stages was sufficient to fire the trigatrons was confirmed by visual observations. Tests were carried out with S_2 opened to a value sufficiently great to prevent breakdown occurring in this gap when S_1 was triggered. When breakdown occurred in S_1, a faint spark was visible in the annular gaps of the trigatrons in the second-stage gap S_2.

It seems certain that for all impulse generators larger than that described in this experiment, a similar effect would occur. The reason for this is that, for larger impulse generators, both the stray capacitance between stages and the charging voltage would be greater. The voltage pulse occurring across the annular gaps of the trigatrons would then be greater than for the impulse generator described here (even allowing for the non-uniform voltage distribution across the main spark gaps of the generator), and would thus be easily sufficient to cause sparkover in the annular gaps.

Time lag and voltage measurements. With a high-speed cathode-ray oscillograph, the time delay between the breakdown of S_1 and the breakdown of S_3 was measured for the circuits of Figs. 1 and 2. In both cases, the time delay between the firing of the first and last stages was small (less than about 0·1 μs) over most of the operating range of voltage. Oscillographic measurements confirmed that t output waveform of the circuit shown in Fig. 1 was t same as that for the circuit shown in Fig. 2, using only stra capacitance coupling between stages. The fact that the pe output was the same in the two cases was confirmed sphere-gap measurements of voltage.

Effect of capacitive load. Experiments were carried out find whether or not the performance of the circuit shown Fig. 1 could be significantly improved (so as to approach t performance of the circuit of Fig. 2) by the use of capaciti loads on the output. A capacitance of 250 pF was connecte between earth and the output of the second stage and similar load between earth and the output of the third (fina stage. The capacitance per stage of the generator w 0·25 μF. S_2 and S_3 were each made 2·6 cm, correspondi to a value of S_2/S_1 of 1·53 cm. With the circuit shown Fig. 1 thus loaded, the working range was 33% for bo positive and negative charging polarity. This compares wi a working range of 27% (positive charging voltage) and 24 (negative charging voltage) for the circuit of Fig. 1 with load. With the circuit of Fig. 2 with no capacitive loa and using only stray-capacitance coupling between stages, th working range was 48%. Thus, even with substanti capacitive loading the performance of the circuit shown i Fig. 1 is significantly below that of the circuit of Fig. 2.

Effect of altering stage capacitance. The experiments we continued using the same impulse generator as in the exper ments already described but with a capacitance of 0·005 μ per stage instead of 0·25 μF as previously. Curves relati working range with S_2/S_1 were plotted for the circuit of Fig. 1 and for that of Fig. 2 with only stray-capacitance coupli between stages. The results are shown in Fig. 4. Again i is seen that the circuit of Fig. 2 gives much better results than the circuit of Fig. 1. As an example, with S_2/S_1 equa to 2·0, the circuit of Fig. 2 gives a working range of 31% as against 7% (positive charging voltage) and 4% (negative charging voltage) for the circuit of Fig. 1. Thus the improved characteristics obtained with the new circuit are retained even when the capacitance per stage is altered by a factor of 50, as above.

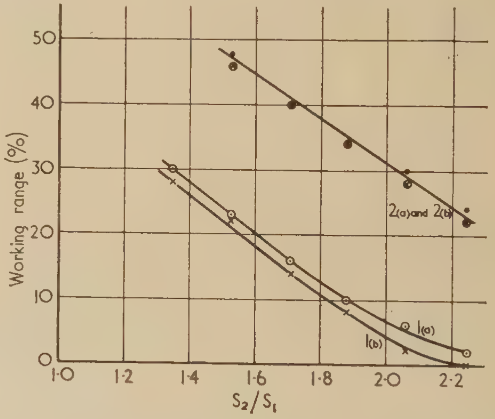

Fig. 4. Comparison between performance of circuits shown in Figs. 1 and 2. Three-stage impulse generator; charging voltages up to 50 kV; stage capacitance, 0·005 μF

Curve 1(a) ⊙ Positive } Conventional circuit
Curve 1(b) × Negative } (as in Fig. 1)

Curve 2(a) ⊗ Positive } New circuit
Curve 2(b) ● Negative } (as in Fig. 2)

(No extra coupling capacitors, stray capacitance only)
Polarities quoted above are those of charging voltage

Effect of reversing connexions to trigatrons. With the ircuit of Fig. 2 with capacitance per stage of 0·005 μF, nd with only stray-capacitance coupling between stages, xperiments were carried out to find the effect of reversing he connexions between the trigger rod and the spherical lectrode of each trigatron. These experiments showed that with the connexions reversed, the working range was rather ower than that obtained when using the circuit of Fig. 2. With S_2/S_1 equal to 1·88 ($S_2 = S_3 = 3{\cdot}2$ cm) the working range dropped from 35% to 27% when the connexions were reversed. With S_2/S_1 equal to 2·06 ($S_2 = S_3 = 3{\cdot}5$ cm) the corresponding drop in working range was from 29% to 20%. These results show that the circuit as drawn in Fig. 2 gives better results than a similar circuit with the connexions to the trigger rods and the spherical electrodes of the trigatrons reversed. This is as might be expected, since the stray capacitance between one stage of the impulse generator and the spherical trigatron electrode in the next stage will be greater than that between the one stage and the trigger rod (nearly all of which is shielded by the spherical trigatron electrode) of the next stage. In the latter case, the stray-capacitance coupling between stages may well be insufficient to ensure sparkover in the trigatron annular gaps when breakdown occurs in the preceding stage.

Experiments using small impulse generator. Experiments similar to those described above were carried out using the small impulse generator having a capacitance per stage of 0·005 μF and trigatron electrode diameters of 0·5 in. The maximum allowable charging voltage was 20 kV. Preliminary experiments with this impulse generator showed that the stray-capacitance coupling between stages was insufficient to enable a trigger spark to occur in the trigatrons when the preceding stage broke down. With only stray-capacitance coupling between stages identical working-range curves were obtained for the circuits of Figs. 1 and 2. The probable reason for this was that, since the charging voltage was as small as 10–20 kV, the voltage occurring across the trigatron annular gaps (which depends on the relative value of the stray capacitance between stages and the capacitance of the trigatron annular gaps) might not be sufficient to cause breakdown of these gaps. The fact that no spark occurred in the annular gaps of the second-stage trigatrons when the first-stage spark gap broke down was confirmed by visual observations.

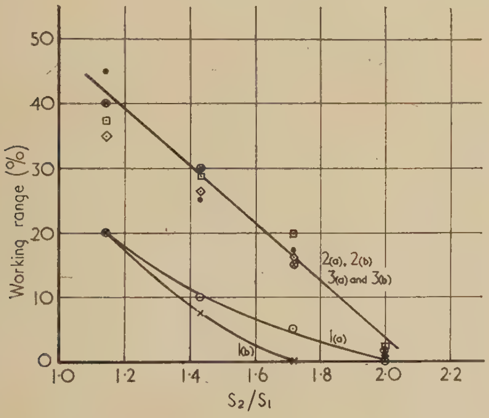

Fig. 5. Comparison between performance of circuits shown in Figs. 1 and 2. Small three-stage impulse generator; charging voltages up to 20 kV; stage capacitance, 0·005 μF

Curve 1(*a*) ○ Positive } Conventional circuit
Curve 1(*b*) × Negative } (as in Fig. 1)

Curve 2(*a*) ⊗ Positive } New circuit
Curve 2(*b*) ● Negative } (as in Fig. 2)
(Extra coupling capacitors, 50 pF each)

Curve 3(*a*) ⊡ Positive } New circuit
Curve 3(*b*) ◊ Negative } (as in Fig. 2)
(No extra coupling capacitors. Artificially increased stray-capacitance coupling between stages)

Polarities quoted above are those of charging voltage

Experiments with extra coupling capacitors of 50 pF (provided by 2·5 ft lengths of coaxial cable) in each of the positions shown dotted in Fig. 2 showed that the trigatrons operated satisfactorily. It thus seemed clear that if the stray capacitance between stages could be increased to a sufficiently high value, the trigatrons should operate. To find whether or not this were so, a short length of wire (about 15 in.) was connected to the spherical electrode of each of the trigatrons in the second and third stages. Each wire was bent round towards the vicinity of the previous stage so as to make the stray-capacitance coupling reasonably high. Using this system, with no extra coupling capacitors, satisfactory operation occurred. Thus, for very small impulse generators it is necessary either to increase the stray capacitance between stages artificially, or to use coupling capacitors. These can conveniently be made from short lengths of coaxial cable.

Working-range curves for the impulse generator were obtained as a function of S_2/S_1, S_1 being fixed throughout at 0·7 cm. The results are shown in Fig. 5. The working-range curve using 50 pF coupling capacitors between stages was virtually coincident with the curve obtained using no extra coupling capacitors but with the stray capacitance between stages artificially increased as described above. It will be seen that, as in the case of the larger impulse generator already described, the circuit of Fig. 2 gives a much higher working range than that of Fig. 1.

Conclusions

The results of the experiments described in this paper demonstrate that the circuit shown in Fig. 2 overcomes the inherent disadvantages (described in the Introduction) of the conventional impulse-generator circuit of Fig. 1. With the new circuit, a multi-stage impulse generator operates over a much greater range of voltage for given spark-gap spacings than is the case with the conventional circuit. Conversely, for a given charging voltage, the spacings of the spark gaps in the various stages of the generator may be set at any values within wide limits. Thus none of the spark gaps in the various stages needs to be critically set. This is in marked contrast to the conventional circuit in which the spark gap in each stage (other than the first, if a trigatron is used in this gap) has to be critically set to just withstand the charging voltage. The likelihood of the gaps failing to operate when triggered, or breaking down spontaneously prior to triggering, is thus much reduced when the new circuit is used. It is also unnecessary, using the new circuit, for the spark gaps in the various stages to be in line. For all multi-stage impulse generators other than very small ones the stray capacitance coupling between stages is sufficient to operate the trigatrons and no extra coupling capacitance is required. It is therefore a simple matter to convert an existing impulse-generator circuit such as is shown in Fig. 1 to the circuit of Fig. 2, since the existing spherical or hemispherical electrodes can be used as the main trigatron electrodes. The cost incurred in such a modification is negligible and the characteristics of the impulse generator are greatly improved. Distributed wave-front resistance can be incorporated in the generator in exactly the same way as with the conventional circuit.

Although the performance of only two particular impulse generators has been investigated, previous investigations into the characteristics of trigatrons(3, 5) indicate that the results quoted will be fairly typical of other impulse generators of any size, including the very large machines used for testing high-voltage equipment. With any particular large multi-stage generator, the degree of improvement in the operating characteristics derived by using the new circuit can easily be established by carrying out a few tests on the first two or three stages only.

References

(1) Edwards, F. S., Husbands, A. S., and Perry, F. F. *Proc. Instn Elect. Engrs*, **98**, Part 1, p. 155 (1951).

(2) Craggs, J. D., Haine, M. E., and Meek, J. M. *J. Ins Elect. Engrs*, IIIA, **93**, p. 963 (1946).

(3) Broadbent, T. E. *Brit. J. Appl. Phys.*, **8**, p. 37 (1957

(4) U.K. Patent Application No. 2851/60.

(5) Broadbent, T. E., and Fernandez, A. *J. Sci. Instrum* **36**, p. 452 (1959).

Magnetically operated mass-marker

by J. J. BROWN, R. I. REED, Ph.D., and W. SIMPSON, The University, Glasgow

[*Paper first received* 15 *February, and in final form* 30 *March*, 1960]

Abstract

The construction and operation of a magnetically operated mass-recorder which is suitable for use with the mass-spectrometer, type M.S.2 (by Metropolitan-Vickers Electrical Co. Ltd.), is described. Certain precautions in its operation are discussed. On the present evidence it operated with such accuracy as to be useful in a mass-range of up to 500 *mass-units.*

Introduction

It is often found that one of the most time-consuming tasks in the practice of mass-spectrometry is the assignment of mass-units to the individual fragment ions. This is particularly so in the higher mass-ranges where it is often necessary to count up each ion and occasionally even interpolate for regions in which ions are absent.

One solution to this problem is an accurate measurement of the field strength of the magnet. At least three methods of accurate measurement are available and these have all been applied. The difficulties of the vibrating magnetometer* and the use of coils of bismuth wire† arise in the present case from the difficulty of inserting the probe into the gap between the poles of the electromagnet. The second method is further complicated by the necessity of thermostatically controlling the probe coil to prevent variations in its temperature. The use of proton-resonance phenomenon has also been investigated, but it was found that to cover the range of mass-numbers necessary, several probes were required. The inconvenience of having to interrupt a scan for this purpose is greater than the ease of calibration.

Accordingly, the following apparatus which measures the increments in magnet current has been devised in an effort to minimize these problems. It has the advantage that it is independent of the field of the magnet and whilst precautions are necessary to avoid the problems of hysteresis in the magnet, it has given satisfactory service. It has been used in conjunction with a mass-spectrometer, type M.S.2 (by Metropolitan-Vickers Electrical Co. Ltd.), but can be used with any instrument in which the scanning of the various masses is effected by varying the strength of the magnetic field.

Design and operation of the instrument

It is assumed that the magnet current is below 50 mA an is increasing, which is the direction in which the mass-marke operates. Initially the reference grid of V_{1B} in the circui diagram is the more positive and acts as the control of th double triode V_1. The grid of the section V_{1A} of this valv is connected through a 350 Ω resistor, a current-limitin device in series with the magnet coils and earth. As th current through the magnet coils increases, the potential o the grid of V_{1A} rises. When the magnet current of 50 m is reached, the potential on the grid becomes 17·5 V. A this point, control of the valve transfers to this grid, and th steady current of 6 mA flowing through V_{1B} is momentaril transferred to the anode of V_{1A}, with a consequent rise i the potential at the anode of V_{1B}. This, in effect, supplies positive sharp-edged pulse to the grid of the valve V_2 through C_2, R_2. Accordingly, V_2 becomes conducting for a tim which depends on the magnitude of C_2 and R_2 and the setting of the potentiometer VR_3. This valve actuates the rela RA/2. Contact RA/2 is closed and applies a current puls to the uniselector, moving the contact from position 1 t position 2. In this move, the grid of V_{1A} falls to eart potential, and control of the double triode is returned to V_{1B}. Moreover, the positive pulse applied to V_2 has by this time died away and V_2 is cut off. The relay RA/2 returns to its original operative condition and the contact RA/2 opens. The system has now returned to its original condition with one important difference. In moving from contact 1 to 2, the uniselector has introduced a 20 kΩ resistor in series with the 100 kΩ resistance already connected to this grid, which now has an applied potential of 14·6 V. The cycle is now repeated: the grid of V_{1A} becomes more positive (17·5 V) than grid V_{1B}, initiating the pulse which moves the uniselector from position 2 to 3 and again restoring the system to its usual position. Now, however, a 40 kΩ resistor is connected in series with the grid resistor of the V_{1A}, which returns to a potential of 15·0 V. This process is continued with increasing magnet current, and will operate until the potential at grid V_{1A} is so near to that at the reference grid of V_{1B} that the valve cannot distinguish reliably between the two potentials. In the present arrangement, the insertion of the 20 kΩ resistor results in a pulse operating the uniselector at 10 mA intervals.

The contact RA/1 of relay RA/2 also closes as the uni-

---

* Caldercourt, V. J., and Adler, S. E. *Rev. Sci. Instrum.* **25**, p. 953 (1954).

† Beynon, J. H., and Clough, S. *J. Sci. Instrum.*, **35**, p. 289 (1958).

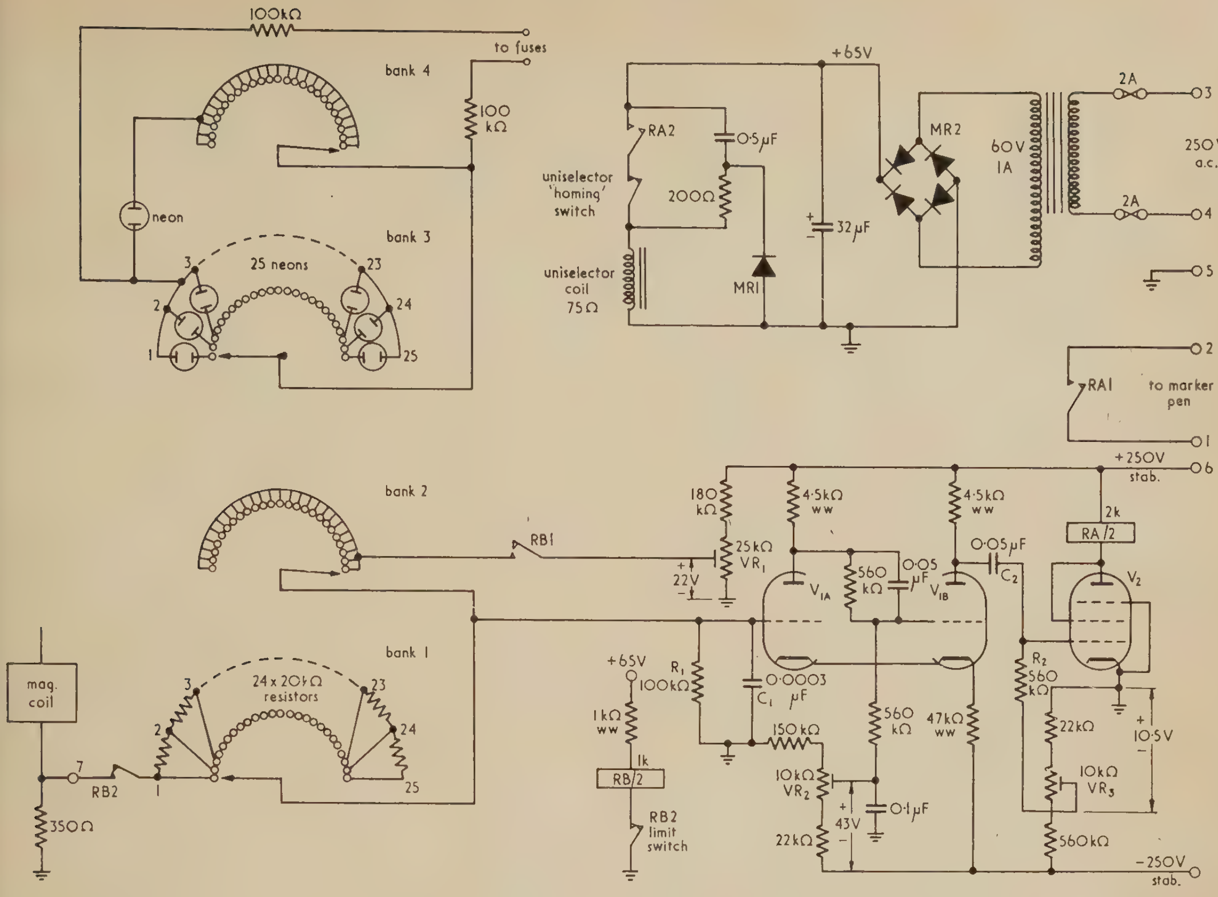
100kΩ
to fuses
bank 4
100 kΩ
neon
bank 3
25 neons
3
23
2
24
1
25
+65V
RA2
0·5μF
uniselector 'homing' switch
200Ω
uniselector coil 75Ω
MR1
32μF
MR2
60V 1A
2A
3
250V a.c.
2A
4
5
2
RA1
to marker pen
1
+250V stab.
6
bank 2
RB1
180 kΩ
25kΩ VR1
22V
4·5kΩ ww
4·5kΩ ww
560 kΩ
0·05 μF
V1A
V1B
0·05μF
C2
2k
RA/2
V2
bank 1
mag. coil
24x20kΩ resistors
3
23
2
24
7
RB2
1
25
350Ω
+65V
R1 100kΩ
0·0003 μF
C1
1kΩ ww
1k
RB/2
RB2 limit switch
150kΩ
560 kΩ
47kΩ ww
10kΩ VR2
43V
0·1μF
22kΩ
R2 560 kΩ
22kΩ
10·5V
10kΩ VR3
560kΩ
-250V stab.

Circuit of mass-marker for mass-spectrometer

selector moves, and operates a small pen upon the recorder, thus marking the current upon the trace itself. Also, for practical convenience, a bank of signal lights is present on the mass-marker, which give a visual indication of the position of the uniselector at any given time.

The voltages at which the potentiometers were set are shown beside them on the diagram. The encircled numbers refer to pin-numbers on an 8-pin Painton Plug used to connect this instrument with the appropriate supplies on the mass-spectrometer. The rectifier MR1 may be any 250 V metal rectifier capable of passing 100 mA. Its function is to minimize the development of any back e.m.f. which might hold the uniselector in its operational position longer than is needed for the change to an adjacent contact.

The 250 a.c. and d.c. supplies are taken from the appropriate points on the mass-spectrometer, whilst the −250 V d.c. stabilized supply comes from an additional power pack (Solartron High-Stability Power Supply, Sub Unit).

Once the upper limit of operation of the uniselector, in this instance position 26, has been reached, corresponding to a magnet current of 290 mA, the selector remains at this position for the rest of the upward scan. When the magnet current has reached its maximum and starts to diminish this circuit is broken by a switch operated by the scan-reversing motor. This breaking of the circuit de-energizes a second relay RB/2, closing RB/1, and opening RB/2. The grid of V_{1A} is now connected to a 22 V potential through a second bank of the uniselector in which all positions are equivalent. The uniselector now rapidly traverses all these positions until it returns to position 1 where it remains. When the magnet is again reversed, at about 40 mA, the change in direction of scan closes the switch, energizing relay RB/2, opening RB/1, and closing RB/2. The grid of V_{1A} is thus reconnected with bank one of the uniselector and the whole cycle of operations associated with the upward scan begins once again.

The useful range of this particular instrument, which operates at regular 10 mA increments, is from 50–290 mA. Above this, the variations in the potential of grid of V_{1A} are too small for the reliable operation of the instrument. The effective range of the instrument might be increased by increasing the intervals of operation from 10 mA to 14 mA. The range of operation would then be extended to 380 mA—the useful range of many instruments, including the M.S.2 instrument. This result may be achieved in two ways: firstly, by utilizing only 250 Ω (of the 350 Ω resistance shown on the circuit diagram), to provide a potential on grid of V_{1A}, and secondly, by replacing the 20 kΩ resistors by others of suitable value. This latter method may be extended to the use of a series of resistors of different values such that mass-marks are put on the trace at the values of suitable mass-numbers rather than at equal current intervals. An independent method which further extends the useful range of this device is to reduce the ion-accelerating voltage. If the machine operates at a potential of 1 kV instead of the customary 2 kV, the range of mass-number covered by the mass-marker is doubled, but so equally is any error in the measurements.

The most serious errors may arise from hysteresis in the electromagnet, the more so because, at the upper end of a scan, the magnet must be nearly saturated. This effect is particularly noticeable if a scan is interrupted at some point and then restarted. In such cases, the reproducibility of the magnet-current/ion-mass curve is destroyed and no continuity exists between the two portions of the graph. Consequently the scan must cover the full range of the magnet current and this operation must be carried out at a uniform rate or, at least, in a strictly reproducible way. For the best results, it has been found that a standard procedure (although not necessarily the one given above) should be employed for returning the magnet current to the lower limit. The limited evidence now available indicates that interruption in the magnet scan, if necessary, is best done at higher magnet currents and during the downward part of the cycle. When the scan is restarted, the current is allowed to fall to the minimum value and reverse without interruption. A useful precaution, if the magnet has been switched off for some hours, is to allow a preliminary cycle of the magnet current before undertaking measurements.

A series of measurements has been made upon a variety of known organic compounds, and the values of the magnet current calibrated against the mass-numbers of the fragment ions. As $M/_e\alpha H^2$ errors in the reproducibility of the mass-marker will be exaggerated in the apparent value of M, in the present instance, an error of about 0·3 mA in the magnet current of 286 mA will produce an error of one unit at a mass of 500, the highest so far examined. This is the magnitude of experimental error which has been found and thus places an upper limit on the utility of the device.

Practically, it has been found most useful to assign the mass-numbers of the fragment ions which appear at the values of the magnet current recorded by the mass-marker and to interpolate for others. This method has the advantage that, for small variations in the reproducibility of the marker, the correct fragment ion is still chosen. Occasionally, however, particularly with aromatic compounds which give rise to few fragment ions, the alternative procedure is necessary. The magnet current corresponding to a fragment ion is obtained by interpolation from the known values of the current and the mass of the ion determined.

Initially the making and breaking of the various contacts proved troublesome until suitable values of R_2 and C_2 wer found by trial and error. Certain technical advantages migh accrue if the level of operation of the uniselector could b made dependent upon the actual level of the 2 kV repeller plate potential, and also if the marker operated on th downward rather than the upward scan. These possibilitie are now being investigated.

Acknowledgements

The authors wish to express their indebtedness to th Hydrocarbons Research Group of the Institute of Petroleu for financial assistance and to Professor P. I. Dee and Dr. W McFarlane for extending to them the facilities of the Department of Natural Philosophy of the University of Glasgow for the construction of this instrument.

Appendix

Components used

Resistors

One 200 Ω ± 5%; one 1 kΩ ± 5%, w.w.; Two 4·5 kΩ ± 5%, w.w.; Twenty-four 20 kΩ ± 1%, h.s.; Two 22 kΩ ± 1% h.s.; One 47 kΩ ± 5%, w.w.; One 150 kΩ ± 1% h.s.; On 180 kΩ ± 1%, h.s.; Two 200 kΩ ± 5%; Three 560 kΩ ± 1%, h.s.; Two 10 kΩ w.w. preset potentiometers; One 25 kΩ w.w. preset potentiometer.

Capacitors

One 0·0003 μF; Two 0·05 μF; One 0·1 μF; One 0·5 μF One 32 μF, electrolytic, 350 V.

Miscellaneous

One 50-way P.O. uniselector; One 3000-type relay; 1 kΩ 1 make, 1 break; One 3000-type relay; 2 kΩ, 2 make; One metal rectifier, 1–345/14/1 FW; One metal rectifier, 1–RM Twenty-six neon tubes, CV988; Twenty-six neon-tub holders, M.B.C.; One 9-pin B9A valveholder, CV402 One 7-pin B7G valveholder, CV4014; One transformer 250 V primary, 60 V, 1A secondary; Two 2A fuses; Tw fuseholders; One chassis; One 8-pin Painton plug.

Liquid-nitrogen cryostat for single-crystal X-ray diffraction

by A. E. ATTARD and LEONID V. AZÁROFF, Illinois Institute of Technology, Chicago 16, Illinois, U.S.A.

[*Paper first received* 19 *January, and in final form* 8 *March*, 1960]

Abstract

The cryostat employs a continuous flow of precooled gas to maintain a small single crystal mounted on a fibre at −190° ± 2° *C. The cooling chamber is completely enclosed so that a relatively small amount of coolant is required. Higher temperatures can be maintained to within two degrees by simply decreasing the gas flow rate.*

X-RAY diffraction arrangements employing low temperatures have been used in the past to study the thermal properties of crystals and to investigate crystals having melting points below room temperature. Although it was recently suggested that low temperatures be used in the study of ordinary crystals as well,(1) no reported use of this procedure has been made in crystal-structure determinations. By reduction of the thermal motions of atoms in a crystal, the intensities of crystalline reflexions are increased, while the background scattering is decreased. With the advent of direct-ionization detectors in X-ray diffraction analysis, this has become particularly important since both the accuracy and the sensitivity of the analysis can be greatly increased thereby. Experience has shown that temperatures between −150 and −200° C are sufficient, in most instances, to obtain optimum peak-to-background ratios.

Cooling arrangement

There are several ways that a crystal can be cooled. Pro- ded it is sufficiently large, it can be placed in direct contact th a metal plate that forms the side of a liquid nitrogen ntainer. The very small size of the crystals usually used X-ray diffraction studies, however, makes the cooling of em by conduction impractical. The crystal, mounted at e end of a thin fibre, therefore, is usually cooled by passing refrigerated gas directly over it.(2–4) The cryostat described elow also uses this arrangement. It has the following portant advantages over previous devices: (1) the tem- erature of the crystal can be maintained as low as -190° ± 2° C for extended periods of time; (2) a higher mperature can be maintained with equal accuracy by mply adjusting the rate of gas flow, the refrigerant used, or oth; (3) the amount of coolant materials used is a small action of that required by other arrangements. This last ctor becomes particularly important when a very large umber of X-ray reflexions is to be measured, and is probably e principal reason why low temperatures have not been sed in routine analyses despite the advantages in doing so.

Design features

A cross-sectional view of the cryostat is shown in the igure. It consists of two parts: the cryostat proper, shown o the left, and a base containing the goniometer head, to which the crystal is affixed. The cryostat slides over the goniometer head and is held in place by three external clips (not shown). The cryostat consists of a liquid-nitrogen chamber, which is insulated by a vacuum chamber surrounding it, a $\frac{1}{4}$ in. copper coil passing through the liquid nitrogen, and a small chamber wherein the crystal to be examined is located when the two parts are joined together. Liquid nitrogen is supplied to the chamber through an opening $\frac{1}{2}$ in. in diameter in its top by means of a siphon placed in a liquid-nitrogen reservoir. A dry gas, say helium, is forced through the copper coil in this chamber and is thereby cooled to the temperature of liquid nitrogen. As it leaves the coil, it strikes the crystal which is located approximately $\frac{1}{4}$ in. from the orifice. When it is desired to cool the crystal to −190° C, the gas is precooled in an auxiliary cryostat consisting of a copper coil placed in a one-litre Dewar flask containing liquid nitrogen. By adjustment of the flow rate of the gas between 5 and 15 l./min, any temperature between −150 and −190° C can be obtained by this arrangement. For higher temperatures, the precooling stage can be omitted.

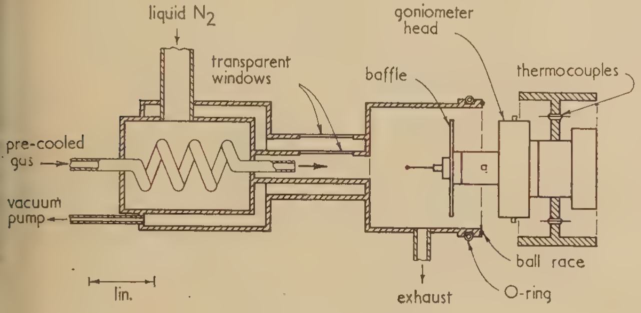

Cross-section of cryostat

A double, transparent window of 0·01 in. lucite surrounds the crystal and allows diffraction over a 200° C range about the goniometer axis and from +40 to −15° C about a transverse plane containing the direct beam. The crystal and goniometer head assembly is free to rotate about its own axis. This rotation is made possible by using a graphite coated O-ring and a ball-bearing race at the base, as shown in the figure. A circular baffle placed between the crystal and goniometer head prevents the coolant from striking the goniometer head directly. To further minimize the cooling of the goniometer arcs, a small heater coil is attached to the rear of this baffle. Thus, when the crystal is cooled to −190° C, the temperature of the goniometer head is only −52° C. After passing over the baffle, the coolant gas is allowed to escape through an outlet in the bottom of the goniometer-head chamber. Insulated, feed-through seals in the base provide outlets for two thermocouples and the heater leads.

Utilization

This cryostat was designed for use with a special single-crystal diffractometer based on a design by M. J. Buerger. The cryostat is supported in a horizontal position by means of a clamp and stand attached to the diffraction unit. The goniometer head is then made to oscillate about various settings of the crystal by a motor drive in the diffractometer. Before beginning a series of measurements, the insulation chamber is evacuated and sealed. The crystal chamber is next evacuated through the outlet, and the gas flow is started. The crystal reaches the desired temperature within a couple of minutes. (The optimum flow rate, etc., is previously determined by placing a thermocouple in the position of the crystal.) If desired, the same gas can be used again by connecting the inlet and outlet tubes of the cryostat to a recirculating pump. The temperature of the crystal chamber and the goniometer head can be checked with the aid of two thermocouples placed on opposite sides of the baffle. When Ag$K\alpha$ X-radiation is used, the diffracted beams suffer an attenuation of approximately 10%. This is a very small loss and is more than offset by the very much larger increase in intensity resulting from the decreased thermal scattering. In fact, experience has shown that reflexions, the intensities of which could not be measured at room temperature, can be detected quite readily with this cryostat. Incidentally, it should be noted that because the lucite window is cylindrically disposed about the crystal, any correction for absorption can be included in the usual correction made for cylindrical crystals.(5)

Acknowledgement

The authors would like to thank Mr. H. Deptolla for his help in constructing this cryostat.

References

(1) Burbank, R. D. *Rev. Sci. Instrum.*, **23**, p. 321 (1952).

(2) Abrahams, S. C., Collins, R. L., Lipscomb, W. N., and Reed, T. B. *Rev. Sci. Instrum.*, **21**, p. 396 (1950).

(3) Post, B., Schwartz, R. S., and Fankuchen, I. *Rev. Sci. Instrum.*, **22**, p. 218 (1951).

(4) Woods, E. A. *Rev. Sci. Instrum.*, **24**, p. 325 (1952).

(5) Buerger, M. J., and Niizeki, N. *Am. Mineral*, **43**, p. 726 (1958).

Large storage binary-to-decimal converter

by G. DEARNALEY, M.A., Ph.D.,* L. G. LAWRENCE, M.A., and H. C. TRESISE, B.Sc.,
Cavendish Laboratory, Cambridge

[*Paper first received* 27 *July*, 1959, *and in final form* 18 *January*, 1960]

Abstract

An accurate binary-to-decimal converter is described capable of dealing with numbers up to 2^{24}. *The instrument is designed for manual input with display on dekatron indicators, and a speed of operation of four bits per second.*

Introduction

There are many instruments using a display in the binary system, and several methods have been described for converting this display into the more familiar decimal system.(1,2) However, where complete accuracy, speed of operation and large capacity are required, it was felt necessary to use a digital computer design. The method described fulfils these requirements, and some features may have other applications where very high speed is not essential.

General principles

The basis of the design is the pulse source of separate but synchronized groups of 1, 2, 3 . . . 9 pulses, which are permanently connected to the requisite contacts of seven banks of a 25-way uniselector. The banks correspond to powers of ten up to 10^6 and successive wiper positions correspond to successively higher powers of two. Thus the $(n+1)^{th}$ wiper position relates to $2^n = \ldots dcba$, and the first bank contact would be connected to the source of a pulses and so on, as illustrated by Fig. 1 for the first few banks and contacts. From the wipers the pulses are fed to the corresponding dekatron stage of the seven-decade display.

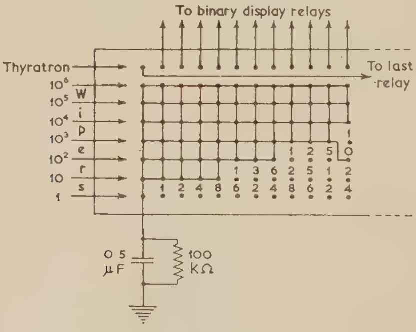
To binary display relays
Thyratron
10^6
10^5
10^4
10^3
10^2
10
1
W
i
p
e
r
s
To last relay
1 2 5
1 3 6 2 5 1
1 2 4 8 6 2 4 8 6 2
1
0
2
4
0 5 µF
100 kΩ

Fig. 1. Connexions of pulse sources to the first few banks and contacts

Outline of the design

The block diagram is shown in Fig. 2. The input is by a pair of push-buttons A and B, the operation of which corresponds to the addition, or not, of the particular pow of two into the storage display.

Button A operates a scale-of-two gate which in turn ope a suppressor-gated amplifier allowing pulses from a co tinuously running multivibrator to pass through. The puls

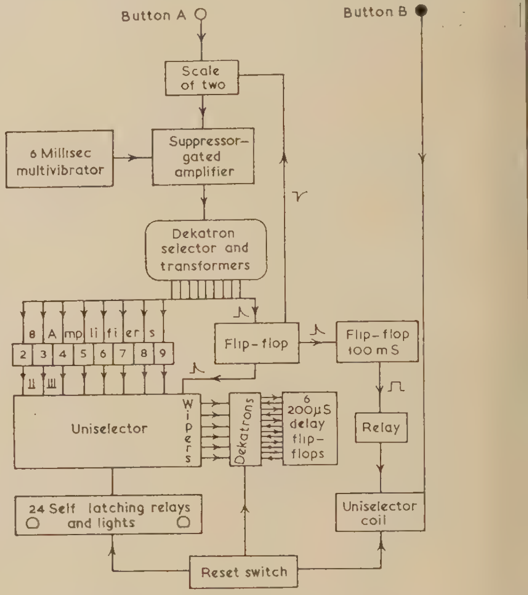
Button A
Button B
Scale of two
6 Millisec multivibrator
Suppressor-gated amplifier
Dekatron selector and transformers
8 Amplifiers
2 3 4 5 6 7 8 9
II III
Flip-flop
Flip-flop 100 mS
Uniselector
Wipers
Dekatrons
6 200µS delay flip-flops
Relay
24 Self latching relays and lights
Uniselector coil
Reset switch

Fig. 2. Block diagram of the circuit

V_1, V_3 = ECC91 (6J6 CV858)
V_9 = 1/2 CV858
V_2 = CV329
V_4 = GS126 dekatron selector
V_5 = 1/2 ECC81 (12AT7 CV455)
V_6, V_7 = ECC81
V_8 = EN91 (2D21) thyratron
V_{10} = GC10B/5 (CV2271)
V_{11} = ECC83 (12AX7 CV492)

D_1 = EA50 (CV1092) hot diode
All other diodes crystal diodes CV448

R_1, R_3, R_4, R_{16}, R_{32}, R_{47}, R_{61}, R_{70}, R_{79}, R_{80} = 470 $k\Omega$
R_2, R_{48} = 15 kΩ
R_{84} = 1·5 MΩ
R_5, R_{11}, R_{18}, R_{22} = 560 kΩ
R_6, R_{10}, 3 W., R_{67} = 33 kΩ
R_7, R_8 = 330 kΩ
R_9 3 W., R_{26}, R_{46}, R_{72} = 22 kΩ
R_{12}, R_{13}, R_{37}, R_{40}, R_{49}, R_{60}, R_{77} = 1 MΩ
R_{14}, R_{41} = 68 kΩ
R_{15} = 50 Ω
R_{17}, R_{19}, R_{21}, R_{28}, R_{30}, R_{31}, R_{32}, R_{33}, R_{34}, R_{35}, R_{36}, R_{38}, R_{54}, R_{58} = 100 kΩ
R_{24}, R_{25}, R_{27}, R_{55}, R_{59}, R_{64}, R_{65} = 47 kΩ
R_{29}, R_{43} = wire wound potentiometer
R_{51} = wire wound potentiometer
R_{66} = 10 kΩ
R_{20}, R_{62}, R_{81} = 39 kΩ
R_{23}, R_{63}, R_{71} = 150 kΩ
R_{53} = 3·9 MΩ
R_{57} 6X6 W.12 Ω = 72 Ω

R_{74} wire wound potentiometer = 5 k
R_{69} = 82 kΩ
R_{39}, R_{42}, R_{50} = 330 Ω
R_{45} = 820 k
R_{56} = 3·9 k
R_{68}, R_{75} = 680 k
R_{76} 3 W. wire wound = 50 k
R_{73} = 6·8 kΩ
R_{78} = 56 kΩ
R_{82} = 18 kΩ
R_{83}, R_{84} = 100 Ω
R_{44}, R_{52} 6 W. wire wound = 3 k
M_1, M_2, M_3 = metrosils 110 V, 1 W.
R_{85}, 1 kΩ in series with 1 kΩ relay c
T_1–T_9 intervalve transformers 5 : 1
S_1 button A (yes); S_2 button B (no)
RS, reset switch

C_1, C_6, C_7 C_{16}, C_{19}, C_{27}, C_{36}, C_{38} = 0·01 µF
C_2, C_5, C_8, C_{10}, C_{11}, C_{17}, C_{18}, C_2 C_{22}, C_{39}, C_{40}, C_{41} = 0·1 µF
C_9, C_{20}, C_{31}, C_{32} = 0·02 µF
C_3 = 0·005 µF
C_{13} = 0·05 µF
C_{33} = ~200 µµF
C_{24} = 0·05 µF
C_{28} = 0·25 µF
C_{34} = 1500 µµF
C_{23} = 1 µF (electrolytic)
C_4, C_{30} = 100 µµF
C_{12} = 2000 µµF
C_{14}, C_{35} = 1000 µµF
C_{25}, C_{26} = 0·5 µF
C_{29} = 680 µµF
C_{15} = 100–300 µµF

---

* Now at Atomic Energy Research Establishment, Harwell, Berkshire.

ve a period of 6 ms and a mark-to-space ratio of 1 : 2. hese pulses are fed into a twelve-position dekatron selector be (type GS12C by Ericsson Telephones Ltd.) which is the ulse source. As the method of obtaining the requisite umbers of pulses is novel, it is best described in some detail, ith reference to Fig. 3. The first ten separate cathodes of e tube are connected to the primaries of a chain of nine nall transformers (Radiospares intervalve type, ratio 1 : 5), nd one end of the chain is earthed. One side of each condary is earthed, the output being taken from the other. iodes can be used across the primaries to eliminate nwanted pulses and the associated ring of the transformer, ut this was only found to be necessary with the last one in e chain (the unit pulse transformer).

As the discharge invests cathode x from the second guide ectrode, current flows through the primaries of the x ansformers up to this point in the chain, producing pulses each of these x secondaries. When the discharge leaves is cathode, a pulse of the same size but of opposite sign is roduced at the same secondaries. The glow moves around e nine cathodes in the chain, the first transformer giving ine pulses, the second eight, and so on; the pulses are, of course, synchronized and the single pulse from the last transformer coincides with the last pulse in each group. The

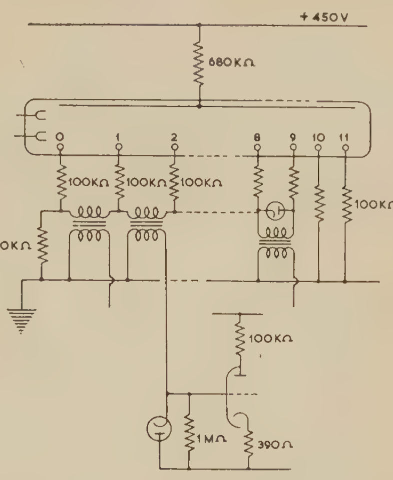
+450V
680KΩ
C
C
0
1
2
8
9
10
11
100KΩ
100KΩ
100KΩ
100KΩ
10KΩ
100KΩ
1MΩ
390Ω

Fig. 3. Pulse source and amplifier

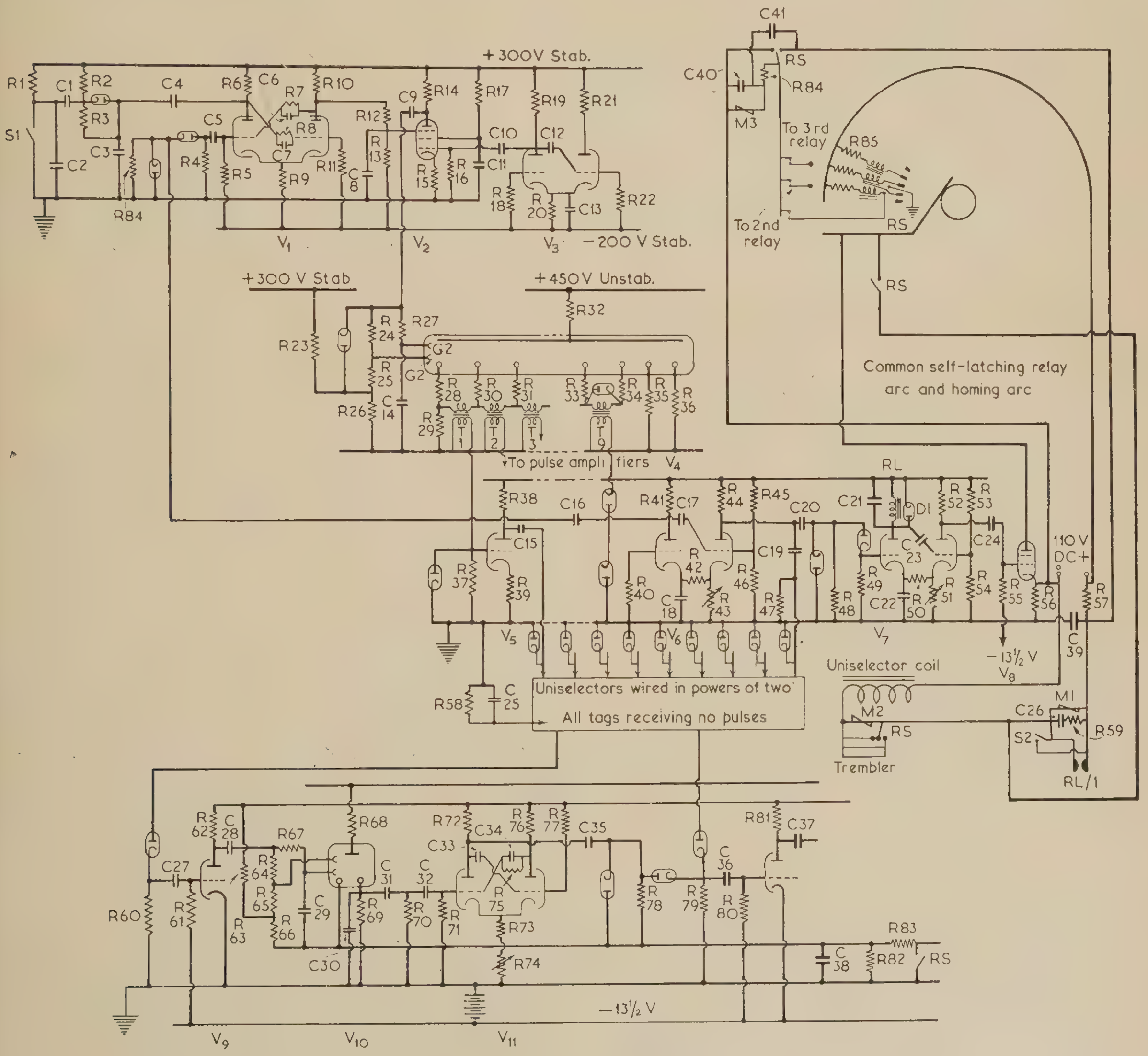
+300V Stab.
R1
C1
R2
R3
C4
R6
C6
R7
R10
R8
C5
C7
S1
C2
C3
R4
R5
R9
R11
C8
R12
R13
C9
R14
R15
R16
R17
C10
C11
R18
R19
R20
C12
C13
R21
R22
R84
V1
V2
V3
−200 V Stab.
+300 V Stab
+450V Unstab.
R32
R23
R24
R27
G2
R25
G2
R26
C14
R28
R29
R30
R31
R33
R34
R35
R36
T1
T2
T3
T9
To pulse amplifiers
V4
C40
C41
RS
R84
M3
To 3rd relay
R85
To 2nd relay
RS
RS
Common self-latching relay arc and homing arc
RL
R38
C16
R41
C17
R44
R45
C20
C21
D1
R52
R53
C15
R37
R39
R40
C18
R42
R43
R46
R47
C19
R48
R49
C22
C23
R50
R51
R54
R55
R56
C24
110V DC+
R57
C39
V5
V6
V7
−13½ V
V8
Uniselector coil
M2
RS
Trembler
M1
C26
S2
R59
RL/1
R58
C25
Uniselectors wired in powers of two
All tags receiving no pulses
R62
C28
R67
R68
R72
C34
R76
R77
C35
R81
C37
C27
R64
C31
C32
C33
R60
R61
R63
R65
R66
C29
R69
R70
R71
R75
R73
R78
R79
C36
R80
C30
R74
C38
R82
R83
RS
−13½ V
V9
V10
V11

Fig. 4. Circuit diagram

positive pulse from the last transformer triggers a univibrator,(3) from which are taken a negative pulse to close the gate and a positive pulse to trigger a second univibrator (having a relay coil as anode load) for the purpose of resetting and moving the uniselector on. From the other eight transformers negative pulses (about 8 V high) are fed into amplifiers. The outputs from these, together with a positive pulse from the first univibrator, are fed into the uniselector as described above, and from there into the dekatron display. Thus at each operation of button *A*, separate groups of 9, 8, 7 . . . 1 pulses are produced and fed into the appropriate dekatron.

A miniature thyratron (type 2D21) and self-latching relays are used to give an indication, by light bulb, of the addition of this binary digit, so that there are always equivalent binary and decimal displays. An eighth bank of the uniselector is used for the relays.

If button *B* is pressed, the uniselector is simply moved to its next position, and no change is made in the displays.

In order to avoid difficulties from the coincidence of pulses fed into a dekatron stage, and the carry pulses from the previous one, a univibrator is used to delay the carry pulses by a time of about 200 μs.

Speed of operation is limited, by resetting and uniselector time constants, to about five bits per second. If greater speed were required, an increase by a factor of ten could be achieved by another dekatron drive circuit, and by using larger current pulses with shorter time constants for the relays.

A switch is provided in order to reset the instrument to zero. For this the dekatrons are reset in the usual manner; the uniselector has a homing arc (making nine banks required in all) and trembler, and the binary display circuit of self-latching relays and lights is opened.

Details of circuits and construction

The circuit diagram is given in Fig. 4. It should be not that the complications in the binary display circuit are d to the same uniselector bank being used for the homing a as for the binary display relays. The supplies required a 450 V, 5 mA, unstabilized, 300 V, 100 mA and −200 10 mA stabilized, with 50 V, 2 A for the uniselector an relays, and 6·3 V, 8 A for heaters and lights. A lo impedance bias supply of −13½ V is best supplied by d batteries.

The input push-buttons are micro-switches for positi action. These and the reset switch are conveniently mounte in a small unit which can be close to the binary display bei read. Connexion to the main converter is by twelve-co cable.

In order to avoid spurious pulses, it is necessary to ear all unused uniselector tags, to magnetically isolate t uniselector from the transformers and to use Metrosil spa suppression on the uniselector operating contacts.

Acknowledgements

We are grateful to Messrs. Ericsson Telephones Ltc Beeston, Nottinghamshire, for readily providing informati regarding their dekatron tubes.

References

(1) Shire, E. S. *Cavendish Laboratory Electrostatic Generat Circuit.* Unpublished.
(2) Setterwall, M. *J. Sci. Instrum.*, **33**, p. 18 (1956).
(3) Chance, B., Hughes, V., MacNickol, E. F., Sayre, D and Williams, F. C. *Waveforms*, M.I.T. Radiatio Laboratory Series, Section 5 (New York: McGra Hill Book Co. Inc., 1949).

Growth of single crystals of anthracene

by J. N. SHERWOOD, B.Sc., Ph.D., A.R.I.C., and S. J. THOMSON, B.Sc., Ph.D., F.R.I.C., Chemistry Department, University of Glasgow

[*Paper received 16 February*, 1960]

Abstract

Single crystals of anthracene have been grown from melts of zone-purified material, in an all-glass oven. The important factors which governed the successful growth of single crystals by the moving-vessel technique have been investigated, viz. the purity of the anthracene, the temperature gradient, the shape of the growth vessel and the growth rate.

Introduction

Growth of organic crystals from the vapour phase usually results in slow growth of very thin crystals.(1–5) Thus, when large single crystals are required, these must be grown from the melt, or from saturated solution. In the case of anthracene, the latter method is of doubtful applicability, because the limiting factor in growth from solution(6) is solubility. Solubilities of 20–50% by weight are required for tolerable growth rates, and anthracene solu bilities are much lower. There is also the disadvantage o possible solvent occlusion.

Growth from the melt has none of these disadvantage and reports(7–13) are available on the growth of anthracen crystals by this method. Though the Kyropoulos pro cedure(14, 15) may not be used because of the volatility o anthracene, and the likelihood of atmospheric oxidatio the moving-vessel(13, 16–19) and the stationary-vessel tech niques(16, 20, 21) can be used. These have the advantage tha crystals can be grown from highly purified material in a inert atmosphere. The moving-vessel technique was chose for the present study. The investigation is concerned wit several important criteria to be observed before crystals ca be grown successfully, namely, the purity of materials, th temperature gradient, the rate of crystal growth, and th shape of the growth vessel.

Growth oven

vertical oven, in which the whole process could be erved, was constructed from three concentric tubes of ex glass (Fig. 1). The vessel containing the anthracene suspended in the upper part of the furnace, where the

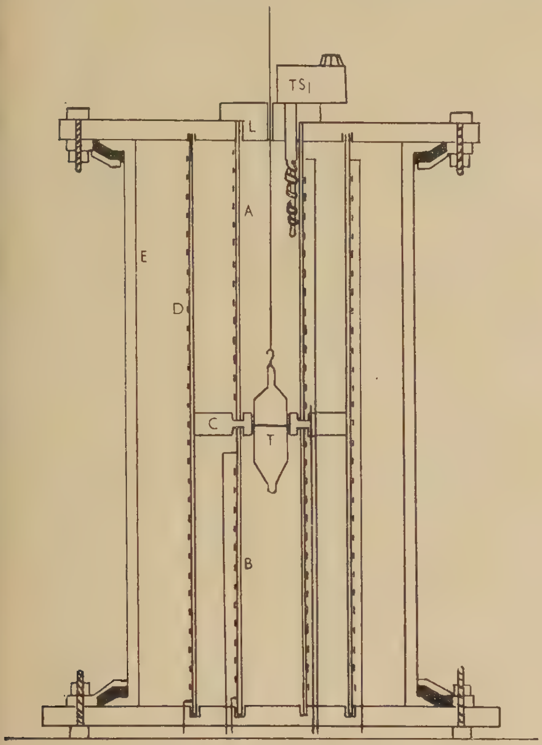

Fig. 1. Crystal-growing oven

mperature was above the melting point of anthracene. he vessel was then lowered slowly down the temperature radient. As the tip of the vessel passed the isothermal at 17° C, crystallization began. Continued lowering resulted crystal growth.

Two heating coils A and B of resistance 80 and 130 Ω espectively, were wound from 33 Ω/yd "Nichrome" heating ape (0·025 × 0·002 in.) on the two 2 in. diameter Pyrex lass tubes A and B. The heaters were wound with the coils loser together at the lower ends, in order that an even temerature could be maintained along as much of the length f the coil as possible. The two coils were separated by a Sindanyo" asbestos baffle C, the central hole of which was ust large enough to admit the crystal growth tube T to the ower half of the oven. The outside diameter of C was cut o 2·6 in. so that a third Pyrex glass tube D of that internal iameter would slip over this, and lie concentrically with A nd B. On D a 100 Ω heating coil was uniformly wound ith wire similar to that used for A and B.

The tubes A, B and D were supported at the top and ottom by two circular "Sindanyo" sheets, and were enclosed y the thick-walled, 12 in. diameter, Pyrex glass pipe E. In he upper "Sindanyo" sheet was cut a hole 2 in. in diameter o that access could be gained to the oven. When the oven as in use, this hole was closed by means of the lid L, which lso served as a support for the thermostat TS_1. The crystal rowth tube T was supported by a fine wire which passed hrough a small hole in this lid.

The oven was protected from draughts by enclosing it in a hardboard box which also served as a support for the control panel for the heaters and the lowering mechanism. The growing crystal could be viewed through a small hole in the front of the box.

The heaters A and B were arranged in parallel, and operated from 250 V, a.c. stabilized mains, *via* adjustable rheostats. Heater D was a thermostatically governed control coil, which was fed through a "Sunvic" circuit F102/3M, incorporating a thermostat TS_1 energy regulator, and hot-wire vacuum switch.

Temperature gradient

Suggested gradients vary between a gradual change between the upper and lower limits$^{(17, 22)}$ and those which have a very steep gradient.$^{(7)}$ The optimum condition found for anthracene growth, was a steep gradient: heaters A and B were arranged to operate at 10° C below the required temperature, viz. 240 and 190° C, and heater D was used as a control coil to raise the temperature over the last 10° C. The temperature was uniform for 2–3 in. above and below the baffle, where the temperature fell 50° C over the thickness of the baffle, 0·5 in.

Growth vessels

The initiation of good seed crystals is difficult for organic crystals. Tammann$^{(23)}$ used a vessel with a long capillary and the first experiments were conducted with the growth vessel shown in Fig. 2(a). Though some workers report$^{(17)}$ that this aids single-crystal growth, we found, like others,$^{(22)}$ that about twelve small crystals were produced surrounded

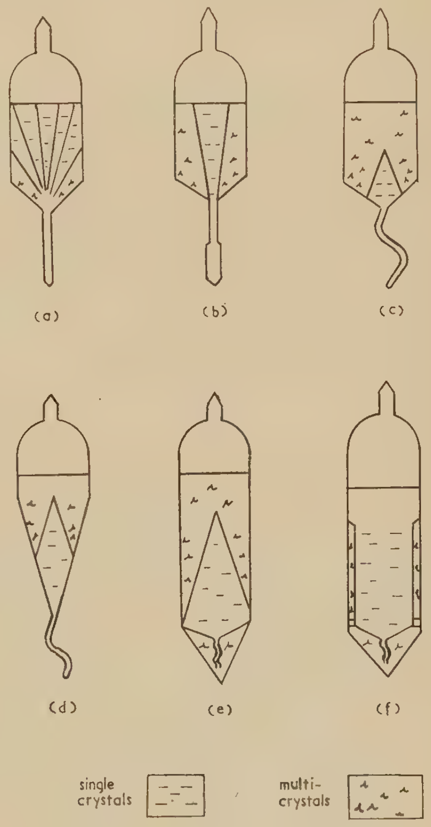

Fig. 2. Crystal-growing tubes

by polycrystals. In Fig. 2(*b*), the modified design had a bulb on the capillary and a limited number of crystals grew into the capillary to produce about six single crystals in the vessel.

While investigating the growth of stilbene crystals, Scott, Hutchinson and Lapage(16) used a bent capillary, Fig. 2(*c*), and a single crystal was produced. With anthracene, single crystals were grown in the upper part of the vessel, but these were in the form of inverted wedges, and they were surrounded by polycrystals. These had been seeded in the lower corners of the vessels, either because of temperature fluctuations, or because outward growth of the single crystals was slow.

Design 2(*d*) was introduced to remove the shoulders of the growth vessel but once again polycrystals were formed. To reduce their interference with the single crystal, the baffle(16) in 2(*e*) was used. Larger single crystals resulted, but polycrystals were initiated at the top of the baffle, perhaps because of local cooling.

In the final successful design, Fig. 2 (*f*), a vessel was constructed, with an inner growth tube. The anthracene in the annular space between the inner and outer vessels acted as a thermal insulator. The bent capillary aided single-crystal initiation, and the conical shape obviated "corner" effects as the single crystal grew into the wider tube.

The single crystals produced completely filled the inner tube, and the best crystals were finally grown with high-purity anthracene from the zone-melting process. The boules were 4 cm long and 2·5 cm in diameter and the crystals had a beautiful blue fluorescence.

Crystal orientation

The factors which affect this aspect of the crystal growth are discussed by Scott, Hutchinson and Lapage.(16) We have found that, for anthracene, if θ, the angle of inclination of the capillary to the vertical, was less than 45°, then the crystals grown in the vessel had the 001 cleavage plane vertical. If θ is greater than or equal to 45°, re-orientation occurred and the cleavage planes of the crystal were horizontal, the crystals produced after re-orientation were, unexpectedly, single crystals. This was probably the result of using highly purified material, and growing the crystals very slowly. For the purpose of the present study, crystals were usually grown in which the cleavage planes were horizontal.

Rate of crystal growth

The rate of crystal growth sets an upper limit to the rate at which the crystal-growing vessel can be lowered in the oven. A rate of 1–2 mm/h has been recommended(16) as an upper limit for organic crystals, in contrast to 20 mm/min for metals(24) and 1–4 mm/h for ionic crystals.(15, 25)

The crystal-growing tube was lowered by means of a geared-down synchro-clock motor. It was found that rates greater than 1–2 mm/h always resulted in the formation of multi-crystals, whereas lower rates resulted in satisfactory growth. Large crystals could be grown in 8 to 10 days at 0·5 to 1 mm/h.

Purification of anthracene

Attempts to grow crystals from Messrs. B. D. H's. Blue Fluorescent Anthracene were unsatisfactory. Even in an inert atmosphere in the growth vessel, brown multi-crystals were produced. A chromatographic purification,(22, 26 which 40–60° petroleum ether was the elutriant, left sev impurity bands on the alumina column. Use of this mate gave an improvement in crystal growth, but the product rate of purified anthracene was inadequate.

Recrystallization(13) from acetic acid followed by th distillations in vacuum, and further crystallization fr acetic acid and then toluene, gave very pure material. original had absorption bands in the region 270–300 mμ 400–460 mμ: Hutchinson and Lapage(13) attributed these the impurities naphthacene, perylene, and carbazole. Wh as chromatography reduced the absorption in these regio the recrystallization procedure gave an even purer prod The u.v. absorption spectrum of the final product in the ra 290–380 mμ compared well with that reproduced Friedel and Orchin.(27)

The quality of the crystals grown from recrystalli material was very much better than that of crystals gro from material purified by chromatography. However, cl observation of crystal growth led to an even better meth of purifying anthracene. After the seed crystal had initia growth from the upper end of the capillary tube, and grow had continued into the upper part of the tube, the apparen perfect crystal gave way to a region with increasing dens of faults, cracks, and striations. It appeared as if impurities remaining in the anthracene were concentrat in the melt, until a limit was attained, when they crystalli out and disrupted the lattice. This concentration impurities in the melt is characteristic of the process of zo refining,(28) and it was decided to use this technique purification of the anthracene.

Zone refining

Powdered anthracene was packed into a thick-wall Pyrex tube, which was then thoroughly evacuated. T anthracene was consolidated to form a compact mass. Th was repeated until a solid mass of anthracene 50 cm lo had been prepared. The tube was evacuated and pump for at least two hours at sticking vacuum. Argon w admitted to a pressure of 12 cm of mercury, and the tu sealed. The inert gas prevented bumping of molten anthr cene. The sealed tube was supported in a vertical positi and a cylindrical furnace, 2 cm long, slipped over it. Th furnace, at 250° C, was lowered down the column at a spe of 2·5 cm/h. Thus a molten band of anthracene, whi contained the impurities, 3–4 cm wide, passed down th column. This process was repeated ten times. The quali of the anthracene in the upper part of the tube was exceller in so far as good single crystals could be grown from th material.

The anthracene was transferred to another apparatu from which it was distilled under a small pressure of argo into the growth vessel. This was evacuated for two hou at sticking vacuum, argon to a pressure 12 cm of mercu admitted, and the vessel was sealed off for crystal growt After crystal growth was complete, the vessel was placed an annealing oven at 180° C for two days. This furna was cooled slowly to room temperature over the next tw days.

Conclusions

The successful growth of single crystals depends partly o the production of the highly purified anthracene and on th e of the vessel with its inner growth tube. The crystals, he form of boules 4 cm long and 2·5 cm in diameter, ld be cleaved easily along the 001 plane, into pieces × 1·5 × 0·75 cm.

he specimens of single crystal were used subsequently in usion experiments.(29) These were examined for sin-arity under the polarizing microscope, and were found e free of all striations, and visible imperfections.

Acknowledgements

We wish to thank Mr. K. T. B. Scott, Dr. R. Lapage, and . S. K. Hutchinson for most useful discussions and advice. N. S. also acknowledges gratefully awards from the Durham lleges and the Gas Council. We also wish to thank the partment of Scientific and Industrial Research for the n of equipment.

References

1) Buckley, H. E. *Crystal Growth* (New York: Wiley and Sons, 1951).
2) Lawson, W. D., and Neilsen, S. *Preparation of Single Crystals* (London: Butterworths, 1958).
3) Dawson, I. M., and Vand, V. *Proc. Roy. Soc., A*, **206**, p. 555 (1951).
4) Craig, D. P., and Hobbins, P. C. *J. Chem. Soc.*, p. 2309 (1955).
5) Brandstätter, M. *Z. Elektrochem.*, **56**, p. 968 (1952).
6) Holden, A. N. *Discuss. Faraday Soc.*, **5**, p. 312 (1949).
7) Mette, H., and Pick, H. *Z. Physik*, **134**, p. 566 (1953).
8) Bell, P. R. *Phys. Rev.*, **73**, p. 1405 (1948).
9) Feazel, C. E., and Dixon-Smith, C. *Rev. Sci. Instrum.*, **19**, p. 817 (1948).
0) Ross, B. *Proc. National Electronics Conference*, **6**, p. 531 (1950).
(11) Deutsch, M. *Nucleonics*, **2**, p. 58 (1948).
(12) Sangster, R. C. *M.I.T. Technical Report on Electronics*, No. 55 (1952).
(13) Hutchinson, S. K., and Lapage, R. *A.W.R.E. Report*, No. 0–73/54 (1955).
(14) Kyropoulos, S. *Z. Anorg. Chem.*, **154**, p. 308 (1926); also *Z. Physik*, **63**, p. 849 (1930).
(15) Menzies, A. C., and Skinner, J. *Discuss. Faraday Soc.*, **5**, p. 306 (1949).
(16) Scott, K. T. B., Hutchinson, S. K., and Lapage, R. *A.W.R.E. Report*, No. 0–4/53 (1953).
(17) Bridgman, P. W. *Proc. Amer. Acad. Arts Sci.*, **60**, p. 305 (1925).
(18) Hendricks, S. B., and Jefferson, M. E. *J. Opt. Soc. Amer.*, **23**, p. 299 (1933).
(19) Baret, C., *et al. C.E.A. Report*, No. 74 (1951).
(20) Rousset, A., and Lochet, R. *J. Physique*, **3**, p. 146 (1942).
(21) Stöber, F. *Z. Krist*, **61**, p. 299 (1925).
(22) Leininger, R. F. *Rev. Sci. Instrum.*, **23**, p. 127 (1952).
(23) Tammann, G. *Metallography*, translated by Dean and Swanson (New York: The Chemical Catalog Co., 1925).
(24) Goss, A. J., and Weintroub, S. *Nature (London)*, **167**, p. 349 (1951); also *Proc. Phys. Soc., B*, **65**, p. 561 (1952).
(25) Stockbarger, D. C. *Discuss. Faraday Soc.*, **5**, pp. 294, 299 (1949).
(26) Curran, S. C. *Luminescence and the Scintillation Counter* (London: Butterworths, 1953).
(27) Friedel, R. A., and Orchin, M. *U.V. Spectra of Aromatic Compounds* (New York: Wiley and Sons, 1951).
(28) Pfann, W. G. *Solid State Physics*, **4**, p. 423 (1957).
(29) Sherwood, J. N., and Thomson, S. J. To be published.

Revised edition of *Notes for authors*

The Institute of Physics has recently published a 36-page revised edition of its booklet intended to assist less-experienced authors and to serve as a reference booklet for all those who wish to contribute to the Institute's publications. Under its new title *Notes for authors*, it gives hints on the preparation of scripts and diagrams, on the layout of mathematics, the correction of proofs and so on. In addition to a bibliography of reference books and works on technical writing, the pamphlet also contains lists of the spellings, symbols and abbreviations used by the Institute. These conform with British Standard 1991: Part I: 1954: *Letter symbols, signs and abbreviations, Part I, General* which authors of mathematical papers are also advised to consult.

Authors preparing contributions for submission to this *Journal* are invited to make use of the guidance available in the booklet, copies of which may be obtained from The Institute of Physics, price 3*s*. 6*d*. (including postage).

Wide-band detector for micro-microampere low-energy electron currents

by T. E. EVERHART, Ph.D.,* and R. F. M. THORNLEY, B.A., Department of Engineering, University of Cambridge

[*Paper received* 25 *January*, 1960]

Abstract

Electrons with a mean energy of a few electron volts emerging from a source a few millimetres in diameter are accelerated on to a positively biased plastic scintillator. The light generated in the scintillator is guided by a Perspex light-pipe to a photomultiplier. If the scintillator bias is greater than 10 *kV, no noise is introduced by the scintillator-light-pipe-photomultiplier system. If the original electron signal is modulated, the maximum modulation frequency transmitted by the system is greater than* 10 *Mc/s. The minimum detectable current is limited by the photomultiplier dark current, and may be less than* 10^{-15} *A with a suitably chosen tube.*

Introduction

The properties of the detector described in this paper were largely determined by the instrument for which it was designed, the scanning electron microscope. In this instrument, a fine electron probe is scanned in a rectangular raster across the surface to be examined. Secondary electrons leaving the surface are collected, amplified and used to control the brightness of a cathode-ray tube scanned in synchronism with the probe. Details of the instrument and the contrast mechanism have been published by McMullan,(1) Smith and Oatley,(2) and Everhart, Wells and Oatley.(3) For the full capabilities of the instrument to be realized, relatively noise-free amplification of the modulated secondary electron current is required. As this current ranges from 10^{-13} to 10^{-10} A, and contains frequency components up to 200 kc/s, conventional thermionic amplifiers cannot comply with the low-noise and bandwidth requirements. Early workers used secondary emission electron multipliers, but these were not very satisfactory, electrically or mechanically.

General description

The new detector (shown in Fig. 1) consists of a cylindrical brass shield which is closed at the end facing the specimen by a grid of copper gauze (etched in nitric acid to increase the grid porosity) and is biased positively in order to attract the low-energy electrons. Once through the grid, the electrons are accelerated toward the hemisphere of plastic scintillator, the surface of which is covered with a 700 Å layer of aluminium (maintained at 7 to 12 kV positive). The intense electrostatic field, shaped by the focusing electrode, causes most electrons to strike the hemisphere near its ap The light generated in the scintillator is guided by a Pers light pipe to a commercial photomultiplier tube which t converts the light back to an electron signal and prov most of the required amplification.

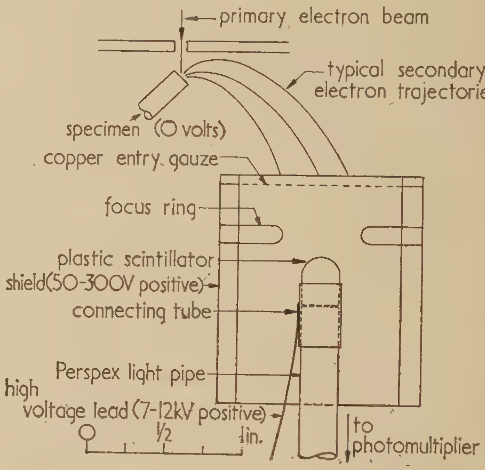

Fig. 1. Diagram showing collector geometry

Theoretical performance

For such a system to be reasonably noise-free, each electr entering the collector must liberate, on the average, at lea one electron from the photomultiplier cathode. The numb of photoelectrons produced by one zero-energy seconda electron entering the collector is given by:

$$n = \{(E_s - E_a)C_pC_0C_ef(\nu_p)\}/E_p$$

where E_s = energy of the electron striking the scintillat surface (eV),
E_a = energy lost by the electron in passing throu the aluminium film (eV),
C_p = energy conversion efficiency into photons average energy E_p,
C_0 = efficiency of the optical system,
C_e = conversion efficiency of the photocathode,
$f(\nu)$ = spectral response of the photocathode photons of energy E_p (eV).

E_a can be calculated from the Thompson–Whiddington la

$$E_a = \sqrt{(E_s^2 - axd)}$$

where x is the film thickness in cm, a is 4 × 10^{11} $(\text{eV})^2$ cm^2 and d is the density in g/cm³.

---

* Now at Department of Electrical Engineering, University of California, U.S.A.

n the early work on the collector, the manufacturer's ure for C_p was used and C_0 was assumed to be unity. is gave n equal to 2·2 for $E_s = 7$ kV, indicating that der these conditions no noise was introduced. It was ınd in practice that noise was being introduced and a ailed investigation of C_p and C_0 was carried out.

Scintillator efficiency

Several workers(4–6) have reported that the conversion iciency of scintillators falls as the incident particle energy reduced below 50 keV, but the losses quoted vary con-lerably. It was therefore necessary to measure C_p at the ergy levels in question.

Two makes of plastic scintillator were investigated—melon, made by Isotopes Development Ltd.; and Naton 11, ade by Nash and Thompson Ltd. No significant difference performance was detected.

A 10 kV electron beam carrying about 10^{-12} A was ranged to strike the scintillator surface, the potential of nich could be varied between +10 and −10 kV. It was und that the response varied approximately linearly with cident energy for energies above a threshold value which ried between 2 and 10 kV. Typical curves are shown in ig. 2. Further investigation showed that the method used o prepare the scintillator surface was of critical importance n determining the performance for low incident energies. Scintillators machined under water-cooled conditions and olished with French chalk in water showed threshold nergies of 2 to 2·5 keV. This energy is that required to enetrate the 700 Å aluminium film used to make the cintillator surface conducting. Dry machining and/or olishing with proprietary brands of metal polish raised the hreshold into the 5 to 10 keV range. Any slight overheating luring the metallizing had a similar deleterious effect on the erformance.

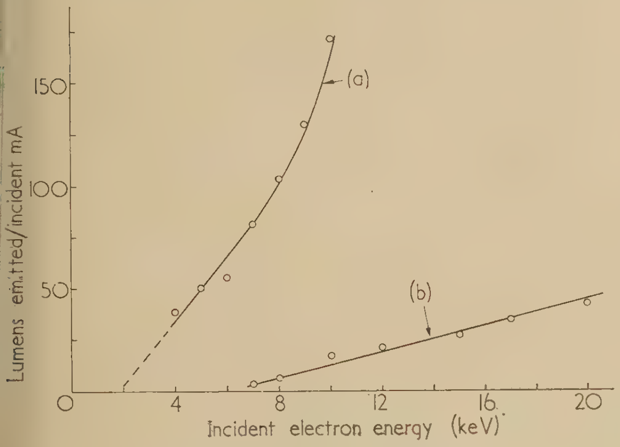

Fig. 2. Scintillator performance

Curve (*a*), wet machined, French chalk polished; curve (*b*), dry machined, polished with metal polish

Measurements with a calibrated photomultiplier showed hat the conversion efficiency of a well prepared scintillator vas 0·02 ± 0·005 for 7 keV electrons. This figure agrees, vithin the limits of experimental error, with the manu-acturer's value.

The scintillator did not show any saturation effects until he input current density reached about 1 A/cm². Under normal operating conditions, the input current density is less than 1 μA/cm² so saturation is not a limiting factor in the performance of the collector.

Optical system efficiency

The optical efficiency of the scintillator-light-pipe system is estimated by assuming that all electrons entering the collector shield (see Fig. 1) strike the scintillator near the apex of the hemisphere. The critical angle θ_c of the scintillator material (measured from a surface normal to the ray path) is 40·5°. If no light is absorbed by the scintillator, and no loss occurs at surface reflexions, then by using a simple geometrical argument, over 90% of the generated light is found to enter the light-pipe. Further, all these light rays entering the light-pipe subtend an angle to the surface normal greater than the critical angle of the light-pipe material, Perspex. Thus in the absence of absorption in the light-pipe, all light entering the pipe should reach the photomultiplier. If it is assumed that a 10% loss of intensity occurs at each surface reflexion in the scintillator, about 80% of the generated light enters the light-pipe.

The transmission efficiency of the light-pipes used was measured with a special neon light source having an intensity distribution similar to that expected from a scintillator hemisphere. The light-pipes were made from $\frac{3}{8}$ in. diameter Perspex rod cut in lengths varying from 9 to 11 cm. The ends were polished. Bends of 45° and 90° with a radius of 2·5 cm were made on some light-pipes by gently warming the rod in a low bunsen flame and then bending to the desired shape. It was found that in no case did the transmission exceed 65%, and if extreme care was not taken with the surface finish, the transmission fell below 40%. The bends did not increase the loss by more than 10% in any case. This loss, which is rather surprising in view of the high transparency of Perspex, is believed to be mainly caused by reflexion losses on entering and leaving the pipe. A drop of vacuum oil placed in a joint between two pipes increased the transmission by about 5% provided the oil did not spread along the ferrule supporting the joint. If this occurred, the loss was greater than for a dry joint.

Measured performance

Putting $C_0 = 0·4$, $C_p = 0·02$ and $n = 1$ in the transfer equation gives $E_s = 8$ keV. This analysis depends on the accuracy of the photomultiplier calibration which was not better than 20%. An independent check on the result was made by observing the signal/noise ratio of the photomultiplier output for a constant input current, with the scintillator voltage varied to give values of E_s between 0 and 20 keV. This gave the curve shown in Fig. 3, indicating

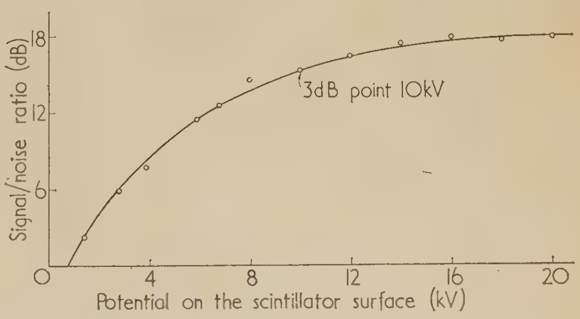

Fig. 3. Signal/noise ratio variation with scintillator potential

that the noise is effectively constant for scintillator potentials greater than 10 kV. (The 18 dB signal-to-noise ratio is determined by the shot noise in the primary electron beam plus the noise introduced in the secondary emission process.)

Conclusions

A wide-band detector for micro-microampere secondary electron currents has been constructed and tested. Noise-free current gains ranging from 10^5 to 10^8 have been observed with a bandwidth exceeding 200 kc/s. The minimum signal which can be detected is set by the dark current of the photomultiplier used. For the tube used in this investigation, an E.M.I. type 6094B, this dark current is less than 10^{-15} A, and it could be reduced further by cooling the photocathode.

The maximum bandwidth is set by the decay time of the scintillator or the transit time spread of the photomultiplier, or both. The decay time for Pamelon is stated to be less than 10^{-8} s, and the transit time spread for the photomultiplier used is about 10^{-8} s. Thus the bandwidth of the present system is estimated to be greater than 10 Mc/s.

As used in the scanning electron microscope, this detector offers important advantages. The mechanical flexibility is much better than that of the old secondary electron detector. A movement of the detector input requires only a new piece of light-pipe bent to the proper shape with the new detector, while previously an entire new brass bottom plate for the specimen chamber had to be constructed.

Previously, the input of the electron multiplier was necessarily near ground potential, requiring the output be approximately 6 kV positive. This in turn required t the initial stages of valve amplification float at 6 kV positi With the new detector, the output of the photomultip can be at ground potential, making a direct-coupled vid amplifier possible.

Acknowledgements

We wish to express our thanks to our supervisor, M C. W. Oatley, for much useful advice and encouragement.

One of us (T. E. E.) was supported by a Marshall Schol ship, while the other (R. F. M. T.) was in receipt of D.S.I.R. Research Studentship.

References

(1) McMullan, D. *Proc. Instn Elect. Engrs*, **100**, Part p. 245 (1953).
(2) Smith, K. C. A., and Oatley, C. W. *Brit. J. Appl. Ph* **6**, p. 391 (1955).
(3) Everhart, T. E., Wells, O. C., and Oatley, C. *J. Elect. & Control*, **7**, p. 97 (1959).
(4) Taylor, C. J., Jentschke, W. K., Remley, M. E., E F. S., and Kruger, P. G. *Phys. Rev.*, **84**, p. 10 (1951).
(5) Birks, J. B., and King, J. W. *Phys. Rev.*, **86**, p. 5 (1952).
(6) Belcher, E. H. *Brit. J. Radiol.*, **30**, p. 103 (1957).

LABORATORY AND WORKSHOP NOTES

Modified cylindrical cell for the microelectrophoresis of suspended particles

by E. J. Ambrose, M.A., and J. Ryder, B.Sc., Chester Beatty Research Institute, Institute of Cancer Research: Royal Cancer Hospital, London, S.W.3

[*Note received* 6 *January*, 1960]

Satisfactory chambers for the measurement of the electrical mobility of very small particles have been known for some time.(1) An apparatus suitable for the measurement of suspended bacteria with a rectangular chamber (0·5 × 25 mm cross-section) has been described by Loveday and James.(2) In these cases the particles remain continuously in suspension and they can always be observed at the stationary level, where the true electrophoretic mobility can be measured. The stationary level lies at a distance of 0·21 times the total depth of chamber from the chamber wall and parallel to the wall. Larger particles sediment under gravity and their mobility can only be measured accurately if they are allowed to fall freely, in the plane of the stationary level, while the electric field is applied at right angles to this direction. The rectangular chamber must therefore be arranged vertically so that the particles can fall through the whole depth of the chamber.(3) This arrangement is reasonably satisfactory but is most sensitive to small thermal changes owing to the vertical depth (25 mm)(4) within which convection currents can arise. The location of the large particles (up to 20 μ in diameter) at the stationary level in the small total depth (500 μ) of the chamber also presents difficulties.

Bangham, Flemans, Heard and Seaman(5) described apparatus using a cylindrical chamber which has sever advantages. The height of the chamber is only equal to t diameter of the tube (2·33 mm) and convection curren leading to drift are therefore not troublesome. The dep of the chamber (2330 μ) is relatively much larger in relatio to the diameter of the particles (20 μ). The apparatus satisfactory for moderately large particles, such as red bloo cells, but larger particles sediment extremely rapidly in th small depth of the tube and it is difficult to take more tha ten readings after filling the chamber, even when working great speed. To enable more readings to be taken, and wit greater accuracy, a method of resuspending the cells in th chamber has been devised.

A small piece of Mumetal (approximately 3 mm lon sealed into thin-walled capillary tubing (Fig. 1) is placed i the electrophoresis chamber. It is drawn along through th chamber by a magnet (Fig. 2). Its passage stirs up the suspension and resuspends the cells without disturbing th thermal equilibrium. The magnet is moved along a meta

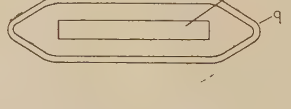

Fig. 1. Enlarged view of stirrer
r, Mumetal; *q*, thin glass

ough, suspended under the chamber from the sides of the ermostat tank, by a pulley. While the cells are timed the irrer rests in one electrode chamber and the magnet is illed just beyond the electrode chamber. In these positions here is no apparent effect on the values of timings. The tirring can be repeated until a sufficient number of results re obtained.

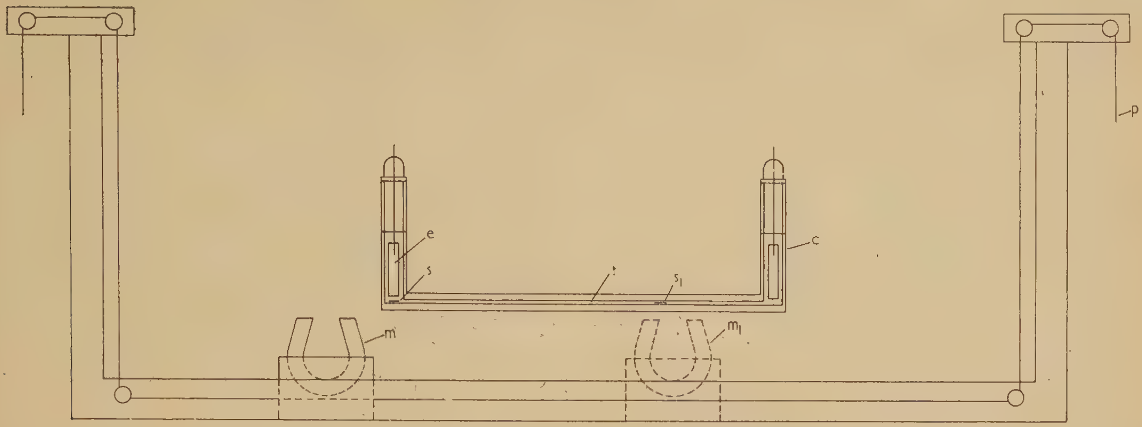

Fig. 2. Electrophoresis chamber with stirrer and magnet.
c, electrophoresis chamber; *s*, s_1, stirrer in alternative positions; *m*, m_1, magnet in alternative positions; *e*, electrode; *p*, pulley; *t*, 2·33 mm capillary

The cylindrical chamber has another disadvantage in that he optical conditions for viewing the particles are unsatisactory owing to the curvature of the wall. This was overome to a considerable extent by grinding and polishing a flat surface 0·1 mm from the inner wall of the tube and immersing the chamber *and* microscope objective in the water thermostat tank.$^{(5)}$ However, the concave cylindrical lens provided by the chamber wall still introduces some distortion (Fig. 3) and Henry's correction$^{(6)}$ must be applied. It is also necessary to locate the centre of the chamber accurately to be at the point of minimum depth of the chamber wall.

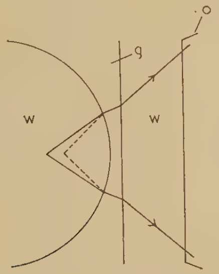

Fig. 3. Diagram of light rays passing through plane ground cell
g, glass; *w*, water; *o*, microscope objective

As an alternative, thin-walled capillary tubing of accurate bore can be obtained, but the wall thickness is approximately 0·6 mm with the result that image definition is poor. A more satisfactory chamber (Fig. 4) has been prepared in which a portion of the wall (12 × 1 mm) is ground down evenly to give a cylindrical wall 0·1 mm thick. The grinding is done using a diamond lathe and rotating the capillary tube at an angle of 60°. With this arrangement vertical alinement of the chamber is not so critical and the deflexion of light rays by the wall is very small (Fig. 5) so as to be negligible for usual numerical apertures. The image definition is considerably improved.

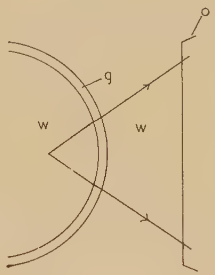

Fig. 5. Diagram of light rays passing through cylindrically ground cell
g, glass; *w*, water; *o*, microscope objective

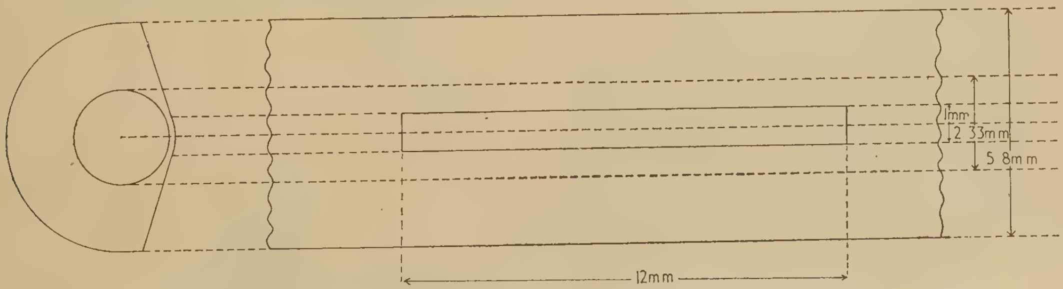

Fig. 4. Diagram of electrophoresis chamber to show the thin-walled portion

We should like to thank Dr. A. D. Bangham, Dr. D. H. Heard and Dr. G. V. F. Seaman for helpful discussions. This investigation has been supported by grants to the Chester Beatty Research Institute from the Medical Research Council, the British Empire Cancer Campaign, the Jane Coffin Childs Memorial Fund for Medical Research, the Anna Fuller Fund, and the National Cancer Institute of the National Institutes of Health, U.S. Public Health Service.

References

(1) Abramson, H. A., Moyer, L. S., and Gorin, M. H. *The electrophoresis of proteins* (New York: Reinhold Publishing Corporation, 1942).
(2) Loveday, D. E. E., and James, A. M. *J. Sci. Instrum.*, **34**, pp. 97–98 (1957).
(3) Purdom, L., Lowick, J. H. B., James, A. M., and Ambrose, E. J. To be published.
(4) Brinton, C. C., Jr., and Lauffer, M. A. *Electrophoresis, theory, methods and application* (Ed. Milan Bier), p. 446 (New York and London: Academic Press Inc., 1959).
(5) Bangham, A. D., Flemans, R., Heard, D. H., and Seaman, G. V. F. *Nature* (*London*), **1820**, pp. 642–644 (1958).
(6) Henry, D. C. *J. Chem. Soc.*, p. 997 (1938).

Instruments for measuring the temperature of a running thread-line, and of a jet of viscous liquid

by M. F. Culpin, Ph.D., and K. A. Martin, British Nylon Spinners Ltd., Pontypool, Monmouthshire.

[*Note received* 21 *March*, 1960]

The instrument for measuring the temperature of a running thread-line, described in a previous issue of this *Journal*,* consisted essentially of the parts shown in Fig. 1. A thermocouple *A* was joined to a source of heat *B* by means of a piece of material *C* of fairly low thermal conductivity. When the temperature of the thermocouple *A* had settled down, the thread-line *D* was moved quickly down to the position *E*, touching the thermocouple. If the temperature of the thread-line differed from that of the thermocouple, the latter would, through a suitable potentiometer and galvanometer, indicate a change of temperature. The operation of the instrument required the adjustment of the thermocouple temperature, by means of the heater, until the thermocouple showed no change of temperature on contact with the thread-line. This temperature of the thermocouple was taken to be the same as that of the thread-line.

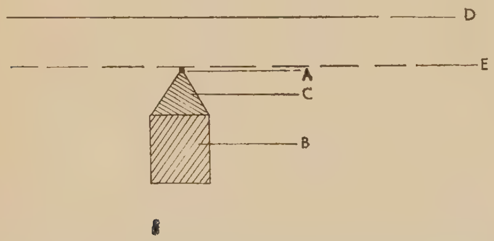

Fig. 1. Basic details of instrument for measuring the temperature of a running thread-line

For measurements on a running thread-line, two improv ments in the design were sought: firstly, to increase th sensitivity, so that measurements could be made on threa lines of smaller size; and secondly to reduce the time require for the thermocouple to settle down to a new temperatu when the temperature of the heater was altered. The instr ment head shown in Fig. 2 satisfied these requirements. Th heater *F* consists of a piece of thin nickel strip folded back o itself, the tails being formed into split tubes to which hea copper leads are attached for electrical connexion. Thes leads pass through a Tufnol bush *I*, and are used to suppo the heater assembly. The latter is mounted in an enclosin copper tube *J*, arranged so that the centre of the fold *G* i the heater appears at a hole *H* in the centre of a piece o Teflon sheet *K*, shaped as shown to fit the end of the tube *J*. Behind the centre of the fold *G* in the nickel strip, a thermo couple is silver-soldered with a minimum of solder. I practice, the instrument is brought up to the thread-line *L* so that the latter runs against the nickel foil at *H*. Th thermocouple being in contact with the heater itself ensure a minimum of thermal lag, while the small thermal capacit of the nickel strip ensured good sensitivity of the device. (A further point in favour of the design is its simplicity o construction.)

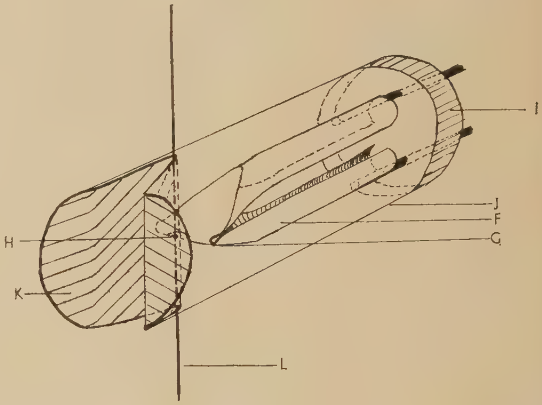

Fig. 2. Improved instrument head

To measure the temperature of a jet of viscous liquid, an instrument of more robust design, which could be easily cleaned after each test, was required. Such a device is shown in Fig. 3. A nickel strip *N* carries a thermocouple *O* and thick copper leads *P*. It is held inside a square metal tube *Q* by means of fire clay plugs *T*, and insulated electrically by

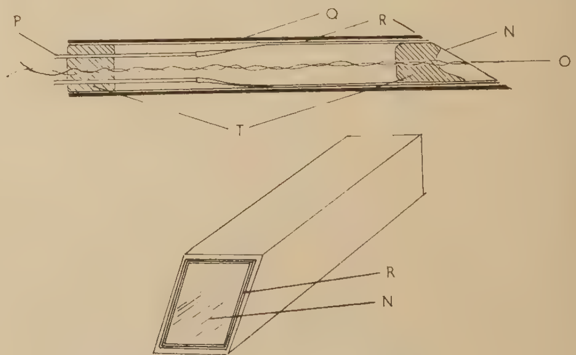

Fig. 3. Instrument for measuring the temperature of a jet of viscous liquid

ca strips *R*. When the temperature of the thermocouple *O* s settled down, the device can be "dabbed" into a vertical of liquid so that the latter impinges at *O*. As in the case a thread-line, the temperature at *O* is adjusted until it es not change on contact with the liquid. Care must be ken, of course, that the flow of the jet *above* the dabbing int is not disturbed by the dabbing operation, and that ost of the liquid adhering to the tip is removed after each st.

---

* Culpin, M. F., and Madoc Jones, D. *J. Sci. Instrum.*, **36**, p. 28 (1959).

Experience of the use of these devices has shown that the mperature of the thread-line or jet can be estimated to thin about ±1° C, in the range from 20 to 200° C for read-lines, and up to 300° C for jets. With suitable design should be possible to make similar instruments for tempera- res up to at least 500° C. The cheapness and simplicity of e instrument is such that it may be used freely in circum- ances where its life may be short.

We are indebted to British Nylon Spinners Ltd. for ermission to publish this note.

Bakeable bellows-type differential pressure manometer

by A. E. D. Heylen, B.Sc., Ph.D., Electrical Engineering Department, Queen Mary College, London

[*Note first received* 3 *March, and in final form* 30 *March,* 1960]

ince the introduction of a bakeable null-reading absolute anometer(1) for use in ultra-high-vacuum systems, there has een a need for a similar device which forms an integral part f the ultra-high-vacuum side and need not be dismantled each ime on bake out. Other manometers(2, 3) have been described hich are not as sensitive and are not suitable for quantity roduction. It is the purpose of this paper to describe a evice which has the desirable characteristics of the first-entioned manometer and also need not be disturbed for ake out. Apart from saving the labour of dismantling, voiding the risk of breakage and a change in the null reading, vacuum is maintained at all times across the sensitive bellows, hus protecting it from corrosion when at higher temperatures.

The principle used is the detection of a change in capaci-ance between two parallel-plate disks, one of which acts as a et-zero probe, the other being connected to a sensitive ellows system which responds to a difference in pressure. The instrument shown in the diagram is bolted upright on to a thick base pad (*A*) which forms part of the floor of the bake-out oven. The upper bakeable half is connected to the ultra-high-vacuum side and the lower half leads to a high-vacuum system which incorporates oil and mercury manometers and a needle valve for the controlled introduction of a balancing gas. The bellows (*B*) (by Palatine Surbiton Ltd.) consists of twenty convolutions made up of diaphragms which are argon arc-welded together forming a stack 1·8 in. in length; end plates are welded on, the lower one consisting of the movable parallel-plate disk (*C*), whilst the upper plate is made of Nilo-K, and has a glass-to-metal matched seal attached to it. The whole is supported by an argon arc-welded seam and is enclosed in a stainless-steel shell (*D*). The probe (*E*) is screwed on to a shaft (*F*), which projects through the base pad and is guided in the bakeable chamber by means of a $\frac{1}{4}$-in. hole through a plate glass disk (*I*). The shaft is spring-loaded (at *G*) to prevent large stresses being set up on inadvertent introduction of atmospheric pressure to one side of the bellows, and is insulated from an adjustable micrometer (*J*) which transmits motion through a bellows (*K*), by means of a double-matched glass-to-metal seal (*H*). Electrical connexion is made *via* a tungsten seal (*L*) and a nickel wire, spot-welded at both ends.

The instrument is shown just prior to final assembly. Two halves were held in the chucks of a vertically erected glass-blower's lathe and brought together to the right distance. A spring was inserted (at *G*) and the two parts of the shaft (*F*) screwed together. The glass annulus (*M*) was then lowered

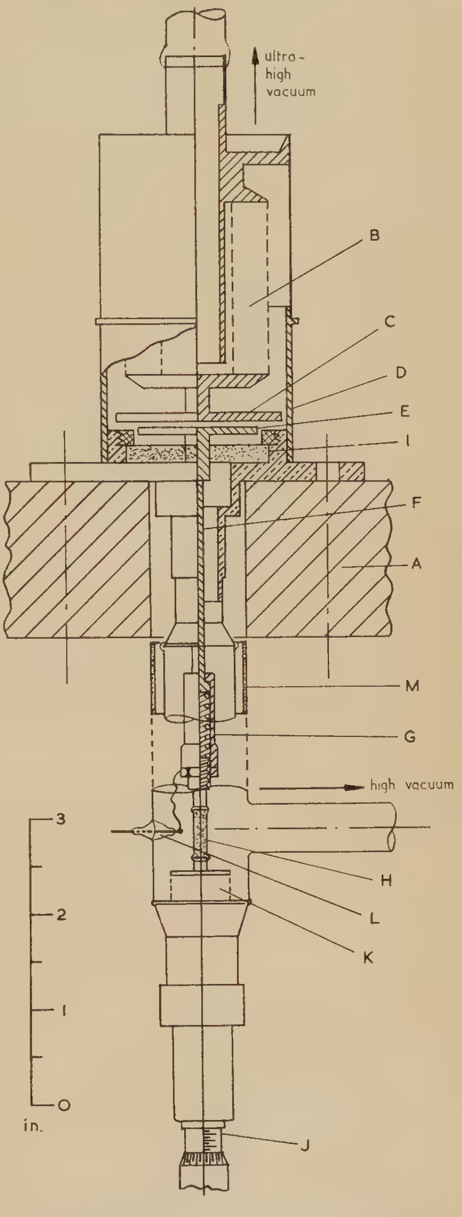

Outbakeable differential pressure manometer
(all parts not to scale)

A, 2-in. thick base pad covered with $\frac{1}{2}$-in. asbestos board; *B*, stainless steel (18/8) bellows consisting of forty $1\frac{7}{16}$-in. O.D. and $\frac{3}{4}$-in. I.D. diaphragms, 0·007-in. thick; C, moveable parallel-plate disk, $1\frac{13}{16}$-in. dia.; D, stainless-steel shell, 2-in. O.D., 0·040-in. thick; *E*, set-zero probe, $1\frac{1}{4}$-in. dia.; F, supporting shaft, spring-loaded at (*G*) and having a double-matched seal at (*H*); *I*, $\frac{1}{4}$-in. thick plate-glass insulating and guiding disk; *J*, adjustable micrometer (accuracy, 10^{-4} in.); *K*, brass bellows $\frac{9}{16}$-in. O.D., 8 convolutions, double ply (by Power Flexible Tubing Co. Ltd.) *L*, tungsten seal for electrical connexion; *M*, glass annulus into position and sealed at each end. The capacitance between the parallel plates is read on a commercially available proximity meter (by Fielden Electronics Ltd.). To prevent stray capacitances affecting the reading, the high-vacuum glass tubulation is coated with colloidal graphite.

The sensitivity of the manometer can be adjusted by varying a potentiometer on the proximity meter and by altering the parallel-plate gap by means of the micrometer. A useful working distance was found to be 0·040 in. which corresponds to a capacitance of 9 pF in parallel with a further stray 19 pF. With the mechanical sensitivity of the bellows being 0·0005 in./mm of mercury, a linear relationship could be obtained on the proximity meter from anything in the region of 25 mm of mercury/100 div. F.S.D. to 3 mm of mercury/100 div. F.S.D. In this latter range, the reading becomes susceptible to mechanical vibrations but allows 10^{-2} mm of mercury to be detected. The mechanical sensitivity could further have been increased by a factor of four without increase in the size of the bellows by using diaphragms 0·005-in. thick which are available. The instrument has been repeatedly baked at 430° C and vacua less than 10^{-10}mm of mercury have been obtained against a leakage of 5×10^{-9} clusecs.

The device described equals the performance of previous such instruments, and requires no dismantling for bake out. The ultra-high-vacuum part is at all times surrounded by a high vacuum of 10^{-6} mm of mercury and separated from it by argon arc-welded stainless-steel seams. It can also support other apparatus which may need bake-out.

Acknowledgements

The technical skill of Messrs. L. W. Borroff, A. E. Barnard, L. Vinton and L. C. Morgan materially assisted the construction of the apparatus. The award by the University of London of an I.C.I. Fellowship is gratefully acknowledged. Thanks are due to Professor M. W. Humphrey Davies for facilities provided.

References

(1) Alpert, D., Matland, C. G., and McCoubrey, A. O. *Rev. Sci. Instrum.*, **22**, p. 370 (1951).
(2) Johnson, J. B., and Williams, N. T. *Rev. Sci. Instrum.*, **25**, p. 393 (1954).
(3) De Crescente, M., and Janz, G. J. *Rev. Sci. Instrum.*, **28**, p. 468 (1957).

Method of finding the focal curve of a photographic spectrometer

by J. F. James, M.Sc., Department of Physics, Queen's University of Belfast

[*Note received* 4 *March*, 1960]

The purpose of this note is to describe a simple and convenient technique whereby the focal curve of a spectrograph may be determined by the exposure of a single photographic plate. Essentially, the method is to replace a broad extra-focal image by a pair of much narrower lines at the edges of the broad image.

When the initial adjustments of the instrument are completed, a mask is fitted over the dispersing element. The mask should be a strip of opaque material, the width of which is approximately one-third that of the prism or grating, and should be mounted with its edges parallel to the slit to cover the centre third of the prism. The effect is to div into two parts the monochromatic convergent beams t fall on to the photographic plate to form the images o line spectrum. If the plate lies inside or outside the fo curve, two images of each line are produced, the separat of which depends on the distance of the plate from the fc curve. A series of exposures is made, with some suita optical component being adjusted between each exposu With a Rowland grating, the grating itself is moved, or w a prism spectrograph, the focusing lens or the plate. possible, the plate should be moved, since a change position of the focusing lens may alter the shape of the fo curve. The movements may be quite coarse, a few mi metres each time, and should be such that some exposu positions lie on either side of the proper focusing positio The distance moved in each case is recorded, and a gra plotted of the separation of the doublet components again this position. From this graph it is possible to interpola with great accuracy the position for zero doublet separatio and if a many-line spectrum such as that of an iron arc employed, the focal curve for a considerable range of wa lengths can be deduced.

If the instrument is to be used with a light source of sm angular aperture, the correct alinement of the source m also be determined by making a series of exposures with t plate out of focus and with small adjustments to the late position of the source. The proper position for the sour may then be decided by observing which of the exposur shows the doublet members with equal intensity.

If an external Fabry–Pérot étalon is to be used with t spectrograph, the same procedure may be used to focus fringes on to the spectrographic slit. In this case the ma should be arranged perpendicular to the slit, that is, paral to the fringes at the point where they cross the slit.

When the instrument to be focused is an optical spect meter, all these adjustments may be made visually with t aid of a travelling microscope.

Improved sample loading technique for solid source mass spectrometry

by R. E. Powell, Atomic Weapons Research Establishment, Aldermaston, Berkshire

[*Note received* 7 *March*, 1960]

In solid source mass spectrometry the sample is loaded b evaporation of an aqueous solution, drop by drop, on tungsten filament (0·001 × 0·030 × 0·3 in.). This is usual

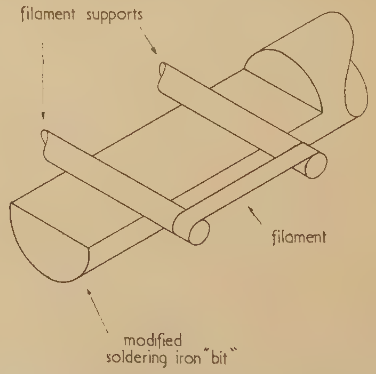

Arrangement for heating tungsten filament through the filament supports ieved by the use of a heat lamp or by passing a current ough the filament. For maximum efficiency, the sample uld be deposited at the centre of the filament. This comes increasingly important if the amount of sample ilable is small. The above-mentioned methods of loading ve the disadvantage that the centre of the filament is warmer n its ends, causing the sample to run away from the centre. It is found that the effect of heating the filament *via* its pports reverses this condition and restricts the sample to centre. The supports can be heated by contact, a 25 W dering iron with a modified bit being ideal. The figure ows the arrangement for the triple filament (only one side ament being shown) but is equally suited to the single ament source. If there is risk of contamination of the it" it should be made from stainless steel and boiled in tric acid between loadings.

Automatic gas-sampling device for gas chromatography

by D. W. HILL, M.Sc., A.Inst.P., A.M.I.E.E., and J. R. HOOK, A.I.B.S.T., Research Department of Anaesthetics, Royal College of Surgeons of England, Lincoln's Inn Fields, London

[*Note first received* 26 *October*, 1959, *and in final form* 8 *December*, 1959]

he application of the techniques of gas-solid and gas-liquid hromatography to the analysis of the permanent gases and naesthetic vapours encountered in anaesthetic practice and spiratory research offers several advantages.(1) If the gas hromatograph is designed on the lines of a plant-type nstrument as used in routine chemical process control, then s operation can be simpler than many of the physical nethods now in use.(2) For routine use of the gas hromatograph in medicine and surgery it must be possible o read the analysis directly from the recorder chart. This neans that the analysis must be in terms of peak heights nd not areas. For this to be so, it is necessary that the amples of gas or vapour are of a closely reproducible volume.

With gases or vapours, the use of a valve system in conjunction with a sampling loop of known volume is standard practice.(3,4) In the automatic sampling system to be described, both the timing sequence and the sample introduction are effected by a single standard synchronous electric clock motor.

The sampling valve is similar in operation to that described by Timms, Konrath and Chirnside.(4) The construction has been modified so that the valve disks need only rotate through twenty degrees and the valve ports are so arranged that no dead-space gas is added to the sample volume injected into the carrier-gas stream. The valve disks which are shown in Fig. 1 are made from stainless steel with the mating surfaces ground flat. No lubrication is used because oils and greases will readily adsorb anaesthetic vapours. Disk 2 is normally set so that the centre line at *A* is vertical. In this position, carrier gas passes directly to the column, whilst the sample loop is purged with sample gas. On rotating disk 2 so that the centre line *B* moves into the vertical position, the carrier-gas stream is made to sweep the volume contained in the sample loop on to the column. The sample-gas stream meanwhile escapes to the atmosphere.

For the application in this note, the timing mechanism is arranged so that the sampling valve can be set to operate in the range: once every minute to once every twenty minutes, in steps of one minute. A view of the mechanism is shown in Fig. 2, with a section in Fig. 3.

Shaft *A* is driven from a synchronous clock motor and revolves at the rate of one revolution per minute. It carries the cam *C* and the driving disk *B*. The pin in disk *B* engages in a spring-loaded ratchet wheel *D* carrying it forward one tooth per revolution until the screw head *E* assumes a position just clearing the small arm *F* attached to beam *G*. At the end of the following minute screw-head *E* engages with arm *F* lifting beam *G*. This releases the spring-loaded lever *H* which rotates valve disk 2, injecting the sample volume into the carrier-gas stream. Slide *J* is also operated, lifting a pawl clear of ratchet wheel *D*. After an interval of fifteen seconds, cam *C* returns slide *J*, thus resetting the valve.

The period between injection and successive samples is

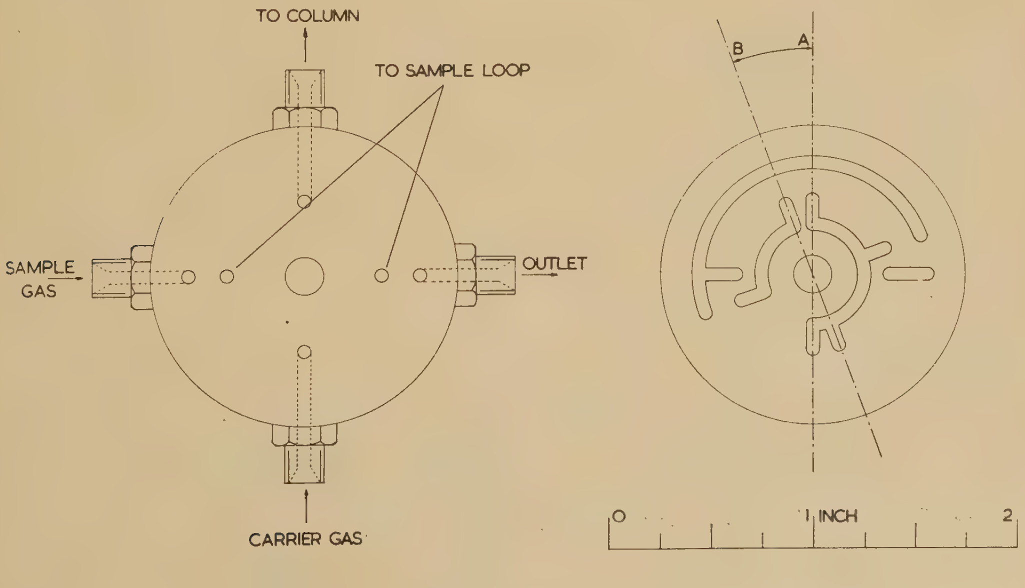

DISK 1 DISK 2

Fig. 1. Sampling-valve porting arrangement

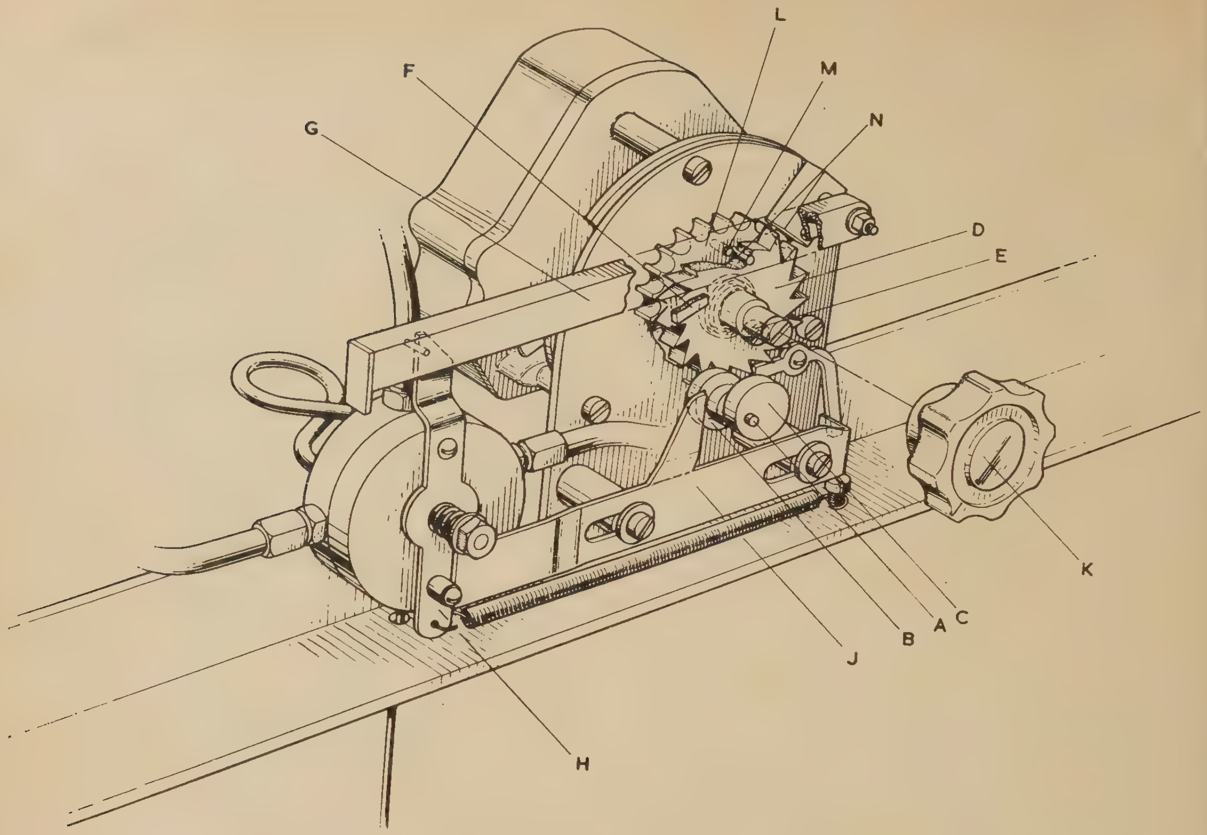

Fig. 2. Pictorial view of sampling valve and timing system

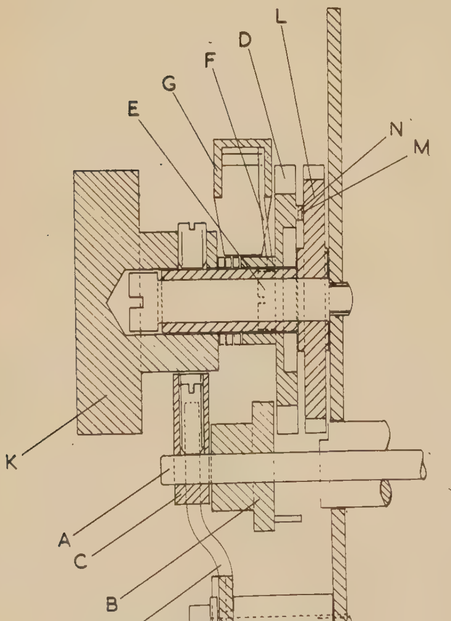

Fig. 3. Section of valve-operating mechanism

governed by the position of peg *M*. This forms a stop for peg *N* in wheel *D* when it is returned, on lifting the pawl, by a watch mainspring fitted inside. Peg *M* is positioned b knob *K* attached to the knotched wheel *L* which is held b a spring-loaded plunger located under the pivot of beam G

The maximum column inlet pressure used is 450 mm c mercury above atmospheric pressure with the outlet a atmosphere pressure. Hence it has not been found necessar to surround the sampling valve with carrier gas at the colum inlet pressure to reduce any possible leakage.

When the gas chromatograph is connected to a anaesthetic circuit, connexion to the sampling valve is mad *via* a length of flexible corrugated stainless steel tubing. A small flow of gas to be analysed is continuously drawn alon this tube by means of a small diaphragm pump. For us with syringe samples, such as in the study of nitrogen wash out curves or oxygen consumption studies, the pump i disconnected. The timing operation is set to operate onc each minute and the mains supply to the clock motor switche off. The syringe is now connected to the sampling valve *vi* a Luer–Lok fitting and the syringe emptied. The moto switch is then closed and within a minute the valve transfer the volume of the loop into the carrier-gas stream. Th volume of the syringe used must be chosen to be greate than the volume of the sample loop and its connecting tubing Each operation of the sampling valve actuates a micro-switc causing a signal to be sent to the event-marker pen of th chromatograph pen recorder.

The earlier work on the gas-chromatographic analysis o permanent gases was performed with solid adsorption columns The application of partition columns to this work opens u the use of capillary columns which can be made to have muc shorter retention times.(5) With a 0·1 ml. sample volum d a flow-dividing device placed after the valve in the rier-gas stream, the valve may be used with a capillary lumn and the chromatogram displayed on a cathode-ray e.

To cover the analysis of a mixture of permanent gases and aesthetic vapours, it is convenient to use two different romatographic columns operating in parallel. Two npling valves are used ganged together and the sample lumes chosen to suit the analysis. In practice, a 3 ml. mple is used with one column to analyse for ether, halothane, loroform, etc. A second column uses a 3 ml. sample and alyses for oxygen, nitrous oxide and carbon dioxide. Both mpling valves operate at room temperature, the first lumn at 75° C and the second column at room temperature.

Acknowledgements

It is a pleasure to acknowledge the encouragement of Prof. Ronald Woolmer in this work.

References

(1) Adlard, E. R., and Hill, D. W. To be published.
(2) Woolmer, R. *Brit. J. Anaesth.*, **25** p. 315 (1953).
(3) Hooimijer, J., Kwantes, A., and Van de Craats, F. *Gas Chromatography* 1958, edited by Desty, p. 288 (London: Butterworths Scientific Publications, 1958).
(4) Timms, D. G., Konrath, J. H., and Chirnside, R. C. *The Analyst*, **83**, p. 600 (1958).
(5) McWilliam, I. G. *J. Appl. Chem.*, **9**, p. 379 (1959).

ORRESPONDENCE

he theory of stresses in two-component glass to metal tube seals

have just noted an error in my paper, published under the bove title in this *Journal* (**26**, p. 25, January 1949).

Although equation (7) which gives the expression for A_2 correct, equation (8) which gives the same expression in implified form is incorrect, the values of E_1 and E_2 having een interchanged. The correct form of equation (8) is

$$A_2 = \frac{\delta}{(2\sigma - \beta)/E_2 + \{\alpha(\gamma - 2\sigma)\}/E_1}$$

The equation for the stresses p_r and p_θ for rings 1 and 2 should ead

or ring 1

$$P_r = \frac{\alpha\delta}{(2\sigma - \beta)/E_2 + \{\alpha(\gamma - 2\sigma)\}/E_1}[1 - a^2/r^2]$$

$$P_\theta = \frac{\alpha\delta}{(2\sigma - \beta)/E_2 + \{\alpha(\gamma - 2\sigma)\}/E_1}[1 + a^2/r^2]$$

For ring 2

$$P_r = \frac{\delta}{(2\sigma - \beta)/E_2 + \{\alpha(\gamma - 2\sigma)\}/E_1}[1 - c^2/r^2]$$

$$P_\theta = \frac{\delta}{(2\sigma - \beta)/E_2 + \{\alpha(\gamma - 2\sigma)\}/E_1}[1 + c^2/r^2]$$

The equations for p_z are correct.

Fortunately the correct equations were used in deriving the design curves given in Figs. 2 to 4.

Associated Electrical Industries (Rugby) Ltd.,
Research Laboratory,
Rugby, Warwickshire.

H. Rawson
[27 *May*, 1960]

Measurement of cyclic strain

In our paper under the above title which appeared in the April 1960 issue of the *Journal* the circuit diagram (Fig. 2) on p. 140 contained an error. The error has been corrected in the portion of the circuit diagram shown below with the contact shown as open instead of closed as it appeared in the original diagram.

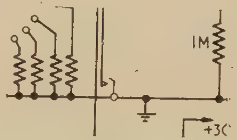

National Engineering Laboratory,
East Kilbride,
Glasgow.

T. M. Dowell
J. A. MacKinnon
[18 *May*, 1960]

Apparatus for the measurement of Young's modulus, between −200 and 700° C by tranverse vibration in vacuum

In view of the considerable interest shown in my paper published under the above title in this *Journal* (37, p. 117, April, 1960), it may be of value to readers to know that since the paper was prepared the temperature range of the equipment has been further extended. This was achieved by mounting the specimen on wires, spot welded to the nodal points, as suggested for internal friction measurements in the original paper, thus reducing the loss of energy at the points of support. By this means it was found possible, using a titanium specimen, to determine Young's modulus at temperatures up to 850° C, the limit being imposed by the furnace at present in use.

Research Department,
Imperial Chemical Industries Limited,
Metals Division,
Birmingham.

H. J. Stokes
[27 *May*, 1960]

Notes and comments

Elections to The Institute of Physics

The following elections have been made by the Board of The Institute of Physics:

Fellows: J. R. Barker, R. S. Barnes, D. E. Caro, M. F. Culpin, T. Charnley, J. R. Drabble, K. Greenwood, A. C. Groom, J. S. Halliday, J. A. Huggill, E. R. Johnson, C. Jones, J. Lamb, K. E. Pattinson, E. Pitts, C. D. Pomeroy, H. Steels, R. T. Whitfield, J. M. Ziman.

Associates: J. W. S. Allen, R. C. Andrews, H. C. Angus, R. K. Angus, H. M. Assenheim, P. J. Bateman, R. E. Belin, P. Benjamin, D. Bennett, J. C. Brice, A. R. Bugden, N. J. Canny, D. D. Carruthers, P. Catterall, J. Caudwell, S. Clough, C. H. Copley, C. A. Crofts, J. O. Cutter, R. H. A. Davies, J. R. de Laether, A. M. Dowler, G. M. Dyche, W. R. Eadington, C. Evans, L. Freedman, K. G. Freeman, J. B. Garg, S. K. Ghosh, W. Gibson, L. A. Gilbert, R. W. Goodley, D. W. Goodwin, B. O. C. Grieves, S. Grundy, I. D. C. Gurney, R. D. J. Hammond, D. V. Harris, J. Harwood, S. S. Hasan, J. A. Hey, R. Hine, K. J. Hughes, D. F. Jephcott, F. B. Johnson, C. R. Johnes, C. S. Jones, P. D. Lee, H. G. Leventhall, J. P. Llewellyn, A. E. J. Poultney, B. A. Proctor, I. T. Pye, A. N. Rapsey, W. E. Read, H. Ridley, T. W. Roberts, J. L. Rouse, R. A. Saunders, E. N. Shaw, R. W. Snell, G. Stuart-Monteith, P. R. Stuart, J. S. Sutherland, G. M. Thomas, R. H. Thomas, G. Underwood, R. C. Valentine, N. Washington, P. P. Williams, W. Woodside, R. E. Worsley.

Seventy-seven Graduates, ninety-three Students and eight Subscribers were elected.

1960 Waverley Gold Medal essay competition

This competition, sponsored by the magazine *Research*, is designed to draw attention to the problem of communicating scientific information to the layman and also to scientists engaged in other fields.

The Waverley Gold Medal and £100 will be awarded for the best essay of about 3000 words based on some recent scientific research or new development (whether the author's work or not), giving some indication of the scientific background, the experimental results and its potential application in industry. The essays will be judged for technical content, by specialists in that field, and for clarity of presentation and style.

A second prize of £50 will also be awarded and an additional prize, also of £50, for the best entry from a competitor under 30 years of age on the 31 July, 1960. The competition is open only to persons at present engaged in scientific work and the closing date for entries is 31 July, 1960.

An additional competition has been introduced this ye and candidates, who must be practising scientists under t age of 30, are invited to write an essay of some 5000 word This should be based on any new idea, concept or exper mental result put forward in the recognized scientific liter ture in the last two years and should discuss the commerci exploitation in the next decade. The first prize will be £ and the second prize will be £30. Entries should be su mitted not later than 31 July, 1960. Further details may b obtained from the Editor, *Research*, 4–5 Bell Yard, Londo W.C.2.

Fifth International Instrument and Measurements Conferen

This conference, organized by The Royal Academy Engineering Sciences and The Swedish Association Technical Physicists will be held in Stockholm, 13–16 Se tember, 1960. Further information may be obtained fro the Secretary General, The Royal Institute of Technolog Stockholm 70, Sweden.

Erratum

In the paper on the "Weight-in-air basis of adjustment precision weights", which appeared in the August 1959 iss of this *Journal*, three errors occurred in the table printed page 361. The bottom figures in the second and third colum should read −0·30 and −0·29 and not −0·030 and −0·02 In the heading of the third column, 8·0 gm/l. should re 8·0 g/ml.

British Journal of Applied Physics

Contents of the July issue

PAPERS

Design and performance of a compact surge generator. By E. Thornton.
Optical methods for the study of flames in turbulent pre-mixed gas streams. M. D. Fox and F. J. Weinberg.
A study of large strains and the effect of different values of Poisson's ratio. H. Fessler and B. H. Lewin.
Strength of irradiated drawn and undrawn nylon. By C. C. Hsiao, Y. C. Da and A. Haynes.
Variation of permanent-magnet properties with crystal orientation in columna crystal alloys. By M. McCaig and W. Wright.
Power law for creep. By B. J. Rigby.
Experimental and theoretical investigations on the oscillating cylinder viscomete for Newtonian liquids. By Ali Abdel Kerim Ibrahim and Abdel Monem Kabiel.
Method of recording low-angle X-ray scattering when intensity scattered b specimen changes rapidly with time. By P. W. Teare.
Influence of temperature on the spectral composition of the zinc sulphid luminescence. By I. Soudek.
Thermal propagation of a normal region in a thin superconducting film and it application to a new type of bistable element. By R. F. Broom and E. H Rhoderick.
Etch pits and dislocations in cadmium sulphide crystals. By J. Woods.
Half-life of iridium 192. By J. W. Allison.

CORRESPONDENCE

Evaporated films of niobium. From D. Shaw and B. N. Watts.
Glow-discharge characteristics of helium-argon mixtures. From G. F. Westo
Comments on the A.S.T.M. Powder Data File—5. From J. W. Hughes, Isabe E. Lewis and A. J. C. Wilson.

THIS *JOURNAL* is produced monthly by The Institute of Physics, with the co-operation of the National Physical Laboratory. It deals with the principles, construction and use of scientific instruments. All rights reserved. Responsibility for the statements contained herein attaches only to the writers.

EDITORIAL MATTER. Communications concerning editorial matter should be addressed to the Editor, The Institute of Physics, 47 Belgrave Square, London, S.W.1. (*Telephone:* Belgravia 6111.) Prospective authors are invited to prepare their scripts in accordance with the *Notes for Authors.* (Price 3*s.* 6*d.* including postage.)

REPRODUCTION. The Institute of Physics is a signatory to The Royal Society's Fair Copying Declaration. Details may be obtained upon application from The Royal Society, London, W.1.

ADVERTISEMENTS. Communications concerning advertisements should be addressed to the agents, Messrs. George Jackson (Fleet St.) Ltd., Cliffords Inn, Fleet Street, London, E.C.4. (*Telephone:* Holborn 3611–2.)

CLAIMS FOR MISSING JOURNALS. Claims from regular subscribers to this *Journal* for missing numbers will only be considered if received within 60 days of the date of mailing plus normal outward time of transit and time for lodging the claim. Losses attributable to failure to notify a change of address or to similar omissions will not be considered.

SUBSCRIPTION RATES. A new volume commences each January. The charge is £6 per volume ($17 U.S.A.), including index (post paid) payable in advance. Single parts, so far as available, may be purchased at 12*s.* 6*d.* each ($1.75 U.S.A.), post paid, cash with order. Orders should be sent to The Institute of Physics, 47 Belgrave Square, London, S.W.1, or to any bookseller.

PRINTED IN GREAT BRITAIN BY UNWIN BROTHERS LIMITED, WOKING AND LONDON

Tomograph for industrial radiography

By D. CHARLES, B.Sc., Grad.Inst.P.,* Imperial Chemical Industries Ltd., Witton, Birmingham, 6

[Paper first received 29 September, 1959, and in final form 8 April, 1960]

Abstract

Tomography is a radiographic technique originally developed for medical purposes, in which relative movements of X-ray tube, subject and film are controlled so that a defined section of the subject is recorded as a sharp image, superimposed on a diffuse background due to blurred images of the rest of the subject. A tomograph for industrial use has been developed, and its capabilities assessed by tests on an assembly of wire mesh gauzes. Its practical application has been demonstrated with two types of heat exchangers, on which useful detailed observations were made. Tomography is considered to be particularly effective for examination of such assemblies in which repetitive detail is masked by overlying layers.

Introduction

As a radiograph is a two-dimensional representation of a three-dimensional object, the problem of resolving detail in planes parallel to the film often occurs. Stereo-radiography may be applied, but the interpretation of stereo photographs is difficult, especially when repeating patterns are present in the object under examination. Tomography, an alternative approach, is often to be preferred.

All tomographic methods involve relative movement of the X-ray tube, the object and the film. This movement is arranged so that all the points in a chosen plane of the object are projected on to the same points on a film throughout the exposure. When this condition is satisfied, a sharp image of the chosen plane will appear on the film, superimposed on a diffuse background due to blurred images of the rest of the object.

The theory of tomography and its applications have been described in medical literature.† Constructional details of an apparatus for tomographic examination of industrial samples are described, and an illustration of its use is given.

Constructional details

The object and film move in horizontal planes and are connected by a rigid rod, fixed to the object cradle at the height of the selected plane and free to oscillate about its attachment point. The extremities of the rod slide through freely oscillating joints, one being fixed to the framework on an axis through the X-ray tube focus, and the other attached to the film tray.

To ensure steady motion and eliminate vibration, a rigid open frame of 1 in. angle iron was constructed, its main features being shown in Fig. 1. The object under examination rides in a cradle, with an aluminium base, running on rails, and the film is supported on a light tray running on rails attached to the cradle and parallel to and immediately below it. The cradle attachment point is variable over a vertical range of 7½ in. and any object plane within this distance may be rendered in focus.

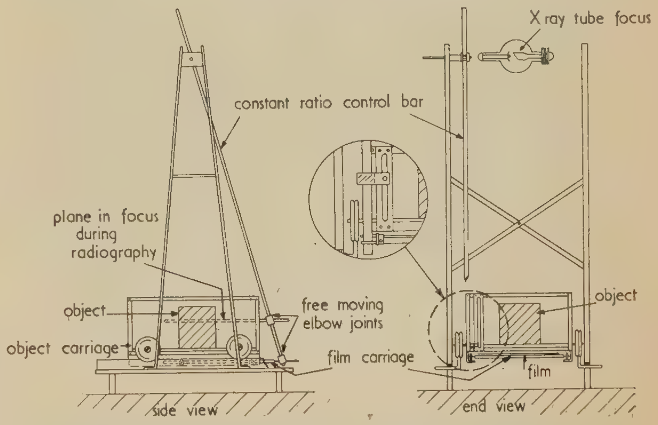

Fig. 1. Diagrammatic sketches of tomographic apparatus

Theoretically it should be possible to make an exposure of any duration, whilst the object traverses back and forth. However, when this method was employed in practice, backlash in the moving parts produced inferior tomographs. Therefore, a system of gears was devised to produce various traverse speeds so that each exposure would be made during a single traverse.

An accurately machined feed screw drives the object carriage. Power is provided by a 1/40 h.p. motor coupled to two gearboxes and a variable gear system. The time of a single traverse can be changed from 2 min to 30 min for X-ray exposures, or from 1 h to 64 h for γ-ray exposures. In this way a wide range of object densities and thicknesses can be accommodated. To eliminate accidental damage, limit switches which reverse the motor are provided at each end of the traverse. However, if the equipment had to be left unattended it would be a simple matter to alter the limit switches to ensure complete shutdown.

The accepted operational sequence is as follows: choose a gear system to provide a traverse interval slightly longer than the necessary exposure time for the particular object. With the object carriage near and approaching one end of its run, adjust the X-ray controls and set exposure time. Switch on the tomograph motor and wait for reversal to occur, then make the X-ray exposure.

The exposure conditions required for a tomograph are the same as those for a normal radiograph of the same subject.

---

* Now at Nuffield Central Research Laboratories, Courthouse Green, Coventry.

† McDougall, J. B. *Tomography* (London: H. K. Lewis and Co. Ltd., 1938).

To reduce overall fog due to scattered radiation, the film is sandwiched during exposure, between lead screens, 0·0015 and 0·006 in. thick, front and back respectively. It is also helpful, with a thick or dense sample, to surround it with a lead shield placed at the level of the selected plane to reduce blackening at the edges of the sample.

Assessment of the method

Wire gauzes were used in assessment of the effectiveness of the tomographic apparatus. Five wire gauzes of mesh size 5, 8, 10, 16 and 18 were arranged in random order in parallel planes, each 2 in. above its neighbour. A normal radiograph of the five gauzes is shown in Fig. 2(*a*). None of them is clearly recognizable.

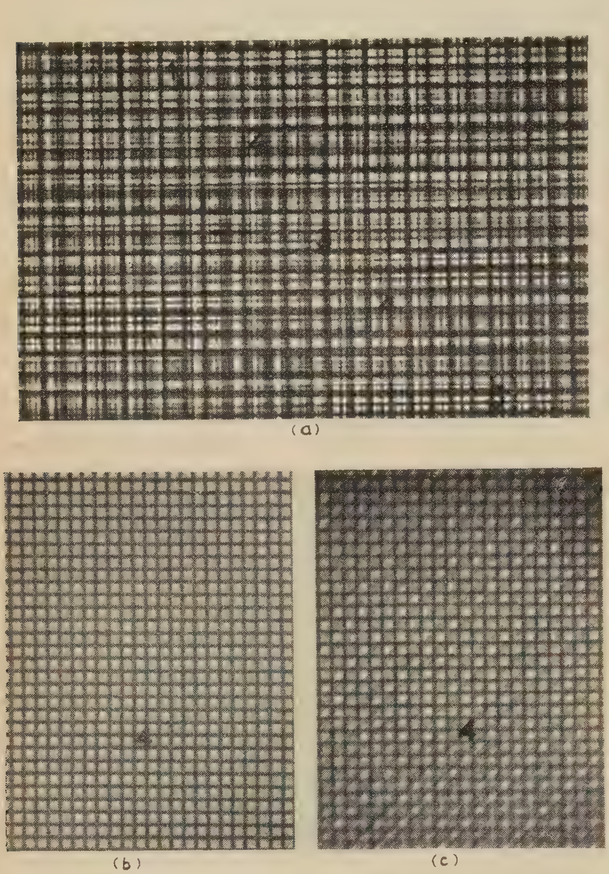
(a)
(b)
(c)

Fig. 2. (*a*) Radiograph of assembly of five wire gauzes
(*b*) Radiograph of single 8-mesh gauze
(*c*) Tomograph of 8-mesh gauze in assembly, inclined 1 in 8 to film to show "depth of focus"

A stationary radiograph of a single 8-mesh gauze is reproduced in Fig. 2(*b*) to illustrate the best definition obtainable. For comparison the tomograph, Fig. 2(*c*), of the entire assembly shows part of the 8-mesh gauze in focus. In this tomograph the assembly was inclined 1 in 8, so that the clearly defined area is a measure of "depth of focus" which is approximately 0·1 in.

Applications of tomography

Heat exchangers. Because corrugations of identical pattern are arranged in parallel layers throughout their thickness, heat exchangers are difficult subjects for standard radiographic examination. However, application of the tomographic technique enables any particular layer to be examined in detail, without mechanical sectioning which may obliterat fine structure; an example is illustrated in Fig. 3.

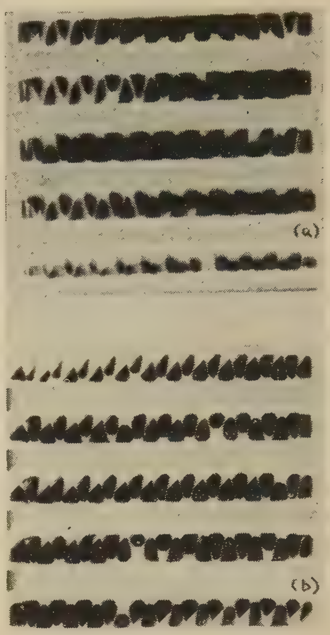

Fig. 3 (*a*) Radiograph of aluminium bronze heat exchanger
(*b*) Tomograph of same showing excess brazing metal at a number of joints

This is a small experimental heat exchanger in aluminium bronze, in which tomography has been used to define quality of brazing throughout the assembly. No detail of the quality of brazing on corrugations parallel to the X-ray beam is revealed in the normal radiograph illustrated in Fig. 3(*a*). However, a tomograph, Fig. 3(*b*), shows examples of good and bad quality brazing which occurred in the same sample.

A light alloy heat exchanger has also been examined, after pressure testing to failure. One such failure, an internal blister, had caused external damage, but subsequent tomographic examination revealed a secondary much smaller blister. The tomographs proved that damage was due to failure of the brazed joints rather than to tearing of the metal.

Conclusions

The tomograph has proved effective for radiographic sectioning of industrial samples. It is particularly effective for the examination of assemblies, such as heat exchangers, in which detail in any one layer is masked by overlying layers.

Acknowledgement

The author wishes to express sincere appreciation t Dr. N. P. Inglis, Research Director, I.C.I. Metals Division for permission to publish this paper.

A 450J spark discharge for shadowgraph photography

by L. WHITLOW, National Gas Turbine Establishment, Pyestock, Farnborough, Hampshire

[*Paper first received* 21 *March, and in final form* 25 *April*, 1960]

Abstract

To allow shadowgraph photographs to be taken of jet engines in altitude test cells, a 450 *J spark discharge is used. This emits sufficient light to illuminate a large working area and to allow armour plate and heat-resistant glass to be used for the cell windows. The design and construction of a suitable spark gap is given. The size of the light source is about* 1 *mm diameter and the flash duration is* 1·9 *μs. Details are also given of tests carried out on various insulating and electrode materials.*

Introduction

Spark shadowgraph photography of jet-engine intakes calls for a working area large enough to show the profile of the engine intake and the shock pattern on it. This means the image has to be projected on to a ground-glass screen, which must be far enough away from the intake to prevent it being damaged. The dimensions of the system are fixed by these considerations because, to obtain good resolution, the distance from the light to the object must be several times the distance from the object to the screen. When the engine is in an altitude-test cell, the light source and camera are outside and the ground-glass screen is inside the cell. Windows are provided in each side of the cell so that the light reaches the camera after passing through the working area and the ground-glass screen. These windows are made of a sheet of armour plate and a sheet of heat-resistant glass.

In this particular case, the object is 22 ft away from the light source—which is 1 mm in diameter and subtends an angle of less than 1 minute of arc at the object—and the ground-glass screen is 3 ft away from the object. The light transmission through each of the windows is 60 and 50% through the ground-glass screen. Under these conditions only a fraction of 1% of the light emitted actually reaches the camera. To provide sufficient light, a spark gap is used that releases 450 J every time it is discharged. It is not possible to put the spark gap in the test cell, since the cell operates over a wide range of temperature and pressure which would make the setting up of the electrode spacing impossible.

Construction of spark gap

The spark gap assembly is shown in Fig. 1. This is based on a design by Melton, Prescott and Gayhart* and is known as the Libessart gap after General Libessart of the French Army, who is credited with the basic design. It consists of two spark gaps in series; one between the earthed and intermediate electrodes, and the other between the intermediate and high-voltage electrodes. The second gap is a constricted gap, the discharge being confined to a cylinder of 1 mm diameter inside the constricting insulator. This constricted gap is used as the light source; the light is emitted through a small hole in the high-voltage electrode in line with the hole in the constricting insulator. The gap between the earthed electrode and the intermediate electrode allows the e.h.t. to be connected across the spark-gap assembly without it breaking down until it is triggered. This gap is adjustable and may be set so that the spark gap can be triggered with an e.h.t. of 7 to 30 kV. A trigger electrode is fitted coaxially with the earthed electrode to initiate the discharge. The spark-gap assembly is connected directly to the terminals of a 1 μF capacitor to reduce the self-inductance of the circuit. The earthed and high-voltage electrodes are connected to the capacitor terminals, and the intermediate electrode is left disconnected.

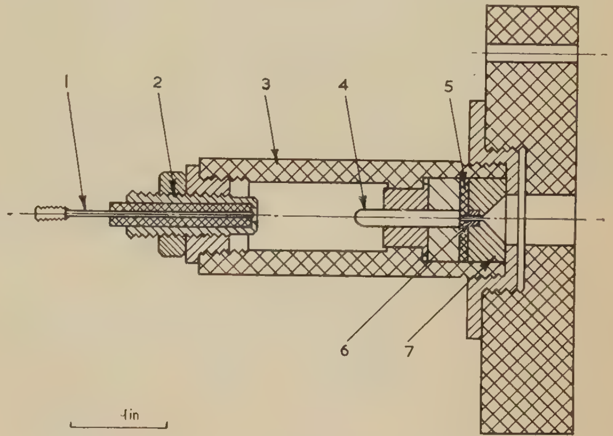

Fig. 1. Cross-section of the spark gap

1, tungsten trigger electrode; 2, stainless steel earthed electrode; 3, polythene body; 4, tungsten intermediate electrode; 5, constricting insulator (Bakelite laminate DH19057); 6, tungsten carbide insert; 7, stainless steel high voltage electrode

When the capacitor discharges through the spark gap, the temperature of the gas in the constricted gap rises rapidly, and since the discharge is confined to a small cylinder of 1 mm diameter and 3 mm long, the pressure will also increase rapidly. This build-up of pressure during the discharge has the effect of increasing the luminosity of the gas. The rapid increase of temperature and pressure in the constricted gap causes erosion of the constricting insulator and the high-voltage electrode. This erosion enlarges the holes in the constricting insulator and high-voltage electrode, and causes the apparent size of the light source to increase.

---

* Melton, B. S., Prescott, R., and Gayhart, E. *A Working Manual for Spark Shadowgraph Photography*, Bumble Bee Report No. 90, 1948. The Johns Hopkins University, Applied Physics Laboratory.

Originally, pyrophyllite was used for the constricting insulator, and stainless steel for the high-voltage electrode. The pyrophyllite insulators shattered after a few discharges—frequently after the first one. The stainless-steel electrodes eroded away quickly, the hole diameter being increased by 100% after about ten discharges. Silica tubing was tried for the constricting insulator, but this shattered after the first discharge. Polythene was tried next but this was unsuitable because small pieces of metal from the high-voltage electrode became embedded in it near the inner surface of the central hole; this caused pre-triggering breakdown. P.T.F.E. was also used but this suffered from erosion, the central hole being enlarged by 100% after seven or eight discharges.

Two insulating materials suggested by Bakelite Ltd. were tried next. One of these, an alkyd moulding material, type X17349, was found to shatter after the first few discharges, but the other one, an epoxide/glass laminate, type DH19057,* was found to be suitable. With this material, the erosion was found to be much less than that of P.T.F.E. Some of the laminations peeled off after a few discharges but this had no effect on the operation of the spark gap. The hole size increased by about 50% after fifty discharges.

With the Bakelite laminate DH19057 and for the constricting insulator, tests were carried out to find a suitable material for the high-voltage electrode. The materials were made into small inserts and fitted into a stainless-steel holder to form the high-voltage electrode. The results of these tests are shown in Table 1, which shows tungsten carbide to be the most suitable material tested. Tests were then carried out, with tungsten carbide used for the high-voltage electrode and Bakelite laminate DH19057 as the constricting insulator, to find out how the hole diameter increased with a larger number of discharges and the results are shown in Table 2.

Table 1. *Erosion of electrode materials*

Material	*Original diameter (mm)*	*Final diameter (mm)*	*No. of discharges*
Molybdenum	1·0	2·3	50
Platinum/Rhodium	1·2	2·5	50
Platinum	1·1	2·2	50
Tungsten	1·2	1·9	50
Tungsten	1·2	1·7	20
Tungsten Carbide	1·2	1·5	50

Table 2. *Erosion of constricting insulator and high-voltage electrode*

No. of discharges	*Insulator hole diameter (mm)*	*Electrode hole diameter (mm)*
0	1·4	1·2
50	2·0	1·5
75	2·3	1·8
100	2·4	1·9
125	2·4	2·0
150	2·6	2·1
175	2·9	2·2
200	3·0	2·2
250	3·4	2·5
300	3·4	2·5
350	3·8	2·5
400	3·9	2·5
500	3·9	2·5

Initially, the discharge takes place between the intermediate electrode and some point inside the hole in the high-voltage electrode. It is probable that after about 250 discharges the hole in the constricting insulator has enlarged enough to allow the discharge to take place between the intermediate electrode and the face of the high-voltage electrode. This would account for the diameter of the high-voltage electrode not being enlarged after 250 discharges. Because this could mask some of the light from the discharge, it is proposed to change both the constricting insulator and high-voltage electrode after 150 discharges.

Power supply and trigger unit

The e.h.t. supply is derived from a voltage-multiplier circuit; the output voltage is adjusted by a variable transformer on the mains input. Remote indication and interlocking for the camera circuit is provided by a relay which operates when the capacitor has charged up to the predetermined voltage. The spark gap is triggered by discharging a capacitor through the primary of a pulse transformer by means of a cold-cathode discharge tube. The secondary voltage of the pulse transformer breaks down the gap between the trigger and earthed electrodes and so initiates the main discharge.

Performance

The duration and relative intensity of the light emitted from the spark gap is shown in Fig. 2. The flash duration—when the light intensity is greater than 50% of the peak—is 1·9 μs. The subsidiary peaks occurring after the main peak is due to insufficient damping. From observation of the decay and frequency of the discharge current, the peak current was calculated as 40 000 A and the total circuit inductance as 0·53 μH. After several thousand discharges the spark gap remained stable and showed no signs of self-firing.

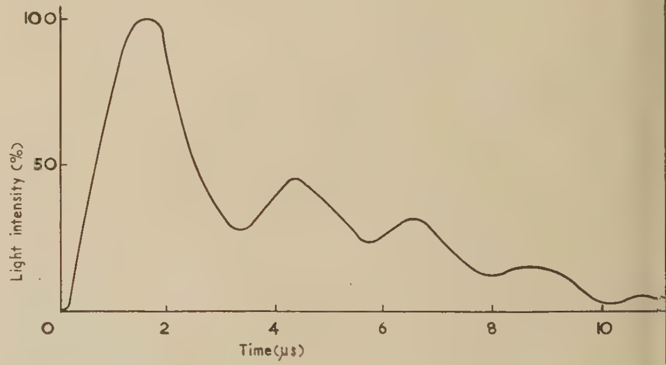

Fig. 2. Light-intensity of discharge plotted against time

Acknowledgements

The author would like to thank Bakelite Ltd., who kindly supplied samples of insulating materials. Thanks are also due to his colleagues Messrs. J. W. Brand and F. Gillians, who carried out the tests on the insulating and electrode materials, and Mr. J. W. Harris, who was largely responsible for the mechanical design of the power supply unit.

---

* This has now been superseded by type DH19073, but the author has not had the opportunity of testing it yet.

Moiré fringe reading head for use with a fine grating

By D. A. PALMER, B.Sc., Ph.D., D.I.C., A.R.C.S., National Physical Laboratory, Teddington, Middlesex

[*Paper received* 12 *April*, 1960]

Abstract

In the usual moiré fringe measuring system, practical difficulties arise in the use of very fine gratings. An optical system is described in which the use of a separate index grating is avoided, the moiré fringes being formed between the scale grating and the image formed by its reflexion in a concave mirror. This arrangement has the particular advantage that the sensitivity is doubled. A working model has been constructed to demonstrate the principle.

THERE have been many recent developments in the application of moiré fringe techniques to digital methods of processing and machine tool control with gratings.(1–5) The accuracy with which such devices can operate depends to a large extent on the grating quality, and it might seem that a good spectroscopic grating would be very suitable, as it would have a large number of very accurately spaced rulings, forming an extremely sensitive and accurate scale. On the other hand, it is often found easier in practice to use a fairly coarse grating, higher accuracy being obtained by subdividing each fringe electronically.(3, 6, 7) The latest developments suggest that an accurate subdivision into hundredths of a fringe may soon be possible in this way. This approach seems to hold the most immediate promise, but even in view of this trend it was considered that it might be worth following up the suggestion of using a very fine grating, to obtain some experience of the problems involved.

In the moiré fringe technique, the "scale" grating is usually held in close proximity to an "index grating", a small section of grating of similar pitch, to form the fringes, and by arranging at least two photoelectric detectors to be in phase quadrature in the fringe pattern, it is possible to operate a bidirectional counter.(8) In such a system it is usually essential that the two gratings should be maintained in the correct relative orientation. For example, should the moving grating "pitch" as a result of imperfections in its carriage, an error might easily be introduced into the fringe count, which would become more serious the smaller the ruling space, and might vitiate any attempts to improve the accuracy by the use of a fine grating.(3)

J. W. Gates(3) suggested that this particular difficulty might be overcome if only one grating were used, the index being replaced by an image of the single grating, reflected back by means of a suitable optical system, working at a magnification of -1, so that the returned image would be reversed. Thus any rotation of the grating would produce exactly the same rotation of the image, so that any pitching movements in the slide would be completely compensated. On the other hand, for a pure translation at right angles to the direction of the rulings on the grating, the grating and its image would move in opposite directions, and this would allow a further advantage in that the sensitivity would be doubled. In the normal system, the gap thickness between index and scale is very critical, especially with a fine grating where the gap is sometimes so small that there is a danger of the two gratings fouling. In the self-imaging system, this difficulty does not arise.

To demonstrate the practicability of this type of reading head, a model has been constructed using a replica of a 14 400 l.p.i. grating (Fig. 1). To achieve the optical imaging, a concave mirror of good optical quality and 5 in. in radius was used, of sufficient aperture to collect the zero and one first-order beam diffracted by the grating (these beams emerge at an angle of about 20° to each other). With such a mirror and grating, the working area of the image where the moiré fringes can be "fluffed out" without distortion, is only about $\frac{1}{8}$ in. in diameter. This is a result of the off-axis aberrations of the mirror, which even if small can have a considerable effect on so fine an image. This small working area was a serious disadvantage because of the small amount

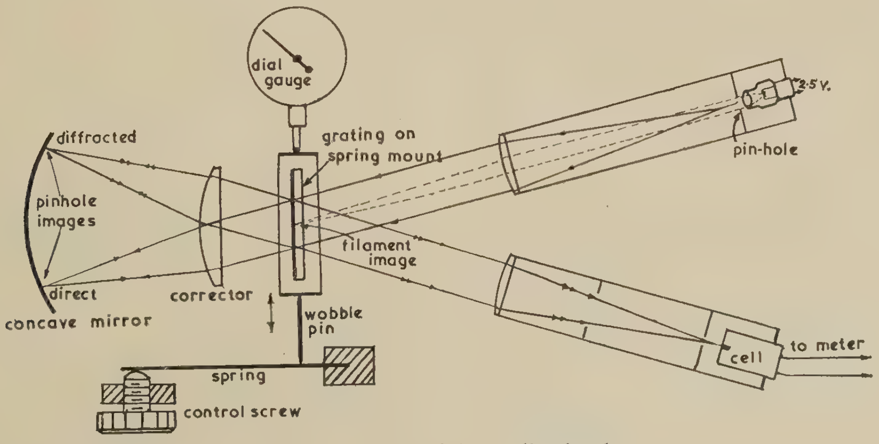

Fig. 1. Model of the reading head

of light which could pass through it. Dr. J. M. Burch suggested that the situation could be improved if the Petzval sum of the system could be reduced. For this purpose he suggested the use of a glass hemisphere of suitable refractive index and radius, concentric with the mirror (Fig. 2).

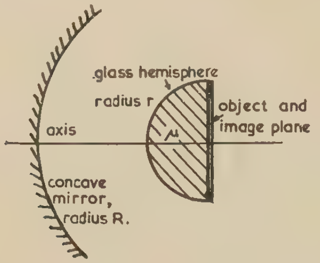

Fig. 2. Proposed system, with zero Petzval sum, for imaging grating on to itself

The condition for zero Petzval sum is given by

$$\frac{1}{R}+\frac{\mu-1}{r\mu}=0$$

where R is the radius of the mirror; r the radius of the hemisphere; μ the refractive index of the glass in the hemisphere.

As an approximation to the hemisphere a plano-convex lens of suitable radius and refractive index was used, the plane face of which cannot affect the Petzval sum. This gave a very great increase in the usable field area although no special precautions had been taken to ensure that the above conditions were rigidly fulfilled. The diameter of the "fluffed out" fringe region was increased to about $\frac{3}{4}$ in., making the problem of the lack of light much easier. Shortly after this model was completed, J. Dyson mentioned quite independently in a private communication that he was writing a paper on this type of system. This has since appeared in the *Journal of the Optical Society of America.*(9)

As arranged for the purpose of demonstration, the light source in the illumination system consists of a 2·5 V lens-ended pentorch bulb, with a pin-hole about $\frac{1}{32}$ in. in diameter immediately in front of it. The lens on the bulb forms an approximately collimated beam from the filament, which is limited in aperture by the pin-hole. This beam is focused by another lens, to produce an enlarged image of the filament on the surface of the grating within the working area of good fringe visibility. The pin-hole is at the focus of this same lens, so that light considered as originating from the plane of the pin-hole emerges collimated and passes through the grating as a parallel beam. This beam is diffracted at the grating, and the zero and one of the first-order diffraction spectra are collected by the reflector system. It so happens that when the Petzval sum condition is satisfied, the power of the plano-convex corrector is such that a parallel beam entering the system will be focused as a point on the surface of the mirror. Thus the pin-hole in front of the source will be imaged as two small spots on the mirror surface, one representing the direct beam, and the other the first-order diffracted beam. Only a small portion of the mirror is thus used, and it might be sufficient in practice to have two much smaller mirrors in suitably adjustable mounts to produce the same effect. The function of the mirror is to return the light from these two pin-hole images back along the same path to the grating, where both beams undergo further diffraction before collection at the detector. The detecting system is so arranged that the light which is to be collected from the diffracted pin-hole image on the mirror surface passe straight through the grating on its way back, without furthe diffraction, whilst the light from the direct image has t undergo diffraction to reach the detector. Using the notatio adopted by Guild,(2) the order sequences of the two inte fering beams are (0, 1) and (−1, 0). To obtain maximum efficiency, therefore, the grating should be blazed to give tw equal first-order spectra, each of amplitude one-half tha of the zero order beam. This condition was not well satisfie in the model, with the consequence that there was som shortage of light.

The phase relation between the two beams collected by th detector depends upon the position of the grating, so tha when this is moved at right angles to the direction of it rulings, the combined beam shows periodic fluctuation corresponding to the passage of the grating spaces. Becaus of the properties of the reflecting system, two complet fringes are registered for each ruling on the grating, thu doubling the sensitivity. The interfering beams are focuse on to a photocell by means of an optical system very simila to that in front of the source. For visual demonstration Schwartz-type photoconductive cell has been used togethe with a one-stage d.c. transistor amplifier, working a millia meter to display the fringes as the movement of a needle o a dial. To obtain a sufficiently fine control over the move ment without a precision slide, the grating has been su ported on a parallel spring mounting, driven by a cantileve spring, which reduces the movement of the micromete adjusting screw by about fifty times (see Fig. 1). Thi particular arrangement has been adopted for convenience o demonstration, but there is no limit other than the length o the grating to the magnitude of the displacement which thi system can measure. A Schwartz cell is not suitable fo rapid operation because of its poor response at high fre quencies. Nevertheless, the system seems satisfactory as fa as the optical components are concerned, and has an advantage in that it employs pure two-beam interference, so that the output signals are sinusoidal. This waveform is ver suitable for fringe subdivision, and opens up the possibilit of dividing each fringe into twentieths, or even hundredth when the electronic techniques have been perfected, to giv a sensitivity of less than a microinch with this type of system

This work forms part of the research programme of the National Physical Laboratory, and this paper is published by permission of the Director of the Laboratory.

References

(1) Guild, J. *The Interference Systems of Crossed Dif- fraction Gratings* (London: Oxford University Press 1956).

(2) Guild, J. *Diffraction Gratings as Measuring Scale* (London: Oxford University Press, 1960).

(3) Burch, J. M. *The Possibilities of Moiré Fringe Inter- ferometry.* NPL Symposium on Interferometry, June 1959 (London: H.M.S.O., in the press).

(4) Sayce, L. A. *Trans Soc. Instrum. Tech.*, **9**, p. 139 (1957)

(5) Blake, D. V., and Sayce, L. A. *Trans Soc. Instrum. Tech.*, **10**, p. 190 (1958).

(6) Barber, D. L. A., and Atkinson, M. D. *J. Sci. Instrum.*, **36**, p. 501 (1959).

(7) Williamson, D. T. N. *Machinery Lloyd* (European Ed.), **26**, p. 51 (1954).

(8) Peck, E. R., and Obetz, S. W. *J. Opt. Soc. Amer.*, **43**, p. 505 (1953).

(9) Dyson, J. *J. Opt. Soc. Amer.*, **49**, p. 713 (1959).

Production of islands and dice in semi-conductor slices with an ultrasonic drill

By R. D. KNIGHT, A.M.I.Mech.E., A.M.I.Prod.E., Services Electronics Research Laboratory, Baldock, Herts

[*Paper first received* 11 *February, and in final form* 7 *April,* 1960]

Abstract

The production of islands of less than 0·002 *in. in diameter with an ultrasonic drill is described along with the tools and the additions made to the equipment to achieve the degree of accuracy required. A novel feature is a frictionless gauge to indicate depth and rate of cutting. Also described is a method of bulk dicing and bulk islanding by the use of laminated tools. Each of these tools has a protruding "pilot-blade" to locate the work so that dicing can be correctly related to islanding and/or to any strip plating, markings, etc., put on the slice in earlier operations.*

A novel self-aligning work table, essential to the bulk islanding process, ensures that the exposed face of the semi-conductor slice is in intimate contact with the tool face.

---

1. Introduction

Two important stages in the manufacture of certain semi-conductor devices are the cutting of the semi-conductor slice into dice, and the forming of an island or mesa on each die. Several methods of performing these operations are available but we are here concerned only with the ultrasonic drilling techniques: the limitations and difficulties associated with the alternative techniques prompted the work reported here.

The ultrasonic drill is a familiar tool widely used in a variety of fields; since full information on the principles and construction has been available for some years,(1) it is unnecessary to repeat this here.

Fig. 1 shows a semi-conductor slice secured to a ceramic block by shellac. The slice has been cut into dice and then an island has been cut on each die. These operations are explained with particular reference to the design of the tools used and the steps taken to adapt the ultrasonic drilling equipment to provide the accuracy and control required. Further, a technique is described whereby a semi-conductor slice is islanded and diced in four cutting strokes of the drill.

Mullard ultrasonic drills (supplied by Kerry's Ultrasonics Ltd.) were used for this work. The 60 W bench type drill is shown in chain dotted lines in Fig. 2 for the purpose of showing the additions made to it; these additions mainly concern the islanding operations and are described under that heading.

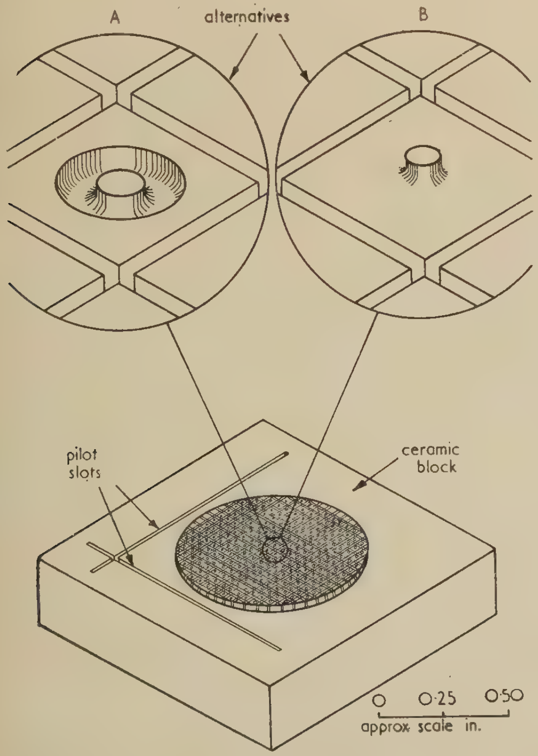
A
alternatives
B
pilot slots
ceramic block
0 0·25 0·50
approx scale in.

Fig. 1. Semi-conductor slice islanded and diced

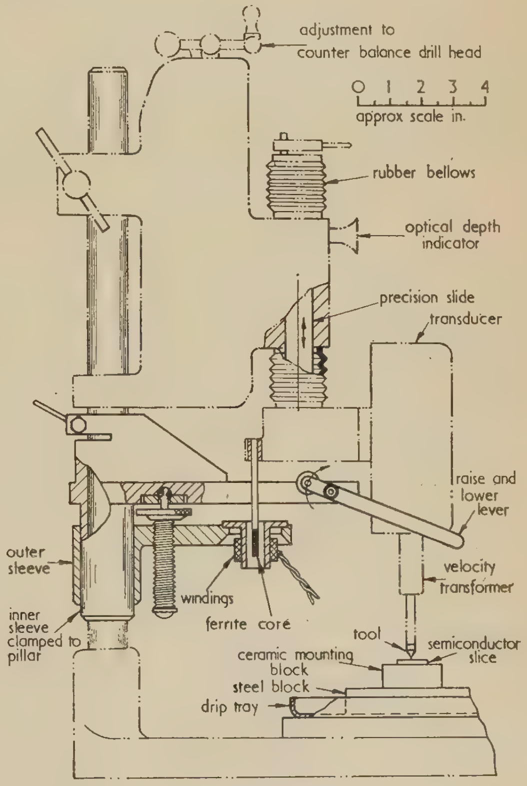
adjustment to counter balance drill head
0 1 2 3 4
approx scale in.
rubber bellows
optical depth indicator
precision slide
transducer
raise and lower lever
outer sleeve
velocity transformer
windings
ferrite core
inner sleeve clamped to pillar
tool
semiconductor slice
ceramic mounting block
steel block
drip tray

Fig. 2. Additions to 60 W ultrasonic drill

2. Cutting of islands on the 60 W drill

Islands of varying sizes down to less than 0·002 in. diameter, are cut, one at a time, on a mounted slice that has been cut into dice in the previous operation.

2.1. *Equipment.* Three additions were made to the standard equipment to give the fine control and accuracy needed for the consistent reproduction of these islands. The first is shown in Fig. 2. A sleeve fitting over the drill pillar is fitted with a simple mechanism attached to a stationary arm so that the drill head can be sensitively raised and lowered. This mechanism does not interfere with the free movement of the tool during cutting since the lift lever swings clear after lowering the head on to the work. A secondary or outer sleeve mounted on the first one has an arm designed to take a dial gauge or other depth indicator so that the depth and rate of penetration of the tool into the work can be observed. This secondary sleeve is raised or lowered on the stationary sleeve, by means of the screw provided, to adjust the depth gauge to zero.

The second addition concerns the actual gauge used for determining the depth and rate of islanding. It was found that the load applied by the springs and friction of a standard dial gauge reduced the sensitivity of balance in the vertical lift movement of the drill head. This gauge was therefore replaced by a frictionless type developed for the purpose, shown in position in Fig. 2. It is a differential transformer comprising a ferrite rod core attached to the drill head by a glass tube and moving freely in coil windings mounted on the secondary arm. The transistorized gauge unit indicates depth of cutting on a microammeter and provides a choice of two ranges, 0·0025 in.–0–0·0025 in and 0·025 in.–0–0·025 in. respectively. Incorporated in the circuit is a zero adjustment control which accommodates errors in the slice mounting of the order of 0·020 in. without affecting the accuracy or linearity of response; this feature enables the operator to process a complete semi-conductor slice without having to reset the mechanical adjustment.

The third addition is that of a power control. The makers have provided tappings for the addition of a switch to cut off the ultrasonic power to the head without switching off the generator. This facility has been incorporated and, in addition, a potentiometer has been fitted so that with the switch in the "ON" position the power can be varied from full to very low. An adjustable stop limits the movement of this power control on the low side and is reset at a suitable intensity for every tool. With this arrangement the control is used on full power for initial tuning and occasional cleaning of the tool, and on a selected lower power for cutting islands.

2.2. *Islanding tools.* The working end of a typical tool is machined in the form of a tube to produce type *A* island (Fig. 1) and in the form of a solid square with a fine hole up the centre in the case of type *B* islands. A small exhaust hole is drilled across the tool to break into the vertical hole so as to encourage circulation of the slurry across the cutting face of the tool. An alternative method of manufacture is to soft solder or braze a length of drawn tubing into the end of the tool body. A soft copper washer between the tool and the velocity transformer stub ensures an efficient coupling and therefore maximum power transmitted to the tool tip.

2.3. *Procedure.* The procedure is exactly as for drilling small holes except that the additions described above are utilized to give the fine control necessary. The slurry used here is 1200 grit silicon carbide in water. Typical rates for cutting islands in silicon range from 0·0005 in./s for a 0·012 in. diameter island to 0·0001 in./s for a 0·002 in. diameter island.

3. Cutting of dice in bulk

A typical bulk dicing tool is shown in Fig. 3. This tool ha a cluster of 0·005 in. mild steel blades spaced at 0·045 in pitch and riveted together before being brazed or sof soldered to the drill stub. The blades protrude sufficientl to allow them to be re-ground several times to clean up afte uneven wear. The blade at one end protrudes about 0·020 in beyond the others for the purpose of locating the workpiec under the tool; a matching slot is provided in the mounting block.

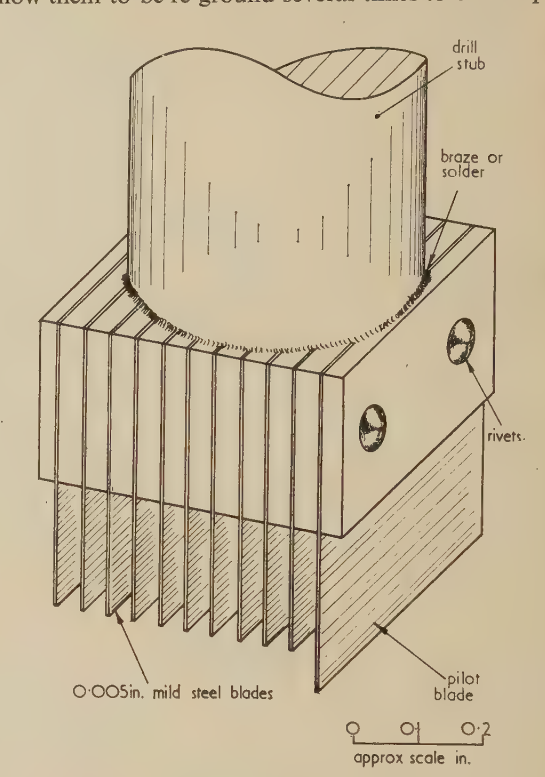

Fig. 3. Bulk dicing tool

3.1. *Procedure.* The tool is lowered on to a mounted semi-conductor slice so that the protruding blade locates i one of the two pilot slots (Fig. 1). A slurry of 600 grit silicon carbide in water is applied and cutting produces a series o 0·040 in. strips in the slice. A second cut, with the protruding blade locating in the second pilot slot (at right angles to the first) completes dicing of the area under the tool.

This operation presents no difficulties and can be carried out with the standard equipment as bought. Where it is considered that the optical depth indicator is not adequate for judging when the tool has completely penetrated the semi-conductor slice an alternative arrangement is used. The slice is secured to a piece of glass instead of to a ceramic block; a mirror is placed face upwards under the mounted slice and in it the operator can observe the blades penetrating the slice.

3.2. *Work location.* The system of locating the work by a pilot blade in the tool ensures the correct angular relationship between the two cuts without the need for an indexing table or fixture. Such fixtures require positive location for the block on which the slice is mounted and their moving parts have to be adequately protected from the slurry. Besides ensuring correct angular location the blade and slot technique offers a means of locating bulk dicing relative to ny markings, islands, gold bands, etc., processed on the ice in earlier operations.

3.3. *Dice size.* These tools produce dice of 0·040 in. quare, but any convenient size can be produced down to bout 0·030 in. square when the bond between the slice and he shellac is not at present adequate at the desirable cutting peeds. However, if a requirement arose for small dice a ombination of slower cutting rate, finer grit slurry and hinner cutting blades would reduce this size limitation.

4. Cutting of islands in bulk

The technique of bulk islanding is an extension of the bulk licing system. A $\frac{7}{8}$ in. square cluster of 0·005 in. blades ested in close pairs (say 0·006 in. apart) at a pitch spacing f 0·045 in. produces islands slightly smaller than 0·006 in. quare all over the surface of a semi-conductor slice in two trokes of the drill, as in Fig. 4 (type *A*). An alternative type f island produced by a tool with thick blades is also shown n Fig. 4 (type *B*).

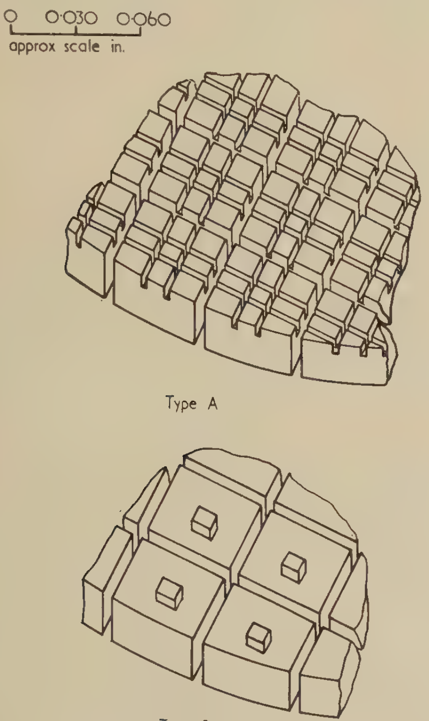

Type A

Type B

Fig. 4. Islanded slice after dicing

The square island produced by this process is usually acceptable in place of the more conventional circular island. It will be obvious that substituting a tool with a different blade spacing for the second islanding cut will produce rectangular islands; this finds an application in some transistor configurations. Using an islanding tool with a series of suitable equispaced cuts across the blades will result in each island being a square (or rectangular) counterpart of the island in Fig. 1(*A*), where the "moat" is restricted to the vicinity of the island.

4.1. *Equipment.* For this bulk islanding process a Mullard 2 kW ultrasonic head is used, driven by a 500 W generator.* This arrangement combines adequate power with a high degree of tool stability; the latter arising out of the fact that the transducer stub is anchored at the nodal point by a flange instead of by a clamp such as is employed to retain the stub on the 60 W drill head.

4.1.1. *Special fixture.* A further piece of equipment that is essential to the success of this technique is the universal work table shown in Fig. 5. This was designed to compensate for out-of-parallel errors between the tool and the workpiece.

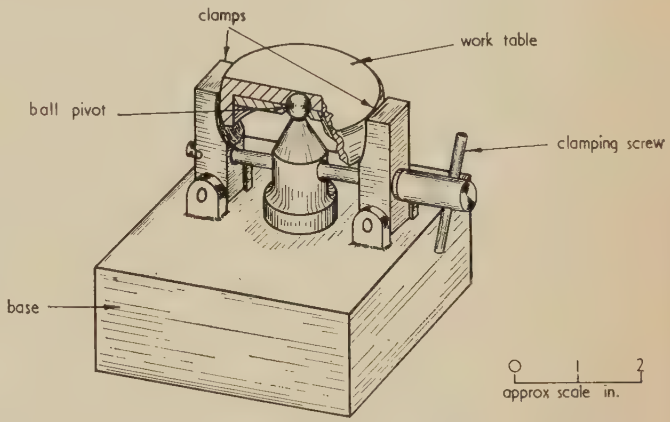

Fig. 5. Ball-joint work table

A work table pivots freely on a small ball fixed to a solid base. The pressure applied when the tool is lowered on to the workpiece has the effect of aligning the face of the workpiece into intimate contact with the face of the tool; the work table is locked in this position by tightening the clamp and the first islanding cut is made. The clamp is then released so that the work table can be reset for the second islanding cut.

Acknowledgements

The author wishes to acknowledge the most valuable assistance of Mr. J. J. Low, who was responsible for the design and manufacture of both the 500 W generator and the transistorized version of the frictionless depth gauge unit. Acknowledgement is also made to the Admiralty for permission to publish this paper.

Reference

(1) Neppiras, E. A. *J. Sci. Instrum.*, **30**, p. 72 (1953).

---

* Designed by Mr. J. J. Low of Services Electronics Research Laboratory, Baldock, Herts.

Single tube sedimentation apparatus for the measurement of particle size distribution

by J. KOBAK, A.M.Inst.F., and D. J. LOVERIDGE, B.Sc., The British Coal Utilisation Research Association, Randall
Road, Leatherhead, Surrey

[*Paper first received* 21 *March, and in final form* 25 *April*, 1960]

Abstract

The equipment described is of the "liquid column with sediment extraction" type which enables dilute suspensions, 0·05% solids concentration by volume, to be used. Thus the sedimenting conditions approximate to those required for unhindered settling of the particles. The apparatus is simple in design and does not require any specialized skills in its operation; one operator can easily control two sizings. Two similar sedimentation tubes have been shown to be devoid of individual characteristics and to be capable of giving reproducible results. The results compared well with those obtained in other laboratories using different sedimentation methods.

1. Introduction

For the development work carried out in B.C.U.R.A. on cyclone dust collectors and a centrifugal separator, it became necessary to determine the size distribution of a sub-sieve test dust. Various methods of determining particle size distribution were considered before the "liquid column with sediment extraction" method was selected as the most suitable for the work in hand. The principle of this method had been known for some time and Stairmand(1) designed an apparatus embodying this principle, in which the sediment was removed discontinuously. A modified form of that apparatus has since been reported(2) elsewhere.

The apparatus to be described employs the same principle, but consists of a single tube. This new design facilitates the continuous collection of the sediment and after extensive testing a very simple and reliable experimental technique has been evolved.

2. Design and use of equipment

2.1. *Theoretical considerations.* An initially homogeneous suspension of the particles is prepared from which the particles settle at their free falling velocities. The time (t_d) taken for particles of size d to settle through the total depth (h) of the suspension can be calculated from Stokes* equation. At time t_d after sedimentation has commenced, the sediment will be composed of all particles of size d and larger, together with some smaller particles which have settled through depths less than h. Measurements are made of the total weight of sediment deposited after calculated times. Methods based on such data are described as "cumulative".

The single tube method is based on that described by Stairmand(1) and is essentially "cumulative" in nature. The size range (this can be determined visually by a microscopical examination) of the sample is divided into a number of size classes the limits of which lie in a $\sqrt{2}$ geometric progression. The geometric mean size is used to characterize each class and the settling times* for particles of these mean sizes ar calculated. The sediment deposited in the time interval between these settling times is collected and weighed and from these data the size distribution of the sample can be calculated by using the relationship given below, the derivation of which is fully treated by Stairmand.(1) Suppose that the mean size particle of the top size class is 76 μ then

$$\begin{aligned} W_{76} &= X_{76} - \chi_{53} \\ W_{53} &= 2\chi_{53} - \chi_{38} \\ &\ldots\ldots\ldots\ldots\ldots\ldots \\ W_{6\cdot7} &= 2\chi_{6\cdot7} - \chi_{4\cdot7} \\ W_{<5\cdot6} &= 2\chi_{4\cdot7} + \chi_{\infty} \end{aligned}$$

where $W_{76}, W_{53} \ldots$ = weight of material in size class of mean size 76, 53 . . . μ

$W_{<5\cdot6}$ = weight of material below size class of mean size 6·7 μ. (Limits 8 to 5·6 μ

X_{76} = weight of sediment collected in time (t_{76}) for 76 μ particles to settle

$\chi_{53}, \chi_{38} \ldots$ = weight of sediment collected in time interval t_{76} to t_{53}, t_{53} to t_{38} . . .

χ_{∞} = weight of material that would settle between $t_{4\cdot7}$ and $t = \infty$; this is found by difference

In this way the weight of material in each size class is determined and a cumulative under- or over-size distribution can be calculated as required.

2.2. *Description of apparatus.* The apparatus is shown in the figure.

The sedimentation tube is constructed of glass and is closed at the top by a removable stopper fitted with a tap; this is replaced by the funnel during filling and stirring. The tube is tapered at the bottom with the tip of the taper ground flat at right angles to its axis. With the exception of the size of the opening at the tip of the taper, which needs to be 1 to 2 mm internal diameter, the dimensions are not considered to be critical, and those shown in the figure were found to be convenient.

The sedimentation tubes are housed in a thermal stabilizing bath, maintained at 25 ± 0·05° C, and are fitted into holes in the bottom of it with about 1 cm protruding on the underside. Adjustable clamps are fitted inside the bath to locate the tubes vertically.

---

* $v = \dfrac{h}{t} = \dfrac{gd^2(\sigma - \rho)}{18\eta}$ where v = free falling velocity (cm s^{-1})

h = height of fall (cm)
t = settling time (s)
d = particle diameter (cm)
η = viscosity of suspending liquid (P)
σ = density of particles (g cm^{-3})
ρ = density of suspending liquid (g cm^{-3})

The glass sediment collection tubes are approximately 1 cm ameter and 1·5 cm deep, having a capacity of approximately ml.

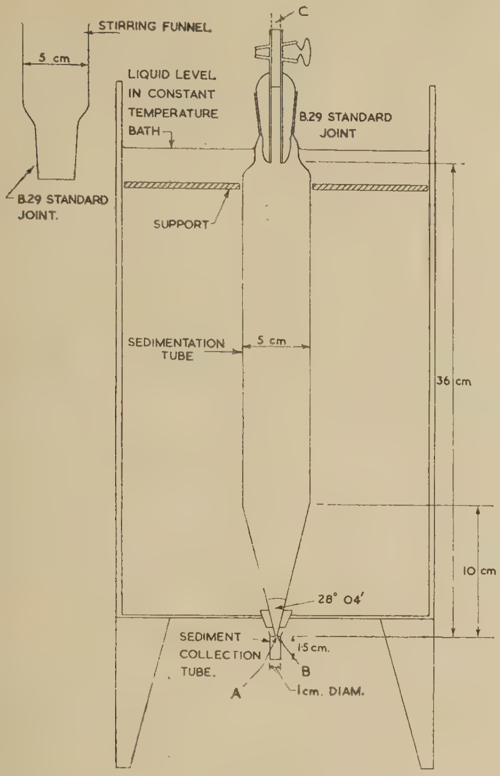

Diagram of the apparatus

A = outlet diameter 0·2 cm; *B* = level of liquid in sediment collection tube; *C* = internal diameter of 0·5 cm (approx.)

2.3. *Method of operation.* The height of fall *h* (see figure) and the volume of the tube with the stopper in position, are measured; the latter measurement gives the final volume of the suspension. The tube is then fitted into the stabilizing bath and thoroughly cleaned *in situ.*

At the start of sedimentation the concentration of the suspension should be 0·05% of solids by volume; hence the weight of analysis sample used varies with the density of the powder. The analysis sample is well dispersed in a dispersing agent, by shaking or swirling in a suitable container, until an apparently homogeneous slurry is obtained. The outlet *A* (see figure) of the sedimentation tube is closed with a clipped rubber tube which is connected to a source of clean, dry compressed air.* The funnel is placed in the top of the sedimentation tube which is then approximately two-thirds filled with suspending liquid; to this a suitable quantity of suspending agent is added. An additional quantity of suspending liquid, for topping-up purposes, is placed in the stabilizing bath in a separate container. The liquid in the tube is stirred by bubbling compressed air through it, and allowed to stabilize to the temperature of the bath; for temperature differences of a few degrees this takes about 15 to 30 minutes. Stirring is continued as the dispersed analysis sample is washed into the sedimentation tube and while the suspension is adjusted to its final volume.

The efficiency of the dispersion can be checked at this stage by examining a small drop of the suspension under the microscope. If the particles are aggregated the sizing should be abandoned.

After stirring the suspension for a total of about 5 minutes the compressed air supply is stopped by closing the clip on the connecting tube; settling times are measured from this instant. The funnel is then removed and the stopper, with the tap open, is inserted into the top of the sedimentation tube; the tap is then closed. Thus the sedimentation tube should be completely filled by the suspension. The air supply tube is detached from the outlet *A* and the first weighed sediment collection tube, containing about 0·7 ml. of suspending liquid, is placed in position under the outlet so that the two liquid surfaces are in contact. The two surfaces join readily to give a continuous liquid medium through which the particles settle into the collection tube.

The sediment collection tubes are changed in accordance with the calculated settling times and in this way a series of sediment fractions are obtained. Finally the tubes containing the sediment are dried and the weight of sediment collected in each is determined by difference.

3. Performance of equipment

3.1. *Experimental procedure.* Two similar tubes were constructed and tested for individual sizing characteristics; the reproducibility of the results was also estimated from these tests. The two tubes were used simultaneously and four samples of silica dust, which were selected at random from a batch of eight, were sized in each. The samples of silica dust were prepared from a bulk sample, which was coned and quartered repeatedly to extract eight samples. The tests using silica were followed by a series of tests using a sample of zircon dust, which provided a second estimate of the reproducibility of the results for a dust of higher density.

3.2. *Results.* The results of the individual sizings of the silica dust are shown in Table 1, together with the mean for each group of four sizings. The overall means, standard deviation, and confidence limits of these results are shown in Table 2, and the cumulative undersize distribution is shown in Table 3. The results of the similar series of sizings carried out on the sample of zircon dust are shown in Tables 4 and 5.

Table 6 gives a comparison of results obtained by sizing

Table 1. *Size analysis of silica dust: General table of results*

Tube 1 *Mean size of class* (μ)	*Class limits* (μ)	*Weight % in class* *Sample* 1	2	3	4	*Mean*
76	90·5 – 64	6·3	0·3	—	—	1·7
53·7	64 – 45·2	10·4	10·2	6·2	9·8	9·2
38	45·2 – 32	15·0	20·7	17·8	18·8	18·1
26·9	32 – 22·6	15·6	14·5	16·6	16·4	15·8
19	22·6 – 16	9·0	12·7	12·5	13·2	11·9
13·4	16 – 11·3	9·2	9·9	10·2	9·5	9·7
9·5	11·3 – 8	9·4	9·8	8·5	8·1	8·9
6·7	8 – 5·6	4·2	4·7	5·2	6·0	5·0
	< 5·6	21·0	17·2	23·0	18·1	19·8
Tube 2		1	2	3	4	*Mean*
76	90·5 – 64	1·5	—	—	—	0·4
53·7	64 – 45·2	11·1	8·4	8·0	6·7	8·6
38	45·2 – 32	16·6	18·0	18·1	16·5	17·3
26·9	32 – 22·6	14·3	16·0	16·1	16·1	15·6
19	22·6 – 16	12·7	12·6	12·3	13·4	12·8
13·4	16 – 11·3	10·5	8·5	9·3	9·4	9·4
9·5	11·3 – 8	6·6	7·4	7·9	8·1	7·5
6·7	8 – 5·6	4·7	5·7	6·0	5·4	5·5
	< 5·6	21·9	23·4	22·2	24·4	23·0

---

* When using compressed air from a main some trouble may occasionally be caused by the presence of very fine oil mist.

Table 2. *Silica dust: Overall mean, standard deviation and 95% confidence limits*

Mean size of class (μ)	*Class limits (μ)*	*Overall mean (weight %)*	*Standard deviation of observations*	*Standard deviation of the mean*	*95% Confidence limits or single sizing*	*95% Confidence limits for mean*
76	90·5 — 64	1·0	2·2	0·8	±5·2	±1·8
53·7	64 — 45·2	8·9	1·8	0·6	±4·3	±1·5
38	45·2 — 32	17·7	1·7	0·6	±4·0	±1·4
26·9	32 — 22·6	15·7	0·9	0·3	±2·0	±0·7
19	22·6 — 16	12·3	1·4	0·5	±3·3	±1·2
13·4	16 — 11·3	9·6	0·6	0·2	±1·5	±0·5
9·5	11·3 — 8	8·2	1·0	0·4	±2·4	±0·9
6·7	8 — 5·6	5·2	0·7	0·2	±1·6	±0·5
	< 5·6	21·4	2·5	0·9	±6·0	±2·1

Table 3. *Silica dust: Cumulative size distribution*

Particle size (μ)	*Weight % undersize*
90·5	100
64·0	99
45·2	90
32·0	72
22·6	57
16·0	44
11·3	35
8·0	27
5·6	21

the same sample of silica dust by a number of sedimentation methods, including the single tube.

3.3. *Discussion of results.* To test for a significant difference between the sizings carried out in the two tubes the "*t*" test was applied, at each size class, to the differences between the means of the two groups of sizings. The results showed that there was no significant difference between the two groups of sizings at the 95% level; hence there was no evidence that the tubes possessed individual sizing characteristics. The results of the eight sizings could thus be regarded as one group. The overall mean, standard deviation, and confidence limits at the 95% level, were then calculated.

Table 4. *Size analysis of zircon dust: General table of results*

Mean size of class (μ)	*Class limits (μ)*	*Weight % in class*						
			2	3	4	5	6	*Mean*
18·9	22·5 — 15·9	—	—	—	—	—	—	—
13·4	15·9 — 11·2	3·5	6·3	6·1	5·0	5·9	0·7	4·6
9·5	11·2 — 7·9	21·8	25·7	23·1	23·0	21·1	21·4	22·7
6·7	7·9 — 5·6	23·2	25·4	23·6	23·5	22·4	24·0	23·7
4·7	5·6 — 4·0	18·4	16·0	18·5	18·9	17·7	20·1	18·3
3·3	4·0 — 2·8	11·9	7·4	12·2	12·7	13·1	13·4	11·8
	< 2·8	21·3	19·2	16·6	16·9	19·7	20·5	19·0

Table 5. *Size analysis of zircon dust: Overall mean, standard deviation and 95% confidence limits*

Mean size of class (μ)	*Class limits (μ)*	*Mean*	*Standard deviation of observations*	*Standard deviation of the mean*	*95% Confidence limits single sizing*	*95% Confidence limits mean*
18·9	22·5 — 15·9	—	—	—	—	—
13·4	15·9 — 11·2	4·6	2·2	0·9	±5·7	±2·3
9·5	11·2 — 7·9	22·7	1·7	0·7	±4·4	±1·8
6·7	7·9 — 5·6	23·7	1·0	0·4	±2·6	±1·0
4·7	5·6 — 4·0	18·3	1·4	0·6	±3·6	±1·5
3·3	4·0 — 2·8	11·8	2·2	0·9	±5·7	±2·3
	< 2·8	19·0	1·9	0·8	±4·9	±2·1

Table 6. *Comparison of methods of sizing by comparing results of sizings carried out on silica dust*

Method / *Particle size (μ)*	*Sedimentation balance*	*Photo-sedimentation*	*I.C.I. liquid column*	*Pipette 1*	*Pipette 2*	*B.C.U.R.A. liquid column*
	Percent undersize (by weight)					
64·0	—	91	94	—	—	99
45·2	90	86	85	82	84	90
32·0	76	74	70	69	74	72
22·6	60	58	55	55	61	57
16·0	47	44	43	43	48	44
11·3	38	34	32	32	36	35
8·0	31	26	22	25	27	27
5·6	21	16	17	20	22	21
4	17	9	12	15	17	—

These showed that over the middle range of the size distribution the results could be reproduced to between 3 and 8%. For the coarsest and finest size classes the reproducibility of the results was not as good; this is to be expected since an initial timing error and any effects due to the shape of the apparatus would have their greatest effect in these size classes.

The results of the sizings carried out on the sample of zircon dust were examined for reproducibility only. This was found to be similar to that for the sizings carried out on the silica dust.

The results of sizings of the silica dust by other sedimentation methods were available; a comparison of these results (Table 6) with those obtained by the single tube method shows that there is very fair agreement between the values obtained by all the methods quoted.

It is assumed in the theory of the method of calculating e results that the sedimentation tube is of uniform cross-ction over its whole length. Thus if any errors are intro-iced by the conical portion of the apparatus they are nored. It is also possible for the amount of fine material be over-estimated by the deposition of sediment on the ne. In such circumstances it may be preferable to determine $_0$ directly rather than by difference.

4. Acknowledgements

The authors wish to express their thanks to Mr. W. Bostock imon Carves Ltd.), Dr. H. Heywood (Mechanical Engineer- g Department, Imperial College of Science and Technology, University of London), Dr. B. A. Scott (Research Laboratories, British Aluminium Co. Ltd.), and Dr. C. J. Stairmand (Engineering Research Department, Imperial Chemical Industries Ltd., Billingham), who supplied data for Table 4 in private communications. The paper is published by permission of the Director General of the British Coal Utilisation Research Association.

5. References

(1) Stairmand, C. J. *Sym. Particle Size Analysis*, p. 128 (London: Inst. Chem. Eng. and Soc. Chem. Ind., 1947).

(2) Kobak, J. *J. Sci. Instrum.*, **32**, p. 153 (1955).

Multipoint digital temperature recorder with punched tape output

y T. S. HOLDEN, B.Sc., Division of Building Research, Commonwealth Scientific and Industrial Research rganization, Melbourne, Australia

Paper first received 5 *January, and in final form* 25 *March*, 1960]

Abstract

A sixty-five point potentiometric recorder, which gives its utput in binary form on punched tape directly suitable or use with a digital computer, is described. The instrunent operates intermittently, and provides reference times nd parity and logical sum checks with the other data on he output tape. Although designed for recording temeratures, the instrument may be readily adapted to other pplications.

Introduction

Detailed experimental studies in various fields of physics often yield a large amount of numerical data which may be analysed quickly and conveniently in n automatic digital computer. In such cases considerable ffort is usually required to collect the data and to present hem in a form suitable for processing in the computer, and t appeared to be worthwhile to investigate the possibility of ecording the data in a new way.

An experimental investigation of the thermal behaviour of uildings required that the air temperature be measured at a umber of points at hourly intervals over a period of several veeks. For this type of work no high degree of accuracy f measurement was required, but the quantity of data to be ecorded and analysed was considerable. The recorder lescribed in this paper was built to collect data of this type, nd to produce its output in the form of punched paper tape lirectly suitable for input to an automatic computer.

General description

The basic principles of the recorder are illustrated in the lock diagram, Fig. 1. The temperature measuring system mploys thermocouples as sensing elements, a slide wire, ibrator, amplifier, and balancing motor. The e.m.f. due to he temperature difference between the point being measured nd a reference thermojunction is compared with the e.m.f. etween the moving contact and one end of a slide wire; this out-of-balance e.m.f. is converted to a.c. by a vibrator, amplified, and the resulting signal applied to one winding of a balancing motor which drives the moving contact of the slide wire until a balance point is reached. At balance the position of the shaft which carries the moving contact is a function of the temperature at the point being measured. This shaft also carries a digitizer which generates an eight-digit binary code, depending on its position. This code is fed to an interpreter circuit which changes the code as described below, and the resulting code is punched four digits at a time on to paper tape. The sequence of operations is controlled by a programmer, which commences each set of data with a cue and codes for the time, date and month, selects each temperature measuring circuit in turn, and concludes each set with a column parity check and a code. The codes for the time and data and the signal to commence each set of measurements are supplied by a clock unit. The whole equipment weighs 250 lb and is housed in a steel cabinet 2 × 2 × 3 ft high, mounted on four castors.

Components

The various components of the instrument can be seen in Fig. 2.

Slide wire, balancing motor, and amplifier. The temperature measuring system employed is typical of commercial potentiometric recorders, and in the present case the slide wire, balancing motor and some components of the amplifier are commercial items. The system is capable of reaching balance in three seconds, and as high speed is not necessary for the particular application, readings are made every five seconds.

Digitizer. In coding (digitizing) the position of a shaft, various systems are possible; in the present instance a binary system was chosen because of its inherent electrical simplicity and because programming for many digital computors is simpler with binary numbers. The particular code chosen was the unambiguous Gray cyclic code (see Appendix), which has the advantage that each successive increment of rotation alters only one digit at a time, a feature which widens the permissible tolerance considerably.

As the temperatures being measured are subject to rando fluctuation of the order of 0·5° F, and small changes of tl position of a measuring thermocouple can yield changes temperature of the same order, it is unnecessary to measu to a greater degree of accuracy. For convenience the rang of the instrument was chosen as 30 to 158° F, obtained wit 256 (2^8) half-degree increments, requiring eight binary digit The comparatively slow recording speed made it possible t allow the slide wire shaft to come to balance, remove tl driving power, and then, whilst the shaft was stationary, t bring the microswitches to bear on their respective cam which could thus be cut with square teeth.

Hot box. The reference thermojunction is embedded i (but electrically insulated from) a box fabricated from ½ tl 3 in. and ½ by 4 in. brass strip. The box is insulated wit ½-in. thick compressed cork, is 5 × 6 × 7 in. overall, and maintained at a temperatre of 160 ± 0·2° F by means of heater and a stem-type bimetallic thermostat. The pow supply for the slide wire is located in a cavity inside the ho box. Although it is usual in potentiometer circuits to use dry battery or lead accumulator for this purpose, and t standardize the potentiometer against a standard cell intervals, it has been found quite satisfactory to use a voltag regulator valve and a voltage reference valve in series supplie from the a.c. power supply provided for the amplifier. Thes valves supply a constant current to a voltage divider, acros a portion of which is the slide wire. The voltage dividin resistors and the two valves, being located inside the h box, are at a constant temperature, and it has been foun that fluctuations of the voltage across the slide wire are le than 0·01% for large variations in mains voltage. Provisio has been made for comparison with an external standa cell, but this is required only as a long-term check and usually done when the instrument is first turned on.

Clock unit. A five-digit code for the hour of the day generated by means of five digitizing cams and micr switches on a shaft which rotates once in twenty-four hour driven by an electric time-switch motor. This shaft al

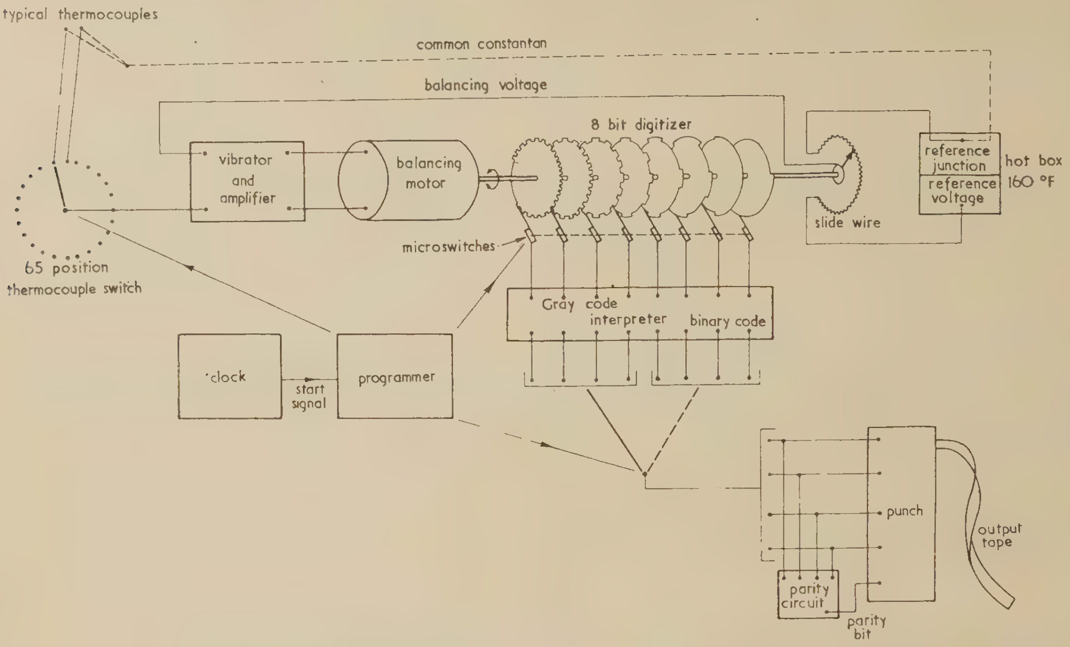
typical thermocouples
common constantan
balancing voltage
8 bit digitizer
vibrator and amplifier
balancing motor
reference junction
reference voltage
hot box 160 °F
slide wire
microswitches
65 position thermocouple switch
Gray code interpreter
binary code
clock
start signal
programmer
punch
output tape
parity circuit
parity bit

Fig. 1. Block diagram of multipoint digital temperature recorder

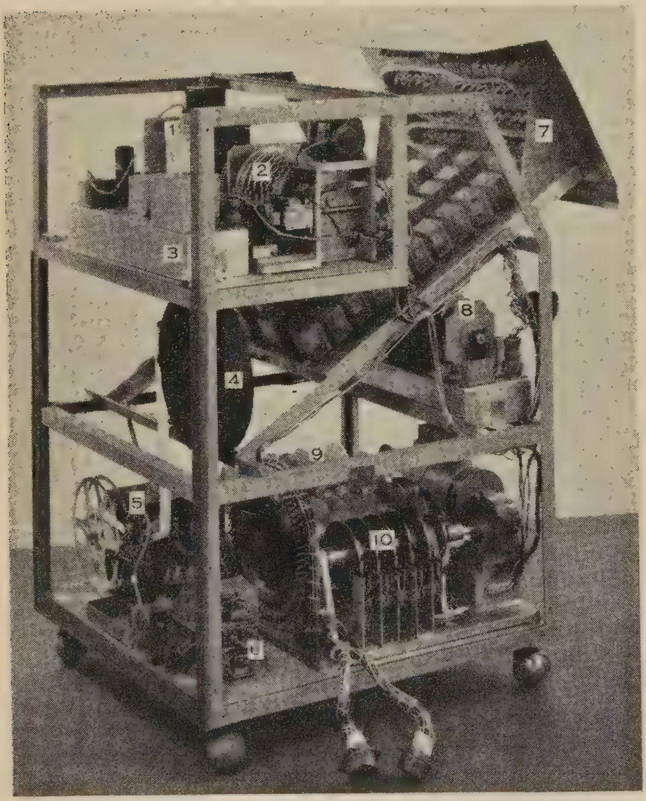
1
2
3
4
5
6
7
8
9
10

Fig. 2. Assembly of the recorder

(1) hot box; (2) digitizer; (3) amplifier; (4) tape holder; (5) tape winder; (6) punch; (7) interpreter; (8) power supply; (9) clock; (10) programmer.

rries a cam which provides the signal for initiating each corder cycle; by changing this cam the recorder may be ade to operate any integral number of times per day, though a minimum time of six minutes must be allowed r each operation. A second shaft on the same unit, rotated 31 of a turn for every complete revolution of the first shaft means of a ratchet, also carries five digitizing cams nerating codes for the day of the month. There is prosion for manual resetting of these shafts, e.g. at the end the month, or after a power failure.

Interpreter, parity check, and control relays. Signals from e slide wire digitizer, from the hour and day digitizers, and om the month hand-set register are all in the cyclic Gray ode previously mentioned. The interpreter is a set of lays, one for each digit, interconnected in such a manner at the code is changed to pure binary code; examples of ese two codes with the decimal equivalents are given in the ppendix. Each four-digit group (half of an eight-digit roup denoting a temperature) is accompanied in the punch gister by a parity check digit, generated by a set of four lays which produces a signal only if an even number of on-zero digits is already in the punch register. These relays, nd those controlled by the programmer microswitches for ontrolling the various operations, are mounted on a separate lug-in chassis; the type of relay chosen is built on to a plug or easy replacement and has a transparent dust cover. ontact arrangements were kept to three types to reduce the umber of spares required. The functioning of the various ircuits is monitored by neon indicating lights located on a anel integral with the relay chassis.

Programmer and thermocouple switch (Fig. 3).—The equence of operations of the recorder is controlled by a rogrammer unit consisting of two shafts carrying cams which operate the microswitches that initiate the various operations. The thermocouple switch is a sixty-eight position single-pole switch, sixty-five positions being used for thermocouples and the other three reserved for operations described below. The design of the switch is copied from a smaller (twenty-five position) commercial thermocouple switch, the contact studs and contact brush being taken from commercial switches. The first programmer shaft carrying six cams is directly driven at 12 rev/min by a small induction motor, and the second shaft carrying seven cams and the thermocouple switch is rotated 1/68 of a turn for every complete revolution of the first shaft. The sequence of operations is as follows:

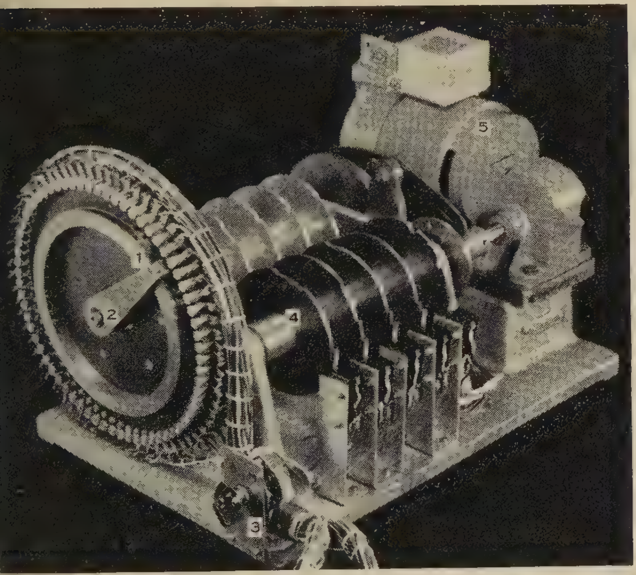

Fig. 3. Programmer and thermocouple switch
(1) thermocouple switch; (2) switch shaft; 1 rev for each set of data; (3) automatic-manual switch; (4) motor shaft; 1 rev for each switch position; (5) motor.

1st cycle. The cue signal, the function of which is to indicate the start of a group of data, is switched to the punch register and then punched, then the code for the hour of the day is similarly recorded. All cycles conclude with the thermocouple switch arm being moved to the next position.

2nd cycle. The code for the day of the month is first recorded, then the code for the month is next recorded from a hand-set register of five switches. Throughout this cycle the column parity check is rendered inoperative, leaving it reset ready to receive the first data from the next cycle.

Thermocouple cycles. Power is supplied to the amplifier and balancing motor for the first three seconds of each thermocouple cycle, allowing the slide wire arm to come to balance. The power is then removed and the solenoid is actuated, bringing the eight digitizing microswitches to bear on their respective cams; the resulting eight-digit signal is divided into two groups of four digits, and these groups of four digits are recorded successively. The solenoid is next released, the thermocouple switch turned to the next position, and power is restored to the amplifier and balancing motor for the next cycle.

Final cycle. During each of the sixty-five thermocouple cycles the successive signals sent to the punch register are accumulated by a column parity check register; actually a cumulative digit by digit inequality* is formed. This cumulative inequality or column parity check is recorded first in the final cycle, then a code to designate the project for which the recorder is being used is also recorded, and lastly the programmer motor is switched off to wait until the whole sequence is again initiated by the clock.

Punch. The punch is basically a telegraphic reperforator, but has been modified to operate from a separate wire for each channel, instead of the five channels being set by a series of successive impulses over the same wire. Other components such as tape holder, tape winder, and power supply can be seen in Fig. 2.

Data processing

Data from the recorder are being processed by the "CSIRAC" computer at the University of Melbourne. The data are first checked by a separate test programme which passes it through the tape reader, checking that each set of data has its correct cue, that the hour, day, and month are compatible with those on the previous set, that there is the correct number of items of temperature data and that the row and column parity checks are correct. If any errors occur the computer types out sufficient information to enable the error to be identified and investigated. Other programmes are then used to process the tested data.

---

* A cumulative inequality has the following truth table:

$0 + 0 = 0$ $\quad$ $1 + 0 = 1$
$1 + 1 = 0$ $\quad$ $0 + 1 = 1$

Discussion

There are a number of points of design which require some comment. The mechanical arrangement of cams and microswitches in the digitizer is robust, but has the great advantage that it is simple to construct, reliable in operation and considerably cheaper than a commercial unit. It would have been possible to include translation from the cyclic Gray code to pure binary code as part of the input routine of the computer, instead of achieving this in the recorder by means of the interpreter. This possibility was rejected for two reasons: first, a simple visual indication of the temperature being measured is impossible if only the Gray code is available, and, secondly, a conversion routine occupies valuable storage space in the computer and increases computation time. For applications with a fast recording rate the advantage of simpler design of the recorder might well outweigh the disadvantages mentioned, and conversion to binary code could be done in the computer. Similarly, the decisions to include row and column parity checks were influenced by their comparative simplicity in an instrument of such slow speed; a final decision as to the necessity of such checks will have to be deferred until more experience with the system has been obtained.

Conclusion

A description has been given of the design and construction of an automatic recorder which can record data in form suitable for an electronic computer, and in far greate quantity than was possible by previous methods with a sma staff.

Apart from some initial difficulties due to oversights an faulty components, very little servicing of the equipment ha been necessary over a period of several months of continuou operation. More practical experience is necessary to asses the long-term reliability of the recorder as a whole.

Acknowledgements

The author wishes to thank Mr. G. W. Hill, Division Mathematical Statistics, C.S.I.R.O., for helpful suggestion with regard to programming techniques and methods data checking. Mr. B. C. Bautovich, of the State Electricit Commission of Victoria at present seconded to the Divisio of Building Research, gave valuable assistance with som aspects of the mechanical design. The modifications to th telegraphic reperforator were carried out by the Telegraphi Equipment Section, Postmaster General's Department, wh supplied the unit.

Appendix

Gray code and binary code

Decimal	*Gray code*								*Binary code*							
	Switch number															
	8	7	6	5	4	3	2	1	2^7	2^6	2^5	2^4	2^3	2^2	2^1	2^0
0	0	0	0	0	0	0	0	0	0	0	0	0	0	0	0	0
1	0	0	0	0	0	0	0	1	0	0	0	0	0	0	0	1
2	0	0	0	0	0	0	1	1	0	0	0	0	0	0	1	0
3	0	0	0	0	0	0	1	0	0	0	0	0	0	0	1	1
4	0	0	0	0	0	1	1	0	0	0	0	0	0	1	0	0
5	0	0	0	0	0	1	1	1	0	0	0	0	0	1	0	1
6	0	0	0	0	0	1	0	1	0	0	0	0	0	1	1	0
7	0	0	0	0	0	1	0	0	0	0	0	0	0	1	1	1
8	0	0	0	0	1	1	0	0	0	0	0	0	1	0	0	0
9	0	0	0	0	1	1	0	1	0	0	0	0	1	0	0	1
10	0	0	0	0	1	1	1	1	0	0	0	0	1	0	1	0
11	0	0	0	0	1	1	1	0	0	0	0	0	1	0	1	1
12	0	0	0	0	1	0	1	0	0	0	0	0	1	1	0	0
13	0	0	0	0	1	0	1	1	0	0	0	0	1	1	0	1
14	0	0	0	0	1	0	0	1	0	0	0	0	1	1	1	0
15	0	0	0	0	1	0	0	0	0	0	0	0	1	1	1	1
16	0	0	0	1	1	0	0	0	0	0	0	1	0	0	0	0
32	0	0	1	1	0	0	0	0	0	0	1	0	0	0	0	0
64	0	1	1	0	0	0	0	0	0	1	0	0	0	0	0	0
128	1	1	0	0	0	0	0	0	1	0	0	0	0	0	0	0
255	1	0	0	0	0	0	0	0	1	1	1	1	1	1	1	1

High vacuum high temperature X-ray camera

By B. A. HATT, M.Sc., P. J. C. KENT and G. I. WILLIAMS, B.Sc., Ph.D., Fulmer Research Institute Ltd., Stoke Poges, Bucks

[Paper received 4 *April*, 1960]

Abstract

A camera suitable for the examination of reactive metals such as titanium and zirconium up to temperatures of 1000° C in a vacuum better than 1×10^{-6} *mm of mercury is described.*

The high vacuum is obtained by constructing the camera in glass without demountable seals, and the use of a radiant heater in place of a conventional furnace assembly.

Application of the camera to studying the $\beta - \alpha$ *transformation in Ti – Cr and Ti – Zr alloys is described.*

Introduction

THE camera was designed specifically for studying the $\beta - \alpha$ transformation in titanium and zirconium alloys but in basic design it is equally suitable for a variety of problems where the following considerations apply:

(*a*) The maximum temperature is about 1000° C.

(*b*) A high degree of vacuum, preferably better than 1×10^{-6} mm of mercury is to be maintained, with ease of outgassing specimen and camera interior a major consideration.

Existing types of high temperature X-ray cameras were regarded as unsuitable for such applications because of specimen contamination introduced by the relatively poor vacua attainable and the difficulties of outgassing the camera interior, particularly the furnace assembly. Essential features of the new design are the construction of the camera in glass and the use of a radiant heater situated outside the camera. The latter eliminates contamination due to the conventional furnace assembly within the instrument while the clean smooth interior walls and use of sheet specimens simplify the outgassing procedure.

Description of the camera

Vacuum system. The camera body consists of a Pyrex glass envelope joined directly to a glass liquid air trap which is attached to the pumping system, as shown in Fig. 1. Two circular windows allow the passage of incident and diffracted X-ray beams. They are of Al–Si alloy⁽¹⁾ 0·0015 in. thick, permanently bonded to ports carried from the side of the camera so avoiding demountable seals. A lead borosilicate glass cement is used for metal-to-glass bonding and the ports themselves form a graded seal matching the expansion of this glass to that of Pyrex.⁽²⁾ The windows are positioned according to the nature of the problem. For example, in the work on Ti–Cr and Ti–Zr alloys they enable the (200) diffractions of the high temperature β phase (cubic) and the $(10\bar{1}2)$ and $(11\bar{2}0)$ diffractions of the low temperature α phase (hexagonal) to be recorded with MoKα radiation. The pressure is measured by an ionization gauge-head joined to the camera.

With this type of system avoiding demountable seals above the liquid-air trap, vacua of 1×10^{-7} mm of mercury are obtained after suitable outgassing of the camera walls, with heater tapes at about 400° C for several hours.

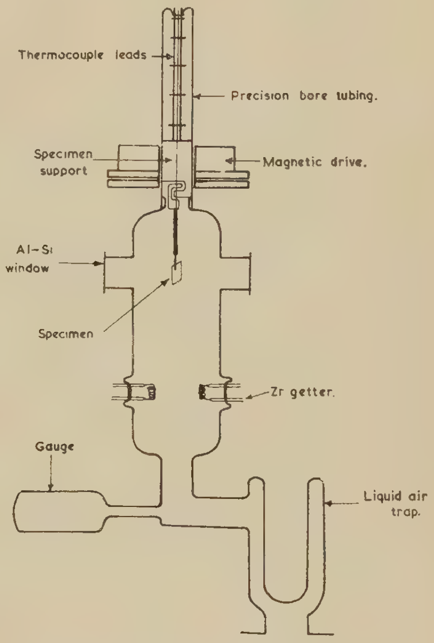

Fig. 1. Vertical section through camera body

Provision is made for operating two zirconium getters, one at high temperature to getter oxygen, and the other at about 200° C to take in hydrogen. The getters are made by coiling thin zirconium strip around a molybdenum wire core which is itself wound into a coil of about 10 turns. The zirconium strip is held in position by thin molybdenum wire wound over it and heated by passing a current along the molybdenum core. Before installing in the camera, the getters are "formed" and outgassed by heating them to about 1750° C in a subsidiary vacuum apparatus. This causes the zirconium strip to melt and flow evenly over the core. When installed in the camera they can, if desired, be operated with the zirconium molten; it is held in position by the outer winding. The getters were designed with a view to sealing off the camera, and then "gettering" to a higher vacuum. Alternatively, as in the present work, they can be used as vacuum boosters in conjunction with the dynamic pumping system.

Specimen mounting. Fig. 2 shows the specimen support consisting of a hollow aluminium cylinder (*b*) machined so that the blind hole (*e*) is coaxial with the cylinder axis. A soft iron armature (*d*) is carried on the spindle (*c*) which rests on a ball-bearing located in (*e*) and is supported at the other end by the bushed bearing (*a*). The specimen is joined to (*c*) by the bracket (*g*) and moves with the armature which can be rotated about a vertical axis by means of an external magnet with shaped pole pieces moving over a graduated scale. The entire assembly can be positioned vertically along the length of the precision glass tubing constituting part of the camera body.

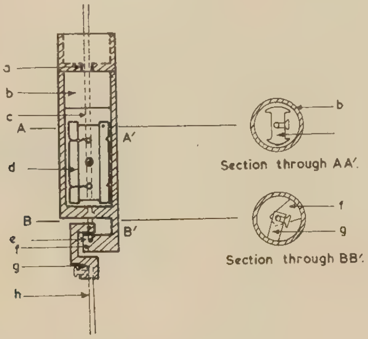

Fig. 2. Vertical section through specimen support

The movement provided by this type of support is suitable for both single crystal and polycrystalline specimens. The specimen size and shape is limited essentially by the power and focus of the radiant heater. The single crystal studies reported later were made on pieces of sheet material 1 cm × 0·5 cm and 0·1 mm thick in which suitable crystals had been grown. The specimen was then spot-welded under argon to a 0·020 in. platinum wire attached to the spindle (*h*).

Radiant heater. The conventional type of furnace is precluded since it is difficult to outgas without contaminating the specimen. In studying phase transformations it is desirable that the specimen be held at one end only to avoid stress induced effects. One method of heating which satisfies these requirements consists of focusing an intense beam of light onto the specimen.$^{(3)}$ The source is a 1000 W projection bulb (type Philips 7242 C/OS) which is situated at one focus of a (semi) ellipsoidal reflector with minor and major axes 8 and 13 in. respectively. The specimen is at the second focus. The reflector spun by Warwick Production Ltd. from commercial aluminium gives fairly strict geometrical focusing so that the intense focus at the specimen extends over an area less than one square inch. With the specimen turned to intercept the maximum light flux, temperatures up to 1000° C are obtained. If the specimen is to be rotated more than a few degrees on either side of this position, a second reflector suitably placed is required to minimize temperature fluctuations.

Electron bombardment heater. In order to obtain temperatures higher than about 1000° C a method of bombarding the specimen with electrons emitted from a heated filament was investigated. The filament consisted of a few turns of tungsten wire situated some 3 cm from the specimen. With a filament temperature of 2000° C and a voltage difference of 1000 V, a specimen of tantalum attained temperatures of about 1500° C. The upper limit of temperature to be obtained by this method appears to be governed primarily by excessive contamination of specimen by evaporation of the filament material. By using thoriated tungsten with its lower work function, or carefully siting the filament, it shoul be possible to minimize contamination from this source.

Temperature measurement. A 0·010 in. Pt/Pt–13% R thermocouple is spot-welded to a small lug of the she containing the specimen. The leads are insulated with silic quills and mica spacers, and taken out of the camera throug glass-to-metal seals placed at the top of the camera in region not subjected to severe temperature variations, so th errors due to spurious e.m.f.'s are minimized. The thermo couple leads are over 10 cm long and give no appreciab resistance to movement of specimen.

Operation. The X-ray system is shown in Fig. 3. lithium fluoride curved crystal monochromator produces focused beam of MoKα radiation from a sealed-off X-ra

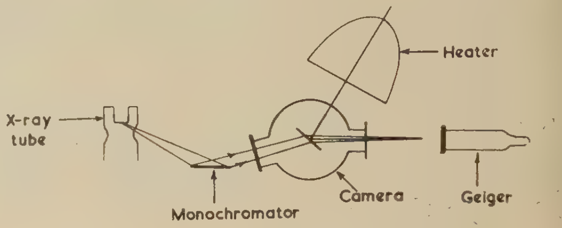

Fig. 3. Plan of camera and auxiliary equipment

tube. It may be remarked that a sealed-off tube is highl desirable for use with this type of camera since to attain th highest degree of vacuum, the camera is rigidly attached t the pumping system and therefore the X-ray source must b movable to permit alinement. Film or Geiger–Mülle counter recording is made at the exit window.

Applications

The camera has been used for studying the β (B.C.C.) t α (H.C.P.) phase transformation in Ti–Cr and Ti–Zr alloy Fig. 4(*a*) shows a film obtained from a single crystal c Ti 10 at.% Cr in the β field at 700° C. The specimen wa oscillated about the [001]β axis during the exposure. I Fig. 4(*b*) taken with the same specimen still within the camer but cooled to 20° C additional diffractions corresponding t the appearance of the α phase can be seen.

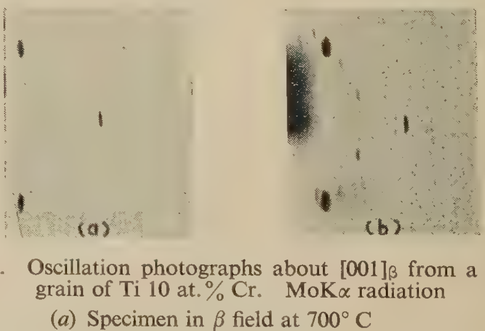

Fig. 4. Oscillation photographs about $[001]_\beta$ from a single grain of Ti 10 at.% Cr. MoKα radiation

(*a*) Specimen in β field at 700° C
(*b*) Specimen quenched from α + β field

It has been shown$^{(4)}$ that the orientation relationship o the β − α transformation in these alloys is

$$(110)_\beta//(0001)_\alpha$$
$$[111]_\beta//[11\bar{2}1]_\alpha$$

nsequently, when a single β grain transforms it gives rise twelve possible orientations of α. In order to determine relative amounts of phases present it is thus necessary record information from all these possible orientations. g. 5 shows a film obtained from a Ti 2 at.% Cr specimen enched from the $\alpha + \beta$ region. This was taken outside he camera in order to show the disposition of the diffractions vailable at the camera window whose equivalent position is dicated by the circle. The analysis of the diffractions merging is given in the table where θ is the Bragg angle nd η the angle through which the crystal must be rotated om that position where the [100]β direction is parallel to he incident beam in order for the appropriate plane to iffract. The orientations of α are labelled 1–12 and the ositions of the diffractions are given by *a*–*d*. Four of the orientations diffract to each of the *a* and *b* positions and wo to each *c* and *d* positions. The diffraction from the 200) plane of the β phase appears at *e*.

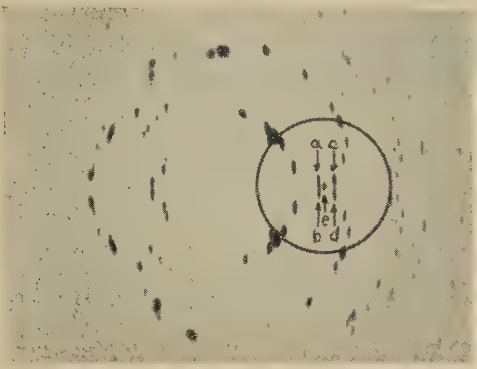

Fig. 5. Oscillation photographs taken outside the camera from a single grain of Ti 2 at.% Cr water-quenched from $\alpha + \beta$ field. Specimen oscillated about $[001]_\beta$ with $[100]_\beta$ oscillating between 0 and 15° with respect to direct beam. Equivalent position of X-ray window indicated by circle. MoKα monochromatic radiation

In the case of Ti 50 at.% Zr alloys the rates of decomposiion of the β phase on quenching to lower temperatures have een measured. A Geiger counter was used to record the ntensity of the $(200)_\beta$ diffraction. The family of curves btained on quenching to different temperatures is shown in ig. 6.

As a check on the amount of contamination introduced during a high temperature exposure a specimen of pure titanium was heated in the camera. The hardness figure of titanium is a sensitive index of the contamination introduced during the heating. For example, addition of 0·03 at.% oxygen increases the hardness by about 10 points. After 3 hours at 900° C the hardness increased from 69·3 V.P.N. to only 71·9 V.P.N. No significance is attached to this increase since it is of the same order as the experimental accuracy of such determinations. It was concluded that the contamination introduced during heating would not materially affect the transformations under investigation.

Crystallographic data for $(10\bar{1}2)_\alpha$, $(11\bar{2}0)_\alpha$ and $(200)_\beta$ diffractions emerging through camera window

hkl	α *Orientation*	*Diffraction*	η	2θ
$(10\bar{1}2)_\alpha$	1	*a*	7°	22°
	2	*b*		
$(10\bar{1}2)_\alpha$	3	*a*	7·5°	22°
	4	*b*		
$(11\bar{2}0)_\alpha$	5	*c*	8·2°	26°
	6	*d*		
$(200)_\beta$		*e*	11·0°	23°
$(10\bar{1}2)_\alpha$	7	*a*	13·5°	22°
	8	*b*		
$(10\bar{1}2)_\alpha$	9	*a*	14·0°	22°
	10	*b*		
$(11\bar{2}0)_\alpha$	11	*c*	16·0°	26°
	12	*d*		

It is interesting to note that despite the 12 possible orientations of α which can arise from a β grain, and the 6 orientations of β which can result from each of these α orientations, repeated thermal cycling through the $\beta - \alpha$ transformation does not break up the grain size; the original β grain reappears as do the relative amounts of α occurring on each orientation.

The above examples show how the camera can be used for determining phases present at temperature and their rate of transformation using single crystals and transmission X-ray methods. A similar experimental arrangement can be used for fine grained polycrystalline specimens. With specimens of greater X-ray absorption back reflexion or glancing angle techniques would be used with the camera windows suitably positioned.

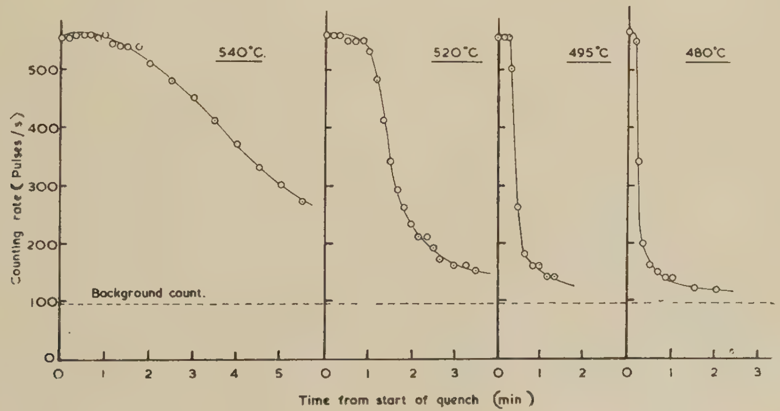

Fig. 6. Rate of decomposition of β phase in Ti 50 at.% Zr alloy when quenched from 580° C to various temperatures in the α field

Acknowledgements

Thanks are due to the Director of A.E.R.E. Harwell for permission to publish the results on Ti–Zr alloys and to Imperial Chemical Industries Ltd., Metals Division, for permission to publish the photographs obtained from Ti–Cr specimens.

Thanks are also due to Dr. M. Waldron and Mr. B. Butcher of Metallurgy Division A.E.R.E. for encouragement during development of the camera and to Mrs. M. K. McQuillan of Imperial Chemical Industries Ltd. for supplying specimens of pure titanium and titanium–chromium.

References

(1) Provan, A. G., Shaw, B. A., and Williams, G. I. *J. Sci. Instrum.*, **33**, p. 445 (1956).
(2) Kent, P. J. C. *J. Sci. Instrum.*, **34**, p. 72 (1957).
(3) Weisberg, L. R., and Gunther-Mohr, G. R. *Rev. Sci. Instrum.*, **26**, p. 896 (1955).
(4) Burgers, W. G. *Physica*, **1**, p. 561 (1934).

Sensitive and simple integrator

by J. P. FUNK, Dr.Phil., Commonwealth Scientific and Industrial Research Organization, Division of Meteorological Physics, Aspendale, Victoria, Australia

[*Paper received* 1 *March*, 1960]

Abstract

A sensitive and simple battery-operated current integrator is described. It uses as sensing element a standard millivoltmeter or microammeter, the pointer position of which is sampled at regular intervals by electromechanical means, the required movement of a feeler then being converted into rotation of a counter. The integrator accepts signals of varying polarity and also indicates the extreme signal level during any chosen period. It is particularly suited for the integration of quantities such as daily totals of net or global radiation.

Introduction

The need has long existed for a simple and sensitive means of integrating signals in the millivolt range, such as those obtained from net-radiometers or solarimeters. Without such aid the analysis of the records to give daily radiation amounts is very laborious, particularly so when broken cloud causes the radiation to fluctuate very widely. Some solutions to this problem are undesirably complex and expensive, e.g. the use of amplifiers and integrating motors and integrators attached to recording potentiometers.

An electromagnetic integrator of the Gilbert type$^{(1, 2)}$ did not prove entirely reliable in the above applications. (In this case the signals usually faded gradually to zero, thereby tending to leave the moving pointer at rest against one of the contacts without activation of the crossover circuit. This frequently prevented a future start of the armature even on reappearance of a strong input signal.)

The integrator described in the following was designed for simplicity, cheapness and to be suitable for use at places having no electricity supply. It was based on the well-known technique of periodically clamping a galvanometer pointer and detecting its position each time by bringing up a feeler, but was designed to be capable of accepting signals of reversible polarity. It has the further advantage of indicating the highest absolute signal level during any chosen time interval—an important quantity in radiation work and many other applications.

Integrator design and operation

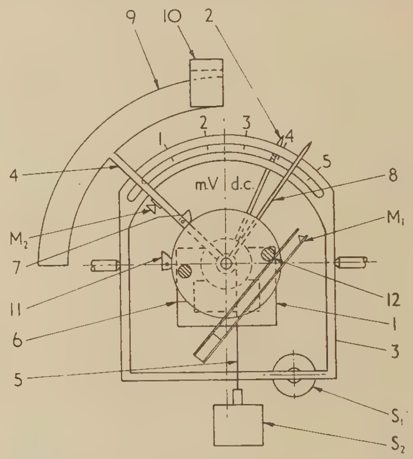

Fig. 1. General arrangement of integrator mechanism

The design and operation of the actual integrator mechanism is best understood by reference to Fig. 1. It consists of a standard moving coil galvanometer (1), the pointer (2) of which is clamped at fixed time intervals by means of a slotted clamping bar (3) activated by a solenoid (S_1). This type of clamping reduces strain on the pointer. While the galvanometer pointer is clamped, a spring-loaded feeler arm (4) is activated by another solenoid (S_2) through a fusee chain (5) and, from a position slightly on the negative side of the movement zero, moves up against the pointer, thus sampling its position. This sampling method is somewhat similar to that used in certain mechanical recording potentiometers. In moving up, the feeler arm also rotates a wheel (6) through a continuous ratchet$^{(3)}$ (7). Whenever the pointer deflexion exceeds the position of the freely movable maximum value indicator (8), the feeler arm also moves the latter to the new extreme deflexion.

The angle between the feeler zero and the pointer zero is made as nearly as possible equal to the backlash of the ratchet. Eddy current damping generated by an aluminium vane (9) and a magnet (10) is used to lessen the impact of the feeler arm. During the return of the feeler after each sampling, the wheel (6) maintains its position on account of another continuous ratchet (11). Twice per revolution of the wheel (6) the pins (12) close a contact (M_1) which activates a register. Clearly the number of turns of wheel (6) in time t is proportional to $\int_0^t idt$, where i is the input signal.

In order to integrate signals which may change sign, another contact (M_2) is provided, also activated by the feeler arm, and opened when the latter has progressed beyond a point slightly before the pointer zero position. If the input signal drives the pointer in a negative direction this contact remains closed and initiates a reversing mechanism, described later.

The full operation of the integrator, as seen from Fig. 2, is as follows. A timer closes contact M_3 (in the prototype for about 2 s every minute), thereby activating the clamping solenoid (S_1) as well as relay A, the latter through a delay network (R_1C_1). Relay A operates the feeler solenoid (S_2) and also causes a delayed pulsed action of relay B by means of R_2, C_2, R_3 and C_3; the discharge of C_3 through R_2 and relay B providing the pulse, whereas R_2 C_2 causes the delay. If the pointer deflexion is positive no further action takes place since M_2 is open. If the pointer deflexion becomes negative, contact M_2 stays closed and, after a delay, relay B operates the latching relay D, which reverses the polarity of the meter and also changes over the registers. The counts on the registers are thus proportional to the positive and to the negative parts of $\int_0^t idt$.

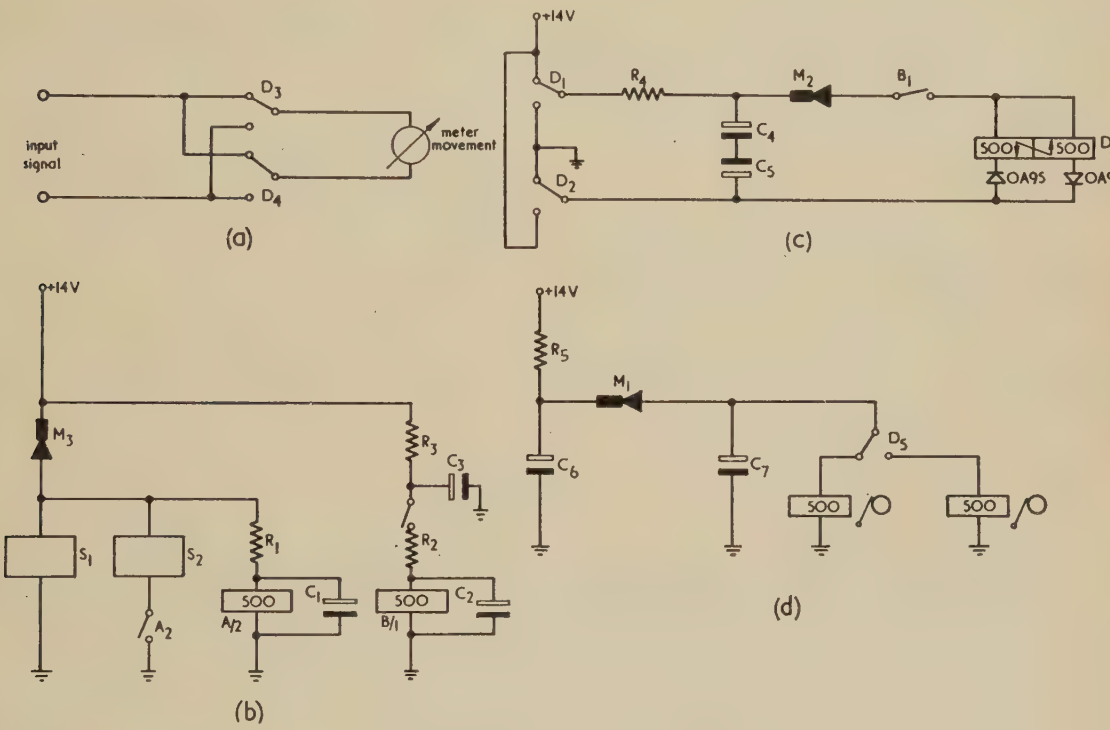

Fig. 2. Complete circuit of integrator

R_1, R_2 = 200 Ω
R_3 = 10 kΩ

R_4, R_5 = 5 kΩ

C_1, C_2 = 250 μF
C_3 = 1000 μF

C_4, C_5, C_6 = 500 μF
C_7 = 20 μF

The sequential operation of relays A and B is necessary in order that (a) the feeler should not operate before the pointer is clamped, and (b) the latching relay D should neither operate before the feeler has a chance to get away from its zero position, nor immediately after it has returned to zero at the end of the cycle. In cases of small deflexions the latter could cause a polarity reversal due to unwanted operation of relay D.

As can be seen from Fig. 2, battery drain has been minimized by operating most relays and all registers from capacitor discharges. The latching circuit [Fig. 2(b)] is very positive and does not require accurate relay adjustments.

Often integrated values are required for periods of time, at the beginning and end of which the registers cannot be read due to unavailability of personnel. Usually printing counters or photographic methods are used under such circumstances, but provided the number of periods is not too numerous a simple method can be used. For each period two pairs of registers (one pair if the input signal cannot change sign) are provided, each of them connected for the specified period on alternate days. Thus on each day the previous days' recordings can be read off at leisure.

In the particular case of net-radiation integration at Melbourne, two positive counters (daytime radiation) are required but only a single negative one (night time), since, negative signals only being observed at night, the night register can be read at any time during the day.

The sensitivity of the integrator can easily be made different for negative and positive signals by switching attenuators into the circuit. For unipolar operation a continuous mechanical counter directly driven by wheel (6) can be used.

Performance

Apart from sampling errors the accuracy of the integrator when used on unipolar signals is, as near as one can tell, equal to the accuracy of the galvanometer used, since the slight backlash of the ratchet is compensated by slightly offsetting the feeler zero with respect to the pointer zero.

When used with signals of reversible polarity, errors of two principal kinds may occur:

(i) since one ineffective sampling must take place while the meter polarity is being reversed, the corresponding rotation of wheel (6)—generally small—is lost;

(ii) on all reversals except those where wheel (6) is midway between activiations of M_1, an effective positive or negative error of up to one count (depending on the wheel position) will occur.

To minimize both effects and, in general, since the degree of fluctuation tolerable in the input signal is obviously limited by the sampling rate of the integrator, this rate must be made sufficiently high. If required, it could easily be made ten samples per minute or better. The effect of error (ii) alone can be reduced by increasing the number of counts per revolution of wheel (6).

If polarity changes are so frequent as to cause excessive error, two non-reversible integrators connected back to back, one integrating positive and the other negative signals, must be used.

Errors due to inaccurate location of the point of reversal can be made negligible. For the particular movement used in the prototype (7 mV, full-scale deflexion, 100 Ω) the reversing mechanism operates at an inverse voltage of only 20 μV.

Acknowledgement

The design owes much to discussions with many people of the Division of Meteorological Physics. Mr. G. Harris carried out the careful construction of the integrating mechanism.

References

(1) Gilbert, R. W. *Rev. Sci. Instrum.*, **18,** p. 328 (1947).

(2) Dyer, A. J. *J. Sci. Instrum.*, **35,** p. 240 (1958).

(3) Jones, D. J. *Ingenious Mechanisms for Designers and Inventors*, **1,** p. 49 (New York: The Industrial Press, 1948).

Accurate measurements of phase differences with the Babinet compensator

by P. HARIHARAN, Ph.D., A.Inst.P., and D. SEN, M.Sc., Ph.D., National Physical Laboratory of India, New Delhi, India

[*Paper received* 5 *January*, 1960]

Abstract

A considerable increase in accuracy is possible in measurements of phase differences with a Babinet compensator by reflecting the beams emerging from the compensator back through it. The first part of this paper deals with a new system of fringes produced in this fashion, in which the intensity distribution undergoes a periodic modulation as the path difference introduced by the compensator is varied, while the second section shows how the Babinet compensator can be converted into a uniform-field compensator by reflecting the beams emerging from the compensator back through it. By using a suitable half-shade device with such an arrangement, readings can be repeated to a few ten-thousandths of a wavelength.

Introduction

The Babinet compensator$^{(1, 2, 3)}$ is commonly used for measurements of the phase difference between the two components of an elliptically polarized beam of light, produced, for instance, by the introduction of a birefringent plate in a plane-polarized beam. This compensator, as is well known, consists of two right-angled quartz wedges, usually of equal angle, placed with their hypotenuse faces in contact, so that together they form a plane-parallel plate. These wedges are cut so that when they are mounted in the compensator, the optic axis of each wedge is parallel to its outer face, and the optic axes of the two wedges are at right-angles to one another. One of the wedges is stationary and has a reference mark engraved on it, while the other can be moved in a longitudinal direction by means of a micrometer screw, so as to vary the total thickness of the parallel plate formed by the two wedges.

In the normal method of use, the Babinet compensator is placed in azimuth $\pi/4$ between crossed polarizers. When illuminated with monochromatic light, a system of equally-spaced dark fringes is seen covering the field. The instrument is initially calibrated by noting the number of turns of the micrometer screw between settings of the reference mark on consecutive dark fringes, which corresponds to a phase difference of 2π. The crystal plate of unknown retardation is then introduced in azimuth $\pm\pi/4$. This results in a lateral displacement of the fringes which can be compensated for by an appropriate movement of the micrometer screw. From this, the value of the phase difference introduced by the plate can be calculated.

The accuracy with which measurements can be made with such a compensator therefore corresponds to the accuracy with which settings can be repeated on a given dark fringe. This is limited primarily by the $\sin^2$ intensity distribution in the fringes. Under normal conditions, settings can be repeated with an accuracy of the order of a hundredth of the spacing between fringes, i.e. $0{\cdot}01 \times 2\pi$, though better results are possible if advantage is taken of the subjective sharpening of the dark fringes resulting from very high field brightnesses.

A much higher accuracy is, however, possible when a photometric setting criterion is used, as in the various types of half-shade compensators described in the literature.[(3)] The present paper describes two methods by which such a criterion can be applied to the Babinet compensator. In these the beams emerging from the compensator are reflected back through it; this may be briefly termed "double-passing" the compensator. In the first method, a new system of fringes is formed in which the intensity distribution undergoes a periodic modulation as the phase difference between the beams is varied; in the second, the Babinet compensator is converted into a uniform-field compensator which can be used in conjunction with a suitable half-shade device.

Double-passed fringes

(*a*) *Experimental arrangement.* Fig. 1 is a schematic diagram of the optical system used for producing double-passed fringes in the Babinet compensator. The compensator, which is set in azimuth $\pi/4$ between the crossed polarizers P_1 and P_2, is illuminated with roughly parallel light from the collimator L_1. The beam of light emerging from the compensator is then reflected back through it once again by the lens L_2 and the plane mirror M_1 which is placed at its focus. The distance of L_2 and M_1 from the compensator is adjusted so that an inverted image of the compensator is formed in its own plane, as shown by the dotted lines in Fig. 1. This adjustment is not very critical and can easily be made with a sufficient degree of accuracy by checking that the fiducial mark engraved on the inner face of the fixed wedge is imaged on itself. The double-passed fringes are viewed by means of an auxiliary semi-reflecting mirror M_2 and a low-power telescope T which is focused on the compensator.

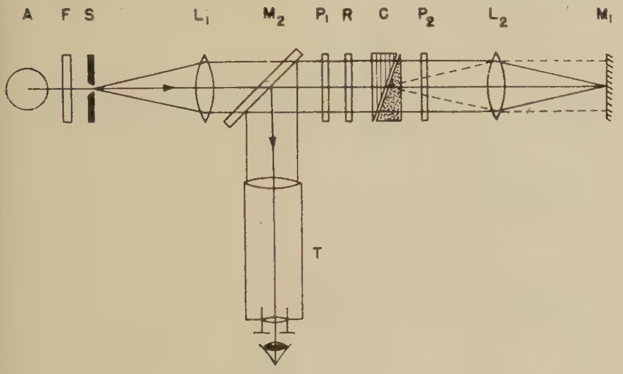

Fig. 1. Schematic diagram of the optical system used to produce double-passed fringes with the Babinet compensator

A, mercury arc lamp; *F*, green filter; *S*, slit; L_1, collimator lens; L_2, lens; P_1, P_2, polarizers; *R*, retarding plate; *C*, compensator; M_1, plane mirror; M_2, semi-reflecting mirror; *T*, low-power telescope

(*b*) *Theory.* One can assume for the purpose of deriving the theoretical intensity distribution in the fringes that the polarizer P_1 is in azimuth zero, the compensator in azimuth $\pi/4$ and the polarizer P_2 in azimuth $\pi/2$. Assume also that a crystal plate producing an unknown path difference r is introduced in azimuth $\pi/4$ at R, as shown in Fig. 1, between the polarizer P_1 and the compensator.

A ray polarized in the horizontal plane by P_1 and incident on the compensator in a section at a distance x from the axis of the optical system is then resolved, within the crystal plate as well as the compensator, into two rays having equal amplitudes but polarized in azimuths of $+\pi/4$ and $-\pi/4$ respectively. These travel with different velocities in the crystal plate as well as the two wedges, the total optical path difference Δ_1 introduced between the two rays being given by the relation

$$\Delta_1 = (t_1 - t_2 - 2\,x\,\theta)\,(\underset{o}{\mu} - \underset{e}{\mu}) + r \qquad (1)$$

where t_1 and t_2 are the thicknesses of the two wedges in the section containing the axis of the optical system, θ is the angle of the wedges, and $\underset{o}{\mu}$ and $\underset{e}{\mu}$ are the ordinary and extraordinary refractive indices of quartz.

The polarizer P_2 transmits only the vertical components of these two vibrations, giving a single plane-polarized vibration. Assuming that the transmission of the polarizers P_1, P_2 is 100% when they are set in the same azimuth, the complex amplitude of the resultant vibration, which is equal to the sum of the complex amplitudes of the resolved components of the two vibrations polarized in azimuths of $+\pi/4$ and $-\pi/4$ respectively, is given by the relation

$$A' = (A/2)\{1 - \exp - i(\phi + \delta - \psi)\} \qquad (2)$$

where A is the amplitude of the original incident beam,

$$\phi = (2\pi/\lambda)(t_1 - t_2)(\underset{o}{\mu} - \underset{e}{\mu}), \quad \delta = (2\pi/\lambda)r \quad \text{and}$$

$$\psi = (2\pi/\lambda)2\,x\,\theta(\underset{o}{\mu} - \underset{e}{\mu}).$$

When this ray is reflected back from the mirror M_1 and is incident on the compensator once again, it is resolved as before into two vibrations in azimuths $+\pi/4$ and $-\pi/4$. The path difference Δ_2 introduced by the wedges and the crystal plate between these two components on the return journey is given by the relation

$$\Delta_2 = (t_1 - t_2 + 2\,x\,\theta)(\underset{o}{\mu} - \underset{e}{\mu}) + r \qquad (3)$$

since the ray is now incident in a section at a distance $-x$ from the axis of the optical system.

The polarizer P_1 transmits only the horizontal components of these two vibrations, giving a single plane-polarized vibration. As before, the complex amplitude of the resultant vibration is equal to the sum of the complex amplitudes of the two resolved components and is given by the relation

$$\begin{aligned} A_x &= (A'/2)\{1 - \exp - i(\phi + \delta + \psi)\} \\ &= (A/4)\{1 - \exp - i(\phi + \delta - \psi)\} \\ &\qquad \{1 - \exp - i(\phi + \delta + \psi)\} \qquad (4) \end{aligned}$$

The corresponding value of the intensity I_x is obtained by multiplying A_x by its complex conjugate A_x^* and is given by the relation

$$\begin{aligned} I_x &= (A/4)\{1 - \exp - i(\phi + \delta - \psi)\} \\ &\qquad \{1 - \exp - i(\phi + \delta + \psi)\} \\ &\times (A/4)\{1 - \exp i(\phi + \delta - \psi)\} \\ &\qquad \{1 - \exp i(\phi + \delta + \psi)\} \\ &= I_0\{\cos(\phi + \delta) - \cos\psi\}^2 \qquad (5) \end{aligned}$$

where $I_0 = (A/4)^2$.

The interference pattern seen with the compensator under these conditions consists, as in the conventional Babinet compensator, of equally-spaced straight fringes which are located in the plane of the wedges. However, a change in the setting of the movable wedge now results, not in a shift of the fringes, but in a change in the intensity distribution.

This is easily seen from Fig. 2, which shows the fringe system for three different settings of the movable wedge corresponding to values of $(\phi + \delta)$ of $\pm 2n\pi$, $\pm(2n + 1)\pi/2$ and $\pm(2n + 1)\pi$, where n is an integer. The theoretical intensity distribution curves for these settings are shown in Fig. 3. When $(\phi + \delta) = 2n\pi$ or $(2n + 1)\pi$, alternate fringes in the pattern are suppressed, while when $(\phi + \delta) = (2n + 1)\pi/2$, all the fringes have the same intensity. At the latter point, a very small change in the position of the movable wedge results in an appreciable difference in brightness between adjacent fringes. Consequently, this criterion can be used as a sensitive photometric null-setting.

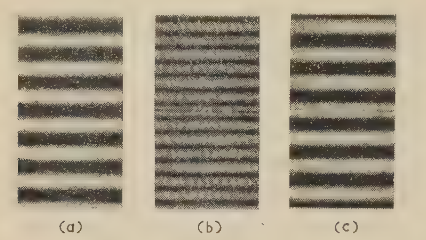

Fig. 2. Double-passed fringes obtained with the Babinet compensator for settings of the movable wedge corresponding to values of $(\phi + \delta)$ of (a) $2n\pi$, (b) $(2n + 1)\pi/2$, and (c) $(2n + 1)\pi$ respectively

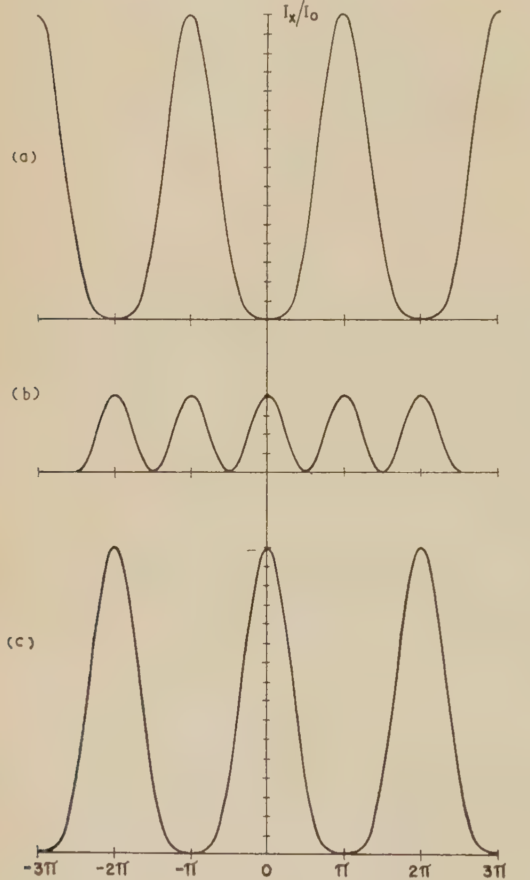

Fig. 3. Theoretical intensity distribution in the double-passed fringe system formed with the Babinet compensator for values of $(\phi + \delta)$ of (a) $2n\pi$, (b) $(2n + 1)\pi/2$, and (c) $(2n + 1)\pi$

(c) *Calibration and use.* The compensator is calibrated by noting the readings of the micrometer screw for several successive settings for equality of illumination of adjacent fringes. The difference in these readings gives the change in the reading of the micrometer screw corresponding to a change in the value of ϕ of π.

To use the compensator, it is first set so that the intensity of adjacent fringes is the same, and the reading of the micrometer screw is noted. The corresponding value of ϕ is then defined by the equation

$$\phi_0 = (2n + 1)\pi/2 \tag{6}$$

The crystal plate is then introduced in azimuth $\pi/4$, between the polarizer P_1 and the compensator as shown in Fig. 1, and the movable wedge is adjusted so that the adjacent fringes are once again equally bright. The phase difference ϕ_1 corresponding to the final reading of the micrometer screw is then defined by the equation

$$\phi_1 + \delta = (2n + 1)\pi/2 \tag{7}$$

so that the phase difference δ introduced by the crystal plate is given by the relation

$$\delta = \phi_0 - \phi_1 \tag{8}$$

(d) *Sensitivity.* The accuracy with which the setting for equality of illumination of adjacent fringes can be made is obviously proportional to the relative difference in intensity $(\Delta I/I)$ of adjacent fringes, caused by a small change $\Delta\phi$ in the phase difference introduced by the compensator from the true null-setting. It can be shown from equation (5) that this is given to a first approximation by the relation

$$(\Delta I/I) = 4\Delta\phi \tag{9}$$

It is fairly obvious that the photometric setting is rather unfavourable in the present case, as the fringes to be compared are separated by a darker region. However, a relative difference in intensity of about 5% may be taken as the discernible minimum.(4, 5) This would correspond to an accuracy in the measurement of ϕ of $0{\cdot}002 \times 2\pi$. In practice, settings can be repeated with an accuracy slightly better than this, without much difficulty.

Uniform-field compensator

(a) *Experimental arrangement.* The optical system which is used for converting the Babinet compensator into a uniform-field compensator is similar to that used to produce the double-passed fringes, and is shown schematically in Fig. 4. Parallel light from the collimator L_1, polarized in

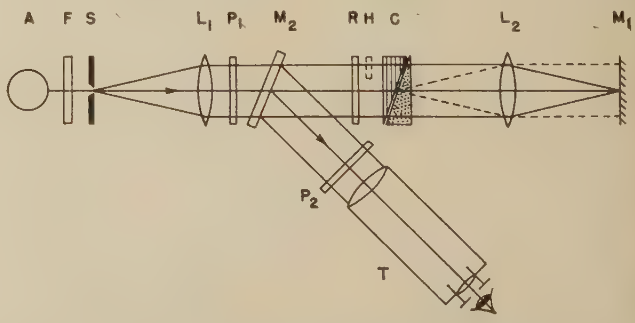

Fig. 4. Schematic diagram of the optical system used to convert the Babinet compensator into a uniform-field compensator

A, mercury arc lamp; F, green filter; S, slit; L_1, collimator lens; L_2, lens; P_1, P_2, polarizers; R, retarding plate; H, half-shade plate; C, compensator; M_1, plane mirror; M_2, semi-reflecting mirror; T, low-power telescope

azimuth zero by the polarizer P_1, is incident on the compensator which is in azimuth $\pi/4$. The beam of light emerging from the compensator is reflected back through it once again by the combination of the lens L_2 and the plane mirror M_1 placed at its focus. The distance of this combination from the compensator is adjusted, as before, so that an inverted image of the compensator is formed in its own plane. The beam returning back through the compensator is reflected to one side by means of the semi-reflecting mirror M_2 and is received in a low-power telescope T which is focused on the compensator. The polarizer P_2 is set in azimuth $\pi/2$, so that, in the absence of the compensator, no light is transmitted. (To ensure complete extinction with the compensator, the residual ellipticity introduced by the reflexion at M_2 for a ray polarized in azimuth $\pm\pi/4$ must be negligibly small. This can be ensured by using a plate coated with a $\lambda/4$ thick dielectric film of high refractive index for the semi-reflecting mirror M_2, and by keeping the angles of incidence and reflexion at it as small as possible.)

(*b*) *Theory*. It is assumed, as before, that a crystal plate producing a path retardation r is introduced in azimuth $\pi/4$ between the polarizer P_1 and the compensator (see Fig. 4). A ray polarized in azimuth zero by P_1 and incident on the compensator in a section at a distance x from the axis of the optical system is then resolved into two rays having equal amplitudes, but polarized in azimuths $+\pi/4$ and $-\pi/4$ respectively, which travel with different velocities in the crystal plate as well as in the wedges of the compensator. These rays, when reflected back by the plane mirror M_1, return through the compensator in a section at a distance $-x$ from the axis of the optical system. From equations (1) and (3) it is then easily seen that the total optical path difference Δ between these two rays is given by the relation

$$\Delta = \Delta_1 + \Delta_2 = 2(t_1 - t_2)(\mu_o - \mu_e) + 2r \qquad (10)$$

Since this expression does not involve x, it follows that the retardation introduced is the same in all sections, and the field is uniform. With the polarizer P_2 set in azimuth $\pi/2$, the field will be dark when the phase difference between the two beams, $(2\pi/\lambda)\Delta = 2(\phi + \delta) = 2n\pi$, and bright when $(2\pi/\lambda)\Delta = 2(\phi + \delta) = (2n + 1)\pi$, where n is any integer.

(*c*) *Calibration and use*. The uniform field compensator is calibrated by noting the readings of the micrometer screw for several successive settings yielding complete darkness of the field. The difference in these readings gives the change in the reading of the micrometer screw, corresponding to a change in the value of ϕ of π.

To use the compensator, it is first set so that the field is completely dark, and the reading of the micrometer screw is noted. The value of ϕ corresponding to this setting is defined by the relation

$$2\phi_0 = 2n\pi \qquad (11)$$

The crystal plate is then introduced in azimuth $\pi/4$ between the polarizer P_1 and the compensator, as shown in Fig. 3, and the movable wedge is adjusted so that the field is completely dark. The value of ϕ corresponding to this setting is then defined by the equation

$$2(\phi_1 + \delta) = 2n\pi \qquad (12)$$

so that the phase difference δ introduced by the crystal plate is given, as before, by the relation

$$\delta = \phi_0 - \phi_1 \qquad (13)$$

(*d*) *Sensitivity*. The sensitivity of the Babinet compensator when used as a uniform field compensator, as described above, is not very high, partly because the eye cannot judge a minimum of intensity very accurately, and partly because the intensity minimum itself is quite broad. A considerable increase in sensitivity can, however, be obtained by using a suitable half-shade device. The most convenient one is one due originally to Szivessy⁽²⁾ and consists of a plane-parallel plate of muscovite mica covering part of the field. This plate is introduced at H as shown in Fig. 4 and covers about one-third of the field. (The appearance of the photometric field is then similar to that in a triple-shade polarimeter, since beams which are passing through the centre of the field do not pass through the half-shade plate, while beams passing through both edges of the field pass through it once.) The theory of such a half-shade device has been discussed in detail by Jerrard,⁽⁶⁾ who has shown that a plate with a retardation of about $\pi/5$, placed in an azimuth giving a suitable low brightness of the test fields at the matching point, is most satisfactory. With such a half-shade device, readings can be easily repeated to a few ten-thousandths of a wavelength. This limit is of the same order as that set by mechanical imperfections of the compensator.

(*e*) *Discussion*. The set-up described has two theoretical advantages. In the first instance, since the beam traverses the crystal plate twice, the theoretical sensitivity should be twice that of a conventional uniform-field compensator, such as the Soleil compensator. Secondly, in this arrangement, one has a uniform-field compensator which can be considered as being formed by the Babinet compensator and its inverted image. Consequently, a uniform field will be obtained even if the angles of the two wedges in the original Babinet compensator are not strictly equal. It is only essential that the two wedges in the Babinet compensator should be set with their optic axes at right angles, an adjustment which can be performed fairly easily by examining the compensator between crossed polarizers.⁽⁷⁾ Because of this, it is possible to realize a fairly good uniform-field compensator even with a comparatively inexpensive Babinet compensator.

Conclusion

The two methods described in the present paper permit a considerable improvement in the accuracy of measurements with the Babinet compensator. Of the two, the uniform-field technique is capable of greater accuracy and can be conveniently utilized for such purposes as the precise calibration of retarding plates in the laboratory.

Acknowledgement

The authors wish to thank the Director, National Physical Laboratory of India, for permission to publish this paper.

References

(1) Bravais, A. *C.R. Acad. Sci.* (*Paris*), **32**, p. 115 (1851).

(2) Szivessy, G. *Z. Phys.*, **29**, p. 372 (1924).

(3) Jerrard, H. G. *J. Opt. Soc. Amer.*, **38**, p. 35 (1948).

(4) Zernike, F. *J. Opt. Soc. Amer.*, **40**, p. 326 (1950).

(5) Hariharan, P., and Sen, D. *J. Sci. Instrum.*, **36**, p. 70 (1959).

(6) Jerrard, H. G. *J. Sci. Instrum.*, **28**, p. 10 (1951).

(7) Jerrard, H. G. *J. Sci. Instrum.*, **26**, p. 353 (1949); **27**, p. 62 (1950).

Some modifications to an oscilloscope camera, and the construction of a control unit

by M. H. EVANS, Ph.D.,* and G. PIERSON, Medical Research Council, Institute of Orthopædics, Brockley Hill, Stanmore, Middlesex

[*Paper first received* 4 *January, and in final form* 7 *March,* 1960]

Abstract

A Langham-Thompson series 200 *camera has been modified to provide facilities for printing frame numbers along the edge of the photographic film, and to give warning when the supply of film is exhausted. The camera is used in conjunction with a control circuit that can provide either fully automatic operation or photography of single sweeps that have been preselected manually.*

Modifications to standard camera

As the camera is always used with the shutter open, the shutter closing spring is disconnected, and the shutter is prevented from closing by altering the position of the beam switch operating cam. The beam switch is no longer needed, so its connexions to the wander plug sockets on the camera body are broken.

A Unitor eight-pole fixed plug (by Belling-Lee Ltd.) is mounted on the underside of the camera body at the feed end, so that connexions to the control unit can be made. The frame feed switch is connected in parallel with pins 1 and 4 on the plug, *via* the tag board in the camera. Pins 7 and 8 are connected to two of the wander plug sockets on the camera body to carry the supply for the printing lamp of the numbering mechanism. Pins 5 and 6 are used to carry the 15 V supply to the end-of-film warning microswitch.

End-of-film warning

A Honeywell type V4–14 microswitch is mounted in the camera at the feed end, behind the film gate. The switch is held in the "off" position by a lever, which rests on the film where it runs between the feed cassette and the gate. The lever is arranged to touch the film just below the upper row of perforations, so that should any scratches be produced by the lever, they will not interfere with the records. Leads are taken from the microswitch to pins 5 and 6 on the control unit connecting plug P_1. When the film runs out, the switch closes and operates a warning light and a buzzer in the control unit.

Frame numbering mechanism (Fig. 1)

Operation. In the numbering mechanism, two counters are driven from an extension of the frame feed switch operating shaft, which revolves once for each frame. One counter *C* is mounted beneath the camera and gives a visual indication of the frame number. The second counter, which is synchronized with the first one, is mounted in the light-tight box *E* screwed to the underside of the camera hood *F* near the oscilloscope end. A right-angle prism is mounted in this box in front of the counter and a lamp (8 V, 0·2 A) is arranged to illuminate the figures when it is required to print the number on the film. The image of the figures is reflected upwards by the prism, through a rectangular hole cut in the camera hood, on to a second prism, mounted so that it projects about one inch inside the hood and reflects the image of the figures through the camera lens on to the film. Both the oscilloscope screen and the frame number must be in focus on the film; therefore the prisms and counter are arranged so that the length of the light path from counter to lens is equal to that from the oscilloscope screen to the lens.

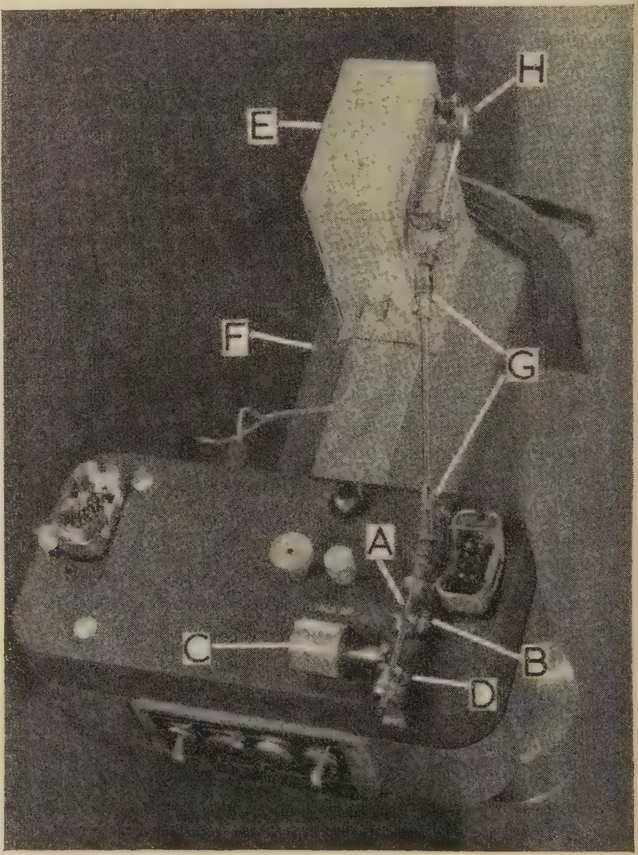

Fig. 1. Underside of modified camera

---

* Now at National Institute for Medical Research, Mill Hill, London, N.W.7.

A mechanical counter drive was used in preference to an lectro-mechanical system, as the magnetic fields generated by some electro-mechanical counters cause serious interference with high-sensitivity electro-physiological recordings.

Construction. The existing frame feed switch drive-shaft is eplaced by a longer shaft that extends through a hole cut n the bottom of the camera casing. A short transverse shaft A is mounted in Oilite bushes (by the Manganese Bronze and Brass Co. Ltd.) on brackets beneath the camera and connected to the drive shaft by a pair of bevel gears B (by Bonds O'Euston Rd. Ltd.). One end of this transverse shaft drives the external counter C through another pair of bevel gears D. The other end of the shaft drives the second counter (inside the light-tight box E) through a pair of universal couplings G and a pair of bevel gears H.

In order to facilitate servicing, the hole for the drive shaft in the bottom cover of the camera is made large enough to allow the bevel gear to pass through. The two long cover retaining screws at the "take-up" end are replaced by studs and nuts. The cover can thus be removed without disturbing the gearing.

The two prisms are mounted on a sub-frame within the light-tight box E. The lower prism is initially provided with a vertical adjustment to enable the image of the figures to be focused on the film. When this has been done the prism is permanently locked in position. The upper prism is made to tilt, so that minor alterations to the position of the number on the film can be made.

The supply for the printing lamp is brought from the camera control unit through pins 7 and 8 of the Unitor plug and socket to the wander plug sockets on the camera body, and from there into the light-tight box through miniature plugs and sockets (by Oxley Developments Ltd.).

Camera control unit

The camera control circuits are required to operate the modified Langham–Thompson camera in conjunction with a Nagard DT103 oscilloscope. Two alternative modes of operation are necessary; either automatic, photographing each consecutive sweep of the oscilloscope, or manual, when a single sweep can be preselected and photographed. In either case, the control unit has to perform an operation cycle as follows:

(i) at the start of the sweep the Nagard oscilloscope spot is brightened by changing a potential applied to the external beam brightening socket from +105 V to 0 V;
(ii) at the end of the sweep the +105 V beam blanking potential is restored;
(iii) at the end of the sweep, a lamp in a light-tight box (Fig. 1, E) is flashed for about 0·5 s to print the number on the edge of the exposed frame;
(iv) the camera motor operates for about 3 s to wind on the film to the next frame.

To provide sufficiently rapid spot-brightening and blanking, an electronic switch of the bistable multivibrator type (Eccles–Jordan trigger) is used, and this switch also enables the circuit to be built with some interlocking between the various stages in the operation cycle. The frame-numbering lamp and camera motor are controlled by relays in conventional unistable multivibrators ("flip-flops"), and a Schmitt trigger is used to provide sharp pulses from the oscilloscope flyback.

The method of operation is described below. When the apparatus is switched on and the valves have warmed up, the 5 kΩ relays A and B (Fig. 2) are energized because they are in the normally conducting halves of the flip-flops V_3 and V_4. Consequently when the apparatus is switched on and passive, the contacts of the relays A and B are in the opposite positions to those shown in Fig. 2, $A1$ and $B1$ being closed, while $A2$, $B2$ and $B3$ are open. With the automatic/manual selector switch S_3 in the automatic position as shown in the circuit, the 75 Ω relay C cannot be energized at any time and its contacts will remain as shown.

Automatic operation. The oscilloscope sweep is initiated by an external triggering pulse, and a coincident negative trigger pulse of about −40 V peak amplitude and 100 μs duration initiates the operation of the camera control unit. This negative trigger pulse is fed into P_2, through relay contacts $C1$, $A1$ and $B1$, and capacitor C_9, and trips "on" the bistable multivibrator V_2. The voltage of the left-hand anode in V_2 falls and can be set to 0 V by adjusting the 10 kΩ variable resistor RV_2. This anode potential is taken from P_3 to the external beam brightening input of the Nagard oscilloscope and brightens the spot for photographing the sweep.

The oscilloscope time-base going positive from about +150 to +280 V, is taken through P_4 and R_7 to the Schmitt trigger V_1, "cocking" it during the sweep and "firing" it during the flyback. The trigger output from R_{10} is differentiated by C_6 and $R_{14} + R_{15}$, the positive "cocking" pulse is clipped by MR_6 and the negative flyback pulse is fed through C_7 to trip "off" the bistable multivibrator V_2. This blanks the oscilloscope beam by restoring the potential of about +105 V at the left-hand anode of V_2, and a differentiated positive pulse from this potential is fed from R_{20}, *via* C_8 and MR_8, to trigger the flip-flop V_3, and relay A is operated (de-energized) for about 0·5 s. Contact $A1$ opens to prevent any trigger pulse from brightening the oscilloscope beam during this stage of the cycle, while $A2$ closes to illuminate the frame-numbering counter with a lamp (8 V, 0·2 A), connected through pins 7 and 8 of the Unitor eight-pole plug P_1. The brightness of this lamp is controlled by the 100 Ω variable resistor RV_1, and monitored by the panel lamp PL_3. Switch S_2 is spring loaded to "off", and can be pressed to check the functioning of this illumination circuit. Relay contacts $A3$ provide a changeover 15 V signal that can be used as an "end of sweep" event marker when ancillary apparatus is being used.

When the flip-flop V_3 reverts to the passive state, a positive pulse is taken from R_{26} through C_{11} and MR_9 to trigger the flip-flop V_4 and operate (de-energize) relay B for about 2·5 s. Contact $B1$ opens, taking over from $A1$ the function of keeping V_2 paralysed during the camera cycle. Contact $B2$ closes and starts the Langham–Thompson camera by closing a circuit connected in parallel with the camera's single frame feed switch, *via* pins 1 and 4 of plug P_1. When the camera is driven by a 1500 rev/min motor, frame transport takes about 3 s. It is only necessary to close the single-frame feed circuit for about 1 s, as a microswitch in the camera controls the completion of the operation. However, the flip-flop V_4 was designed to operate for 2·5 s in order to maintain $B1$ open until film transport was almost completed.

As soon as relay B is re-energized and $B1$ closes, the control unit is then ready for another cycle of operation. With the 1500 rev/min motor and flip-flop durations as given, sweeps can be photographed automatically every 3 to 4 s.

Manual operation. With S_3 in the manual position, relay C will be energized through contact $B3$ (either on switching on, or during a previous cycle of automatic operation). Contact $C4$ will hold relay C energized through R_4, and in this condition *C*1 will earth the negative-trigger input to V_2 and *C*2 will earth the grid of the Schmitt trigger valve V_1. The control circuit is then paralysed and, although the oscilloscope time-base may be triggered, the sweeps are not photographed.

When one wishes to photograph a sweep, the manual button (either S_4 or the remote control extension S_5) is momentarily pressed to de-energize relay *C* by breaking its earth return. Contacts *C*1 to *C*4 return to the positions shown in Fig. 2. The next sweep-triggering pulse will trip V_2 and an operational cycle will commence as described above. As relay *B* operates, relay *C* will re-energize through contact *B*3, and upon completion of the cycle the apparatus will revert to the "waiting" conditions until the manual button is again pressed. It should be noted that even if the manual button is pressed during the latter part of a sweep, the oscilloscope spot will not brighten until the beginning of the next sweep, as V_2 can only be tripped "on" by a negative time-base trigger pulse arriving when contacts *C*1, *A*1 and *B*1 are all closed.

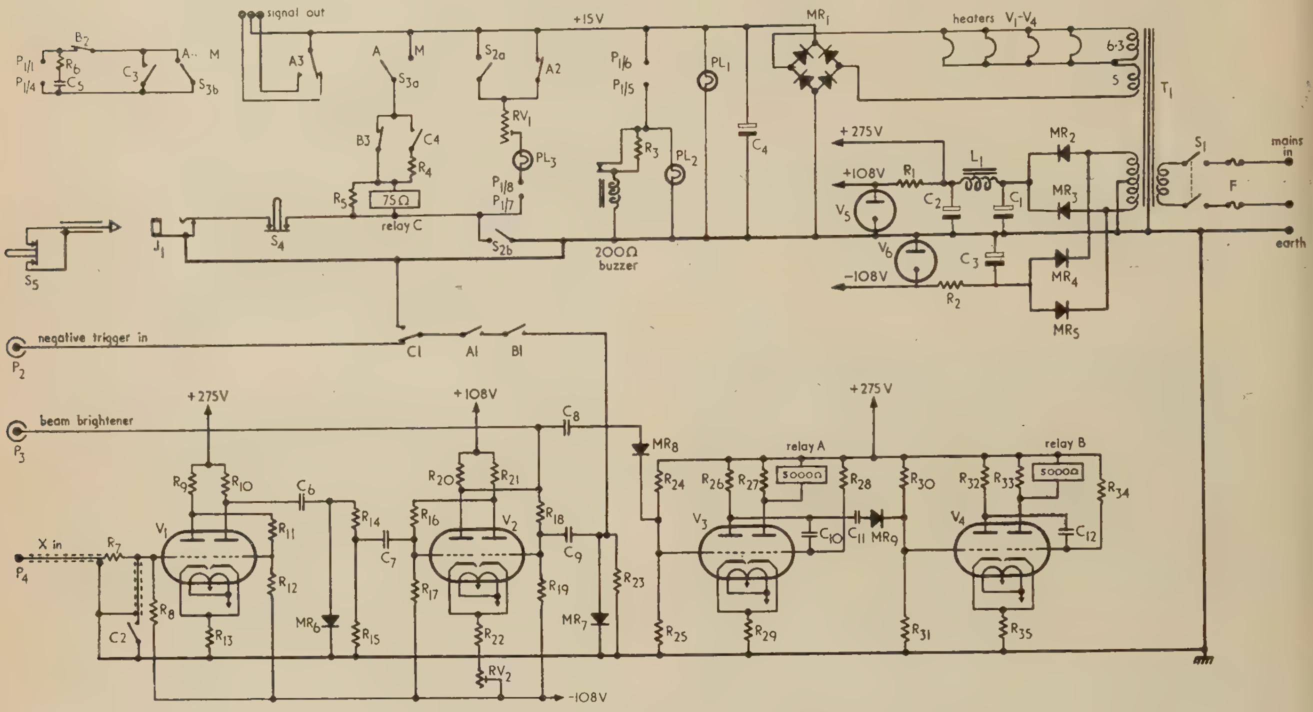
signal out
+15V
MR1
heaters V1-V4
6·3
5
T1
B7
R6
C5
P1/1
P1/4
C3
A
M
S3b
A3
S3a
S2a
A2
RV1
PL3
P1/6
P1/5
PL1
C4
B3
C4
R4
R5
75Ω
relay C
P1/8
P1/7
R3
PL2
+275V
MR2
S1
mains in
+108V
R1
L1
C2
C1
MR3
F
V5
S5
J1
S4
S2b
200Ω buzzer
V6
C3
earth
-108V
R2
MR4
MR5
negative trigger in
P2
C1
A1
B1
+275V
+108V
+275V
beam brightener
P3
C8
MR8
relay A
5000Ω
relay B
5000Ω
R9
R10
C6
R20
R21
R24
R26
R27
R28
R30
R32
R33
R34
V1
R11
R14
R16
V2
R18
V3
C10
C11
MR9
V4
C12
X in
R7
C7
C9
P4
R12
R17
R19
R23
R8
MR6
MR7
C2
R13
R15
R22
R25
R29
R31
R35
RV2
-108V

Fig. 2. Circuit diagram of camera control unit

All fixed resistors are ½ W ± 10% unless otherwise stated. High stability (h.s.) resistors are all ½ W ± 5%

R_1, R_2 = 12 kΩ, 5 W
R_3 = 10 kΩ
R_4 = 33 Ω, 1 W
R_5, R_6 = 270 Ω
R_7 = 2 MΩ h.s.
R_8 = 1 MΩ h.s.
R_9 = 47 kΩ. 1 W
R_{10} = 27 kΩ, 1 W
R_{11} = 1·5 MΩ h.s.
R_{12} = 1 MΩ h.s.
R_{13} = 6·8 kΩ, 1 W
R_{14}, R_{15} = 1 MΩ
R_{16} = 1·5 MΩ h.s.
R_{17} = 510 kΩ h.s.
R_{18} = 1·5 MΩ h.s.
R_{19} = 510 kΩ h.s.
R_{20}, R_{21} = 18 kΩ, 1 W
R_{22} = 2·2 kΩ
R_{23} = 1 MΩ
R_{24} = 560 kΩ
R_{25} = 150 kΩ
R_{26} = 47 kΩ, 1 W
R_{27} = 22 kΩ
R_{28} = 2·2 MΩ h.s.

R_{29} = 6·8 kΩ, 1 W
R_{30} = 560 kΩ
R_{31} = 150 kΩ
R_{32} = 47 kΩ, 1 W
R_{33} = 22 kΩ
R_{34} = 2·7 MΩ h.s.
R_{35} = 6·8 kΩ, 1 W

RV_1 = 100Ω, 5 W
RV_2 = 10 kΩ, 1 W

C_1 = 16 μF, 350 V
C_2 = 32 μF, 350 V
C_3 = 16 μF, 450 V
C_4 = 500 μF, 25 V
C_5 = 0·1 μF, 1000 V
C_6 = 500 pF, 500 V
C_7, C_8 = 220 pF, 500 V
C_9 = 100 pF, 500 V
C_{10} = 0·5 μF, 1000 V
C_{11} = 100 pF, 500 V
C_{12} = 2 μF, 600 V

L_1 = 10 H, 60 mA smoothing choke

V_1–V_4 = ECC 82
V_5, V_6 = 108 Cl

F = 1 A fuse

J_1 = Break circuit jack socket

MR_1 = 12 V, 3 A bridge rectifier
MR_2, MR_3 = 250 V, 60 mA rectifier
MR_4, MR_5 = 250 V, 20 mA rectifier
MR_6–MR_9 = OA81 diode

PL_1 = 16 V, 0·2 A green
PL_2 = 16 V, 0·2 A red
PL_3 = 8 V, 0·2 A colourless

P_1 = 8-pole connector
P_2, P_3 = coaxial sockets
P_4 = screw terminal 4 B.A.

T_1 = 250–0–250 V, 80 mA, 6·3 V, 4 A, 5 V, 2·5 A. Mains transformer

Relay *A* = type P.O. 3000, 5 kΩ. *A*1, light-duty make; *A*2, heavy-duty (2*A*) break; *A*3, light-duty changeover
Relay *B* = type P.O. 3000, 5 kΩ. B_1, light-duty make; B_2, heavy-duty break; B_3, heavy-duty break
Relay *C* = type P.O. 3000, 75 Ω. C_1, light-duty changeover; C_2, light-duty make; C_3, heavy-duty make; C_4, heavy-duty make

S_1 = double-pole, single-throw "on/off"
S_2 = double-pole, single-throw spring-loaded off. "Press to test"
S_3 = double-pole, double-throw "automatic/manual operation"
S_4, S_5 = single-pole, single-throw, press button switches, spring-loaded on, "manual control"

Superimposed sweeps. By holding the manual buttons S_4 or S_5 pressed, with S_3 at "manual", the earth returns of both the counter illumination and relay *C* are broken. Neither the frame-numbering flash nor the frame feed circuits can operate for as long as the manual button is pressed, and successive sweeps of the oscilloscope will be superimposed upon the same frame of film. This is a technique frequently used in biological research, but it should be noted that as relays *A* and *B* will continue to operate at the end of every sweep, the time-base repetition rate must not be faster than about 1 in 3 s. If it is desired to superimpose sweeps at a higher repetition rate, an additional switch will have to be incorporated to hold the flip-flop circuits paralysed during the opening of S_4 or S_5.

Temperature regulator for close temperature control

By E. N. HERZBERG, E.M.E., M.Sc., Ministry of Defence, Scientific Department, Hakiya,
Tel Aviv, Israel

[*Paper first received* 18 *September*, 1959, *and in final form* 4 *March*, 1960]

Abstract

The design and performance of an electronic temperature regulator for an analytical oven of special construction is described. Stable temperature control with a resettability of better than 1 *deg C is obtained over the range of* 150–550° *C. Residual peak-to-peak temperature fluctuations in the oven are less than* 0·015 *deg C.*

Introduction

THE instrument described was designed to guarantee a temperature constancy of ±0·02 deg C in an oven over the range of 150–550° C. Such instruments are not readily available, because close control is seldom attained over a wide temperature range exceeding temperatures of about 350 or 400° C. Most instruments hitherto described in literature were either not suitable for the above requirement, or were rather elaborate.

In the development of the regulator, it was considered desirable to avoid the use of moving elements or, as far as possible, of materials and components not readily available. A saturable reactor was chosen as the output element in preference to thyratrons or relays. The instrument has already proved its worth, being in unattended daily use for nearly a year.

The primary requirement was the temperature regulation of a glass tube 16 mm in diameter, which forms a part of an intricate vacuum system. The external dimensions of the oven are only 24 × 23 × 31 cm, and the weight is 17 kg. The temperature-equalizing mass is a brass cylinder 2·5 kg in weight which fits into a brass tube carrying the heater element.

The instrument described maintains close temperature control over the range 150–550° C, limiting peak-to-peak fluctuations in the specially constructed oven to less than 0·015 deg C. The presetting of the temperature is performed by a simple panel control with a resettability of better than ±1 deg C. After thermal equilibrium has been reached, temperature drifts in the oven do not exceed 0·015 deg C, even for long runs. Temperature overshoots occurring after any resetting of the temperature are usually less than ±0·5 deg C, and are quickly damped out.

Intimate thermal contact between the heater element and the brass cylinder, a short time-constant of the temperature-sensing element, the large mass of the cylinder, and good thermal insulation are all essential for optimum temperature regulation. It was necessary to construct a special platinum resistance thermometer as the sensing element.

The control characteristic of the regulator ensures close regulation by proportional control for small temperature deviations, and rapid heating by a control similar to "on–off" for the initial warming-up period. Power consumption of the regulator proper is only 65 W. No voltage-stabilizing element is necessary in the supply to the oven, because compensation against line variations is automatically given by the control action of the regulator.

Block diagram and general circuit description

The block schematic diagram is shown in Fig. 1, and the detailed circuit diagram in Fig. 2. The temperature-sensitive element R_1 in Fig. 2 constitutes one arm of a Wheatstone fed from an a.c. supply. The balance point of the bridge is preset by a 10-turn helical potentiometer P_1 equipped with a multi-turn dial. The error voltage of the bridge is amplified and detected by a phase-sensitive detector V_5. The detector output governs the control tube V_6, which supplies the control current of the saturable reactor T_3. The a.c. windings of the saturable reactor regulate the current through the heating element in the oven.

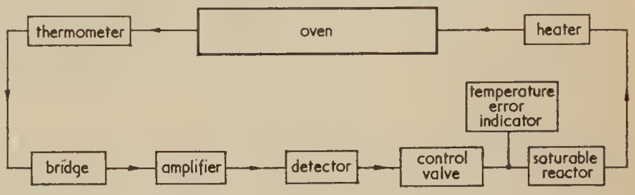

Fig. 1. Block schematic diagram

Description of main circuit elements

Thermometer. The thermometer is the most critical part of the instrument, and the behaviour of the whole system depends to a great extent on its design. The type of the thermometer and the physical phenomena on which it is based determine the characteristics of the associated electronic control equipment.

The advantages and disadvantages of the most widely used types of thermometer are:

(*a*) Thermocouples require a stable high-gain d.c. amplifier(1) and the preservation of the "cold junction" at a standard reference temperature.

(*b*) Thermistors can only be used up to 400° C, but they have high temperature sensitivities.(2–4)

(*c*) Resistance thermometers have characteristics which depend on the material used. The properties of platinum are outstanding and consequently only the use of this metal is considered. Resistance thermometers using this material have long-term stability and can be used without difficulty up to 550–600° C (at higher temperatures, crystallization may set in).

In the absence of information concerning the availability of a suitable commercial thermometer designed for control purposes, it was decided to design one. The value of the resistance must be a compromise between the large values which permit the effective utilization of the reference potentiometer and the mechanical limitations of the thermometer pocket. A platinum wire having a diameter of 0·12 mm (Reference Grade) was selected. This is wound over a thin mica card *A* (Fig. 3). The thermometer, insulated by further mica cards, is clamped tightly by segment *B* to the brass cylinder *C*. This ensures good thermal contact and hence a short time constant of the thermometer. Thermometer resistance R_1 at room temperature is 34·5 Ω. Connexion to the thermometer is made *via* the microphone connector *E* which is held by a stainless-steel tube *D*, 20 cm long, equipped with five cooling fins. The temperature at the far end of the steel tube never exceeds 50° C, even at oven temperatures of 550° C. The thermometer has been aged at 600° C for several hours prior to calibration and use.

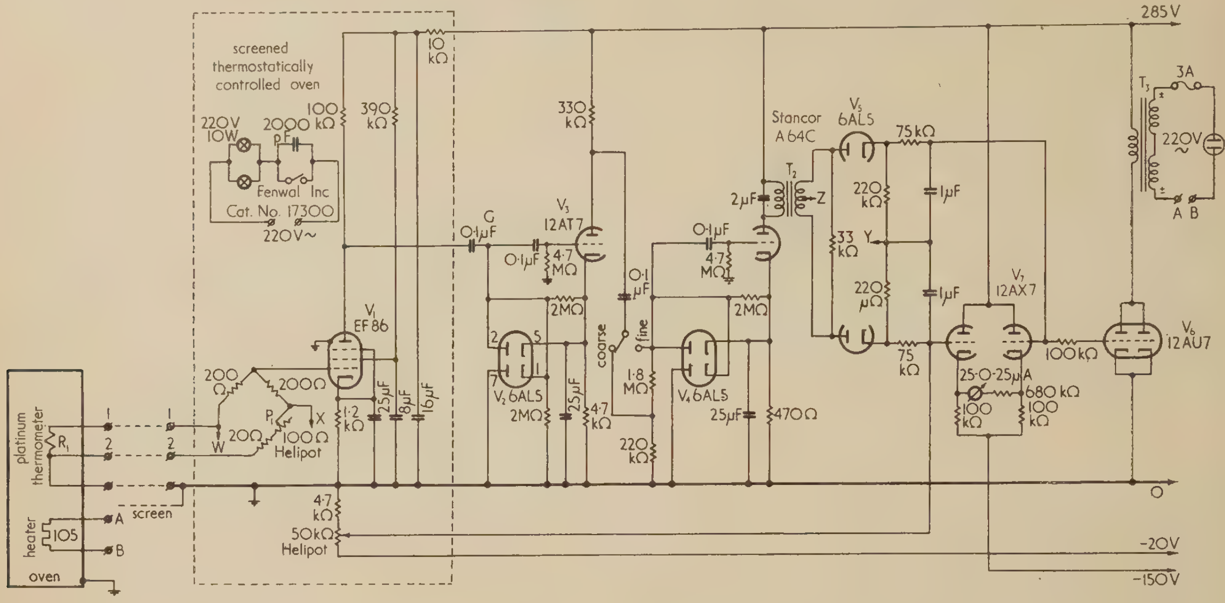
screened
thermostatically
controlled oven
220V
10W
100
2000 kΩ
pF
390 kΩ
10 kΩ
Fenwal Inc
Cat. No. 17300
220V~
330 kΩ
G
0·1μF
V₃
12AT7
0·1μF
4·7 MΩ
2MΩ
V₁
EF86
200 Ω
2000Ω
P₁
X
1·2 kΩ
25μF
8μF
16μF
W
20Ω
100Ω
Helipot
1
2
platinum thermometer
R₁
screen
A
B
heater
105
oven
4·7 kΩ
50kΩ
Helipot
7
2
5
1
V₂ 6AL5
2MΩ
25μF
4·7 kΩ
coarse
fine
0·1 μF
1·8 MΩ
220 kΩ
V₄ 6AL5
25μF
470Ω
0·1μF
4·7 MΩ
2MΩ
Stancor
A64C
T₂
2μF
Z
V₅
6AL5
75kΩ
220 kΩ
33 kΩ
Y
220 μΩ
1μF
1μF
75 kΩ
V₇
12AX7
25-0-25μA
680 kΩ
100 kΩ
100 kΩ
100kΩ
V₆
12AU7
285V
T₃
3A
220V~
A B
0
−20V
−150V

Fig. 2. Circuit diagram

Bridge and first-amplifier circuits. The connexion between the thermometer and the other arms of the bridge is a shielded, compensated three-lead cable.(5) This artifice compensates for small resistance changes in the connecting cable caused by variations in ambient temperature. That this refinement is necessary may be simply illustrated. The lead resistance (both directions) in the instrument is 0·14 Ω. An ambient temperature variation ΔT_a of 5 deg C (which may well occur during a working day) will cause a resistance change which will be interpreted by the equipment as a temperature shift in the oven of $\Delta T'$. This temperature shift is given by:

$$\Delta T' = \frac{\alpha_{Cu} R_{Cu} \Delta T_a}{\alpha_{Pt} R_{Pt}}$$

where α_{Cu}, R_{Cu} are the temperature coefficient and resistance of the connecting lead, and α_{Pt}, R_{Pt} are the temperature coefficient and resistance of the platinum. Thus:

$$\Delta T' = \frac{0\cdot 003\,93 \times 0\cdot 14}{0\cdot 003\,92 \times 34\cdot 5} \times 5 = 0\cdot 21 \text{ deg C.}$$

The equipment was initially found to have a settling time (after switching on) of three to four hours, which fell to

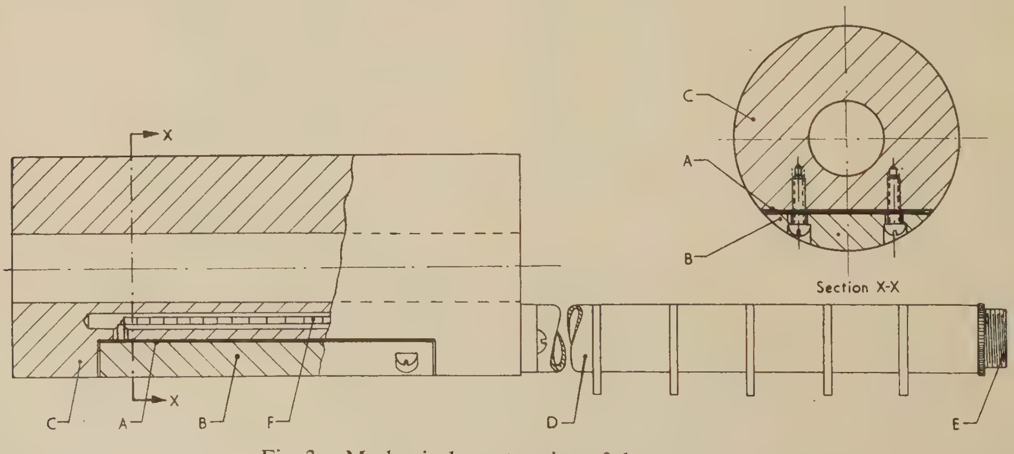
X
X
C
A
B
F
D
E
Section X-X
C
A
B

Fig. 3. Mechanical construction of thermometer

A, thermometer; *B*, damping segment; *C*, temperature-equalizing mass; *D*, stainless-steel tube; *E*, connector; *F*, ceramic insulating beads

5 minutes after the fitting of a thermostatically controlled ven (55° ± 1° C) containing the bridge, the input elements nd the first amplifier valve. This additional control was ecessary despite the fact that only deposited-carbon resistors r wire-wound units were used in these circuits. (The eference thermometer P has a temperature coefficient of nly 0·000 02.) The thermostatic enclosure also serves as a agnetic shield screening the low-level circuits from the trong stray magnetic fields of the saturable reactor.

The advantages arising from the use of a signal frequency ifferent from the mains frequency did not justify the amount f additional equipment that would be required. Hence the ridge is supplied by a 1·8 V, 50 c/s signal, the low level of hich minimizes self-heating effects.

Clippers and phase-sensitive detector. A difficulty someimes encountered with temperature regulators is the loss of ontrol when temperature errors exceed a certain value. This irregularity may occur every time the preset temperature s changed, or during the initial warming-up period. The resent regulator achieves stable control at all degrees of ridge unbalance and avoids overloading of the amplifier and etector by symmetrical limiting. The clipping action may e elucidated by considering the first double diode V_2. Small signals pass unclipped. The potential of point G is nidway between that of the cathode of V_3 and earth, and is 1·2 V. Positive-going signals which raise the potential of G to 2·4 V or more are clipped by anode "2" and cathode "5" of V_2. Negative half-cycles which reduce the potential of G below zero are clipped by the lower diode. Thus signals with a peak-to-peak amplitude greater than 2·4 V will appear at G as a symmetrical square wave. Clipping commences at V_4, which is preceded by two stages of amplification with a total voltage gain of about 5500 times. Thus, linear regulation ceases at r.m.s. values of bridge unbalance exceeding 2·4/(2·8 × 5500) or 150 μV. The first clipper stage V_2 limits large signals, which may otherwise overdrive the first half of V_3, distorting the waveform and causing erratic operation of the phase-sensitive detector V_5.

The phase-sensitive detector V_5, which is quite conventional, is fed at the points Z and Y with a 20 V, 50 c/s, signal at correct phase relation to the bridge input at X and W. Both voltages are derived from a special double-screened line transformer. T_2, which is a conventional interstage transformer (single plate to push–pull grids) with a turns ratio of 1 : 4 and a primary inductance of 2·5 H. The approximate specification is: Core, EI625, 16 mm high; Primary, 800 turns; Secondary, 3200 turns centre-tapped, both 0·08 enamelled-copper wire.

Thermionic diodes are preferred to semiconductor units in the clippers as well as in the phase-sensitive detector, since their use simplifies the problem of non-linearity at low signal amplitudes.

Saturable reactor. As a control element for this instrument, a saturable reactor was considered superior to both relays and thyratrons. The initial cost of all three elements is similar, so that, with its much greater life-expectancy, the saturable reactor is the preferred component.

Standard silicon–iron stampings (Allegheny Ludlum Steel Corp. "Transformer C", EI36, stacked 7·5 cm high) were used because they were available at the time. The size of the reactor was offset by low cost of materials and simple assembly. The a.c. windings (load windings) consist of two coils of 300 turns each, connected in antiphase. The d.c. control winding consist of 25 000 turns of 0·16 mm diameter enamelled-copper wire.

Special care was taken in orientating the reactor on the chassis, because strong stray fields are generated by it, especially in the saturated condition. The average power amplification of the reactor is over 50 times.

The oven. The requirements of size, mobility and temperature range indicated the use of a "solid oven" with a heavy brass cylinder as the temperature-equalizing element. The alternative of a liquid bath was considered to be inappropriate.(8)

One of the most important parts of the system is the thermal insulation surrounding the brass cylinder, which determines the losses and hence the power to be supplied. The material finally selected was 6·3 cm thick fire blocks, type JM16, by Johns Manville. The bricks are loosely inserted in a rugged sheet-metal box of external dimensions 24 × 23 × 31 cm, which guards them against mechanical abuse. The specific power consumption of the oven is about 0·4 W/° C, indicating that good thermal insulation has been achieved.

The heater element, which must be in intimate thermal contact with the brass cylinder and electrically insulated from it, must be designed with care. The element should work at its upper limit of electrical rating in order to increase the speed of heat transfer. Thin mica sheeting, 0·2–0·3 mm thick, was found adequate for good insulation.

Power supplies. Unregulated a.c. power is supplied to the heater of the oven, as compensation for line variations are automatically provided by the regulating mechanism. Electronic regulation of the main h.t. supply (285 V) was necessary to insure control stability.

Type of control and indication of error

The bridge output is proportional, near balance, to the temperature error, which is defined as the difference between oven temperature and the temperature preset by the reference thermometer. Linear regulation is maintained up to temperature errors of either ±0·15 deg C or ±0·2 deg C, depending on the position of the sensitivity switch. For temperature errors outside of this range, limiting occurs, and control passes to the "on–off" mode. These relations are shown schematically in Fig. 4. The use of the "coarse" range minimizes the swing-in time by a factor of about seven.

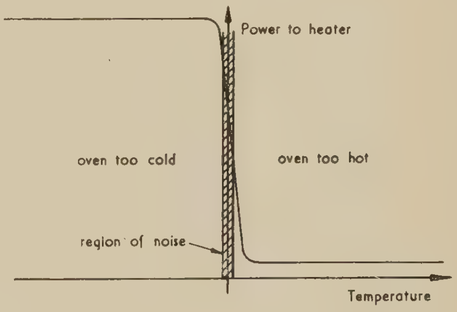

Fig. 4. Power supplied to the heating element plotted as a function of oven temperature

The inherent sensitivity is given by the smallest signal error which will rise over the noise level induced by hum pickup, microphony and the first-stage noise. The region of uncertainty caused by noise is shown schematically as the cross-hatched region in Fig. 4 (not to scale). A typical example stressing the importance of noise suppression is a tenfold increase of temperature swings when the earth connexion of the a.c. heater circuit is intentionally broken, and a twofold increase if the first stage is heated by alternating instead of direct current.

As the control is completely automatic and no external signs of regulation are detectable, a 25–0–25 μA meter in the VTVM circuit (V_7) was fitted. The meter shows the sign of the temperature error and its approximate value. The absolute reading of the meter is dependent upon the amplifier gain and other variable circuit parameters. The linear range, in which each small division equals 0·015–0·02 deg C, is limited to deflexions of 10–0–10 μA because clipping sets in at ± 15 μA.

Calibrations and adjustments

The temperature calibration of the multi-turn dial is a near-linear function, as shown in Fig. 5. Non-linearity arises from two sources:

(1) The second-order term in the expression:

$$R_t = R_0(1 + \alpha t - \beta t^2)$$

for the temperature coefficient of platinum, where $\alpha = 0{\cdot}003\,92$ and $\beta = 0{\cdot}000\,000\,588$ (Rhodes(6) or, in tabular form, Werner(7)).

(2) The non-linearity of the multi-turn potentiometer (0·5% guaranteed tolerance). Any resultant deviations from linearity were not significantly detectable on the calibration curve.

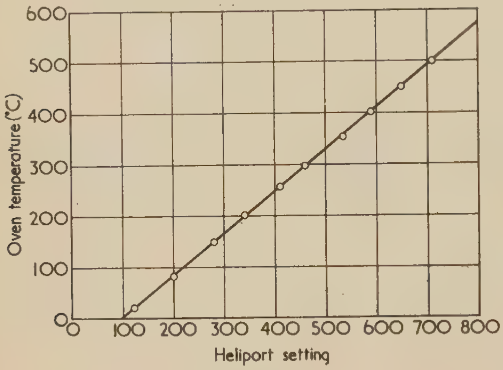

Fig. 5. Oven temperature plotted as a function of potentiometer setting

The detector output, which changes sign as the bridge passes through balance, is added to a constant preset grid bias. The "static" d.c. bias is adjusted to ensure that the power supplied to the oven varies with the preset temperature, because for every temperature there is one particular value of heater power which gives optimum regulation. This is achieved by a ganged connexion between the bias potentiometer and the reference potentiometer of the bridge. As the heater power does not change linearly with the bias voltage on the control valve, a "best-fit" linear-bias combination had to be used (Fig. 6). As a result, the maximum deviation over the whole range of heater power (15–280 W) will not be more than 5 W. These small deviations are smoothed out by the control action of the instrument. The only indication of the misfit is a small displacement of the balance position relative to the meter zero (1–2 μA).

Performance and conclusion

Before giving performance figures, some words of caution concerning temperature measurements are necessary. All absolute temperatures referred to in this paper were measured on a precision mercury thermometer with its bulb at the central part of the brass cylinder cavity. This positioning implies that some 10 cm of the stem were within the oven. The temperature recorded will of course depend on the thermal contact between the thermometer bulb and the oven wall, axial positioning and the thermal conductivity of the glass.(9) Thus the temperature is not absolute, but is in any case within the specified ± 1 deg C.

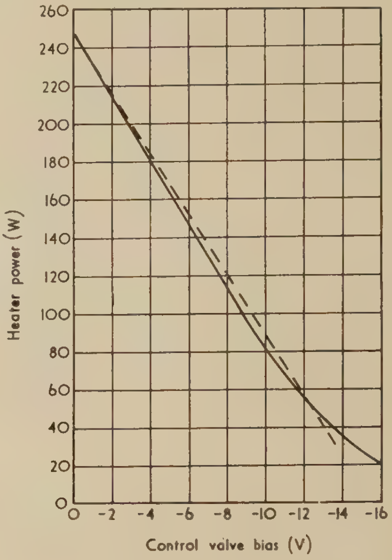

Fig. 6. Heater power plotted as a function of control-valve bias

Axial temperature gradients of the cavity were measured using a thermocouple brazed to a brass disk of diameter just less than that of the cavity bore. These measurements show that a constant temperature within $\pm 0{\cdot}5$ deg C is maintained over the central section (3 cm long) of the cavity. Temperature overshoots occurring after any temperature reset depend both in amplitude and number on the preset temperature. Even at the lower part of the operating range (150–200° C) where cooling is much slower, overshoots do not exceed 0·5 deg C in amplitude and ten in number. Above 300° C, overshoots decrease to about 0·2 deg C and five in number. These depend largely on the thermal characteristics of the oven (insulation, thermal mass, etc.) and not on the electronic regulator because all electrical time constants are very much shorter than the thermal time constant of the oven.

The swing-in characteristic for a temperature step of 100 deg C is given in Fig. 7, in which ΔT designates the

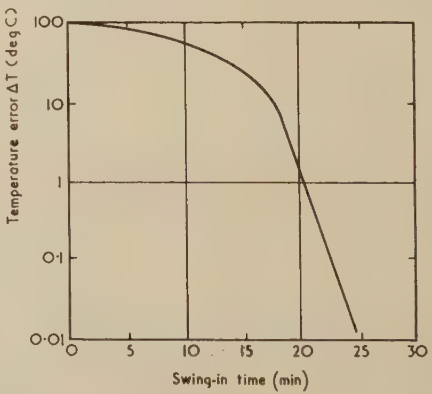

Fig. 7. Swing-in time for temperature step of 100 deg C.

sidual temperature error after the elapse of t min. The ontribution of changes in line voltage may be estimated from he result of a performance test. While the input line voltage as changed from 205 to 235 V, the oven temperature hanged only by 0·033 deg C. This corresponds to a shift f 0·001 deg C/V in the absolute temperature calibration. (This test was carried out at 325° C.)

Rapid corrective regulation is achieved as the overall pecific power sensitivity is as high as 280 W/deg C. The pecific power sensitivity n is defined as $\Delta N/\Delta T$, where ΔN is the corrective power increment supplied to the oven nd ΔT is the temperature error.

During the first two hours of operation, temperature drifts f 0·02–0·04 deg C may occur. After this "transient" eriod, thermal steady-state conditions prevail in the oven, nd temperature drifts are so small that they could not be etected, even after runs of eight hours. Ultimate stability may well be much better than 0·015 deg C, but was not recisely determined because of the difficulties which arise when fluctuations of the order of 0·001–0·005 deg C are to e measured (at 400–500° C).

The regulator has only two controls, one for temperature resetting and one for sensitivity. Any temperature in the range 150–550° C may be preset to ±1 deg C with a esettability of better than ±0·5 deg C. The upper temerature limit was chosen to ensure an adequate margin of afety for the platinum thermometer. During performance ests, close regulation could be maintained at temperatures p to 700° C. The range of regulation might be extended elow 150° C, if need should arise, by minor changes in the thermal insulation of the oven. The regulator proper may be adapted to any other temperature range, only a few readjustments being required.

Acknowledgements

The design and engineering of the regulator was carried out under the auspices of the Scientific Department, Ministry of Defence, Israel, and is published with its permission. The author also wishes to express his gratitude to Mr. E. Gross for his valuable help which contributed much to the speedy and successful completion of the project.

References

(1) DAUPHINEE, T. M. *Rev. of Sci. Inst.*, **26**, p. 693 (1955).
(2) MALMBERG, P. *Rev. of Sci. Inst.*, **27**, p. 136 (1956).
(3) NOLTINGK, B. E. *J. Sci. Inst.*, **30**, p. 349 (1953).
(4) WOLFE, H. C. *Temperature, its Measurement and Control in Science and Industry*, p. 288 (New York: Reinhold Publishing Co., 1955).
(5) *The Instrument Manual*, p. 270 (London: United Trade Press, 1953).
(6) RHODES. *Industrial Instruments for Measurement and Control*, p. 158 (New York: McGraw-Hill, 1941).
(7) WERNER. *Rev. of Sci. Inst.*, **23**, p. 163 (1952).
(8) WOLFE, H. C. *Temperature, its Measurement and Control in Science and Industry*, p. 617 (New York: Reinhold Publishing Co., 1941).
(9) *Loc. cit.*, pp. 236–240.

Time analyser using a crystal-controlled trochotron tube

by T. DOBROWOLSKI, and J. WALKER, Ph.D., F.Inst.P., Department of Physics, University of Birmingham

[*Paper received* 2 *February*, 1960]

Abstract

A nine-channel timing system is described in which a crystal oscillator has its output switched by a starting signal and is then used to drive a beam-switching tube (Burroughs, type MO-10R). An accurate sequence of voltage impulses is thus produced and these operate conventional circuits which gate the signals to be timed. The accuracy of the system is discussed briefly.

Principle of operation

The trochotron, or beam-switching tube, when controlled by a crystal oscillator, provides an accurate and convenient method of generating successive timing waves for the study of random, or other, processes. The arrangement described here has as its particular aim the measurement of the decay-time of thermal neutrons in moderators and in a sub-critical assembly of uranium and water; mean lifetimes in the region 10^{-4}–10^{-3} s are to be measured.

The Burroughs beam-switching tube, type MO-10R, has been used as the basis of the equipment; the characteristics of this tube have been described in some detail by Fan* so that a very brief description only is needed here. A combination of a magnetic field perpendicular to the plane of the diagram in Fig. 1, and an electric field produced between the spade electrodes and the cathode directs a beam of electrons to any one of the targets. This beam can be switched successively from target to target by application of suitable potentials to the grids.

In the present application, the trigger pulses are generated initially by a crystal-controlled oscillator so that pulses of very accurate duration and spacing are produced on the targets of the beam-switching tube. These pulses are used to switch electronically the signals from the neutron detector to nine recording channels. The tenth (or zero) target is used for the rest position of the beam. For the first experiment, the duration of each channel is 40 μs, but this time can be altered by having suitable frequency-dividing circuits between the oscillator and the trochotron. In the application mentioned, the thermal neutrons are produced by moderation of a burst of fast neutrons which, in turn, are the result of a burst of deuterons impinging on a target containing deuterium or tritium. The end of the deuteron burst initiates the operation of the timing sequence but a delay of some 200 μ s is injected before the beam-switching tube starts its cycle. This delay, which does not have to be known accurately, ensures that the neutron measurements in moderators are concerned with thermal neutrons only. For other types of measurement, the delay may be zero; a measurement of the half-life of Po^{214} (RaC′) made with the equipment is an example. In this case, a β-particle from Bi^{214} (RaC) initiates the trochotron cycle and the α-particles from Po^{214} are recorded in the timing channels.

---

* FAN, S. P. *J.Brit.I.R.E.*, XV, p. 335 (1955).

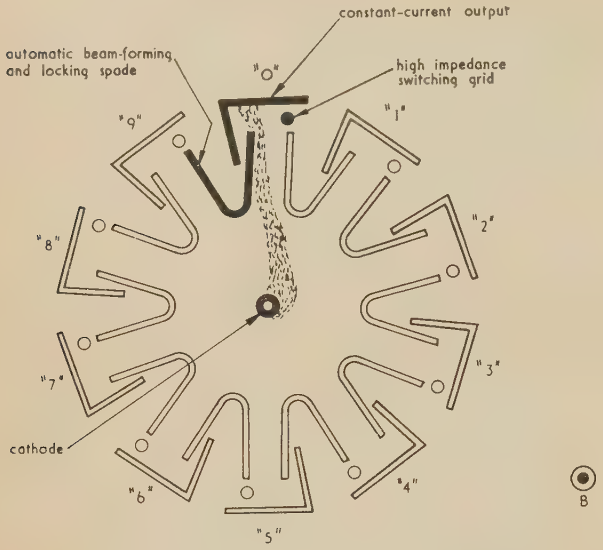
constant-current output
automatic beam-forming and locking spade
"0"
high impedance switching grid
"1"
"2"
"3"
"4"
"5"
"6"
"7"
"8"
"9"
cathode
B

Fig. 1. Schematic diagram of beam-switching tube

Scheme of operation

A schematic diagram of the equipment is shown in Fig. 2. To some extent, the design of the unit was arranged to employ equipment which was easily available. For example, the 1 Mc/s oscillator and the following scale-of-ten actually used could be replaced, for the measurements being made at present, by a 100 kc/s oscillator, although it may be advantageous in later work to gate the 1 Mc/s waves. The three units shown in the dotted enclosure were obtained by using a standard scaler (Philips type PW 4032); the only modification required was the minor one of bringing to an output socket the waveform from a suitable point between the second binary stage and the first decade counter. The operation of the system is as follows: The starting pulse, a pulse from the deuterium target or β-particle detector for the cases mentioned, is shaped and then triggers the monostable multivibrator which is used to produce the delayed pulse. The end of this pulse starts the switching wave, from a bistable multivibrator, and thus opens the timing gate. Pulses from the crystal oscillator are then passed through the scale-of-four circuit to the driving circuit for the beam-switching tube. Here, two sets of pulses are produced to operate the odd and even switching grids. This separation of the grids into two groups means that the triggering pulses can be of reasonable length without any risk of double jumps by the beam. The scale-of-four also drives a decade scaler, the output of which coincides with the end of the beam-tube cycle and, thus, it is used to end the switching wave and so to close the timing gate. Of course, a pulse from the beam-switching tube itself could be used to close the cycle, but the decade scaler was available in the equipment used and is a convenience in fault-tracing. During each cycle, a pulse of 40 μs duration is obtained from each target in the beam-switching tube and, as the transit time from target to target is so short (about 0·2 μs), the target, or channel, pulses are practically contiguous. This condition is not essential for the measurement of a single decay constant, but a sharp edge to the channel pulses helps to maintain the accuracy in width and spacing set by the crystal oscillator. Each of the nine channel pulses is used to operate the suppressor grid of a pentode gating tube with the signals to be timed on the control grid; the output on each anode is recorded.

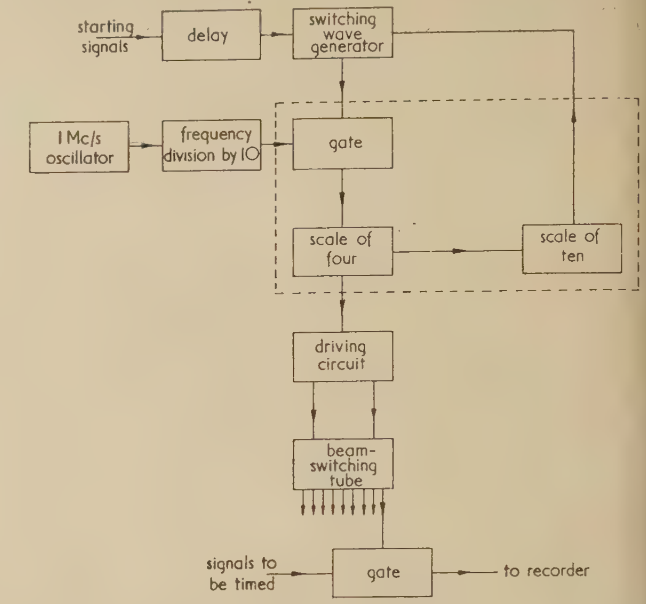

Fig. 2. Block diagram
(Pulse shapers are not shown. The circuits for the last three blocks are shown in Fig. 3)

Circuit details and waveforms

No details will be given here of the two standard pieces of equipment, the 1 Mc/s oscillator and Philips' scaler. The PW4032 handbook gives complete circuit details for the latter, and the only modification is to extract the output from the driving tube for the first decade counter (anode *a′* of tube B_1 in the handbook). The timing impulses (100 kc/s) are supplied to the normal input of the scaler and the switching wave to the remote control point (Bu_3^4 in the handbook). The output of the first decade stage (Bu_1^3) is used to terminate the switching wave. The delay circuit and switching wave generator will not be described in detail as they are of fairly orthodox design* and, in any case, the latter is almost identical with the multivibrator used in the control circuit for the beam-switching tube. This circuit and the tube connexions are shown in Fig. 3. Here are produced the two trains of pulses, each at 50 kc/s, for operating the even and odd grids. When the apparatus is first switched on, it is important to ensure that the beam rests on the zero target and that the driving multivibrator is in the correct state (V_2 conducting) to supply the even grids, and therefore grid zero, with the first pulse. The setting switches S_1 and S_2 ensure that these conditions are satisfied and the neon lamp *N* and the meter *M* act as indicators for them. The switch S_2 lowers appreciably the potential on all the spade electrodes of the trochotron and when S_2 is opened, the capacitor on spade 0 delays the rise in voltage relative to that on the other spades so that the electron beam is driven to the zero target.

---

* MILLMAN, J., and TAUB, H. *Pulse and Digital Circuits* (New York: McGraw-Hill Book Co. Inc., 1956).

Some indication of pulse waveforms are given in Fig. 3, and a few others are given in Fig. 4 to clarify the operating sequence. In Fig. 4, the double pulse at the beginning of the timing waveforms is used to represent the possible movement of the whole sequence relative to the time zero by up to 10 μs. This arises because the starting waveform and the 100 kc/s wave are not synchronized. The uncertainty at the end of the switching waveform is due to the same cause. For the present measurements, this movement of the whole sequence does not matter, but the stability of the channels relative to each other is very important.

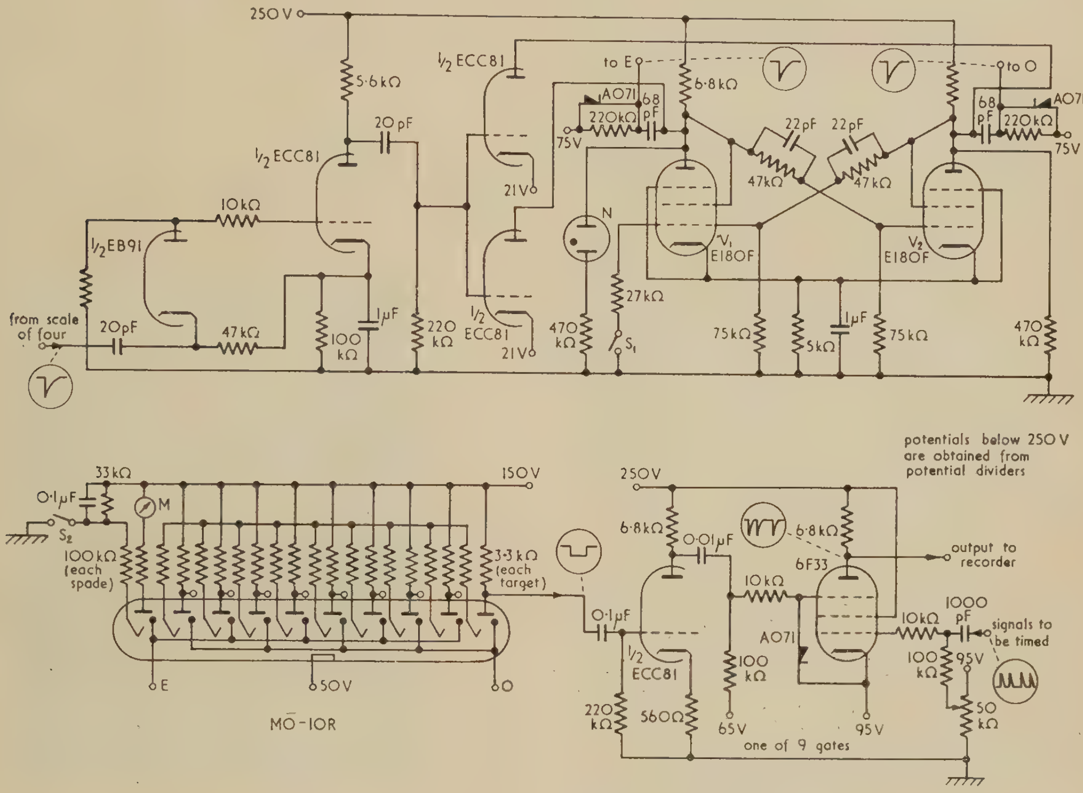
250 V
5·6 kΩ
½ ECC81
20 pF
½ ECC81
10 kΩ
½ EB91
from scale of four
20 pF
47 kΩ
100 kΩ
1 µF
220 kΩ
½ ECC81
21 V
21 V
to E
AO71
220 kΩ
68 pF
75 V
N
470 kΩ
27 kΩ
S₁
6·8 kΩ
22 pF
22 pF
47 kΩ
47 kΩ
V₁ E180F
V₂ E180F
75 kΩ
5 kΩ
1 µF
75 kΩ
470 kΩ
to O
AO71
68 pF
220 kΩ
75 V
33 kΩ
0·1 µF
S₂
M
100 kΩ (each spade)
150 V
3·3 kΩ (each target)
E
50 V
O
MO-10R
250 V
6·8 kΩ
0·01 µF
0·1 µF
½ ECC81
220 kΩ
560 Ω
6·8 kΩ
6F33
10 kΩ
AO71
100 kΩ
65 V
95 V
one of 9 gates
potentials below 250 V are obtained from potential dividers
output to recorder
1000 pF
10 kΩ
signals to be timed
100 kΩ
95 V
50 kΩ

Fig. 3. Circuits associated directly with beam-switching tube

Brief comments on accuracy and stability

Details of measurements of lifetimes made with this equipment will be reported elsewhere and it is sufficient to state here that the timing channels are stable and closely equal in duration. The rise- and fall-times of the pulses supplied to the signal gates do not exceed 0·2 μs, and a similar time applies to all the earlier stages which are of importance, so that fluctuations in the width of the timing channels should be small compared with this figure. Oscillograph measurements of the gating waves and the output signals showed that the channels were equal to within the accuracy of the measurement, which was about $\pm\frac{1}{2}\%$. Another check is the equality of random events recorded in each channel when the signals being measured are not correlated with those triggering the apparatus. Measurements of this type have again shown the equality in channel width is accurate to $\pm\frac{1}{2}\%$.

Acknowledgements

Discussions with Mr. H. R. Shaylor were valuable in the early stages of this work and the authors are grateful to Mr. R. H. Morle for help in the construction of the apparatus, and to the Department of Scientific and Industrial Research for financial assistance. During the period of the work, one of us (T. D.) was on leave of absence from the Institute for Nuclear Research, Warsaw.

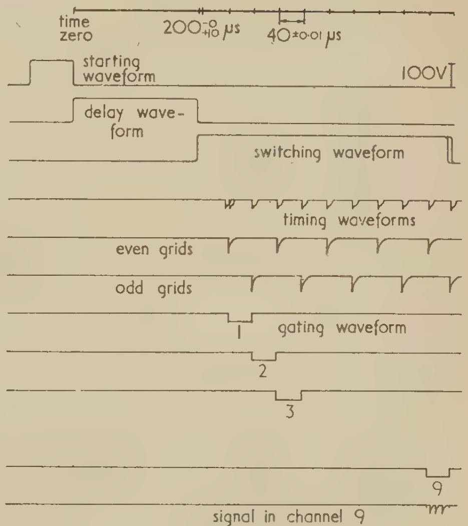
time zero
200^{-0}_{+10} µs
40±0·01 µs
starting waveform
100V
delay waveform
switching waveform
timing waveforms
even grids
odd grids
gating waveform
1
2
3
9
signal in channel 9

Fig. 4. Some waveforms

The torsiometer—an instrument for the study of gels considered as elastic solids

by W. A. SOUTHORN, Ph.D., A.R.I.C., Rubber Research Institute of Malaya, Kuala Lumpur, Federation of Malaya

[*Paper first received* 3 *March*, 1959, *and in final form* 4 *April*, 1960]

Abstract

A new instrument has been developed for studying changes in development of structure in the weak hydrogels produced when natural rubber latex from Hevea braziliensis *is coagulated. The instrument records on a chart the progressive changes in torque required to give a fixed small value of deformation in an annular sample. The machine can be used for gel systems other than rubber, and may therefore have applications in other fields. Results may be expressed directly as a modulus of rigidity for materials with properties approximating to those of an elastic solid. For visco-elastic materials the modulus is a complex function including viscosity components. The range of sensitivity of the instrument is from* 1 *to* 100,000 *dyn/cm*^{2}.

Introduction

When natural rubber latex from *Hevea braziliensis* is destabilized, the precipitated rubber is usually in the form of a coherent hydrogel or coagulum. The physical properties of this material, including its rigidity, are of considerable technological interest, but are difficult to measure. In the first place the gels are very sensitive to manipulation and their properties are altered by any test which involves substantial deformation or handling. Furthermore, they change fairly rapidly with time so that a series of tests on the same gel is essential if a complete picture is to be obtained. These effects are particularly marked in the case of the weak gels produced in the early stages of coagulation from fresh field latex. Lastly the coagulation of latex is an irreversible process initiated as soon as the destabilizing agents are added, which means that the time available for placing the sample may be short, and difficulties may arise if the test container is not robust and very easily accessible. Although many instruments are described in the literature (a good review is given by Ferry$^{(1)}$), it was difficult to find one suitable for the present purposes.

Most previous workers in the field of rubber coagulation have avoided weak gels and have confined themselves to measuring some property such as modulus or elongation at break, on coagulum which has been allowed to harden long enough to toughen considerably. Examples of this type of measurement are described by de Vries and Van den Tempel$^{(2)}$ and by Madge.$^{(3)}$ Another approach by Medalia, Townsend and Grover$^{(4)}$ involves the use of temporary supports for the gel, but this limits the types of coagulation which can be studied. To extend this work, a special recording instrument has been developed which may find applications to similar problems in other fields, and it has come to be known as a torsiometer. This has the general appearance of a cup-and-bob viscometer (Fig. 1), but its mode of operation is very different. It is a recording instrument and its results are produced as a chart in which one axis is time and the other is the value of torque which has to be applied to the gel to produce a small fixed value of deformation. The torque is applied at frequent intervals starting from the moment when the sample is placed in the testing cup. Some hundreds of measurements can thus be made at the site of coagulation and the results give a complete history of the development of structure throughout the coagulation and subsequent maturing processes.

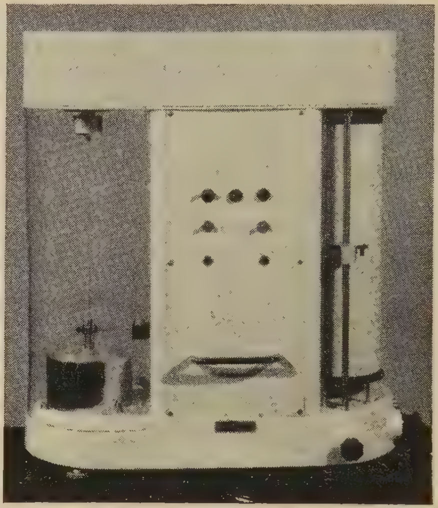

Fig. 1. Torsiometer (H.L. Instruments version)

Principles of measurement

The principles of the measurement are simple and are shown diagramatically in Fig. 2. The system to be investigated, for example latex plus acid, usually starts in a liquid state and is poured into a cup of standard dimensions in which a cylindrical bob hangs from a torsion wire fixed at its upper end to a driving and measuring head. When this head is rotated, a torque is transmitted down the wire which causes the bob to move, but because of the resistance from the contents of the cup, the motion of the bob lags behind that of the head. When the torsiometer bob has been rotated by a standard small amount, chosen by experience to be less than that required to cause permanent deformation in the system under test, the rotation of the driving head is stopped through a sensing device on the bob. The head motion is then reversed so that the strain in the system is first released and then built up again in the opposite direction. The whole process is carried on automatically and the head otion is measured and recorded on the instrument chart at ch reversal.

As the material in the cup increases in rigidity, the wire as to be twisted by an increasing amount and this is shown in the chart produced (Fig. 3). In each cycle of operations, the motion of the head minus the motion of the bob is a measure of the torque applied. The motion of the bob indicates the small constant deformation which this torque produces, so that the head motion is related to the modulus of rigidity of the material under test.

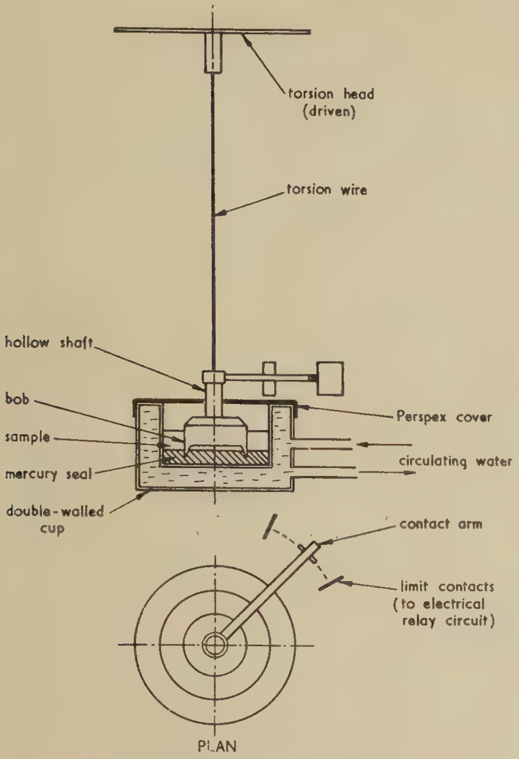

Fig. 2. Principles of measurement with diagrammatic section of cup and bob showing disposition of the liquids in the cup

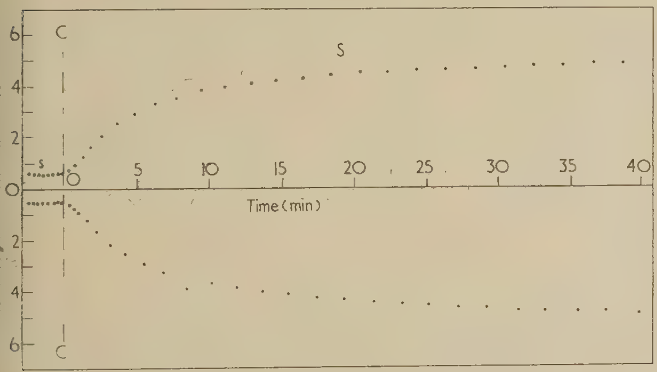

Fig. 3. Torsiometer chart

The dotted traces show the pen positions at each reversal. These are related to the head rotations required to give a fixed small movement of the bob, first in one direction then in the other. The gelling agent was added at point *C*. Thereafter the widening separation of the traces shows the progress of gelation. The ordinate gives the traces separation in centimetres from which the modulus of rigidity at any given time may be calculated. The "effective separation" is $S - s$ (cm)

With a fluid material, the instrument behaves like a cup-and-bob viscometer and the bob lags by an amount depending on the viscosity and the rate of shear chosen. The torsiometer is adjusted to give a rate of shear so low that for many purposes the effects of viscosity can be neglected. The annulus between cup and bob is relatively large (the diameter of the cup is $2\frac{1}{2}$ in. and the diameter of the bob is $1\frac{1}{2}$ in.), whilst the speed of rotation is very slow (several minutes per revolution), With these characteristics, the instrument is insensitive to viscous effects, but is very sensitive to structural effects such as occur on gelation.

The torsion head is driven by a small but powerful reversing electric motor suitably geared to give a choice of three slow speeds (approximately 4 rev/h, 12 rev/h, and 40 rev/h). The head motion is transmitted by means of a cord to a recording pen which strikes a chart moving at constant speed. One end of this cord is attached to the circumference of a drum fixed to the head, the cord then passes over a pulley and the other end is attached to the pen which runs on vertical guides. As the head oscillates, the pen moves up and down, maintaining the cord in approximately uniform tension by virtue of its own weight. For most of its journey the pen clears the chart without making any mark, but at each reversal of the head motion, a solenoid tilts the guides momentarily, so that the pen pecks at the chart. There is thus no friction between the pen and the chart and only the points of reversal are recorded. The chart is carried on a vertical cylindrical drum driven by a small synchronous clock unit. These clock units are available with a wide variety of shaft speeds and they can be quickly interchanged. The speeds found to be most useful are 1 rev/h and 1 rev/day.

The torsion wires are of standard length (9·5 in.) and are sweated into brass bushes at either end. These bushes fit into chucks in the torsion head and the bob, so that they may easily be interchanged. A series of calibrated torsion wires allows the sensitivity of the instrument to be varied over a very wide range.

The bob is of stainless steel and hangs from the torsion wire symmetrically in a double-walled cup. The bob has a stem, which carries an arm terminating in twin electrical contact points (Fig. 2). When the bob moves, the arm moves with it until it makes electrical contact with one or other of two contact plates which intercept its path in either direction. When contact is made, a small current passes down the torsion wire and fires a series of sensitive relays which reverse the motor and cause the pen solenoid to operate. The whole cycle of operations is then repeated. The permitted arc of travel depends on the position of the contact plates and the spacing of the twin contact points on the contact arm. For routine use, it is convenient to fix the position of the contact plates and use a series of arms which are calibrated so that the arc of travel is known accurately for each. For most work, a value of 5° is convenient but the angle can be varied between 1 and 10° as required. This represents the total swing between two reversal positions, so that the maximum deformation of the sample can be regarded as half of this.

The permitted arc of travel of the bob is always chosen so that the deformation of the material is insufficient to alter its properties irreversibly. This must be determined with reference to the system being investigated, but in most cases there is considerable latitude. Within these limits the measurement is not altered by adjusting the gap setting providing the new angle is used for calculation purposes. This can be used to alter the sensitivity of the instrument when necessary during the course of an experiment.

The cup is double-walled so that the temperature of the system can be controlled. Most gel systems are very dependent on temperature and to get comparable results it is necessary to circulate water at constant temperature through the wall of the cup. The cup is made of chrome-plated brass. For experiments with *Hevea* latex where copper can exert a disturbing catalytic effect even in trace quantities, a glass liner is used to guard against the possibility of pinholes in the plating. This liner can be removed to give better thermal contact if required. The whole cup assembly slides out for cleaning. To avoid troubles from evaporation, the cup is fitted with a Perspex lid through which the torsion wire is threaded.

When the machine is working with very sensitive torsion wires or in unusually draughty locations, it may be necessary to use Perspex covers (Fig. 1) which envelope the whole of the torsion system, but in normal circumstances they are not needed. Levelling screws are provided so that the bob may be centred in the cup. The machine illustrated in Fig. 1 is now in commercial production by Messrs. H. L. Instruments of Poole Road, Dorset.

To carry out a test, the first step is to fit a torsion wire and a contact arm suitable for the system to be investigated, and level the instrument. In tests on rubber latex the following procedure is adopted which eliminates end effects (Fig. 2). About 20–25 ml of well-cleaned mercury are placed in the bottom of the cup, and the bob is lowered, by adjusting the chucks, till its bottom rim just dips into the surface of the mercury pool. The bob ordinarily used is cylindrical and the bottom edge is turned so as to leave a knife edge at the rim. It is this knife edge which makes contact with the mercury and seals off the bottom face of the bob. The sample is destabilized and poured quickly into the space round the bob and above the mercury. In this way, a true annulus of coagulum develops and no complications from end effects can arise. For any system for which mercury can be used, this will probably be the best way to operate.

The machine produces its results in the form of two dotted traces which should be symmetrical (Fig. 3). Each trace represents the positions of the torsion head required to produce the fixed deformation in one direction. Any temporary disturbance is shown by a point out of line and not duplicated in the second trace so that the two traces serve as a check on each other. When the machine is operated with no material in the cup, the traces appear as parallel lines, the separation between them being a measure of the free travel of the bob between the contact limits, together with a very small lag arising from mechanical factors which will be discussed later. By running the machine for a few minutes in this way before the sample is poured on, a "blank" value is obtained. When the sample is added and gelation starts, the traces begin to separate at a rate which depends on the speed with which gel structure is built across the annulus between bob and cup. At any given time the separation between the traces, less the "blank" separation due to free travel of the bob between contacts, indicates the deflexion of the head required to produce the fixed value of deformation (set by the limit contacts) in the material under investigation. This quantity will be known as the "effective separation" of the traces.

Theory

For a material approximating to an elastic solid, the results may be expressed directly as a modulus of rigidity. Since the stress is applied between the inner and outer walls of an annulus which are of equal length but unequal area, the stress distribution is not even throughout the sample. A mathematical treatment of this problem is given by Smith.$^{(5)}$ Since in the torsiometer the angle of deflexion is always small, the higher terms in Smith's equations may be neglected for practical purposes, giving the simple expression:

$$\alpha = \frac{T}{4LG}\left(\frac{1}{r_1^2} - \frac{1}{r_2^2}\right), \tag{1}$$

where α is the angle of deflexion (rad), L is the length of inner and outer walls (cm), r_1 is the radius of bob (cm), r_2 is the radius of cup (cm), G is the modulus of rigidity (dyn/cm^2), and T is the torque (dyn/cm). Substitution for the operational constants of the torsiometer and rearrangement give:

$$G = S\left(\frac{W}{h\theta}\right)\left[\frac{4{\cdot}55}{L}\left(\frac{1}{r_1^2} - \frac{1}{r_2^2}\right)\right], \tag{2}$$

where S is the effective separation of the torsiometer traces (cm), W is the "wire constant", i.e. the couple required to twist the end of the torsion wire through one degree when the other end is fixed (dyn cm/deg.), h is the "head constant", i.e. the distance the pen moves per degree rotation of the torsion head (cm/deg.), and θ is the whole angle of swing of the bob between successive reversals (deg.). The factors L, r_1 and r_2 now represent the length of the bob, the radius of the bob, and the internal radius of the cup respectively.

Providing the standard cup and bob are used with a fixed volume of sample, then the quantity inside the square bracket in equation (2) is constant; for a 50-ml sample and the dimensions mentioned in this paper, it has a value of 0·428. The factor $W/h\theta$ is under the control of the operator according to the wire and machine settings chosen, and enables the sensitivity of the instrument to be adjusted.

Errors due to viscosity factors

The range of sensitivity available by choosing suitable wires and machine settings, is from 1 to 100,000 dyn cm^2. A "perfectly elastic" solid and a "Newtonian liquid" are both abstractions never realized in practice, and it is clear that at the lower end of this range of sensitivity, the elastico-viscous materials are far from being perfectly elastic solids. The torsiometer is commonly used to take readings through the whole range of the sol/gel transition. In the sol state the properties are predominantly those of a liquid and in the gel state they are mainly those of a solid. It follows that the record given by the instrument when used in, this way includes both viscous and elastic elements. As already mentioned, the instrument is much more sensitive to elasticity than to viscosity because of the low rates of stress application. If the instrument is considered as a cup and bob viscosimeter, the following expression may be used to calculate the viscosity η required to give a particular chart reading on the torsiometer:

$$\omega = \frac{T}{4\pi\eta L}\left(\frac{1}{r_1^2} - \frac{1}{r_2^2}\right), \tag{3}$$

where ω is the angular velocity in rad/s and T is the couple acting on the wire when the bob has attained the same velocity as the head. For example, using a sensitive setting with a wire factor of 45 dyn cm/deg., a head factor of 0·1315 cm/deg., a head velocity of 3·9 rev/h and with a 50 ml sample over mercury between a cup and bob of standard dimensions, this indicates a viscosity of 2,500 cp for a 1 mm increment of chart separation. This is a high viscosity corresponding to a heavy gear oil. If the same constants are substituted in equation (3), then a similar result would be ven by a solid structure having a rigidity of only 2·7 dyn/cm², hich corresponds to a very weak solid which would be nable to retain shape against gravity, and therefore would be assed as a liquid for most purposes.

Nevertheless, because of viscosity components, the modulus ven by the torsiometer for a visco-elastic material must be garded as a complex function depending on the rate of hear. Since the machine is provided with means of varying he rate of head motion, the significance of the viscosity actor can readily be checked for the system under examination. For most gels (including rubber hydrogels) it is not arge enough to impair the usefulness of the instrument. With weak gels from fresh natural rubber latex, a ten-fold ncrease in shear rate may increase the chart reading by 10 o 20% in some cases because of the increased contribution rom viscosity. Comparative tests on visco-elastic materials hould therefore be made as nearly as possible at the same shear rate. Since quite large errors from other factors are iable to be encountered in this kind of work, such as the ifficulty of preparing any two gels with identical properties, he viscosity effect is less serious in practice than in theory, ut it must be borne in mind, particularly as the rate of shear s not usually constant throughout a torsiometer experiment.

It cannot therefore be claimed that the modulus calculated s an absolute measure of rigidity except for materials which pproximate fairly closely to elastic solids. However, it is ufficiently near to be of value for many purposes, providing hese qualifications are understood. As a check tests have een made in which the torsiometer was used alongside other methods for determining the elasticity of gels. For example, he apparatus described by Saunders and Ward⁽⁶⁾ has been sed very successfully, for gelatine gels. A sample of commercial gelatine dissolved as a 6% wt/vol solution in water y heating to 70° C for 10 min and then set for 16 h at 24° C gave a value of 10,160 dyn/cm² in an apparatus of this type nd 10,570 dyn/cm² in the torsiometer. This is a good greement in view of the different techniques. The Saunders nd Ward apparatus cannot be used effectively with rubber coagulum because of the difficulty of forming a suitable bottom meniscus in a column of this type of gel.

Errors due to mechanical factors

Possible sources of error are as follows:

1. Lost motion between gears, drive cords, etc.
2. Delays resulting from the pressures required to establish electrical contacts when the motion of the bob is intercepted.
3. Electrical delays resulting from the time taken for relays to establish new circuits.
4. Inertia of the motor system which may cause the head to overshoot.
5. Inertia of the bob system.

The pen motion is taken directly from the head itself so that errors could only arise from changes in length of the cord connecting the pen to the head. Tests made at different humidities and temperatures show that such errors are negligible.

Delays arising from contact pressures, electrical delays and inertia of the motor armature and the head mechanism, all have features in common: they tend to cause excessive pen travel and they come into effect on reversal so that they are independent of the arc of travel of the bob. Their extent may therefore be ascertained by running the machine in air at different gap settings and plotting the results, as in Fig. 4. If there were no errors of this type, the values should form a straight line passing through the origin. In fact, they lie on a straight line which passes slightly above the origin. The intercept shows the magnitude of the small constant error which is for most purposes negligible. Since the normal way of conducting a test is to run a "blank" determination for a few minutes and subtract this from the gross separation of the traces to give an effective separation, a correction is automatically applied, because the "blank" includes the machine errors. Contact pressures are the major source of these errors which may be regarded as small if the contacts are clean and the triggering relay is in good order. Some such check as the above should be made at intervals to ensure this.

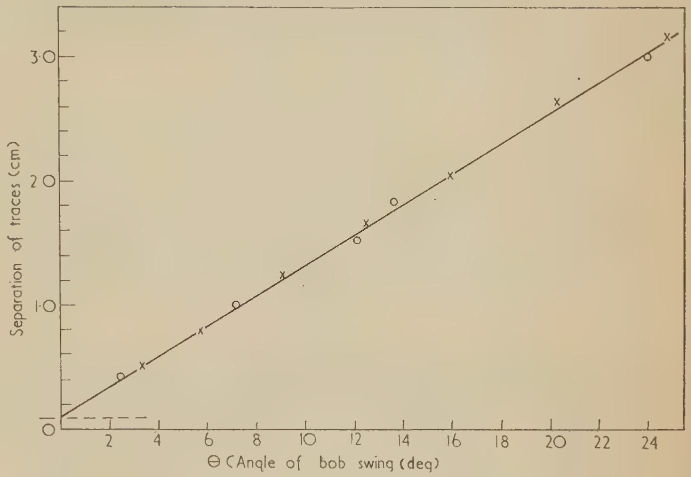

Fig. 4. Separation plotted against θ for varying gap settings

For this experiment a torsiometer was modified to give wider variations in θ than are normally required. Two sets of experimental results are shown (circles and crosses). The intercept on the vertical axis gives the total error due to machine factors which is approximately 0·10 cm

Inertial errors, both of the bob and of the drive mechanism, may be checked by running the head at different speed settings. No significant differences due to the inertia of the drive mechanism are found, presumably because the motor armature always runs at constant speed and the head itself only moves very slowly. The bob can, however, introduce small errors resulting from inertia when combinations of the fastest head speeds and finest wires are employed. At speeds of 3·9 rev/h or even 12 rev/h, the energy stored in the bob is small and tests in which the machine is run at these speeds, with the bob hanging free in air, show no difference as between fast and slow. To sum up, provided the contact and relays are in good order, which may be checked as above, and provided combinations of fast head speeds and fine wires are avoided, the machine errors are negligible and are in any case largely self-correcting by the normal method of operation.

Conclusion

The main value of the instrument is to provide a very convenient test which gives a recorded history of the progress of a sol/gel transformation directly and without requiring any special manipulative skill. For an elastic material, the results may be expressed in absolute units as the modulus of rigidity of the material. The properties of many gel systems are such that this may be used as an adequate approximation, but for visco-elastic materials in which there is a strong viscosity element, the modulus is a complex function including a variable component. The significance of this component for a particular system may be estimated by using the facilities provided for varying the rate of application of stress. The machine is useful even in cases where the results do not have an absolute significance, since comparison of actual charts given by gels prepared in different ways enables the effects of the treatment to be evaluated.

Acknowledgements

The author wishes to record his thanks to Mr. W. G. Wren of the Rubber Research Institute of Malaya at whose suggestion this work was started and who has helped with very valuable criticism and advice. Also the author wishes to thank Yee Shin Meng and Maulud bin Marahasa for their great help in building the first five working models. Lastly, thanks are due to Messrs. H. L. Instruments of Poole Road, Dorset, for their work in developing the production model illustrated in this paper.

References

(1) Ferry, J. D. *Rheology, theory and applications*, Vol. 2, p. 433, edited by F. R. Eirich (New York: Academic Press, 1958).

(2) de Vries, A. J., and van den Tempel, M. *Proc. 2nd Int. Congr. Rheology* (1953).

(3) Madge, E. W. *Trans I.R.I.*, **28**, p. 207 (1952).

(4) Medalia, A. I., Townsend, H. B., and Grover, H. N. *Anal. Chem.*, **26**, p. 697 (1954).

(5) Downie-Smith, J. F. *J. Appl. Mech. A*, **6**, p. 159 (1939).

(6) Saunders, P. R., and Ward, A. G. *Proc. 2nd Int. Congr. Rheology* (1953). Communication No. 34.

Portable electrometer voltmeter

by W. E. K. GIBBS, B.E.E., Australian Defence Scientific Service, Defence Standards Laboratories, Department of Supply, Maribyrnong, Victoria, Australia

[*Paper received* 1 *February*, 1960]

Abstract

This paper describes a portable high impedance d.c. voltmeter for measuring voltages up to two volts at impedances of up to 10^{10} *ohms. The accuracy attained is about* 2% *of full-scale deflexion and the short-term zero drift is also of this order.*

The principle of the electronic voltmeter is shown in Fig. 1. The high-gain d.c. amplifier with gain A, grid current I_g and feedback resistor R, supplies a moving coil voltmeter V. The earth point of the system is at the amplifier output instead of at the input, as is usual. The voltage to be measured is E with a source resistance R_1. Analysis of the circuit yields:

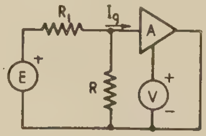

Fig. 1. Principle of instrument

$$V = (E - I_g R_1)\left\{\frac{1}{\left(1 + \frac{1}{A}\right)\left(1 + \frac{R_1}{R}\right)}\right\},$$

or:

$$V \simeq E,$$

since, for 2% accuracy:

$$\frac{1}{A} + \frac{R_1}{R} < 0{\cdot}02,$$

and:

$$I_g R_1 < 0{\cdot}02E.$$

These conditions are met by using an electrometer as the input to a transistor amplifier with an overall voltage gain of about 300, and a value of R equal to $10^{12}\ \Omega$, as shown in Fig. 2.

The use of transistors with the Mullard electrometer, type ME1401, fulfilled the need for portability and obviated high-voltage supplies. One feature of the amplifier, the use of germanium and silicon transistors in cascade, is of note. The silicon transistor *Tr*3 (Fig. 2) has better temperature stability than the germanium transistor *Tr*1, and its higher base-to-emitter voltage enables direct cascade connexion. Another feature is the use of transistor *Tr*2 as the load for *Tr*1 in an attempt to cancel the effects of the temperature-sensitive leakage current of *Tr*1. However, this is somewhat of a refinement and could be omitted in many instances. The 0·01 μF capacitor from the base of *Tr*2 stabilizes the amplifier for all values of source resistance. A zero adjustment is provided in the bias circuit of the electrometer. The instrument, complete with batteries and meter, is conveniently mounted in a 10 × 8 × 6 in. metal box.

Acknowledgement is made to the Chief Scientist, Australian Defence Scientific Service, Department of Supply, Melbourne, Australia, for permission to publish this paper and to Messrs. S. A. Lott and P. H. Mathieson of the Defence Standards Laboratories, Maribyrnong, Victoria, Australia, for their helpful advice.

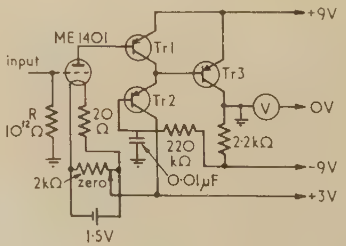

Fig. 2. Detailed circuit

*Tr*1, *Tr*2, germanium transistors, OC71
*Tr*3, silicon transistor, OC470
V, voltmeter, 20 kΩ/V, 2 V

Novel displacement detector and its application n a recording thermobalance

y J. C. VAN DER BREGGEN and H. J. WOUTERLOOD, Chem. Docts., African Explosives and Chemical ndustries Ltd., Northrand, Transvaal, South Africa

Paper received 1 *February*, 1960]

Abstract

transducer has been developed to detect changes in position of a balance beam. Its operation is based upon a differential capacitor. Variations in capacitance are made to produce directly a d.c. voltage corresponding in sign to the sense of deflexion of the balance beam. The construction of the transducer is described, and its application in automatic apparatus for thermogravimetric analysis is illustrated by results obtained on the dehydration of copper sulphate and the decomposition of quinoline phosphomolybdate.

The sensitivity of the instrument can be varied in nine steps to give full-scale deflexions from 10 *to* 5000 *mg. An accuracy of about* 1·5 *mg or* 0·75% *of full scale was obtained for the* 200 *mg range.*

Introduction

In the course of thermogravimetric investigations it became necessary to develop an instrument which would be capable of handling a large range of weight changes. Although several conversions of ordinary analytical balances into recording instruments have been described,(1–7) the inherent limitations of each of these instruments necessitated a more extensive investigation into the properties of electromechanical transducers.(8) The transducer which was finally developed is described below.

Operating principle

The beam of the balance is rigidly connected to the central plate of a differential capacitor C_1C_2 (Fig. 1). Movements of the beam are thus translated into capacitance changes.

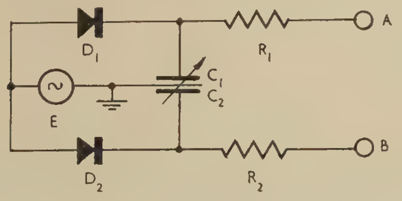

Fig. 1. Transducer circuit

D_1, D_2 = OA72 R_1, R_2 = 470 kΩ, ½ W, high stability

The differential capacitor is energized *via* two crystal diodes D_1 and D_2 by the r.f. oscillator *E*. If a movement of the beam results in an increase of C_1 and a decrease of C_2, the current through D_1 increases and that through D_2 decreases. The result of the rectifying effect of D_1 and D_2 is that a d.c. voltage is produced between *A* and *B*. If the beam moves in the opposite direction, C_1 decreases and C_2 increases and reversal of polarity at *A* and *B* takes place. The sign of the d.c. voltage thus corresponds to the sense of deflexion of the balance beam and no separate phase-sensitive rectification of an a.c. transducer output signal is therefore required.

Construction

To minimize the influence of stray capacitances the transducer is constructed in the form of a double-walled metal box. The inner box containing the diodes and resistors is kept at the r.f. potential; the outer box is earthed (Fig. 2). Connexions are made *via* the Perspex lid facing one end of the balance beam. The stationary plates of the differential capacitor measure 12 × 6 × 1 mm approximately. The distance between the plates is 6 mm. The needle-shaped central plate, measuring 35 × 2 × 1 mm, projects through a hole in the Perspex plate. This arrangement prevents excessive movement of the central plate which would result in short-circuiting of the differential capacitor.

Application in a recording balance

When a differential capacitor is used as displacement detector in an ordinary analytical balance, special precautions are required because the detector must respond only to rotation of the beam around the horizontal axis. The usual construction of agate plane and knife edge, however, permits translations of the beam over the plane as well as rotation around a vertical axis. It was found that the construction mentioned did not respond to unwanted movements of the beam.

As the changes in weight usually encountered in practice are greater than 10 mg, some form of weight loss compensation must be employed. In this instrument compensation is obtained by the force exerted by an electric current acting in the field of a permanent magnet. The "voice coil" of a loudspeaker magnet assembly was therefore attached to the end of the beam bearing the sample holder (the other end of the beam being connected to the transducer) (see Fig. 2). The current through the coil is directly proportional to the loss in weight of the sample, provided the coil moves in the homogeneous part of the magnetic field. It was possible to fulfil this condition fairly well by careful positioning of the permanent magnet. Recording of the compensating current thus forms a convenient method of obtaining a continuous record of weight changes.

In order to perform the weight loss compensation automatically, the transducer and the restoring force unit must be linked in a closed loop. One way of carrying this out is to have the output signal from the transducer generate a restoring current which is proportional to the transducer signal. The balance beam then assumes a different position for each value of the restoring current. The operation of the instrument is thus based upon the "error signal" principle.

The deviation from the initial position, required to generate the balancing current, can be made extremely small (of the order of a few thousands of a millimetre) by employing a high-gain servo-amplifier. This is an essential condition to retain proportionality between restoring current and change in weight.

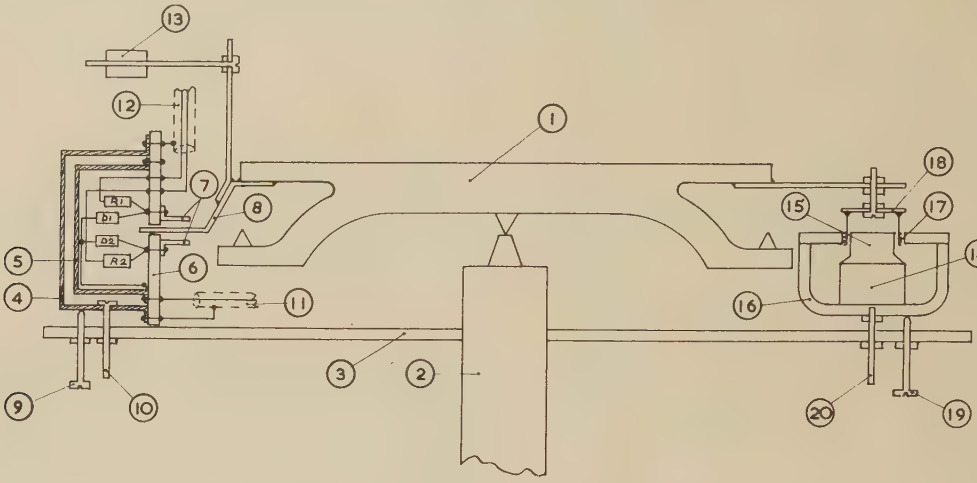

Fig. 2. Construction of transducer and restoring force magnet assembly

(1) beam (drawn schematically); (2) central column (drawn schematically); (3) base plate; (4) outer box; (5) inner box; (6) Perspex lid; (7) stationary plates; (8) central plate; (9) adjusting screws (three); (10) locking screw; (11) shielded cable to oscillator output; (12) shielded cable to amplifier input; (13) counterweight; (14) permanent magnet; (15) pole piece; (16) yoke; (17) "voice coil"; (18) "voice coil" bearer plate; (19) adjusting screws (three); (20) locking screw

Oscillator and servo-amplifier

The r.f. oscillator (Fig. 3) operates at 12 to 15 V, 2 Mc/s approximately. The use of one of the diode plates of V_6 permits an easy control of the output voltage.

The circuit-diagram of the high-gain starvation-type d.c. amplifier is shown in Fig. 4. The restoring force coil (resistance 3 Ω) requires about 4·5 mA/g. It is shunted by R_{34} to bring the total current consumption to 5 mA/g or 1 mA for 200 mg. This produces 10 mV output over R_{35} for the 200 mg full-scale deflexion range. For the lower ranges (i.e. 10, 20, 50 and 100 mg full-scale deflexion) the restoring force coil is shunted by R_{25} to R_{28}; for the higher ranges (i.e. 500, 1000, 2000 and 5000 mg full-scale deflexion) R_{35} is shunted by R_{29} to R_{32}. The values of R_{25}, R_{26}, R_{29} and R_{30} deviate from the calculated values because of the internal resistance of the generator V_3V_4.

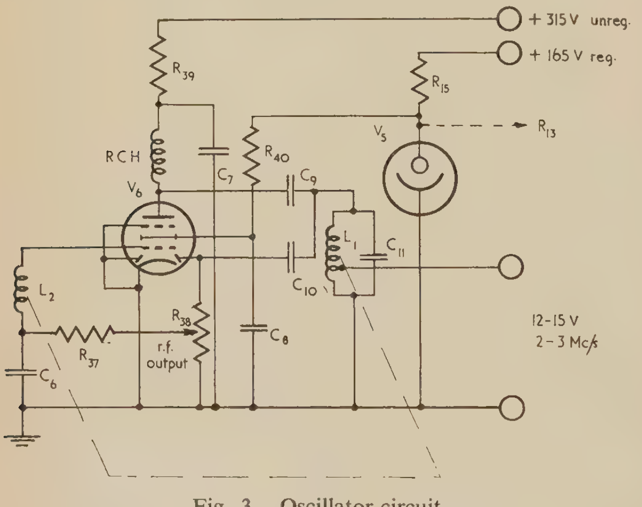

Fig. 3. Oscillator circuit

R_{37} = 75 kΩ, ½ W carbon
R_{38} = 500 kΩ potentiometer
R_{39} = 18 kΩ, 1 W carbon
R_{40} = 25 kΩ, ½ W carbon

C_6 = 47 pF mica, 350 V
C_7, C_8 = 0·01 μF paper, 250 V
C_9 = 100 pF mica, 350 V

C_{10} = 47 pF mica, 350 V
C_{11} = 68 pF mica, 350 V

L_1 = 100 μH, tap 1 : 1
L_2 = ¼ of number of turns of L_1 on same former
RCH = 2·5 mH, r.f. choke
V_6 = EBF 80

A microswitch S_1, operated by the arresting-mechanism of the balance, short-circuits the output of the transducer in the arrested position, thereby preventing overloading of the amplifier.

A 0–10 mV strip chart recorder was used to record the weight loss and the furnace temperature. It appeared necessary to filter the output from R_{35}. To prevent an excessive increase in response time of the recorder, the RC-time of the filter $R_{36}C_5$ cannot be made as large as would be required to obtain completely smooth curves. For a given RC time a small value of R and a large value of C is desirable to keep the output resistance to the recorder at a low value.

An electronically stabilized power pack was used for the anode supply voltage and additional stabilization was provided by V_5.

Performance

The accuracy and proportionality between restoring current and change in weight were checked by placing known weights on the balance pan and observing the recorder-pen deflexion. The results for the 200 mg range (Table 1) showed that the accuracy is about 1·5 mg or 0·75% of full scale. Further, that the desired proportionality between restoring current and change in weight was achieved.

Of the numerous analyses carried out with this instrument two examples are quoted below.

1. *The dehydration of copper sulphate.* It was claimed by Taylor and Klug and others(9, 10) that during the dehydration of copper sulphate the intermediate compound $CuSO_4 . 3H_2O$ is formed. The existence of this compound is not generally

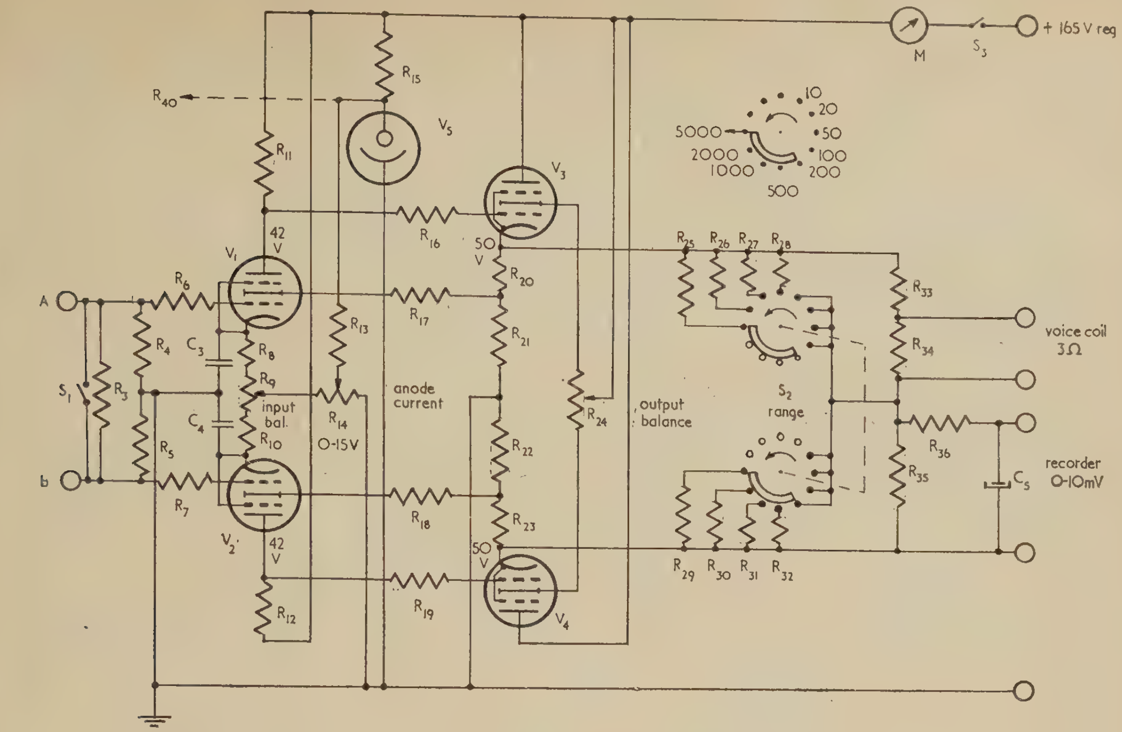
+ 165 V reg
M
S3
R40
R15
V5
R11
V3
10
20
50
100
200
500
1000
2000
5000
42 V
V1
R16
50 V
R20
R25 R26 R27 R28
R33
A
R6
R17
R13
R21
voice coil 3Ω
R4
C3
R8
R34
S1
R3
R9
input bal.
anode current
output balance
S2 range
C4
R14 0-15V
R24
R5
R10
R22
R36
recorder 0-10mV
b
R35
C5
R7
R18
R23
V2
42 V
50 V
R29 R30 R31 R32
R12
R19
V4

Fig. 4. Amplifier circuit multipoint digital temperature recorder

R_3 = 2·2 MΩ, ¼ W carbon
R_4, R_5 = 10 MΩ, ¼ W carbon
R_6, R_7 = 150 kΩ, ½ W carbon
R_8 = 33 kΩ, ½ W carbon
R_9 = 25 kΩ potentiometer
R_{10} = 33 kΩ, ½ W carbon
R_{11}, R_{12} = 3·9 MΩ, 1 W carbon
R_{13} = 220 kΩ, 1 W carbon
R_{14} = 50 kΩ potentiometer
R_{15} = 15 kΩ, 1 W carbon

R_{16} = 10 kΩ, ¼ W carbon
R_{17}, R_{18} = 150 kΩ, ¼ W carbon
R_{19} = 10 kΩ, ¼ W carbon
R_{20}–R_{23} = 500 Ω, 5 W w.w.
R_{24} = 5 kΩ potentiometer, w.w.
R_{25} = 0·26 Ω w.w., manganin
R_{26} = 1·2 Ω w.w., manganin
R_{27} = 5 Ω w.w., manganin
R_{28} = 10 Ω w.w., manganin
R_{29} = 0·434 Ω w.w., manganin

R_{30} = 1·263 Ω w.w., manganin
R_{31} = 4 Ω w.w., manganin
R_{32} = 6·66 Ω w.w., manganin
R_{33} = 7·35 Ω w.w., manganin
R_{34} = 22·8 Ω w.w., manganin
R_{35} = 10 Ω w.w., manganin
R_{36} = 100 Ω, 1 W carbon

C_3, C_4 = 0·5 μF paper, 250 V
C_5 = 2000 μF, electrolytic 12 V

V_1, V_2 = EF40
V_3, V_4 = 6Y6
V_5 = 85 A2

S_1 = microswitch
S_2 = nine position range switch
S_3 = single-pole, single-throw toggle switch

M = 0–150 mA

Table 1. *Calibration of balance*

On balance pan (mg)	*Calculated from chart (mg)*
20	19·4
40	40·0
60	60·0
80	80·6
100	100·6
120	122·0
140	143·0
160	162·8
180	183·0

accepted. The authors' results, however (Table 2), are in agreement with those of Taylor and Klug.

Although a good plateau was not obtained a marked change in the rate of weight loss was observed at 95° C and this point was used to calculate the loss in weight. This loss agreed well with that calculated for the compound $CuSO_4 . 3H_2O$.

2. *The decomposition of quinoline phosphomolybdate.* This compound is formed as a precipitate in the gravimetric analysis of phosphate using the method of Wilson.(11) It is therefore required to know at which temperature this precipitate can be dried without undergoing a change in composition. The results obtained (Table 3) indicated that quinoline phosphomolybdate decomposes according to the reaction equations:

$$(C_9H_8N)_3PO_4 . 12MoO_3 \rightarrow (C_9H_8N)H_2PO_4 . 12MoO_3 + 2\,C_9H_7N$$

and: $$2(C_9H_8N)H_2PO_4 . 12MoO_3 \rightarrow P_2O_5 . 24MoO_3 + 2\,C_9H_7N + 3\,H_2O$$

Conclusions

Initially some difficulty was experienced in alining the transducer and the magnet assembly and also in matching the amplifier to different recorders. After these difficulties

Table 2. *Dehydration of copper sulphate*

Plateau	*Decomposition temperature (° C)* *started*	*completed*	*Compound*	*Weight loss (%, cumulative* *theoretical*	*found*
1	50	95	$CuSO_4 . 3H_2O$	14·43	14·84
2	95	125	$CuSO_4 . H_2O$	28·87	29·44
3	205	270	$CuSO_4$	36·08	36·96
4	640	850	CuO	68·14	69·40

Table 3. *Decomposition of quinoline phosphomolybdate*

Plateau	*Decomposition temperature (° C)*	*Compound*	*Weight loss (%, cumulative)* theoretical	*Weight loss (%, cumulative)* found
1*	(200)	$(C_9H_8N)_3PO_4 . 12MoO_3$	—	(29·61)
2	∼360	$(C_9H_8N)H_2PO_4 . 12MoO_3$	11·67	11·87
3	∼450	$P_2O_5 . 24MoO_3$	18·73	18·85

* Loss of water from wet precipitate completed at about 200 °C.

had been overcome, however, the instrument has given reliable service over a period of about one year.

An accuracy of about 1·5 mg or 0·75% of full scale was obtained for the 200 mg range.

Acknowledgements

The authors wish to thank Messrs. African Explosives and Chemical Industries, Ltd., for permission to publish this paper. They are also greatly indebted to Mr. A. Lensink for carrying out the construction and checking of the electronic apparatus and to Mr. C. S. Bergström for performing the thermogravimetric analyses.

References

(1) Bartlett, E. S., and Williams, D. N. *Rev. Sci. Instrum.*, **28**, p. 919 (1957).

(2) Garn, P. D. *Analyt. Chem.*, **29**, p. 839 (1957).

(3) Groot, C., and Troutner, N. H. *Analyt. Chem.*, **29**, p. 835 (1957).

(4) de Keyser, W. L. *Bull. Soc. franc. céram.*, **20**, p. 2 (1953).

(5) Mauer, F. A. *Rev. Sci. Instrum.*, **25**, p. 598 (1954).

(6) Waters, P. L. *Nature* (*London*), **178**, p. 324 (1956).

(7) Wendlandt, W. W. *Analyt. Chem.*, **30**, p. 56 (1958).

(8) van der Breggen, J. C. To be published.

(9) Taylor, T. I., and Klug, H. P. *J. Chem. Phys.*, **4**, p. 601 (1936).

(10) Schultz, R. D., and Dekker, A. O. *J. Phys. Chem.*, **60**, p. 1095 (1956).

(11) Wilson, H. N. *Analyst*, **76**, p. 65 (1954).

Ratiometer phase angle indicator

by K. L. MORPHEW, M.Sc.(Eng.), A.M.I.E.E., Electrical Engineering Department, The University, Southampton

[*Paper first received* 25 *January and in final form* 4 *April*, 1960]

Abstract

The principle of the moving coil ratiometer is described together with the circuit used with it for phase angle measurement. The mode of operation, performance, adjustment, and calibration are given.

Introduction

The principle of the ratiometer is essentially that of a permanent-magnet moving-coil instrument with two separate coil windings. When the coil pivots are, conventionally, in the middle of the ends of the coil, the angular movement is limited to about 90° Another form of construction, as used in the Sangamo Weston ratiometers,(1) employs two separate coils, pivoted about one side, with the other side free to move in a long, radially directed magnetic field, as shown in Fig. 1. This permits an angular coil movement of about 270°, and also allows control of the scale calibration by using shaped pole pieces.

In normal use, the ratiometer coils are joined at one end to the d.c. supply, while one of the other ends is connected to a variable resistor, Fig. 2*a*. Alternatively, both free ends may be joined as in Fig. 2*b*. In practice the moving coils have shunts and series resistors fitted in the instrument case to make the instrument stable and to limit currents to the right magnitude. The torques of the coils are in opposition. This means that control springs are not required, for when the coils carry equal currents, and if the pole faces are similar, the movement will rest mid-way between the ends of the air gap.

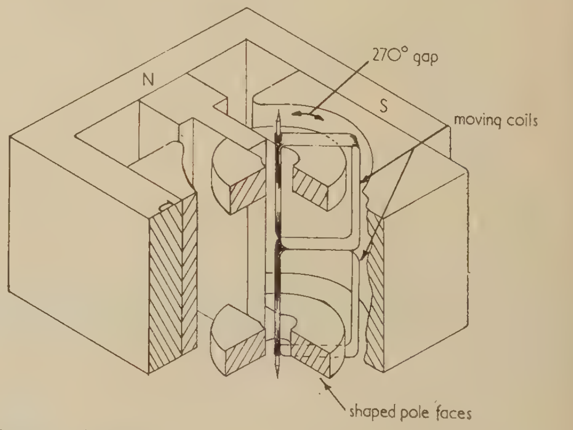

Fig. 1. Construction used in Sangamo Weston ratiometer

Description

A ratiometer of this type has been used as a phase-angle indicator by making it compare two alternating currents, one of which is used as a reference of phase angle. The urrents have to be rectified before the ratiometer will spond, and the resulting circuit, Fig. 3, shows what is in fect a form of phase-sensitive bridge. The reference phase from the supply E, and, from it, half-wave rectified currents

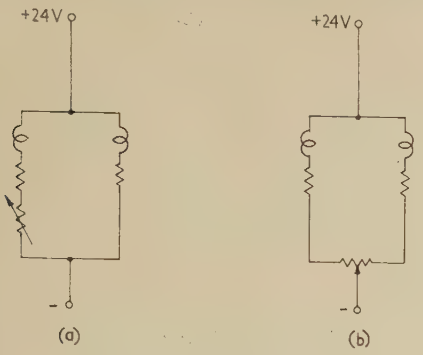

Fig. 2. Ratiometer coils

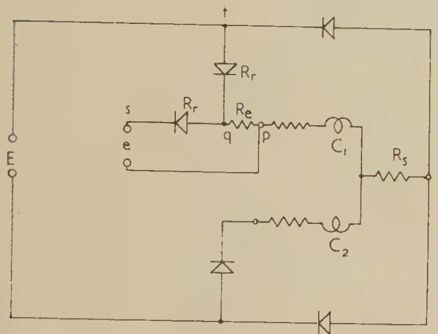

Fig. 3. Rectifying circuit

low through the two ratiometer coils C_1 and C_2. Coil C_1 s joined to the external resistor R_e, which in other appli-ations is varied with the quantity being measured. In this ase, it carries rectified current from e, the supply of a.c., the hase of which is to be measured with reference to E.

Operation

(*a*) When points s and t are in phase and positive, the current through R_e will be due to E alone. This current passes through C_1 together with any small current which passes round qsp due to E overcoming e in that circuit.

(*b*) When points s and t are in phase and negative there wil be no current due to E, except through C_2, but e can drive a current through R_e and also through C_1. Thus R_e carries consecutive half waves of current in opposite directions and the upper trace in Fig. 4*a* shows this. The lower trace in Fig. 4*a* is the potential difference across the rectifier in series with e, both sides of which are positive in (*a*), and which offers a low resistance in (*b*).

(*c*) When s and t are in antiphase, with t positive, the current in R_e will be low because e and E are in series *via* *tqsp*; but the current in C_1 will be greater than in (*a*).

(*d*) When t is negative in case (*c*), then s will be positive and there will be no current in R_e nor in C_1. This is shown by the flat portions in the upper trace of Fig. 4*c* which correspond in time to the complete half-waves of the potential difference across the rectifier shown in the lower trace.

The traces in Fig. 4*b* are clearly of a stage midway between conditions (*a*), (*b*) and (*c*), (*d*). The current, I_2, in C_2 is virtually constant, the small fluctuation being due to the voltage drop across the series resistor (R_s) which will be affected by changes in I_1.

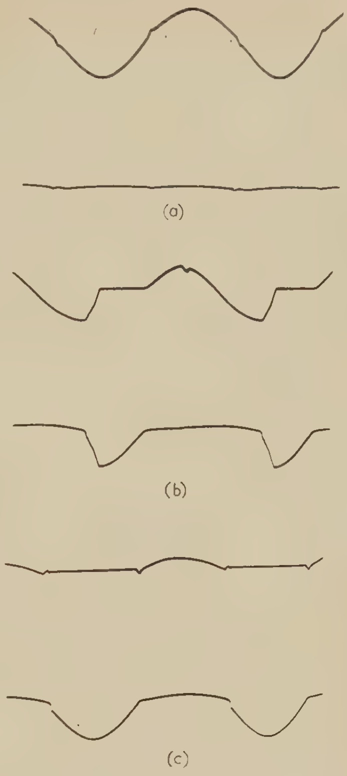

Fig. 4. Variations of potential in rectifier circuit
(*a*) $\phi = 0°$; (*b*) $\phi = 90°$; (*c*) $\phi = 180°$

Adjustment

The current I_2 in the coil C_2 is effectively constant and the torque it provides acts like a control spring. The current I_1 in C_1 determines the position of the pointer and the ratio of I_{1max} to I_{1min} is called the *overall ratio* in the maker's literature. Centre-scale indication obtains when I_1 equals I_2 for the instrument used. By ignoring the circuit of C_2 the connexions to R_e may be redrawn as shown in Fig. 5. If the rectifiers are assumed to have linear characteristics, then the

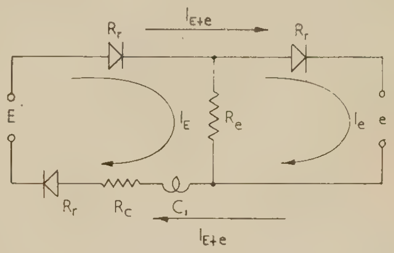

Fig. 5. Currents in phase comparator circuit

equations may be written, using instantaneous values of current and voltage:

$$E \sin \omega t = (I_E + I_{E+e})(2R_r + R_c) + (I_E - I_e)R_e \qquad (1)$$

$$e \sin (\omega t + \phi) = (I_e + I_{E+e})R_r + (I_E - I_e)R_e \qquad (2)$$

$$E \sin \omega t + e \sin (\omega t + \phi) = (I_E + I_{E+e})(2R_r + R_c) + (I_e + I_{E+e})R_r) \qquad (3)$$

Now these expressions are only true when $0 > \omega t > \pi$. Furthermore, the solutions for E, e and $(I_E + I_{E+e}) = I_1$ require to be obtained as mean values, as the currents determine the coil torques. This is a cumbersome process. It is more effective to find the value of $I_1 = I_2$ by adjusting R_e when e is open-circuited and the pointer is at mid-scale. Then with e connected and set to $\phi = 90°$ phase shift with respect to E, R_e should be readjusted to bring the pointer back near to mid-scale. The pointer positions should be checked with $\phi = 0$ and $\phi = 180°$, making small adjustments each time. By using this process, iteratively, the most desirable value of R_e will be quickly obtained.

Many ratiometers have a "no-signal" device which will hold the pointer at one end of the scale when the supply potential is below about one half of the nominal value. The author found it necessary to render this ineffective.

Performance

The instrument used was a Sangamo-Weston ratiometer with a 270° pointer movement and a centre-zero scale calibrated linearly from −6 to +6 in steps of 0·2 division. It was found possible to use the whole scale for a phase shift of 180° by adjusting R_s to 600 Ω with e equal to 3·75 V and E equal to 24·5 V.

The calibration was done by supplying e from the rotor of a Muirhead "Selsyn" which had a guaranteed accuracy of ±0·25° angle. Changes of 1° in the phase of e were easily detected and would have been measurable had the scale been more finely divided. The accuracy of calibration depended upon the three-phase supply to the Selsyn having an angle of 120° between the phases. This was tested by measuring the inter-phase angular separation by means of a precision Gall–Tinsley a.c. potentiometer. The three-phase mains used was usually within 0·5° of 120° and variations of this order did not introduce significant errors in the calibration curve (Fig. 6). An artificially large inter-phase angular shift of 4·5° in one phase was produced by introducing an inductor into the Selsyn stator circuit. The effect on the calibration is shown by the dotted line.

The instrument was calibrated at a frequency of 50 c/s. Simultaneous changes in the frequency of E and e of ±10% did not affect the calibration, and it is reasonable to suppose that the indicator will operate over a wide frequency band, as does the Sangamo–Weston ratiometer frequency meter.

Tests were made to determine the effect of harmonic distortion in e, with E remaining sinusoidal. To the given value of e were added, separately, 10% of the 3rd, 5th, 7th, and 9th harmonics. In each case, the pointer varied by ±0·35 divisions according to the phase angle between e and the added harmonic. At harmonics above the 9th, the pointer fluctuation decreased, becoming imperceptible at the 25th harmonic. Fluctuations of 4% in the supply produced changes of only 2° in indicated phase angle. In general, the pointer response was rapid and sensitive, but the performance of the indicator would have been improved had there been some air-damping vane to steady the movement and pointer.

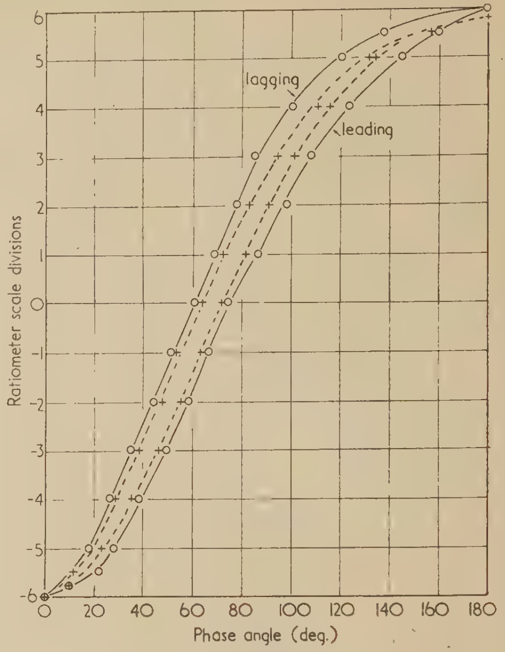

Fig. 6. Calibration curve
. . . balanced supply, —— unbalanced supply

As is well known, the non-linear character of the phase-sensitive bridge rectifier may produce different signals for a given phase shift according to whether the angle is leading or lagging. This is also true of the ratiometer circuit and accounts for the form of the calibration curve.

References

(1) Brit. Pat. 567435/1945.

(2) Hague, B. *A.C. Bridges*, p. 567 (London: Pitman and Sons Ltd., 1946).

(3) de Gruchy, J. *Trans Soc. Inst. Tech.*, **2**, p. 3 (1950).

(4) Bell, J. "Data Transmission Systems", *J. Instn Elect. Engrs*, **94**, IIA, p. 221 (1947).

(5) Lamson, H. W. *Proc. I.R.E.*, **28**, p. 541 (1940).

Transistor operation of electromechanical registers

by J. C. Barton, B.Sc., Ph.D., Northern Polytechnic, London, N.7

[*Note received* 13 *April*, 1960]

he usual method of operating an electromechanical device a transistor circuit is to make it the collector load for one a pair of transistors connected as a univibrator. An ternative technique of adding a second winding so that the vice may be operated in a blocking oscillator circuit has ree advantages: (*a*) only one transistor is needed; (*b*) the urrent drain is extremely small except when actually ounting; and (*c*) there is no need to stabilize the circuit gainst voltage and temperature variations.

The diagram shows a circuit which has been used for perating electromechanical, "Post Office", registers. The rcuit is stable without including a capacitor in the base connexion, which is fortunate as a very large capacity would be needed. The circuit operates successfully with the recently introduced S.T.C. 5-digit register type 59-LAA-1AA (G.P.O. type 150), as well as with earlier types. In the former case the most satisfactory windings are 5000 turns for the collector and 2000 turns for the base, each of 38 g synthetic enamelled wire. Under these conditions the circuit can be used with any supply voltage between -6 and -18 V and is stable up to at least 35° C. The maximum counting rate is about $6\,\mathrm{s}^{-1}$ at -9 V and rather more at higher voltages. The circuit may be triggered by a negative pulse on the base or a positive one on the collector. One unit has now been in use for over a year without attention.

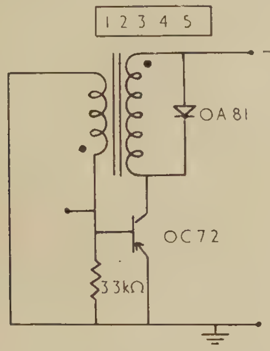

Circuit used for operating electromechanical registers

It has been stated by Chaplin and Williamson* that it is impossible to operate registers as blocking oscillators because the time constant of the driving coil is too short. These authors seem to have overlooked the fact that the pulse length of a blocking oscillator can be several times longer than this time constant. For the circuit described the collector coil time constant is 23 ms but the pulse length, at -9 V, about 55 ms. A theoretical analysis shows that the ratio of these times is about what would be expected.

This type of circuit should also be useful for the operation of other electromechanical devices such as relays and control valves.

---

* Chaplin, G. B. B., and Williamson, R. *Proc. Instn Elect. Engrs*, **105 B**, p. 231 (1958).

Cut-off for the vacuum manipulation of chlorine

by M. Green, Ph.D., and K. H. Maxwell, Ph.D., Zenith Radio Corporation, Chicago 39, Illinois, U.S.A.

[*Note received* 14 *March*, 1960]

In a recent study of the interaction of gaseous chlorine with clean germanium surfaces(1) it was necessary to have a device which could function as a high vacuum "stop-cock". Such a "stop-cock" has been developed and used for some time. A brief description of the device and its characteristics is given in this note.

The device is basically a cut-off using fused silver chloride. It has been known for some time(2) that silver chloride forms a vacuum-tight seal with glass. Stasiw and Teltow(3) and Mitchell(4) point out that the wetting of glass by molten silver chloride, and the adhesion of the solid to glass, requires the presence of silver oxide at the interface. The cut-off, made from Pyrex glass, is drawn to scale in the figure. A stick of cast silver chloride was placed in the upper reservoir *A*, and, with the cut-off in a near horizontal position, gently melted under vacuum. This operation served to degas the silver chloride. The cut-off was then ready for use. The device was operated in the following manner. A small amount of silver chloride was melted, whereupon it flowed down to the capillary and solidified (*B* in the figure). The top two-thirds of the silver chloride thread was carefully remelted, using a hand torch (pointed "air–gas" flame). The thread solidified starting from the bottom, and formed a solid thread of silver chloride which was leak-tight. If, as sometimes happened, there was a chain of bubbles or a fine thin dark line running up the silver chloride thread, the silver chloride was remelted until a section of thread was free of any visible flaws. To open the cut-off, the silver chloride thread and the glass down to point *C* were gently warmed, whereupon the silver chloride flowed easily into the lower

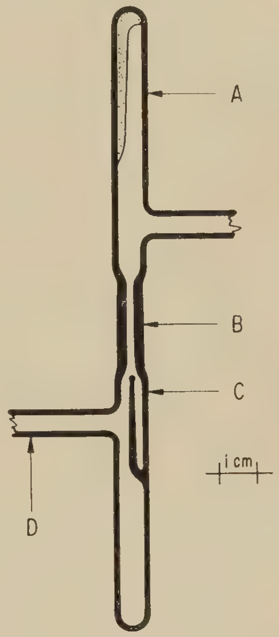

Scale drawing of silver chloride cut-off
Diameter of capillary tube = 1·5 mm

reservoir. The cut-off was used many times before a fresh charge of silver chloride was required.

The outgassing characteristics of a new silver chloride cut-off were determined, using a VacIon pump(5) to measure the total amount of gas desorbed. (The VacIon pump is a titanium ion pump, working on the principle of the Penning gauge, and was obtained from Varian Associates of Palo Alto, California.) The melting of the whole silver chloride stick was accompanied by the evolution of approximately 20 mm–cc of gas (1 mm–cc $\equiv 3{\cdot}2 \times 10^{16}$ gas molecules at 27° C). About 10^{-1} mm–cc of gas came off when some of the silver chloride was melted and flowed into the capillary to form a plug. Remelting about two-thirds of the plug and measuring gas evolution on side *D* gave approximately 10^{-2} mm–cc of gas. The room temperature outgassing rate was such that the pressure was less than 10^{-8} mm of mercury with a VacIon pump having a maximum pumping rate of 1 l/s.

REFERENCES

(1) Green, M., and Maxwell, K. H. To be published.

(2) Strong, J. *Procedures in Experimental Physics*, p. 557 (New York: Prentice-Hall Inc., 1939).

(3) Stasiw, O., and Teltow, J. *Z. Anorg. Chem.*, **257**, p. 109 (1948).

(4) Mitchell, J. W. *Progress in Semiconductors*, **3**, p. 56 (London: Heywood and Co., 1958).

(5) Hall, L. D. *Rev. Sci. Instrum.*, **29**, p. 367 (1958).

Test tube adaptor for use in optical density measurements

by J. B. Dawson, Ph.D., Dept. of Medical Physics, The General Infirmary, Leeds 1

[*Note received* 18 *January*, 1960]

Many of the photoelectric colorimeters and spectrophotometers in current use employ "matched test tubes" to contain the solution under test. Such tubes, while having the advantage of economy, lack reproducibility of optical density readings when compared with the more expensive plane-faced "fused glass cells". The reproducibility of the "test tube" cell may be improved by using the same tube oriented in the same position for all readings, but this is inconvenient where it is desirable to develop and read the colour without transfer to another tube.

The relatively poor reproducibility of the "test tube" cell appears to be due to irregularities in the shape and thickness of the wall of the tube; such irregularities will produce deviation of light by refraction at the glass surface.

The adaptor illustrated in the figure minimizes refraction at the outer surface of the test tube by immersion of the tube in toluene, the refractive indices of glass and toluene being almost identical (1·52 and 1·50 respectively). As the adaptor forms, in effect, a parallel-sided cell and is common to every measurement, the reproducibility of measurement is considerably improved. The effect of the internal surface cannot be eliminated in the same manner but as, in general, the liquids contained have a refractive index of 1·3 or greater, refraction at this interface should not be serious.

Commercial adaptors have been produced having windows with plane outer and concave inner surfaces matching the curvature of the test tube, but with no provision for liquid filling; in our hands this type of adaptor gave no improvement in reproducibility over the tube without an adaptor.

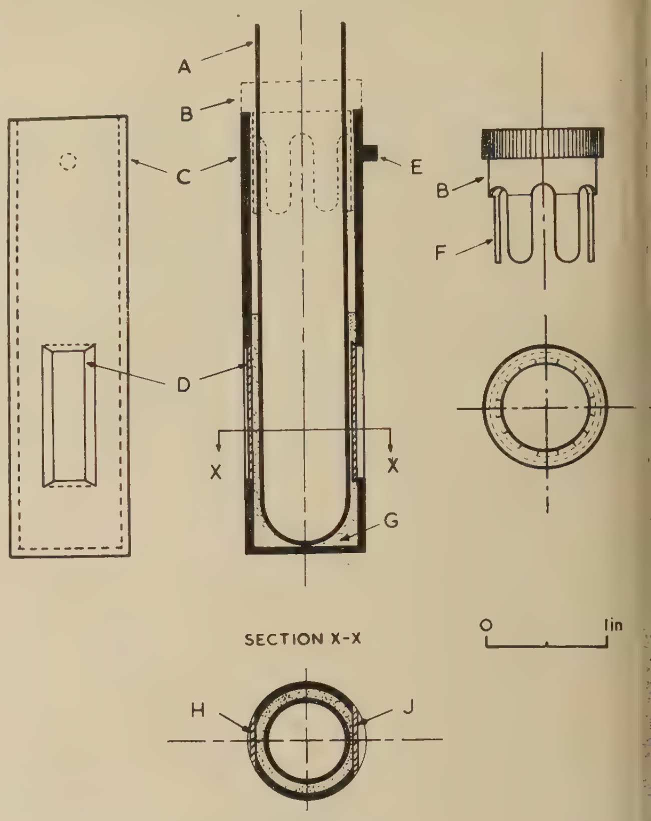

Test tube adaptor

A, test tube; *B*, test tube locator; *C*, brass tube; *D*, glass window dovetailed into brass tube and cemented with Araldite; *E*, locating spigot; *F*, spring support for test tube; *G*, toluene; *H*, front window; *J*, rear window

The reproducibility of optical density measurements with and without the two types of adaptor has been examined using the Unicam S.P. 400 spectrophotometer and the results are summarized in the accompanying table.

Reproducibility of optical density measurements

Type of adaptor	*Standard deviation expressed as percentage of the mean. 1 observation on each of 10 tubes*	*Standard deviation expressed as percentage of the mean. 10 observations on the same tube in different positions*
None	1·25	1·00
Commercial	1·5	0·75
Liquid-filled	0·5	0·5

The liquid-filled adaptor described has been in regular use for the last three years and has been found to be quite satisfactory. Although the adaptor was designed for use with the Unicam S.P. 400 spectrophotometer the principle should be applicable to other colorimeters and spectrophotometers.

I am indebted to Dr. A. Hodgkinson of the Medical Research Council's Unit for Metabolic Disturbances in Surgery who posed the problem and for his helpful comments on this note, and to Mr. S. Taylor of the Department of Medical Physics who constructed the adaptor.

Simple high temperature X-ray camera

by G. Farrow, Ph.D., B.Sc.(Tech.), and D. Preston, Research Department, Fibres Division, Imperial Chemical Industries Ltd., Harrogate, Yorkshire

[*Note received* 7 *March*, 1960]

uring some recent work on polyethylene terephthalate and her related polymers* it became necessary to obtain X-ray fraction patterns of samples at high temperatures. In order do this a simple high temperature furnace, particularly itable for polymer specimens, which could be used with a nicam S. 25 standard X-ray goniometer was constructed. he whole assembly is shown in the figure.

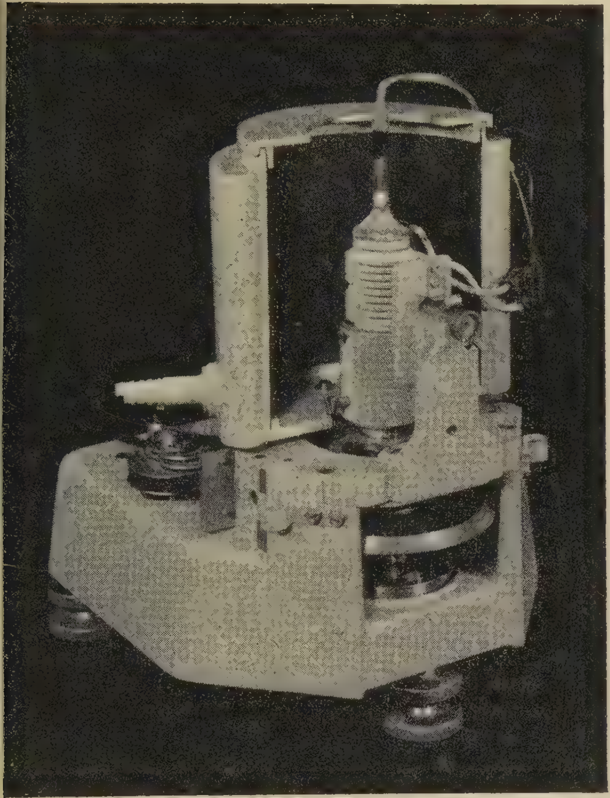

Simple high temperature X-ray camera

A material known as Agalain (from Geo. Bray and Co. Ltd.) was used for the construction of the furnace. It is a naturally occurring block material which is readily machined and easily workable. When fired at 1200° C—the maximum working temperature—there is an increase in tensile strength. The furnace has an outside diameter of 1·3 in. and an nternal chamber diameter of 0·625 in. The height is approximately 1·75 in.

The heating elements consisted of Brightray resistance wire, hreaded through silica thermocouple tubing and controlled by a Variac transformer. They were arranged vertically and concentrically, in the internal chamber of the furnace, around the specimen. Two of the six silica tubes were approximately one-third the length of the other elements in order to allow the entry of the collimator and the fitting, diametrically opposite, of a beryllium window (0·005 in. thick, 0·625 in. in diameter); which was sufficiently wide to allow the passage of the principal X-ray reflexions of any polymer. The heating elements and window were fixed into position with a refractory cement; the top of the furnace was sealed with a lid of Agalain through which was threaded a copper/constantan thermocouple used to measure the temperature of the specimen. The base of the furnace was sealed with a disk of Agalain having a 0·125 in. diameter hole passing through its centre to allow adjustment and movement of the specimen mount. Cooling fins were machined on the outside of the furnace.

To enable the furnace to be used with the Unicam goniometer (see figure) a brass base of identical size and dimensions to the base of the 6 cm X-ray camera normally used with this goniometer was made. Fitted to this was a threaded column and screwed onto this a knurled collar to carry the furnace. Height adjustment of the furnace with respect to the X-ray beam was carried out by means of the knurled collar. The correct radial orientation was achieved by turning the furnace in the machined seating at the top of the collar and then locking it by two screws.

The central spindle of the goniometer had a small collett chuck mounted on it which was capable of holding a range of stainless steel tubes of small diameter (0·5 to 3·0 mm). These tubes served as specimen holders, height adjustment being carried out by viewing the sample through the collimator aperture and altering the height accordingly.

The film holder (see figure) of 11·46 cm diameter locked into position on the Unicam goniometer. Cold water was circulated through the cooling jacket fitted to the outside of the holder to keep the temperature of the film down to 20° C. The beam trap fitted diametrically opposite the collimator was of tubular construction and designed to reduce the amount of air scattered radiation reaching the film.

The high temperature camera was successfully employed to take X-ray diffraction photographs from room temperature up to 270° C. Temperatures were held to within ±1° C.

---

* Bateman, J., Richards, R. E., Farrow, G., and Ward, I. M. *Polymers*, **1**, p. 63 (1960).

Stabilized high-intensity light source

by C. M. Hurd, B.Sc., Department of Physics, University of Hull

[*Note first received* 23 *February, and in final form* 29 *March*, 1960]

An ex-cinema carbon-arc lamp has been modified to provide, for periods up to 40 min, a light beam of up to 48 cm^2 cross-sectional area in which the fluctuations lasting longer than 2 s are less than 4% of the total intensity. Previous attempts to stabilize d.c. carbon-arc lamps have resulted in either constant arc current$^{(1, 2)}$ or constant arc power.$^{(3)}$ In this laboratory and elsewhere$^{(4)}$ it has been shown that constancy of the arc current does not necessarily mean constancy of the light intensity.

In this controller the position of each carbon rod tip is automatically maintained throughout burning to within 0·005 cm. This is achieved by projecting, with a magnification of ×20, a side view of the arc on to a screen. The light from part of the image of a rod is passed through a vertical slit in the screen and focused on to a photoelectric cell. This cell is part of a tetrode-thyratron on/off circuit in which the rod driving motor is connected. As the rod burns away the movement of its image alters the light intensity at the photocell and switches on the driving motor. The rod is driven forward at a greater rate than that at which it is burning away until it reaches its initial position. A movement of less than 1 mm of either image is sufficient to actuate the appropriate motor switch. Each rod is controlled separately in this way. This control alone is sufficient to produce for limited periods (up to 5 min) a light-beam in which the fluctuations lasting longer than 2 s are less than 3% of the total intensity. To obtain stabilized running for longer periods, and at a predetermined level, a further control is added in the form of an intensity-sensitive reversing switch, controlling the motor-driven Variac which supplies the rectifiers feeding d.c. to the arc. The reversing switch is a simple optical-arm arrangement, the galvanometer current being supplied by a photomultiplier tube in the light beam. A change of less than 2% in the intensity is sufficient to actuate the appropriate switch.

Under normal conditions between 40 and 50 A d.c. are passed through the Morganite "Flamex" carbon rods. It is found that it is the reduction of the diameter along the length of the rods which limits their lifetimes. The rods and the basic Kalee "Vulcan" arc unit were not designed to meet anything approaching the rigorous specifications for light-sources used in research. It has thus been shown that by simple methods such equipment can be modified to give satisfactory service. Fig. 1 shows a typical record of light intensity against time obtained with this system. The part of the record shown was chosen because it shows the effect upon the intensity of the introduction of the intensity-sensitive device. At *A* the arc is 24 min old; between *B* and *C* the intensity-sensitive device is not actuated; at *D* the limits set by this device are seen as the galvanometer light-beam oscillates from one switch to the other due to insufficient damping. Acknowledgements are due to Prof. G. F. J. Garlick who has supervised this work, to Mr. N. Taylor for attention to mechanical design problems, and to the Department of Scientific and Industrial Research for a Research Studentship.

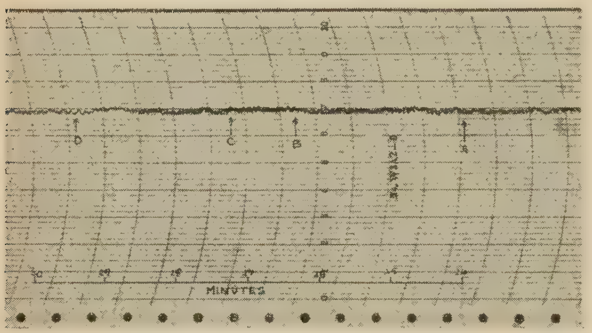

Part of a typical record of light intensity against time

REFERENCES

(1) Smith, D. M., and Wiggins, G. M. *Analyst*, **74**, p. 95 (1949).

(2) Potter, E. V., and Scott, A. *Rev. Sci. Instrum.*, **18**, p. 722 (1947).

(3) Gersing, R. *Z. Wiss Mikr*, **63**, p. 257 (1957).

(4) Dieke, G. H., Loh, H. Y., and Crosswhite, H. M. *J. Opt. Soc. Amer.*, **36**, p. 185 (1946).

Simple detector for small leaks using a thoriated tungsten emitter with oxygen as probe gas

by R. N. Bloomer, A.Inst.P., and W. C. Brooks,
Associated Electrical Industries Ltd., Research Laboratory, Harlow, Essex

[*Note received* 20 *April*, 1960]

It is well known that the thermionic emission of electrons from some cathodes is changed by the presence of even a partial monolayer of gases like oxygen. Thoriated tungsten filaments are very sensitive to such gases(1) and can be used in a leak detection method, applicable to well-baked high vacuum systems, in which oxygen is used as a probe or jacket gas, replacing air entering through any remaining leaks.

The sensitivity of the device depends upon the temperature of the filament, for this determines both the extent of the coverage of the tungsten by a monatomic layer of thorium and the rest time t of adsorbed gas on the surface (as given by the Frenkel formula $t = t_0 \exp - E/kT$ where E is the binding energy on a substrate with lattice vibration period t_0 at a temperature T° K, and k is Boltzmann's constant). Following Langmuir(2) the procedure is known for attaining and maintaining a thorium coverage of the tungsten surface, and with filaments of known diameter the necessary temperatures for thorium diffusion can be controlled by the heating currents(3) used. Initially, and normally once only,(4) the filament temperature is raised to 2800–2900° K for 5–15 s, to reduce thoria to thorium. Then the temperature is kept at about 2400° K and emission current drawn until this steadies, before lowering the filament temperature to the best operating value for the conditions of particular leak detections.

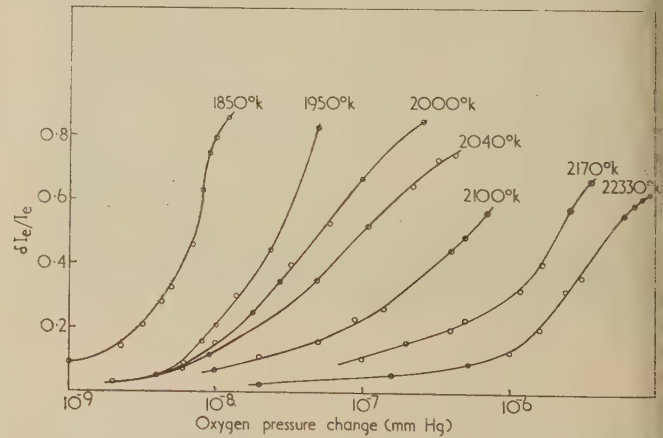

Variation of sensitivity to oxygen pressure changes for various filament temperatures

The condition, or sensitivity, of the leak detector is conveniently defined by the fractional change $\delta I_e/I_e$ in the emission current I_e from the filament. [In a leak detector diode the anode for collecting the current can be of any convenient shape. For example, a piece of thicker wire can be placed near enough to the hottest part of the filament so that at modest voltages (<100 V) the current flow is limited by the filament temperature.] The greatest sensitivity is at temperatures just below about 1900° K, when the tungsten surface is partly covered with thorium, such as can be obtained when only leaks of 10^{-6} l. μ/s or less are remaining in a well-baked system pumped at a speed of 0·1 l./s. A lesser sensitivity, adequate for the detection of leaks of order

$^{-5}$ l. μ/s at a speed of pumping of 0·1 l./s, is obtained at nperatures higher than about 2000° K, when the surface of e tungsten is covered with a monolayer of thorium. As ell as filament temperature, the pressure of oxidizing gases so influences the coverage of the surface by thorium. The gure is a plot of typical sensitivities for different tempera- res and pressures, of a short filament of diameter 0·005 in. is seen that higher sensitivities are obtained at lower mperatures as the pressure is reduced. Furthermore, in der to obtain the highest sensitivity in a search for the nallest leaks, the setting and control of the filament heating rrent has to be done increasingly exactly as the vacuum nditions improve and the filament temperature is reduced.

A warning must be given about a third state, of very low nsitivity, in which leaks less than 0·1 l. μ/s at speeds of umping 0·1 l./s can go undetected. This occurs when the ament becomes carburized. It is because of the danger of is happening in the presence of hydrocarbon vapours and the like, and because of the influence of residual water vapour upon the emission of electrons from the thoriated tungsten, that the detector is not suitable for use in unbaked apparatus. If it should happen that a filament becomes carburized accidentally it must be replaced: no thermal treatment cycle will bring it to a sensitive state again. But in a well-baked system thoriated filaments can, if necessary, always be restored to a desired state of sensitivity again and again by a short period of running at a temperature of about 2400° K.

REFERENCES

(1) Nottingham, W. B. *Phys. Rev.*, **49**, p. 78 (1936).
(2) Langmuir, I. *Phys. Rev.*, **22**, p. 357 (1923).
(3) Ribaud, G., and Nikitine, S. *Ann. Phys.* (*Paris*), **7**, p. 5 (1927).
(4) Schneider, P. *J. Chem. Phys.*, **28**, p. 675 (1958).

CORRESPONDENCE

Foam viscometer

oams for fire-fighting use are non-Newtonian fluids, and s such cannot be compared in terms of their coefficients of iscosity. When subjected to a steady rate of shear they do, owever, exhibit a well-defined critical shear stress; after the nitial shear at the critical stress, a lower constant value, enerally referred to as the "continuous shear stress", can e measured. The critical shear stress is used in the study of re-fighting foams, as it is closely related to the specific urface of the foam and is a measure of its surface energy. t gives also a good indication of the flow properties of the oam.

These shear stresses are measured at the Joint Fire Research Organization by means of a torsional-vane viscometer described in this paper. The instrument has been developed rom an earlier type in use for the past fifteen years, which was itself derived from the instrument used by N. O. Clark* at the National Chemical Laboratory.

The present form of the foam viscometer consists essentially of a rotating torsion wire and vane which can be made to dip into a stationary bowl containing the foam sample (see igure).† The torsion wire and vane are rotated by a motor and gearbox in the head of the instrument, and these are arranged to slide on a vertical column, against the tension of a long phosphor-bronze spring. The torsion wire and its enclosing tube are fixed to the downward-facing gearbox spindle, and the lower end of the tube carries a circular scale, held to it by a friction device for adjustment purposes. It also carries a stainless-steel bearing, which has two narrow ands spaced about 1½ in. apart to give a low-friction bearing for the stainless-steel spindle on which the vane is mounted. This spindle carries a weight to keep the wire taut and a pointer adjacent to the circular scale. The vane itself is a ¼ in. square of 18 s.w.g. stainless steel. The sliding head is fitted with adjustable stops which can be set so that, when the head is depressed, the vane is just fully immersed in the foam sample, the container for which is made of brass, 4 in. in diameter and 3 in. deep.

The size of the torsion wire can be selected to give an instrument constant suitable for the range of critical shear stresses being measured. In the instrument described here, the torsion wire was made of steel piano wire, 0·016 in. in diameter × 9·7 in. effective length giving a constant of 3·5 dyn/cm^2 per degree (480 dyn/cm^2 is equivalent to

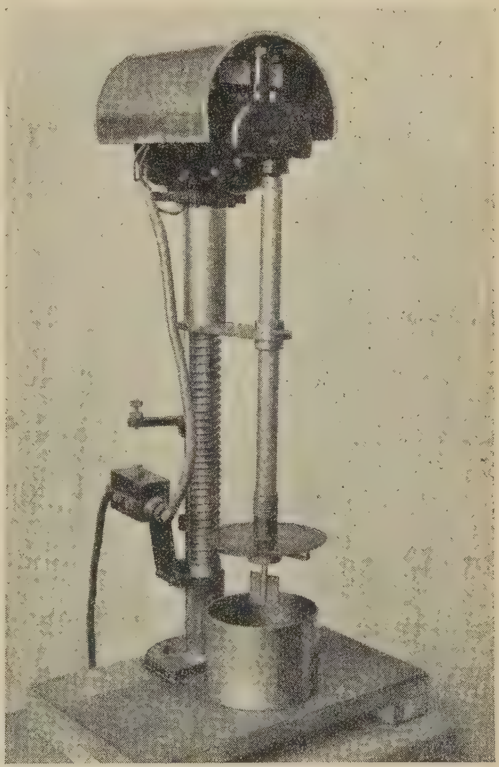

---

* Clark, N. O. *Chemistry Research Special Report*, No. 6 London: H.M. Stationery Office, 1947).

† Copies of the working drawing of the viscometer are available rom the Joint Fire Research Organization.

1 lb/ft^2). On one version of this instrument, a microswitch is arranged to start the motor just as the vane becomes immersed. In a later version, a manual switch is fitted. The speed of rotation of the torsion head is 8·5 rev/min.

This instrument has certain advantages over those formerly used, namely:

1. Rapid determinations can be made; it is possible to take a reading only ten seconds after collection of the foam.
2. The wire, being enclosed, is not unduly subject to corrosion and has been found to retain its characteristics over a period of at least three years.
3. No sliding mechanism is required in the drive system.
4. The electrical gear is above the foam container so that there is the minimum chance of its becoming wet.

The instrument described in this paper was designed as part of the programme of the Joint Fire Research Organization of the Department of Scientific and Industrial Research and Fire Offices' Committee; the paper is published by permission of the Director of Fire Research.

Department of Scientific and
Industrial Research and Fire
Offices' Committee Joint Fire
Research Organization,
Boreham Wood,
Hertfordshire.

R. J. French
[4 *May*, 1960]

NOTES AND NEWS

New instruments, materials and tools

The Editor invites manufacturers of instruments and light machine tools to keep him informed of their new or improved products. The Institute of Physics assumes no responsibility for the statements given below: information for these has been taken from literature supplied.

Transistor output power meter. Dawe Instruments Ltd., 99 Uxbridge Road, London, W.5.

This meter is designed to measure the output power of audio oscillators, amplifiers, and networks and source impedances of equipment operating in the range from 10 c/s to 50 kc/s. The instrument measures output power by providing between its input terminals a resistive load of high power wire-wound resistors for the equipment under test. Forty values of the resistance between 2·5 Ω and 20 kΩ can be switched into circuit by rotary switches. The voltage across the selected load resistor forms the input of the transistor amplifier which drives the meter circuit. A variable attenuator is ganged to the resistance selector switches to give a direct reading of output power, irrespective of the setting of the selector switches. A four-position "power-range" switch extends the power scale from 0·1 mW to 10 W in four ranges. An auxiliary calibration shows the power level in decibels with reference to a level of 1 mW.

It is stated that, unlike designs using a multi-range transformer, the accuracy of ±0·5 dB on the ×1, ×10, ×100 ranges and ±1·0 dB on the ×1000 range (from 20 c/s to 20 kc/s) is unaffected if direct current is superposed on the a.c. signal through the load.

The source impedence of the equipment under test is determined directly by adjusting the resistance (impedance) selector switches until a load is found which draws maximum power from the source. Accuracy of measurement of the source impedance is ±2% from 20 kΩ down to 20 Ω, and ±5% below 20 Ω.

The instrument is fully transistorized, thus eliminating warm-up delay, so that the instrument can be switched on and off intermittently. Dry batteries last approximately 700 h operation, and a test position of the supply switch indicates when the batteries need renewing. The overall dimensions are 6 × 5 × 11 in.

Blood pressure follower. Winston Electronics Ltd., Shepperton, Middlesex.

This apparatus, type 1108, measures blood pressure by the use of a finger cuff instead of the conventional arm cuff or arterial cannulation. It records pressure continuously by a dial in the front panel, a mercury sphygmomanometer, and on a heat-sensitive chart calibrated from 0–300 mm of mercury, giving visible indication of pressure being too high or too low. The top section of the apparatus is a self-contained unit with built-in power supply. It is portable and can be detached and used as a separate unit. With the additional use of the control panel the equipment can be used to control the infusion of hypo- or hypertensive drugs into a patient. The panel operates an alarm system if blood pressure is above or below pre-set levels.

Scintillation counter. Ekco Electronics Ltd., Southend-on-Sea, Essex.

This scintillation counter has been produced for use on the laboratory bench. Beta emitters, including tritium and carbon 14, are immersed in a liquid phosphor for counting, whilst gamma emitters are enclosed in a thallium-activated sodium-iodide crystal. A high-gain amplifier, for which good overload characteristics are claimed, is included in the unit.

For counting from the liquid, the lead-shielded well is fitted with a shutter/sample holder assembly, enabling the sample pot to be loaded into the instrument while the photomultiplier is covered by an interlocked light-tight shutter. When the shutter is closed, the photomultiplier shutter interlock is released. The sample pot is then automatically lowered directly on to the photomultiplier face when the lead cover is closed; no intermediate glass window is fitted, so that the optical coupling between the sample pot and photomultiplier is as close as possible. The sample chamber is shielded in all directions by 2·5 cm of lead.

For gamma counting, the sample may be prepared (*a*) in a test tube, (*b*) in a polythene annular container, or (*c*) in a 50 ml. flat beaker. It can then be counted for (*a*) in a well crystal, (*b*) with a small crystal, or (*c*) with a 1½ in. diameter crystal. The shutter assembly used for liquid counting is replaced by a top-plate assembly on which the crystals are mounted. Lifting the counterbalanced lead lid exposes the crystal for sample changing.

w-drift d.c. amplifier. The Solartron Electronic Group Ltd., 45 Thames Street, Kingston, Surrey.

is d.c. amplifier with a wide frequency band range has n designed for the distortion-free amplification of very /-level signals from transducer sources such as pressure k-ups, thermocouples, and photocells. It is also stated be particularly useful for medical research, and numbers already in use in the development of earth satellite trumentation in the U.S.A.

GAIN
SOLARTRON

Low-drift d.c. amplifier

The band width is from direct current to 40 kc/s, the ceptionally low equivalent input drift is less than 2 μV in) h, and the gain factor is from 20 to 1000 in nine steps. he low drift and noise achieved have been possible, it is aimed, by the use of advanced negative feedback techniques, ıcluding continuous "chopper" correction. Noise and round loop problems are minimized by holding the common oltage rail above the chassis, and the input above the ominal earth.

recision vernier d.c. potentiometer. Doran Instrument Co. Ltd., Stroud, Gloucestershire.

t is stated that this potentiometer measures from 1 μV to ·899 99 V in two ranges. The main dial has eighteen steps f 0·1 V each; the second dial comprises ninety-nine steps f 0·001 V and is a vernier on the first, and the third ninety-ine steps of 0·000 01 V. The reading of the potentiometer ials is given directly by observation windows on the cover anel.

Standardization of the instrument is effected by balancing standard cell against an auxiliary potential divider, which as a range of adjustment from 1·018 00 to 1·019 00 V. This djustment, which is carried out by means of the coarse and ne rheostats provided, may be made without disturbing the etting of the potential dials and checked at any time without nterrupting a test. The instrument is intended for use with n external galvanometer, a standard cell and a 2 V accumulator, the latter supplying the potentiometer current. The circuit is arranged so that two e.m.f.'s in turn can be measured by a selecting switch.

The terminals are of copper, the potentiometer network of aged manganin and the switch contacts of precious metal; all of which are stated to ensure that there is a low temperature coefficient of resistance and low thermal e.m.f.'s. The galvanometer tapping switch is of the dual pressure type, a light pressure connecting the galvanometer to the circuit through a protective resistance, and further pressure giving direct contact to the galvanometer.

The dimensions of the instrument are 23 × 13½ × 8½ in.; it is claimed to have a high accuracy of measurement and long-term stability.

Speed regulator for compressed air. Baldwin Instrument Co. Ltd., Dartford, Kent.

A speed regulator has been developed for use with the compressed air cylinders produced by this firm. It is claimed to have a regulation capable of a more accurate setting than the earlier model, but is of the same micrometer type. The bore sizes are ¼, ½, ¾, and 1 in. The model is slightly larger, and utilizes the same two-piece construction as its predecessor. The regulator is of anodized duralumin, and has a friction device incorporated to prevent the micrometer adjustment from slipping due to vibration.

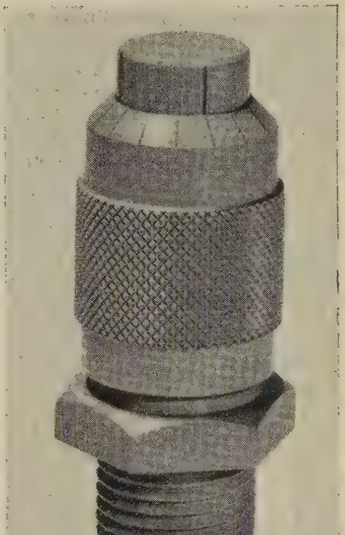

Speed regulator for compressed air cylinders

Where the speed of the air jet is required to be different in different directions of projection, it is claimed that the unit forms a simple means of producing this. It screws directly into the exhaust ports of the directional control valve, and thereby throttles the escape of air from the exhaust end of the cylinder. This method of speed regulation is claimed to be satisfactory where steadiness of motion is required.

All these regulators are made to conform to nominal bore size, and should be sealed to the valve body by a soft metal washer, or bonded seal. The maximum working pressure is 150 lb/in^2.

Tong-type a.c. detector. Dawe Instruments, Ltd., 99 Uxbridge Road, London.

The clip-on probe of this instrument permits the detection of current in a conductor without interrupting the circuit. Unlike many instruments of this type, the probe has been reduced to the dimensions of a large crocodile clip and is mounted at the end of a flexible lead to make it possible to insert it in otherwise inaccessible positions.

The clip-on probe forms the secondary of a transformer, where the single-turn primary is the conductor carrying the current. It is claimed that negligible impedance is reflected back into the circuit under test and special feedback arrangements provide a voltage output proportional to the primary current over the whole frequency range from 10 c/s to 200 kc/s. After amplification, the signal is fed to the output of the instrument, and then to a valve voltmeter for measurement of current or to a cathode-ray oscilloscope for monitoring the waveform. A wide current range is given by the sensitivity control, the three settings providing an output of 1 V for an input of 50 mA, 1 and 20 A. The maximum output is 1 V into 10 kΩ and the accuracy is 3% above 1 mA.

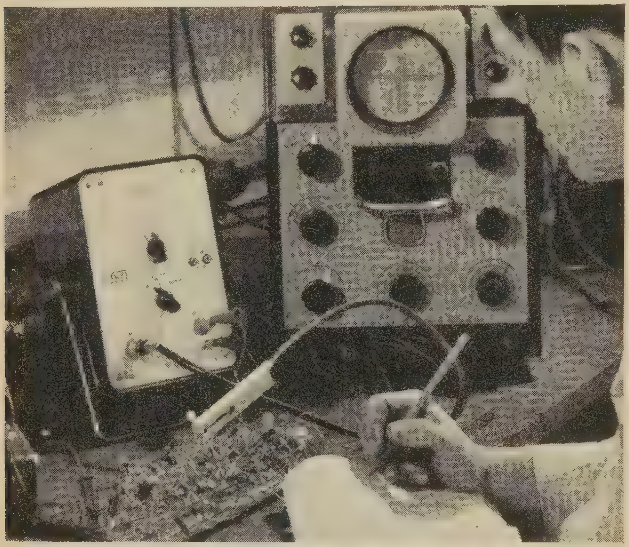

Tong-type a.c. detector

The instrument is applicable to transistor and other semiconductor circuits, in which current is of greater importance than voltage, as, for instance, measurement of short-circuit gain in transistors. There are also obvious advantages for printed circuits, where unsoldering is undesirable. It can be used for null measurements on a.c. bridges, or current measurements in magnetic amplifier circuits.

The instrument is fully transistorized and may be mains- or battery-operated, a dry battery lasting 50 h of operation. The dimensions are 6 × 5 × 11 in. approximately.

Servo-multiplier. The Solartron Electronic Group Ltd., 45 Thames Street, Kingston, Surrey.

It is claimed that this servo-multiplier (also available as a resolver) will operate with less than 1° phase lag at full-scale amplitude up to 10 c/s. It permits multiplication of up to five analogue variables by one other variable, or the generation of up to the sixth power of one variable. A six-section potentiometer is standard, one section having additional taps for the connexion of loading resistors to achieve special functions of a variable. In the servo-resolver there are five potentiometer sections, three linear, and two conforming to the sine/cosine law.

Both these non-linear computing units are entirely self-contained and incorporate highly efficient transistorized power supplies. Thus the units may easily be incorporated into existing computer installations using a mounting unit; or they may be operated independently, directly from the mains supply.

The instrument uses 110 or 220 V power supply and its ambient temperature limit is about 100° F; a cut-out is incorporated to guard against damage in the event of fan failure or excessive temperature. The dimensions are 5¾ in. wide, 7 in. high and 16½ in. long.

Sensitive hygrometer. Shaw Moisture Meters, Rawson Road, Bradford, Yorks.

The hygrometer is intended as a means of checking the humidity of "dry" gases such as those in drying ovens and those used in the chemical and semiconductor industries. It consists of a detecting instrument and a measuring unit. The principle is as follows. The small detecting element consists of a capacitor with a hygroscopic dielectric only a few microns thick, with 24 carat gold electrodes. The variation in capacitance caused by the alteration of the moisture content of this dielectric is indicated on the dial of the measuring unit. The detector is contained in a strong fine-wire gauze protector which plugs into a coaxial cable connecting it to the recorder. It is 1 cm in diameter and 6 cm long, and can be used with any length of cable. Two types of elements are available: (*a*) the "ordinary", which operates between temperatures of −50 and 150° C, and has a humidity range of 10–80% at room temperatures; and (*b*) the "sensitive", which is suitable for dewpoints of −130° C to −20° C; the temperature range is the same as before.

It is claimed that the "ordinary" type will detect the change in humidity between ground level and 4 ft above the ground. The sensitive type will record one part of water vapour per million parts of gas, and is suitable for testing the efficiency of dessicants, where it will detect the difference between the operation of P_2O_5 and silica gel. Further, the time lag is only of the order of a second, and so rapid changes in humidity can be measured and recorded. Both elements are available with ambient and pressure-type mountings.

Four modifications of the measuring unit are available: (1) indicating, (2) recording, (3) recording and controlling, and (4) adjustable alarm.

This hygrometer with its immediate response, stable characteristics and provision for easy checking and standardization, as well as remote reading, is claimed to be essentially robust and reliable, and to operate in adverse climatic conditions. An individual calibration of the element supplied is provided with each instrument.

Air velocity indicators. Shandon Scientific Co. Ltd., 6 Cromwell Place, London, S.W.7.

The larger of these two instruments is circular with a die-cast housing 4 in. in diameter and 1¾ in. deep. The rotating peripheral scale 8 in. long gives direct readings in ft/min or miles/h. Two-scale reading are available, 0–1000 ft/min and 0–3000 ft/min, the latter scale bearing also miles/h markings. The readings are automatically averaged over an area 3 in.

diameter, and the accuracy is within 2% of the full-scale ding. A zero adjustment is provided.

In operation the instrument is simply held in the air eam and the reading taken. The rotor is magnetically mped to level out insignificant variations in velocity, and ing the scale rapidly to rest. A scale lock is provided so at when the instrument is in an inaccessible place, as when ld on a long extension rod, its reading can be preserved. e instrument is suitable for ventilating engineers and for ecking flow conditions in exhaust pipes, cooling air, etc., d for laboratory work.

Air velocity indicator

The smaller type is a pocket instrument, 4⅝ × 2⅞ in. having 2¼ in. long scale graduated in divisions from 0–1000 ft/min. is entirely self-contained and requires no auxiliary fittings. works on the deflecting vane principle, the air entering rough a small hole in the base of the plastic case. A zero djustment is provided. It is claimed that the instrument is s simple to use as a pocket compass, and is particularly uitable for checking and balancing in heating, ventilating nd other air-circulating systems.

agnetic tape data recorder. The Solartron Electronic Group Ltd., 45 Thames Street, Kingston, Surrey.

his standard data recorder using magnetic tape is designed pecifically for industrial applications, and is intended as a omplement to a former precision data system made by the rm which is already applied generally in research and uided weapon instrumentation.

The present data recorder is a scaled-down version of the ormer instrument and is intended for the many applications here extreme refinement is not needed. It is smaller and ore movable and employs direct 50 c/s mains synchroniza- ion; it incorporates precision-machined plate and tape drive- ssemblies, together with separate record-reproducing ampli- ers for each channel. These last two parts are directly nterchangeable with those in the precision instrument.

The instrument has seven (or fourteen) record and seven or fourteen) reproducing channels; it takes approximately 000 ft of tape, weighs 750 lb, and has dimensions 5½ ft high, ½ ft wide and 2½ ft deep.

Gauge-quality cabinet projector. Watson, Manasty and Co. Ltd., Orleans House, Manor Road, Teddington, Middlesex.

This instrument is a portable cabinet projector, with a high optical accuracy. It can be employed in either a vertical or horizontal position. Two magnifications of ×10 and ×25 are obtained with interchangeable lenses. The table for holding the specimen has a glass insert on which the specimen is placed, supported on a slide. Standard charts for the measurement, in addition to mechanical measuring facilities, are supplied by the firm.

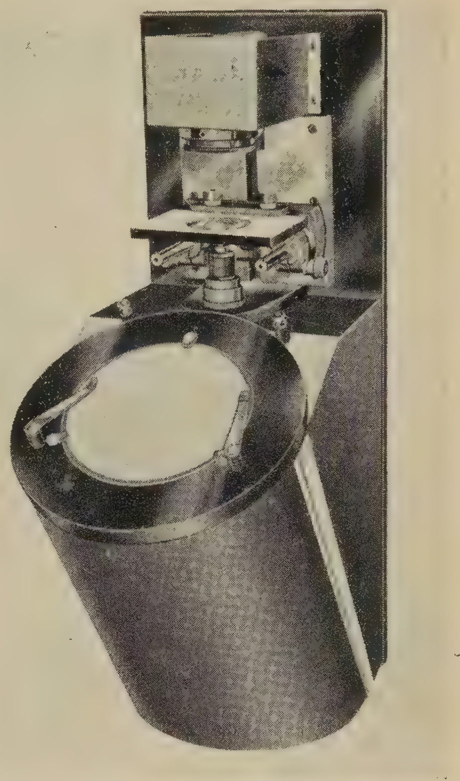

The projector design with vertical table

It is stated that one of the chief applications has been the inspection of screw thread forms, including Whitworth, B.A., etc. The screw is mounted in the fixture and compared to a standard on a chart. It is claimed that the optical system is designed for the highest fidelity of reproduction, so that the inspection of small parts may be made with precision and confidence. The screen is 6 in. in diameter and the instrument is 28 in. long.

Rhenium. Chase Brass and Copper Co., Waterbury 20, Conn., U.S.A.

Wrought rhenium, in the form of rod, wire, and strip is now in commercial production by this firm. It is an extremely dense, silver-coloured metal, forming an engineering material with a high melting point and high strengths at elevated temperatures. With a melting point of 3180° C, surpassed only by tungsten and carbon, rhenium finds important applications in the highly critical measurement and control aspect of high-temperature technology. Thermocouples of rhenium and tungsten, for instance, make possible the measurement and control of temperature up to 2500° C.

Rhenium itself is not a structural metal, but it seems to be a good welding material for molybdenum and research on this is proceeding. Tests over extended periods have shown that molybdenum-rhenium alloys have considerable advantages over the pure metals; they have better mechanical properties than pure molybdenum and are cheaper than rhenium.

The metal is stated to have excellent electrical properties, and is considered to be extremely reliable as a material for electrical components. It is claimed that for certain applications in electronic equipment, electrical contacts of rhenium have a life expectancy of twenty times that of the material currently being used. It is wear resisting, offers greater stability to high-temperature arcing, as well as having the resistance to corrosion of the precious metals. It is suitable for filaments and structural components of cathode-ray tubes, for at room temperatures it allows working and welding, and has a high purity. It is also suitable for the metallic components of vacuum gauges.

The following data is given: density, 21·0 g/cm^3; melting point 3180° C; thermal expansion $6\cdot7 \times 10^{-6}$ per deg. C; and modulus of elasticity, $4\cdot7 \times 10^{13}$ dyn/cm^2.

Notes and comments

Elections to The Institute of Physics

The following elections have been made by the Board of The Institute of Physics:
Fellows: W. Ashhurst, V. Balashov, G. A. Bell, J. G. Campbell, J. H. Coupland, D. E. Davies, L. W. Davies, M. Davis, R. Jones, R. D. Lowde, G. B. F. Niblett, D. W. Pashley, W. G. H. Schwietzke, S. P. Thong. H. Tunley.
Associates: J. E. Allen, D. W. Ballentyne, G. G. Bowman, E. A. Braun, A. F. C. Brown, L. D. Brown, J. R. Butler, R. W. Cotterhill, J. Daley, R. R. Davis, G. E. H. Deadman, M. E. Delany, N. Gerald, M. J. Goodman, W. A. Heslop, H. Hofer, A. Hood, R. Hughes, F. W. E. Jackson, G. J. Johnson, K. V. Krishna Rao, A. G. Little, H. Lockett, M. C. Lovell, N. A. Lynch, A. F. McFarlane, M. H. McTaggart, G. A. Manning, I. F. Mayer, J. I. Missen, A. O'Connor, N. J. Peacock, R. Phillips, M. R. Piggott, B. Pounder, R. R. Preston, J. B. Rich, G. W. Rowe, M. C. Sexton, D. Shaw, G. R. Sothern, R. C. Spragg, F. S. Ward, P. G. Williams, J. A. Woodward.

Thirty-five Graduates, twenty-six Students and four Subscribers were elected.

Isotope Information Bureau

The United Kingdom Atomic Energy Authority has recently opened an Isotope Information Bureau at its London Office in Charles II Street, S.W.1. This bureau has been established to provide industry with a convenient central point of enquiry when seeking information on the production and uses of radioisotopes. A display in the bureau outlines developments in the industrial applications of radioisotope and informative catalogues and other literature provide a more detailed account of the work which is, and has been, proceeding in the field.

A qualified staff in constant attendance can provide visitors with a basic introduction to the industrial uses of radioisotopes and can specify reference works for study by those with further interests. Enquirers can be placed in touch with the appropriate departments of the Authority in those cases where detailed information is sought.

Information and advice is provided by the bureau free of charge.

British Journal of Applied Physics

Contents of the August issue

CONFERENCE REPORT

Summarized proceedings of a conference on some aspects of magnetism, Sheffield, September 1959. By R. S. Tebble and D. E. G. Williams.

PAPERS

Gaseous diffusion in porous media. Part 1.—A non-steady state method. By J. A. Currie.
Gaseous diffusion in porous media. Part 2.—Dry granular materials. By J. A. Currie.
Contact electrification of semiconductors. By W. R. Harper.
Rolling-sphere viscometer for structured liquids. By G. W. Scott Blair and J. C. Oosthuizen.
Observations of the magnetization reversal process in thin films of nickel-iron, using the Kerr magneto-optic effect. By M. Prutton.
Skeleton strength and critical porosity in set sulphate plasters. By K. K. Schiller.
Calibration of manganese and gold foils for relative neutron flux measurements. By K. G. Stephens and W. M. Cooper.
Interpretation of γ-ray scintillation spectra from fission-product mixtures. By D. H. Peirson.
Measurement of crystallinity in drawn polyethylene terephthalate fibres by X-ray diffraction. By G. Farrow and D. Preston.
Variable ultrasonic water delay line. By G. W. Williams.
Wall effect in the flow of lubricating greases in plunger viscometers. By A. D. Bramhall and J. F. Hutton.
Application of photoelectric densitometry to the assessment of respirable dust samples. By A. R. Bugden, R. J. Hamilton and G. H. S. Jones.
Photo-electric method for the analysis of fluctuation records and its application to electrical noise. By J. Scott.
Effects of oil vapour contamination on the adhesion of zinc sulphide films to glass and silica. By L. Holland and S. K. Bateman.
Explanation of the enhanced arc velocity on magnetic electrodes. By P. E. Secker.

CORRESPONDENCE

Thermal transients in graphite-copper contacts. From J. A. Greenwood and J. B. P. Williamson; W. Davies.
Measurement of coupling coefficient and Q of low-Q piezo-electric ceramics. From R. M. Glaister.

THIS *JOURNAL* is produced monthly by The Institute of Physics and The Physical Society, with the co-operation of the National Physical Laboratory. It deals with the principles, construction and use of scientific instruments. All right reserved. Responsibility for the statements contained herein attaches only to the writers.

EDITORIAL MATTER. Communications concerning editorial matter should be addressed to the Editor, The Institute of Physics and The Physical Society, 47 Belgrave Square, London, S.W.1. (*Telephone:* Belgravia 6111.) Prospective authors are invited to prepare their scripts in accordance with the *Notes for Authors*. (Price 3*s*. 6*d*. including postage.)

REPRODUCTION. The Institute of Physics and The Physical Society is a signatory to The Royal Society's Fair Copying Declaration. Details may be obtained upon application from The Royal Society, London, W.1.

ADVERTISEMENTS. Communications concerning advertisements should be addressed to the agents, Messrs. George Jackson (Fleet St.) Ltd., Cliffords Inn, Fleet Street, London, E.C.4. (*Telephone:* Holborn 3611–2.)

CLAIMS FOR MISSING JOURNALS. Claims from regular subscribers to this *Journal* for missing numbers will only be considered if received within 60 days of the date of mailing plus normal outward time of transit and time for lodging the claim. Losses attributable to failure to notify a change of address or to similar omissions will not be considered.

SUBSCRIPTION RATES. A new volume commences each January. The charge is £6 per volume ($17 U.S.A.), including index (post paid) payable in advance. Single parts, so far as available, may be purchased at 12*s*. 6*d*. each ($1.75 U.S.A.), post paid, cash with order. Orders should be sent to The Institute of Physics and The Physical Society, 47 Belgrave Square, London, S.W.1, or to any bookseller.

PRINTED IN GREAT BRITAIN BY UNWIN BROTHERS LIMITED, WOKING AND LONDON

rror of rectifier-type milliammeters in low-resistance circuits

J. WILBUR-HAM, B.Sc., and W. E. K. GIBBS, B.E.E., Defence Standards Laboratories, Department of Supply,
lbourne, Australia

per first received 3 *December*, 1959, *and in final form* 22 *March*, 1960]

Abstract

though a bridge-rectifier meter indicates r.m.s. current en the current is sinusoidal, a sinusoidal voltage produces non-sinusoidal current, and hence an error in the indica- n, because the resistance of a copper-oxide rectifier is n-linear, varying as the −0·7 *power of the current. ries resistance tends to swamp the non-linearity, and the ror, calculated by arithmetical integration, is shown on nomogram relating error, series resistance and meter dication. Experiment confirms the results.*

Introduction

AN ideal meter rectifier would have zero impedance in the forward direction and infinite impedance in the reverse direction. Copper oxide rectifiers depart from is ideal in several respects, notably in that their forward sistance is not only finite but variable, becoming lower as e applied voltage is increased.(1) Other semi-conductor ctifiers also suffer from this defect and are less suitable for eters because conduction does not begin until appreciable rward voltage is applied. Copper oxide rectifiers are erefore likely to continue in use for some time and this aper deals only with this type of rectifier.

The rectifier characteristic, i.e. the variation of its resistance ith current, introduces non-linearity such that when a nusoidal voltage is applied the current waveform depends n the circuit resistance external to the rectifier (see Fig. 1).

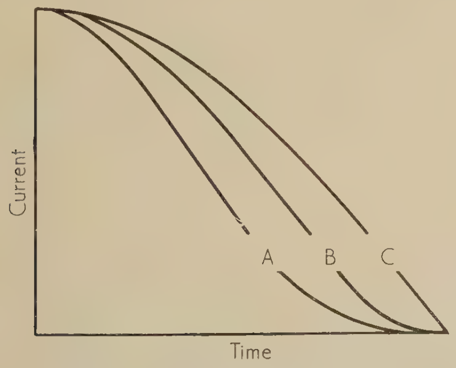

Fig. 1. Waveform of a quarter cycle of the current when the series resistance S is (A) zero, (B) R_{min} and (C) infinite

f this resistance is much smaller than the rectifier resistance, he current waveform is badly distorted from sinusoidal, lthough the voltage across the rectifier is sinusoidal. If, owever, it is much greater than the rectifier resistance, the urrent is sinusoidal with the voltage across the rectifier istorted. Between these two extremes the form factor of the current changes appreciably, as does the meter indication for the same r.m.s. current through the meter.

For this reason the meter indication is not reliable when the resistance of the circuit is low, but no accurate estimate of the error involved seems to have been made.

Resistance of a rectifier in circuit

The practical circuit is shown in Fig. 2(a), with the equivalent circuit in Fig. 2(b). The circuit to be analysed is Fig. 2(c) and the equivalent circuit is Fig. 2(d). In the diagrams E is the energizing voltage, i the instantaneous current, k the current transformer ratio, S the fixed effective series resistance (which includes the resistance of the moving coil) and R the varying resistance of the rectifier; R is equal to e/i where e is the instantaneous voltage between the bridge rectifier input terminals when the output terminals are short circuited.

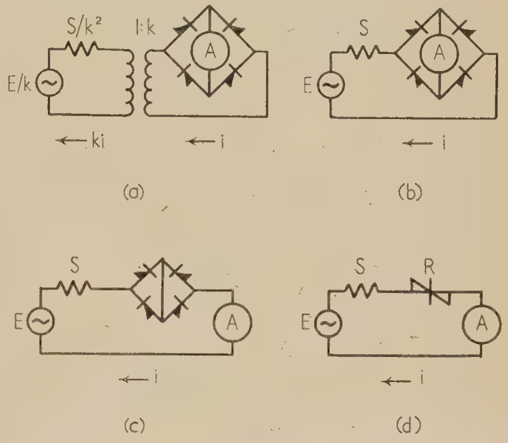

Fig. 2. Practical and equivalent circuits of an ammeter

Figs. 2(b) and (c) are equivalent for half a cycle because the current that leaks through the non-conducting elements of the rectifier is negligible. This was demonstrated by setting up the two circuits (b) and (c) and measuring the resistance of the rectifier on direct current. A fixed resistor simulated the coil of the meter in circuit (b), its value being subtracted from the measured resistance between the input terminals. The result is shown in Fig. 3. The circles were obtained with a 1 mA rectifier and a 1 kΩ resistor in circuit (b), and line A with the same rectifier in circuit (c). Similarly, the dots and line B were obtained with a 5 mA rectifier and a 100 Ω resistor.

Plotted on log-log scales as in Fig. 3, the characteristics are practically straight lines over the whole working range of the rectifiers. The gradient of the 1 mA and 5 mA lines is

$-0{\cdot}70$ and that of the 10 mA line is $-0{\cdot}74$; Hughes[2,3] in 1934 reported a gradient of $-0{\cdot}8$. Because 1 mA and 5 mA rectifiers are the more common, the gradient of $-0{\cdot}7$ will be used in the analysis that follows.

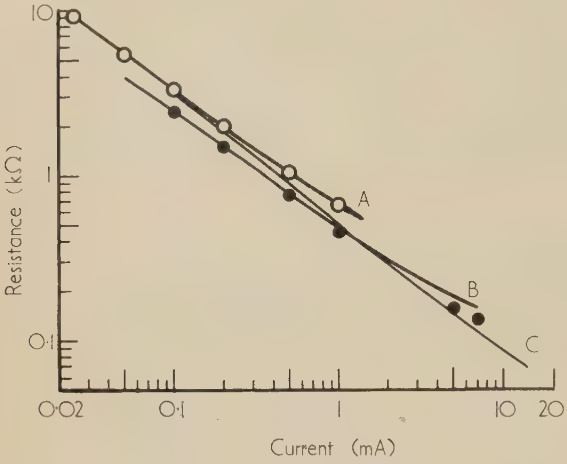

Fig. 3. Characteristics of commercial meter rectifiers rated at (*A*) 1 mA, (*B*) 5 mA and (*C*) 10 mA

Analysis

Consider an alternating current of symmetrical waveform where the instantaneous value i is related to its maximum value i_{max} by

$$i/i_{max} = n \tag{1}$$

where n is a periodic function of the electrical angle θ, which is proportional to time. Over a quarter cycle, the average current i_{av} is

$$\begin{aligned} i_{av} &= i_{max}\frac{2}{\pi}\int_0^{\pi/2} n d\theta \\ &= i_{max}P, \text{ say} \end{aligned} \tag{2}$$

and the root-mean-square current i_{rms} is

$$\begin{aligned} i_{rms} &= i_{max}\sqrt{\left(\frac{2}{\pi}\int_0^{\pi/2} n^2 d\theta\right)} \\ &= i_{max}Q, \text{ say} \end{aligned} \tag{3}$$

The form factor F is defined by

$$\begin{aligned} F &= i_{rms}/i_{av} \\ &= Q/P \end{aligned} \tag{4}$$

The meter responds to the average current, and its scale is marked in such a way that the indicated current i_{ind} is

$$i_{ind} = \phi i_{av} \tag{5}$$

When the current is sinusoidal, equations (1) to (4) yield

$$\left.\begin{aligned} n &= \sin\theta \\ P &= 2/\pi \\ Q &= 1/\sqrt{2} \\ F &= \pi/2\sqrt{2} \end{aligned}\right\} \tag{6}$$

Since in most applications it is the r.m.s. current that is required, and since the waveform is usually substantially sinusoidal, the scales of rectifier milliameters are marked on the basis of ϕ equal to $\pi/2\sqrt{2}$, that is, $1{\cdot}1107$, so that when the current is sinusoidal the indicated current i_{ind} is equal to the r.m.s. current i_{rms}.

For other waveforms the indicated current differs from the r.m.s. current. The difference or error ϵ, as a proportion of i_{ind}, is given by

$$\begin{aligned} \epsilon &= (i_{ind} - i_{rms})/i_{ind} \\ &= 1 - (F/\phi) \end{aligned} \tag{7}$$

which can be found by calculating the form factor F.

Consider the circuits of Fig. 2 when the energizing voltage E is sinusoidal:

$$E = E_{max}\sin\theta \tag{8}$$

i.e.

$$i(R + S) = i_{max}(R_{min} + S)\sin\theta \tag{9}$$

the suffixes *max* and *min* denoting corresponding maximum and minimum values in the cycle. The rectifier characteristic can be written

$$R/R' = (i/i')^{-0{\cdot}7} \tag{10}$$

where R' is the rectifier resistance at some assigned current i'. Hence from equations (9) and (10)

$$\theta = \text{arsin}\,\frac{n(n^{-0{\cdot}7} + S/R_{min})}{1 + S/R_{min}} \tag{11}$$

When this is substituted in equations (2) and (3) to obtain P and Q, the integrals cannot be evaluated analytically. However, on integrating by parts, equation (2) becomes

$$\begin{aligned} P &= 1 - \frac{2}{\pi}\int_0^1 \theta dn \\ &\simeq 1 - \frac{2}{\pi}\Delta n \sum_{j=0}^{1/\Delta n} \theta_j \end{aligned} \tag{12}$$

and similarly equation (3) becomes

$$Q \simeq \sqrt{\left(1 - \frac{4}{\pi}\Delta n \sum_{j=0}^{1/\Delta n} n_j\theta_j\right)} \tag{13}$$

These integrals can now be evaluated arithmetically by the trapezoidal rule, and hence the error ϵ may be calculated for particular values of S/R_{min}. To relate it to the indicated current i_{ind}, equations (2), (5) and (10) are combined to obtain

$$(i_{ind}/i')^{0{\cdot}7}S/R' = (\phi P)^{0{\cdot}7}S/R_{min} \tag{14}$$

where the expression on the right-hand side is a function of S/R_{min} only. The calculated error ϵ is next plotted against the corresponding values of this expression, so as to allow graphical interpolation. Finally, a convenient value is assigned to i', namely, such that $i_{ind}/i' = 1$ at full-scale deflexion.

This is the derivation of Fig. 4, which is a nomogram relating:

left, i_{ind}/i', the meter indication as a percentage of full scale;

centre, S/R', the ratio of the equivalent series resistance S (including the meter resistance) to the rectifier resistance R' (R' being measured at a direct current i' equal to the nominal meter current at full-scale deflexion, e.g. 1 mA d.c. for a 1 mA a.c. instrument);

right, ϵ, the error, i.e. the difference between the indicated current i_{ind} and the r.m.s. current i_{rms}, as a percentage of i_{ind};

for the case in which the energizing voltage E in Fig. 2 is sinusoidal.

The summations in equations (12) and (13) were evaluated h $\Delta n = 0{\cdot}05$. For sinusoidal current, when $S = \infty$, s gave $1{\cdot}1109$ as the value of ϕ, which agrees closely with true value of $1{\cdot}1107$; the former value was used in equa- n (7) when calculating ϵ.

When $S = 0$, the error is about -20%.

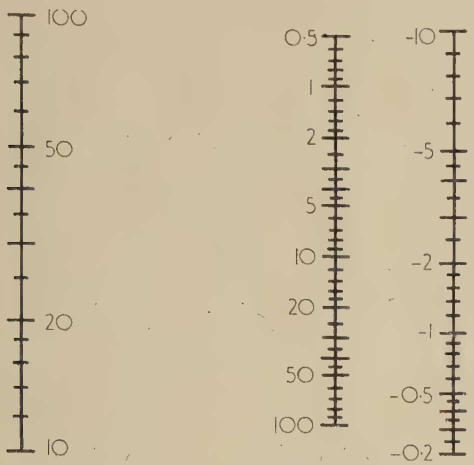

Fig. 4. Nomogram relating the meter reading, series resistance and error (see text)

Experimental confirmation

To check the analysis, a thermocouple meter, which ieasures r.m.s. current irrespective of waveform, was con- ected in series with a 1 mA rectifier meter and a resistance ox. The circuit was energized from a pure 50 c/s sinusoidal oltage source and the thermocouple meter readings com- ared for various values of resistance, the rectifier meter eading being kept constant at 1 mA by adjusting the voltage ource. The error ϵ so obtained is plotted in Fig. 5 for values f S which include the meter resistance.

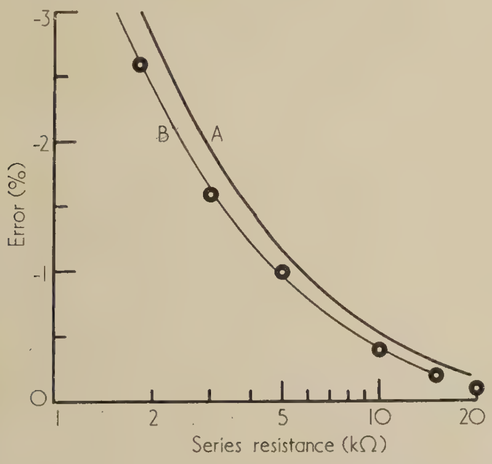

Fig. 5. Error of a meter indicating 1 mA when the rectifier resistance R' is (A) 660 Ω and (B) 550 Ω

The rectifier resistance R' was 660 Ω at 1 mA, and the iomogram predicted the error shown by curve A. Curve B, vhich is closer to the measured points, is the predicted error f $R' = 550$ Ω. The difference is of little practical importance, out it is explained if the rectifier is represented by the sum of two resistances, one obeying equation (10) (550 Ω at 1 mA) and the other constant (110 Ω). This also explains why the curves in Fig. 3 start to flatten at very high currents.

Discussion

These results are of importance in the calibration of rectifier current meters. A rectifier voltmeter does not present difficulties because it is calibrated on sinusoidal voltage and the circuit resistance, represented by its range multiplier, does not change between calibration and use. The effect of non-sinusoidal current can be seen from the non-linear scale of low-range voltmeters where the circuit resistance is not very high.

When calibrating a rectifier milliammeter, however, sufficient circuit resistance must be introduced to enforce sinusoidal current; the value in keeping with the accuracy of the meter can be obtained from Fig. 4. When a rectifier milliammeter is in use, the circuit must have sufficient resistance if the calibration is to be valid. The error given in Fig. 4 should not be applied as a rigorous correction because of the approximations involved in equation (10), the dependence of R' on temperature, and the possible uncertainty in the value of S in a practical circuit.

The turns ratio k of the current transformer reduces the resistance required in the primary circuit by a factor of k^2, so at high currents quite small resistances are ample. This is shown in the table, which was derived from Fig. 4 for the example of a 1 mA 1 kΩ moving-coil meter and a bridge rectifier for which $R' = 500$ Ω when $i' = 1$ mA. In this case no external resistance is needed to attain an accuracy of 4% because the resistance of the meter alone is sufficient.

Resistance needed in the primary circuit of a milliammeter

Range (mA)	1	10	100
Error at full-scale deflexion (%)	*Resistance in primary circuit (Ω)*		
−0·25	11 000	110	1·1
−0·5	7 000	70	0·7
−1	3 200	32	0·32
−2	1 200	12	0·12
−4	0	0	0

Instrument comprises (a) 1 mA 1 kΩ moving-coil meter, (b) 1 mA 500 Ω bridge rectifier and (c) multi-range current transformer.

Acknowledgements

This investigation was initiated and encouraged by Dr. R. E. Bauer and is published by permission of the Chief Scientist, Australian Defence Scientific Service, Department of Supply, Melbourne, Australia.

References

(1) Harris, F. K. *Electrical measurements*, pp. 418–28 (New York: John Wiley and Sons, Inc., 1952).

(2) Hughes, E. *J. Instn Elect. Engrs*, **75**, p. 453 (1934).

(3) Golding, E. W. *Electrical measurements and measuring instruments*, 3rd ed., p. 636 (London: Sir Isaac Pitman and Co. Ltd., 1940).

Daylight factor meter

by D. P. TURNER, Pilkington Bros. Ltd., St. Helens, Lancashire

[*Paper first received* 12 *February, and in final form* 20 *April,* 1960]

Abstract

A brief survey and criticism of existing methods of measuring daylight factors is followed by a description of an improved daylight factor meter, in which the current outputs of two photoelectric cells are compared by a null-balance method. When one cell is exposed inside the building and the other outside, the ratio of the illuminations at the two positions is indicated directly on a calibrated scale by the balance position of the potentiometer. The circuit is so arranged that the load resistances of the cells are unchanged by changes in the balance position and, for a constant daylight factor, the balance position is not affected by changes in the average luminance of the sky. The instrument can be calibrated directly on an optical bench, either for use with the outside cell exposed to a full hemisphere of sky or for use with the outside cell so masked that light is only received from a part of the sky.

Introduction

THE daylight factor, as defined by the International Commission on Illumination, 1955, is a measure of the daylight illumination at a point on a given plane, expressed as a ratio of the illumination on the given plane at that point and the simultaneous exterior illumination on a horizontal plane from the whole of an unobstructed sky, of assumed or known luminance distribution. Direct sunlight is excluded from both interior and exterior values of illumination.

In the design of some buildings calculations are made of the daylight factors to be expected at various positions in the working plane and, after occupation of the building, measurements can be made to check the predicted values of daylight factor.

Present methods of measurement

Two methods of measuring daylight factor are at present generally available.

(i) Comparison of the current obtained from a selenium photocell, exposed within the building, with that obtained from the same or a different cell, when exposed out of doors to a complete hemisphere of sky. The disadvantages of this method are:

(*a*) since the condition of the sky can change very quickly, the time interval between "indoor" and "outdoor" readings is often sufficient to produce inaccurate results;

(*b*) the method normally requires a change of range of the current meter when the cell is changed from "indoors" to "outdoors". Different instrument ranges impose different resistive loads on the photocell and so change the cell characteristics. It is therefore necessary to refer to calibration curves for the use of the cell on each instrument range before the two readings can be compared.

(ii) Use of the Building Research Station/Evans Electroselenium Ltd. daylight factor meter.* This consists essentially of a single photoelectric cell, the output of which is indicated on a moving coil meter shunted by a variable resistor. In use the cell is masked by a special mask, exposed to the sky and the variable shunt adjusted until the meter reads at a calibration mark. The instrument is then transferred to the test position, the mask removed and the daylight factor read directly from the scale. This daylight factor meter is very compact, light and portable but has the following limitations:

(*a*) even under sky conditions which are comparatively stable it is not advisable to take daylight factor readings at more than two or three points without checking the calibration setting of the instrument. Repeated journeys to the window or some other outdoor observation point must therefore be made, and may mean that the method is impracticable for the survey of a large factory area where there is no ready access to the outside;

(*b*) care must be taken in the transfer of the instrument from the window to the test position to avoid alteration to the setting of the variable resistor. The time interval between the calibration at the window and reading the daylight factor is therefore, in practice, of the order of 15 s, and during this time the sky brightness may change sufficiently to invalidate the calibration setting made.

Instrument requirements

The foregoing criticisms indicate the requirements for a satisfactory daylight factor meter:

(i) simultaneous comparison of the levels of illumination inside and outside the building. This implies the use of two photoelectric cells;

(ii) the use of a suitable circuit to compare the outputs of the two cells at the same time;

(iii) the comparison circuit should present a suitable constant resistance as the load for each cell.

Instrument design

The circuit diagram of the new daylight factor meter is shown in Fig. 1. Two selenium photocells are used as the nsing elements, one of which is exposed at the test position thin the building and the other exposed outside. The otocells are 45 mm diameter cosine corrected cells (by vans Electroselenium Ltd.). The output currents from the o photocells are compared in the resistance network *AOB* ig. 1). The resistors R_1 and R_2 of the potentiometer chain e a pair of 250 Ω wire-wound potentiometers which are nged together, the sliding contacts being driven by a mmon shaft. In this arrangement, and for a particular tio of output currents from the two cells, there is a unique osition of the potentiometer sliders, *X* and *Y*, for which no otential difference exists between them. This null position indicated by a 25–0–25 μA, centre zero, moving coil meter , of 990 Ω resistance, which is connected between the ders. The slider position is indicated on a circular scale y a pointer on the control knob.

---

* LONGMORE, J., and HOPKINSON, R. G. *J. Sci. Instrum.*, **31**, pp. 214–217 (1954).

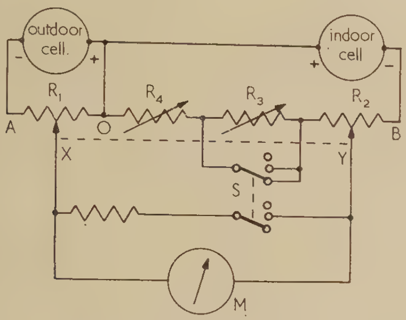

Fig. 1. Circuit diagram of daylight factor meter

If the potentiometer chain were to consist of the resistors R_1 and R_2 only, for equality of cell currents, the null-reading osition would occur at the point where the tapped resistances vere half the full values. Since, in practice, the daylight lumination inside a building is always less than that outside, is desirable to avoid the ambiguity which would be introuced by the central 100% position, and also to make use of the full length of the resistances by bringing the 100% osition to one end of the total slider travel. For these easons, the preset resistors R_3 and R_4, 0–300 Ω each, are added in series with the resistor R_2 and the switch *S* is used o short out resistor R_3.

For the measurement of daylight factor as defined, the outdoor cell should be exposed on a horizontal plane to the full hemisphere of sky and the indoor cell exposed in the working plane at the required position. In this mode of operation the short is removed by the switch *S* from the resistor R_3, which is preset to give no meter deflexion when the sliders are in the 100% position and both cells are subected to the same illumination.

It is often impossible to put the outdoor cell in such a position that it can "see" a full hemisphere of sky. To overcome this difficulty the Building Research Station designed a mask for use with their original daylight factor meter which confined the field of view of the outdoor cell to a band of sky 40 to 45° above the horizon. This same mask can be fitted to the outdoor cell of the present instrument. The scales on the B.R.S./E.E.L. meter indicate that the mask reduces the illumination on the cell from an overcast sky in the ratio 40 : 1. When the mask is in use the switch *S* is set to short out the resistor R_3. The resistor R_4 is then preset to give no meter deflexion when the sliders are in the 100% position and the illumination of the indoor cell is forty times the illumination on the outdoor cell.

Calibration of the instrument

The calibration of the instrument and the presetting of resistors R_3 and R_4 was carried out on an optical bench. The two photocells were set up on opposite sides of a single lamp and the distances of the cells from the lamp were adjusted until the illuminations of the cells, as measured by a calibrated photometer, corresponded to those to be expected in the field for various values of daylight factor with an outdoor illumination of 500 lm/ft^2 on the horizontal plane. This level of outdoor illumination is commonly used in design calculations. The meter was balanced for each value of daylight factor and a calibration curve (Fig. 2) was drawn, from which it is possible to prepare a dial graduated directly in daylight factor.

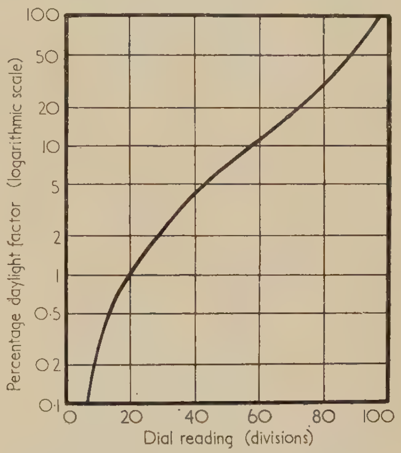

Fig. 2. Typical calibration curve for masked outdoor cell

Advantages

(i) The luminance of the sky is subject to rapid changes, and it is rare for the sky conditions to be sufficiently constant for outdoor and indoor readings taken consecutively to be a reliable measure of the daylight factor. The meter described here overcomes this difficulty by making a simultaneous and continuous comparison of the outdoor and indoor illuminations.

(ii) When the meter is adjusted to the null-balance condition there is no current in the meter circuit and therefore no shunt effect on the potentiometer chain. The effect of this is to present constant load resistances to the photoelectric cells over the full range of daylight factor readings from 0 to 100%.

(iii) The instrument can be calibrated directly on the optical bench for use both with and without a mask. Recalibration for the use of a mask which views the sky at a different angle is only dependent on a knowledge of the effective reduction factor of such a mask. The instrument should therefore prove to be of value for use with any style of mask which may be developed.

(iv) The meter is readily portable and also easy to operate since there is only one adjusting knob.

Acknowledgement

Thanks are due to the Directors of Pilkington Bros. Ltd. for permission to publish this paper.

Time-sorter for use in the nanosecond range

by G. JONES, Ph.D.,* Physics Department, University of British Columbia, Vancouver, Canada

[*Paper received* 1 *January*, 1960]

Abstract

The paper presents the design of a time-to-amplitude conversion circuit employing delayed fast coincidence techniques for use in the nanosecond region. This circuit has a linear time calibration over the range 1 *to* 10 *ns, a resolution time of less than* 0·05 *ns and a variation of time calibration less than* 0·03 *ns per day is achieved. A resolution time of* 0·8 *ns was found when detecting coincidence between* γ*-rays from a* ^{60}*Co source.*

Introduction

THE basic qualities required of a time-sorter, based on time-to-pulse height conversion for the measurement of lifetimes of the order of one nanosecond or less, are good time resolution, a linear time response and, perhaps most difficult to achieve and most important, high electronic stability. The circuit is a development of that described by Jones and Warren(1) in which the good time resolution, and hence large operating frequency bandwidth, is facilitated by the use of small signal levels and crystal diodes are used as the sensitive element in the converter circuit. The block diagram of the instrument and the principle of operation have been presented in the earlier paper,(1) the major modifications described here consisting of an improved time-to-pulse height converter, employing microwave mixer diodes, and a limiter circuit which develops pulses more nearly constant in amplitude, both over an extended time period and over a wide range of counting rate.

The circuit now provides:

(i) an intrinsic electronic resolution time of less than 0·05 ns;

(ii) a resolution time using the prompt γ-rays from ^{60}Co and type 1P21 photomultipliers of 0·8 ns;

(iii) an electronic stability of better than 0·5% over the course of a day (i.e. a drift of less than 0·03 ns);

(iv) a linear time calibration down to an overlap of about 1 ns, the linearity over the range 1 to 10 ns havin been checked in detail experimentally.

Time-to-pulse height converter

As shown in the circuit diagram, Fig. 1, the converter i essentially a fast current switch consisting of two microwav diodes followed by a Miller integrator. Preceding the diod switch is a shorted stub clipping line, employed in the manne described by Bell, Graham and Petch.(2) In contrast to th type 6BN6 gating pentode time-sorter system of Neilson an James,(3) in which separate clipping lines are incorporate into each limiter, this system uses a single stub for bot channels.

In the quiescent state the input diode conducts a constant current of 1 mA to ground from the 250 kΩ resistance, while the second diode is biased off by about 0·75 V. The occurrence of a single pulse (of 0·47 V amplitude) at the input merely causes a rise in voltage at the diode junction, with the second diode remaining cut off. The superposition of two coincident pulses, however, which produces a step amplitude

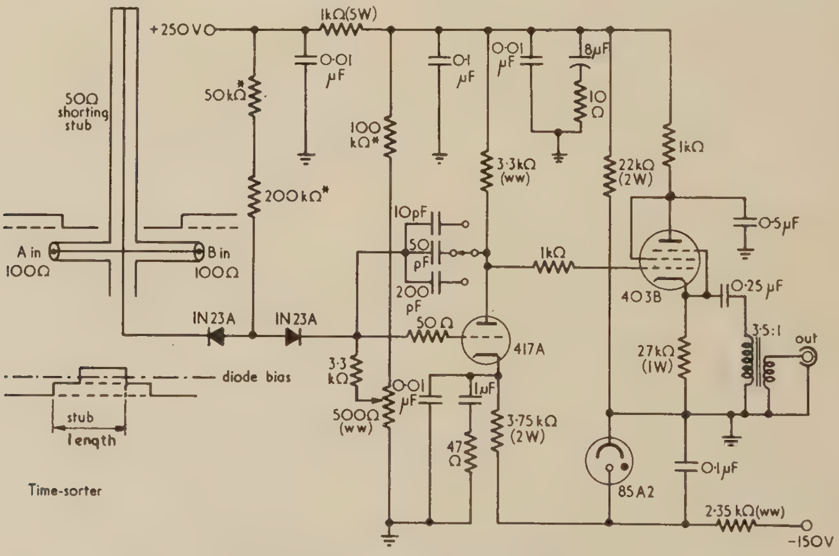

Fig. 1. Time-to-pulse height converter circuit

---

* Now at the Clarendon Laboratory, Oxford.

0·94 V, a voltage exceeding the bias of 0·75 V, switches ie constant current into the integrator as the first diode cuts f. Since the first diode is cut off during the switching time, ie loading effect of the converter on the incoming pulses is nall; only 1 mA of the incident 20 mA is required for vitching.

This idealized description of the operation is not strictly alized in practice. Since the characteristics of the diode vitch are not infinitely sharp, a small current is conducted y the second diode during a single pulse or during the edestal surrounding a partial overlap. The d.c. switching aracteristic of the diode switch, incorporating type 1N23A iodes, is shown in Fig. 2, in which the output d.c. current s plotted as a function of an input d.c. voltage, zero bias eing applied to the second diode. As is evident from this iagram, a limited pulse of amplitude greater than 0·4 V is equired to switch the output from zero to full current. Also, o prevent conduction during single pulses, a bias of about ·25 V more than the limited pulse amplitude must be selected. When operating the time-sorter under the conditions described arlier, a coincident overlap to single pulse output ratio of greater than 20 to 1 is easily achieved.

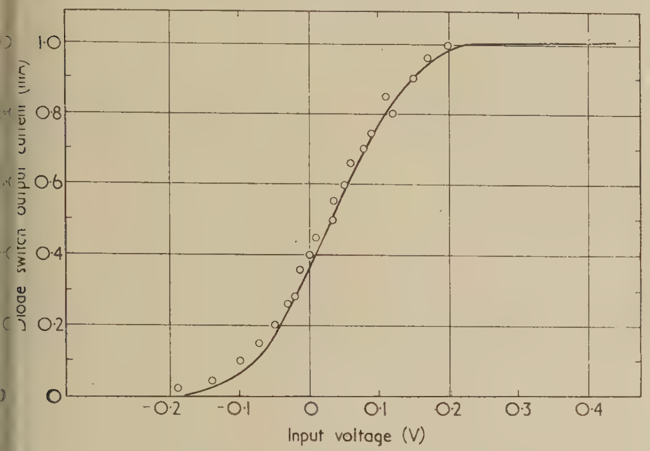

Fig. 2. D.C. operation of the diode current switch

○ = measured values; —— = curve calculated from diode characteristics

Hole storage effects

If the d.c. characteristics of the current switch (Fig. 2) also applied to the nanosecond pulse operation, the time-sorter behaviour would be independent of input pulse amplitude, providing this were large enough to give complete switching of the current. Unfortunately, owing mainly to hole storage effects, this is not quite the case.

The switching characteristics under pulse conditions are illustrated in Fig. 3. The deviation in the amplitude of the integrated output pulse, for the 10 ns input pulse, from that expected on the basis of the integrated output pulse being one-tenth that obtained with a 100 ns input pulse, is attributed to minority carrier conduction in the first diode when it is supposedly cut off. Since the relative amount of minority carrier conduction is strongly dependent on the input pulse width, the linearity of response is also dependent on this parameter. As can be seen from Fig. 3, this deviation from linearity is small if the bias is adjusted so that the current switched by the overlap pulse corresponds to the operating point indicated by the voltage *L*. Under these conditions the linearity is good down to overlap pulse lengths of about 1 ns. This operating condition greatly increases the stability requirement of the limiter circuit however.

Minority carrier conduction in the second diode would remove some of the charge switched into the integrator when the input signal returns to ground level. Since minority carrier lifetimes are probably a few nanoseconds for microwaved iodes of the type employed, this loss of integrated charge was reduced by preventing the converter input signal from returning to ground for a period of several nanoseconds after the overlap signal. This was accomplished by using a shorted stub of electrical length about 10 ns greater than the overlap width of interest. Hence, by delaying the limiter pulse by about 10 ns, a single pulse pedestal of 10 ns following the overlap pulse is produced, thus allowing the second diode to recover before the input signal returns to ground level.

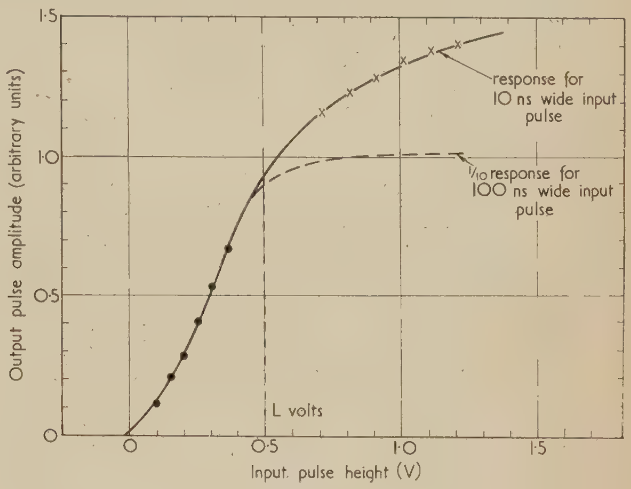

Fig. 3. Pulse operation of the diode current switch

Fig. 4 shows a plot of the total time-sorter response as a function of the delay inserted in one channel. The loss in output pulse amplitude near complete overlap, and hence zero pedestal length, is attributed to the hole storage effect in the second diode.

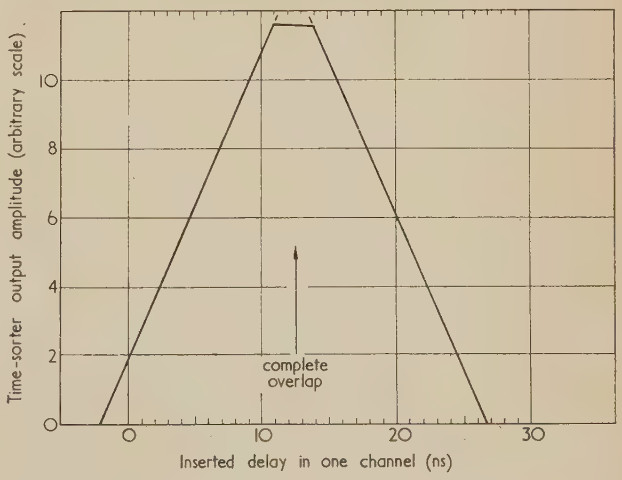

Fig. 4. Complete time-sorter response

Choice of microwave diodes

The qualities governing the choice of diode for the diode switch were:

(*a*) good high-frequency response and hence a short minority carrier lifetime. Associated with this is the need of a fast turn-on time for the diode;

(*b*) high back resistance, to lessen the temperature dependence of the switching circuit by reducing the magnitude of the strongly temperature-dependent reverse leakage currents;

(*c*) high forward conduction in order to produce a sharp switching action.

Of the several easily available microwave mixer diodes examined at the time of construction of this instrument, the type IN23A was selected. This diode is designed for use as a microwave mixer up to 9000 Mc/s, and, in addition, it has an inverse leakage current of less than 20 μA at a reverse voltage of 1 V at room temperature, while its forward conduction is about 15 mA at 1 V. Some recently developed diodes such as the Bell Telephone types IN696 and the "Sharpless" diode, characterized by fast turn-off times, should offer a significant improvement in this part of the circuit. The type IN696, for example, is quoted as having a reverse leakage current of 0·001 μA at 1 V, a forward conduction of 25 mA at 1 V, and a recovery time of less than 5 ns on switching from 10 mA forward to 10 mA reverse current.

Limiters

The requirements for the limiter tube and associated circuit, besides that of high stability in the output pulse amplitude, are:

(*a*) the limiter tube must be a sharp cut-off tube capable of producing an anode pulse with a rise time of less than 1 ns;

(*b*) the tube must be capable of conducting a d.c. plate current of 20 mA in order to produce the desired 1 V output pulse across an effective plate load of 50 Ω;

(*c*) the circuit must be insensitive to count rate, so that the output pulse amplitude is uniform and independent of channel counting rate. The total fluctuation in the d.c. value of the limiter current must be less than 0·3% if time measurements to a precision of $\pm 0{\cdot}1 \times 10^{-10}$ s are to be achieved, as discussed later under "Performance".

The secondary emission pentode limiter previously used[1] did not give quite the stability and uniformity of pulse amplitude required for the author's work on positron lifetimes in metals, to be reported elsewhere. New limiters were designed around the recently developed high-gain, high-current pentodes such as the Western Electric type 404A or Philips type E180F. The limiter circuit (Fig. 5) is shown with a type 404A tube, but a type E180F may be substituted, the only change needed being a rather higher screen voltage than the +50 V indicated. The high d.c. stability is achieved by operating the tube with constant current from both the control and screen grids to the cathode. Since the plate current is essentially determined by the screen and grid currents rather than their voltages, a stable plate current results when both the screen and grid currents are stabilized. These currents were, in turn, supplied by approximately constant current sources, namely large resistances connected to the h.t. positive line. Some negative feedback is also introduced by connecting the grid supply resistor R_2 to the screen grid. By this means, if the screen current tends to decrease, thus indicating reduced tube conduction and decreased plate current, the screen voltage rises and this automatically increases the control grid current, and hence the total tube conduction.

The screen voltage supply is set so that in the quiescent state the diode D_1 is cut-off by a few volts. When the limiter tube is cut-off by a pulse from the photomultiplier, D_1 comes into conduction and the screen current is shunted into the power supply. Thus the current stabilizing tendency of the circuit is only operative in the quiescent state, not when the tube is cut off. The use of a small screen decoupling capacitor C_1 (22 pF), and hence a short recovery time, $R_1C_1 = 1$ μs, further ensures count-rate insensitivity.

The use of a positive grid bias also enables operation with low screen and plate voltages (60 and 90 V respectively), and

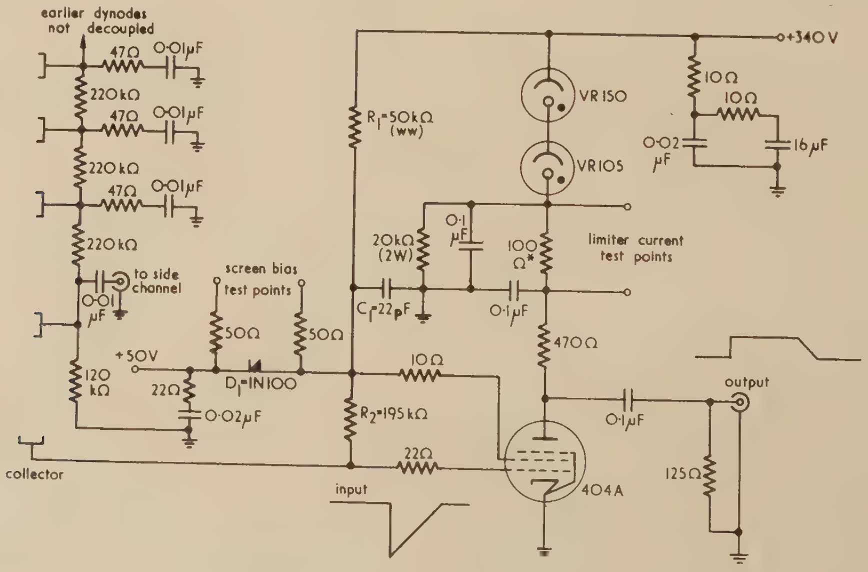

Fig. 5. Circuit of type 404A pentode limiter

ence ensures that the screen and plate power dissipations are well within their rated limits, even with a plate current of 20 mA. The value of the grid supply resistor R_2 was chosen to recharge the grid circuit to its nominal value of $-0\cdot5$ V within 1 μs after pulsing of the photomultiplier. An important benefit gained by this technique of grid clamping is that an approximately constant value of recharge current is supplied to the capacity of the grid circuit to ground, when this capacity is charged negatively by the photomultiplier collector pulse. Thus a waveform of the type shown at the grid point of Fig. 5 is obtained, rather than the usual exponential recovery which approaches the baseline slowly, making count-rate insensitivity difficult. In addition, the use of a negative photomultiplier h.t. facilitates direct coupling between the collector of the photomultiplier and the grid of the limiter tube, thus enabling another possible source of count-rate shifts, the coupling capacitor, to be eliminated. Most recent photomultipliers are characterized by much less after after-pulsing than that of the 1P21, and so inject less integrated charge on to the limiter input capacity. For these photomultipliers a larger value of R_2 (hence smaller recharge current) than that indicated in Fig. 5 is required for a 1 μs recovery time. With such photomultipliers a larger value of R_2 is needed.

Monitoring of the mean d.c. plate current also affords a convenient means of determining the limiter count-rate, as the fractional decrease in the mean d.c. plate current is equal to the fractional mark-to-space ratio to a first order.

Operation of the circuit as shown in Fig. 5 yielded an output pulse of 0·94 V amplitude into a 100 Ω cable. When this pulse is incident on the junction of the 50 Ω shorting stub and the other 100 Ω cable, a 50% reflexion occurs producing a single pulse of 0·47 V amplitude at the input to the diode switch. The cable used to transmit the limited pulses from limiters to converter was a 100 Ω type with good h.f. characteristics (Telcon type AS48 by the T.C.M. Co., London). The 50 Ω shorting stub was a rigid one formed by mounting a $\frac{3}{16}$ in. copper rod within a $\frac{7}{16}$ in. inner diameter brass tube and using a homogeneous polystyrene plastic foam spacer to give a dielectric constant close to that of air.

Performance

Time calibration of the apparatus was obtained by two methods. The first involved varying the relative time delay between the two channels, either by inserting calibrated cable lengths or by moving a source of coincident γ-rays between the two counters. The second consisted of varying the overlap pulse width by varying the shorting stub length.

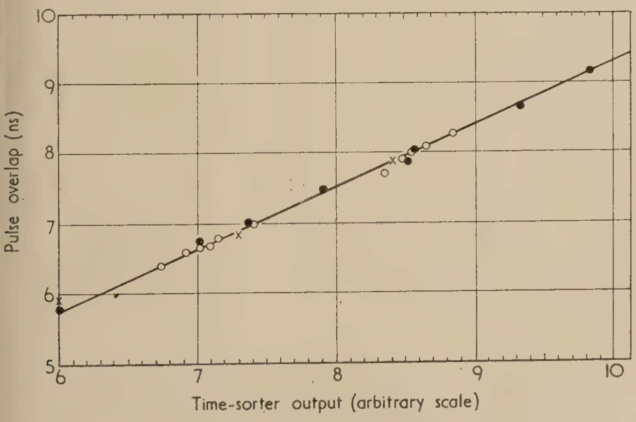

Fig. 6. Inserted delay time calibration curve

γ-ray time-of-flight time calibration } ● = first calibration curve
○ = calibration curve two months later
× = variable shorting-stub time calibration

Comparison of time delays inserted into a channel by altering the γ-ray flight path with that produced by insertion of a length of type AS48 cable, gave a value of $(2\cdot48 \pm 0\cdot05)10^{10}$ cm/s for the velocity of pulses in this cable, which is in good accord with other measurements of the velocity in this laboratory using h.f. resonance methods. Fig. 6 is an example of a detailed time calibration curve obtained by the inserted delay method. Each group of points, corresponding to a particular cable delay, is in itself a time calibration by γ-ray time of flight, wherein a positron source was placed between the two counters and its position along the line joining the counters was varied. The side-channel, single-channel, pulse-height analysers were in this case set to cover a major fraction of the Compton spectrum of the 510 keV annihilation radiation. This time calibration held exceedingly well over a period of two months.

The resolution of the complete instrument is shown in Fig. 7. Curve A illustrates the intrinsic electronic resolution of the apparatus when it is driven by artificial prompt pulses produced by a mercury relay pulse generator. The 0·05 ns width at half height is much smaller for this curve than for curve C, which results from a prompt γ-ray source. Curve B is the resolution curve resulting when both limiters are driven by the same counter. The increased width of this curve over that of curve A illustrates the effect of pairs of pulses coincident in time, but varying somewhat in rise time and perhaps amplitude. The resolution curve C for ^{60}Co radiation is characterized by a resolution time of 0·8 ns, and shows that the limit in time resolution for γ-ray detection is due to the radiation detectors at the present time.

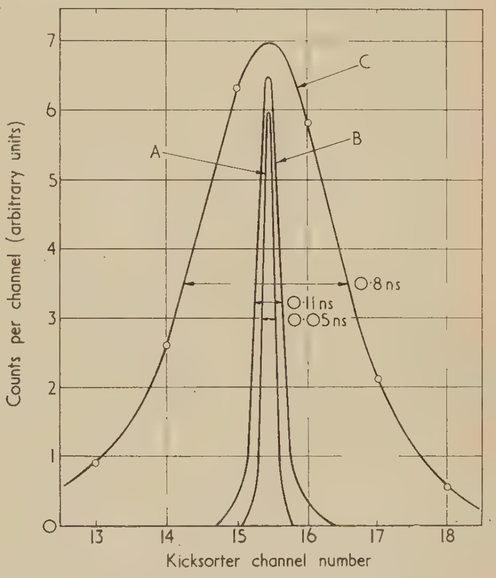

Fig. 7. Prompt resolution curves

Curve A, electronic resolution; curve B, single scintillation counter resolution curve; curve C, ^{60}Co prompt resolution curve

A semilogarithmic plot of a ^{60}Co resolution curve is shown in Fig. 8, as recorded with one side-channel analyser biased to detect γ-rays of energy greater than 700 keV and the other analyser set to cover the top one-third of 0·51 meV

γ-ray Compton spectrum. The values of the width at half-height $11 \cdot 0 \times 10^{-10}$ s and the slope of the sides of the curve, a factor of 2 in $1 \cdot 2 \times 10^{-10}$ s on the left and in $1 \cdot 9 \times 10^{-10}$ s on the right, are somewhat worse than those obtained by Green and Bell(4) with a recent type 6BN6 time-sorter, namely $8 \cdot 5 \times 10^{-10}$ s width at half-height and $1 \cdot 4 \times 10^{-10}$ s for the slope on the right-hand side of the curve. The difference between the two sets of curves probably lies in the types of photomultiplier used; Green and Bell used diphenylacetylene crystals on R.C.A. type 6342 photomultipliers operated at 2100 V, while the circuit described here was used with type 1P21 photomultipliers with internal photocathodes operated at 2000 V, one scintillator being diphenyl acetylene and the other plastic.

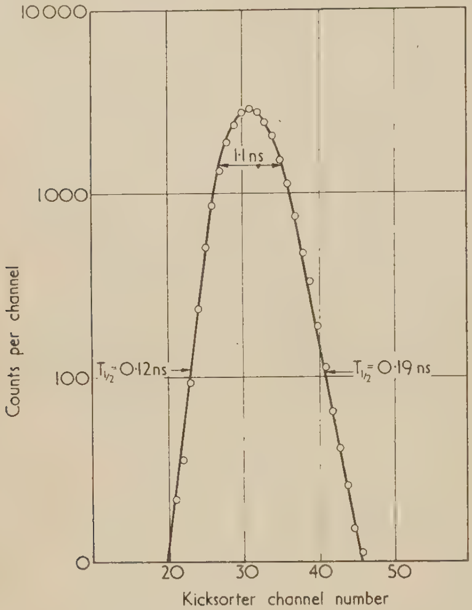

Fig. 8. Prompt resolution curve taken with cobalt 60 source
Time calibration, $1 \cdot 31 \times 10^{-10}$ s/channel

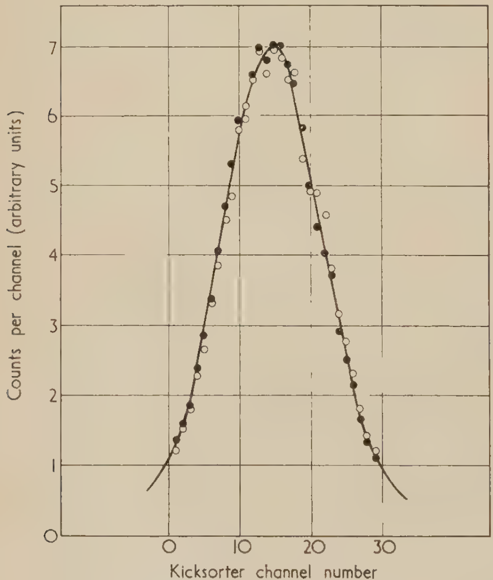

Fig. 9. Count rate effect on resolution curves
Time calibration $1 \cdot 0 \times 10^{-10}$ s/channel
○ = 22 000 counts/s ● = 850 counts/s
—— = annihilation γ-ray resolution curves

The effect of variations in count rate on the experimental resolution curves is shown in Fig. 9. The rates quoted, 850 and 22 000 pulses/s, were those counted at the outputs of the side-channel analysers, the biases of which were set just above noise level so that most of the Compton spectrum from annihilation radiation was dected. It is clear that for these rates no significant effects, such as a broadening or displacement of the coincidence resolving curves, is observed. The very small shift apparent in Fig. 9 can be attributed to different γ-ray flight paths in the two cases.

The overall stability of the time calibration for the instrument was checked by periodically repeating the γ-ray time-of-flight calibration curve during an interval of two months. No significant alteration of the slope of the curve was observed over this time period, although slight translations of the various time calibration curves relative to each other did occur with slight variations in the operating voltages.

A detailed study of the stability of the complete system was made by varying the operating conditions of each of the various elements of the instrument in turn, and observing the corresponding time shift of the resulting resolution curves. These measurements were obtained while driving both limiters with one scintillation counter, an arrangement which yielded narrow resolution curves of the type shown as curve *B* in Fig. 7, with the following results.

(i) Variations in the rise time of the scintillation pulses, as a result of variations in photomultiplier gain, resulted in time shifts of less than $0 \cdot 01$ ns for h.t. variations of less than ± 50 V in the 1850 V employed. This is a somewhat over-optimistic estimate of this dependence, since in actual practice two scintillation counters are used, so differences in the characteristics of the two counters would result in different gain and transit time variations, resulting in turn in greater time shifts than would be observed in this test with just one counter. In use, of course, photomultiplier h.t. variations of less than 1 V may easily be achieved.

(ii) A.C. mains input variations of $\pm 10\%$ resulted in time shifts of less than $0 \cdot 02$ ns.

(iii) Variation in the time-sorter power supply of ± 1 V in the 250 V used resulted in time shifts of about $\pm \frac{1}{2}\%$, i.e. $\pm 0 \cdot 25 \times 10^{-10}$ s for the pulse overlap employed.

(iv) The temperature of the diodes in the fast current switch unit of the time-sorter had to be kept to within $\pm 0 \cdot 8^\circ$ C for errors of less than $0 \cdot 005$ ns in the time measurements. This was ensured in practice by keeping the room temperature constant to about 1° C. Temperature lagging of the fast diode assembly was also incorporated by mounting the diode unit in a styrofoam insulated box.

(v) Variation in the d.c. limiter current of $0 \cdot 15\%$ resulted in a time uncertainty of $\pm 0 \cdot 01$ ns. With the limiter circuit of Fig. 5, the limiter currents were observed to remain constant to $0 \cdot 2\%$ over the course of a day. A slow decline of the limiter plate current of 6% occurred over the course of half a year's continual operation.

Conclusions

The stability of the time-sorter described is sufficient for the measurement of time intervals to an accuracy of $\pm 1 \times 10^{-11}$ s over the course of a day. This accuracy has been achieved in the measurement of positron lifetimes in various metals, to be described elsewhere. A significant improvement in the time stability would require a limiter and time converter of still higher stability. Either a limiter circuit of greater stability than the 0·2% mentioned above, or a diode current switch with less dependence on the input pulse amplitude would be required. Achieving the former, while still maintaining a high degree of count-rate stability, is a difficult problem. The latter may be a more promising approach in view of the continuing improvement of the new fast recovery switching diodes. On the other hand, the ability to obtain coincidence resolution curves of significantly reduced width must await the development of scintillation counters of faster response.

Acknowledgements

I am grateful to Dr. J. B. Warren for his help and encouragement with this work and to Dr. B. L. White for many useful suggestions. I am indebted to the National Research Council for scholarships held by me during the time this instrument was developed and to the University of British Columbia's Research Fund for financial support of this work.

References

(1) Jones, G., and Warren, J. B. *J. Sci. Instrum.*, **33**, p. 429 (1956).

(2) Bell, R. E., Graham, R. L., and Petch, H. E. *Canad. J. Phys.*, **30**, p. 35 (1952).

(3) Neilson, G. C., and James, D. B. *Rev. Sci. Instrum.*, **26**, p. 1018 (1955).

(4) Green, R. E., and Bell, R. E. *Radiation Lab. Report* (Montreal, Canada: University of McGill, 1958).

Isotopic analysis of boron in boron trifluoride by mass spectrometry, and measurement of natural boron 10 concentration

by P. G. BENTLEY, B.A., United Kingdom Atomic Energy Authority, Research and Development Branch, Capenhurst, Chester

[*Paper first received* 6 *March*, 1959, *and in final form* 17 *May*, 1960]

Abstract

A conventional mass spectrometer is used for precise measurements of the isotope ratios of boron in boron trifluoride samples with widely differing concentrations of boron 10. "*Memory*" *effects caused by the adsorption of boron trifluoride on to the surfaces of the inlet system have been investigated, and it is found that these can be reduced to a workable level by careful design of the inlet system. By blending together enriched and depleted boron trifluoride, standard samples with known isotopic constitutions are prepared and used to calibrate the mass spectrometer. The true and measured isotope ratios are thus found to differ by several per cent, an effect attributed to mass discriminations in the ion source. After correcting for this error, the boron* 10 *atomic concentration in some naturally-occurring boron is found to be* 19·27 ± 0·13%.

Introduction

Measurements of isotopic concentration are usually made most accurately by mass spectrometry, and boron is no exception in this respect. Results quoted by different workers, however, range from 18·4 to 19·9 at.-1% for the atomic concentration of boron 10 in naturally-occurring boron. There are three possible explanations for this diversity in results—first, that there is an actual variation in the isotopic content of boron from different minerals; secondly, that variations have been introduced during processing; and thirdly, that the mass spectrometer measurements are in error. The question of whether variations in nature occur or not is one which still remains to be finally settled. The present evidence is contradictory in that Thode and others$^{(1)}$ and Shuittse$^{(2)}$ find considerable variations, whereas Osbergaus$^{(3)}$ and Parwell and others$^{(4)}$ find none. The possibility of variations arising during processing is, of course, possible, but it seems unlikely that such large variations could be introduced during large-scale commercial processing, which is the source of many workers' materials. The third possibility of errors in mass spectrometry seems to be a very probable explanation. In particular, it is often assumed$^{(5, 6)}$ that absolute (rather than relative) results can be obtained by satisfying certain experimental conditions, but this is not necessarily justified.

No attempt has been made here to resolve the question of whether variations in nature occur or not. However, the experimental errors have been "short-circuited" by the use of isotopic standards, and a carefully prepared natural sample has been used to obtain a particular value for the natural abundance of boron 10.

In order to prepare the standards and make the comparison, it was first necessary to have a reliable method of making relative mass spectrometric measurements over a wide range of isotopic concentrations. The first part of the paper describes apparatus for this and gives the results of investigations into the way in which boron trifluoride adsorbs on metal surfaces to give "memory" effects.

Mass spectrometry

Mass spectrometer measurements are made on boron trifluoride using a conventional electron-bombardment ion source and a type M.S.3 mass spectrometer manufactured by

Associated Electrical Industries Ltd., Manchester. An instrument of this kind using gas rather than solid sample is essential for the work described here (even though the "memory" effects are more serious), since it must be assumed that mass discriminations cannot change between successive measurements. Boron trifluoride is preferable to other gaseous boron compounds because it is easily prepared in a sufficiently pure state for accurate blending.

Boron trifluoride gives principal peaks B^+, BF^+ and BF_2^+ in the proportions 3, 5, and 92. The BF_2^+ peaks are used for all measurements given here (even though they suffer from much worse interference than the B^+ peaks) because they are the largest and because the relatively small fractional mass difference between $^{10}BF_2^+$ and $^{11}BF_2^+$ implies small mass discrimination effects.

Interference peaks are produced by products of reaction of boron trifluoride with traces of water vapour and any glass which may be present. Compounds are formed which give peaks such as $^{11}BFH_2O^+$, $^{10}BF_2H^+$, $^{29}SiF^+$ and $^{30}SiF^+$ at the same masses as $^{10}BF_2^+$ and $^{11}BF_2^+$. It is found that, if samples are reasonably pure, appreciable quantities of these reaction products can be prevented from reaching the ion source by cooling the samples to −80° C with solid carbon dioxide. Similar reactions occurring in the inlet system or ion source can be reduced to negligible proportions by flushing with sample. Remaining interference could be examined, if necessary, by using modern high-resolution analytical instruments; in the present case, however, the necessary corrections could be estimated by measuring associated peaks like $^{10}BFH_2O^+$, $^{11}BF_2H^+$ and $^{28}SiF_3^+$. No corrections were necessary in the work described here.

Under normal operating conditions, the flow of gas into the mass spectrometer through the glass pinhole leak (see below) is predominantly molecular in character. Changes in sample composition arising from pump-out through the leak are not appreciable, because of the small size of leak compared with the volume of the handling system and the short time spent in making measurements. Measurements of isotope ratio on the same sample are reproducible over long periods to within 0·5% (at the 95% confidence level), provided that the same ion source is used. More accurate measurements are very difficult because of day-to-day changes in mass discriminations.

"Memory" effects

"Memory" effects are caused by boron trifluoride which is adsorbed on to the surfaces of the inlet system and ion source. When samples of differing isotopic concentration are being analysed, exchange occurs between the adsorbed boron trifluoride from old samples and the boron trifluoride of the new sample; measured isotope ratios are thus modified by the isotope ratios of previous samples. There are three ways of attacking this problem: first, to try to build the inlet system from materials which do not adsorb much boron trifluoride; secondly, to remove adsorbed boron trifluoride by chemical treatment; and thirdly, to design the inlet system so that surface adsorption has a minimum effect.

Copper and nickel inlet systems have been tried but no significant difference could be detected between them as adsorbents for boron trifluoride; from experiments on the "memory" effect (described below), the total adsorption was found to be about 7×10^{-8} mol./cm². Melton and others⁽⁷⁾ have done similar experiments with glass apparatus, and from their results the adsorbed layer is calculated to be about 5×10^{-9} mol./cm². Some of this marked difference between metals and glass will arise because, in this case, the metal surface is rough (i.e. not specially prepared) and has an effective area for adsorption greater than the apparent area. Glass has not been used in apparatus described here (except for the gas leak), since it is difficult to make glass valves which can be heated to high temperatures and because of the large interference effects which could be caused by formation of silicon tetrafluoride.

Several attempts have been made by previous workers to remove adsorbed boron trifluoride by chemical methods. Melton and others⁽⁷⁾ have used boron trichloride with some success, but the added trouble and expense do not seem to justify its use. Kilpatrick and others⁽⁵⁾ report that ammonia gas can be used, but this has been tried at this Laboratory and by Melton and others⁽⁷⁾ without success. When tried at this Laboratory it appeared that, although no boron trifluoride was removed, the complex formed between the two compounds slowed down the rate of exchange of the boron trifluoride and so produced an apparent reduction in the size of "memory" effect. Because of the consequently longer time needed to eliminate "memory" effects by flushing, the use of ammonia seems a positive disadvantage. It is suggested that only very reactive compounds like fluorine or chlorine trifluoride could be of use in removing adsorbed boron trifluoride; these cannot be tried with the present apparatus because of the probably disastrous effects on the glass leak; they might be tried with advantage, however, if a metal leak were used.

"Memory" effects can be reduced to a workable level by careful design of the inlet system. Before the system in current use is described, further consideration must be given to the way in which "memory" effects appear. Referring to Fig. 1, the inlet system can be divided into high- and low-pressure parts, separated by the leak which reduces the pressure from a few centimetres of mercury to about 10^{-3} mm of mercury. When boron trifluoride is introduced into the high-pressure side it exchanges with adsorbed material left by previous samples. The $^{10}BF_3$ molar concentration in the gas phase thus starts at the true value and changes with time in the direction of that for the previous sample. In the low-pressure side, boron trifluoride is continually flowing through and exchanging with adsorbed boron trifluoride from previous samples. The $^{10}BF_3$ molar concentration in the gas phase is therefore altered at first and only returns to its true value after all the adsorbed boron trifluoride is replaced by the new sample.

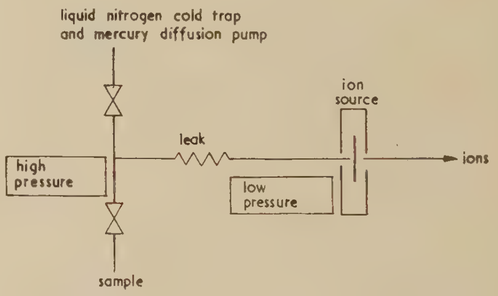

Fig. 1. Schematic diagram of the inlet system

When low-pressure "memory" is predominant, the measured $^{10}BF_3$ molar concentration approaches its true value asymptotically, and it is often difficult to decide when all the "memory" has disappeared and what the true value is. It is therefore very important to reduce low-pressure "memory" by good design, even if this means that high-pressure "memory" will be increased.

"Memory" effects in the high-pressure side can be reduced by designing the system to have a small surface/volume ratio and by working with large pressures of boron trifluoride; those in the low-pressure side can be reduced by designing it to have a small surface area and by working with a large flow rate of boron trifluoride. Low-pressure "memory" effects have been reduced to negligible proportions by using a leak situated inside the ion box of the ion source. The leak is made by imperfectly sealing up a piece of (boron-free) glass tube, evacuating it and then sparking through with a high-frequency spark generator. (It is found, incidentally, that the sparks are much less fierce, and the size of hole more easily controlled, if the glass is supported by an electrical non-conductor.) It is almost impossible in this way to make leaks which give reasonable flow rates with more than a few centimetres of mercury of boron trifluoride in the high-pressure side of the inlet system; high-pressure "memory" effects will therefore tend to be much larger than they would be if a more conventional leak were used. The high-pressure side of the inlet system is made from ¼ in. Danfoss valves (by Danfoss Mfg. Co., Nordborg, Denmark) in order to give a small surface/volume ratio ($8\ \mathrm{cm}^{-1}$) and high pumping speed without the need for excessively large samples. Strip heaters are fitted so that the system can be baked to 300° C.

High-pressure "memory" effects should follow the relationship:

$$\frac{C_t - C_f}{C_0 - C_f} = \exp - \left(\frac{N+n}{Nn} \cdot r.t\right) \qquad (1)$$

which is derived in Appendix 1. Here C_f, the equilibrium $^{10}\mathrm{BF}_3$ molar concentration after a long time, is given by

$$\frac{C_0 - C_f}{C_f - C_0'} = \frac{N}{n} \qquad (2)$$

and C_t is the $^{10}\mathrm{BF}_3$ molar concentration in the gas phase at time t, C_0 is the true $^{10}\mathrm{BF}_3$ molar concentration of the new sample, C_0' is the $^{10}\mathrm{BF}_3$ molar concentration of adsorbed boron trifluoride from previous samples, N and n are the number of boron trifluoride molecules adsorbed and in the gas phase, respectively, and r is the rate of exchange between adsorbed and gas molecules.

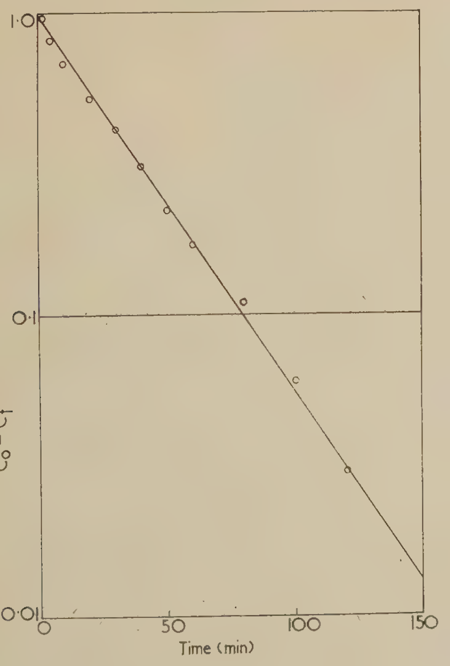

Fig. 2. A high-pressure "memory" effect curve

This relationship is obeyed, as shown in Fig. 2, and can be used to calculate values of N and r. (Measured values of concentration are sufficiently accurate for this purpose and mass discriminations are neglected.)

Table 1. *Adsorbed layers of boron trifluoride on a nickel surface*

(Figures may be in error by up to a factor of two)

Experiment	*Layer*	*Layer size (moles/cm²)*
Desorption of boron trifluoride by heating to 300° C	A_1	$1{\cdot}8 \times 10^{-8}$
Memory effect at room temperature after removing A_1	A_2	$1{\cdot}8 \times 10^{-8}$
Memory effect at 300° C after removing A_1	$A_2 + A_3$	$4{\cdot}9 \times 10^{-8}$
—	A_3	$3{\cdot}1 \times 10^{-8}$
—	$A_1 + A_2 + A_3$	$6{\cdot}7 \times 10^{-8}$

It appears, from the results of experiments summarized in Table 1, that the boron trifluoride behaves as if it is adsorbed as three distinct layers of approximately equal size. The first layer A_1 is removed by hearing to 300° C. The second layer A_2 provides boron trifluoride which cannot be removed in this way, but which exchanges with gaseous boron trifluoride reasonably quickly (40 min) at room temperature and very quickly at 300° C. The third layer A_3 cannot be removed by heating and exchanges at a much slower rate than A_2 (24 h at room temperature, and about 30 min at 300° C). This third layer causes most of the trouble in isotopic analysis; only by being able to heat to 300° C has it been possible to eliminate "memory" completely and make true measurements. The usual method is to bake and pump the inlet system, to remove A_1 (about 30 min is sufficient), and then to flush with new sample, changing it at thirty-minute intervals, until no "memory" effect is detectable. By flushing with boron trifluoride at a pressure of 2 cm of mercury it is possible to change the sample molar concentration from 5 to 95% $^{10}\mathrm{BF}_3$, and at the end of eight hours to have no detectable "memory" effect, i.e. less than 0·01% $^{10}\mathrm{BF}_3$.

Break-seal tubes of boron-free glass are used for storing samples, since it is found that concentration changes are very marked when using Pyrex. Sample tubes are never opened directly to the inlet system, since this could cause an undetected "memory" effect; a detachable polythene diaphragm valve fits between the inlet system and the sample tube. This can be dismantled and effectively cleaned with hot water.

Standards

Primary isotopic standards are prepared by blending a known amount of boron trifluoride, which is highly enriched in boron 10, with another known amount, which is greatly depleted in boron 10. The blending is done conventionally by measuring the pressure of each component gas in the same fixed volume and at a fixed temperature. Blending materials are shown to be sufficiently free from impurities, such as silicon trifluoride, during their mass spectrometric analysis, and errors caused by boron trifluoride being not a perfect gas(8, 9) are negligible at the low pressures (approximately 10 cm of mercury or less) at which the components are measured. In order to reduce "memory" effects, the apparatus is constructed from small polythene diaphragm valves and boron-free glass; from the results given above it is calculated that "memory" effects are sufficiently small to be neglected.

Since neither of the blending materials is isotopically pure (in either boron 10 or 11), some correction is necessary to allow for the effect of the other isotope on the blend. This is done by analysing the blending materials with the mass spectrometer; since the effect of mass discriminations is to introduce a small fractional error in the isotope ratio, it follows that the correction of an almost 100% isotopic concentration will only introduce very minor errors from mass discrimination (see also Appendix 2).

If one defines a mass-discrimination constant k by

$$R = kR' \qquad (3)$$

where R is the true $^{11}B/^{10}B$ isotope ratio and R' is the measured $^{11}B/^{10}B$ isotope ratio; it is to be expected that k will be the same for all values of R. To prove this point, and to provide extra checks on the method, duplicate blends are made at both the 25 and 75% boron 10 concentration levels, and k_1 (for the 25% concentration blend) and k_2 (for the 75% concentration blend) are calculated independently.

Table 2. *Measurements taken during standardization*

Sample	(±0·0010)	*R′* (±0·5%)
Blend (*a*)	0·2488	0·348
Blend (*b*)	0·2517	0·354
Enriched blending material		0·0402
(Bulk material)		(0·0443)
	Ion Source changed	
Blend (*c*)	0·7421	2·479
Blend (*d*)	0·7469	2·468
Depleted blending material		19·62
Bulk standard		4·07
(Enriched blending material, repeat)		(0·0409)
(Bulk material, repeat)		(0·0448)

The experimental results are given in Table 2. All errors quoted here and elsewhere are at 95% confidence limits. Values of f are limited in accuracy by statistical reading errors of the mercury meniscus and possible surface-tension effects. The random errors assigned to R' are those already discussed in the section on mass spectrometry. The ion source had to be changed in the middle of these measurements, but fortunately it was possible to repeat some of them and so calculate the change in mass discriminations.

The duplicate blends provide a check on the blending and mass spectrometry; blends (*a*) and (*b*) compare favourably but there is a slight discrepancy (about twice the estimated error) between blends (*c*) and (*d*). The discrepancy probably arises from an unfortunate summing of errors; the estimated error has been increased to cover the discrepancy and remove any possibility of inaccuracy. An outline of the subsequent calculations is given in Appendix 2.

After correcting k_2 to k_2' to allow for the change in mass discriminations caused by the change in ion source, the mass-discrimination constants are found to be:

$$k_1 = 1{\cdot}034 \pm 0{\cdot}011 \qquad (4)$$

$$k_2' = 1{\cdot}031 \pm 0{\cdot}007 \qquad (5)$$

There is no significant difference between the values of k_1 and k_2, as was expected. The mean value of k_1 and k_2' is used to find the true isotope ratio of the bulk secondary standard and hence the true $^{10}BF_3$ molar concentration, which is 19·23 ± 0·10%.

Measurement of the natural boron 10 abundance

In order to make the ultimate check on the boron 10 abundance in nature, it would be necessary to make isotopic measurements on a very wide range of boron-containing ores. This raises the problem of satisfactory chemical treatment of the ores in order to obtain representative samples—a major problem in itself. It has already been pointed out that although several workers(1–4) have investigated the possible variation in nature of boron isotopic composition, the results are conflicting in that some have found variations while others have not. No attempt has been made here to resolve this point. However, in view of the discrepancy between the generally accepted(10) value of 18·8% for the natural boron 10 abundance and the results of other workers, it seems desirable to make some check with the aid of the standards which have been prepared.

The bulk secondary standard has therefore been compared with a sample of boron trifluoride which has been carefully prepared from naturally-occurring boron. This sample is one supplied by Herr von Ubisch and has been shown by him and his co-workers to contain boron with the same isotopic composition as that obtained from a wide range of other minerals.(4) The boron 10 atomic concentration of this sample of natural boron is found to be 19·27 ± 0·13%. This has been briefly communicated elsewhere.(11)

Discussion

The values for the mass discrimination constant show that directly measured values of the $^{11}B/^{10}B$ isotope ratio are too small by 3–4%. This is a much larger error than most mass spectrometrists would expect. Fractionation of the sample cannot account for it, since the effects of fractionation in the gas leak and the ion box should cancel out; in any case the maximum error of this sort should be less than 1%. Possible errors arising from non-linearity in the measuring circuits have been checked and found to be absent. The magnetic field is varied rather than the ion accelerating voltage when changing between ion beams, and there are therefore no gross changes in drawing-out efficiency from the ion source. The conclusion must be either that there is a difference between the effective ionization cross-sections for the different isotopic species, as suggested by Lehmann and Shapiro,(12) or that there is some difference in the ion optical efficiency for the different ions after they are formed.

Whichever explanation is finally accepted, the literature references show no reason why errors of this sort should be absent from previous workers' results. In the present work, errors of this type have been obviated by using isotopic standards. While it is accepted therefore that there may be some variation in the boron 10 abundance in nature, it is suggested that the figure of 19·27 ± 0·13% may be nearer the truth than the present generally accepted value of 18·8%.(10)

Acknowledgements

This paper is published by permission of Sir William Cook, anaging Director, and Dr. H. Kronberger, Director of esearch and Development, of the United Kingdom Atomic nergy Authority (Development and Engineering Group).

I am indebted to Herr H. von Ubisch of A.B. Atomenergi, tockholm, for supplying the "natural" sample of boron ifluoride. The blending of materials for the standard mples was done by Dr. A. N. Hamer and Mr. B. Grundy f this Laboratory.

References

(1) Thode, H. G., Macnamara, J., Lossing, F. P., and Collins, C. B. *J. Amer. Chem. Soc.*, **70**, p. 3008 (1948).

(2) Shuittse, V. *Soviet Physics* (*JETP*), **2**, p. 402 (1956).

(3) Osberghaus, O. *Z. Phys.*, **128**, p. 366 (1950).

(4) Parwel, A., Ubisch, H. von, and Wickman, F. E. *Geochim. et Cosmoch. Acta*, **10**, p. 185 (1956).

(5) Kilpatrick, M., Hutchinson, C. A., Taylor, E. H., and Judson, C. M. *Separation of the Boron Isotopes* (National Nuclear Energy Series, III–5) (Oak Ridge: United States Atomic Energy Commission, 1952).

(6) Palmer, G. H. *J. Nuclear Energy*, **7**, p. 1 (1958).

(7) Melton, C. E., Gilpatrick, L. O., Baldock, R., and Healy, R. M. *Oak Ridge National Laboratory. Report* 2006 (Undated).

(8) Booth, H. S., and Martin, D. R. *Boron Trifluoride and its Derivatives*, p. 21 (New York: John Wiley and Sons, Inc., 1949).

(9) Rumold, C. F. Ph.D. Thesis (Western Reserve University, Cleveland, Ohio, 1931).

(10) Ingham, M. G. *Phys. Rev.*, **70**, p. 653 (1946).

(11) Bentley, P. G., and Hamer, A. N. *Nature* (*London*), **182**, p. 1156 (1958).

(12) Lehmann, W. J., and Shapiro, I. *J. Inorg. Nuclear Chem.* (To be published.)

Appendix 1

High-pressure memory effect

Consider N molecules of adsorbed boron trifluoride, with an original $^{10}BF_3$ molar concentration C_0', exchanging with n molecules of gaseous boron trifluoride, with an original $^{10}BF_3$ molar concentration C_0.

A relationship between C_t and C_t', the $^{10}BF_3$ molar concentrations in the gas and adsorbed phases at time t after the exchange begins, is obtained by equating numbers of ^{10}B molecules at times t and $t = 0$.

$$NC_t' + nC_t = NC_0' + nC_0 \qquad (6)$$

When the exchange is complete, the final $^{10}BF_3$ molar concentrations in the gas and adsorbed phases are the same, i.e. C_f.

$$NC_f + nC_f = NC_0' + nC_0 \qquad (7)$$

and so

$$\frac{N}{n} = \frac{C_0 - C_f}{C_f - C_0'}$$

Another relationship between C_t' and C_t is obtained by considering exchange of ^{10}B molecules during a time interval δt. If r is the rate of exchange of gas and adsorbed molecules, the numbers of ^{10}B molecules entering and leaving the gas phase are $(r\,.\,C_t'\,.\,\delta t)$ and $(r\,.\,C_t\,.\,\delta t)$, respectively, the $^{10}BF_3$ molar concentration being thereby changed from C_t to $\left(C_t + \frac{dC_t}{dt}\cdot\delta t\right)$.

$$n\left(C_t + \frac{dC_t}{dt}\cdot\delta t\right) = nC_t + r\,.\,C_t'\,.\,\delta t - r\,.\,C_t\,.\,\delta t$$

and so

$$n\frac{dC_t}{dt} = (C_t' - C_t)\,.\,r$$

$$= \frac{N+n}{N}(C_f - C_t)\,.\,r \qquad (8)$$

from equations (6) and (7). Integrating this and putting $C_t = C_0$ at $t = 0$, one obtains:

$$\frac{C_t - C_f}{C_0 - C_f} = \exp - \left(\frac{N+n}{Nn}\cdot r\,.\,t\right)$$

Appendix 2

Calculation of mass discriminations

The $^{10}BF_3$ molar concentration of a blend is given by

$$C_m = fC_d + (1-f)C_e \qquad (9)$$

where C_m is the $^{10}BF_3$ molar concentration of the blend, C_d is the $^{10}BF_3$ molar concentration of the blending material depleted in ^{10}B, C_e is the $^{10}BF_3$ molar concentration of the blending material enriched in ^{10}B, and f is the molar fraction of depleted material used in the blend. The mass-discrimination constants k_1 and k_2 are then given by

$$R_{m1} = k_1 R_{m1}' \qquad (10)$$

$$R_{m2} = k_2 R_{m2}' \qquad (11)$$

where R_{m1} and R_{m2} are the true $^{11}B/^{10}B$ isotope ratios for the blends at the 25% ^{10}B and 75% ^{10}B concentration levels, respectively {calculated from values of C_m given by equation (9)}, and R_{m1}' and R_{m2}' are the measured $^{11}B/^{10}B$ isotope ratios for these two blends.

Values for C_d and C_e are obtained from the mass spectrometer results given in Table 2. These measured values will contain an error arising from mass discriminations which, although small, is just significant. A correction can be made by utilizing the mass-discrimination constant which should be the same for all samples. In case there is any slight variation in this mass-discrimination constant, it seems reasonable to use k_1 when correcting for C_d (since k_1 applies to the blend which is closest in isotopic composition to C_d), and similarly to use k_2 when correcting for C_e. If this is done, examination of Table 2 reveals that the changes in mass discrimination introduced by the change in ion source will result in a systematic difference between k_1 and k_2. Corrections for the change in ion source can then conveniently be left until values of k_1 and k_2 are obtained.

Equations can be set up which give k_1 and k_2 directly in terms of the experimental results. These, however, lead to quartic equations which are unnecessarily complicated. An alternative is to assume that either k_1 or k_2 can be used to correct for C_d and C_e; this leads to simple quadratic equations which are easily solved, but also necessitates estimating the errors introduced by the assumption. A simpler way, preferred by the author, is to neglect the mass-discrimination error in C_d and C_e at first, and to obtain preliminary values for k_1 and k_2. These preliminary values can be used to correct C_d and C_e, and hence to obtain better values for k_1 and k_2. By a series of rapidly converging approximations, it is possible to obtain precise values for k_1 and k_2 and at the same time to see the effect of the corrections applied to C_d and C_e.

Using this last method, the first preliminary values are

$$k_1 = 1{\cdot}027 \pm 0{\cdot}010$$
$$k_2 = 1{\cdot}037 \pm 0{\cdot}005,$$

and after three successive approximations the results converge on

$$k_1 = 1{\cdot}034 \pm 0{\cdot}011$$
$$k_2 = 1{\cdot}045 \pm 0{\cdot}005$$

These must be corrected for the change in mass discrimination which occurs when the ion source is changed. Duplicate measurements on the enriched blending material and enriched bulk material are consistent with a fractional change in isotope ratio of 0·014 ± 0·005. Correcting k_2 to bring it into line with k_1 gives:

$$k_1 = 1{\cdot}034 \pm 0{\cdot}011$$
$$k_2' = 1{\cdot}031 \pm 0{\cdot}007$$

Ratiometer for low-current mass spectrometry

by F. D. S. BUTEMENT, B.Sc., Ph.D., Department of Inorganic and Physical Chemistry, University of Liverpool
and N. P. FINKELSTEIN, M.Sc., Ph.D.*

[*Paper received* 22 *April*, 1960]

Abstract

A new technique for the measurement of isotopic abundance ratios has been developed. Individual ions in the beam are detected, and an automatic switching device counts the total number of ions in each of the two mass beams being compared. The system is simple to operate and has been found to give very accurate results. No elaborate stabilization of ion-source emission or other operating conditions is necessary.

Introduction

This paper describes a new technique for the measurement of isotopic abundance ratios in mass spectrometry which combines the maximum possible sensitivity (the counting of individual atoms in the ion beam) with high accuracy, and dispenses with the need for any elaborate stabilization of ion-source emission or other operating conditions.

In ratiometry, the two relevant ion currents may be measured either simultaneously, or alternately and repeatedly, thus eliminating from their ratio any inaccuracy due to random fluctuations. Several ratiometers have been described since Strauss(1) first used the technique in 1941. These fall into two broad classes, double- and single-beam ratiometers. In instruments of the first type, the two ion currents are detected simultaneously at separate detectors;(2) in single-beam ratiometers they are brought alternately to the same collector.(3–5) The single-beam type was preferred in our work for the following reasons:

(i) Double-beam ratiometers are subject to errors due to changes in the gain of the two separate detection/amplifying measuring systems.

(ii) With a suitable beam-switching system it is a simple matter to select and change the ionic species being compared, whereas with dual collection this is generally more difficult.

(iii) All the advantages of simultaneous collection are retained, if the two species are alternated with sufficient frequency.

At low beam strengths, the counting of individual atoms has advantages over the more common method of integrating the collected charges. This simplifies the problems of single-beam ratiometry. While single-beam ratiometers have been described(3, 4) which employ integrated current measurement, the determination of the relative strengths of two currents which are not simultaneous is not a simple matter; and this is reflected in the complexity and difficulty of operation of these devices. On the other hand, with single-particle counting, each species can be channelled to a different scaler. Comparison of the number of counts recorded gives the ratio of the two beam strengths during any period. Furthermore, since this ratio is, in fact, the ratio of the total number of ions of the two species arriving at the collector slit, errors due to differential evaporation in the thermal emission source can be eliminated by prolonging measurement over the whole life of a sample. In their paper on positive ion counting as a means of measuring mass spectrometer ion currents, White and Collins(5) refer to a single beam ratiometer, but do not give any details of its performance.

Description of apparatus

The ratiometer is conveniently described under three main headings: (*a*) Detection, (*b*) Measurement, (*c*) Beam control; that is, the means by which ion peaks are selected and brought reproducibly, and under identical conditions, to the collector slit.

---

* Now at Central Metallurgical Laboratory, Anglo-American Corporation of South Africa Ltd., Johannesburg, South Africa.

(*a*) *Detection of ions.* The ion beam was detected by a ovel method first used by Schütze and Berhardt(6) and cently developed by Daly.(7) The beam emerging from e detector slit S_4 (see Fig. 1) is accelerated through a high otential V_D on to a polished aluminium disk K (the "conersion dynode"), where it gives rise to secondary electrons.

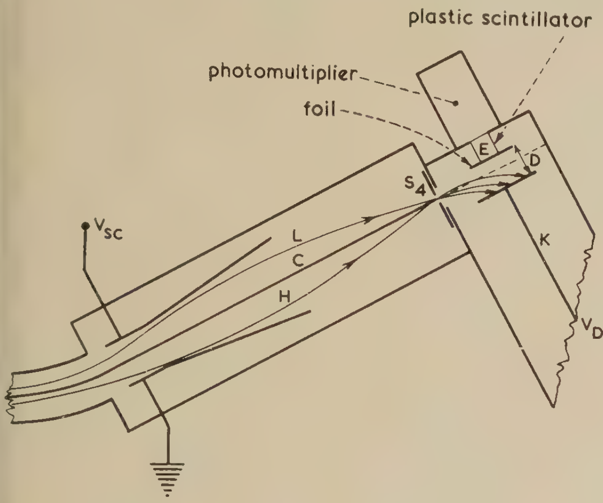

Fig. 1. Method of ion-beam detection

These are, in turn, accelerated on to the earthed surface of the phosphor of a conventional photomultiplier scintillation detector E, which uses a sheet of plastic scintillator covered with a thin (0·5 mg/cm^2) aluminium foil through which the electrons pass. This device, to a large extent, combines the advantages and eliminates the drawbacks of the simple scintillation ion detector and the electron multipler.

The detector used in the present work was developed more or less concurrently with that of Daly, and differs from it in some details. The conversion dynode is operated at a potential 60 kV negative to earth, and the separation of the dynode and phosphor D is 1·7 cm. Thus the potential gradient is 35 kV/cm. Under these conditions, the signal pulses arising in the detector are large enough to allow complete discrimination against photomultiplier dark current. The total recorded level due to field emission from the conversion dynode is generally less than 5 pulses per second. The efficiency of detection is greater than 99%, and mass discrimination is very low. (Under identical conditions, argon-40 and krypton-86 are both detected with greater than 99% efficiency.) The detection-efficiency/dynode-voltage characteristic of the detector has a flat maximum extending about 10% above and below 60 kV, thus ensuring that the efficiency will be constant under all normal running conditions.

(*b*) *Measurement.* The measuring system is shown schematically in Fig. 2. The output from the photomultiplier tube (type 6097, by E.M.I.) is amplified by a pulse amplifier (type 1430A, by Dynatron Radio) and then fed through a discriminator to both a ratemeter and the ratiometer display and switching unit. A second input to the display and switching unit was taken from the diode pump of the ratemeter (q.v.). The output from the ratiometer is fed into two sets of counters, each consisting of two Labgear scalers, type D4019, in series. The resolving time of this system is 6·25 μs. Some advantage would be gained from the use of ultra-fast scaling units, but these were not available for the present work.

(*c*) *Beam control.* The position of the mass-spectrometer beam relative to the collector slit is normally controlled by varying either the ion accelerating voltage or the magnetic analyser field. The former is not practicable with the present instrument, while magnetic field control introduces problems of speed of response and, more serious, of ensuring the reproducible switching between the two positions which is so essential in single-beam ratiometry. It was decided to adopt the unconventional expedient of scanning electrostatically by means of a pair of plates between the magnetic analyser and the collector slit. In practice, this technique proved satisfactory, and no loss in performance due to defocusing or geometrical discrimination was observed.

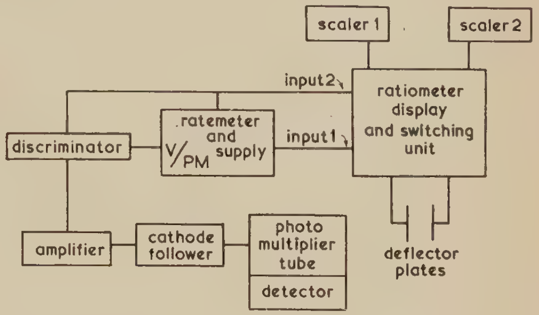

Fig. 2. Measuring system

An essential feature of the ratiometer is that it allows the positions of the ion beams under investigation to be adjusted relative to the collector slit while measurements are actually in progress. This reduces the effect on the precision of measurement of changes in ion energy, and in the strength of the magnetic analyser field. In previous ratiometers(3, 4) where the position of the peaks is present, these factors have seriously limited the performance. It also increases the flexibility of the instrument, by making the selection of the peaks for comparison a simple and rapid process.

This facility was accomplished by means of a special switching and display system, shown in Fig. 3. The switching cycle t is taken to be the interval between successive counts on the same ionic species. During each switching cycle a sequence of events takes place. In the first interval of $t/2$, a portion of the mass spectrum, previously selected by adjustment of the magnetic field strength, is swept across the collector slit by a varying potential on the electrostatic deflector plates, and the response of the detector is displayed on a long-persistence cathode-ray tube so that the pattern of peaks in the relevant part of the spectrum may be observed. During each of the following intervals of $t/4$, fixed potentials are applied to the deflector plates, causing two spots to appear on the horizontal scale of the c.r.t. Their positions can be adjusted, by comparison with the displayed spectrum, so as to bring any pair of peaks in the mass spectrum to the slit. The response of the detector in each interval is now channelled to a separate scaler. Once in operation the process is continuous, the only attention required being an adjustment of the two fixed potentials to compensate for any drift in the mass scale. The ratio of the total counts accumulated on the two scalers during any series of cycles gives the mean relative strengths of the two ion beams during that period.

The ratiometer requires two different types of signal from the detector electronics. For counting, individual short pulses are necessary. These (Input 2) are taken directly from the output of the discriminator. Secondly, a rate-dependent d.c.

voltage is required for the c.r.t. display. This is obtained as follows: The discriminator output is fed into a conventional type of ratemeter, tapped off the diode pump of this instrument as a 120 V, 20 ms sawtoothed pulse, and taken to the display as "Input 1". Satisfactory smoothing of this signal is effected by an RC filter of about 0·01 s time-constant without imposing an objectionable delay on the trace which normally takes 5 s to cross the screen.

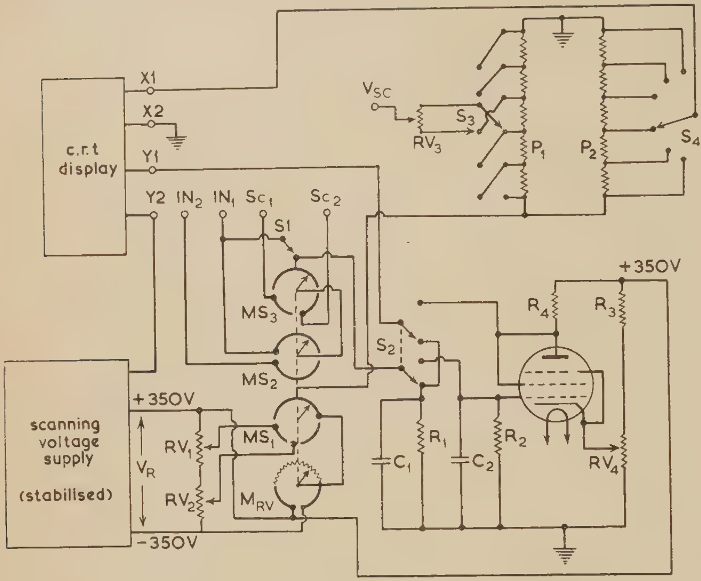

$C_1 = 1\ \mu F$
$C_2 = 0{\cdot}25\ \mu F$

$R_1 = 170\ k\Omega$
$R_2 = 100\ k\Omega$
$R_3 = 22\ k\Omega$
$R_4 = 75\ k\Omega$

V = 6K7

VR = control voltage

P_1 = deflector potential output potential divider [5 × 1 MΩ resistors]
P_2 = C.R.T. time-base output potential divider [5 × 1 MΩ resistors]

Mechanical switch
MRV = rotary potentiometer, approx. 67 kΩ
MS_1, MS_2, MS_3 = rotary switches

Controls
RV_1, RV_2 = 50 kΩ. Control of position of beam during counting periods
RV_3 = 1 MΩ. Fine control for amplitude of electrostatic scan
RV_4 = 20 kΩ. Amplifier bias control

S_1 = by-pass, MS_3
S_2 = display signal selector
S_3 = coarse control for amplitude of electrostatic scan
S_4 = control for X-sweep amplitude

Input 1 = display signal input
Input 2 = counting signal input

Sc_1, Sc_2 = outputs to scalers

X_1, X_2 = C.R.T. X-plates

Y_1 = first c.r.t. Y-plate
Y_2 = second c.r.t. Y-plate and Y-shift

V_{sc} = output to electrostatic deflector plates

Fig. 3. Ratiometer display and switching unit

As is to be expected, the d.c. level developed in this filter is not linearly dependent on rate, and thus peaks tend to become flattened at high rates. This effect was found to be unobjectionable in quantitative work at rates below 1000 atoms per second, and, in fact, was found to be very useful for qualitative work, when the accentuation of the smaller peaks is an advantage.

At rates in excess of 1000 per second, peak flattening reduces the certainty with which the maxima can be distinguished. Their sharpness is restored by applying the signal from the filter to the grid of a variable-mu pentode amplifier, the bias of which can be adjusted (RV_4) so that the valve operates at maximum mutual conductance at the top of the peak. The output of this valve is then applied to the Y-plates. This circuit has the disadvantage that it involves operating the c.r.t. with its Y-plates at 100–150 V above earth potential, with some loss in focus, but this is not sufficient to reduce the precision of measurement.

The voltage V_R used in scanning the ion beam and the c.r.t. time-base is generated by a stabilized power supply and fed by a rotary mechanical switch to potential dividers P_1 and P_2 in parallel. These allow appropriate fractions of the potentials produced by the switch at any time to be applied to the X-plates of the cathode-ray tube, and the electrostatic scanning plates in the mass spectrometer tube. In this way, the c.r.t. spot is kept precisely in step with the position of the beam in the tube.

The mechanical switch comprises three rotary switches MS_1, MS_2, MS_3 and a rotary potentiometer M_{RV} with their wipers mounted on a common insulating shaft. This is driven by a synchronous motor and gearbox. Allowance is made for some variation in the speed of rotation, but advantage is seldom taken of this in practice. A speed of 6 rev/min is used as this is most convenient with a screen persistence of 5–10 s. The switch is so mounted that the end of the driving shaft protrudes from the front panel of the display and switching unit, thus making manual control possible. The rotary switches are constructed of semi-circular or quadrant plates of stainless steel on heavy Perspex mounts. They are so designed that their phosphor-bronze wipers snap sharply and reproducibly from stage to stage as the shaft rotates. M_{RV} is an ordinary 100 kΩ, 15 W rotary potentiometer, modified so that only 180 deg. of its winding is operative. The relative positions of the plates of MS_1, MS_2, MS_3, and of the winding of M_{RV}, and the alinement of their wipers is indicated in Fig. 3.

The functions of the mechanical switch are to control and distribute pulses, display voltages, and scanning potentials. Each revolution consists of a display half-cycle, and two measuring quarters. During the display half-cycle a varying fraction of V_R is supplied by M_{RV} to MS_1, and thence to the output potentiometers P_1 and P_2; thus the ion beam is scanned across the collector slit, and the spot across the c.r.t. screen. At the same time, a signal is applied from Input 1 through MS_2, MS_3, and the appropriate filter to the Y-plates of the cathode-ray tube. During the measuring quarters, steady potentials from the potentiometers RV_1 and RV_2 are in turn applied through MS_1, and P_1 and P_2, fixing both the beam and the position of the spot; and the pulse signal from Input 2 is fed in turn to each scaler. The trace produced during the display half-cycle persists through the counting quarters, enabling each stationary spot to be brought to the maximum of a peak by adjustment of RV_1 or RV_2. Switch S allows the d.c. signal to be applied to the c.r.t. either with RC filtering or through the valve, as desired.

The procedure used in locating a pair of peaks and measuring their relative strengths is as follows:

(a) The source is adjusted to give a convenient ion current.

(b) The spectrum in the region of the masses under investigation is located using magnetic-analyser field control.

(c) Electrostatic scanning is commenced with the output potentiometer to the deflector plates (P_1) set for maximum amplitude of sweep. The magnetic field is adjusted to bring the two peaks of interest to the centre of the screen; then the amplitude of scan is reduced until they, and any peaks lying between them, are displayed.

(*d*) According to the circumstances, either the filter or filter-amplifier display is selected and, in the latter case, the bias adjusted to give the optimum displayed peak shape.

(*e*) Using RV_1 and RV_2, the stationary spots are set on the maximum of the peaks.

(*f*) Both sets of scalers are switched on, care being taken to perform this operation during a display half-cycle.

(*g*) As the machine is running, RV_1 and RV_2 are adjusted as necessary to compensate for any shift in the mass scale.

(*h*) After a period of time, the scalers are switched off, again during a display half-cycle, and the counts recorded by each scaler noted.

(*i*) Each of these figures is corrected for lost counts, using the accurately known dead-time of the measuring system, and the strengths of the ion beams (determined before and after each run using the ratemeter). The ratio of the resulting totals is multiplied by a factor Q to compensate for inequality in the effective length of the two counting quadrants. The factor Q is measured as the ratio of counts recorded when pulses from a pulse generator are applied to the ratiometer, and was constant to 0·08%. The final corrected ratio represents the relative strengths of the two ion beams.

Performance

The operation of the ratiometer in its present form is complicated by the fact that both the means of scanning and the detector used impose changes of trajectory on the ion beam, after it has emerged from the magnetic analyser. Fig. 1 shows on exaggerated scale the paths followed by a heavy mass H and light L as they are brought to the collector slit by the scanning voltage V_{sc} and then accelerated on to the conversion dynode of the detector. C is an intermediate mass which is undeviated by V_{sc}. L and H enter the detector at different angles to the path of C, and strike the dynode at different places, and at different angles. Therefore, they may be detected with differing efficiencies; and mass discrimination might consequently result. This possibility was investigated by determining the relative efficiencies with which the same mass was detected at varying values of V_{sc}. It was found that with the detector geometry used (that is, $D = 1{\cdot}7$ cm), the efficiency is constant for mass separations up to 5%. This range can be extended by reducing D, but this was not necessary in the present application. The performance of the ratiometer was studied by carrying out a series of determinations of the relative abundance of ^{84}Kr and ^{86}Kr. Ions were produced in a simple gas-discharge source since its characteristically unstable ion beam would allow the device to be tested under the most exacting conditions.

About 100 determinations were made of the abundance ratio ^{84}Kr/^{86}Kr. The duration of the measurements, and the strength of the ion beam were systematically varied: the counting times ranged from 5 to 25 min, and the strength of the mass-86 current from 100 to 2800 atoms per second. The mean value of ^{84}Kr/^{86}Kr obtained was 3·270. The standard deviation of the individual ratios from this value varies regularly with the duration of the run, that is, with the number of alternations of the peaks. This is shown in the Table. The standard deviation falls from 0·77% for a 5 min (30 rev) run to 0·15% for runs of 25 min (150 rev).

Standard deviations

Duration of run *(min)*	*(rev)*	^{84}Kr/^{86}Kr	*Standard deviation from* ^{84}Kr/^{86}Kr = 3·270	
5	30	3·269	0·025	(0·77%)
10	60	3·271	0·015	(0·45%)
15	90	3·271	0·011	(0·34%)
20	120	3·271	0·007	(0·21%)
25	150	3·268	0·005	(0·15%)

No dependence of the standard deviation on the total number of counts in readings of constant duration is apparent. This is explained by the fact that the standard deviations recorded are greater than can be attributed purely to statistical fluctuation of the total number of atoms counted.

The precision of the above determinations is, therefore, limited by the unsteadiness of ion beam and any irreproducibility in setting up the maxima of the peaks. It should be mentioned that one of the modes of instability in the discharge source is a random sharp extinction of duration in the region of 0·1–1 s, and repetition rate anything upwards of 5 s. If one considers that the counting periods were 2·5 s in length, and 10 s apart, it can be appreciated that this is the type of fluctuation with which the ratiometer is least fitted to deal. It is, therefore, fair to regard the observed performance as a lower limit. The ultimate precision of the ratiometer is, of course, determined by statistical fluctuation of the steady rate of count of the ion beams. This limit is determined by the lowness of the beam currents used and the duration of the runs, and is independent of the techniques used in measurement.

It was found that abundance ratios measured on different days had a standard deviation of less than 0·1% from the mean value. This may be taken as a measure of the reproducibility of the instrument.

The accepted values of the relative abundances of the isotopes of krypton are due to Nier.(8) In his very careful measurements he obtained the value ^{84}Kr/^{86}Kr as 3·276 ± 0·006. The present value, 3·270 ± 0·005, agrees well with this, but it is possible that this agreement is fortuitous. As the main interest of this investigation was the precision of the instrument, no attempt was made to define the gas-flow conditions in the ion source. Thus it is not known whether they are likely to introduce mass discrimination.

Conclusion

The precision of the instrument is of the same order as that of other recent ratiometers which employ integrated current methods of measurement,(2, 4, 9) although the currents compared are several orders of magnitude lower. No data are available as to the performance of the ratiometer of White and Collins,(5) but it is considered that the shorter switching cycle (10 s as against 40 s), and the fact that the position of the peaks is monitored and can be adjusted while measurement is in progress, must confer some advantage on our instrumentation.

It was found that the instrument was extremely simple to operate, and placed no strain on the operator. The adjustments involved in the process of selecting the peaks to be compared are all performed consecutively, and are independent. This operation seldom took longer than 5 min. Once measurements are in progress, the adjustment required to maintain the correct position of each of the relevant peaks is instantly made using a single control knob. Furthermore, it was found in practice that this adjustment did not have to be performed very often. In this respect the ratiometer compares very favourably with that of Reutersward,(4) where the long series of interacting adjustments necessary apparently make considerable demands on the operator.

It is evident that the performance could be even further improved in several ways. A moderate stabilization of ion-source emission against large short-period fluctuations would be advantageous. At present, the scaler resolving time of $6{\cdot}25\ \mu$s necessitates a rather large correction for lost counts at rates above about 10000 per second, and this correction will not be precise if based on the mean counting rate. Since scintillation counters with a plastic phosphor can give pulses of only 10^{-8} s duration, the use of a fast transistorized scaler(10) with a resolving time of 10^{-8} s would enable counting rates of up to 10^{6} per second to be employed.

Acknowledgement

One of us (N. P. F.) wishes to express his gratitude to the South Africa Council for Scientific and Industrial Research for financial support during the period of this research.

References

(1) Strauss, H. A. *Phys. Rev.*, **59**, p. 430 (1941).
(2) Nier, A. O., Ney, F. P., and Inghram, M. G. *Rev. Sci. Instrum.*, **18**, p. 274 (1947).
(3) Reutersward, C. *Arkiv för Fysik*, **10**, p. 501 (1956).
(4) Reutersward, C. *Arkiv för Fysik*, **8**, p. 18 (1954).
(5) White, F. A., and Collins, F. M. *Appl. Spectroscopy*, **8**, p. 17 (1954).
(6) Schütze, W., and Bernhardt, F. *Z. Phys.*, **145**, p. 44 (1956).
(7) Daly, N. R. Private communication, April 1959.
(8) Nier, A. O. *Phys. Rev.*, **79**, p. 450 (1950).
(9) Stevnes, C. M., and Inghram, M. G. *Rev. Sci. Instrum.*, **24**, p. 987 (1953).
(10) Baldinger, E., Santschi, P., and Wehrli, P. *Nuclear Instruments*, **4**, p. 117 (1959).

Measurement of space density of charge in flowing liquids

by A. SCHURINGA and C. LUTTIK, Koninklijke/Shell-Laboratorium, Amsterdam, Netherlands

[*Paper first received* 11 *December*, 1959, *and in final form* 23 *May*, 1960]

Abstract

A description is given of an instrument for the detection and measurement of the space density of charge in electrically charged flowing liquids, such as white petroleum products. It is based on the measurement of the dielectric displacement at a metal rod placed in the axis of a pipe carrying the liquid under test. The advantage over existent measuring methods is that no pipe-line section or other part of the installation need be insulated.

Introduction

If a liquid flows through a pipe, electric charges are generated in the fluid by the adsorption of ions of one sign on the surface, whilst the mobile ions of the other sign are carried away by the flowing fluid, resulting in a net charge of the fluid. By conduction these charges leak away. As a result of these two effects the charge accumulates until a balance is attained between generation and leakage. If the conductivity is low, it may build up to such a level that an electric breakdown in the form of a spark can result, with the possibility of ignition of combustible vapour resulting in fires and explosions. This may occasionally occur in handling white petroleum products during pumping. In recent years much research has been devoted to the cause of this "electrostatic charging" and to ways of reducing it.* Experimental methods were developed and used for the determination of the properties of the product pumped (conductivity and charging tendency), for monitoring the electrostatic fields in the tanks and for measurement of the amount of charge pumped per unit of time (streaming current). The streaming current can be measured in small installations by collecting the charged liquid in an insulated tank and measuring the current to earth.

Another possibility is the installation of an insulated widened section in the pipe. The bulk of the charge carried with the flow, and generated in the preceding section of the line, flows to earth through the wall of the insulated part, *via* a current meter. The amount of charge generated in the section itself is small, the flow velocity being low here.

Both methods call for a rather complicated mechanical construction with very good electrical insulation, which it is difficult to maintain under most experimental conditions. With the instrument described in this paper only minor structural changes and a light insulation are required.

Principle of the method

In the axis of the pipe *P*, through which the charged liquid flows, a cylindrical rod *R* is placed (Fig. 1). Both rod and pipe are earthed and, owing to the electric charges present between rod and pipe, an electric field is formed at the surface of the rod. This field can be measured by incorporating a cylindrical rotating field meter in a section of this rod. It measures the electric field perpendicular to the axis of the rod. The signal generated is proportional to the dielectric displacement and will, apart from secondary effects, be pendent only on the amount of charge and its spatial stribution. In practically all cases where electrostatic arging is important, pumping speeds are high and pipe ameters large. Hence the flow is very turbulent and a iform charge distribution can be assumed to exist.

---

* Klinkenberg, A., and van der Minne, J. L. *Electrostatics in the Petroleum Industry* (Amsterdam: Elsevier Publishing Co., 1958).

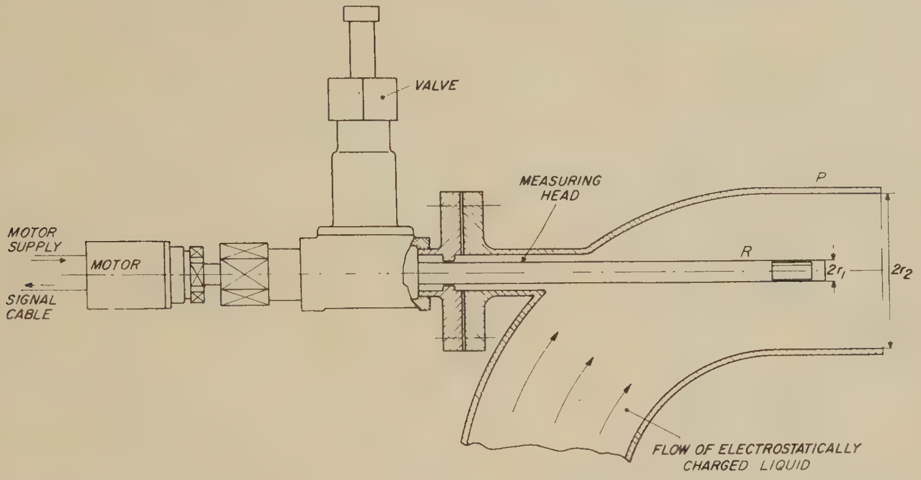

Fig. 1. Position of measuring head in charge density meter

Description of the instrument

Fig. 2 is a block diagram of the complete instrument. It omprises a measuring head (1), junction box (2), cable reels or motor supply and signal cable (3), electric unit (4), scilloscope (5), valve voltmeter (6), and recorder (7).

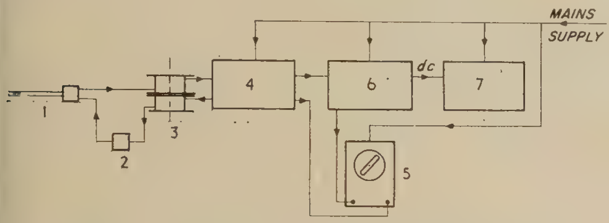

Fig. 2. Block diagram of charge density meter

Mechanical part. The measuring head is brought into the ipe-line at a bend *via* a $1\frac{1}{2}$ in. gate valve (Fig. 1) and is onnected with the electric equipment by two cables (lengths ip to 150 m have been used). This valve permits the measurng head to be installed in and withdrawn from a pipe under ressure.

The measuring head consists of an earthed 800 mm long netal tube, of 24 mm outer and 18·5 mm inner diameter. t the place where the field is measured it is provided with ectangular slots, 55 mm in length and covering 90°. Inside his tube rotates an insulated identically slotted metal tube f 16·5 mm outer diameter, driven by a synchronous motor Fig. 3). The rotation will alternately expose the inner tube rotor) to the field and screen it by the outer tube ("chopping"). y induction a small a.c. voltage is generated, its magnitude nd frequency depending on the rotor speed, number of slots nd impedance between rotor and earth. For a four-pole notor run on 50 c/s and with two slots a signal of the same requency is obtained.

It was possible to use the mains frequency because the ignal was fairly strong (1–50 mV) so that mains intererence could be neglected; this has the advantage of easier andling of the signal. The voltage of the signal is proportional to the dielectric displacement at the surface of the rotor and its phase corresponds with the sign of the charge. This voltage is indicated by a commercial valve voltmeter and may be recorded if needed.

A small 22 W synchronous motor (Fig. 4) is used to drive the rotor; the motor consists of the rotor and stator of a type 77311 synchronous chart-drive motor (by Honeywell Brown Ltd.) equipped with ball bearings. It is contained in an explosion-proof housing of 75 mm diameter, sealed with an O-ring, and drives the rotor by a magnetic coupling, thus providing a gas-tight and low-friction transmission which prevents hydrocarbons and water from entering even in the case of submersion. The signal is picked-up from a rhodium-plated slip ring by a small gold brush.

The lower bearing consists of a stainless steel pin in a porous bronze bush lubricated with molybdenum disulphide. The upper bearing is a stainless steel microball bearing, lubricated by the product pumped.

This construction can only be used in cases where contamination by magnetic particles is unlikely, because these might stick to the magnet and cause stalling of the rotor.

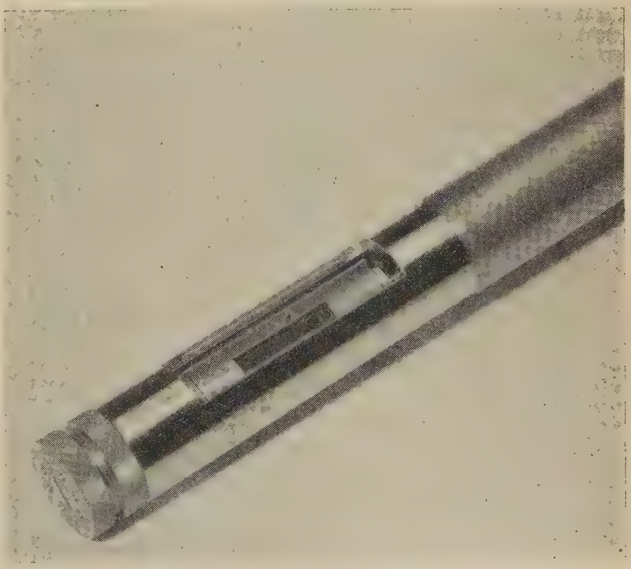

Fig. 3. Slotted cylinders in measuring head

Polytetrafluoroethylene is used throughout as insulating material. O-ring seals make it possible to use the instrument where large positive pressures occur (up to 10 atm). It was found to be important for the rotor shaft to be perfectly straight. Otherwise rotation will cause a variation of the gap between shaft and housing which may give rise to erroneous readings.

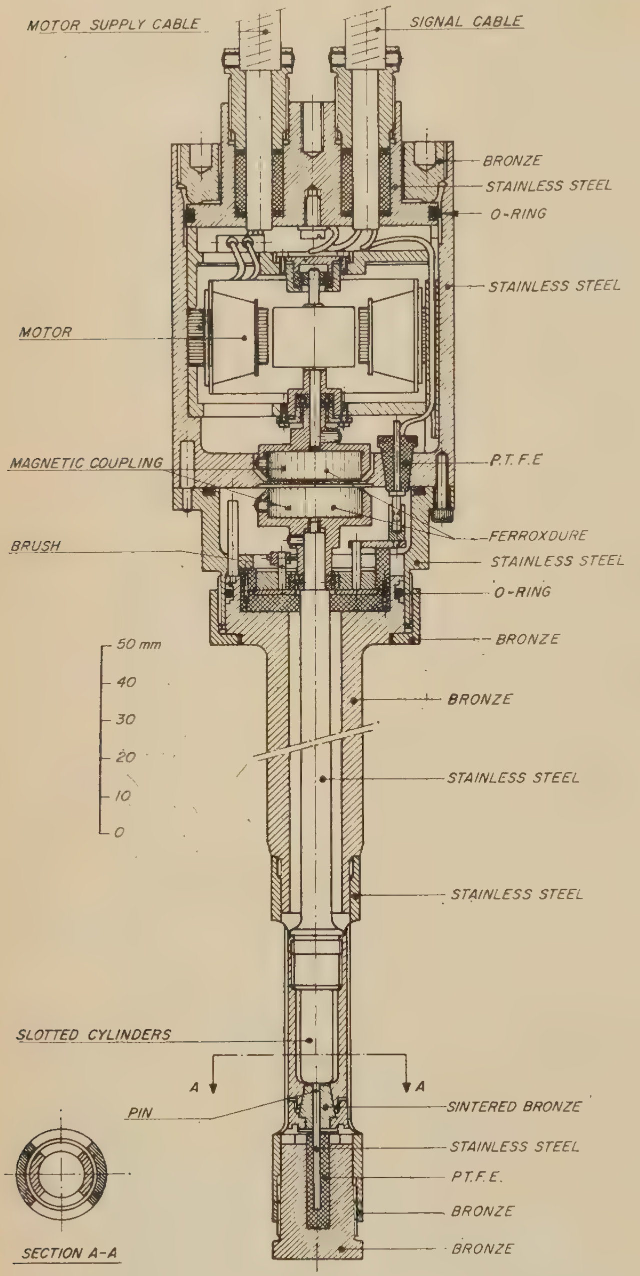
MOTOR SUPPLY CABLE
SIGNAL CABLE
BRONZE
STAINLESS STEEL
O-RING
STAINLESS STEEL
MOTOR
MAGNETIC COUPLING
P.T.F.E
FERROXDURE
BRUSH
STAINLESS STEEL
O-RING
BRONZE
50 mm
40
30
20
10
0
BRONZE
STAINLESS STEEL
STAINLESS STEEL
SLOTTED CYLINDERS
A
A
PIN
SINTERED BRONZE
STAINLESS STEEL
P.T.F.E.
BRONZE
SECTION A-A
BRONZE

Fig. 4. Diagram of measuring head of charge density meter

Electric circuit. Fig. 5 is a representation of the electric circuit used between the measuring head and the valve voltmeter. It contains a power supply for the motor and a switch S_2, with which it is possible to check the instrument from a distance and to determine the sign of the charge. This must be done separately, as the indication of the valve voltmeter is not phase-sensitive and the sign of the charge would otherwise be lost. By pressing push-button S_2 a voltage difference of $+22\cdot5$ V is applied between rotor and stator of the measuring head, creating a positive field between the two cylinders. This field is superimposed on the measured field and, from the resulting increase or decrease in the reading of the voltmeter, it can be decided whether the original field was positive or negative.

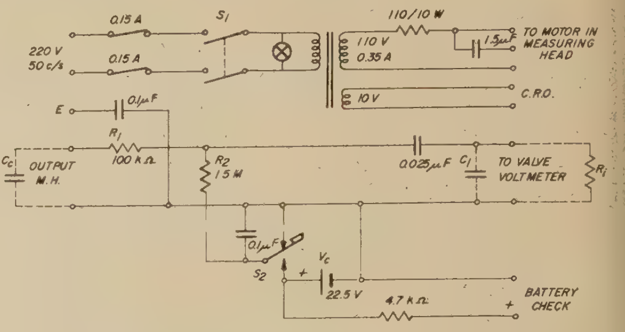
0.15 A
S1
110/10 W
220 V
50 c/s
0.15 A
110 V
0.35 A
1.5μF
TO MOTOR IN MEASURING HEAD
10 V
C.R.O.
E
0.1μF
R1
100 kΩ
Cc
OUTPUT M.H.
R2
15 M
0.025μF
C1
TO VALVE VOLTMETER
Ri
0.1μF
Vc
S2
+
22.5 V
4.7 kΩ
+
BATTERY CHECK

Fig. 5. Circuit used between the measuring head and the valve voltmeter

C_c = cable capacitance
R_i = input resistance of valve voltmeter

Connexion of a small oscilloscope to the a.c. output of the valve voltmeter is very useful for checking phase and waveform of the signal. In experiments where the sign may vary rapidly, a more elaborate circuit with phase-sensitive detection is recommended; such a circuit has been used for field-strength measurements and has been described elsewhere.*

The measuring-head circuit is intrinsically safe: the battery voltage is low and a current-limiting resistor eliminates any danger of a spark forming between the rotor and stator. A conventional d.c. potentiometer recorder can be used, the d.c. signal being derived from the moving-coil meter circuit.

Calculation

The quantities used in the calculations are expressed in the units of the practical system (m, kg, s, V, A, etc.). For the annular space between measuring head (radius r_1) and pipe (radius r_2) the relation between space-charge density and dielectric displacement is:

$$\operatorname{div} D = s \qquad (1)$$

In cylindrical co-ordinates it is:

$$\frac{1}{r}\frac{d(rD)}{dr} = s \qquad (2)$$

with D the dielectric displacement at radius r and s the space density of electric charge.

Measuring head and pipe wall are at the same potential (both are earthed) hence:

$$\int_{r_1}^{r_2} E dr = \int_{r_1}^{r_2} \frac{D}{\varepsilon\varepsilon_0} dr = 0 \qquad (3)$$

where ε is the dielectric constant of the liquid and ε_0 is a universal constant.

---

* Klinkenberg, A., and van der Minne, J. L. *Electrostatics in the Petroleum Industry*, Appendix III (Amsterdam: Elsevier Publishing Co., 1958).

From equations (2) and (3) one obtains for the relation etween the dielectric displacement at the measuring head nd the charge density:

$$D = sr_1/2A \tag{4}$$

here

$$A = 1\Big/\left\{1 - \left(\frac{r_2^2}{r_1^2} - 1\right)\Big/\ln \frac{r_2^2}{r_1^2}\right\}$$

Now derive a relation for the e.m.f. generated. If S enotes the rotor surface area at time t (maximum value $_0$), the charge induced on it will be DS. Variation of the xposed surface area causes an inductive current $d(DS)/dt$ to ow to earth *via* the circuit connected between rotor and arth, developing a voltage v over it. Let this circuit be omposed of a capacitance C and a resistance R in parallel. ne then has:

$$\frac{v}{R} + \frac{d(Cv)}{dt} = \frac{d(DS)}{dt}. \tag{5}$$

In reality three additional currents may have to be taken nto consideration. These are due to:

(*a*) charge generation by the flow at the interface liquid-rotor (current i_1);
(*b*) charge dissipation due to the conductivity of the liquid causing a leakage current i_2 *via* the rotor surface over the input circuit to earth;
(*c*) charge generation by the movement of the rotor relative to the fluid and increasing with speed of rotation (current i_3).

The phenomena (*a*) and (*b*) are analogous to what normally ccurs at the pipe wall. The currents from these two causes re very small compared with the inductive current, as is hown by a rough calculation. Current i_3 from internal harging effects was measured in experiments in a stagnant iquid and was found to be negligible. Hence relation (5) dequately describes the electrical behaviour of the instrument.

If, as an approximation, one supposes that the exposed surface area varies sinusoidally with an angular frequency ω, the relation between the r.m.s. voltage and the dielectric displacement is:

$$V = 0{\cdot}35\, DS_0\Big/\left\{C\sqrt{\left(1 + \frac{1}{\omega^2R^2C^2}\right)}\right\} \tag{6}$$

Combination of equations (4) and (6) gives the relation between charge density and voltage generated

$$s = \frac{5{\cdot}7\, AVC}{S_0 r_1}\sqrt{\left(1 + \frac{1}{\omega^2R^2C^2}\right)}(C/m^3) \tag{7}$$

Determination of constants. The construction used does not permit of easy calculation of the above given relation, because the active surface area S_0 is much smaller than the geometric area, owing to screening by the depth of the slots of the outer cylinder and incomplete chopping: if the rotor is behind the stator it is still exposed to part of the field. Calibration of the instrument is therefore necessary.

The calibration can be carried out by measuring the relation between output voltage and dielectric displacement, assuming that the screening effects remain the same, and calculating with relation (4) the unknown charge density from the signal voltage.

The measuring head is placed axially in a cylinder (radius r_c) brought at a known d.c. potential P, so that at the inner cylinder (radius r_0):

$$D = \frac{\varepsilon\varepsilon_0 P}{r_0} \times \frac{1}{\ln r_c/r_0}\ (C/m^2) \tag{8}$$

If the generated e.m.f. is V_c the calibration constant is

$$\frac{\varepsilon\varepsilon_0 P}{V_c r_0} \times \frac{1}{\ln r_c/r_0}\ (Cm^{-2}\,V^{-1}) \tag{9}$$

In combination with equation (4) one obtains the relation between e.m.f. generated and charge density, if the instrument is used as a charge density meter:

$$s = \frac{2AD}{r_1} = \frac{2A\varepsilon\varepsilon_0 P}{V_c r_0 r_1}\,\frac{1}{\ln r_c/r_0}\ (Cm^{-3}\,V^{-1}) \tag{10}$$

Another, more reliable, but inconvenient method of calibration is obtained by placing the instrument in an earthed metal pipe through which kerosene with good charging properties is pumped into an insulated tank. The electric current I from this tank to earth and the rate of volume flow F are measured; the charge density is then given by I/F. Two independent sets of experiments agreed with the values calculated according to equation (10) within 20%.

For a 5 in. pipe using the circuit of Fig. 5 with

cable capacitance $C_c = 3000$ pF
shunt capacitance $C_i = 0$
input resistance of valve voltmeter $R_i = 1\ \text{M}\Omega$

it was found that $s = 4 \times 10^{-3}\ Cm^{-3}\ V^{-1}$.

The instrument has been successfully used in recent years in several experiments on electrostatic charging in refinery operations, loading of tankers and aircraft fuelling with gasolines, kerosenes and jet fuels.

Reduction of dead-time in halogen-quenched Geiger counters

by B. B. TROTT, B.Sc., Ph.D.,* Viriamu Jones Laboratory, University College, Cardiff

[*Paper first received* 30 *October*, 1959, *and in final form* 20 *May*, 1960]

Abstract

A new type of charge-reduction has been found with a halogen-quenched X-ray Geiger counter. A practical circuit has been developed which reduces the effective dead-time of the counter by a factor of ten. The dead-times were measured by a new method.

Introduction

At the end of a Geiger-counter discharge, a cylindrical sheath of positive ions lies around the anode wire. Normally it must drift well away from the anode before the counter will count again. Simpson(1) was the first to try reversing the voltage applied to the counter immediately after the discharge, so as to collect the positive ions on the anode. Using a nine-valve circuit, he obtained dead-times down to 20 μs. Hodson(2) obtained a dead-time of 30 μs with a simple two-valve circuit.

Collinge(3) showed that Hodson's results (in long cosmic-ray counters) were really due to *localization* of the discharge to a small fraction of the full length of the tube. Later(4) he showed that positive ion collection did occur in some cases.

Thus two versions of the system arose:

(*a*) in short Geiger counters, the ion-collection principle was employed. Simpson reduced the anode voltage to several hundred volts *below* the cathode potential, hoping to collect *all* the positive ions, but later workers such as Smith(5) found this impracticable. The usual compromise was to lower the anode-cathode voltage to zero for say 5–10 μs, thus collecting most of the positive ions on the anode.(1–6)

(*b*) in long cosmic-ray counters, a small voltage drop (e.g. 300 V) was used to localize the discharge, so that most of the length of the tube became active as soon as the voltage pulse ceased (after a few microseconds). This principle has been used widely.(1–5, 7–12)

All the above work was done with counters using an organic quenching gas (usually alcohol). McKeown and Ubbelohde(13) applied a typical circuit to a halogen-quenched X-ray counter, reducing the anode-cathode voltage to zero, and obtained dead-times of about 30–40 μs. Apparently they did not investigate the subject in detail.

The original aim of the present work was to try the effect of a wide range of voltage reductions and pulse lengths on a halogen-quenched X-ray counter. It was intended to measure the charge passing through the counter, as well as the dead-time produced.

A flexible monostable multivibrator circuit was built (Fig. 1), and used with a Philips (Eindhoven) type PW 1962/00 counter (threshold voltage 1360 V). The balanced attenuators enable the anode waveforms of V_1 and V_2 to be observed on an oscilloscope without the circuit being disturbed. The part of the circuit associated with V_3 prevents the anode potential of V_2 from falling more than a few volts below its steady value. This prevents positive overshoot at the grid of V_1, and hence increases the sensitivity of the circuit, since the bias on V_1 is normally set 2·0 V from oscillation point. A quench pulse 3–6 μs long is produced.

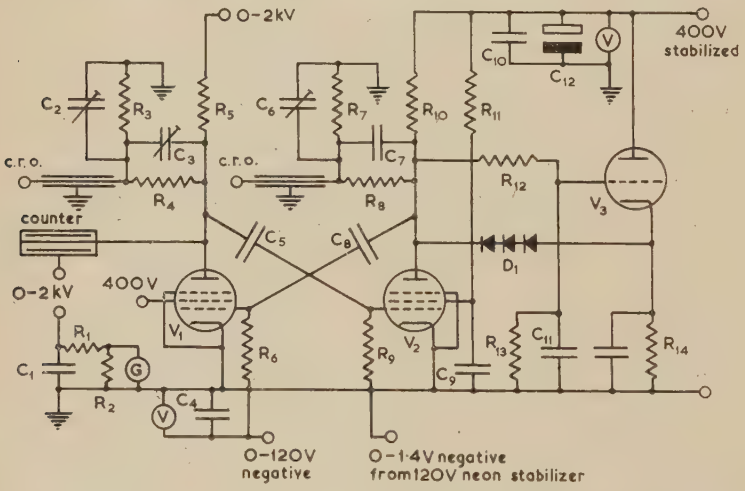

R_1, R_2 = 0·5 MΩ
R_3 = 250 kΩ
R_4 = 20 MΩ
R_5 = 30 kΩ
R_6 = 40 kΩ
R_7 = 170 kΩ
R_8 ≃ 10 MΩ
R_9 = 50 kΩ
R_{10} = 15 kΩ
R_{11} = 36 kΩ
R_{12} = 250 kΩ
R_{13} = 3 MΩ
R_{14} = 50 kΩ

C_1 = 0·1 μF
C_2 = 10–100 pF
C_3 = 2–4 pF
C_4 = 0·1 μF
C_5 = 20 pF
C_6 = 10–100 pF
C_7 = 5 pF
C_8 = 60 pF
C_{11} = 0·1 μF
C_{12} = 8 μF
C_{13} = 0·2 μF

V_1 = EL 38
V_2 = SP 61
V_3 = 6J5

D_1 = 3 × GEX54/3

Fig. 1. Two-valve circuit

The charge Q passing through the Geiger counter was measured by means of the galvanometer in the cathode e.h.t. circuit. The results (Fig. 2) are interpreted as follows:

When the quench-pulse magnitude v is small, the counter behaves almost as though it was operating normally at the e.h.t. value obtaining during the pulse. Larger values of v produce an increase in Q (the peaks in the curves). These are associated with abnormal effects in the counter, e.g. "oscillatory" counts,(14) and the "double pulse" effect,(15) induced by the very low effective anode resistance with which the counter is working during the pulse, and by the presence of a negative ion sheath (formed by electron capture at the beginning of the count).

---

* Now at Brush Electrical Engineering Co. Ltd., Loughborough.

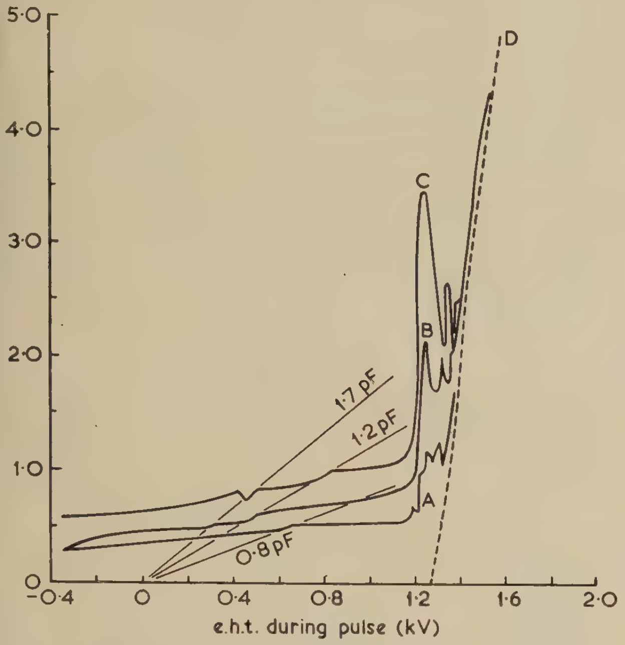

Fig. 2. Effect of the e.h.t. reduction during the pulse on the charge passing per count

A, standing e.h.t. = 1·4 kV
B, standing e.h.t. = 1·5 kV
C, standing e.h.t. = 1·6 kV
D, (broken line) normal (charge/e.h.t.) characteristic of Geiger counter

The charge Q falls sharply when V, the anode voltage during a pulse, falls below 1220 V; this is due to the prevention of avalanche breeding. Breeding normally ceases at 1280 V, but the negative ion sheath increases the field near the anode. As V decreases below 1220 V, Q approaches a steady value, the reduction from normal being entirely due to the halting of the discharge. At still lower values of V, Q is further reduced by ion *collection*. This explains the discontinuities in the curves between 400 and 800 V.

Now collection will occur when the field between the ion sheath and the counter anode is reversed. Let the anode radius of the counter be a, the cathode radius be b and the length of the counter be l. Then, assuming that the ion sheath is close to the anode, the field within it will be reversed when Q/V exceeds $l/2 \ln (b/a)$, if the discharge is spread evenly over the full length of the counter. If the discharge is localized, the field will be reversed within the main concentration of charge at lower values of Q/V. Ion collection should therefore occur when Q/V exceeds a critical value, which may be $l/2 \ln (b/a)$ or some lower figure. For the counter used, $l/2 \ln (b/a) \simeq 1 \cdot 5\ \mu$F, which agrees with Fig. 2 if the discharge covers most of the tube at 1500 and 1600 V, but is partially localized at 1400 V. The second discontinuity in the 1 500 and 1 600 V curves is possibly explained by interaction between the part of the anode which projects clear of the cathode and the tube in which the Geiger counter is mounted.

The reduced value of Q for $V = 800$–1200 V is therefore due to the halting of a discharge which is already building up evenly over almost the entire length of the tube—not to localization of the discharge or to Simpson-type collection. It is well known that in halogen-quenched counters the discharge spreads rapidly, but builds up slowly at any one point (e.g. see Ref. 16). The full length of the counter therefore recovers at almost the same time, which is particularly important in an X-ray or β-particle counter, where the incident particles are not evenly absorbed along the length of the tube.

Measurement of effective dead-time

It was decided to measure the effective dead-time of the system by means of a foil method, as the use of paired γ-ray sources with an X-ray counter is always suspect, especially when the discharge is known to be partially localized. The analogous method involving two pinholes in a screen placed across the X-ray beam(17) requires excessively accurate and rigid construction of the apparatus. The application of external quench-pulses(18) would not have given a clear indication of dead-time if the individual insensitive periods varied in length, and would not have shown possible counting losses due to effects such as abnormal electron capture in the Geiger counter. Facilities were not available for direct comparison of the system with a proportional or scintillation counter.

Usually a number of matched foils is employed in a dead-time measurement, the assumption being that each foil produces exactly the same attenuation of the X-ray beam when in place. If the foils are blemished or unequal in thickness, if stray radiation reaches the counter, or if the X-ray beam is not monochromatic, this method is inaccurate. Also it is laborious to carry out, and not flexible.

It was therefore decided to use a single nickel foil, mounted on a pivoted arm so that it always fell into the same position relative to the X-ray beam. It could be lowered and raised instantly by remote control, thus speeding the work. The attenuation of the single foil is constant if the spectral composition of the X-ray beam remains constant. The high sensitivity of the "multiple-foil" method to non-characteristic radiation, which causes the foils to attenuate unequally, is therefore avoided. The effect on the attenuation of variations in the percentage of non-characteristic radiation, and the effects of this radiation on the form-factor of the dead-time, should be relatively insignificant when a strong diffracted beam is used for the measurements. In the present work these effects were further reduced by the use of a fixed nickel filter, which removed most of the high-energy radiation which would otherwise have been attenuated abnormally by the movable foil.

Now if:

true counting rate with the foil out is	N_2
true counting rate with the foil in is	N_1
apparent counting rate with the foil out is	N_2'
apparent counting rate with the foil in is	N_1'
true attenuation factor of the foil is	A
apparent attenuation factor of the foil is	A'
effective dead-time of the counter is	T

then:

$$A = N_2/N_1 \tag{1}$$

$$A' = N_2'/N_1' \tag{2}$$

$$N_2 = N_2'/(1 - N_2'T) \tag{3}$$

$$N_1 = N_1'/(1 - N_1'T) \tag{4}$$

Therefore

$$\frac{N_2}{N_1} = A = \frac{N_2'(1 - N_1'T)}{N'(1 - N_2'T)} = \frac{A'(1 - N_1'T)}{(1 - N_2'T)} \qquad (5)$$

Therefore

$$\begin{aligned} A' &= A(1 - N_2'T)\{1 + (N_1'T) + (N_1'T)^2 + \dots\} \\ &= A[1 - (N_2' - N_1')T - \{(N_2' - N_1')T(N_1'T)\} - \dots] \end{aligned} \qquad (6)$$

If $N_1'T$ is small, $A' \simeq A - AT(N_2' - N_1')$.

A graph of A' against $(N_2' - N_1')$ then gives A (from the intercept on the A' axis) and then T (from the slope, assuming that T is effectively constant so that the graph is a straight line. If the losses are somewhat greater, then a reasonable result may be obtained by plotting A'' against $(N_2' - N_1')$ where

$$\begin{aligned} A'' &= A\{1 - (N_2' - N_1')T\} \\ &\simeq \left\{\frac{A'}{A} + (N_2' - N_1')(N_1')T^2\right\}A \\ &\simeq A' + A(A - 1)T^2 \cdot (N_1')^2 \end{aligned} \qquad (7)$$

The corrections are calculated using the initial value of T, or preferably an estimate of the final value.

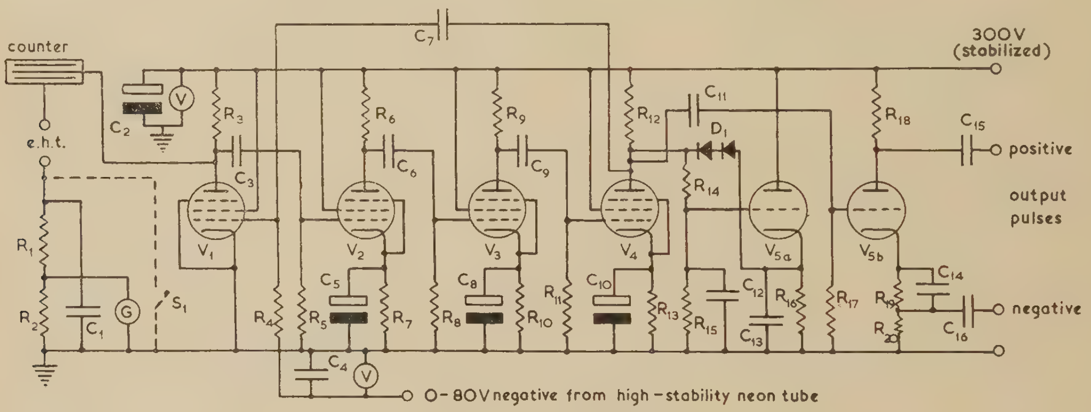

Fig. 3. Multivalve circuit

R_1, R_2 = 0·5 MΩ
R_3, R_4 = 30 kΩ
R_5 = 15 MΩ
R_6 = 370 Ω
R_7 = 1 kΩ
R_8 = 8 MΩ
R_9 = 10 kΩ
R_{10} = 2 kΩ
R_{11} = 50 kΩ
R_{12} = 10 kΩ
R_{13} = 110 Ω
R_{14} = 250 kΩ
R_{15} = 2·5 MΩ
R_{16} = 400 kΩ
R_{17} = 2 MΩ
R_{18} = 2 kΩ
R_{19} = 50 kΩ
R_{20} = 2 kΩ
C_1 = 0·1 μF
C_2 = 8 μF
C_3 = 0·01 μF
C_4 = 0·1 μF
C_5 = 25 μF
C_6 = 0·01 μF
C_7 = 50 pF
C_8 = 25 μF
C_9 = 20 pF
C_{10} = 25 μF
C_{11} = 2·5 pF
C_{12} = 0·1 μF
C_{13} = 1 μF
C_{14} = 0·1 μF
C_{15}, C_{16} = 0·01 μF
V_1 = KT67
V_2–V_4 = Z77
V_5 = ECC83
S_1 = short-circuiting switch for galvanometer system
D_1 = 2 × GEX54/3

Where counting losses are too large for the A'' correction at the highest rates used, a graph can be plotted of A' against N_1', and the true counting losses found by a step-by-step calculation, starting at low rates where the losses may be found from the A' or A'' plot.

The circuit of Fig. 1 gave effective dead-times (on a self-rectifying X-ray source with copper target) of 130 μs, with quench pulse heights of either 300 V or the full e.h.t. value (the two cases of practical importance). Used with an orthodox R–C circuit, the counter exhibited an effective dead-time of 780 μs.

Since the circuit of Fig. 1 was unduly affected by changes in e.h.t. and bias, a more sensitive multivalve circuit, using the same basic principle with a 300 V quench pulse, was built (Fig. 3). The maximum output signal from V_2 is too small to drive V_3 into the grid-current region. This circuit gave dead-times of 40–50 μs over a 70 V range of e.h.t., and for bias values of 4–14 V from oscillation point. The use of R–C connexions to the counter increased the dead-time to 70–80 μs. A 2400 pF capacitor was used for C and the resistor R was chosen so that the counter anode voltage did not rise or fall at high counting rates. In all three cases the counter was used with a 25 pF cable (e.g. 4 ft at 6 pF/ft). The experiments are described in greater detail elsewhere.(19)

When producing large quench pulses (e.g. 1500 V), the circuit of Fig. 1 draws excessive e.h.t. currents and subjects the grid of V_1 to excessive negative voltages. When it is producing small (300 V) quench pulses the e.h.t. and bias voltages must be maintained within close limits to keep the dead-time low. The multivalve circuit of Fig. 3 is therefore more suitable for practical use, in addition to giving a shorter dead-time. It will operate from normal quench-circuit power supplies; that is, 300 V valve-stabilized, at least 60 V bias from a high-stability neon tube and normal stabilized e.h.t. supplies (from which less current than normal is drawn). A calibrated potentiometer would suffice for setting the bias. The circuit therefore offers a very simple method of improving the performance of at least some halogen-quenched Geiger counters.

Acknowledgements

The author wishes to thank Dr. J. W. Hughes for his supervision during the research in the course of which the above work was performed, and the Department of Scientific and Industrial Research for a maintenance allowance.

References

(1) Simpson, J. A. *Phys. Rev.*, **66**, p. 39 (1944).
(2) Hodson, A. L. *J. Sci. Instrum.*, **25**, p. 11 (1948).
(3) Collinge, B. *Nature* (*London*), **162**, p. 853 (1948).
(4) Collinge, B. *Proc. Phys. Soc.* (*London*) *B*, **63**, p. 15 (1950).
(5) Smith, P. B. *Rev. Sci. Instrum.*, **19**, p. 453 (1948).
(6) Thamer, B. J., and Voit, A. F. *Phys. Rev.*, **74**, p. 1261 (1948).
(7) Elliot, H. *Proc. Phys. Soc.* (*London*) *A*, **62**, p. 369 (1949).
(8) Den Hartog, H., and Muller, F. A. *Physica*, **16**, p. 17 (1950).

(9) Porter, W. C., and Ramsay, W. E. *J. Franklin Inst.*, **254**, p. 153 (1952).
10) Porter, W. C. *Nucleonics*, **11**, p. 32 (1953).
(11) Fenyves, E., and Haiman, O. *MTAIII Osztály Közleményei*, **2**, p. 351 (1952).
12) Fenyves, E. *Acta Phys. Hungar.*, **4**, p. 363 (1955).
13) McKeown, P. J. A., and Ubbelohde, A. R. *J. Sci. Instrum.*, **31**, p. 321 (1954).
(14) Liebson, S. H., and Friedman, H. *Rev. Sci. Instrum.*, **19**, p. 303 (1948).
(15) van Zoonen, D. *Appl. Sci. Res., B*, **5**, p. 368 (1955–56).
(16) van Zoonen, D. *Appl. Sci. Res., B*, **4**, p. 237 (1954–55).
(17) Barieu, R. E. *Rev. Sci. Instrum.*, **26**, p. 729 (1955).
(18) Cochran, W. *Acta Cryst.*, **3**, p. 268 (1950).
(19) Trott, B. B. Ph.D. Thesis (University of Wales, 1959).

Apparatus for the measurement of gas velocity in furnaces and models

by A. E. PENGELLY, B.Sc., A.Inst.P., The United Steel Companies Ltd., Moorgate, Rotherham

[*Paper first received* 30 *November*, 1959, *and in final form* 5 *April*, 1960]

Abstract

A range of Pitot tubes is described together with an electromagnetic transducer micromanometer. The assembly is designed for the measurement of gas velocity over a large range of temperature, and pollution with velocities as low as 40 *cm/s. Some applications are described.*

1. Introduction

In recent years the aerodynamics of furnace chambers and ducts has received considerable attention. Measurements have been made in actual plant and in both cold and hot models. Theories have been proposed with the general objectives of improving combustion and heat release, and of analysing and eliminating wear due to erosion by gas-borne solids.(1, 2)

Experience at the International Flame Research Foundation, Ijmuiden, Holland,(3) has led to the development of a range of equipment capable of measuring gas velocity in virtually any circumstances of temperature and pollution ordinarily to be encountered, providing that the stream direction is approximately known, and providing also that the precision required is not greater than about 3%, particularly in slowly moving zones.

Fast work is essential when measurements of gas flow are to be made in production furnaces which do not, in general, work in an equilibrium state, and a feature of the equipment to be discussed is that it has been designed to give a maximum of information in unit time.

2. Range of variables of interest

Short descriptions are given of the type of furnaces and models on which the equipment has been developed and of the general levels of velocity, temperature and solid loadings encountered.

Cold models

Cold aerodynamic models to study flow patterns are generally designed to carry clean air with tracer gases such as carbon dioxide or smoke. In general, the greatest internal dimension of such models is of the order of 150 cm, with temperature below 150° C and velocity above 50 cm/s. Equipment suitable for work in these models is also applicable to ducts carrying similar fluid flows.

Hot models

The use of fired pilot size models of furnaces is increasing. Those on which work has been done are between 1 and 4 m in length with wall temperatures between 700 and 1600° C and fired with oil or gas. The mean flow velocities are generally about 2 m/s at up to 1500° C.

Large furnace chambers

At the Flame Research Station, Ijmuiden, two large furnace chambers exist.(3) Both run with wall temperatures up to 1450° C. Temperatures in the flame cores in either commonly reach 1700° C. In the oil- or gas-fired tunnel the flame jet velocity may be as high as 150 m/s, whilst in the pulverized fuel tunnel the maximum velocity so far attained was 70 m/s. The dimensions of the tunnels are respectively $2 \times 2 \times 6\cdot50$ m long and $1\cdot5 \times 1\cdot5 \times 10$ m long. Solid loading of the gases in furnace No. 1 is at its heaviest about 150 mg per n.t.p. litre in the active flame, with effectively clean gas in the outer zones. The maximum solid particle size is usually not greater than a few microns, but liquid oil drops may exist near the burner. Solid particle loading in furnace No. 2 is much greater; both inside and outside the flame, particle size is larger and solids persist in the whole chamber (ash) with minimum concentration 5–25 mg/l. Frequently the general gas temperature in the chambers is of the same order as the ash fusion temperature of the coal fuel (i.e. about 1400° C). The overall flow velocity is in each case of the order of 1 m/s at 1400° C.

In production units, such as the open hearth steel-melting furnace, temperatures higher than 1700° C are common and the probe equipment has been designed to withstand incident radiation up to 23 cal cm^{-2} s^{-1}, equal to that emitted from a black source at 1750° C.

3. Design of Pitot head

The Pitot tubes described are based upon the National Physical Laboratory shape of hemispherical headed Pitot static tube (Fig. 1). Work has been limited to this type of tube because of its well-known characteristics and its insensitivity to small errors in orientation towards the stream velocity. The principal difficulty in Pitot tube design is in arranging for the static pressure sensing to be accurate and independent of velocity. In general, there is a point on the surface of a body in an airflow at which the pressure is equal to the ambient static level, but its position is a fairly weak function of Reynolds number (pp. 56–64, Ref. 4). The N.P.L. probe of Fig. 1 was designed with the static holes placed to minimize static pressure error. For this work it has been found that if changes in the dimensions of the N.P.L. probe are made as specified on Fig. 1—to facilitate insertion through small doors—no error greater than 3% occurs.

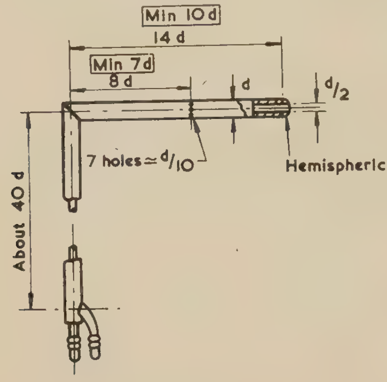

Fig. 1. Round-nosed Pitot static tube, based on the National Physical Laboratory standard

(Figures in boxes indicate minimum dimensions for this work)

Uncooled Pitot tubes

Two designs of uncooled stainless steel Pitot tubes are used; the first, and more critical, is shown in Fig. 2.

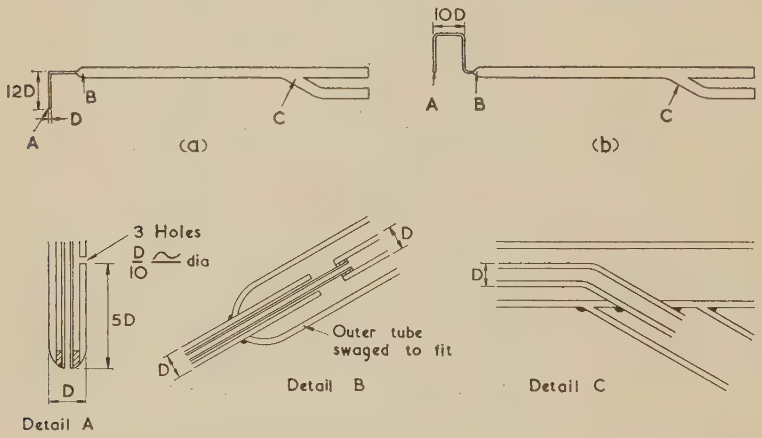

Fig. 2. Small stainless steel uncooled Pitot tubes

(*a*) Straight tip
(*b*) Hooked tip

The designs of Fig. 2 are used for heads of diameter less than 3 mm; the resistance of pressure lines is kept reasonably low by using a wider tube as close to the head as possible. Although an all-welded version of this small Pitot tube has been made for use in a duct at 900° C, the design is more suitable for brazing. The minimum size that has been successfully used is 1·2 mm outer diameter, and it has a time response of 0·3 s for half reading, when used with the micromanometer described in Section 4.

In traverses across jets, the outer boundary of which may coincide with the inner boundary of a negative flowing (recirculation) zone, the "shepherd's crook" shape [Fig. 2(*b*)] permits continuation of the traverse line with the head pointing in the opposite sense.

The second design of uncooled Pitot tube has been made in all sizes from 3 to 20 mm outside diameter and in lengths from 30 to 450 cm. Various specifications of stainless steel have been used and no physical failure has occurred, other than by operating the tubes at temperatures above 1200° C. The design differs only from that of Fig. 2 in that the nose section continues without enlargement to the tail. Most of the calibration work described in Section 5 was done with a tube of this type at temperatures between 20 and 750° C.

Water-cooled Pitot tubes

Two designs of cooled probe are in common use. The larger is 20 mm in diameter and is suitable for work in large chambers and with high solid loading of the gas. A second design, external diameter 6 mm, is suitable for use in flames and hot gases in small enclosures, such as models or ducts carrying gas too hot for the uncooled tubes.

Large cooled Pitot tube. The construction of this head is shown in an exploded view in Fig. 3. It may be fitted to any appropriate water-cooled jacket provided with an internal bore large enough to carry the two $\frac{1}{2}$ in. water supply pipes, together with the two $\frac{1}{4}$ in. outer diameter pressure signal lines. The reason for arranging a separate water supply to the head is that the resistance to water flow is so high that insufficient cooling would be obtained in the supporting probe if it were in series circuit with the head. A water flow of 125 gal/h at 35 lb/in.^{2} is required in order that the temperature rise shall be less than 40° C under the worst possible conditions (black flame at 1700° C = 20·6 cal cm^{-2} s^{-1} incident radiation).

In order to allow sufficient room for water cooling in the minimum practical outside diameter, the total head sensing hole and connexion have been reduced far below the N.P.L. standard size ($d/2$) (Fig. 1). Calibration and comparison with the criterion that $R_e > 30$ when referred to hole diameter (p. 252, Ref. 5) shows that the response of the instrument is unaffected by this modification, and work in highly dust-laden flames has proved it to be an advantage in that the penetration of blocking matter into the probe is less deep than with wider mouthed heads. No difficulty has ever been encountered in clearing the tube with compressed air blown from the back. Under the worst conditions of molten ash found in pulverized fuel flames, no appreciable build-up of solid matter on the probe has occurred, though a layer of fine dust is ordinarily deposited.

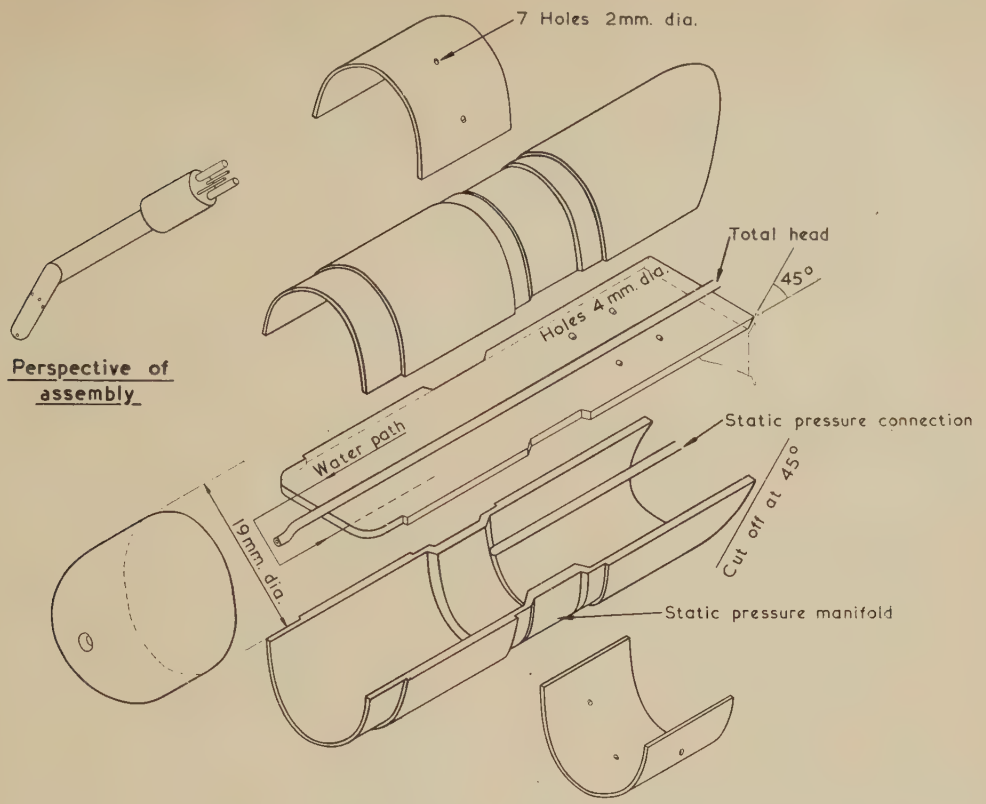
7 Holes 2mm. dia.
Total head
45°
Holes 4 mm. dia.
Perspective of assembly
Water path
Static pressure connection
Cut off at 45°
19mm. dia.
Static pressure manifold

Fig. 3. Exploded view of large water-cooled Pitot head

Small cooled Pitot tube. Fig. 4 shows a water-cooled Pitot tube which has the same external form as the type previously described, but has been made with outside diameter 6 mm. The instrument is constructed of cold drawn multi-bore stainless steel tube (see Fig. 4 for cross-section). Owing to the small bore of the sensing tubes, similar remarks regarding time response apply as to the small uncooled tubes described in Section 2. A water pressure of 25 lb/in.^{2} is required to ensure adequate cooling in the hottest conditions.

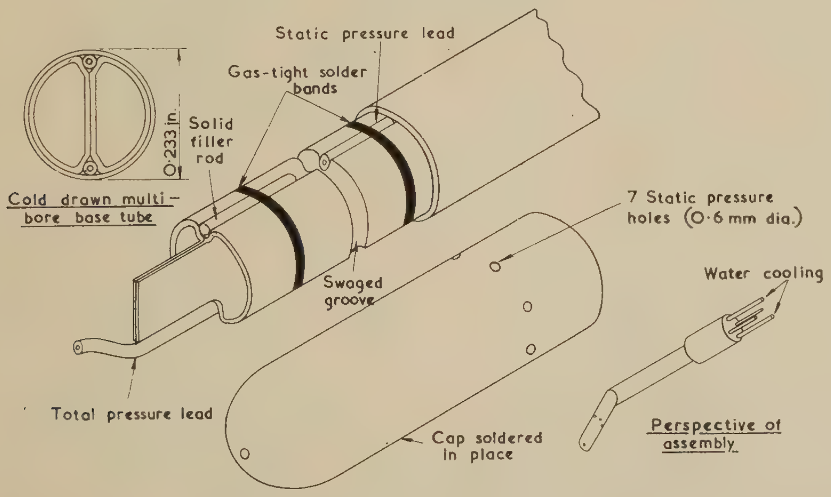
Static pressure lead
Gas-tight solder bands
Solid filler rod
0·233 in.
Cold drawn multi-bore base tube
Swaged groove
7 Static pressure holes (0·6 mm dia.)
Water cooling
Total pressure lead
Cap soldered in place
Perspective of assembly

Fig. 4. Head construction of 6 mm water-cooled Pitot tube

Effect of design modification on Pitot characteristics

A Pitot tube of standard design facing a gas stream of velocity V cm/s, the density of which is ρ (g/cm^3) yields a differential pressure between its static and total tappings equal to Δp (dyn/cm^2), where Δp is given by the equation:

$$V = \sqrt{\{2(\Delta p)/\rho\}}K$$

K is a coefficient, near to 1·0 for standard instruments, which is a function of Reynolds' number. For the minimum head length probe (Fig. 1) of diameter 9 mm, it would be expected that $K = 0{\cdot}97$ (pp. 56–64, Ref. 4) when $V = 100$ cm/s at laboratory temperature (Reynolds' number 560). Depending on the tube diameter and the ambient temperature, the same Reynolds' number, and therefore K value, would occur in a furnace for V between 200 and 500 cm/s. It is worth noting that when velocities of this order occur in furnaces, they are usually in recirculation or unstable zones and subject to fluctuations much greater than 3%. The value of K for $R_e > 600$ is not different by more than 2% from unity and is neglected.

The effect of solid particles suspended in the gas has been the subject of experiments by other workers.(6) Opinions differ as to the quantitative effect, but for the solid concentration levels encountered in all but the burner mouth regions of coal flames, the maximum error to be expected, in neglecting solids altogether and taking ρ equal to the clean gas density, is 5%. A better estimate of V may be obtained by using the mean density of the suspension in the calculation. In the outer zones of the flame the maximum error due to solids is unlikely to be greater than 2%.

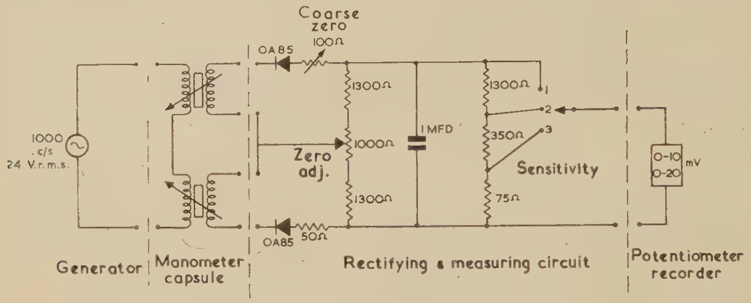
Coarse zero
100Ω
OA85
1300Ω
1MFD
1300Ω
1
2
3
1000 c/s 24 V.r.m.s.
Zero adj.
1000Ω
350Ω
Sensitivity
0-10
0-20
mV
1300Ω
75Ω
OA85
50Ω
Generator
Manometer capsule
Rectifying & measuring circuit
Potentiometer recorder

Fig. 5. Circuit diagram of Beaudouin mutual inductance pressure sensing head

4. Requirements for micromanometers measuring differential pressures of Pitot tubes

(*a*) The speed of response of all Pitot tubes is dependent upon the resistance of the pressure transmission lines and the total volume of the system under pressure (lines plus manometer). It is, therefore, desirable to have the smallest possible included volume in the micromanometer.

(*b*) To allow estimation of the real value in turbulent jets; to obtain a reasonable speed of work, and to help eliminate the human error, a recording instrument is required.

(*c*) A readily variable sensitivity, from the maximum possible to such a value as will allow measurement of the highest differentials expected, is of great assistance when traversing jets.

(*d*) Any non-absolute instrument should be capable of ready calibration against a standard.

The Beaudouin micromanometer

An instrument combining the qualities required uses the Beaudouin mutual inductance pressure sensing head (obtainable from Ateliers de Construction Beaudouin, Paris, or S.F.I.M. (G.B.) Ltd., Slough). The complete system consists

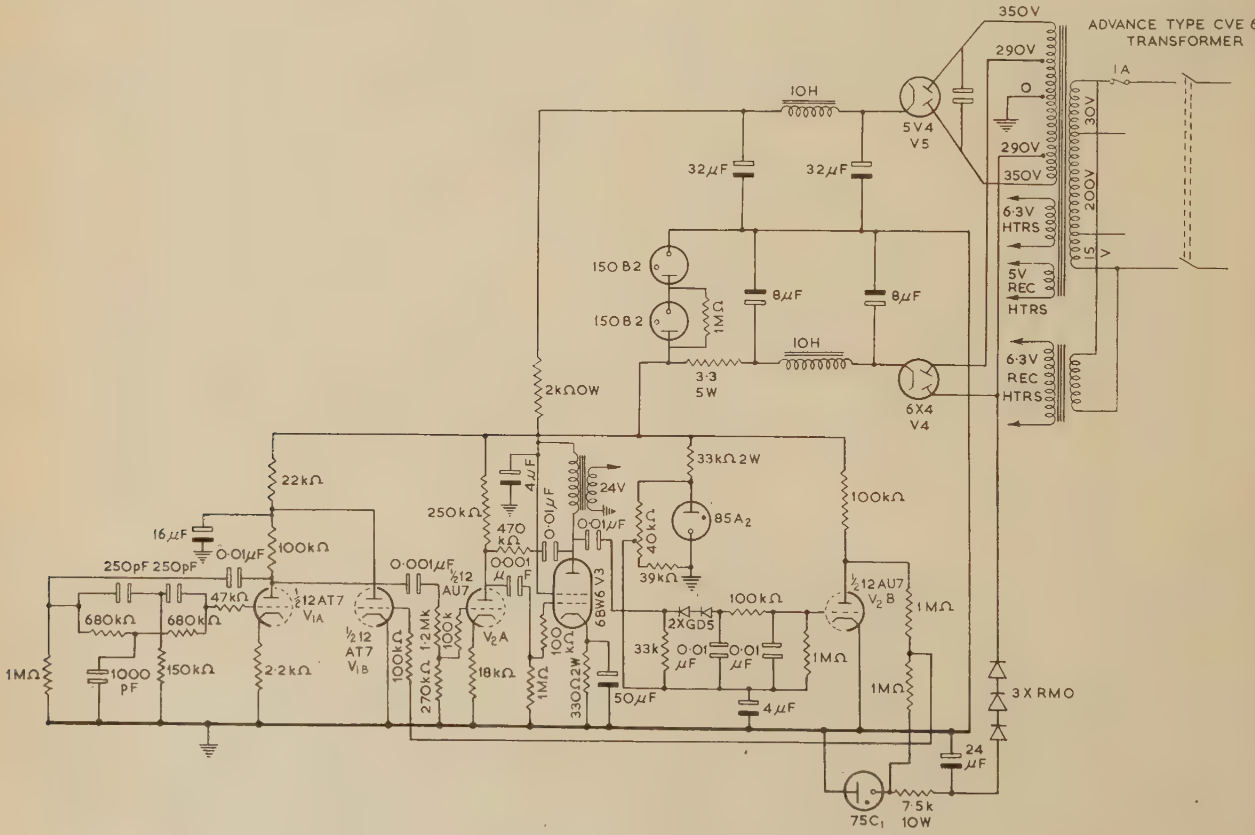
350V
ADVANCE TYPE CVE 60 TRANSFORMER
290V
1A
0
10H
5V4
V5
30V
290V
350V
200V
32μF
32μF
6·3V HTRS
15V
150B2
150B2
1MΩ
8μF
8μF
5V REC
HTRS
10H
3·3 5W
6X4
V4
6·3V REC HTRS
2kΩ0W
33kΩ 2W
22kΩ
4μF
24V
100kΩ
250kΩ
0·01μF
0·01μF
85A2
16μF
470 kΩ
40kΩ
0·01μF
100kΩ
250pF 250pF
0·001μF
0·001 μF
39kΩ
½12 AU7 V2 B
47kΩ
½12AT7 V1A
½12 AU7
6BW6 V3
100kΩ
2XGD5
1MΩ
680kΩ
680kΩ
½12 AT7 V1B
100k
V2A
33k
0·01 μF
0·01 μF
1MΩ
1MΩ
1000 pF
150kΩ
2·2kΩ
100kΩ
1·2MΩ
270kΩ
18kΩ
1MΩ
100 kΩ
330Ω2W
50μF
4μF
1MΩ
3 X RMO
24 μF
75C1
7·5k 10W

Fig. 6. Circuit diagram of 1000 c/s oscillator unit

f an a.c. generator feeding a differential transformer sensing ead, which gives a d.c. millivolt signal after rectification. ig. 5 shows the arrangement.

enerator

The principal required characteristic of the supply generator s stable output voltage. The circuit shown in Fig. 6 has een found to be suitable and stable to better than 1% n time and for mains input variations of ±15%. It has ufficient output to supply one sensing head. A further mplifying valve for each head is used when more than one nit is needed.

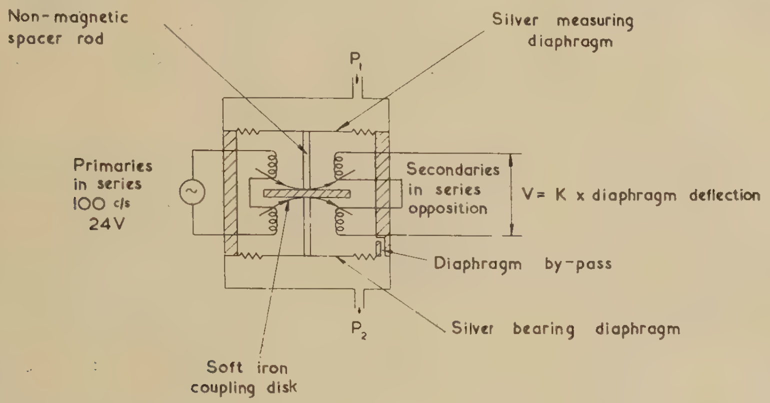
Non-magnetic spacer rod
Silver measuring diaphragm
P_1
Primaries in series 100 c/s 24V
Secondaries in series opposition
V = K x diaphragm deflection
Diaphragm by-pass
P_2
Silver bearing diaphragm
Soft iron coupling disk

Fig. 7. Principle of the Beaudouin differential transformer micromanometer

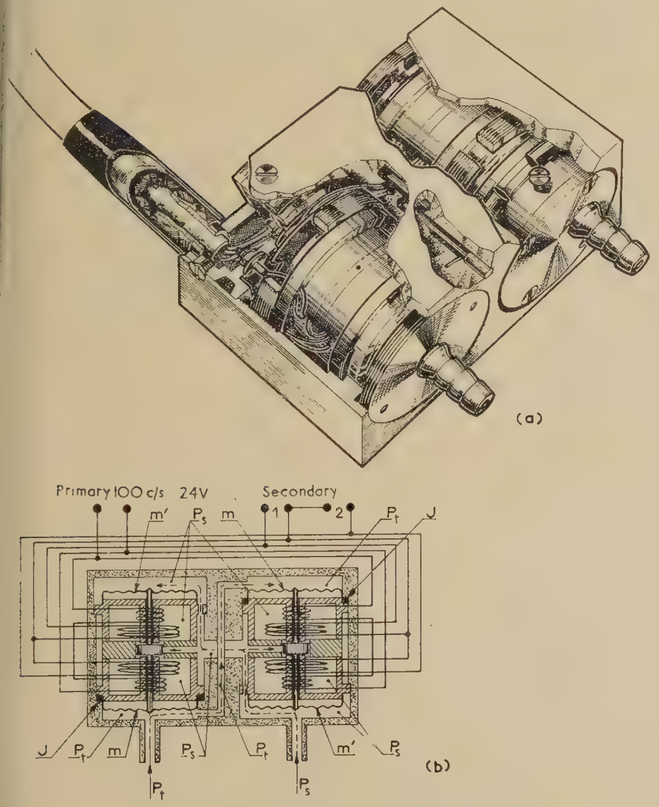

Fig. 8. Micromanometer sensing head

(*a*) Detailed cross-section
(*b*) Internal electrical system

P_s = static pressure; P_t = total pressure; J = gasket; m = measuring diaphragm; m' = bearing diaphragm

Sensing head

The schematic drawing of the sensing head (Fig. 7) makes clear the principles of its construction, and the detailed cross-section (Fig. 8) shows its appearance, size and robust construction. Various sensitivities and maximum pressure tolerances are available from the manufacturers, but those most useful for the Pitot tube applications discussed have maximum pressure tolerances of 4 and 10 cm water gauge (w.g.) respectively. To eliminate errors due to orientation of the sensitive capsule, two units are built into one case [Fig. 8(*a*)] and connected in the self-compensating manner indicated in Fig. 8(*b*), which also shows the internal electrical system.

Rectifying circuit

The circuit shown as part of Fig. 5 has been developed and found to be quite stable and to be unaffected by ambient temperature variations in the range 0–50° C.

Calibration of the micromanometer assembly—sensitivity

Calibration of the system is quickly done against a standard zero-setting water micromanometer. In general, the minimum reliable reading of such instruments is 0·05 mm w.g., but the calibration line may confidently be extrapolated since it is straight and the extrapolation passes through the origin of co-ordinates.

The maximum sensitivity obtainable with the 4 cm w.g. maximum range Beaudouin head is 10 mV/mm w.g. When this signal is fed to a 10 mV full-scale deflexion recorder, the random zero drift is of the order of 0·05 mV or less when using the circuits described. Thus signals greater than 0·1 mV may be detected. The equivalent differential pressure of 0·01 mm w.g. corresponds to velocities of about 40 cm/s at 20° C or 100 cm/s at 1500° C. When special precautions are taken to protect the equipment from ambient temperature changes, from electrical interference and from vibrations, the minimum pressure detectable is 0·003 mm w.g. With the 0–10 cm w.g. range sensing head, corresponding sensitivity figures are reduced by about 30%.

5. Overall test of the equipment

At the time of the development of the water-cooled Pitot tube, it was not certain either that its behaviour would be unaffected by the temperature of the surrounding gas, or that the classic relation (Section 3) would be applicable under the various conditions shown in the table below.

Reynolds' numbers referred to various Pitot tubes and operating conditions

Gas properties			*Reynolds' number referred to Pitot tube and diameter*			
Velocity (m/s)	*Temperature (° C)*	*Approx. Δp (mm w.g.)*	*2 mm uncooled*	*6 mm cooled*	*10 mm uncooled*	*19 mm cooled*
1	20	0·06	120	350	600	1100
10	20	6	$1{\cdot}2 \times 10^3$	$3{\cdot}5 \times 10^3$	$5{\cdot}8 \times 10^3$	$11{\cdot}2 \times 10^3$
1	1000	0·015	—	30	55	105
2	1000	0·06	—	60	110	210
1	1500	0·01	—	20	30	60
2	1500	0·04	—	40	70	130
100	1500	100	—	2×10^3	$3{\cdot}3 \times 10^3$	$6{\cdot}3 \times 10^3$

An overall calibration was therefore undertaken.

The two large furnaces at Ijmuiden are supplied with combustion air at up to 750° C through a common horizontal brick-lined duct of internal diameter 46 cm. A straight portion, 7 m long, of this duct was used as a wind tunnel and traverses made across it with standard form water-cooled and stainless steel Pitot tubes. The distribution curves obtained were integrated and the calculated flow rate compared with the value passing through a metering orifice on the cold side of the air heater, which, together with the rest of the system had been pressure tested and found to be effectively leak free.

Overall calibration

Fig. 9 shows the results of traverses made at mass velocities of the order of 4 m/s; they show a typical flat-topped turbulent distribution shape. The minimum mass velocity at which fully turbulent conditions may reasonably be supposed to exist (Reynolds' number = 2000) in the pipe are about 7 cm/s at 20° C and 50 cm/s at 700° C; both velocities being below the values of interest.

A number of complete traverses and integrations was made for mass velocities between 1·2 m/s at 700° C ($R_e = 4650$) and 35 m/s at 20° C ($R_e = 9{\cdot}5 \times 10^5$) and agreement between integrated and measured mass flow values was obtained with 2% standard deviation. From this, it would be expected that the ratio between mass flow and peak velocity would be a function of Reynolds' number and pipe roughness, but it was found during the experimental work that for all the values tested, the ratio (axial velocity/mean velocity) was 1·09 ± 2%. Detailed calculations based on the work of Stanton and Nikuradse (pp. 33–35, Ref. 4, and pp. 336–339, Ref. 5) suggest that within the range of velocities and temperatures used, it would be expected that the velocity ratio would fall about 2% between 2 and 30 m/s and be

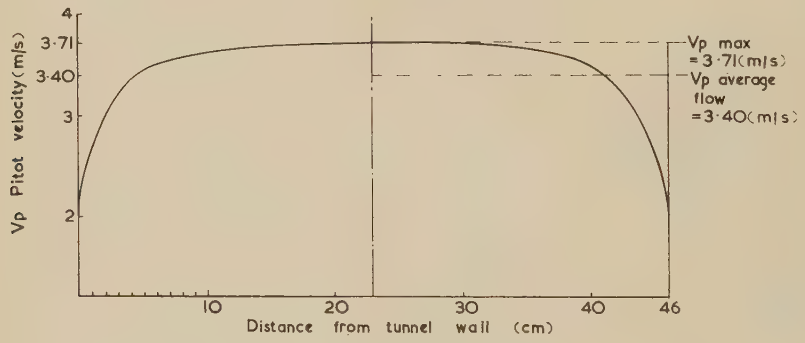

Fig. 9. Typical velocity distribution across hot wind tunnel $V_p = \sqrt{(2\Delta p/\rho)}$.

Temperature = 460° C.

Mean velocity calculated from orifice reading 3·34 m/s

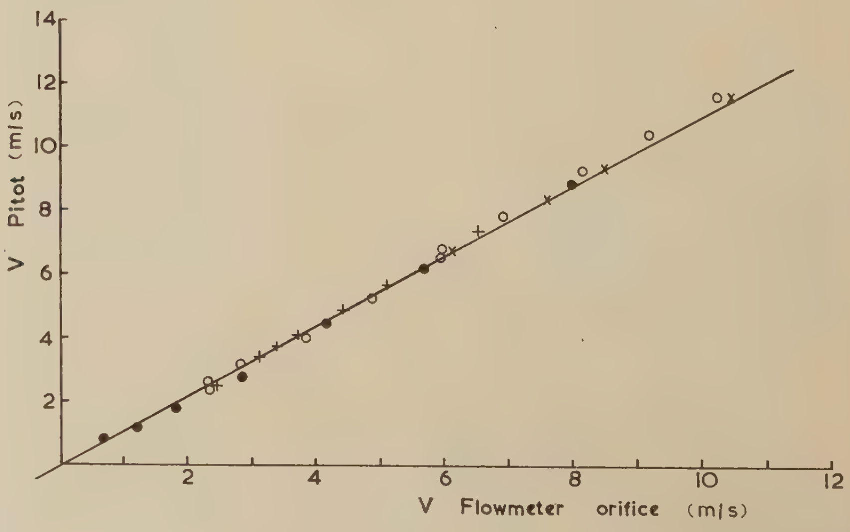

Fig. 10. Relation between axial velocity (Pitot tube) in wind tunnel and mass flow velocity (orifice)

× = 650° C + = 460° C
● = 260° C ○ = 20° C

rtually independent of temperature, within the range of perimental error.

Turbulent distribution having been proved, and unit rrelation between orifice reading and maximum value ving been demonstrated, Pitot heads were placed in the nnel axis and readings made comparing the orifice measure- ent with that of the Pitot head for different flow rates.

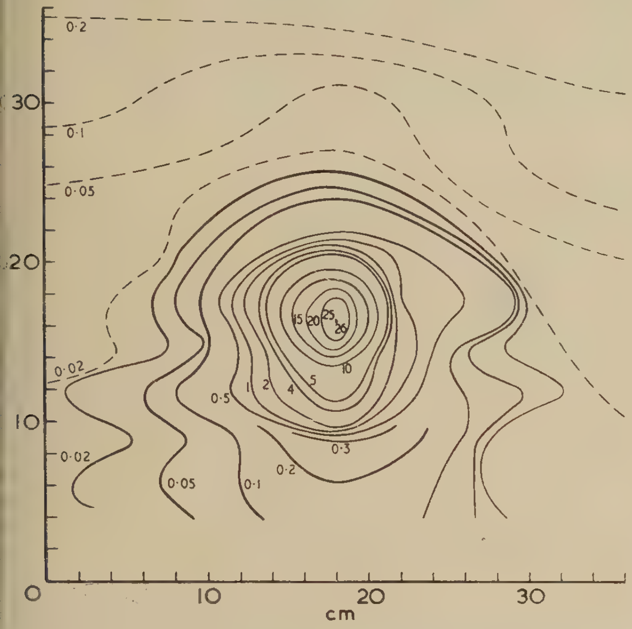

Fig. 11. Velocity cross-section of a hot model furnace
– – – – = recirculation (negative velocities)
(Figures are equivalent Δp in mm water gauge)

ig. 10 shows the results of experiments of this type. The act that the line is straight and passes through the origin ith a slope of 1·09 demonstrates that the Pitot head behaves ithin practical limits according to the classic equation for ll the values shown.

From the well-established laws of flow round Pitot tubes pp. 52–64, Ref. 4) it would be expected that the value of K ould rise from 0·97 at $R_e = 560$ to 1·00 at $R_e = 250$, and thereafter increase rapidly. The lowest point of Fig. 10 corresponds to $R_e = 260$, and its position is subject to accidental errors of ±3%. From known behaviour and from the calibration it may therefore be concluded that for Reynolds' number referred to a given Pitot tube, practicable results can be obtained for values down to $R_e = 250$. For Reynolds' numbers between 50 and 250, work in cold air has shown that K rises to about 1·1 at $R_e = 50$. Below $R_e = 50$, worthwhile measurement could not be made. From the table it can be seen that in most circumstances, it is possible to choose, from the range of Pitot tubes available, one physically suitable for measurement in given circumstances.

6. Application of equipment

To illustrate the scope of the assembly of equipment some examples of its application are given.

The greatest advantage of the equipment over other systems of Pitot-manometer assembly is the low response time and the fact that signals may be recorded. Thus mechanically-propelled traverses may be made.

Work in small scale models

Fig. 11 shows a cross-sectional contour plan of isokinetics in a small hot model furnace which was fired with town's gas.

In order to scan both the positive flowing and recirculation zones of the whole cross-section, the length of the Pitot tip was made equal to the distance between vertical slots of the furnace. Thus, to scan at a given slot the Pitot tube was passed through the next rearward slot for positive-flowing zones, and the next forward slot for recirculation areas. Evidently this method requires that the two zones should be measured at different times, but it will be noticed how well the shapes of the "just positive" and "just negative" regions correlate. In order to construct such cross-sections, ten horizontal traverses were made in the forward and in the negative facing directions. The total working time required was about 40 min.

Work in the large tunnels

A special device for holding and traversing large water-cooled probes in the Ijmuiden flame tunnels allows relatively easy handling, and thus greatly speeds velocity measurement.

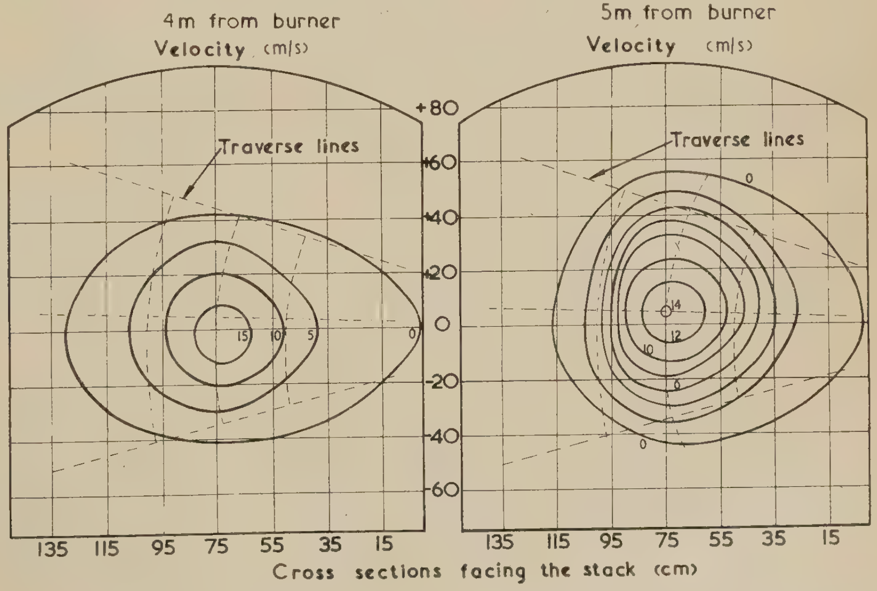

Fig. 12. Pulverized coal flame furnace velocity contours

Interest in velocity contours in these tunnels is usually confined to the positive flowing (jet) zone. Equipment used enables traverses to be made over the region and along the *loci* indicated on Fig. 12, which also shows isokinetics at an early slot, when burning high ash pulverized coal. Only in the very mouth of the burner, where the solid concentration is of the order of 1 g/l, is it impossible to complete a traverse of the jet before the Pitot tube is blocked. No difficulty has, however, been experienced in clearing by blowing compressed air from the rear of the Pitot tube.

One horizontal and three or five radial double traverses are made at each slot where the jet still effectively exists. Each traverse takes approximately 90 s so that information for completing the contour shown may be obtained in 18 min working time.

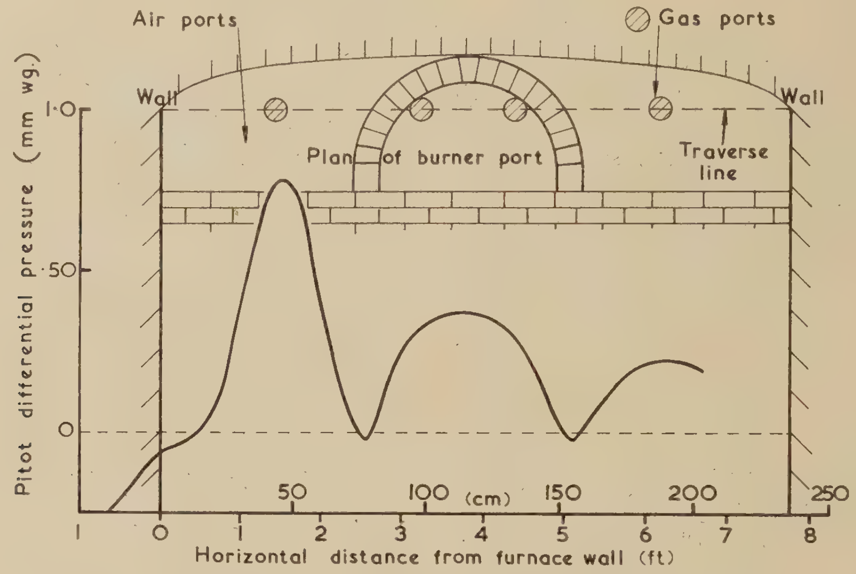

Fig. 13. Velocity head traverse across gas-fired soaking pit burner ports (Standard 20 mm water-cooled Pitot tube)

An industrial application

There are numerous industrial furnace and duct problems, the solutions of which can be accelerated if equipment for reasonably accurate and fast gas velocity measurement is available. Fig. 13 shows the results of a traverse across the inlet port of a furnace in a steelworks. The asymmetry of the incoming gas is effectively demonstrated and a reason for the reported unevenness of slag deposits in the furnace is indicated.

7. Summary and conclusions

General background and critical details have been given of the development of equipment for fast and reasonably reliable measurement of gas velocities in a known direction. The scope of the equipment is wide in that it may be used in gases at widely different temperatures and with high dust loadings.

8. Acknowledgements

The author wishes to thank the Joint Committee of the International Flame Research Foundation, and Mr. F. H. Saniter, Director of The United Steel Companies Ltd. Research Laboratories, for permission to publish this work. He also acknowledges his indebtedness to the Electronics Department of the above Laboratories for the circuit design of Fig. 6.

References

(1) Thring, M. W. *Brit. J. Appl. Phys.*, **8**, p. 89 (1957).

(2) Chesters, J. H. *Iron and Steel*, **32**, p. 3 (1959).

(3) Saunders, O. A. *Nature (London)*, **173**, p. 1160 (1954).

(4) Ower, E. *The Measurement of Air Flow*, 3rd Ed., pp. 33–35, pp. 52 *et seq.* (London: Chapman and Hall Ltd.).

(5) Goldstein. *Modern Developments in Fluid Dynamics*, **1** to p. 330; **2**, pp. 331 *et seq.* (Oxford: Clarendon Press).

(6) Dalmon, T., and Lowe, H. 2*nd Conference on Pulv. Fuel* (London, November 1957, published by Inst. Fuel).

Simple continuous chart and integrating device or a Joyce-Loebl microdensitometer Mk. I

y G. FARROW, B.Sc.(Tech.), Ph.D., and D. PRESTON, Fibres Division, Imperial Chemical Industries Ltd., arrogate, Yorkshire.

[*Paper first received* 7 *March, and in final form* 10 *May*, 1960]

Abstract

Two simple devices are described which may be added to Joyce–Loebl microdensitometer. The continuous chart evice enables a chosen expansion ratio of any film being canned by the microdensitometer to be recorded on one iece of chart paper. The existing mechanical link etween the original chart table and film carriage table as been preserved. The integrating attachment allows he area beneath the recorded trace to be determined while the trace is being produced.

Introduction

A METHOD has recently been devised for the measurement of crystallinity in drawn polyethylene terephthalate fibres by an X-ray technique.(1) The X-ray reflexions are recorded on photographic film which is then scanned by a microdensitometer (by Messrs. Joyce–Loebl and Co. Ltd.), based on a design by Walker.(2) The Joyce–Loebl microdensitometer Mk I suffered from the defect, for certain applications, of only being able to record the trace on a piece of graph paper 28 cm in length. This meant that a number of pieces had to be joined together to give an expanded trace, which was found to be more convenient for the accurate measurement of crystallinity. Furthermore, it was necessary to know the integrated area of the trace for the measurement of crystallinity. A simple integrating device was incorporated into the instrument to do this while the trace was being produced.

Description of chart device

The general arrangement of the instrument may be seen from the schematic diagram in Fig. 1. The existing small movable table (11 × 8·75 in.) on which the graph paper was pinned has been replaced by a fixed table (22 × 8·75 × 0·25 in.), secured in position by six Allen screws tapped into the top of the microdensitometer. The spindle *A*, mounted on the top of the table, is detachable (held in position by a spring-loaded bar) and is threaded through the centre of a roll of chart paper (150 ft × 8·75 in. in width). The paper is passed under the removable rollers *B* and *C* (retained in position by spring-loaded ball bearings at either end) which keep the paper flat as it passes beneath the pen of the instrument. It is then taken up on to the feed roll *D* which is driven directly from the gear-box (connected to the motor) by the connecting rod *E*, with two universal couplings for flexibility, and the worm drive *F*. The idler roller *G* is again spring-loaded and presses the chart paper against the circumference of the feed roll, giving it a greater angle of contact and preventing "jumping" of the paper off the roller. The paper overhangs the end of the microdensitometer when it leaves the feed roll and falls freely to the floor. Its complete passage is indicated by the letter *H*. The existing ratio arm *I*

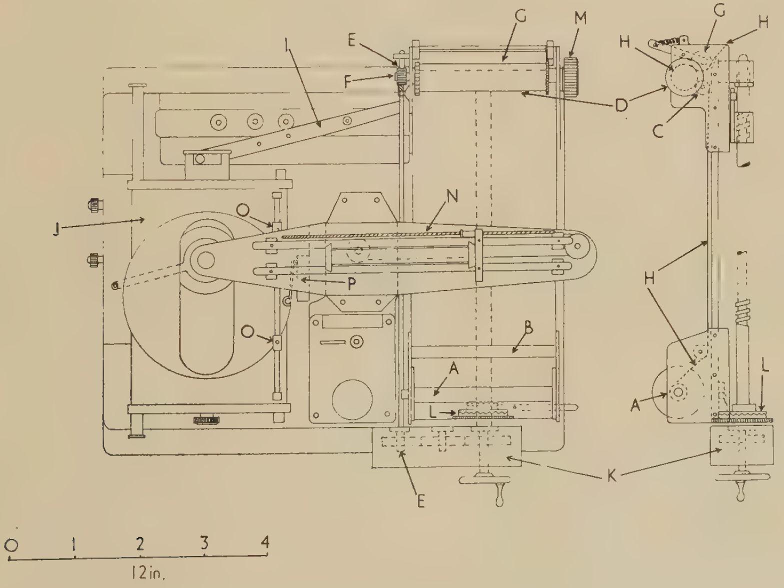

Fig. 1. General arrangement of the Joyce–Loebl microdensitometer Mk. 1

(fixed on a 1 : 1 ratio and passing underneath the new table), connecting the film table *J* with the motor *via* the old table, has been preserved, so that any variation in the speed of the motor will affect the movement of the film table and chart to the same extent (see integrating device, however). The 1 : 1 position on the ratio arm is kept in this fixed position.

The actual ratio of expansion obtained from a film is governed by the speed of the chart, which in itself is governed by the selected gear ratios in the gear-box *K*, various ratios being available between 1 : 1 and 24 : 1, or even higher if desired. The faster the chart speed the greater the expansion. The gears are made of hard brass. If a compound train of gears is necessary to produce a particular ratio, adjustable studs and a banjo plate are available in the gear-box. The gears are numbered and the ones necessary to give particular gear ratios have been engraved on the side of the sliding panel of the gear-box.

In order to place the film table into a suitable position it is sometimes necessary to traverse it by hand. Two clutches have been provided, one *L* disengages the lead screw from the motor and the other, a torsion spring under the knob *M*, when held by the hand, disengages the feed roll from the drive.

Principle of integrating device

A modified Honeywell–Brown slide wire *N* (total resistance 650 Ω) is fitted parallel to the pen traverse (19 cm) of the microdensitometer and in contact with a low-resistance wiper arm. Any change, therefore, in the position of the pen will produce a corresponding change in the resistance of the slide wire. The slide wire and wiper are potentiometrically coupled to an integrating motor, the speed of which varies in proportion to the position of the pen.

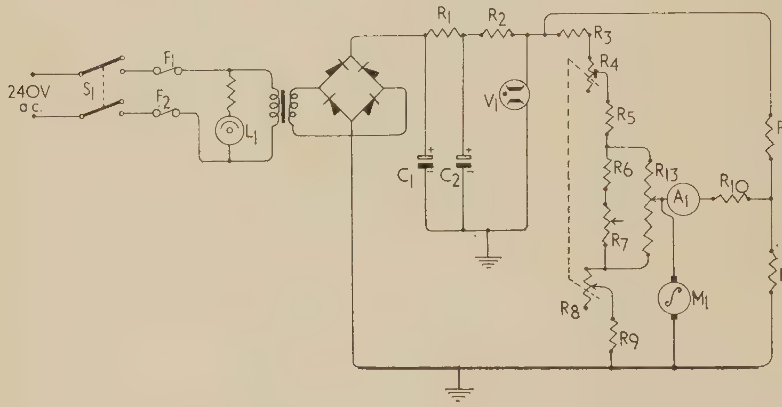

$R_1 = 680\ \Omega$
$R_2 = 330\ \Omega$
$R_3 = 3{\cdot}9\ \text{k}\Omega$
$R_4 = 250\ \Omega$
$R_5 = 180\ \Omega$
$R_6 = 1\ \text{k}\Omega$
$R_7, R_8 = 250\ \Omega$
$R_9 = 430\ \Omega$
$R_{10} = 10\ \text{k}\Omega$
$R_{11} = 82\ \text{k}\Omega$
$R_{12} = 10\ \text{k}\Omega$
$R_{13} = 650\ \Omega$, slide wire
$C_1 = 16\ \mu\text{F}$
$C_2 = 32\ \mu\text{F}$
V_1 = 90C1
S_1 = double-pole switch
F_1, F_2 = 20 A fuses
L_1 = indicator lamp
A_1 = 0–100 μA
M_1 = low inertia integrating motor

Fig. 2. Theoretical circuit of electronic area integrator

Electronics

Integrating motor. The motor (by Electro Methods Ltd.) is mechanically coupled to a calibrated dial, capable of recording 10 000 counts. In order for the motor to function in a linear manner (i.e. the speed or number of counts recorded by the motor is directly proportional to the applied voltage), as necessary for the measurement of area, the voltage input had to lie between 7·0 and 25 V d.c. The upper limit was set by the allowed voltage on the armature of the motor and the lower limit was found experimentally. A linear count rate was not reached until the input voltage attained 7·0 V.

Circuit and method of biasing. The circuit (Fig. 2) is designed to give a stable d.c. supply and to allow the voltages fed to the integrating motor from the contacts on the slide wire (connected to the pen of the microdensitometer) to fall within the stated range.

The stabilized d.c. supply is fed into the slide wire through a series resistance which reduces the voltage at the top of the slide wire to the maximum input voltage of the integrating motor (24·0 V), so that this value is reached when the pen is at maximum optical density. A second resistance, placed at the end of the slide wire, ensures that the minimum input voltage (7·0 V) is maintained. As a minimum input must be maintained on the armature of the integrating motor, even if an area is not being integrated, it is not possible to set the recorder pen of the microdensitometer to give a zero count. An artificial zero, called the basic count, is therefore used. It is a fixed number which, on deduction from the total number of counts, obtained from scanning a particular set of intensities, gives the true number of counts. In order to keep this basic count constant, irrespective of pen position of the microdensitometer, over a certain range of movement (0–6 cm), a backing-off or biasing device was constructed. The spindles of two 250 Ω potentiometers were mechanically coupled together so that by incorporating them with the slide wire (Fig. 2), and with suitable adjustment, the potential dividing network would maintain a constant voltage, independent of the position of the pen over the specified range (as the resistance of one potentiometer is rising the other is falling by the same amount). The amount of adjustment required by the backing-off device is indicated on a centre zero microammeter coupled to the integrating device in a bridge circuit (Fig. 2). The bridge is balanced with the microammeter needle at zero and the integrating motor running at the basic counting rate.

Measurement of area. The measurement of area by the integrating device may be readily understood from Fig. 3. The shaded part of the drawing represents the area it is

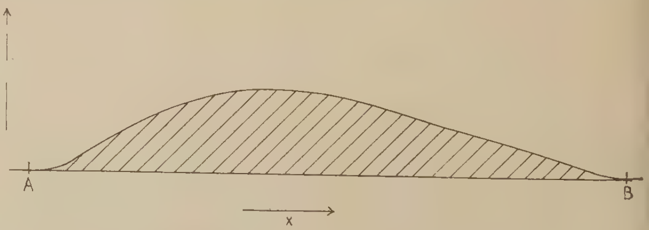

Fig. 3. Measurement of area by the integrating device

quired to measure. The two parameters necessary to do is may be designated x and y respectively. The movement the recording pen of the microdensitometer will be along e y direction and the chart paper will move along the direction. The count recorded by the integrating motor ill depend on two things; the length of time that the chart aper takes to travel from A to B (the chosen points of the an) and the movement of the pen along the y direction. he former will depend on the speed of the chart motor (or e gearing from the motor) and the latter on the intensity the X-ray film being scanned. The speed of the chart aper must, therefore, be constant during any one measureent and this was ensured by fitting a synchronous motor the microdensitometer in place of the existing variable eed motor.

It is desired to measure the area between points A and B. hese points are located by two movable cams O (Fig. 1) n a bar, set in relation to the film, which is alined and unched before exposure on a jig. This allows it to be ccurately located each time on the movable table of the icrodensitometer. As the film traverses under the scanning bjective of the microdensitometer the first cam trips a icro-switch P (Fig. 1) at point A (Fig. 3), which starts the tegrating device. When the second cam reaches the icro-switch, at point B, the device is switched off. Initially, he film table is wound into position A by hand (denoted by he "click" of the micro-switch) and the backing-off device adjusted until the microammeter needle reads zero.

The speed of the dial type integrator has been adjusted (by shunting the slide wire) so that one digit on the dial is equal to one square centimetre. From the total count recorded on the dial the basic count must be deducted. The basic count is most readily obtained by a linear scan between the cams without a film. The basic count for this particular work has been in the region of 2500 reproducible to ± 2 counts. Areas can be measured to an accuracy of $\pm 1{\cdot}5\%$.

In the case of polyethylene terephthalate (as with other polymers) there is a slight rise in film background due to incoherent scatter, which must be added on to the basic count before deduction from the total. As the scatter has been shown to be a linear function(1) it is easily read off from a specially prepared graph.

Acknowledgement

The authors wish to acknowledge the help given by Mr. E. Bakker and Mr. L. Varley in the design and for most of the construction of the instruments; also Dr. K. W. Hillier for helpful criticisms of the manuscript.

References

(1) Farrow, G., and Preston, D. *Brit. J. Appl. Phys.*, **11**, p. 353 (1960).
(2) Walker, P. M. B. *J. Sci. Instrum.*, **30**, p. 162 (1953).

Measurement of thermal diffusivity of semiconductors by Ångström's method

y A. GREEN, B.Sc., Ph.D., and L. E. J. COWLES, Research Laboratories of The General Electric Co. Ltd., Wembley, England.

Paper received 11 *April*, 1960]

Abstract

An apparatus for the accurate determination of the thermal diffusivity of semiconductors, which utilizes the thermoelectric properties of such materials, is described. In its present form, the apparatus can be used between room temperature and 180° C. The application of the method is illustrated by an experiment using a single-crystal specimen of bismuth telluride.

Introduction

When a temperature wave is propagated in a medium, the amplitude and phase at any point depend on the properties of the medium and the frequency of the wave. Comparison of the amplitude and phase at two points enables the thermal diffusivity to be determined. In Ångström's method, attention is restricted to a sinusoidal wave propagated in a semi-infinite bar. It can be shown(1) that

$$k = \frac{K}{\rho s} = \frac{\pi L^2}{T\beta \ln \alpha}, \qquad (1)$$

where k is the thermal diffusivity, K the thermal conductivity, ρ the density, s the specific heat, L the distance between the points, T the periodic time, β the phase difference, α the ratio of amplitudes.

Modifications of Ångström's method have been applied to metals,(2) insulators,(3) and semiconductors.(4, 5) In each case the temperature wave has been generated by a resistance heater, and the temperature variations measured with conventional thermocouples.

This paper describes a novel form of temperature-wave generator, which can be applied to all classes of material, and a method of recording the temperature variations which is applicable to semiconductor specimens.

If the input temperature wave is not sinusoidal, it is convenient to measure the temperature variations of the bar beyond the point where the higher harmonics have been attenuated sufficiently to give a sensibly sinusoidal temperature wave. This enables direct measurements to be made from the temperature-time records, without the need to determine the first Fourier component.

An electrical resistance heater, used under "on-off" conditions gives rise to an asymmetric temperature wave, with consequent introduction of even harmonics. This means that the main sinusoidal component becomes predominant at a greater distance from the source than if a symmetrical input wave had been generated. Consequently, the temperature excursions are small and difficult to record. A further disadvantage of the resistance heater is that the time-average of the heat supplied during each cycle cannot be equal to zero. This leads to an increase in the mean temperature of the bar during cycling, which precludes measurements at the initial ambient temperature. These disadvantages can be overcome by using the Peltier effect.

The heating and cooling of a semiconductor thermojunction by periodic reversal of the current offers a method of generating a symmetrical temperature wave in which the time-average of the heat supplied during each cycle is equal to zero. For semiconductors, the sensitivity of the temperature recording can be increased by utilizing the high Seebeck coefficient of such materials. Since only relative amplitudes are needed, the temperature variations at any point can be determined by recording the variation of thermoelectric voltage between that point and the end of the bar at the ambient temperature.

Apparatus

A diagram of the apparatus is shown in Fig. 1. The temperature wave generator was constructed by first sandwiching a thin sheet of mica between two blocks of bismuth telluride, one *p*-type and the other *n*-type, and bonding with Araldite resin. The unit so constructed was a rectangular block 1·2 × 0·8 × 1·0 cm. A piece of thin copper foil 1·2 × 0·8 cm was then soldered to the upper faces of the blocks, so forming a thermojunction having low thermal capacity and electrical resistance. The lower faces of the two blocks were soldered to two *D*-shaped copper plates, cemented together with Araldite resin to form a disk. This disk acted as the heat reservoir. Copper wires attached to the two halves of the disk served as current leads for the thermojunction. The cooling capacity of this unit was 0·5 W for a current of 5 A.

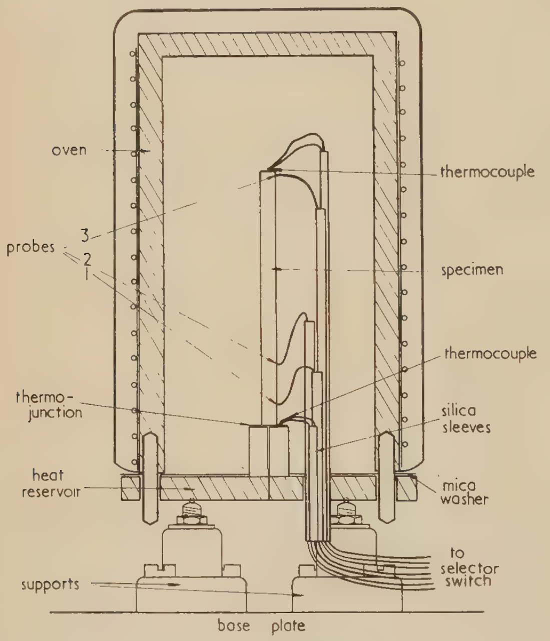

Fig. 1. Sectional diagram of apparatus inside the vacuum chamber

Generation of a temperature wave was effected by periodic reversal of the current through the thermojunction using the circuit shown in Fig. 2. The reversing switch was a heavy-duty relay operated periodically by an electrically-driven time-switch. A variable resistance was used to adjust the current during the heating half-cycles.

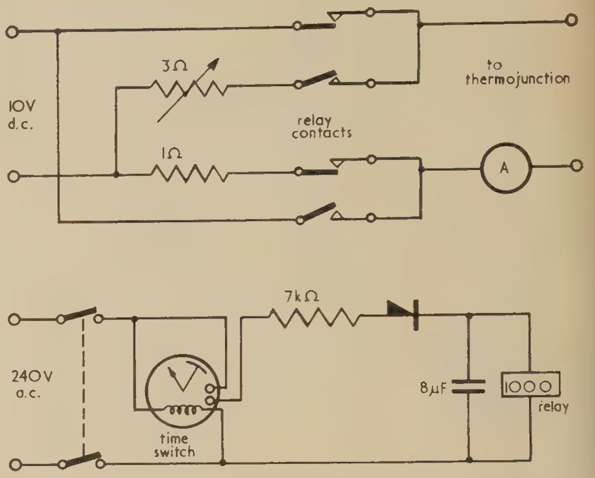

Fig. 2. Circuit for current supply to temperature wave generator

The supports for the disk were four porcelain stand-off insulators, each with a small steel ball brazed to the end of the central screw. These balls were located in triangular grooves cut on two diameters at right-angles on the underside of the disk. This method of mounting the disk minimized heat losses and allowed free expansion when the apparatus was used at elevated temperatures. The use of soft solder in the construction of the temperature-wave generator limited the upper temperature to 180° C but, in principle, the method can be used at higher temperatures.

The specimen was cut from a single crystal ingot of undoped bismuth telluride. It was 5·0 cm long with a rectangular cross-section of 0·3 × 0·4 cm, the cleavage planes running parallel to its length. One end face was nickel-plated, tinned and soldered to the thermojunction.

Three probes of 0·05 mm diameter chromel wire were pulse-welded to the specimen as shown in Fig. 1. The low thermal conductivity of the probe material minimized distortion of the isothermals. The separation of the probes was measured with a travelling microscope. In order to monitor temperature variations at each end of the specimen, a chromel-alumel thermocouple was pulsed-welded to the top and a similar thermocouple was embedded in the solder at the base. The probes and thermocouple leads were brought out through silica sleeves.

For experiments at elevated temperatures an oven consisting of a closed copper cylinder on which was wound a 200 Ω heater lagged with refractory cement, was used. This oven also served as a radiation shield for room-temperature experiments. It was mounted by two studs located in peripheral holes in the copper disk. A mica washer prevented the oven from short-circuiting the two halves of the disk.

The entire assembly was mounted in a vacuum chamber, electrical connexions to external equipment being made through an Edison connector type 3295. The probes and thermocouples were connected *via* reference junctions to a selector switch. Since only the alternating components of the e.m.f.'s were required, the selected output was applied a potentiometer, and the out-of-balance potential amplified d recorded, using a d.c. microvoltmeter (by Pye) and plifier feeding a Record pen recorder.

Experimental details

Temperature cycling was carried out with a 30 s periodic ne, compensation for the Joule heating being effected by ing unequal heating and cooling currents. When the ratio the currents was correctly adjusted, no temperature adient existed along the specimen and the mean temperature the specimen was equal to that of the enclosure. At room mperature a cooling current of 6 A and a heating current 3·6 A gave a temperature excursion of 23° C at the base the specimen.

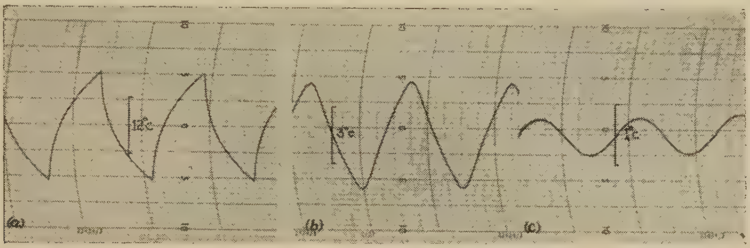

(*a*) Input temperature wave-form

(*b*) Temperature wave-form at probe 1

(*c*) Temperature wave-form at probe 2

Fig. 3. Typical traces obtained for Bi_2Te_3 using a periodic time of 30 s

Records were taken of the temperature variations at the ase of the specimen, at probe 1, and at probe 2; some ypical traces are shown in Fig. 3. On each half-cycle the nput temperature varied as the square-root of the time, and ook the form shown in Fig. 3(*a*). For probe 1, distant ·41 cm from the base, the trace became more nearly inusoidal because of attenuation of harmonics, as shown in ig. 3 (*b*). The trace for probe 2, distant 1·2 cm from the ase, showed a marked difference of amplitude and phase vhen compared with that for probe 1, as shown in Fig. 3 (*c*). Analysis of the probe 1 trace showed a ratio of 40 : 1 between he first and third harmonics, indicating that probe 1 had been ositioned sufficiently far from the base to enable phase ifference and amplitude ratio to be measured directly on the race. The specimen was regarded as semi-infinite since ariations of the free-end temperature were undetectable.

Results

The thermal diffusivity k of the bismuth telluride specimen vas determined as $0{\cdot}0136 + 0{\cdot}0005$ cm²/s at 20° C from the ollowing results:

Probe separation $L = 0{\cdot}790 \pm 0{\cdot}001$ cm
Phase difference $\beta = 2{\cdot}16 \pm 0{\cdot}04$ rad
ln (amplitude ratio) $= 2{\cdot}24 \pm 0{\cdot}02$
Periodic time $T = 30$ s

arge heat losses were undesirable since they would have led o a diminished amplitude at the second probe, and a smaller hase difference, with consequent reduction in accuracy of neasurement. A measure of the heat losses is the departure f the ratio of $\ln \alpha$ to $|\beta|$ from unity, a small departure ndicating small heat losses; the results showed that this ondition was satisfied.

The semi-infinite boundary condition was assumed to be atisfied when the temperature amplitude at the free end of he specimen was negligible compared with that at probe 2. he observed attenuation showed that the temperature amplitude at the free end was about 10^{-5} deg. C for an input temperature amplitude of 10° C; thus, the specimen was effectively semi-infinite.

Conclusion

Although the apparatus was primarily designed for specimens having low thermal diffusivities, the method could be applied to materials having higher thermal diffusivities. The important points when designing such an experiment are:

(1) With an approximate value for thermal diffusivity, the ratio of the square of sample length to periodic time must be chosen to give negligible temperature variations at the free end of the specimen. For materials of high thermal diffusivity, short periodic times would have to be used to prevent the specimen becoming inconveniently long. This, in turn, would necessitate a larger cooling power for the temperature-wave generator.

The table below gives some representative values of thermal diffusivity for some semiconductors, together with ratios of the square of sample length to periodic time necessary to give an amplitude ratio of 10^5 between the input end and the free end.

Table of representative values

Semiconductor	Bi_2Te_3	PbTe	InAs	InSb	GaSb	GaAs	InP
Thermal diffusivity (cm²/s)	0·014	0·015	0·15	0·086	0·14	0·25	0·17
$\dfrac{(\text{length})^2}{\text{periodic time}}$	0·59	0·63	6·3	3·6	5·9	10·6	7·2

(2) The lower probe must be positioned so that the third-harmonic contribution is negligible.

(3) The upper probe must be positioned to give a measurable phase difference and amplitude ratio.

References

(1) Carslaw, H. S., and Jaeger, J. C. *Conduction of Heat in Solids*, 2nd ed., p. 136 (Oxford: Clarendon Press, 1959).
(2) Sidles, P. H., and Danielson, G. C. *J. Appl. Phys.*, **25**, p. 58 (1954).
(3) Billington, N. S. *J. Sci. Instrum.*, **26**, p. 20 (1949).
(4) Nii, R. *J. Phys. Soc. Jap.*, **13**, p. 769 (1958).
(5) Kanai, Y., and Nii, R. *J. Phys. Chem. Solids*, **8**, p. 338 (1959).

Heavy-water electrolysis unit for generation of deuterium gas provided with automatic switch-off and safety devices

by P. K. DUTT, M.Sc., Saha Institute of Nuclear Physics, Calcutta, India

[*Paper first received* 28 *January, and in final form,* 10 *March,* 1960]

Abstract

An electrolysis apparatus has been constructed for the safe and trouble-free generation of deuterium gas from heavy water for experimental purposes. It has been found particularly suitable for introducing the gas at a rate of millilitres per minute (S.T.P.) into a vacuum system without the use of an extra pumping unit, because the electrolysis is done under atmospheric pressure and not in a vacuum. The apparatus is equipped with electrical control-relays and needs little attention. It operates within a specified pressure range of the liberated deuterium gas, and is automatically shut off if the pressure exceeds a certain value. There is an almost complete absence of danger of explosion arising from the electrical devices should the generated deuterium gas be accidentally mixed with air.

A SKETCH of the apparatus is given in Fig. 1 and the electrical circuit is shown in Fig. 2. The electrodes for electrolysing heavy water are in the form of platinum foils held in the soda-glass U-tube containing the acidulated heavy water by platinum-wire seals. The deuterium gas generated passes from the moisture absorber* through the Pyrex tube T_1 of 8 mm bore. The tube T_1 is let into a wider tube T_2 of 25 mm bore through a seal in its side wall, and is held concentrically within it. The open end of T_1 rests at about 5 millimetres above the open end of T_2. Both ends are immersed in the mercury contained in the reservoir M. The delivery end E of T_2 is connected to the vacuum system and the rate of entry of the gas is controlled by the needle valve N. At the start, when N is opened to the vacuum system, a mercury column rises in the tube T_2 through the annular space between T_1 and T_2, and assumes the barometric height. Care is taken to ensure that the mercury level within the reservoir M is a few millimetres (3 mm in this case) above the open end of T_1. The deuterium gas generated in T_1 has to build up a pressure equivalent to this few millimetres of mercury above atmospheric pressure in order to pass into the gas container G by displacement of mercury in T_2. As more and more gas is liberated in G, it develops greater pressure, and the mercury column M_1 in T_2 falls. The change in the column height denotes the gas pressure within the container. For operation with this apparatus (the maximum pressure within the deuterium container being 50 cm of mercury) the gas pressure in T_1 was such that the difference in heavy-water levels in the two arms of the U-tube was never more than 9–10 cm. The quantity of liquid in the U-tube must be sufficient to ensure that, under this extreme condition, the electrodes are well immersed in the liquid. To prevent excessive jerky movement of the mercury column in T_2 when the gas escapes through it to the container, glass beads are embedded at places inside its wall.

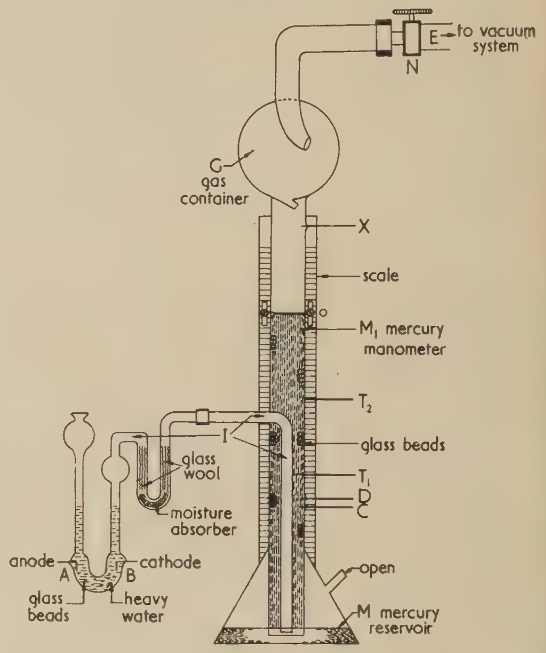
E
to vacuum system
N
G
gas container
X
scale
o
M_1 mercury manometer
T_2
glass beads
I
glass wool
T_1
D
C
moisture absorber
anode
A
B
cathode
open
glass beads
heavy water
M mercury reservoir

Fig. 1. Heavy-water electrolysis unit

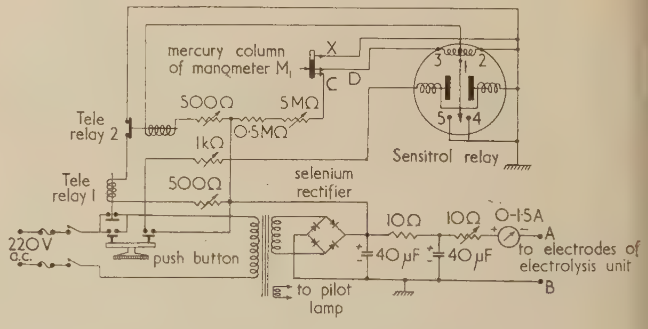
mercury column of manometer M_1
X
C
D
3
1
2
5
4
Sensitrol relay
500Ω
5MΩ
Tele relay 2
0·5MΩ
1kΩ
Tele relay 1
500Ω
selenium rectifier
220V a.c.
push button
10Ω
10Ω
0-1·5A
A
40μF
40μF
to electrodes of electrolysis unit
B
to pilot lamp

Fig. 2. Automatic control circuit

The tube T_2 is provided with three tungsten wires sealed to it at C, D and X. The mercury column in T_2 serves as a manometer, and also operates the automatic devices by switching actions between C and D and D and X. The electrical circuitry comprises a "Sensitrol" relay (Weston Mod. 705), telephone relays and a 28 V selenium rectifier which supplies power for the electrolysis as well as for the ays. Electrolysis can be started by pressing the push-tton switch (Fig. 2) if the mercury column is above *D*. e push-button is a double-pole switch. One pole serves to mplete the primary circuit of the transformer, and the ner releases the magnetic needle-clutch of the Sensitrol ay ready for operation. Subsequently, the primary circuit completed through the contacts of the Tele-relay 1 for all ading positions of the Sensitrol relay needle. The contacts the Tele-relay 2 are normally closed for operation. When e Sensitrol relay needle is at the end positions, the coil of e Tele-relay 2 is energized and its contacts break, thereby eaking the primary circuit. The circuit will then remain en until and unless the push-button is again pressed for eration.

---

* In this work, complete freedom from the inevitable trace of oxygen was not required. If it is, a catalytic re-combination agent should be introduced before the moisture absorber.

When the gas pressure inside the container exceeds 50 cm mercury, the contact between *C* and *D* through the mercury lumn is broken and the entire electric power supply to the ectrolysis unit and the control circuit is disconnected. For eration to restart, the gas pressure has to be reduced to low 50 cm of mercury, and the push-button pressed. metimes it may happen, if the gas generation is very rapid, at the upward jerky movement of the mercury column ight damage the glass apparatus. To prevent this, as the ercury column makes contact with the tungsten wire at *X* ere will be a switch arrangement to short circuit the coil the Sensitrol relay, and the input power will be cut off before.

The mercury-column switch carries only currents of the der of a few microamperes flowing through the Sensitrol lay-coil. There is, therefore, little chance of this switching using an explosion if there is an accidental mixture of air ith the generated deuterium gas.

There is one disadvantage with this type of apparatus. hen operation is started, some air is trapped in the portion *I* (Fig. 1). This gets diluted gradually with the generated deuterium gas and escapes through the mercury column. After a run of about an hour or so, the portion becomes free from air for all practical purposes and the deuterium gas should only then be collected and stored. In all subsequent runs, however, no question of contamination with air arises, and pure deuterium gas is obtained because *I* always remains filled with the liberated deuterium gas.

There is another way of shutting down the electrolysis unit when the gas pressure in the container exceeds the desired value. This is done by adjusting the amount of the heavy water in the electrolysis U-tube in such a way that, as soon as the gas exceeds that pressure, the electrolyte level in an arm of the tube goes below the electrode housed in it. However, the method does not ensure a dependable and consistent arrangement without external controls as in the previous case. Nevertheless, it does provide an extra precaution in case the control-unit fails. In this apparatus, the amount of heavy water is such that, if the gas pressure exceeds 55 cm of mercury, the electrolyte level goes below one of the electrodes.

In the event of an accident (for example, if the gas-container or the manometer cracks), the mercury goes back to the reservoir and no spilling of the heavy water out of the U-tube can occur.

The apparatus has been supplying deuterium gas to the ion-source of the Calcutta 37 in. Cyclotron for a couple of years and requires little attention for its operation. Normally it runs with an electrolysis current of 1 ampere.

Acknowledgements

The author wishes to thank Prof. B. D. Nag and Prof. D. N. Kundu for constant encouragement.

Temperature-controlled permanent magnet for high-resolution nuclear magnetic resonance

y B. A. EVANS, M.Sc., Mullard Research Laboratories, Salfords, Surrey, and R. E. RICHARDS, M.A., D.Phil., F.R.S., hysical Chemistry Laboratory, University of Oxford

Paper received 4 *February*, 1960]

Abstract

he design and construction of a large temperature-ontrolled permanent magnet is described and the con-iderations given towards obtaining a high degree of field niformity. Using current shims and a spinning sample, resolving power and stability of a few parts in 10^8 *may e obtained at any time and, with care,* 1 *part in* 10^8 *can e achieved.*

Introduction

SEVERAL accounts have been given of magnets for high-resolution nuclear magnetic resonance in which the time stability of the magnetic field is achieved electronically. This paper described a relatively simple high-resolution ermanent magnet which provides a good performance with-out electronic stabilization.

Magnet design

The basic design of the magnet is governed by three main considerations, namely, high field strength, stability and field uniformity.

The signal-to-noise ratio of a nuclear resonance increases as $H^{7/4}$, provided the line width remains constant. If the magnet inhomogeneity exceeds the line width, and is assumed to be proportional to H, then the maximum absorption intensity increases only as $H^{3/4}$. A high field is desirable in order to increase the chemical shift with respect to spin-spin coupling constants. The maximum field is also governed by the gap size. The gap must be large enough to allow a reasonable working space, and to minimize the effects of inhomogeneities in the pole-piece material. A gap of $1\frac{1}{2}$ in. was chosen. Optically flat pole pieces are used of sufficient diameter to give a satisfactory region of high uniformity.

Purcell(1) has shown that to obtain field uniformities of the order of a few parts in 10^8 one must have a diameter-to-gap ratio of at least 5 : 1 when plane, flat cylindrical pole pieces are used. For this reason a pole diameter of 8 in. was chosen.

There is one further consideration which will affect the dimensions of the magnetic material to be used. Fig. 1 shows typical field variations for a 13 in. diameter, 3 in. thick block of Ticonal G magnetic material measured in a 0·15 in. gap. The three plots correspond to three lines from the circumference to the centre, at angles 120° apart. The falling-off near the origin is partly due to the edge effect, but towards the centre, field variations of the order of 500 G in 8000 G must be considered. Some yoke saturation was present in this test but this does not appreciably affect the relative magnitudes. In order to overcome these variations very thick pole pieces of high permeability may be used. It was pointed out by Purcell,(1) however, that if a pole piece is divided into a number of slabs of high permeability magnetic material separated by small air gaps, then the pole piece would behave as a filter for the inhomogeneities of the permanent magnet material. Since, however, the front face of the pole piece was to be optically polished, and in order to avoid undue distortion of this surface, it was necessary to make the end slab of soft iron $1\frac{1}{2}$ in. thick. The remainder of the pole piece was divided into two slabs of soft iron $\frac{7}{16}$ in. thick, separated from each other and the front slab by a $\frac{1}{16}$ in. thick ring of aluminium.

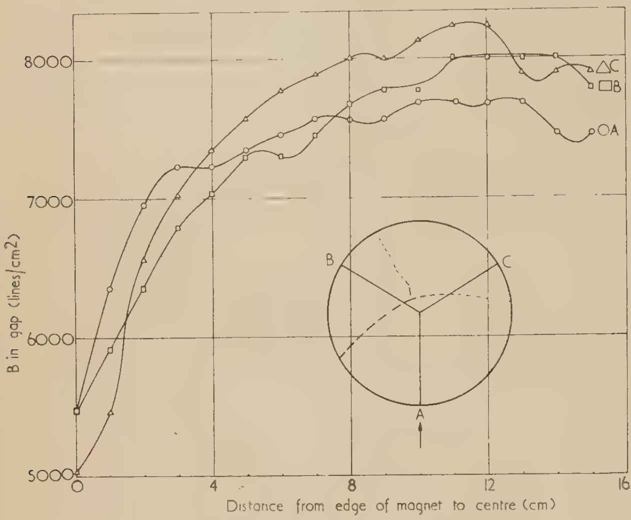

Fig. 1. Field variation of magnet material

Each slab of iron was initially machined to approximately $\pm\frac{1}{32}$ in. all over and then annealed in a hydrogen atmosphere by soaking at 850° C for three hours and then allowing to cool at approximately 45° C per hour down to 350° C. After annealing the surfaces were carefully ground and the whole joined together with Araldite type 15 epoxy resin. The outer surfaces were then turned to size, the front face ground and subsequently polished to better than one wavelength over the 8 in. diameter.

The pole faces were protected by an evaporated layer of chromium and then a coating of Frigilene varnish. Additional protection was provided by detachable disks of Perspex acrylic sheet. The total length of air gap used was, therefore, $1\frac{3}{4}$ in. of which $\frac{1}{4}$ in. was used for filtering.

The magnetic poles were made up of four slabs of Ticonal G magnetic material, each of which was 13 in. diameter and 3 in. thick. The slabs were joined together with Araldite type 15 epoxy resin.

The dimensions of the yoke were chosen for mechanical stability. A photograph of the assembled magnet is shown in Fig. 2. The magnet is used with the plane of the yoke horizontal. The two side members are under compression and the two end members to which the magnets are attached are tending to bend from the magnetic attraction of the poles (approximately 500 lb) and tending to twist from the weight of each pole (600 lb). Hence, the end members of the yoke were made 6 in. thick and the two side members 4 in. thick. The distance between the magnets and the side members is $8\frac{1}{2}$ in. so as to minimize the non-symmetrical leakage to the yoke. In fact, as will be shown later, no significant asymmetry was produced.

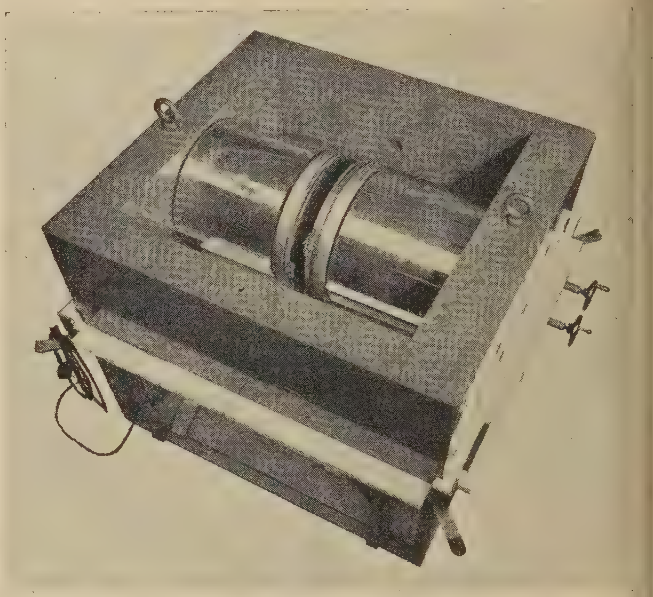

Fig. 2. Photograph of the assembled magnet

Adjustment of the gap

A method basically similar to that employed by Gutowsky and Hoffman(2) was used. Six phosphor-bronze rods are tightly screwed into a brass ring which fits closely over a shoulder on the pole caps. The rods pass through six holes in the yoke at the base of the poles and are held by nuts with a fine thread. A small disk of phosphor-bronze 0·020 in. thick and 2 in. diameter, centrally placed between the Ticonal poles and the pole pieces enables the parallelism of the pole pieces to be adjusted by altering the tension in the phosphor-bronze rods. The axial alinement of the pole pieces is made after magnetization. Lateral supports were found to impede the smooth operation of the six adjusting rods, and were not required. This method of adjustment proved to be very convenient, though temperature-sensitive.

Magnetization

In order to magnetize the whole assembly two layers of heavy welding cable were wound evenly along the magnet poles, pole pieces, and gap. A pulse of 223 000 ampere-turns was applied for $1\frac{1}{2}$ seconds.

The field strength of the magnet after magnetization was

0 G but this was stabilized to 7049 G for use on the oton resonance at 30 Mc/s.

A magnet assembly of this type has a temperature coef- ent of field of about 0·02 to 0·03% per deg. C, so it is irable to control its temperature.

Temperature control

The magnet rests on a 1 in. layer of Jablite polystyrene um which is in turn supported by a steel cradle. The whole embly is enclosed by a box of Jablite 2 in. thick which is otected by an aluminium outer casing. A circulating fan ces air from the space below the magnet, over the magnetic terial, and back again. The air is heated by two electric ht bulbs before it enters the fan, and the heat is controlled a small platinum resistance thermometer, just above the n, through an a.c. bridge temperature controller. The air nperature cycles above and below the mean temperature about ±0·03° C every minute or so. The temperature riation of the magnet is then less than ±0·0001° C because its very large thermal capacity.

Removable panels are provided at suitable places for casional access to the magnet box. Nuclear resonance mples are inserted through the top of the magnet box.

Magnetic field investigations

The field was plotted with a small nuclear resonance obe using a regenerative detector.(3) Typical field contours e shown in Fig. 3. These show that the field in the plane the gap is symmetrical about the centre, where it has a inimum, with peaks 300 mG high at 3·2 in. diameter. here is, however, a field gradient across the centre of the ap of about 150 mG in ½ in. Longer and more intense nagnetization currents did not have any effect on the 300 mG eaks, and the symmetry was maintained. On interchanging the pole pieces, the gradient across the gap changed in direction but very little in magnitude, suggesting that it was due to a centre weakness in the pole piece material.

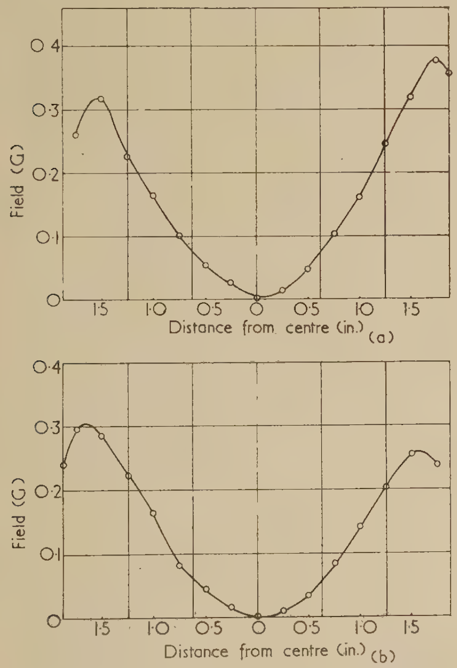

Fig. 3. (*a*) Field plot in horizontal plane perpendicular to axis of magnet

(*b*) Field plot in vertical plane perpendicular to axis of magnet

In order to eliminate the gradient across the gap several experiments were carried out. The first was to try to reduce the pole strength of one pole by reverse pulses of current of up to 1200 ampere-turns, but the gradient changed very little. Windings in opposition on the high side to those on the low side for both pulses and steady currents also had no appreciable effect on the field contours. This procedure was then repeated with a mild steel "collar" 2 in. wide and ½ in. thick on the outside of the high pole piece to increase the leakage, but this again merely reduced the field without having a very great effect on the contours. Finally a 16 s.w.g. mild steel cylinder was made to enclose completely the high field pole with a collar of 2 × ½ in. steel at the pole-piece end, but this again had a negligible effect on the field gradient across the gap at the centre, but reduced the field by over 400 G.

No further attempts were made to modify the field contours by external influences and it was accepted that, with such a large diameter-to-gap ratio, the total flux out of one pole piece equals the total flux into the other pole piece, as far as the centre portions of the gap is concerned, and the contours can only be modified by internal modifications.

It was found that the field contours could easily be improved by rings of nickel wire and current-carrying coils within the gap. For example, two printed circuit coils of eight turns and 2½ in. mean diameter completely eliminated the field gradient across the centre of the gap, when 80 mA was passed through each coil in order to increase the field of the low pole and decrease the field of the high pole. With such a simple coil system, and using an $0\cdot02\ \mathrm{cm}^3$ spinning sample, the resolution is of the order of 1 part in 10^7 and, for example, the CH_3 triplet of ethyl alcohol is completely resolved.

This magnet forms the basis of a particularly simple high-resolution spectrometer.(4) A more elaborate set of current shims, designed by Golay,(5) is used and these are continuously energized from a constant current source. The resolving power obtained with a cylindrical sample of 4 mm diameter, spinning about its axis, is then a few parts in 10^8 at any time. No readjustment of the sample probe in the gap is necessary except when it is removed for cleaning. With care, a resolving power of 1 part in 10^8 can be achieved.

Acknowledgements

We are indebted to Mr. A. J. Tyrrell of Mullard Ltd. for much helpful advice on the early stages of the design of the magnet. We are also grateful to Prof. Purcell for making available to us some of the results of his calculations. One of us (R. E. R.) wishes to express his appreciation to the Royal Society, to the Department of Scientific and Industrial Research, and to the Shell Petroleum Co. for grants towards the cost of the magnet, and also to Mullard Ltd. for their generous and helpful co-operation.

References

(1) Purcell, E. M. Private communication.
(2) Gutowsky, H. S., and Hoffman, C. J. *J. Chem. Phys.*, **19**, p. 1259 (1951).
(3) Pound, R. V. *Prog. Nuclear Phys.*, **2**, p. 31
(4) Leane, J. B., Richards, R. E., and Schaefer, T. P. *J. Sci. Instrum.*, **36**, p. 230 (1959).
(5) Golay, M. J. E. *Rev. Sci. Instrum.*, **29**, p. 313 (1958).

Improved design for an auto-focus range-finder

by H. ASHER, Physiology Department, University of Birmingham, L. DODIN, Montpellier, Hérault, France, and H. P. MULHOLLAND, Department of Mathematics, The University of Exeter

[*Paper first received* 21 *December*, 1959, *and in final form* 30 *May*, 1960]

Abstract

Various designs for a camera range-finder with parallel mirrors and a variable prism unit have been described.(1–3) *In each design certain parts of the range-finder shared the motion of the camera lens in focusing. Here a further design of this type is described in which there is no relative movement of the mirrors.*

List of symbols

a = distance of L from centre M_1 of opaque mirror
b = distance between centres M_1, M_2 of mirrors
c = distance of pin C from pivot P
h = distance of P behind anterior focal plane of (movable portion of) camera lens when focused on infinity
ρ = distance of object O from this plane
f = focal length of (movable portion of) camera lens
μ = refractive index of glass used in prism-unit
x = forward displacement of (movable portion of) camera lens from its "infinity" position
ϕ = inclination of PC to its "infinity" position PX
ψ = inclination of reflected ray to PLM_1 on entering prism-unit

Introduction

As in previous papers,(1,2) camera range-finders are considered in which the usual two mirrors (one semi-transparent) remain always parallel, while the incoming rays that they reflect are caused to deviate appropriately by a variable prism unit between the mirrors. This unit consists of a pair of lenses, of which one is fixed to the camera and the other moves with the camera lens. Sufficiently accurate automatic focusing would be obtained if the mirrors could be fixed with their centres in the anterior focal plane of this lens (see Ref. 1, p. 403), or, alternatively, if the semi-transparent mirror, as well as one lens of the prism unit, moved with the camera lens (see Ref. 2, Fig. 1, and Ref. 3). However, the former alternative is impracticable, and the latter requires an expensive precision mounting for the moving mirror. The arrangement shown in Fig. 1 avoids these drawbacks by having both mirrors mounted on a swinging arm. This lengthens the effective base of the range-finder when the arm swings forward, and so offsets the effect of placing the range-finger behind the anterior focal plane [for details see formulae (1) and (7) below].

The variable prism unit now consists of a plano-convex lens fixed to the camera and a plano-concave lens mounted (together with the mirrors) on the swinging arm. The curved surfaces of the two lenses have the same radius PL, so that they can slide over one another: together they act like a prism of angle ϕ, where ϕ is the angle through which the arm has swung from its original (or "infinity") position PX, which is parallel to the focal planes of the camera lens. The mirror nearer to the pivot P is semi-transparent, and the centres M_1, M_2 of the mirrors and a pin C, linked to the camera lens, are all in line with P. The mirrors are set at 45° to the line PM_2CM_1. This line and the line PX are the axes of the plano-concave and plano-convex lenses, respectively.

Theory

Fig. 2 shows (for simplicity) the path of the reflected ray (from the object O) that passes through the point L where the line PM_2CM_1 meets the curved surfaces of the lenses in the prism unit. It is supposed that the thickness of the prism unit is negligible and that the range-finder is adjusted, as usual, to bring this reflected ray into coincidence with the

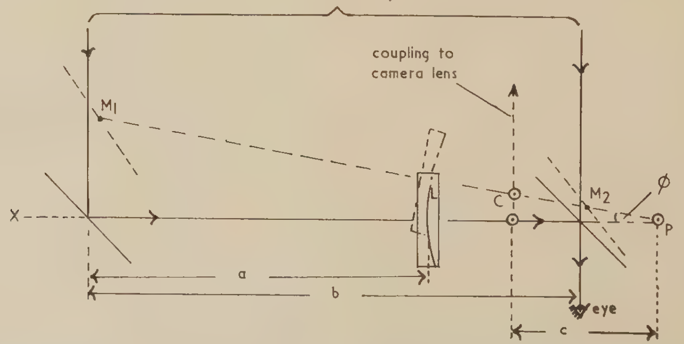

Fig. 1. The optical system of the range-finder, the rays shown being from an object at infinity. For a near object the mirrors and one lens are carried on a swinging arm, pivoted at P, to positions such as are shown in broken lines: the plano-convex lens remains fixed to the camera

ect ray from the object before the rays reach the eye. w the deflexion $\phi - \psi$ of the reflected ray by the prism it at L must equal the angle L_1OL_2 between the two rays m O. Also the angle $OL_1L_2 = 45° + \psi$. Hence

$$\frac{\sin(\phi-\psi)}{L_1L_2} = \frac{\sin(45°+\psi)}{OL_2} = \frac{(\sin\psi + \cos\psi)\cos 45°}{OL_2}$$

it $L_1L_2 \cos 45° = M_1M_2 = b$, and $OL_2 = OQ - L_2Q =$ $+ h - L_2Q$, where Q is the intersection of PX with OL_2

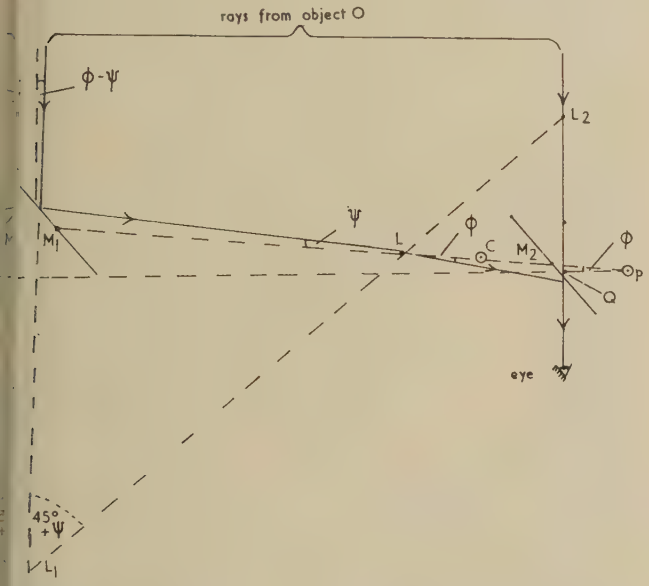

Fig. 2. A reflected ray from a near object at O is deflected at L by the prism unit. L_1 and L_2 are the images of L in the mirrors. PX is parallel to the focal planes of the camera lens

roduced, so that L_2Q is approximately equal to $L_2M_2 =$ $M_2 = b - a$. Replacing the sines above by the corresponding angles (in radian measure) and $\cos\psi$ by 1, we nd that $(\phi - \psi)/b$ is approximately equal to

$$(1 + \psi)/(\rho + h - b + a),$$

e.

$$b(1 + \phi) \simeq (\rho + h + a)(\phi - \psi) \qquad (1)$$

The expression on the left of formula (1) may be regarded s the effective base of the range-finder [see also equation (1) n Ref. 2].

The prism unit is equivalent to a prism of angle ϕ, and it roduces a deviation $\phi - \psi$: hence

$$\phi - \psi \simeq (\mu - 1)\phi \qquad (2)$$

Combining expressions (1) and (2) we have

$$b(1 + \phi) \simeq (\rho + h + a)(\mu - 1)\phi \qquad (3)$$

On the other hand, when the camera lens has moved a distance x from its "infinity" setting it will be correctly focused on objects at a distance ρ', from its original anterior focal plane, given by Newton's formula $x(\rho' - x) = f^2$, so that $x\rho' = f^2 + x^2$. Neglecting x^2 in comparison with f^2 we get

$$x\rho' \simeq f^2 \qquad (4)$$

But the linking of the pin C to the camera lens involves the relation

$$x \simeq c\phi, \qquad (5)$$

so that $\rho' \simeq f^2c^{-1}\phi^{-1}$. Since the distance ρ of the object actually sighted satisfies expression (3) we thus get

$$(\rho' - \rho)(\mu - 1) \simeq \{f^2c^{-1}(\mu - 1) - b\}\phi^{-1} - b + {} + (\mu - 1)(h + a) \qquad (6)$$

The error $\rho' - \rho$ in range will thus be small if we make

$$bc = (\mu - 1)f^2, \quad b = (\mu - 1)(h + a) \qquad (7)$$

It may be verified without much difficulty that the error in the approximate equality (6) consists of some terms of the order of ϕ and others of the order of $d/(h + a)$, where d is the thickness of the prism unit; and $d/(h + a)$ will usually be quite small. The following is a set of possible dimensions (in centimetres): $f = 5$, $h = 8{\cdot}5$, $a = 4{\cdot}5$, $b = 6{\cdot}5$, $c = 25/13 = 1{\cdot}923\ldots$, $PL = 3$, $d = 0{\cdot}3$, with $\mu = 1{\cdot}5$. We then find that $d/(h + a) = 0{\cdot}023$. With these figures accurate calculations of the error $\rho' - \rho$ and of the corresponding error Δx in the displacement of the lens, for three specimen ranges (from the original position of the camera lens), have yielded the following results (in centimetres):

$\rho'+f$	$\rho+$	$\rho'-\rho$	Δx
100	96·15	3·85	−0·0112
300	298·47	1·53	−0·00045
900	899·26	0·74	−0·000023

These errors would be tolerable, except at 100 cm with apertures wider than $f/6{\cdot}3$. Further, the dimensions, instead of satisfying equations (7) exactly, could be chosen so as to obtain greater accuracy at the minimum range required.

The practical work was carried out at the second author's private laboratory at Montpellier.

References

(1) Asher, H. *J. Sci. Instrum.*, **29**, p. 402 (1952).

(2) Asher, H. *J. Sci. Instrum.*, **30**, p. 402 (1953).

(3) Naumann, H., and Faulhaber, F. *Deutsches Patentamt*, Patentschrift No. 838540, Fig. 9 (8 May, 1952).

Vernier scale arrangement for the measurement of peak heights on mass spectrometer charts

by J. R. Richards, M.Sc., Ph.D., Australian National University of Canberra, Australia

[*Note received* 1 *March*, 1960]

The relative intensities of ionic species in mass spectra are usually obtained from a recorded chart by measurement of the vertical distance between the effective zero at the base of the peak and the peak top which precedes it (Fig. 1). Since the effective zero is, in general, different for each amplifier sensitivity range, a separate reference zero-line must be drawn for each peak measured. When a number of replicate groups of peaks is drawn to gain greater precision, this procedure leads not only to an unnecessary consumption of time, but also to a multiplication of possible sources of error, both from personal fatigue and from inaccuracies of pencil work. A device which has been constructed to minimize these effects will be described in three parts—the rule, the method of mounting it, and the desk on which the device is supported.

The rule (Fig. 1) consists of two rectangular pieces of $\frac{1}{8}$ in. Perspex sheet, with squared edges. The main scale, 30 cm long and graduated in millimetres, is inscribed, in the reverse of customary direction, on the near edge of one piece, size 7 × 32 cm. The vernier is inscribed on the corresponding edge of the other piece, which is 7 cm square. Parallax is avoided by having the graduations on the lower surface, next to the paper. The two zero lines, about 5 cm long, are inscribed at a distance of 1 cm from the end. Readings are obtained by placing the main-scale zero-line on the effective zero of the peak (in the middle of the ink line), and the vernier zero against the peak top. In such a system a bevelled edge is unnecessary.

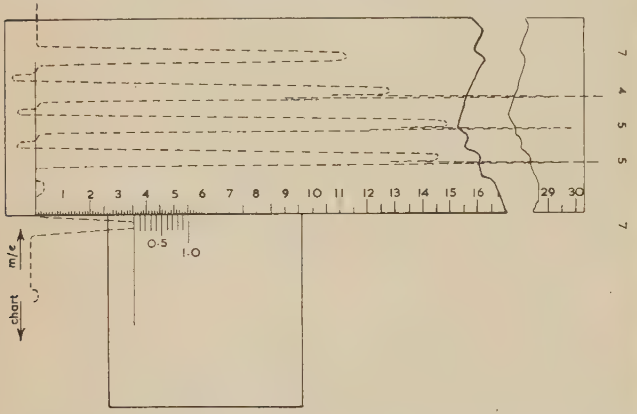

Fig. 1. Scale and vernier (full lines) superimposed on a typical mass spectrum (broken lines) to illustrate the measuring position. Note that the zero, on the high mass side of each peak, is at a different level for each sensitivity range

It may be assumed, when the electronic system is operating stably, that the average zero line is parallel to the chart edge. Thus, if the main rule is mounted on a pantograph system, one adjustment of the zero line parallel to the paper edge should suffice for the measurement of a number of peak heights. The vernier is operated as an independent piece. An Air Force chartboard (type D), which consists of a pantograph mounted on a plastic board approximately 18 in. square, has proved suitable when covered with a sheet of plain white filter-paper. The roughness of this backing, in combination with two rulers held in place by heavy rubber-bands, provides sufficient friction to keep the chart paper flat and in position.

It has been found that this measuring table is most conveniently used when mounted against the recorder unit (of a Metropolitan-Vickers type MS2 mass spectrometer) in such a way that the chart can be measured as it feeds over the table direct from the instrument. For this purpose a light frame has been constructed from $\frac{3}{4}$ in. Duralumin angle which hooks (by means of a length of 2 × 1 in. Duralumin channel) on to the cabinet framework immediately below the recorder mechanism, and rests against the top three drawers, between the handles (Fig. 2). The top members, on which the chart-board rests loosely, slope downwards towards the operator in the traditional desk-style. The whole structure forms a rigid and comfortable desk which, when not required, can be unhooked quickly and stored elsewhere.

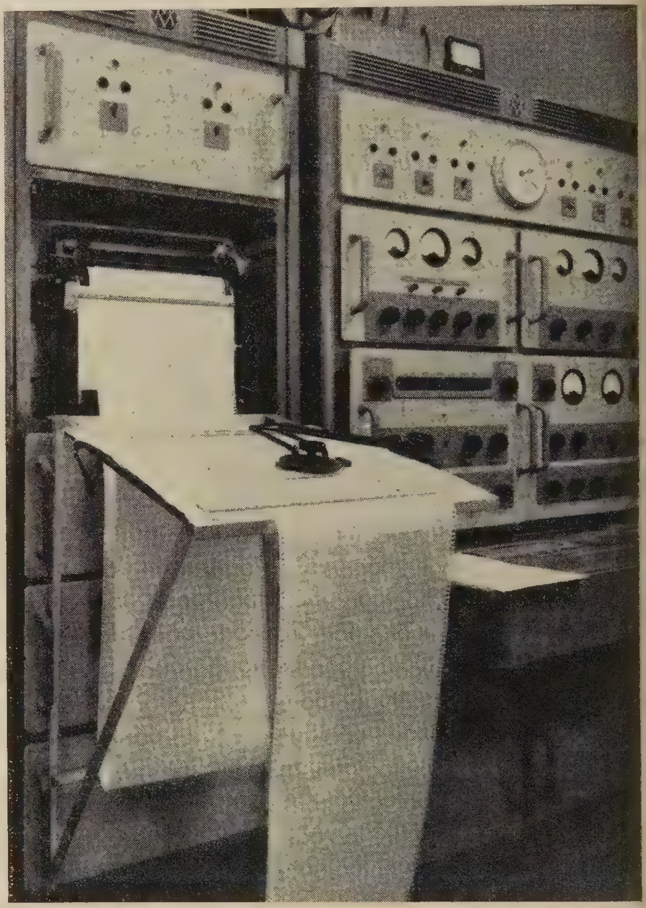

Fig. 2. The desk in operating position

Insulated terminals for high-vacuum systems using demountable glass-metal seals

by R. S. Nelson, B.Sc., Metallurgy Division, Atomic Energy Research Establishment, Harwell, Berks

[*Note first received* 28 *March, and in final form* 26 *April*, 1960]

It is often required to have demountable insulated terminals passing high voltages through the metal wall of a high-uum system. Such terminals should be simple in design l should be as small and as compact as the electrical itations allow, e.g. tracking distances, etc. Many such rices using organic materials are in existence; these are ually only suitable for pressures down to 10^{-6} mm of rcury. For higher orders of vacuum it is necessary to use tal and glass components only which may be baked at nperatures up to 500° C.

This note describes a simple technique in which the vacuum ht is made between the glass insulator and the metal uum wall. Other methods employing an intermediate tal support sealed to the glass insulator, which is used to ke a demountable metal-to-metal vacuum joint with the uum wall, have been successful. The main advantages of method described here are its size and simplicity of nstruction. Vacuum seals with indium and aluminium e gaskets have been used widely in recent vacuum hniques.* Indium is used for non-bakable systems ilst aluminium may be baked to 500° C. In order to mpress the wire sufficiently to make a seal comparatively ge forces are required, especially in the case of aluminium; us when compressing the wire between glass and metal rfaces a uniform force must be maintained over the glass rface to prevent it from cracking. A simple technique sed on a method for glass-to-glass seals using standard rex pipe line fittings with tapered ends† has proved very ccessful. The Pyrex was pulled down on to the wire sket by means of a backing flange cushioned from the ss by an asbestos insert, as illustrated in the figure.

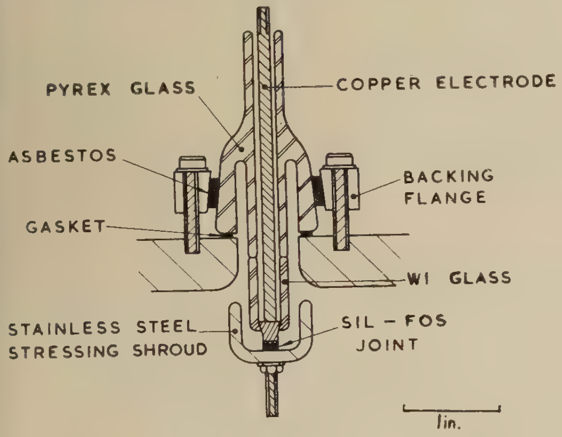

High-voltage terminal

Six or more bolts are needed to maintain a uniform force, ese being tightened by only a little at a time. The quality f the finish of the metal sealing surfaces plays a large part making good seals, especially in the case of aluminium askets. Scratchless surfaces finished to better than 8 μ in. ave been used. The bakable seals were made by com-ressing annealed aluminium wire of 0·01 in. diameter down 0·002 or 0·003 in. For sealing with indium, wire of and $\frac{1}{32}$ in. diameter was used. It is worth noting that hen baking to 500° C the difference in expansion between yrex and stainless steel is taken up by the plasticity of the asket. It is essential, however, to ensure slow heating and cooling rates during the bake-out, otherwise the glass may fracture.

It only remains to bring the high-voltage lead in through the glass support. In most cases, for voltages below 5 kV, a tungsten wire was simply sealed into the sealed end of the Pyrex tube at a convenient distance above the backing flange, that is providing the wire was less than 1 mm in diameter; otherwise tungsten sealing glass must be used intermediate between the Pyrex and tungsten. For higher voltages, such as those employed in accelerators, etc., a slightly more elaborate device must be used. The figure shows a typical terminal suitable for voltages of the order of 40 kV. A standard copper-to-W1 glass stem seal was joined to the Pyrex glass insulating support at a distance of about $\frac{1}{2}$ in. from the seal, as shown in the diagram. This $\frac{1}{2}$ in. of W1 glass was sufficiently long to prevent damage to the seal when joining the two glass components. The copper electrode was then sealed into the copper-glass seal by a silver-phosphorous-copper alloy solder (Sil-fos made by Johnson Matthey and Co. Ltd., London), which is suitable for bakable vacuum systems using mercury diffusion pumps. A copper-silver eutectic solder could be used equally well; in this case, however, Sil-fos was chosen because it needs no flux.

The phosphorus in Sil-fos appears to have no ill effect on the vacuum system when baked at 500° C. Slight oxidization of the copper occurs during brazing, but after a quick dip in nitric acid, followed by a rinse in acetone, the terminal is ready for use. The terminal is shown complete with a potential stressing shroud to shield the lines of force from the copper-to-glass seal; this is simply secured by a nut screwed on to the threaded copper rod. The construction is quite robust and has been used to support electrostatic lens elements in an accelerator.

---

* Holden, J., Holland, L. and Laurenson, L. *J. Sci. Instrum.*, , p. 281 (1959).

† Green, L. A., Miles, H. T., and Richardson, A. C. *J. Sci. strum.*, 36, p. 324 (1959).

Cosine correction of a weatherproofed photovoltaic cell

by E. T. Weston, B.E., A.M.I.E.Aust., and D. Paix, M.Sc., Commonwealth Experimental Building Station, Sydney, Australia

[*Note first received* 21 *January, and in final form* 21 *April,* 1960]

The response of a barrier-layer photovoltaic cell to a light beam of intensity I is ideally proportional to $I \cos \theta$, where θ is the angle of incidence of the beam. To obtain this proportionality it is necessary to mount the photoelement beneath a special correcting device, commonly known as a "cosine corrector".(1, 2)

The Commonwealth Experimental Building Station required such a cosine-corrected cell, which would be quite impervious to the weather, for its programme of recording illumination from the sky. Accordingly, a cosine-corrector of the Pleijel–Longmore type was developed for an hermetically-sealed weatherproof photocell (Weston type 856W). The corrector has the advantage that it is completely external to the cell, and therefore does not disturb its weatherproof case or hermetic sealing.

The corrector assembly is depicted in Fig. 1, and the essential dimensions of its components are shown in section in Fig. 2. The metal parts are blackened brass and the central disk is white translucent Perspex, grade 040, carefully depolished on upper and lower surfaces. Glass paper was used for depolishing to avoid discolouring the surfaces.

Difficulty was experienced in early designs in preventing the ingress of water and water vapour through the joint

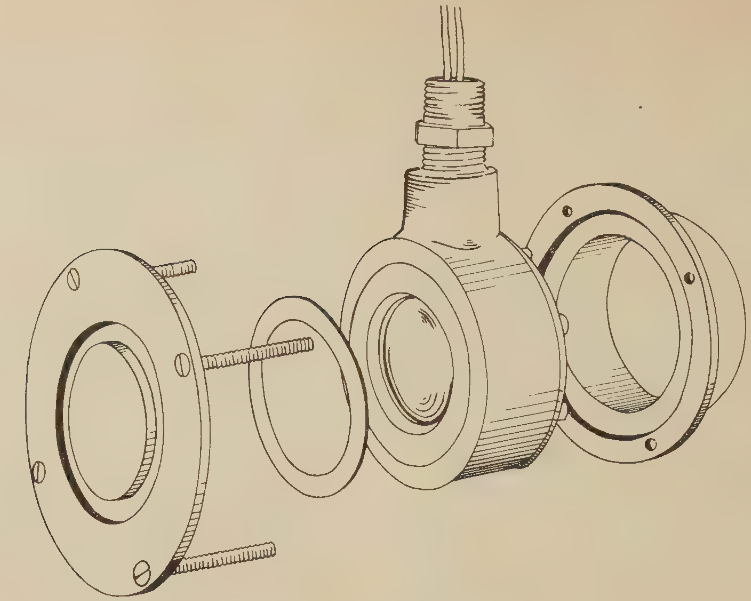

Fig. 1. Assembly of photocell and cosine corrector

between the brass and Perspex, presumably because of the high coefficient of thermal expansion of the latter.(3) The problem was solved by sealing the joint with the same $\frac{1}{32}$ in. thick neoprene gasket used to seal the corrector assembly to the cell. A clearance of 0·005 in. was allowed at room temperature between the two diameters of the Perspex disk and those of the corresponding openings in the brass. The clearance, which reduces to zero at about 120° F, allows free expansion of the Perspex and eliminates the risk of distortion when the cell is exposed, as it normally is, to large fluctuations in temperature.

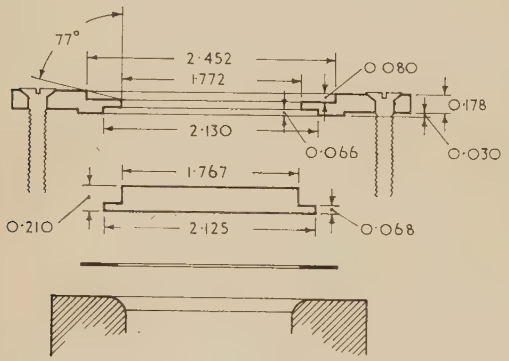

Fig. 2. Section through cosine corrector. All dimensions shown in inches

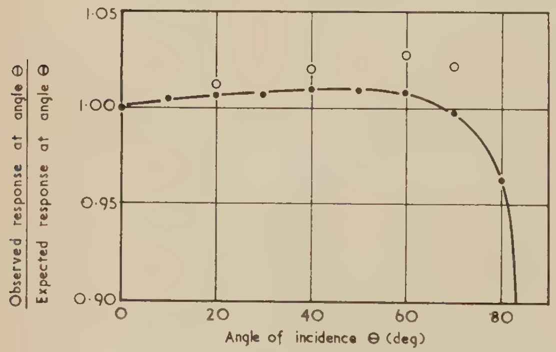

Fig. 3. Cosine correction of photocell type 856W

The curve and solid points in Fig. 3 show the response of a corrected cell (expressed as a decimal of the expected response) plotted as a function of the angle of incidence θ. The open points in Fig. 3 have been included to give some indication of the tolerances which apply; they represent the results obtained from a prototype corrector in which the parts of the disk visible in Fig. 1, and the screening ring surrounding it, were 0·040 in. thicker than in the final design.

The sensitivity of the cell to normally-incident light was reduced to about one-third of its original value by the addition of the corrector.

REFERENCES

(1) Pleijel, G., and Longmore, J. *J. Sci. Instrum.*, **29**, p. 137 (1952).

(2) Reeb, O., and Tosberg, W. *Building Research Stn. Lib. Comm. No.* 745 (Garston, Herts: April 1956).

(3) *Perspex Acrylic Materials, Part* 1—*Nature and Uses*, p. 4 (Imperial Chemical Industries Ltd.).

Automatic silver concentration control for nuclear emulsion fixing baths

by E. Dahl-Jensen, Institute for Theoretical Physics, University of Copenhagen, Denmark

[*Note first received* 8 *January, and in final form* 28 *April*, 1960]

The maintenance of a fixed silver concentration in the hypo bath, when fixing thick nuclear emulsions, is worth while. If the silver concentration is too low the surface grains in the emulsion will be etched away, and it will thus be difficult or impossible to follow near minimum tracks through the top 10–15 μ emulsion. On the other hand, distortion resulting from the tanning effect of the silver thiosulphate complex may be caused by high silver concentrations. In practice, satisfactory results have been obtained when the silver ncentration was maintained in the region of 2–6 g of silver litre throughout fixation.*†

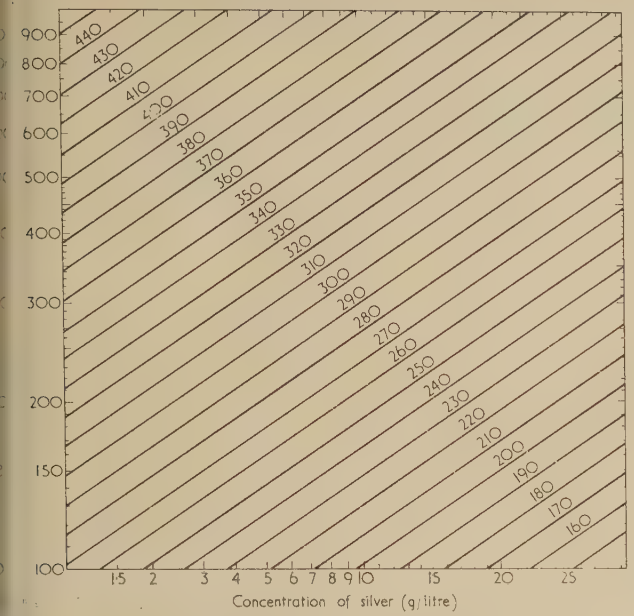

Fig. 1. Graphic representation of measurements using a silver electrode and a calomel electrode, connected to a *p*H-meter.

This note describes a convenient electrometric method in hich the potential between a silver electrode and a calomel lectrode in the hypo bath is used to determine the silver oncentration. A circuit which can be used to maintain the ilver concentration at a fixed level is also described.

The potential (in millivolts) of the silver electrode in an argentiferous hypo bath is given by the formula

$$-58{\cdot}2\log_{10}\left[1{\cdot}02\times10^{-13}\{b/(a-2b)^2\}\right]+ \\ +29{\cdot}1\sqrt{(3a+b)}-800$$

where a = g hypo/l/248
b = g silver/l/108

The potential difference between the silver and calomel electrodes is obtained by subtracting the potential of the calomel electrode (−219 mV) from the above formula. The theoretical result is consistent, within ±1 mV, with the values obtained experimentally for hypo concentrations from 100 to 600 g/litre and for silver concentrations varying from 1 to 20 g/litre. Measurements (consistent with the above equation), using a type P161 silver electrode and a type K4022 calomel electrode, connected to a type 22 *p*H-meter (all by Radiometer, Copenhagen), are represented graphically in Fig. 1.

These measurements were made at 20° C. In general, fixing is carried out at about 5° C. Nevertheless, with any pair of electrodes at any temperature between 0–25° C the accuracy of the estimate of the silver concentration, derived from Fig. 1, will be better than 10%. This is better than is required to control the silver concentration when fixing thick nuclear emulsions.

The potential is not affected by the addition of sodium bisulphite, sodium sulphite, sodium acetate, acetic acid or gelatine to the hypo bath. Changes of *p*H will not have any influence on the potential within the limits of ±1 mV.

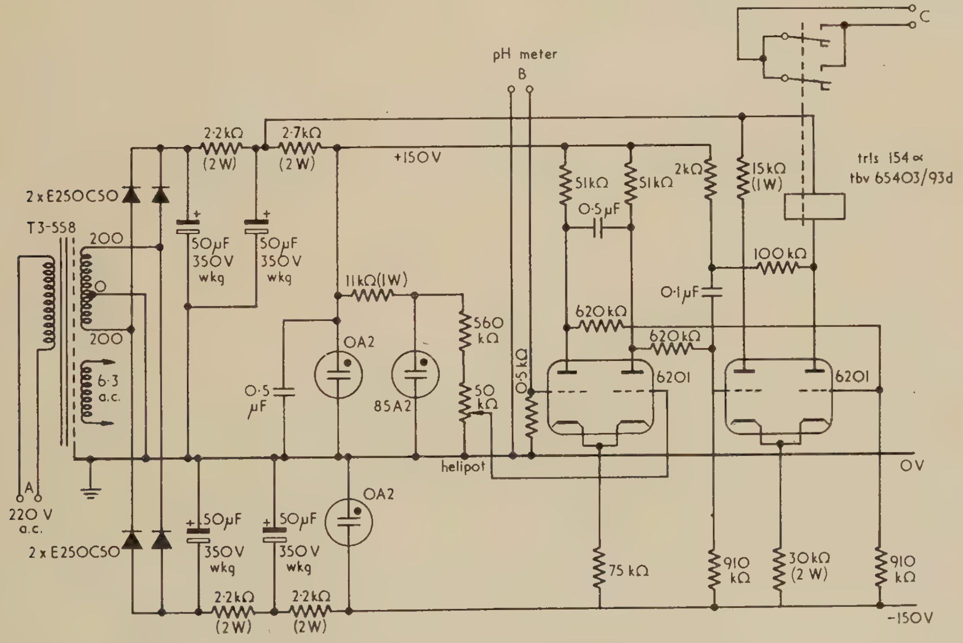
C
pH meter
B
2·2kΩ
(2W)
2·7kΩ
(2W)
+150V
2xE250C50
T3-558
200
0
200
6·3
a.c.
50μF
350V
wkg
50μF
350V
wkg
11kΩ(1W)
560
kΩ
OA2
0·5
μF
85A2
50
kΩ
0·5kΩ
helipot
51kΩ
51kΩ
2kΩ
0·5μF
15kΩ
(1W)
trls 154∝
tbv 65403/93d
100kΩ
0·1μF
620kΩ
620kΩ
6201
6201
0V
OA2
A
220 V
a.c.
2xE250C50
50μF
350V
wkg
50μF
350V
wkg
2·2kΩ
(2W)
2·2kΩ
(2W)
75 kΩ
910
kΩ
30kΩ
(2 W)
910
kΩ
-150V

Fig. 2. Relay circuit

If the hypo between the electrodes is not static, the direction of the line connecting the electrodes should be perpendicular to the flow vector.

Should it be desired to maintain automatically the silver concentration level in the fixing bath, the signal from the electrodes, after amplification in the *p*H-meter, can be used to control the flow of fresh hypo into the bath. This may be done by allowing the signal to operate a relay instrument which in turn switches on and off some suitable device (e.g. a solenoid valve) in the piping system.

---

* Burge, E. J., Davies, J. H., van Heerden, I. J., and Prowse, . J. *Nuovo Cimento*, **12**, p. 1005 (1957).

† Hooper, J. E., Dahl-Jensen, E., and Neergaard, E. B. *uovo Cimento Suppl.*, **15**, p. 211 (1960).

The relay circuit used in this laboratory is shown in Fig. 2. The instrument is fed by 220 V, a.c. at *A*. Jacks *B* are connected to the pH-meter jacks for an external recording circuit. The electrical circuit for the solenoid valve is passed through jacks *C* to the switches of the relay. The instrument is adjusted in such a way that the scale on the variable resistance Helipot potentiometer indicates the potential at which the instrument is working. The sensitivity of the instrument is such that the solenoid valve is opened if the potential between the electrodes is 5 mV less than the potential set on the Helipot potentiometer, and the valve closes again if the potential is 5 mV more than the instrument setting.

The way in which the instrument works can be illustrated by the following example. If the desired silver concentration in a 400 g hypo/litre fix bath is 10 g/litre, the corresponding potential can be read from Fig. 1 to be 313 mV. The Helipot potentiometer resistance of the relay instrument is then set at 313. If, for instance, the silver concentration in the fix bath is 12 g/litre (306 mV) the relay opens the solenoid valve and fresh hypo will flow into the system. As the silver concentration falls, the potential increases until it reaches 318 mV (9 g silver/litre). The relay then closes the solenoid valve. The silver concentration now increases as the silver–hypo-complexes diffuse out of the emulsions. When a concentration corresponding to 308 mV (11 g silver/litre) is reached the solenoid valve again opens and fresh hypo flows into the fixing bath; the silver concentration falls, and so on.

The author would like to express his particular thanks to cand. mag. Børge Madsen who designed and constructed the relay circuit.

Robust and sensitive spoon gauge

by B. J. Aylett, M.A., Ph.D., Chemistry Department, University of Aberdeen

[*Note first received* 21 *March, and in final form* 11 *April,* 1960]

Conventional types of spoon gauge* of high sensitivity are inconveniently fragile. This is particularly true if they incorporate a magnifying link mechanism with glass fibre pivots. The apparatus described in this note overcomes this difficulty without the use of expensive electrical sensing equipment, and is quite easy to construct.

The diagram shows the essential parts of the gauge. The lower end of the pointer *B*, actuated by the spoon *A*, is fused to a stirrup-shaped piece of platinum wire *C*(0·014 in. diameter) which passes through a hole of 0·015 in. diameter in the periphery of a small clock balance-wheel *D*, about $\frac{1}{2}$ in. in diameter.† The balance-wheel is held in a support *E* made from glass rod, which has two conical depressions to accommodate the pointed ends of the spindle. The wheel also carries a short length of thin glass rod, pointing downwards from its lowest point and fixed with picien wax. A small galvanometer mirror *F* is attached to this thin rod, also with picien wax. An essential feature is the hair-spring *G*, which is under slight compression, i.e. it is wound up about one complete turn. The free end is then cemented to a small piece of rod protruding from the side of the support *E*. This effectively prevents any backlash in the system. The whole assembly is made of soda glass, as a springy, sensitive spoon is most easily blown from this material; it is then enclosed, *via* a graded seal, in a Pyrex jacket of the usual type, in which the pressure can be varied and also measured accurately by means of a precision mercury manometer.

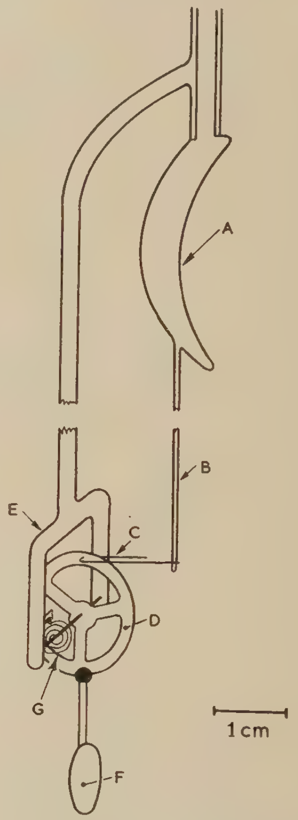

General view of the apparatus

A typical gauge of this type, used with a scale one metre distant, had a sensitivity of 5 cm scale-deflexion/mm of mercury for deflexions in each direction up to about 10 cm. Above this value, the sensitivity decreased somewhat, particularly with an excess pressure in the spoon. Zero shift over a period of some months corresponded to a pressure change of 0·04 mm, while hysteresis effects were seldom greater than 0·01 mm during the course of a day. The gauge several times withstood a pressure difference of about 5 cm in each direction without damage.

In making the support *E*, the bearing depressions are first produced by heating the ends of the glass with a small flame and then indenting them with a small pin. The support is then put on its side and arranged so that the balance-wheel axle can just be inserted. One arm of the support is then heated, and allowed to fall by its own weight on to the axle. In this way, a satisfactorily tight bearing is produced.

---

* Foord, S. G. *J. Sci. Instrum.*, **11**, p. 126 (1934).

† That from a Westclox "Baby Ben" alarm clock is very suitable.

New instruments, materials and tools

The Editor invites manufacturers of instruments and light machine tools to keep him informed of their new or improved products. The Institute of Physics and The Physical Society assumes no responsibility for the statements given below: information for these has been taken from literature supplied.

Portable radiation background measuring instrument. Plessey Nucleonics Ltd., Weedon Rd., Northampton.

This lightweight portable measuring instrument, Type P.N.I. 1072, has been developed to meet the frequent need for an accurate means of measuring any background activity quickly and easily. Detection is accomplished by a built-in halogen-quenched Geiger–Müller tube with measurement on a transistor rate-meter giving direct reading of dose rate on a 2½ in. scale moving coil meter. The instrument has a range of from 0 to 3 mr/h on a two decade quasi-logarithmic scale, with a minimum scale calibration of 30 μr/h. The unit is powered by a 9 V dry battery and weighs 8 lb.

Vibrating reed electrometer. Ekco Electronics Ltd., Southend-on-Sea, Essex.

This electrometer is designed to measure very small direct currents and voltages with high zero stability, by converting applied d.c. to a.c. by means of a vibrating reed capacitor, and finally amplifying it by a stable a.c. amplifier. Seven ranges are provided, from 3 mV to 3 V, and the output is rectified and measured on a 5 in. meter calibrated to give the d.c. voltage at the input.

It is claimed that the accuracy for voltage measurement is about $\pm 5\%$, while that for current measurement is the same, provided that the total value of the input resistance is known and the calibration control adjusted as necessary.

Trace reading equipment. Southern Instruments Ltd., Frimley Road, Camberley, Surrey.

The TRE 12 trace reading equipment shown in the figure is designed for the analysis of oscillograph traces. The chart on which the record has been made can be moved in either direction by a push-button controlled motor drive; fine control of the chart position is by a large thumb-wheel. The record may contain up to 12 traces. In a single scan, each trace is read in turn and the output is obtained in digital form. The output can be by electric typewriter, tape perforator or card punch, either singly or simultaneously. A visual display is also provided. Non-linear calibration can be introduced into the reading of each trace on the chart. The calibration charts are produced on graph paper fitted to a drum beneath the trace display window, and both calibration curve and record are traversed by a single short cursor. The cursor is set over the point to be read from the trace, and the calibration drum is rotated to bring the calibration curve beneath the cursor. A voltage proportional to the drum rotation is fed to the calibration unit, where it is scaled and combined with a zero shift voltage. The output from the calibration unit is compared with a reference voltage and the result is displayed in decimal digital form. Readout is controlled by push-button or foot switch. Stepping on to the next channel is automatic, and the operative channel is shown on a digital display above the trace window. The reader can handle records in the form of paper up to 12 in. wide and up to about 200 ft in length. 35 and 70 mm film can also be read by using a projector attachment. An accuracy of 0·2% of full scale is claimed.

Trace reading equipment

Hygrometer alarm. Shaw Moisture Meters, Rawson Road, Westgate, Bradford, Yorkshire.

This hygrometer alarm uses a special sensing element which continuously records the humidity of any low- or high-pressure atmosphere (up to 3000 lb/in.^{2}). It gives immediate warning of any change in dewpoint or humidity. The range of working is 10^7 to 1 for the humidity, and dew points down to −150° C can be measured. It is claimed that the instrument is at least 100 times as sensitive as the ordinary conventional methods, and it will work in dusty conditions without attention. Its working temperature range is −50 to −150° C.

The instrument has chart recordings and the chart speed is ½ in./h; it is transistorized and is stabilized for 190 to 260 V; it is remote reading and independent of the flow rate of the gas to be measured; its response time is 1 s.

High-sensitivity leak detector. Leland Instruments Ltd., 22 Millbank, London, S.W.1.

The type THM 105A leak detector is made by the French Thomson-Houston Co., and is distributed in the United Kingdom by Leland Instruments. The apparatus is based on the principle of detection of helium gas by a miniature mass spectrometer using double deflexion of 180 degrees to obtain stability of operation and a high sensitivity. It is claimed to be capable of detecting, locating and measuring leaks of 10^{-12} cc/s measured at atmospheric pressure. Detection is stated to require a concentration of helium in any other gas of 1 part in 10^7. The instrument incorporates two pumping units in the vacuum circuit. The first is a two-stage mechanical pump of high capacity; the second is a silicone-oil-diffusion pump cooled by compressed air. This pumping assembly can maintain a pressure of 10^{-6} mm of mercury in the test cavity. A helium flow meter, controlled helium jet, and a helium sensing probe are additional features of this instrument, and provision is also made for remote indicating meters and audible alarms.

Stirrer. Jones and Stevens Ltd., Long Lane, Littlemore, Oxford.

This newly developed stirrer is designed to give optimum power output at the required speeds, and to give increased power as speed decreases.

The powerful induction motor is said to ensure there is no danger of sparking, and a choice of six secondary shaft speeds is available. Hollow stirring shafts, accurate speed control and 5/16 in. capacity chuck are other advantages claimed by the manufacturers of this unit.

Automatic electrophoretic strip scanner. Evans Electroselenium Ltd., St. Andrew's Works, Colchester Road, Halstead, Essex.

The "Eel" automatic scanner is designed to draw automatically a dye concentration curve for an electrophoretic strip. The sample carriage will accept a paper strip 5 × 17 cm, and the instrument will scan a length of 15 cm, the complete curve being drawn in 3 min. The sample holder is mounted on a movable table which also carries the roll chart. The table is driven by a slow-speed motor which may be engaged or disengaged by a lever at the right-hand side of the instrument. The sample is illuminated by a focused beam of light from a festoon-type lamp, the light transmitted being received by a photomultiplier mounted behind a narrow slit beneath the movable table. One of a range of interchangeable colour filters is inserted in the light beam to obtain the greatest extinction of light in conjunction with the dye employed. The photomultiplier operates a logarithmic detector circuit, the output of which feeds an amplifier. This, in turn, operates the recording milliammeter to deflect the pen arm. Controls to adjust the zero balance and sensitivity are provided, their range being such that either thick or thin papers may be employed for the electrophoretic separation, with or without the use of a clarifying liquid. A change in optical density of 0·6 suffices to give full-scale deflexion of the pen arm.

Automatic delay switches. Electrical Remote Control Ltd., Elremco Works, Harlow New Town, Essex.

The type SE time switch is a solenoid-operated mechanical escapement operating a changeover switch at the end of an adjustable time delay. The switch can be supplied for one of two alternative switching actions. In the type SE/A, the delay time commences on energization of the solenoid. At the end of the adjustable time delay, the changeover switch is operated and will remain in the operated position until the solenoid is de-energized. On de-energization of the solenoid, the unit resets within 0·5 s. In the type SE/B, energization of the solenoid instantly resets the unit and operates a changeover switch. The time delay commences on de-energization of the solenoid, and the changeover switch is operated at the end of an adjustable time delay. The units can be supplied for the time ranges 1–10 s, 3–30 s, 5–60 s, or 1–5 min. They can be supplied to operate off voltages up to 440 V a.c. or 110 V d.c. and to switch currents of 5 A at 230 V a.c. or 24 V d.c.

Low capacitance bridge. Marconi Instruments Ltd., St. Albans, Hertfordshire.

Capacitances from 1·111 pF down to 0·002 pF can, it is claimed, be measured with 0·2% accuracy by means of this three-terminal transformer ratio-arm bridge. It is suitable for such applications as the measurement of the temperature coefficient of capacitors or changes in valve interelectrode capacitance. The bridge measures the capacitance between any two terminals of a three-terminal network; and is virtually unaffected by the impedance between either of these terminals and the third point. As a result, connexion to the component under test can be made through long leads without affecting the measurement accuracy. This feature allows *in situ* measurements of remote or wired-in components without the need to disconnect associated circuits; and is particularly valuable where it is important to include inherent shunt and stray capacitances, which cannot be disconnected for conventional measurement.

The resistive and reactive components of the unknown capacitor are separately balanced out in a transformer ratio arm bridge, the unknown and standard impedances being connected in opposite sides of the bridge. Effective shunt resistance of the component under test is balanced by a standard resistor fed through three transformer tappings and a continuously variable potentiometer. The total range is said to be from 1 MΩ to at least 1000 MΩ. Decade switching and readout is provided; automatic decimal point indication ensures that the readout is the direct reading.

The bridge is complete with internal oscillator (1000 c/s) and detector. The detector gain can be switched to provide high or low sensitivity and, to facilitate balancing, automatic gain control is used to give progressive increase in sensitivity as the balance point is approached.

Frequency meter and tachometer. Airmec Ltd., High Wycombe, Buckinghamshire.

The type 265 frequency meter is claimed to measure the frequency of a repetitive waveform in the range 10 c/s to 100 kc/s with an accuracy of ±1%. The input waveform is squared and limited, and applied to an integrating circuit, the voltage on which is applied to a large panel meter. The circuits are arranged so that the meter reading is independent of the amplitude or waveform of the input voltage.

The instrument can be used to measure the speed of a rotating shaft by arranging that the shaft makes or breaks a contact at each revolution thus applying a square-wave potential to the frequency meter. Alternatively, by employing the optical probe type 283 in which the rotation is detected by reflexion of a light beam from a painted line on the shaft, speed measurements may be made without loading the equipment under test.

The frequency meter is fully transistorized, light and portable, and may be powered from a.c. mains or the internal batteries. Power supply and signal connexion for the optical probe are available at a rear socket. An internal calibration check is provided by means of a stable 5 kc/s oscillator, and the meter is direct-reading in frequency and rev/min. An external meter or recorder may be fed from a socket on the front panel.

Oscilloscope camera. J. Langham Thompson Ltd., Bushey Heath, Hertfordshire.

The series 400 is a single-shot camera, the body of which is a Polaroid-Land fast-processing unit. All processing of the film takes place inside this, thus eliminating the necessity for darkroom and developers. The camera, when fitted with the appropriate hood, can be used on almost every general-purpose oscilloscope at present commercially available. Loading of the roll film is carried out in daylight in the normal manner. The camera is fitted with a Dallmeyer lens with a fixed aperture of $f/3\cdot5$ and a focal length of 3 in. in a focusing mount. The sensitized material is Polaroid roll film, which is available in two types: one producing black and white prints and the other black and white transparencies. The format is 4 × 3 in., and each roll of film is sufficient for 8 exposures.

A simple spring-loaded, manually-operated shutter is fitted, it having been found unnecessary to incorporate a multi-speed shutter because of the ease with which the brightness of the cathode-ray spot can be controlled. The shutter is interconnected with a switch which terminates in sockets beneath the camera and permits a circuit to be either "made" or "broken" when the shutter is fully open. For recording transients, provision is made for locking the shutter in the open position.

A ground glass graticule bearing an engraved black line is fitted into the camera so that the line lies along the centre of the optical path and at the focal plane. Focusing is achieved by illuminating the line, thus projecting it through the optical system on to the cathode-ray-tube face.

Electric melting point apparatus. Electrothermal Engineering Ltd., 270 Neville Road, London, E.7.

This instrument which, it is claimed, will give regularly reproducible results for the determination of melting points between 20 and 360° C to an accuracy of ±1° C consists of a base which houses the controls; a framework which acts as a draught screen for the operating area; a heater with a specially designed metal block to receive three capillary tubes and a specially designed and calibrated thermometer; an optical system for illuminating and viewing the capillaries and a transformer in the base which also gives stability to the apparatus. Disadvantages associated with heat transfer through liquids are eliminated by the use of a metal block.

Digital printer. Radiatron, 7 Sheen Park, Richmond, Surrey.

A fast printer has been designed for recording digital information collected by electronic scalers without destroying the scaler indication. Unlike an electrical typewriter, it prints up to 14 characters simultaneously. The Kienzle type D.1.E printer includes the essential electronic circuits so that it can be connected to commercially available scalers with little or no addition to the existing circuits. The principle of operation is that on receiving the print command, an electric motor turns all print wheels (one for each digit) by one complete revolution, sending during this process 10 interrogation pulses to the scaler, corresponding to numbers 0–9 embossed on each print wheel. These pulses are sent to all decades of the scaler simultaneously, each resulting in stepping all scaler digits by one position. Whenever one of the scaler digits passes its zero position, it sends back to the printer a locking pulse. This is passed through an amplifier to a solenoid and locks the corresponding print wheel in a position to match the indication of the scaler digit. The scaler itself continues to step until it again reaches its original position. The whole interrogation process takes only 90 ms. Immediately after interrogation, simultaneous printing of all digits takes place. All locking amplifiers and the interrogation pulse generator are transistorized and are contained in the printer.

The printer is capable of printing 3 lines/s of up to 14 digits each on 80 mm paper strip. A serial number can be printed alongside the record; this number may step automatically, or may be remotely controlled. A date printer may also be incorporated, printing year, month and day. The printer is available in a larger model in which 30 columns or more (depending on the number of digits) can be printed on a 600 mm paper roll. Translator circuits are available for operating the printer from dekatron, hard valve flip-flop, and hot-cathode indicating-tube counters. The printer also operates from electro-mechanical counters (type D.10.E).

Numeral indicator tube. Standard Telephones and Cables Ltd., Valve Division, Footscray, Kent.

The GN-1 tube is a cold-cathode, gas-filled numeral indicator intended for use as a direct read-out device operating from a.c., unsmoothed rectified a.c., or d.c. power supplies. The numerals 0–9 are arranged as a series of wire cathodes one behind the other; the primary anode is in the form of a black box which masks reflexions and stray light. The normal operating supply for the tube is about 3 mA at 200 V, but both a.c. and unsmoothed rectified a.c. supplies are stated to give good cathode-glow coverage at lower mean currents. Thus, by reducing the current, the light output can be dimmed without loss of cathode coverage. It is stated that the numerals can be read at a distance of 40 ft and at a viewing angle of 45 degrees.

Rugged alphabetical indicator tubes and a plus and minus sign indicator are also available.

Stable power supply for spectrophotometer. Doran Instrument Co. Ltd., Stroud, Gloucestershire.

The power supply required for the operation of the amplifier and tungsten lamp of the Union S.P. 500 spectrophotometer is normally obtained from two 6 V accumulators. With this mains unit, however, the inconvenience of changing and re-charging batteries is avoided, and also the drift of the instrument's pointer, due to changes in power supply, is eliminated.

It is claimed that the degree of stabilization afforded by the mains unit is such that the readings of the spectrophotometer are unaffected by variations of ±50% in the voltage of the power supply, or by small variations in frequency.

The unit, connected to the a.c. mains (200–250 V, 50 c/s), provides a stabilization 6 V, 6 A supply for the tungsten lamp of the spectrophotometer, and a stabilization 6 V d.c. output (tapped at 2 V) for the amplifier. By means of a switch, the former supply may be disconnected. The unit is contained in a metal case, ventilated to keep the temperature low.

Although designed primarily for use with the Unicam S.P. 500 spectrophotometer, it is stated to be suitable with simple adaptors for providing a stable 6 V and 76 mA (maximum) for many purposes. A 60 c/s model is also available. The dimensions are $17\frac{3}{4} \times 9\frac{1}{2} \times 9\frac{1}{2}$ in.

New books

Progress in semiconductors. Vol. 4. Edited by A. F. Gibson, F. A. Kröger, and R. E. Burgess. (London: Heywood and Co. Ltd., 1960.) Pp. viii + 292. Price 63*s*.

This volume contains a number of excellent articles on subjects of topical interest in semiconductor physics. The first by Krömer explains the concept of negative effective mass, how it could arise in different types of crystal and its possible application in the negative mass amplifier. The second paper by Green discusses oxidation phenomena on clean and etched germanium surfaces and relates them briefly to the electronic properties. Yamashita presents the theory of avalanche multiplication by strong electric fields in non-polar crystals, particularly in *p–n* junctions. The related subject of internal field emission is treated by Chynoweth, and includes electronic and hole injection, Zener breakdown, field ionization and dielectric breakdown. Sautter gives an account of noise in semiconductors, i.e. thermal noise, generation-recombination noise and $1/f$ noise, all in homogeneous specimens. Bardsley discusses the generation of dislocations in semiconductors with the diamond-type lattice, and the associated electrical effects, while Volger discusses the interaction between lattice imperfections and dielectric properties.

Finally there is an important paper by Ioffe and Regel on amorphous and liquid semiconductors, showing that semiconducting properties are by no means restricted to periodic crystal lattices, that in many semiconductors the mobility is not determined by scattering by the vibrations of the crystal lattice, but by the transfer process from one ion to another, and that short range order is of vital importance in determining the semiconducting properties of a solid or liquid. This paper gives a more completely co-ordinated account of Russian investigations and thought on these subjects than the writer has seen previously, and should be of considerable interest in the West. In fact, while the standard of this series of volumes has been high throughout, this particular volume is perhaps the most stimulating so far produced. D. A. Wright

British glass industry. Directory and buyers' guide. 7th ed. (London: Illiffe & Sons Ltd., for The Society of Glass Technology, 1959.) Pp. 376. Price £2.

The directory in its new format comprises four main sections; the "Catalogue of firms" consisting of names, and addresses, branch offices and oversea agencies, of approximately 600 firms; the "Buyers' guide" containing over 13,000 names of firms alphabetically arranged under approximately 1200 classified headings, and "Proprietary and trade names, and Display announcements."

Process integration and instrumentation. Electricity and productivity series, No. 8. (London: Electrical Development Association, 1959.) Pp. xx + 204. Price 8*s*. 6*d*.

The preface to this book notes the "large and bewildering variety of most types of apparatus" that is now available for instrumentation-process control, and goes on to state that the book will "assist in helping to achieve the conceptual aim" in relation to process integration. This tautological claim the reviewer begs leave to doubt. The final bewilderment is likely to be as great as the first. In fact, an impossibly large task has been attempted in so small a compass. A useful introduction to process control (the case for "process integration" is not too clear) and its associated concepts and components would be better divorced from the associated measuring instruments; and to deal adequately with industrial instrumentation would require much more space and greater lucidity of classification than is in evidence here.

In short, the book fails to be either a satisfactory primer or an adequate catalogue. R. E. Fischbacher

Materials and techniques for electron tubes. By W. H. Kohl. (New York: Reinhold Publishing Corporation; London: Chapman and Hall Ltd., 1960.) Pp. xviii + 638. Price £6 12*s*.

This book is a revised version of the author's previous work *Materials Technology for Electron Tubes*. It is thus primarily intended to provide information for the valve engineer or the technician in the laboratory.

Before writing the book, the author wisely circulated a questionnaire among a large number of users of his former work, in order to obtain some guidance as to the most useful chapters and what new subjects to include in the revised version. The result, as demonstrated in this new volume, has been eminently satisfactory.

The book contains sixteen chapters: eleven of these give clear, but concise, accounts of the various metals and non-metals used in the manufacture of electron tubes; the remaining five deal with manufacturing processes, such as glass-to-metal sealing, brazing of metals and so on. On the whole, the subject-matter is well written and each chapter is liberally supplied with references. The diagrams are well drawn and very clear. One minor criticism which could be made is that the author has a penchant for constructing rather long sentences. This makes reading somewhat tedious at times, and one is sometimes forced to refer back to the beginning of a sixty- or seventy-word sentence to refresh one's memory as to the original subject being discussed.

The author index is extremely helpful. It lists not only the pages on which the name appears in the text, but also the appropriate reference number in a specified chapter. This book will no doubt become a most useful reference source for those engaged in the manufacture of valves, cathode-ray tubes and the like. D. G. Anderson

Kleines Handbuch technischer Regelvergange. By W. Oppelt. (Weinheim/Bergstr: Verlag Chemie, 1960.) Pp. 632. Price DM 39.60.

This is an extremely useful book, since it gives a very large number of practical examples of all types of control systems and the components that are included in them. Mechanical, electrical, hydraulic and pneumatic elements are all treated fully and the fields from which the systems' examples are taken include process control, automation, electric power, guided missiles and nuclear power. It is copiously illustrated with diagrams giving mechanical details as well as block-schematic and response diagrams. So well is it illustrated that there is little need to understand German to follow the text.

All the usual methods used in the design of control systems are given in considerable detail and there are extremely useful tables giving the frequency and transient response and pole-zero configurations for difficult types of system. There are also useful tables giving different types of measuring instruments, amplifiers and other components.

Having dealt exhaustively with simple linear systems, there is a useful chapter on multivariable systems. Then follows a chapter on non-linear systems, in which the describing function and phase-plane techniques are dealt with and this is followed by chapters on digital controls and simulators, respectively. A comprehensive bibliography and index complete the volume.

In the matter of documentation, the reader is given full measure, since the appropriate references are also given as footnotes, which are very much more convenient to use than the general bibliography.

J. F. Coales

Programming programme for the BESM computer. By A. P. Ershov. Translated from the Russian by M. Nadler. Edited by J. P. Cleave. (Oxford: Pergamon Press Ltd., 1959.) Pp. 158. Price 60*s*.

This is a most valuable book which gives the first account of Russian work on automatic programming which has been made available to Western scientists.

The book gives a detailed account of the structure of the BESM computer and then describes both the theory of algorithmical processes and the way in which this theory can be used to enable a computer to interpret a mathematical formula and then to construct a programme for its arithmetical evaluation.

Unfortunately the translation is bad and no attempt seems to have been made to make the result follow normal English sentence structure. Likewise the technical Editor has failed to reduce the untechnical raw translation to current usage, the most glaring example being that "Programming Programme" should be "Automatic Programme".

A. D. Booth
K. H. V. Booth

Laboratory instruments. 2nd ed. By A. Elliott and J. Home Dickson. (London: Chapman and Hall Ltd., 1959). Pp. xvi + 514. Price 55*s*.

The first edition of this very useful work was published in 1951, since when there have been some quite considerable advances in laboratory techniques and materials. The authors have spared no pains in bringing the book up to date, even though this has involved the inclusion of a good deal of new matter as well as the revision of many details. Major additions refer to plastics, adhesives, corrosion of metals, optical and infra-red materials, photometry and radiation. The authors' decision to exclude electronic and purely biological instruments was certainly wise, since it has enabled them to discuss the principles of design and construction of mechanical-optical instruments much more thoroughly than would otherwise have been possible. Indeed, its pre-occupation with principles is one of the more attractive features of the book, rendering it not only eminently readable but even at times absorbingly interesting, to a physicist at least. For those who have need of further detail there are frequent bibliographical references.

In its revised form the book is even more valuable, one might almost say indispensable, to all those who have occasion to construct or design instruments for any type of physical measurement. The production, the diagrams and the index leave nothing to be desired.

W. E. Curtis

Electronics for spectroscopists. Edited by C. G. Cannon. (London: Hilger and Watts Ltd., 1960). Pp. 333. Price 60*s*.

The fourteen chapters by nine expert contributors provide a thorough going and comprehensive basis for the understanding of the electronic circuits and devices upon which spectroscopy is becoming more and more dependent. The problem of dependence is, of course, not peculiar to spectroscopy but this book is clearly designed to answer the needs particularly of the spectroscopist in comprehending his apparatus either to employ it to the maximum of its potentialities or to extend them by additions or modifications for special research problems.

The book progresses from subject-matter of very general importance (a.c. theory, amplifier design, power supplies) to considerations of noise; and then proceeds to discuss in turn the various devices used either in detecting the radiation or in its accurate measurement. On the whole the infra-red region is more fully treated than the ultra-violet.

In this type of book there is a need for a glossary to help the reader over the many unfamiliar terms. In fact there is no glossary. In addition the index is very thin. Apart from these weaknesses, the working spectroscopist (who is not already an electronics expert) will be glad to have this up-to-date book at his elbow.

H. L. Fisher

Zone refining and allied techniques. By N. L. Parr. (London: George Newnes Ltd., 1960.) Pp. xvi + 184. Price 40*s*.

The author of this book states that he has aimed first at surveying the technique of zone refining and secondly at providing practical information on methods and equipment. He has been the more successful in the second of these aims. The descriptions of well-tried apparatus are good, and the text is supported by many diagrams which, though detailed, are usually very clear. On the other hand, a number of the plates are of little value and can only add to the price.

As a survey of the zone-refining technique the book is incomplete; it is felt that the basic considerations of the first three chapters could well have been expanded and clarified. This volume is, therefore, not ideal as an introduction to the zone-refining process, but it does provide much useful information to the man who has to construct and operate zone-refining equipment and practise the allied techniques.

H. J. Goldsmid

Automatic titrators. By J. P. Phillips. (New York: Academic Press Inc.; London: Academic Books Ltd., 1959.) Pp. viii + 225. Price 48*s*.

Written for the analytical chemist, this volume provides a clear and concise review of its subject. Fundamentals of titrator design are dealt with, and a number of typical commercially available instruments are described and discussed. Results of analyses taken from published work are tabulated and form a useful guide to applicability. Although the book and its author (a professor of chemistry at the University of Louisville, Kentucky) are American, a useful selection of non-American instruments is included in its scope.

The text is well illustrated with explanatory diagrams, and there is a good index, together with a large number of useful literature references to original work. Although it cannot be considered as a textbook on the subject, and was not so intended, it should prove to be a useful reference work in a field where comprehensive books are at present lacking.

W. Sebborn

Notes and comments

The amalgamation of The Institute of Physics and The Physical Society

The incorporation of a new body on 17 May, 1960, under the name of "The Institute of Physics and The Physical Society" marks the fulfilment of the desire expressed by the overwhelming majority of the members of the Institute and Society that the "necessary action" should be taken to implement the scheme for amalgamation prepared by a Joint Committee. The originating bodies have now been formally wound up and their assets handed over to the new one.

The first President of the amalgamated body is Sir John Cockcroft and the four Vice-Presidents are Dr. J. Topping, Dr. W. H. Taylor, Professor R. W. Ditchburn and Mr. A. J. Philpot, each responsible to the Council for a defined area of the many activities taken over by the new organization from its predecessors. The Presidents of the predecessors (Sir George Thomson and Mr. J. A. Ratcliffe) are also members of the new Council. The other Officers are Dr. J. Taylor (Honorary Treasurer) and Dr. C. G. Wynne (Honorary Secretary).

The Physical Society of London, as it was then called, was founded in 1874 and on the initiative of that Society's Council The Institute of Physics was founded 45 years later. The original scheme envisaged a kind of federation of societies interested in physics, to provide among other objects, rooms for meetings, a library, and a common secretariat. In fact the Institute's offices were in the Society's present rooms in South Kensington from 1927 to 1949 and the Institute provided the secretariat for The Physical Society and The Optical Society which themselves amalgamated in 1931.

At the time of its establishment no one could have foreseen the spectacular growth and influence of physics in the modern world. Broadly speaking before the war the scientific meetings and publications of the Institute were confined to applied physics while those of the Society were concerned more with pure physics. As, however, the boundary between these two aspects became less definite there has been increasing overlap in the activities of the two bodies and in their membership. It is not, therefore, surprising that during the past 20 years proposals for the amalgamation of the two bodies have been made repeatedly and from time to time detailed proposals examined, until eventually a satisfactory solution was worked out.

The qualification for the award of Fellow of The Institute of Physics, Associate of The Institute of Physics, and Graduate of The Institute of Physics will remain unchanged and members of the new body holding these diplomas will also be Fellows of The Physical Society. Besides the three Institute of Physics' grades of membership of the new body there will also be the grade to be known as "Fellow of The Physical Society". All the Fellows of the old Society will be automatically transferred to this new grade, but new candidates for election to the grade will be required to possess a degree or diploma in physics recognized by the Council, or to satisfy the Council that they have a sufficient knowledge of physics.

Provision has been made for other scientists and engineers to participate in the scientific and educational work of the new body. Activities relating to the practice of the profession as such, will be strictly confined to those possessing one of the Institute's diplomas.

The executive Officers of the new body are *Secretary:* Dr. H. R. Lang; *Editor and Deputy Secretary:* Dr. A. C. Stickland; and *Deputy Secretary:* Mr. N. Clarke. The registered offices and headquarters are at 47 Belgrave Square, London, S.W.1, and for the present, offices will also be retained at 1 Lowther Gardens, South Kensington, London, S.W.7.

British Journal of Applied Physics

Contents of the September issue

CONFERENCE REPORT

Summarized proceedings of a conference on X-ray analysis, London, November 1959. By G. J. Bullen and A. L. Mackay.

PAPERS

Pumping characteristics of a titanium droplet getter-ion pump. By L. Holland and L. Laurenson.

Numerical investigation of a range of unipotential electron lenses. By J. Vine.

NEW BOOKS SECTION

Reviews and notices.

PAPERS (continued)

Emission of negative ions of oxygen during the activation of oxide-coated cathodes. By N. A. Surplice.

Sorption and desorption of gas in a hot-cathode ionization gauge. By F. A. Baker and T. A. Giorgi.

Solution of ladder networks containing non-linear resistances. By T. Kovattana and J. R. Barker.

Passage of current through the glass envelope of a receiving-type valve. By H. N. Daglish.

Temperatures reached in a bimetallic brake drum. By T. P. Newcomb.

NOTES AND NEWS

Notes and comments

THIS *JOURNAL* is produced monthly by The Institute of Physics and The Physical Society, with the co-operation of the National Physical Laboratory. It deals with the principles, construction and use of scientific instruments. All rights reserved. Responsibility for the statements contained herein attaches only to the writers.

EDITORIAL MATTER. Communications concerning editorial matter should be addressed to the Editor, The Institute of Physics and The Physical Society, 47 Belgrave Square, London, S.W.1. (*Telephone:* Belgravia 6111.) Prospective authors are invited to prepare their scripts in accordance with the *Notes for Authors.* (Price 3*s.* 6*d.* including postage.)

REPRODUCTION. The Institute of Physics and The Physical Society is a signatory to The Royal Society's Fair Copying Declaration. Details may be obtained upon application from The Royal Society, London, W.1.

ADVERTISEMENTS. Communications concerning advertisements should be addressed to the agents, Messrs. George Jackson (Fleet St.) Ltd., Cliffords Inn, Fleet Street, London, E.C.4. (*Telephone:* Holborn 3611–2.)

CLAIMS FOR MISSING JOURNALS. Claims from regular subscribers to this *Journal* for missing numbers will only be considered if received within 60 days of the date of mailing plus normal outward time of transit and time for lodging the claim. Losses attributable to failure to notify a change of address or to similar omissions will not be considered.

SUBSCRIPTION RATES. A new volume commences each January. The charge is £6 per volume ($17 U.S.A.), including index (post paid) payable in advance. Single parts, so far as available, may be purchased at 12*s.* 6*d.* each ($1.75 U.S.A.), post paid, cash with order. Orders should be sent to The Institute of Physics and The Physical Society, 47 Belgrave Square, London, S.W.1, or to any bookseller.

PRINTED IN GREAT BRITAIN BY UNWIN BROTHERS LIMITED, WOKING AND LONDON

Magnetic probes of high frequency response

by S. E. SEGRE, Dottore in Fisica, and J. E. ALLEN, B.Eng., Ph.D., A.M.I.E.E., Laboratorio Gas Ionizzati del C.N.R.N., c/o Laboratori Nazionali di Frascati, Roma, Italy

[*Paper received* 24 *June*, 1960]

Abstract

Probes for the measurement of the magnetic field distribution in fast pulsed discharges have been constructed. Their frequency response has been measured and agrees well with that calculated from an equivalent circuit. The probes described have an attenuation flat (*to within* 1%) *up to* 20 *Mc/s.*

A criterion is given which states the optimum value for the impedance of the recording circuit.

Introduction

In some experimental studies of the behaviour of plasma in a magnetic field, it is desirable to obtain the spatial distribution of the magnetic field as a function of time. Such measurements have been carried out by means of magnetic probes,(1) both in "slow" discharges with characteristic times of the order of 1 ms(2) and in "fast" discharges with characteristic times ~ 1 μs.(3) The probes consist essentially of small coils which are inserted in the magnetic field B and which give a signal proportional to dB/dt. This signal, after integration, is displayed on an oscillograph and measurements made with the probe in different positions enable one to determine the distribution of the magnetic field in space. This paper reports on measurements of the frequency response of magnetic probes for use in fast discharges and gives a criterion for obtaining the best frequency response. The probes described are being used to measure the distribution of the magnetic field in orthogonal pinch experiments.(4)

The probe circuit

The measurements reported in this paper, which refer to frequencies up to 30 Mc/s, show that the circuit of Fig. 1(*a*) can be used to describe the behaviour of a magnetic probe in this frequency range. The voltage of the generator G is equal to that induced in the coil by the changing magnetic field, L and r are the inductance and the resistance of the coil respectively and C is the capacitance of the coil, leads and connector.

The circuit used in practice is that shown in Fig. 1(*b*), where R is a matching impedance for the coaxial cable and is followed by a high-impedance RC integrator. Thus the frequency response of the probe can be calculated using the circuit of Fig. 1(*c*), and it is easily shown that the attenuation $|A|$ and the phase shift ϕ as function of angular frequency ω are given by

$$|A| = \{(R+r)^2/R^2 + \Omega^4 - \Omega^2(2 - r^2/R_0^2 - R_0^2/R^2)\}^{-1/2} \quad (1)$$

and $$\phi = \tan^{-1}\left\{\frac{\Omega}{\Omega^2 - (r+R)/R}\left(\frac{R_0}{R} + \frac{r}{R_0}\right)\right\} \quad (2)$$

where $R_0 = \sqrt{(L/C)}$ and $\Omega = \omega\sqrt{(LC)}$. From equation (1) it can be shown that if $R > R_0(2 - r^2/R_0^2)^{-1/2}$ the attenuation curve has a resonance at

$$\omega = \omega^* = [\{1 - r^2/(2R_0^2) - R_0^2/(2R^2)\}/LC]^{1/2} \quad (3)$$

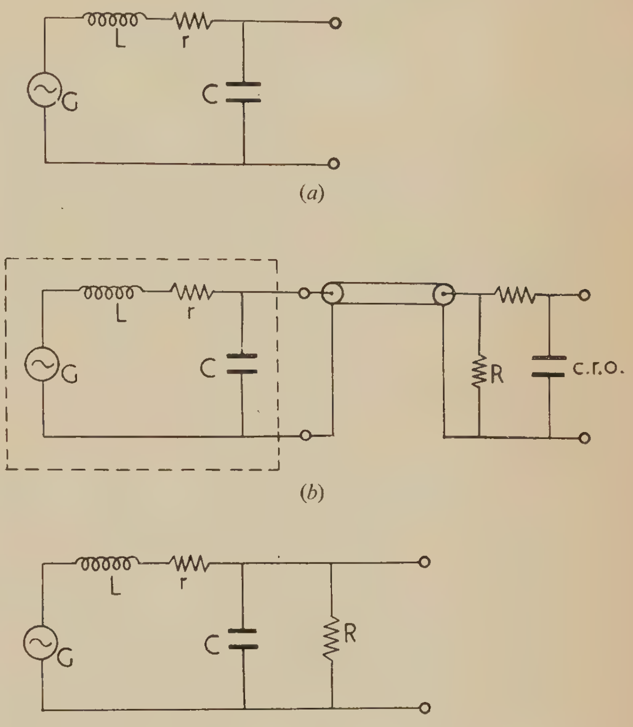

(*a*)

(*b*)

(*c*)

Fig. 1. (*a*) Equivalent circuit of the magnetic probe; (*b*) Circuit used in practice to measure magnetic fields; (*c*) Equivalent circuit pertaining to the calculation of the frequency response of the magnetic probe

For typical probes $r^2/(2R_0^2) \simeq 1\%$ so that, if R is large enough

$$\omega^* = (LC)^{-1/2} \quad (4)$$

to within less than 1%. It can be seen from equation (3) that, if R is decreased, the resonant frequency decreases until it becomes zero when

$$R = R_0(2 - r^2/R_0^2)^{-1/2} \simeq R_0/\sqrt{2} \quad (5)$$

For values of R less than that given by equation (5) the attenuation curve does not have a resonance. Attenuation curves calculated from equation (1), for a particular set of values of L, C, and r, are shown in Fig. 6. For these curves $R_0/\sqrt{2} = 197\ \Omega$ and it can be seen that for this value of

R one obtains the flattest attenuation curve. {It can be shown from equation (1) that, if R is given by equation (5), $d|A|/d\omega = 0$, $d^2|A|/d\omega^2 = 0$ and $d^3|A|/d\omega^3 = 0$ at $\omega = 0$ i.e. at this point the attenuation curve has a contact of third order with the horizontal tangent.}

Construction of the probe

The probes (see Fig. 2) consist of a double layer coil of 60 turns, of 0·03 mm copper wire wound on a small glass rod. The coil is 1 mm long and 0·7 mm in diameter. The leads to the coil are twisted together (to avoid induced voltages) and pass through a silvered glass tube of 0·5 mm external diameter. The coil and the metallized tube are inserted and fixed with a drop of glue in a quartz tube 15 cm long and 3 mm external diameter, the axis of the coil being perpendicular to the axis of the quartz tube. The latter is attached to a connector (not shown in Fig. 2) which can be connected directly to a coaxial cable. At the connector, one of the leads and the silvered tube are connected together. The silvered tube is an electrostatic shield, but the thickness of the metallic layer is so small ($\sim 0\cdot01$ mm) that diamagnetic currents in the layer will not shield the external magnetic field and so will not perturb it.$^{(5)}$

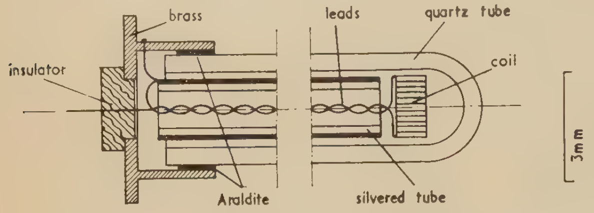

Fig. 2. Construction of the magnetic probe

Measurements

Experimental curves of attenuation versus frequency were obtained by inserting the probe radially in a coil of low resistance which was fed by an oscillator of variable frequency (1 to 30 Mc/s).

The probe was connected directly to the input of the oscillograph (c.r.o.). The voltage across the coil, which was proportional to the voltage of the generator G (see Fig. 1), was measured with a valve voltmeter. A resistor R was connected in parallel with the probe at the c.r.o. input. The attenuation curves shown in Fig. 3 were obtained by plotting the ratio of the c.r.o. deflexion to the voltmeter reading as a function of frequency, ν, for different values of R and by normalizing the curves so that $|A| = R/(R+r)$ at low frequencies.

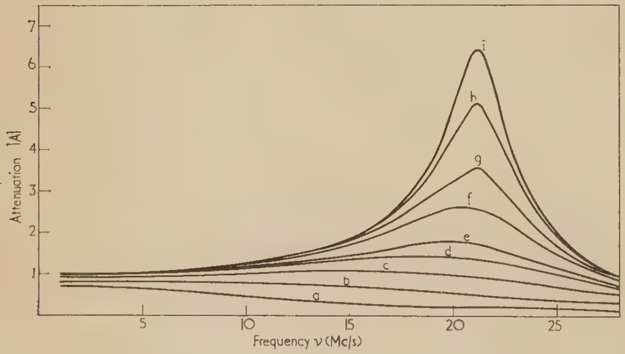

Fig. 3. Experimental attenuation curves of the probe (plus c.r.o. input) for different values of R

(*a*) $R = 51\cdot5\ \Omega$; (*b*) $R = 105\ \Omega$; (*c*) $R = 197\ \Omega$; (*d*) $R = 299\ \Omega$; (*e*) $R = 427\ \Omega$; (*f*) $R = 720\ \Omega$; (*g*) $R = 1\cdot125$ kΩ; (*h*) $R = 2\cdot62$ kΩ; (*i*) $R = 6\cdot67$ kΩ

Actually the c.r.o. has an effective input impedance of 1 MΩ shunted by a capacitance $C_0 = 34$ pF (which includes the capacitance of the connectors used between the probe and the c.r.o.). For this reason the curves of Fig. 3 refer to a circuit similar to that of Fig. 1(*c*) with an effective capacitance C_e that is the sum of the probe and the c.r.o. capacitance (i.e. $C_e = C + C_0$).

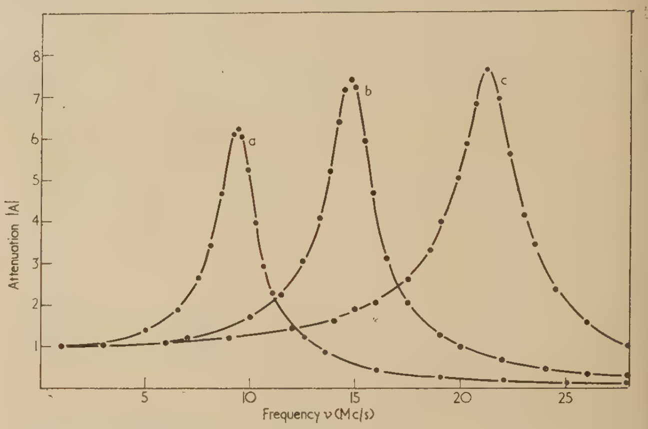

Fig. 4. Experimental attenuation curves of the probe (plus c.r.o. input) for three values of C_1

(*a*) $C_1 = 206$ pF; (*b*) $C_1 = 51$ pF; (*c*) $C_1 = 0$

Attenuation curves were also obtained (see Fig. 4) by connecting a known capacitor C_1, in parallel with the probe, in place of the resistor R. The resonant frequencies of these curves, using equation (4), are given by

$$2\pi\nu^* = (LC_e)^{-1/2},\ 2\pi\nu_1^* = \{L(C_e + C_1)\}^{-1/2},$$

and so they can be used to determine L and C_e and hence R_0. The value of r was determined by comparing the experimental and the calculated values of $|A|$ at resonance.

As the main source of error was the instability of the r.f. oscillator, the error in the measurement of the resonant frequency was less than 1%. This was confirmed by measuring ν_1^* for two values of C_1 (see Fig. 4), when it was found that the resulting two sets of values of L, C_e and R_0 agreed to within less than 1%. The determination of r is less accurate, because it involves absolute measurements of $|A|$. The error in r is $\lesssim 10\%$.

Using the curves of Fig. 4, the following values were found:

$$L = 1\cdot14\ \mu\text{H},\ C_e = 49\cdot5\ \text{pF},\ r = 21\ \Omega,$$
$$R_0 = 152\ \Omega,\ \nu^* = 21\cdot2\ \text{Mc/s}.$$

Calculated attenuation curves referring to these values of the parameters are shown in Fig. 5 together with experimental points, for three values of R. The deviations may be due to the fact that L, C_e, r and R are not rigorously independent of frequency (for d.c. $r = 9\ \Omega$) and at high frequencies the bandwidth limit of the c.r.o. (25 Mc/s) introduces some attenuation.

The resonant frequency of the probe has also been measured directly with the c.r.o. by shock-exciting the probe and, by adding a capacitor C_1 in parallel, ν_1^* was determined. These measurements are simpler but less precise than those described above. There is agreement (within the experimental errors) between the two types of measurement.

Conclusions

The measurements described in the previous paragraph show that the equivalent circuit of Fig. 1 and the corresponding frequency response equations (1) and (2) can be used to analyse the behaviour of the probe.

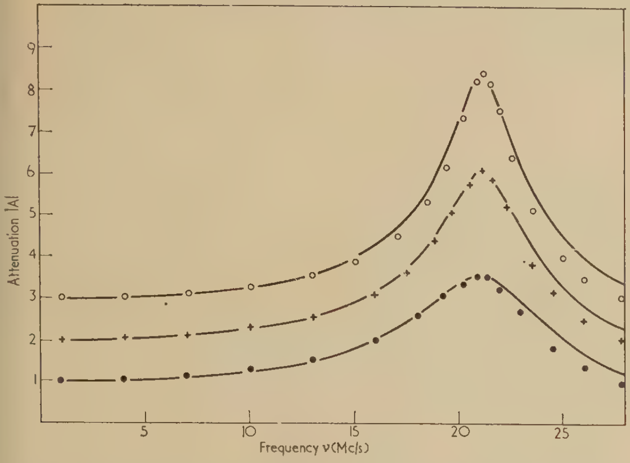

Fig. 5. Calculated attenuation curves (full lines) and experimental points (corresponding to the experimental curves of Fig. 3) for three values of R. The two upper curves have been displaced vertically for clarity

—○— $R = 6\cdot67$ kΩ
—+— $R = 2\cdot62$ kΩ
—●— $R = 1\cdot125$ kΩ

The parameters L, C_e and r determined above refer to the probe closed on the input impedance of the c.r.o. The corresponding parameters for the probe alone [Fig. 1(*a*)] are the following:

$$L = 1\cdot14\ \mu\text{H},\ C = C_e - C_0 = 15\cdot5\ \text{pF},\ r = 21\ \Omega,\ R_0 = 271\ \Omega,\ \nu^* = 37\cdot8\ \text{Mc/s}.$$

Attenuation curves calculated with these parameters, for different values of R, are shown in Fig. 6. (At the higher frequencies, of course, Fig. 6 is purely indicative because measurements to show the adequateness of the equivalent circuit have not been made above 30 Mc/s.)

With the probe described above it is obviously convenient to use a cable of 197 Ω impedance because for this value of R the condition given by equation (5) is realized and the attenuation curve is flat up to 20 Mc/s (to within 1%). Therefore the probe has a time resolution of the order of $0\cdot01\ \mu$s.

The phase shift $\phi(\omega)$ has been plotted for $R = 197\ \Omega$ [using equation (2)] and it was seen to be linear to a good approximation, as it should be for a faithful reproduction of the signal.

The bandwidth of the probe may be increased [provided the condition given by equation (5) is satisfied, so that the attenuation curve is flat], by increasing ν^*, i.e. by decreasing L and C. In practice it is difficult to reduce C beyond 10 pF and, if L is reduced, the signal produced at G (Fig. 1) becomes smaller, so that L has a lower limit corresponding to the minimum signal which is to be measured. The probe described above gives a signal (unintegrated) of 2 V, for $dB/dt = 1$ kG/μs.

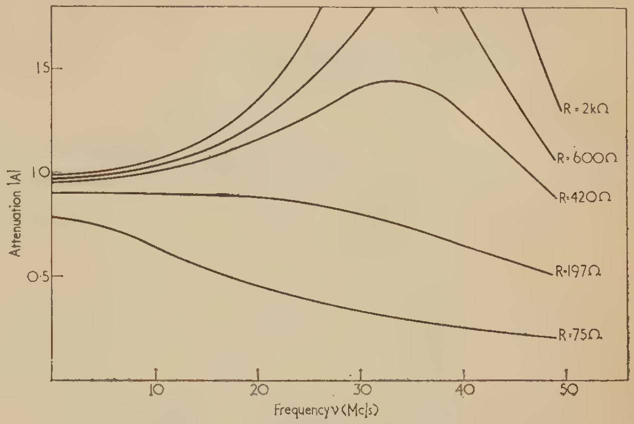

Fig. 6. Calculated attenuation curves of the probe referring to the circuit of Fig. 1(*c*)

The probes described in this paper were designed for use in fast transient discharges.⁽⁴⁾ They can also be used in stationary r.f. discharges⁽⁶⁾ at a fixed frequency. In this case one can use probes which are resonant at the applied frequency so that an amplification of the signal is obtained.

Acknowledgements

The authors wish to thank Dr. F. Magistrelli for constructing the probes used in the earlier part of this work, and Mr. L. Ricciardi, for his help in making the measurements. They also wish to thank Professor B. Brunelli for his interest and support.

References

(1) Lovberg, R. H. *Ann. Phys.* (*New York*), **8,** p. 311 (1959).

(2) Harding, G. N., Dellis, A. N., Gibson, A., Jones, B., Lees, D. J., McWhirter, R. W. P., Ramsden, S. A., and Ward, S. *Proc. 2nd Intl. Conf., Geneva*, 1958, Vol. 32, p. 365 (Geneva: United Nations, 1958).

(3) Burkhardt, L. C., Lovberg, R. H., and Phillips, J. A. *Nature* (*London*), **181**, p. 224 (1958).

(4) Allen, J. E., and Segre, S. E. *Proc. 4th Intl. Conf. on Ionization Phenomena in Gases, Uppsala*, 1959, Vol. II, p. 1073 (Amsterdam: North-Holland Publishing Co. Ltd., 1960).

(5) Smythe, W. R. *Static and Dynamic Electricity*, p. 415, n. 14 (New York: McGraw-Hill Book Co. Inc., 1939).

(6) Dippel, K. H., and Teckenburg, W. *Proc. 4th Intl. Conf. on Ionization Phenomena in Gases, Uppsala*, 1959, Vol. I, p. 533 (Amsterdam: North-Holland Publishing Co. Ltd., 1960).

Transistorized frequency stabilization for reflex klystrons used in magnetic resonance

by P. JUNG, Docteur en Sciences, European Research Associates, Brussels

[*Paper first received* 11 *April, and in final form* 10 *June*, 1960]

Abstract

The description of a fully transistorized frequency stabilizer for reflex klystrons is given. This is suitable for magnetic-resonance experiments and other microwave applications, where frequency stability is essential. In a typical case (klystron, type 2K25, *cavity* $Q = 3000$) *the effect of ripple and drift of the power supply is reduced by a factor of* 1000.

Introduction

A SIMPLE E.S.R. spectrometer can be improved by the addition of automatic frequency stabilization of the reflex klystron, thereby reducing both amplitude noise and ripple introduced by the reflector. Many different systems have been proposed.(1–5) This system is, in principle, not different from the one of Ref. 3, but it is fully transistorized and very versatile.

Principle of the stabilizer

The block diagram of the stabilizer is shown in Fig. 1. The reflector voltage of the klystron is amplitude-modulated at 50 kc/s. The resulting frequency modulation is transformed into an amplitude-modulated wave, the cavity acting as a frequency discriminator. The rectified signal at terminal I or II contains a 50 kc/s component which is proportional to the difference between the klystron frequency and the resonant frequencies of the cavity or the wavemeter respectively, provided that this difference is small. The 50 kc/s "error" signal is amplified, demodulated and fed back to the reflector, reducing the error signal by an amount of $1/G$, where G is the open loop gain of the system.

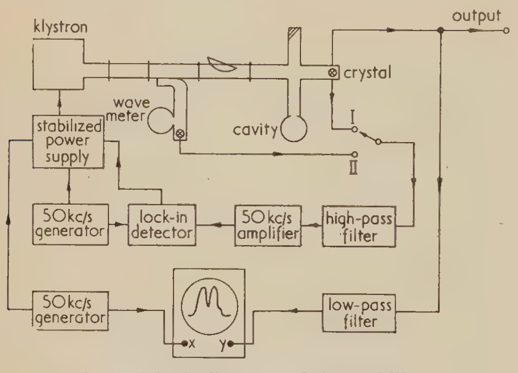

Fig. 1. Block diagram of the stabilizer

In order to achieve a quick-acting and accurate frequency correction, the gain-bandwidth product of the open-loop system should be high. It will be shown in the Appendix that, for a stable system, this product is given approximately by:

$$GB < \frac{\omega_m}{2\pi}$$

where G is the low frequency gain, B the bandwidth and ω_m the modulation angular frequency. By choosing a frequency of 50 kc/s and a gain of 1000, the bandwidth of the system is limited to 50 c/s.

Detailed description of the circuits

The circuits are fully transistorized. The circuit diagram is shown in Fig. 2. The reflector of the klystron is modulated by a 50 kc/s generator followed by a buffer amplifier. Transformer T_5 is a coupling transformer the secondary winding of which is in series with the reflector power supply. The high degree of insulation of this transformer makes the system very flexible.

The error signal is introduced by the crystal to the input of the signal amplifier. The latter is a four-stage broad-band amplifier. The output transistor delivers the power to the lock-in detector by means of an isolating transformer T_1. The reference signal is provided by T_2. Two separate secondary windings couple the buffer amplifier to the four switching transistors, type OC77 (by Mullard). The amplitude and phase of the reflector sweep voltage can be adjusted.

The four separate units are built in a single box. An internal shield suppresses any direct coupling between the

Transformer characteristics

	Mullard Ferroxcube	*Primary numbers of turns*	*Wire diameter (mm)*	*Second. numbers of turns, I*	*Wire diameter (mm)*	*Second. numbers of turns, II*	*Wire diameter (mm)*
T_1	E 907.36/3A I 740.09/3A	200	0·18	550	0·1	550	0·1
T_2	E 907.36/3A I 740.09/3A	280	0·18	100	0·18	100	0·18
L_3	EE 907.44/3A	225	0·1				
T_6	E 907.36/3A I 740.09/3A	280	0·18	140	0·18	140	0·18

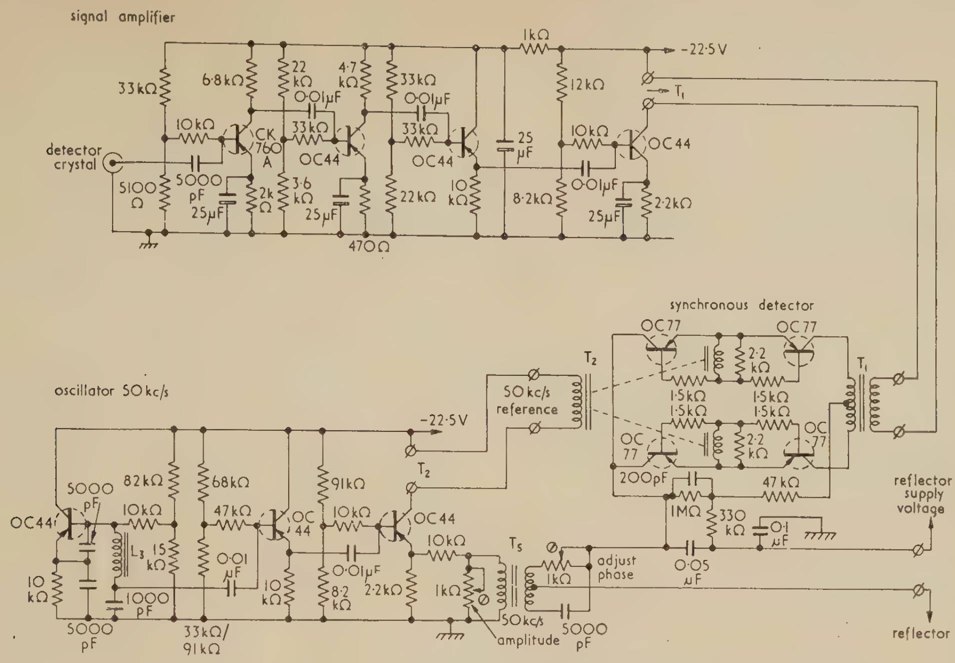
signal amplifier
1kΩ
-22·5V
33kΩ
6·8kΩ
22 kΩ
4·7 kΩ
33kΩ
0·01μF
0·01μF
12kΩ
T₁
10kΩ
CK 760 A
33kΩ
OC44
33kΩ
OC44
25 μF
10kΩ
OC44
detector crystal
5100 Ω
5000 pF
25μF
2k Ω
3·6 kΩ
25μF
22kΩ
10 kΩ
8·2kΩ
0·01μF
25μF
2·2kΩ
470Ω
synchronous detector
OC77
OC77
T₂
T₁
2·2 kΩ
1·5kΩ
1·5kΩ
1·5kΩ
1·5kΩ
OC 77
OC 77
2·2 kΩ
oscillator 50kc/s
50kc/s reference
-22·5V
T₂
200pF
47kΩ
1MΩ
330 kΩ
0·1 μF
reflector supply voltage
5000 pF
82kΩ
68kΩ
91kΩ
OC44
10kΩ
47kΩ
OC 44
10kΩ
OC44
L₃
15 kΩ
0·01 μF
10kΩ
T₅
adjust phase
1kΩ
0·05 μF
10 kΩ
1000 pF
10 kΩ
0·01μF
8·2 kΩ
2·2kΩ
1kΩ
50kc/s amplitude
5000 pF
reflector
5000 pF
33kΩ/ 91kΩ

Fig. 2. Circuit diagram of the stabilizer

signal generator and detector. The table gives the characteristics of the transformer used in this device.

The phase of the signal depends on the polarity of the crystal and on the kind of discriminator used (for example, transmission or reflexion cavity). A switch can be inserted at the primary of T_5 in order to invert the phase of the reference signal readily. It may be convenient to replace the batteries by a regulated power supply. The diagram of such a unit is given on Fig. 3. This unit can be built to the same dimensions as the 22·5 V, *B* battery (National Carbon 778 or equivalent). It delivers 20 mA with a ripple of 2·5 mV.

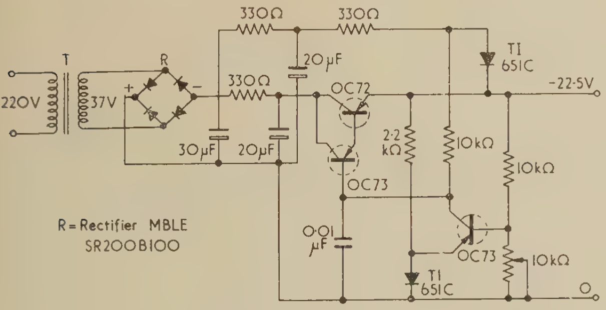
330Ω
330Ω
T
R
20μF
TI 651C
220V
37V
330Ω
OC72
-22·5V
30μF
20μF
2·2 kΩ
10kΩ
10kΩ
OC73
R = Rectifier MBLE SR200B100
0·01 μF
OC73
10kΩ
TI 651C

Fig. 3. Circuit diagram of stabilized power supply

The microwave components are first put into operation and the klystron mode-centred about the cavity, by means of a 50 c/s sweep signal. After the 50 c/s sweep has been reduced, the frequency stabilizer is put into operation. Its regulating range extends to ±10 V. The amplitude of the 50 kc/s sweep should be adjusted. It depends upon the Q of the cavity and the total gain needed. In any case, the sweep should be small, otherwise the microwave frequency spectrum is spread out.

Conclusion

A high-gain quick-acting stabilizer can be built by choosing a high-frequency sweep. As we were principally interested in eliminating ripple and microphonics, a d.c. gain of 1000 together with a 50 c/s bandwidth was convenient. A drawback of this system is the introduction of noise components centred at 50 kc/s into the low-frequency channel of the resonance signal. A higher sweep frequency improves this situation, as the noise of the crystal decreases with frequency. The amplitude of the sweep may be kept very small if the gain of the amplifier is increased. The noise of the input transistor will put a limit to the useful amplification.

Acknowledgement

The author takes this opportunity to express his thanks to the Union Carbide Corporation, New York, which sponsored this work.

Appendix

The stabilizer is a closed-loop system involving a modulation and demodulation process. It is thus necessary to smooth the carrier or modulation frequency so that the open-loop gain at this frequency is less than 1 which is generally achieved by an RC network producing a single time lag. This also assures the stability of the feedback system.(6) The frequency dependence of the gain can then be expressed by:

$$G(\omega) = \frac{G}{\left\{1 + \left(\frac{\omega}{\omega_c}\right)^2\right\}^{1/2}},$$

where ω_c is 2π times the cut-off frequency determined by

$\omega_c = 2, \pi B = 1/RC$. The requirement that $G(\omega_m) < 1$ applied to the above equation gives the relation:

$$GB < \frac{\omega_m}{2\pi},$$

provided that $G^2 \gg 1$.

References

(1) Pound, R. V. *Rev. Sci. Instrum.*, **17**, p. 490 (1946).

(2) Peter, M., and Strandberg, M. W. P. *Proc. I.R.E.*, **43**, p. 869 (1958).

(3) Varian Associates data sheet for E.P.R. Spectrometer V-4500.

(4) Bruin, F., and Van Ladensteyn, D. *Physica*, **25**, p. 1 (1959).

(5) Hirshon, J. M., and Fraenkel, G. K. *Rev. Sci. Instrum.*, **26**, p. 34 (1955).

(6) Nyquist, H. *Bell System Techn. J.*, **11**, p. 125 (1932)

Cyclic shearing interferometer

by P. HARIHARAN, Ph.D., A.Inst.P., and D. SEN, M.Sc., Ph.D., National Physical Laboratory of India, New Delhi, India

[*Paper received* 4 *February*, 1960]

Abstract

A wavefront shearing interferometer is described which can be conveniently used for routine tests of optical systems with relative apertures of f/6 *or less. The necessity of equalizing the two optical paths has been eliminated in this instrument, making it extremely easy to adjust and handle. At the same time, the shear can be continuously varied, so that zonal errors can be easily identified.*

Introduction

A major obstacle in the way of more general use of shearing interferometry in optical testing has been the lack of an interferometer in which the shear is continuously variable, and which, at the same time, is comparatively easy to adjust and handle. Thus, while the interferometer described by Drew$^{(1)}$ represents a considerable simplification over the original shearing interferometer of Bates,$^{(2)}$ it is still necessary to equalize the two optical paths to obtain fringes of high visibility. This adjustment is usually rather critical, since coherence conditions dictate the use of a narrow slit for through-type testing and, consequently, a bright source such as a high-pressure mercury arc, which normally has relatively broad lines. The present paper shows how, within certain limitations, this difficulty can be avoided by the use of a simple cyclic shearing system.

Optical system

The optical system of the instrument is shown schematically in Fig. 1. The basic interferometer consists of a plane-parallel plate M_0, with a semi-reflecting coating on one face, and three plane mirrors. Any ray incident on M_0 from the right is divided into two rays, which traverse the path M_0, M_1, M_2, M_3, M_0, in opposite directions before they are recombined at M_0 and emerge on the left. Since both these rays traverse very nearly the same path in this interferometer, the path difference between them is always very small, eliminating the necessity for any path length adjustment. Further, in an interferometer of this type, while it is possible to introduce a tilt between two such rays in the horizontal plane (i.e. the plane of the figure) by rotating any one of the mirrors, it is not possible to introduce tilt between them in the vertical plane. In this plane it is only possible to introduce a lateral separation between them. This is reduced to zero when all the four mirrors are parallel to one another in the vertical plane.

In order to use this interferometer as a shearing interferometer, the convergent beam from the system under test is allowed to fall on M_0 and the instrument is initially adjusted so that the two cones of rays, which are formed by division of the incident beam at M_0, are brought to a focus at the same point P on the surface of M_2. If the mirrors are set so that there is no tilt between the rays, the two cones emerging from the interferometer will overlap exactly, so that the whole field presents a uniform interference colour. However, if M_2 is rotated by an angle θ about a vertical axis passing through P, the two cones emerging from the interferometer will be rotated in opposite directions by an angle 2θ about this point, as shown by the dotted lines in Fig. 1. An eye placed at O will then see two displaced images of the system under test, sheared through an angle 4θ in the horizontal plane. For an incident cone of angular aperture η, there will be an overlap region of angular aperture $(\eta - 4\theta)$ in this plane in which interference will occur. As can be seen from Fig. 1, if the axis of rotation of M_2 passes exactly through the foci of the two cones, and if one assumes the beam-dividing plate M_0 to be of zero thickness, such a rotation of M_2 will not introduce a path difference between interfering pairs of rays in the two cones.

Residual aberrations

Since the two sheared cones traverse the beam-dividing plate M_0, which has to be of finite thickness, at slightly different angles, residual deviations are introduced in the interference pattern. However, since the difference in the angles of incidence of the two cones in this interferometer is only half what it is in the Bates interferometer for the same shear, the residual aberrations are much smaller. Numerical calculations of the residual aberrations, according to the procedure given by Bates in the appendix to his paper,$^{(2)}$

show that with cones of moderately large angular aperture, the residual aberrations can be made negligibly small in this interferometer merely by reducing the angle of incidence of the rays on the beam divider.

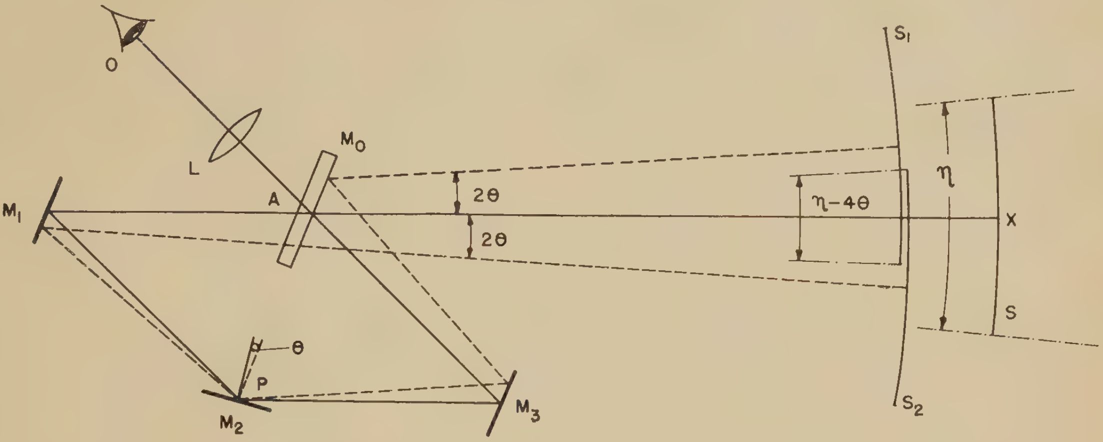

Fig. 1. Schematic diagram of the interferometer

M_0, semi-reflecting plate; M_1, M_2, M_3, plane mirrors; L, field lens; S, spherical wavefront from system under test; S_1, S_2, sheared images of the incident wavefront

Thus, when the angle of incidence of the principal ray on the beam divider is equal to 15°, the residual astigmatism (which is the principal residual aberration), for an $f/6$ cone, sheared edge over centre, is only $0{\cdot}03\,\lambda$ for a 3 mm thick beam-dividing plate, while the corresponding figure for the primary coma is only of the order of $0{\cdot}002\,\lambda$. Measurements made with this interferometer, under these conditions, should therefore be quite reliable.

The residual path difference which is introduced between the two beams under the same conditions is less than $20\,\lambda$. Even with a source such as a high-pressure mercury vapour lamp, this should not result in any appreciable decrease in the visibility of the fringes.

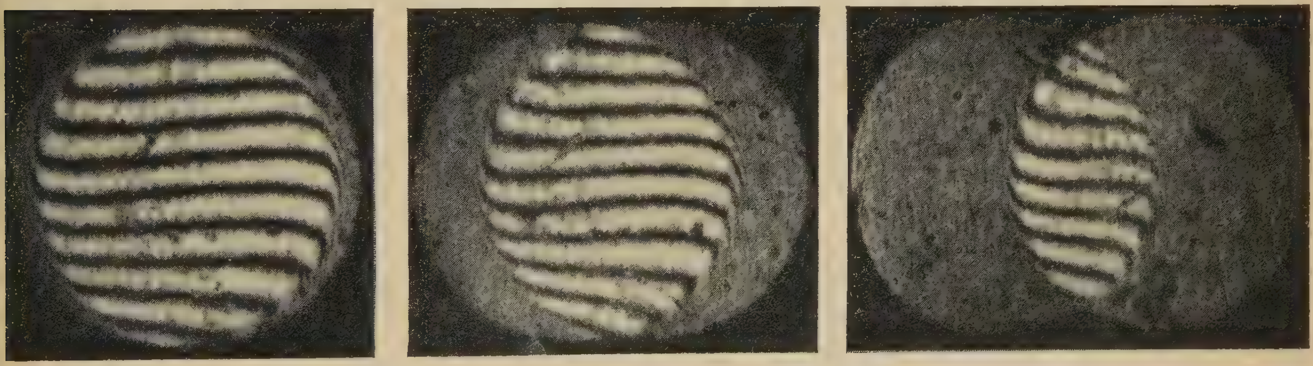

Fig. 2. Typical interferograms of a partly figured $f/8$ lens obtained with the cyclic shearing interferometer at three different settings of the shear control

Adjustment and operation

For maximum convenience in use, the entire interferometer, which can be made quite compact, is mounted on a slide on an optical bench so that the axis XA coincides with the axis of the system which is being tested. Construction is simplified by providing only the mirror M_1 with controls for tilt about horizontal and vertical axes as well as for movement through a short distance. The mirror M_2 should have provision for rotation about a vertical axis (the shear control) while M_0 and M_1 need only be provided with rough, screwdriver adjustments.

The initial adjustment of the interferometer is best carried out in two steps. Using a fairly wide slit source, the mirrors are first adjusted so that the paths of the two beams traversing the interferometer in opposite directions coincide with each other as far as possible, and the two images of the slit source formed by the system under test on the ursface of M_2 coincide with one another and with the axis of rotation of M_2. After this, the fringes formed in diffuse light in the interferometer are observed, and final adjustments of M_1 about a horizontal axis and M_2 about a vertical axis are made until the zero-order fringe fills the whole field. The instrument is then adjusted for zero shear. After removing the diffuser, the images can be sheared as required by tilting M_2 about a vertical axis. Horizontal fringes can be introduced in the field by tilting M_1 slightly about a horizontal axis, so that the two images of the source formed on M_2 are separated by a small distance in the vertical plane.

If the foci of the two cones do not coincide exactly with the surface of M_2, vertical fringes may appear in the field as the shear control is operated. These can usually be eliminated by moving the slide bearing the interferometer nearer to or farther away from the system under test.

Typical interferograms of a partly figured $f/8$ lens obtained with this interferometer at three settings of the shear control, using a high-pressure mercury vapour lamp and a Wratten 77A filter, are shown in Fig. 2. The turned-down edge is clearly evident in all the three interferograms.

Acknowledgements

The authors wish to thank the Director, National Physical Laboratory of India, for permission to publish this paper.

References

(1) Drew, R. L. *Proc. Phys. Soc.* (*London*), *B*, **64**, p. 1005 (1951).
(2) Bates, W. J. *Proc. Phys. Soc.* (*London*), **59**, p. 940 (1947).

Automatic range-changing of a linear ratemeter

by S. LOVETT, A.R.I.C., Microbiological Research Establishment, Porton, nr. Salisbury, Wiltshire

[*Paper first received* 15 *February, and in final form* 10 *May*, 1960]

Abstract

A circuit is described which automatically changes the range of a linear ratemeter as the count rate from a flow Geiger counter increases or decreases. The counter voltage is switched off when the count rate exceeds the maximum that the counter is designed to accept and is switched on at intervals to sample the count rate and remains on when the rate has diminished to an acceptable level.

Introduction

A study of the phosphorus metabolism of bacteria using radioactive phosphorus as a tracer involved the fractionation of the compounds containing the radioactive phosphorus on an ion-exchange resin column and recording the radioactivity of the effluent with a flow Geiger counter.* The count rate was recorded on a chart recorder operated from a linear ratemeter. The variation of the count rate in the column effluent was considerable, and some fractions had peak count rates of 5–10 counts per second above background while others, in particular the fraction containing unmetabolized orthophosphate, reached rates of up to and greater than 3000 counts per second. Since it was not practicable to remove orthophosphate and since a fractionation may carry on for 36 h it was essential to have an automatic system to alter the range switch of the ratemeter as the count rate changed. Further, the apparatus must switch off the high voltage to the Geiger counter when the count rate exceeded the maximum that the counter was designed to accept. A logarithmic ratemeter could be used to record the widely varying count rates but a linear ratemeter possesses the advantages of being considerably cheaper and is more accurate.

Circuit

The circuit was designed for use with an A.E.R.E. linear ratemeter, type 1037, or with the commercial equivalent. However, the principle could be adapted to operate with other types of ratemeter. The principle of operation of the circuit is as follows. A chart recorder which has movable upper and lower contacts is used or such contacts are fitted to a recorder or to the meter which displays the count rate. Normally the upper contact is positioned to operate at a full-scale reading of the recorder and the lower contact is set at a position less than one-tenth full scale. When either of these contacts are closed, a circuit is completed which operates the appropriate coil of a bi-directional stepping switch. Two banks of the stepping switch are connected to the banks of the range-changing switch in the ratemeter. The operation of the stepping switch can be confined to preselected ranges and at the upper limit the high-voltage supply to the Geiger counter is switched off and a time interval, determined by a synchronous motor, elapses and the counter voltage is again switched on. If the count rate has decreased to a suitable level the voltage remains switched on but if the rate is still too high the voltage is again switched off and the cycle is repeated.

The circuit diagram of the range-changer is shown in Fig. 1. After switching on the apparatus, the stepping switch is reset to the starting position *RMA* 1.1 by depressing SW_2. When in this position, $D/1$ is energized and contacts D_1 open and prevent the closure of the lower recorder contacts RC_1 operating the circuit which moves the stepping switch in an anti-clockwise manner to the unconnected position 11 on *RMA* 1–5. When the count rate increases and the upper recorder contact RC_2 closes, $B/3$ is energized. Contacts B_1 change over and C_3 is discharged through *RMB*11/5 and the stepping switch is moved to position 2. $B/3$ remains energized through B_2, HWSB1, earth and the heater of the hot wire switch HWSB/1 is supplied through B_3. When HWSB1 open, $B/3$ relaxes and C_3 is recharged through R_4 and R_5. The resistor R_5 is inserted to reduce sparking at B_1 at the moment of discharge of C_3. R_6 allows C_3 to discharge on switching off the apparatus. Further closing of RC_2 moves the stepping switch on to positions 3 or 4 as determined by the position of SW_4. When $E/4$ is energized

---

* To be published.

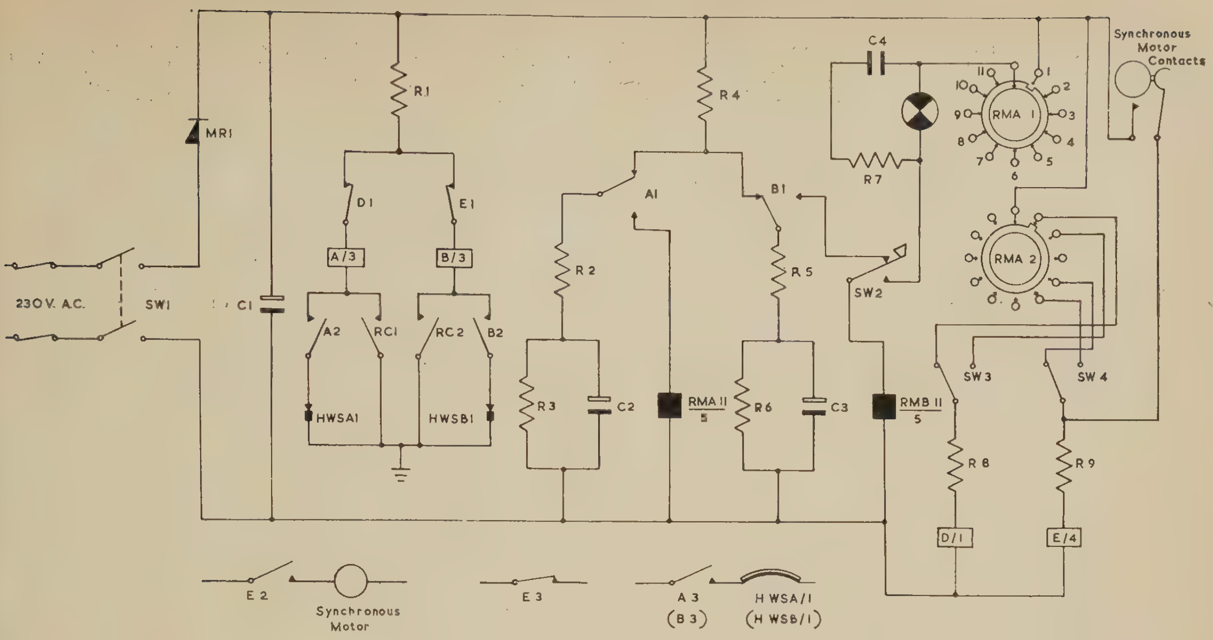
230 V. A.C.
SW1
MR1
C1
R1
D1
E1
A/3
B/3
A2
RC1
RC2
B2
HWSA1
HWSB1
R4
A1
B1
R2
R3
C2
RMA 11/5
R5
R6
C3
SW2
RMB 11/5
C4
R7
RMA 1
RMA 2
Synchronous Motor Contacts
SW3
SW4
R8
R9
D/1
E/4
E2
Synchronous Motor
E3
A3
(B3)
HWSA/1
(HWSB/1)

Fig. 1. Circuit diagram of range-changer

$R_1 = 22\ \text{k}\Omega$
$R_2, R_5 = 100\ \Omega$
$R_3, R_6 = 120\ \text{k}\Omega$
$R_4 = 2{\cdot}2\ \text{k}\Omega$
$R_7 = 470\ \Omega$
R_8, R_9 depend on the coil rating of $D/1$ and $E/4$

$C_1 = 8\ \mu\text{F}$
$C_2, C_3 = 50\ \mu\text{F}$
$C_4 = 1{\cdot}0\ \mu\text{F}$
MR_1 = Sentercel, C57

A/3 and *B*/3 are relays having operating currents appropriate to the recorder contacts
D/1 and *E*/4 are suitable P.O., type 3000 relays
*RMA*11/5 and *RMB*11/5 are the coils of a Ledex bi-directional stepping switch having four standard, eleven-position, single-pole wafer sections and one control section with commutating switch (by N.S.F. Ltd., London)
HWSA/1 and *HWSB*/1 are time delay switches, type *TYEM* (by Sunvic Controls Ltd., Harlow, Essex)

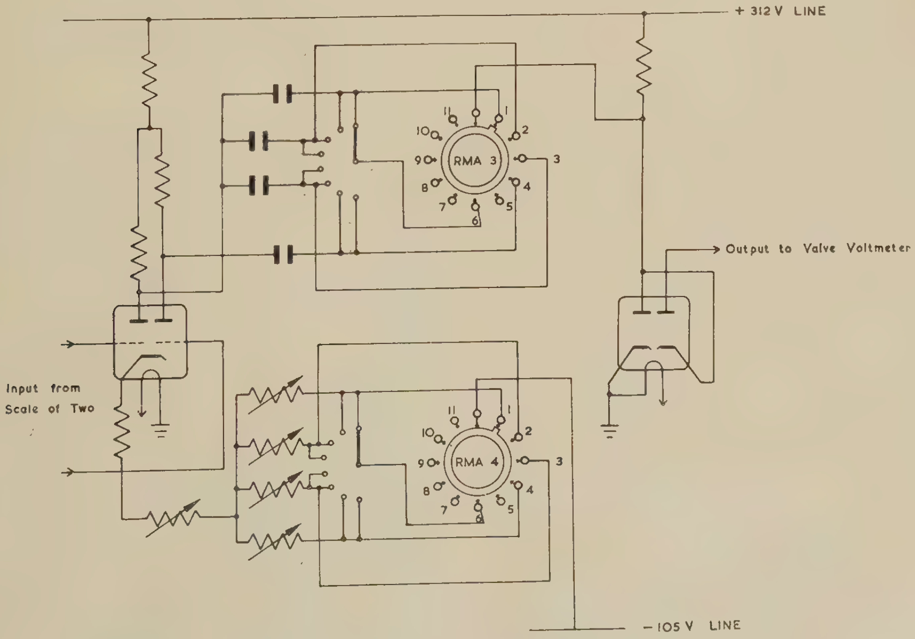
+ 312 V LINE
RMA 3
Output to Valve Voltmeter
Input from Scale of Two
RMA 4
− 105 V LINE

Fig. 2. The limiter and diode pump section of the type 1037 ratemeter

through SW_4, E_1 open and prevent further operation of $B/3$, the synchronous motor is switched on through E_2 and the high-voltage supply to the counter is interrupted by E_3. These contacts are connected in series with the switch controlling the h.t. unit in the ratemeter. Contacts E_4 are connected to a warning light. The contacts on the synchronous motor break soon after the motor begins to turn and $E/4$ remains energized when the recorder reaches the lower contact RC_1 and moves the stepping switch on to a lower position. As the recorder will now remain on the lower contact, $A/3$ remains energized and further movements of the stepping switch do not occur. When the synchronous motor completes a revolution and the cam-operated contacts open, $E/4$ relaxes thus stopping the motor and switching on thecounter voltage. The recorder will again record the count rate and if this is sufficiently high, RC_2 will close and the cycle will be repeated.

Practical notes

When recording the count rate of the effluent of the ion-exchange resin column, integrating time constants of 20 s or longer were used and the hot-wire switches were set to operate after 10 s. This delay period was necessary because the recorder pen frequently bounced against the contacts owing to the random changes in count rate, and caused the stepping switch to move several positions. The period of revolution of the synchronous motor found to be most suitable was 5 or 10 min. These values for the hot-wire switch delay and the synchronous motor period were adequate for rates of change of count rate up to 300 counts per second in 5 min.

The stepping switch was mounted on the ratemeter chassis to keep the leads from the limiter section of the ratemeter as short as possible and the necessary connexions to the rest of the circuit of the range-changer, which was built on a separate chassis, were made using a suitable multi-way plug and socket. The ranges of the ratemeter were trimmed in the usual way using the variable resistors provided. The operation of the stepping switch caused no interference with the ratemeter. Fig. 2 shows how banks 3 and 4 of the stepping switch are connected to the ratemeter range-changing switch. The wipers of the ratemeter switch are connected to position 6 on the two stepping switch banks and an extra resetting switch can be inserted to reset the stepping switch to this position and allow the ratemeter to be used without the automatic range-changer. Selection of the ×3 and ×10 ranges of the ratemeter is carried out with the ratemeter range switch. Positions 1–4 on bank 5 of the stepping switch are connected to neon indicator lamps to indicate the range being used.

Production of a pulsed magnetic field using an electrolytic capacitor bank

by D. G. BATE, B.Sc.(Eng.), and R. F. SAXE, Ph.D., Queen Mary College, University of London

[*Paper first received* 13 *April, and in final form* 2 *June*, 1960]

Abstract

An economical system for obtaining magnetic fields of the order of 10^4 *G lasting for times of the order of milliseconds is described. A switch is operated by a falling mercury column and performs two switching operations separated by an adjustable, repeatable delay of a few milliseconds. Currents of the order of* 10^4 *A flow through the switch during operation. The source of stored energy is a capacitor bank of large capacitance and low voltage, and this is discharged through a solenoid by means of the switch.*

Introduction

The work to be described here was carried out as part of a research project on plasma physics. It was required to produce magnetic fields of up to 20 kG, over a cylindrical volume approximately 30 cm long by 6 cm in diameter, as economically as possible. A further condition set by the nature of the projected experiments was that, if a pulsed method was to be used, the pulse length should be of at least a few milliseconds duration.

Although most convenient experimentally, a continuous d.c. field was ruled out not only by the cost of the required motor generator set, but also by the additional cost and complexity of the cooling system necessitated by the high rate of heat dissipation in the magnet coil. The use of a bank of heavy-duty batteries for short duration d.c. working at first seemed attractive, but the disadvantages here are the large storage space needed, the cost of a circuit breaker capable of breaking the high currents involved and the problem of the removal of acid fumes produced during recharging.

Turning to pulsed methods, and in particular to those which involve the discharge of a capacitor bank through the magnet coil, the problem is one of choosing the best type of capacitor for the purpose. It is found that a bank of electrolytic capacitors working at 500 V is to be preferred to another economically possible system using "uncanned" paper insulated capacitors working at, say, 10 kV. The two systems are comparable in terms of energy storage per unit cost and per unit volume. However, for a pulse rise time of a few milliseconds duration, a high capacitance is required and further consideration of insulation and charging problems leads to the choice of the low-voltage system.

Basic design

The basic design, achieved by reference to Champion,(1) is as follows.

Capacitor bank. This consists of one hundred units, each having a nominal capacitance of 400 μF (-20%, $+50\%$ tolerance) and a working voltage of 500 V d.c. The measured capacitance for parallel connexion is 0·058 F, giving a maximum energy storage of 7·25 kilo-joules in a space of 80 × 80 × 20 cm. According to information received from the capacitor manufacturers, a small series protection resistor is required for each capacitor unit to prevent random breakdowns occurring in large parallel banks of this type, and consequently 0·5 Ω of resistance wire is connected in series with each capacitor. The charging equipment is capable of supplying 250 mA at 600 V.

Magnet coil. The coil consists of sixty turns of 1 × 0·5 cm, high-conductivity, rectangular copper bar wound "on edge". The turns are separated by a 1 mm gap which is filled with an epoxy resin, acting both as an insulant and as a bonding agent to hold the coil rigid. To obtain a good bonding between the resin and the metal the coil was initially silver-plated. Great strength is not required, however, as the electromechanical forces set up can be shown to be small.(2) The principal coil parameters are as follows:

Total capacitance	0·058 F
Working voltage	500 V
Maximum energy storage	7·25 k-joules
Coil inside diameter	7 cm
Coil length	36 cm
Coil inductance	43·5 μH
Coil resistance	$5 \times 10^{-3}\ \Omega$
Total circuit resistance	$10^{-2}\ \Omega$

Circuit. Connexion is made between capacitor bank, coil and switch (see later) by high-conductivity copper bar 0·65 × 1·9 cm giving a total resistance of $10^{-2}\ \Omega$, half of which is due to the resistors associated with the individual capacitors. The natural period of oscillation of the circuit is 10 ms. The peak current is 12·5 kA, producing a peak magnetic field of 23 kG. The magnetic field is 62% of the value calculated for a circuit having zero resistance and a coil of infinite length.

Switching requirements

The main problem involved in the development of this system is that of switching. The discharging switch must carry the peak current of some 10^4 A and this fact, together with the low operating voltage, excludes the use of electronic switching if the cost of the apparatus is to be kept at a low figure. Further, since electrolytic capacitors can be easily destroyed by the application of a voltage of the wrong polarity, it is necessary to protect them against reversed voltage, and a second switch is thus required for "crowbarring". This is illustrated in Figs. 1 and 2. Ideally, the crowbar switch closes at a time one-quarter cycle later than the time at which the discharge switch closes, i.e. when the current has reached its maximum value. If one considers the simple circuit shown in Fig. 1, then, for this condition, the waveform of the current will be as indicated (Fig. 2, curve *a*). This waveform will vary with the crowbarring time and Fig. 2 gives two other possible conditions; when the crowbar switch closes early, curve (*b*), and late, curve (*c*). After crowbarring the current decays exponentially with a time constant $L/(R_1 + R_2)$.

It should be noted, however, that the circuit will not be the simple one of Fig. 1, Fig. 3 showing a more practical representation. The pulse length is considerably increased by the use of the crowbar switch, provided that $(R_1 + R_2)$ is sufficiently small. An electronic switch is again impracticable since the crowbar switch is required to operate at zero voltage and must also carry the peak current.

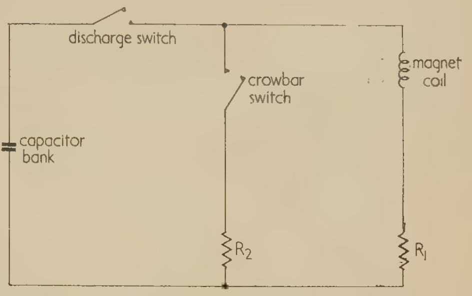

Fig. 1. Simplified circuit for capacitor bank, magnet coil and switch

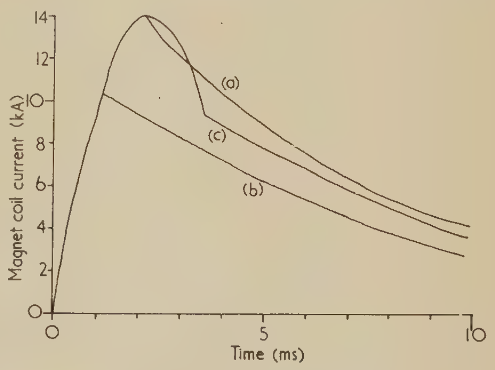

Fig. 2. Current pulses illustrating (*a*) ideal, (*b*) early and (*c*) late crowbarring

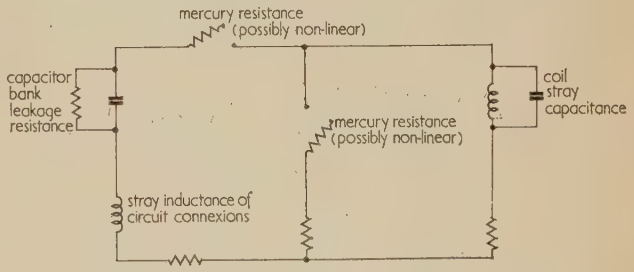
mercury resistance (possibly non-linear)
capacitor bank leakage resistance
coil stray capacitance
mercury resistance (possibly non-linear)
stray inductance of circuit connexions

Fig. 3. Practical circuit for capacitor bank, magnet coil and switch

It was decided that two mechanical switches should be used, the main considerations being that their closing actions should be free from "bounce" and that there should be an accurately controllable delay of a few milliseconds between their closing times.

Mercury crowbar switch

The principle of switching is illustrated in the schematic diagram (Fig. 4). A column of mercury is accelerated to a velocity of approximately 1500 cm/s, and then makes contact with electrodes *A*, *B* and *C* in turn. When the electrodes *A* and *B* are connected by the mercury column the capacitor bank starts to discharge through the coil. At a later time, the mercury reaches electrode *C* and the circuit is crowbarred, the delay depending on the distance *x* (see Fig. 4). For successful operation the mercury column must be prevented from breaking up and its final velocity must be reproducible. If the mercury is accelerated only by gravity, any irregularity in its release will persist down to the electrodes and may cause the switch to break and remake a number of times. In practice, the acceleration is achieved by a combination of gravity and gas pressure. A quantity of mercury, with a slide-fitting plunger floating on top, is initially supported between two diaphragms. An impulsive pressure of gas, released by the rupture of the upper diaphragm, breaks the lower diaphragm and accelerates the mercury down a tube. This ensures that the mercury will reach the electrodes as a solid column and with a uniform front. The electrode geometry is such as to give mainly tangential contact with the mercury and so reduce bounce as much as possible. If the mercury rebounds from a surface a thread of liquid is most probably drawn out and electrical contact is not entirely lost.

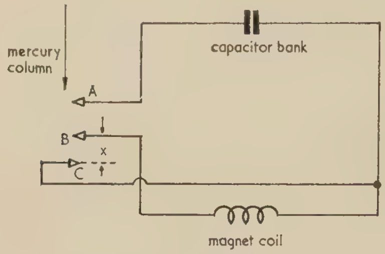

Fig. 4. Schematic illustration of the mercury switch principle of operation

Fig. 5 shows the construction of the switch. The metal parts which are periodically in contact with the mercury are made of brass, protected from corrosion by a thick deposit of nickel (applied by the Kanigen plating process) and an overall deposit of $0{\cdot}0002_5$ cm rhodium. The upper and lower diaphragms are made of cellophane of thickness 0·0025 cm and melinex of thickness 0·000 65 cm respectively, the former being ruptured mechanically to release nitrogen at 25 lb/in.^{2} from a cylinder. On being released, the mercury passes down a 5 ft length of Perspex tubing of $\frac{7}{8}$ in. inside diameter, reaching electrodes *A* and *B* at the bottom. These consist of brass disks each with a $\frac{3}{4}$ in. diameter central hole through which the mercury falls. This slight reduction in the internal diameter of the system serves to ensure a good contact and also to arrest the fall of the steel plunger, preventing it from damaging the third electrode *C*. This latter is cone-shaped and its position relative to electrode *B* may be adjusted by means of a fine screw thread. When the plunger has come to rest, the gas pressure is released *via* the upper side tube which, together with the lower side tube, also allows the air initially in the system to be pushed out ahead of the mercury. These two outlets are arranged to prevent the egress of mercury vapour.

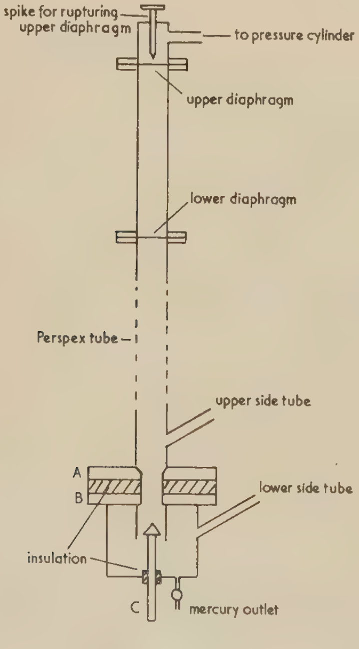

Fig. 5. Mercury switch construction

Operation of the equipment

In testing the equipment, oscillograms of the magnet coil current, of the coil voltage and of the magnetic field strength are recorded. The current is measured by means of a small non-inductive resistor and the magnetic field strength by a small electrostatically shielded search coil. Fig. 6 [curve (*a*)] shows the trace obtained for the current under conditions where the crowbar has been applied slightly late. If this is compared with the corresponding curve in Fig. 2 it may be seen that the behaviour of the system differs from that predicted from the simple circuit. No sudden change of slope can be observed at the crowbar point, indicating that the crowbar probably does not act as a perfect switch (with an infinitely short closing time). This is in agreement with published work on most other crowbarred systems, where switching has been by means of an ignitron. (For example, see Spitzer$^{(3)}$).

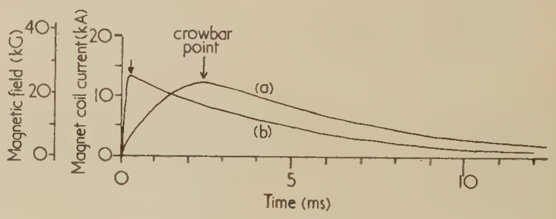

Fig. 6. (See text)

The experiments for which the pulsed magnetic field system has been designed involve the use of r.f. electric fields in the megacycle frequency range. Both the rise and decay of the magnetic field pulse are, therefore, sufficiently slow to allow the required measurements to be made. The pulse shape which could be obtained from a high-voltage, low-capacitance bank of similar energy storage is shown in curve (*b*), Fig. 6. The rise time here is too fast for this application and only the decay could be utilized.

Conclusion

The combination of an electrolytic capacitor bank and the mercury crowbar switch has been shown to be an economical means of producing a pulsed magnetic field. After a large number of operations, no capacitor breakdown has occurred. The switch performs reliably and reproducibly.

Acknowledgements

One of us (D. G. B.) wishes to thank the Department of Scientific and Industrial Research for the award of a Research Studentship, during the tenure of which this work was performed.

Both authors wish to thank the Atomic Energy Research Establishment for their interest in this work and for a grant for the purchase of equipment.

References

(1) Champion, K. S. W. *Proc. Phys. Soc.* (*London*), *B*, **63**, p. 795 (1950).
(2) Cockcroft, J. D. *Trans Roy. Soc.*, **227**, p. 317 (1928).
(3) Spitzer, L. *Proceedings of the Second Geneva Conference on the Peaceful Uses of Atomic Energy*, **32**, p. 181 (Geneva: United Nations Organization, 1958).

Transformer bridges for use with resistance strain gauges and similar transducers

by L. N. CLARKE, M.I.Mech.E., B.Eng.Sc., A.M.I.E.E., Division of Forest Products, Commonwealth Scientific and Industrial Research Organization, Melbourne, Australia

[*Paper received* 17 *May*, 1960]

Abstract

A method of balancing a.c. bridges having transformer ratio arms is described which is particularly suitable for use with resistance transducers such as electrical-resistance strain gauges. The long-time stability and accuracy of reading can be readily made better than required for most static testing by the use of an auxiliary transformer. The bridge can be combined with a commercial potentiometric recorder to form a multi-channel self-balancing a.c. bridge which can provide different ranges on successive channels. The balancing system lends itself to the control of testing machines, especially for the production of a given time-pattern of load or strain. The use of other types of transducers is considered.

Introduction

Although the basic principle of operation and some of the advantages of a.c. bridges having tightly coupled inductive or transformer ratio arms have been known for many years, it is only in the last ten years or so that the possibilities of such bridges have been exploited to any extent. Clark and Vanderlyn$^{(1)}$ made use of the ability of this type of bridge to reject shunt admittances to a third point for measuring components *in situ*. Thompson$^{(2)}$ and others have used this property along with the long-term stability and accuracy of ratio for the precise measurement of three-terminal capacitors.

In all these bridges an unknown impedance is measured in terms of a known and similar impedance. The bridge balance may be obtained by means of a variable known impedance and a fixed ratio, a variable ratio and a fixed standard, or a combination of the two. There is a very favourable application of transformer ratio arms with transducers such as resistance strain gauges which usually involves the provision of a similar gauge as the fourth arm of the bridge. This is necessary to compensate for temperature changes and in the case of measurements on hygroscopic materials for dimensional changes produced by moisture movement. Also it is often advantageous to use two transducers in a differential arrangement, for example, two strain gauges to measure bending, shear, or torsion. In none of these cases is there a place for a variable arm.

The most common method of balancing these bridges is shown in Fig. 1. There are two main disadvantages of this circuit. The resistor Y shunts one or other of the gauges to a variable extent and hence alters the effective "gauge factor" of the transducers. This is more serious as the measuring range is increased; a range of ±5% would involve a change of 5% in gauge factor at the ends of the range. Also the range of the bridge, for a given value of Y, depends on the resistance of the gauges.

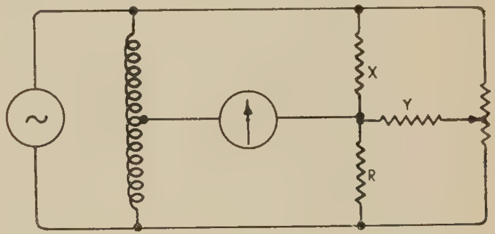

Fig. 1. A common method of balancing resistance strain-gauge bridges. X and R are the transducer elements

Both these disadvantages can be overcome by the use of a variable ratio as shown in Fig. 2. It is shown in the next section that, near unity ratio, the change in position of the tapping point to restore balance bears a simple relation to the fractional change in resistance of X or R.

The basic requirements for a strain-gauge bridge for static testing are usually long-term stability, a measuring range of up to ±5% about a unity ratio and a subdivision of ratio to about 2 in 10^6. Accuracy of measurement of ratio is usually

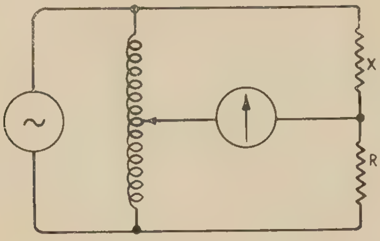

Fig. 2. Simple variable ratio transformer bridge

not required to better than 1 in 10^3 but a change in ratio of 0·1% or greater should be measurable to about 1%. A long-term stability of the order of 1 in 10^6 is often desirable.

Variable-ratio method of balancing a transformer bridge

Moving the tapping point along the turns of the transformer to balance the bridge, as shown in Fig. 2, is not usually a practical proposition if a reasonable degree of subdivision is required. If it is desired to read to 2 in 10^6 then the coil would require 2×10^6 turns. The simplest way of getting greater subdivision is to connect a resistive divider between two taps on the transformer as shown in Fig. 3. In some cases it may be desirable to use a separate winding to supply the divider as shown in Fig. 4. If this is done, the bridge can then be used with transducers which incorporate a full four-arm bridge, as shown in Fig. 5.

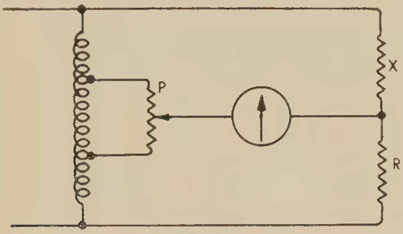

Fig. 3. Variable ratio obtained by the use of a resistive divider

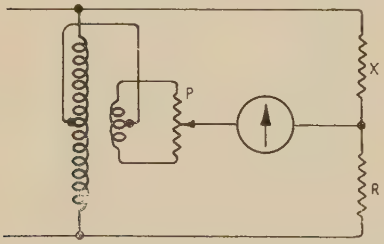

Fig. 4. The use of a separate winding to feed the divider

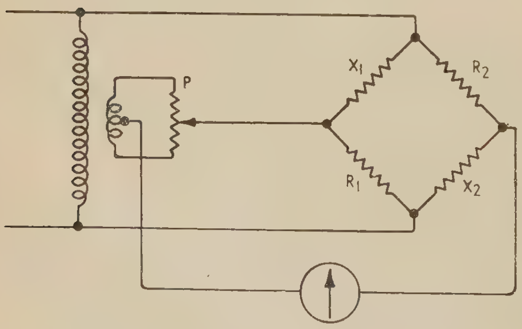

Fig. 5. A bridge for use with four active transducer elements

Although the use of a separate winding instead of tappings on the main ratio arms will introduce a small error in the measurement of ratio, this will not normally be a problem in transducer bridges, because direct measurement of ratio is not usually required. The fact that subsequent discussion refers exclusively to the use of tappings does not imply that there is normally any disadvantage in the use of a separate winding as far as transducer bridges are concerned.

For the bridge of Fig. 3 it can be shown that, if the bridge supply voltage is e, then the voltage change δv at the moving arm of P necessary to restore the balance when X is changed by δX is given by:

$$\frac{\delta v}{e} = \frac{R\delta X}{(X+R)(X+R+\delta X)}.$$

If $R = X$ then:

$$\frac{\delta v}{e} = \frac{\delta X}{2(2X+\delta X)}$$

$$\simeq \frac{\delta X}{4X}.$$

The percentage error involved in the approximation $\delta v/e = \frac{1}{4}\delta X/X$ is half the percentage change in resistance and hence a correction can easily be made if required. Even if R and X initially differ by 5%, the error in the approximation is not greatly affected. If both R and X are changed simultaneously by amounts $-\delta R$ and $+\delta X$ then

$$\frac{\delta v}{e} = \frac{(R\delta X + X\delta R)}{(R+X)(R+X-\delta R+\delta X)},$$

and if $\delta R/R = \delta X/X$, then:

$$\frac{\delta v}{e} = \frac{2R\delta X}{(R+X)(R+X-\delta R+\delta X)}.$$

If $R = X$ then $\delta v/e = \frac{1}{2}\delta X/X$ exactly. For the bridge of Fig. 5 with four equal active elements, $\delta v/e = \delta X/X$. There is no shunting of the transducer elements and the range is independent of the transducer resistance.

One great advantage of this type of bridge is that the requirements for accuracy and stability imposed on the two main parts, the ratio arms and the variable ratio device, can be easily met. An accuracy of 1 in 10^5 and a stability of 1 in 10^6 can be readily obtained with unity-ratio transformers. The performance required of the variable-ratio device depends on the range required, for example, to accommodate a change of ratio of 1% and to measure the ratio to 1 in 10^6 this system would require an accuracy and stability of 1 in 10^4, which is readily attainable with the circuit of Fig. 3 if the element P is an inductive or other stable divider.

The variable-ratio device can be fed from a separate transformer connected across the bridge supply although it is not usually economical to do so. If for some reason the impedance of P is considerably greater than that of X and R, it may be desirable to place P directly across the bridge supply and feed the output from P to a precision cathode follower and then through a suitable step-down transformer.(3)

Development of basic circuit

(*a*) The basic circuit of Fig. 3 can be used as a simple but effective bridge especially if P is a multi-turn helical potentiometer. The resistance of P is not critical, the lower limit being governed by the impedance of the winding supplying *P* and the upper limit by the increased source impedance presented to the detector. Values from 100–500 Ω are usually suitable. There is no restriction in temperature coefficient of resistance of *P* as long as it is constant along the length of the winding. It is possible to increase the degree of subdivision by switching *P* successively turn by turn along the winding.

(*b*) If an initial zero adjustment is required, this can be provided by a voltage divider *Q* connected across an auxiliary winding on the ratio arms as shown in Fig. 6. This circuit is very suitable for use in conjunction with a load cell for the automatic control of testing machines. *X* and *R* can consist of strain gauges mounted on a suitable elastic link. *Q* can be used for zero setting and *P* can be used for load setting. The machine loading system is then controlled by the amplified error signal from the detector. If the element *P* is suitably chosen and motor-driven it is possible to produce loading patterns that vary in a given manner with time, for example, if *P* is a "sine pot" and driven at 1 rev/h, the machine will produce sinusoidal loading at the rate of 1 cycle/h. If the controlling gauges are mounted on the specimen under test, it is possible to control the machine in terms of the strain in the specimen instead of the load.

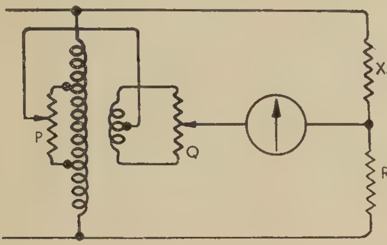

Fig. 6. A method of providing zero adjustment

(*c*) If a multi-channel bridge is required, zero-setting voltage dividers are connected in parallel across the auxiliary winding and the detector is switched to each pair of transducer elements and their zero setting unit in turn as shown in Fig. 7.

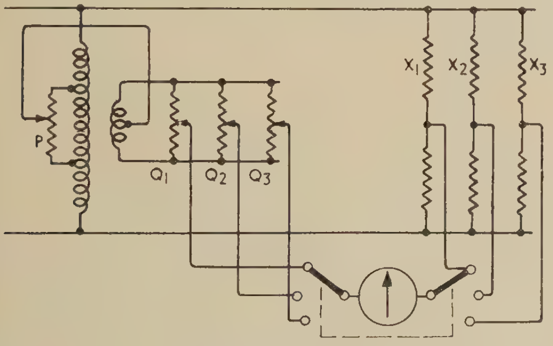

Fig. 7. A multi-channel bridge with individual zero adjustment for each channel

This circuit is very suitable for use as a multi-channel self-balancing bridge as it is only necessary to use the out-of-balance signal from the detector to control a motor which drives the element *P*. It is usually quite easy to modify a self-balancing d.c. potentiometer to this type of bridge if it uses a chopper to convert the incoming direct current to 50 or 60 c/s alternating current before amplification. Use can then be made of the a.c. amplifier, driving motor and slide-wire, along with suitable ratio arms, to make an a.c. self-balancing bridge.

An advantage of this type of recording bridge is that it is possible to have different ranges on some of the channels. This is done by having tapping points on the main winding and is shown in Fig. 8. If the number of turns between the tapping points is 10% of the whole, then the allowable range of X_1 and R_1 is ten times that of X_2 and R_2. This feature can be very useful when measuring strains in a composite structure with resistance strain gauges; for example, the strains in wood and steel for the same load are in the ratio of about 10 : 1.

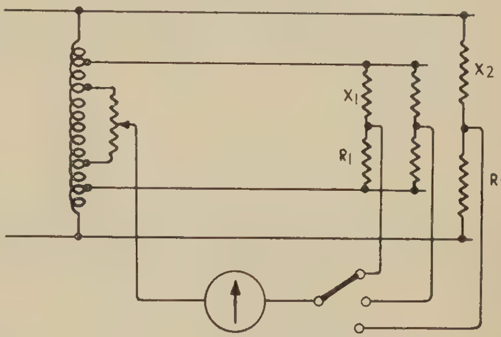

Fig. 8. A method of providing different ranges in a multi-channel bridge

(*d*) The degree of subdivision and stability of the basic circuit of Fig. 3 can be improved by the method shown in Fig. 9. In a typical bridge operating at 500 c/s, the main ratio transformer T_1 consists of a winding of 200 turns on a mumetal toroid. Another toroid T_2 has a 100-turn winding tapped every 10 turns and a 10-turn winding tapped at every turn. The 100-turn winding can be switched across each turn of portion of the main ratio transformer. Each turn of the main ratio transformer represents a change of 2% in *X* or *R* and hence for resistance gauges with a strain factor of 2, each turn is equivalent to 1% strain. The second and third switches thus represent steps of 0·1% and 0·01% strain, and the variable element, divided into 100 parts, gives 0·001% and 0·0001%. This latter strain is 1 μ in./in. The subdivision could be carried further by using another toroid with two windings instead of the variable resistive element.* Care must be taken in the layout to avoid direct induction from one toroid to another.

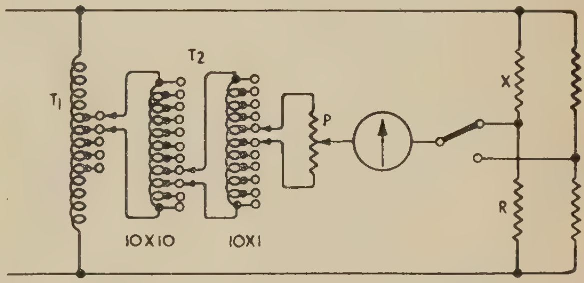

Fig. 9. The use of an auxiliary transformer to extend the degree of subdivision

---

* Commercial units of this type of divider are available, for example, from Gertsch Products Inc., 3211 South La Cienega Boulevard, Los Angeles 16, California, U.S.A.

This type of bridge is unusual in that no accurately known resistors are required and the temperature coefficient is practically zero. Several bridges of this type are in use in this laboratory for static strain measurement with resistance gauges. Laboratory tests indicate that the long-time stability of this bridge is very good. True assessment of stability proved difficult because of lack of suitable resistances for X and R, but tests have indicated that the readings are repeatable to 0·0001% for periods of weeks. This represents a stability of about 1 in 10^6 in the ratio arms and about 1 in 10^4 in the divider system.

General comments

The design of the ratio transformer itself may be governed by the allowable flux density or by the degree of subdivision required. If the bridge is to be self-balancing or part of a machine controller, it is usually operated from the supply mains at 50 or 60 c/s; in this case the maximum allowable flux density usually determines the minimum number of turns and size of core. A mumetal toroid 1 in. wide, inner diameter 2 in. and outer diameter $2\frac{1}{2}$ in. ($\frac{1}{4}$ in.^{2} core area) with a total of 400 turns has been found suitable for use across 6 V at 50 c/s. On the other hand, a bridge of the type shown in Fig. 9 may work at a frequency of 500–1000 c/s, and the minimum number of turns may well be governed by the subdivision necessary. The winding would require 400 turns if each turn is to represent 1% change in resistance of X or R.

The two sections of the ratio transformer should be tightly coupled and as similar as possible. Both these objects can be achieved by ensuring mechanical symmetry in the windings and the use of a high permeability core. It is desirable that the ratio of winding resistances should be kept the same as the turns ratio to minimize phase-angle errors.

If reactive balancing is necessary because of stray circuit capacitances, etc., it can be provided as shown in Fig. 10. In the circuit of Fig. 10(*b*) the variable element Z should be low enough not to introduce significant resistive shunting of X or R. At 500 c/s and with $C = 300$ pF, Z can be as high as 1000 Ω without changing X or R by 1 in 10^6 if X and R are 100 Ω or less.

Applications to other transducers

The bridges can be used with any transducers which produce an out-of-balance voltage in phase with the excitation. This is the case with any resistance-type transducer, with most capacitance types but not with all inductive types. The various bridges shown are readily used with resistance-type temperature elements, either metal wire or semi-conductor. The circuit of Fig. 6 can be used for a controlled temperature enclosure and can be made to follow a given temperature programme if P is a motor-driven multi-tapped potentiometer. The basic circuit of Fig. 3 is suitable for use as a tolerance bridge and if the variable element P is motor-driven it would form a self-balancing unit for automatic component testing.

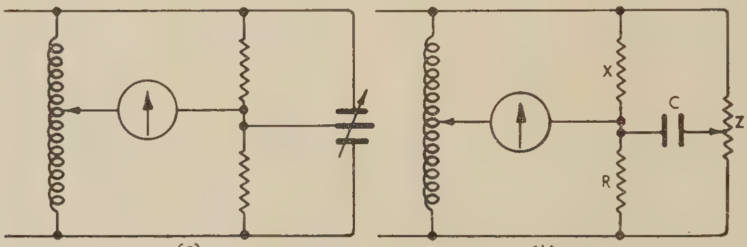

(a) (b)

Fig. 10. Methods of providing reactive balance

Conclusions

A type of a.c. bridge has been described which is particularly suited to measuring resistance strain gauges in static or v.l.f. tests. The bridge can be readily combined with a potentiometric recorder to form a self-balancing multi-channel bridge. It can also be used with suitable load cells to control a testing machine either at constant load or through a given cycle of loading. The design does not require critical values in any of the components and has very good long-term stability and accuracy. The bridge can be used with many other transducers besides resistance strain gauges.

References

(1) Clark, H. A. M., and Vanderlyn, P. B. *Proc. Inst. Elect. Engrs*, **96**, Part III, p. 189 (1949).

(2) Thompson, A. M. *Trans I.R.E. Instrumentation*, **1–7**, p. 245 (1958).

(3) Clarke, L. N. *J. Sci. Instrum.*, **31**, p. 300 (1954).

Production of millimicrosecond current pulses using a pressurized spark gap

by J. H. ADLAM, B.A., A.M.I.E.E., and L. S. HOLMES, Atomic Energy Research Establishment, Harwell, Berks

[*Paper first received* 19 *May, and in final form* 16 *June*, 1960]

Abstract

A pressurized spark gap has been designed to discharge a number of coaxial cables in parallel, thus producing a current pulse of 10^4 *A with a rise time of* 4·5 *mμs. It is intended to use a number of these spark gaps in parallel, and to test the feasibility of doing this, measurements have been made of the statistical variation of the time lag for breakdown after triggering.*

1. Introduction

The spark gap which is described has been designed to carry out experiments on the shock heating of a plasma. In order that as much energy as possible may be delivered to the plasma, and also to simplify the interpretation of the results, the current is made to rise in as short a time as possible. The total current delivered is 54 kA and the voltage developed across the point where the current is fed into the system is estimated as 20 kV.

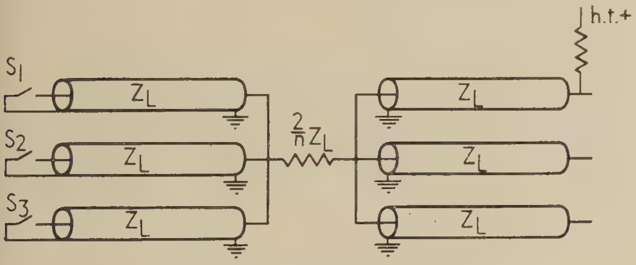

Fig. 1. Coaxial line circuit

To make the time for the rise of current as small as possible the circuit due to Blumlein, which has been described by Wilkinson,⁽¹⁾ is used. This is shown in Fig. 1; charged coaxial lines Z_L are here used to store the energy, and these lines are switched by the spark gaps S_1, S_2, S_3, here shown as switches. The shock heating apparatus, which is shown as a resistive load, was a cylindrical tube 11 cm long and 3 cm diameter with electrodes at each end, and was filled with hydrogen at 5–10 μ pressure. This gas was first pre-ionized by a preliminary discharge. When the Blumlein circuit is made to operate, the plasma contracts under pinch-effect forces, the self-inductance L of the tube increases and the voltage across the tube is given by

$$V = (d/dt)(LI) = L(dI/dt) + I(dL/dt) \qquad (1)$$

Once the current I has attained a steady value the first term on the right-hand side of equation (1) vanishes and the tube appears to have a resistance equal to dL/dt.

In order to make the rise time of the current through the load approximately equal to the rise time of the current flowing through each spark gap, the spark gaps must be arranged to break down in a time which is less than the rise time. To achieve this end the spark gaps are all triggered from a single master spark gap, and the spark gaps must be designed so that the statistical variation in the time lag for breakdown is small. When used in this way the requirements for the spark gap are:

(i) the probability of breakdown before the gap is triggered must be less than 0·1%;
(ii) the statistical variation in the time lag for breakdown after the triggering pulse has been applied must be less than 2 mμs;
(iii) the time constant for the rise of current must be less than 5 mμs.

Fletcher⁽²⁾ has used pressurized spark gaps as switches for circuits consisting of coaxial lines, and has obtained voltage pulses with rise times of 0·4 mμs. The spark gap to be considered in this paper is pressurized and closely resembles Fletcher's. It differs, however, in three ways. First, each spark gap is to be used to switch a number of coaxial cables in parallel. Second, these cables are short-circuited at one end by the spark gap, rather than switched into another cable. Third, the spark gaps are to be designed so that when a number are used in parallel, the times of breakdown all lie within 2 mμs. This means that the statistical variation in the time lag for breakdown is small.

2. Method of operation

The following method of operation has been devised to make the overvoltage ratio of a gap, that is the ratio of voltage applied to the voltage required for breakdown, as large as possible. This is done because it is found that the larger the overvoltage ratio is made, the smaller is the statistical variation in the time lag for breakdown.

The spark gap used was a three-electrode gap; the method of operation is illustrated in Fig. 2 by the sequence (*a*)—(*b*)—(*c*)—(*d*). The circuit used is shown in Fig. 3; here S' represents the master spark gap. When the gap S' fires,

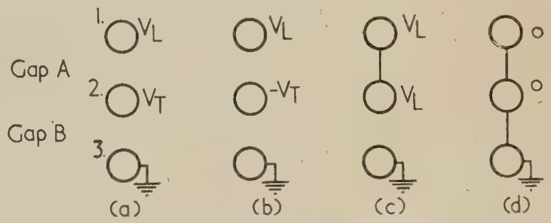

Fig. 2. Voltages applied to the electrodes of a spark-gap (*a*) Initially; (*b*) on triggering; (*c*) after the breakdown of gap *A*; (*d*) after the breakdown of gap *B*

a current wave travels along the cable Z_T; on reaching electrode 2 this wave is reflected, the voltage changing from $+V_T$ to $-V_T$.

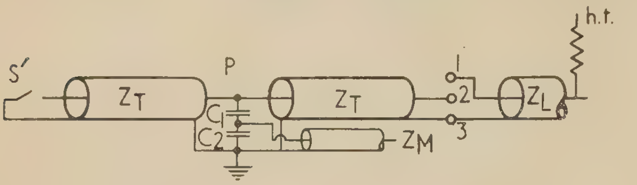

Fig. 3. Circuit for the measurement of the time delays for breakdown (t_A and t_B)

Write the overvoltage ratio of gaps A and B, r_A and r_B respectively. Then

$$r_A = \frac{1}{\alpha}\frac{V_L + V_T}{V_L - V_T} \quad r_B = \frac{1}{\alpha}\frac{V_L}{V_T} \tag{2}$$

where α is a factor of safety greater than 1. If the value of V_L/V_T is adjusted to make $r_A = r_B$, then

$$V_L/V_T = 1 + \sqrt{2} = 2{\cdot}414 \quad r_A = r_B = 2{\cdot}414/\alpha \tag{3}$$

By making V_L/V_T larger than 2·414, r_B is increased but r_A decreased, and by making V_L/V_T smaller than 2·414, r_A is increased but r_B decreased.

3. Construction of spark gap

When pressurized spark gaps are used under the conditions considered in this paper, it is found that after breakdown the voltage is dropped almost entirely across the inductance associated with the spark gap. If L is the inductance associated with the spark gap and Z_L is the impedance of all the cables in parallel connected to the spark gap, there is a time constant L/Z_L for the rise of current. Thus the number of cables which can be connected to a spark gap is limited if condition (iii) of Section 1 is to be satisfied. For this reason seven 14 Ω cables are connected in parallel to the spark gap, making $Z_L = 2\,\Omega$.

The maximum charging voltage was 24 kV and the maximum current obtainable was therefore 12 kA. This means that nine spark gaps have to be used in the circuit shown in Fig. 1. The energy per pulse switched by each spark gap is 6 J and the energy dissipated within the gap will be less than this.

The 14 Ω cable used was Uniradio 42; this is a coaxial polythene insulated cable with a braided inner conductor. A cross-section through the spark gap is shown in Fig. 4. Three of the 14 Ω cables are shown as C, C' and C'', the connexions of these cables to the plate J are arranged in a circle about the axis of symmetry. The outer conductors make electrical connexion with the plate J, while the inner conductors make electrical connexion with the plate K. Insulation between plate K, which is charged up with the inner conductors of the cables, and earth is provided by the Nylon insulator D and by pressurized gas, which fills the region within the O-ring seals. The live electrode (1) and the earth electrode (3) are carried on the ends of spindles G and F respectively. These screw into the body of the apparatus and allow micrometer adjustment of the gaps to be made.

In the region between plates J and K the polythene insulation of the cable is subject to the gas pressure. It is found that even with a gas pressure of 500 lb/in.^{2} there is no flowing of the polythene. The breakdown between plates J and K, due to tracking across the surface of the polythene, is inhibited owing to the presence of the gas under pressure; this effect has been discussed elsewhere.$^{(3)}$ The trigger voltage is fed in through an Araldite bush E which is matched in electrical impedance to the trigger cable. The voltage gradient between the electrodes before they are overvolted is approximately 1 kV per 0·001 in.

In operating an earlier spark gap, it was found that material from the spark was deposited on all surfaces exposed to the spark. When this material was deposited on insulators, they rapidly lost their insulating property. Here the polythene insulation of the cables between the plates J and K is not exposed to the spark, and the lead to the electrode 2 is brought through a small hole so that the Araldite bush E is also protected.

4. Measurement of static breakdown

If static breakdown is measured with a high resistance between the voltage source and the spark gap, to limit the current passed on breakdown to a few milliamperes, values

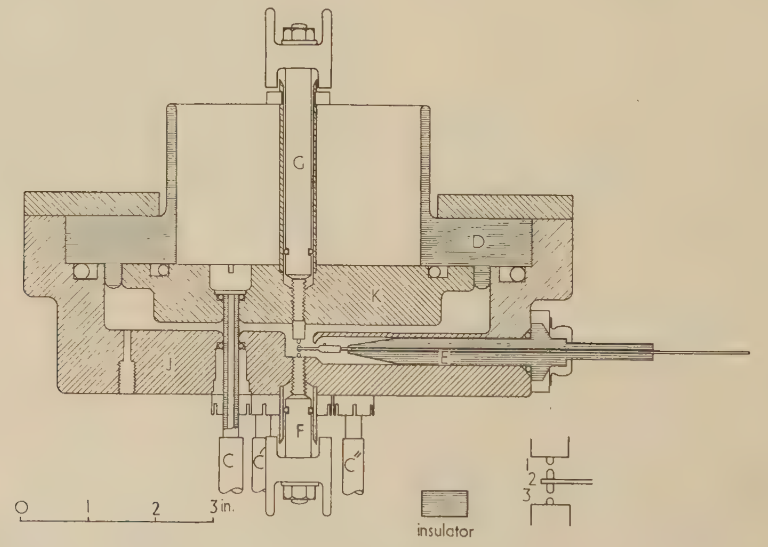

Fig. 4. Diagram of pressurized spark-gap

are obtained for the breakdown voltage which are consistent to within ±2%. Further, if the electrodes are smooth this breakdown voltage will be larger than for rough electrodes. When a spark gap passes a high current after breakdown the electrodes will be left in a rough pitted condition, and this causes the breakdown voltage to change after each discharge. In order to form an estimate of the spread in the value of the breakdown voltage, the following experiment was made. The coaxial cables connected to the spark gap were charged through a large resistor, the resistor being of such a value as to give a time constant for charging of about 30 s. The coaxial lines then slowly charged until breakdown occurred when they were rapidly discharged, the process being repetitive. An electrostatic voltmeter was connected across the spark gap and the voltage of each breakdown was noted. When about one hundred breakdowns had been noted a histogram was constructed, plotting the number of breakdowns in a given interval against the voltage.

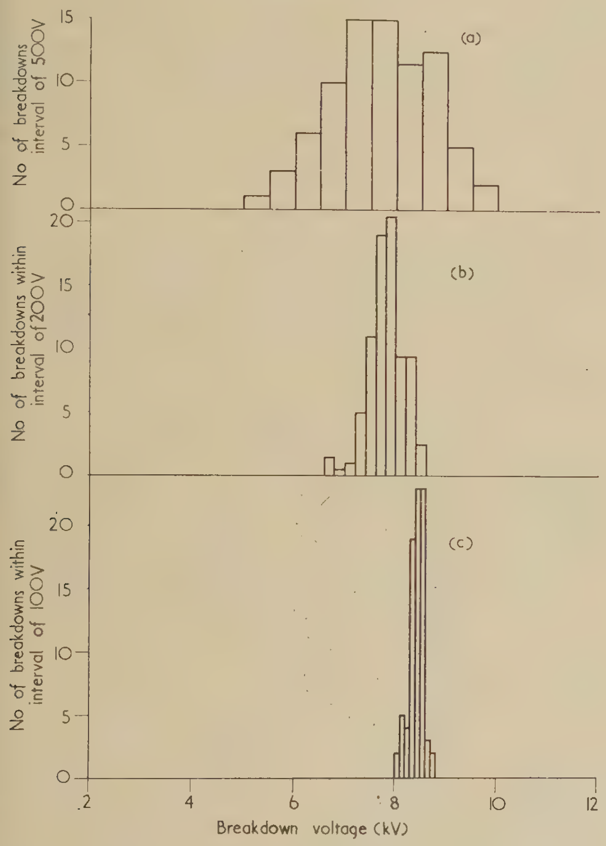

Fig. 5. Histograms for the static breakdown of a pressurized spark-gap, showing the number of breakdowns within a given interval of voltage

(*a*) For nitrogen, pressure 150 lb/in.^{2}, gap 0·011 in., molybdenum electrodes;
(*b*) for air, pressure 150 lb/in.^{2}, gap 0·008 in., molybdenum electrodes;
(*c*) for oxygen, pressure 150 lb/in.^{2}, gap 0·009 in., molybdenum electrodes.

Fig. 5 shows three such histograms obtained with nitrogen, air and oxygen as the insulating gas at high pressure. These histograms show that, for consistency in the value of the breakdown voltage, oxygen is best, followed by air and then nitrogen. This effect presumably depends upon the state of the electrode surface after a discharge in the various gases. Further experiments showed that carbon dioxide is intermediate between air and nitrogen in this respect. Molybdenum and copper were tried for the electrode material and it was found that copper electrodes have the disadvantage of wearing away more rapidly. Electrodes made from 0·060 in. diameter rods with hemispherical ends, as shown in the inset to Fig. 4, were more consistent than nearby plane electrodes. When sharply pointed electrodes were used the cold emission current before breakdown was large. When molybdenum electrodes were used, oxygen at 150 lb/in.^{2} gave more consistent values for the breakdown voltage than oxygen at 300 lb/in.^{2} This may have been because, when experiments were made with oxygen at 300 lb/in.^{2}, the gaps were set rather close together (0·005 in.) in order to obtain a breakdown voltage of convenient value. The ratio of the depth of irregularities in the electrode surface to the gap width is now larger.

5. Measurements of time lags for breakdown

If the spark gap is made to operate as described in Section 2, by measuring the variation of the voltage on electrode 2 with time, the time between the overvolting of the gaps *A* and *B* (Fig. 2) and their breakdown is obtained. This variation is shown in Fig. 6(*b*); the times to be measured are shown as t_A and t_B. Since it is not practicable to measure the voltage at electrode 2, it is instead measured at a point *P* roughly half-way along the triggering cable. The voltage measured at *P* is shown in Fig. 6(*a*). As the current wave travels along the cable the voltage is seen to drop from V_T to earth potential. When the current wave is reflected as a reversed potential, the voltage changes from earth potential to $-V_T$. Thereafter the voltage waveform at *P* is the same as at the electrode 2; the times t_A and t_B can therefore be measured.

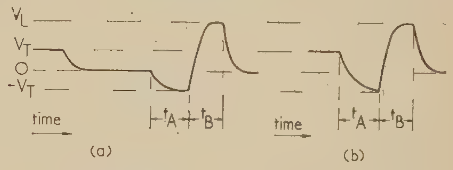

Fig. 6. (*a*) Voltage at point *P*. (*b*) Voltage at electrode 2

The voltage at point *P* was measured by a capacity divider, the equivalent circuit of which is shown in Fig. 7. Capacitor C_1 was made equal to 1·6 pF; to obtain this capacitance a piece of foil was wrapped round the polythene insulation of the cable from which the outer braid had been removed, the continuity of the outer being maintained by a brass tube. Capacitor C_2 was made equal to 820 pF, and was made from a piece of mica silvered on both sides and wrapped round into a small cylinder. All connexions were made as short as possible to reduce the effect of inductance. The value of resistor Z_T was 91 Ω and Z_M was 70 Ω. From a consideration of Fig. 7, it can be shown that the shortest time interval which can be resolved is $\frac{1}{2} C_1 Z_T$, which is, in this case, 0·07 mμs. The oscilloscope used was one designed at the Atomic Weapons Research Establishment; it contained a General Electric Company cathode-ray tube No. VCRX410 (now obsolete). The input to this tube was matched to

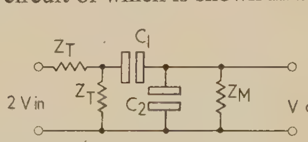

Fig. 7. Equivalent circuit of capacity voltage divider

70 Ω cable. The signal passed along a helix to produce the deflexion, which was a maximum for 40 V. Clear photographs were obtained from a single pulse with a time base of 10 mμs.

The spark gap was operated a number of times with the gaps at a particular setting. A histogram was then constructed by plotting the number of breakdowns for which t_A lay in a certain interval against the value of t_A, and similarly for t_B. These histograms are shown in Fig. 8 for various values of the overvoltage ratio of gap A and of gap B. From Fig. 8 it is evident that, for a given overvoltage ratio, the spread in the values of t_A is greater than the spread in the values of t_B. The measurements of t_A and t_B were made using both oxygen and air as the insulating gas. When oxygen was used, although the breakdown voltage was more consistent as shown in Fig. 5, it was found that sets of measurements of t_A and t_B were not reproducible from day to day. The measurements shown in Fig. 8 refer to air.

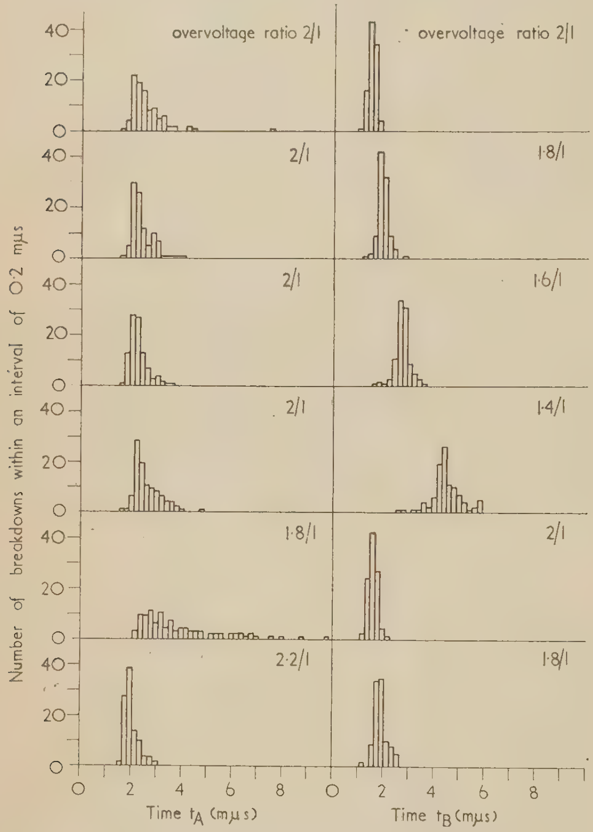

Fig. 8. Histograms for the time delays for breakdown in a pressurized spark-gap (t_A and t_B), showing the number of breakdowns within a certain interval of delay time

The total delay between triggering and breakdown is $t_A + t_B$ and, as mentioned in Section 1, the spread in the value of this quantity must be made less than 2 mμs. This condition is satisfied by making the overvoltage ratio on gap A 2·2/1 and on gap B 1·8/1. The histogram for this case is shown in Fig. 8.

6. Conclusion

These experiments show that the statistical variation of the time lag between the triggering and breakdown of a pressurized spark gap can be made as small as 2 mμs. Thus it is possible to use a number of spark gaps in parallel to produce a current pulse with a rise time of about 5 mμs.

7. Acknowledgements

The authors are indebted to Dr. J. E. Allen for help in the earlier part of the work, to the group at the Atomic Weapons Research Establishment, Aldermaston, led by Mr. S. D. Abercrombie, for the provision of a fast oscilloscope, and to Mr. H. S. Cockroft of Ferranti Ltd. for helpful suggestions.

References

(1) WILKINSON, K. J. R. *J. Instn Elect. Engrs*, **93**, p. 1090 (1946).
(2) FLETCHER, R. C. *Rev. Sci. Instrum.*, **20**, p. 861 (1949).
(3) MEEK, J. M., and CRAGGS, J. D. *Electrical Breakdown of Gases*, p. 339 (Oxford: University Press, 1953).

Electronic apparatus for the study of X-rays with proportional counter

by N. PATLA, M.Sc., Sir John Cass College, London

[*Paper received* 29 *March*, 1960]

Abstract

The design and construction of an electronic pulse recording system for use with a proportional counter suitable for X-ray studies is described. The performance of the high gain amplifier and pulse amplitude analyser for X-ray wavelength discrimination is discussed in detail.

Introduction

THE use of the proportional counter as a detector of X-rays was first reported by Trost(1) and later by Lang,(2) Arndt and Riley(3) and Skertchly.(4) The radiation detector to be employed for X-rays should have a high quantum efficiency, stability, linearity and good signal-to-noise ratio as well as a large response to individual photons. The wavelength discrimination possible with the proportional counter(5) considerably widens their field of application. In other words, they lend themselves well to an electronic method of monochromatization. Proportional counters have resolving times which are so short that counting losses become completely negligible in any normal X-ray application. In recent years, its use for crystallographic studies in the field of X-rays has increased and, therefore, it was decided to introduce this system with existing X-ray equipment. Proportional counters require, of course, more elaborate electronic circuits than do Geiger–Muller counters. Fig. 1 shows the block diagram of the whole apparatus.

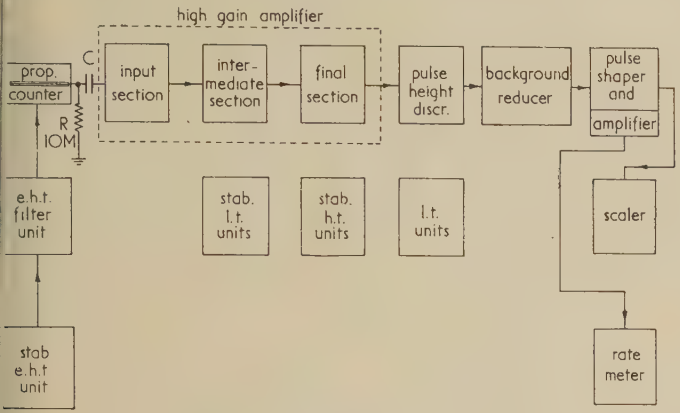

Fig. 1. Basic diagram of the recording system

Proportional counter

At present few proportional counters suitable for X-ray work are commercially available. Bernstein, Brewer and Rubinson(6) have published the possible constructional details of such a counter. Arndt, Coates and Crathorn(7) used a continuous gas-flow counter. Curran, Angus and Cockroft(8) described the behaviour of a proportional counter in the analysis of low-energy spectra. Rossi and Staub(9) have given data on the variation of gas multiplication with pressure and counter geometry for a number of gas mixtures. West and Rothwell(10) have dealt with the improvement of proportional counters for X-ray work when extreme demands are made on the wavelength resolution of the counter. The present experimental proportional counter (type PX28B) was made by 20th Century Electronics Ltd., England. The details of its size, filling, etc., are described in a paper by Kiss and Patla.(11) The gas mixture used was selected because of its linearity in energy response and extreme stability.(12) The counting rates at various X-ray tube voltages and currents for CO*K*α radiation are given in Figs. 2(*a*) and 2(*b*) which show good linearity of counting rate with X-ray intensity. (Recently type PX28E and F has been made by the same firm and claimed to give good energy resolution with X-rays.)

High gain amplifier

The function of the pulse amplifier is to raise the small pulses (100 μV to 5 mV) of the proportional counter to a level, usually in the range 5 to 50 V, at which they are suitable for feeding to the subsequent equipment, which measures pulse rate per second and pulse amplitude distribution for the analysis of energy spectrum. The significant properties of the proportional counter in so far as they affect the performance demanded from the amplifier are:

(i) time T for charge collection ($0{\cdot}5$ to 2μs), and
(ii) pulse amplitude across the coupling condenser C.

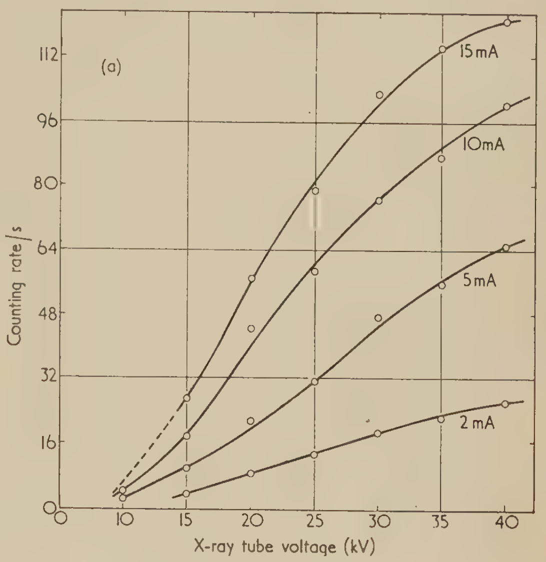

Fig. 2(*a*). Variation of counting rate with X-ray tube voltage

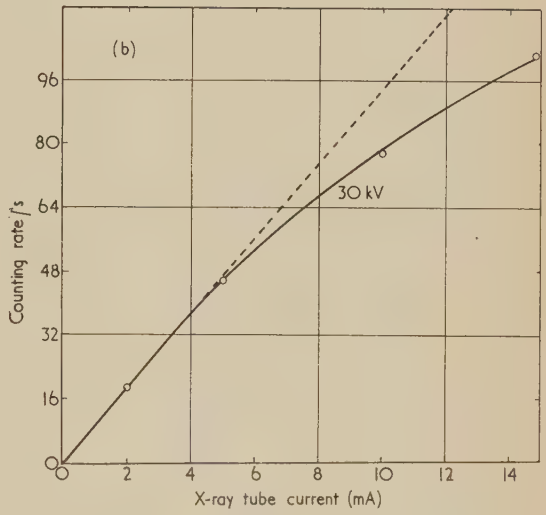

Fig. 2(*b*). Variation of counting rate with X-ray tube current

The amplitude of the pulse after discharge at the wire of the proportional counter is given by

$$\Delta V_0 = n_0Ae/C'$$

where n_0 = the number of ion pairs formed in the counter by each photon
A = the gas amplification factor
C' = the total capacitance of the anode and the grid system
e = the charge per ion = $1{\cdot}59 \times 10^{-19}$ C.

If the voltage gain of the amplifier is F, then the output signal V is given by

$$V = FAn_0e/C'$$

With $A = 10^4$, which is a rarely used practical upper limit even in gases, such as methane, and setting $V = 5$ V, a suitable value for the output signal, and reducing the capacity $C' = 20$ pF at the input grid to a practical minimum for maximum sensitivity,

$$Fn_0 = 6{\cdot}3 \times 10^4$$

This equation shows clearly the great sensitivity of the device if operated at such high values of A. A value of $F = 6{\cdot}3 \times 10^4$ is easily attained, hence the device should be able to record a single ion pair. Amplitude measurements on the pulse have little significance in such extreme cases on account of the statistical fluctuations in the value of n_0 in any experiment. However, with n_0 of the order of 10, measurements can be made and F need have a value of only about 10^4.

It can also be shown in another way that a proportional counter can theoretically measure the number of ion pairs formed within the counter down to the limit of $n_0 = 1$. Thus from $\Delta V_0 = n_0 Ae/C'$ with $A = 10^4$, $e = 1{\cdot}59 \times 10^{-19}$ C and $C' = 20 \times 10^{-12}$ F

$$\Delta V_0 = 80 n_0 \ \mu\text{V}.$$

Now a well designed amplifier has an input noise voltage of the order of 10 μV (r.m.s.) and a signal of 80 μV can easily be measured above the noise peak voltages. Hence n_0 may be as small as unity. It must be noted now that the proportional tubes operating at very small values of n_0 should be carefully constructed. The insulation of the leads must be good and electrical screening of the input terminal is essential.

It is not always convenient to have A as high as 10^4 and it usually ranges between 10^2 and 10^4. It is clear, however, that in almost all practical cases, the smaller value of A may be successfully countered by larger values of F of the order of 10^6, for an output noise voltage of about 10 V (r.m.s.) In the determination of an energy distribution, the curve drawn is the differential bias curve showing the counting rate of pulses occurring within a given pulse height interval. Here it is most essential that the amplifier supplying the pulses to the differential analyser should have a very high degree of gain stability and linearity. In such an experiment where a very wide range of pulse amplitudes may have to be encountered, the larger pulses can cause overloading of the amplifier output stages, and grid blocking (wherein the amplifier is rendered insensitive for a reasonably long period of time) may result. Further troublesome features in such a high gain amplifier are its two components of random noise, both arising from the input valve. The first is anode current

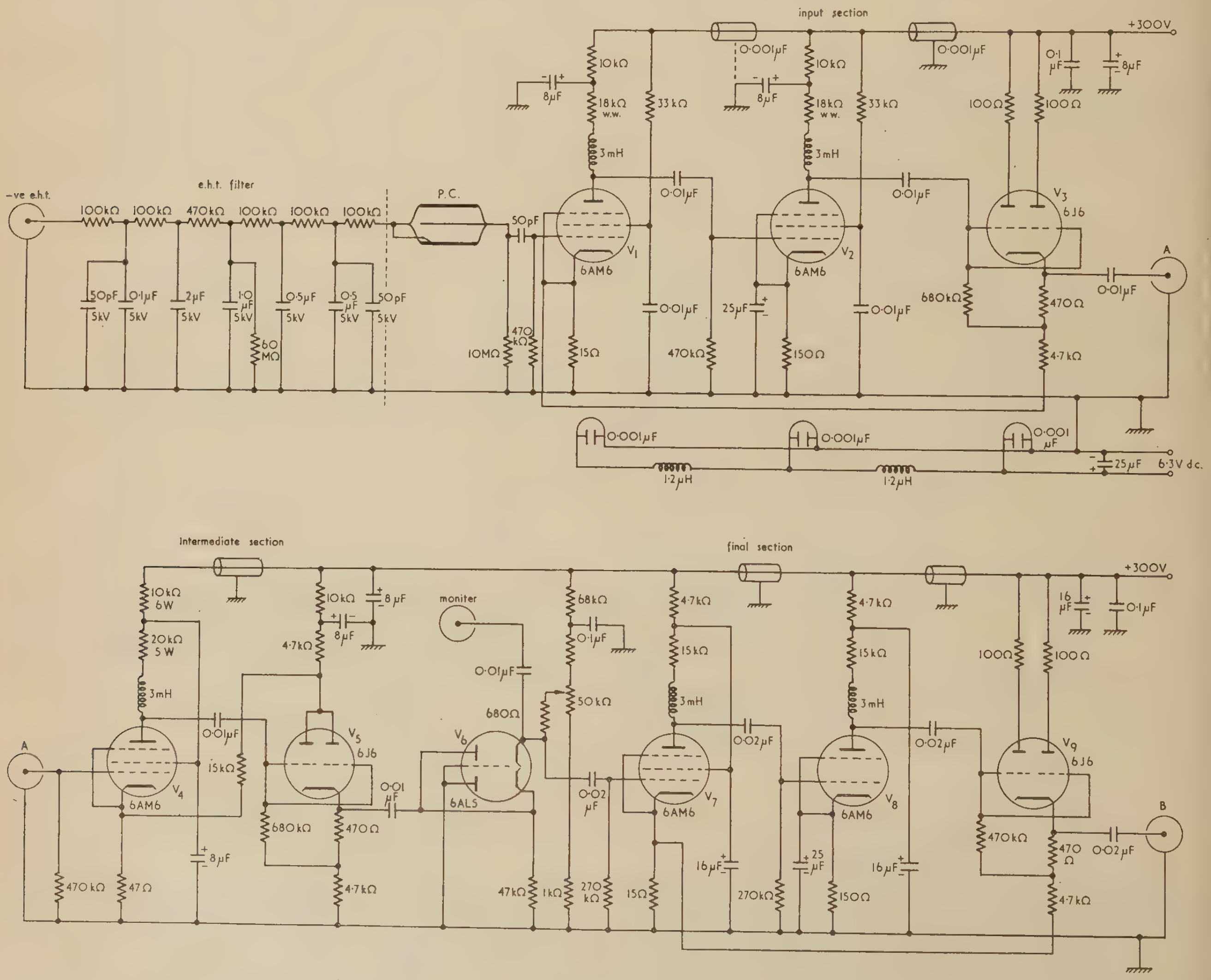
input section
+300V
−ve e.h.t.
e.h.t. filter
100kΩ
470kΩ
50pF
0·1μF
2μF
1·0 μF
0·5μF
0·5 μF
5kV
60 MΩ
P.C.
10MΩ
470 kΩ
15Ω
10kΩ
8μF
18kΩ w.w.
33kΩ
3mH
0·001μF
0·01μF
6AM6
V1
V2
25μF
150Ω
V3
6J6
100Ω
680kΩ
470Ω
4·7kΩ
A
0·001 μF
1·2μH
6·3V d.c.
intermediate section
final section
10kΩ 6W
20kΩ 5W
4·7kΩ
monitor
68kΩ
50kΩ
680Ω
V4
V5
V6
6ALS
V7
V8
V9
15kΩ
0·02μF
16μF
270kΩ
1kΩ
47kΩ
270 kΩ
B

Fig. 3. Proportional counter and high gain amplifier system

shot noise which has been reduced by selection of the high slope valves. The other is grid current noise, so called because it refers to the noise voltage set up across the input capacity of the first stage by the random fluctuations of the valve grid current. This noise component has been kept small by using valves under conditions of very low grid current. Proper layout, screening between the control grid and the anode of each valve, adequate heat dissipation, wire wound resistors as anode loads, non-microphonic valves, high quality soldering and many other precautions help to avoid self-oscillation and undesired feedback as well as to reduce noise to a minimum. The importance of the amplifier noise on the X-ray wavelength discrimination was discussed by Kiss and Patla.(11) It is most necessary to make the stabilized e.h.t. supply for the proportional counter associated with such a high gain pulse amplifier free from 50 c/s hum. For this a filter unit (Fig. 3) has been built and the e.h.t. supply is filtered again before passing to the proportional counter through 30 ft of double screened coaxial cable. The d.c. high voltage supplies (h.t. units) are all stabilized, primarily to keep the supply impedance very low as a guard against unwanted coupling between the low level input and the high level output stages. This also contributes towards the overall gain stability of the amplifier. To reduce hum, the filaments are heated by 6·3 V d.c. supply, stabilization of which is essential when accurate energy determination is required.

In the present apparatus, the whole amplifier (Fig. 3) consists of three separate sections. The input section is a small compact unit intended to be housed inside the X-ray chamber as well as very near to the spectrometer table containing the proportional counter. This keeps the total capacitance as low as possible and the voltage pulse is consequently high. The cathode follower output from the input section is passed through a long coaxial cable to an intermediate stage situated some distance away outside the X-ray chamber, for further amplification, and thence to the final amplifier on the recording table. Provision has been made to exclude an amplifying section (intermediate or final stage) and to include an attenuator(13) between the intermediate and final section of the amplifier according to requirements. Overall gain is adjusted between 10^5 and 10^6 by the help of the pulse generator unit.(13) The rise and fall of the output pulse in every stage (complete within $0\cdot3\ \mu$s) has been made more rapid by introducing a coil of inductance L (3 mH) in series with the anode load resistor. This inductance also increases the amplification of the circuit without loss of steepness of the rise and fall of the output pulse. The maximum noise amplitude is $2\cdot8$ V peak to peak before the final section. The amplifier is found to have excellent response to a step signal, good linearity and the gain remains constant within 3 dB up to 500 Kc/s. The function of V_6 in the final section is to allow all pulses below any predetermined level to be rejected, i.e. to exclude noise pulses, if required. The transmission of output pulses from the cathode follower of each section is made through 72 Ω coaxial cables (uni-radio 32) which was not found to introduce any harmful attenuation or pulse distortion over the distances used.

Pulse height analyser

A pulse amplitude analyser is an instrument designed to measure the amplitude distribution of pulses. This enhances

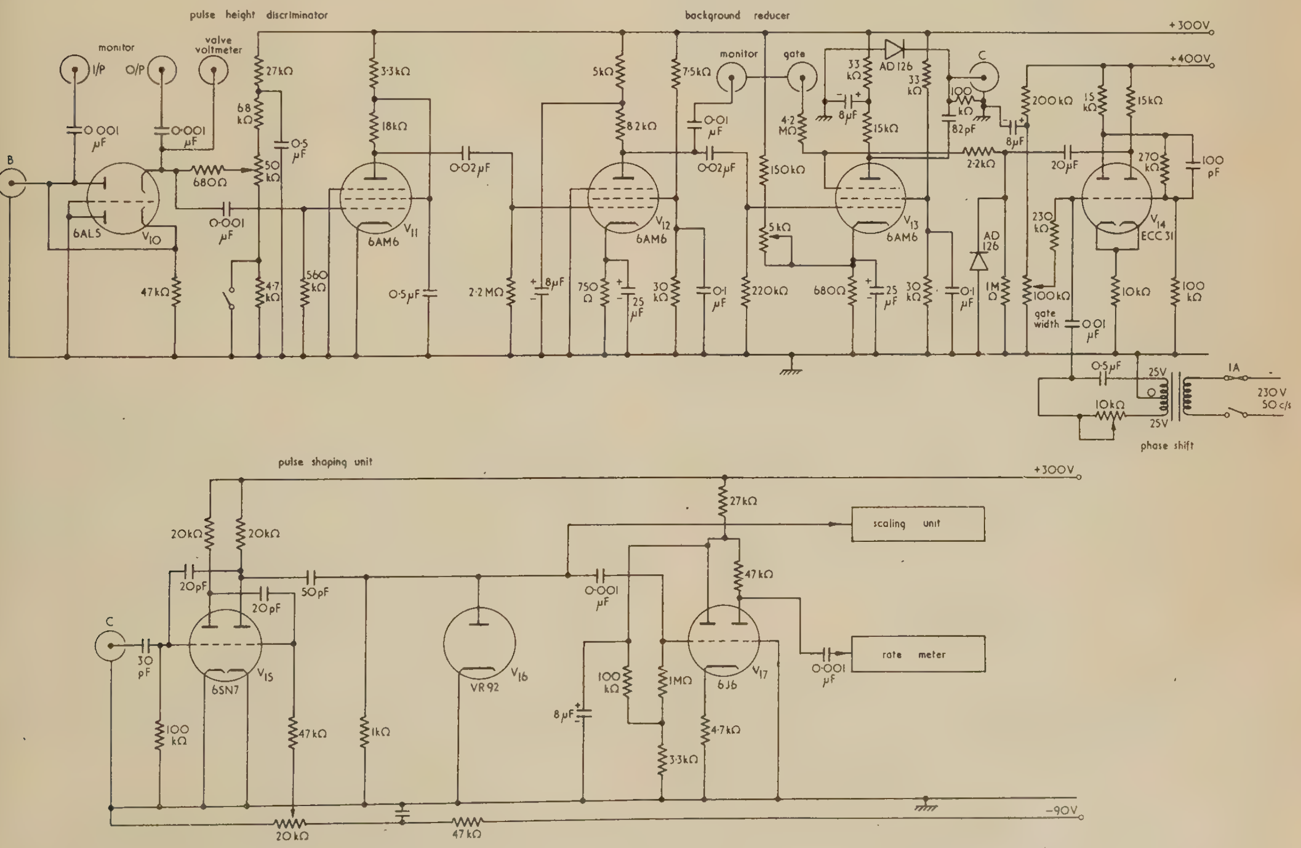

Fig. 4. Pulse height discriminator, background reducer and pulse shaping unit

the usefulness of a proportional counter system for X-rays, because the total ionization and hence the pulse height is proportional to the energy of the photons (total ionization only proportional to E if absorption is true absorption) and hence inversely proportional to the wavelength of the radiation. The possibility of wavelength resolution of X-rays by a proportional counter was first considered by Lang.$^{(2)}$ Later$^{(5)}$ he discussed the problem of detecting CuKα radiation in the presence of a slightly softer fluorescent background excited by the CuKα rays. Considerable work has been done on the design of multichannel and single channel pulse height analysers whose degree of complexity depends on the nature of the pulses to be analysed. An excellent review of the subject was published by Van Rennes.$^{(14)}$ A more recent review was presented at the Geneva Atoms for Peace Conference by Kelley.$^{(15)}$

In the present work, in order to test the overall performance of the completed proportional counter system, an experiment was carried out on the wavelength discrimination using CuKα radiation from the crystal monochromator. Positive pulses from the final section of the amplifier system were fed to one anode of a double diode V_{10} (Fig. 4), to the cathode of which a positive bias (V) of any value between 0 and x V could be applied. Only those pulses whose amplitudes exceed this threshold value will then be passed to the next stage. The other half of the diode acts as a d.c. restorer and any negative spikes will be by-passed to earth. Counting rates were obtained at one volt intervals of discriminator bias when a steady reflected beam of constant intensity from a large plane calcite crystal passed through the counter. The pulse height distribution was found by subtracting successive readings to give the number of pulses in a channel of width 1 V. This corresponds approximately to wavelength intervals of about 0·22 Å, at the wavelength of CuKα. A calibrated valve voltmeter was used to measure the bias voltage at the cathode of the diode. The pulse height distribution curves are shown in Figs. 5(*a*), (*b*), (*c*) and (*d*).

Results

(1) Crystal reflected CuKα (X-ray tube 40 kV, 10 mA). Three components can be seen in Fig. 5(*a*) corresponding to the CuKα $\lambda = 1{\cdot}54$ Å at 7·5 V and its harmonics $\lambda/2$ and $\lambda/3$ at 15·0 V and 22·5 V respectively.
(2) As (1) but with a nickel β-filter [Fig. 5(*b*)]. This materially reduces the effect of the white radiation scattered from the crystal monochromator relative to the Kα line.
(3) As (1) but with X-ray tube at 19 kV, 15 mA [Fig. 5(*c*)].
(4) As (3) but with a nickel β-filter [Fig. 5(*d*)]. Here only λ and $\lambda/2$ appear as the X-ray tube voltage is too low to generate $\lambda/3$.

During the experiment the constancy of the X-ray tube output was checked by the monitoring system.$^{(13)}$

Background reduction

The background pulses arising from cosmic rays and local radio active matter may, with the high gain counting system used, be augmented by pulses due to local magnetic and electrical disturbances. For the measurement of low X-ray intensities, it is necessary to keep this recorded background rate as low as possible. An increase in the ratio of the number of counts due to X-rays to the number due to overall background may be obtained by arranging that the X-rays arrive in pulses of short duration and ensuring that counts are recorded only when the X-rays are incident. Such an ideal is partially realized in the case of the output from a self-rectifying X-ray tube, as the characteristic X-rays are only emitted during about a third of the a.c. supply cycle. A circuit has been designed (Fig. 4) to act as a gate between the pulse height discriminator unit and the pulse shaping unit so that it will only allow pulses to pass during a certain fraction of the a.c. cycle. This gate whose "open" phase and width are adjustable, is obtained from the same a.c. supply that operates the X-ray tube. Sequences of X-ray pulses, gate and background pulses are shown in Fig. 6. Referring to this figure, the X-ray counting rate is n/T for $t \geqslant t'$ and $(n/T)\,(t/t')$ for $t < t'$, while for the background the counting rate is $(t/T)N$ where N is the number of ionizing events in the counter due to background effects. Thus if t is reduced until $t = t'$, all the X-ray pulses are registered and the fraction of background pulses recorded is then $N(t'/T)$.

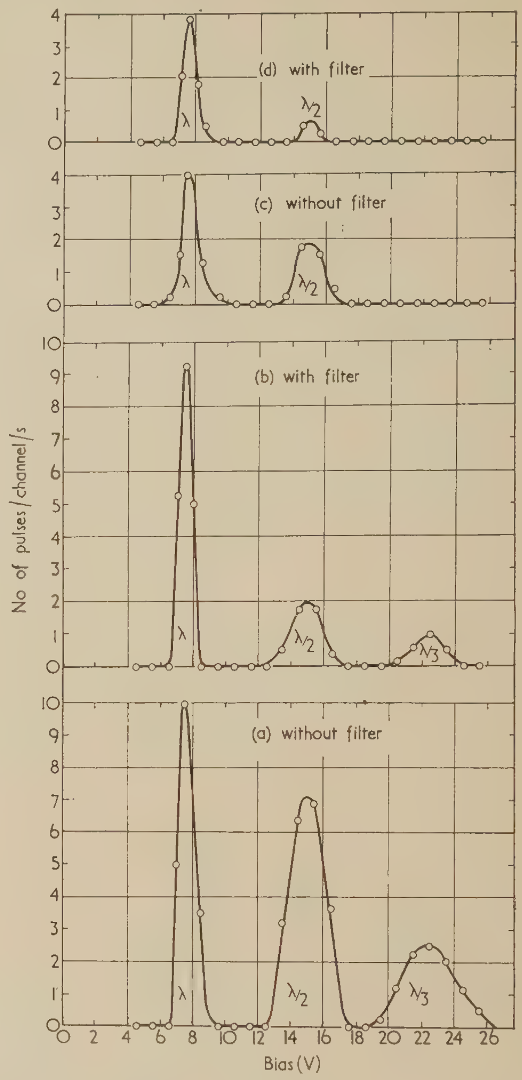

Fig. 5. Wavelength discrimination curves for CuKα

Pulse shaping unit

Successful operation of the pulse counting units requires that the duration of the input pulses should be about the same as that of interstage pulses within the scaling circuit (approximately 1 μ s) and the height of the pulses must be fairly uniform. In the present design (Fig. 4) the multivibrator is asymmetrically biased so that there is only one stable state for no signal instead of two in the symmetrical case. When operating at a supply potential of +300 V, the negative pulse taken from the anode of diode VR92 was found to be of the order of 18 V in height and 1 μs in duration. The response is essentially the same throughout the counting range of the scaler and rate meter (2000 counts/s).

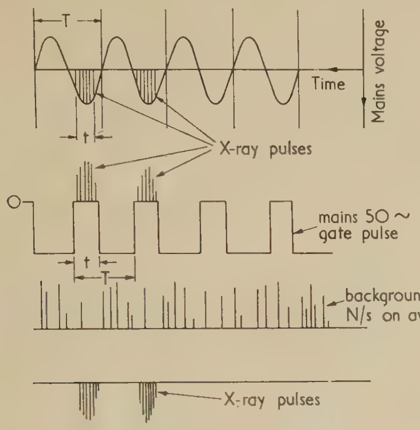

Fig. 6. Sequences of X-ray pulses, gate and background pulses

Scaling, rate meter, e.h.t., h.t. and l.t. units

The output from the pulse shaping unit is fed directly to the scaling unit type 200 (Atomic Energy Research Establishment, Harwell) and through an amplifying stage (Fig. 4) to the counting rate meter (Monitor, Radiation No. 1021, A.E.R.E., Harwell). The e.h.t. unit is also a part of the scaling unit type 200, capable of supplying both positive and negative stabilized potential with respect to earth. The h.t. power units are electronically stabilized(13) using series stabilizer and d.c. feedback amplifier, the reference voltage being derived from a neon stabilizer. The l.t. units for the high gain amplifier sections are stabilized using transistors and zener diodes.(16)

Conclusion

An account has been given of the principles governing the use of proportional counter and the electronic circuits designed for use with it in X-ray studies, where the requirements for crystallography are quite different from those for nuclear investigations The various units have been in constant use for more than five years working faithfully without failure, which indicates the stability of the entire system. The apparatus has been used for measuring the quantum efficiency of a specially designed proportional counter at various characteristic X-ray wavelengths.(11,13) The apparatus could be used for measuring the absolute intensity of the X-ray beam, for testing the efficiency of X-ray tube and for experiments where the losses due to monochromatizing filters would be excessive.

Acknowledgements

The experimental work described in this paper was carried out at Sir John Cass College, London. The author wishes to thank Mr. R. H. Humphry, head of the Department of Physics, for his interest and encouragement and to Mr. A. E. Kiss for constant help and valuable discussion during the course of the work.

References

(1) Trost, A. Z. *Angew. Phys.*, **2,** p. 286 (1950).

(2) Lang, A. R. *Nature* (*London*), **168,** p. 907 (1951).

(3) Arndt, U. W., and Riley, D. P. *Proc. Phys. Soc.* (*London*), **A65,** p. 74 (1952).

(4) Skertchly, A. R. B. *J. Sci. Instrum.*, **33,** p. 209 (1956).

(5) Lang, A. R. *Proc. Phys. Soc.* (*London*), **A65,** p. 372 (1952).

(6) Bernstein, W., Brewer, H. G., and Rubinson, W. *Nucleonics*, **6,** p. 39 (1950).

(7) Arndt, U. W., Coates, W. A., and Crathorn, A. R. *Proc. Phys. Soc.* (*London*), **B67,** p. 357 (1954).

(8) Curran, S. C., Angus, J., and Cockroft, A. L. *Phil. Mag.*, **40,** p. 36 (1949); *Nature* (*London*), **162,** p. 302 (1948).

(9) Rossi, B. B., and Staub, H. H. *Ionization Chambers and Counters* (New York: McGraw-Hill, 1949).

(10) West, D., and Rothwell, P. *Phil. Mag.*, **41,** p. 873 (1950).

(11) Kiss, A. E., and Patla, N. *Brit. J. Appl. Phys.*, **10,** p. 376 (1959).

(12) Parry, J. K., Rathgeber, H. D., and Rouse, J. L. *Proc. Phys. Soc.* (*London*), **A66,** p. 541 (1953).

(13) Patla, N. M.Sc. Thesis, University of London (1958).

(14) Van Rennes, A. B. *Nucleonics*, **10,** p. 20 (July 1952); p. 22, Aug. (1952); p. 32, Oct. (1952) and p. 50, Oct. (1952).

(15) Kelley, G. G. *Proc. Intl. Conf., Geneva*, 1955 (Paper 8/P/66) (New York: United Nations, 1956).

(16) Brown, T. H., and Stephenson, W. L. *Electronic Engng*, **29,** p. 425 (1957).

X-ray fluorescence method for determination of the transition-metal content in very small specimens of alloys

by P. J. Brown, Crystallographic Laboratory, Cavendish Laboratory, Cambridge

[*Paper received* 16 *June*, 1960]

Abstract

A method is described for the quantitative determination of the transition metal content in very small quantities of alloys containing transition metals of the first long period. The method depends upon measurement of the intensity of the fluorescent X-rays emitted by the specimen, and the results are evaluated by comparison with a series of standards. An accuracy of better than 1% *can be achieved in specimens containing as little as* 0·2 *mg of the transition metals.*

1. Introduction

This method has been developed in an attempt to remove one source of uncertainty from the interpretation of results of crystal structure determinations of transition metal alloys. Very often in such investigations, and particularly in ternary systems, crystals are extracted from an inhomogeneous alloy and there is available for analysis only a very small quantity of material with composition known to be the same as that of the crystal used for the structure determination. These quantities are seldom sufficient for chemical microanalysis, therefore if the structure analysis is to be at all complete some other method of determining the chemical composition must be found. The fluorescence spectrometer described in this paper has been developed for this purpose.

The absolute intensity of the characteristic fluorescent X-rays emitted by an irradiated specimen depends to a large extent on the spectrum of the incident radiation and the density and composition of the specimen. The form of the dependence has been investigated by Priestly.[1] This relationship, however, makes no allowance for absorption, which will be important for the longer wavelengths, and depends to a great extent on the physical state of the specimen; and it is not applicable in cases where more than one fluorescing element is present. For this reason a direct quantitative analysis has not been attempted; instead, a comparative technique has been adopted. The principle of this method is to measure the ratio between the intensities of the characteristic X-rays emitted by two fluorescing elements in the specimen, and to compare this with measurements of the same ratio made for a number of specimens of known composition in the same physical state. If only one fluorescing element is present in the alloy a known percentage of a second must be added.

2. The principle of the spectrometer

Fig. 1 shows a schematic plan of the spectrometer. The analysing crystal is a plate of lithium fluoride with faces parallel to the (001) planes; these planes are bent to the arc of a cylinder of radius $2R$ and subsequently the inner surface is ground to radius $R = 2{\cdot}25$ in. This crystal is situated at O on the circumference of the focusing circle of radius R and centre C. White X-rays from a tungsten target irradiate the specimen and a beam of fluorescent X-rays is allowed to fall on the analysing crystal. The condition for fluorescent X-rays of wavelength λ to be focused at the point B on the circle is that $B\hat{C}O = A\hat{C}O = 2\theta$ where $\lambda = 2d \sin\theta$ and $d = 2{\cdot}01$ Å [the spacing of the (002) planes in LiF]. In order to record the complete fluorescent spectrum emitted by the specimen, the detector must be driven round the circumference of the focusing circle whilst the crystal is rotated so that the normals to the reflecting planes bisect the angle between the incident and diffracted X-rays. Fig. 2 is a drawing of the spectrometer and illustrates the method by which this motion is achieved.

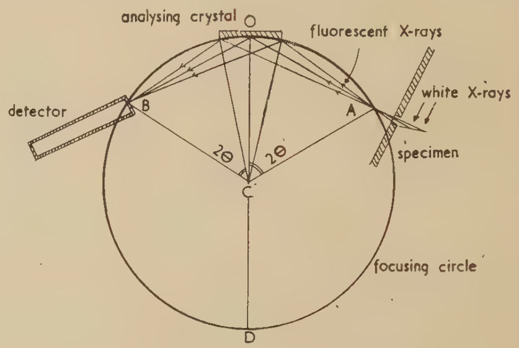

Fig. 1. Schematic plan of the spectrometer

The motors, which for simplicity are not shown in Fig. 2, are mounted on plate (2). This plate can rotate about the bed of the instrument [plate (1)] on a vertical axis through O. The analysing crystal (3) is mounted at O on the platform (4) which can also rotate about the axis through O. As angle AOB changes the block (5) slides on the rod (6) and the direction of OC is maintained as the bisector of angle AOD by means of the two equal bars (7) and (8) which are pivoted at their ends. The point C at distance R from O is the centre of the focusing circle and is linked to B by the bar (9), also of length R, and pivoted at both ends. The point B is thus maintained on the circumference of the focusing circle and is the point at which the entry slits to the detector are placed. The detector itself is mounted on the carriage (10) which can move backwards and forwards along the line OBE. The instrument is driven by means of two motors, giving a fast and a slow speed; these work through a differential to rotate the lead screw (11) and drive the nut (12) which is fixed to the detector carriage.

The position of the detector at any time is shown by a

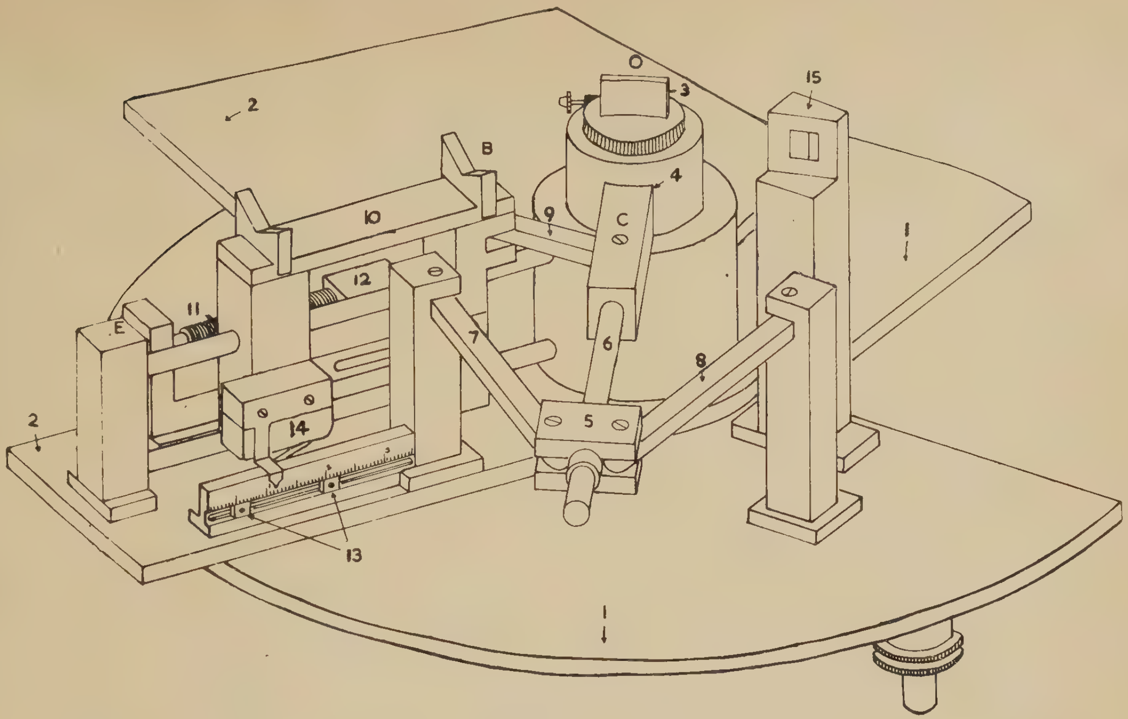

Fig. 2. Diagram of the spectrometer

pointer attached to the carriage which moves over a scale on plate (2). The positions of the detector carriage which correspond to the characteristic radiations of particular elements can be marked on this scale by fixing the stops (13) in the appropriate positions. These stops operate a micro-switch (14) attached to the carriage. Limit switches (not shown) operated by the nut (12) are fixed at either end of the lead screw to prevent over-running.

3. The detection system

The fluorescent X-rays are detected by means of an argon filled halogen quenched Geiger counter with a thin mica end window (Mullard type MX118). The stabilized e.h.t. supply is fed to the Geiger counter *via* a quench unit having a variable quench time of 100 to 250 μs. The pulse output from the quench unit is passed to a linear ratemeter and to a scaler. The output of the ratemeter can be registered on a chart recorder.

4. Adjustment of the spectrometer

Before making any measurements, the orientation of the analysing crystal must be adjusted so that the normals to the reflecting planes pass through the point on the focusing circle diametrically opposite *O*. It is convenient to adjust the crystal position using the fluorescent Kα peak from an iron specimen since the wavelength of this peak (1·94 Å) lies in the middle of the useful range of the instrument. The crystal is first set as accurately as possible by eye; then using a wide slit at the detector the approximate position of the FeKα line is found; successive reductions of the slit width are then made and each time the crystal is adjusted for maximum counting rate at the peak of the line. The last small adjustment is made by observing the change in the profile of the FeKα line with small movements of the crystal; the position giving the sharpest single peak is chosen. Finally the width of the slits is adjusted to give the best compromise between peak counting rate and resolution of the FeKα from the MnKβ line.

5. Operation of the spectrometer

The spectrometer may be used to obtain a qualitative analysis of a specimen by recording the fluorescent spectrum in a straightforward way. The detector on its carriage is driven to the end of the lead screw remote from *O* so that it accepts the longest wavelength of which it is capable; this is about 3·0 Å since for longer wavelengths the absorption in the air path is very high, and in addition the driving system becomes inefficient. The detector is then driven by the slow motor towards *O* and meanwhile the output of the ratemeter is registered by the chart recorder. The chart record so obtained shows peaks corresponding to the characteristic fluorescent radiations emitted by the specimen, and interpretation of the record is particularly easy for owing to the method of driving the spectrometer, equal distances on the chart represent equal differences in wavelength. In Fig. 1

$$OB = 2R \sin\theta \quad (R = 2\cdot 25 \text{ in.})$$

and since

$$\lambda = 2d \sin\theta \quad (d = 2\cdot 01 \text{ Å})$$

$$OB = R\lambda/d$$

therefore as the slow driving speed is $\frac{1}{4}$ rev/min, the pitch of the lead screw is $\frac{1}{32}$ in. and the speed of the chart recorder is $\frac{1}{2}$ in./min; one inch on the chart represents 0·014 Å. The short wavelength limit of the instrument is fixed by the size of the central pillar which houses the bearings; this prevents close approach of the detector carriage to *O* so that it is impossible to record wavelengths less than about 1·1 Å.

To obtain a quantitative analysis of the specimen some measurement of the intensity of the characteristic peaks must be made. This may be done in one of two ways; either the peak counting rate corresponding to each fluorescent line, or else the total number of counts registered by the scaler as the detector moves at uniform speed through the position of the fluorescent peak, may be measured. With the present instrument the latter method is preferred as it does not require the detector to be positioned accurately at the centre of the fluorescent peak. The control system for the instrument has therefore been designed to facilitate this method of measurement.

In order to measure the intensity of a particular fluorescent peak, one of the stops (13) (Fig. 2) is set at a position which corresponds to the long wavelength edge of the peak. If the motors are then started the instrument will drive itself to this position and then stop. The background counting rate in this position can then be measured. The distance over which the peak extends is found from a preliminary chart recording, and the distance through which the detector must move to record the whole peak can be set on a series of switches on the control panel; it may be any multiple up to 32 of $\frac{1}{256}$ in. (0·0035 to 0·112 Å). If the slow motor is now started the scaler will automatically count all incoming pulses until the detector has moved through the specified distance. At this stage the slow motor stops and the scaler gate is closed; if less than 10 000 counts have been recorded the fast motor will drive the detector back to the beginning of the peak and a further slow run through will be made automatically. When more than 10 000 counts have been recorded the instrument will wait at the short wavelength end of the peak so that the total number of counts, and the number of runs through the peak can be written down, and a further measurement of the background made. If the intensities of several peaks are to be measured a stop is placed at the long wavelength end of each peak.

Corrections must be made to the numbers of counts recorded for non-linearity in the response of the Geiger counter which arises from its long dead time. This is done using the method described by Cochran(2) by making measurements using different quench times.

6. Preparation of specimens

In order to obtain reproducible results when using a comparative technique of X-ray fluorescence analysis it is necessary for all the specimens compared to be closely the same in their physical state. When comparing the composition of a very small quantity of an alloy with a range of standards, a very satisfactory method of obtaining uniformity between specimens and standards is to dissolve the alloy in about two drops of a suitable reagent (one which does not contain a fluorescing element); a small piece of filter paper soaked in this solution and allowed to dry is used as the specimen. A range of standard specimens is easily produced in the same form by soaking pieces of filter paper in solutions containing the appropriate elements in known concentrations. A plan of the specimen holder which is used with this type of specimen [(15) Fig. 2] is shown in Fig. 3.

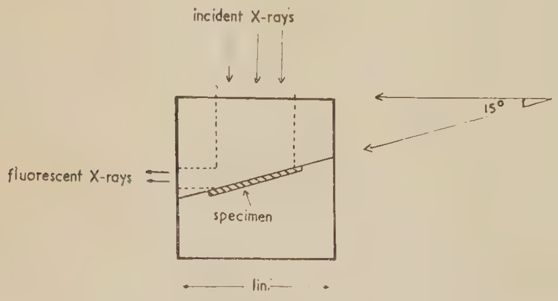

Fig. 3. Plan of the specimen holder

7. Determination of the iron to copper ratio in (FeCu)Al_6

The technique described above has been used to determine the iron/copper ratio in some specimens of (FeCu)Al_6; in all cases only a few small crystals were available for analysis.

Fig. 4 shows the ratio of the intensities of the iron and copper Kα peaks, after dead time and background corrections have been made, plotted against composition for a range of standard specimens. The ratio of iron and copper intensities measured for specimens prepared from three different samples of the ternary alloy which were obtained from different sources, are shown in the table together with the composition deduced from the calibration curve. The value found for the crystals obtained from Dr. P. Spiegelberg agrees well with the value found by Phragmen(3) using chemical methods and the cell dimensions of these crystals are those quoted in this paper. The crystals of specimen 2 were probably cored with $FeAl_3$ which explains the high iron content; those of specimen 3 had been specially selected for the absence of cores.

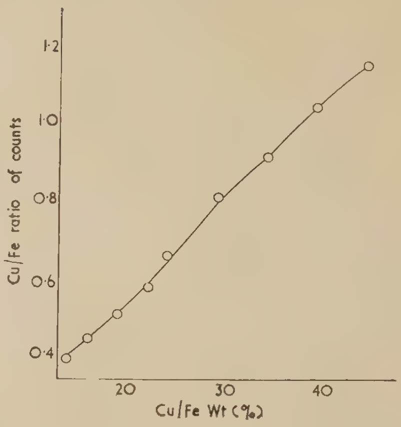

Fig. 4. Standardization curve for copper to iron ratios

Copper to iron ratios for specimens of (FeCu)Al₆

Specimen	*Source*	*Cu/Fe counts*	*Cu/Fe % by Wt*
1	Dr. P. Spiegelberg, Metallografiska Institutet Stockholm	0·961 ± 0·010	36·4 ± 0·4
2	Dr. B. Ward, Department of Metallurgy, University of Birmingham	0·515 ± 0·008	19·8 ± 0·4
3	Mrs. J. Halnan, Aluminium Research Laboratories Ltd., Banbury	0·845 ± 0·008	31·6 ± 0·4

8. Summary

The method described above can be used to measure the relative concentration of two or more metals in an alloy. The useful range of the spectrometer covers the wavelength range 1·1 to 3·0 Å and includes the Kα lines of the elements from Scandium to Germanium. The sensitivity of the instrument is such that the ratio between the weights of two metals may be determined with 1% accuracy if more than 0·2 mg of the metals is present; metals present in less than one hundredth of this quantity can be detected qualitatively.

9. Acknowledgements

I am indebted to Mr. E. F. Priestly of the A.R.D.E. for his helpful advice and also for making the analysing crystal used in the spectrometer. This research forms part of a project supported by the Air Force Office of Scientific Research of the Air Research and Development Command, United States Air Force, through its European office, under Contract No. AF 61(052)–50.

I should like to thank Prof. N. F. Mott and Dr. W. H. Taylor for provision of facilities and for their interest and encouragement. I am indebted to the Department of Scientific and Industrial Research for the award of a Research Fellowship.

References

(1) Priestly, E. F. A.R.D.E. Report (M) 1/56 (1956).
(2) Cochran, W. *Acta cryst.*, **3**, p. 269 (1950).
(3) Phragmen, G. *J. Inst. Metals*, **77**, p. 489 (1950).

LABORATORY AND WORKSHOP NOTES

Pyrolytic coating of quartz and ceramic vessels used for zone melting

by R. Beels and W. De Sutter, European Research Associates s.a., 95 rue Gatti de Gamond, Brussels 18, Belgium

[*Note received* 16 *May*, 1960]

Some metals have a very strong tendency to react with silica-containing materials like quartz or ceramics. The result is generally a contamination of the metal or the formation of a bond between the metal and the vessel with the consequence that the vessel is broken after the first melting. Generally one overcomes this difficulty by coating the vessel with a layer of "Aquadag" graphite applied as a colloidal suspension in water. But this colloidal graphite suspension is not a particularly pure substance and, furthermore, the layers are not mechanically very strong.

We have found that pyrolytic carbon gave far better results from the point of view of both purity and mechanical resistance. The process is the following: If the vessel is transparent quartz, in order to achieve good adhesion, the internal surface must be slightly abraded. This is done with an "SS. white airbrasive unit". After that, the vessel is introduced in a refractory tube heated at 1050° C. It is essential that the furnace be long enough so that the temperature along the vessel does not vary by more than about 20° C. The system is then flushed with a stream of pure nitrogen. After flushing, the stream of pure nitrogen is mixed with a stream of nitrogen having bubbled through toluene at room temperature.

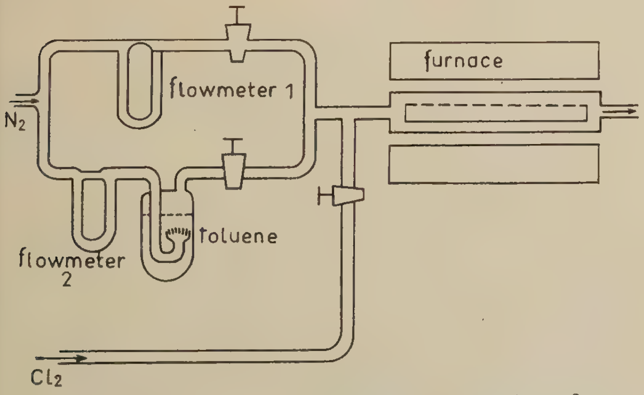

Experimental set-up for the pyrolytic coating of quartz vessels

The respective flows of gas are adjusted in such a way that one gets a mixture of 4/5 pure nitrogen and 1/5 nitrogen charged with toluene. The total flow is such that the gas velocity *inside the reaction chamber* (that is, at 1050° C) is about 40 cm/s. The total duration of one run is about ten minutes. Using this method we have obtained uniform deposits on vessels 50 cm long. After coating, the vessel may be treated at the same temperature in the same apparatus with a stream of chlorine to eliminate possible impurities. The experimental set-up is indicated by the figure.

This work is part of a research project sponsored by the Union Carbide Corporation, New York.

Furnace for the uniform heating and mixing of powders in controlled atmospheres

by H. Monk, B.Sc., and F. F. Kierys, Research Department, Imperial Smelting Corporation Ltd., St. Andrew's Road, Avonmouth, Bristol

[*Note received* 12 *May*, 1960]

Many white pigments are made commercially by precipitation from solutions and, after a preliminary drying, require a subsequent calcination stage at temperatures in the range 700–1000° C. This produces the growth in particle size which is necessary for the development of optimum pigmentary properties. Thus, lithopone and other zinc-sulphide pigments have an average size of about $0{\cdot}02$–$0{\cdot}03\ \mu$ when they are first precipitated from zinc-sulphate solution; this is much too small to produce an effective scattering of light. Calcination, under suitable conditions, increases the particle size to approximately $0{\cdot}5$–$0{\cdot}7\ \mu$ and pigmentary strength is thereby developed. Zinc and titanium oxides may also be produced by similar means.

The calcination stage of pigment manufacture is, therefore, of prime importance. One essential requirement is that the dried particles of precipitate should all be exposed to carefully controlled temperature conditions, and, hence, adequate mixing must occur during the heat treatment. Furthermore, it is frequently necessary to control the atmosphere in the furnace and, for example, provide an inert gas which will avoid any risk of oxidation taking place.

To study the effects of various calcination conditions on particle size growth and pigmentary properties, the furnace to be described was designed and constructed. It is capable of producing a pound or more of product per batch, a quantity sufficient for testing, on a small scale, in paints.

The heating chamber (Fig. 1) consists of a closed silica tube 6 in. long by 3 in. diameter, heated electrically and rotating at a speed which can be varied over the range 0–2 rev/min. The electrical connexions are made by means of copper-carbon brushes bearing on brass slip rings. A steady mean temperature is maintained by the manipulation of an energy regulator. A thermocouple, protected by a silica cap which protrudes into the heating chamber, passes through the centre of the shaft on which the furnace rotates. The gas, used to control the furnace atmosphere, passes through the annular space (Fig. 2) between the inner and outer linings of the axle shaft. It is then preheated in a silica tube located between the heating element and the outer furnace wall and enters the charge through the perforated end of the tube. Finally, spent gas escapes around the porous lid of the furnace.

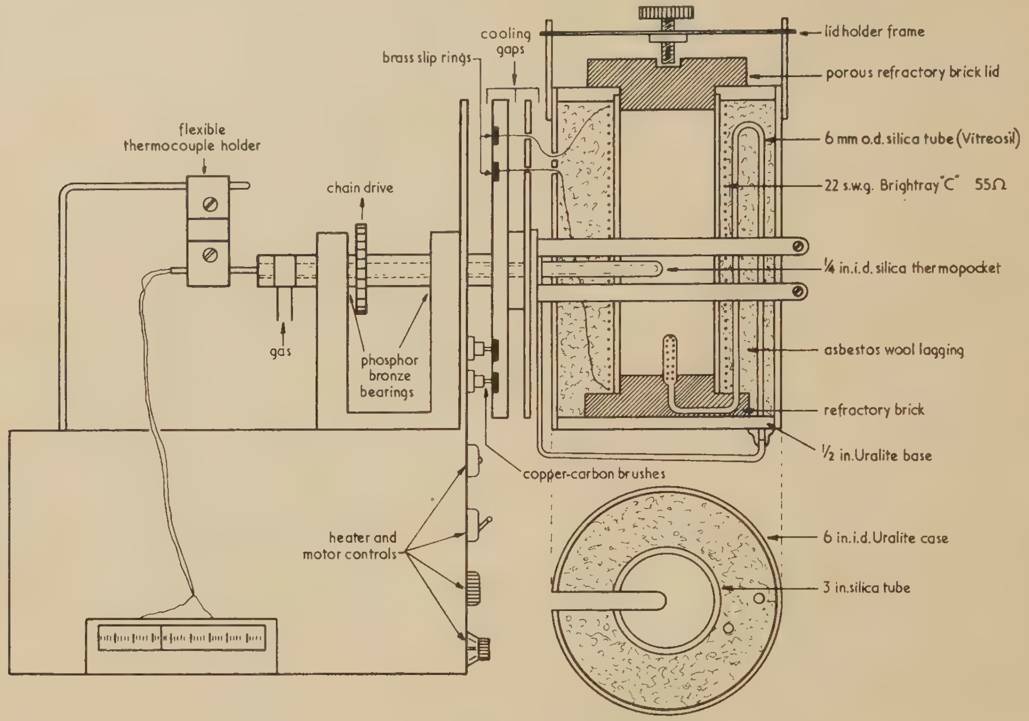
cooling gaps
brass slip rings
lid holder frame
porous refractory brick lid
flexible thermocouple holder
6 mm o.d. silica tube (Vitreosil)
chain drive
22 s.w.g. Brightray "C" 55Ω
¼ in. i.d. silica thermopocket
gas
phosphor bronze bearings
asbestos wool lagging
refractory brick
½ in. Uralite base
copper-carbon brushes
heater and motor controls
6 in. i.d. Uralite case
3 in. silica tube

Fig. 1. Rotating electric furnace

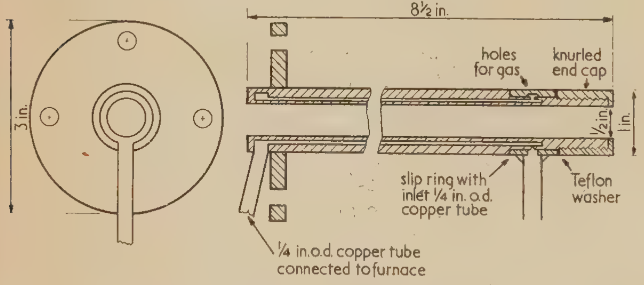
8½ in.
3 in.
holes for gas
knurled end cap
½ in.
1 in.
slip ring with inlet ¼ in. o.d. copper tube
Teflon washer
¼ in. o.d. copper tube connected to furnace

Fig. 2. Shaft for rotating furnace

When in use, the temperature in the heating chamber is adjusted to the desired level, the charge is dropped into it with the aid of a wide-necked funnel, the lid is fitted and the motor is switched on. Suitable adjustments of the energy regulator compensate for the temperature drop caused by the cold charge. In practice, it is found that the temperature has resumed its original value within ten minutes. When the calcination is complete, the hot charge is quenched in a suitable receptacle by first stopping the furnace in an upright position, removing the lid and restarting the motor at a slow speed, in order to empty the heating chamber.

It is important that the bore of the furnace should not be too small. This was demonstrated in a furnace whose bore was only 2 in. by placing a small quantity of a coloured pigment on top of the zinc-sulphide charge and observing the product after several rotations of the furnace. The defect was rectified by increasing the diameter of the lining to 3 in. The presence of small aggregates, up to ¼ in., in very fine powders proves beneficial to the stirring action.

ACKNOWLEDGEMENTS

The authors wish to express their thanks to the Directors of the Imperial Smelting Corporation Ltd. for permission to publish this information.

Frequency stabilization of klystrons

by M. J. A. Smith, B.Sc., Grad.Inst.P., Department of Physics, University College of North Staffordshire

[*Note first received* 5 *May, and in final form* 9 *June*, 1960]

This note describes a new method that has recently been designed and successfully applied to stabilize the frequency of microwave klystrons. The actual application in this particular case was to stabilize the microwave source for a high-sensitivity microwave spectrometer but since the method is very straightforward and has considerable advantages over other methods that have been previously employed it is felt that it might prove useful in a large number of other cases where frequency stabilization is required.

The methods most commonly used previously for locking a reflex klystron to a high-Q cavity, whether it is the sample cavity or an external reference cavity have been:

(1) frequency modulation of the klystron so that an amplitude modulation is produced on the microwave output from the cavity if the resonant frequency of this drifts from that of the klystron;
(2) the Pound System in which an external reference cavity is used;
(3) mechanical modulation of the cavity resonance where an output from the cavity identical to that of method (1) is obtained.

The first of these methods has the disadvantage that the microwaves are no longer monochromatic and all the output has a frequency modulation superimposed on it. The second method is somewhat complicated and requires half of the available klystron power for its operation. The third method avoids frequency modulation of the microwaves but permits only the use of an audio-frequency modulation which automatically increases the time delay between the onset of a drift and its correction.

The main features of the present method are:

(*a*) its relative simplicity;
(*b*) the absence of reflector modulation and hence frequency modulation of the main signal;
(*c*) the high-correction speed which is obtained by using 465 kc/s modulation frequencies.

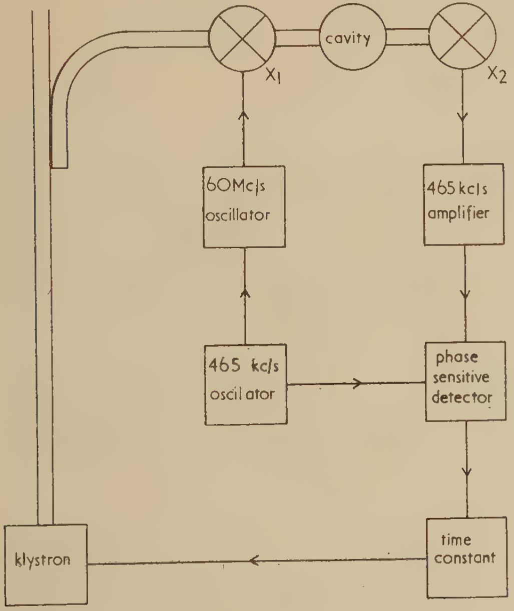

Block diagram of the klystron frequency stabilizer

The present scheme is illustrated by the block diagram shown in the figure. It will be seen from this that a fraction of microwave power is taken from the main wave-guide system by a directional coupler and passed on to a crystal X_1 placed across the wave-guide. R.F. power at 60 Mc/s is frequency modulated at 465 kc/s by two reverse-biased germanium junction diodes and is fed to X_1. By this means, frequency-modulated sidebands are produced in the microwaves without affecting the main system, provided that the directional coupler is correctly matched. The magnitude of the deviation required is one-half of the cavity bandwidth which for a Q of 6000 corresponds to three-quarters of a megacycle per second. An amount different from this reduces the accuracy of stabilization and, if smaller, the magnitude of the error signal also. The cavity is tuned to one of the sidebands and the detector crystal X_2, which is placed after the cavity, is connected to a 465 kc/s narrow-band amplifier and phase-sensitive detector. If the microwave frequency drifts, an output from X_2 is obtained, the amplitude of which is dependent on the amount of drift and the phase of which depends on the direction of drift. The sign of this phase is detected and an appropriate error signal is fed on to the klystron reflector. The correction speed is controlled by an *RC* filter connected between the phase sensitive detector and the klystron. This is a maximum when *RC* is equal to zero and corresponds to a delay of approximately 2 μs.

For the satisfactory operation of this unit, the 60 Mc/s oscillator should be carefully made to minimize drift of this frequency and therefore of the klystron. The overall stability is certainly better than 0·5 Mc/s and this can be improved further by surrounding the cavity with a constant temperature oven.

Oscillating flat-specimen holder for an X-ray powder camera*

by J. D. Wilkinson and L. D. Calvert, B.A., B.Sc., M.Sc., Ph.D., Division of Applied Chemistry, National Research Council, Ottawa, Canada

[*Note received* 27 *June*, 1960]

For some years 114·6 mm diameter Norelco X-ray cameras have been used in this laboratory with conventional powder specimens. Recently it was necessary to examine a number of flat specimens similar in composition to powder specimens previously examined. In order to compare the two sets of films directly, the specimen holder described here was designed. The holder provides positive alignment of flat-specimens, is readily interchangeable with the existing holder, and the design is applicable to any similar camera.

The holder is made from stainless steel and consists of a half-cylinder *C* (see figure) whose face *E* locates the surface of the specimen on the axis of the film cylinder. The specimen *A* is lined up by eye against the line *B* scribed on the end face of *C* and is held in place by the rubber band *D*. The collar *F* rides freely in a well in the camera and projects into the camera to prevent specimens from rubbing against the camera wall. The shaft *G* is carefully fitted ($\pm 0{\cdot}0008$ cm) to the bearing in the camera hub. After long use the tension of the drive belt tends to cause this bearing to wear unevenly so it is wise to check the bearing and rework if necessary to bring the centre of the bearing coincident with the film axis. Drum *P*, which fits freely over the camera hub, is tightly gripped by the split-cylinder *Q* to which the arm *K* is silver-soldered opposite the split. The closed end of *P* is enlarged and knurled to form a hand grip and is drilled to receive shaft *G*. The taper pin *V* locks *G* to *P* so that when the specimen is parallel to the X-ray beam the pointer *H* (screwed to the open end of *P*) is opposite zero on a scale graduated from −20 to +200°. This scale, which is omitted from the figure for clarity, is clamped rigidly to the hub of the camera. The two arms *R* and *U* are silver-soldered to opposite sides of the split in cylinder *Q*. Lever *S* is silver-soldered to shaft *T* carried between these arms. *Q* can be freed from *P* by squeezing *S* and *U* together. Before taking a photograph the angle between the surface of the specimen and the X-ray beam is set by freeing *Q* from *P* and setting pointer *H* at the required angle. The specimen is oscillated by the light plastic arm *L*, the lower end of which is drilled with a hole *M* which is an easy push fit over the wide end of the taper pin *N* driven into the existing drive pulley *O*. There are two holes *J* and *J′* in the upper end of *L* which are easy push fits over taper pins *I* and *I′* in arm *K*. When the drive pulley rotates, the two positions of *L* on *I* or *I′* provide a specimen oscillation of 10 or 20° respectively. To replace the original holder, *P* is removed from *G* by tapping out pin *V*. The total time to change holders is less than two minutes. A taper pin was chosen as the simplest way to lock *P* to *G* and to recover the original alignment after reassembly. It also minimizes the effects of wear occurring in any demountable locking system.

---

* Issued as N.R.C. Paper No. 5905.

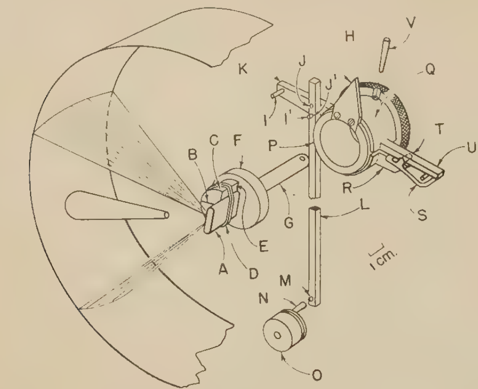

A perspective drawing of the oscillating specimen holder shown in relation to the X-ray beam and film. The camera body and angle scale are omitted for clarity. No dimensions are given since the exact values will depend on the individual camera

This holder extends the usefulness of existing cameras and provides photographs which are directly comparable with an existing library of films. It was found convenient with the specimens studied here (multi-layer oxide scales on iron alloys) to record one-half of the photograph with the specimen stationary and the other half with the specimen oscillated in order to accentuate any variations in crystal size between the phases present in the specimen. For fine-grained specimens stationary photographs are possible and the holder without the oscillating mechanism is sufficient. The oscillating mechanism can be improvised by putting a pin in the drive pulley and fastening a suitable arm on the camera pulley with plasticine. This arrangement is only satisfactory for a limited number of specimens because the angle between specimen and X-ray beam has to be set by eye. The clearances inside the camera limit the maximum dimensions of the specimen to about 3 × 2 × 1 cm, when the ordinary collimator and beam stop are used, or to 7 × 3 × 2 cm if the collimator and beam stop from a 57·3 mm camera are used. The narrow band recorded in this type of camera may not be enough for preferred orientation studies. The use of a flat plate camera is more appropriate in such cases. The angular velocity of the specimen oscillation is not uniform but this has been unnecessary for any of the samples studied here; if it were necessary the drive pin and arm could be replaced by an appropriate cam follower mechanism.

The authors wish to thank Mr. E. Niman who constructed the holder.

Editorial office—change of address

Readers are requested to note that all correspondence of an editorial nature should now be sent to the following address:

The Editor,
The Institute of Physics and The Physical Society, 1 Lowther Gardens, Prince Consort Road, London, S.W.7 (Kensington 0048).

Correspondence concerning subscriptions, missing journals, and sales of publications should continue to be sent to:

The Institute of Physics and The Physical Society, 47 Belgrave Square, London, S.W.1 (Belgravia 6111).

British Journal of Applied Physics

Contents of the October issue

CONFERENCE REPORT

Summarized proceedings of a symposium on the generation of temperatures below 1° K—London, December, 1959. By D. H. Parkinson.

PAPERS

Pre-breakdown conduction in continuously-pumped vacuum systems. By W. K Mansfield.
Use of an electrical analogue for the solution of a variety of torsion problems. By S. C. Redshaw.
Importance of insulating inclusions in arc initiation. By R. Hancox.
Measurement of convective heat transfer by means of the Reynolds analogy. By R. A. Granville and G. Boxall.
Determination of preferred orientation in polycrystalline metal foils using a sputtering technique. By R. S. Nelson.

CORRESPONDENCE

On the nature of whiskers. From A. Grohman and J. Krylow.
Dynamic measurement of elasticity using resonance methods. From G. Bradfield.

THIS *JOURNAL* is produced monthly by The Institute of Physics and The Physical Society, with the co-operation of the National Physical Laboratory. It deals with the principles, construction and use of scientific instruments. All rights reserved. Responsibility for the statements contained herein attaches only to the writers.

EDITORIAL MATTER. Communications concerning editorial matter should be addressed to the Editor, The Institute of Physics and The Physical Society, 1, Lowther Gardens, Prince Consort Road, London, S.W.7. (*Telephone:* Kensington 0048.) Prospective authors are invited to prepare their scripts in accordance with the *Notes for Authors*.

REPRODUCTION. The Institute of Physics and The Physical Society is a signatory to The Royal Society's Fair Copying Declaration. Details may be obtained upon application from The Royal Society, London, W.1.

ADVERTISEMENTS. Communications concerning advertisements should be addressed to the agents, Messrs. George Jackson (Fleet St.) Ltd., Cliffords Inn, Fleet Street, London, E.C.4. (*Telephone:* Holborn 3611–2.)

SUBSCRIPTION RATES. A new volume commences each January. The charge is £6 per volume ($17 U.S.A.), including index (post paid) payable in advance. Single parts, so far as available, may be purchased at 12*s.* 6*d.* each ($1.75 U.S.A.), post paid, cash with order. Orders should be sent to The Institute of Physics and The Physical Society, 47 Belgrave Square, London, S.W.1, or to any bookseller.

CLAIMS FOR MISSING JOURNALS. Claims from regular subscribers to this *Journal* for missing numbers will only be considered if received within 60 days of the date of mailing plus normal outward time of transit and time for lodging the claim. Losses attributable to failure to notify a change of address or to similar omissions will not be considered.

PRINTED IN GREAT BRITAIN BY UNWIN BROTHERS LIMITED, WOKING AND LONDON

Low-compliance diaphragm-capacitance gauge for measurement of liquid pressures of the order of 1 in. water

by A. S. LODGE, M.A., D.Phil., British Rayon Research Association, Heald Green Laboratories, Wythenshawe, Manchester 22

[*Paper first received* 6 *May, and in final form* 7 *July*, 1960]

Abstract

The construction of a compact "diaphragm-capacitance" gauge suitable for pressure measurement in viscous liquids is described. Sensitivities in the range 1 *to* 12 *pF/in. water are obtained by using different diaphragm units, and the overall zero stability is about* 0·002 *in. water over a few hours. The response time is about* 5 *s when the gauge is filled with a* 50 *P liquid and the outlet hole is* 0·5 *mm in diameter and* 2 *mm in length.*

Introduction

Recent rheological investigations call for the measurement of pressure distributions in flowing polymer solutions of appreciable viscosity (100 P or more). Capillary gauges have been used(1) for the purpose, but take as much as an hour to reach equilibrium, owing to the appreciable volume of liquid which has to flow (through a small hole) in response to a change of pressure. The corresponding volume of liquid is usually much less if diaphragm-capacitance gauges are used but no such gauge, commercially available or described in the literature, satisfied our particular requirements of high sensitivity coupled with low compliance (i.e. volume change for a given pressure difference), overall compactness and ability to be used when filled with liquid.

The present paper describes the construction and performance of a new diaphragm-capacitance gauge which, in comparison with a similar gauge due to Pressey,(2) has a 100 times smaller compliance and about equal sensitivity, and in comparison with a similar gauge due to Hansen,(3) has a 5000 times greater sensitivity but a 100 times greater compliance. In view of the extensive literature on the subject, the design is here discussed only briefly; special reference is made, however, to the electrode mounting and to the construction of pre-tensioned diaphragm units.

General description

The figure is a scale drawing of a central section and of an end-view of the gauge. Before use, the chamber *L* is filled through the standard laboratory gas tap *I* with the liquid under test up to the top of the small hole *A*; the tap is then closed and more liquid is poured on to the plate *B*. Any change of pressure at *A* is transmitted through the liquid in *L* and causes the diaphragm *K* to deflect and change its capacity to the electrode *D*. In our apparatus, this change of capacity was measured by a method due to Attree,(4) the output arrangement of his circuit having been slightly modified in order to reduce the sensitivity to changes of h.t. voltage. The gauge was used as a null indicator, a balancing air pressure of known magnitude being applied to the electrode side of the diaphragm by means of the tube *G*. Water near room temperature from a tank thermostatically controlled to 0·1° C or better was circulated through horizontal holes (not shown) in the plate *B* which made good thermal contact with the gauge body *M*. The air temperature in the room was also controlled to about $\pm\frac{1}{2}$° C. Ground and lapped surfaces gave liquid-tight joints between the pairs *B* and *M*, *M* and *J*; to give an air-tight joint between the body *H* and the rim of the diaphragm unit *JK*, the former was ground and lapped, the latter was lightly rubbed on fine emery paper, and a thin layer of oil was used between the two. The tap *I* was soft-soldered to the body *M*.

In the rheological measurements for which the present gauge was designed, the plate *B* formed the lower plate of a cone-and-plate apparatus similar in principle (though different in detail) to the Weissenberg Rheogoniometer.(1) A polymer solution sheared between a rotating wide-angled cone with vertical axis and the horizontal stationary plate *B* gave rise to a distribution of pressure on *B* determined by certain rheological properties of the solution. The distribution was measured by using three gauges and holes of the type described and by moving horizontally (relative to the cone) the plate *B* with its attached gauges. Similar measurements were also made with the cone replaced by a circular flat plate. Results of both measurements together with a detailed description of the rest of the apparatus are to be published elsewhere.

The response time of the gauge assembly is determined by the change of volume associated with the diaphragm movement, by the dimensions of the small hole *A*, and by the viscosity of the test liquid. The response time would be greatly increased by the presence of air bubbles in the chamber *L*; these were easily avoided in practice by filling the gauge slowly from below, using a pressure head of not more than 2 or 3 in. water so as to avoid overstraining the diaphragm. The response time could be reduced by filling the chamber *L* with a liquid less viscous than that under test, but this possibility was rejected since any such liquid to be effective would have to fill the small hole *A* and could there at the interface with the test liquid give rise to contamination and to non-negligible pressure differences associated with surface tension.

Diaphragm units. Several methods of clamping the diaphragm were tried in order to avoid the instability due to buckling which is liable to occur when thin diaphragms are clamped between flat rings. In one method, the rings were slightly chamfered (so that their surfaces were parts of cones of semi-vertical angle about 89°) in order to give the

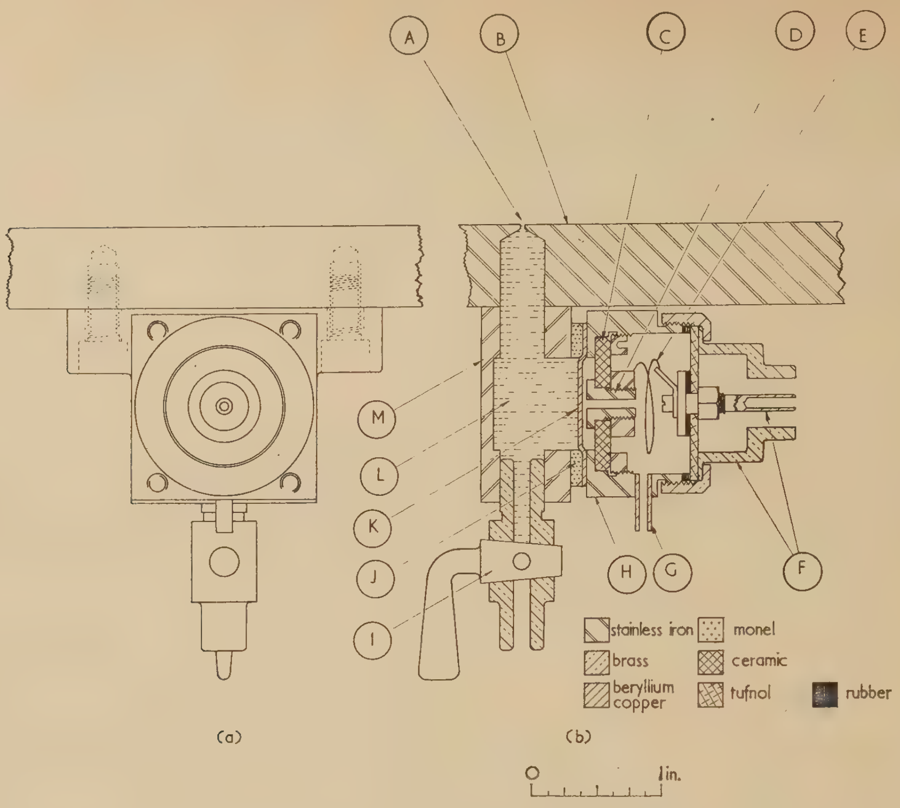

A low-compliance diaphragm-capacitance gauge

(*a*) End view. (*b*) Side view, central section. (Diaphragm thickness and diaphragm-electrode gap exaggerated)

diaphragm a slight initial curvature; in another method, a small V-groove was machined in the rings to give a slight initial tension to the diaphragm; initial tension was also given in another method by means of a third ring screwed against a diaphragm already tightly clamped between flat rings. None of these methods proved very satisfactory in the rather limited tests made of them: the disadvantages found were loss of sensitivity, leakage of liquid, and difficulty of reproducible manufacture.

Ultimately, it was found both satisfactory and simple to make up a pre-stressed diaphragm unit by soft-soldering beryllium-copper foil *K* to one side of a flat-sided monel metal ring *J*; on cooling after soldering, the foil contracts more than the ring and remains in a state of tension. Units so made are found to give adequate sensitivity and stability and moreover are robust and interchangeable. The diaphragms are invariably found to be slightly "dished" (for an unknown reason), i.e. the free part of the diaphragm lies in a plane parallel to the ring face but displaced by about 0·001 in. towards the ring. This displacement gave just about the gap required for our purposes [when the faces of the electrode and its mounting were coplanar (see below)] and no further adjustment of gap (e.g. by lapping the electrode face) was made. There was, of course, some variability between units, presumably due to differences of tension and gap, but it was not difficult to select units giving nearly the same performance: for example, three units having nearly equal sensitivities (4, 5 and 6 pF/in. water) were selected from a batch of eight units (made from foils of two different thicknesses) whose sensitivities covered a tenfold range (1·2 to 12 pF/in. water).

Electrode mounting. As was to be expected with a gap of only 0·001 in. between diaphragm and electrode, stability with regard to changes of temperature proved to be a matter of overriding importance. Of the various possible sources of thermal instability considered by Pressey[(2)] in relation to gauges of this type, the differential expansion of electrode *D*, insulator *C*, and mounting *H* appeared likely to be of greatest importance. The effect of this source was minimized by choosing metal and insulator to have linear thermal expansion coefficients as nearly equal and as low as possible and by keeping their dimensions in the direction normal to the diaphragm as small as possible. The insulator was of Frequentite (stock disks No. R. 52072 from Messrs. Steatite and Porcelain Products Ltd., Stourport-on-Severn, Worcs.) and the metal was a stainless iron of type En 56AM. After the insulator, electrode and mounting had been fitted together, the surfaces of electrode and mounting were ground flat in the same plane in order to avoid difficulties which might have arisen from lack of flatness of the ceramic member which had not been specially ground.

The electrical connection to the electrode unit was made by soft-soldering a wire *E* sufficiently fine to preclude transmission of force to the electrode from the coaxial plug connection *F*.

Gauge dimensions. It is known that a precise use of elasticity theory to design diaphragm gauges is not feasible owing to uncertainties about the boundary conditions at the diaphragm rim. Nevertheless, some use of theory is essential because gauge sensitivity changes very rapidly with change of diaphragm dimensions.

Without going into detail, we may observe that the requirements of high sensitivity and low compliance are in opposition, and can only be met by using gaps so small that thermal stability must be taken into account. Standard expressions⁽⁵⁾ for sensitivity and volume change enable one to derive inequalities which show whether any proposed values for compliance, sensitivity, electronic circuit drift and gap change (from temperature change) are mutually compatible and (if they are) enable one to choose appropriate values for the diaphragm dimensions and diaphragm-electrode gap.

The tension in the diaphragm is rather an uncertain factor, owing to possible lack of flatness before soldering and to "dishing" after soldering, but estimates of tension made with neglect of these complications on the basis of the nominal differential thermal contraction of diaphragm and ring give theoretical values for sensitivity which, on the average for twelve diaphragm units, are only twice the measured values; in these calculations the diaphragm stiffness is ignored, a procedure which is found to be justified by further calculation which showed that sensitivities calculated for a stiff diaphragm with zero tension proved to be 10 to 100 times greater than those observed.

The final dimensions are: diaphragm diameter 0·709 in. (1·8 cm); diaphragm thicknesses 0·002 in. and 0·0007 in.; diaphragm-electrode gaps about 0·001 in.; electrode diameter 0·4 in. (1·0 cm).

The overall size of the gauge is such that three gauges can just be accommodated on the same plate when mounted directly below collinear holes A_1, A_2, A_3 such that $A_1A_2 = 1$ in., $A_2A_3 = 1 \cdot 75$ in.

Performance

The overall performance is such that a pressure of 0·1 in. water can be measured reproducibly to about 1% or 2% accuracy. The detailed performance is given in the table below for a typical set of four units selected (for brevity) out of a batch of twelve, together with comparative performance figures for the gauges of Hansen⁽³⁾ and Pressey.⁽²⁾

Zero stability. About 0·001 or 0·002 in. water over a period of hours.

Hysteresis. 0·005 in. water at 10 s and 0·001 in. water at 60 s after release of pressure of 1 in. water applied for 3 min.

Linear range. ½ to 1 in. water for linearity to within 2%.

Capacity. Gap: 20 to 40 pF; stray, 6 to 7 pF.

Dynamic temperature coefficient. About 0·5 in. water/° C/min for gauge filled with 50 P liquid to outlet hole 0·5 mm diameter and about 2 mm long; no detectable coefficient for gauge filled with air.

In this table, the gap was calculated from the measured capacity and the compliance was calculated from the measured sensitivity, using formulae appropriate to a stretched membrane of zero stiffness. The linear range quoted is that of the gauge alone; the Attree circuit has a smaller linear range.

The rather high sensitivity of the gauges to *changing* temperatures is presumably due to liquid expansion giving rise to a transient pressure as the liquid flows through the small hole. Through an oversight, the volume of the liquid-containing chamber *L* was made larger than it need have been; it is estimated that (by suitable redesigning) this volume could be reduced about seven times, which would be expected to result in a similar reduction in the dynamic temperature coefficient. Despite this sensitivity, it was found possible to keep the plate and gauge temperature sufficiently constant to give the overall zero stability recorded above.

It is perhaps of interest to remark that the observed zero stability (0·002 in. water) implies a constancy of gap near the centre of the diaphragm to within 7 to 40 Å.

Detailed performance of gauge for typical set of four units

Gauge no.	*Diaphragm unit no.*	*Diaphragm thickness (in.)*	*Diaphragm-electrode gap (in.)*	*Sensitivity (pF/in. water)*	*Equilibrium temperature coefficient (in. water/° C)*	*Compliance (cm⁵/dyn × 10⁸)*
2	12	0·002	0·0012	0·6	—	2
5	7	0·002	0·0008	3·6	0·022	4
4	6	0·0007	0·0006	4·7	0·016	3
6	11	0·0007	0·0009	6	0·035	9
Hansen		0·014	0·0006	0·001	—	0·025
Pressey		0·010	0·004	6	0·0014	320

Acknowledgements

I would like to express my thanks to the following: Messrs. Steatite and Porcelain Products, for samples of Frequentite disks; Messrs. Johnson Matthey, for a sample of 0·002 in. Be–Cu foil; Vacuumschmelze A.G., Hanau, Germany, for a sample of 0·0007 in. Be–Cu foil; Mr. R. E. Blakeley and Mr. J. Baker for assistance in design and drawing; Mr. G. Berry and Mr. D. F. Williams for machining; Dr. D. W. Saunders for advice, and to Mr. N. Adams for measurements.

References

(1) Weissenberg, K. *Nature*, **159**, p. 310 (1947).
Roberts, J. E. *Proc. 2nd Int. Cong. on Rheology*, p. 91 (London: Butterworths Scientific Publications, 1954).

(2) Pressey, D. C. *J. Sci. Instrum.*, **30**, p. 20 (1953).

(3) Hansen, A. T. *Acta Physiologica Scand.*, **19**, Suppl. 68 (1949).

(4) Attree, V. H. *Electronic Engng*, **24**, p. 284 (1952).

(5) Lilley, J. C., Legallais, V., and Cherry, R. *J. Appl. Phys.*, **18**, p. 613 (1947).

Lens mass-spectrometer leak detector

by D. COSSUTTA, Dipl.Ing.,* and W. STECKELMACHER, B.Sc., F.Inst.P., Edwards High Vacuum Ltd., Manor Royal, Crawley, Sussex

[*Paper first received* 28 *March, and in final form* 13 *July*, 1960]

Abstract

A new mass-spectrometer leak detector was investigated based on the use of an iron-shrouded axially symmetrical magnetic lens for focusing ions in the low mass range. By taking precautions to keep the hydrogen background at a low and stable level (by the use of a mercury-vapour pump, liquid-air traps and clean construction) it was possible to use hydrogen as a search gas. Leaks of 5×10^{-10} *torr litre/s corresponding to an indication of a change in ion current reading of about* 3×10^{-13} *A (for hydrogen) were consistently detected with an almost instantaneous response when testing equipment of a few litres volume using either hydrogen or helium as search gas. Some measurements of the mass spectrum obtained with this instrument are given. A very reliable and convenient version of a compressed-powder leak is also described.*

Introduction

Leak testing is important whenever equipment is constructed which must be gas or liquid tight, and is of special significance in the operation of all kinds of vacuum plant. With the recent interest in the large-scale applications of very low pressures has come the demand for testing to more and more exacting specifications of tightness. Leak-test methods based on the use of search gases have the advantage that the leak-proving test can be very simply followed by a leak-location test.(1, 2) Of the different search-gas methods, the mass spectrometer leak detector is the most sensitive. This is due to its ability to measure very small changes in the partial pressure of search gas. There now exists an extensive literature covering different designs, methods of use and applications.(11–18, 20–30)

Various principles have been employed to separate and detect gases in a mass spectrometer, one of the most straightforward relying on the deflexion of ions in a uniform magnetic field.(3, 4) Gas is ionized in an ion source and the ions are projected into the magnetic field of the analyser through 30, 60, 90 or 180 deg. according to the magnet system employed.

In a uniform magnetic field, the ion beam is focused in the plane perpendicular to the magnetic lines in the direction of the collector electrode. There is no focusing in other planes. Mass spectrometers have been described in which this limitation is overcome, for example, by using specially shaped magnet pole pieces. The prevailing tendency has been to reduce the focusing error of simple directional focusing fields or to obtain some re-focusing action in the plane perpendicular to that previously mentioned. In this way a better resolving power at a given sensitivity, or *vice versa*, is obtained depending on the application. In mass-spectrometer leak detectors, an increase in sensitivity at the expense of resolving power is preferred.

It is also known from the literature on β-ray spectrometers(5) that helical spectrometers, in which the focusing action is based on the use of an axially symmetrical magnetic field, have a higher transmission figure for a given resolution than "flat" spectrometers based on a uniform-field focusing system. This feature is naturally an advantage in the design of high-sensitivity leak detectors.

Magnetic lenses, although extensively used in electron optics, are rarely used in ion optics.(6) However, M. V Ardenne(7) describes the use of a magnetic lens in an ion monochromator for deuterons. Magnetic lenses of the axially symmetric type have not previously to our knowledge been used as analysers in mass spectrometers or leak detectors. A successful leak detector using this principle was completed in 1958(8) using hydrogen as search gas and some of its features and experimental results are here reported.

The mass spectrometer consists essentially of an ion source assembly *IS*, a magnetic lens and a collector assembly *C* as shown in the schematic diagram in Fig. 1. Search gas applied to the leak will pass into the ion source, where it is ionized by collision with electrons emitted from the hot filament. The ions are accelerated and projected into the lens. For various ions of mass m and ion accelerating voltage V volts it is possible to calculate the focusing condition. The following expression may be used to calculate the focal length (in cm) of a simple lens having an internal bore diameter D cm:

$$f = mVD(IN)^{-2} \times 8\cdot 87 \times 10^{4}, \qquad (1)$$

where IN is the number of ampere turns of the lens coil. It is seen that with fixed ion accelerating voltage V and lens current I, ions of increasing mass come to a focus in succession at increasing distances along the lens axis, the distance between the different mass foci decreasing with increasing mass number. The best resolution is obtained at the shortest focal lengths corresponding to ions of small mass such as those of hydrogen and helium and these gases are therefore preferred as search gases.

To a fixed value of the lens field strength corresponds a certain value of ion accelerating voltage for which the search gas ions will be focused onto the ion collector electrode. An essential feature of this method is a baffle in the centre of the lens to screen the collector from all relatively undeflected ions of other gases.

When search gas is applied to a leak it will therefore be indicated by an increase in the collector current. This current may be measured by a sensitive d.c. amplifier (preamplifier *Pr* and amplifier *A*) and observed on the leak indicator *RI* which may be mounted remotely to suit the operator.

---

* Now at 20th Century Electronics Ltd.

Description of the mass spectrometer leak detector

Referring to Fig. 1, the equipment to be tested (E) is attached to the input port IP. The equipment under test can be isolated from the leak detector by the isolation valve V. The trap T_1 is connected between the isolation valve and the ion source of the mass spectrometer. The purpose of this is to protect the ion source from contamination of condensable gases and vapours possibly evolved from the equipment. The calibrated leak RL which is used for checking the sensitivity is connected to the mass-spectrometer system between the valve V and the trap T_1.

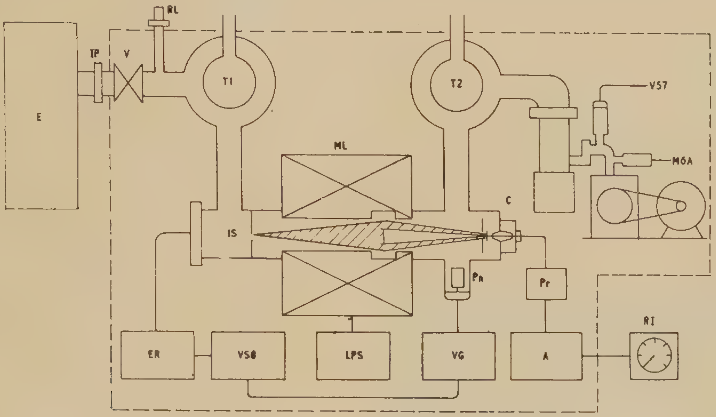

Fig. 1. Schematic diagram of leak detector

The pumping system of the mass spectrometer consists of a liquid air trap T_2, mounted directly on top of a 30 litre/s mercury-vapour pump which is backed by a single-stage gas-ballasted rotary pump.

The vacuum in the spectrometer is measured by a Penning vacuum gauge. A Pirani gauge head and a discharge-vacuum switch head are mounted in the backing line to indicate the backing pressure, and to switch the vapour-pump heater on or off according to the pressure in the line. The pumping system is thus fully protected in case of a sudden rise of pressure or mains failure and the filament in the leak-detector ion source is protected by a Penning relay unit PR.

Ion source assembly

A simple ion source designed for use with the lens leak detector is shown in Fig. 2. In the centre is situated a wire-gauze box on the two opposite sides of which are filaments with shields attached on one end of each filament support. In operation one filament only is operated. Although the filament is protected by the Penning relay unit, it has a limited life and will require periodic replacement. Therefore, the second spare filament has been fitted which may be brought into use when required.

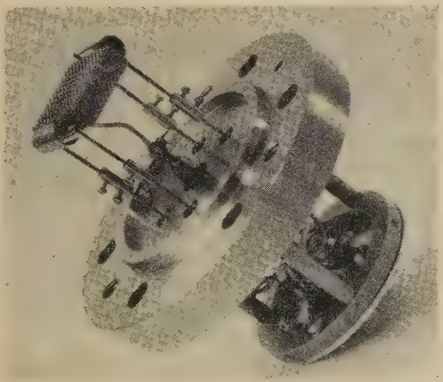

Fig. 2. Photograph of simple ion source

The ions are produced in the wire-gauze box and accelerated by the potential applied between the latter and a plate with a circular hole in the ion-source housing. Two small permanent magnets fixed outside the housing serve to collimate the ionizing electron beam in the centre of the box from one filament to the other. An electron accelerating voltage of 65 V was found to be satisfactory.

Magnetic ion lens

The lens used in this work, together with the ion source and collector-electrode assembly, is shown in Fig. 3. The lens coil is fully shielded by a mild-steel casing except for an internal axial gap where the whole magnetic field is concentrated. The distance from the ion source to the centre of the lens is equal to the distance from the centre of the lens to the collector, that is, the magnification of the lens is unity. The lens was designed primarily for focusing hydrogen ions at some 300 V and for this purpose a field of the order of 2000 G was required in an axial gap of 20 mm. To collect any undeflected ions, a cup-shaped baffle was supported in the centre of the lens by thin wires.

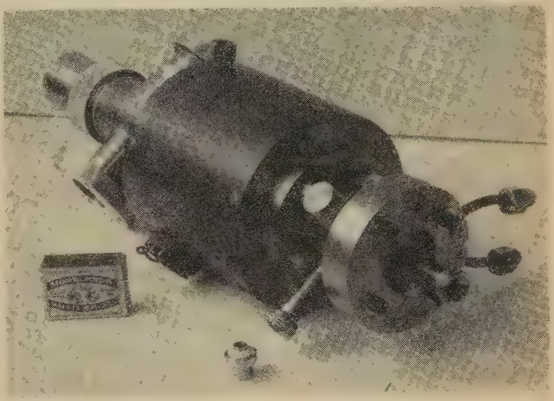

Fig. 3. Photograph of ion source, lens unit and ion collector assembly

Collector assembly

A simple collector electrode was used to begin with but it was found that considerable improvement was obtained by mounting a suppressor electrode system in front of the collector. The electrodes of the suppressor system are made with circular holes instead of the system of slits usually used in uniform-magnetic-field instruments. The suppressor electrode itself was connected to a positive potential of the same value as the wire gauze box in the ion source.

Electrical supplies

As seen from the photograph (Fig. 4), all electrical supplies and circuits were mounted on a drawer accessible from the front of the unit. All circuits have been kept as simple as possible bearing in mind the stability required in the face of possibly relatively large mains fluctuations when used in some industrial applications.

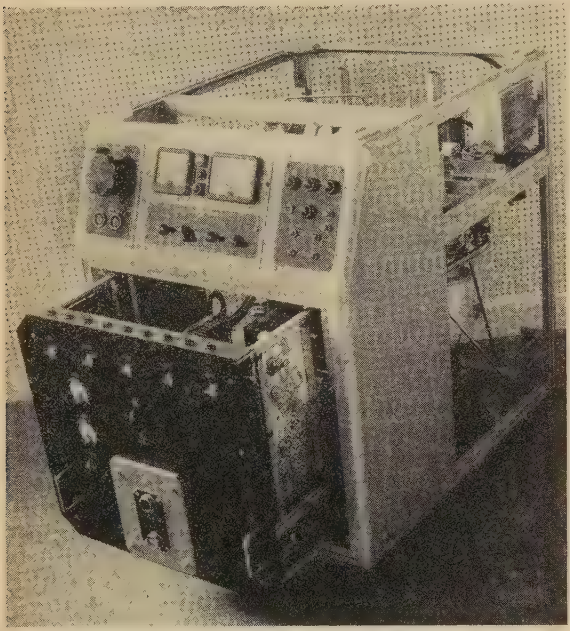

Fig. 4. Photograph of prototype mass spectrometer leak detector

The lens was supplied by a simple current stabilizer *via* a series-connected power valve. The lens current was applied to a precision resistance and the resulting voltage compared with a reference voltage. The series valve was controlled by a degenerate difference amplifier so that the lens current was held to within $\pm 0{\cdot}1\%$.

The electron emission in the ion source was stabilized by a modification of a circuit described in Ref. 9, and shown schematically in Fig. 5. The filament was supplied from the transformer T_1 the primary windings of which were controlled by the double-triode power valve V_1. The voltage on the preset variable resistance RV_1 is proportional to the electron emission current and is compared with the voltage derived from the stabilizing tubes V_2 and V_3. The power valves are controlled by the degenerative difference amplifier V_4. The setting of RV_1 determines the actual emission current to be stabilized (range 1–10 mA), whereas RV_2 determines the ion accelerating voltage.

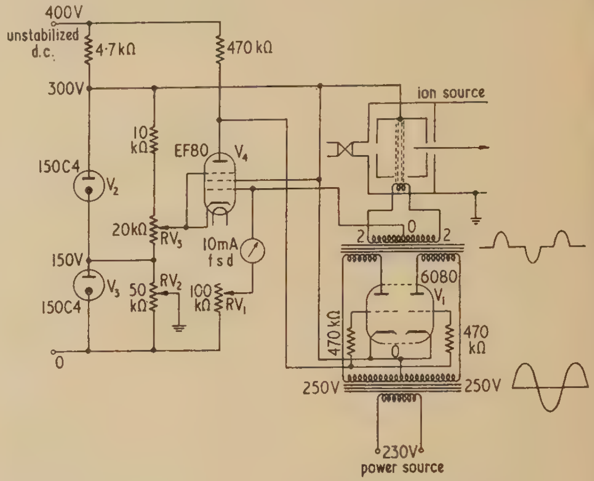
400V
unstabilized d.c.
4·7kΩ
470 kΩ
300V
ion source
10 kΩ
EF80
V4
150C4
V2
20kΩ
RV3
10mA f s d
150V
V3
50 kΩ
RV2
100 kΩ
RV1
150C4
0
2
0
2
6080
V1
470 kΩ
470 kΩ
250V
250V
230V
power source

Fig. 5. Schematic circuit of emission control unit

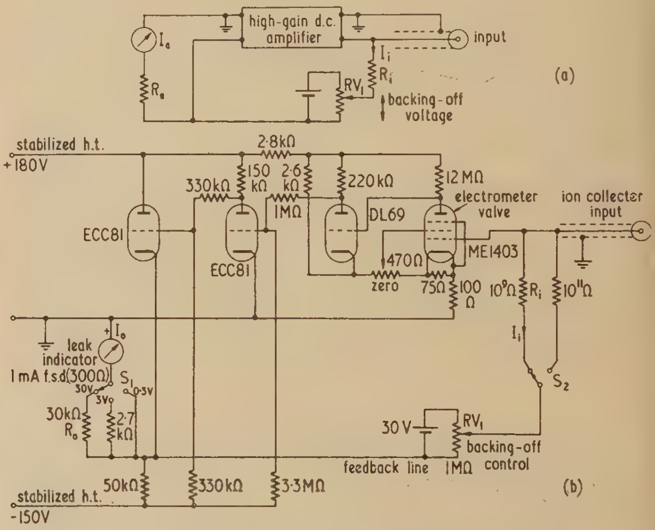
high-gain d.c. amplifier
I0
input
Ii
Ri
RV1
R0
backing-off voltage
(a)
stabilized h.t. +180V
2·8kΩ
330kΩ
150 kΩ
2·6 kΩ
1MΩ
220kΩ
12 MΩ
electrometer valve
ion collecter input
ECC81
ECC81
DL69
ME1403
470Ω
zero
75Ω
100 Ω
10⁹Ω
Ri
10¹¹Ω
leak indicator
1 mA f.s.d(300Ω)
I0
S1
30V
3V
0·3V
30kΩ
R0
2·7 kΩ
Ii
S2
30 V
RV1
backing-off control
feedback line
1MΩ
50kΩ
330kΩ
3·3MΩ
stabilized h.t. -150V
(b)

Fig. 6. (*a*) Block diagram of feedback d.c. amplifier
(*b*) Schematic circuit of d.c. amplifier

The d.c. amplifier is shown schematically in Fig. 6(*a*) and (*b*). A preamplifier can be placed in close proximity to the ion collector containing the electrometer valve together with two remotely switched input resistances of 10^{11} and $10^9\ \Omega$. With 100% negative voltage feedback, the electrometer grid operates virtually at a fixed potential even at relatively high input currents. Hence, in Fig. 6, the voltage developed at the input resistance R_i is repeated at the meter series resistance R_0 and

$$I_0 = I_i R_i / R_0.$$

With a suitable choice of R_0 ion currents ranging from 3×10^{-8} to 3×10^{-12} A for full-scale deflexion of the meter could be measured.

Steady background currents could be backed-off by injecting an inverse voltage into the feedback line as indicated by RV_1. This facilitates the measurements of small changes in ion current in the presence of relatively high, steady background currents.

The leak-indicating meter together with S_1, S_2 and RV_1 were mounted in a portable indicating unit so that leakage could be observed from any convenient position.

Experimental results

The focusing conditions for H, H_2, He and H_2O ions were calculated according to equation (1) and the required lens current plotted as a function of the ion accelerating voltage as shown in Fig. 7. The values determined experimentally for these ions are also indicated. It will be noticed that the focal lengths obtained experimentally are somewhat smaller than the calculated values, the differences being in some cases up to 10%.

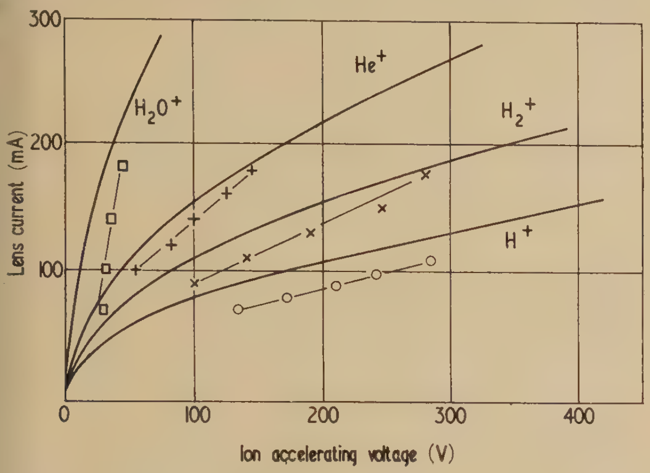

Fig. 7. Focusing conditions for H, He and H_2O. Lens current plotted against ion accelerating voltage

To determine the distribution of ion density in the plane of the collector electrode, a collector system consisting of eight concentric ring electrodes was used. The latter is shown in Fig. 8 and a diagram illustrating the density distribution with focusing conditions set for H_2 ions is given in Fig. 9.

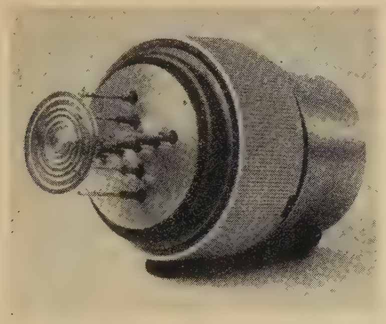

Fig. 8. Experimental collector system used to determine distribution of focused ions

The dimensions of the concentric ring electrodes are shown under the ordinate. The broken curve represents the H_2^+ background and the full-line curve the response to hydrogen when this was introduced into the ion source *via* a leak of 10^{-5} torr litre/s. Although the ion-source exit hole was relatively large in order to obtain high sensitivity, the focusing action can be considered well pronounced. On the central collector electrode (2 mm dia.) the current density of the focused H_2 ions is about 13×10^{-9} A/mm². The ions collected on the concentric electrodes away from the centre consist of scattered ions of H_2^+ in addition to unfocused ions of other gases such as H^+, H_2O^+.

The amplifier showed very good performance and stability. After a brief warming-up period, the short-term stability was better than ±1 mV on the most sensitive range (corresponding to an input-current stability of better than $\pm 10^{-14}$ A). A similar amplifier with an input resistance 10 times higher than in this leak detector has been used satisfactorily for experimental work, but at present (see discussion below) the additional sensitivity obtained could not generally be exploited in industrial leak detection.

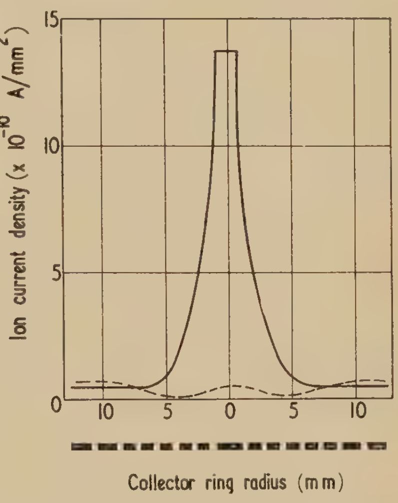

Fig. 9. Plot of ion distribution measured at special collector system

A typical background spectrum of the leak detector is shown dotted in Fig. 10. The measurements were taken at a constant lens current of 120 mA by varying the ion accelerating voltage, and they indicated the presence of water and

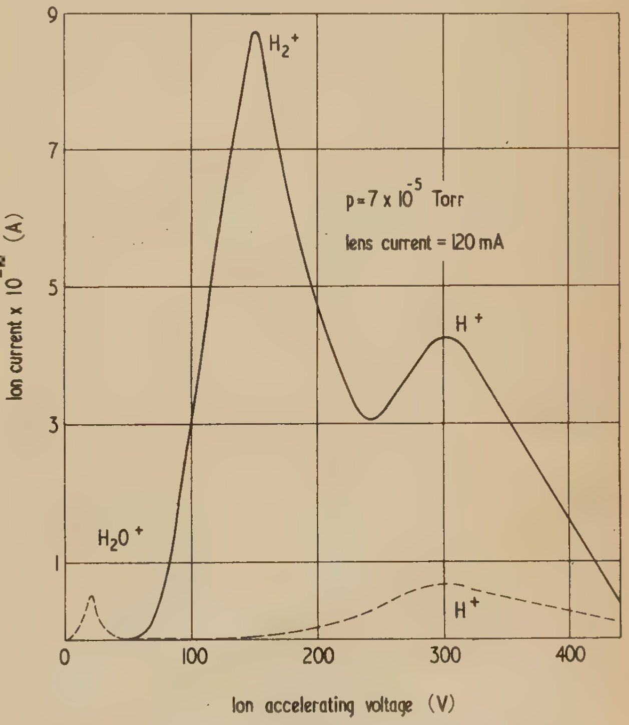

Fig. 10. Typical background spectrum

H^+ ions. The peaks were broad, as would be expected from an instrument designed for high sensitivity rather than high resolution. The background current at the accelerating voltage corresponding to the focusing condition for H_2 ions was usually found to be of the order of 10^{-11} A, while the stability of the ion current was of the order of $\pm 1 \times 10^{-13}$ A. The relatively high hydrogen background as such is not disturbing as long as it is at a steady level and the amplifier indicating the ion current contains a backing-off facility to reduce steady readings to zero.

When hydrogen is applied to a leak connected to the ion source a response is obtained as indicated by the full line in Fig. 9. It can be seen that the H^+ peak also increases to about a third of the H_2^+ peak. A response would also be obtained with helium when focusing this gas according to the conditions shown in the diagram in Fig. 7.

The advantage of hydrogen compared with helium (widely used for leak detection with the mass spectrometer) is its availability and lower cost. A disadvantage generally put forward is that it is present as background in a vacuum system and is formed in the spectrometer ion source as a breakdown product of hydrocarbons and water vapour especially when these come into contact with the spectrometer filament. Special precautions have therefore been taken in the construction: the vapour contamination from the equipment under test is kept out of the spectrometer by a liquid-air trap in the inlet line to the ion source, the ion-source construction is "clean" in that organic materials are avoided and the demountable seals use metal foil gaskets.(10) Finally, the mass-spectrometer pumping system is based on a mercury diffusion pump with its own liquid-air trap resulting in a significantly lower hydrogen background.

Sensitivity of the leak detector

The maximum sensitivity of the leak detector is at present of the order of 5×10^{-10} torr litre/s corresponding to a meter deflexion of about 3×10^{-13} A. It should be noted that this current is some 100 times higher than is usually obtained with other mass spectrometers(11–17) and therefore the amplifier sensitivity requirements at this order of leak are not too exacting. Alternatively, this would suggest that with a more sensitive amplifier it would be possible to have a more sensitive leak detector. However, as with any such device, the limitation of sensitivity is due to the presence of background fluctuations which in the present instrument may give rise to currents of the order of 1×10^{-13} A. It is hoped that the background fluctuations can be further reduced so that the sensitivity of the leak detector could be readily increased.

With helium, the sensitivity was about half that for hydrogen. Normally the background stability is, however, greater in the mass-4 region so that with helium the limiting sensitivity is about the same, and the required ion accelerating voltage is half the value of that for hydrogen. However, the instrument could not be used with other search gases as these have a much greater mass number and with a reasonable value of accelerating voltage a very powerful magnetic field would be required for their satisfactory focusing. With the source and collector electrode designed for high resolution, a more powerful lens would undoubtedly give a more complete spectrum covering a number of gases in the low mass range, but the quality of the spectrum would probably be worse than that obtainable with the more conventional uniform magnetic-sector-field mass spectrometer.

Calibration of leak detector

A useful method of calibrating the leak detector is to compare its response with that obtained when search gas is applied to a calibrated reference leak. Reference leaks may be independently calibrated in terms of their flow rates. In making a reference leak, the nature of the leakage path has to be considered, for the search gas has to displace the air initially filling the leak or diffuse through this air before it can enter the vacuum system. The response time of the leak is the time which elapses until the detector responds to the application of search gas to the leak and is largely determined by the nature of the leak. Obviously reference leaks are preferred which have a reasonably short response time. Another difficulty is that leaks exposed to normal atmospheric conditions may be blocked by dust particles, particularly if there is only one leakage path, and leaks may require frequent re-calibration if this is suspected. A leak using a compressed or sintered powder has the advantage that it consists of a number of leakage paths in parallel and therefore generally has a greater stability and longer life. Our experience in the construction and performance of an easily reproducible reference leak may therefore be of some interest. It is difficult to make leaks having small leakage rates which at the same time have the desired properties of stability, long life and short response time. It is therefore of advantage to make leaks of comparatively large leakage rates and use the linear response of the mass spectrometer so that leaks of widely dissimilar flow rates may be compared. The larger sized leaks also have the advantage that their performance at any time may be readily checked using a simple pressure-rise test.(18)

A small quantity of a metal powder mixture was placed into a $\frac{1}{16}$ in. demountable vacuum union linear and compressed using the special jig shown in Fig. 11. The leakage rate could be adjusted by the degree of compression employed and with a metal powder susceptible to cold welding a sufficiently coherent mass was obtained so that the jig could be removed after compression leaving a porous disk inside the vacuum union connexion. In this way leaks could be made covering leakage rates of 10^{-6}–10^{-4} torr litre/s. Provision was made to have such a leak connected permanently to the input of the leak detector. In practice, these leaks were found to have a good long-term stability and life. Of a batch of 25 leaks, about 70% have continued

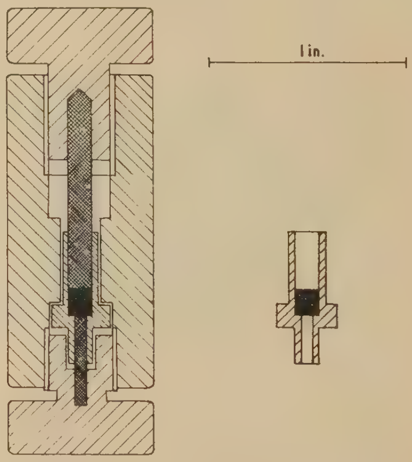

Fig. 11. Sectional diagram of reference leak and special jig used in compressing powder

o give good service after six months of day-to-day use and did not change in value while the other 30% were blocked after two to three months of use. Damp atmosphere does not seem to have any effect on the leaks. This was also shown experimentally by pumping moist air through a reference leak for 24 hours after which no change in the leak value could be observed.

Discussion

The relatively high output current at the ion collector for small leakage rates at the input of the leak detector (that is, 3×10^{-13} A for a leak rate of 5×10^{-10} torr litre/s with hydrogen as search gas) can be shown to be due to a number of factors of which the following are the most important*:

1. In this detector, all the search gas applied to the leak passes through the ion source and is available for ionization. Some other leak detectors are fed into the vacuum line between the equipment under test and the pump so that a proportion of search gas may be pumped away and lost.
2. The ion source has a relatively large exit aperture of 5 mm diameter.
3. The relatively high transmission figure of the symmetrical axial lens system as compared with the more conventional uniform magnetic field instruments.
4. The exit aperture in the ion source also acts as a throttle in the pumping line with the effect that the pressure in the ion source is increased while maintaining a relatively low pressure in the analysing section. This is preferable to restricting the pumping in the whole mass spectrometer as is sometimes advocated (see, for example, Ref. 11). To decide on the optimum degree of throttling, a compromise has to be made between high sensitivity and a reasonably fast response time. The response time also depends in the usual manner on the volume of the equipment under test. The above figures relate to testing vessels up to a few litres internal volume when an almost instantaneous response is observed on the leak indicating meter. For testing equipment having a very large volume, the backing-space technique may be used with advantage, involving an auxiliary pumping system. In this case, a high-speed mercury-vapour pump is interposed between the equipment under test and the mass-spectrometer inlet, and a fast response is then obtainable with equipment having relatively large volumes.

An examination of the actual contribution of each of these factors to the leak conversion factor* found with this instrument will be dealt with in an investigation to be published later. In any case, there is at present insufficient data on the detailed performance of other mass spectrometers to make any very definite comparisons in this respect.

Axially symmetrical ion sources of a different design were also tried. Of the two designs shown schematically in Fig. 12, type (*a*) was found to be the more satisfactory. The direction of the electron beam relative to the ion beam is different in these two types. The application of an axial-type ion source is of special interest if a permanent magnet lens is used for ion focusing. In such a case, the stray field of the permanent magnet lens is sufficiently strong and in the required direction to collimate the electron beam so that no additional source magnets are required. These simple sources were not investigated sufficiently to give a complete explanation of their performance and more work is planned in the future. However, it would appear that simple axial ion sources of this type do not produce sufficiently mono-energetic ions, and it is intended to consider a more complicated design. (A number of possible designs have been described elsewhere.(6, 19))

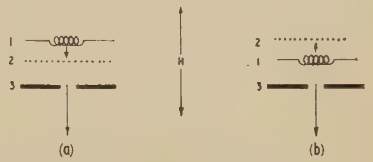

Fig. 12. Diagram of axially symmetrical types of ion sources

It is evident from the above formula [equation (1)] that, with a set lens current and ion accelerating voltage, ions of different mass are focused in succession along the lens axis with decreasing distances between the different mass foci. It should therefore also be possible to collect, for example, two different ion masses (providing the mass numbers are low enough) with two collectors at their respective foci along the axis. However, in any such application, the use of a baffle in the form of a cup to collect any undeflected ions in the centre of the lens would be an essential feature. This may also be worthwhile investigating.

Finally, a leak detector having a higher sensitivity is always of interest and this is mainly a matter of reducing the background fluctuation since it is easy to use greater amplification for the output signal. It is hoped that the use of high-quality mono-energetic ion sources in connexion with suitably positioned baffles may give a further increase in sensitivity. There is undoubtedly scope for further extensive investigation, and this work can therefore by no means be considered complete. However, a number of leak detectors designed according to the simple lines indicated have already given valuable service in routine testing to a consistently high standard.

From the operational experience gathered over the last year it appears that these leak detectors required little maintenance, showed no change in performance and could be readily operated by ordinary test staff.

Acknowledgements

We would like to acknowledge the help given by Mr. D. Tinsley and Mr. H. Wingate in much of the experimental investigations, Mr. T. Chapman for his help in the mechanical work and the many others in the Instrument Division who have made contributions to the final design. We would like to thank Mr. F. D. Edwards, Managing Director of Edwards High Vacuum Ltd., for encouragement and permission to publish this work.

References

(1) Steckelmacher, W. *Nuclear Engng*, p. 450 (1959).
(2) Cross, S. H., and Steckelmacher, W. *Research*, p. 124 (1956).
(3) Barnard, G. P. *Modern Mass Spectrometry* (London: The Institute of Physics, 1953).

---

* The ratio of leakage rate to ion current (that is, $1{\cdot}67 \times 10^3$ torr litre/s A in this case) could be termed the "leak conversion factor" of the instrument. This should be distinguished from the "sensitivity" of the detector, a term usually used to denote the minimum detectable leakage rate in the presence of a general noise level (caused by instrument or "background" fluctuations).

(4) WALDRON, J. D. (Edited by). *Advances in Mass Spectrometry* (Proceedings of Conference, London, 1958), (London: Pergamon Press, 1959).
(5) PERSICO, E., and GEOFFRION, C. *Rev. Sci. Inst.*, **21**, p. 945 (1950).
(6) ARDENNE, M. V. *Tabellen der Elektronenphysik, Ionenphysik und Uebermikroskopie, Band* 1 (Berlin: VEB Deutscher Verlag, 1956).
(7) ARDENNE, M. V. *Phys. Z*, **43**, p. 91 (1942).
(8) *Handbook of Scientific Instruments and Apparatus*, p. 324 (London: Physical Society, 1959).
(9) STECKELMACHER, W., and VAN DER MEER, S. *J. Sci. Instrum.*, **27**, p. 189 (1950).
(10) BRYMNER, R., and STECKELMACHER, W. *J. Sci. Instrum.*, **36**, p. 278 (1959).
(11) CHARPENTIER, D. E. *A Simplified Mass Spectrometer Type Helium Leak Detector* 1956 *Nat. Symp. Vac. Trans*, p. 117 (London: Pergamon Press, 1957).
(12) DRAWIN, H. W. *Vakuum Tech.*, **8**, p. 215 (1959).
(13) DRAWIN, H. W., and KRONENBERGER, K. *Vakuum Tech.*, **8**, p. 128 (1959); also *Zs. f. Instrumkd.*, **67**, p. 157 (1959).
(14) MONGODIN, G. *Proc.* 1*st Int. Cons. Vac. Tech.*, 1958, *Namur*, **1**, p. 229 (London: Pergamon Press, 1960, Ref. 14—referred to below as: 1958, Namur); see also: *Le Vide*, **73**, p. 15 (1958).
(15) WARMOLTZ, N. (1958, Namur, Ref. 14), p. 257.
(16) WARMOLTZ, N., and DE GREFTE, H. A. M. *Le Vide*, **12**, p. 202 (1957).
(17) PETERS, J. L. *Rev. Sci. Instrum.*, **30**, p. 1093 (1959).
(18) OCHERT, N., and STECKELMACHER, W. *Vacuum*, **2**, p. 125 (1952). (This reference also contains an extensive bibliography of early papers on mass spectrometer leak detection.)
(19) LE POOLE, J. B. *Some Designs in Electron and Ion Optics* (Thesis, Delft, 1954).
(20) BARNES, A. H., SMITH, F. A., and WIMUNC, E. A. *Symposium on Non Destructive Tests in the Field of Nuclear Energy* (Am. Soc. Test. Mat., 1958).
(21) BELL, R. L. *J. Sci. Instrum.*, **33**, p. 269 (1956).
(22) CASSIGNOL, C., GELLER, R., and MOREAU, J. *Le Vide*, **8**, p. 1415 (1953).
(23) CHARLES, D., and WARNECKE, R. J. *Le Vide*, **12**, p. 25 (1958). See also: 1958, Namur, Ref. 14, p. 251.
(24) CHOUMOFF, S. *Le Vide*, **12**, p. 193 (1958).
(25) CHOUMOFF, S., and LAPLUME, J. *An Industrial Leak Detector for Helim* (1958, Namur, Ref. 14), p. 233. See also: LAPLUME, J. *Le Vide*, **12**, p. 46 (1958).
(26) GELLER, R. *Le Vide*, **10**, p. 119 (1955). See also: *Le Vide*, **12**, p. 3 (1958); *Le Vide*, **12**, p. 398 (1958).
(27) LINEWEAVER, J. L. *I.R.E. Trans on Electr. Devices*; p. 28 (1958).
(28) MOODY, R. E. *Nat. Vac. Symp. Trans* 1956, p. 28 (London: Pergamon Press, 1957).
(29) PETERS, J., and RAIBLE, F. *Nat. Vac. Symp. Trans*, 1956, p. 107 (London: Pergamon Press, 1957).
(30) VARADI, P. F., and SEBESTYEN, L. G. *J. Sci. Instrum.*, **33**, p. 392 (1956).

Apparatus for the floating-zone refining of gallium arsenide

by F. A. CUNNELL, B.Sc., Ph.D., and R. WICKHAM, Services Electronics Research Laboratory, Baldock, Hertfordshire

[*Paper first received* 18 *May, and in final form* 8 *August*, 1960]

Abstract

The design and operation of equipment to purify and to grow single crystals of gallium arsenide are described. Features of the design include a demountable quartz system, adjustment of the relative position of the ends of the gallium arsenide rod during operation, excellent visibility, a traversable heater system and close control of the arsenic pressure in the tube. The latter feature has reduced the problem of ejection of molten material from the zone found in previous work.(7)

Introduction

THE technique of floating-zone refining was developed originally by Keck and Golay(1) for the processing of silicon. Subsequently it has been applied to refractory metals(2,3) and more recently to the compound semiconductor, gallium arsenide(4) (melting point 1,250° C). The principal advantage of the method, as applied to gallium arsenide, is that it enables refining and single-crystal growing to be conducted under conditions in which the quartz work tube is never in contact with the liquid semiconductor and is always at a temperature much lower than the melting point of the semiconductor.

Previous work

The general problem of processing compounds in which one of the components is appreciably volatile has been described by Boomgaard, Kröger and Vink.(5) Boomgaard and Schol(6) have shown that the dissociation pressure of arsenic over gallium arsenide at the melting point is 0·9 atmospheres. Consequently, zone-refining and crystal-growing equipments for gallium arsenide are normally designed to incorporate a temperature-controlled arsenic reservoir which provides this pressure. The reservoir must be the lowest temperature point of the enclosure confining the arsenic vapour (approximately 600° C).

The floating-zone equipment used by Whelan and Wheatley(4) to refine gallium arsenide has been described in some detail. With it, single crystals up to 6 mm diameter and 15 cm length have been grown. Similar equipment, though possibly less refined, has been operated by one of the present authors.(7) Both items of equipment involved sealing the gallium arsenide rod in an evacuated quartz envelope in such a way that the material on either side of the liquid zone remained independently supported and in alinement. This has been achieved by slightly different methods in the two cases. The work performed in this laboratory showed that considerable effort was required in the initial mounting of the specimen and this effort had to be repeated with each ingot. Furthermore there was no provision for adjustment of the relative positions of the two portions of the rod above and below the molten zone. This manipulation during zone-refining can prove most valuable as a means for controlling the cross-section of the ingot and it is a feature of most equipment used in the processing of silicon and the refractory metals.

Much of the early work was made difficult by poor visibility through the quartz tube. This was caused by a layer of small crystals of gallium arsenide on the inner wall which originated as droplets of molten material ejected from the zone. The ejection was believed to be a consequence of the loss of arsenic vapour from the zone caused by an unbalance between the dissociation pressure of arsenic over the liquid and the ambient pressure of the arsenic in the tube. Whelan and Wheatley also have experienced visibility problems. They have incorporated an inner slotted quartz liner which can be rotated periodically to expose a new portion of the outer tube.

The problem of zone stability has been discussed by Heywang.(8) The diameter of the zone is limited in practice by the necessity for producing a complete melt-through, consistent with a stable zone length, when the r.f. input power to the zone is dissipated primarily in a thin surface skin. The problem is aggravated in the particular case of gallium arsenide since close coupling of the r.f. coil and the ingot is not possible because the water-cooled coil has to be spaced away from the quartz tube in order to maintain the latter at a temperature greater than 600° C. (In the apparatus to be described it has been found necessary to interpose an auxiliary wire heater wound on a cylindrical quartz former between the work tube and the r.f. coil.)

Design considerations

Previous work at S.E.R.L. has shown that several important features should be considered in designing gallium arsenide floating-zone equipment.(7) These are as follows:

(1) A demountable quartz work tube to contain the gallium arsenide and the arsenic vapour;
(2) A mechanical control of the length of the liquid zone during the operation;
(3) A temperature-controlled arsenic reservoir maintaining a constant arsenic pressure of about 0·9 atm.;
(4) Minimization of vibration in the molten zone;
(5) Good visibility;
(6) Safety of the operator.

A demountable quartz work tube which can be used repeatedly reduces substantially the time required to mount a specimen for zoning and eliminates the need for the regular services of a skilled quartz worker. Suitable design of the work tube makes a mechanical control of the liquid-zone length quite simple. The work tube may be sealed at its lower end and closed at the top by a quartz plug fitting accurately in the bore of the tube yet able to slide freely along its axis. If the gallium arsenide rod is attached to the plug at one end and held stationary relative to the work tube at the other end, a convenient adjustment of zone length can be made.

It is impossible to prepare a sliding quartz "lock" capable of making a perfect seal, and some arsenic loss must therefore be tolerated. For a lock of given dimensions, the rate of arsenic loss from the tube can be influenced by adjusting the external gas pressure. The most unfavourable conditions occur when an external vacuum is maintained. The loss rate can be reduced appreciably by introducing an external "blanket" gas at a pressure greater than the arsenic pressure. This permits the loss of arsenic by diffusion only, but complicates the design of the heater system which surrounds the work tube by introducing convection and conduction heat losses. The latter condition is chosen for the operation of the equipment although vacuum operation could be adopted without excessive arsenic loss provided the lock is made with sufficient precision.

The zone-traversal mechanism may be designed to move either the heater system or the work tube. Moving the work tube has the disadvantage that it is difficult to avoid introducing some vibration at the zone emanating from the motor drive. The alternative choice involves a more complicated design since the r.f. coil and the heaters must be moved in unison. The additional complication is accepted in the present equipment in return for a rigid vibration-free support of the work tube.

Provision has to be made in the equipment for evacuating the work tube and its immediate surroundings before closing the lock and then establishing the background gas pressure. It is also essential to protect the operators from arsenic vapour in the event of the work tube breaking during operation. It is convenient, therefore, to mount the work tube and heater system inside a rigid, water-cooled metal box capable of withstanding an excess internal gas pressure. The box should be provided with large doors giving easy access to the interior and a large quartz window giving good visibility.

Mechanical design

The general arrangement of the equipment is shown in Fig. 1 with a more detailed arrangement of the work tube in Fig. 2. The chamber is fabricated by argon arc welding of 1 in. precision-rolled plate of a 3 to 5% magnesium-aluminium alloy to B.S.S.1477/N.P.5/6, supplied by Messrs. James Booth and Co. Ltd., Birmingham, as M.G.5. Grooves for water cooling are cut externally in the chamber and covered with plates on which water manifolds are fitted. Each box face has its own cooling system which is arranged so that all O-rings are adequately cooled. There are further water supplies to the current-carrying heater supports and coaxial r.f. assembly. To avoid condensation within the chamber when open to the atmosphere, the water is pumped from a static tank which is kept at room temperature by a continual small addition of cold water. A detachable, transparent, quartz window, 10 × 3 × $\frac{3}{8}$ in., is fitted into a large water-cooled door on the front of the chamber. This door is held closed by wing nuts and sealed by a large O-ring. The window ensures perfect viewing during operation. A similar window, 3 × 3 × $\frac{3}{8}$ in., is fitted to a back door for further observation. The chamber is evacuated from the side through an O-ring stop valve which has combined with it a gas inlet valve, a let-down valve and a Pirani fitting.

The work tube consists of three separate pieces of quartz ware fused together. The lower piece is a length of 15 mm precision bore tubing with a re-entrant formed at its lower end to house an external thermocouple. The middle section is a piece of tubing of slightly larger bore which has first been shrunk on to a specially-prepared molybdenum mandrel and then lapped and polished with a diamond abrasive compound. The concentricity and diameter of the bore does not vary by more than 0·0001 in. The third and top section is a piece of tubing with a bore slightly larger than the shrunk section. The upper end is immersed in a recess bored in the top plug of the water-cooled box. Any arsenic vapour escaping through the lock is confined within this top quartz section and condensed on the tube walls. The lower end of the work tube is supported by a piece of thick-walled quartz tube which goes out through a rubber seal at the bottom of the chamber. Inside this tube is a second quartz tube with a closed upper end which encloses the thermocouple and fits into the re-entrant portion of the work tube. The thermocouple wires emerge at the lower end through a rubber bung. The work tube is held in a vertical position by entering a centreless-ground quartz rod the lower end of which has been lapped and polished over 2½ in. so that its diameter is only 0·0003 in. smaller than the shrunk portion of the work tube. Four longitudinal grooves, ½ in. in length, at the end of the polished portion of the rod make it possible for the work tube to be evacuated when the rod is only just entered into the shrunk portion. The upper end of the quartz rod passes through a seal in the top plug of the chamber, and the position of the rod relative to the work tube is adjusted by a lever system attached externally to the rod by a removable collet.

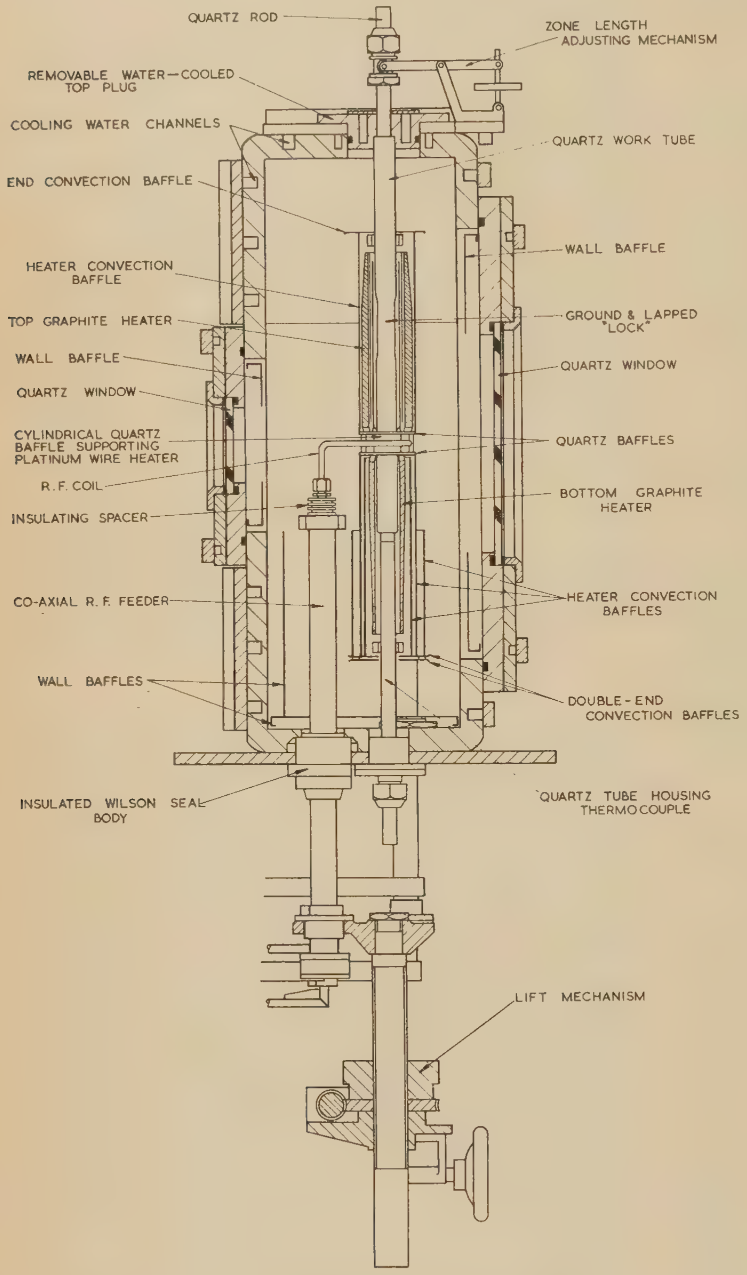
QUARTZ ROD
ZONE LENGTH ADJUSTING MECHANISM
REMOVABLE WATER—COOLED TOP PLUG
COOLING WATER CHANNELS
QUARTZ WORK TUBE
END CONVECTION BAFFLE
WALL BAFFLE
HEATER CONVECTION BAFFLE
TOP GRAPHITE HEATER
GROUND & LAPPED "LOCK"
WALL BAFFLE
QUARTZ WINDOW
QUARTZ WINDOW
CYLINDRICAL QUARTZ BAFFLE SUPPORTING PLATINUM WIRE HEATER
QUARTZ BAFFLES
R.F. COIL
BOTTOM GRAPHITE HEATER
INSULATING SPACER
CO-AXIAL R.F. FEEDER
HEATER CONVECTION BAFFLES
WALL BAFFLES
DOUBLE-END CONVECTION BAFFLES
INSULATED WILSON SEAL BODY
QUARTZ TUBE HOUSING THERMOCOUPLE
LIFT MECHANISM

Fig. 1. The general arrangement of the equipment

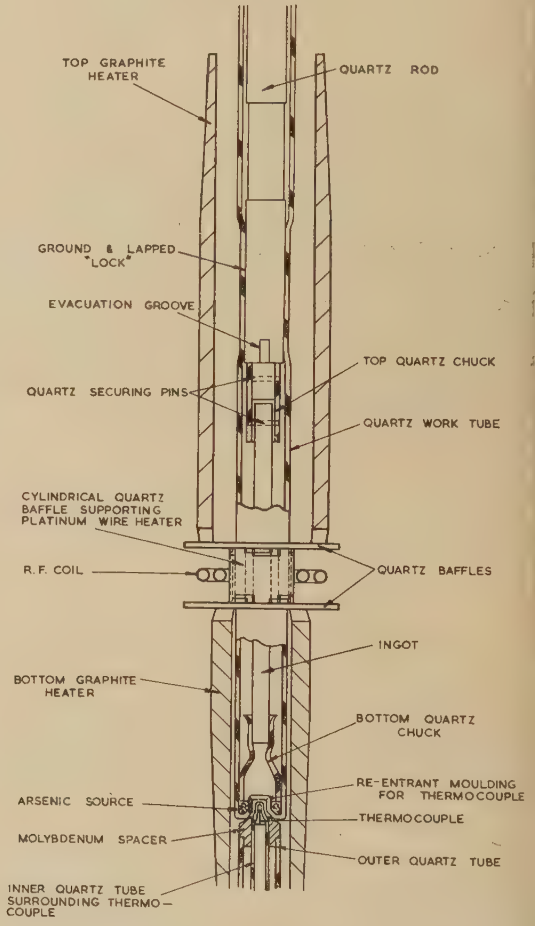
TOP GRAPHITE HEATER
QUARTZ ROD
GROUND & LAPPED "LOCK"
EVACUATION GROOVE
TOP QUARTZ CHUCK
QUARTZ SECURING PINS
QUARTZ WORK TUBE
CYLINDRICAL QUARTZ BAFFLE SUPPORTING PLATINUM WIRE HEATER
R.F. COIL
QUARTZ BAFFLES
INGOT
BOTTOM GRAPHITE HEATER
BOTTOM QUARTZ CHUCK
RE-ENTRANT MOULDING FOR THERMOCOUPLE
ARSENIC SOURCE
THERMOCOUPLE
MOLYBDENUM SPACER
OUTER QUARTZ TUBE
INNER QUARTZ TUBE SURROUNDING THERMO-COUPLE

Fig. 2. The detailed arrangement of the work tube and heaters

The lower end of the quartz rod is reduced in diameter over a ½ in. length and the gallium arsenide specimen supported on it in the manner shown in Fig. 2. The other end of the gallium arsenide is mounted in a quartz holder also shown in Fig. 2.

The heaters are hollow graphite cylinders cut lengthwise at intervals around the circumference in order to present a high resistance path to the heating current. The cross-section of the graphite varies along the heaters in such a way that a relatively uniform temperature around 650° C may be obtained down the length of the heater system. Convection baffles are used to assist in the attainment of a flat temperature distribution. The detailed arrangement is shown in Fig. 1. The power delivered to the lower heater is controlled by a temperature regulator so that the temperature of the thermocouple junction at the bottom of the work tube is maintained at 610° C independent of the position of the heater system within its operating traverse. A small quantity of metallic arsenic (roughly 200 mg) is placed at the bottom of the tube. The pressure of the arsenic vapour will be determined by the temperature of this reservoir provided the remainder of the tube is always at a higher temperature. The power into the upper heater is set to establish this condition over the upper portion of the work tube, and an auxiliary heater is fitted between the graphite heaters to eliminate a cold "spot" produced by the proximity of the water-cooled r.f. coil. This takes the form of a platinum wire wound non-inductively on a quartz spool (see Fig. 2). Visibility of the zone is impaired only very slightly by this arrangement. Fig. 3 is a photograph of a molten zone during operation and illustrates the quality of visibility. Under the conditions of the experiment there is some r.f. power coupled to the ends of the graphite heaters adjacent to the r.f. coil and this assists in eliminating a cold region under the coil.

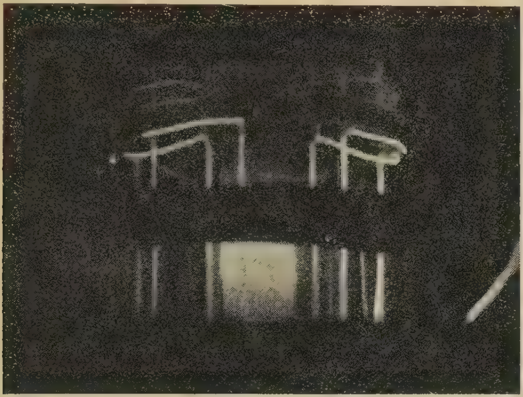

Fig. 3. Photograph of molten zone

The two-turn flat r.f. coil is fed with water through a rigid coaxial assembly coupled via flexible leads to a 4·3 Mc/s Radyne r.f. generator. This coaxial line and the heater support rods pass through vacuum seals at the bottom of the chamber and are fixed to a moving platform driven by a variable speed servo-motor *via* a screw thread and spring-loaded half nuts. The half nuts may be opened to allow movement of the carriage by a hand-wheel.

Operation of equipment

A square-section rod of gallium arsenide is cut from a polycrystalline ingot which has been cast in a quartz boat. A small hole is bored ultrasonically through the rod at the centre of one face and roughly ¼ in. from one end. Surface contamination is removed by etching in a mixture of four parts by volume of hydrochloric acid and one part of nitric acid and then washing in de-ionized water.

The cleaned gallium arsenide together with the quartz chucks and additional arsenic are placed in the cleaned work tube which is evacuated to a pressure of 10^{-5} mm of mercury and baked at 300° C for several hours. The ingot and chucks are assembled as shown in Fig. 2 so that the ingot is resting on the constriction of the lower chuck when the lock is fully closed. The top of the lower chuck is flared out to the walls of the work tube to act as a guide in entering the gallium arsenide rod. The top plug of the box is fitted to the quartz rod and the work tube lowered into position through the heater assembly until the re-entrant base rests on the thermocouple tube. The plug is then clamped to the box by three "butterfly" screws. A small clearance (approximately 0·020 in.) between the top of the work tube and the plug is allowed for expansion of the quartz. With the work tube in position, the quartz rod is withdrawn from the lock until the evacuation channels cut in the bottom of the rod are exposed at the top of the lock, thereby putting the work tube into direct communication with the box. The rod is clamped, and the box and work tube evacuated to a residual air pressure of $2 \cdot 5 \times 10^{-3}$ mm of mercury. The work tube and contents are outgassed further during evacuation. The lock is closed by lowering the quartz rod into a pre-determined position and dry oxy-free nitrogen introduced to the box at a pressure of 24 lb/in². Power is delivered to the upper graphite heater and to the wire-wound platinum heater for a period of about twenty minutes before warming the lower heater. This is important since it is necessary to establish a temperature gradient which ensures that the arsenic reservoir is the coldest point in the work tube at all times. The r.f. power dissipated in the extremities of the graphite heaters adjacent to the r.f. coil makes a significant contribution to the total power input to the heater system. It is necessary, therefore, in raising the temperature of the lower heater to supply r.f. power to the coil at a level which is insufficient to melt a zone in the gallium arsenide rod but sufficient to prevent a "cold region" developing at the top of the bottom heater.

When the temperature of the bottom of the work tube is controlled at its preset value, a liquid zone is formed by increasing the r.f. power input. The length of the zone must be sufficient to ensure a complete melt-through of the rod, consistent with stability. For ¼ in. diameter rods the normal operating zone length is roughly ¼ in. and is maintained within close limits by small adjustments in the r.f. power level. The mechanical adjustment of zone length is employed primarily in the initial joining of the gallium arsenide rod to a seed crystal. The zone is traversed from bottom to top of the rod. This helps to prevent the inclusion of cavities in the solid material since any arsenic-vapour bubbles formed in the liquid tend to rise to the top of the liquid zone away from the freezing interface. The rate of traverse of the zone is normally about 7 cm/h.

Single crystal rods ¼ in. diameter, approximately 4 in. in length and very uniform in section have been produced by "seeding" a polycrystalline rod to a selected single-crystal seed (Fig. 4). A seed is normally a square-section rod about 1½ in. in length cut from a horizontally grown poly-

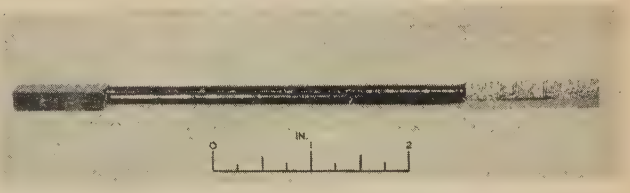

Fig. 4. Photograph of a single-crystal gallium arsenide rod

crystalline ingot in such a way that it is tipped by one large crystallite of arbitrary orientation.

After operation, the heater system is cooled in the reverse order to the warming procedure. The lower heater power and r.f. power are shut off first, thus ensuring that the solid arsenic remains in the reservoir. When the vapour pressure of the arsenic has fallen to a small value, the other heaters are allowed to cool.

The zoned gallium arsenide rod is removed by withdrawing the quartz rod together with the specimen from the work tube. The work tube is ready for use again after cleaning in AnalaR acids.

Discussion

The equipment enables zone refining of gallium arsenide to be conducted in an accurately controlled arsenic atmosphere. One consequence of this control is an improvement in visibility compared with previous work$^{(7)}$ because of the reduction in the quantity of molten material ejected from the liquid zone. The rate of loss of arsenic from the work tube varied from one quartz lock to another, but in every case proved to be small (roughly 10 mg/h).

A detailed study of the effect of multiple zone passes on the purity of gallium arsenide has not yet been completed. However, in general, material of very high resistivity is obtained after several passes. This behaviour is being investigated.

Single crystals may be grown on a routine basis by seeding. The dislocation density has been examined across a (111) face of a typical crystal. Near the centre of the rods the density is about 5×10^3 cm^{-2}, but increases by about one order of magnitude in approaching the surface.

Conclusion

The apparatus permits rapid loading of a gallium arsenide rod into a quartz work tube which may be used repeatedly. The visibility through the work tube during operation is very good, there is only a small rate of loss of arsenic through the lock, and vibration of the ingot is negligible.

Acknowledgements

The authors are indebted to the following members of the Services Electronics Research Laboratory for their assistance in this work: Mr. F. E. Birbeck for much of the detail in the mechanical design and for his valuable assistance in the operation of the equipment; Mr. W. Lester and Mr. R. Mitchell for the development of precise techniques for grinding and lapping the quartz lock; Mr. C. H. Beaumont for helpful suggestions and for the fabrication of the work tubes, and Mr. P. Gurnell for reading the manuscript. The authors also wish to make acknowledgement to the Admiralty for permission to publish this paper.

References

(1) KECK, P. H., and GOLAY, M. J. E. *Phys. Rev.*, **89**, p. 1297 (1953).

(2) CALVERLEY, A., DAVIS, M., and LEVER, R. F. *J. Sci. Instrum.*, **34**, p. 142 (1957).

(3) SMITH, R. L., and RUTHERFORD, J. L. *J. Metals*, **9**, p. 478 (1957).

(4) WHELAN, J. M., and WHEATLEY, J. H. *J. Phys. Chem. Solids*, **6**, p. 169 (1958).

(5) VAN DEN BOOMGAARD, J., KRÖGER, F. A., and VINK, H. J. *J. Electronics and Control*, **1**, p. 212 (1955).

(6) VAN DEN BOOMGAARD, J., and SCHOL, K. *Phillips Res. Reports*, **12**, p. 127 (1957).

(7) CUNNELL, F. A., EDMOND, J. T., and HARDING, W. R. *Solid-State Electronics*, **1**, p. 97 (1960).

(8) HEYWANG, W. *Z. Naturforsch.*, **11a**, p. 238 (1956).

Rapid counter for small particles in suspension

by J. B. CORNWALL, Grad.I.E.E., Auckland Industrial Development Laboratories, D.S.I.R., New Zealand,
and R. M. DAVISON, M.Sc., Ph.D.(Lond.), Fruit Research Division, D.S.I.R., New Zealand

[*Paper received* 27 *June*, 1960]

Abstract

Equipment based on a photoelectric detection method is described which has been designed for counting apple cells (approximate size distribution 70–500 μ *length) but which may be used with any reasonably opaque particles of suitable size which can be held in suspension in a clear low-viscosity liquid. The accuracy of a single run is about* $\pm 3\%$ *including sampling errors. This error may be reduced by averaging several samples.*

Introduction

In studies of the growth of apple fruits the need arose for a rapid and accurate method of counting the number of cells present in samples of tissue of known volume in order to estimate average cell volume. Techniques are available for macerating such tissue into single cell units (Letham$^{(1)}$). In the shape the cells approximate to oblate spheroids or spheres. Within any one sample, cell lengths may vary within the range 70–500 μ. Various types of counters have recently become available for counting and sizing blood cells,$^{(2)}$ but the cost of such equipment is often beyond the means of biological laboratories. The following paper describes a simple particle counter which has been devised for the specific purpose of counting apple cells. It is likely, however, that the counter could readily be adapted for use with a range of other particles.

Macerated cells are first stained evenly over their walls with a suitable stain which is chosen to accord with the sensitivity of the photo cell used in the apparatus. Trypan blue has been found to give satisfactory results with apple tissue.

A suitable aliquot of cell suspension is diluted in 25 ml. of distilled water in a small beaker. A syphon is arranged so that when a solenoid operated valve is opened, the suspension of cells streams through a glass tube which is attached to a microscope stage. A lamp illuminates a constricted region of the tube, an image of which is focused by means of the optical system on to a photo transistor mounted together with a two-stage amplifier above the eyepiece.

As the image of cells passing the constriction is focused on the photo-transistor, electrical pulses are formed which are amplified and used to trigger an electronic counter.

When the beaker is nearly empty the solenoid valve is automatically closed and the beaker may then be refilled. A second run is necessary to flush the liquid remaining in the glass tube before the constriction. This may contain up to 10% of the cells. A third run yields only a further 0·5 to 1% of cells and since these are carried over into another count, they can be neglected where samples of the same order of count are being run through consecutively.

The time required to syphon 25 ml. from the beaker, using a suction head of 1 m of water and a tube bore of 3 mm, constricted to 500 μ for a length of 2·5 cm, is 40 s. The two runs can therefore be easily completed in 2 min, and the count is read directly from the electronic counter. An electrically operated stirrer is used to prevent the cells from settling.

The apparatus

Fig. 1 shows a photograph of the unit. The photocell, two-stage amplifier, "set zero control" and setting up meter are housed above the eyepiece of the microscope. The microscope objective has a focal length of 16 mm and the eyepiece a magnification of 4.

The illuminated capillary tube may be focused on to ground glass slides mounted in the same plane as the photo-transistor by opening a turret on top of this section. This must be closed during operation, however, to exclude outside light from the photocell.

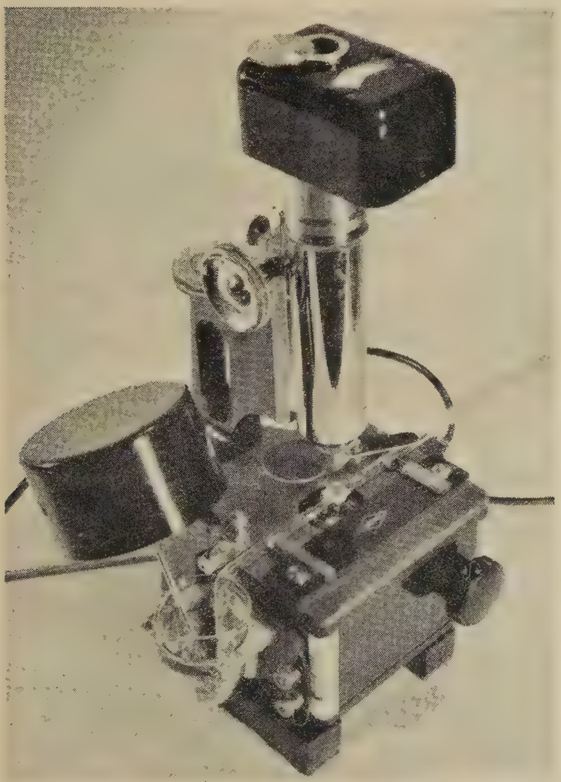

Fig. 1. Microscope unit with capillary tube on stage and photocell assembly above eye-piece

The stirrer shown mounted on the left of microscope has been constructed from a Venner synchronous motor and the shaft has two propelling blades to keep the suspension in circulation.

The box mounted beneath the stage contains the lamp housing, "intensity" control and a relay to operate the control apparatus when the liquid level has dropped below that of two adjacent electrical contacts.

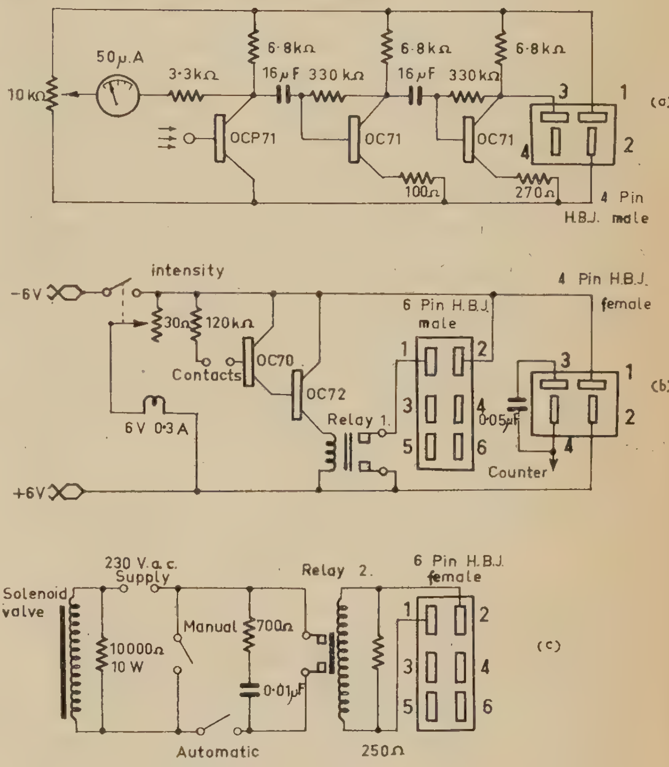

Fig. 2. Circuit diagrams
(*a*) Eyepiece unit; (*b*) Substage unit; (*c*) Control unit

The capillary tube is held in place by two metal brackets attached to a plate which can be adjusted in a horizontal plane relative to the stage. This allows the tube image to be alined accurately with the most sensitive portion of the photo-transistor. Although the capillary constriction has a diameter larger than that of the largest cell, it is probable that the effective diameter of the flowing column of cells is less, since plastic suspended particles are known to assume axial flow in narrow bore tubes.

A length of polythene tubing connects the capillary tube to the control box, where the liquid passes through a solenoid valve, and then down a further length of polythene tube to a waste container 1 m below the level of the platform.

The control box contains, as well as the solenoid valve, a 6 V d.c. relay with 230 V a.c. contacts, and switches for either automatic or manual control. Once the syphon system is filled the tubing is never allowed to empty, and with the controlling equipment described, the level of liquid in the beaker can be arranged to stop a little above the entrance of the tube. Since the bottom of the beaker has been drawn to a funnel of small cross-sectional area, the volume of liquid retained is very small. The circuit of each unit is shown in Fig. 2. The "set zero control" is used to set the meter to zero when the light is blocked off between the capillary tube and the objective lens, by the shutter provided. When the tube is filled with distilled water, and the shutter removed, the "intensity" control is used to set the meter to a predetermined point. This method of setting up has been chosen to compensate for changes in the transistor operating conditions due to temperature variations, and for changes in the light intensity due to ageing of the lamp, and falling battery voltage. It has been considered desirable to carry out the above adjustments before each count, although the changes in the settings that have been experienced after a reasonable warm-up time have been negligible. A small quantity of common salt is added to the wash water to ensure high conductivity. The contacts shown in the power unit diagram are completely immersed in this liquid so that current flows into the input of the two-stage d.c. transistor amplifier causing the associated relay to operate. This operates the heavy duty relay in the control box and the equipment is ready for use.

When the suspension of cells has been added to the beaker, the counting cycle is started by closing the switch marked "auto". This applies suction to the capillary and pulses with a period of approximately half a millisecond are formed by the photo-transistor as the cells intercept the light beam. After two stages of amplification these pulses are fed directly to the Philips type PW 4032 counter.

When the liquid level falls below the contacts, the power unit relay switches off the control unit relay and hence the solenoid valve. The automatic switch is then reset, the beaker refilled with filtered and salted water and the second run may begin.

Selection of operating-gain

Because fragmented material is present in the suspension, some form of selection has been necessary. The background material which is mostly cell contents tends to be smaller than the smallest apple cells, and size differentiation is used. For this reason the image of the capillary tube is arranged by choice of objective and eyepiece to be smaller than the width of the sensitive photocell area so that the pulse from the photocell corresponds to the size of the particle in the capillary tube. The relationship between count and amplifier gain has been plotted in Fig. 3 for a typical cell sample. A figure determined by a careful haemocytometer slide count has also been drawn in. The curve indicates that while there is no clear distinction between apple cells and background fragments, by operating with a sensitivity giving a count which agrees with the manual count, an error of ±3·5% will result from ±10% change in gain. Negative feedback throughout the amplifier should hold gain variations well within these limits.

A comparison of manual and automatic counts for two-cell suspensions

	Approx. mean cell length (μ.)	*Manual count*	*Automatic count*
Variety I	250	1699 ± 36	1741 ± 13
Variety II	325	1493 ± 41	1498 ± 11

A comparison of manual and automatic counts for two additional cell suspensions from different apple varities is given in the table. These samples cover the range of cell sizes usually encountered in apple fruit tissue. The manual count represents the mean of seven slide counts and the automatic count, the mean of five counts. Agreement between results obtained by the two methods is satisfactory. As the standard errors show, there is considerably more variation between manual counts than between automatic counts, a reflexion of the errors inherent in the respective methods.

As a further check on the instrument, samples of cells were counted and then recounted after a 10% dilution. In three experiments the recount values of equal aliquots of the diluted suspension were 90·5, 88·7 and 90·1% of the original undiluted sample.

Maximum counting rate

The scaler counter used has a maximum counting rate of 120 000 periodic pulses per second. Since the interval of the pulses formed by the photo-transistor is of the order of half a millisecond it would seem that the limit of count could approach 2000 per second. This means that the 25 ml. suspension, which is passed through the syphon tube in 40 s, could contain up to 40 000 cells, assuming the cells occupy half the liquid volume.

In practice the cells have a tendency to adhere to one another, and the maximum number which can be suspended in 25 ml. of solution without this effect taking place to a serious degree sets the maximum counting rate. The possible loss of counts in this way was determined by counting multiple aliquots of cell preparations so as to increase successively the number counted in the standard volume of

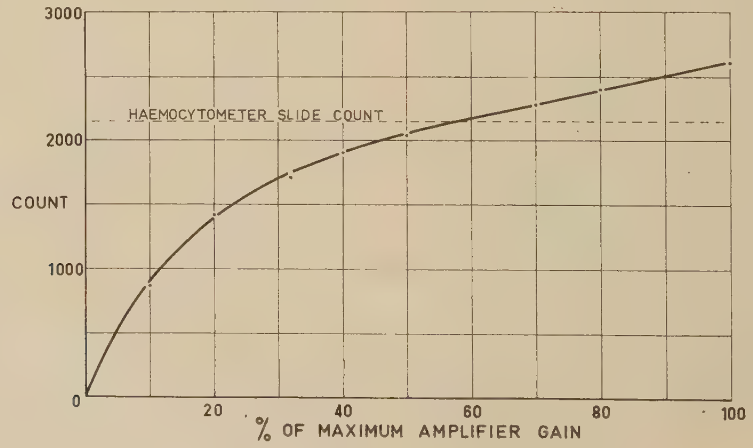

Fig. 3. Count at different amplifier gains

25 ml. of wash water in the beaker. Results of two runs are shown in Fig. 4. Each point representing the multiple aliquots (e.g. single, double) is the mean of five counts. Between 3000 and 4000 counts, the graph diverges slightly from a straight line which is drawn through the value of the single aliquot and zero. Taking the count of the single aliquot as a true estimate, this means that some coincidence loss is occurring at high suspension concentrations. Results of a number of similar runs suggest that, as might be expected, this coincidence loss appears predictable, and if necessary an adjustment could be made to compensate for the error involved.

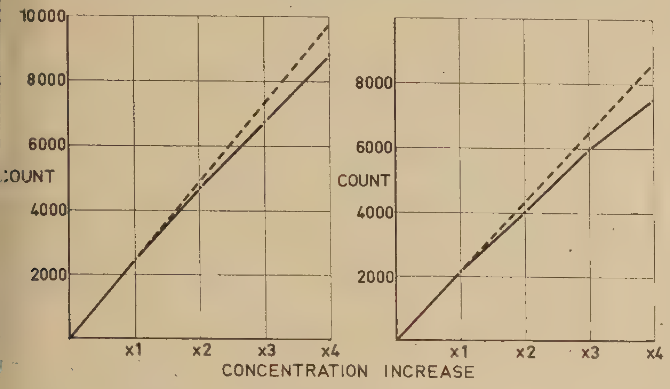

Fig. 4. Effect of suspension concentration on counting efficiency

Errors

Some pulses are induced in the equipment by operation of the relay and solenoid and these have been reduced by the usual suppression methods. The total error count due to these pulses is less than 0·5% over the two runs required.

It is essential to ensure a supply of bubble-free water since bubbles are readily counted. The reservoir supply is deaerated before use and considerable care exercised in filling the sample beaker to avoid splashing. Errors arising from bubbles generated in the aliquot transferred from an agitated bulk suspension are minimized by mixing samples on a slowly rotating wheel. Additions of suitable antiform agents will also assist.

Conclusions

Consideration of the apparatus suggests that with little adaptation, the counter could record accurately many other types of particles. For example, preliminary experiments have indicated that, with the instrument set up as described above, suspensions of certain protozoa are readily counted. A change in the magnification of the optical system and corresponding changes in the bore of the syphon tube would, within limits, extend the range of the instrument.

Further investigations are under way to determine the limits of use of the instrument for counting a wider range of biological particles.

Acknowledgement

The authors' thanks are due to Mr. J. Boyes for the mechanical construction required on the microscope.

References

(1) Letham, D. S. *Nature*, **181**, p. 135 (1958).
(2) Brecher, G., Schneiderman, M., and Williams, G. Z. *Amer. J. Clin. Path.*, **26**, p. 1439 (1956).

Measurement of the optical thickness of absorbing specimens with the three-beam interferometer

by P. HARIHARAN, Ph.D., A.Inst.P., and D. SEN, M.Sc., Ph.D., National Physical Laboratory of India, New Delhi, India

[*Paper received* 23 *June*, 1960]

Abstract

A simple modification of the three-beam interferometer is described which permits measurements of the optical thickness of absorbing specimens with a high degree of accuracy.

Introduction

PRECISE measurements of the optical thickness of absorbing specimens by conventional interference methods present difficulties because the amplitudes of the interfering beams differ considerably. This results in an appreciable decrease in the visibility and sharpness of the fringes and leads to poor accuracy. The use of three-beam interference⁽¹⁾ is one method of obtaining higher accuracy in this case. The present paper outlines a simple modification to the three-beam interferometer described by the authors in an earlier publication⁽²⁾ which makes it particularly suitable for such measurements.

Optical system

The optical system of the modified three-beam interferometer is shown in Fig. 1. As can be seen from the diagram, the main difference between the new instrument and the earlier one is that the incident and emergent beams in the present arrangement are approximately at right angles to the axis of the instrument, instead of parallel to it. With this arrangement, I_1 and I_3, the intensities of the two outer beams, are equal and are given by the relation

$$I_1 = I_3 = I_0 R^2 r^2 t^2 \qquad (1)$$

where I_0 is the intensity of the incident beam, R is the reflectivity of the outer faces of the beam-dividing plates, and r and t are the reflexion and transmission coefficients, respectively, of the inner, semi-reflecting faces of the beam-dividing plates. Under the same conditions, I_2, the intensity of the central beam, is given by the relation

$$I_2 = I_0 R^2 t^4 \qquad (2)$$

The ratio of the intensities of the middle beam and the outer beams is then, obviously,

$$(I_2/I_1) = t^2/r^2 \qquad (3)$$

This ratio can therefore be made to take any required value in this arrangement merely by a suitable choice of the optical constants of the beam-dividing film.

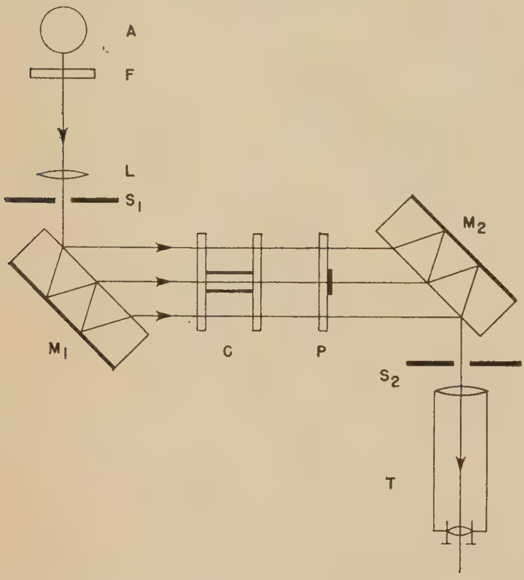

Fig. 1. Schematic diagram of the optical system of the modified three-beam interferometer

A, source; *F*, monochromatic filter; *L*, condensing lens; S_1, S_2, stops; M_1, M_2, beam-dividing plates; *C*, compensating cell; *P*, absorbing specimen; *T*, telescope

Theoretical considerations

The optimum value of the reflectivity of the beam-dividing film in any given case is easily found as follows. If we ignore the effects of the phase coherence factors of the beams, the intensity distribution in the interference pattern is given by the relation⁽³⁾

$$I(x, \phi) = 2I_1\{1 + \cos(2\pi x/a)\} + \\ + I_2 + 4(I_1 I_2)^{1/2} \cos(\pi x/a) \cos \phi \qquad (4)$$

where x is the distance from the centre of the pattern, a is the fringe spacing and ϕ is the phase difference between the central beam and the two outer beams. As before, all the fringes will have the same intensity when the phase difference between the central beam and the outer beams is equal to an odd multiple of $\pi/2$. The relative difference in intensity between adjacent fringes caused by a small change $\Delta\phi$ in the phase of the central beam from the value corresponding to equality of illumination of all the fringes is then given, to a first approximation, by the relation

$$\begin{aligned}(\Delta I/I) &= 8\{(I_1 I_2)^{1/2}/(4I_1 + I_2)\}\Delta\phi \\ &= 8\{\sigma^{1/2}/(4 + \sigma)\}\Delta\phi \qquad (5)\end{aligned}$$

where $\sigma = (I_2/I_1)$.

Assuming that a relative difference in intensity of 5% between adjacent fringes corresponds to the setting limit,⁽¹⁾ the variation of the theoretical setting accuracy with (I_2/I_1) has been calculated and is shown in Fig. 2. The validity of this curve over a fairly wide range was confirmed by experimental measurements of the setting accuracy at various values of (I_2/I_1), the results of which are also plotted on the same figure. As can be seen, the experimental points follow the theoretical curve reasonably closely, though the accuracy obtained in practice is rather higher than that predicted by the simple theory at large values of (I_2/I_1). This is presumably because the dark minima between adjacent fringes then become quite faint, so that the photometric setting is made under more favourable conditions.

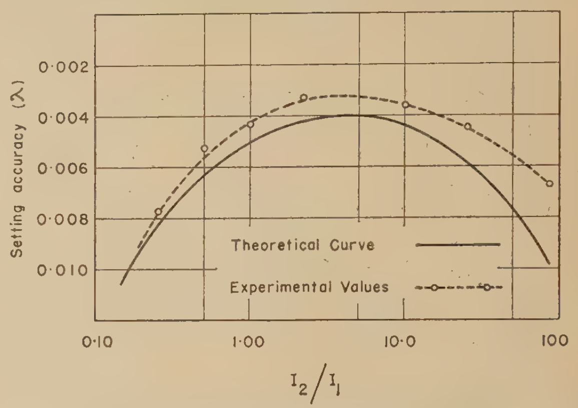

Fig. 2. Variation of the setting accuracy with (I_2/I_1), the ratio of the intensities of the central beam and the outer beams

Measurements with absorbing specimens

As can be seen from Fig. 2, the setting accuracy is a maximum when $(I_2/I_1) = 4$, that is to say, when the amplitude of the central beam is twice that of the outer beams. From the shape of the curve, it is also easily seen that the loss in accuracy in measurements with an absorbing specimen can be minimized by choosing the initial value of (I_2/I_1) so that the geometrical mean of the final value of (I_2/I_1) (with the specimen in the central beam) and the initial value is equal to this optimum value. Since the maximum of the curve is rather flat, the loss in accuracy under these conditions is fairly small. Thus, when $(I_2/I_1) = 22$, settings can still be repeated with an accuracy of $\lambda/175$. This initial value of (I_2/I_1) can be obtained with a beam dividing film having a reflexion coefficient $r = 0{\cdot}17$, and a transmission coefficient $t = 0{\cdot}83$, such as, for instance, a zinc sulphide film of suitable thickness. Measurements can then be carried out with at least the same accuracy on specimens with transmissions as low as 3%, corresponding to a final value of $(I_2/I_1) = 0{\cdot}7$. This range has been found quite adequate, in practice, for measurements on such specimens as retarding films for phase contrast microscopy, since these are rarely made with densities greater than 1·5.

Conclusions

The simple technique described permits accurate measurements on absorbing specimens with the three-beam interferometer. In practice, it eliminates the necessity of using such devices as an auxiliary polarizing system to adjust the relative intensities of the central beam and the outer beams⁽⁴,⁵⁾

in all instances except where the very highest precision is required, or where very highly absorbing specimens are to be studied.

Acknowledgement

The authors wish to thank the Director, National Physical Laboratory of India, for permission to publish this paper.

References

(1) Zernike, F. *J. Opt. Soc. Amer.*, **40**, p. 326 (1950).
(2) Hariharan, P., and Sen, D. *J. Sci. Instrum.*, **36**, p. 70 (1959).
(3) Vittoz, B. *Helv. phys. Acta*, **26**, p. 400 (1953).
(4) Fleischmann, R., and Schopper, H. *Z. Phys.*, **130**, p. 304 (1951).
(5) Paris, D. *Z. Phys.*, **141**, p. 507 (1955).

Digito-analogue computer for solving linear simultaneous equations and related problems

by E. V. KRISHNAMURTHY, M.A., M.Sc., Ph.D., Department of Physics, University of Madras

[*Paper first received* 21 *March, and in final form* 27 *June*, 1960]

Abstract

This paper describes Līlāvati model III, a digito-analogue computer for solving simultaneous and secular equations by a variety of iterative processes. Unlike the other computers in this field, multiplication is carried out by using Ohm's law and addition by null methods. The familiar Kelvin–Varley slide forms the basic circuit of the computer. This, in addition to simplifying the number of components involved in the computer, provides a method of feeding in and taking out the data as numbers, correct to three significant figures. An accuracy of between one and two parts in a thousand is readily obtainable.

1. Introduction

A number of electrical analogue computers have been constructed for the solution of simultaneous linear algebraic equations and secular equations, and an excellent review of the subject is available in Soroka.(1) In all these machines the physical quantities used as analogues are voltages, and the product and the sum of two numbers are obtained either by transformers or potentiometers and high resistors. These methods are not strictly accurate because of the non-linearity involved in loading the potentiometer during the process of multiplication, and because current is being drawn from the circuit in which voltage is measured. As a result, elaborate auxiliary circuit arrangements have to be used in order to obtain a nominal accuracy of one part in a thousand. These difficulties can be obviated if all measurements are made at the null-setting. Multiplication can be carried out exactly by using Ohm's Law, and addition can be simulated by connecting the individual voltages in series. The analogue machine constructed on these principles has been named Līlāvati after a book by the Indian mathematician Bhaskaracharya.* This machine can be adapted to solve any problem based on linear algebraic equations, e.g. solution of a set of simultaneous equations or secular equations.

In models I and II(2, 3) the analogue of the coefficient a in equation (1) is a resistance, while that of the variable x is a current, the product ax giving a voltage. The sum of a set of several such products such as $a_{11}x_1 + a_{12}x_2 + \ldots$ is the analogue of a single equation. It is evident that the solution of simultaneous or secular(4) equations involve n such equations represented by

$$\sum_{j=1}^{n} a_{ij}x_j = g_i (i = 1 \text{ to } n) \tag{1}$$

or in matrix notation

$$AX = G \tag{2}$$

The analogy of equation (2) therefore requires $(n+1)$ columns and n rows of resistances. In model I the coefficients a_{ij} are represented as resistances fed into the $(n \times n)$ volume controls by using an auxiliary Wheatstone network and g_i's are preset as voltages measured by a high resistance voltmeter. The signs of these are also preset using plus-minus switches. The resistors in each column are in series and form a current circuit. The interconnexions for each row forming the analogue of equation (1) are made by means of a selector switch through a galvanometer, to adjust for null deflexion. This switch thus sets up the analogy of each one of the equations of equation (1) at its various settings 1 to n. In order to satisfy all the n-equations, the familiar Gauss–Seidel iterative process is carried out varying the ith variable at the ith setting of the switch, namely in the ith equation. When the process converges, the currents in each circuit gives the solution and they are read with an ammeter.

In model II, all meters are dispensed with and accurate potentiometric methods are used for measuring both currents and voltages. This model can also give the solution of secular equations making use of a relaxation method as used by Frost and Tamres.(5)

Both these models, however, suffer from the serious disadvantage that the processes employed in them for solving the equations do not necessarily converge in all cases. It therefore becomes necessary to design a computer which is somewhat more versatile, in the sense that it can utilize one or the other of different iterative processes,(4, 6–8) according to the requirements of the particular problem. The advantage is that, even if one iterative method fails or is slow in a particular case, some other iterative method in which convergence is ensured can be readily substituted although the latter method would not be commonly used, because it requires a larger number of operations. Thus it should be readily possible to switch over from one sequence of operations to another, according to the choice of the iterative process. Naturally, this led the author to study the various iterative processes that are available in the literature. A discussion of these mathematical aspects of model III are being published elsewhere.(4)

---

* Apart from several old Sanskrit editions of this ancient book, an English translation by Dr. H. T. Colebrook has been published by Punjab Sanskrit Book Depot, Lahore (1927).

The methods that can suitably be mechanized in this computer are (1) Gauss–Seidel Process, (2) Richardson–Hotelling Process, (3) Relaxation Process and (4) Choleski's Process for the solution of simultaneous equations, and (1) Matrix Power Method and (2) Relaxation Method for the solution of secular equations. It will thus be seen that the computer must be capable of performing a variety of sequences. Consequently, the design of the earlier model was so modified that any one of a series of iterative processes could be selected by means of a suitable selector switch, called "Sequence Selector". Having selected the sequence, the different steps in an iteration could be performed by setting the "Step Selector" switch at each of its positions.

A new idea which has been incorporated in model III is to have all the data fed in and read as numbers, although the operation of the instrument itself is based on analogue principles. In models I and II, the coefficients were fed in as resistances in a set of wire wound volume controls, using an auxiliary post-office box arrangement. These volume controls have several disadvantages:

(1) They are not strictly non-inductive and so the operation of the computer with a.c. will not be accurate.

(2) A coefficient which is less than 5% of the total value of the volume control cannot be set, if ordinary radio volume controls are used.

(3) The feeding in of the data by means of a standard post-office box arrangement (other types of computers reported in the literature use a standard potentiometer for this) consumes a longer time than even the actual solution of the problem. This is a serious drawback, and the data cannot be checked by visual examination after being fed in.

(4) Since all the coefficients in a column are in series in a current circuit, the resistance becomes very large and consequently a high voltage power supply is required.

Some of these difficulties, particularly (2) and (3), can be avoided by using accurate Helipot type potentiometers, while difficulties (1), (2) and (3) can be avoided only by using three-decade resistance boxes (for 0·1% accuracy), but the cost of the computer would then be prohibitive as $n(n+1)$ coefficient potentiometers or resistance boxes would be required.

By making use of a three-decade Kelvin–Varley arrangement of resistors, in which the total resistance is constant, all the four difficulties can be obviated, and further the values of the coefficients can be set as dial readings on a series of decade switches. At the same time, only $(n+1)$ resistor units are required, which brings about a great saving in the number of components and therefore also in the cost. So, also, the voltages and currents can be read off as dial readings by making use of potentiometric methods. Only the basic circuits illustrating the principles are described here. For fuller details reference should be made to the publication mentioned earlier.

This Līlāvati model, therefore, should be considered to be a new type of computer (which might be called "digito-analogue computer"), in which data are fed in and taken out as numbers recorded by dial settings, while the analogy of the mathematical equations is furnished by electrical quantities. (An altogether different type of digito-analogue computer, using punched cards for programming the problem and parallel high-resistance additive network voltage divider circuits for representing the coefficients, has been designed by Walker.(9) Unfortunately, this work has not been referred to in several of the publications since that date.) An accuracy of three significant figures is readily obtainable, which is higher than most pure analogue computers, but of course lower than the purely digital computers. The Līlāvati principle has recently been applied by the author to the design of a Fourier synthesizer, a polynomial equation solver giving complex roots and related problems like a structure factor computer for X-ray crystallography. Some of these designs are actually being constructed and they will be described in due course.

An advantage of the digital setting of data is that the machine can be made to operate automatically by means of standard telephone uniselectors; the techniques for carrying this out are also being worked out and the next model (model IV) for solving twelve linear equations is expected to be automatic in its operation.

Model III is the first analogue machine to be developed in which the various *iterative* processes used in numerical analysis for the solution of both simultaneous and secular equations have been mechanized, and it contains no relays of any sort.

2. Basic steps in the various iterative processes and their analogues

The various iterative methods used for solving simultaneous and secular equations require only two types of basic operations which may be called (*a*) matrix multiplication of an arbitrary vector and (*b*) transfer of data or feeding back a fraction of the multiplied vector.

The operation of matrix multiplication may be represented by the equation

$$AX = G \tag{3}$$

or

$$\sum_{j=1}^{n} a_{ij}x_j = g_i \; (i = 1 \text{ to } n) \tag{4}$$

The analogy of equation (4) requires $(n+1)$ columns and n rows. Here a_{ij}'s are represented by resistances, x_j by currents and g_i by voltages. The essential idea is to vary either one of the x_j's (currents) or the g_i's (voltages) so as to obtain zero. In the Gauss–Seidel iterative process(2, 3) the former is done, while in simple matrix multiplication, i.e. multiplying a vector $X^{(0)}$ by the matrix A,

$$AX^{(0)} - G = 0 \tag{5}$$

the resultant vector components are g_i.

Some of the steps in other iterative processes are also of this type, with a small extension. Thus, in the Richardson–Hotelling(10) process for the solution of simultaneous equations, the iterative sequence is given by

$$(A - bI)X^{(p)} - G = -bX^{(p+1)} \tag{6}$$

where b is an arbitrary scalar parameter chosen in such a way that the convergence is fast.(4, 11)

Now equation (6) may be written in the form

$$A'X^{(p)} - G + R^{(p)} = 0 \qquad (7)$$

and

$$X^{(p+1)} = R^{(p)}/b \qquad (8)$$

where A', G and $X^{(p)}$ are known and $X^{(p+1)}$ to be found out, which is done in two steps:

The step given by equation (7) requires $(n + 2)$ columns and n rows, but otherwise the basic arrangement is the same as that for the matrix multiplication. The step given by equation (8) requires the transfer of the result in the previous step with a multiplying factor $1/b$.

So also, in solving secular equations by the matrix power method(6–8) and the subsequent standardization of the Eigenvector (i.e. making one of the components unity) the same two steps are involved, as may be seen from equations (9) and (10).

$$AX^{(p)} + R^{(p)} = 0 \qquad (9)$$

where

$$X^{(p+1)} = - R^{(p)}/\lambda \qquad (10)$$

(*a*) *Analogue of matrix multiplication.* The block diagram of the arrangement for this is shown in Fig. 1(*a*) and the circuit diagram for a simple two equation example of equation (7) is shown in Fig. 1(*b*). The quantities marked at the top of Fig. 1(*b*) are the currents through the various circuits and the quantities marked against the resistors are their values.

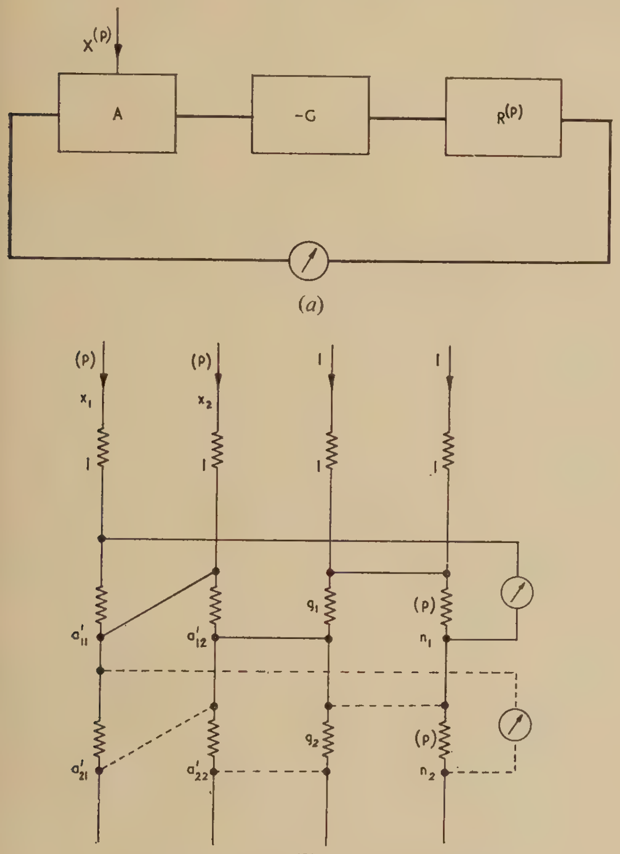

(*a*)

(*b*)

Fig. 1. (*a*) Block diagram for the analogy of matrix multiplication. (*b*) Two equation analogy of matrix multiplication

(*b*) *Transfer of data (feed-back).* The block diagram of the arrangement corresponding to the equation $X^{(p+1)} = R^{(p)}/b$, where b is given is shown in Fig. 2(*a*). The circuit diagram for a (2×2) matrix is shown in Fig. 2(*b*). The current through $r_1^{(p)}$ and $r_2^{(p)}$ which was originally unity is changed to $1/b$, the multiplying factor, and the transfer is done by effecting the diagonal connexions shown in Fig. 2(*b*). It should be mentioned that the circuit diagrams in Figs. 1(*b*) and 2(*b*) are intended only to clarify the ideas. Actually in the computer they are arranged in an entirely different way, as will be clear from succeeding sections.

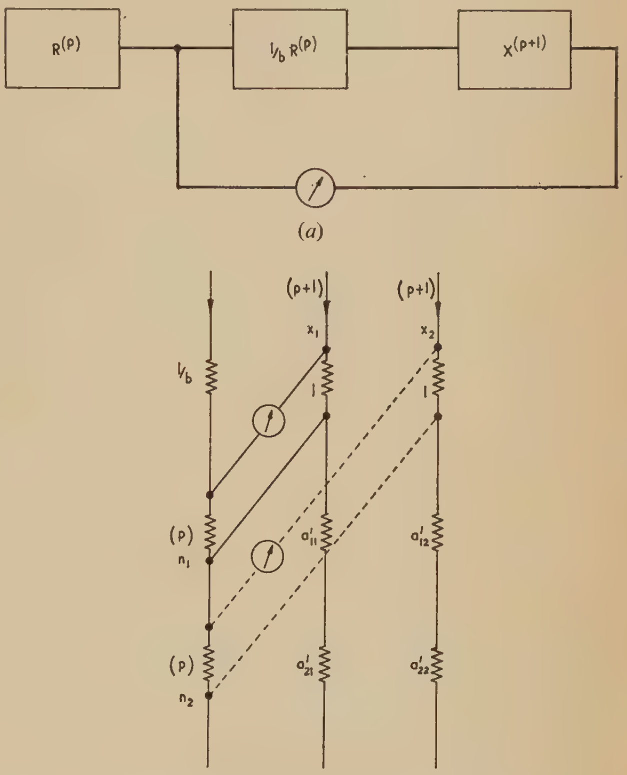

(*a*)

(*b*)

Fig. 2. (*a*) Block diagram for the analogy of transfer of data. (*b*) Two equation analogy for the transfer of data

3. The Kelvin–Varley bridge

In models I and II(2, 3) separate resistances were used to represent each of the coefficients a_{ij}. As mentioned earlier, by using the Kelvin–Varley arrangement, it is possible to have only $(n + 2)$ resistance boxes from which the appropriate values of a_{ij}, g_i, and r_i corresponding to each row can be tapped and connected up as required by means of selector switches.

The Kelvin–Varley arrangement of resistances providing a three-decade range in value is shown in Fig. (3). The top row consists of eleven coils each of resistance "r" Ω. Connected across two of these coils is another row of eleven coils, each of resistance $r/5$ Ω, the shunting connexions being made through two sliding contacts which always move together, so that two coils of resistance $2r$ in the upper row are shunted by the total resistance $2r$ in the row below, at each step. Again, two of the coils in this second row are shunted in the same way by a series of ten coils whose total resistance is equal to that of the two coils which it shunts, namely $2r/5\ \Omega$. Since in each case the two coils are shunted by a resistance equal to their own resistance, the resistance of the combination is the same as the resistance of one coil so that the total effective resistance of each of the rows in the system is in each case that of ten coils only, and the total effective resistance of the system across the points connected to the input E_{in} is always $10r$, irrespective of the settings of the contacts. On the other hand, the output E_{out} can be made equal to any integral multiple of $0{\cdot}001\ E_{in}$ (from 0 to 1000) by suitably setting the three decade switches A, B and C. The dial readings of these switches would give the three digits of the number represented by E_{out} if $0{\cdot}001\ E_{in}$ is taken as the unit. On the other hand, irrespective of the setting of these switches, the total resistance of the box is a constant and so the current flowing through the box does not vary with the switch settings, provided the contact resistance of the switches is negligible.

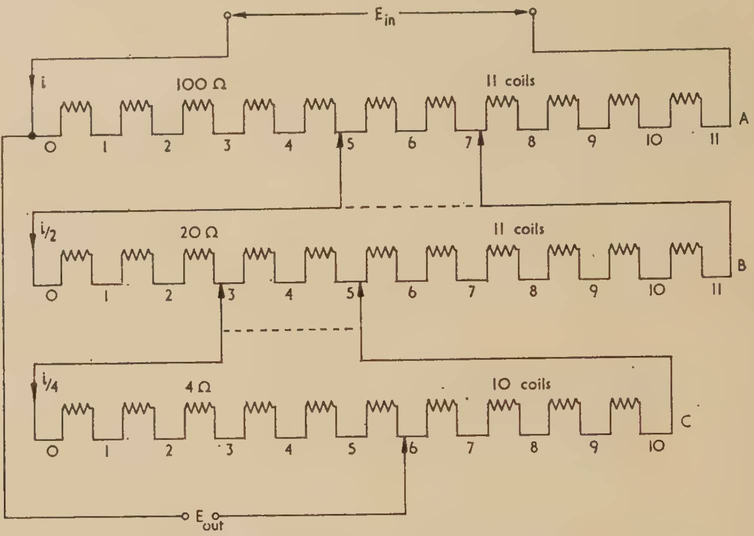
E_{in}
i
100 Ω
11 coils
A
0
1
2
3
4
5
6
7
8
9
10
11
i/2
20 Ω
11 coils
B
i/4
4 Ω
10 coils
C
E_{out}

Fig. 3. The Kelvin–Varley Bridge

In the arrangement used in the present computer the total resistance is 1000 Ω.

4. Selector switches

(*a*) *The step selector.* In order to mechanize the various processes it is enough if the analogy of a single equation at a time is set up. Consequently, the data for the n different equations can be fed in by making use of n groups of switches for each box, to which the potential points of the particular potentiometer are all brought. The arrangement for one of the boxes (say box 1) is shown in detail in Fig. 4. The points A_{i1}, A'_{i1} are the two poles of a two-pole ten-way switch, A'_{i1} having its ten ways connected to the points 0 to 9 and A'_{i1} having its ten ways connected to the points 2 to 11 of the series of coils in the row A of the Kelvin–Varley bridge in the first box. B_{i1} and B'_{i1} are similar poles of a two-pole ten-way switch having their ten ways connected to the points 0 to 9 and 2 to 11 respectively of the series of coils in the second row B. C'_{i1} is the pole of a one-pole eleven-way switch having its ways connected to the points 0 to 10 of the third series of coils in the row C.

Exactly similar connexions are made to $(n-1)$ other series of three-decade switches (single-pole or double-pole switches, as the case may be). Thus, n sets of switches arranged in a vertical column having their ways all connected in parallel to the various points of the first box as described above, represents a column of the matrix (i.e. a_{ij} $(i = 1$ to $n)$.

Similarly each of the boxes is connected to n sets of three switches arranged in a vertical row. Thus there are $n(n+2)$

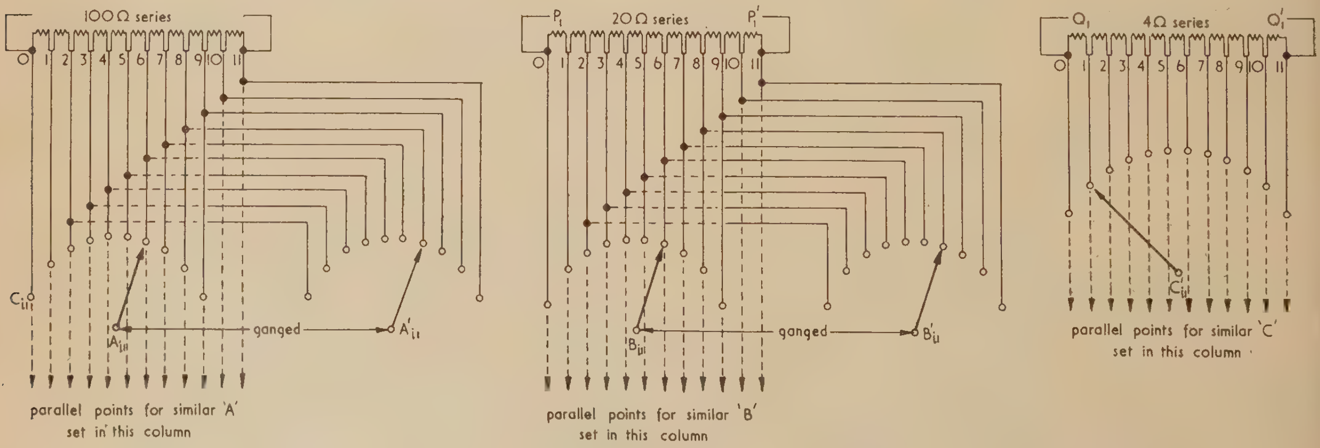
100 Ω series
0
1
2
3
4
5
6
7
8
9
10
11
C'_{i1}
A_{i1}
ganged
A'_{i1}
parallel points for similar 'A' set in this column
P₁
20 Ω series
P'₁
B_{i1}
ganged
B'_{i1}
parallel points for similar 'B' set in this column
Q₁
4 Ω series
Q'₁
C_{i1}
parallel points for similar 'C' set in this column

Fig. 4. Three-decade set switches for a column

sets consisting of three setting switches, arranged in a rectangular array for representing the quantities a_{ij}, g_i and r_i. Since the present computer is designed to solve six simultaneous equations by the Gauss–Seidel method (and five equations by the Richardson–Hotelling process for simultaneous equations) or six secular equations, there are six rows and seven columns in the computer (and therefore only seven resistance boxes).

The purpose of the step selector is to connect the poles of the three-decade switches, representing each one of the coefficients in a column, to the end terminals of the corresponding resistance box and add up all the resulting voltages corresponding to a row, through plus-minus switches, as in the earlier models.[2, 3] Thus the analogy of $\sum_{j=1}^{n} a_{1j}x_j$ is set up for the first setting of the step-selector and this is connected to g_1 with the opposite sign through the galvanometer. The analogy of each row at a time is thus set up in the n settings of the step selector. This corresponds to the matrix multiplication process discussed above.

For transfer of data, at each setting of the step-selector switch, one of the picked-out voltages from a particular column [which may conveniently be arranged to be the last or the $(n + 2)$th column] is compared with the voltages across unit resistance in one of the columns [i.e. making the diagonal connexions as shown in Fig. 2(*b*), unit resistance being the input resistance of the Kelvin–Varley resistance box]. Which of these processes is done, is predetermined by a sequence selector switch, to be described below.

(*b*) *The sequence selector.* This switch determines the interconnexions made by the step selector between the several voltages picked out, for adding in series. If this switch is set in the matrix multiplication position, or the Gauss–Seidel process, which also requires the same connexions, all the picked-out voltages are connected in series, a current unity is made to flow in the $(n + 1)$th and $(n + 2)$th columns (g_i and r_i) and the galvanometer is brought to the right position for balancing.

If this switch is set in the feed-back position, i.e. for transfer of data, the galvanometer is used to compare the voltages in the various rows of the $(n + 2)$th column, with the voltage developed across unit resistance, in each of the columns. The current through the $(n + 2)$th column is changed to $1/b$ if a multiplication by such a factor is required as in equation (8). The same arrangement is also used for measuring the current through each one of the columns if the current through the $(n + 2)$th column is made equal to unity, which is also done in one of the settings of the sequence selector. This change in current is easily achieved if two current potentiometers are used for feeding in the $(n + 2)$th Kelvin–Varley resistance box, of which one or the other can be connected to send either unit current or a current $1/b$. In practice, it is more convenient to have the initial current as b and so after multiplication by $1/b$, the new value becomes unity.

The sequence selector is also used for standardizing the current through the circuits using a reference cell.

5. Operational routine for iterative processes

The previous section contained an account of how the computer can set up the analogues of equations (7) and (8) or (9) and (10). We will now describe how some of the more important iterative techniques are carried out on the computer. The other processes are not described as they do not involve any new principle. For the sake of convenience the two-equation example will again be considered.

(*a*) *Gauss–Seidel process for simultaneous equations.* In order to solve the equation $A'X = G$, consider Fig. 1(*b*). The coefficients a'_{ij} and g_i are all fed in and r_i's are kept at zero. The sequence selector is kept in the standardizing positions and the current through the $(n + 1)$th and $(n + 2)$th (3rd and 4th) circuits is kept at some standard value (say unity). With arbitrary currents $x_1^{(0)}$ and $x_2^{(0)}$ in the first two circuits, the sequence selector is set in the matrix multiplication position. The step selector is now kept in the first position to set up the analogue of the first equation

$$a'_{11}x_1^{(1)} + a'_{12}x_2^{(0)} - g_1 = 0 \qquad (11)$$

by varying the current $x_1^{(0)}$ to $x_1^{(1)}$ for balance. The step selector is then moved to the next position to set up the analogue of

$$a'_{21}x_1^{(1)} + a'_{22}x_2^{(1)} - g_2 = 0 \qquad (12)$$

by varying the current $x_2^{(0)}$ to $x_2^{(1)}$ for balance, thus completing one cycle of operations.

This cycle of operations is repeated until convergence, i.e. until the two equations are simultaneously in balance. The sequence selector is now set in the current reading position and the step selector is set at the two positions to set up the analogue of

$$1 \, . \, x_1^{(p)} = r_1^{(p)} \, . \, 1 \qquad (13)$$

and

$$1 \, . \, x_2^{(p)} = r_2^{(p)} \, . \, 1 \qquad (14)$$

Thus the values of the unknowns are read off as $r_1^{(p)}$ and $r_2^{(p)}$.

(*b*) *Richardson–Hotelling process for simultaneous equations.* This process requires matrix multiplication and feed-back operations represented by equations (7) and (8). After feeding in the coefficients a'_{ij} and g_i the sequence selector is kept in the standardizing position and the current through the third circuit is set to unity. The sequence selector is then set in the position where comparison is done between the third and fourth circuits and the current through the fourth circuit is set at the properly chosen value b by adjusting the b-current potentiometer. The fourth circuit is also standardized with the unit current potentiometer in another position of the sequence selector [compare Section 4(*b*)].

The sequence selector is now set in the matrix multiplication position and the step selector is set in the first position. With arbitrary currents $x_1^{(0)}$ and $x_2^{(0)}$ the first row sum

$$a'_{11}x_1^{(0)} + a'_{12}x_2^{(0} - g_1 = r_1^{(0)} \, . \, b \qquad (15)$$

is read by varying r_1 to $r_1^{(0)}$. The step selector is set in the second position and the second row sum

$$a'_{21}x_1^{(0)} + a'_{22}x_2^{(0)} - g_2 = r_2^{(0)} \, . \, b \qquad (16)$$

is read by varying r_2 to $r_2^{(0)}$.

Now the sequence selector is set in the feed-back position whence the current through the fourth column is changed from b to unity automatically. Then the step selector is set in the first two positions, thereby effecting the diagonal connexions as shown in Fig. 2(*b*). The iterated vectors $x_1^{(1)}$ and $x_2^{(1)}$ are thus fed-back. With these as the components of a new trial vector a new cycle of operation is started. These cycles of operations are carried out until convergence is obtained and the solution is read off in the usual way.

(*c*) *Matrix power method for secular equations.* The solution of these equations is exactly similar to that of the Richardson–Hotelling process except that one of the components of the Eigenvector, preferably the largest found out by trial, is taken as unity (say $x_1^{(0)} = 1$) and x_2 and λ are obtained as successive approximations.

The procedure therefore starts with $x_1^{(0)} = 1$ and $x_2^{(0)}$ having any arbitrary value. The sequence selector is kept in the matrix multiplication position. With the step selector in the two positions 1 and 2 the first row sum

$$a'_{11}x_1^{(0)} + a'_{12}x_2^{(0)} = \lambda^{(0)} . x_1^{(0)} \qquad (17)$$

or

$$a'_{11} . 1 + a'_{12}x_2^{(0)} = \lambda^{(0)} . 1$$

and the second row sum

$$a'_{21}x_1^{(0)} + a'_{22}x_2^{(0)} = \lambda^{(0)} . r_2^{(0)} \qquad (18)$$

or

$$a'_{21} . 1 + a'_{22} . x_2^{(0)} = \lambda^{(0)} . r_2^{(0)}$$

are obtained by varying the current λ to $\lambda^{(0)}$ and resistance r_2 to $r_2^{(0)}$ respectively in the two positions.

The feed-back of the standardized vector is now carried out by dividing the vector by $\lambda^{(0)}$ and transferring it for the next matrix multiplication. This is done exactly in the same way as described above for the Richardson–Hotelling process.

As usual, after convergence, $x_2^{(p)}$ and $\lambda^{(p)}$ are read off. This would give the largest eigenvalue and its associated vector. Knowing the largest value, the other eigenvalues are obtained by modifying the matrix in the usual way adopted in numerical analysis.(6–8)

It should now be mentioned that the above explanation is only intended to clarify the ideas. In the computer, selector switches are arranged in a convenient way and pilot lamps are provided for guiding the operator who need follow only certain routines which have been tabulated for solving a set of n equations. These pilot lamps are controlled by the sequence selector, so that once the sequence is selected everything goes on as a routine process.

6. The description of the model

The photograph of the front view of the computer constructed for solving six equations is shown in Fig. 5. the inclined top-panel contains the coefficient setting switches and the sign switches.

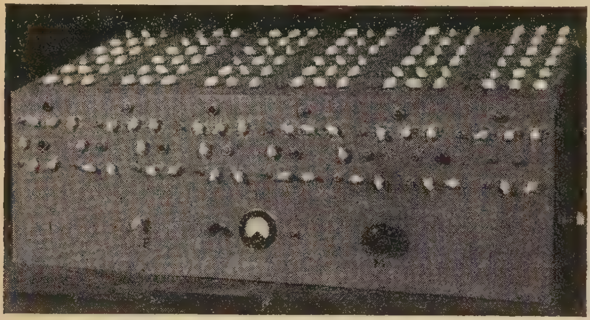

Fig. 5. A digito-analogue computer for solving linear simultaneous equations and related problems

The lower front panel is the operating panel and this contains all the current adjusting potentiometers and their sign switches, on-off and range switches for currents, the r_i switches and their sign switches, the guiding lamps, the step selector M and the sequence selector F. By means of the toggle switch to the right of the galvanometer, the shunt can be switched in or out.

All the resistance boxes are fixed to the back panel through octal-sockets.

Ordinary Eveready flash-light cells (4·5 V) were found to be satisfactory as power supplies for all the columns except the seventh, for which an accumulator was used. Since these batteries will not have long-term stability, occasional check-up is necessary for at least one of the columns with respect to which the other columns can be compared. For this purpose the seventh column is standardized (r_i set switches) with reference to a standard cell. This standardization is done in one of the settings of the sequence selector as already described.

The components used in the computer are indigenous radio components that are readily available.

7. Performance and other applications

The computer has been tested on a variety of problems and has proved itself satisfactory. Since data can be fed in and read off as dial settings, tiresome meter readings are avoided. An accuracy of between one and two parts in a thousand is obtained in most of the problems dealing with simultaneous and secular equations (of course, ill-conditioned equations are difficult to solve accurately even by numerical methods).

The computer can be used for several other problems which can be converted into linear algebraic forms. For example, the solution of simultaneous equations by factorization of the matrix can be carried out. Also since the solution of polynomials can be readily converted into the solution of an eigenvalue problem, the computer can be directly used for this purpose.(12) In order to obtain complex roots of real matrices, the matrix power method itself can be used and from the knowledge of three successive values of the oscillating iterates, it is possible to determine them.(13) However, if there is provision for complex multiplication, this problem becomes easier. The construction of such a modification to this machine is now complete and will be reported elsewhere.

8. Acknowledgements

The author wishes to express his deepest sense of gratitude to Prof. G. N. Ramachandran for the helpful guidance and encouragement received during the progress of this work. Thanks are due to Messrs. V. R. Sambandam and T. Shanmugam, laboratory assistants, for the help rendered in the construction of the model.

9. References

(1) Soroka, W. W. *Analog Methods in Computation and Simulation* (New York: McGraw-Hill Book Co. Inc., 1954).
(2) Ramachandran, G. N., and Krishnamurthy, E. V. *Proc. Indian Acad. Sci.*, **48a**, p. 152 (1958).
(3) Krishnamurthy, E. V. *Proc. Indian Acad. Sci.*, **48a**, p. 269 (1958).
(4) Ramachandran, G. N., and Krishnamurthy, E. V. *J. Madras Univ.* (1960). (In press.)
(5) Frost, A. A., and Tamres, M. *J. Chem. Phys.*, **15**, p. 383 (1947).
(6) Bodewig, E. *Matrix Calculus* (Amsterdam: North Holland Publishing Co., 1959).
(7) Buckingham, R. A. *Numerical Methods* (London: Sir Isaac Pitman and Sons Ltd., 1957).
(8) Hartree, D. R. *Numerical Analysis* (London: Oxford University Press, 1952).
(9) Walker, R. M. *Proc. Inst. Radio Engrs*, **37**, p. 1467 (1949).
(10) Hotelling, H. *Ann. Math. Stat.*, **14**, p. 1 (1943).
(11) Krishnamurthy, E. V. Ph.D. Thesis (University of Madras, 1959).
(12) Krishnamurthy, E. V. *Quart. J. Mech.* (1960). (In press.)
(13) Wilkinson, J. H. *Proc. Cambridge Phil. Soc.*, **50**, p. 536 (1954).

Inexpensive graph plotter for five-track paper tape

by L. MOLYNEUX, B.Sc., Ph.D., and E. E. SCHNEIDER, Dr.Phil.Nat., F.Inst.P., Physics Department, King's College in the University of Durham, Newcastle upon Tyne

[*Paper first received* 18 *January, and in final form* 17 *June*, 1960]

Abstract

The device will produce a graph from data in the form of five-track paper tape. The rate of plotting is 20 *points per minute at an accuracy of up to one part in* 1000. *Apart from a standard ten-millivolt potentiometric recorder and tape reader, the device requires* 21 *transistors,* 2 *valves and* 22 *relays.*

Introduction

The increasing use of electronic digital computers in scientific research, both for the processing of experimental data and for the performance of theoretical calculations, has created a need for the automatic graphical presentation of output data. The instrument to be described converts data into graphical form from the punched five-track paper tape which is the input and output medium of many computers. The plotting mechanism is an ordinary ten-millivolt potentiometric recorder such as is available in many laboratories. Since the recorder requires only minor modifications, its occasional use for plotting does not interfere with its ordinary work.

General problem

The presentation of coded information in graphical form is a special case of the general problem of decoding or converting digital information into analogue form. In the present case, the coded information consists of a set of numbers, $y_n = f(x_n)$, which are samples taken at values x_n (at equal intervals) of a continuous function $y = f(x)$. The analogue is the length Y_n of the ordinate of a point (or other mark) plotted on the graph paper such that $Y_n = ky_n$. The abscissae of the points are the analogues of the values x_n at which the samples were taken.

It should be emphasized that the plotter merely executes automatically the first stage of graphical interpretation as normally understood. It is usual to regard some smooth curve drawn through the plotted points (or marks) as a representation of some original continuous function $f(x)$. We do not consider in this paper the difficulties underlying any such interpretation; these are present in any processes of data handling. They belong to two distinct fields: firstly data sampling and digital recording⁽¹⁾ and secondly finite-difference analysis⁽²⁾ which is necessarily involved in electronic digital computing. As regards the former, the sampling interval and the number of digits recorded together determine whether or not the variation of the input function has been adequately represented. As regards the second, the possibility of interpolating the output function depends also on the suitable choice of any intermediate numerical procedures.

The conversion of coded data into the position of a marker pen takes place in two stages. In the first stage the coded number is converted into a voltage analogue. In the second, the voltage is fed into a potentiometric recorder so that the position of its marker pen becomes the analogue of the coded number.

The paper of the recorder is moved either intermittently in equal steps, or continuously at a constant rate. In either case, the distance of the plotted points along the direction of travel of the graph paper is the analogue of x_n. The range of the input numbers y_n determines the maximum number of discrete positions of the plotting device.

A range of three decades in the values of the y_n implies a graph in which the ordinate Y should have 1000 discrete values, and is said to have a precision of one part in 1000. These values must be equally spaced which means that the plotting factor $k = Y_n/y_n$ must be constant over the whole range. The accuracy is then defined in terms of the error in attaining any of these 1000 positions. There are two ways in which errors can arise. Firstly the voltage corresponding to the number on the tape may have an incorrect value, secondly the response of the recorder to this voltage may be incorrect. These errors as well as those concerning the abscissae of the graph are dealt with in a later section.

Punched paper tape

Information is conveyed by the presence of holes punched in rows across the tape. Each row has in addition a smaller perforation which is used to feed the tape through the tape reader. A "character" consists of a row of holes or a mixture of holes and spaces. The character represented by spaces only—that is, the complete absence of holes apart from the perforation—is called "blank tape". A binary digit or "bit" has a value of 1 or 0 and is represented by a hole or space respectively. A character on five-track tape thus contains five bits and can be used to represent any number up to 32 ($2^5 = 32$). As $2^4 = 16$, a decimal digit can be represented by four bits. "Code" is used to mean the way in which the bits of a character represent a decimal digit, while "pattern" is used to describe a group of characters which are always repeated in the same order and in which the function of each character is determined by its position within the group.

Input pattern

The input pattern contains three decimal digits and a "starting character". The numbers to be plotted are arranged on the tape in the following order: starting character, hundreds character, tens character, units character and then the starting character of the next number. Fig. 1 represents two complete numbers and the starting character of a third. In this case, the starting character is a complete row of holes, but only the hole in the top track (Fig. 1) is essential. This hole is called the "synchronizing hole". The other bits of the character may be used to convey other information. For instance, one of them might be used to control a marker pen on the edge of the plotting paper. In the numerical characters, the bits representing the decimal digits occupy the four lower tracks, and the top track is always blank.

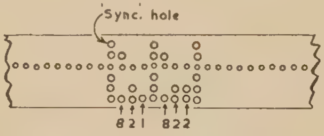
Sync. hole
821
822

Fig. 1. Paper tape punched with two numbers in the input pattern

Production of numbers in the input pattern

The exact form in which a computer punches its output is determined by its programme, and the particular part of the programme responsible is usually referred to as the "print sub-routine". Sub-routines that will cause a Ferranti "Pegasus" computer to punch its output in the correct pattern have been developed,* and there should be little difficulty in the development of sub-routines for other computers. Numbers in the correct pattern can also be produced from the digitized output of a measuring instrument.† In this case, the spare bits of the starting character are of particular use for recording additional information.

Number code

The code in which a decimal digit is represented on the tape is not important, provided that any decimal digit can be represented by four consecutive bits. If the plotter is to be used only to display the output from a computer, a simple binary representation is to be preferred as the decoding arrangements are then comparatively simple. The code actually used by our machine is "Watts reflected decimal"‡ as numbers in this code are produced by a digitizer attached to an existing measuring device. The tapes from this equipment can therefore be checked on the plotter before being fed into the computer for processing.

Block diagram (Fig. 2)

The tape reader converts information on the paper tape into electrical signals which are routed by the distributer to the appropriate set of decoding relays. The contacts of the decoding relays are connected to the potential-forming network in such a way that the numbers on the tape finally appear as a potential proportional to their value, and this forms the input of the recorder. The functions of the separate units are co-ordinated by the control unit.

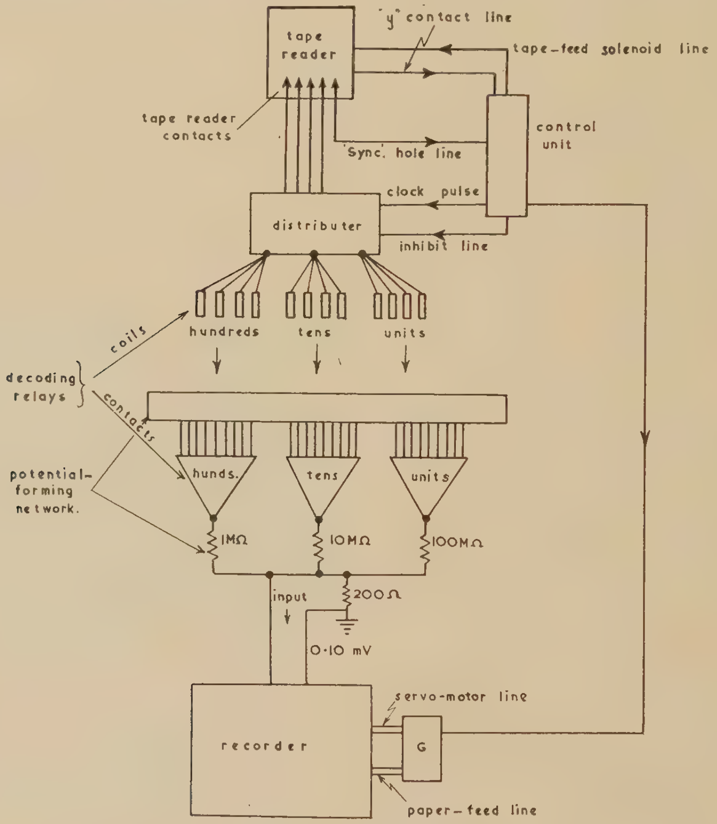
"y" contact line
tape reader
tape-feed solenoid line
tape reader contacts
control unit
'Sync.' hole line
clock pulse
distributer
inhibit line
coils
hundreds
tens
units
decoding relays
contacts
potential-forming network.
hunds.
tens
units
1MΩ
10MΩ
100MΩ
input
200Ω
0·10 mV
servo-motor line
recorder
G
paper-feed line

Fig. 2. Block diagram

---

* G. C. Midgley has written sub-routines which enable a Ferranti "Pegasus" computer to read and punch numbers in the required input pattern. The routines are available for both "machine orders" and "auto-code, Mk. 4".

† A description of a device which will convert the output digitizer to the required input pattern is being prepared for publication.

‡ "Watts reflected decimal" code is used by some of the digitizers produced by Hilger and Watts Ltd.

Tape reader

Mechanical tape readers for paper tape are fitted with contacts which close in accordance with the combination of holes of the character in the reading position. The characters are brought into the reading position by a tape-feed mechanism which in our tape reader (a high-speed tape reader, type 92, by Creed Ltd.) is operated by a solenoid. The tape feed mechanism is also fitted with a pair of contacts (*y*, Fig. 3) which close when a new character is in position.

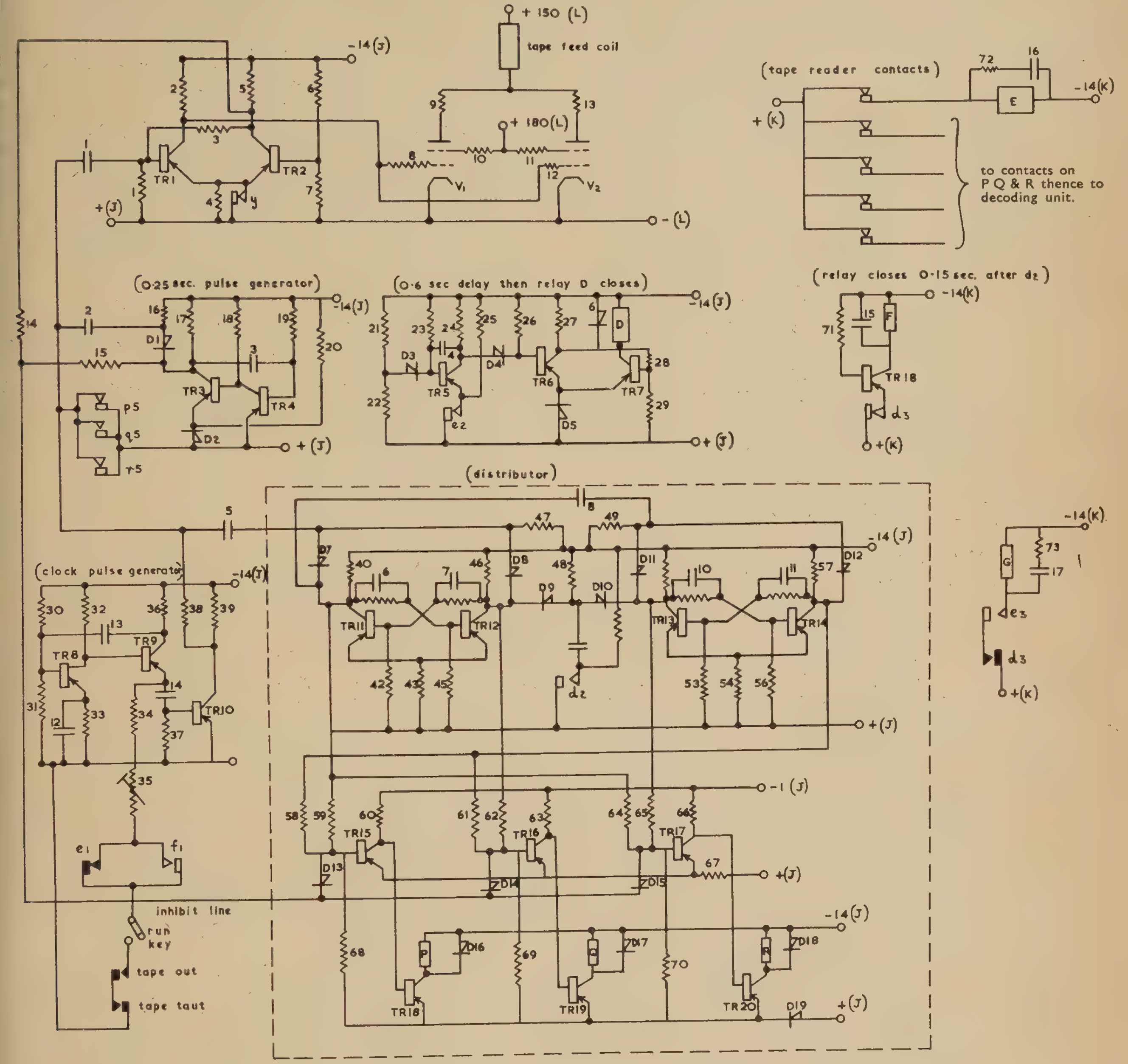
+ 150 (L)
tape feed coil
- 14 (J)
2
5
6
3
9
13
+ 180 (L)
TR1
TR2
8
10
11
12
V₁
V₂
1
4
y
7
+ (J)
- (L)
(tape reader contacts)
72
16
- 14 (K)
E
+ (K)
to contacts on P Q & R thence to decoding unit.
(0·25 sec. pulse generator)
(0·6 sec delay then relay D closes)
(relay closes 0·15 sec. after d₂)
14
2
16
17
18
19
D1
-14 (J)
20
15
3
TR3
TR4
p5
q5
r5
D2
+ (J)
21
23
24
4
25
26
27
6
D
D3
D4
TR5
TR6
TR7
28
22
e₂
D5
29
+ (J)
- 14 (K)
71
15
F
TR18
d₃
+ (K)
(distributor)
5
8
47
49
- 14 (J)
(clock pulse generator)
-14 (J)
D7
40
6
7
46
D8
48
D9
D10
D11
10
11
57
D12
30
32
36
38
39
13
TR8
TR9
TR11
TR12
TR13
TR14
14
TR10
31
12
33
34
37
42
43
45
d₂
53
54
56
+ (J)
35
58
59
60
61
62
63
64
65
66
- 1 (J)
TR15
TR16
TR17
e₁
f₁
D13
D14
D15
67
+ (J)
inhibit line
run key
tape out
tape taut
- 14 (J)
68
P
D16
69
Q
D17
70
R
D18
TR18
TR19
TR20
D19
+ (J)
- 14 (K)
73
G
17
e₃
d₃
+ (K)

Fig. 3. Circuit diagram of graph plotter

R_1 = 100 kΩ
R_2 = 4·7 kΩ
R_3 = 47 kΩ
R_4 = 1 kΩ
R_5 = 10 kΩ
R_6 = 47 kΩ
R_7 = 10 kΩ
R_8 = 4·7 kΩ
R_9 = 68 Ω
R_{10} = 120 Ω
R_{11} = 120 Ω
R_{12} = 4·7 kΩ
R_{13} = 68 Ω
R_{14} = 120 Ω
R_{15} = 120 Ω
R_{16} = 47 kΩ
R_{17} = 6·8 kΩ
R_{18} = 10 kΩ
R_{19} = 100 kΩ

R_{20} = 10 kΩ
R_{21} = 10 kΩ
R_{22} = 820 Ω
R_{23} = 120 kΩ
R_{24} = 12 kΩ
R_{25} = 33 kΩ
R_{26} = 120 kΩ
R_{27} = 10 kΩ
R_{28} = 4·7 kΩ
R_{29} = 10 kΩ
R_{30} = 82 kΩ
R_{31} = 100 kΩ
R_{32} = 10 kΩ
R_{33} = 15 kΩ
R_{34} = 1·5 MΩ
R_{35} = 1 MΩ
R_{36} = 470 Ω
R_{37} = 3·9 kΩ
R_{38} = 1·8 kΩ

R_{39} = 10 kΩ
R_{40} = 10 kΩ
R_{41} = 39 kΩ
R_{42} = 68 kΩ
R_{43} = 820 Ω
R_{44} = 39 kΩ
R_{45} = 68 kΩ
R_{46} = 10 kΩ
R_{47} = 33 kΩ
R_{48} = 33 kΩ
R_{49} = 33 kΩ
R_{50} = 22 kΩ
R_{51} = 10 kΩ
R_{52} = 39 kΩ
R_{53} = 68 kΩ
R_{54} = 820 Ω
R_{55} = 39 kΩ
R_{56} = 68 kΩ
R_{57} = 10 kΩ

R_{58} = 120 kΩ
R_{59} = 120 kΩ
R_{60} = 10 kΩ
R_{61} = 120 kΩ
R_{62} = 120 kΩ
R_{63} = 10 kΩ
R_{64} = 120 kΩ
R_{65} = 120 kΩ
R_{66} = 10 kΩ
R_{67} = 150 Ω
R_{68} = 56 kΩ
R_{69} = 56 kΩ
R_{70} = 56 kΩ
R_{71} = 27 kΩ
R_{72} = 220 Ω
R_{73} = 220 Ω

C_1 = 0·005 µF
C_2 = 0·005 µF
C_3 = 3 µF
C_4 = 4 µF
C_5 = 0·05 µF

C_6 = 0·01 µF
C_7 = 0·01 µF
C_8 = 0·01 µF
C_9 = 0·05 µF
C_{10} = 0·01 µF

C_{11} = 0·01 µF
C_{12} = 50 µF
C_{13} = 0·1 µF
C_{14} = 1 µF
C_{15} = 300 µF

C_{16} = 0·25 µF
C_{17} = 0·25 µF

D_4 = type OA5

All other diodes = type OA81 (Mullard Ltd.)

TR_7, TR_{16}, TR_{17}, TR_{18}, TR_{21} = type OC72

All other transistors = type OC71 (Mullard Ltd.)

Power supplies = (J) 13 to 15 V at about 40 mA (ripple 0·1%)

(K) 13 to 15 V at about 200 mA (ripple 50%)

Note these supplies must be separate.

(L) 150 ± 5 V able to supply pulses of 200 mA
180 ± 5 V able to supply pulses of 30 mA

Note the pulses will not be longer than 40 ms.

Operation of the device as a whole

Except when a starting character is in the reading position, the tape moves through the reader at a rate determined by the "clock-pulse" generator (Fig. 3) of the control unit. The clock-pulses are also fed to the "distributor" (Figs. 2 and 3). The distributor can be considered as a four position "switch" which is turned from one position to the next by the clock-pulses. Three of the positions of the switch are connected to the coils of relays (*P*, *Q*, *R*, Fig. 3) while the fourth is left blank. Between the distributor switch and the relays there is a further circuit called the "inhibitor" (D_{13}, D_{14}, D_{15}, Fig. 3) which is operated by the "inhibit line" (Figs. 2 and 3). When in operation it prevents the distributor relays from closing, or, if they are already closed, it opens them. Each distributor relay operates contacts (p_1, p_2, p_3, p_4; q_1, q_2, q_3, q_4; r_1, r_2, r_3, r_4; Fig. 4) which can connect any of the three groups of decoding relays to the tape reader.

The clock-pulse initiates the supply of current to the tape-feed solenoid and at the same time moves the distributor into a new position. As the distributor switch is composed of transistors, it takes up its new position within a few microseconds and, if no other action were taken, a distributor relay would close shortly afterwards. However, the current operating the distributor relays has to pass through the inhibiter, and this it is not allowed to do until the closure of the contacts on the tape-feed mechanism (*y*, Fig. 3) indicates that the new character is in the reading position. When these contacts close, the current supply to the tape-feed solenoid is interrupted so that the mechanism returns to its starting position and is then ready to feed the next character. The clock-pulse also operates a circuit (see Fig. 3) which produces a pulse of about 0·25 s duration. At the end of this pulse, the inhibiter is again brought into operation and the distributor relay opens. The distributor relays are

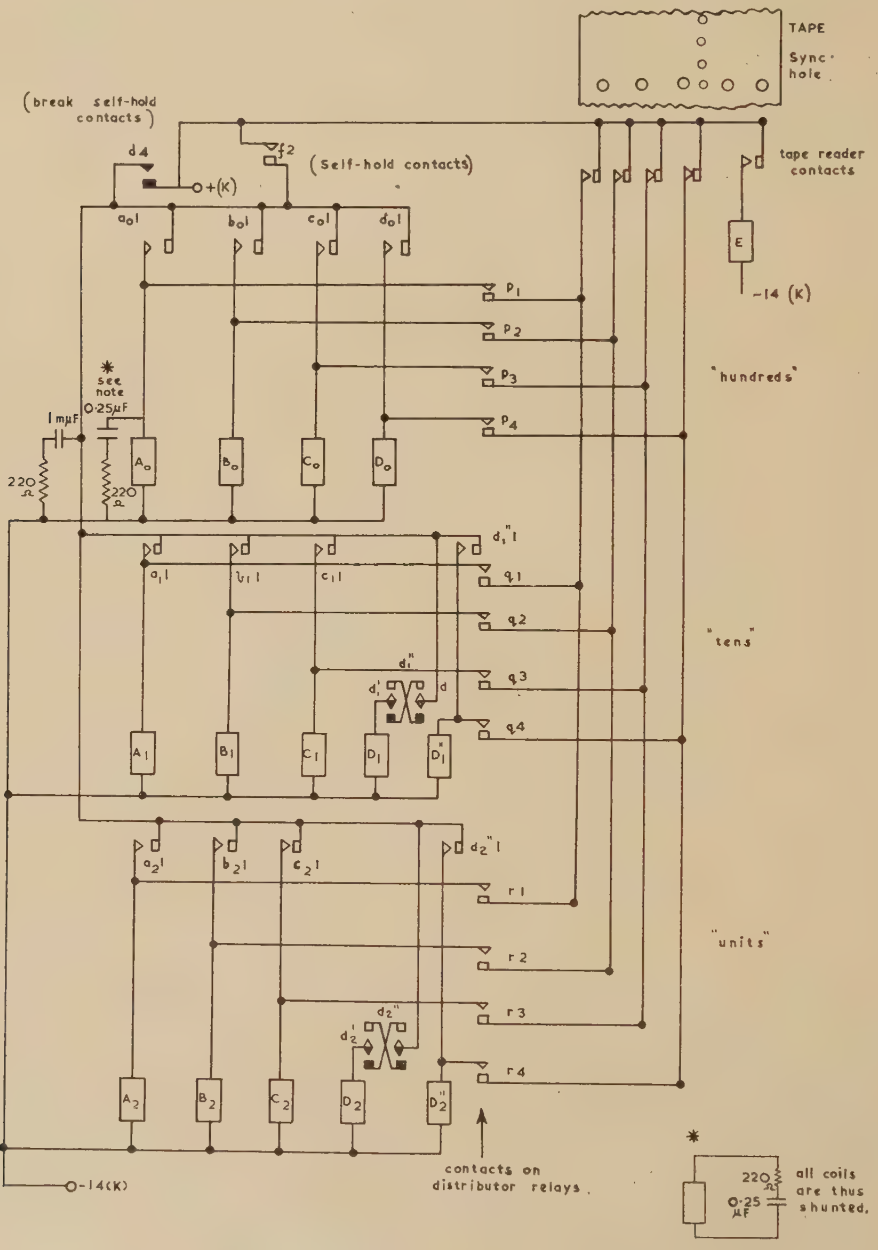
TAPE
Sync-hole
(break self-hold contacts)
d4
f2
+(K)
(Self-hold contacts)
tape reader contacts
a0'
b0'
c0'
d0'
E
-14 (K)
p1
p2
p3
p4
"hundreds"
✱ see note
0·25µF
1 mµF
220 Ω
220 Ω
A0
B0
C0
D0
d1''1
a1'
b1'
c1'
q1
q2
q3
q4
"tens"
d1''
d1'
d
A1
B1
C1
D1
D1''
a2'
b2'
c2'
d2''1
r1
r2
r3
r4
"units"
d2''
d2'
A2
B2
C2
D2
D2''
contacts on distributor relays.
-14(K)
✱
220 Ω
0·25 µF
all coils are thus shunted.

Fig. 4. Coil connexions of the decoding relays

all fitted with a fifth pair of contacts (Fig. 3, p_5, q_5, r_5) which, when closed, prevent the formation of clock-pulses. This arrangement prevents the tape from being moved while the tape reader contacts are connected to the decoding relays. It is in the nature of a safety precaution as the clock-pulses are normally spaced about 0·5 s apart so that they occur about 0·25 s after the end of the 0·25 s pulse. The actions of the control unit just described may be summed up by stating that the distributor relays cannot close until the tape has moved to the new position and will open before it moves again.

It is easier to make clear the other functions of the control unit by describing its actions. Suppose that the tape in the reader is composed of a short length of blank tape followed by some numbers in the correct input pattern. The first five characters following the blank tape will then be as follows. First, there will be a starting character, and then one representing the hundreds digit. The next two characters will represent the tens and the units digits respectively, while the next will be the starting character of the following number.

When the plotter is switched on (run key, Fig. 3), it feeds the blank tape through the reader at a rate of one character per clock-pulse (about two characters per second). While the tape reader is reading blank tape, the distributor relays close in the normal sequence of hundreds, tens and units. After that, a gap of one clock-pulse occurs before the sequence is repeated. The important function of the first starting character encountered is to set the distributor to the blank position. The next clock-pulse then advances the distributor into the hundreds position and at the same time feeds the hundreds character into the reading position. Similarly the other characters are fed in turn by the distributor to the correct decoding relays. It should be mentioned here that the decoding relays are each fitted with an extra pair of contacts (called "self-hold" contacts) which maintain them closed even though the supply from the tape reader is interrupted. In this way, the decoding relays will remain in the positions determined by the tape characters. When the starting character of the new number is reached, the bits of all three decimal numbers are "remembered" as the settings of the twelve relays. The interconnected contacts on these relays are connected to a potential forming network (Figs. 5, 6) which produces a potential proportional to the value of the decimal digits on the tape. This potential forms the input of the recorder.

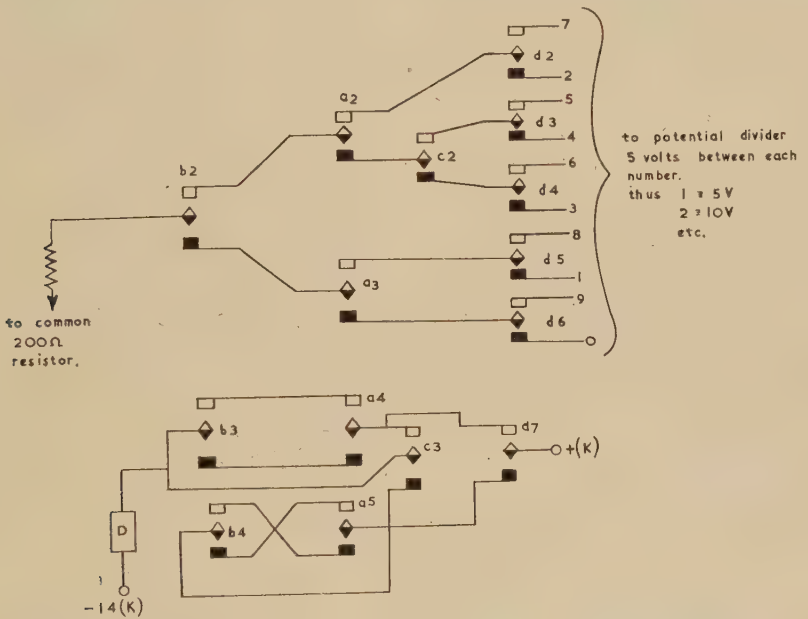

Fig. 5. Decoding relay-contact connexions for "Watts reflected decimal" code

The synchronizing hole in the tape operates relay *E* (Fig. 3) with the following results. (The appropriate contacts are specified in lower-case letters.)

(1) The clock-pulse generator is stopped (e_1, Fig. 3).

(2) Relay *G* (Fig. 3) is energized (e_3, Fig. 3) and its contacts start the paper drive of the rceorder and energize the servo-motor so that the pen of the recorder starts to move to a position corresponding to the input potential of the recorder, and therefore the decimal number on the tape.

(3) A time-delay circuit (Fig. 3) is started (e_2, Fig. 3). This circuit will close relay *D* (Fig. 3) after a delay of about 0·6 s.

While the time-delay circuit is operating, the pen of the recorder is able to move to the new position and the paper moves forward by about 0·5 mm. At the end of the time-delay period, relay *D* closes with the following results:

(i) The supply to relay *G* is interrupted (d_3, Fig. 3) so that the paper stops moving, and the pen, which by this time will be in the new position, is prevented from moving any further.

(ii) The supply to the self-hold contacts (a_0' to c_2', Fig. 4) on the decoding relays is interrupted (d_4, Fig. 4) and all these relays open.

(iii) The distributor is set (d_2, Fig. 3) to the blank position.

(iv) A potential is connected to the delay network (R_{71}, C_{15}, Fig. 3) of relay *F*. Relay *F* closes about 0·15 s after the potential is applied to the delay network with the following results:

(*a*) The self-hold supply to the decoding relays is restored (f_2, Fig. 4).

(*b*) The clock-pulse generator is restarted (f_1, Fig. 3). The following clock-pulse will then advance the distributor and the tape, thus completing the cycle of operations.

Though it was supposed that the numbers were preceded by blank tape, this is not necessary in practice. However, the first number may be incorrectly plotted if the tape is not started with the starting character in the reading position of the tape reader.

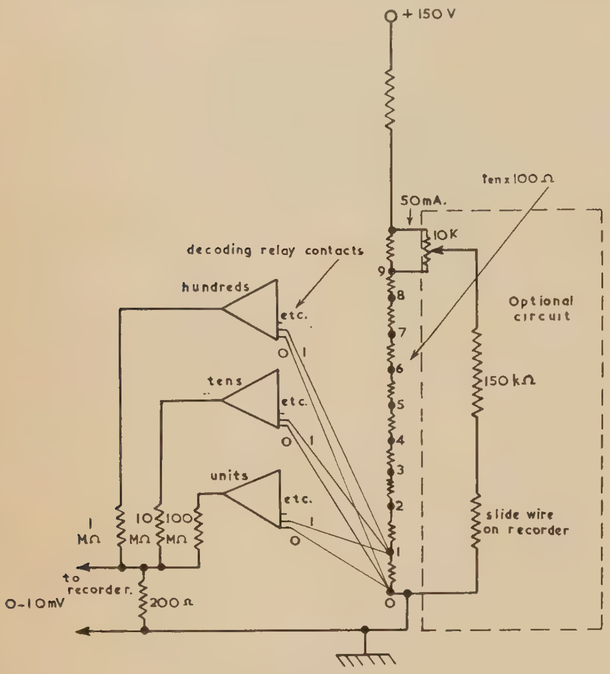

Fig. 6. Potential-forming network

Modifications to the recorder

The nature and extent of modifications to the recorder depend on a balance between the appearance of the final graph and the ease of converting the recorder back again to normal use. The minimum modification is as follows. It is essential that the servo-motor of the recorder should be prevented from moving in between the plotting of numbers. In most recorders, the servo-motor is a two-phase induction motor and it can be prevented from moving at the wrong time by supplying one of its phases *via* contacts on relay *G* (Fig. 3). This relay should be mounted inside the recorder itself as otherwise the switching transients may disturb the transistor circuits. If this is the only modification, the paper drive must be run continuously and the graph has a stepped appearance. The distance between points along the paper is determined by the rates of paper feed and plotting. The appearance of the graph can be slightly improved by allowing the paper to run only while the servo-motor is energized. This can be arranged by supplying the motor *via* contacts on relay *G* (Fig. 3). If the paper is driven by a two-phase motor, only one of the phases should be supplied *via* relay *G* as there will then be little movement of the paper after the relay has opened.

A big improvement in the appearance of the graph may be made by replacing the continuously writing pen by one that makes a single dot for each number plotted. We have arranged this on our recorder by fitting a "Uno" pen worked by a relay (P.O. type 600) mounted on the sliding carriage which normally carries the continuously writing pen. The relay is operated by an extra pair of contacts on one of the distributor relays so that the pen makes a brief contact with the paper once for each number. Finally, the supply to the slide-wire of the recorder may be obtained from the optional part of the potential-forming network (Fig. 6).

Decoding unit

The contacts and coils of the decoding relays are arranged as shown (Figs. 4 and 5). This arrangement will decode Watts reflected decimal code and represent the decoded numbers as a potential such that $V = 10N/1000$ mV, where N is the number on the tape and can have any value from 0 to 999. If the optional part of the potential-forming network (Fig. 6) is used, so that the slide wire of the recorder is supplied from the same source as the potential-forming network, then the supply to this circuit does not need to be specially stable (± 5 V). However, if the slide wire is not connected in this way the supply to the potential-forming network must be stable to the required accuracy of plotting. A stability of $\pm 0{\cdot}1\%$ would be suitable.

Errors

The error in the second stage of conversion is determined by the details of the potentiometric recorder, mainly the uniformity and pitch of the winding of the potentiometer and the gain and stability of the feedback system. Many commercial instruments have an accuracy of better than three parts in 1000 while an accuracy of one part in 1000 is sometimes offered to special order.

The errors in the first stage, in which the numbers are converted into a voltage analogue, are of two kinds. (1) Errors in the values of the resistors in the potential-forming network. (2) Inherent errors in the method of forming and combining the analogues of the three decade digits. Errors of the first kind can be kept within acceptable limits by using resistors of the required accuracy. The design of the potential-forming network is such that, even if the errors are distributed in the worst possible combination, the error in the voltage analogue will be no worse than that of the individual resistors. The accuracy of the individual resistors should therefore be of the same order as the precision of the input-code (for example, one part in 1000).

Inherent error

The graph plotter is initially set up so that the number 900 on the tape gives a mark on the graph paper of exactly 900/1000 of full-scale deflexion. If the resistors in the potential divider (100 Ω resistors, Fig. 6) are all of exactly the correct value the potential of the junction points of the resistors will be in the ratio of the resistors, that is, 9 : 8 : 7, etc., but when any of the feed resistors (1, 10, 100 MΩ, Fig. 6) are connected, the ratios will be disturbed. The error is greatest for the "hundreds" feed resistor. However, the circuit values have been chosen so that it does not exceed one part in 4000 in the worst case.

Finally, there is the error due to the combination of the three separate digital analogues. Basically the digit analogues are formed as currents and the final potential, that is, the potential that forms the input to the recorder, is formed by passing the combined current through a common resistor. The potential across this resistor decreases the applied potential across the feed resistors and so changes the current through them. The effect can be allowed for in any single decade, and the setting-up procedure does this for the "hundreds" digits. The error in the other digits is then negligible.

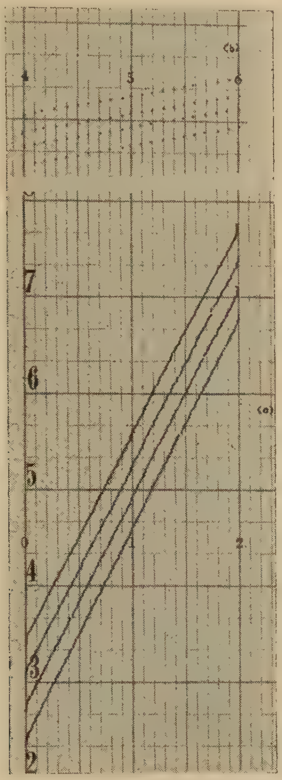

Fig. 7. (*a*) Steps of one unit 0–200 (0–2 on paper)
(*b*) Steps of ten units 400–600 (4–6 on paper)
It should be noted that as the recorder is adjusted to be correct at 0 and 900 the greatest possibility of error will occur at about 450 (4·5 on paper)

Performance

Our machine plots twenty points per minute, and at this rate there is ample allowance for changes in the performance of the various timing circuits and/or changes in the mechanical characteristics of the relays. We have used resistors of 0·1% accuracy and the accuracy of the plotted points is limited by the recorder* to about two parts in 1000. Fig. 7 gives an idea of the repeatability and accuracy of plotting under practical conditions.

The individual steps along the abscissa show some fluctuation. As the steps are small it is not easy to measure this directly, but the maximum variation is estimated (from measurements made over ten successive steps) not to exceed 3% of the step length. A variation of this size does not seriously affect the shape of the graph but if better constancy were needed it could be obtained by driving the paper continuously with a synchronous motor and locking the clock-pulses to the mains frequency.

Acknowledgements

The authors gratefully acknowledge the assistance of G. C. Midgley (Department of Philosophy) and the staff of the Durham University Computing Laboratory in all matters concerning the computer. One of us (L. M.) would also like to acknowledge a prolonged and most informative discussion on the problems of handling data in digital form with F. A. Johnson of the Royal Radar Establishment, Malvern.

References

(1) Susskind, A. K. *Notes on Analog-Digital Conversion Techniques*, pp. 2–1 (London: Chapman and Hall Ltd., 1958).

(2) Hartree, D. R. *Numerical Analysis*, p. 34 (London: Oxford University Press, 1952).

---

* The recorder at present in use is made by Messrs. Honeywell and Brown, type 153 × 18. A recorder made by Elliot Ltd. has also been used.

Apparatus for measurement of sorption of reactive, condensable vapours up to 350°C

by R. M. BARRER, F.R.S., and S. WASILEWSKI, Physical Chemistry Laboratories, Chemistry Department, Imperial College, London, S.W.7

[*Paper first received* 19 *January, and in final form* 25 *April,* 1960]

Abstract

An apparatus for the measurement of sorption of reactive, condensable vapours at temperatures up to 350° *C and pressure range* 0·1–760 *mm of mercury is described. It is composed essentially of a wholly enclosed Pyrex-glass balance system, incorporating a silica spring balance, a sensitive platinum resistance thermometer and a spiral pressure gauge; the whole unit being surrounded by electric furnaces. The pressure and temperature measurement and control are also described. The amount sorbed can be measured with accuracy to* 0·03 *mg; pressure to at least* 0·05 *mm of mercury; temperature to* 0·01° *C.*

Introduction

SINCE its introduction by McBain and Bakr(1) the silica spring balance has been an important means of studying the sorption of gases and vapours by solids. It has been used successfully not only at ordinary temperatures and pressures but also at high pressures and at low temperatures. During a study of sorption equilibria, we have had to make measurements under exacting conditions which led us to develop the apparatus, involving the silica spring balance, described below. Accurate sorption isotherms were required under the following conditions:

(i) the sorbate was not readily volatile (for example, I_2, S, $AlCl_3$, $FeCl_3$, $HgCl_2$), or was corrosive towards mercury or tap grease (I_2, Br_2, S);
(ii) the sorption studies were to be conducted up to about 350° C, at pressures up to one atmosphere.

The apparatus comprised several component parts which will be briefly described.

Balance system

The conditions (i) and (ii) were met, as in Fig. 1, by constructing a wholly enclosed Pyrex-glass balance system (Fig. 2) consisting of an upper section, in which was suspended the spring (20) carrying a small bucket of sorbent, and a bottom reservoir (24), containing the sorbate and joined to the upper section by a narrow tube. In-sealed into the balance case was a tube carrying a platinum resistance thermometer (21) appropriately placed in relation to the bucket carrying the sorbent. A Pyrex-glass spiral gauge (22) was used for pressure measurement, this gauge being in-sealed into a glass tube which in turn was in-sealed into the upper balance case. The inside of the spiral then had direct contact with the vapour in the balance case, while the outside surface was in contact with nitrogen gas, introduced at regulated pressures through a tube entering by way of a suitable small aperture in the surrounding furnace (3). By adjustment of the nitrogen pressure, the gauge could always be brought to zero deflexion, and the nitrogen pressure then equalled the pressure of sorbate vapour in equilibrium with the sorbent. Movement of the spiral gauge was registered by the movement of a platinum-coated mirror, attached to the spiral, which reflected a beam of light through an optically flat glass window on to a galvanometer scale. The detail of this manometer is indicated in Fig. 2.

A second side-arm passing through a small opening in the furnace (3) served to evacuate the balance case, and to outgas the sorbent. When outgassing was complete a sealed glass tube, containing pre-distilled sorbate and placed in the bottom reservoir, was broken by means of a magnetic hammer and the sorbate was frozen out with liquid air until furnace (2) was brought into position, and the experiment was commenced. Before this stage, however, the side-arm was sealed off, completing the isolation of the sorption system. There was an additional side-arm used for careful admission of air to the system when, after completion of a series of experiments, it was desired to change either sorbate or sorbent. This was a glass tube, very narrow at the end, which could be broken after covering by a rubber tube closed by a screw clip.

Furnaces

Three furnaces were used: the topmost furnace (1) heated the upper chamber of the balance case; the bottom furnace (2) heated the sorbate reservoir. The middle furnace (3) was designed to eliminate any temperature drop at the junction between the upper furnace (temperature T_1) and the lower furnace (temperature T_2). It is essential that no part of the system should fall below T_2 or distillation of sorbate out of the reservoir would occur.

The first two furnaces were mounted on steel railings and were counter-weighted so that they could be moved in vertical directions, and then rotated sideways to give easy access to the balance case. The third furnace was in the form of two semi-circular segments which could be removed separately. To ensure the most even temperature distribution, the inside cores of the furnaces were made of stainless-steel tube.

In the main furnace (1) the inner steel tube was 110 cm long and 3⅜ in. diameter, and was fitted with five optically flat quartz windows, to allow measurements of the length of the silica spring and observation of the mirror attached to the spiral gauge. The steel tube was covered with asbestos or silica cloth and on it the heating wire (Nicalloy A) of total resistance 270 Ω (7·16 Ω/yd) was wound in such a way as

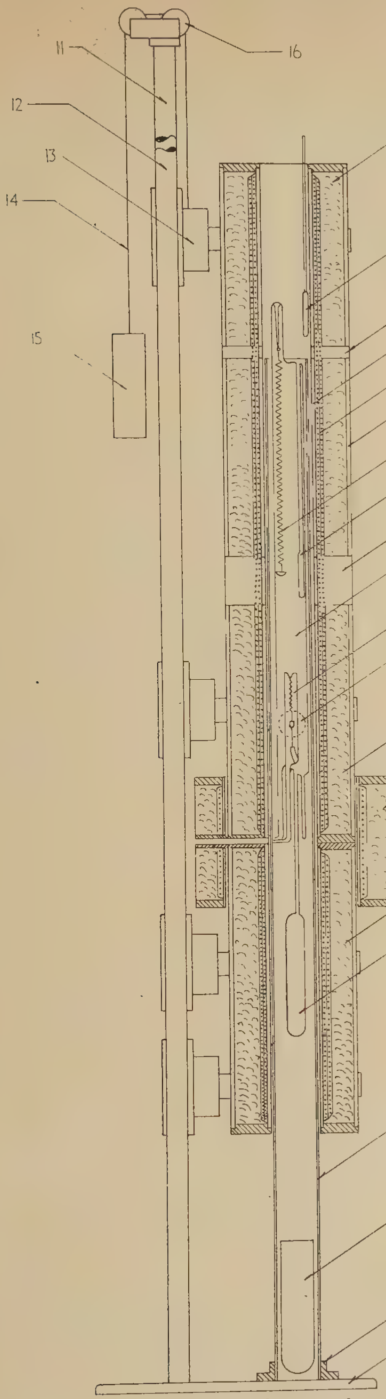

Fig. 1. Diagram of measuring apparatus

1 Furnace No. 1
2 Furnace No. 2
3 Furnace No. 3
4 Stainless-steel tube
5 Heating wire and insulating material
6 Asbestos wool
7 Asbestos tube
8, 9 } Windows
10 Stainless-steel tube supporting balance case
11, 12 } $1\frac{1}{2}$ in. diameter steel rod
13 Sliding clamps
14 Steel cord
15 Counter-weight
16 Pulleys
17 Cast-iron base
18 Independent support for (10) with levelling device
19 Balance case
20 Quartz spring
21 Platinum thermometer for measuring temperature
22 Pressure-measuring device
23 Optical window
24 Vessel for sorbate
25 Dewar flask
26 Platinum thermometer for temperature control

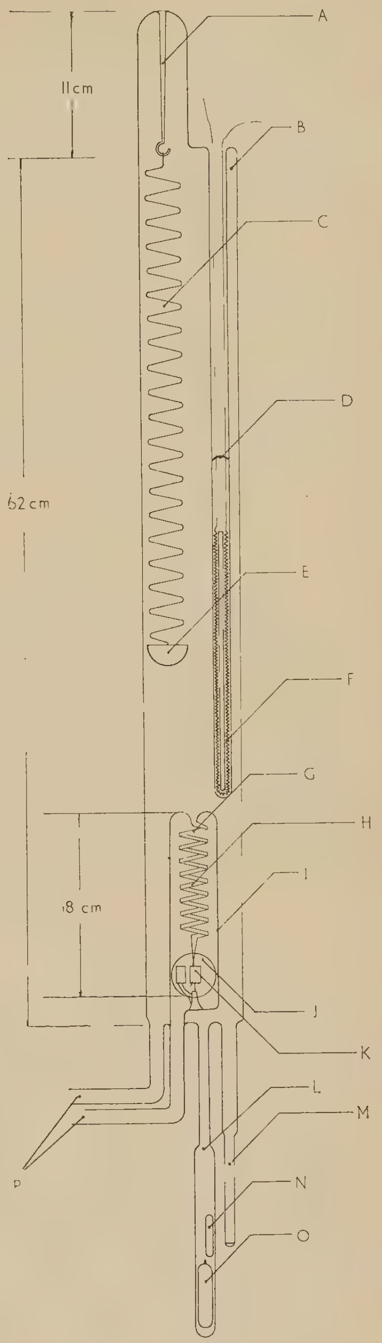

Fig. 2. Balance case

A, glass hook; *B*, balance case; *C*, silica spring; *D*, in-seal; *E*, glass bucket with sorbent; *F*, platinum thermometer; *G*, spiral gauge; *H*, hollow spiral; *I*, outer wall; *J*, optical flat; *K*, platinized glass mirror; *L*, reservoir for sorbate; *M*, device for admitting air; *N*, magnetic hammer; *O*, sealed tube with sorbate; *P*, to pumping system and pressure measuring and levelling devices to secure uniform heat distribution along the tube. The heating wire was fixed in position by alumina cement and covered with asbestos or silica cloth. On it was wound the main heating element (Kanthal wire of resistance 0·66 Ω/yd and total resistance 27 Ω). It was secured in position and covered as for the inner winding. The resultant furnace core was placed inside an asbestos tube of 1 ft in diameter, fitted with five optically flat Pyrex windows. The free space between the tubes, except for that of the windows, was packed with asbestos wool. The two tubes were held in position at both ends by asbestos rings which were bound together by two steel rods diametrically spaced inside the furnace.

The lower furnace (2), 40 cm long, was constructed in the same way as the furnace (1). The total resistance of the main heating element was 36 Ω (1·60 Ω/yd), and that of the subsidiary element was 250 Ω (10·8 Ω/yd). Each semi-circular part of the central furnace (3) had windings in a form of a uniform wire coil 0·5 cm diameter. The windings were uniformly and vertically distributed along the inner wall and secured by Pyruma cement.

Temperature measurement

The temperature inside the sorption balance case was measured by means of a platinum resistance thermometer, the glass sheath of which was only 0·1 mm thick so as to minimize the time lag in heat conduction. The thermometer responded to temperature variations of less than 0·001° C. The thermometer and its compensating leads were connected to a modified form of Callendar–Griffiths bridge, which was checked on a new type of Smith difference bridge(2) with an accuracy of 0·000001 Ω, as supplied by the Cambridge Instrument Co. The balance point was indicated by a mirror galvanometer of sensitivity 740 m/μA.

Temperature control

The temperature was controlled by a modified form of Roberts controller,(3) changes in temperature being detected by a sensitive platinum resistance thermometer placed in close proximity to the inner metal wall of the furnace. Furnaces (1) and (2) were heated by the main heating element to a temperature a few degrees below that required, the voltage being maintained by a constant voltage regulator and adjusted by an 8 A Variac. Fine control was then obtained by switching on the auxiliary heating element, the current of which passed through the Roberts controller. Across the switch of the controller a variable resistor was connected so that, in effect, the current through the auxiliary heating element was automatically decreased or increased, as the switch opened or closed, so as to keep the resistance of the platinum resistance thermometer constant. With this equipment the furnace temperature was maintained constant within 0·1–0·05° C. The temperature of the third furnace was regulated by means of a Variac.

Pressure measurement

The spiral-gauge manometer already referred to gave a 1 mm deflexion on the galvanometer scale for 0·1 mm pressure difference, so that in a pressure range 1–760 mm of mercury the pressure could be read to at least 0·05 mm. Since the counter-balancing nitrogen pressure was read by a cathetometer in a manometer at room temperature, the connecting tube was made not less than 1 cm diameter, to avoid thermomolecular pressure effects.

Silica spring

A silica spring convenient for the purpose of our experiments contained 60 turns and had a sensitivity of 36 cm/g. The spring length was measured by a cathetometer, reading to 0·01 mm. An extension of 1 mm corresponded to 3 mg weight, so that the amount sorbed could be measured with accuracy to 0·03 mg.

The apparatus has been in constant use for more than a year, at temperatures up to 300–350° C. The upper limit of temperature is set by the thermal properties of the glass of the silica spring and of the spiral gauge. Hysteresis begins to appear in heating and cooling cycles above about 350° C. Fig. 3 shows a typical family of isotherms, obtained in the apparatus described, for occlusion of iodine by a near-faujasite (Linde Sieve X). The thermodynamic analysis of these and other isotherms will be given elsewhere.

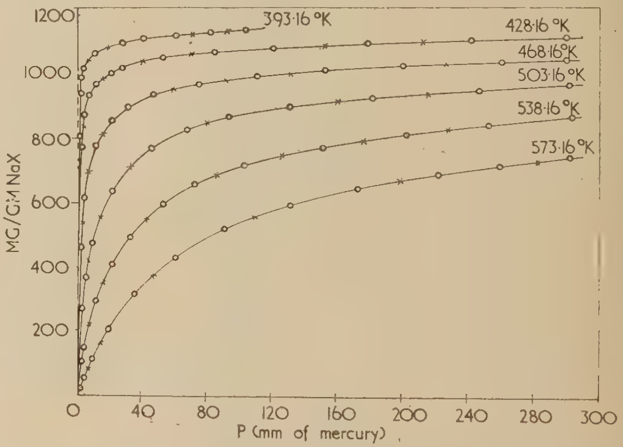

Fig. 3. Family of isotherms for sorption of iodine on sodium near-faujasite (Na–X)

○ sorption
× desorption

References

(1) McBain and Bakr. *J. Amer. Chem. Soc.*, **48**, p. 690 (1926).
(2) Smith, F. E. *N.P.L. Collected Researches*, **9**, p. 219 (1913).
(3) Roberts, M. H. *Electronic Engng*, **23**, p. 51 (1951).

Instrument for the measurement of specular reflectivity of bright metal surfaces

by B. A. SCOTT, A.R.C.S., Ph.D., F.R.I.C., F.I.M. The Research Laboratories of The British Aluminium Co. Ltd., Chalfont Park, Gerrards Cross, Buckinghamshire

[*Paper first received* 10 *May, and in final form* 10 *August*, 1960]

Abstract

A simple modification of the gloss head for painted surfaces, described in Defence Specification DEF/1053 (*Method* 11), *enables it to be used for the measurement of the surface quality of bright anodized aluminium in terms of specular reflectivity. The instrument has a high sensitivity, and readily discriminates between surfaces of differing appearance. Good reproducibility between two instruments after modification, and satisfactory correlation with visual assessments of surface quality, have been obtained. The instrument should prove useful for the evaluation of bright finishes on other metals, but is not suitable for matt or highly diffusing surfaces.*

Introduction

THE current use of chemical brightening solutions for the production of a bright appearance on aluminium and certain of its alloys has revealed that the Guild photometer(1) is not entirely reliable as a means of assessing the quality of the surface, and the results often disagree with the evidence of visual observation. A characteristic feature of all chemical brightening treatments is the production of a surface showing a varying degree of rounded irregularity described as "grain", "orange peel", "pebble", etc., which gives the reflected image a broken or distorted appearance, but to which the Guild instrument is relatively insensitive. For example, the accepted method of estimating surface quality with this instrument is by means of the ratio S/T of specular to total reflexion factor, and the respective figures for the best mirror-like finish and a chemically-brightened surface showing only a "fuzzy" reflected image are 0·992 and 0·985 respectively, a difference of less than 0·8%.

These limitations of the Guild photometer appear to result from the arrangement of the optical system, which was originally designed to deal with surfaces of all types, ranging from highly diffuse to highly specular. The instrument consists of an integrating sphere, whitened internally, having a small circular aperture against which the surface under test is closely applied. A convergent beam of light is allowed to fall on the surface of the specimen, which then acts as a secondary source of light shining into the sphere. The reflected cone may be intercepted at will by a blackened cavity which is intended to trap the light specularly reflected. The light intensity within the integrating sphere is measured by means of a photoelectric cell and galvanometer. With the absorbing cavity in position, the instrument responds to the diffusely reflected light only, while the total reflexion is determined with the cavity swung out of the way.

It will be realized that specular reflexion, unlike total reflexion, is an arbitrary parameter defined, in this instance, by the angle of the light cone and the dimensions of the blackened cavity. In the Guild instrument, it is possible that some light not necessarily reflected specularly, i.e. such that the angle of reflexion is nearly equal to the angle of incidence within relatively narrow limits, may be intercepted by the absorbing cavity owing to the conical beam.

Gloss head instrument

Many of these disadvantages appear to be overcome by the gloss head originally designed for the evaluation of painted surfaces, and described in Defence Specification DEF/1053 (Method 11). The apparatus is available complete with a combined reflecting galvanometer and constant-voltage source for the lamp, making a convenient portable assembly. The instrument is only capable of measuring specular reflectivities relative to a standard surface, and cannot be adapted to measure total reflectivity, for which another head (the P.R.S. head(2)) is available for attachment to the same measuring instrument.

The optical system on the gloss head is shown diagrammatically in Fig. 1. The light from the lamp is rendered parallel by means of a lens, and meets the surface of the specimen, which must be held flat against the base of the instrument, at an angle of 45°. The specularly reflected light is collected by means of a similar lens, which forms an image of the lamp filament at its focal distance. An orifice plate with a rectangular aperture, slightly larger than the filament of the lamp, is placed at this point, and the reflected light is then allowed to fall on the measuring photocell. As in the case of the Guild photometer, the size of this aperture, or rather the effective angle of acceptance of the instrument subtended at the metal surface, defines the specular reflectivity

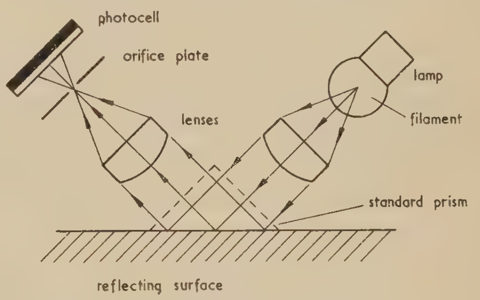

Fig. 1. Optical system of gloss head

on an arbitrary basis. The angle of acceptance of the photocell diaphragm subtended at the surface of the specimen under test is about 0·001 15 steradian, as against 0·2 steradian for the Guild photometer. Another advantage of the instrument appears to lie in the fact that a parallel rather than a convergent beam of light impinges on the specimen, and that rays departing only slightly from parallelism, because of irregularities of the surface, will miss the rectangular aperture. Specular reflectivities are compared directly over a relatively large area (about ½ in. diameter), which tends to reduce sampling errors, particularly with specimens showing a fairly coarse grained finish.

Standard reflecting surface for gloss head

Since the instrument is only capable of giving comparative readings, it would be advantageous if a surface of known specular reflectivity could be employed as a standard. The most obvious choice of a surface-silvered mirror suffers from the disadvantage of susceptibility to tarnishing and mechanical damage, while in a back-silvered mirror, the glass introduces variable errors because of displacement of the reflecting surface from the measuring plane of the instrument.

Both these objections appear to be largely overcome by the use of a 45°, right-angle prism with its hypotenuse face as the reference surface. Such prisms are obtainable fairly readily with optically worked faces, and a high degree of dimensional precision, which makes them particularly suitable for use as standards. Dimensions of a suitable prism are 1 × 1 × 1·41 in. In use, the prism is placed with its hypotenuse face in contact with a plane sheet of black plate glass. The measuring aperture of the gloss head is placed over the prism and in contact with the black glass without fouling the prism, with the light beam normally incident on one of the 45° faces, and the reflected beam emerging normally from the other.

Allowing for the losses caused by reflexion at the glass/air interface (4–5%) and absorption in the glass (2%), the theoretical specular reflectivity of the prism with total internal reflexion at the hypotenuse face should be almost exactly 90%, provided it is kept clean and grease-free.

It was found by experiment that minor displacements of the prism from a central position with its axis at right-angles to the optic axis of the measuring head, did not produce any significant change in photo-cell response as indicated by the galvanometer, and reproducible readings to within ±1% would be easily obtained after removal and replacement of the prism without any special precautions other than judgement by eye. Five different prisms also gave similar readings within the same limits.

Comparison of gloss head and Guild photometer

After alinement of the optical system, the reading of the gloss head with the prism in position was set at 100 units on the galvanometer scale, and a series of readings of specular reflectivity was taken on a number of bright anodized aluminium samples. Four measurements were made on each 6 × 3 in. specimen, two in the direction of rolling, and two at right-angles. In Table 1 the mean reading in the rolling direction is placed first. In general, this reading was slightly the higher. Table 1 also shows the ratio of specular to total reflectivity as measured by the Guild photometer, and the corresponding ratio of gloss head to P.R.S. head readings, multiplied by a factor of 0·90 to allow for the specular reflectivity of the standard prism. The last column gives the maximum distance in metres at which the reflected image at approximately 45° of an illuminated Gardam grid[3] with ⅜ in. black lines could be resolved.

Table 1. *Specular reflectivity and image resolution*

Sample	*Gloss head, Prism = 100*	*Guild S/T*	*Gloss head, S/T × 0·9*	*Gardam grid, (m)*
A	89/88	0·989	0·895/0·885	9·5
B	88/87	0·983	0·875/0·865	9·5
C	84/83	0·987	0·85/0·84	9·5
D	83½/82	0·990	—	8·5
E	78/73	0·990	0·78/0·73	5·5
F	71/71	0·963	0·725/0·725	9
G	69/59	0·980	0·705/0·605	3
H	69/58	0·983	0·705/0·595	2
I	67½/62½	0·980	0·68/0·63	1·5
J	60/60	0·969	0·61/0·61	1·5
K	62/55	0·983	0·62/0·55	1·25
L	60/52	0·980	0·61/0·53	1
M	57/51	0·985	0·57/0·51	1·25
N	62/45½	0·985	—	1
O	49/45	0·981	0·495/0·455	0·5
P	44/38	0·917	0·48/0·41	6
Q	37/36	0·946	0·375/0·365	0·3
R	34/30	0·975	0·345/0·305	0·25
S	21/20	0·952	0·22/0·21	1·25

Although, with the Guild photometer, it is more usual to employ the ratio of specular to total reflectivity S/T as a criterion of surface quality, it seems more appropriate to use the specular reflectivities obtained directly with the gloss head for this purpose, in view of the extremely limited range of total reflectivity (87–90½%) recorded by the P.R.S. head in comparison with a standard magnesium carbonate surface. This has the advantage that only one kind of measurement is required for metal surfaces of similar type, while the relative order of merit of the specimens remains substantially unchanged.

The most striking observation from Table 1 is the increased sensitivity of the gloss head as compared with the Guild photometer, as exemplified by the difference in readings between the best and worst samples *A* and *S*. The improvement in discrimination obtained with the gloss head is illustrated in Fig. 2, which shows four brightened aluminium

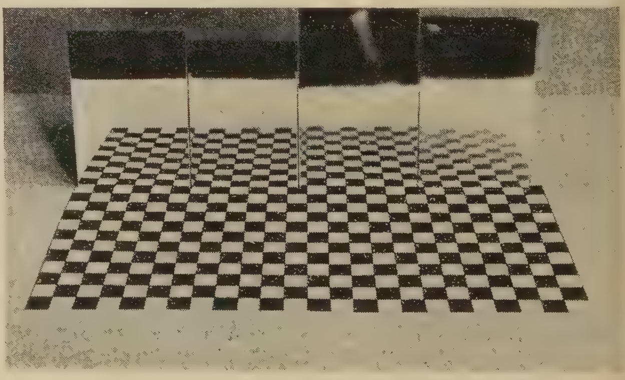

Fig. 2. Appearance of bright anodized samples

Sample	*B*	*E*	*I*	*M*
Guild, S/T	0·983	0·990	0·980	0·985
Gloss head, mean (%)	87·5	75·5	65·0	54·0

urfaces of widely differing appearance, together with their respective Guild photometer and gloss head readings. Although the increased sensitivity of the gloss head is gained at the expense of some loss of apparent reproducibility, it is possible that some of the variations encountered are caused by real differences from point to point of the metal surfaces.

The interpretation of the instrument readings in terms of the subjective appearance of the surface is complicated by the ability of the human eye to take into account a number of different factors when assessing the quality of a bright metal surface. These include the overall brightness of the reflexion, the clarity and resolution of the reflected image including image contrast, and the presence and relative size of surface irregularities. Another complication is that these factors are not necessarily independent of each other, and are themselves of a complex character. For this reason, it is not possible to express a visual assessment in the form of a figure, other than the relative order of ranking, which is also apt to vary with different observers.

The use of the Gardam grid, which concentrates mainly on image clarity or resolution, enables an observer to assign a figure, which is reasonably reproducible between different observers, to any reflecting surface. This measurement represents the maximum distance at which the reflected image of the individual lines of an illuminated rectilinear grid may be resolved. The image is viewed at an angle of 45°. The results obtained for a grid made up of black and white lines $\frac{1}{8}$ in. wide is shown in the last column of the table.

Although the reflectivity measurements with the gloss head may be considered to be associated more closely with the brightness of the reflexion, while the Gardam grid figures tend to emphasize the effect of image resolution, the correlation between these two sets of observations was quite good. The Guild photometer readings on the other hand showed poor correlation, as well as a limited range between extremes.

In the case of three samples lettered *F*, *P*, and *S* in Table 1, the Gardam grid results appeared to be higher than would be expected from the reflectivity figures. A closer examination of the specimens concerned revealed that each had a milky or finely diffusing surface that reduced image contrast without a corresponding effect on resolution. The lack of correlation in these cases is not surprising in view of the different criteria of measurement of the two methods.

Modified gloss head

A large number of determinations of specular reflectivity have been carried out using two gloss heads on a range of brightened surfaces, in order to test the reproducibility of the method. These experiments revealed that variations in reading could be obtained from the use of the lamp filament as an image source. Agreement between the two instruments was not very good, and replacement of one lamp by another of the same type produced systematic differences in reading, even after careful alinement. This was finally traced to variability of the filament shape and position, as well as lack of uniformity of the glass envelope, in the small 6 V, 3 W motor-car side-lamp bulbs used. Typical results are shown in Table 2 below.

A considerable improvement was obtained by frosting the bulb of the lamp with emery cloth moistened with turpentine, and covering it with a cylindrical brass cap carrying a central $\frac{1}{16}$ in. hole, which acted as a secondary-image source, while the slit diaphragm in front of the photo-cell was replaced by a similar circular aperture. The brass cap just covered the bulb of the lamp, and was conveniently held in position by means of the clamping screw provided for securing the bulb in its holder. The metal gauze placed behind the slit to reduce the photocell response was also removed, since the amount of light available had been decreased.

Table 2. *Comparison of reflectivity measurements with two gloss heads*

Sample No.	*Gloss head reading: Prism = 100* *Instrument A*			*Instrument B*		
1	84/83	85/83	—	—	—	—
2	71/71	76/74	73/72	78/76	79/77	78/76
3	69/59	72/60	71/59	72/62	74/64	75/63
4	69/58	68/59	67/58	73/62	72/63	73/63
5	60/52	63/53	62/52	62/55	64/55	64/57
6	49/45	50/46	49/45	54/50	54/51	55/51
7	44/38	46/40	45/40	47/42	47/40	47/43
8	34/30	36/32	36/32	37/35	38/35	38/36
9	21/20	24/23	23/23	24/23	23/24	25/23

The modified arrangement is shown diagrammatically in Fig. 3 in which it can be seen that the lampholder assembly has been moved back so that the circular aperture now occupies the focal position previously held by the filament. This new position was located by means of a split collar on the tubular support of the illuminating system, arranged so that a circular spot of light could be seen in sharp focus on a screen at about 10 feet distant, when the instrument was tilted upwards. The alinement of the illuminating system was carried out using the three alinement screws in the base of the lamp housing in the same manner as for the unmodified gloss head.

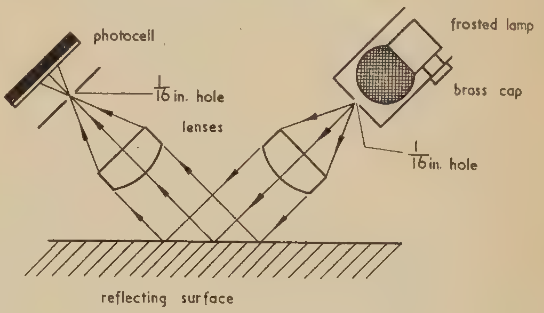

Fig. 3. Modified gloss head

Table 3 below shows the mean results of several groups of readings taken at different times using two similar gloss

Table 3. *Comparison of reflectivity measurements with modified instruments*

Sample No.	*Gloss head readings: Prism = 100* *Instrument A*	*Instrument B*	*Mean*
1	84, 84, 85, 85, 85, 86	85, 85, 87, 84, 84, 86	85·0
2	75, 75, 76, 75, 76, 77	76, 75, 77, 75, 76, 74	75·6
3	73, 73, 74, 73, 74, 74	74, 73, 75, 73, 73, 74	73·6
4	68, 67, 70, 68, 68, 68	68, 69, 70, 68, 68, 68	68·3
5	68, 67, 69, 68, 69, 68	68, 67, 69, 68, 67, 67	67·9
6	59, 59, 59, 59, 59, 60	59, 59, 60, 59, 58, 59	59·1
7	47, 46, 48, 47, 47, 47	47, 47, 47, 47, 46, 48	47·0
8	44, 44, 45, 44, 45, 46	44, 44, 45, 44, 43, 46	44·5
9	28, 28, 29, 29, 29, 29	29, 28, 29, 29, 29, 29	28·8

heads modified as described above. Agreement between the two instruments was good, even although the illuminating system of each was dismantled and re-alined several times during the course of the test.

The overall standard deviation for both instruments together was ±1·1 and it can be shown that there is no significant difference between the two sets of readings for instruments *A* and *B*.

With this arrangement, the readings at right-angles and parallel to the rolling direction were close together within the range of reproducibility of the instrument, in contrast to the previous readings with the linear image of the filament. This difference is probably due to the change from an elongated image to a more nearly uniformly illuminated circular spot, in which case a single mean figure can represent the specular reflectivity of the surface in question. Correlation with Gardam grid results was again satisfactory. The values of reflectivity obtained were higher than with the unmodified instrument. These values, as mentioned previously, are dependent on the acceptance angle of the photocell in conjunction with the geometry of the optical system. The angle of acceptance of the modified instrument is 0·001 25 steradian. Table 4 shows the effect of varying the size of the aperture, and hence the angle of acceptance, on the reflectivity of three of the previous samples.

Table 4. *Effect of aperture size on specular reflectivity*

Sample No.	*Gloss head readings: Prism* = 100 *Aperture diameter* (*in.*)				
	1/32	1/20	1/16	1/8	3/16
1	79½	85	84	88½	91
5	52½	66	69½	78½	83
9	14	24	29	50½	63½

Table 4 strikingly illustrates the increase in specular reflectivity and reduction in discrimination between samples with increasing angle of acceptance. The $\frac{3}{16}$ in. aperture corresponds to a solid angle of acceptance of about 0·0113 steradian, as compared with 0·0003 steradian for the $\frac{1}{32}$ in. aperture. It is not surprising that the Guild photometer tends to give high results with a relatively low degree of differentiation between samples, because of its high acceptance angle of about 0·2 steradian. In some cases, the relative order of the samples may vary with the acceptance angle of the measuring instrument, because of differences in the polar distribution of the reflected light.

The choice of any particular angle of acceptance is necessarily arbitrary, but the $\frac{1}{16}$ in. aperture selected for the modified gloss head shows good correlation with visual assessment while still affording a reasonable photoelectric-cell response.

Conclusions

The gloss head, modified in the manner described above, is a versatile, sensitive instrument for the assessment of specular reflectivity of bright metal surfaces. The correlation of the readings with visual observations of surface quality is good. Although the measurements in this paper have been confined to bright anodized aluminium, it would seem that the gloss head could also be employed for the assessment of other surfaces, such as mill finish or mechanical polishing on aluminium and other metals.

Standardization of the instrument is conveniently carried out using a 45° right-angle prism with total internal reflexion on the hypotenuse face. Such an arrangement has an absolute specular reflectivity of 90%. For convenience, the reading of the instrument with the prism in position is set arbitrarily at 100%.

Acknowledgements

The author is indebted to his colleague, Mr. R. W. Thomas, for suggesting the use of a prism as a standard of reflectivity. Thanks are also due to The British Aluminium Co. Ltd., for permission to publish this paper.

References

(1) Guild, J. *J. Sci. Inst.*, **17**, p. 178 (1940).
(2) *Paint Research Station Technical Paper No.* 141.
(3) Gardam, G. E. *Metal Finishing*, **49**, p. 61 (1951).

Simple method for stopping a radiation chopper in a preferred position

by M. F. Kimmitt, B.A.(Sc.), Royal Radar Establishment, Malvern, Worcester

[*Note received* 3 *June*, 1960]

In our infra-red vacuum spectrometer, the radiation is interrupted by a two-bladed chopper so as to produce a signal from the detector suitable for a.c. amplification. As the spectrometer is also used with pulsed sources, it is necessary to have a reliable method of stopping the chopper with neither blade in the radiation path, and without destroying the vacuum. The 6 in. diameter chopper blade is driven by a small a.c. motor, servo-controlled at speeds from 150–3000 rev/min. Even a small out-of-balance component causes much vibration (and, presumably, considerable strain on the bearings) so it is not possible to achieve a preferential rest position by increasing the weight of one of the blades.

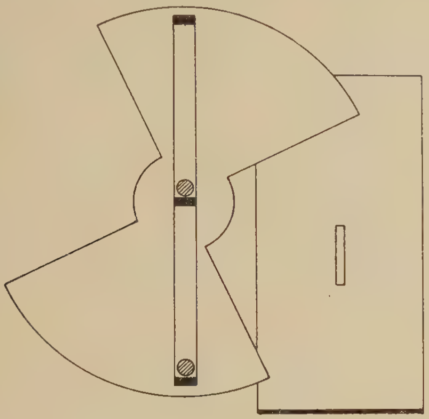

Illustration of method of stopping chopper in preferred position

The problem has been overcome by attaching a small-diameter tube to the face of the chopper blade. This is blocked at the centre and, after a ball-bearing has been inserted in each half, at both ends. At speeds greater than about 120 rev/min, centrifugal force carries the balls to the ends of the tube and the blade can be balanced dynamically. When the motor is switched off and the blade slows down, one ball drops to the end of the tube and the other to the centre. Consequently, the tube comes to rest in a vertical position. (In fact, as there is some residual friction, the tube stops within ±5° of the vertical.) By altering the position of the tube on the face of the chopper blade, the angle at which the blade comes to rest can be varied. The diagram shows how the method is used in the spectrometer where the radiation focus to be chopped is lower than the axis of the motor.

Flap-valve for long narrow apertures

by G. W. King, B.Sc., Ph.D., Department of Chemistry, McMaster University, Hamilton, Ontario, Canada

[*Note received* 9 *June*, 1960]

In large vacuum spectrographs the photographic plate is usually mounted in a chamber that can be isolated by a valve. Air can then be admitted separately to this chamber and the plate changed, without releasing the vacuum in the main body of the instrument. The isolating valve must close a long slot, through which a spectrum can be projected on to the plate during exposure, when the chamber is evacuated and the valve open. A satisfactory design for such a valve, used in a recently-constructed 21 ft vacuum spectrograph, is shown in the figure.

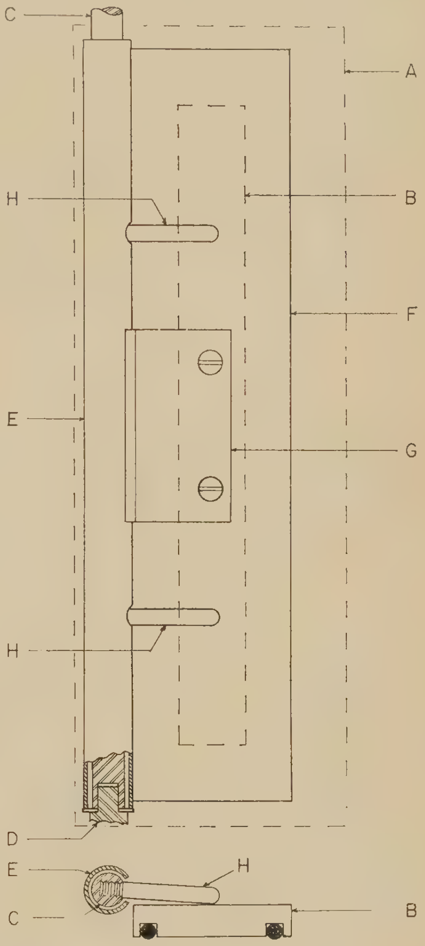

Flap-valve for long narrow apertures

The plate chamber was connected to the instrument proper by a steel duct, with internal dimensions $4\frac{1}{4}$ by $12\frac{1}{2}$ in. The inside of this duct is shown in section by the dashed rectangle *A*. The rectangular slot *B*, of size 1 by 10 in., through which the spectrum normally passes was cut in a flat metal plate welded across the end of the duct. The flap valve covering this slot had to meet three requirements; first, that it should be sufficiently compact to fit inside the duct; secondly, that it should not impede the passage of light when open; and thirdly, that it should have sufficient flexibility to bed properly when closed.

The upper end of a $\frac{1}{2}$ in. diameter steel rod *C* passes through a Wilson seal to a handle outside the duct (not shown). The lower end of *C* pivots on a bearing *D*, made by turning down the end of a $\frac{5}{8}$ in. steel bolt that is threaded through the bottom of the duct. A length of copper tube *E*,

$\frac{3}{4} \times \frac{1}{16}$ in., fits loosely over *C* and rests on a washer on *D*. The flap *F* is a brass plate $2\frac{1}{2} \times 11\frac{3}{4} \times \frac{1}{2}$ in. with a rectangular O-ring groove on its far surface. This groove was made by milling four straight cuts close to the sides of the plate, and then slightly rounding the edges where these cuts intersect. With the flap closed, the O-ring makes contact with the surface around the slot *B* at a $\frac{1}{2}$ in. distance from the edges of the slot. The flap *F* is bolted to a piece of $\frac{3}{16}$ in. brass sheet *G*, which is hard-soldered to the outside of the tube *E*. The two steel pegs *H*, of $\frac{1}{4}$ in. diameter steel rod, are threaded into the rod *C* and project through $\frac{3}{8}$ in. holes in *E*, as shown in the lower sectional view.

It can be seen that the flap *F* has some freedom of play due to the flexibility of the brass sheet *G* and the clearance between the tube *E* and the rod *C*. This enables it to bed properly when closed. Pressure can be applied to the back of the flap through the pegs *H* by rotating *C*, to hold the valve closed. When *C* is rotated in the opposite direction, the pegs *H* swing away from the flap, causing *E* to rotate and the valve to open.

In use, pressure need only be applied to the back of the valve by turning *C* while air is being admitted to the chamber; atmospheric pressure in the latter holds the valve closed and free of leaks.

Hot tube Nylon cord cutter for balloon flights

by J. A. Phillips, B.Sc., Grad.Inst.P., H. H. Wills
Physics Laboratory, University of Bristol

[*Note received* 21 *July*, 1960]

The release of equipment from non-bursting high altitude balloons is conveniently achieved by cutting the Nylon suspending cord with either an electrically heated wire, carrying 2–5 A, or an explosive chisel, firing on 0·1 A. These systems are actuated by a clockwork timing mechanism or by radio command from the ground. The hot-wire method is unreliable if the batteries become too cold due to increased internal resistance, as may occur on night flights, while the explosive chisel is a relatively complicated and expensive device. An electric detonator can also be used to sever a cord, but a safer method is preferred for balloon flights.

An alternative, and very effective type of cord cutter, has been tried recently in which a gasless heating composition, contained in a metal tube, is ignited with an electric detonator fuse-head (Fig. 1). The asbestos fibre above the composition traps all sparks which could ignite hydrogen-air mixtures. The cord is held in tension against the tube, as shown in Fig. 2. This arrangement can be fixed to the cord at any point without cutting the latter, as the tube can be screwed into position after the cord has been passed over it. On firing, the surface temperature of the tube rises 400° C or more, and the cord is melted through within a few seconds. (The melting point of Nylon 6.6 is about 265° C.) If required, several cords can be cut with the same tube. To reduce the horizontal bending force on the tube, the cord is passed through two grooves in the shackle; the grooves also serve to keep the cord central (Fig. 2). Satisfactory tests of the device have been made on balloons at altitudes of around 30 km, as well as in a vacuum chamber at a pressure of 6 mm of mercury. Copper tubes were used for test purposes, of length 10 cm, inner diameter 0·6 cm and outer diameter 0·8 cm, but larger diameter steel tubes are intended for cord loads of many kilogrammes.

The gasless composition employed consisted of an intimate mixture of 80% red lead and 20% silicon powder, of particle size less than 5 μ. This mixture ignites readily on exposure to a flame, burning in accordance with the reaction

$$Pb_3O_4 + 2Si \rightarrow 3\,Pb + 2\,SiO_2$$

yet is difficult to ignite by friction or impact. Gasless mixtures giving higher temperatures contain up to 92% of red lead, the amount required to burn all the silicon. If this latter figure is exceeded, the compositions become explosive when fired confined, as free oxygen is produced. A number of other gasless compositions are also suitable.*

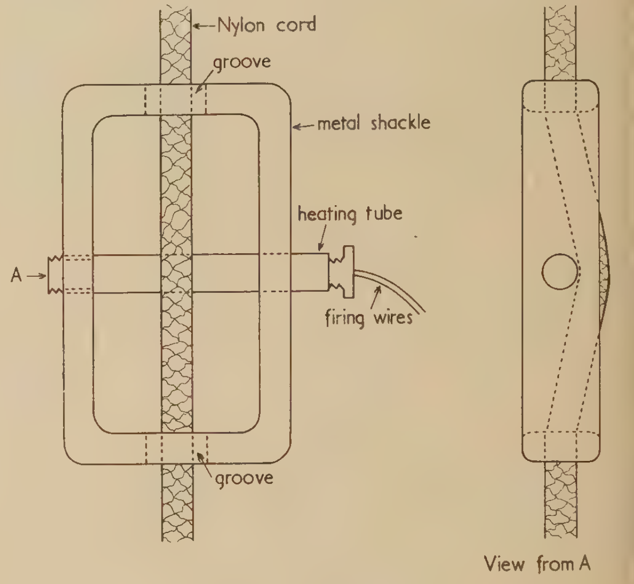

Fig. 1. The heating tube

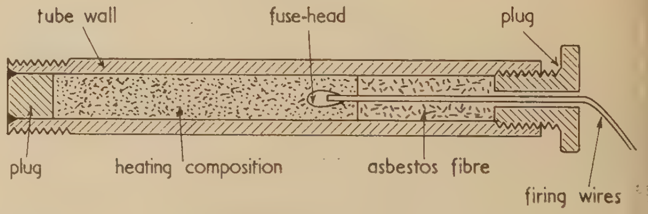

Fig. 2. Arrangement of cord through shackle

To fire the fuseheads, which ignite on 0·1 A d.c. at 2 V, a battery or charged capacitor is convenient. With capacitors of 2–8 μF, the fuse-heads fired on a minimum energy of 0·5 mJ, compared with the several Joules necessary for effective operation of the hot wire. A short circuit often develops in the tube after firing, allowance for which must be made if the battery operates other equipment, e.g. by putting a fuse in the circuit or, with a battery-capacitor system, by charging the capacitor through a high resistance. Adequate thermal insulation of the battery and capacitor (if electrolytic) is required, especially at night, as at the low temperatures experienced on the balloons the internal resistance rises, while the e.m.f. and capacity fall. Only the latter two quantities affect the performance of the battery-capacitor system, which is preferable to a battery used alone. The e.m.f. of a 30 V dry cell was measured as 7 V at −50° C and 1 V at $-75°$ C, while a 2000 μF electrolytic capacitor dropped to 300 μF at $-70°$ C.

---

* British Patent No. 760,360 (1956).

Cord cutters of the above type are intended for use on balloons of all sizes, from meteorological balloons to ones carrying loads of 500 kg or more. Other applications of the device also seem possible.

The author would like to thank Mr. J. Davies for many valuable suggestions, and Mr. D. Bye who helped with the experiments. Imperial Chemical Industries Ltd. kindly supplied the fuse-heads.

Film carrier for the analysis of oscillograms by means of a travelling microscope

by T. M. Parnell, Ph.D.Grad., Inst.P., Department of Electrical Engineering, University of Queensland

[*Note received* 10 *May*, 1960]

Oscillograms of voltage and current pulses on 35 mm film may be analysed conveniently and accurately by means of a two-coordinate travelling microscope. Experience at this laboratory has shown that the difficulty in alining the timebase or X-axis of an oscillogram with the appropriate axis of motion of the microscope may be a major source of error in such measurements. This note describes a film stage which facilitates rapid and accurate alinement of a calibration line on an oscillogram with either axis of the travelling microscope.

The device is illustrated in the figure. The main stage *A* is cut from ¼ in. thick Perspex sheet and carries a ball-race *B* of 2¼ in. internal diameter in a recess at its centre. The film stage *C* is a stepped circular Perspex plate whose central portion fits firmly inside the inner race of *B*. The centre of rotation of the ball-race is marked by a dot and interrupted cross on the upper surface of the film stage *C*. The arm *D* consists of an ⅛ in. diameter brass rod screwed into the upper edge of the film stage and permits finely controlled rotation of the film stage from outside the frame of the travelling microscope. The film is held flat on its stage under a hinged Perspex cover-plate *E* which is clamped by means of the spring clip *F*. To provide sufficient friction to prevent unwanted rotation of the film stage, the ball-race *B* is packed with a heavy grease.

The alinement procedure is as follows: The carrier is fixed in the frame of the travelling microscope in place of its original plate-glass stage, and the cross-hairs of the microscope are alined on the centre dot of the film stage. The film is then inserted under the cover plate and its position adjusted by hand so that the timebase line is centred on the cross-hairs. The cover plate is then clamped by means of the clip *F*. The microscope is next moved off centre along, say, its X-axis and the timebase line brought back on to the cross-hairs by appropriate rotation of the film stage. The timebase line is thus made parallel with the X-coordinate of the microscope. A final check of parallelism is made by observing whether the cross-hairs track accurately along the timebase line as the microscope is returned to its original position.

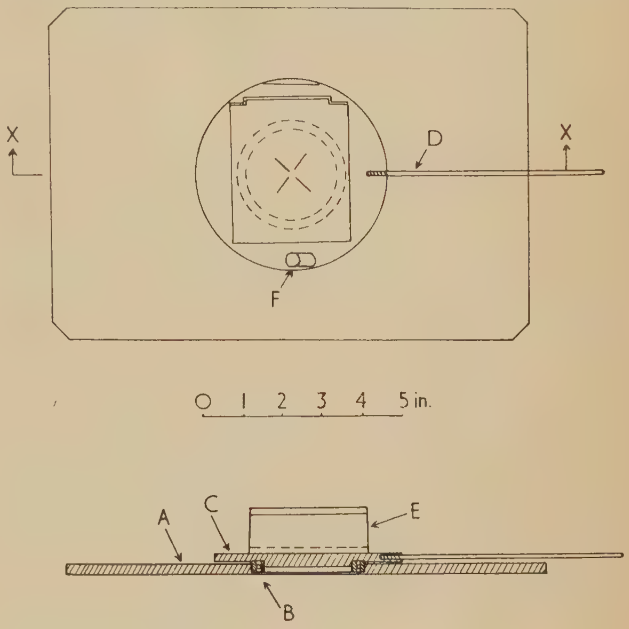

section X–X

Film carrier assembly

The microscope and film carrier have been mounted over an illuminating box having an inclined top which gives the operator a comfortable working position. For simple measurements, such as the ratio of pulse height to the distance between voltage calibration lines, the repeatability of a single determination is usually better than 0·25% for an individual operator and better than 0·5% for measurements by different operators.

New instruments, materials and tools

The Editor invites manufacturers of instruments and light machine tools to keep him informed of their new or improved products. The Institute of Physics and The Physical Society assumes no responsibility for the statements given below: information for these has been taken from literature supplied.

Non-reset electromagnetic counter. Counting Instruments Ltd., 5 Elstree Way, Boreham Wood, Herts.

This small electromagnetic counter is designed to operate on 230 V, a.c. in its standard design, but other voltages can be accommodated. It cannot be reset, and the cover is made to fix through the base of the frame, so that it cannot be removed without dismantling the counter. It is intended to meet the need for a compact counter which is safe from unauthorized interference.

Medical scintillation counter. Ekco Electronics Ltd., Southend-on-Sea, Essex.

This lightweight scintillation counter, with a directional shield, is constructed in a stainless steel container enabling it to be cold-sterilized. The output from the photomultiplier tube is fed *via* a cathode follower stage to the permanently attached cable. Connexions from this can then be made to a suitable ratemeter or scaler. Although the counter can be connected directly to some ratemeters, it requires the use of a separate amplifier when connected to those requiring a minimum output of 5 V.

The directional shield holds the scintillation counter by means of a simple clamp ring, and it can be fitted with any one of three standard collimators which provide alternative angles of acceptance. To facilitate accurate repositioning in relation to the patient, a continuously adjustible coincident light-spot range-finder is incorporated.

High-stability pulse amplifier. Ekco Electronics Ltd., Southend-on-Sea, Essex.

This general-purpose, high-stability pulse amplifier has a wide frequency response. It is designed for use with scintillation counters without built-in amplifiers and will drive ratemeters and scalers requiring an input of 5 V or more. A six-position gain selector is incorporated and the low impedance output is positive-going for a negative-going input. A simple modification, however, enables negative-going output to be obtained if desired. The power supplies are obtained from the associated ratemeter or scaler. It is claimed that the gain is approximately constant from 50 c/s to 200 kc/s and there is an upper half-power frequency of 1 Mc/s. The instrument is housed in a strong metal case of dimensions $12\frac{1}{8} \times 7\frac{3}{8} \times 5\frac{3}{4}$ in.

Strain gauge power supply. The Solartron Electronic Group Ltd., 45 Thames Street, Kingston, Surrey.

When working from transducers into a high-gain amplifier, a normal stabilized power supply may produce a large amount of hum. In order to eliminate this, a fully transistorized six-channel strain gauge power supply unit has been introduced by this firm, primarily for use with their own strain gauge pressure transducers. However, it is stated that the unit has been designed to work in bridges of a nominal 350 Ω resistance, but it may also be used with resistance bridges of a higher impedence, so that it is suitable for energizing most types of strain gauges, bonded or unbonded.

In the instrument special transformers are employed to reduce the undesirable feed-through which produces the mains hum. Taking up only $5\frac{1}{4} \times 19$ in. panel space, this mains energized power supply incorporates six individual, "fully-floating," stabilized power sub-units. Each sub-unit is capable of providing a nominal 5 V of regulated direct current at up to 20 mA. A "sensitivity" control allows variation of the output voltage by ±5%.

Also incorporated is a "balance" control capable of correcting initial bridge unbalance of up to 10% of full scale. Adjustments to the "sensitivity" controls (for each channel) may be clamped by use of concentric control locks.

High intensity cobalt container for use in industrial radiography. Associated Electrical Industries Ltd., Trafford Park, Manchester 17.

A cobalt container, which houses a source of 1500 c, has been produced by this firm. The cobalt 60 source provides rays which will penetrate materials such as steel plates 6 in. thick. Any flaws will be shown on the resultant radiograph. It has the following features. It is largely independent of mains and water supplies, for if these fail, provisions are made for batteries to take over the protective mechanisms. The container is dust-proof and damp-proof, and so is suitable for the most adverse climatic conditions.

A steel cylinder surrounds the container, which can thus be rolled about the site; an attachment is also provided for use by a crane. Rotating gears are provided to allow the beam to be moved throughout 360°. The shutter is a disk which moves 180° from the protected to the exposed position and stops of tungsten copper alloy serve to adjust the diameter of the beam.

A powerful light source, which shines along the beam direction before the exposure, is used for positioning the beam. The operator places the film behind the welded joint to be checked and then returns behind the source before he exposes the beam. Relays can be arranged to prevent unauthorized people from intercepting the beam during the exposure. Lights indicate when the source is exposed, and continue to operate if the power suddenly fails. The exposure is controlled by an automatic timer; the shutter then returns to the protected position. With these protections it is claimed that risk to the operator from radiation is avoided.

Tool shank material. Johnson, Matthey and Co. Ltd., 73–83 Hatton Garden, London, E.C.1.

Mallory "No-Chat" is a sintered material with a modulus of rigidity of $13 \cdot 2 \times 10^{11}$ dyne cm^{-2}, density of $16 \cdot 96$ g/cm^3, and coefficient of linear expansion of 5×10^{-6} per deg. C between

100 and 200° C. Because of these properties, the material is stated to be superior to steel for tool-shank material. Steel shanks tend to "chatter" (i.e. vibrate so that the end of the tool strikes the boring material intermittently), but, it is claimed, with this material, it does not occur. Further, tips are often made of tungsten carbide, which has approximately the same coefficient of expansion as this material; thus thermal strains set up due to heating of the tip in working are eliminated, and cracking is prevented. Finally, the material does not anneal, even at high temperatures, so that a tip may be removed and a new one brazed on without destroying the hardness properties of the tool shank.

The advantages and improvements resulting from the use of this material are most apparent where the conditions of working are at their worst. When it is necessary to have extended tool overhang, a thinner shank, higher cutting speeds or deeper cuts, it is claimed that the advantages of the material are considerable.

Liquid nitrogen purity gauge. Research and Control Instruments Ltd., 207 King's Cross Rd., London, W.C.1.

This purity gauge, which is intended for operation with liquid nitrogen, is a hydrometer, consisting of a vertical tube of narrow bore, opening into a glass bulb which contains just sufficient mercury for the instrument to float upright. The factors affecting the density of liquid nitrogen are (*a*) the atmospheric pressure and (*b*) the oxygen content. It is stated that argon, which might be expected in less pure specimens, is present only in negligible amounts in "pure" nitrogen. It is therefore possible to calibrate the instrument so that a given reading on the scale, together with the atmospheric pressure, gives the purity of the nitrogen.

The measuring range is 0–1% of oxygen, and the accuracy is claimed to be better than 0·2%. The barometer range is 58–78 cm, of mercury (or 0–2000 m above sea level).

Counter for detecting particle size. Coulter Electronics Ltd., 4 Auriol Mansions, Edith Rd., London, W.14.

This instrument uses a technique in which the required particle-size control is attained by the use of a device which sizes the particles by the change in electrical resistance which occurs when the particles pass through a tiny hole of the order of only 5 or 10 times the size of the particles. The instrument needs calibration for each kind of suspension—but once calibrated it is effective for testing samples in emulsions and suspensions which are used commercially in great quantities, as for example in some kinds of ink. The instrument counts particles having the same resistance; so that with a symmetrical distribution for example, counts are taken through the range in suitable steps and the median size determined.

Small synchronous cam-operated timer. Electrical remote control Co. Ltd., Harlow New Town, Essex.

A typical example of these timers is the one with six changeover switches which has dimensions of only 7 × 3 × 3 in. approximately; thus showing their compact nature. Each is capable of dealing with currents of the order of 10 A non-inductive, or 6 A (with a maximum surge of 30 A) inductive current; the voltage being 250 V a.c. mains.

All the switches are capable of base or end mounting, have shafts mounted in oil-retaining bearings, have friction clutches between motors and cam-shaft, and a cam-shaft spindle projecting beyond the end-plate with a hand for resetting to zero. A wide variety of input voltages, with 50–60 c/s a.c. or even d.c. is catered for; and the number of separate switches can be as many as twelve.

The time intervals can be obtained using cam-shaft speeds from 1 rev in 5 sec to 1 rev in 28 days. One of the switches can be wired to the motor circuit thus switching off the motor at a predetermined time. The time of operation of every cam can be independently adjusted, so that a wide range of time intervals can be covered; and processes controlled which need different circuits to operate for different lengths of time.

Electronic registration and control unit. Electronic Machine Co. Ltd., Mayday Rd., Thornton Heath, Surrey.

This instrument consists of two parts (*a*) the scanning head, consisting of a reflector type photocell and light head, and (*b*) the power supply and amplifier unit.

A small rectangle is printed on the main design on the front of a package on a supply line. Light is projected through a small opening in the scanning head across the supply line. The light, when reflected from the package, is picked up by a pair of photocells; and changes in the reflected density depending on the colour of the material of the package, produce different voltages in the photocells, which when amplified are easily distinguishable. When the rectangle passes the beam, the resultant change in voltage is amplified and passed to a relay which will perform any required control function. There are many applications for this type of control unit.

Frequency meter. Venner Electronics Ltd., Kingston By-pass, New Malden, Surrey.

This instrument is a transistorized analogue frequency meter and gives direct frequency measurements over a range of 3 c/s to 300 kc/s in ten steps; and each sub-range is capable of expansion by 3 or 10. Extra damping of the meter is available on the lower ranges, and the accuracy of the instrument is largely independent of the input wave form. It is capable of measuring frequencies whose amplitudes may vary from 200 mV to 250 V r.m.s. for sine waves, or from 0·5 to 500 V peak for pulse wave-form.

It may be used to measure the speed of a rotating shaft or wheel by using, in addition, a combined photohead and light source. A socket in the rear provides the necessary power source and the signal lines to the photohead unit. A remote indicator or recorder may also be used with the instrument, operating from a further socket at the rear.

The input impedance is 250 kΩ shunted by 50 pF, and the instrument may be operated from an internal 12 V battery, an external 12 V battery, 200 to 250 V, 50 c/s mains or 100 to 125 V 50 c/s mains. It consumes 70 mA and its dimensions are 10 × 7 × 8 in.

The ambient temperature over which it will function satisfactorily is −10 to 50° C, and the accuracy claimed is ±2% of the range switch setting.

Magnetic amplifiers. R. B. Pullin & Co. Ltd., Phoenix Works, Great West Road, Brentford, Middlesex.

The R603 amplifier is intended to supply a phase reversible a.c. output signal to the control phase of a size 18 servo motor. The unit operates on 115 V 400 c/s a.c. and delivers, at the mid-point of its control range, 18 W at 115 V in quadrature with the amplifier excitation voltage. Control is by two d.c. coils each of 5600 Ω resistance; a differential of 12 mA in the current through these coils produces an output of 30 W. The amplifier operates over an ambient temperature range of −55 to +71° C. In a different version of the amplifier—designated RH603—the upper temperature limit is raised to 125° C.

Crystal chronometer. Communications Systems Ltd., Norfolk House, Norfolk Street, London, W.C.2.

The general appearance of the chronometer is shown in the figure. In the front of the cabinet is a 6 in. diameter clock; on the left is a hinged door giving access to the control panel and on the right is an opening through which a multi-point jack feeds the power supply and from which three different timing pulses can be fed to a distribution block. The chronometer has been designed to operate with most types of slave clock, including those with sweep seconds hand. The chronometer can also be modified so as to operate synchronous clocks.

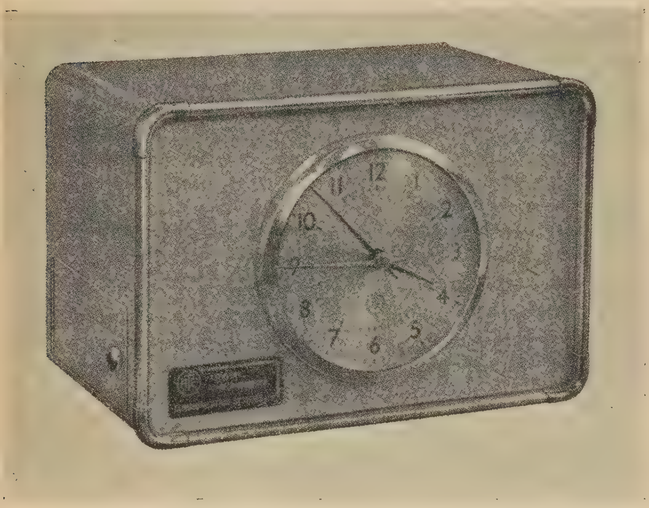

General view of crystal chronometer

The crystal-controlled oscillator uses a crystal cut so as to have zero temperature coefficient of frequency at normal room temperature. It is claimed that the normal accuracy under temperature changes likely to be encountered indoors in a temperate climate is of the order of one second per month. The output is fed through a buffer amplifier to a series of binary dividers which produce 20–24 V square pulses at second, half-minute and minute intervals, the pulse duration being ½ s for the fastest and 1 s for each of the other pulses. The master clock and each slave train is controlled by a 3-position switch. The central position gives normal running, the upper position stops the pulses and the lower position speeds up the pulse rate to 2 pulses/s in the case of the 1 s chain and 1 pulse/s in the case of the other chains. This lower switch position advances the slave clocks when changing from G.M.T. to B.S.T. The whole instrument is transistorized and operates from 24 V d.c. supply with a current consumption of 200 mA.

Frequency synthesizer. Aveley Electric Ltd., Ayron Road, Aveley Industrial Estate, South Ockendon, Essex.

The XUA synthesizer, manufactured by the German firm of Rohde and Schwarz, and distributed in the United Kingdom by Aveley Electric Ltd., is based on a 100 kc/s standard frequency derived either from a built-in crystal oscillator or an external source. Frequency dividers generate a 1 kc/s signal from this. A multiple of the 100 kc/s signal may be selected and combined with a multiple of the 1 kc/s signal, thus producing any frequency from 0–30 Mc/s which is a multiple of 1 kc/s. The frequency selection is made by two dials which are continuously variable, but calibrated at intervals of 100 and 1 kc/s respectively. Selection is obtained by turning the dial to the calibration mark required, fine adjustment being made by setting so that a panel meter reads a maximum. A third dial controls an oscillator over the frequency range 9–10 kc/s; this is mixed with the other signals so as to produce an increment of 0–1 kc/s on the frequency selected by the other dials. It follows that, with three-dial control, it is possible to set up any frequency from 0–30 Mc/s with an accuracy of 0·5 c/s. The makers claim that this accuracy is maintained over long periods. It is also claimed that the attenuation of unwanted frequencies with respect to the desired signal is at least 60 dB.

The output signal is adjustable between 0·1 and 1 V, and its magnitude is indicated on a meter. A subsequent attenuator, calibrated in 10 dB steps, and having a constant output impedance of 60 Ω, enables the output voltage to be reduced by a further factor of 1000.

Digital reading oscilloscope. Leland Instruments Ltd., Abbey House, Victoria Street, London, S.W.1.

The type 425 oscilloscope, manufactured by The Allen B. Du Mont Laboratories of New Jersey, is claimed to incorporate the first direct digital reading system in an oscilloscope. The type 425 is a high-frequency instrument for use from d.c. to 60 Mc/s (down 3 dB at 35 Mc/s), designed round a new Du Mont tube which operates with 12 000 V acceleration

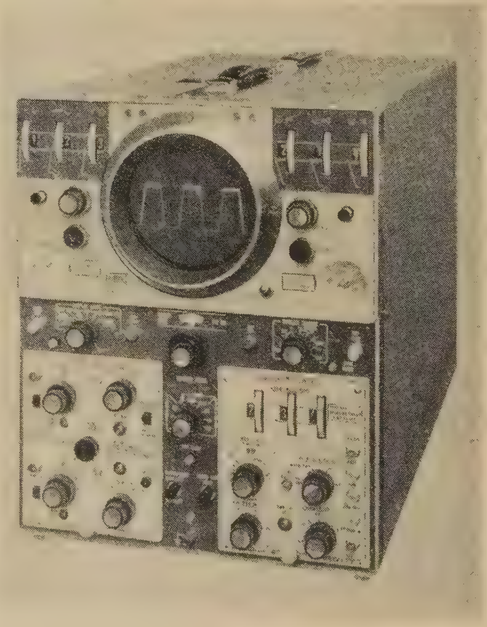

Digital reading oscilloscope

potential giving high sensitivity, high light output and high resolution on its 10 cm × 5 cm display area. The instrument is built on the modular construction system and a variety of plug-in modular units are available which enable the range and performance of the oscilloscope to be varied and extended in a number of ways. Its construction in five easily replaceable units appreciably reduces the normal maintenance problems. The unique numerical read-out system ensures increased accuracy because the possible errors of interpolating and converting mathematically have been eliminated. In addition, the instrument may be connected directly to punched-card equipment for recording and analysis.

Transistorscope. Microcell Electronics Ltd., Blackwater, Camberley, Surrey.

Modern semiconductor circuit techniques have been used to produce a fully portable, self-contained Transistorscope. Measuring 12½ in. long × 7 in. wide × 8½ in. high and weighing 10 lb, it contains a Y-amplifier of bandwidth d.c.—10 Mc/s (3 dB) with a basic sensitivity of 100 mV/cm, specially designed for faithful pulse response. The time-base with a sweep range from 1 μs to 3 s is designed for synchronized or triggered operation, the trigger signals being generated either internally or externally, and their level controlled by an input amplifier of special design. A 3½ in. diameter tube is used with an optically flat screen. Time and voltage measurement to an accuracy of 5% is carried out with the aid of a calibrated graticule. Power is provided from a battery pack of high capacity silver–zinc cells: a charging circuit is incorporated which can be connected to the mains supply.

Gas chromatography for medical gas analysis. Shandon Scientific Co. Ltd., 6 Cromwell Place, London, S.W.7.

The Clinical Gas Partitioner made by the Fisher Scientific Co. of America and recently introduced into this country by the Shandon Scientific Co. Ltd., is stated to employ gas chromatography for the first time in medical gas analysis. It will provide qualitative and quantitative analyses of oxygen, nitrogen and carbon dioxide in whole blood, and in respiratory gases; and of the carbon dioxide content of blood serum. In eight minutes it will also determine the carbon monoxide content of blood. As against the 1 ml. sample required for determinations by the Van Slyke method, the Clinical Gas Partitioner needs a sample of only 0·1 ml. of whole blood—and results are of comparable accuracy. The sensitivity is dependent on the size of the sample and the sensitivity of the recorder. Using a 0·1 ml. sample and a 1 mV recorder, oxygen in whole blood can be determined down to 2% by volume, and carbon dioxide down to 10% by volume. With a 1 ml. sample these figures are improved to 0·2% and 1% respectively.

Resistance analogue field plotter. Servomex Controls Ltd., Crowborough, Sussex.

This analogue, type FP.92, uses a special resistance paper, with conducting electrodes painted on, to which the FP.92 is connected. The internal power supply sets up a voltage between the electrodes and also across the measuring potentiometer system. By a probe joined to the galvanometer the voltage at any point on the paper can be measured, and a map prepared of lines of equipotential, crossed by lines of current flow. The analogy between this field and the fields of electrostatics, magnetism, heat flow, fluid flow, etc., enables the solution of diverse problems to be found.

"B-W" moulded electric heating elements. Barlow-Whitney Ltd., 2 Dorset Square, London, N.W.1.

These elements are stated to provide a convenient and economic answer to many of the higher temperature heating problems which arise so frequently on experimental and prototype work. The variety of shapes which can be supplied enables temporary heating chambers and tunnels to be built up in the laboratory or research department and special forms can also be made for permanent installation in production equipment. Two types are available—series E1000 MHE to 1000° C and series E1200 MHE to 1200° C.

X-ray tubes for fluorescence analysis. Watson and Sons (Electro-Medical) Ltd., Industrial Division, East Lane, North Wembley.

The spurious characteristic radiation generated in X-ray tubes is one of the factors limiting the sensitivity of the X-ray fluorescence method. In these new tubes it is claimed that the characteristic radiation from impurities in the tube anode is reduced to a very low intensity. The new tubes allow an improvement in sensitivity to be obtained, especially for copper and nickel, and the effect of target impurities is now insignificant. The AEG–50–S and OEG–50–S tubes have 5 mm × 5 mm foci and are available with tungsten or platinum anodes. The OEG–60–S tube has a 6 mm × 6 mm focus and is available with tungsten, platinum and molybdenum anodes. All the new tubes have beryllium windows and operate up to 50 kV.

High stability computor reference power supply. Solartron Electronic Group, Kingston, Surrey.

The AS 756.2 Reference Power Supply comprises two high-stability power supply sub-units with drift-corrected feedback control, using a Weston cadmium–mercury cell as a basic reference. The feed-back control operates by comparing the output of the Weston cell against a fraction of the negative supply, any error voltage being amplified and applied as a correcting signal to the stabilizing control valve of the negative supply sub-unit. The positive output is then stabilized by reference to the "corrected" negative supply, via a summing network and a second drift-corrected amplifier. The outputs are ±100 V, which can each be loaded up to 200 mA. Long-term stability of the negative supply is better than 0·1%, and the positive supply remains within 5 mV of the negative output. The stabilization ratio is 1000 : 1, d.c. source impedance less than 0·05 Ω, and ripple and noise is less than 15 mV peak to peak.

New books

Collection de l'A.N.R.T.: Études de pyrométrie pratique. By R. Alègre and others. (Paris: Éditions Eyrolles and Éditions Gauthier-Villars, 1959.) Pp. 231. Price 3300 fr.

As the title implies, the book consists of a collection of articles on various aspects of pyrometry. Each part has a different author or group of authors, with the inevitable result that there is a certain unevenness of treatment, some subjects not being considered and some being treated more comprehensively than others. Apart from an introductory chapter on choice of method of temperature measurement, the book is divided into three parts under the titles of thermoelectric, thermistor and optical pyrometry. The last mentioned, however, is devoted exclusively to flame-temperature measurement, and accounts for two-thirds of the book. The most valuable part of the book is the detailed description with numerous photographs and diagrams of apparatus for the automatic recording of flame temperatures. A short summary at the end of this section deals with the pyrometry of hot gases by aspiration methods. The book is certainly of considerable value to all concerned with practical pyrometry and, in particular, to those interested in the rather difficult techniques of flame-temperature measurement. C. R. Barber

Health physics instrumentation. By J. S. Handloser. (Oxford: Pergamon Press Ltd., 1959.) Pp. x + 182. Price 42*s*.

This is a useful book, describing instruments and techniques for the measurement of ionizing radiations at low dose rates—roughly between the limits represented by the natural background and the maximum permissible occupational exposure level. Circuit diagrams are provided, with elementary discussion of design and operating principles. Portable survey instruments, air monitors and neutron monitors receive particular attention, as do the design and equipping of counting rooms for radioactive assay.

J. M. A. Lenihan

Instrumentation in scientific research. Electrical input transducers. By K. S. Lion. (London: McGraw-Hill Co. Ltd., 1959.) Pp. xv + 324. Price 74*s*.

Nothing is more important in this day and age than the application of transducers to instrumentation and control, particularly in this country where we live on the "balance of trade". It is therefore a pleasure to see a book devoted to the most interesting side of instrumentation, namely, electrical input transducers. And yet the name is a little unfortunate. Professor Lion intends it to mean a transducer "converting a non-electrical quantity into an electric signal". It is a little difficult to reconcile input with electrical.

The scope of the book is wide. Indeed the author has qualms about the wisdom of compressing it into one volume. But he has performed his task adequately and has added something of considerable value to the literature. In the preface he disallows criticism of certain aspects by saying that the book is not meant to be "modern-minded". Nevertheless, it is a pity that certain modern electrical transducers have not been mentioned, or have only received cursory treatment in view of their increasing importance to large sections of industry. The absence of mention of moiré fringe techniques, the short and very elementary discussion of the measurement of flow by ultrasonic methods, the lack of appreciation of the importance of the Wallmark diode, are all blemishes which it is difficult to understand, particularly as they are all elements which are capable of transforming the instrumentation of certain processes and tools.

Nevertheless the book should be read by every young instrument engineer, if only because it covers the subject in a manner which will prove to the reader that electrical transducers can perform almost any function in instrumentation. Professor Lion is to be congratulated. J. Thomson.

Diffraction gratings as measuring scales. By J. Guild. (London: Oxford University Press Ltd., 1960.) Pp. x + 211. Price 35*s*.

This book is written for engineers and scientists who might with advantage use the recent developments in moiré fringe techniques for continuous precision measurement and machine tool control, but who have not got the basic knowledge of optics or electronics, or the time, to follow the theoretical arguments expounded in Mr. Guild's former book *The interference systems of crossed diffraction gratings, theory of moiré fringes*. An elementary description is given of the formation of moiré fringes by the superposition of two diffraction gratings, and sufficient mathematical analysis without proof is given for an appreciation of the various technical problems encountered in using the combined grating pair with the accompanying optical system and photosensitive detector unit. For complete understanding it would, however, be necessary to follow up the numerous references given to the former publication.

While the book deals mainly with the industrial requirements for "automatic readout" of lengths either for machine tool control, or for measurement (with digital readout), some indications are given of the possibility of the use of this system in the laboratory for high precision measurements by visual fringe counting for the accurate comparison of very nearly equal lengths. The description of the gratings used, in contrast to the description of counters, does not mention the firms who have been working on them. This chapter gives the possible user useful information about the types which he should select for his purpose, and also mentions recent methods of replication on steel tapes as well as on glass. Some notes are given in a separate chapter on the application of the moiré fringe technique to angular measurement and there is a useful discussion of phototransistors and silicon diodes as detectors.

While the book itself amply fulfils its avowed object of giving a detailed introduction to the novel new "tool" provided by the moiré fringe technique, the second appendix provides the really interesting information about recent developments with special reference to dynamic metrology and servocontrol of machine tools among the many uses to which this recently developed technique can be applied.

It is stimulating to realize that this technique sprang from Lord Rayleigh's method of testing diffraction gratings described in 1874 and that now the grating itself is being used as an accurate means of linear measurement.

G. A. Whipple

Notes and comments

Elections to The Institute of Physics

The following elections were made at its final meeting by the Board of The Institute of Physics on 22 June, 1960.

Fellows: J. Dutton, J. Dyson, A. Franks, R. J. Hamilton, E. W. Jones, C. A. Ramm, W. Steckelmacher, S. G. Tomlin, F. Tyler, G. I. Williams.

Associates: W. E. Armstrong, T. H. Baker, D. D. Bayes, C. Birch, H. C. Buckingham, A. Bowling, G. Bullock, D. M. Burns, E. W. Burdett, G. W. Canning, D. G. Christie, M. D. Clark, E. Coen, R. Collins, T. K. Dean, R. H. de Vere, J. G. Forrest, J. B. Forsyth, H. G. Frost, F. Gardner, H. I. Glass, G. L. Gooberman, A. Green, W. Haddock, N. J. Hidden, G. S. Holister, A. R. Joy, D. W. Lewin, G. D. Lill, R. E. Loughhead, V. E. Miller, T. P. Moorhead, K. A. Morley, J. L. Parmee, T. I. Putner, R. M. Rees, E. A. Richards, P. E. Richmond, P. O. Rogers, W. Salter, D. M. Schlapp, E. Shuttleworth, D. A. Silverston, J. R. Thompson, F. R. Tipping, S. Turner, A. L. Wallis, J. A. Warburton, G. M. Ward, E. J. Wheeler, K. B. Whiting, W. T. Wilkinson, P. R. Williams, R. V. Williams.

Thirty-four Graduates, twenty-four Students and four Subscribers were also elected.

Annual Report of The Institute of Physics, 1959

The Annual Report of The Institute of Physics for 1959 which was adopted at the final meeting of the Institute before its amalgamation with The Physical Society shows that at the end of the year the total membership in all grades was 6,754, an increase of 445 on the previous year. The number of applications for membership continued to increase and reached a new record of 933 during the year. The Report records that at a General Meeting on 1 December, the Scheme for amalgamation was unanimously adopted and the Board was requested to take the necessary action to implement the proposals.

The number of candidates entering for the Graduateship examination of the Institute continued to increase at a very satisfactory rate; 119 candidates took papers compared with 80 the previous year. Only 39 candidates were successful and of these 13 held university degrees and 26 the Higher National Certificate in applied physics.

The Report again records the expanding activities in many fields including education, scientific publications, conferences and symposia and meetings arranged by the Branches and specialist subject Groups.

During the year the Institute's Benevolent Fund gave assistance to ten cases where members of the Institute or their dependents had met with misfortune.

Optics and Spectroscopy

We have received from the Optical Society of America a copy of the Society's translation of the Russian journal, *Optika i Spektroscopiva.* This monthly journal of the USSR Academy of Sciences commenced publication in 1956, and publishes the work of leading Russian scientists in all branches of optics and spectroscopy, including X-ray, ultraviolet, visible infra-red and microwave, thin layer optics, filters, detectors, diffraction gratings, electroluminescence, thermal radiation backgrounds, infra-red polarizers and their many other applications in science and industry. The English translation, which is being published with a grant-in-aid from the National Science Foundation, starts from Volume 6, January 1959, and it is the aim of the Society that *Optics and Spectroscopy* will appear within four months of the Russian original.

The subscription rate is \$28, including postage, and further information can be obtained from the Society, 1155 16th Street, N.W., Washington 6, D.C., U.S.A.

Laboratory and Workshop Notes, 1956–58

Dr. Ruth Lang has compiled a fifth volume of laboratory and workshop notes from the *Journal of Scientific Instruments*, and this has been published by Edward Arnold (Publishers) Ltd., 41 Maddox Street, London, W.1. (Price 40*s.*)

As the royalties from this book will be donated to the Benevolent Fund of The Institute of Physics and The Physical Society, members are specially invited to do what they can to ensure that this new volume is purchased in large numbers.

Conference on irreversibility and statistical mechanics

The Institute of Physics and The Physical Society announces that it is arranging a conference on statistical mechanics (with special reference to irreversibility). It will be held at Queen Mary College, London, on Monday and Tuesday, 19 and 20 December, 1960.

A full programme has already been arranged. The topics include the general theory of irreversibility, random processes, liquids (theory and experiment) and irreversibility in gases and in plasma.

Further information and preliminary programmes can be obtained from The Secretary, The Institute of Physics and The Physical Society, 47 Belgrave Square, London, S.W.1.

The Postgraduate Training of Physicists in British Universities

A distinguished committee appointed by The Institute of Physics and The Physical Society has now issued its report, *The Postgraduate Training of Physicists in British Universities*, in which it records its opinion that the Ph.D. degree in physics is severely criticized by employers of physicists. In the committee's opinion this criticism is often justified. A strong recommendation is made that universities should require postgraduate students to attend co-ordinated courses of advanced lectures in physics as part of their preparation for the Ph.D. degree. Universities should be more critical in their selection of research students and should be willing to fail candidates who do not show evidence of an appropriate degree of scientific originality. Copies of the report are available (price 2*s.* including postage) from The Institute of Physics and The Physical Society, 47 Belgrave Square, London, S.W.1.

Radioactive sources and chemicals

Two catalogues have recently been issued by the Radiochemical Centre of the United Kingdom Atomic Energy Authority. *Radioactive chemicals*—deals with the primary isotopes and labelled compounds which are of interest to all who use radioactive tracer methods and with radioactive pharmaceuticals. It also includes radioactive reference sources for calibrating instruments. *Radioactive sources*—deals with sealed radioactive sources and appliances which will be of interest to radiotherapists and to industrial users of ionizing radiations. It also includes a great variety of radioactive sources which can be used for research purposes.

Both catalogues give the tariff for irradiation in the research reactors at Harwell. Most of the chemicals and sources in regular production are listed and users are recommended to choose these whenever possible on grounds of economy and ready availability: but the Centre welcomes inquiries for other materials or appliances which can often be made to special order and is willing to advise users as to the most suitable product for this particular purpose.

Only the briefest technical information is given in the catalogues but detailed specifications for most products can be supplied on request. The Centre's scientific staff will gladly advise on technical matters generally.

Copies of the catalogue are obtainable on request from the Radiochemical Centre, Amersham, Buckinghamshire.

Solid-state electronics

We have received the first issue of a new bi-monthly periodical entitled *Solid-state electronics.* The publishers state that "It is the function of this *Journal* to bring together in one publication outstanding papers reporting original work in various areas of applied solid-state physics, including transistor technology in all its aspects, transistor theory and design, crystal growing and handling, preparation of junctions, and transistor process technology. Also of interest are applications of intermetallic and other binary and ternary semiconductors, applications of ferrites and ferroelectrics, the design and performance of galvanomagnetic devices, thermoelectric properties and their applications, electroluminescent and related devices, photoconductors, and photovoltaic cells and solid-state batteries. The *Journal* will also consider problems of packaging, stability, reliability, and device life. Papers covering novel topics extending the frontiers of existing solid-state technology are, of course, invited. Review papers covering important topics in the field of solid-state electronics will be presented at intervals."

The Editor-in-Chief is Dr. W. Crawford Dunlap, Jr., of the Raytheon Company, Waltham, Mass., U.S.A. The publishers are Pergamon Press Ltd., of Oxford.

Cryogenics

We have received the first issue of a new journal dealing specifically with low temperature engineering and research, and published under the above title.

The *Journal* will appear quarterly, publishing original papers on all aspects of cryogenic research and technology, together with shorter technical notes, book reviews and correspondence. It will also contain a bibliography of recent cryogenic literature, together with 4-language summaries.

Cryogenics is to be edited jointly by Dr. K. Mendelssohn, of the Clarendon Laboratory, Oxford; R. B. Scott, chief of the N.B.S. Cryogenic Engineering Laboratory, Colorado; and Professor L. Weil of the Institut Fourier, Grenoble University. In addition, a panel of twelve experts will act as advisory editors.

The first issue contains a contribution by Dr. N. Kurti, who discusses the prospects of nuclear cooling. There are also nine original papers from Britain, America, France and the Netherlands.

In addition to the work devoted to fundamental issues, *Cryogenics* will also publish papers dealing with the increased use of cryogenic propellants as rocket fuels, new methods of handling, storage and transport, low temperature electronics and other technical problems related to cryogenics.

The *Journal* is published by Heywood and Co. Ltd., Drury House, Russell Street, Drury Lane, London, W.C.2. The annual subscription is £5.

Erratum

In the paper entitled "Novel displacement detector and its application in a recording thermobalance" by J. C. Van Der Breggen and H. J. Wouterlood, which appeared in the August issue of this *Journal*, the caption to Fig. 4 should read "Amplifier circuit". The words "Multipoint digital temperature recorder" should be deleted.

British Journal of Applied Physics

Contents of the November issue

CONFERENCE REPORT

Summarized proceedings of a conference on the borders of X-ray analysis—Reading, April, 1960. By R. P. Ferrier and B. T. M. Willis.

PAPERS

Contrast of electron micrographs. By J. S. Halliday and T. F. J. Quinn.

Production of resonance radiation in discharge tubes of non-circular cross-section. By M. A. Cayless.

X-ray microscopy of beryllium. By J. Sawkill and D. R. Schwarzenberger.

Selected-area diffraction in the electron microscope. By R. Phillips.

Study in background structure in platinum/carbon shadowing deposits. By D. E. Bradley.

Smoke density integrator. By R. M. Storey.

Some electrical and surface properties of sintered nickel matrix cathodes. By R. W. Fane.

Wear of the hard and soft phases in cobalt-bonded tungsten carbide. By J. Golden and G. W. Rowe.

Fifth order spherical aberration of magnetic lenses. By G. D. Archard.

CORRESPONDENCE

Static and dynamic elastic constants. From L. Gold.

X-ray stress determination in austenitic steel. From J. H. S. Neilson.

NOTES AND NEWS

Notes and comments

THIS *JOURNAL* is produced monthly by The Institute of Physics and The Physical Society, with the co-operation of the National Physical Laboratory. It deals with the principles, construction and use of scientific instruments. All rights reserved. Responsibility for the statements contained herein attaches only to the writers.

EDITORIAL MATTER. Communications concerning editorial matter should be addressed to the Editor, The Institute of Physics and The Physical Society, 1, Lowther Gardens, Prince Consort Road, London, S.W.7. (*Telephone:* Kensington 0048.) Prospective authors are invited to prepare their scripts in accordance with the *Notes for Authors.*

REPRODUCTION. The Institute of Physics and The Physical Society is a signatory to The Royal Society's Fair Copying Declaration. Details may be obtained upon application from The Royal Society, London, W.1.

ADVERTISEMENTS. Communications concerning advertisements should be addressed to the agents, Messrs. George Jackson (Fleet St.) Ltd., Cliffords Inn, Fleet Street, London, E.C.4. (*Telephone:* Holborn 3611–2.)

SUBSCRIPTION RATES. A new volume commences each January. The charge is £6 per volume ($17 U.S.A.), including index (post paid) payable in advance. Single parts, so far as available, may be purchased at 12*s.* 6*d.* each ($1.75 U.S.A.), post paid, cash with order. Orders should be sent to The Institute of Physics and The Physical Society, 47 Belgrave Square, London, S.W.1, or to any bookseller.

CLAIMS FOR MISSING JOURNALS. Claims from regular subscribers to this *Journal* for missing numbers will only be considered if received within 60 days of the date of mailing plus normal outward time of transit and time for lodging the claim. Losses attributable to failure to notify a change of address or to similar omissions will not be considered.

PRINTED IN GREAT BRITAIN BY UNWIN BROTHERS LIMITED, WOKING AND LONDON

Further experiences with aluminium wire seals for bakeable vacuum systems

by L. ELSWORTH, L. HOLLAND, F.Inst.P., and L. LAURENSON, Vacuum Deposition Research Division, Edwards High Vacuum Ltd., Crawley, Sussex

[*Paper first received* 6 *July, and in final form* 19 *August*, 1960]

Abstract

The use of aluminium cemented *seals in vacuum systems has been further investigated to find the effect of the flange surface finish on the adhesion of the aluminium joint and the performance of such seals in bakeable apparatus. Aluminium wire clamped between stainless-steel flanges and baked at* 300° *C formed more adherent joints as the surface finish was decreased from* 50 *to* 10 μ *in. (average height of asperities). The aluminium joint would not cold weld with a force of 4 tons per inch of* 20 *s.w.g. wire using flanges with a surface finish of* 10 μ *in., and the flanges were indented by the wire. With constant surface finishes, the strength of the aluminium joint was directly proportional to the baking temperature above a forming temperature* (250° *C at* 10 μ *in.) and was greatest when the aluminium wire was perpendicular to the direction of the machining marks. Seals made between flanges with a* 10 μ *in. finish had an adhesion strength of* 354 *lb/in. of wire after forming with a force of* 5000 *lb per inch of wire and baking at* 400° *C. Vacuum seals using a total length of 9 ft of wire were successfully employed in a stainless-steel vacuum plant with a* 28 *litre volume chamber. The plant was exhausted by an oil diffusion pump (baffled speed* 40 *l./s) with a liquid nitrogen trap and gave an ultimate pressure of* 7×10^{-10} *mm of mercury, and* 10^{-10} *mm of mercury using a titanium evaporated getter. The seals had to be uniformly heated to avoid unequal expansion breaking the "cemented" joints.*

Introduction

It has recently been shown* that aluminium wire gaskets flow and adhere to the steel mating flanges of vacuum couplings when they are baked at a high temperature providing the aluminium has been sufficiently compressed. Such "cemented" joints can be easily broken and are suitable for use in demountable vacuum apparatus which must be degassed by baking. It is necessary to know the compression force and baking temperature at which the aluminium sticks to the flanges to avoid the couplings parting on cooling, and some information on this has been given.* When the "cemented" aluminium seal is formed, the steel clamping bolts become slack as the joint is cooled, and it is important to know the strength of the joint because it may be stressed by the weight of pipelines or other components. To provide information for general use in the design of bakeable vacuum plant, it was decided to investigate the influence of the baking conditions and flange surface finish on the strength of the "cemented" joint. Experience has also been gained of using aluminium seals in a vacuum plant constructed for preparing pure evaporated metal films, and these recent investigations are dealt with here.

Flange surface finish and adhesive strength of aluminium seal

Apparatus and procedure. The strength of the aluminium wire seals and their dependence on the baking temperature and flange surface finish were determined as follows. A 1 in. length of super-pure aluminium wire (20 s.w.g.) was annealed at 350° C for one hour and then clamped between two stainless-steel blocks (BSS.EN58B) of 1⅛ in. diameter using a hydraulic ram. The surface finish of the machined blocks was determined with a Philips's roughness tester (type PR.9151) which measured the average height of the surface asperities. The clamping blocks were enclosed and heated by a circular resistance element of 175 W and the temperature of the joint was measured with a chromel-alumel thermocouple inserted in one of the blocks. In every case the clamping blocks were heated to the required temperature as quickly as possible, held there for 10 min and then allowed to cool.

For simplicity, a constant force was exerted on the wire as it underwent plastic flow during the baking cycle. In practice, with bolted steel flanges, the compression would rise and fall as the expansion of the aluminium was restrained by the bolts. However, if one designs a bolted coupling to give at normal temperature the compressive stress specified here, then this will ensure that the compressive force will be more than adequate to form the seal when the joint is baked. The adhesive or breaking strength of the joint formed after baking was measured at right-angles to the clamping surfaces either by hanging weights on one of the clamping blocks or by a lever mechanism.

The machined surfaces used in the tests were either turned on a centre lathe or ground. When turned finishes were used, the blocks were machined off-centre so that the parallel turning marks ran almost straight across the mating surfaces and the aluminium wire could be placed in a known relation to the turning grooves. Surfaces with grooves of 35 μ in. in height were obtained by machining, and smoother finishes by polishing turned or ground surfaces with fine emery cloth to remove the tops of the corrugations.

Surface finish and breaking strength at constant temperature. A series of experiments was made to determine the relationship between surface finish of the clamping blocks and breaking strength of the aluminium joint with the aluminium wire placed at right-angles to the direction of the turned grooves.

A preliminary test was made with a 10 μ in. finish to see if the aluminium seal could be made to adhere to the blocks when compressed at very high pressures. However, even with a force of 4 tons per inch of wire the aluminium would not adhere to the blocks and the gasket indented the stainless-steel surfaces. If the flanges of a coupling are indented by a wire seal then they have to be frequently remachined and, in view of this, the attempt to form a cold-welded junction was abandoned.

---

* HOLDEN, J. T., HOLLAND, L., and LAURENSON, L. *J. Sci. Instrum.*, **36**, p. 281 (1959).

In subsequent experiments, a force of 5000 lb was applied to 1 in. lengths of aluminium wire in the clamping blocks, and the seals baked at 300° C, which is the lowest baking temperature likely to be used with a metal vacuum system. It is shown in Fig. 1 that the breaking strength of a seal increases as the surface becomes smoother.

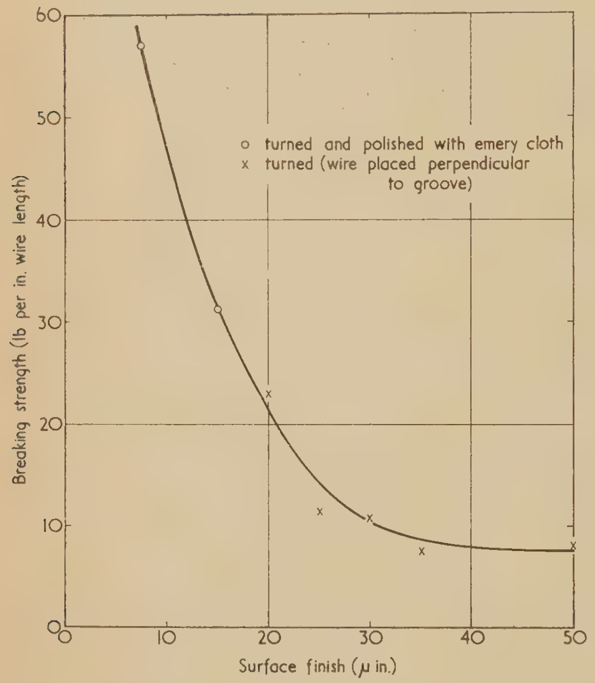

Fig. 1. Dependence of breaking strength of aluminium seal on surface finish of flanges after baking at constant temperature of 300° C. All seals made under a constant force of 5000 lb per inch of wire

Baking temperature and direction of the machining grooves. The effect of the baking temperature on the adhesive strength of the aluminium joint was investigated. Constant surface finishes were used of 10 and 35 μ in. with the aluminium wire either parallel or perpendicular to the direction of the machining marks. The joints were formed under a force of 5000 lb per inch of wire as used before, and their breaking strength as a function of the baking temperature is shown in Fig. 2. These curves show that the minimum baking temperature required to form a cemented joint decreases from about 350 to 250° C as the surface finish is improved. With machined surfaces and the wire perpendicular to the machining marks, the joints made with a ground finish were stronger than those prepared by turning. When a turned finish was used, a smooth curve could not be drawn through the breaking values for joints made with the wire parallel to the surface grooves, as shown in Fig. 2.

It is believed that the breaking strength of seals made between smooth surfaces is higher than those made between ground or turned faces because the breaking force acts normal to the seal interface. That is, the measured breaking strength is equal to the true strength of adhesion, wherea with irregular surfaces the breaking force is not everywher normal to the aluminium/steel interface and the aluminiu joint fails because of shear. Thus weak joints formed o rough machined surfaces show that bonding of the aluminiu to the steel does occur because traces of aluminium are lef

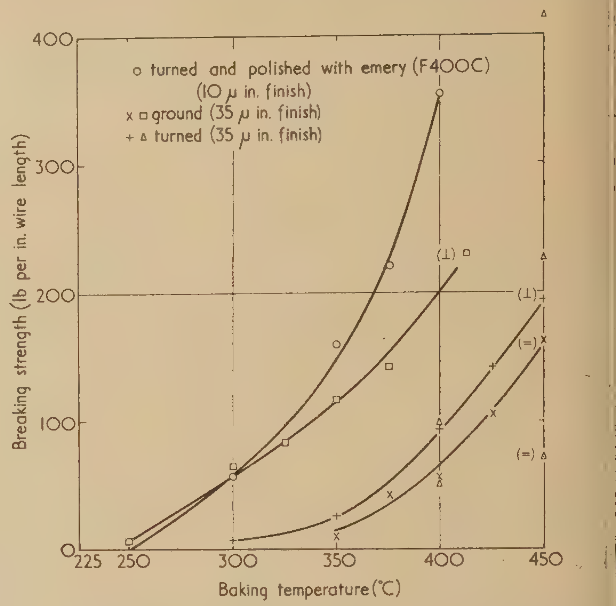

Fig. 2. Dependence of breaking strength of aluminium seal on baking temperature using different surface finishes and with wire parallel and perpendicular to direction of machining grooves. All seals made under a constant force of 5000 lb per inch of wire

within the surface tracks when the joint is broken. Also such joints are normally free from leaks. Dr. Ransley of the British Aluminium Research Laboratories has sectioned a cemented joint prepared by the writers above 400° C anc found evidence of an intermetallic compound formed by the iron and aluminium at the interface of the joint.

The reason for the low breaking strength obtained wit the wire parallel to the direction of the machining groove is more obscure. It is believed that a cemented seal is forme because the oxide on the aluminium fractures as the meta yields and frictionally rubs against the flange surface. Whe the wire is perpendicular to the grooves and plasticall deformed at high temperature, the flattened wire will move sideways in contact with and rub against the whole of the groove surface, whereas when it is parallel to the tracks, the greatest rubbing action during flow will occur on the tops o the asperities with the metal expanding to fill the base of the grooves.

Performance of a bakeable vacuum plant with aluminium seal

A high-vacuum plant intended for use in producing pure evaporated metal films was made using aluminium seals fo the demountable joints. The vacuum chamber was 12 in diameter and 14 in. high (28 litre in volume) and mounte on a base-plate with a flange seal. Four glass/metal lead-i electrodes were sealed in the base-plate with aluminiur gaskets. The plant was made with stainless-steel components A tungsten spiral was mounted in the chamber for evaporating a titanium getter to assist the pumping at low ressures. The vacuum pressure was measured with an lpert type ionization gauge.

The chamber was pumped by a 4 in. diameter fractionating-il diffusion pump (250 l./s) with a water-cooled baffle and a in. liquid nitrogen trap mounted on top of the pump. n the experiments described here, silicone 704 was used as he diffusion-pump fluid. The baffled speed of this com-ination for permanent gases was 40 l./s. The system was ealed with aluminium wire gaskets throughout, and a total ength of 9 ft of aluminium wire was used in eleven bakeable oints.

The flange on the bottom of the chamber was 15 in. outer iameter by 12 in. inner diameter by 1 in. thick, and some arly difficulties were experienced in sealing it to the base-late because the flange had slightly distorted during welding. he distortion resulted in the gap between the flanges at the nner diameter of the flange being 0·008 in. greater than at he outside of the flange. The highly compressed aluminium vire forms, when baked, a ribbon about 0·005 in. thick and he distortion in the flange resulted in the outer side of the lange making contact with the base so that the aluminium vas incompletely compressed. The flange was remachined o a tolerance of ±0·0005 in. and satisfactory joints were nade. The seals were all assembled using a constant torque panner, and it was found empirically that a torque of 95 lb ft ad to be applied to each of the sixteen bolts on the chamber lange to compress the aluminium gasket sufficiently for the oint to become cemented on baking. Each bolt compressed 2½ in. of wire and the bolts had sixteen threads per inch, so gnoring the friction losses in the threads, etc., the force per nch of wire was $95 \times 2\pi \times \frac{2}{5} \times 16 \times 12$ or 45 700 lb,* which is in fair agreement with the figure (34 900 lb/in.) given previously for small test flanges. Also, with the torque values used here, the aluminium was initially compressed to orm a ribbon of 0·012 in. thick as previously used.

Trouble was experienced in making vacuum tight seals o the flanges of the lead-in electrodes because they were made of mild steel electro-plated with nickel which peeled after the plant had been baked several times.

Experience has shown that once the cemented joints have formed it is essential to keep to the same temperature distri-bution during baking and temperature/time cycle as that nitially used because, once the aluminium has flowed plastically to form a thin ribbon, there is insufficient metal o take up any new strains. On one occasion, the aluminium oints broke simultaneously because the plant was unevenly baked after the seals had become cemented.

After baking the chamber and liquid-nitrogen trap for hree-and-a-half hours with the temperature rising to 320° C, n ultimate pressure of $3{\cdot}5 \times 10^{-9}$ mm of mercury was attained at the end of a total cycle time of 7 h, as shown in he dashed curve in Fig. 3. When the nitrogen trap was illed immediately on removing the oven, a pressure of 7×10^{-10} mm of mercury was obtained after a total time of 7 h (full curve in Fig. 3). With the titanium getter, an ultimate pressure of less than 10^{-10} mm of mercury was reached, as shown in Fig. 4. The titanium was degassed and prefused to the tungsten spiral at a pressure of 3×10^{-7} mm of mercury and evaporated after baking the system at 350° C and charging the cold trap.

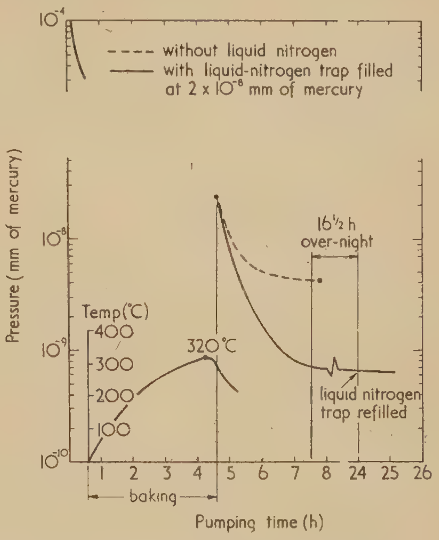

Fig. 3. Pumping cycles of ultra-high-vacuum deposition unit baked to 320° C. (1) with diffusion pump alone, (2) with liquid-nitrogen trap charged

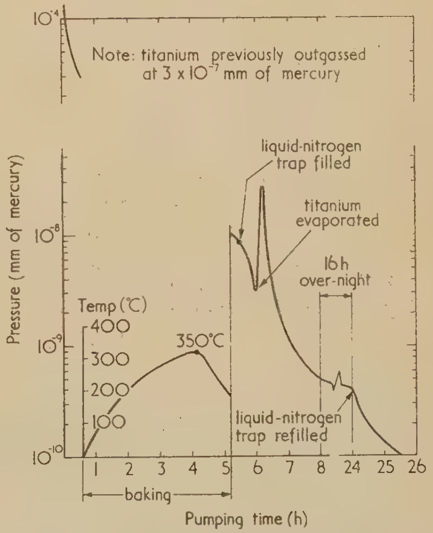

Fig. 4. Pumping cycle of ultra-high-vacuum deposition unit baked to 350° C and using liquid-nitrogen trap and titanium getter

---

* The apparent compression determined from the torque applied o the bolts is some ten times that required to make a seal by direct hrust. The difference is due to the transmission loss in the bolts.

Wide-angle photoelectric integrating flashmeter

by J. EDWARDS, W. R. LANE, B.Sc., F.Inst.P., and B. R. D. STONE, Chemical Defence Experimental Establishment, Porton, Wiltshire

[*Paper received* 4 *July*, 1960]

Abstract

The design, construction and calibration of a compact portable battery-operated photoelectric integrating photometer, which was developed for measuring very low levels of luminous energy incident on a surface from a distant light flash at night, is described. The instrument has a linear response and on its most sensitive range gives full-scale deflexion for an exposure of 0·004 *lx s. Drift, arising from the photocell dark current and night-sky background illumination, is neutralized by feeding into the integrating capacitor a variable compensating current. Six ranges of sensitivity are provided, and colour filters can be inserted for measurements in restricted wavebands.*

Introduction

In the course of a study of the transmission and scattering of light by the atmosphere, a need arose for a compact portable battery-operated integrating photometer, capable of measuring very low levels of luminous energy incident on a surface from a distant light flash at night. Measurements of this nature had previously been made by photographic photometry, but a supplementary method capable of indicating the integrated flux immediately, without the delay and tedious work associated with the processing and densitometry of photographic plates, was desirable, both to serve as an independent check and to increase the rate at which atmospheric transmission data could be accumulated.

Photoelectric exposure meters, which indicate the time-integral of a flash or of a varying illumination, have previously been designed and used by several workers. In the instruments described by Preston(1) and by Edgerton,(2) as in the one described in the present paper, the light received by a photocell generates a current, which is integrated in a capacitor. The voltage appearing across the capacitor is proportional to the time integral of the illumination at the receiving surface, and it is recorded by means of a valve voltmeter. Preston's flashmeter is a reliable and compact instrument but, in its original form, it is not sufficiently sensitive for the present purpose; other disadvantages are that only a single range of sensitivity is normally provided and the response of the instrument is not linear over the whole scale. Edgerton's instrument utilizes a similar principle but, being intended for measurement of the light from photographic flash tubes, also falls short of the required sensitivity.

The flashmeter described here operates on the same principle of integration as the earlier instruments but, by embodying certain modifications (some of which were proposed by Preston in his original report), the sensitivity is considerably increased without undue loss of stability. Six ranges of sensitivity in steps of 5 : 1 are available, and the instrument has a linear response throughout each range. A number of instruments of the type described below have been constructed and, over several years, they have given very satisfactory field service in measurements of the time integral of the illumination at distances up to twenty miles from a source emitting 3 × 10^7 cd s, mostly within 300 ms.

Principle of operation

The electrical circuit of the flashmeter is shown in Fig. 1. The light received by the photocell *A* generates a photocurrent proportional to the flux. The resulting charge flowing into the integrating capacitor causes an increase in potential difference, proportional to the time integral of the illumination at the receiving surface, and this is recorded with the aid of a suitable valve voltmeter, as a deflexion on the indicating meter *M*.

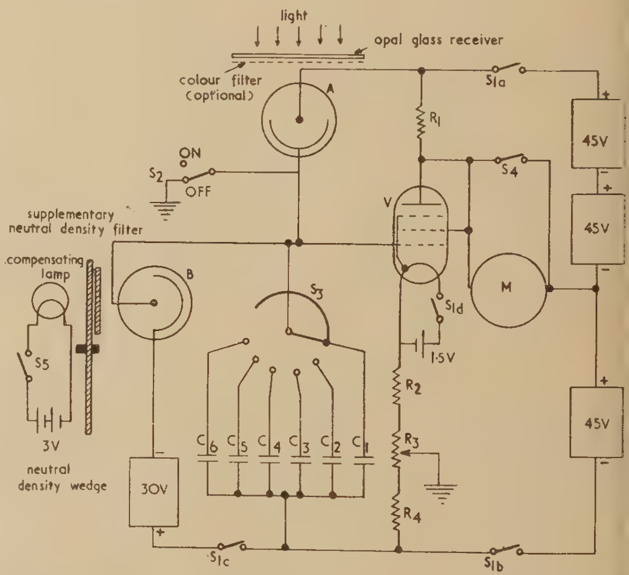

Fig. 1. Circuit diagram of the flashmeter

$R_1 = 220\ \text{k}\Omega$
$R_2 = 3{\cdot}3\ \text{k}\Omega$
$R_3 = 2{\cdot}5\ \text{k}\Omega$ potentiometer
$R_4 = 1\ \text{k}\Omega$

$C_1 = 40$ pF self-capacitance

$$\left.\begin{array}{l} C_2 = 220\ \text{pF} \\ C_3 = 1000\ \text{pF} \\ C_4 = 4700\ \text{pF} \\ C_5 = 0{\cdot}02\ \mu\text{F} \\ C_6 = 0{\cdot}1\ \mu\text{F} \end{array}\right\}\ \text{Suflex plastic film type}$$

S_1 = power supply switch
S_2 = operating switch (ceramic)
S_3 = range switch (ceramic)
S_4 = meter shunt switch
S_5 = compensating lamp switch

A = Cintel VA39 photocell
B = G.E.C. BMV31 photocell
V = CV1758 (IL4)
M = Turner model 605 microammeter (0–100 μA)

Batteries: 45 V Ever Ready B109
30 V Ever Ready B105
1·5 V Ever Ready AD35
3 V Ever Ready 800

The valve grid current, photocell dark current and photourrent due to background illumination are also integrated y the capacitor, resulting in a steady drift of the pointer. his is offset by feeding into the capacitor an opposing comensating current provided by the photocell *B*. Continuous mooth variation of the compensating current is achieved by otating an annular neutral density wedge, situated between hotocell *B* and the lamp *L*.

The measuring photocell, Cintel type VA39, has peak esponse at 4300 ± 500 Å, but any vacuum photocell having low dark current (less than 10^{-10} A) would be suitable. The spectral response should be appropriate to the colour f the light under investigation; cells type VS39 have been sed for measurements in the near infra-red region. The ompensating photocell, G.E.C. type BMV31, was specially hosen for its low dark current, which in selected cells is as low s $2{\cdot}5 \times 10^{-14}$ A. It is, of course, essential that the dark urrent of cell B should not exceed that of cell A plus the rid current of the valve. The integrating capacitors C_2 to C_6 are of the plastic film dielectric type, having a very igh insulation resistance; C_1 is the self-capacity of the wiring.

The valve, type CV1758 (1L4), is selected for low grid urrent after ageing for about 50 h with 45 V applied to its node and to g_2; it is operated as a triode with the anode onnected to g_2.

With the power supply switch S_1 on, the meter shunt witch S_4 (provided to damp movement in transit) open, the operate switch S_2 off and the sensitivity range switch S_3 at position 6 (to ensure equal potential difference across each of the capacitors C_1–C_6), R_3 is adjusted to give zero meter deflexion. The valve grid bias is now approximately −2 V; he anode current is approximately 0·4 mA, giving 90 V across R_1, and therefore zero current through the meter. Switch S_3 is now set to the appropriate sensitivity range, and witch S_2 is put on. The meter deflexion rises, at a rate depending on the background illumination, the valve grid current and, of course, on the sensitivity range in use. If compensation is required, switch S_5 is closed and the pointer eturned to zero and held there by adjusting the annular neutral wedge. On receipt of the flash, the resulting change n the voltage across the capacitor(s) is indicated by a rapid deflexion of the pointer to a steady reading, which is proportional to the time-integral of the illumination. If the meter deflexion exceeds full scale, the range switch is moved o successively higher settings until the pointer returns on o the scale. If the capacitor selected initially is much too mall, the resulting high grid voltage will cause excessive grid current to be drawn before the range is changed. Tests have hown, however, that valid readings are obtained after witching up not more than two ranges. Full-scale deflexion of the 100 μA meter results from a grid voltage change of only approximately 0·3 V, and since the characteristic is very nearly straight over this range, the instrument has a inear calibration.

The flashmeter reading will not be a true measure of the ntegrated light if, at any time during the flash, the light eaching the photocell exceeds a value above which the photocurrent ceases to be directly proportional to the flux. Tests on a typical type VA39 cell in a flashmeter subjected o known steady illuminations (a microammeter having been ubstituted for the integrating capacitors) showed, however, a constant sensitivity for illuminations up to at least 2000 lx. The brightest flashes measured had peak intensity about 350 × 10^6 cd, and the illumination at the nearest observation point (1 mile) therefore never exceeded 134 lx.

Constructional details

Fig. 2 shows the layout of components of the instrument; front and rear views of the flashmeter are shown in Fig. 3. All components, including the batteries, are housed in two boxes made from ½ in. plywood, which clip together forming a single unit of approximate dimensions 11 × 10 × 6 in., suitable for tripod mounting. The smaller box contains the battery, lamp and annular neutral density wedge, which together provide the variable illumination for the compensating photocell; the remaining components are housed in the larger box, the inside of which is spray-coated with aluminium to provide electrical screening.

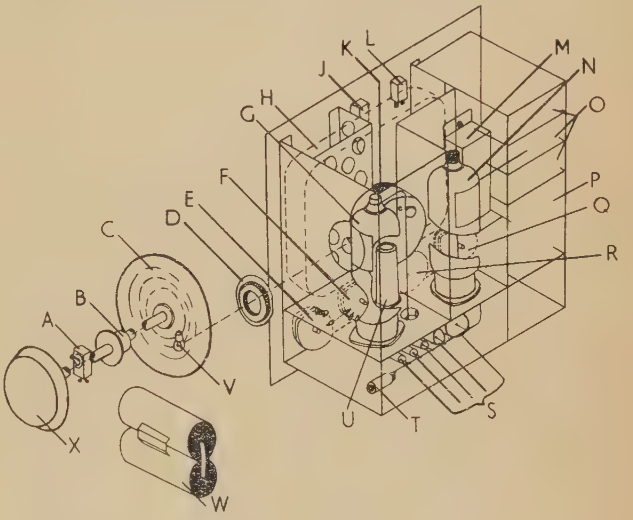

Fig. 2. Layout of components in flashmeter

A, compensating lamp switch; *B*, 12 : 1 reduction gear; *C*, neutral density wedge; *D*, supplementary filter holder (attached to wooden case); *E*, operating switch; *F*, range switch; *G*, compensating photocell; *H*, drying agent compartment; *J*, meter shunt switch; *K*, microammeter; *L*, panel light switch; *M*, B105 battery; *N*, measuring photocell; *O*, B109 batteries; *P*, AD35 batteries; *Q*, power supply switch; *R*, set zero potentiometer; *S*, integrating capacitors C_2 to C_6; *T*, stand-off insulator; *U*, screening can covering CV1758 valve; *V*, compensating lamp; *W*, type 800 battery; *X*, compensating control knob

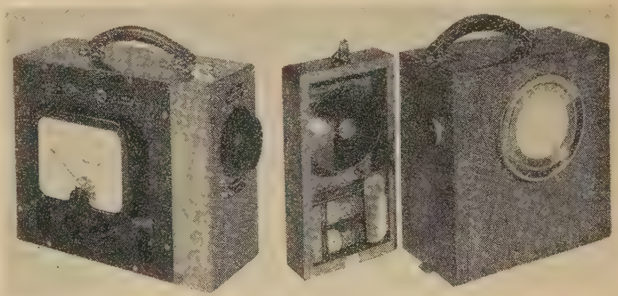

Fig. 3. Views of flashmeter

The drying agent (about 6 oz activated alumina contained in a twill bag) ensures high surface insulation of the components, which is essential for electrical stability. The indicating meter (scaled 0–50 divisions) is internally illuminated, and adequate illumination for the controls is provided by replacing the standard opaque plastic panel, fitted in the base of the meter, by a transparent panel.

The light receiver consists of a disk of matt-surfaced flashed opal glass of 3 in. effective diameter. This is retained in position by an aluminium holder having a very shallow rim to allow a wide angle of light acceptance (about 160°). Glass or gelatin colour filters can be accommodated behind the receiving surface.

The internal arrangement of the components in the background compensation control box can be seen from Figs. 2 and 3. Light from the lamp, after attenuation by the adjustable annular neutral density wedge and a supplementary attenuating filter (chosen according to the level of background illumination), enters the main instrument case and falls on the compensating photocell.

Calibration procedure

The method used in calibrating the instrument will depend upon the purpose and precision of the measurements for which it is to be employed. In the authors' application, since the mean colour temperature of the flash was in the neighbourhood of 2800° K, calibration with light of about this colour temperature was desirable. A tungsten filament lamp, operated at 2750° K and standardized with the aid of a calibrated photometer, is used as the source. An aperture in the lamp box accommodates a precision camera shutter, providing a range of exposure times which are measured (to within $\pm 2\%$) by means of an electronic timer. Using conventional photometric procedures, the flashmeter is calibrated by controlled exposures to light of a constant measured intensity. To avoid any possibility of error arising from departure from a perfect reciprocity relationship, the calibration flashes are arranged to be of about the same duration as the flashes to be measured.

Sensitivity

The relation between the meter deflexion and the time-integral of the illumination (taken as the product of the known illumination at the receiver surface and the measured exposure time) is strictly linear for all six sensitivity ranges. Values of the integrated illumination required to produce full-scale deflexion on each range of a typical instrument are as follows:

Range	1	2	3	4	5	6
Integrated illumination (*lx s*)	0·0042	0·024	0·165	0·70	3·0	14·4

Angular sensitivity

Light transmitted through the atmosphere for several miles will often have suffered considerable scattering and strike the receiver surface at all angles. Ideally, the response of the instrument should vary as the cosine of the angle of incidence at the receiver surface. Such a characteristic is only obtainable, however, by sacrificing considerable sensitivity, due to attenuation of light by the diffuser, and for this reason a compromise between ideal response and high sensitivity has to be accepted. The response curve is shown in Fig. 4. Deviation from cosine response amounts to 11% at an angle of 60° and increases rapidly at angles greater than 70°. Corrections for these deviations can be applied if the angular distribution of the light reaching the instrument is known; alternatively a closer approach to a true cosine response could probably be attained if required.

When the flashmeter is used in fog the diffuser may become wet, but as can be seen from Fig. 4, which includes measurements made immediately after the diffuser had been swabbed with wet cotton wool, the angular response of the instrument is not significantly affected.

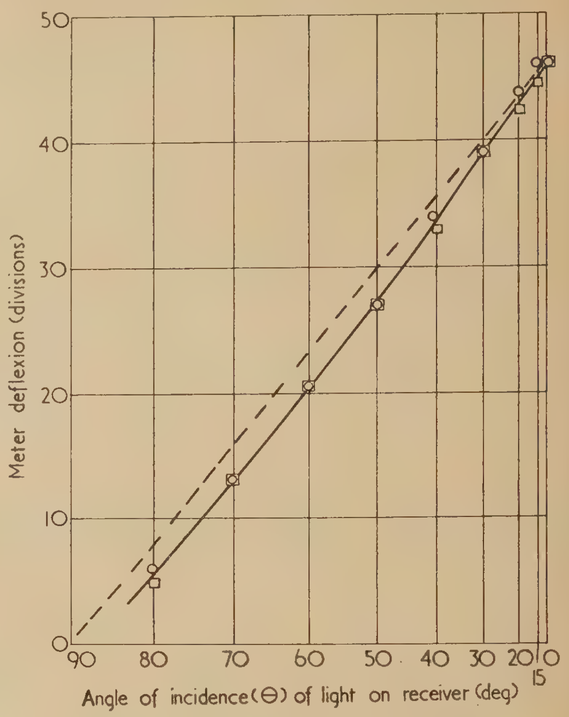

Fig. 4. Angular sensitivity of flashmeter

———— = ground-flashed opal glass receiver; ○ = glass dry
□ = glass wet
— — — = ideal receiver with cosine law response

Compensation for background illumination

The level of background illumination for which compensation can be provided is limited, because high background and compensating photocurrents reduce the stability of the instrument and the accuracy with which exact compensation can be achieved. Tests have shown that if a flashmeter is used on its most sensitive range, where full-scale deflexion on the meter corresponds to approximately 0·004 lx s, satisfactory compensation is possible provided that the background illumination is not greater than 0·1 lx. Correspondingly higher background illuminations can be tolerated on the less sensitive ranges.

Acknowledgements

The authors wish to thank Mr. J. S. Preston (National Physical Laboratory) for advice on flashmeter design.

This paper is published with the permission of H.M.S.O., and Crown copyright is reserved.

References

(1) PRESTON, J. S. *The N.P.L. Integrating Photoelectric Flashmeter* (Teddington: National Physical Laboratory, 1944).

(2) EDGERTON, H. G. *Electronics*, **21**, p. 78 (March 1948).

Portable water velocity meter

y J. M. EDINGTON, B.Sc., and L. MOLYNEUX, B.Sc., Ph.D., Grad.I.E.E., Departments of Zoology
ıd Physics, King's College, University of Durham, Newcastle upon Tyne

Paper first received 9 *May, and in final form* 19 *August,* 1960]

Abstract

Vilkie(1) *has described an instrument for measuring the elocity of water, in which the rate of rotation of a small olystyrene rotor is measured by electronic means, using alves as the active circuit elements. The present paper escribes a circuit in which the valves are replaced by ransistors and which is designed so that compensation for hanges in the conductivity of the water occurs auto- ıatically. As the instrument is small and light and owered by a self-contained battery it is particularly uitable for field work.*

General description

THE measuring head is identical with that described by Wilkie.(1) It consists of a polystyrene rotor with five helical blades, mounted on a stainless-steel spindle unning in jewel bearings. The swept diameter of the rotor s 1 cm. The rotor is protected by a frame, which is mounted n a stainless-steel tube. A gold wire, insulated from the ube, passes down inside it and finishes about 0·1 mm clear of the propeller blades. The measuring head is connected to the electronic unit by coaxial cable.

The resistance between the tip of the central gold wire and the stainless-steel tube, when the head is in water, varies slightly as each blade passes the tip.

In the detection part of his circuit Wilkie uses a Wheatstone bridge, of which the cable and measuring head form one arm. In the new version the bridge is replaced by a transformer and transistor (T_2, TR_2, Fig. 1).

The circuit as a whole may be described as follows. An oscillator TR_1 supplies the detector TR_2. The output from the detector is filtered and amplified (TR_3–TR_4) and then used to trigger a bi-stable pair (TR_6–TR_7) which is coupled to a diode-pump integrator.

The detector circuit

If other factors remain constant, the potential [Fig. 2(*a*)] across the secondary of T_2 (VZ) (Fig. 1) is determined by the resistance between the gold wire and the steel frame. Its value varies at the rate at which the tips of the blades pass

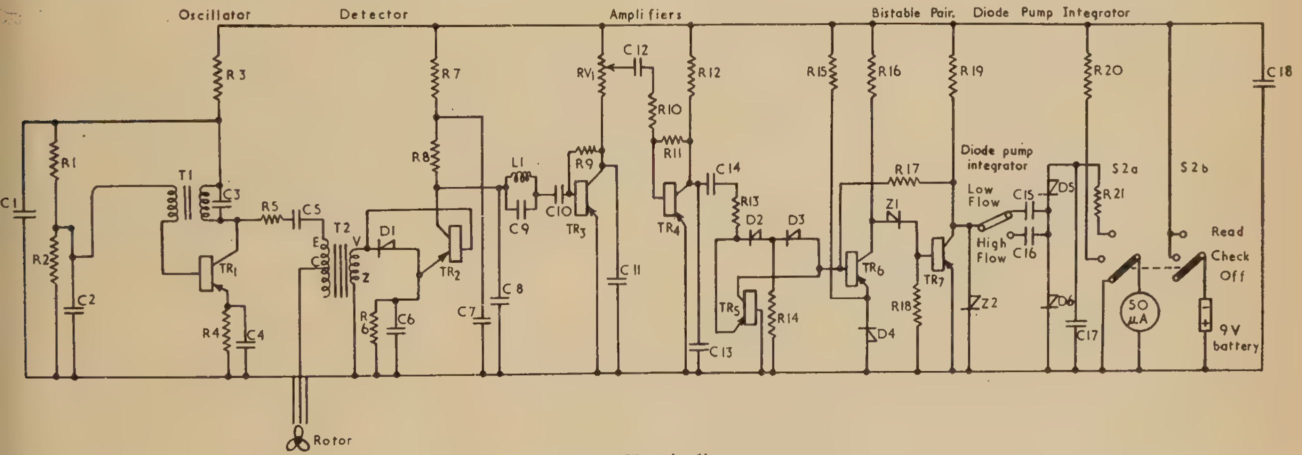

Fig. 1. Circuit diagram

R_1 = 10 kΩ
R_2 = 1 kΩ
R_3 = 1·5 kΩ
R_4 = 3·9 kΩ
R_5 = 4·7 kΩ
R_6 = 12 kΩ
R_7, R_8 = 4·7 kΩ
R_9 = 1 MΩ
R_{10} = 8·2 kΩ
R_{11} = 1 MΩ
R_{12} = 6·8 kΩ
R_{13} = 8·2 kΩ
R_{14} = 10 kΩ

R_{15} = 12 kΩ
R_{16} = 10 kΩ
R_{17} = 150 kΩ
R_{18} = 10 kΩ
R_{19} = 6·8 kΩ
R_{20} = 200 kΩ
R_{21} = 470 Ω

P_1 = 5 kΩ

C_1 = 50 μF
C_2 = 1 μF

C_3 = 0·02 μF
C_4 = 3 μF
C_5 = 0·05 μF
C_6, C_7 = 50 μF
C_8 = 0·05 μF
C_9 = 0·001 μF
C_{10} = 50 μF
C_{11} = 0·05 μF
C_{12} = 50 μF
C_{13} = 0·02 μF
C_{14} = 50 μF
C_{15} = 0·05 μF
C_{16} = 0·025 μF

C_{17} = 25 μF
C_{18} = 100 μF

D_{1-4} = OA81
D_5, D_6 = OA200
Z_1 = OAZ204
Z_2 = OAZ203
(all by Messrs. Mullard Ltd.)

TR_1 = OC71
TR_2 = OC45
TR_3 = OC71

TR_4 = OC75
TR_5 = OC45
TR_6 = OC71
TR_7 = OC201

T_1 = core type LA2104 (Messrs. Mullard Ltd.)
T_2 = type MM1A (Messrs. Fortiphone Ltd.)
L_1 = core type LA2104 (Messrs. Mullard Ltd.)
Inductance mm = 0·07 H

Notes

(1) The battery should be replaced if less than 40 μA flows through the meter in the "check" position of switch 2.
(2) C_{15} and C_{16} should have polystyrene dielectric.
(3) The capacity of the cable connecting the rotor head to T_2 should be less than 0·0008 μF.
(4) C_9 is adjusted so that L_1, C_9 resonates at 15 kc/s.

the end of the gold wire. The frequency at which the variations occur will be called the rotor tip frequency.

A short time (of the order of seconds) after the rotor is placed in water, C_6 charges *via* D_1 to about the mean value of the potential across the secondary of T_2 [Fig. 2(*b*)]. This potential, which is negative with respect to the neutral line, is applied to the emitter of TR_2. The secondary of T_2 is also connected directly to the base of TR_2. The potential between the emitter and base of TR_2 [Fig. 2(*c*)] is therefore the difference between the mean and instantaneous value of the secondary potential of T_2. The collector current of a transistor connected in the common emitter configuration (as TR_2 is) is an amplified version of the current flowing in the base-emitter circuit. However, little current flows unless the base is negative with respect to the emitter. The waveform of the collector current of TR_2 [Fig. 2(*d*)] is therefore composed of pulses of current with a repetition rate equal to the oscillator frequency (15 kc/s). These pulses are modulated in amplitude at the rotor tip frequency. The capacitor C_8 in parallel with the collector load of TR_2, together with the rejector circuit L_1, C_9, eliminates most of the oscillator frequency component (15 kc/s) of the waveform, while leaving the rotor tip component relatively unchanged [Fig. 2(*e*)]. The rotor tip signal is then amplified (TR_3–TR_4) until it is sufficient to trigger the bi-stable pair (TR_6–TR_7). The triggering action is as follows. Suppose TR_7 is "off", then about 60 μA flows through R_{17} into the base of TR_6, maintaining it "on". If a current of 60 μA or more flows through R_{13} in the positive direction (with respect to the neutral line) then the current flowing through R_{17} will be diverted to TR_5, thus turning TR_6 "off". When TR_6 is "off", TR_7 is maintained "on" by the current flowing through Z_1. The emitter of TR_6 is maintained at about $-0{\cdot}5$ V (with respect to the neutral line) by the potential drop across D_4; TR_6 can only be turned on if its base is taken more negative than its emitter, and R_{14} ensures that this can only take place if more than 60 μA flows through R_{13}. The flow must be in the negative direction with respect to the neutral line. Thus TR_7 is turned "off" if more than 60 μA passes through R_{13} in the positive direction, and is turned "on" if more than 60 μA passes through R_{13} in the negative direction. This unusual trigger action is most effective in distinguishing the rotor tip signal from the noise of the system. When TR_7 is "on", the potential of its collector is virtually that of its emitter; when it is "off" its collector potential is defined by the Zener diode Z_2. The collector voltage waveform is used to drive a diode-pump integrator.

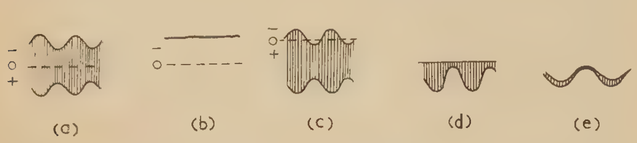

Fig. 2. Circuit waveforms

(*a*) Waveform across secondary of T_2 (15 kc/s carrier modulated at rotor tip frequency. The depth of modulation has been exaggerated).

(*b*) Waveform across R_6 (virtually no rotor tip or carrier frequency present).

(*c*) Waveform between emitter and base of TR_2. (Polarity shown relative to emitter.)

(*d*) Collector waveform of TR_2. (Not to scale.)

(*e*) Waveform at the base of TR_3. (Not to scale.)

The detector may be looked upon as a self-balancing "slide-back" peak voltmeter, in which the reference potential (across C_6) adjusts itself to nearly the peak value of the input waveform. The waveform applied to the "voltmeter" is modulated so that the peak amplitude (and the output of its detector) varies at the rotor tip frequency. A change in the conductivity of the water will change the peak value of the input potential, but, as the reference potential (derived from the same source) also changes by about the same amount, the input (and output) of the detector remains much as it was, and no manual adjustment of the circuit is necessary.

The diode-pump integrator

The diode-pump integrator can be shown to give an output which is linear with frequency, provided that the driving voltage waveform is very much greater than the potential developed across the output meter (see Earnshaw[(2)]). As the driving voltage waveform has a magnitude of about 7 V, while the potential across the output meter never rises above 100 mV, the condition is fulfilled. Earnshaw also shows that the current through the meter is given by $I = nVC$ where I is the average current through the meter, n is the frequency of the driving voltage waveform and V its magnitude and C is the value of the feed capacitor (C_{15} or $_{16}$, Fig. 1). The magnitude of the driving voltage waveform (provided the battery voltage is greater than 8 V) is determined mainly by the characteristics of the Zener diode. {The battery voltage may be checked by going to the "check" position of switch 2. For correct operation a reading of more than 40 μA should be obtained (1 V = 5 μA).} Both the Zener diode and the feed capacitor have low temperature coefficients (less than one part in 1000 per deg C), so that the calibration of the instrument would be expected to vary little with temperature. In fact, the results of calibration with the instrument at 4 and 35° C are not distinguishable (probably because of the scatter of the readings) from those taken at room temperature.

Setting-up procedure

The rotor is placed in still water and RV_1 is advanced until the meter shows occasional small kicks; the control is then rotated backwards by about ten degrees. The instrument is now ready for use and further adjustment should only be necessary if any of the components change their characteristics. The exact relationship between the velocity of the

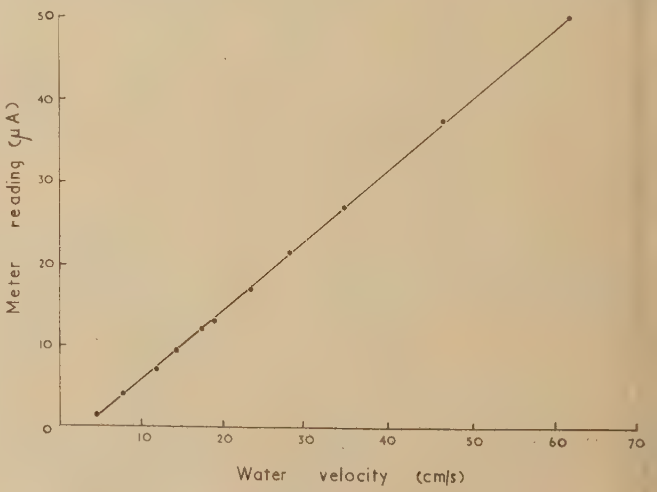

Fig. 3. Calibration of instrument-meter readings and corresponding velocities

vater and the meter reading is determined mainly by the form f the rotor, the Zener voltage of the diode (Z_2) and the exact alue of the feed capacitor (C_{15} or C_{16}). Of these factors the irst two may be regarded as constant and the value of the eed capacitor adjusted to give a suitable scale. With a feed apacitor of 0·05 μF and a rotor of the form described by Dedow and King(3) (type B), full-scale deflexion was obtained or a water velocity of about 60 cm/s.

Calibration and performance

The measuring head was rotated in a circular flume at arious speeds and the deflexions of the meter noted. Fig. 3 hows a typical calibration run for the lower speed range. The failure of the best straight line to go through the origin s presumably due to friction of the rotor bearings. The alibration has been extended up to 170 cm/s with similar inearity and scatter of readings.

An important feature of the instrument is its ability to vork in water of various conductivities without adjustment. The instrument has been shown to work in sea water, tap vater and a mixture consisting of one part tap water to two parts of distilled water. (The conductivity of the mixture was about 100 μmhos/cm.)

Construction

All the electronic components, including the meter and the battery, may be fitted into a case 23 cm long, 15 cm wide and 9 cm deep. The weight of the present instrument is less than 1·4 kg. The battery consumption is less than 5 mA at 9 V.

Acknowledgements

We should like to thank the Civil Engineering Department, not only for making the measuring head, but also for providing facilities for its calibration. One of us (J. M. E.) holds a Nature Conservancy research studentship.

References

(1) Wilkie, M. J. *J. Sci. Instrum.*, **32**, p. 350 (1955).
(2) Earnshaw, J. B. *Electronic Engng*, **28**, p. 26 (1956).
(3) Dedow, H. R., and King, R. F. *Engineering* (*London*), **178**, p. 396 (1954).

Swept Langmuir probe system for intense gas discharges

by H. W. JONES, B.Sc., and P. A. H. SAUNDERS, B.Sc., A.R.C.S., A.E.R.E., Harwell

[*Paper received* 2 *August*, 1960]

Abstract

The apparatus described provides a pulse of biasing voltage to a probe system so that electron temperatures up to 2 × 10⁵ °*K and ion densities up to* 5 × 10¹⁴/*cc can be measured. The system consists of a low impedance voltage sweep generator, a transformer-coupled measuring circuit and a logarithmic amplifier. The apparatus can be used to sample a portion or the whole of the electron energy distribution by using double probes of equal or greatly unequal areas. The probe plots are displayed directly on an oscilloscope.*

Introduction

Johnson and Malter(1) have described a Langmuir probe technique for measuring the electron temperature and ion density in a gas discharge. There are two principal difficulties in applying this method to a high intensity pulsed discharge where the electron temperature and ion density may be as high as 2 × 10⁵ °K and 5 × 10¹⁴ ions/cc respectively:

(1) It is not possible to maintain a bias of more than about 30 V between the probes without an arc occurring;
(2) there may be rapid random variations in the parameters to be measured.

It has been found that a complete probe plot can be obtained without arcing if the biasing voltage is applied in the form of a fast sawtooth pulse.(2) If the rise time of this pulse is long compared with the time taken for a positive ion to cross the probe sheath, there is no distortion of the probe plot. The rise time must, however, be short compared with the time in which there are significant changes in ion density and electron temperature.

The electron temperature must be known in order to calculate the ion density, and the concept of electron temperature is only meaningful if the electron energy distribution is Maxwellian. Johnson and Malter have shown that in a typical system consisting of two probes of equal area, less than the top 1 % of the electron energy distribution is sampled. If probes of unequal area are used and the ratio of areas is greater than $(m_{ion}/m_{electron})^{1/2}$, the whole of the energy distribution can be sampled, and departures from Maxwellian distribution should be seen on the probe plots. Such a system is essentially similar to the classical single Langmuir probe,(3) with the advantage that the probes are floating and thus no current is drawn from the discharge.

For probes of equal area, the electron temperature can be obtained directly from the probe plots by the equivalent resistance method described by Johnson and Malter. With probes of unequal area, however, the electron temperature is obtained from the slope of the semi-log plot of probe current against biasing voltage. For this purpose, it is useful to be able to display the semi-log plot directly on an oscilloscope, and a circuit to do this is described below.

For some applications, the probe system must be floating from earth, so coupling transformers which must not distort the shape of the voltage sweep must be used.

Description of apparatus

A block diagram of the apparatus is shown in Fig. 1. The sweep generator consists of a bootstrap sawtooth generator giving a maximum sweep of 120 V with a sweep length variable from 1 to 20 μs. Since probe currents of up to 10 A can be drawn, a very low output impedance is necessary. This is obtained by using the voltage sweep to drive four White cathode followers connected in parallel. The output from this stage can be fed to the probes either directly and superimposed on a d.c. bias variable from 0 to ± 30 V, or through an isolating transformer. The whole system is balanced about earth to avoid pick-up, and the voltage sweep can also be fed through a balance to unbalance unit to the X-plates of an oscilloscope.

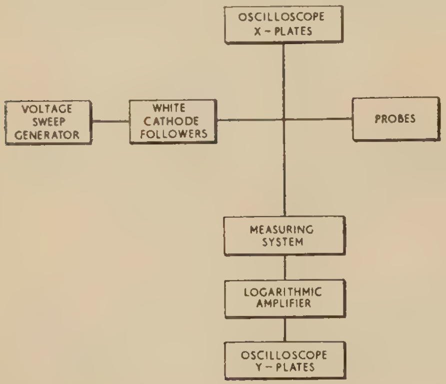
OSCILLOSCOPE X - PLATES
VOLTAGE SWEEP GENERATOR
WHITE CATHODE FOLLOWERS
PROBES
MEASURING SYSTEM
LOGARITHMIC AMPLIFIER
OSCILLOSCOPE Y - PLATES

Fig. 1. Block diagram of complete system

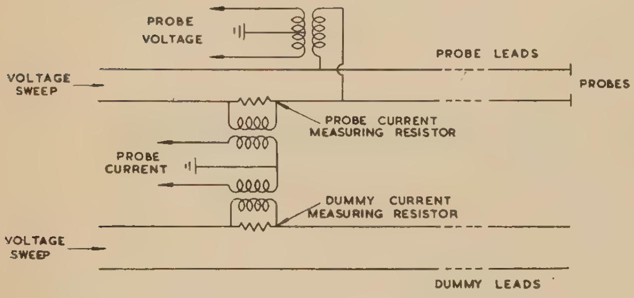
PROBE VOLTAGE
PROBE LEADS
VOLTAGE SWEEP
PROBES
PROBE CURRENT MEASURING RESISTOR
PROBE CURRENT
DUMMY CURRENT MEASURING RESISTOR
VOLTAGE SWEEP
DUMMY LEADS

Fig. 2. Probe current and voltage measuring system

The measuring system, Fig. 2, which consists of a series of resistors of accurately known values through which the probe current flows, is balanced and transformer-coupled. The transformers have a rise time of 0·1 μs and a 10 μs flat top, and are fed by and feed into cathode followers. The whole measuring system is isolated from earth and powered by batteries to avoid pick-up. The system measures an additional current, produced by the voltage sweep charging up any stray capacitances, such as the capacitance of the cables. There is a second complete measuring system which is connected to a dummy cable the same length as the cable from the sweep generator to the probes and in parallel with it. The current in this system is then subtracted from the measured probe current. This is not entirely satisfactory as the terminations of the two cables cannot be identical but, in practice, the remaining capacitance current can usually be neglected.

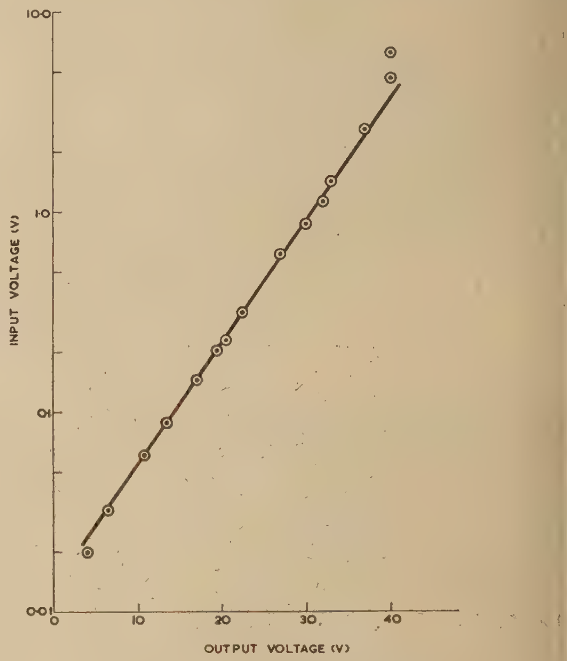

Fig. 4. Performance of logarithmic amplifier

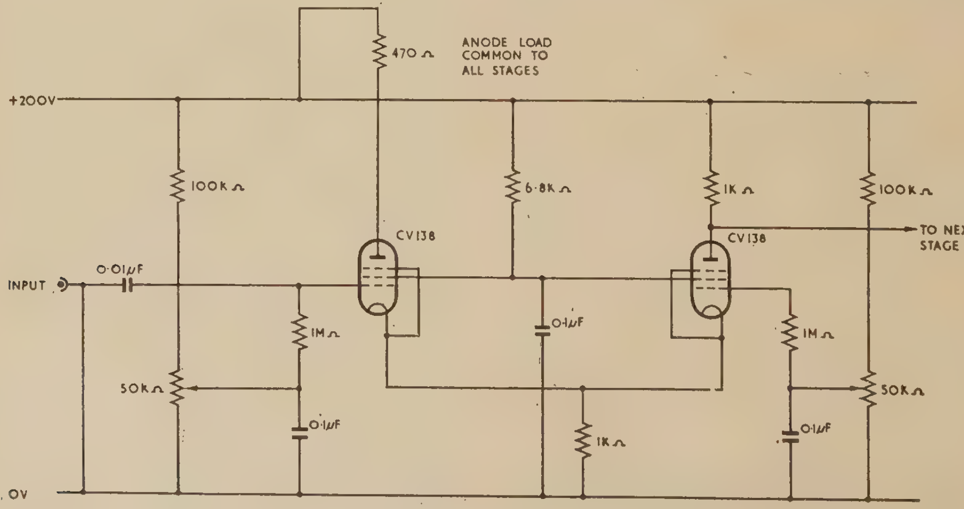
470 Ω
ANODE LOAD COMMON TO ALL STAGES
+200V
100K Ω
6·8K Ω
1K Ω
100K Ω
CV138
CV138
TO NEXT STAGE
INPUT
0·01μF
1M Ω
0·1μF
1M Ω
50K Ω
50K Ω
0·1μF
1K Ω
0·1μF
0V

Fig. 3. One stage of logarithmic amplifier

The logarithmic amplifier consists of five identical stages, ch being a long-tailed pair as shown in Fig. 3. The anodes the first valves of each stage are connected to a common node load so that the output from each stage is added. The final output is taken from this common anode load through a cathode follower. The second valve of each pair is used to feed the next stage.

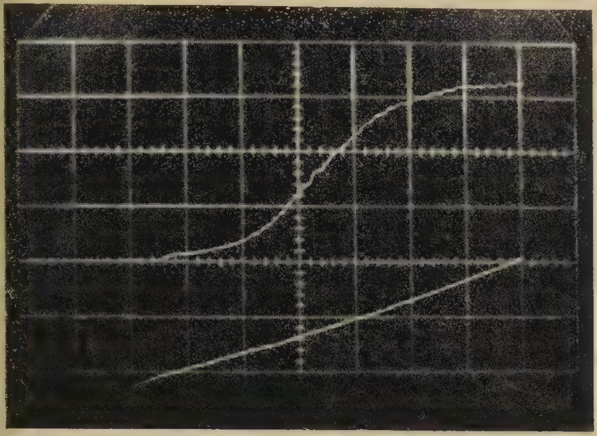

Fig. 5. Top trace, typical probe current-voltage characteristic Lower trace, probe voltage; *x*-deflexion provided by probe voltage sweep

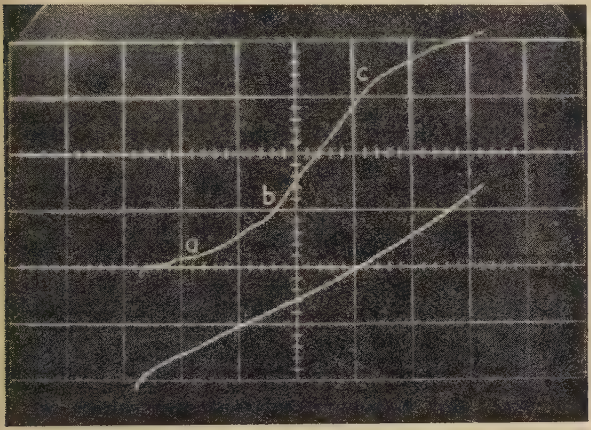

Fig. 6. Top trace, semi-logarithmic probe plot

a to *b*—the last stage of the log amplifier is not saturated so its response is not logarithmic; *b* to *c*—straight line portion of semi-log plot. *c*—break point

Lower trace, probe voltage; *x*-deflexion provided by probe voltage sweep

The principle of the circuit(4) is best seen by considering the amplifier to have n identical stages, each with gain G. Assume that an input voltage of x just saturates the last stage. The total output signal will be $G^n x$ + smaller contributions from previous stages. The gain per stage must be large enough to make the contributions from previous stages negligible. If the input is now multiplied by G, the $(n - 1)$th valve will just saturate and the total output signal will be $G^n x + G^n x$ (neglecting contributions from previous stages). Thus a multiplication of the input by G has added $G^n x$ to the output and a further multiplication of the input by G will add a further $G^n x$ to the output. This gives the required logarithmic characteristic, but only the points where each stage saturates lie on the logarithmic curve. A valve has to be selected whose characteristic just before saturation gives the closest approach to a complete logarithmic response for the amplifier.

The circuit used was logarithmic over two decades (see Fig. 4) and its frequency response was flat up to 2 Mc/s. The logarithmic range can, of course, be extended by adding further stages.

Results

The system has been used to measure electron temperatures and ion densities in Zeta-type discharges.(5) Fig. 5 shows a plot obtained using equal-area probes with a standing d.c. bias of 20 V. Fig. 6 shows a semi-log plot obtained with the logarithmic amplifier using probes with an area ratio of 100 to 1.

Under some conditions it is possible to obtain a d.c. probe plot by applying a standing voltage to the probes, varying this from discharge to discharge, and measuring the probe current at the same time in each discharge. The values obtained for electron temperature and ion density in this way were found to agree with those measured by the swept system to 10%.

The final limitation to the use of the swept system is likely to be the arcing that still occurs in very intense discharges; this is probably due to charging and dielectric breakdown of insulating inclusions present as impurities in the probe material.(6) This may be reduced by evaporating a layer of metal on to the probes under clean vacuum conditions.

References

(1) Johnson, E. O., and Malter, L. *Phys. Rev.*, **80**, p. 58 (1950).

(2) Mamyrin, B. A. *Zh. Tekh. Fiz.*, **23**, p. 904 (1953).

(3) Langmuir, I., and Mott-Smith, H. M. *Gen. Elec. Rev.*, **27**, pp. 449, 538, 616, 762, 810 (1924).

(4) Chambers, T. H., and Page, I. H. *Proc. I.R.E.*, **42**, p. 1307 (1954).

(5) Harding, G. N., *et al. Proc. Second Intern. Conf. Peaceful Uses Atomic Energy, Geneva*, **32**, p. 365 (1958).

(6) Hancox, R., and Walker, C. H. *AERE-R* 3254.

Photomultiplier soft X-ray spectrometer

by L. JACOB, Ph.D.,[*] R. NOBLE, Ph.D.,[†] and H. YEE, B.Sc.,[‡] Nuclear Physics Research Laboratory, University of Liverpool

[*Paper first received* 11 *December*, 1959, *and in final form* 31 *August*, 1960]

Abstract

A description is given of a soft X-ray spectrometer which uses a Be–Cu photomultiplier as detector. Unlike most spectrometers of this type it is not a modification of a previously existing photographic instrument, but was designed specifically to take advantage of the new technique. In particular the photo-detector is made to move around the Rowland circle by the simple expedient of mounting it on a radial arm. Its method of use is described and the emission band spectra of Al, Mg, Na and Li are given as examples of results obtained with it.

Introduction

In recent years there has been a tendency in soft X-ray spectroscopy to replace the photographic plate by a photoelectric method of recording. This has been due to the development of the beryllium–copper photomultiplier, which has an efficiency in this X-ray region high enough to make it a much more sensitive method of detection than the photographic method. This means that lower target voltages and currents can be used with consequent reduction of target contamination. A more important reason for adopting the photoelectric detector is that it makes possible the direct measurement of intensities, and should give more accurate spectra than the photographic method. A third advantage is that there is no processing stage between an exposure and the first examination of results. This speeds up work by making target adjustments and control of other necessary conditions easier, and leads to fewer futile exposures. A typical soft X-ray spectrum band can be obtained in ten minutes or less. Additionally, only the X-ray tube needs evacuating after a change of target, the main body of the spectrometer being permanently evacuated.

Several instruments of this type are in use, typical examples being those at the National Physical Laboratory,(1) the Massachusetts Institute of Technology,(2, 3) and the University of Western Australia. Most of these instruments have been modifications of existing photographic spectrometers. It was decided in the present instance to design an instrument expressly to meet the needs of the new technique.

The Rowland type of mounting is normally used in soft X-ray spectrometers and in the new instruments the primary slit and grating mounting are as used in the photographic instruments. The spectrum, however, is examined with a photomultiplier placed behind a slit, which is required to move around the Rowland circle. In the modified photographic instruments it has been the practice to remove the curved casette, by means of which the plate is constrained to follow the Rowland circle, and replace it with curved rails. A trolley or slide, carrying the slit and photomultiplier, moves round the curved rails, usually driven by link arms and a leadscrew which can be operated from outside the instrument.

Constructional details

In building the present spectrometer it was decided to adopt the more straightforward system of mounting the detector system at the end of a radial arm pivoted at the centre of the Rowland circle. This meant a departure from the customary cylindrical vacuum tank and the instrument case was made in the shape of a sector of a circle. This approach was made possible by use of a 1 m grating and ½ m radius Rowland circle. The use of a grating of larger radius would result in a prohibitively large casing. The main details described below can be seen in the schematic diagram in Fig. 1.

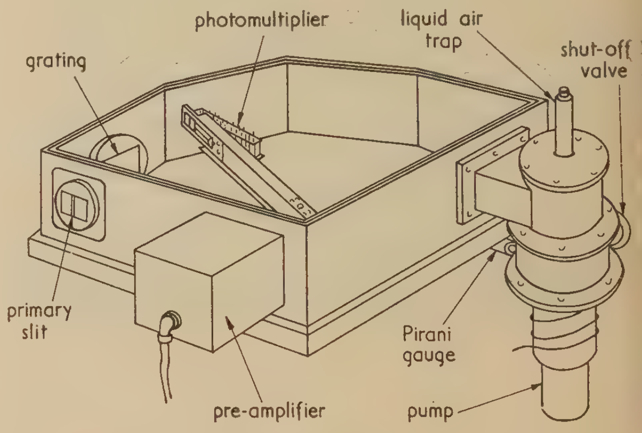

Fig. 1. General appearance of spectrometer

The base was made from mild steel plate 2 in. thick. The walls of 1 in. thick mild steel were welded to the base and to one another. A slot, made around the top of the walls, held an endless rubber seal upon which rested the spectrometer lid made from an aluminium alloy of 1 in. thickness. The outer 3 in. of the underside of this lid were milled flat to obtain a good vacuum seal. The thickness of the base and walls prevents any flexing and relative movement of the important parts, while the use of a light alloy for the lid permits its removal without any special lifting tackle.

Two rectangular ports were cut in one of the long radial walls of the casing. A ground flange, carrying the primary slit to which the X-ray tube could be fixed, was fitted over the first port. A rectangular Perspex flange with vacuum-tight terminal posts was fitted over the second port to bring out the connexions to the photomultiplier.

A larger port was cut in the other radial wall, over which was fitted a flange and tube of rectangular cross-section, eading to a liquid air-trap chamber. The liquid air-trap was made from stainless steel and supported from the top of the hamber by a long neck, folded back on itself to provide a ong heat conduction path. Evaporation from this trap was uite slow, one filling lasting more than an hour.

---

[*] Now at Royal College of Science and Technology, Glasgow.
[†] Now at M.S.S. Recording Co. Ltd., Colnbrook, Bucks.
[‡] Now at English Electric Ltd., Luton, Beds.

Immediately below the liquid air-trap chamber was a arge chamber containing a flap-seal valve operated by a andle on the side. A 4 in. oil diffusion pump, with an ltimate pressure of 10^{-5} mm of mercury, was fitted below he flap-seal chamber. The valve served to cut off the instrunent case from the pump and also, to some extent, to baffle he pump.

In order to make it possible to seal off the vacuum casing ompletely, a valve was also fitted to close off the primary lit. There being no room on the outside, the valve had to e fitted inside the case behind the primary slit flange. A rass block faced with rubber was mounted on levers in uch a way that it could be pressed over the hole behind the lit or swung back out of the path of the X-ray beam when not in use. It was operated by means of a dog-clutch on the nd of a rod passing through the lid of the instrument. A ever was fitted to the top of the rod and a clamp to the top of the lid to enable the valve to be closed firmly as, in this ase, atmospheric pressure does not assist the closing of the eal.

The grating used was a concave glass grating of 1 m radius of curvature, ruled with 30 000 lines per inch. It was mounted n a brass mount provided with facilities for rotating it about orizontal and vertical axes (Fig. 2). This mount was fitted t the base into a dovetail slide to permit radial movement.

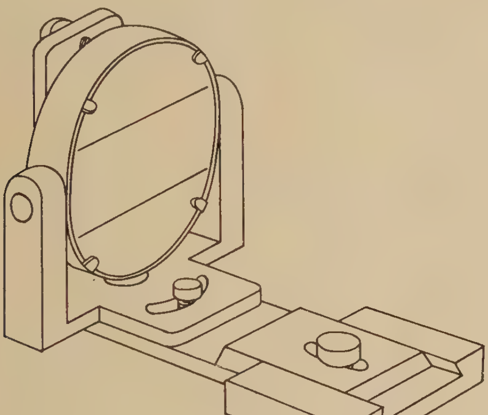

Fig. 2. Grating mounting

The base of the dovetail slide could be bolted to the spectrometer base in one of several positions, thus permitting some adjustment of the angle of incidence of the radiation to the grating. A vertical knife edge was attached to the mount in such a way as to cut off direct reflexion from the grating and pass only the diffracted radiation to the photomultiplier.

The radial arm to carry the photomultiplier was made from a mild steel girder of I-shaped cross-section, fixed at one end to a 1 in. diameter steel rod passing through the base of the spectrometer, forming a pivot. The bearing of the pivot consisted of a thrust roller bearing inside the spectrometer and a locating ball bearing outside the spectrometer. The pivot was made vacuum-tight with Gaco hat seals in suitable housings, and a pointer and scale were attached to the pivot on the outside to give an indication of the position of the arm within. The lower end of the steel pivot was coupled to a precision gear-box driven by a reversible induction motor. The gear-box reduction ratio was approximately 300 to 1.

A variable width slit was fitted to the outer end of the radial arm; this slit was also capable of radial adjustment, to allow it to be located accurately on the Rowland circle. The photomultiplier was mounted on a bracket behind the slit at an angle suitable for the entry of the X-ray beam to the first dynode of the multiplier. It would appear desirable that the detector assembly should be arranged to make the plane of the slit normal to the X-ray beam in all positions of the arm. This is not so much because of the change in effective area of the slit, as this should be quite small over any given band and easily corrected for, but rather because as the arm moves, the X-ray beam strikes a different part of the first dynode. Though possible, such an arrangement would be complicated and was not used.

Electronics of instrument

The photomultiplier was a fifteen-stage beryllium–copper device of the type described by Allen,(4) and was made by Dr. Owen at the Atomic Energy Research Establishment, Harwell; it will not be described further.

The connexions to the individual stages of the photomultiplier were made with small clips to facilitate rapid fitting and removal and prevent prolonged exposure of the beryllium–copper surfaces to the atmosphere. The body of the spectrometer was normally kept evacuated to this end.

The leads from the dynodes were taken along the top of the radial arm in glass tubes and then over from the pivot to the Perspex terminal board by means of polythene-covered wires, shaped into spiral coils for flexibility.

The supply voltages to the dynodes were provided by a chain of eight megohm resistances across the output of a variable 4 kV regulated power supply. This value of resistor was chosen so as not to load the supply unduly, and at the same time to pass a "bleeder" current large in comparison with the dynode currents. This is important to prevent voltage variations with signal current. The regulation of the dynode supply must be good, as the effects of voltage variations in early stages are magnified by large factors in the subsequent multiplication stages.

There are two ways of making use of a photomultiplier detector in this application. One is to use it in conjunction with a pulse amplifier and counter or pulse-ratemeter. A second is to integrate the pulses by using a d.c. amplifier to amplify the average current from the multiplier. The difficulties associated with each method differ widely and only the latter method will be described. This method was finally chosen because of the availability of equipment and because it did not appear to have been attempted previously.

The signal from the final stage was fed into a pre-amplifier built directly over the Perspex terminal board on the side of the spectrometer. This pre-amplifier, shown in simplified form in Fig. 3, contained an electrometer valve as the first stage of the d.c. amplifier. The rest of the amplifier was housed on a nearby rack. The amplifier had a voltage gain of about 10^4, which was reduced to unity by the application of negative feedback in a circuit of the virtual earth type. The gain was thus made extremely stable against the usual variations. The feedback resistor forms the load for the multiplier and a choice of two values, $10^{10}\ \Omega$ or $10^{11}\ \Omega$, was available. Resistors of such high values require that the parallel leakage resistance, which may be variable, should be at least 10^{13} Ω and considerable care was exercised to achieve this value. The chassis of the pre-amplifier was made of Perspex, the electrometer valve base was cut away around the grid pin and a direct connexion made to this pin. The Perspex was cleaned carefully at intervals to reduce surface leakage. The pre-amplifier was electrostatically screened to prevent pick-up of stray voltages and avoid capacity effects with nearby moving objects.

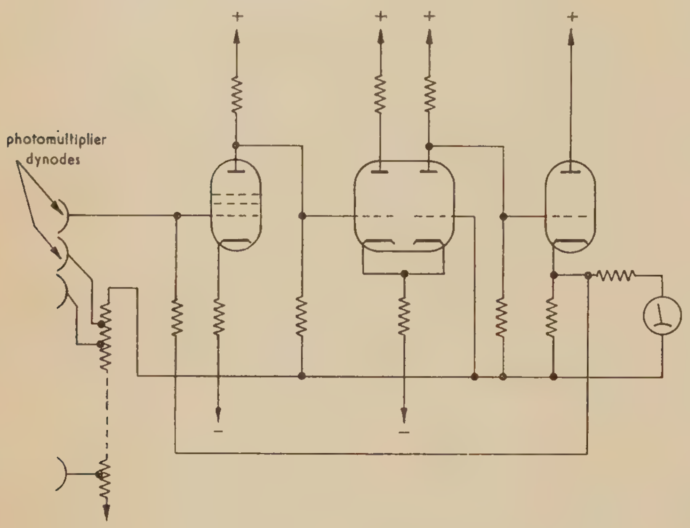

Fig. 3. Schematic circuit of amplifier

The output from the d.c. amplifier came from a cathode follower and was fed to a pen recorder driven by a synchronous induction motor.

The X-ray tube used was of the now familiar type used by Skinner,(5) and consisted essentially of a spherical glass bulb fitted with glass-pinch arms to carry the target, filaments and evaporators. A brief description of the mechanism by which the soft X-ray emission bands are excited may be of interest. Electron bombardment of the target results in ejection of electrons from the inner shells of the target atoms. As the atoms revert to their lowest energy states, electrons from the valence or conduction bands fall into the vacancies in these inner shells. Since the inner levels of the atom are comparatively sharp, the bands of radiation produced by this type of transition are representative of the distribution of energy levels in the valence or conduction bands. The emission intensity at any point within the band is not directly proportional to the density of energy levels but is modified by the transition probabilities. Briefly, in the lighter elements for example, the K spectra are representative of the level densities of the p-type electrons, while the L spectra are representative of the level densities of the s- and d-type electrons. Additionally, since emission intensity is proportional to the cube of frequency, it is necessary to plot a graph of emission intensity, $I(E)$ divided by ν^3 to obtain a true picture of the level densities.

The voltage supply to the target must be maintained constant and this was done manually with the aid of a Variac transformer, which was, however, fed from a constant voltage transformer.

Method of operation

The adjustment of the slits and grating was made first by careful measurement, then by an optical method and finally by trial experiments on the emission edges of aluminium and magnesium.

The photomultiplier slit width was set normally to a width of 0·004 in., and a resolution of about 1 Å was obtained. The width was made less for a number of experiments in order to examine detail; in particular to obtain the L_2 edges in the cases of aluminium and magnesium. The target voltages used were of the same order as those used with the photographic method (2 to 3 kV), but the currents were normally less by factors from about two to ten. These target powers may seem large when compared with those used by Piore and others,(2) but this is to some extent due to the difference in photomultiplier slit widths used, and also to the fact that the present authors tended to use the photomultiplier in a less sensitive condition. This was done to overcome the random fluctuations which appear on the output when small target powers and high photomultiplier sensitivities are used. These appear as noise on the desired output signal, but if the power input to the system is increased the signal-to-noise ratio is improved. The fluctuations were also reduced to some extent by artificially reducing the amplifier bandwidth and making the photomultiplier track the band more slowly. This corresponds to increasing the integration time in a counting ratemeter. An alternative method is that used by Caterall and others,(1) in which the multiplier is moved in a series of discrete steps, a count being taken in each stationary position. Each count is made sufficiently large to reduce statistical variations to the required degree. This last method is probably the most convenient to apply if accuracy is required, but all three methods are based upon a sacrifice of bandwidth for signal-to-noise ratio, and a compromise can be made in each experiment depending on whether the requirements are high resolution, accurate

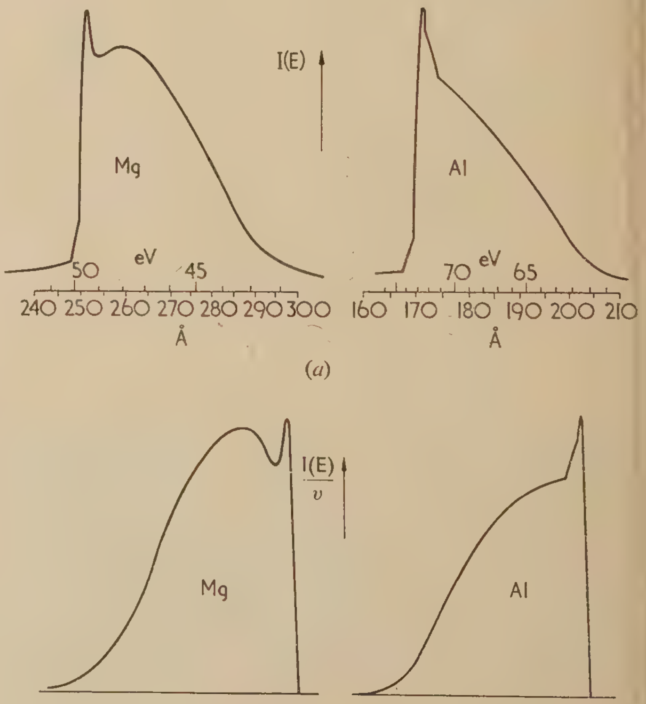

(a)

(b)

Fig. 4. Aluminium and magnesium. (a) Spectrometer traces. (b) Plots of $I(E)/\nu^3$ giving a more correct representation of electron band forms

ntensity measurement or rapid operation. A convenient nethod of working is to make a rapid scan of the band, to letermine the general form, followed by a more accurate xamination of the interesting details.

Some expreimental results

The instrument was tested by determining the band forms of several well-known elements. The bands of aluminium, magnesium, lithium and sodium are shown in Figs. 4 and 5.

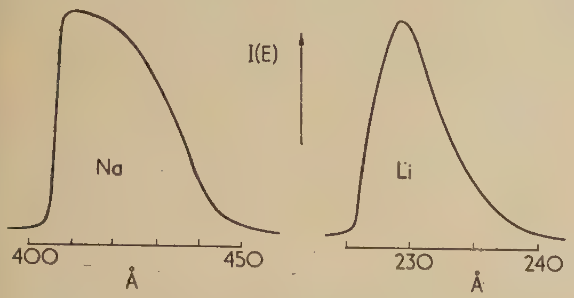

Fig. 5. Spectrometer traces of sodium and lithium

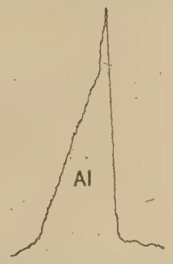

Fig. 6. Copy of pen tracing of aluminium band

These bands agree well with those previously published but the intensities are probably more accurate than those obtained by the photographic method. In the case of sodium the band is more "parabolic" than that published by Skinner and the small kink near the edge which he described does not appear to be present. However, owing to the experimental difficulties met in obtaining the band, the authors are inclined to be a little doubtful about the validity of this result. Fig. 6 is a careful copy of an original pen tracing included to give some indication of the amount of smoothing produced by the averaging process used to obtain Figs. 4 and 5.

Acknowledgements

The work described was carried out at the Nuclear Physics Research Laboratory of the University of Liverpool under the direction of Dr. Louis Jacob. Acknowledgement is due to the late Prof. Skinner who gave valuable advice on the design of the spectrometer.

References

(1) Catterall, J. A., Wilson, L. F., and Trotter, J. *J. Sci. Instrum.*, **35**, p. 393 (1958).

(2) Piore, E. R., Harvey, G. G., Gyorgy, E. M., and Kingston, R. H. *Rev. Sci. Instrum.*, **23**, p. 8 (1952).

(3) Gale, B., and Trotter, J. *Phil. Mag.*, **1**, Series 8, p. 759 (1956).

(4) Allen, J. S. *Phys. Rev.*, **55**, p. 966 (1939); *Rev. Sci. Instrum.*, **18**, p. 739 (1947).

(5) Skinner, H. W. B. *Phil. Trans Roy. Soc. A*, **239**, p. 95 (1946).

Stability of some reactance standards

by L. H. FORD, M.Sc., National Physical Laboratory, Teddington, Middlesex

[*Paper received* 22 *July*, 1960]

Abstract

Examples are given of the behaviour over several years of the working standards of inductance and capacitance maintained at the National Physical Laboratory. The information is supplementary to that contained in previous papers.

Introduction

The performances of the working standards of reactance in use at the National Physical Laboratory, for measurements of both inductance and capacitance, have been described in a number of previous papers.(1-4) A brief account of the subsequent behaviour of some of these instruments is given in the present paper; examples have been chosen that may be of general interest to the users of reactance standards, without attempting any comprehensive survey of the stability of such standards. Most of the instruments referred to are good quality commercial products; only a few were designed and made at N.P.L.

The measured values given in the paper are for a frequency of 1000 c/s and a temperature of 20° C, unless otherwise stated; they are all based on the assumption that the primary standard of mutual inductance has remained constant throughout the whole period covered by the measurements.

Mutual inductometer

The standard variable mutual inductor now in use was designed and made at N.P.L. in 1937(5,6) the windings are fully screened and are oil-immersed. Fig. 1 shows the departures from the mean value of every calibration at the 10 mH setting over the period 1937 to 1960, made at a frequency of 10 c/s. This mean value is the same to within 0·2 parts in 10^5 of that given previously(1) for the period 1937 to 1948. The apparent improvement in stability over the years is probably illusory. The high stability achieved was not anticipated, and the earlier calibrations were uncertain to about one part in 10^5, since the temperature was only observed to the nearest 1° C; only in the last decade has the room, in which the instrument is kept, been temperature controlled and the temperature been observed to 0·1° C during calibrations.

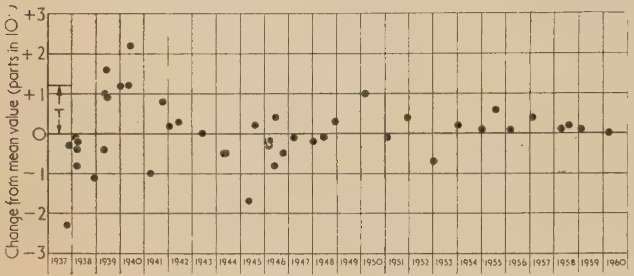

Fig. 1. Departures from the mean value of every calibration made on the mutual inductometer at 10 mH (10.0.0) setting, at a frequency of 10 c/s and a temperature of 20° C

T, change for 1° C rise in temperature

The stability of the instrument at the intermediate settings is not as good as at the 10 mH setting. At the 5 mH setting, which is much used in measurements of self inductance, a fairly steady drift has taken place, relative to the 10 mH setting, of about 0·5 parts in 10^5 per annum. Thus, if the instrument were used to measure a self inductance of 10 mH on a Campbell–Heaviside bridge, the value obtained today would be almost exactly one part in 10 000 in error if the first calibration made in 1937 were used to evaluate the results.

The construction of this inductometer is such that the fixed winding is sandwiched between two equal sub-divided secondary windings, the axis of the windings being vertical. The changes in calibration observed are consistent with a steady subsidence of the secondary windings over the years under the influence of gravity: the individual 1 mH mutual inductances between the fixed winding and each of the five sections of one secondary winding have increased, while those of each of the five sections of the other secondary winding have decreased by almost equal amounts.

Self inductors

The set of inductors(6) from 1 μH to 1 H in value, referred to briefly in a previous paper,(1) have now been under observation for more than ten years. They are constructed with two end cheeks of laminated paper Bakelite that support longitudinal members of loaded ebonite on which the coil is wound. The inductance of these coils is dependent on atmospheric relative humidity, but only one, of 10 mH, is maintained in an atmosphere of constant relative humidity; the remainder are subject to the fluctuations occurring in the room in which they are kept. When measured under these conditions over the period 1946 to 1960, the larger coils, of 200 μH and more, have shown a spread between the highest and lowest observation of coil inductance which ranges from 22 to 5 parts in 10^5, as shown in Table 1. With one or two exceptions, there is little sign of any permanent drift in value in either direction, and the changes are probably largely due to variations in the relative humidity from one test to another. The 0·2 and 0·5 mH coils, however, have probably decreased in inductance by about 5 parts in 10^5 for constant humidity.

Table 1. *Spread in inductance of standard coils*

Inductance (mH)	0·2	0·5	1	5	20	100	1000
Parts in 10^5	21	22	14	8	5	6	13

Since 1954, the 10 mH coil has been kept in a container with a saturated solution of potassium carbonate, which maintains the atmospheric relative humidity at 44%. Its observed inductance has remained within ±1 part in 10^5 of that recorded for July 1955 in the previous paper,(2) over the past five years.

The performances of the coils of 100 μH and less, which are more susceptible to changes in atmospheric relative humidity, are inferior to those of the larger coils. For example, the values obtained on the 100 μH coil show a spread of 33 parts in 10^5, with little sign during the years of any systematic change other than that with relative humidity, and the values on the 1 μH coil show a spread of 0·003 μH, with an increase in inductance of about 0·002 μH, over the period 1946 to 1960.

A 10 mH inductor of commercial manufacture, in the form of a toroid in a hermetically sealed case, has now been under observation for two and a half years. In that period its inductance has varied over an extreme range of 3 parts in 10^5 and has tended to decrease in value.

Capacitors

Considerably more information has been published(3, 4, 7, 8) concerning the capacitors maintained at N.P.L. than the inductors, and in all cases, except one, little more need be said. The exception is the mica capacitor of 0·01 μF which was kept in a desiccator for a year and then hermetically sealed in a container with silica gel.(4) The results on this instrument, manufactured in 1932, are shown in Fig. 2 for the eight years that have passed since it was sealed.

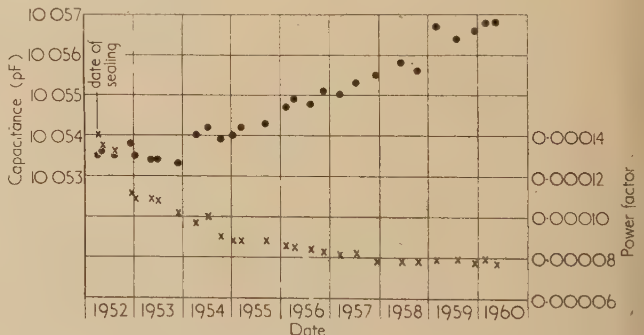

Fig. 2. Results of measurements on the sealed mica capacitor at a frequency of 1000 c/s and a temperature of 20° C

● = capacitance
× = power factor

The power factor, which was 0·0005 when drying commenced and had fallen to 0·000 14 at the time of sealing, continued to decrease and has now been steady at 0·000 08 for four years. The capacitance, which was 0·010 065 μF when drying commenced, remained reasonably steady at 0·010 053 5 μF for two years after sealing, but it has now been increasing fairly uniformly over the last six years. The absence of any corresponding rise in power factor shows that this capacitance increase is not due to the ingress of moisture. The capacitance was probably drifting upwards throughout the whole period covered by Fig. 2, but over the first two years the increase was balanced by a decrease due to the drying action of the silica gel; the fall in power factor over the period supports this hypothesis.

A rise in capacitance with time is not unusual on small mica capacitors of clamped construction, for a few years after manufacture. Some values obtained on another 0·01 μF capacitor during the first twenty years of its life are given in Table 2, and these may be taken as representative; this instrument showed a power factor of about 0·000 08 throughout the period.

Table 2. *Capacitance change on* 0·01 *μF mica capacitor*

Time (years)	0	1	5	9	15	21
Capacitance (pF)	0	+1	+4	+5	+6	+7

It is exceptional for a mica capacitor to show a rate of increase of capacitance as great as is shown in Fig. 2 for thirty years after manufacture. However, in an N.P.L. standard capacitor(3) covering the range 0·01 to 0·1 μF, one of the two units of 0·01 μF has continued to increase in capacitance at the same rate as it did over the period 1944 to 1950 for the next ten years, 1950 to 1960; the average rate is still plus 3 parts in 10^5 per annum. In contrast to this, the other 0·01 μF unit of the same box had a mean value of capacitance of 0·010 011 3 μF over the period 1944 to 1950 and has had a mean value of 0·010 011 8 μF over the past two years; this change is less than the seasonal changes of capacitance with atmospheric relative humidity. Both these units are nearly thirty years old; it is clearly impossible to say how capacitors of modern construction will behave after a similar period.

Large mica capacitors of clamped construction show considerably greater stability than small ones. Of the units in the N.P.L. standard capacitor covering the range 0·1 to 1·0 μF, the best is one of 0·2 μF. The mean capacitance of this was 0·199 846 μF over the period 1944–1950,(3) and has been 0·199 847 μF over the last two years; the capacitance has only fluctuated over a range of 3 parts in 10^5 over the last ten years. The performances of the other units of this capacitor have been almost as good; the worst, a unit of 0·1 μF, has varied over a range of 6 parts in 10^5 in this period. Of all mica capacitors at N.P.L., this is the best.(8)

The power factors of all except one of the units in these two standard capacitors have remained substantially unchanged for the last ten years. The exception is the 0·1 μF unit referred to above, which has increased in power factor from a mean value of 0·000 07 over the period 1944 to 1950 to a value of 0·000 13 in 1959. Measurements at higher and lower frequencies than 1000 c/s show that this increase is not due to a rise in series resistance, such as would be caused by a defect in the connecting leads to the terminals, but is inherent in the capacitor.

The standard variable air capacitor of N.P.L. design and make(6) has continued to be exceptionally stable. The calibration for a capacitance change of 2000 pF, when corrected for changes in atmospheric humidity, has remained constant within ±5 part in 10^5 of its mean value over the last ten years. The calibration of a commercial variable air capacitor, manufactured in 1939, after an initial increase has remained constant within ±10 parts in 10^5 over the last ten years, for a capacitance change of 5000 pF. Some values obtained on a three-terminal commercial instrument during the first twelve years of its life are given in Table 3.

Table 3. *Capacitance of variable air capacitor at setting* 90

Time (years)	0	1	3	7	13
Capacitance (pF)	1311·2	1311·4	1311·5	1311·6	1311·6

Conclusion

Experience at N.P.L. has shown that standards of reactance of commercial make can be obtained which will have stable values to within ±5 parts in 10^5 over a period of ten years or more, starting a few years after manufacture. For inductors the best performance is found with values from 10 to 100 mH, and for capacitors it is found with values from 0·1 to 1·0 μF. The stability for lower values of either inductance or capacitance is unlikely to be as good.

Acknowledgement

This paper, describing work undertaken as part of the programme for maintenance of standards at the National Physical Laboratory, is published by permission of the Director of the Laboratory.

References

(1) RAYNER, G. H., and FORD, L. H. *J. Sci. Instrum.*, **27**, p. 19 (1950).

(2) RAYNER, G. H., and FORD, L. H. *J. Sci. Instrum.*, **33**, p. 75 (1956).

(3) RAYNER, G. H., and FORD, L. H. *J. Sci. Instrum.*, **28**, p. 168 (1951).

(4) RAYNER, G. H., and FORD, L. H. *J. Sci. Instrum.*, **31**, p. 3 (1954).

(5) ASTBURY, N. F., and FORD, L. H. *Phil. Mag.*, **25**, p. 1009 (1938).

(6) HAGUE, B. *Alternating Current Bridge Methods*, pp. 565, 137, 173 (London: Sir Isaac Pitman and Sons Ltd., 1943).

(7) *N.P.L. Notes on Applied Science*, No. 13 (London: H.M. Stationery Office, 1955).

(8) RAYNER, G. H., and FORD, L. H. *Proc. Instn Elect. Engrs B*, **107**, p. 185 (1960).

Monitor for the quantitative determination of beryllium in the atmosphere

by M. S. W. WEBB, B.Pharm., F.P.S., F.R.I.C., R. J. WEBB, B.Sc., and P. C. WILDY, B.Sc., United Kingdom Atomic Energy Authority (Research Group), Woolwich, London, S.E.18

[*Paper first received* 16 *June, and in final form* 29 *July*, 1960]

Abstract

The air is drawn through a triggered intermittent arc and the intensity of the beryllium doublet at 3130 *Å is monitored, together with the adjacent background, and the ratio of these intensities is recorded on a ratio recorder. Provision is made for frequent calibration by means of an aerosol of known concentration, produced by an auxiliary spark between beryllium-copper electrodes. The accuracy and sensitivity of the instrument are not materially affected by the chemical form of the beryllium, and are unaffected by the sizes of particles normally encountered in atmospheric dust. The instrument is mobile, fully automatic and rapid in operation, one result being produced each minute. The limit of detection is* 1 $\mu g/m^3$ *for a twenty-second sampling time. The instrument is considered to have potentialities for the determination of other elements in air, apart from beryllium.*

Introduction

THE health hazard associated with airborne particles of beryllium and its compounds has received considerable attention during the past decade as a result of the increasing use of these materials in industry. The medical problems have been summarized by a number of workers(1, 2) and, whilst there is no official code of practice for the handling of beryllium and its compounds in this country at the moment (March 1960), the United Kingdom Atomic Energy Authority, and the Medical Research Council have given provisional acceptance(3) to the tolerances laid down by the Beryllium Advisory Committee of the Atomic Energy Commission Division of Biology and Medicine for use on United States Atomic Energy Commission projects. These tolerances may be summarized as follows:

(i) the atmospheric concentration of beryllium should not exceed 2 $\mu g/m^3$. This refers to the average concentration throughout an eight-hour working day;

(ii) in no circumstances and at no time should the concentration of beryllium in the air exceed 25 $\mu g/m^3$, even though the daily average might be satisfactory;

(iii) in the neighbourhood of plant handling beryllium, the maximum permissible monthly average concentration is 0·01 $\mu g/m^3$.

Monitoring techniques used in industry have involved the removal of beryllium and its compounds from the air by filtration, and subsequent analysis of the filter by chemical,(4–7) nuclear chemical(8) and spectrographic methods.(9–13) Precise and accurate results are obtainable with all these methods and their application is appropriate when no inconvenience is occasioned by a delay in obtaining results. Under carefully controlled conditions of laboratory and workshop hygiene, the monitoring of air for conformity with the limits outlined in (i) and (iii) above can be carried out conveniently by such a filter technique. It is essential, however, to have a continuous monitoring device with as near an instantaneous response as possible, to ensure that the requirements of (ii) are fulfilled.

In an effort to avoid cumbersome and time-consuming methods, Churchill and Gillieson developed a spectrographic method for the direct monitoring of industrial atmospheres.(14) In principle, the method involved passing the air to be sampled through a condensed spark, the emitted light being dispersed in a grating monochromator and photoelectrically recorded. The instrument was calibrated with artificially produced beryllia aerosols. Subsequently, however, it was recognized that the indication of this instrument was only semi-quantitative,(15) since the response was affected by particle size. Furthermore, since no automatic calibration device was built into the instrument, it had to be assumed that once the instrument had been calibrated it would hold its calibration over a long period of time.

The work described below had for its object the development of a fully automatic monitor for the concentration range 1 to 100 $\mu g/m^3$, the sensitivity of which would be unaffected by the chemical and physical form of the beryllium present in the atmosphere.

Preliminary considerations and experiments

A direct spectrographic method for the monitoring of beryllium in the air would of necessity be similar to the Churchill–Gillieson monitor, in that the air to be sampled must be drawn through a suitable spectrographic source, the light beam dispersed with a monochromator and the intensity of the selected beryllium line detected photoelectrically. Apparatus for the last two stages was adequately provided for by conventional equipment, but the main problem lay in the design of a suitable spectrographic source to meet the following requirements:

(i) a reproducible portion (or preferably all) of the particles in the air stream must pass through the zone of excitation;

(ii) the air flow should be sufficient to give a detectable line-to-background ratio, and the velocity of flow must be low enough to permit complete vaporization and excitation of the particles, irrespective of their chemical form or particle size,

(iii) the excitation source should be as near to the air intake as practicable, to eliminate the possibility of fractionation and deposition of particles.

The inefficient excitation of particulate matter in previous monitors appeared to be due to the following factors:

(*a*) the linear velocity of air through the spectrographic source was very high, it being calculated that the time occupied by a particle between the electrodes was about 10 μs;

(*b*) the cross-section of the spark plasma was small compared with sources operating under arc-like conditions;

(*c*) the time constant of the simple condensed spark was such that only about 5% of any one cycle of the mains was occupied by a discharge passing between the electrodes;

(*d*) the possible fractionation and deposition of particles in the hollow sampling probe used to convey the sample into the spark.

The inherent sensitivity to particle size of the Churchill–Gillieson monitor was originally overcome in this laboratory by the temporary expedient of collecting the beryllium oxide contained in the air on a filter pad, and subjecting the pad to simple condensed spark excitation.(10) Subsequently it became necessary to determine beryllium metal and other compounds of beryllium in air, and this method gave low results for beryllium metal, beryllium ammonium fluoride and beryl ore. However, it was found that by using a modification of the triggered intermittent arc devised by Davis and Campbell,(16) quantitative results could be obtained for all the materials mentioned.

Bearing in mind the necessity for retaining the particle to be excited in the zone of excitation for the longest period of time, and for the need for a discharge with a cross-section and time constant approximating to that of arc-like characteristics, a new arc chamber(17) was developed and an intermittent triggered arc was used as spectrographic source.

Arc chamber. A number of arc chambers were designed to have the desired characteristics, the most satisfactory being that shown in Fig. 1 in which air was drawn at 40 l./min through a conical shaped annulus which directed the flow of air into the centre of the arc gap and along the length of the arc column. The relative dimensions of the annulus and the channel containing the electrodes were designed to give a low linear velocity of air through the arc chamber. The fact that particles travelled along the length of the arc plasma ensured that airborne dust remained in the excitation zone for a maximum period (1 ms).

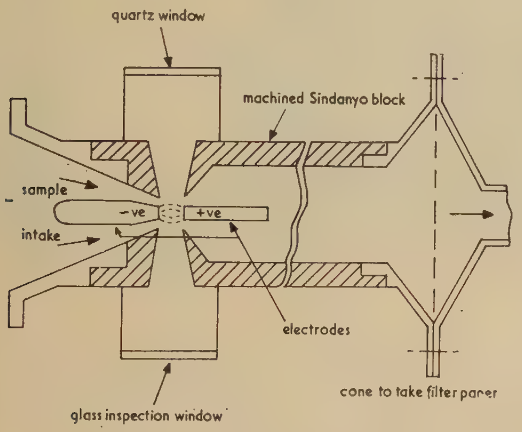

Fig. 1. The arc chamber

Spectrographic source. A triggered 50 c/s discharge operating under arc-like conditions was found to give a suitable source. The cross-section of the arc plasma was broad, and the time constant of the discharge was such that approximately 25% of any one cycle was occupied by a discharge passing between the electrodes. A variety of electrode materials were tried in the analytical gap, including copper, tungsten and platinum. The first two metals oxidized fairly quickly and resulted in instability of the source. This disadvantage did not occur with platinum, and the background associated with this material was considerably less than with copper or tungsten. It was found convenient to use a $\frac{1}{4}$ in. diameter copper rod tipped with platinum as negative electrode and a piece of 14 s.w.g. platinum wire as positive electrode, the air flow through the source being from negative to positive.

Primary calibration. In a quantitative instrument it was necessary that provision should be made for frequent and rapid calibration. Experiments carried out with a simple spark discharge between beryllium copper electrodes showed that beryllium was evolved at a constant rate. The air was first filtered by passage at a constant rate through a commercial filter (methylene blue penetration less than 0·001%) and then through a spark discharge between beryllium–copper electrodes. The resulting aerosol was then piped to the arc chamber and the monitor response noted. The concentration of beryllium in the aerosol was determined by filtering the effluent air from the arc chamber and analysing the filter by an independent method.(9)

Recording system. Before deciding upon the method of recording the photomultiplier response, the errors associated with the sampling of different volumes of air containing a fixed concentration of beryllium, in the form of discrete particles distributed at random, were considered. It appeared likely that the errors would follow the Poisson law and, on the assumption that the air contains spherical particles of beryllium oxide of uniform diameter, Table I gives the volume which must be sampled to ensure that the sampling errors are not greater than 10, 20 and 50% respectively at the tolerance level of 2 μg/m^3.

Table 1. *Volume of air and associated sampling error*

Particle size: diameter (μ)	*Sampling error* (2 σ) ±10% *(litres)*	 ±20% *(litres)*	 ±50% *(litres)*
1	0·3	0·1	—
2	2·5	0·6	0·1
3	8·5	2·1	0·3
4	20	5·0	0·8
5	39	9·8	1·6
10	310	78	12
15	1060	270	42

The fact that an intermittent arc was being used for excitation meant that the effective volume of air sampled would be a fraction of the actual air flow, so that with practicable air velocities of 30 to 50 l./min, and a normal airborne particle distribution of up to 2 μ, an actual sampling time of 10 to 30 s would be required. Thus a method involving integration of the appropriate beryllium radiation was decided upon.

Use of the source conditions given above resulted in the 3130/3131 Å doublet being the most intense lines in the beryllium spectrum. Any conventional monochromator having sufficient dispersion to resolve this doublet from any interfering lines could be used, but clearly, the greater the dispersion the better the line-to-background ratio that could be expected. A two-channel detector system was favoured in view of the low line-to-background ratio likely to be encountered.(18) The exit slit of the monochromator was ruled on an aluminized quartz flat and mounted so that the background adjacent to the line was reflected on to one photomultiplier, the beryllium doublet passing through the slit on to another photomultiplier.

Feasibility trials were carried out on a prototype monitor made from components which were readily available in the laboratory.(19) A diagrammatic representation of the apparatus is shown in Figs. 2 and 3. Details of the arc chamber have been described above, and the unit used for secondary calibration consisted of a Paxolin tube with a pair of beryllium copper alloy electrodes mounted transversely, so that filtered air was drawn laterally across the spark discharge. A shutter controlled the intake of air into the arc chamber and determined whether the air was passed directly into the intake annulus to be monitored, or was drawn through a filter and thence through the calibration source, enabling a determination to be made or a calibration of the instrument to be effected. For the monochromator a folded 3-metre Eagle type mounting, having a reciprocal linear dispersion of 5 Å/mm, was used.

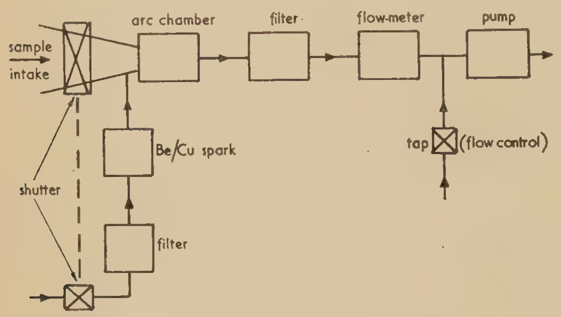

Fig. 2. Diagrammatic layout of prototype monitor

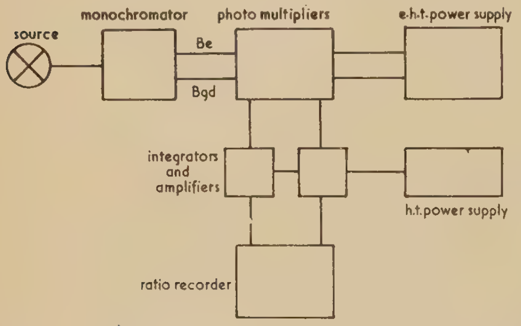

Fig. 3. Schematic diagram of electronic unit for prototype monitor

Quartz-windowed photomultipliers (by E.M.I. Ltd.) were used throughout. A schematic diagram of the electronic units is shown in Fig. 3. Conventional stabilized power supplies were used and the integrator and amplifier circuits have been described elsewhere.(18) The output from these was suitably attenuated and fed into a ratio recorder, in which the ratio of the intensity of the beryllium doublet to the intensity of the adjacent background was recorded by a pen on a moving chart. The whole cycle of operations (initiation of the arc, integration, recording, etc.) in a particular determination was automatically controlled by a synchronous sequence timer, which could be initiated by a single push-button control. For automatic operation a pre set repetitive programme, involving the determination o blank, calibration of the instrument and the evaluation of number of samples was controlled by means of a uniselecto switch.

This instrument was somewhat large (3 ft 6 in. × 2 ft × 6 f high) and cumbersome, but it served to demonstrate that device incorporating the principles outlined above wa capable of giving adequate sensitivity and accuracy.

Final instrument

In view of the encouraging results produced with th prototype instrument, it was decided to design a monito which would be much smaller and more flexible for use i monitoring laboratory and workshop atmospheres, so tha the air in the immediate vicinity of an operator could b sampled without hindrance to his movements. A flexibl sampling probe leading to the monitor was not permissibl because of the possibility of fractionation of the dust at th air velocities used; thus a "sampling head" was designed t incorporate the spectrographic source, the monochromato and detectors, together with the associated component shown in Fig. 2. This was connected to the main consol housing the pump and other heavy units (i.e. the powe supply units, recorder, etc.), by means of flexible hos (10 ft long) which, in addition to providing the suction lin from the pump, carried the necessary electrical connexion (Fig. 4).

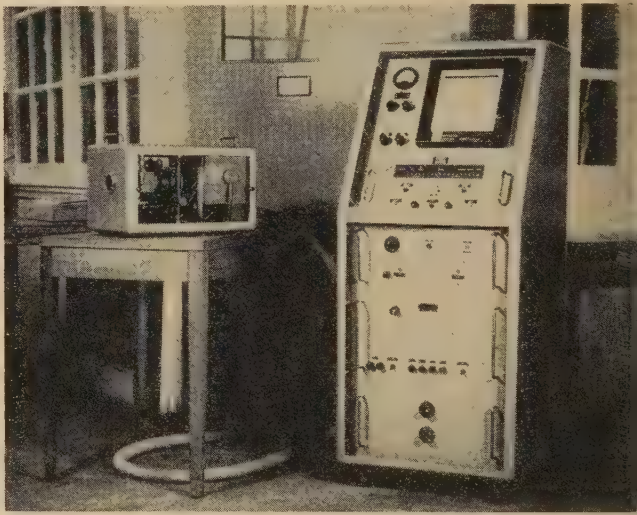

Fig. 4. Photograph of final monitor

The monochromator was a Czerny–Turner type mountin with 27 cm focal length mirrors and a 30 000 lines/in. plan grating. This, used in the third order with an Ilford OX filter at the entrance slit to act as order sorter, gave a recip rocal linear dispersion of approximately 5 Å/mm. The exi slit was set to give approximately a 1 Å band pass. Th complete monochromator with the two photomultiplier was fabricated as a flat box measuring 14 × 6 × 3 in. whic formed the base of the sampling head. Above this wa mounted the arc chamber with its associated component and the trigger unit for the arc source, the whole uni measuring 19 × 10 × 11 in. high. The arc chamber wit the two platinum-tipped electrodes was made as an inter changeable and readily detachable unit, to facilitate servicin of the monitor. In practice, it was found that the electrodes needed changing or adjusting after about eight hours of continuous operation.

As a compromise between the sampling errors involved and the medical requirement that at no time should the concentration exceed 25μg/m^3, a flow rate of 40 l./min. was used and the monitor was set to complete one determination, based on a 20 s sampling time, every minute. The automatic programme was arbitrarily set on a 25 min cycle involving five calibration runs (blanks and standard) and twenty sample determinations.

Performance

Calibration. The device used to calibrate the instrument produces a concentration of beryllium depending upon the spark characteristics of the particular unit. Initially therefore, it was necessary to collect the aerosol on a filter paper and determine the amount of beryllium on the paper by an independent method.(9) Provision was made in the "sampling head" for placing a filter paper immediately after the arc chamber, to collect the aerosol after it had passed through the source. For the particular instrument described in this paper the average amount of beryllium evolved during a sampling period was found to be 0·095 μg ($\pm$0·01 μg) corresponding to a concentration of 7 μg beryllium per m^3. Over a period of three months no drift in the amount of beryllium was noted.

Accuracy and sensitivity. A series of trials was carried out using aerosols of narrow particle size range which had been produced by elutriation(20) of samples of beryllium metal powder and beryllium oxide, the elutriated fractions being sized by microscopy.(21) These artificially produced aerosols were used to establish the potentialities of such an instrument in respect of accuracy and sensitivity, and to study the effect of particle size and chemical form of the beryllium. Finely dispersed samples of beryllium metal and various compounds were produced by passing the air intake of the monitor over the finely divided powders contained in an aspirator. A sample was taken of the air actually passing through the arc chamber during a monitor determination by means of a filter paper, situated behind the arc, and this was subsequently analysed by an independent spectrochemical method,(9) (compare the primary calibration of the instrument). The results obtained by the monitor and by analysis of the filter pad are shown in Tables 2 and 3.

Table 2. *Comparison of results (beryllium metal)*

Particle size (see Fig. 5)	*Concentration of beryllium (μg Be/m^3)* Spectrochemical	Monitor
Fraction 1	116	94
	23	25
(over 40 μ diameter)	11	10
Most of the weight carried	28	26
by particles of 85 μ	54	75
diameter	43	31
	29	38
	12	6
Fraction 6	14	16
	35	33
(All particles less than	71	62
25 μ diameter)	55	43
	1·5	2
	44	43
	31	24
	15	11
	13	12

Table 3. *Comparison of results (beryllium compounds)*
(All results given as μg Be/m^3)

Beryllium hydroxide		*Crushed beryllia crucible (see Fig. 5)*		*Beryllium ammonium fluoride*	
Spectro-chemical	*Monitor*	*Spectro-chemical*	*Monitor*	*Spectro-chemical*	*Monitor*
19	12	14	10	51	37
52	44	62	32	9	16
37	27	19	13	4	5
23	13	2·5	2	56	82
62	46	23	13	51	45
13	9	33	24	11	10
18	14	2·5	2		
		46	27		
		59	36		
		36	26		
		66	37		
		18	14		

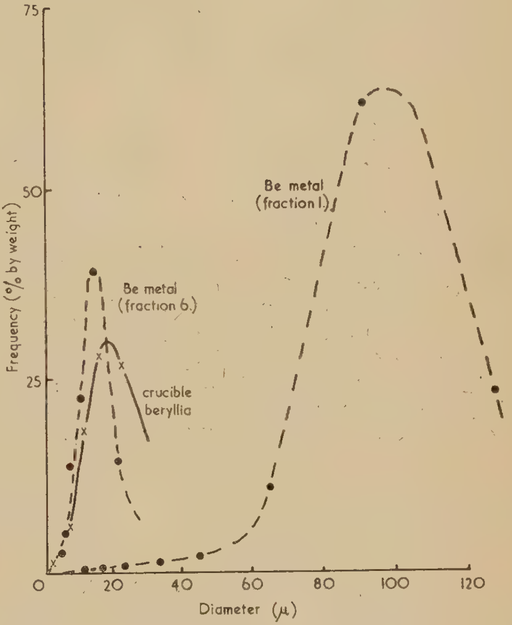

Fig. 5. Size distribution of beryllium metal and crucible beryllia

In the experiments involving "high-fired" crucible beryllia, the particle size distribution of the material reaching the excitation chamber was determined by collecting the deposit on a microscope slide smeared with glycerine and determining the particle size/frequency distribution by microscopy.(21)

The accuracy of the results obtained by the monitor when used to determine different beryllium compounds is summarized in Table 4. In this context the accuracy is quoted as the monitor reading expressed as a percentage of the spectrochemical figure. No correction has been made for the error in the spectrochemical determination (coefficient of variation 8%).

It is interesting to note that the range of accuracy for individual samples is approximately the same for the crucible beryllia and fraction 6 of the beryllium metal, both of which had similar particle size distributions, whilst for the coarser metal fraction a much wider range was recorded, indicating that this uncertainty is associated with the sampling error. The mean figures indicate that there is some bias with the highly refractory compounds, but it is considered that the overall performance of the monitor is adequate for an instrument of this type. The fact that the monitor was calibrated with a fine aerosol produced by a spark between beryllium-copper electrodes, and that the results above are on airborne particles of up to 20 μ diameter (85 μ in the case of metal), indicates its independence of particle size, at least up to these sizes.

Table 4. *Accuracy of the monitor*

Material	*Accuracy (mean %)*	*Range of accuracy (%)*
Beryllium metal (fraction 1)	95	50–140
Beryllium metal (fraction 6)	91	73–109
Beryllium hydroxide	71	57–84
Crushed beryllia crucible	66	53–78
Beryllium ammonium fluoride	130	73–178

In trials over periods of up to eight hours, a slow drift in the readings has been noted on occasions, but as calibration runs are included every 25 min this has little effect on the sensitivity. The variation on sample readings taken in a beryllium-free atmosphere indicates a limit of detection of 1 μg Be/m^3.

Field trials. Field trials using the monitor were carried out by the courtesy and co-operation of ICI Metals Division at Witton, Birmingham. Samples were taken simultaneously by a conventional filter paper device, and the results obtained by spectrochemical analysis of the filters were compared with the results given by the monitor over periods of 10 to 20 min. The results obtained are shown in Table 5, from which it will be noted that the monitor detects significantly high concentrations of beryllium which are of too short a duration to be detected by conventional filter techniques.

It should be noted that the levels of concentration given in Table 5 were encountered near to an item of experimental plant; all personnel in the area were wearing breathing apparatus.

Table 5. *Comparison of results obtained by the automatic monitor and filter samples under factory conditions using beryllium metal*

Monitor		
Individual readings (μg/m^3)	*Mean (μg Be/m^3)*	*Spectrochemical (μg Be/m^3)*
1 2 1 0 0 0 2 1 0 0 0 1 2 2 0 0 1 1 0 0	0·7	0·8
1 0 3 0 0 3 0 0 0 0 0 0 0 0 0 1 3 0 4 21	1·8	2·3
1 0 0 1 0 0 0 0 0 0 1 0 0 42 10 2	3·6	2·0
0 0 0 0 0 0 5 0 4 53 4 2 10 3 2 7 3 0 2 0	4·8	4·2
1 3 2 1 2 3 3 1 3 3 1 2 0 3 8 4 3 3 6 3	2·8	4·2
0 2 5 1 3 2 1 0 0 1	1·5	1·2
0 0 1 0 3 0 3 4 1 3	1·5	1·7
0 0 8 3 3 2 3 1 3 2	2·5	2·3
2 7 2 4 1 3 0 3 1 0	2·3	2·8
3 1 1 9 17 7 4 3 0 0	4·5	3·8

Memory effects and interferences. A memory effect amounting to about 10% of the previous determination has been noted on very high concentrations (100 μg/m^3), but for concentrations approaching tolerance level (25 μg/m^3) the memory effect is negligible. A concentration of 100 to 200 μg Be/m^3 would require three or four determinations before the monitor returned to unbiased readings.

The common elements normally found in atmospheric dust, namely calcium, aluminium, silicon, iron and sodium do not affect the reading of the monitor even when they are present as a visible cloud. Vanadium, titanium and magnesium gave positive readings when present in comparatively high concentrations. Of these magnesium is the most important and a concentration of 1 mg/m^3 gives a reading approximately equivalent to 1 μg Be/m^3. Although there is a direct spectral interference by the mercury line at 3131·5 Å, it is not sensitive enough for mercury vapour at room temperature to cause any interference.

Conclusions

The monitor described has a number of marked advantages over previously described instruments:

(i) the instrument is fully automatic and a result can be recorded in one minute;

(ii) the precision of the instrument is unaffected by ranges of particle sizes likely to be encountered in the atmosphere;

(iii) beryllium metal and its intermediates can be determined.

Acknowledgements

Grateful acknowledgements are made to the following: Mr. F. W. J. Garton for preliminary discussion, Mr. H. L. Youens for considerable help in the constructional work, the Workshop staff of the Chemical Inspectorate, Ministry of Aviation for assistance in making the monochromator, the Electronics Section of the Woolwich Outstation, Chemistry Division, Atomic Energy Research Establishment for providing some of the electronic equipment, and Mr. J. C. Cotterill for spectrochemical analysis.

References

(1) Williams, K. *A.E.R.E. Report MED/MISC/*3 (February 1956).

(2) Hardy, H. L., and Tabershaw, I. R. *Industr. Hyg. Toxicology*, **28**, p. 197 (1956).

(3) Brooks, R. O. R. *Nuclear Pwr*, **3**, p. 112 (1958).

(4) Wolowicz, F. R. Private communication (November 1958).

(5) Trowell, F., Trelease, V., and Hall, D. M. Private communication (1955).

(6) Molyneaux, H. F. Private communication (June 1958).

(7) *Beryllium Symposium at Massachusetts Institute of Technology. A.M.A. Archives of Ind. Health*, **19**, pp. 91–263 (1959).

(8) Gold, R. *Nucleonics*, **15**, p. 114 (1957).

(9) Garton, F. W. J., Webb, M. S. W., and Sayer, J. A. *Chemical Inspectorate, Report C.I./R.*42 (Ministry of Supply, June 1952).

(10) Davis, H. M., Webb, R. J., and Parker, A. *Chemical Inspectorate, Report C.I./R.*82 (Ministry of Supply, October 1953).

(11) Fitzgerald, J. J. *A.M.A. Arch. Industr. Health*, **15**, p. 68 (1957).

(12) Thomason, F. E. Private communication (January 1956).

(13) *U.K.A.E.A. Analytical Method IGO-AM/S.*127. (Springfields: Chemical Services Department, United Kingdom Atomic Energy Authority, 1958).

(14) Churchill, W. L., and Gillieson, A. H. C. P. *Spectrochimica Acta*, **5**, p. 238 (1952).

(15) Gillieson, A. H. C. P. *Atomics*, **1**, p. 15 (1955).

(16) Davis, H. M., and Campbell, J. T. *Atomic Energy Res. Establ.* (*Harwell*) *Rep., AERE. C/R.*2605 (June 1959).

(17) Webb, M. S. W., Webb, R. J., and Wildy, P. C. Brit. Pat. Appl. 11652/59 (March 1960).

(18) Davis, H. M., and Webb, R. J. Brit. Pat. Spec. 772250 (April 1957).

(19) Webb, R. J., Webb, M. S. W., and Wildy, P. C. *Atomic Energy Res. Establ.* (*Harwell*) *Rep.*, AERE-R 2868 (March 1959).

(20) Pryor, E. J., Blyth, H. N., and Eldridge, A. *Recent Developments in Mineral Dressing.* Proceedings of Symposium held at Imperial College, London, 23–25 September, 1952), p. 11 (London: Institute of Mining and Metallurgy).

(21) Fairs, G. L. *J. Roy. Microscopical Soc.*, **71**, pp. 209–222 (1951).

Vibrating reed magnetometer*

by D. C. DOUGHTY, B.Sc., A.M.I.E.E., and P. MOSSMAN, Grad.Inst.P., Research Laboratories of The General Electric Co. Ltd., Wembley, England

[*Paper received* 4 *July*, 1960]

Abstract

This instrument is a development of the pendulum magnetometer for the measurement of saturation magnetization: it has been found especially useful for exploratory work on new materials, since the test samples it requires are small and of simple shape.

The specimen is attached to the end of a flat non-magnetic spring, maintained in continuous vibration in a non-uniform magnetic field: by observing the resonant frequency with and without the field, the magnetization can be calculated by comparison with a reference sample. Accuracies of about 1% *can be obtained on materials with specific magnetizations of* 50 *e.m.u., while the lower limit of usefulness of the instrument is determined primarily by the accuracy required. The device is robust, inexpensive to construct and, in its present form, may be used from room temperature up to* 400° *C.*

Introduction

A KNOWLEDGE of the saturation magnetization per unit mass, or specific magnetization, of a magnetic material, and its variation with temperature, is important for the design of many magnetic devices and the advent of ferrite materials, suitable for use at microwave frequencies, has currently increased the interest in its measurement.

Methods of measurement which can utilize small specimens of simple shape are most useful for exploratory work on new materials, which may be difficult to machine, or which are available only in small quantities. The methods used in the laboratory can be grouped into those requiring measurement of the induced field due to a specimen, or the measurement of the force exerted on the specimen in a non-uniform field; in both cases a polarizing field sufficient to saturate the specimen, must be applied. Such methods are seldom absolute but rely on a comparison with a standard, the properties of which are already known.

In 1926 Weiss and Förrer measured the magnetic properties of nickel over a wide temperature range by an induction method.(1) A small nickel sample was placed symmetrically between the plane pole-pieces of an electromagnet, and was surrounded by a search coil that measured the change of induction when the specimen was suddenly withdrawn from the field. More recently, D. O. Smith and his colleagues(2) have developed a successful vibrating coil magnetometer, in which the dipole field set up by a fixed specimen is converted into an alternating voltage by means of a vibrating pick-up coil. Such an arrangement is convenient in principle, but at first, considerable trouble was experienced with spurious voltages picked up by the vibrating coil; this was found to be due to non-uniformities and lack of constancy in the electromagnet field, and mechanical instability in the drive to the vibrating coil. An improved model has now been briefly reported in which these difficulties are said to have been largely overcome. Foner has avoided some of these design problems, but with some loss of convenience, by making the pick-up coil fixed and causing the specimen to vibrate.(3)

A well-known force method is due to Sucksmith.(4) In its simplest form, the non-uniform field is provided by an electromagnet with pole-pieces specially shaped to provide a region of uniform field gradient, in which the specimen is situated; the instrument is then insensitive to small errors in the centring of the specimen between the pole-pieces. The force is measured as a small displacement of the specimen against the restoring action of the suspension, in a direction at right angles to the axis of the field. The suspension must be carefully designed to permit free movement in the desired direction, but resist any sideways pull towards the pole-pieces.

---

* G.E.C. Communication No. 884.

Rathenau and Snoek have described(5) a simple pendulum magnetometer, in which the specimen moves in simple harmonic motion about a central position between the hemispherical pole-pieces of an electromagnet. The specimen and its carrier are suspended such that they can swing freely under gravity in a given vertical plane, but cannot readily move towards the pole-pieces. The magnetization of the specimen is determined from measurements of the period of oscillation with and without the magnetic field. The authors constructed a magnetometer of this type, which gave good results, but since the average period of a large number of swings had to be taken with a stop-watch, the method tended to be tedious; in addition the apparatus was susceptible to draughts, and was not easily adapted for measurements at other than room temperature. The new magnetometer uses the same basic principle, but the pendulum is replaced by a continuously vibrating metal spring or reed excited by a piezoelectric transducer and oscillator: the amplitude of vibration of the reed is now controlled, and its frequency can be read off directly from the oscillator calibration, with a considerable improvement in speed and convenience.

Design and operation of a modified magnetometer

In the modified magnetometer, the specimen is mounted in a simple holder at the free end of a flat beryllium copper spring or reed, the other end of which is rigidly clamped (Figs. 1 and 2). This reed is mounted horizontally with the specimen and holder in the rest position lying on the common axis of the hemispherical poles of an electromagnet. The broad face of the reed is parallel to this axis; thus the specimen may vibrate freely at right angles to the direction of the field, but is not easily drawn towards the pole-pieces. The spring is maintained in continuous vibration by a piezoelectric transducer employing a barium-titanate type material (G.E.C. vibration strain gauge type SP 1101), which is fixed to the spring close to the support, and which is energized by a variable low-frequency oscillator. A second transducer, mounted on the opposite face of the spring, measures the deflexion, which is a maximum at resonance; the transducer output is measured on a sensitive millivoltmeter. The whole spring assembly with its mounting is located on guide rails, such that it may be withdrawn completely from the magnetic field, as is required during part of the measurement. For temperature variation measurements a small electric oven can be positioned between the pole-pieces, enclosing the specimen. The specimen temperature is measured by a small thermocouple in close contact with it; the thermocouple wires run along the sides of the reed, supported and insulated by fused quartz beads. The screws for the specimen holder are of silicon-copper, as these were found to have no detectable magnetic moment.

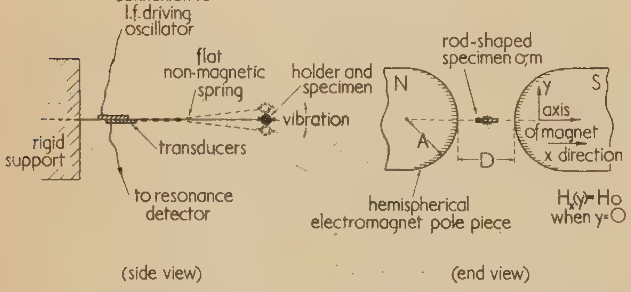

Fig. 1. Diagrammatic view of vibrating reed magnetometer
Electromagnet—Newport Instruments type A; reed—$13 \times 0{\cdot}5 \times 0{\cdot}07$ cm

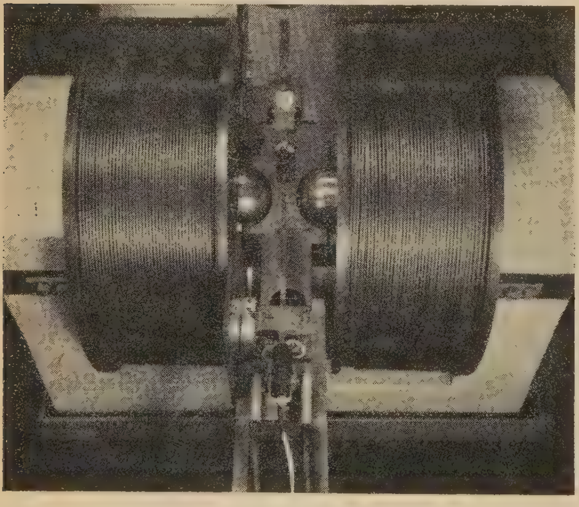

Fig. 2. Layout of magnetometer, showing oven drawn back clear of the specimen

With no field, the resonant frequency of the spring is about 15 c/s, and can increase up to about 30 c/s when the field is applied, depending on the specimen magnetization and mass. The oscillator, on which the accuracy of measurement largely depends, has been calibrated throughout its range against a precision frequency meter; it can be checked, and corrected if necessary, at several fixed points in its range by forming Lissajous figures on an oscilloscope with a 40 c/s sine wave; this is locked in frequency to a crystal-controlled standard, which has an accuracy of one part in 10^7.

Theory of magnetometer

With reference to Fig. 1, let

σ = specific magnetization of specimen
m = mass of specimen
M = effective mass of the reed system, considered as concentrated at the specimen
S = elastic stiffness of the reed
F_H, F_0 = resonant frequencies of the vibrating reed with and without the magnetic field
D = minimum air gap between the pole-pieces
A = radius of curvature of the pole-pieces
$H_x(y)$ = magnetic field in x-direction, at position y of the specimen
H_0 = maximum value of the field, at the axis of the magnet, where $y = 0$.

An exact analysis of the field distribution is difficult, but Rathenau and Snoek have shown experimentally,(5) that near the centre of the air gap, the field $H_x(y)$ may be represented with sufficient accuracy as follows:

$$H_x(y) = H_0(1 - Ky^2), \qquad (1)$$

where K is a term dependent on the geometry of the air gap.

Force exerted on specimen in the y-direction equals

$$m\sigma\{\partial H_x(y)/\partial y\} = m\sigma(-2KH_0y). \qquad (2)$$

This restoring force increases the stiffness of the vibrating system by an amount proportional to the magnetic moment, when the specimen is moved into the magnetic field. This increase is determined by measuring F_0 and F_H.

With no field, the equation of motion of the specimen is

$$(m + M)\ddot{y} + Sy = \text{periodic driving force.} \qquad (3)$$

At resonance,

$$F_0 = \frac{1}{2\pi}\left\{\frac{S}{(m + M)}\right\}^{1/2}. \qquad (4)$$

With the field, the resonant frequency increases to

$$F_H = \frac{1}{2\pi}\left(\frac{S + 2KH_0 \, . \, m\sigma}{m + M}\right)^{1/2} \qquad (5)$$

since the mechanical damping is very small in both cases.

From equations (4) and (5), one obtains

$$\sigma = \frac{2\pi^2}{KH_0}(F_H^2 - F_0^2)\left(1 + \frac{M}{m}\right). \qquad (6)$$

Because the gradient constant KH_0 can never be measured or calculated with sufficient precision in regions where the gradient is large, an absolute calibration is not attempted, nor is it required; as in other force (and some induction) methods, the apparatus is calibrated under the same conditions with a reference sample of pure nickel, the properties of which are known very accurately,$^{(4,5)}$ giving

$$\sigma' = \sigma'' \frac{(F_H'^2 - F_0'^2)\{1 + (M/m')\}}{(F_H''^2 - F_0''^2)\{1 + (M/m'')\}} \qquad (7)$$

where the single and double dashes refer to the specimen and calibrating sample respectively.

Sensitivity and performance

Equation (6) shows that the sensitivity, or change of frequency for a given specimen, depends on the gradient constant KH_0; to gain an insight into the factors affecting this parameter, assume that, as an approximation in the region close to the axis of the magnet, $H_x(y)$ is inversely proportional to the length of the air gap measured parallel to the magnet axis.

Then, if terms higher than y^2 are neglected, it may readily be shown that

$$H_x(y) = H_0\{1 - (y^2/DA)\}. \qquad (8)$$

A series of measurements based on equation (6) using a nickel sample, in which H_0, D and A were varied in turn, indicate that in fact KH_0 is nearer $0{\cdot}8\ H_0/DA$, but the simple analysis* is adequate to show that for the ultimate sensitivity H_0 should be as large as possible, and D and A as small as possible. The air gap D is limited by the length of the specimen, or the width of the oven, if used. For a given air gap, the maximum field H_0 is then set by saturation of the pole-pieces. The radius of curvature A must be large compared with the amplitude of vibration, if the specimen is to remain in a region of linear gradient. An advantage over the simple pendulum magnetometer is that the resonant amplitude of oscillation can be made very small (less than 1 mm in this apparatus), limited only by the sensitivity of the detector. Changes of frequency of as small as 0·025 c/s can readily be observed as a change of detector output, since the mechanical damping of the vibrating reed is very low. (Transient vibrations may be set up when either the vibrational frequency of the reed, or the tuning of the oscillator is suddenly altered, and some practice is needed in setting the oscillator quickly to the position of maximum steady-state amplitude.)

In this magnetometer $D = 1{\cdot}5 - 2{\cdot}5$ cm
$A = 3$ cm
specimen = 0·3 cm diameter, up to 1 cm long
$H_0 = 4$–14 k-oersteds.

The effective mass M of the reed (which includes the specimen holder) is determined in an initial experiment by loading the specimen holder with a series of known masses, and measuring the resonant frequencies. A value of 2·15 g ± 1% has been obtained by a linear extrapolation from the graph of $1/F_0^2$ against the added mass m (Fig. 3). The error in M always tends to cancel, since the term appears in both numerator and denominator of equation (7). For example, if $m' = 332{\cdot}5$ mg, $m'' = 259{\cdot}6$ mg, a 1% error in M introduces an error of only 0·02% in σ'. Any error may be made to cancel completely by making $m' = m''$, but this may be undesirable if the volumes of specimen and reference sample differ appreciably. It is more important that the two should be of the same size and shape, so that the field distribution over the volume of each shall be the same. When two rods of nickel, 0·3 cm diameter and initially both 1 cm long, were compared, a reduction of 5% in the length of one caused a discrepancy of 0·1% in the magnetization of one measured relative to the other: small changes of diameter had negligible effect.

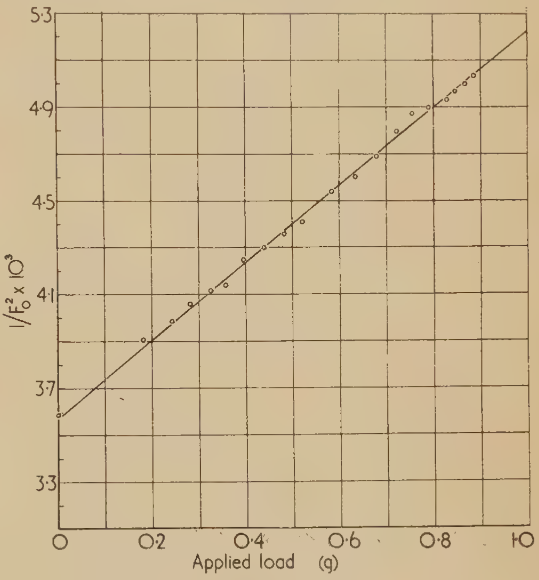

Fig. 3. Graphical determination of effective mass of reed

By sliding the reed assembly up to a locating mark on the horizontal guide rails, the long axis of the specimen can be made coincident with the axis of the magnet; a high degree of precision is, in fact, not necessary, as the region of linear field gradient extends over a region of at least 2 mm about the true centre, and small differences of position between sample and specimen, in either horizontal or vertical plane, are unimportant. (The small differences in the vertical plane are such as might be caused by differences in mass and specific magnetization.) When the specimen was displaced to one side of the holder, there was no change of F_H, for displacements up to 1 mm, in a specimen 1 cm long. Since it may be positioned well within this limit, no inaccuracy due to centring errors should be introduced. Provided that reasonable care is taken, the reed assembly may be drawn back clear of the pole-pieces, the specimen removed from the holder and the procedure repeated in reverse, without causing any measurable change in the original frequency setting.

---

* An alternative, but less simple, approach assumes that the lines of flux intersect the surfaces of the unsaturated pole-pieces normally, and follow paths which are the arcs of large circles: the agreement with the experimental results is then very good.

No change of frequency with amplitude of vibration was observed, up to the maximum amplitude of 1 mm: a change would be expected if higher order terms in equation (1) were significant. No error is thought to be introduced by the comparison of a reference standard of a solid metal with magnetic materials of high resistivity,$^{(6)}$ since no detectable change of resonant frequency or amplitude of vibration was seen with a pure copper specimen in the holder, when the field was applied.

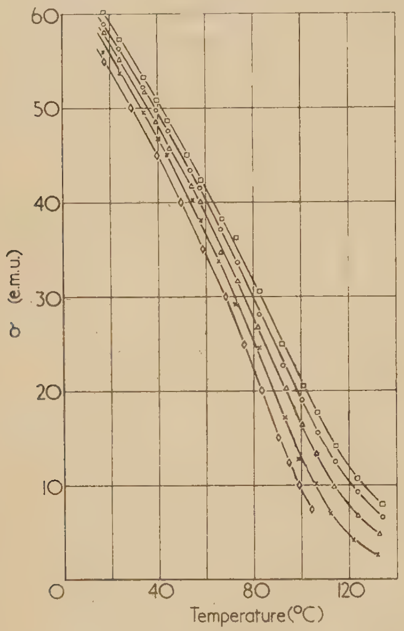

Fig. 4. Variation of specific magnetization with temperature for an experimental ferrite material. (The curve of spontaneous magnetization *versus* temperature was obtained by extrapolation to zero field)

□ = H_0, 13 500 oersteds
○ = H_0, 11 000 oersteds
△ = H_0, 8 000 oersteds
× = H_0, 5 000 oersteds
◇ = spontaneous magnetization

As an example, the magnetization of an experimenta ferrite material is plotted in Fig. 4 as a function of temperature and over a range of fields. From these results the spontaneous magnetization of the specimen has been obtained, by an extrapolation back to zero internal field.

At the lower field values, the change of frequency of the reed is smaller because the field gradient is also reduced, and errors in σ' tend to increase; due to the form of equation (6), the errors will not increase by an amount proportional to the decrease in field. Estimates are made in the accompanying table of possible errors in the magnetization of this ferrite material at fields of 13 500 and 5 000 oersteds, at a fixed temperature of 17·5° C.

Assessment of results

Specific magnetization of calibrating sample, 54·54 e.m.u. ± 0·25%
Mass of calibrating sample, 259·6 ± 0·05 mg
Mass of ferrite specimen, 332·5 ± 0·05 mg
Error introduced by uncertainties in the value of the effectiv mass of the reed, ± 0·02%
Temperature, 17·5 ± 0·5° C

	Calibrating sample	*Specimen*	*H_0 (oersteds)*
F_0 (c/s)	15·85	15·70	
$F_H - F_0$ (c/s)	10·50 ± 0·05	13·50 ± 0·05	13 500
σ(e.m.u.)		**60·0 ± 1·2%**	
F_0 (c/s)	15·85	15·70	
$F_H - F_0$ (c/s)	4·45 ± 0·05	5·55 ± 0·05	5 000
σ(e.m.u.)		**56·0 ± 2·3%**	

Acknowledgement

The advice of Dr. A. Bloch in the preparation of this paper is acknowledged.

References

(1) Weiss, P., and Forrer, R. *Ann. Phys.* (Paris), **15**, p. 153 (1926).
(See also Vigoreux and Webb. *Electrical and Magnetic Measurements*, p. 376 (London and Glasgow: Blackie and Son, 1946).
(2) Smith, D. O. *Rev. Sci. Instrum.*, **27**, p. 261 (1956).
(3) Foner, S. *Rev. Sci. Instrum.*, **27**, p. 548 (1956).
(4) Sucksmith, W. *Proc. Roy. Soc. A*, **170**, p. 551 (1939).
(5) Rathenau, G., and Snoek, J. *Philips Res. Rep.*, **1**, p. 239 (1945/6).
(6) Foner, S. *Rev. Sci. Instrum.*, **30**, p. 569 (1959).

Geiger counter backgrounds

by B. L. COHEN, D.Sc., Oak Ridge National Laboratory, Oak Ridge, Tennessee, and University of Pittsburgh, Pittsburgh, Pennsylvania

[*Paper first received* 5 *May, and in final form* 22 *July*, 1960]

Abstract

An extensive study of counting backgrounds in ten essentially identical Geiger counters is reported. Important long-term time variations were found; their rate is generally less than ½% per day, they change direction frequently and their total magnitude averages about 6%. They could not be correlated with counter efficiency, and were not, in general, correlated among the different counters. Consecutive day differences were generally less than 1%, although about 20% of the time there were non-statistical variations in the same direction in all counters, averaging 2·3% in magnitude. No day-night variations were detected within an accuracy of one part in 300. Temperature effects were found to be extremely important. An experience with an area-wide air contamination is discussed.

1. Introduction and experimental methods

In measurements of radioactivity with Geiger counters, the subtraction of background is frequently an important correction. However, it is generally not clear how often and with what accuracy this background should be measured, how constant it is with time and what factors are important in keeping it as constant as possible. It is the purpose of this paper to record the results of an extensive experimental study of these matters.

As part of an experiment requiring low-level counting,(1) ten Tracerlab type TGC-2 end-window Geiger counters were operated under essentially identical conditions. In general, samples were counted during the night and background was recorded for five hours during the day, thus giving measurements of the latter with about 1·2% statistical accuracy. The temperature of the room was regulated by an ordinary commercial air conditioner; the room was in constant use as an office and electronics maintenance area by several people, although some care was taken to assure that no intensely radioactive sources were brought in. The samples to be counted were mounted in 1 in. diameter watch glasses and covered with cellophane tape; they had relatively short half lives (17 h, 9 h) and their total counting rates (1/8 in. from the counter window) were never more than 30% of counter background, so that counter contamination from these samples was not a problem.

The counters were housed in standard types of aluminium-lined lead shields; there was no important source of radioactivity nearby, but there were several reactors operating a few miles away—a situation which is becoming not untypical of many areas. The scalars with built-in high voltage supplies were typical commercial types; on every 512th count, they fed a pulse to an Esterline–Angus twenty-pen recorder; this caused the pen for that scalar to draw a pip on the chart which moved uniformly with time. The data were then obtained by counting the number of pips per five-hour interval on the chart with suitable corrections at the end points. Every 64th count from most scalars was also recorded and used for checking. This method of recording assures simple detection of instrumental difficulties or important changes in experimental conditions.

Counter voltage plateaux were measured at about ninety-day intervals; in one case a voltage change was deemed necessary. Counter efficiencies were measured at frequent intervals (see Section 3) by counting cross-calibrated 32P samples in a well-defined geometry; it was assumed that the average efficiency of the ten counters was constant.

2. Variations of background with time

The variations of background with time will be considered under two categories, the long-term variations, which are defined as variations extending over several days, and the short-term variations, consisting of changes over periods comparable with or less than one day.

(*a*) *Long-term variations.* The background count-rate measurements are shown in Fig. 1 plotted as a function of time between November 1955 and June 1956. From June 1956 until June 1957, the scalars and power supplies were turned off; at the end of this period, they were turned on again and measurements were made over a sixty-hour period; these latter measurements are shown by the black squares on the right margin of the figure. The statistical accuracy of the points on the figure is exhibited by the dashed curves associated with the data from counter No. 1; they are three standard deviations above and below the smooth curve through the data.

It is clear from Fig. 1 that long-term variations are present in the data. The smooth curves through the data represent an attempt to fit it with curves having a maximum slope of ½% per day; the fact that these curves follow the data within statistical accuracy indicates that these long-term variations are seldom more than ½% per day; in general, they are very much less.

The difference between the highest and lowest points on the smooth curve are shown for the various counters in Table 1. This variation averages about 6%; one may thus conclude that in experiments where background need be known only to within about 6%, only a very few sporadic measurements are necessary.

The relatively small differences between the detailed data and the "one year later" data of Fig. 1 indicates that there are probably no important long-term time variations extending over periods comparable with a year; if there are such variations, there is some evidence that the trend is toward lower backgrounds.

Some of the long-term variations in Fig. 1 show similarities among the various counters. For example, from 24 February to 15 March, nine of the ten curves are falling; from 25 March to 4 April, nine of the ten curves are rising; and from 4 May to 14 May, nine of the ten curves are falling. These effects may possibly be explained as an increase in air contamination or as a temperature effect. However, the majority of the long-term variations show no correlations among the various counters; their source is difficult to surmise. They do not seem to be due to any factors that change the counting efficiency (see Section 2), so that they must be due to characteristics peculiar to each individual counter.

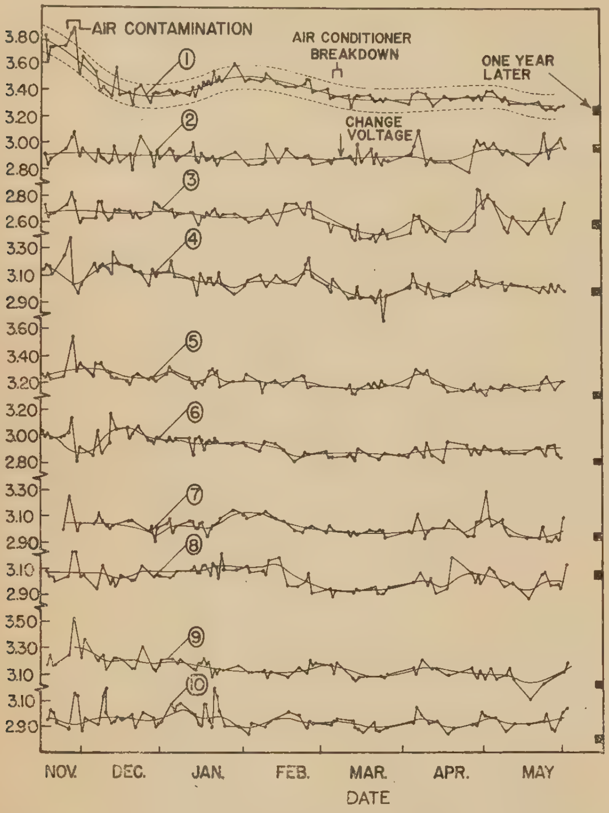

Fig. 1. Counting backgrounds in each counter as a function of time. Smooth solid curves through the data represent an attempt to show the long-term time variations. The dashed curves are three standard deviations in counting statistics above and below the smooth curves

Table 1. *Variations in counting background in the various counters*

Counter No.	*Maximum variation in 200 days (%)*	*Counter-efficiency variation (%)*	*Variation in air conditioner shut-down test (%)*
1	6	4	3
2	3	5	6
3	10	6	45
4	7	5	55
5	6	4	7
6	7	5	11
7	5	5	9
8	6	3	17
9	7	6	15
10	3	3	22
Average	6%	4·6%	

(*b*) *Short-term variations.* One possible short-term variation that could be troublesome is a day *versus* night difference. This was studied on several occasions and no difference was found; in the most complete single test, the difference was found to be zero with a statistical accuracy of one part in 300. This is in agreement with the fact that day-night variations in cosmic-ray intensity are only a few tenths per cent.⁽²⁾ This experimental result justifies the technique of counting samples during the day and background at night, or vice versa.

The other short-term variation studied was the difference between background counts on consecutive days. This was determined for thirty-three pairs of consecutive days (with no one day taken as part of two pairs). For six of these thirty-three pairs, the variations in nine of the ten counters were in the same direction, and at least three of the ten counters showed variations greater than two standard deviations in the counting statistics. The probability of one such case occurring is about one in ten thousand, so that these cases are clearly non-statistical; they are evidently due to air contamination, a room temperature fluctuation, or perhaps cosmic-ray intensity variations. The average consecutive day deviation for these cases was 2·3%.

For the remaining twenty-seven pairs of consecutive days, the distribution of deviations is shown by the points in Fig. 2. The curve in Fig. 2 is the expected distribution due to counting statistics only. The excellent agreement between the experimental points and the curve indicates that the observed deviations can be explained by counting statistics only. If a systematic effect is present, it is less than 1%.

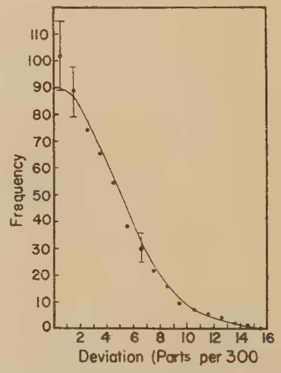

Fig. 2. Difference between background counts on consecutive days. Points are from data, and curve shows distribution expected from counting statistics. Six of the thirty-three sets of consecutive-day data were excluded for reasons described in the text

The results of the consecutive-day studies are, then, that 80% of the time there were no short-term deviations as large as 1%; for the remaining 20% of the cases, a systematic deviation was found, the average deviation for these cases being 2·3%. Of the 300 consecutive-day deviations studied, the largest was 5%, and only five were more than 4%. It thus seems reasonable to conclude that short-term variations may be neglected if accuracy not better than about 2% is required.

3. Counter efficiencies

The counter efficiency corrections are shown in Table 2, and the maximum deviations are shown in Table 1. The counting statistics were about 1% for three standard deviations, but other sources of error, as in positioning and cross calibration of samples, could explain occasional variations as large as 1 or perhaps 2%. The evidence for counter-

Table 2. *Percentage counter efficiency corrections*

Counter number

Date	1	2	3	4	5	6	7	8	9	10
17.11.55	+ 6	+1	−1	0	+2	+4		+3	−5	+2
18.11	+ 6	+2	−1	0	+3	+5		+3	−5	+3
21.11	+ 6	+2	−1	0	+3	+5		+3	−5	+3
23.11	+ 7	0	−3	−1	+2	+5		—	−3	+2
25.11	+ 7	+2	−2	−1	+2	+4	0	+3	−5	+2
26.11	+ 7	+1	−2	−1	+2	+3	0	+3	−5	+3
29.11	+ 6	0	−2	0	+1	+3	0	+3	−4	+3
2.12	+ 7	+1	−1	−1	+2	+2	0	+3	−5	+3
6.12	+ 6	—	−1	−1	+2	+2	0	+3	−5	+3
10.12	+ 7	+1	−1	−1	+3	+3	+1	+3	−5	+3
14.12	+ 7	+1	−1	−1	+3	+2	0	+4	−5	+3
16.12	+ 7	+1	−1	−1	+3	+3	0	+4	−5	+3
22.12	+ 7	0	0	−1	+3	+3	0	+4	−5	+4
10.1.56	+ 8	+1	−2	−2	+4	+3	+1	+2	−6	+2
7.2	+ 9	−1	−1	−3	+5	+4	−1	+2	−5	+3
15.2	+10	−1	−1	−3	+5	+4	−2	+2	−5	+3
21.2	+10	−1	−2	−3	+5	+3	−3	+3	−6	+3
9.3	+ 8	+1	−3	−3	+2	+6	−3	+2	−6	+2
13.3	+10	+3	−6	−2	+3	+7	−1	—	−6	+1
25.3	+10	+2	−4	−3	+3	+6	−2	+2	−9	+2
3.4	+10	+2	−5	−4	+4	+7	−1	+2	−8	+1
10.4	+10	+4	−5	−5	+3	+4	−4	+3	−9	0
25.4	+10	+3	−3	−5	+2	+4	−3	+5	−9	0

efficiency variations from Table 2 is clear; they are generally long-term and tend to be monotonic. Attempts to explain the principal features of the long-term background variation (Fig. 1) by variations in counter efficiency met with no success; there seems to be surprisingly little correlation between the two effects.

4. Temperature and miscellaneous effects

During the running of the experiment, the air conditioner broke down at one point, and it was noticed that counter backgrounds rose markedly. Within a day or two after the air conditioner was repaired, backgrounds returned to their normal values as can be seen in Fig. 1. (Data taken *during* the breakdown is not shown in Fig. 1.)

In order to study the effect in more detail, a prearranged test was made during which the air conditioner was shut off for a fifty-hour period. The room temperature rose very rapidly (within about two hours) by about 15° F and, after the air conditioner was turned on again, the temperature returned almost equally rapidly to its original value. The backgrounds in the various counters during this period are shown in Fig. 3, and the maximum percentage by which they increased is given in Table 1. It is immediately obvious from these that temperature effects are very important, and that they are, approximately at least, reversible. An explanation for temperature effects is given by Korff.⁽³⁾ The fact that the effects come in relatively slowly may be explained by the fact that local temperatures inside the counters (which are, in turn, inside lead shields) change less rapidly than room temperature. It may clearly be concluded that air conditioning with close temperature control is an absolute necessity for low-level Geiger counting.

Two miscellaneous effects observed during these studies seem worth mentioning:

(i) the first few days after a Geiger counter is installed, both the background and the efficiency seem to vary erratically. These effects disappear after two to five days;

(ii) A sharp rise by about 8% in background of all counters on 27–28 November may be noted from Fig. 1. During this period, a routine air sample monitor ten miles away recorded three times its normal count rate.

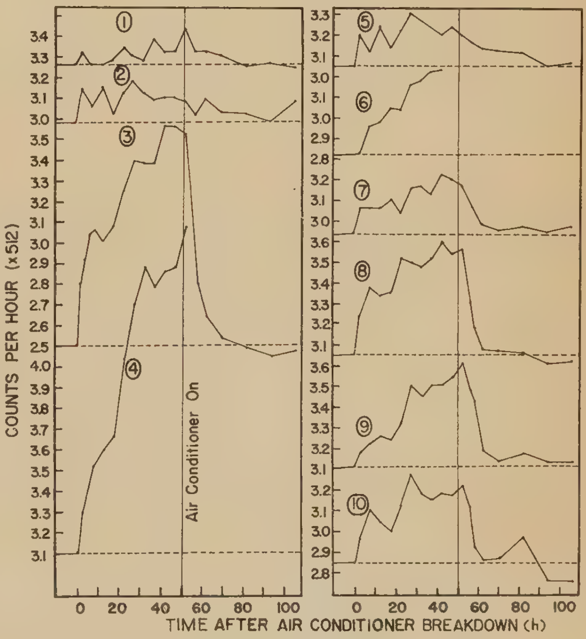

Fig. 3. Background count rate in each counter as a function of time during the air conditioner shut-down test described in the text

The effect is presumably due to air contamination from a bomb test or a reactor exhaust mishap. Thus, if no knowledge of such occurrences is available, the possibility of a sudden 10% change in background must be reckoned with. Such occurrences are presumably sufficiently infrequent that if an experiment is repeated at frequent intervals, no important error would result. In the experiment reported in Ref. (1), data taken during this period had to be discarded.

Acknowledgements

The author would like to acknowledge the assistance of C. B. Fulmer and E. L. Olson in some of these experiments.

Portions of this work were supported by the Atomic Energy Commission, the National Science Foundation and the Office of Naval Research.

References

(1) COHEN, B. L., COHEN, A. F., and COLEY, C. D. *Phys. Rev.*, **104**, p. 1046 (1956).

(2) MONTGOMERY, D. J. X. *Cosmic Ray Physics* (Princeton: University Press, 1948).

(3) KORFF, S. A. *Electron and Nuclear Counters* (New York: D. Van Nostrand Co. Inc., 1946).

Temperature-control system for use with a spectrophotometer

by S. W. THORNE, B.Sc., A.Inst.P., Division of Plant Industry, C.S.I.R.O., Canberra, A.C.T.

[*Paper first received* 29 *July, and in final form* 21 *September*, 1960]

Abstract

A scheme is outlined for the accurate control of the temperature of a standard 5 cm cuvette and contents. Any temperature over, for example, a range of 30–80° C may be selected to an accuracy of ±0·1° C with a subsequent control variation of the order of ±0·05° C. A check-point and interpolation method is described to achieve this selection accuracy. An electromagnetic method designed to provide remote stirring is indicated.

Temperature-control system

A BEAD thermistor (S.T. & C. Ltd., type F15, glass mounted) is used as the sensing element and is included in a bridge circuit. The thermistor follows to a first approximation the law given by

$$\log_{10}R_1 - \log_{10}R_2 \doteq B\{(1/T_1) - (1/T_2)\} \log_{10}e$$

where R_1 is the resistance at temperature T_1 °K and R_2 at T_2 °K, and B is a constant characteristic of the material. Accurate selection of temperature control points over a wide range of temperature is rendered difficult by this temperature-resistance characteristic. The control system evolved utilizes accurate check control points every few degrees. However, interpolation between these accurate check points is carried out on the assumption of a linear régime. Clearly, the closer the check points are located, the more closely the interpolating linear régimes approach the true logarithmic curve. Consider a thermistor of resistance R_1 at a temperature T_1 and R_2 at a temperature T_2. At a temperature T_3, the resistance R_3 will be

$$\log_{10}R_3 = \log_{10}R_1 - B\{(1/T_1) - (1/T_3)\} \log_{10}e.$$

Let the temperatures T_1 and T_3 be accurate check points. Then, under an interpolating linear regime, T_2 would equal $\frac{1}{2}(T_1 + T_3)$, and the mean value of resistance R_m corresponding to this would be $\frac{1}{2}(R_1 + R_3)$. If we now compare the value R_m with R_2 and interpret as a resistance error ΔR, we may calculate the order of magnitude of the error in temperature involved. The temperature coefficient of resistance of a thermistor is given by

$$\frac{1}{R}\frac{dR}{dT} = -\frac{B}{T^2}$$

and, in terms of finite differences to a first approximation

$$\Delta T = -\frac{\Delta R}{R}\frac{T^2}{B} \text{ for } \Delta T \ll T.$$

Calculation then shows that if check points are made every 5° C, the maximum error existing between the logarithmic and linear régimes is less than 0·1° C. If check points are made every 2·5° C, the error is 0·025° C and if made every 1° C the error is 0·004° C. The system described to cover the range 30–80° uses check points every 5° C but, by a system of scale correction, this is rendered equivalent to every 2·5° C so that the error involved in interpolation is considerably less than 0·1° C. The system is thus devised to yield any selected control temperature over the range 30–80° C with an accuracy of 0·1° C without further cumbersome calibration against a standard thermometer and with the size advantage of a bead thermistor as the micro-sensing head.

The circuit diagram of the temperature control system is shown in the figure. A 50 c/s signal voltage is applied to the bridge circuit, the thermistor R_z being located in one arm. The out-of-balance signal is amplified in a simple *RC* coupled amplifier V_1 and V_2. V_3 is a phase-sensitive valve supplied with an a.c. potential to the anode through relay *RL*. The heavy-duty contacts of this relay are used to supply current to the nichrome heater of the sample cuvette. Accurately calibrated control points are provided every 5° C from 30–80° C by means of a selection switch in one arm of the bridge circuit. Before calibration, the thermistor should be artificially aged for several hundred hours at 100° C to minimize aging effects. Calibration of these points is carried out against a standard thermometer to an accuracy of better

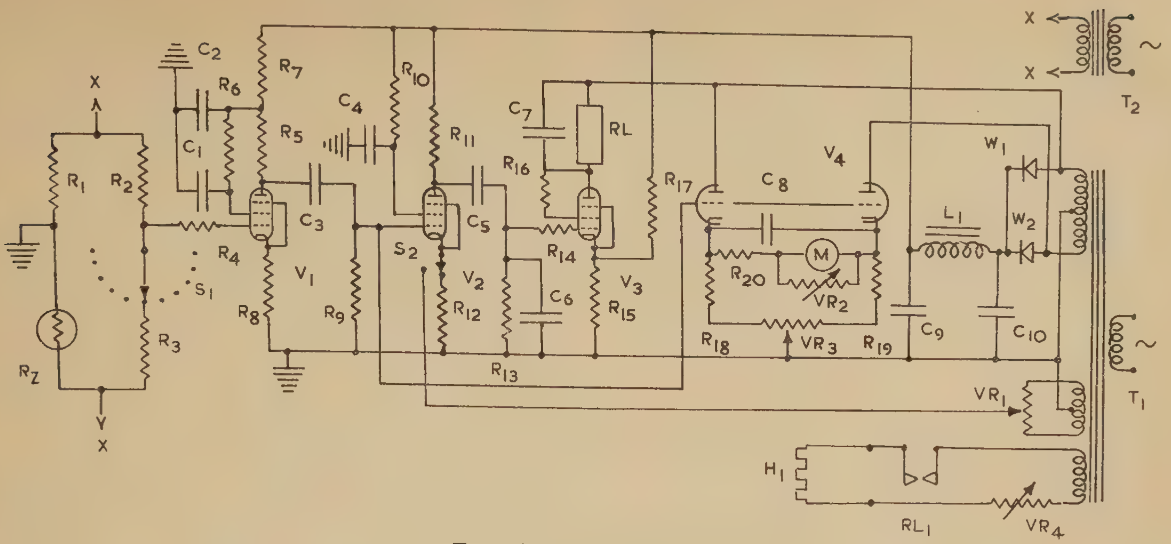

Temperature-control system

C_1 = 8μF, 350 V
C_2 = 8μF, 350 V
C_3 = 0·05 μF
C_4 = 8 μF, 350 V
C_5 = 0·05 μF
C_6 = 0·005 μF
C_7 = 8 μF, 350 V
C_8 = 4 μF, 350 V paper
C_9 = 16 μF, 350 V
C_{10} = 8 μF, 450 V

L_1 = 14 H

M = Meter, 25–0–25 μA

R_1 = 100 kΩ, h.s.
R_2 = 47 kΩ, h.s.
R_3 = Selected values
R_4 = 1 kΩ, h.s.
R_5 = 100 kΩ, h.s.
R_6 = 220 kΩ, h.s.
R_7 = 47 kΩ, h.s.
R_8 = 1 kΩ, h.s.
R_9 = 330 kΩ, h.s.
R_{10} = 220 kΩ, h.s.
R_{11} = 100 kΩ, h.s.
R_{12} = 1 kΩ, h.s.
R_{13} = 330 kΩ, h.s.
R_{14} = 1 kΩ, h.s.
R_{15} = 1 kΩ, h.s.

R_{16} = 1 kΩ, h.s.
R_{17} = 100 kΩ, h.s.
R_{18} = 10 kΩ, h.s.
R_{19} = 10 kΩ, h.s.
R_{20} = 3·3 kΩ, h.s.

R_L = Relay, type 3000
R_Z = Thermistor S.T. & C., type F15, 100 kΩ Thermistor

S_1 = Wafer switch, 1D, 11P
S_2 = Toggle switch

T_1 = Transformer, 230/150–0–150/12.6/6.3
T_2 = Transformer, 230/6·3

V_1 = Pentode, type 6AM6
V_2 = Pentode, type 6AM6
V_3 = Pentode, type 6AM6
V_4 = Double triode, type 12AT7

VR_1 = 5 kΩ linear potentiometer
VR_2 = 2·5 kΩ linear potentiometer
VR_3 = 1 kΩ linear potentiometer
VR_4 = 5 Ω, 25 W, potentiometer

W_1 = Rectifier, Mullard, type OA211
W_2 = Rectifier, Mullard, type OA211

H_1 = Heater, 2 Ω

than ±0·1° C. The gain of the amplifier is such that the relay on-off differential is considerably less than ±0·05° C. Hence operation of the relay is taken as indication of the bridge-circuit balance point.

An out-of-balance signal from V_1 is also fed to both grids of V_4, a double triode, the anodes of which are fed with anti-phased a.c. potentials. The phase and magnitude of this grid signal are displayed effectively on a centre-zero micro-ammeter operating between the cathodes of V_4. In practice a 25–0–25 μA is used and adjustment of the balance control potentiameter VR_3 ensures that the calibrated control-temperature points occur exactly at the balance of this meter. The meter range control VR_2 is adjusted until the 25–0–25 μA movement corresponds to 2·5–0–2·5° C. This may be accurately checked by adjusting until −2·5° C on one control-temperature calibration point corresponds to +2·5°C when the control point immediately lower in temperature is switched in. In practice, the potentiometer VR_2 may be replaced by a stepped resistor operated by a second deck on the temperature control-point selector switch S_1, but for simplicity this has not been shown.

As each control point is selected the meter reading is automatically corrected to read 2·5–0–2·5° C with accuracy to ±0·1° C. Accurate temperature control at intermediate temperatures is obtained by switching VR_1 into circuit by S_2. This control is adjusted until the heater indicator light is just operative when the temperature on the display scale 2·5–0–2·5° C takes up the desired intermediate temperature. It is necessary to ensure that the voltages at the cathode and grid of V_2 are phased in an optimum manner. This is best checked on an oscilloscope, and phasing variation may be carried out by inserting a capacitor in the circuit with VR_1. In any event, operation of the switch S_2 to the interpolation condition should in no way react on the reading indicated by the meter M in the cathode circuit of V_4. The system thus provides an accurate but flexible means of temperature control and may be duplicated so that temperature control may be extended to both the reference and sample-holding cuvettes to facilitate differential temperature studies. The control relay contact RL_1 is used to supply current to the nichrome heater. In view of the wide temperature range, it is necessary to use a variable rheostat VR_4 in series to ensure that the optimum heat-supply level is established for each working temperature. At the same time, this control facilitates rapid temperature changes.

Holder and stirrer

It would be most efficient if the heater unit is placed in direct contact with the liquid. However, practical considerations preclude this. In the first instance, the light path may occupy the full width of the cuvette. Secondly, it is essential for chemical reasons to keep all metals out of contact with the liquid, and thirdly, other types of electrical measurements within the liquid, such as *pH* or redox potentials, were envisaged. The heater then is placed externally to the cuvette, but in as close contact to it as possible. The cuvette is pushed home to a cap of neoprene; this is necessary to avoid loss of liquid by evaporation, particularly at higher temperatures. The thermistor is pushed down into the top of the liquid through this cap. The cuvette is held on both sides by 0·010 in. beryllium-copper sheet. Nichrome heater wires are insulated from this by 0·005 in. sheet mica. The top cover plate is thermally insulated from the beryllium-copper sheath and the thermal capacity of the holder and heater is kept to a practical minimum. Finally, in order to achieve an accurate temperature control, it is essential to have efficient stirring of the liquid. Stirring was carried out by means of a vibrating reed placed in the bottom of the cuvette, the motion taking place in the lower 3/16 in. layer of liquid, clear of the optical path. The stirrer consisted of a polythene-coated strip of silicon–iron $2 \times 0{\cdot}25 \times 0{\cdot}015$ in. with a bend approximately one-third of the way along its length. Externally to the cuvette and immediately below it, an iron-cored coil is subjected to four impulses per second from a power supply. The short section of the silicon-iron strip acts as the armature to this coil and is attracted down four times per second, the greater weight of the long section of this strip ensuring a fall back subsequent to each attractive impulse applied. Careful positioning of the cuvette then allows efficient stirring to be obtained. The impulses are provided by a 1 rev/s electric motor which drives a cam in such a way that a light microswitch M is operated four times per second to apply current from the power source to the iron cored coil. The current level must be adjusted to give a substantial magnetic pull on the stirrer without causing excessive heat dissipation in the coil.

Comments

The system has been used for a period of some six months for the investigation of chemical and biochemical reaction rates with respect to temperature and time, and has given satisfactory performance.

Viscometers having damped torsional oscillation

by B. S. ASHWIN, B.Sc., B.E.(Chem.), T. HAGYARD, B.Sc., Ph.D., I. C. B. SAUNDERS, B.Sc., B.E.(Chem.), and T. E. YOUNG, B.Sc., B.E.(Chem.), Department of Chemical Engineering, University of Canterbury, Christchurch, New Zealand

[*Paper first received* 15 *February, and in final form* 15 *March*, 1960]

Abstract

Two types of torsional pendulum viscometers, having only one solid-fluid boundary, have been developed specifically for use in fluidized solids investigations. They may have utility also in coarse or fibrous suspensions or in melts at high temperatures. The theory of these viscometers is discussed and empirical correlations are presented whereby any instrument of these two types may be used with minimal or no calibration.

List of symbols

D = diameter of working bob (cm)
I = moment of inertia of assembly (g. cm^2)
k, k_1, k_2 = amplitude logarithmic decay constant (s^{-1})
k' = amplitude logarithmic decay constant per cm of cylindrical bob length (s^{-1}cm^{-1})
n = frequency of oscillation (s^{-1})
Re = group D^2n/ν
Z = second polar moment of the surface area of the bob = $\Sigma r^2 dA$ (cm^4)
α, β = exponents
μ = viscosity (g.cm^{-1} s^{-1})
ν = kinematic viscosity (cm^2 s^{-1})
ρ = density (g cm^{-3})

Introduction

SOLIDS in the state of dense-phase fluidization behave in many respects like liquids: they have a well-defined upper surface, appear to flow under near zero stress and appear to exert hydrostatic pressure. Investigation of their fluid properties has hitherto been hindered by lack of viscometers suited to the peculiar circumstances of a fluidized bed. An ordinary viscometer can have quite small clearances, as in the capillary flow and the concentric cylinder type, since the ultimate particles of the fluid are negligibly small compared with the clearance. Fluidized suspensions, on the other hand, have particles generally ranging from 50 to 400 μ and consequently clearances in viscometers of the order of millimetres would be quite unsuitable. Ordinary viscometers may operate at high liquid velocities and high rates of shear without seriously affecting the properties of the fluid, but in fluidized beds the state of fluidization is maintained by upward flow of the gas or liquid medium relative to the solid particles, and this relative velocity is, for cases of gas fluidization, as low as 3 cm/s. It is evident that in such systems the velocity of the fluid and the rate of shear must be kept very low so as to avoid affecting the state of fluidization.

Matheson, Herbst and Holt(1) used a rotating paddle to explore the fluid properties of fluidized systems, but they did not claim that viscosity was the only property measured and the apparatus could not be used to test if the fluized system could even be said to possess such a property. Subsequently, Long(2) used a Brookfield viscometer in which cylindrical bobs were axially rotated in relatively large containers with a gap of about 3 cm between container and bobs, thus avoiding small clearances. In order to obtain measurable torque, relatively high rotational velocities were used, equal to or more than the minimum fluidization gas velocity. This could not fail to disturb the state of the fluidized bed. Under the circumstances of a fluidized bed it would seem to be desirable to avoid constricting the bed, and to avoid velocities even approaching that of the fluidizing gas or liquid.

The drag on a lamina oscillating in its own plane in fluid of infinite extent seemed to fulfil these requirements, but would be mechanically difficult. A solid of rotation, such as a sphere, cone or cylinder, oscillating about its axis of rotation in an infinite fluid, offered easier application and two patterns have been applied already in this Department for studies in fluidized gas-solid systems. The type of calibration required for each is dealt with here, since the instruments may have applications in quite other fields; for example, in suspensions of coarse or fibrous materials, suspensions in which structures or flocs develop, metals and slags at high temperatures and so on.

Type I: fully-immersed bob

If a bob is suspended from a torsion wire and inertial member, as in Fig. 1 and fully immersed in a fluid, the drag may be observed in three ways. Oscillation may be started by momentary torque applied to the wire suspension, and the subsequent decay of the amplitude with time may be observed. Alternatively, an oscillating angular motion may be applied to the top suspension, and its amplitude then adjusted to produce a steady predetermined amplitude of the immersed bob. A third alternative is to determine the power required to sustain vibrations of fixed amplitude. The first method is convenient for observation at the low frequency desired in this work, and leads to very simple apparatus, but to less simple mathematics, since the authors are concerned, not with a simple sinusoidal motion, but with one with exponential damping.

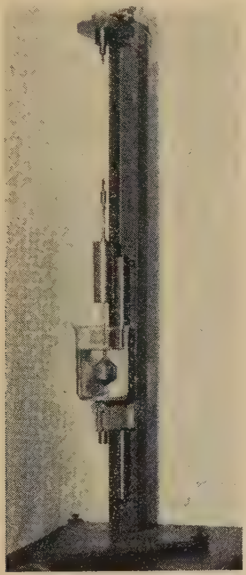

Fig. 1. Viscometer assembly, type I bob

Stokes considered such a system, using a sphere as the immersed body, and others have also developed the theory. For constant sinusoidal oscillation, Lamb (p. 642, Ref. 3) gives a solution for the case where viscosity is small. This does not accord with the present conditions as the viscosity is not small nor is the bob motion undamped. Furthermore, a sphere is not easy to machine and mount accurately centred on a shaft. Consequently a bob of the form shown in vertical cross-section in Fig. 2 is preferable to a sphere, and would appear to have a further advantage in providing less upper, nearly horizontal surface, on which defluidization might occur, especially in nearly quiescent beds. The following analysis applies to bobs dimensionally similar to those of Fig. 2 and Table 1 and completely described by diameter D.

A system, as in Fig. 1, set oscillating torsionally is damped by internal friction in the torsion wire, by air drag on the cylindrical inertial member and shaft and by drag of the fluid on the lower bob. The first two phenomena normally give rise to exponential damping in which log amplitude is inversely proportional to time, the gradient of such a plot being the amplitude logarithmic decay constant k. It is a useful property of such decay constants that, when damping processes are added together, the total decay constant is the sum of those representing the separate processes alone. Consequently, if measurements are confined to any region where the fluid drag also gives rise to exponential damping, then the decay constant of fluid drag may be obtained by subtracting that for internal friction and air drag from the observed decay constant for all three processes. In the apparatus used in the work here described, the decay constant k_1, due to internal friction and air damping, may be observed directly by temporarily housing the lower working bob in the hollow inertial cylinder above it. The value of k_1 so obtained is then subtracted from k_2, the decay constant observed with the working bob in the test fluid, to give k the decay constant for fluid damping alone. A correction to k, to allow for the fact that a small length of shaft exposed to air drag during the k_1 measurement is covered by the lower bob during the fluid drag measurement k_2, has been found to be quite negligible. Such a value for k may be used in a dimensional analysis of the problem, and it is found that if a dimensionless group D^2n/ν is chosen as representing the state of fluid motion, then if the only variables are those below:

$$k/n \text{ is a function of } D^2n/\nu \text{ and of } D^5\rho/I$$

where n = frequency, I = moment of inertia of whole oscillating system, ρ = density and ν = kinematic viscosity of the fluid. This function may be of the type

$$k/n = (D^2n/\nu)^{\alpha}(D^5\rho/I)^{\beta} \qquad (1)$$

or may be more complex. There is only one frequency n in the above correlations because the frequency is unchanged by immersion of the working bob in the test liquid.

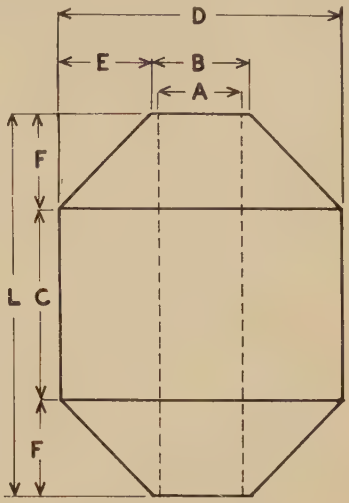

Fig. 2. Type I bob

A bob oscillating in an infinite fluid transmits its oscillations to the fluid, but with diminishing amplitude and increasing phase lag at points increasingly further from the bob surface. In the case of the oscillating lamina treated by Lamb (p. 620, Ref. 3), the fluid oscillation is again in phase with the lamina at a distance from the surface of $\sqrt{(4\pi\nu/n)}$. This wavelength is repeated to infinity, but the amplitude at one wavelength out has diminished by the factor $\exp(2\pi)$ or 535 and hence the containing vessel wall need not, for ordinary accuracy, be further away than one wavelength. For torsional oscillations, the amplitude seems to fall off even more quickly, and the influence of the container wall was found to be negligible, provided that it was at least 28% of the wavelength from the bob. No measurements were carried out with the wall closer than this.

Experimental. The authors have investigated a set of dimensionally similar bobs of dimensions given in Table 1. Fig. 2 shows the dimensions indicated by letters *A*–*F* and *L* (in centimetres).

Table 1. *Dimensions of experimental bobs (cm)*

Bob No.	*L*	*D*	*A*	*B*	*C*	*F*	*E*
I	2·539	1·9055	0·556	0·652	1·274	0·643	0·625
						0·631	0·628
II	3·808	2·8580	0·556	0·989	1·899	0·954	0·935
						0·955	0·933
III	5·080	3·8212	0·557	1·249	2·546	1·266	1·283
						1·266	1·279
ratio II/I	1·500	1·4995		1·517	1·490		
ratio III/I	2·001	2·0050		1·915	1·998		

Table 2. *Experimental fluids*

Fluid	*I*	*II*	*III*	*IV*	*V*
Density ρ at 25° C (g/ml)	0·825	0·879	0·794	2·166	1·419
Viscosity μ at 25° C (cP)	11·26	163·9	2·227	1·59	5·101

Fluids were made from mixtures of hydrocarbons and ethylene dibromide and had densities and viscosities as in Table 2.

Frequencies n between 0·282 and 0·938 oscillations per second were used and at these frequencies the amplitude can readily be observed visually from a galvonometer-type mirror and scale; k was normally obtained from the half amplitude time $T_{1/2}$, from $k = \ln 2/T_{1/2}$ or could be read from a decay curve.

It was found that the log amplitude *versus* time curves were not, in fact, quite straight (see Fig. 3 for air and Fig. 4 for fluid IV). Only for the straight portion of these curves can the k values be additive, and consequently only the lower portions of these curves would seem to be useful. Observations were therefore confined to half amplitudes less tha 0·06 rad and frequencies less than 1 oscillation/s.

It was at first thought that this small change in slope wit amplitude was associated with a change in the flow régim analogous to the change from laminar to turbulent flow However, on any one decay curve the group D^2n/ν is constan and there is thus no relation between this group and th change in slope. However, this group contains no velocit term, so a new dimensionless group was obtained by multiplying it by the amplitude in radians. Inspection of the decay curves showed, however, that the change in slope di not occur at amplitudes that could be related to the ne Reynolds group either, so the original group D^2n/ν was reverted to and used in all correlations.

The oscillating shaft, inertial member and bobs were machined carefully to avoid eccentric oscillation. The mos difficult member to machine was the shaft, which finally exhibited a maximum eccentricity of about 0·0008 cm Small sideways sway purposely induced in the oscillating bo was found to produce insignificant changes in the decay constant, so that it is unlikely that the above eccentricity

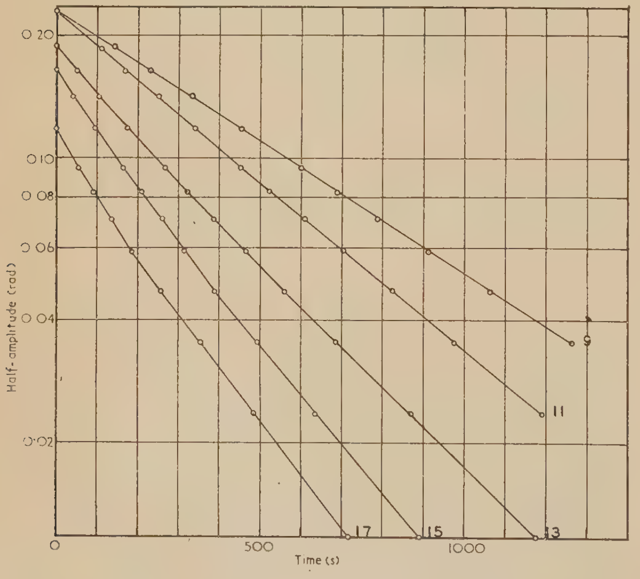

Fig. 3. Amplitude decay curves for air

Run no.	9	11	13	15	17
n(s^{-1})	0·421	0·560	0·675	0·815	0·938

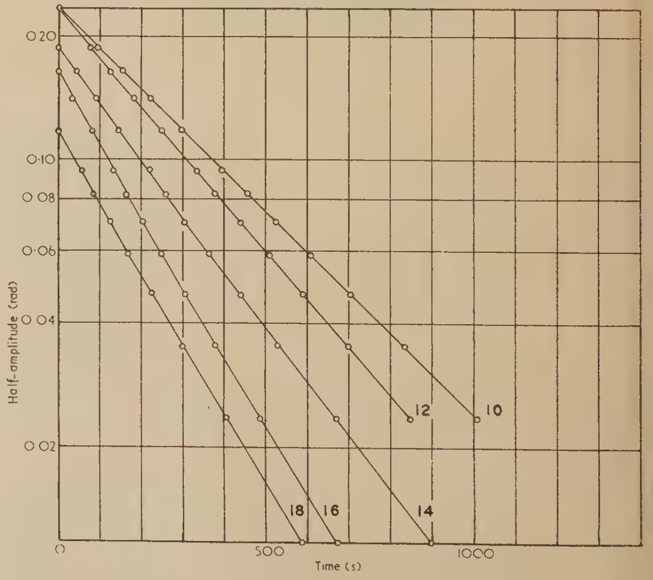

Fig. 4. Amplitude decay curves, fluid IV

Run no.	10	12	14	16	18
n(s^{-1})	0·421	0·560	0·675	0·815	0·938

would have appreciable effects. Depth of immersion has little effect, for example, for fluid IV, bob II could be used as little as 1 mm below the liquid surface with little effect on k. The liquid surface was nevertheless normally at least 1 cm above the bob.

The torsion wire was of hard-drawn phosphor bronze, 0·045 cm diameter. To avoid approaching its elastic limit, torsional strain should be restricted to about 0·02 rad/cm of wire length or to 0·26 rad for the shortest wire used. Actual strains applied were all below this. Fluid temperatures were maintained at 25 ± 0·1° C.

Results. Full tabulated results are recorded in Refs. 5 and 6. As explained above, observations used for the correlations were restricted to the linear portion of the amplitude decay curves and hence to half amplitudes less than 0·06 rad and frequencies less than 1 oscillation/s.

Fig. 5 shows a plot of ln k *versus* ln I for fluid IV, $D = 1{\cdot}906$ cm, $n = 0{\cdot}421$/s. Each point is the average of four runs. The slope of the regression line drawn is $-0{\cdot}992$, not significantly different from $-1{\cdot}000$. It is, therefore, reasonable to take β of equation (1) to be -1 and to write $(k/n)(I/D^5\rho)$ as some function of the Reynolds number D^2n/ν.

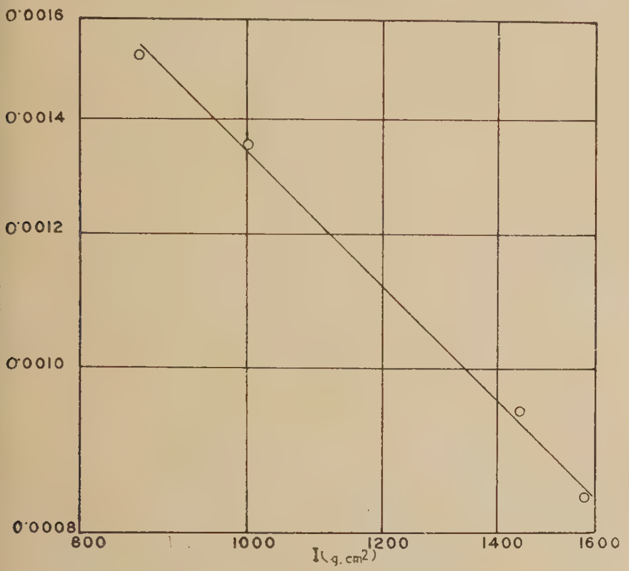

Fig. 5. Logarithmic plot k *vs.* I

Plots of ln k *versus* ln n for constant D, I, ρ and μ gave lines of variable slope, and hence the above function of Reynolds number is more complex than in equation (1). This is possibly due to the incidence of centrifugal effects disturbing the viscous waves leaving the bob surface. All results, however, correlated reasonably well as in Fig. 6, each open print of which represents the mean of four decay observations of half-amplitudes less than 0·06 rad. Solid points in Fig. 6 have also been included, representing half-amplitudes up to 0·2 rad, and hence the non-linear regions of decay curves like Fig. 4. That these points lie on the general correlation line indicates that the use of such large amplitudes does not, in fact, introduce serious error, at least in the range of n, D and ν used by the authors. It is possible that the non-linearity of the decay curves of Fig. 3 and 4 is due to a property of the wire, not of the fluid damping. It is evident from Fig. 6 that deviations are becoming serious at Reynolds numbers exceeding 200, and that the general correlation is unreliable in this region.

By the use of Fig. 6, newly built apparatus using working bobs dimensionally similar to those in Table 1 may be used without calibration, if the total I for the oscillating parts is known. Otherwise a single measurement of $k = k_2 - k_1$, using a fluid of known viscosity, suffices to determine I and so calibrate the apparatus.

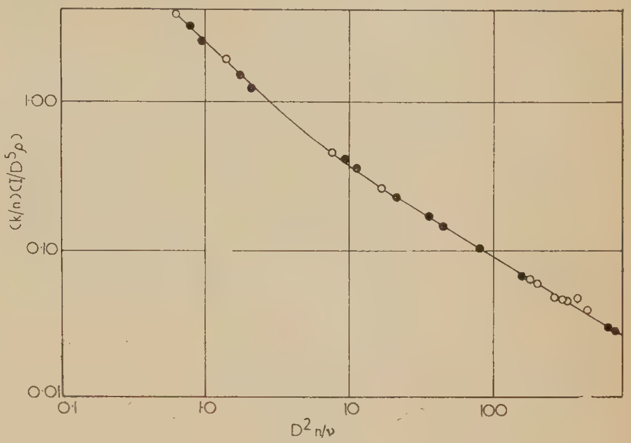

Fig. 6. General correlation, Type I

○ = half-amplitude, 0·06 rad
● = half-amplitude, 0·2 rad

It has been found that aqueous liquids are not very satisfactory calibrating fluids owing to irregular wetting at the immergent shaft, but the addition of a wetting agent can eliminate this source of error. Each value of k is, of course, the difference between k_1 observed in air, with the working bob housed in the hollow cylinder, and k_2 observed with the working bob in the fluid.

Analytical solutions for damped oscillations in infinite fluids are not available, so far as the authors are aware, for such shapes as these. In the limit of very large diameter of very high frequency, the theory of oscillating laminae would perhaps apply. This has been applied to piezoelectric cylinders by Mason,$^{(7)}$ who used continuous oscillation and radio frequencies and found good agreement between lamina theory and observation. The authors have applied lamina theory to bobs of the above form by assuming that each surface particle acted as a lamina oscillating linearly, and that oscillation of the bob was undamped. It was found$^{(6)}$ that

$$\frac{k}{n} = \frac{Z\sqrt{\pi}}{2D^4}\left(\frac{D^5}{I}\rho\right)\left(\frac{D^2n}{\nu}\right)^{-1/2} \qquad (2)$$

This expression implies that $\ln(k/n)\,.\,(I/D^5\rho)$, plotted against ln . Re should give a slope of $-0{\cdot}5$ and an intercept $Z\sqrt{\pi}/2D^4$ which is a bob constant.

This constant is calculated to be as follows:

Bob	I	II	III
Constant	0·643	0·640	0·635

The curve of Fig. 6 has values of the constant ranging from 0·79 and slope $-0{\cdot}56$ at high values of Re to 2·8 and slope $-0{\cdot}85$ at low values of Re, and thus never agrees closely with lamina theory, not surprising in view of the sweeping approximations.

Type II: partially-immersed cylindrical bob

After some use of the submerged bob in measurements in fluidized systems, it was suspected that some defluidization was taking place on the upward-facing horizontal surface, to prevent which it was decided to use a long cylindrical bob, only partially immersed, and thus exposing no upward-facing horizontal surface to the fluidized solids. If the decay constant is observed for such a bob at one depth of immersion and then again at another deeper immersion, then the difference in k characterizes the damping on the extra surface exposed to the fluid in the second test. This therefore is a means of obtaining a value of k' for the cylindrical surface only, since end effects, air drag and internal friction are all eliminated. The value of k' now has dimensions $T^{-1}L^{-1}$. This method requires that the ln amplitude *versus* time curve is straight, and also that air drag on the length of lower bob exposed to air in the first observations is negligible. This was found to be true by measuring the air drag separately by duplicate runs in air, first with the lower bob exposed and then with it housed in the hollow inertia cylinder. It was found that error due to this cause would in all cases be much less than 0·1% and could be neglected.

Correlation of variables. The dimensional analysis for this case differs from the previous case in that there is now an extra length dimension, namely, the difference in immersion between each pair of observations. One now finds that if the same Reynolds group is to be used, then

$$k'D/n \text{ is a function of } D^2n/\nu \text{ and } D^5\rho/I$$

Experimental. Test liquids, range of frequencies and amplitudes were the same as before. The value of k' was determined from the differences between observations when the bobs (length 7·62 cm) were immersed in turn to lines scribed on the bobs at 1·270, 3·810, 6·350 cm from the lower end. Coincidence of liquid meniscus and the scribed lines was observed with a travelling microscope. Fluid temperatures were maintained at 25 ± 0·1° C.

Results. These are given in full in Ref. 8 for bobs of diameters 1·270, 1·905 and 2·540 cm.

Deviations from linearity of the ln amplitude *versus* time curves were found to be in the same range of amplitude and frequencies as before, and observations were therefore restricted to the same range of amplitudes and frequencies, namely, less than 0·06 rad half amplitude and less than 1 oscillation/s. Measurements of three damping runs, each at 1·270, 3·810 and 6·350 cm immersion, gave two values of k' not significantly different. The mean was therefore used in plotting results. Fig. 7 gives the gradient of ln k' *versus* ln I as −1·00.

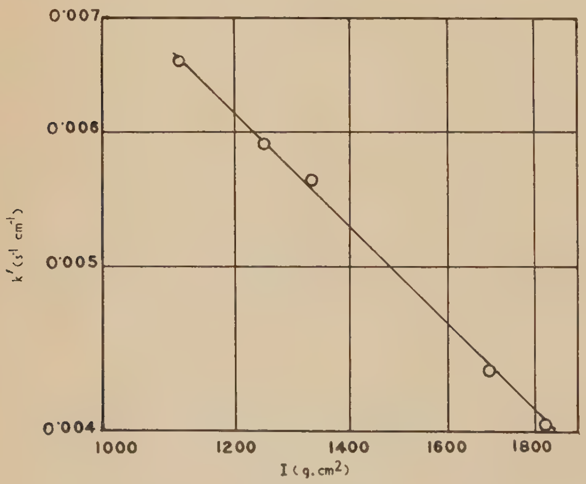

Fig. 7. Logarithmic plot, k' *vs.* I

As before, variable gradients were obtained in plots of ln k' *versus* ln n, and it appears that the function of D^2n/ν is again not simple. The general correlation of results is given in Fig. 8; a rather smoother curve results than Fig. 6 presumably because of the simpler hydrodynamics of cylindrical bobs. The gradient of the curve at D^2n/ν greater than 200 was found to be −0·51, and in this region the general correlation becomes:

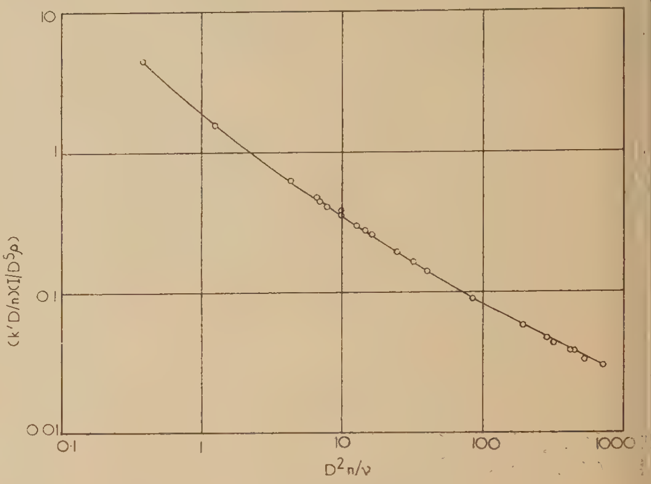

Fig. 8. General correlation, Type II

$$\frac{k'D}{n} = 0{\cdot}80\left(\frac{D^5\rho}{I}\right)\left(\frac{D^2n}{\nu}\right)^{-0.51} \tag{3}$$

or approximately $k' = \{0{\cdot}80\, D^3\sqrt{(n\mu\rho)}\}/I$ (4)

The constant 0·80 is comparable with 0·79 for the same region for the case of the fully-immersed bob.

Although a cylindrical oscillating viscometer was first suggested by Coulomb, analytical solutions to suit the present case are not known to the authors, although a laborious solution for fluid in an annulus around a cylinder is given by Sneddon.(9) This solution does not appear to be capable of being applied when one boundary is at infinity, is unsuitable for routine use and does not include end effects. Consequently, again using equation (2), and bearing in mind that k' refers to damping for 1 cm length:

$$\frac{k'D}{n}\left(\frac{I}{D^5\rho}\right) = \frac{Z\sqrt{\pi}}{2D^3}\left(\frac{D^2n}{\nu}\right)^{-0.5} \tag{5}$$

For cylindrical surfaces 1 cm long, $z = \pi D^3/4$ and

$$\frac{k'D}{n}\left(\frac{I}{D^5\rho}\right) = 0{\cdot}697\left(\frac{D^2n}{\nu}\right)^{-0.5} \tag{6}$$

It is evident that the observed constant, even for high values of D^2n/ν is again somewhat higher than calculated from the theory of laminae.

As before, the general correlation of Fig. 8 can be used for direct calculation of μ for any apparatus for which I is known. Two runs are carried out at two immersions of accurately known differences in depth and the resulting value of k' is used in the general correlation. This method, however, gives a slight error due to the fact that when the immersion is increased, then the air drag is decreased by the additional area of bob now immersed in the liquid. This

Table 3. *Experimental points for Fig.* 6

$\frac{k}{n}\left(\frac{I}{D^5\rho}\right)$	$\frac{D^2 n}{\nu}$
3·93	0·625
1·965	1·405
0·467	7·511
0·262	16·89
0·0645	180·9
0·0587	204·2
0·0461	307·5
0·0470	395·3
0·0478	271·6
0·0450	327·4
0·0396	454·9

Table 4. *Experimental points for Fig.* 8

$\frac{k'D}{n}\frac{I}{D^5\rho}$	$\frac{D^2 n}{\nu}$
4·574	0·378
1·575	1·280
0·637	4·34
0·479	6·56
0·445	6·92
0·410	7·79
0·376	9·94
0·361	9·82
0·301	12·70
0·280	14·8
0·260	16·1
0·193	24·8
0·167	32·0
0·145	40·0
0·0913	84·8
0·0591	191·8
0·0479	283·3
0·0443	320·7
0·0393	412·6
0·0389	444·8
0·0334	521·3
0·0301	707·7

error is negligible with fluids having the range of properties used by the authors, and this method permits the hollow inertia cylinder of Fig. 1 to be replaced by a solid one with a similar value of I. If it is desired to apply a correction for the changed area of working bob exposed to air drag, then the hollow cylinder must be retained so as to house the working bob during measurement of the air drag on the working bob itself.

In spite of the simplicity of using Fig. 8 without such correction, and in spite of the generally better correlations for the immergent cylindrical bob, it is recommended that if surface tension effects are likely to be serious then the fully-submerged bob be used since, with its smaller peripheral length passing through the liquid surface, it is less liable to disturbance from surface tension and irregular wetting.

In order that the general correlation curves may be used by others, Tables 3 and 4 give sufficient points for the curves to be redrawn.

References

(1) Matheson, G. L., Herbst, W. A., and Holt, P. A. *Industr. Engng Chem.*, **41**, p. 1099 (1949).

(2) Long, F. J. M.S.E. Thesis (University of Princeton 1952).

(3) Lamb, H. *Hydrodynamics*, 6th Ed. (Cambridge: The University Press, 1953).

(5) Ashwin, B. S. B.E. Thesis (University of Canterbury, 1955).

(6) Saunders, I. C. B. B.E. Thesis (University of Canterbury, 1956).

(7) Mason, W. P. *Trans Amer. Soc. Mech. Engrs*, **69**, p. 359 (1947).

(8) Young, T. E. B.E. Thesis (University of Canterbury, 1957).

(9) Sneddon, I. N. *Fourier Transforms*, p. 307 (New York: McGraw-Hill Book Co. Inc., 1951).

Elimination of ghost images when using a Kerr-cell shutter

by D. W. Godwin and F. R. Brookes, B.Sc., Grad. Inst.P., Safety in Mines Research Establishment, Ministry of Power, Buxton, Derbyshire

[*Note received* 16 *August*, 1960]

A Kerr-cell electro-optical shutter enables photographic exposures of 1 μs or less to be obtained: it consists essentially of a cell containing nitrobenzene placed between perpendicularly crossed polarizers so that, ideally, no light is transmitted through the cell until an electric field is applied to the nitrobenzene. In practice a certain amount of light passes through the cell even when the polarizers are accurately crossed and there is no electric field across the cell. The ratio of light transmitted through the Kerr-cell when open to that when closed is, in fact, of the order 10 000 : 1, which means that some fogging of the film or the appearance of ghost images can occur, unless a gating shutter is used in conjunction with the cell. Thus, if the light falls on the closed cell for more than 10 ms the effect on the film is greater than that of the light passing through the cell for 1 μs. Thus a gating shutter opening for a millisecond or less is required in order to reduce the effect of a ghost image appreciably for an exposure of 1 μs. A focal plane shutter is not suitable for this purpose and diaphragm shutters of the size and speed needed are not available.

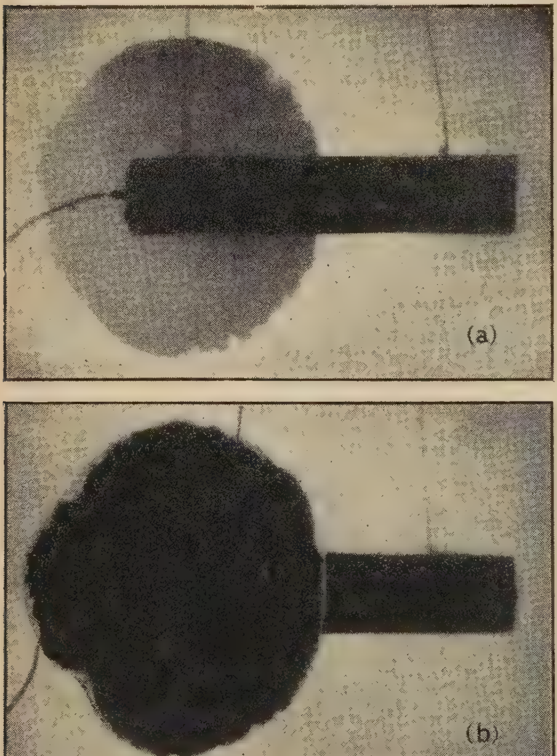

Photographs of a stage in the detonation of a charge of explosive

(*a*) 10 ms gating shutter, stationary film
(*b*) 10 ms gating shutter, moving film

The following simple method of overcoming the difficulty has been used in this laboratory, when the detonation processes in mining explosives are studied photographically with a Kerr-cell shutter with high intensity back lighting from a concave mirror illuminated by an arc lamp, this being an adaptation of the normal arrangement for Schlieren photography. Before entering the cell, light passes through a diaphragm shutter which opens for 10 ms and, after passing through the cell, falls on a rotating drum bearing the photographic film. An oscillograph recording camera capable of giving a film speed of 600 in./s has been found suitable for this purpose.

With an exposure of 1 μs the film moves only 0·0006 in., which is not enough to blur the image; on the other hand, the image of the illuminated field is only $\frac{1}{2}$ in. across and the film moves 6 in. in the 10 ms during which the gating shutter is open, so that fogging is spread over this length of film and has little effect.

This device can also be used for photographing self-luminous events that last longer than the exposure time, and for this purpose it is more convenient than the shatter shutter in which a glass block, placed in front of the Kerr-cell, is made opaque by detonating a small charge of explosive inside it after the photograph has been taken.

The figure shows photographs of a stage in the detonation of a charge of explosive: (*a*) was taken with the 10 ms gating shutter and a stationary film; (*b*) with the 10 ms gating shutter and the moving film. For both photographs the exposure time was 1 μs and high intensity lighting was used to illuminate the charge from behind. In (*a*) the silhouette image of the charge with the detonator protruding from the left-hand end has been formed by the light passing through the Kerr-cell before it was nominally open. The image, formed when the cell was open, of the cloud of opaque products produced by the detonation charge can be seen only faintly. In (*b*) the ghost image has been eliminated and the cloud of opaque products is very much darker; a shock wave can be seen faintly around the edges of the detonation products and the band of light from the detonation wave at the centre of the charge can be seen more clearly.

We wish to thank Mr. J. F. Sheen for his assistance with this work. The illustrations for this note are Crown copyright.

Improved design of portable vacuum manometer

by A. T. J. Hayward, B.Sc., Fluid Mechanics Division, National Engineering Laboratory, East Kilbride, Glagow

[*Note first received* 22 *June, and in final form* 29 *August*, 1960]

It is frequently necessary in the laboratory to measure pressures in the "partial vacuum" range, i.e. between 10 mm of mercury absolute and atmospheric pressure, or more particularly in the lower half of this range, say from 10 to 300 mm of mercury absolute. This range is beyond the limits of the McLeod gauge, and mechanical gauges of the Bourdon or capsule type are inherently inaccurate.

The instrument most commonly used in this range is the portable mercury manometer, which is normally of the form shown in the Figure (*a*). The limb AB is sealed at end A and is completely filled with mercury during manufacture. The scale S is 300 mm long on most commercial instruments, nd when the pressure at D falls below 300 mm, the mercury AB falls below A. It is assumed that a true Torricellian acuum exists at A, so that the pressure there is negligible nd the difference in level between the two limbs is a true easure of the absolute pressure at D.

Unfortunately this assumption of zero absolute pressure t the top of the closed limb is not borne out by practical xperience. It is well known that in this type of manometer mall quantities of air may leak past the mercury into the losed limb, gradually destroying the vacuum. The error ue to small quantities of entrapped gas will be very small at ow readings, but will increase greatly at readings near to ull scale, when the entrapped gas is highly compressed by he rising mercury column.

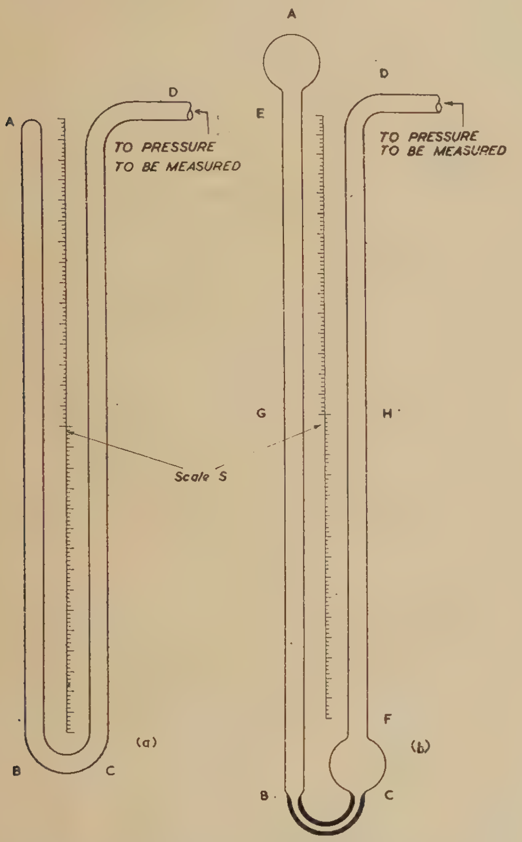

(*a*) Conventional type of portable vacuum manometer
(*b*) The new portable vacuum manometer

It is sometimes suggested that the presence of air in a vacuum manometer may be detected by examining the "zero error" of the manometer, i.e. by connecting it to a complete vacuum, which should give a reading of zero. This, however, is not true. Zero errors due to surface tension effects are liable to mask those caused by entrapped gas. For instance, a manometer has been tested which contained air and had an error of 17 mm at full scale but had a negligible zero error, while another manometer which was free from air had a zero error of 2 mm.

The error due to entrapped air may be reduced substantially by blowing a bulb at A, the top of the closed limb [Fig. (*b*)]. A compensating bulb C, of exactly the same size, is required at the bottom of the open limb to receive the mercury which falls from A when the manometer is connected to vacuum. A short length of narrow-bore tubing between B and C constricts the flow of mercury, and thus prevents the bulb at A from being broken by the "hammer" effect when the vacuum at D is released suddenly.

A manometer of this type has been built in which the bulb at A has three times the volume of the tube from G to E. The accuracy of this new manometer has been compared with that of a commercial instrument of the conventional type which, after only a few months' use, was found to contain an appreciable quantity of air. It will be seen from the table that the new instrument is much more accurate than the conventional manometer at readings near full scale.

Comparison between a conventional manometer and the new manometer

	Errors in conventional manometer			*Errors in the new manometer*		
		Found experimentally			*Found experimentally*	
Manometer reading	*Theoretical* (mm)*	*(mm)*	*(%)*	*Theoretical* (mm)*	*(mm)*	*(%)*
Zero	1	1	—	0·25	1	—
½ scale	2	1	0·7	0·29	1	0·7
¾ scale	4	2	0·9	0·31	1	0·5
Full scale (= 300 mm)	17	17	5·7	0·33	1	0·3

* Based on the assumption of equal masses of entrapped air in each manometer, and ignoring errors due to surface tension effects.

There are two distinct advantages in this design of manometer. Firstly, the total volume above G in the new instrument is four times that in the normal type, so that the mass of air which causes a zero error of 1 mm in the normal instrument causes a zero error of only ¼ mm in the new one. Secondly, since the compression ratio of the new instrument between zero and full scale is only 4 : 3, the full-scale error is only 1·33 times the zero error, whereas the corresponding ratio in the conventional instrument is about 17.

The new manometer is the subject of Patent Application No. 5044/60, and commercial exploitation is being arranged by the National Research Development Corporation.

This note is published by permission of the Director of the National Engineering Laboratory, Department of Scientific and Industrial Research.

Simple force balance for drag measurements

by G. A. Henwood, Chemical Engineering Division, Atomic Energy Research Establishment, Harwell, Berks.

[*Note first received* 20 *June, and in final form* 22 *August*, 1960]

Drag forces acting on spheres submerged in a flowing fluid have been measured as part of an investigation into the fluid dynamics of fluidized beds. Fluidization of 16 B.S. mesh particles in air may occur over a range of Reynolds number of approximately 25 to 100, a condition which has been simulated for the purposes of force measurement by submerging 1·27 cm diameter spheres in water flowing at 0·2 to 0·8 cm/s. The calculated drag force for a single 1·27 cm diameter sphere, in motion through an infinite water medium at velocities in this region, is of the order 10^{-4} g weight. The simple form of balance to be described has proved satisfactory during the course of a series of experiments and is robust enough to require no more than normal care in operation, whilst being capable of measuring forces of $0 \cdot 1 \times 10^{-4}$ g weight.

The method chosen for measuring the drag force was to record the horizontal deflexion of a sphere supported as a simple pendulum, and the forces involved are shown in part (*a*) of the figure. The weight in water of the supporting wire and the sphere W_a acts downwards and the drag force F acts horizontally. The drag is thus given by

$$F = (\delta/l)W_a$$

where l is length of the suspension from the pivot to the intersection of the lines of action of drag and weight forces. This method of measurement is very simple and requires only measurement of the length l, immersed weight of the moving parts W_a and the deflexion δ to give an absolute value of the drag force. Suspension length and weight can be adjusted to give a suitable deflexion for a given force. The deflexion should be sufficiently small to keep the suspension length effectively constant.

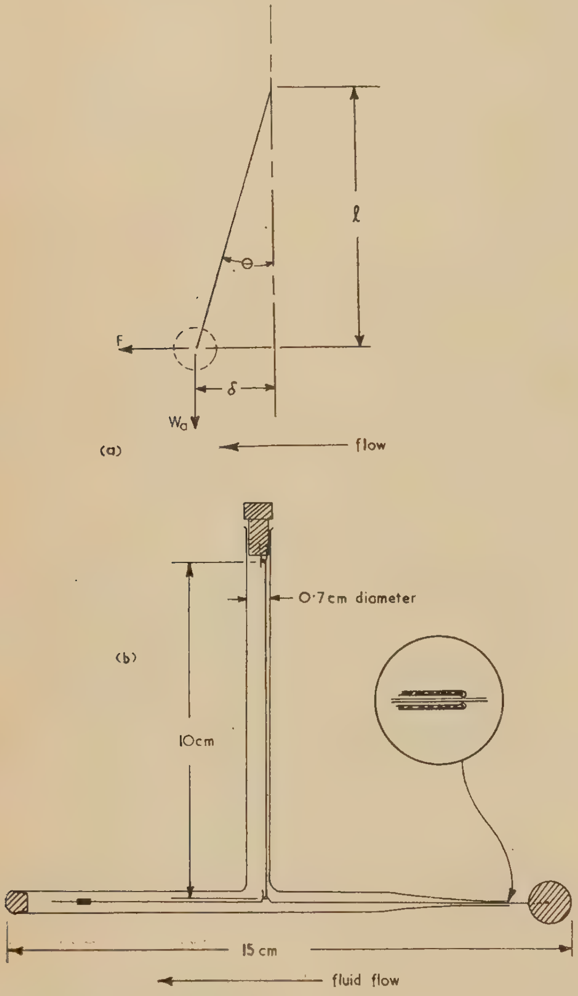

Drag force balance approximately scaled for bodies with a projected area of 1 cm². Mounting not shown

The prototype balances were made with l about 9 cm and W_a about 0·125 g, giving a sphere deflexion of 0·006 to 0·031 cm according to the fluid velocity. The dimensions can be measured with a cathetometer to $\pm 0{\cdot}0005$ cm, whilst W_a can be measured to about $\pm 0{\cdot}0005$ g. The weighing was done with the force balance movement immersed in water, to which a trace of Teepol had been added to reduce surface tension effects. The movement was suspended by means of 48 s.w.g. wire and the weighing was carried out with upward and downward swings of a sensitive chemical balance; several swings were noted and, where the differences were appreciable, the mean was taken as W_a. When a measurement of actual drag force is required, the temperature of the working fluid should be the same as that at which W_a was determined. Where comparative effects are being investigated, the only restriction is that the temperature should be substantially constant during the course of an experiment. The effect of these dimensional tolerances means that the maximum sensitivity of drag measurement is about $\pm 0{\cdot}05 \times 10^{-4}$ g weight.

To minimize flow disturbance in the boundary layer over the sphere, it should be supported from the downstream side. Furthermore, the supporting wire must be screened from the flow to avoid additional drag forces. The assembled apparatus, which meets these requirements, is shown in part (*b*) of the figure. In addition, a mounting to locate the balance and allow triaxial adjustment will be required.

The balance proper consists of an inverted T-shape made from glass tubing, with an adjustable plug of polythene at the end of the vertical limb and another plug to seal one end of the cross member. The remaining end is drawn down to a reduced diameter and the open end flame polished as shown in the enlarged detail, this hole being reduced to a diameter slightly greater than the wire which will be used to go through it. The object of this treatment of the opening is to centralize the wire and reduce to a minimum the possible areas of glass and wire in contact. The ends of a V-shaped piece of 36 s.w.g. Nichrome wire are embedded in the adjustable plug and another length of the same wire with a hook at each end is used as a suspension; 24 s.w.g. wire is used for the horizontal support carrying the polythene sphere. The wires should be straightened by careful stretching before forming hooks and pivots.

Before assembly, the horizontal wire and supported sphere are balanced about the pivot point whilst immersed in water by adjusting a counter weight and, as described previously, the total apparent weight is determined by means of a sensitive laboratory balance. Final assembly is as shown in the diagram; the glass T-tube is completely filled with water and the adjustable plug is used to centralize the horizontal wire in the cross member. The sphere must be removed from its support in order to pass the wire through the opening; care must be taken to restore the sphere to precisely the same position on its support. Finally, the complete balance is mounted in position with the upright limb truly vertical and the horizontal cross member alined with the direction of flow.

As there are only a few millimetres of wire exposed to the fluid flow in the stagnant region immediately behind the body under investigation and friction effects in the balance system are negligible, then the force which is measured is practically that which is due to the drag on the sphere whilst in motion relative to the surrounding fluid. The friction effects were shown to be negligible by the return of the sphere to its neutral position at zero water flow.

The performance of the balance was checked against correlated results for the drag of a sphere in the region Re $0{\cdot}2 \rightarrow 500$ which has been the subject of much investigation. The standard deviation of a single observation of drag force was found to be about $\pm 0{\cdot}1 \times 10^{-4}$ g weight. Nine observations were made on each of two spheres so that an average value was found with a standard deviation of about $\pm 0{\cdot}25 \times 10^{-5}$ g weight. The experimental drag values are in close agreement with those of others at the lower end of the Reynolds number range selected for the experiments, i.e. Re 25, but are high by some 13% at the upper limit Re 100. This discrepancy may possibly be attributed to "blocking" occurring in the experimental water channel which had a width only twelve times greater than the sphere diameter.* On the other hand, there may be a genuine difference between the drag on a freely falling sphere (on which all measurements have hitherto been made in this Reynolds number range) and one that is held rigidly. It has been shown† that even a very low speed of rotation could have an appreciable effect on the drag of a sphere. Observation of this discrepancy was incidental to the principal work and the question was not pursued.

[*] McNown, J. S., and others. *Influence of Boundary Proximity on the Drag of Spheres* (University of Iowa; Iowa Institute of Hydraulic Research, 1948).

[†] See, for example, Goldstein, S. *Modern Development in Fluid Dynamics*, **2**, p. 504 (London: Oxford University Press, 1950).

Liquid-level alarm using internally reflected light

by W. E. Hood and E. Oldham, Imperial Chemical Industries Ltd., Dyestuffs Division, Blackley, Manchester 9

[*Note first received* 28 *October*, 1959, *and in final form* 8 *September*, 1960]

Recently, the problem has arisen of detecting the level of clean organic liquid in a flask. All the liquids used have low dielectric constants so that capacitive methods are insensitive. To avoid the possibility of contamination only Pyrex glass should be in contact with the liquid.

Geake‡ has described a method using a totally internally reflected beam of light in a Perspex rod for liquid-level detection. His method calls for careful machining of the Perspex rod, and the shape would be expensive to obtain in glass. His method also provides only for visual indication. In the apparatus described here the glassware can easily be made by a glass blower, and the instrument can be used to give remote indication, alarm and cut-off.

A piece of glass rod 8 mm diameter is bent into a "U" shape, with a bend diameter of about 1 in. Light is directed largely by internal reflexion down one arm of the "U", round the bend and up the other arm, being finally received on a photocell. If the bend is immersed in a liquid the amount of light emerging is reduced to an extent depending upon the degree of immersion and the refractive index of the liquid. Fig. 1 shows the "U" sealed through a standard ground glass cone. For an 8 in. probe length, a 6 V 3 W lamp gave sufficient light to make a Mullard 90AG photocell operate the relay circuit, Fig. 2. A direct voltage of 85 V is fed from a separate stable power supply to a trigger circuit built around a Mullard ECC81 valve, and a relay mounted with the power supply acts as the load for one anode. Control resistor R_5 sets the condition at which the circuit operates. If it is adjusted so that, with the probe bend in water, the relay is just energized, then for all liquids of higher refractive index the alarm will operate at less immersion of the bend.

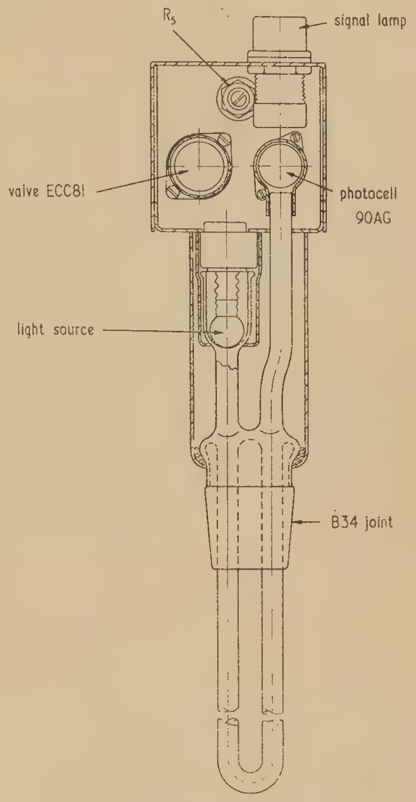

Fig. 1. U-tube sealed through glass cone

The optical system is insensitive to ambient light. However, some light from the source lamp does get to the photocell *via* the ground glass cone, reducing the signal-to-noise ratio. If it were possible to use opaque material instead of the ground glass cone this source of stray light would be eliminated.

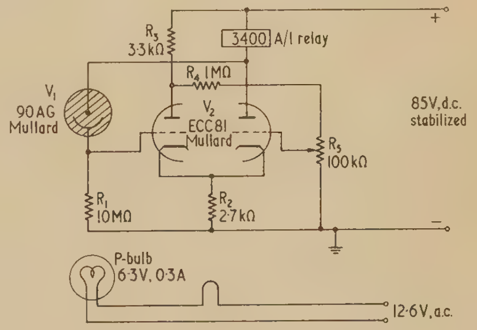

Fig. 2. Electronic circuitry

A feature of the system arranged for the detection of low liquid level is that failure of lamp, valve heater, or stabilized supply, will cause the relay to return to the alarm condition.

[‡] Geake, J. E. *J. Sci. Instrum.*, **31**, p. 260 (1954).

Improved flow-sensitive switch

by H. C. Burford, B.Sc., Grad.I.E.E., Research Laboratory, Associated Electrical Industries (Rugby) Ltd., Rugby

[*Note first received* 4 *July, and in final form* 12 *September*, 1960]

A device has been described* which is designed to give full protection of diffusion pumps against failures of the cooling-water supply.

This note describes another device which has been found to give good results in similar applications. It avoids the use of mercury, and enables the system to be completely sealed. When fitted at the "outlet" end, it gives complete protection to the cooling system, including protection against bursts if a solenoid-operated valve is fitted to the coolant supply.

In currently available flow-sensitive devices which make use of the pressure differential across an orifice, the orifice is of fixed dimensions, except possibly for adjustment of the setting. A disadvantage inherent in such devices is that small amounts of solid matter can accumulate at the orifice, so restricting it. When this occurs, the setting of the instrument is upset, and in extreme cases blockage of the orifice can stop the liquid flow, while maintaining a pressure differential across the blocked orifice and thus indicating full flow.

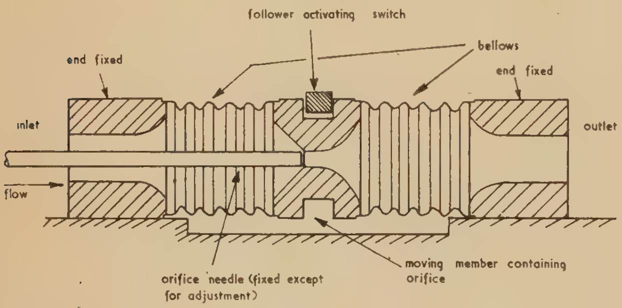
follower activating switch
bellows
end fixed
end fixed
inlet
outlet
flow
orifice needle (fixed except for adjustment)
moving member containing orifice

Diagram showing principal parts of flow-sensitive element (Shown in position when no flow exists)

In the present device, an attempt has been made to overcome this disadvantage by providing an orifice with a variable area. The diagram illustrates the principle of the flow-sensing element. The pressure drop across the orifice causes the movable member to move away from the needle, thus enlarging the effective orifice. At constant flow, a position of equilibrium is reached. An increase of pressure differential at the orifice causes the orifice area to increase further, until a new state of equilibrium is reached. Small particles of solid matter accumulating at the orifice cause an increase of pressure differential, and hence an increase of orifice area, which allows the obstructing matter to pass through the orifice. The system then returns to its normal state.

The moving member is arranged to actuate a microswitch, which controls the electric supplies to the apparatus protected. Since the amount of movement of the orifice varies with flow and also increases with any tendency to blockage, an additional microswitch or switches can be arranged to indicate when excessive movement occurs. The orifice movement can also be made to operate an indicator if required.

A further advantage of this device over fixed-orifice systems is that the device is undamaged by flow rates many times the normal operating value, since the opening of the orifice under such conditions prevents any great increase of pressure differential. By suitable shaping of the orifice and needle, a wide range of flow/movement characteristics can be obtained.

The device is the subject of a patent specification.

---

* Cox, B. C. *J. Sci. Instrum.*, 37, p. 148 (1960).

Method for increasing the range of a flowmeter

by C. C. Harris, B.Sc., Ph.D.,† Mining Department, University of Leeds

[*Note first received* 27 *July, and in final form* 5 *September*, 1960]

The convenience of internal resistance switching in multi-range electrical meters contrasts with the manual interchanging of calibrated orifices, which is necessary for wide-range fluid flow measurement with a single meter. With this in mind, a device sketched in the figure was constructed which, at the turn of a stopcock, provides two extensions to the range of a gas flowmeter. It is particularly useful for dealing with those special cases where the flow rate is so unusually high that the fluid threatens to be ejected from the manometer, or conversely where the flow is so low that the small displacement of manometer fluid impairs the accuracy of reading.

The flowmeter used in this Department is incorporated in a gas permeability apparatus for specific surface area measurement. General information and a bibliography has been given by Orr and Dallavalle.⁽¹⁾ Actual dimensions of the flowmeter are not given here because they will be of little value without details of the complete apparatus; this will be published in due course.

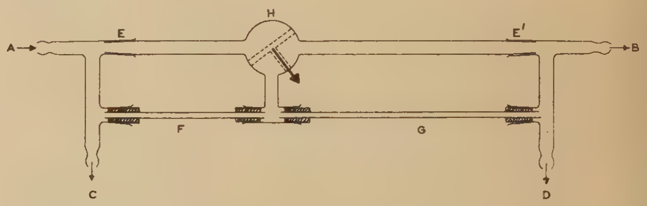

Diagrammatic arrangement of capillary resistances in flowmeter (not to scale)

AB, direction of flow; *C*, to high-pressure manometer; *D*, to low-pressure manometer; *E*, *E*′, standard joints; *F*, *G*, capillary resistances; *H*, three-way stopcock

The resistances *F* and *G* (see Figure) should be in the ratio of about 1 : 2, and the higher resistance should be chosen to cover most of the flow rates normally encountered. Benton⁽²⁾ has given generally accepted design details for gas flowmeters covering small rates of flow. If necessary, calibrated flowmeter capillaries can be purchased. Thus, according to the position of the stopcock *H* the flowpath may pass through: (*a*) the lower resistance for the higher flow rates (→); (*b*) the higher resistance for normal flow rates (←); (*c*) both resistances in series for the lowest flow rates (tap off). The resistances may also be by-passed (↑ or ↓) for zero adjustment. The true flow rate is obtained from a calibration chart of flow against pressure differential. This may be performed by displacement over water,(3) or with a gas meter of the Boys bell type. Alternatively, Barr(4) has described a soap film method.

---

† Now at Mines Department, Columbia University, New York, U.S.A.

This simple arrangement of a single three-way stopcock giving series coupling seems capable of further development by the use of additional components. It is also possible to employ parallel-coupled resistances as described by Harris(5) in connexion with rotameters.

REFERENCES

(1) Orr, C. C., and Dallavalle, J. M. *Fine Particle Measurement* (New York: Macmillan, 1959).
(2) Benton, A. F. *Industr. Engng Chem.*, **11**, p. 623 (1919).
(3) *Brit. Stand.* 146 : 1958; 915 : 1947; 1370 : 1958.
(4) Barr, G. *J. Sci. Instrum.*, **11**, p. 321 (1934).
(5) Harris, C. C. *Brit. Chem. Engng.*, **5**, p. 735 (1960).

CORRESPONDENCE

Measurement of tellurium vapour pressure using electrical discharges

During the investigation of the gallium tellurium phase diagram,(1) it was thought necessary to have a method of measuring millimetric pressures of tellurium vapour. To this end an electrical discharge method was investigated.

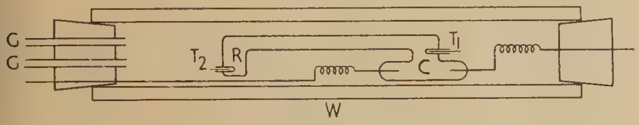

Fig. 1. Apparatus for measuring millimetric pressures of tellurium vapour

C, discharge chamber; *G*, gas inlet and outlet; *R*, tellurium reservoir; T_1, T_2, thermocouples; *W*, furnace

The silica apparatus used is shown in Fig. 1. This consists of a discharge chamber having electrodes of tungsten with 4 mm diameter hemispherical ends. These electrodes were sealed through the silica by means of W10 glass seals. The hemispherical ends were 2 cm apart. The discharge chamber was connected as shown to the tellurium reservoir, which was eventually made the coolest part of the system and used to control the tellurium pressure in the system. Before loading the apparatus was baked under a vacuum of about 5×10^{-6} mm Hg. No chemical cleaning was attempted in order to avoid pitting of the carefully polished electrodes.

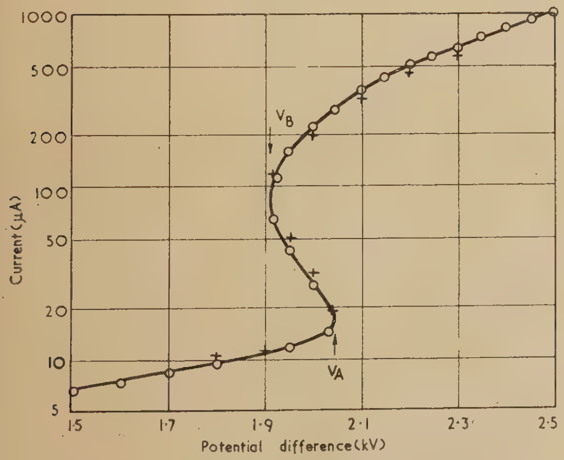

Fig. 2. Typical current/voltage characteristic
Discharge chamber at 762° C. Pressure 11·9 mm
+ = current increasing; ○ = current decreasing

Tellurium (99·999% Mining and Chemical Products Ltd.) which had been etched with concentrated hydrochloric acid and rinsed in alcohol to remove the surface film of TeO_2 was loaded into the apparatus which was then evacuated to about 10^{-6} mm Hg and sealed off. Nickel h.t. leads were connected to the electrodes by spot welding and the apparatus loaded into the two-temperature furnace as shown.

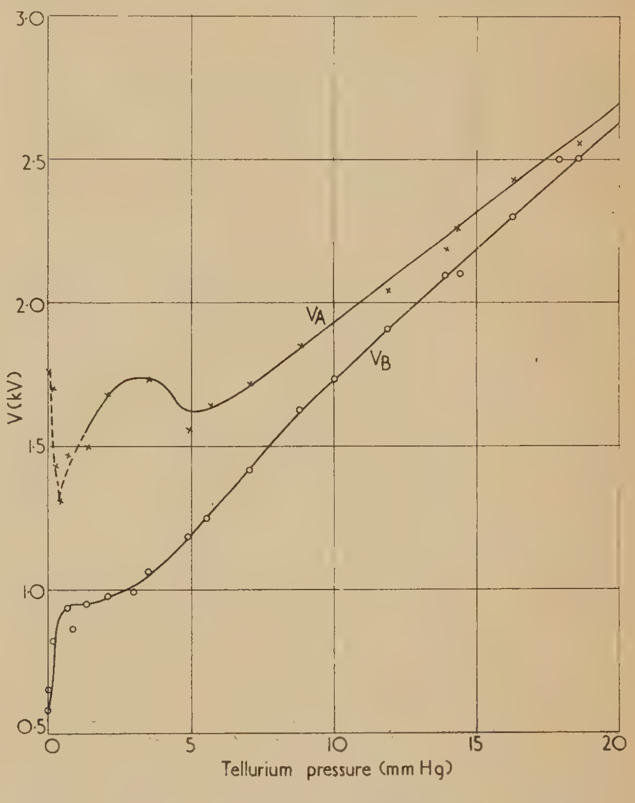

Fig. 3. The variation of V_A and V_B with pressure. Chamber at 762° C

Current/voltage characteristics of the form shown in Fig. 2 were obtained. A plot of the values of V_A and V_B (as defined in Fig. 2) against pressure at 762° C is given in Fig. 3. Similar results were obtained at other temperatures. For pressures greater than 8 mm and temperatures between

700 and 800° C, it was possible to express the experimental results by

$$V_A = (8{\cdot}3 \pm 0{\cdot}1) \times 10^{-4}\, T + (90{\cdot}4 \pm 0{\cdot}4)\frac{p}{T}$$

$$V_B = (1{\cdot}60 \pm 0{\cdot}02) \times 10^{-3}\, T + (75{\cdot}0 \pm 0{\cdot}3)\frac{p}{T}$$

where V is in kilovolts, T is the absolute temperature and p is the pressure in millimetres of mercury calculated from the reservoir temperature using the figures of Machol and Westrum.(2)

The form of the V_A curves at pressures less than 8 mm is probably accounted for by non-uniform field in the discharge.

The method described could be used to measure tellurium vapour pressures from 3 mm up to about 40 mm, and has the advantage that the pressure measuring device can be totally enclosed in a furnace.

The assistance of Mr. E. M. N. Baldwin in the performance of the experiments is gratefully acknowledged, as are many helpful discussions with Mr. G. Weston.

Mullard Research Laboratories,
Salfords,
near Redhill, Surrey.

J. C. Brice

[2 *May*, 1960]

REFERENCES

(1) Newman, P. C., Brice, J. C., and Wright, H. C. *Philips Res. Rep.* To be published.

(2) Machol, R. E., and Westrum, E. F. *J. Amer. Chem. Soc.*, **80**, p. 2950 (1958).

NOTES AND NEWS

New instruments, materials and tools

The Editor invites manufacturers of instruments and light machine tools to keep her informed of their new or improved products. The Institute of Physics and the Physical Society assumes no responsibility for the statements given below: information for these has been taken from literature supplied.

Letter cutting and profiling pantograph machines. Taylor, Taylor and Hobson Ltd., Stoughton Street, Leicester.

The model "A" bench pantograph machine has very many of the facilities of a floor-mounted machine. It is said to be unique in having a pantograph capable of 1 to 1 copying as well as reductions down to 16 to 1. The copyholder and copy letters are interchangeable with those on all other Taylor–Hobson machines. The whole head can be raised 4 in. (101 mm) from table level to accommodate thick work. A work-table 16 × 8 in. (406 × 203 mm) with four tee slots is provided, together with two work-holding clamps.

Generally taper shank cutters are used, but a spindle to take parallel shank cutters may be had on request. A wide range of accessories is available, including copy letters in varying styles, sizes and languages, forming attachment, formers, presser foot for engraving uneven surfaces, extension table, electric etching devices and fillers.

A newly-developed, floor-pedestal machine is the model "D" pantograph machine, of robust construction, with special attention to all pivot and linkage joints to ensure long life (mostly employing ball bearings).

The pantograph is capable of 1 to 1 copying as well as reductions down to 16 to 1. An area 9 × 4½ in. (230 × 115 mm) can be covered at 1 to 1. Eight spindle speeds are provided ranging from 2730 to 18 000 r.p.m. The copyholders and copy are interchangeable with those on all other Taylor–Hobson pantograph machines. A spindle for either taper shank or parallel shank cutters can be supplied, English or metric collets being available.

The deep throat and slide rest enables a large range of work sizes to be engraved or machined; for example, the centre of a 33½ in. (850 mm) disk can be engraved, and work-pieces 11¼ in. (285 mm) high can be accepted between the cutter point and table surface.

Accessories available with the machine include a wide range of copy sizes and styles, a forming attachment and formers, presser foot, extension table, electric etching devices, dividing head, circular table and fillers of various colours.

The machine is suitable not only for engraving but also for many light profiling operations.

The model "JH" engraver/miller is a larger capacity pantograph machine of rugged design with preloaded ball-bearing joints to the pantograph and linkage.

The pantograph is designed to be compact and also have a large coverage—for example, a rectangle 14¼ × 7⅛ in. (362 × 181 mm) at 1 to 1 and corresponding reductions down to 50 to 1. Large plates can be marked and the centre of a 42 in. (1066 mm) disk can be reached, also work-pieces 12 in. (305 mm) high can be accepted under the cutter.

Graduated dials in either English or metric scales are provided for the machine slide handwheels.

The spindle has eight speeds up to 18 000 r.p.m., and will accept parallel or taper shank cutters.

Attachments available include a light milling bracket, forming attachment, dividing head, circular table and a wide range of copy letter styles.

The model "JR" copying, profiling, routing and milling machine is a modest-priced vertical milling machine designed for reproducing any number of further pieces from an existing piece or template by a hand-controlled 3 to 1 lever mechanism guiding the template around a stylus simultaneously guiding the work-piece around the cutter.

The ball-bearing cutter spindle is mounted in the vertical head alongside the stylus at 9 in. (228 mm) centres. Spindle and stylus can be raised and lowered coupled together or they may be disconnected.

Work-piece and template are also mounted side by side at 9 in. (228 mm) pitch on the duplicating table which is on ball slides in both the longitudinal and transverse directions. This duplicating table can be floated in any horizontal direction by a 3 to 1 pantograph lever, guiding the template around the stylus. The work-piece being mounted on the same table must now follow an identical path around the cutter, so ensuring faithful reproduction.

Optical-reading clinometer. Hilger and Watts Ltd., 98 St. Pancras Way, Camden Road, London, N.W.1.

The Hilger and Watts range of optical-reading clinometers has been extended by the introduction of the Microptic precision clinometer (TB 90), which reads direct to 1″, with estimation to 0·5″, over an angular range of 0–360°.

It is suitable for inspecting angular surfaces and gauges, for locating jigs and fixtures, and for setting inclinable tables on jig-boring machines and angular work on grinding and lapping machines. Inclinations are measured by reference to the horizontal plane, indicated by an incorporated spirit-level. Repetition of bubble settings to 1″ is ensured by an optical coincidence-reading system and a slow-motion setting control.

The circular glass scale is totally enclosed and the micrometer microscope eliminates any eccentricity effects in the circle by automatically averaging sub-divisions made on two sides of the circle. The microscope eyepiece is inclined at an angle of 45° and is rotatable for convenience in viewing.

The steel base of the instrument is lapped, with two sides square to each other for reference purposes. Three lapped supports on the back of the clinometer enable it to be used in the horizontal position. Optional accessories are a work-table (TB 116) for measuring angular displacements of small parts, and an adjustable reflector (TB 117) which, in conjunction with an autocollimator, can be used for setting out angles. Both accessories are interchangeable with the spirit-level unit.

The microscope-reading system and the spirit-level are illuminated by separate low-voltage lamps. A transformer for 110/250 V a.c. input is available. The instrument is 9 in. long, 6 in. wide and 12 in. high. It weighs 19 lb.

Other optical-reading clinometers in the range include the TB 100 and TB 104, with direct reading to 10″ and 10′ respectively.

Electron diffraction camera. H. Tinsley and Co. Ltd., Werndee Hall, South Norwood, London, S.E.25.

The KD3 electron diffraction camera, manufactured by the Swiss firm of Trüb Täuber, and distributed in the United Kingdom by Tinsley and Co., is a general-purpose instrument using a cold-cathode electron gun operating over the voltage range 20–50 kV. Diffraction patterns can be observed on a fluorescent screen, or recorded on photographic plates or films. A special motor-driven device permits the continuous recording of structural changes as a function of temperature of the object.

The specimen can be etched under vacuum by ionic etching bombardment. A special ion gun of high current density with seven beams is used for this purpose. It is of great importance in this type of investigation to be able to observe the changes in the diffraction pattern as successive layers of the specimen are etched away. By operating the ion gun simultaneously with the moving film, the progressively changing surface structural pattern may be recorded.

The basic equipment permits recording of both transmission and reflexion patterns at room temperature. The accessories provided consist of a specimen holder for heating the object up to 900° C, and a device for cooling it to low temperatures. The specimen holders can move the object into any desired position and rotate it about its axis during operation without breaking the vacuum. For direct viewing of the specimen, an optical microscope is available with a magnification of ×200.

When working with insulators, the effect of charging up of the specimen can be eliminated by the use of slow electrons from a separate discharge device. Provision is made for the evaporation of materials in the camera. The electron optical system makes possible selected area diffraction as well as magnification of the object up to about ×70.

Compressed air dehydrating unit. Pathfinder Automatic Defroster Co., Hersham, Surrey.

This machine is claimed to supply an uninterrupted flow of air to almost zero humidity, and to clean the air to 0·5 μ; it is portable and capable of operating continually over long periods of time. The applications are in the drying of films, hospital conditions and many industrial processes.

The process is essentially one of refrigeration of the available air and not by the use of supplied cylinders. Two horizontal two-stage compressors of the oil-free carbon ring type are used for pressures up to 60 lb/in^2; for the lower pressures a fully rotary compressor is used. A cooling fan is used before the filtered air is supplied to the compressor. The subsequently cooled air is used with a heat exchanger to cool the air before the compressors. The air from the compressor is also cooled by a heat exchanger with the ambient temperature, and then it is passed to the dehydrating unit, where it is cooled to −40° C and then re-heated. By controlling the temperature at which this unit operates it is possible to obtain any given humidity in the final air, since the process is to remove the ice from the cold air, and then re-heat (the air retaining only that water vapour which was still vapour at the coldest temperature).

The dehydration unit operates with the refrigerant monochlorodifluormethane and is capable of giving a continuous air-outlet dew-point temperature of better than −40° C for a period greater than 12 h. It is constructed in duplicate, so enabling a continuous cycle to be performed indefinitely. The ice produced by the process is dispersed by an automatic defroster. Even if defrosting fails in both sides of the apparatus the machine will function for 12 h before defrosting becomes necessary.

The condensate formed during defrosting is carried away by an automatic drain, and an important feature is that any oil or solid particles which have passed the initial filter are trapped in the ice field and removed by the drain. The drain also provides a reservoir of air, which is washed and therefore cleaner than the air of the room, for subsequent use by the compressors.

The entire equipment works automatically on a time-controlled basis and occupies less than 3 ft square for the base, under 6 ft in height; it is supported on castors.

Semi-conductor convertors. Transipack Electronic Engineers, 29 Burnt Ash Hill, London, S.E.12.

Transipack semi-conductor convertors can transform d.c. voltages of 6, 12, 24 or 28 V into higher d.c. or a.c. voltages without the mechanical disadvantages inherent in rotating or vibrating systems. Hermetically-sealed units and open types are available. They are claimed to be suitable for replacing all types of rotary convertors and vibrator power packs used for the operation of electronic equipment. A complete range of convertors is available varying from sub-miniature 2 W units to 30 W and 100 W models up to the kilowatt region. The Transipack is quiet in operation and requires no additional cooling. The regulation of the unit is good, and the circuit is automatically protected against overload, including a short circuit at the output.

New books

British instruments, directory and buyers' guide, 1960. (London: Scientific Instrument Manufacturers' Association of Great Britain, and United Science Press Ltd., 1960.) Pp. 635. Price 45*s*.

The Scientific Instrument Manufacturers' Association aims to provide a central organization to further the interests of the whole industry and to promote collaboration between member firms. The second edition of the "directory and buyers' guide" has been revised and brought up to date. It contains brief notes on the member firms and the association itself and is afterwards divided into nine sections. The first is a list of specifications directly bearing on instrument matters issued by official bodies. This is followed by a list of consultants, engineers and installers of instrumentation schemes, a list of firms manufacturing single or small batches of instruments to a client's order, and a classified index of products. The five following sections consist of a four-language glossary of headings used in the index of products (in English, French, German and Spanish), an alphabetical list of instrument and component manufacturers with overseas agents, trade names, and manufacturers' announcements.

Sector-focused cyclotrons. (Nuclear Science Series, No. 26.) Edited by F. T. HOWARD. (Washington: National Academy of Sciences—National Research Council, Publication 656, 1959.) Pp. xii + 291. Price $2.50.

The book, which comprises the published proceedings of an informal conference held at Seal Island, Georgia, U.S.A., is divided into six sections corresponding to sessions of the conference. These are headed as follows: orbit calculations and magnetic field design; realization of required field configurations and model magnet work; radio frequency systems; beam quality; beam extraction; external focusing systems, instrumentation, operational experience, and summary of outstanding problems. The book also includes an appendix entitled "Tabulation of sector-focused cyclotrons".

Torsion devices. By P. J. GEARY. (Chislehurst: British Scientific Instrument Research Association, 1960.) Pp. xii + 142. Price 21*s*.

John Michell's invention of the torsion balance in the eighteenth century was a turning-point in the history of scientific instruments. It is the best known of all elastic movements in mechanical design, and it is appropriately the major subject of the latest B.S.I.R.A. Survey of Instrument Parts. This Survey is a valuable compilation of references, together with very useful chapters summarizing both theory and practice. While the torsion balance is as alive as ever, and is even tending to replace the jewelled bearings in shock-proof electrical meters, the B.S.I.R.A. Survey is not confined to the balance alone. Sections on bifilar and trifilar suspensions, coiled torsion suspensions, torsion hinges, and torsion magnifying devices add to the value of the book. The instrument world will be much indebted to the author and to B.S.I.R.A. for the trouble taken in this compilation.

R. V. JONES

F. Friedrichs: Das Glas im chemischen Laboratorium. 3rd revised edition by J. FRIEDRICHS. (Berlin: Springer-Verlag, 1960.) Pp. viii + 154. Price DM18.

This book is concerned almost entirely with the description of standard pieces of glass chemical apparatus. Eighty pages are devoted to descriptions of apparatus such as extraction apparatus, burettes, pyknometers, thermometers, apparatus for the estimation of CO_2 H_2O nitrogen and sulphur to give a few examples. It would appear that where a DIN standard exists reference is made to it.

A short section dealing with the properties of glass is written in general terms and contains no numerical data. No compositions are given for the different glasses, these are referred to as Pyrex, Jena type 20 and so on. The few pages dealing with glass-blowing contain some interesting diagrams.

As the title suggests this book would probably be useful as a reference book in a chemical laboratory.

R. W. DOUGLAS

The relay protection of high voltage networks. By G. I ATABEKOV. (Oxford: Pergamon Press Ltd., 1960.) Pp. xii + 564. Price 84*s*.

This translation of Professor Atabekov's book should be of particular interest to Western protective engineers, since it shows that the Russian approach to protective engineering is quite orthodox but characterized by a sound theoretical and practical approach which has been the result of many years of careful research and experiment.

The book sets out to give the general principles underlying protective engineering and a complete analysis of the performance of the better-known protective systems and relays. It starts from the orthodox method of calculating short circuit currents by means of symmetrical components which is extended to cover transient phenomena, and follows with a comprehensive treatment of symmetrical component filters, and the vector locus method of estimating the performance of certain types of relays which is of particular value for distance and directional relays.

Seperate chapters are devoted to power directional relays distance protection, carrier protection, selection of the faulty phase in single-phase reclosure, differential protection, and systems for preventing incorrect operation of relays due to phase swinging and faults on the secondary windings of voltage transformers.

The author has succeeded in his object and produced a volume which will be of great value to all those concerned with system operation and design.

M. WATERS

Notes and comments

INDEXES AND BINDING ORDERS

The indexes and title-pages of this volume will be dispatched with the January 1961 issue of this *Journal*.

Orders and enquiries about binding this *Journal* should be sent direct to Messrs. E. A. Weeks and Son, 168 Gower Street, London, N.W.1 (EUSton 4674), and *not* to The Institute of Physics and The Physical Society.

The charge for binding is 22*s*. per Volume. Binding cases can be supplied for 13*s*. 6*d*. each.

Subscriptions for 1961 can now be received. See overleaf for full details.

Elections to The Institute of Physics and The Physical Society

The following elections have been made by the Board of The Institute of Physics and The Physical Society:

Fellows: D. J. Maclean, C. G. Morgan, H. Rose, W. A. Runciman.

Associates: R. M. Absalom, D. W. Berry, L. F. Bowles, M. Braden, N. K. Bridge, P. J. Brown, I. D. Campbell, A. V. Cohen, S. M. Crawford, E. Grunbaum, M. A. R. Gunston, M. E. Harper, H. C. Harrison, J. C. Higgins, A. Hogg, C. S. Hope, A. F. Hughes, R. Innes, Z. R. Jeffrey, A. M. Jessop, D. E. N. King, J. E. Knowles, E. J. Langham, D. F. Leach, A. Levy, P. A. Mayer, E. G. Muirhead, B. Peters, J. M. Rollett, R. L. Rouse, N. H. Saunders, J. E. Shaw, B. J. Shepstone, P. F. Smith, K. U. Snowden, P. J. Stevenson, A. V. Stockley, R. W. Strong, B. Stuttard, D. E. Swan, H. F. Symmons, H. H. Thies, R. Webster, M. J. Wheeler, B. J. Williams.

One hundred and eighteen Graduates, fifty-three Students and one Subscriber were also elected.

Annual Exhibition of Scientific Instruments and Apparatus

The 45th Annual Exhibition of Scientific Instruments and Apparatus will be the first to be organized by the recently amalgamated body of The Institute of Physics and The Physical Society. It is to be held, as usual, in the Old and New Halls of the Royal Horticultural Society from 16th–20th January 1961 (inclusive).

Entrance to the exhibition is by ticket only and these may be obtained free of charge, from the offices of the Institute and Society, 47 Belgrave Square, London, S.W.1. The *Handbook of Scientific Instruments and Apparatus*, published in connexion with the exhibition, is also available, price 6*s*., by post 8*s*.

Symposium on Electrical Contacts

The Institute of Physics and The Physical Society announces that it is arranging a symposium on 'Electrical Contacts' in collaboration with The Institution of Electrical Engineers which will take place in the Brunel College of Technology, London, from 5th–7th April 1961.

The symposium is intended mainly for persons concerned with the design and improvement of contacts. There will be a small informal exhibition which will be open during the symposium to those attending the meetings. Abstracts (but not preprints) will be circulated before the symposium, the proceedings of which will not be published in full.

All communications regarding the symposium should be sent to the Secretary, The Institute of Physics and The Physical Society, 47 Belgrave Square, London, S.W.1.

British Conference on Automation and Computation

In 1957 some twenty bodies of the learned society type with interests in the field of automation or in its social and economic implications, set up a central organization, called the British Conference on Automation and Computation, to provide more effective liaison between the interested bodies. However, at meetings held on 10 October, 1960, it was agreed that the Conference would operate more effectively under a central Council and accordingly it was agreed to merge the three autonomous Groups of the Conference. At the first (constitutive) meeting of the Council of the reconstituted B.C.A.C. which followed, it was announced that thirty-two Societies had transferred their membership to the new body, including The Institute of Physics and The Physical Society.

The following were adopted as objects of the Conference: (*a*) To stimulate interest in, to spread knowledge of and to foster the development and applications of automatic control and computation. (*b*) To afford a common meeting ground for the adhering organizations whereby such of their activities as fall within the purview of the Conference can, if they so desire, be co-ordinated and extended. (*c*) To encourage and, if desired, to co-ordinate the presentation at International Conferences of British papers whose subjects fall within the purview of the Conference. (*d*) To maintain, as may be desirable, liaison with other countries which support such international conferences.

Ten representatives from different member organizations were elected to serve with the Honorary Officers as the Executive Committee of the Conference.

At this meeting of the new B.C.A.C. Council, the members of the Conference, through their representatives, made arrangements under which the B.C.A.C. would act as a clearing house for information on their activities in its field and confirmed that details of these should continue to be published in the B.C.A.C. *Bulletin*, copies of which may be ordered from the Secretary of The Institution of Mechanical Engineers by whom the *Bulletin* is published.

The Council re-affirmed that the predominant function of the B.C.A.C. would be to foster action in the fields of automatic control and computation through individual and joint activities on the part of its member organizations.

User experience of electronics in industry

The third number of the *Bulletin of the Electronic Forum for Industry*, recently published, consists of a full report of the twelve papers presented at the E.F.F.I. conference on "User experience of electronics in industry" which was held at the Instruments, Electronics and Automation Exhibition, Olympia, last May.

The 80-page Report covers the three conference sessions—Electronics in data processing, Electronics in factory applications, and Electronics in instrumentation and control.

The individual papers are entitled: A maintenance stores computer application; A production control application; An insurance application; A stock control application; Electronic machine tool control at work; The development of numerically controlled machine tools; Electronics in the steel industry; Induction heating at Ford's; Instrumentation; The uses of electronics in handling and proportioning; the continuous control of machines; Remote control and telemetry.

Copies of this special number of the E.F.F.I. *Bulletin* are obtainable from the Electronic Forum for Industry, 11 Green Street, Mayfair, London, W.1 (price: 21*s*. each, post free).

Nuclear Engineering Abstracts

We have received a new abstracting journal published under the above title which, as its title suggests, deals mainly with nuclear engineering subjects. Its purpose is to present and record developments and trends reflected in the current technical literature and it is mainly designed for engineers, scientists, manufacturers and industrialists either engaged in or connected with the nuclear engineering field.

The abstracts are collected together under one or more of the following main subject headings: *Science and engineering*—General; *Fission:* Research techniques, instrumentation and testing methods, Plant and auxiliaries, Subsidiary processing and handling; *Fusion:* Plant and auxiliaries, Subsidiary processing and handling; *Radiation*, Special associated subjects.

The Editor is Mr. H. L. J. Burgess, former Editor of *Vacuum*, and the journal is published by Silver End Documentary Publications, Ltd., 9–11, Tottenham Street, W.1. The journal is to be issued quarterly and the annual subscription is £6 6*s*. ($18.50), single copies £1 12*s*. 6*d*. ($4.75).

The Physics of Fluids

The American Institute of Physics announces that its journal, *The Physics of Fluids*, will in future appear monthly, instead of bimonthly, effective with Volume IV (1961).

By doubling the number of issues it is hoped that it will be possible to arrange for prompter reporting of the results of research on the structure, statistical mechanics and general physics of gases, liquids, plasmas and other fluids. A before, the journal will continue to offer papers on certai basic aspects of physics of fluids bordering geophysics astrophysics and related fields.

Further information can be obtained from the American Institute of Physics, 335 East 45th Street, New York 17 N.Y., U.S.A.

Editorial and publications sales offices

Readers are requested to note that all correspondence of an editorial nature should now be sent to the following address:

The Editor and Deputy Secretary,
The Institute of Physics and The Physical
Society, 1 Lowther Gardens, Prince Consort
Road, London, S.W.7 (Kensington 0048).

Correspondence concerning subscriptions, missing journals, and sales of publications should be sent to:

The Institute of Physics and The Physical
Society, 47 Belgrave Square, London, S.W.1
(Belgravia 6111).

British Journal of Applied Physics

Contents of the December issue

CONFERENCE REPORT

Summarized proceedings of a conference on applied spectroscopy—Seascale June 1960. By L. Bovey and F. T. Birks.

PAPERS

Deposition of *Lycopodium* spores upon glass slides exposed in a wind tunnel By C. N. Davies.

Some remarks on the conduction current in insulating liquids. By K. Sugita, T. Sato and Y. Toriyama.

Comparison of X-ray and nuclear magnetic resonance measurements of crystallinity in polyethylene terephthalate. By G. Farrow and I. M. Ward.

Image formation by electron bonbardment of metal targets. By E. H. Hirsch.

Measurement of hardness at very high temperatures. By L. M. Fitzgerald.

CORRESPONDENCE

New technique for the direct investigation of fission events. From J. J. Kelsch, O. F. Kammerer and P. A. Buhl.

NOTES AND NEWS

Notes and comments

THIS *JOURNAL* is produced monthly by The Institute of Physics and The Physical Society, with the co-operation of the National Physical Laboratory. It deals with the principles, construction and use of scientific instruments. All rights reserved. Responsibility for the statements contained herein attaches only to the writers.

EDITORIAL MATTER. Communications concerning editorial matter should be addressed to the Editor, The Institute of Physics and The Physical Society, 1 Lowther Gardens, Prince Consort Road, London, S.W.7. (*Telephone:* Kensington 0048.) Prospective authors are invited to prepare their scripts in accordance with the *Notes for Authors*.

REPRODUCTION. The Institute of Physics and The Physical Society is a signatory to The Royal Society's Fair Copying Declaration. Details may be obtained upon application from The Royal Society, London, W.1.

ADVERTISEMENTS. Communications concerning advertisements should be addressed to the agents, Messrs. George Jackson (Fleet St.) Ltd., Cliffords Inn, Fleet Street, London, E.C.4. (*Telephone:* Holborn 3611–2.)

SUBSCRIPTION RATES. A new volume commences each January. The charge is £6 per volume ($17 U.S.A.), including index (post paid) payable in advance. Single parts, so far as available, may be purchased at 12*s*. 6*d*. each ($1.75 U.S.A.), post paid, cash with order. Orders should be sent to The Institute of Physics and The Physical Society, 47 Belgrave Square, London, S.W.1, or to any bookseller.

CLAIMS FOR MISSING JOURNALS. Claims from regular subscribers to this *Journal* for missing numbers will only be considered if received within 60 days of the date of mailing plus normal outward time of transit and time for lodging the claim. Losses attributable to failure to notify a change of address or to similar omissions will not be considered.

PRINTED IN GREAT BRITAIN BY UNWIN BROTHERS LIMITED, WOKING AND LONDON

INDEX TO VOLUME 37

SUBJECTS

(SA) denotes special article, (LN) laboratory notes, (C) correspondence, (NC) notes and comments

Aberration, Angular 95
Abrasive suspensions, Slow-feed dispenser for 36 (LN)
Absolute beta particle counting 201
Absorbing specimens with the three-beam interferometer, Measurement of the optical thickness of 417
Abstracts, Nuclear engineering 494 (NC)
Adapter, Valve and, for the grease-free connexion of glass sample tubes to a mass spectrometer inlet system 69 (LN)
Admittance bridge, R.F., for liquid-dielectric measurements 195
Agitating device, Simple, for partition experiments 222 (LN)
Air aspirator, pump-operated, Report on a 221 (LN)
Airglow photometer, Portable 54
Airspeed, ambient, Effect of, on efficiency of thermal-precipitator 182 (C)
Alarm, Liquid-level, using internally reflected light 489 (LN)
Alloys, very small specimens of, X-ray fluorescence method for determination of the transition-metal content in 394
α-active materials, thin sources of, Vacuum sublimation apparatus for preparation of 169
Aluminium wire seals for bakeable vacuum systems, Further experiences with 449
Amalgamation of The Institute of Physics and The Physical Society, The 368 (NC)
Ambient airspeed, Effect of, on efficiency of thermal-precipitator 182 (C)
Amplification, Parametric 1 (SA)
Amplifier
  integrating 31
  Logarithmic 457
  Tunable galvanometer 136
Analyser, Time, using a crystal-controlled trochotron tube 289
Analysis, high-speed thermal, Gas-quenching apparatus for 108 (LN)
Anemometer, Heat transport, of high stability 166
Anemometer, Transistor cup 189
Ångström's method, Measurement of thermal diffusivity of semiconductors by 349
Angular deflexion, Method of measuring the, in the dynamometer 81
Annual Report of The Institute of Physics, 1959 447 (NC)
Anthracene, Growth of single crystals of 242
Apertures, long narrow, Flap-valve for 439 (LN)
Apparatus for measurement of sorption of reactive, condensable vapours up to 350° C 432
Apparatus, scientific instruments and, Annual exhibition of 493 (NC)
Apple cell counter 414
Arsenide, gallium, Apparatus for the floating-zone refining of 410
Aspirator, pump-operated air, Report on a 221 (LN)
A.S.T.M. Powder Data File—5, Comments on the 183 (C)
Atmosphere, Monitor for the quantitative determination of beryllium in the 466
Atmospheres, controlled, Furnace for the uniform heating and mixing of powders in 397 (LN)
Atomizer, Wax-, for producing spherical dust particles 123
Auto-focus range-finder, Improved design for an 356
Automatic control of an oscilloscope camera 282
Automation and Computation, British Conference on 493 (NC)

Babinet compensator, Accurate measurements of phase difference with the 278
Backgrounds, Geiger counter 475
Bakeable bellows-type differential pressure manometer 251 (LN)
Bakeable vacuum systems, aluminium wire seals for, Further experiences with 449
Baked high vacuum system, Leak detection in 306 (LN)
Balance, Accurate direct-reading hydrostatic 113
Balance, Simple force, for drag measurements 487 (LN)
Balloon flights, Hot tube nylon cord cutter for 440 (LN)
Band spectra of solids 460
Bank, electrolytic capacitor, Production of a pulsed magnetic field using an 378
Barometer, Primary standard, of range 0 to 1200 mb 160
Beam method for the measurement of internal friction 208
Bellows-type differential pressure manometer, Bakeable 251 (LN)
Beryllium, Monitor for the quantitative determination of, in the atmosphere 466
Beta particles, Use of a liquid scintillator counter for 201
Binary-to-decimal converter, Large storage 240

Books, New
  Adhesives guide 111
  Automatic titrators 367
  British glass industry, directory and buyers' guide, 7th edn. 366
  British instruments, directory and buyers' guide, 1960 494
  Cathode-ray tube and its applications, The 110
  Collection de l'A.N.R.T.: Études de pyrométrie pratique 446
  Diffraction gratings as measuring scales 446
  Electronic components handbook. Vol. 3 111
  Electronics for spectroscopists 367
  F. Friedrichs: Das Glas in chemischen Laboratorium. 3rd revised edition 492
  Health physics instrumentation 446
  Instrumentation in scientific research. Electrical input transducers 446
  Kleines Handbuch technischer Regelvergange 366
  Laboratory instruments. 2nd edn. 367
  Materials and techniques for electron tubes 366
  Photomicrography 152
  Process integration and instrumentation. Electricity and productivity series. No. 8 366
  Programming programme for the BESM computer 367
  Progress in semiconductors. Vol. 4 366
  Properties, physics and design of semiconductor devices, The 152
  Relay protection of high voltage networks, The 494
  Sector-focused cyclotrons. (*Nuclear science series, No.* 26) 494
  Techniques modernes et applications de la cryométrie 110
  Tools of biological research 111
  Torsion devices 494
  Zone refining and allied techniques 367
Boron 10
  concentration, natural, measurement of, Isotopic analysis of boron in boron trifluoride by mass spectrometry, and 323
  Isotopic analysis of, in boron trifluoride by mass spectrometry, and measurement of natural boron 10 concentration 323
  trifluoride, Isotopic analysis of boron in, by mass spectrometry, and measurement of natural boron 10 concentration 323
Bridge circuit, Compensated Wheatstone's, for gas-chromatographic catharometry 185
Bridge, R.F. admittance, for liquid-dielectric measurements 195
Bridges, Transformer, for use with resistance strain gauges and similar transducers 381
Bubble method for magnetic susceptibility of liquids 71 (LN)
Burner, High-temperature, for working silica 35 (LN)

- Burning rates, accurate determination of, Simple device for use with platform weighbridges in the 45

- Cadmium sulphide cells 190
- Calibrated reference leak 404
- Calorimeter, Recording, for the measurement of heats of wetting, mixing, or solution 60
- Camera
  - oscilloscope, Some modifications to an, and the construction of a control unit 282
  - Simple high temperature X-ray 305 (LN)
  - X-ray, High vacuum high temperature 273
  - X-ray powder, Oscillating flat-specimen holder for an 399 (LN)
- Cameras, Improved design for an auto-focus range-finder for 356
- Capacitance extensometer for semi-rigid materials 93
- Capacitance gauge, Low-compliance diaphragm-, for measurement of liquid pressures of the order of 1 in. water 401
- Capacitor bank, electrolytic, Production of a pulsed magnetic field using an 378
- Capacitor, Design of a single electrode, for use with moisture meters and similar apparatus 77
- Carbide coding matrix, silicon, An electroluminescent digital indicator with a 47
- Carbon 397 (LN)
- Carbon arc 306 (LN)
- Catharometry, gas-chromatographic, Compensated Wheatstone's bridge circuit for 185
- Cavity resonators 56
- Cell
  - Modified cylindrical, for the microelectrophoresis of suspended particles 248 (LN)
  - Rand soil-pressure, for low pressures, high accuracy and long-term stability 193
  - weatherproofed photovoltaic, Cosine correction of a 359 (LN)
- Ceramic vessels, quartz and, used for zone melting, Pyrolytic coating of 397 (LN)
- Charcoal/methanol wetting 60
- Charge, Measurement of space density of, in flowing liquids 332
- Chart, Simple continuous, and integrating device for a Joyce–Loebl microdensitometer Mk. I 347
- Charts, mass spectrometer, Vernier scale arrangement for the measurement of peak heights on 358 (LN)
- Chlorine, Cut-off for the vacuum manipulation of 303 (LN)
- Chopper, radiation, in a preferred position, Simple method for stopping a 439 (LN)
- Chromatographic catharometry, gas, Compensated Wheatstone's bridge circuit for 185
- Chromatography, gas, Automatic gas-sampling device for 253 (LN)
- Coded scale, Position transducer using a divided circle 125
- Coding matrix, silicon carbide, An electroluminescent digital indicator with a 47
- *Coke and chemistry, U.S.S.R.* 224 (NC)
- Cold hearth melting, New method of 177 (LN)
- Cold traps, Simple refrigerant level controller for 67 (LN)
- Collagen fibres, Apparatus designed for work on 25
- Colorimetry 304 (LN)
- Comité Consultatif de Thermométrie. Proceedings of 112 (NC)
- Comparator, Photoelectric, for Rayleigh fringe electrophoresis patterns 190
- Compensator, Babinet, Accurate measurements of phase differences with the 278
- Compliance diaphragm-capacitance gauge, Low-, for measurement of liquid pressures of the order of 1 in. water 401
- Computation, Automation and, British Conference on 493 (NC)
- Computer, Digito-analogue, for solving linear simultaneous equations and related problems 419
- Conference, British, on Automation and Computation 493 (NC)
- Conference on irreversibility and statistical mechanics 447 (NC)
- *Contemporary physics* 184 (NC)
- Control
  - close temperature, Temperature regulator for 285
- Control—continued
  - system, Temperature-, for use with a spectrophotometer 478
  - temperature, Simple method of 69 (LN)
  - unit, Some modifications to an oscilloscope camera, and the construction of a 282
- Controller, Simple refrigerant level, for cold traps 67 (LN)
- Cooling, inadequate, Protection of diffusion pumps against 148 (LN)
- Copper, Apparatus for the zone refining of 175
- Copper pipe, Welding, to stainless-steel flanges in a laboratory workshop 219 (LN)
- Cord cutter, Hot tube nylon, for balloon flights 440 (LN)
- Cosine correction of a weatherproofed photovoltaic cell 359 (LN)
- Counter
  - backgrounds, Geiger 475
  - diffractometer, Automatically operated balanced filters for 178 (LN)
  - liquid scintillator, for beta particles, Use of a 201
  - proportional, Electronic apparatus for the study of X-rays with 388
  - Rapid, for small particles in suspension 414
- Counters, halogen-quenched Geiger, Reduction of dead-time in 336
- Counting circuits 303 (LN)
- *Cryogenics* 448 (NC)
- Cryostat for use with liquid hydrogen, X-ray diffraction by single crystals at low temperatures: a 41
- Cryostat, Liquid-nitrogen, for single-crystal X-ray diffraction 238
- Crystal-controlled trochotron tube, Time analyser using a 289
- Crystal oscillation mechanism for use with automatic X-ray diffractometers 68 (LN)
- Crystallographic supplies, Index of 112 (NC)
- Crystals of anthracene, single, Growth of 242
- Crystals, X-ray diffraction by single, at low temperatures: a cryostat for use with liquid hydrogen 41
- Cup, Transistor, anemometer 189
- Current pulses, millimicrosecond, Production of, using a pressurized spark gap 385
- Currents, micro-microampere low-energy electron, Wide-band detector for 246
- Cyclic shearing interferometer 374
- Cyclic strain, Measurement of 138, 255 (C)
- Cyclindrical cell, Modified, for the microelectrophoresis of suspended particles 248 (LN)

- Dash pot, Two-way oil-filled 180 (LN)
- Data File—5, A.S.T.M. Powder, Comments on the 183 (C)
- Data processing 269, 425
- Daylight factor meter 316
- Dead-time in halogen-quenched Geiger counters, Reduction of 336
- Decantation, Automatic, for routine sub-sieve sizing 120
- Decimal converter, binary-to-, Large storage 240
- Deflexion, angular, Method of measuring the, in the dynamometer 81
- Deformation at low temperatures 180 (LN)
- Demodulator, Simple photoelectric 107 (LN)
- Demountable glass–metal seals, Insulated terminals for high-vacuum systems, using 358 (LN)
- Densities, low optical, Densitometer wedge for measurements at 33
- Densitometer wedge for measurements at low optical densities 33
- Density
  - measurements, optical, Test tube adaptor for use in 304 (LN)
  - of glass fibres, Determination of the 148 (LN)
  - of liquids, Accurate measurement of 113
  - recorder, Improved smoke 144
- Deposition of a thin film, Instrument for recording the resistance during the 143
- Depth gauge, Capacitor type 141
- Design criterion for correction of parallax at the best focus for definition 95

Designs, Optical 95
Detector
  displacement, Novel, and its application in recording thermobalance 297 (*erratum*) 448 (NC)
  Electronic leak 147 (LN)
  Lens mass-spectrometer leak 404
  Simple, for small leaks using a thoriated tungsten emitter with oxygen as probe gas 306 (LN)
  Wide-band, for micro-microampere low-energy electron currents 246
Deuterium gas, Heavy-water electrolysis unit for generation of, provided with automatic switch-off and safety devices 352
Diaphragm-capacitance gauge, Low-compliance, for measurement of liquid pressures of the order of 1 in. water 401
Dice, Production of islands and, in semiconductor slices with an ultrasonic drill 263
Dielectric measurements, liquid-, R.F. admittance bridge for 195
Dielectric relaxation 195
Differential pressure manometer, Bakeable bellows-type 251 (LN)
Diffraction
  electron, electron microscopy and, Tilting and rotating specimen stage for 199
  patterns, measuring X-ray powder, Improved eye-piece graticule for 134
  photographs, X-ray, Influence of protective paper on 223 (C)
  single-crystal X-ray, Liquid-nitrogen cryostat for 238
  X-ray, by singl ecrystals at low temperatures; a cryostat for use with liquid hydrogen 41
Diffractometer
  counter, Automatically operated balanced filters for 178 (LN)
  Low-angle Geiger, for use with monochromatic radiation 132
  rapid-scanning X-ray, Design and performance of a 6
Diffractometers, automatic X-ray, Crystal oscillation mechanism for use with 68 (LN)
Diffractometry, high temperature X-ray, Vacuum furnace for 172
Diffuse-light integrator 70 (LN)
Diffuse X-ray reflexions 64
Diffusion pumps, Protection of, against inadequate cooling 148 (LN)
Diffusivity, thermal, of semiconductors by Ångström's method, Measurement of 349
Digital indicator, An electroluminescent, with a silicon carbide coding matrix 47
Digital temperature recorder, Multipoint, with punched tape output 269
Digito-analogue computer for solving linear simultaneous equations and related problems 419
Direct-reading hydrostatic balance, Accurate 113
Discharges, electrical, Measuring of tellurium vapour pressure using 489 (C)
Discharges, intense gas, Swept Langmuir probe system for 457
Dispenser, Slow-feed, for abrasive suspensions 36 (LN)
Displacement detector, Novel, and its application in a recording thermobalance 297 (*erratum*) 448 (NC)
Dosage meter, Simple, for high-intensity thermal radiation 73
Drag measurements, Simple force balance for 487 (LN)
Drill, an ultrasonic, Production of islands and dice in semiconductor slices with 263
Droplet size 103
Dust measurement 182 (C)
Dust particles, producing spherical, Wax-atomizer for 123
Dynamometer, Method of measuring the angular deflexion in a 81

Eigenvalue problems, Analogue computer for solving 419
Elastic solids, The torsiometer—an instrument for the study of gels considered as 292
Elections to The Institute of Physics 256 (NC), 312 (NC), 447 (NC)
Elections to The Institute of Physics and The Physical Society 493 (NC)
Electrical
  breakdown of gases at high pressure 385
  contacts, Symposium on 493 (NC)
  resistance, Instrument for recording 143
Electrode capacitor, Design of a single, for use with moisture meters and similar apparatus 77
Electroluminescent digital indicator, An, with a silicon carbide coding matrix 47
Electrolysis unit, Heavy-water, for generation of deuterium gas provided with automatic switch-off and safety devices 352
Electrolytic capacitor bank, Production of a pulsed magnetic field using an 378
Electromechanical low frequency oscillator 149 (LN)
Electromechanical registers, Transistor operation of 303 (LN)
Electrometer circuit, Two-valve 218 (LN)
Electrometer voltmeter, Portable 296
Electromicrobalance for weighing fibres, An 53
Electron
  currents, micro-microampere low-energy, Wide-band detector for 246
  microscope, Device for straining and fracturing thin foil specimens inside an 37 (LN)
  microscopy and electron diffraction, Tilting and rotating specimen stage for 199
  microscopy, Quantitative 33
  microscopy, Simple ultramicro-pipette for 103
  microscopy, transmission, Automatic polishing technique for electro-thinning metals for 216 (LN)
Electronic
  apparatus for the study of X-rays with proportional counter 388
  computing 425
  fluxmeter, An 31
  Guide, The 184 (NC)
Electronics in industry, User experience of 494 (NC)
Electrophoresis patterns, Rayleigh fringe, Photoelectric comparator for 190
Electro-thinning metals for transmission electron microscopy, Automatic polishing technique for 216 (LN)
Elutriator, Laboratory magnetic, for purification and isolation of ferrimagnetic mineral sands 212
Emissivity, Apparatus for investigating total hemispherical 84
Emitter, thoriated tungsten, with oxygen as probe gas, Simple detector for small leaks using a 306 (LN)
Emulsion fixing baths, nuclear, Automatic silver concentration control for 360 (LN)
Encapsulation of semiconductor devices, Equipment for the 197
Epoxy-resin joints for sealed-off, high-vacuum tubes 203
Exhibition, Annual, of Scientific Instruments and Apparatus 493 (NC)
Exhibition, The Physical Society's,—London, 1960 153 (SA)
Extensible tapes, very, Grips for tensile test on 181 (LN)
Extensometer for semi-rigid materials 93
Eye-piece graticule, Improved, for measuring X-ray powder diffraction patterns 134

Factor meter, Daylight 316
Fair Copying Declaration, The Royal Society's 112 (NC)
Ferrimagnetic mineral sands, Laboratory magnetic elutriator for purification and isolation of 212
Fibre surfaces, Technique for replicating, by rolling 210
Fibres
  density of glass, Determination of the 148 (LN)
  mechanical properties of, Apparatus for the measurement of the 25
  weighing, An electromicrobalance for 50
Field, pulsed magnetic, Production of a, using an electrolytic capacitor bank 378
Filament 250 (LN)
Filament winding machine 147 (LN)
Film carrier for the analysis of oscillograms by means of a travelling microscope 441 (LN)

Film, deposition of a thin, Instrument for recording the resistance during the 143
Filter, Low frequency 136
Filters, Automatically operated balanced, for counter diffractometer 178 (LN)
Fixing baths, nuclear emulsion, Automatic silver concentration control for 360 (LN)
Flanges, stainless-steel, in a laboratory workshop, Welding copper pipe to 219 (LN)
Flap-valve for long narrow apertures 439 (LN)
Flashmeter, Wide-angle photoelectric integrating 452
Floating-zone refining of gallium arsenide, Apparatus for the 410
Flowmeter, Method for increasing the range of a 490 (LN)
Flow-sensitive switch, Improved 490 (LN)
Fluidized state—apparent viscosity measurement 480
Fluids, The Physics of 494 (NC)
Fluorescence, X-ray, method for determination of the transition-metal content in very small specimens of alloys 394
Fluxmeter, An electronic 31
Foam viscometer 308 (C)
Focal curve of a photographic spectrometer, Method of finding the 252 (LN)
Focus, auto-, range-finder, Improved design for an 356
Foil, mounting and stretching thin gauze, sheet or, Simple method of 67 (LN)
Foil specimens, Device for straining and fracturing thin, inside an electron microscope 37 (LN)
Force balance, Simple, for drag measurements 487 (LN)
Formation of small molten zone in copper, Method of 175
Fracturing thin foil specimens, Device for straining and, inside an electron microscope 37 (LN)
Frequency
  high, light modulation 205
  oscillator, Electromechanical low 149 (LN)
  stabilization of klystrons 398 (LN)
  stabilization, Transistorized, for reflex klystrons used in magnetic resonance 372
Friction, internal, Beam method for the measurement of 208
Fringe electrophoresis patterns, Rayleigh, Photoelectric comparator for 190
Fringe, Moiré, reading head for use with a fine grating 261
Furnace for the uniform heating and mixing of powders in controlled atmospheres 397 (LN)
Furnace, Vacuum, for high temperature X-ray diffractometry 172
Furnaces and models, Apparatus for the measurement of gas velocity in 339
Furnaces, Design of laboratory 17

Gallium arsenide, Apparatus for the floating-zone refining of 410
Galvanometer amplifier, Tunable 136
Galvanometer reading, Simple technique for recording variations of a few centimetres in 39 (LN)
Gap, pressurized spark, Production of millimicrosecond current pulses using a 385
Gas
  -chromatographic catharometry, Compensated Wheatstone's bridge circuit for 185
  chromatography, Automatic gas-sampling device for 253 (LN)
  deuterium, Heavy-water electrolysis unit for generation of, provided with automatic switch-off and safety devices 352
  discharges, intense, Swept Langmuir probe system for 457
  -quenching apparatus for high-speed thermal analysis 108 (LN)
  -sampling device, Automatic, for gas chromatography 253 (LN)
  velocity in furnaces and models, Apparatus for the measurement of 339
Gauge
  Low-compliance diaphragm-capacitance, for measurement of liquid pressures of the order of 1 in. water 401
  spoon, Robust and sensitive 362 (LN)
  strain, signals, Measurement of 138
  Vacuum 486 (LN)
Gauges, resistance strain, and similar transducers, Transformer bridges for use with 381
Gauges, vibrating-wire, Oscillator measuring equipment for 88
Gauze, sheet or foil, mounting and stretching, Simple method of 67 (LN)
Geiger
  counter backgrounds 475
  counters, halogen-quenched, Reduction of dead-time in 336
  diffractometer, Low-angle, for use with monochromatic radiation 132
Gels considered as elastic solids, The torsiometer—an instrument for the study of 292
Generator circuit, New high-voltage multi-stage impulse 231
Ghost images, Elimination of, when using a Kerr-cell shutter 486 (LN)
Glass
  fibres, density of, Determination of the 148 (LN)
  -metal seals, demountable, Insulated terminals for high-vacuum systems, using 358 (LN)
  sample tubes, Valve and adapter for the grease-free connexion of, to a mass spectrometer inlet system 69 (LN)
  Technology; Physics and Chemistry of Glasses 184 (NC)
  -to-metal seals 203
  to metal tube seals, two-component, The theory of stresses in 255 (C)
Gloss measurement 435
Goniometer, Twin-head, for the study of diffusely reflected X-rays 64
Graph plotter, Inexpensive, for five-track paper tape 425
Graticule, Improved eye-piece, for measuring X-ray powder diffraction patterns 134
Grating, a fine, Moiré fringe reading head for use with 261
Gratings for measuring separation of equidistant parallel straight lines 178 (LN)
Grease-free connexion of glass sample tubes, Valve and adapter for the, to a mass spectrometer inlet system 69 (LN)
Grips for tensile tests on very extensible tapes 181 (LN)

Hall effect, Direct measurement of $\int i^2 dt$ by a method based on the 100
Halogen-quenched Geiger counters, Reduction of dead-time in 336
Head, Moiré fringe reading, for use with a fine grating 261
Hearth melting, cold, New method of 177 (LN)
Heat exchanger, Radiography of 257
Heater (chemical) 440 (LN)
Heats of wetting, mixing or solution, measurement of, Recording calorimeter for the 60
Heavy-water electrolysis unit for generation of deuterium gas provided with automatic switch-off and safety devices 352
Hemispherical emissivity, Apparatus for investigating total 84
High
  frequency response, Magnetic probes of 369
  -intensity light source, Stabilized 305 (LN)
  -intensity thermal radiation, Simple dosage meter for 73
  -resolution nuclear magnetic resonance, Temperature-controlled permanent magnet for 353
  -speed thermal analysis, Gas-quenching for 108 (LN)
  -temperature burner for working silica 35 (LN)
  temperature X-ray camera, Simple 305 (LN)
  temperature X-ray diffractometry, Vacuum furnace for 172
  -vacuum systems, Insulated terminals for, using demountable glass-metal seals 358 (LN)
  -voltage multi-stage impulse generator circuit, New 231
Holder, Oscillating flat-specimen, for an X-ray powder camera 399 (LN)
Hydrogen, a cryostat for use with liquid, X-ray diffraction by single crystals at low temperatures 41
Hydrostatic balance, Accurate direct-reading 113

Illumination—outdoor measurements 359 (LN)
Images, ghost, Elimination of, when using a Kerr-cell shutter 486 (LN)
Impulse generator circuit, New high-voltage multi-stage 231
Index of crystallographic supplies 112 (NC)
Indicator, An electroluminescent digital, with a silicon carbide coding matrix 47
Indicator, phase angle, Ratiometer 300
Industry, User experience of electronics in 494 (NC)
Inertia systems, low-, Yarn-speed meter—a low-torque instrument for measuring the linear speed of 157
Infra-red detector—response times 205
InSb—response time measurement 205
Institute
  of Physics and The Physical Society, Elections to The 493 (NC)
  of Physics and The Physical Society, The amalgamation of The 368 (NC)
  of Physics, Annual Report of The, 1959 447 (NC)
  of Physics, Elections to The 256 (NC), 312 (NC), 447 (NC)
Instrument abstracts 112 (NC)
Instrument and measurements conference, Fifth international 256 (NC)
Instruments and apparatus, scientific, Annual exhibition of 493 (NC)
Instruments, Sighting 95
Insulated terminals for high-vacuum systems using demountable glass–metal seals 358 (LN)
Integrating
  amplifier 31
  device, Simple continuous chart and, for a Joyce–Loebl microdensitometer Mk. I 347
  flashmeter, Wide-angle photoelectric 452
Integrator, Diffuse light 70 (LN)
Integrator, Sensitive and simple 276
Intensity measurements 347
Interferometer, Cyclic shearing 374
Interferometer, three-beam, Measurement of the optical thickness of absorbing specimens with the 417
Internal friction, Beam method for the measurement of 208
Ion sources 130
Ions, Counting of individual 328
Irreversibility and statistical mechanics, Conference on 447 (NC)
Islands and dice, Production of, in semiconductor slices with an ultrasonic drill 263
Isotope Information Bureau 312 (NC)
Isotopic analysis of boron in boron trifluoride by mass spectrometry, and measurement of natural boron 10 concentration 323

Jet of viscous liquid, Instruments for measuring the temperature of a running thread-line, and of a 250 (LN)
Joints, Epoxy-resin, for sealed-off, high-vacuum tubes 203
Journal of Nuclear Energy: Part C 224 (NC)
Joyce–Loebl microdensitometer Mk. I, Simple continuous chart and integrating device for a 347

Kerr-cell shutter, Elimination of ghost images when using a 486 (LN)
Klystrons, Frequency stabilization of 398 (LN)
Klystrons, reflex, used in magnetic resonance, Transistorized frequency stabilization for 372

Laboratory and Workshop Notes, 1956–58 447 (NC)
Laboratory furnaces, Design of 17
Langmuir probe system, Swept, for intense gas discharges 457
Lapping, A slow-feed dispenser for abrasive suspensions 36 (LN)
Leak detector, Electronic 147 (LN)
Leak detector, Lens mass-spectrometer 404
Leaks, small, Simple detector for, using a thoriated tungsten emitter with oxygen as probe gas 306 (LN)
Lens mass-spectrometer leak detector 404
Level controller, Simple refrigerant, for cold traps 67 (LN)
Level, Simple multi-position 220 (LN)
Level alarm, Liquid-, using internally reflected light 489 (LN)
Lifetimes 318
Light
  Diffuse, integrator 70 (LN)
  High frequency, modulation 205
  internally reflected, Liquid-level alarm using 489 (LN)
  source, Pulsed 50
  source, Stabilized high-intensity 305 (LN)
  -spot travel, Recording of 39 (LN)
Linear
  speed, Yarn-speed meter—a low torque instrument for measuring the, of low-inertia systems 157
  ratemeter, Automatic range-changing of a 376
  simultaneous equations and related problems, Digito-analogue computer for solving 419
Lines, equidistant parallel straight, Gratings for measuring separation of 178 (LN)
Liquid
  -dielectric measurements, R.F. admittance bridge for 195
  -flow switch 490 (LN)
  -level alarm using internally reflected light 489 (LN)
  -nitrogen cryostat for single-crystal X-ray diffraction 238
  pressures of the order of 1 in. water, Low-compliance diaphragm-capacitance gauge for measurement of 401
  scintillator counter for beta particles, Use of a 201
  viscous, Instruments for measuring the temperature of a running thread-line, and of a jet of 250 (LN)
Liquids
  density of, Accurate measurement of 113
  flowing, Measurement of space density of charge in 332
  magnetic susceptibility of, Bubble method for 71 (LN)
Loading technique, Improved sample, for solid source mass spectrometry 252 (LN)
Locking klystron to high-Q cavity 398 (LN)
Logarithmic amplifier 457
Low
  -angle Geiger diffractometer for use with monochromatic radiation 132
  -current mass spectrometry, Ratiometer for 328
  frequency filter 136
  frequency oscillator, Electromechanical 149 (LN)
  -optical densities, Densitometer wedge for measurements at 33
  -resistance circuits, Error of rectifier-type milliammeters in 313
  temperatures; X-ray diffraction by single crystals at, a cryostat for use with liquid hydrogen 41
  -torque instrument, Yarn-speed meter—a, for measuring the linear speed of low inertia systems 157

Magnet, Temperature-controlled permanent, for high-resolution nuclear magnetic resonance 353
Magnetic
  elutriator, Laboratory, for purification and isolation of ferrimagnetic mineral sands 217
  field, pulsed, Production of a, using an electrolytic capacitor bank 378
  fields 31
  probes of high frequency response 369
  resonance, high-resolution nuclear, Temperature-controlled permanent magnet for 353
  resonance, Transistorized frequency stabilization for reflex klystrons used in 372
  separation and separators 212
  susceptibility of liquids, Bubble method for 71 (LN)
Magnetically operated mass-marker 236
Magnetometer, Vibrating reed 471

Magnetostriction, Measurement of, within the temperature range −196 to 400° C. 225
Manometer, differential pressure, Bakeable bellow-type 251 (LN)
Manometer, portable vacuum, Improved design of 486 (LN)
Mass
  -marker, Magnetically operated 236
  spectrometer charts, Vernier scale arrangement for the measurement of peak heights on 358 (LN)
  spectrometer inlet system, Valve and adapter for the grease-free connexion of glass sample tubes to a 69 (LN)
  -spectrometer, solid-source, New method of sample interchange in a 130
  spectrometers, Construction of 219 (LN)
  -spectrometry 236
  spectrometry, Isotopic analysis of boron in boron trifluoride by, and measurement of natural boron 10 concentration 323
  spectrometry, low-current, Ratiometer for 328
  spectrometry, solid source, Improved sample loading technique for 252 (LN)
Matrix, silicon carbide coding, An electroluminescent digital indicator with a 47
Measurement
  Apparatus for, of sorption of reactive, condensable vapours up to 350° C. 432
  Direct, of $\int i^2\,dt$ by a method based on the Hall effect 100
  (length) 261
  of cyclic strain 138, 255 (C)
  of gas velocity in furnaces and models, Apparatus for the 339
  of internal friction, Beam method for the 208
  of liquid pressures of the order of 1 in. water, Low-compliance diaphragm-capacitance gauge for 401
  of magnetostriction within the temperature range −196 to 400° C. 225
  of natural boron 10 concentration, Isotopic analysis of boron in boron trifluoride by mass spectrometry, and 323
  of particle size distribution, Single tube sedimentation apparatus for the 266
  of peak heights on mass spectrometer charts, Vernier scale arrangement for the 358 (LN)
  of sorption of reactive, condensable vapours up to 350° C, Apparatus for 432
  of space density of charge in flowing liquids 332
  of specific magnetization 471
  of specular reflectivity of bright metal surfaces, Instrument for the 435
  of strain gauge signals 138
  of tellurium vapour pressure using electrical discharges 489 (C)
  of the mechanical properties of fibres, Apparatus for the 25
  of the optical thickness of absorbing specimens with the three-beam interferometer 417
  of thermal diffusivity of semiconductors by Ångström's method 349
  of Young's modulus, between −200 and 700° C by transverse vibration in vacuum, Apparatus for the 117, 255 (C)
  Two thermocouples suitable for, of temperatures up to 2800° C 15
Measurements
  Accurate, of phase differences with the Babinet compensator 278
  at low optical densities, Densitometer wedge for 33
  drag, Simple force balance for 487 (LN)
  Instrument and, conference, Fifth international 256 (NC)
  liquid-dielectric, R.F. admittance bridge for 195
  of heats of wetting, mixing or solution, Recording calorimeter for the 60
  optical density, Test tube adaptor for use in 304 (LN)
Measuring
  equipment, Oscillator, for vibrating-wire gauges 88
  separation, Gratings for, of equidistant parallel straight lines 178 (LN)
  surface temperatures, Construction of a thermocouple for 221 (LN)
  the angular deflexion in the dynamometer, Method of 81
Measuring—*continued*
  the temperature of a running thread-line, and of a jet of viscous liquid, Instruments for 250 (LN)
  time-resolved spectra, Some techniques for recording and 50
  X-ray powder diffraction patterns, Improved eye-piece graticule for 134
Mechanical properties of fibres, Apparatus for the measurement of the 25
Melting
  cold hearth, New method of 177 (LN)
  reactive metals 177 (LN)
  refractory metals 177 (LN)
Message register, Double-acting reversible 35 (LN)
Metal
  demountable glass-, seals, Insulated terminals for high-vacuum systems, using 358 (LN)
  specimens, strain free, Production and tensile testing of 160
  surfaces, bright, Instrument for the measurement of specular reflectivity of 435
  tube seals, two-component glass to, The theory of stresses in 255 (C)
Metallic surfaces, Apparatus for measuring the hemispherical emissivity of 84
Meter
  Daylight factor 316
  Portable water velocity 455
  Recording weight 27
  Simple dosage, for high-intensity thermal radiation 73
  Yarn-speed, —a low-torque instrument for measuring the linear speed of low-inertia systems 157
Meters, moisture, Design of a single electrode capacitor for use with, and similar apparatus 77
Methanol/charcoal wetting 60
Method of formation of small molten zone in copper 175
Microampere, micro-, low-energy electron currents, Wide-band detector for 246
Microdensitometer 190
Microdensitometer Mk. I, Joyce–Loebl, Simple continuous chart and integrating device for a 347
Microelectrophoresis of suspended particles, Modified cylindrical cell for the 248 (LN)
Micromanometer 339
Micro-microampere low-energy electron currents, Wide-band detector for 246
Microscope, electron, Device for straining and fracturing thin foil specimens inside an 37 (LN)
Microscope, travelling, Film carrier for the analysis of oscillograms by means of a 441 (LN)
Microscopy 210
  electron, and electron diffraction, Tilting and rotating specimen stage for 199
  electron, Simple ultramicro-pipette for 103
  transmission electron, Automatic polishing technique for electro-thinning metals for 216 (LN)
Microwave amplifiers 1 (SA)
Mill, small rolling, Design of a, for use at low temperatures 180 (LN)
Milliammeters, rectifier-type, Error of, in low-resistance circuits 313
Millimicrosecond current pulses, Production of, using a pressurized spark gap 385
Mixing of powders, Furnace for the uniform heating and, in controlled atmospheres 397 (LN)
Models, furnaces and, Apparatus for the measurement of gas velocity in 339
Modulation, High frequency light 205
Modulus, Young's, Apparatus for the measurement of, between −200 and 700° C by transverse vibration in vacuum 117, 255 (C)
Moiré fringe reading head for use with a fine grating 261
Moiré patterns 178 (LN)
Moisture meters, Design of a single electrode capacitor for use with, and similar apparatus 77

Monitor for the quantitative determination of beryllium in the atmosphere 466
Monochromatic radiation, Low-angle Geiger diffractometer for use with 132
Mounting and stretching thin gauze, sheet or foil, Simple method of 67 (LN)
Multi-stage impulse generator circuit, New high-voltage 231
Nanosecond range, Time-sorter for use in the 318

New instruments, materials and tools
  Air velocity indicators 310
  Automatic delay switches 364
  Automatic electrophoretic strip scanner 364
  Blood pressure follower 308
  "B–W" moulded electric heating elements 445
  Circuit magnification meter 40
  Compressed air dehydrating unit 493
  Counter for detecting particle size 443
  Crystal chronometer 444
  Digital printer 365
  Digital reading oscilloscope 444
  Digital-reading slide-wire potentiometer 150
  Directional coupler for measurement of power in coaxial cables 110
  Edgewise electric meter 151
  Electric melting point apparatus 365
  Electric oven 150
  Electron diffraction camera 493
  Electronic registration and control unit 443
  Frequency meter 443
  Frequency meter and tachometer 364
  Frequency synthesizer 444
  Gas chromatography for medical gas analysis 445
  Gauge-quality cabinet projector 311
  High intensity cobalt container for use in industrial radiography 442
  High-sensitivity leak detector 363
  High stability computor reference power supply 445
  High-stability pulse amplifier 442
  High-stability transistorized power units 72
  Hygrometer alarm 363
  L-band signal generator 109
  Letter cutting and profiling pantograph machines 492
  Liquid nitrogen purity gauge 443
  Low capacitance bridge 364
  Low-drift d.c. amplifier 309
  Low-voltage power supply unit 151
  Low voltage soldering iron 150
  Magnetic amplifiers 443
  Magnetic tape data recorder 311
  Medical scintillation counter 442
  Microwave generator 109
  Neutron spectral measurements 109
  Non-reset electromagnetic counter 442
  Numerical indicator tube 365
  Optical-reading clinometer 493
  Oscilloscope camera 364
  Oscilloscope for high-frequency pulse monitoring 72
  Permanent magnet 109
  Portable potentiometer recorder 109
  Portable radiation background measuring instrument 363
  Precision vernier d.c. potentiometer 309
  Production of deionized water 40
  Radiation pyrometer 151
  Recording X-ray diffractometer and fluorescence spectrometer 40
  Resistance analogue field plotter 445
  Rhenium 311
  Scintillation counter 308
  Semiconductor convertors 493
  Sensitive hygrometer 310
  Servo-multiplier 310
  Signal generator 151

New instruments, materials and tools—*continued*
  Small synchronous cam-operated timer 443
  Speed regulator for compressed air 309
  Stable power supply for spectrophotometer 365
  Stirrer 364
  Strain gauge power supply 442
  Thermo-switch 150
  Tong-type a.c. detector 310
  Tool shank material 442
  Trace reading equipment 363
  Transistor output power meter 308
  Transistorized high-speed digital printers 72
  Transistorscope 445
  Vibrating reed electrometer 363
  Vibrator pressure transducer 110
  X-ray tubes for fluorescence analysis 445
Nitrogen, Liquid-, cryostat for single-crystal X-ray diffraction 238
Nuclear
  emulsion fixing baths, Automatic silver concentration control for 360 (LN)
  Energy: Part C, Journal of 224 (NC)
  engineering abstracts 494 (NC)
  magnetic resonance, high-resolution, Temperature-controlled permanent magnet for 353
  particles, velocity of, Direct method for determining the 56
Numbering of photographic oscilloscope records 282
Nylon 210
Nylon cord cutter, Hot tube, for balloon flights 440 (LN)

Oil-filled dash pot, Two-way 180 (LN)
Open channel wave recorder 141
Optical
  densities, low, Densitometer wedge for measurements at 33
  density measurements, Test tube adaptor for use in 304 (LN)
  thickness of absorbing specimens with the three-beam interferometer, Measurement of the 417
Optics and spectroscopy 447 (NC)
Ore dressing 212
Oscillation, damped torsional, Viscometers having 480
Oscillation mechanism, Crystal, for use with automatic X-ray diffractometers 68 (LN)
Oscillator, Electromechanical low frequency 149 (LN)
Oscillator measuring equipment for vibrating-wire gauges 88
Oscillograms, Film carrier for the analysis of, by means of a travelling microscope 441 (LN)
Oscilloscope camera, Some modifications to an, and the construction of a control unit 282
Ovens, Low thermal capacity 69 (LN)
Oxygen as probe gas, Simple detector for small leaks using a thoriated tungsten emitter with 306 (LN)

Paper, protective, Influence of, on X-ray diffraction photographs 223 (C)
Parallax, Design criterion for correction of, and the best focus for definition 95
Parallel straight lines, equidistant, Gratings for measuring separation of 178 (LN)
Parametric amplification 1 (SA)
Particle counting 103
Particle size distribution, Single tube sedimentation apparatus for the measurement of 266
Particles
  beta, Use of a liquid scintillator counter for 201
  producing spherical dust, Wax-atomizer for 123
  small, in suspension, Rapid counter for 414
  suspended, Modified cylindrical cell for the microelectrophoresis of 248 (LN)
  velocity of nuclear, Direct method of determining the 56

Partition experiments, Simple agitating device for 222 (LN)
Patterns, Rayleigh fringe electrophoresis, Photoelectric comparator for 190
Patterns, X-ray powder diffraction, Improved eye-piece graticule for 134
Peak heights on mass spectrometer charts, Vernier scale arrangement for the measurement of 358 (LN)
Permanent magnet, Temperature-controlled, for high-resolution nuclear magnetic resonance 353
Permittivity 195
Phase
  angle, Measurement of 300
  differences with the Babinet compensator, Accurate measurements of 278
  transformations 6
Photoelectric
  comparator for Rayleigh fringe electrophoresis patterns 190
  demodulator, Simple 107 (LN)
  integrating flashmeter, wide-angle 452
  refractometer 38 (LN)
Photographic spectrometer, Method of finding the focal curve of a 252 (LN)
Photographs, X-ray diffraction, Influence of protective paper on 223 (C)
Photography, High speed 486 (LN)
Photography, shadowgraph, A 450J spark discharge for 259
Photometer, Portable airglow 54
Photometry 452
Photomultiplier soft X-ray spectrometer 460
Photo-transistor 414
Photo-voltaic cell 70 (LN)
Photovoltaic cell, weatherproofed, Cosine correction of a 359 (LN)
Physical Society, The amalgamation of The Institute of Physics and The 368 (NC)
Physical Society's Exhibition—London 1960, The 153 (SA)
Pipe, copper, Welding, to stainless-steel flanges in a laboratory workshop 219 (LN)
Pipette, Simple ultramicro-, for electron microscopy 103
Pitot tubes 339
Plane, specific, Radiograph of 257
Platform weighbridges, Simple device for use with, in the accurate determination of burning rates 45
Plotter, Inexpensive graph, for five-track paper tape 425
Polarisation 278
Polishing technique, Automatic, for electro-thinning metals for transmission electron microscopy 216 (LN)
Position transducer using a divided circle and coded scale 125
Postgraduate training of physicists in British universities, The 184 (NC), 447 (NC)
Powder
  camera, X-ray, Oscillating flat-specimen holder for an 399 (LN)
  Data File—5, A.S.T.M., Comments on the 183 (C)
  diffraction patterns, measuring X-ray, Improved eye-piece graticule for 134
Powders in controlled atmospheres, Furnace for the uniform heating of mixing of 397 (LN)
Precipitator, thermal-, Effect of ambient airspeed on efficiency of 182 (C)
Precision weights, Weight-in-air basis of adjustment of (*erratum*) 256
Pressure
  Barometric 162
  manometer, differential, Bakeable bellows-type 251 (LN)
  (measurement) 362 (LN)
Pressures, liquid, of the order of 1 in. water, Low-compliance diaphragm-capacitance gauge for measurement of 401
Primary standard barometer of range 0 to 1200 mb 162
Probe gas, Simple detector for small leaks using a thoriated tungsten emitter with oxygen as 306 (LN)
Probe system, Swept Langmuir, for intense gas discharges 457
Probes (furnace) 339
Probes, Magnetic, of high frequency response 369
Proceedings of Comité Consultatif de Thermométrie 112 (NC)
Profile determination of surge waves 141
Profiles of water waves, Determination of the 141
Properties of fibres, mechanical, Apparatus for the measurement of the 25
Protective paper, Influence of, on X-ray diffraction photographs 223 (C)
Pulsed discharges 369
Pulsed magnetic field using an electrolytic capacitor bank, Production of a 378
Pulses, millimicrosecond current, Production of, using a pressurized spark gap 385
Pump-operated air aspirator, Report on a 221 (LN)
Pumps, Protection of diffusion, against inadequate cooling 148 (LN)
Pyrolytic coating of quartz and ceramic vessels used for zone melting 397 (LN)

Quartz and ceramic vessels used for zone melting, Pyrolytic coating of 397 (LN)
Quick-response micromanometer 432

Radiation
  chopper in a preferred position, Simple method for stopping a 439 (LN)
  high-intensity thermal, Simple dosage meter for 73
  monochromatic, Low-angle Geiger diffractometer for use with 132
Radio frequency melting 177 (LN)
Radioactive sources and chemicals 447 (NC)
Radiography, industrial, Tomograph for 257
Radiometer for field use 128
Rand soil-pressure cell for low pressures, high accuracy and long-term stability 193
Range-changing, Automatic, of a linear ratemeter 376
Range-finder, auto-focus, Improved design for an 356
Ratemeter, linear, Automatic range-changing of a 376
Ratiometer for low-current mass spectrometry 328
Ratiometer phase angle indicator 300
Rayleigh fringe electrophoresis patterns, Photoelectric comparator for 190
Reactance standards, some, Stability of 463
Reciprocity breakdown 50
Recorder, Improved smoke density 144
Recorder, Multipoint digital temperature, with punched tape output 269
Recording
  and measuring time-resolved spectra, Some techniques for 50
  calorimeter for the measurement of heats of wetting, mixing, or solution 60
  resistance, Instrument for, during the deposition of a thin film 143
  thermobalance, Novel displacement detector and its application in a 297 (*erratum*) 448 (NC)
  variations, Simple technique for, of a few centimetres in galvanometer reading 39 (LN)
  weight meter 27
Rectifier-type milliammeters in low-resistance circuits, Error of 313
Reed magnetometer, Vibrating 471
Refining, floating-zone, of gallium arsenide, Apparatus for the 410
Refining of copper, zone, Apparatus for the 175
Reflectivity, specular, of bright metal surfaces, Instrument for the measurement of 435
Reflex klystrons used in magnetic resonance, Transistorized frequency stabilization for 372
Refractometer, Photoelectric 38 (LN)
Refrigerant level controller, Simple, for cold traps 67 (LN)
Register, Double-acting reversible message 35 (LN)
Registers, electromechanical, Transistor operation of 303 (LN)

Replicating fibre surfaces by rolling, Technique for 210
Resin joints, Epoxy-, for sealed-off, high-vacuum tubes 203
Resistance, Instrument for recording the, during the deposition of a thin film 143
Resonance, high-resolution nuclear magnetic, Temperature-controlled permanent magnet for 353
Resonance, magnetic, Transistorized frequency stabilization for reflex klystrons used in 372
R.F. admittance bridge for liquid-dielectric measurements 195
Rolling mill, small, Design of a, for use at low temperatures 180 (LN)
Rolling, Technique for replicating fibre surfaces by 210
Rotating specimen stage, Tilting and, for electron microscopy and electron diffraction 199
Royal Society's Fair Copying Declaration, The 112 (NC)

Safety devices, automatic switch-off and, Heavy-water electrolysis unit for generation of deuterium gas provided with 352
Sample
  interchange, New method of, in a solid-source mass spectrometer 130
  loading technique, Improved, for solid source mass spectrometry 252 (LN)
  tubes, glass, Valve and adapter for the grease-free connexion of, to a mass spectrometer inlet system 69 (LN)
Sands, ferrimagnetic mineral, Laboratory magnetic elutriator for purification and isolation of 212
Scale, coded, Position transducer using a divided circle and 125
Scanning electron microscope, A detector for 246
Scintillator counter, liquid, for beta particles, Use of a 201
Seals
  aluminium wire, for bakeable vacuum systems, Further experiences with 449
  demountable glass–metal, Insulated terminals for high-vacuum systems, using 358 (LN)
  two-component glass to metal tube, The theory of stresses in 255 (C)
Sectioning, Radiographic 257
Sedimentation apparatus, Single tube, for the measurement of particle size distribution 266
Sedimentation—Automatic decantation for routine sub-sieve sizing 120
Semiconductor devices, Equipment for the encapsulation of 197
Semiconductor slices, Production of islands and dice in, with an ultrasonic drill 263
Semiconductors, Measurement of thermal diffusivity of, by Ångström's method 349
Separation, Gratings for measuring, of equidistant parallel straight lines 178 (LN)
Shadowgraph photography, A 450J spark discharge for 259
Shearing interferometer, Cyclic 374
Sheet or foil, mounting and stretching thin gauze, Simple method of 67 (LN)
Short duration light sources 259
Shutter, Kerr-cell, Elimination of ghost images when using a 486 (LN)
Silica, working, High-temperature burner for 35 (LN)
Silicon carbide coding matrix, An electroluminescent digital indicator with a 47
Silver concentration control, Automatic, for nuclear emulsion fixing baths 360 (LN)
Single-crystal X-ray diffraction, Liquid-nitrogen cryostat for 238
Single crystals of anthracene, Growth of 242
Sizing, routine sub-sieve, Automatic decantation for 120
Small molten zone in copper, Method of formation of 175
Smoke density recorder, Improved 144
Society, Physical, Elections to The Institute of Physics and The 493 (NC)
Soil-pressure cell, Rand, for low pressures, high accuracy and long-term stability 193
Solid
  -source mass spectrometer, New method of sample interchange in a 130
  source mass spectrometry, Improved sample loading technique for 252 (LN)
  -state electronics 448 (NC)
Solids, elastic, The torsiometer—an instrument for the study of gels considered as 292
Solvent extraction 222 (LN)
Sorption of reactive, condensable vapours up to 350° C, Apparatus for measurement of 432
Sorter, Time-, for use in the nanosecond range 318
Source mass spectrometry, solid, Improved sample loading technique for 252 (LN)
Space density of charge in flowing liquids, Measurement of 332
Spark discharge, A 450J, for shadowgraph photography 259
Spark gap, pressurized, Production of millimicrosecond current pulses using a 385
Specific heat, An apparatus for measuring 84
Specific gravity of liquids, Accurate measurement of 113
Specimen holder, Oscillating flat-, for an X-ray powder camera 399 (LN)
Spectra, recording and measuring time-resolved, Some techniques for 50
Spectrograph 252 (LN)
Spectrograph, Focusing technique for a 252 (LN)
Spectrographic determination of beryllium in the atmosphere 466
Spectrometer
  inlet system, mass, Valve and adapter for the grease-free connexion of glass sample tubes to a 69 (LN)
  leak detector, Lens mass- 404
  mass, charts, Vernier scale arrangement for the measurement of peak heights on 358 (LN)
  photographic, Method of finding the focal curve of a 252 (LN)
  Photomultiplier soft X-ray 460
  solid-source mass, New method of sample interchange in a 130
Spectrometry
  low-current mass, Ratiometer for 328
  mass, Isotopic analysis of boron in boron trifluoride by, and measurement of natural boron 10 concentration 323
  solid-source mass, Improved sample loading technique for 252 (LN)
Spectrophotometer, Temperature-control system for use with a 478
Spectrophotometry 304 (LN)
Spectroscopy 353
Specular reflectivity of bright metal surfaces, Instrument for the measurement of 435
Sphere, Drag measurement in water 487 (LN)
Spherical dust particles, producing, Wax-atomizer for 123
Spirit levels 220 (LN)
Spoon gauge, Robust and sensitive 362 (LN)
Spring-clip, Improved form of, for holding down a work-piece 38 (LN)
Stability, high, Heat transport anemometer of 166
Stability of some reactance standards 463
Stabilization, Frequency, of klystrons 398 (LN)
Stabilized high-intensity light source 305 (LN)
Stainless-steel flanges in a laboratory workshop, Welding copper pipe to 219 (LN)
Standards, some reactance, Stability of 463
Strain
  cyclic, Measurement of 255 (C)
  -follower for semi-rigid materials 93
  -free metal specimens, Production and tensile testing of 160
  gauge signals, Measurement of 138
  gauges 88
  gauges, Performance of 225
  measurement 381
  Measurement of cyclic 138
Straining and fracturing thin foil specimens, Device for, inside an electron microscope 37 (LN)

Stresses in two-component glass to metal tube seals, The theory of 255 (C)
Stretching thin gauze sheet or foil, mounting and, Simple method of 67 (LN)
Sublimation apparatus, Vacuum, for preparation of thin sources of α-active materials 169
Sub-sieve sizing, routine, Automatic decantation for 120
Surface density variations in paper, Measurement of 223 (C)
Surge waves, Profile determination of 141
Susceptibility of liquids, magnetic, Bubble method for 71 (LN)
Suspended particles, Modified cylindrical cell for the micro-electrophoresis of 248 (LN)
Suspensions, abrasive, Slow-feed dispenser for 36 (LN)
Switch
  Contactless 189
  Improved flow-sensitive 490 (LN)
  Mercury 378
  -off, automatic, and safety devices, Heavy-water electrolysis unit for generation of deuterium gas provided with 352
Symposium on electrical contacts 493 (NC)

Tape, five-track paper, Inexpensive graph plotter for 425
Tape output, punched, Multipoint digital temperature recorder with 269
Tapes, very extensible, Grips for tensile tests on 181 (LN)
Tellurium vapour pressure, Measurement of, using electrical discharges 489 (C)
Temperature
  control, close, Temperature regulator for 285
  control, Simple method of 69 (LN)
  -control system for use with a spectrophotometer 478
  -controlled permanent magnet for high-resolution nuclear magnetic resonance 353
  of a running thread-line, and of a jet of viscous liquid, Instruments for measuring the 250 (LN)
  range −196 to 400° C, Measurement of magnetostriction within the 225
  recorder, Multipoint digital, with punched tape output 269
  regulator for close temperature control 285
  Simple high, X-ray camera 305 (LN)
Temperatures
  low, Design of a small rolling mill for use at 180 (LN)
  surface, Construction of a thermocouple for measuring 221 (LN)
  up to 2800° C, measurement of, Two thermocouples suitable for 15
Tensile testing, Production and, of strain-free metal specimens 160
Tensile tests, Grips for, on very extensible tapes 181 (LN)
Terminals, Insulated, for high-vacuum systems using demountable glass–metal seals 358 (LN)
Testing, Production and tensile, strain-free metal specimens 160
Tests, Grips for tensile, on very extensible tapes 181 (LN)
Thermal
  analysis, high-speed, Gas-quenching apparatus for 108 (LN)
  diffusivity of semiconductors by Ångström's method, Measurement of 349
  precipitator 221 (LN)
  -precipitator, Effect of ambient airspeed on efficiency of 182 (C)
  radiation, high-intensity, Simple dosage meter for 73
Thermobalance, recording, Novel displacement detector and its application in a 297 (*erratum*) 448 (NC)
Thermocouple for measuring surface temperatures, Construction of a 221 (LN)
Thermocouples, Two, suitable for measurement of temperatures up to 2800° C 15
Thermostats, Metal block type 69 (LN)
Thin
  film, deposition of a, Instrument for recording the resistance during the 143
Thin—*continued*
  foil specimens, Device for straining and fracturing, inside an electron microscope 37 (LN)
  sources of α-active materials, Vacuum sublimation apparatus for, preparation of 169
Thoriated tungsten emitter with oxygen as probe gas, Simple detector for small leaks using a 306 (LN)
Thread-line, running, and of a jet of viscous liquid, Instruments for measuring the temperature of a 250 (LN)
Tilting and rotating specimen stage for electron microscopy and electron diffraction 199
Time-resolved spectra, recording and measuring, Some techniques for 50
Time-sorter for use in the nanosecond range 318
Tissue cells in suspension 248 (LN)
Tomograph for industrial radiography 257
Torsiometer—an instrument for the study of gels considered as elastic solids, The 292
Torsional oscillation, damped, Viscometers having 480
Transducer, Position, using a divided circle and coded scale 125
Transducers, similar, resistance strain gauges and, Transformer bridges for use with 381
Transformer bridges for use with resistance strain gauges and similar transducers 381
Transistor 455
  cup anemometer 189
  operation of electromechanical registers 303 (LN)
Transition-metal content in very small specimens of alloys, X-ray fluorescence method for determination of the 394
Transverse vibration in vacuum, Apparatus for the measurement of Young's modulus, between—200 and 700° C by 117
Traps, cold, Simple refrigerant level controller for 67 (LN)
Trifluoride, boron, Isotopic analysis of boron in, by mass spectrometry, and measurement of natural boron 10 concentration 323
Trochotron tube, a crystal-controlled, Time analyser using 289
Tube adapter, Test, for use in optical density measurements 304 (LN)
Tube seals, two-component glass to metal, The theory of stresses in 255 (C)
Tubes, glass sample, Valve and adapter for the grease-free connexion of, to a mass spectrometer inlet system 69 (LN)
Tubes, high-vacuum, sealed off, Epoxy-resin joints for 203
Tunable galvanometer amplifier 136
Tungsten emitter, thoriated, with oxygen as probe gas, Simple detector for small leaks using a 306 (LN)
Tungsten 26 % Rhenium alloy thermocouple 15
Two-valve electrometer circuit 218 (LN)

Ultra high vacuum 449
Ultramicro-pipette, Simple, electron microscopy 103
Ultrasonic drill, Production of islands and dice in semiconductor slices with an 263
Unit, Heavy-water electrolysis, for generation of deuterium gas provided with automatic switch-off and safety devices 352

Vacuum
  Apparatus for the measurement of Young's modulus, between −200 and 700° C by transverse vibration in 255 (C)
  evaporation 147 (LN)
  furnace for high temperature X-ray diffractometry 172
  High, high temperature X-ray camera 273
  high-, systems, Insulated terminals for, using demountable glass–metal seals 358 (LN)
  manipulation of chlorine, Cut-off for the 303 (LN)
  manometer, portable, Improved design of 486 (LN)
  seals 203
  sublimation apparatus for preparation of thin sources of α-active materials 169

Vacuum—*continued*
  systems, bakeable, aluminium wire seals for, Further experiences with 449
  technique 404
  techniques 439 (LN)
  transverse vibration in, Apparatus for the measurement of Young's modulus, between —200 and 700° C by 117
  tubes, sealed-off high-, Epoxy-resin joints for 203
Valve
  and adapter for the grease-free connexion of glass sample tubes to a mass spectrometer inlet system 69 (LN)
  Flap-, for long narrow apertures 439 (LN)
  -voltmeter 218 (LN)
Vapour pressure, tellurium, Measurement of, using electrical discharges 489 (C)
Vapours, condensable, sorption of reactive, up to 350° C, Apparatus for measurement of 432
Velocity
  gas, in furnaces and models, Apparatus for the measurement of 339
  meter, Portable water 455
  of nuclear particles, Direct method for determining the 56
  tachometer 157
Vernier scale arrangement for the measurement of peak heights on mass spectrometer charts 358 (LN)
Vessels, quartz and ceramic, used for zone melting, Pyrolytic coating of 397 (LN)
Vibrating reed magnetometer 471
Vibrating wire gauges, Oscillator measuring equipment for 88
Vibration in vacuum, transverse, Apparatus for the measurement of Young's modulus, between —200 and 700° C by 117, 255 (C)
Viscometer, Foam 308 (C)
Viscometers having damped torsional oscillation 480
Viscous liquid, a jet of, Instruments for measuring the temperature of a running thread-line, and of 250 (LN)
Voltmeter, electrometer, Portable 296

Water
  density, Accurate measurement of 113
  relay 148 (LN)
  velocity meter, Portable 455
  waves, Determination of the profiles of 141
Waverley gold medal essay competition, 1960 256 (NC)
Waves, Profile determination of 141
Waves, water, Determination of the profiles of 141
Wax-atomizer for producing spherical dust particles 123
Wedge, Densitometer, for measurements at low optical densities 33
Weighbridges, platform, Simple device for use with, in the accurate determination of burning rates 45
Weight meter, Recording 27
Weights, precision, Weight-in-air basis of adjustment of (*erratum*) 256
Wheatstone's bridge circuit, Compensated, for gas-chromatographic catharometry 185
Winding machine, Filament 147 (LN)
Wire seals, aluminium, for bakeable vacuum systems, Further experiences with 449

X-ray
  camera, High vacuum high temperature 273
  camera, Simple high temperature 305 (LN)
  diffraction by single crystals at low temperatures; a cryostat for use with liquid hydrogen 41
  diffraction photographs, Influence of protective paper on 223 (C)
  diffraction, single-crystal, Liquid-nitrogen cryostat for 238
  diffractometer, rapid-scanning, Design and performance of a 6
  diffractometers, automatic, Crystal oscillation mechanism for use with 68 (LN)
  diffractometry, High temperature, Vacuum furnace for 172
  fluorescence method for determination of the transition-metal content in very small specimens of alloys 394
  powder camera, Oscillating flat-specimen holder for an 399 (LN)
  powder diffraction patterns, measuring, Improved eye-piece graticule for 134
  spectrometer, Photomultiplier soft 460
X-rays, diffusely reflected, Twin-head goniometer for the study of 64
X-rays with proportional counter, Electronic apparatus for the study of 388

Yarn-speed meter—a low-torque instrument for measuring the linear speed of low-inertia systems 157
Young's modulus, Apparatus for the measurement of, between —200 and 700° C by transverse vibration in vacuum 117, 255 (C)

Zone
  melting apparatus for copper 175
  melting, Pyrolytic coating of quartz and ceramic vessels used for 397 (LN)
  refining of copper, Apparatus for the 175

AUTHORS

(SA) denotes special article, (LN) laboratory notes and (C) correspondence

Ackland, R. G., Simple technique for recording variations of a few centimetres in galvanometer reading 39 (LN)
Adlam, J. H., and Holmes, L. S., Production of millimicrosecond current pulses using a pressurized spark gap 385
Allen, J. E., *see under* Segre, S. E.
Ambrose, E. J., and Ryder, J., Modified cylindrical cell for the microelectrophoresis of suspended particles 248 (LN)
Arndt, U. W., Faulkner, T. H., and Phillips, D. C., Crystal oscillation mechanism for use with automatic X-ray diffractometers 68 (LN)
Asher, H., Dodin, L., and Mulholland, H. P., Improved design for an auto-focus range-finder 356
Ashwin, B. S., Hagyard, T., Saunders, I. C. B., and Young, T. E. Viscometers having damped torsional oscillation 480
Attard, A. E., and Azároff, L. V., Liquid-nitrogen cryostat for single-crystal X-ray diffraction 238
Axson, M., and Magarshack, J. M., Method of measuring the angular deflexion in a dynamometer 81
Aylett, B. J., Robust and sensitive spoon gauge 362 (LN)
Azároff, L. V., *see under* Attard, A. E.

Barker, D., Filament winding machine 147 (LN)
Barrer, R. M., and Wasilewski, S., Apparatus for measurement of sorption of reactive, condensable vapours up to 350° C 432
Barrington, A. E., *see under* Ryder-Smith, S. C.
Barton, J. C., Transistor operation of electromechanical registers 303 (LN)
Bate, D. G., and Saxe, R. F., Production of a pulsed magnetic field using an electrolytic capacitor bank 378
Beels, R., and De Sutter, W., Pyrolytic coating of quartz and ceramic vessels used for zone melting 397 (LN)
Bennett, J. A., and Flanagan, T. P., Instrument for recording the resistance during the deposition of a thin film 143
Bennett, R. G., R.F. admittance bridge for liquid-dielectric measurements 195
Bentley, P. G., Isotropic analysis of boron in boron trifluoride by mass spectrometry, and measurement of natural boron 10 concentration 323
Biddlestone, A. J., *see under* Nutt, C. W.
Bigg, P. H., *see under* Elliott, K. W. T.
Birss, R. R., and Fry, J. P., An electronic fluxmeter 31
Birss, R. R., and Lee, E. W., Measurement of magnetostriction within the temperature range —196 to 400° C 225
Bishop, L., Bruin, de H. J., and Temple, R. B., Simple agitating device for partition experiments 222 (LN)
Bloomer, R. N., and Brooks, W. C., Simple detector for small leaks using a thoriated tungsten emitter with oxygen as probe gas 306 (LN)
Boom, G., *see under* Perdok, W. G.
Brice, J. C., Measurement of tellurium vapour pressure using electrical discharges 491 (C)
Broadbent, T. E., New high-voltage multi-stage impulse generator circuit 231
Brookes, F. R., *see under* Godwin, D. W.
Brooks, W. C., *see under* Bloomer, R. N.
Brown, J. J., Reed, R. I., and Simpson, W., Magnetically operated mass-marker 236
Brown, P. J., X-ray fluorescence method for determination of the transition-metal content in very small specimens of alloys 394
Bruin, de H. J., *see under* Bishop, L.
Burford, H. C., Improved flow-sensitive switch 490 (LN)
Burge, R. E., and Munden, H. R., Tilting and rotating specimen stage for electron microscopy and electron diffraction 199
Burland, J. B., *see under* Jennings, J. E.
Butement, F. D. S., and Finkelstein, N. P., Ratiometer for low-current mass spectroscopy 328

Cairns, J. H., Apparatus for investigating total hemispherical emissivity 84
Calvert, L. D., *see under* Wilkinson, J. D.
Charles, D., Tomograph for industrial radiography 257
Cheney, J. E., *see under* Ward, W. H.
Clarke, L. N., Transformer bridges for use with resistance strain gauges and similar transducers 381
Coates, B. D., Determination of the density of glass fibres 148 (LN)
Cohen, B. L., Geiger counter backgrounds 475
Conaboy, J., High-temperature burner for working silica 35 (LN)
Cornwall, J. B., and Davison, R. M., Rapid counter for small particles in suspension 414
Cossutta, D., and Steckelmacher, W., Lens mass-spectrometer leak detector 404
Cowles, L. E. J., *see under* Green, A.
Cox, B. C., Protection of diffusion pumps against inadequate cooling 148 (LN)
Critchlow, A., *see under* Hodkinson, J. R.
Culpin, M. F., and Martin, K. A., Instruments for measuring the temperature of a running thread-line, and of a jet viscous liquid 250 (LN)
Cunnell, F. A., and Wickham, R., Apparatus for the floating-zone of refining of gallium arsenide 410
Curtain, C. C., Photoelectric comparator for Rayleigh fringe electrophoresis patterns 190

Dahl-Jensen, E., Automatic silver concentration control for nuclea emulsion fixing baths 360 (LN)
Davies, D. A., Two thermocouples suitable for measurement of temperatures up to 2800° C 15
Davison, R. M., *see under* Cornwall, J. B.
Dawson, J. B., Test tube adapter for use in optical density measurements 304 (LN)
Dawson, R. M., Gratings for measuring separation of equidistant parallel straight lines 178 (LN)
Day, A. G., Grips for tensile tests on very extensible tapes 181 (LN)
Dearnaley, G., Lawrence, L. G., and Tresise, H. C., Large storage binary-to-decimal converter 240
De Sutter, W., *see under* Beels, R.
Dickson, E. W., Electrochemical low frequency oscillator 149 (LN)
Dobrowolski, T., and Walker, J., Time analyser using a crystal-controlled trochotron tube 289
Dodin, L., *see under* Asher, H.
Doughty, D. C., and Mossman, P., Vibrating reed magnetometer 471
Dowell, T. M., and Mackinnon, J. A., Measurement of cyclic strain 138
Dowell, T. M., and Mackinnon, J. A., Measurement of cyclic strain 255 (C)
Dowling, D. J., Electronic leak detector 147 (LN)
Dutt, P. K., Heavy-water electrolysis unit for generation of deuterium gas provided with automatic switch-off and safety devices 352
Dyer, A. J., Heat transport anemometer of high stability 166

Edington, J. M., and Molyneux, L., Portable water velocity meter 455
Edwards, J., Lane, W. R., and Stone, B. R. D., Wide-angle photo-electric integrating flashmeter 452
Einstein, P. A., Simple method of mounting and stretching thin gauze, sheet or foil 67 (LN)
Elliott, K. W. T., Wilson, D. C., Mason, F. C. P., and Bigg, P. H., Primary standard barometer of range 0 to 1200 mb 162

Elsworth, L., Holland, L., and Laurenson, L., Further experiences with aluminium wire seals for bakeable vacuum systems 449
Evans, B. A., and Richards, R. E., Temperature-controlled permanent magnet for high-resolution nuclear magnetic resonance 353
Evans, M. H., and Pierson, G., Some modifications to an oscilloscope camera, and the construction of a control unit 282
Everhart, T. E., and Thornley, R. F. M., Wide-band detector for micro-microampere low-energy electron currents 246

Farrow, G., and Preston, D., Simple continuous chart and integrating device for a Joyce-Loebl microdensitometer Mk. I 347
Farrow, G., and Preston, D., Simple high temperature X-ray camera 305 (LN)
Faulkner, T. H., *see under* Arndt, U. W.
Finkelstein, N. P., *see under* Butement, F. D. S.
Flanagan, T. P., *see under* Bennett, J. A.
Ford, L. H., Stability of some reactance standards 463
Forsyth, P. J. E., and Wilson, R. N., Device for straining and fracturing thin foil specimens inside an electron microscope 37 (LN)
French, R. J., Foam viscometer 308 (C)
Fry, J. P., *see under* Birss, R. R.
Funk, J. P., Sensitive and simple integrator 276

Gabriel, A. H., Some techniques for recording and measuring time-resolved spectra 50
Garwood, R. D., Moon, J. R., and Thrush, B. F., Gas-quenching apparatus for high-speed thermal analysis 108 (LN)
Gibbs, W. E. K., Portable electrometer voltmeter 296
Gibbs, W. E. K., *see under* Wilbur-Ham, J.
Godwin, D. W., and Brookes, F. R., Elimination of ghost images when using a Kerr-cell shutter 486 (LN)
Green, A., and Cowles, L. E. J., Measurement of thermal diffusivity of semiconductors by Ångström's method 349
Green, M., and Maxwell, K. H., Cut-off for the vacuum manipulation of chlorine 303 (LN)
Greenough, G. K., Wax-atomizer for producing spherical dust particles 123
Greetham, G., and Martin, A. J., Production and tensile testing of stain-free metal specimens 160
Guile, A. E., *see under* Ryder-Smith, S. C.

Hagyard, T., *see under* Ashwin, B. S.
Hampton, B. F., Direct method for determining the velocity of nuclear particles 56
Hamstead, G. W., Design criterion for correction of parallax at the best focus for definition 95
Hardy, R., Majer, J. R., and Travers, S., Simple ultramicro-pipette for electron microscopy 103
Hariharan, P., and Sen, D., Accurate measurements of phase differences with the Babinet compensator 278
Hariharan, P., and Sen, D., Cyclic shearing interferometer 374
Hariharan, P., and Sen, D., Measurement of the optical thickness of absorbing specimens with the three-beam interferometer 417
de La Harpe, G., *see under* O'Brien, B. J.
Harris, C. C., Method for increasing the range of a flowmeter 490 (LN)
Harrison, P. W., Improved form of spring-clip for holding down a work-piece 38 (LN)
Hatt, B. A., Kent, P. J. C., and Williams, G. I., High vacuum high temperature X-ray camera 273
Hayward, A. T. J., Accurate direct-reading hydrostatic balance 113
Hayward, A. T. J., Improved design of portable vacuum manometer 486 (LN)
Henwood, G. A., Simple force balance for drag measurements 487 (LN)
Herzberg, E. N., Temperature regulator for close temperature control 285
Heylen, A. E. D., Bakeable bellows-type differential pressure manometer 251 (LN)
Hill, D. W., and Hook, J. R., Automatic gas-sampling device for gas chromatography 253 (LN)
Hodkinson, J. R., Critchlow, A., and Stanley, N., Effect of ambient airspeed on efficiency of thermal-precipitator 182 (C)
Holden, T. S., Multipoint digital temperature recorder with punched tape output 269
Holland, L., *see under* Elsworth, L.
Holmes, L. S., *see under* Adlam, J. H.
Hood, W. E., and Oldham, E., Liquid-level alarm using internally reflected light 489 (LN)
Hook, J. R., *see under* Hill, D. W.
Horsfall, F., and Jowett, A., Automatic decantation for routine sub-sieve sizing 120
Huey, R. M., and Lancaster, B. J., Tunable galvanometer amplifier 136
Hughes, J. W., Lewis, Isabel E., and Wilson, A. J. C., Comments on the A.S.T.M. Power Data File—5 183 (C)
Hugo, J. A., *see under* Phillips, V. A.
Hurd, C. M., Stabilized high-intensity light source 305 (LN)

Jackson, N., Vacuum sublimation apparatus for preparation of thin sources of α-active materials 169
Jacob, L., Noble, R., and Yee, H., Photomultiplier soft X-ray spectrometer 460
James, J. F., Method of finding the focal curve of a photographic spectrometer 252 (LN)
Jennings, J. E., and Burland, J. B., Rand soil-pressure cell for low pressures, high accuracy, and long-term stability 193
Jones, G., Time-sorter for use in the nanosecond range 318
Jones, H. W., and Saunders, P. A. H., Swept Langmuir probe system for intense gas discharges 457
Jowett, A., *see under* Horsfall, F.
Jung, P., Transistorized frequency stabilization for reflex klystrons used in magnetic resonance 372

Kado, R. T., *see under* Kolin, A.
Keene, J. P., Two-valve electrometer circuit 218 (LN)
Kendall, B. R. F., New method of sample interchange in a solid-source mass spectrometer 130
Kent, P. J. C., *see under* Hatt, B. A.
Kierys, F. F., *see under* Monk, H.
Kimmitt, M. F., Simple method for stopping a radiation chopper in a preferred position 439 (LN)
King, G. W., Flap-valve for long narrow apertures 439 (LN)
Kinloch, C. D., and Waters, N. E., Extensometer for semi-rigid materials 93
Kitto, P. H., *see under* Nunlist, A.
Knight, R. D., Equipment for the encapsulation of semiconductor devices 197
Knight, R. D., Production of islands and dice in semiconductor slices with an ultrasonic drill 263
Kobak, J., and Loveridge, D. J., Single tube sedimentation apparatus for the measurement of particle size distribution 266
Kolin, A., and Kado, R. T., Simple photoelectric demodulator 107 (LN)
Kouris, M., *see under* Ruck, H.
Krishnamurthy, E. V., Digito-analogue computer for solving linear simultaneous equations and related problems 419

Lambie, R., Improved smoke density recorder 144
Lancaster, B. J., *see under* Huey, R. M.

Lane, W. R., *see under* Edwards J.
Latey, C. W., Photoelectric refractometer 38 (LN)
Laurenson.L, , *see under* Elsworth, L.
Lawrence, L. G., *see under* Dearnaley, G.
Leach, D. F., and Neilson, J. M. M., Design of a single electrode capacitor for use with moisture meters and similar apparatus 77
Lee, E. W., *see under* Birss, R. R.
Leece, J., Welding copper pipe to stainless-steel flanges in a laboratory workshop 219 (LN)
Lewis, Isabel E., *see under* Hughes, J. W.
Littlewood, A. B., Compensated Wheatstone's bridge circuit for gas-chromatographic catharometry 185
Lobb, J., Slow-feed dispenser for abrasive suspensions 36 (LN)
Lodge, A. S., Low-compliance diaphragm-capacitance gauge for measurement of liquid pressures of the order of 1 in. water 401
Loveridge, D. J., *see under* Kobak, J.
Lovett, S., Automatic range-changing of a linear ratemeter 376
Luttik, C., *see under* Schuringa, A.

McGregor, R. R., Transistor cup anemometer 189
McGuire, J. H., and Wraight, H., Radiometer for field use 128
MacKinnon, J. A., *see under* Dowell, T. M.
McKinstry, H. A., and Short, M. A., Automatically operated balance filters for counter diffractometer 178 (LN)
Magarshack, J. M., *see under* Axson, M.
Maggs, F. A. P., and Schwabe, P. H., Recording calorimeter for the measurement of heats of wetting, mixing or solution 60
Majer, J. R., *see under* Hardy, R.
Manley, R. St. J., *see under* Ruck, H.
Martin, A. J., *see under* Greetham, G.
Martin, K. A., *see under* Culpin, M. F.
Martin, W. R. B., Laboratory magnetic elutriator for purification and isolation of ferrimagnetic mineral sands 212
Mash, D. H., An electroluminescent digital indicator with a silicon carbide coding matrix 47
Mason, F. C. P., *see under* Elliott, K. W. T.
Mathai, A. O., Bubble method for susceptibility of liquids 71 (LN)
Maxwell, K. H., *see under* Green, M.
Mølgaard, J., Technique for replicating fibre surfaces by rolling 210
Molyneux, L., *see under* Edington, J. M.
Molyneux, L., and Schneider, E. E., Inexpensive graph plotter for five-track paper tape 425
Monk, H., and Kierys, F. F., Furnace for the uniform heating and mixing of powders in controlled atmospheres 397 (LN)
Moon, J. R., *see under* Garwood, R. D.
Morgan, F. R., An electromicrobalance for weighing fibres 53
Morgan, F. R., Apparatus for the measurement of the mechanical properties of fibres 25
Morley, T. K., *see under* Munden, D. L.
Morphew, K. L., Ratiometer phase angle indicator 300
Mossman, P., *see under* Doughty, D. C.
Mulholland, H. P., *see under* Asher, H.
Munden, D. L., and Morley, T. K., Yarn-speed meter—a low-torque instrument for measuring the linear speed of low-inertia systems 157
Munden, H. R., *see under* Burge, R. E.

Neilson, J. M. M., *see under* Leach, D. F.
Nelson, R. S., Insulated terminals for high-vacuum systems using demountable glass–metal seals 358 (LN)
Noble, R., *see under* Jacob, L.
Nunlist, A., and Kitto, P. H., Report on a pump-operated air aspirator 221 (LN)
Nutt, C. W., and Biddlestone, A. J., Simple refrigerant level controller for cold traps 67 (LN)

O'Brien, B. J., and de La Harpe, G., Portable airglow photometer 54
Oldham, E., *see under* Hood, W. E.
Ongkiehong, L., and van Duijn, J., Construction of a thermocouple for measuring surface temperatures 221 (LN)
Paix, D., *see under* Weston, E. T.
Palmer, D. A., Moiré fringe reading head for use with a fine grating 261
Parnell, T. M., Film carrier for the analysis of oscillograms by means of a travelling microscope 441 (LN)
Patla, N., Electronic apparatus for the study of X-rays with proportional counter 388
Pengelly, A. E., Apparatus for the measurement of gas velocity in furnaces and models 339
Perdok, W. G., and Boom, G., Improved eye-piece graticule for measuring X-ray powder diffraction patterns 134
Phillips, D. C., *see under* Arndt, U. W.
Phillips, J. A., Hot tube nylon cord cutter for balloon flights 440 (LN)
Phillips, V. A., and Hugo, J. A., Automatic polishing technique for electro-thinning metals for transmission electron microscopy 216 (LN)
Pierson, G., *see under* Evans, M. H.
Powell, R. E., Improved sample loading technique for solid source mass spectroscopy 252 (LN)
Preston, D., *see under* Farrow, G.

Rawson, H., The theory of stresses in two-component glass to metal tube seals 255 (C)
Reed, R. I., *see under* Brown, J. J.
Richards, J. R., Valve and adapter for the grease-free connexion of glass sample tubes to a mass spectrometer inlet system 69 (LN)
Richards, J. R., Vernier scale arrangement for the measurement of peak heights on mass spectrometer charts 358 (LN)
Richards, R. E., *see under* Evans, B. A.
Riddiford, L., *see under* Williams, A. W.
Roberts, A. C., *see under* Tolmie, E. D.
Robertson, J. H., X-ray diffraction by single crystals at low temperatures: a cryostat for use with liquid hydrogen 41
Roughton, J. E., Simple device for use with platform weighbridges in the accurate determination of burning rates 45
Ruck, H., Kouris, M., and Manley, R. St. J., Influence of protective paper on X-ray diffraction photographs 223 (C)
Ryder, J., *see under* Ambrose, E. J.
Ryder-Smith, S. C., Guile, A. E., and Barrington, A. E., Direct measurement of $\int i^2 dt$ by a method based on the Hall effect 100
Rymer, T. B., The Physical Society's Exhibition—London, 1960 153 (SA)
Ryves, T. B., Use of a liquid scintillator counter for beta particles 201

Sandover, J. A., and Taylor, C., Determination of the profiles of water waves 141
Saunders, I. C. B., *see under* Ashwin, B. S.
Saunders, P. A. H., *see under* Jones, H. W.
Saxe, R. F., *see under* Bate, D. G.
Sayers, J. F., Epoxy-resin joints for sealed-off, high-vacuum tubes 203
Schneider, E. E. *see under* Molyneux, L.
Schuringa, A., and Luttik, C., Measurement of space density of charge in flowing liquids 332
Schwabe, P. H., *see under* Maggs, F. A. P.
Scott, B. A., Instrument for the measurement of specular reflectivity of bright metal surfaces 435
Segre, S. E., and Allen, J. E., Magnetic probes of high frequency response 369
Sen, D., *see under* Hariharan, P.
Shepherd, W. H., New method of cold hearth melting 177 (LN)

Sherwood, J. N., and Thomson, S. J., Growth of single crystals of anthracene 242

Short, M. A., *see under* McKinstry, H. A.

Silvester, N. R., Densitometer wedge for measurements at low optical densities 33

Simpson, W., *see under* Brown, J. J.

Skertchly, A., Design and performance of a rapid-scanning X-ray diffractometer 6

Smith, M. J. A., Frequency stabilization of klystrons 398 (LN)

Smith, P. G., *see under* Thomas, P. H.

Southorn, W. A., The torsiometer—an instrument for the study of gels considered as elastic solids 292

Stanley, N., *see under* Hodkinson, J. R.

Start, P. L., and Thring, M. W., Design of laboratory furnaces 17

Steckelmacher, W., *see under* Cossutta, D.

Steele, D. J., Recording weight meter 27

Stevens, K. W. H., Parametric amplification 1 (SA)

Stokes, H. J., Apparatus for the measurement of Young's modulus between −200 and 700° C by transverse vibration in vacuum 117, 255 (C)

Stone, B. R. D., *see under* Edwards, J.

Sumner, C. J., Double-acting reversible message register 35 (LN)

Sumner, C. J., Simple multi-position level 220 (LN)

Taylor, C., *see under* Sandover, J. A.

Teare, P. W., Low-angle Geiger diffractometer for use with monochromatic radiation 132

Temple, R. B., *see under* Bishop, L.

Thomas, P. H., and Smith, P. G., Simple dosage meter for high-intensity thermal radiation 73

Thompson, J. E., Beam method for the measurement of internal friction 208

Thomson, S. J., *see under* Sherwood, J. N.

Thorne, S. W., Temperature-control system for use with a spectrophotometer 478

Thornley, R. F. M., *see under* Everhart, T. E.

Thring, M. W., *see under* Start, P. L.

Thrush, B. F., *see under* Garwood, R. D.

Tolmie, E. D., Apparatus for the zone refining of copper 175

Tolmie, E. D., and Roberts, A. C., Design of a small rolling mill for use at low temperatures 180 (LN)

Travers, S., *see under* Hardy, R.

Tresise, H. C., *see under* Dearnaley, G.

Trott, B. B., Reduction of dead-time in halogen-quenched Geiger counters 336

Turner, D. P., Daylight factor meter 316

van der Breggen, J. C., and Wouterlood, H. J., Novel displacement detector and its application in a recording thermobalance 297

van Duijn, J., *see under* Ongkiehong, L.

Van Niekerk, J. N., Vacuum furnace for high temperature X-ray diffractometry 172

Vodden, H. A., Simple method of temperature control 69 (LN)

Walker, J., *see under* Dobrowolski, T.

Ward, W. H., and Cheney, J. E., Oscillator measuring equipment for vibrating-wire gauges 88

Wasilewski, S., *see under* Barrer, R. M.

Waters, N. E., *see under* Kinloch, C. D.

Webb, M. S. W., Webb, R. J., and Wildy, P. C., Monitor for the quantitative determination of beryllium in the atmosphere 466

Webb, R. J., *see under* Webb, M. S. W.

Weston, E. T., and Paix, D., Cosine correction of a weatherproofed photovoltaic cell 359

Whitlow, L., A 450J spark discharge for shadowgraph photography 259

Wickham, R., *see under* Cunnell, F. A.

Wilbur-Ham, J., and Gibbs, W. E. K., Error of rectifier-type milliammeters in low-resistance circuits 313

Wildy, P. C., *see under* Webb, M. S. W.

Wilkinson, J. D., and Calvert, L. D., Oscillating flat-specimen holder for an X-ray powder camera 399 (LN)

Williams, A. W., and Riddiford, L., Two-way oil-filled dash pot 180 (LN)

Williams, G. I., *see under* Hatt, B. A.

Williams, R. L., High frequency light modulation 205

Wilson, A. J. C., *see under* Hughes, J. W.

Wilson, D. C., *see under* Elliott, K. W. T.

Wilson, R. N., *see under* Forsyth, P. J. E.

Wooster, G. A., *see under* Wooster, W. A.

Wooster, W. A., and Wooster, G. A., Twin-head goniometer for the study of diffusely reflected X-rays 64

Wootten, N. W., Diffuse-light integrator 70 (LN)

Wouterlood, H. J., *see under* van der Breggen

Wraight, H., *see under* McGuire, J. H.

Yee, H., *see under* Jacob, L.

Young, I. R., Position transducer using a divided circle and coded scale 125

Young, T. E., *see under* Ashwin, B. S.

PRINTED IN GREAT BRITAIN BY UNWIN BROTHERS LIMITED, WOKING AND LONDON